

TRANSPORTATION RESEARCH
CIRCULAR

Number E-C220

June 2017

**First International
Roadside Safety Conference**

Safer Roads, Saving Lives, Saving Money

June 12–15, 2017
San Francisco, California

TRB TRANSPORTATION RESEARCH BOARD

The National Academies of

SCIENCES • ENGINEERING • MEDICINE

TRANSPORTATION RESEARCH BOARD 2017 EXECUTIVE COMMITTEE OFFICERS

Chair: Malcolm Dougherty, Director, California Department of Transportation, Sacramento

Vice Chair: Katherine F. Turnbull, Executive Associate Director and Research Scientist, Texas A&M Transportation Institute, College Station

Division Chair for NRC Oversight: Susan Hanson, Distinguished University Professor Emerita, School of Geography, Clark University, Worcester, Massachusetts

Executive Director: Neil J. Pedersen, Transportation Research Board

TRANSPORTATION RESEARCH BOARD 2017–2018 TECHNICAL ACTIVITIES COUNCIL

Chair: Hyun-A C. Park, President, Spy Pond Partners, LLC, Arlington, Massachusetts

Technical Activities Director: Ann M. Brach, Transportation Research Board

David Ballard, Senior Economist Gellman Research Associates, Inc., Jenkintown, Pennsylvania, *Aviation Group Chair*

Coco Briseno, Deputy Director, Planning and Modal Programs, California Department of Transportation, Sacramento, *State DOT Representative*

Anne Goodchild, Associate Professor, University of Washington, Seattle, *Freight Systems Group Chair*

George Grimes, CEO Advisor, Patriot Rail Company, Denver, Colorado, *Rail Group Chair*

David Harkey, Director, Highway Safety Research Center, University of North Carolina, Chapel Hill, *Safety and Systems Users Group Chair*

Dennis Hinebaugh, Director, National Bus Rapid Transit Institute, University of South Florida Center for Urban Transportation Research, Tampa, *Public Transportation Group Chair*

Bevan Kirley, Research Associate, Highway Safety Research Center, University of North Carolina, Chapel Hill, *Young Members Council Chair*

D. Stephen Lane, Associate Principal Research Scientist, Virginia Center for Transportation Innovation and Research, *Design and Construction Group Chair*

Ram M. Pendyala, Frederick R. Dickerson Chair and Professor of Transportation, Georgia Institute of Technology, *Planning and Environment Group Chair*

Joseph Schofer, Professor and Associate Dean of Engineering, McCormick School of Engineering, Northwestern University, Evanston, Illinois, *Policy and Organization Group Chair*

Robert Shea, Senior Deputy Chief Counsel, Pennsylvania Department of Transportation, *Legal Resources Group Chair*

Eric Shen, Director, Southern California Gateway Office, Maritime Administration, Long Beach, California, *Marine Group Chair*

William Varnedoe, Partner, The Kercher Group, Raleigh, North Carolina, *Operations and Preservation Group Chair*

TRANSPORTATION RESEARCH CIRCULAR E-C220

First International Roadside Safety Conference

Safer Roads, Saving Lives, Saving Money

June 12–15, 2017
San Francisco, Calif.

Organized by
Transportation Research Board

Sponsored by
TRB Standing Committee on Roadside Safety Design (AFB20)

Co-Sponsored by
Transportation Pooled Fund Program Project No. TPF-5(329)
including
U.S. State Departments of Transportation for
Kentucky, Minnesota, Nebraska, Ohio, Washington, and West Virginia

June 2017

Transportation Research Board
500 Fifth Street, NW
Washington, D.C.
www.TRB.org

The **Transportation Research Board** is one of seven programs of the National Academies of Sciences, Engineering, and Medicine. The mission of the Transportation Research Board is to provide leadership in transportation innovation and progress through research and information exchange, conducted within a setting that is objective, interdisciplinary, and multimodal.

The **Transportation Research Board** is distributing this E-Circular to make the information contained herein available for use by individual practitioners in state and local transportation agencies, researchers in academic institutions, and other members of the transportation research community. The information in this circular was taken directly from the submission of the authors. This document is not a report of the National Academies of Sciences, Engineering, and Medicine.

Roadside Safety Design Standing Committee

Roger Bligh, *Chair*
John Donahue, *Secretary*

Marco Anghileri	Ali Hangul	Stephen Summers
Gerrit Dyke	James Mills	Dean Alberson
Erik Emerson	Brendan Russo	Cheung Joseph
Ronald Faller	Richard Butler	Hardy Donna
Raphael Grzebieta	Marc-Andre Seguin	Dhafer Marzougui
Malcolm Ray	Francesca La Torre	Jennifer Schmidt
Francesca Russo	Wade Odell	Jeff Jasper
Gavin Williams	Gabauer Douglas	Neece Greg
Richard Albin		Joseph Jones

Conference Planning Team

Ronald Faller, Midwest Roadside Safety Facility, University of Nebraska-Lincoln, *Chair*
Roger Bligh, Texas A&M Transportation Institute, *Co-Chair*
Richard Albin, Federal Highway Administration
Marco Anghileri, Politecnico di Milano, Italy
Keith Cota, New Hampshire Department of Transportation
John Donahue, Washington Department of Transportation (Pooled Fund Sponsor)
Mike Dreznes, International Road Federation
Michael Elle, Minnesota Department of Transportation (Pooled Fund Sponsor)
Don Fisher, Ohio Department of Transportation (Pooled Fund Sponsor)
Hampton Clay Gabler, Virginia Tech University
Douglas Gabauer, Bucknell University
Jodi Gibson, Nebraska Department of Roads (Pooled Fund Sponsor and Project Lead)
Raphael Grzebieta, University of New South Wales, Australia
Donna Hardy, West Virginia Department of Highways (Pooled Fund Sponsor)
Joseph G. Jones, Leidos, Inc.
Malcolm Ray, Roadsafes LLC
Jason Siwula, Kentucky Transportation Cabinet (Pooled Fund Sponsor)
Phil TenHulzen, Nebraska Department of Roads (Pooled Fund Sponsor)
Francesca La Torre, University of Florence, Italy
Rod Troutbeck, Troutbeck & Associates, Australia

TRB Staff

Stephen F. Maher, *Associate Director-Design*
Angela Christian, *Associate Program Officer*
Brie Schwarz, *Web Specialist*

Transportation Research Board
500 Fifth Street, NW
Washington, D.C.
www.TRB.org

Preface

This publication contains papers and abstracts presented at the TRB First International Roadside Safety Conference: Safer Roads, Saving Lives, Saving Money; June 12-15, 2017; San Francisco, California. The primary objective of the Conference was to support and advance global efforts to reduce deaths and serious injuries associated with run-off-road crashes. The TRB First International Roadside Safety Conference contributed to this objective through: (1) peer exchange and improved dissemination of information within the international roadside safety community; (2) increased collaboration amongst international roadside safety experts, researchers, government agencies, and engineering consultants; and (3) assisting with a more rapid implementation of new technologies, best practices, and products from around the world.

The E-Circular is organized by the conference subthemes: Advancements in Roadway Safety Features; Innovations in Roadside Safety Hardware and Features; Roadside Safety Design and Hazard Mitigation; Roadway Departure Data Collection and Analysis; Safety Policy, Guidelines, Plans, Programs, and Strategies; Simulation, Testing, and Evaluation Methods; and Vehicle Technologies and Safety Considerations. The views expressed in the papers and the abstracts contained in this publication are those of the authors and do not necessarily reflect the views of the Transportation Research Board, the National Academies of Sciences, Engineering and Medicine, the National Research Council, or the cosponsors of the conference. The papers were subject to a formal TRB peer review process, having a minimum of three reviews.

ACKNOWLEDGMENTS

The conference planning team consisting of: Ronald Faller (Chair), Midwest Roadside Safety Facility, University of Nebraska; Roger Bligh (Co-Chair), Texas A&M Transportation Institute; Richard Albin, Federal Highway Administration; Marco Anghileri, Politecnico di Milano, Italy; Keith Cota, New Hampshire DOT; John Donahue, Washington State DOT; Michael Dreznes, International Road Federation (IRF); Michael Elle, Minnesota DOT; Don Fisher, Ohio DOT; Hampton Clay Gabler, Virginia Polytechnic Institute and State University; Douglas Gabauer, Bucknell University; Jodi Gibson, Nebraska DOT; Raphael Gzrebieta, University of New South Wales, Australia; Donna Hardy, West Virginia DOT; Joseph Jones, Leidos, Inc.; Francesca LaTorre, University of Florence, Italy; Malcolm Ray, Roadsafe, LLC; Jason J. Siwula, Kentucky Transportation Cabinet; Phil TenHulzen, Nebraska DOT; and Rod Troutbeck, Troutbeck and Associates, Australia; assisted with the peer review of the abstracts and papers, as did many others in the international roadside safety community.

Contents

ADVANCEMENTS IN ROADWAY SAFETY FEATURES

Driving Speeds and Speed Tables: Slovenian Research (Abstract only)	3
<i>Marko Rencelj</i>	

Combating Roadway Departures (Abstract only)	4
<i>Richard Albin and Cathy Satterfield</i>	

Safety Impact of High Friction Surface Treatment Installations in the State of Pennsylvania	6
<i>Kimberley Musey, Seri Park, Monica Kares, and Gillian Kennedy</i>	

High-Friction Surfacing Treatment: How A 45-Year-Old Process Has Been Reengineered into the Leading National Safety System Used by Highway Agencies to Reduce Fatalities and Serious Injuries	21
<i>Richard Baker</i>	

Improving Pavement Friction to Advance Roadway Safety on Horizontal Curves (Abstract only)	27
<i>Joseph Cheung</i>	

A MASH TL-3 Compliant Short Radius System (Abstract only)	29
<i>Akram Abu-Odeh, Roger Bligh, Christopher Lindsey, and Wade Odell</i>	

INNOVATIONS IN ROADSIDE SAFETY HARDWARE AND FEATURES

Development of a Continuous Motorcycle Protection Barrier System Using Computer Simulation and Full-Scale Crash Testing (Abstract only)	33
<i>Ali O. Atahan, J. Marten Hiekmann, Jeffrey Himpe, and Joseph Marra</i>	

Relationship between Roadside Hazard Rating and Crash Occurrence	34
<i>Jonathan Wood and Eric T. Donnell</i>	

Initial Investigation into Traversability of Rock Ditch Liners	52
<i>Mojdeh Asadollahi Pajouh, John D. Reid, Cody S. Stolle, Ronald K. Faller, and Erik Emerson</i>	

Development of Crashworthy Road Sign Post Using Energy-Absorbing Modules on the Sign Base Plate (Abstract only)	65
<i>Dukgeun Yun, Mangi Ko, Minhyung Nho, and Jaehong Park</i>	

Challenges in Developing Cost-Effective MASH TL4 Semi-Flexible Barriers (Abstract only)	66
<i>Leigh Brown</i>	
New Zinc-Aluminum-Magnesium Metallic Coating for Guardrails (Abstract only)	67
<i>Richard A. Clausius and Michael Gremling</i>	
New Thrie Beam Terminal End Shoe Connection	68
<i>Akram Abu-Odeh, Roger Bligh, and Christopher Lindsey</i>	
Attachment of a Combination Bridge Rail to Concrete Parapet Utilizing Epoxy Adhesive Anchors	69
<i>Robert W. Bielenberg, Scott Rosenbaugh, and Ronald K. Faller</i>	
Design and Evaluation of a Fascia-Mounted Bridge Rail for Steel Bridges on Local Roadways (Abstract only)	87
<i>Chuck Plaxico</i>	
MASH Equivalency of NCHRP 350-Approved Bridge Railings (Abstract only)	88
<i>William Williams</i>	
Ponderosa Pine Round Posts as Alternative to Rectangular SYP Posts in Retrofit G4(2W) Guardrail Systems	89
<i>Karla A. Lechtenberg, Ronald K. Faller, John D. Reid, Scott K. Rosenbaugh, and David E. Kretschmann</i>	
A Synthesis of MASH-Tested 31-in. Tall, Non-Proprietary, W-beam Guardrail Systems	103
<i>Scott K. Rosenbaugh, Ronald K. Faller, and Robert W. Bielenberg</i>	
Evaluation of Radar Speed Sign for Mobile Maintenance Operations (Abstract only)	121
<i>Ali Jafarnejad and John Gambatese</i>	
Compliance Crash Testing of the CA ST-70 Side-Mounted Bridge Rail (Abstract only)	122
<i>Vue Her</i>	
Development of MASH TL-5 Steel Median Safety Barrier (Abstract only)	123
<i>Richard A. Clausius and Michael Gremling</i>	
MASH TL4 Safety Roller Barrier (Abstract only)	124
<i>Frederick Mauer</i>	
Development of a New MASH Guardrail Terminal (Abstract only)	125
<i>John C. Durkos</i>	

Worksite Safety Screens (Abstract only)	126
<i>Evan Coulson and Daniel Cassar</i>	
Study of an Innovative Type of Junction for Elements of Road Safety Barriers	127
<i>Sergio Marco Bassi, Davide Benetton, Andrea Milanese, Marco Anghileri, and Michele Pittofrati</i>	
Length of Need for Free-Standing, F-Shape, Portable Concrete Barrier	140
<i>Robert W. Bielenberg, John D. Reid, Ronald K. Faller, and Phil Tenhulzen</i>	
A MASH Compliant Sign Mounting Designs for Placement on Concrete Median Barrier (Abstract only)	158
<i>Akram Abu-Odeh and Wade Odell</i>	
Development of a Precast Slim Temporary Concrete Safety Barrier STCSB 50 for Work Zone Applications (Abstract only)	159
<i>Ali O. Atahan, Wolfgang Ganster, Thomas Edl, and Turan Arslan</i>	
 ROADSIDE SAFETY DESIGN AND HAZARD MITIGATION	
Development of a MASH TL-2 Crashworthy Pedestrian Railing System	163
<i>Ronald Faller, Karla Lechtenberg, Jennifer Schmidt, Ana Guajardo, Robert Bielenberg, John Reid, and Erik Emerson</i>	
Vulnerable Road User Serious Injury Impacts into W-Beam Barrier (Abstract only)	183
<i>Raphael Grzebieta, George Rachnitzer, Mario Mongiardini, and Mike Bambach</i>	
Development of Guidance for Minimum Sign Area for Slipbase Sign Supports (Abstract only)	184
<i>Roger Bligh, Chiara Dobrovolny, and Dusty Arrington</i>	
Consideration of Placement Criteria for Utility Poles to Minimize Crash Risk	185
<i>Christine E. Carrigan and Malcolm H. Ray</i>	
Utility Poles, Toleration, or Confrontation	196
<i>Don L. Ivey and C. Paul Scott</i>	
Making Roads (More) Motorcycle Friendly in New Zealand (Abstract only)	208
<i>Julian Chisnall</i>	
Design and Full-Scale Testing of New Retrofit Bridge Rail for 24.8-Mile Long Causeway Bridges Over Lake Pontchartrain, New Orleans, Louisiana	209
<i>William F. Williams</i>	

Safety Procedures for Emergency Responders When High-Tension Wire Rope Systems Are Involved with Run-Off-Road Accidents (Abstract only)	224
<i>Dean C. Alberson</i>	
Design and Analysis of High-Energy-Absorbing Rock Fence	225
<i>Iraj H.P. Mamaghani and Hiroshi Yoshida</i>	
Design of Reinforced Expanded Polystyrene Styrofoam Covering Rock-Sheds Under Impact of Falling Rock	237
<i>Iraj H.P. Mamaghani and Hiroshi Yoshida</i>	
Feasibility Of Predicting Light Vehicle Occupant Injury Disutility from Impacts With Road Safety Barriers	250
<i>Andrew Burbidge and Rod Troutbeck</i>	
Modeling and Simulation of Vehicle Crashes on Curved, Banked Roadway Sections	266
<i>Dhafer Marzougui, Cing-Dao (Steve) Kan, Stefano Dolci, Alberto Morena, and Kenneth S. Opiela</i>	
Commercial Motor Vehicle Safety Measures (Abstract only)	287
<i>John C. Durkos</i>	
New Methodology for Analysis of Sand Barrel Arrays	288
<i>Robert W. Bielenberg, Ronald K. Faller, Joseph G. Putjenter, and John D. Reid</i>	
Evaluation of Energy-Absorbing End Terminals Adjacent to Curbs	306
<i>Jennifer D. Schmidt, Ronald K. Faller, Robert W. Bielenberg, Brock Schroder, and Erik Emerson</i>	
Flail-Space Model – A Review of the Lateral Impact Velocity for Thoracic Injuries (Abstract only)	323
<i>Tana C. Tan, Raphael H. Grzebieta, and Andrew S. McIntosh</i>	
 ROADWAY DEPARTURE DATA COLLECTION AND ANALYSIS	
Standardization of Roadside Safety ISPE Processes Using Data Dictionary for Pre- and Post-Crash Information (Abstract only)	327
<i>Chiara Silvestri Dobrovolny, Charles Stevens, Roger P. Bligh, Madilyn Mendoza, and Carlos Leyva</i>	
A Study of Applying Mobile Mapping Result for Road Safety Audit on Rural roads in Thailand	328
<i>Chakree Bamrungwong, Preecha Soparat, Kawin Saiprasertkit, and Nutvara Jantarathaneewat</i>	

Testing and Analyses of Terrain Effects on Vehicle Trajectories and Kinematics (Abstract only)	344
<i>Dhafer Marzougui, Cing-Dao (Steve) Kan, and Kenneth Opiela</i>	
Evaluating Safety Hardware Identification Methods Durability Using Crash Testing Opportunities	345
<i>Charles R. Stevens Jr., Chiara Silvestri Dobrovolny, Roger P. Bligh, and Ben Zoghi</i>	
Safety Evaluation of Safety Edge Treatment in Iowa (Abstract only)	358
<i>Amrita Goswamy, Shauna L. Hallmark, Michael Pawlovich, and Bo Wang</i>	
Investigating Effectiveness of Centerline Rumble Strips on Rural Two-Lane Roads in Louisiana with Empirical Bayes Method (Abstract only)	359
<i>M. Ashifur Rahman and Xiaoduan Sun</i>	
Safety Impacts of the Safety Edge (Abstract only)	360
<i>Shauna L. Hallmark, Amrita Goswamy, Michael Pawlovich, and Bo Wang</i>	
Safety Impacts of Centerline Rumble Strips in Georgia (Abstract only)	361
<i>Marisha S. Pena</i>	
High Tension Cable Barrier in the Median of a Freeway in Alberta, Canada: A Case Study of Two Successful Projects	362
<i>Paul H. A. Steel, Masood Hassan, Gerard Kennedy, and Bill Kenny</i>	
An Analytical Framework of Systematic Screening of Roadway Departure Crashes on Rural Highways in Montana	378
<i>Md. Shafiul Azam and Patricia W. Burke</i>	
Evaluation of Roadway Departure Characteristics using SHRP 2 Naturalistic Driving Study and Road Information Database Data: Preliminary Results (Abstract only)	392
<i>Nicole Oneyear, Omar Smadi, Shauna Hallmark, and Skylar Knickerbocker</i>	
An Exploratory Analysis on Fatalities of Roadway Departure Crashes	393
<i>Mouyid Islam</i>	
Consideration of Roadside Features in the <i>Highway Safety Manual</i> (Abstract only)	421
<i>Christine E. Carrigan and Malcolm H. Ray</i>	
A New Method to Evaluate Roadside Safety for Rural Two-Lane Roads Based on Reliability Analysis (Abstract only)	422
<i>Mohammad Jalayer and Huaguo Zhou</i>	

Integrating Crash Severity in Roadside Safety Quantitative Analysis: Assessing Partial Proportional Odds Models	423
<i>Carlos Roque and João Lourenço Cardoso</i>	
Estimate of Occupant Ejection and Occupant Head-Slap Prevalence in Real-World Longitudinal Barrier Crashes	437
<i>Douglas J. Gabauer</i>	
Comprehensive Analysis of Bridge-Related Crashes in New Jersey (Abstract only)	450
<i>Mohammad Jalayer and Hooman Parvardeh</i>	
Comprehensive Analysis of Run-Off-Road Crashes in New Jersey (Abstract only)	451
<i>Mohammad Jalayer and Michael O'Connell</i>	
Evaluating the Relevancy of Current Crash Test Guidelines for Roadside Safety Barriers on High-Speed Roads	452
<i>Connie Xavier, Dominique Lord, Chiara Silvestri Dobrovolny, and Roger Bligh</i>	
Design Impact Conditions for Testing and Evaluation of Longitudinal Safety Barriers for Use on High-Speed Roadways (Abstract only)	466
<i>Roger Bligh, Chiara Dobrovolny, and Nauman Sheikh</i>	
Roadside Barrier Issues: Lessons Learned from National Transportation Safety Board Accident Investigations (Abstract only)	467
<i>Donald F. Karol</i>	
The SHRP 2 Roadway Information Database: A Template for Data Collection (Abstract only)	468
<i>Omar Smadi, Neal Hawkins, and Zachary Hans</i>	
The Use of Corporate Crash Data to Assist Companies Improve Road Infrastructure for Workplace Safety	469
<i>Keith Simmons, George Rechnitzer, and Raphael Grzebieta</i>	
Monitoring and Predicting Traffic Safety in Slovenia (Abstract only)	485
<i>Peter Lipar</i>	
Identifying Roadway Risk Factors in Pennsylvania's Delaware Valley Region	486
<i>Kimberley Musey, Seri Park, and Patrick McTish</i>	
Benchmarking the Risks of Roadside Hazards (Abstract only)	497
<i>Christine E. Carrigan and Malcolm H. Ray</i>	

SAFETY POLICY, GUIDELINES, PLANS, PROGRAMS, AND STRATEGIES

Challenges and Opportunities for Improving the Safeside Procedure for Cost-Benefit Assessment of Roadside Safety Intervention Alternatives	501
<i>João Lourenço Cardoso and Carlos Roque</i>	
Road Safety Audit and Proposal for Corridor Extension Plan: Case Study Barapullah Corridor, New Delhi (India)	516
<i>Namit Kumar and Mukesh Kumar</i>	
Roadside Safety Hardware Framework Concept for Enhanced In-Service Performance Evaluation and Asset Management Practices (Abstract only)	528
<i>Charles R. Stevens, Jr.</i>	
Safe System Assessments of Roadside Safety Projects	529
<i>Jamie Robertson, Kenn Beer, and Daniel Cassar</i>	
Utilizing the Safe System Approach to Meet the Challenge of the Decade of Action (Abstract only)	540
<i>Michael Dreznes</i>	
Taxonomy of Roadside Safety Hardware	541
<i>T. Olaf Johnson and Malcolm H. Ray</i>	
Protecting the Most Vulnerable: Which Safety Measures Generate Public Support for Paratransit and Bus Transportation? (Abstract only).....	550
<i>Isabella Guajardo</i>	
Safety Countermeasures For Roadway Departure Crashes: An Overview (Abstract only).....	551
<i>Mohammad Jalayer and Huaguo Zhou</i>	
Initial Developments Supporting a Roadside Tree Removal Marketing Campaign	552
<i>Cody S. Stolle, Karla A. Lechtenberg, Ronald K. Faller, And Taeun (Alexis) Yim</i>	
Retrospective Look at 1998 Strategies to Improve Roadside Safety: Mission 2: Build and Maintain Information Resources and Analysis Procedures.....	574
<i>Kenneth S. Opiela</i>	
Traffic Stopped Ahead: Everything You Wanted To Know About Work Zone Queue Warning Systems (Abstract only).....	606
<i>Joseph “Joe” Jeffrey</i>	
Reducing the Incidence of Impaired Driving Through Globally Effective Countermeasures (Abstract only)	607
<i>Danielle Comeau, Felix J.E. Comeau, and Denise Connerty</i>	

Selection and Placement Guidelines for Test Level 2 Through Test Level 5 Median Barriers (Abstract only)	609
<i>Christine E. Carrigan and Malcolm H. Ray</i>	
Establishing a National Accreditation Scheme for Road Safety Barrier Industry (Abstract only)	610
<i>Daniel Cassar</i>	
Progress Toward a National Harmonisation for Road Side Safety Barrier Training and Accreditations Schemes for Installation and Maintenance in Australia and New Zealand (Abstract only)	611
<i>Paul Hansen</i>	
Advances in Winter Maintenance Practices to Improve Roadside Safety	612
<i>David L. Bergner</i>	
Guidelines for Shielding Bridge Piers (Abstract only)	626
<i>Malcolm H. Ray, Christine E. Carrigan, and Chuck A. Plaxico</i>	
Handling an Instant Hazard (Abstract only)	627
<i>Eric Hemphill</i>	
 SIMULATION, TESTING, AND EVALUATION METHODS	
MGS Dynamic Deflections and Working Widths at Lower Speeds	631
<i>Mojdeh Asadollahi Pajouh, Nicholas A. Weiland, Cody S. Stolle, John D. Reid, and Ronald K. Faller</i>	
Development and Validation of the Surrogate Vehicle Used in ASTM F3016-14 Standard Test Method for Surrogate Testing of Vehicle Impact Protective Devices at Low Speeds	644
<i>Dean C. Alberson, Michael S. Brackin, and Wanda L. Menges</i>	
Correlation between Roadside Safety Hardware and Vehicle Safety Standards Evaluation Criteria (Abstract only)	656
<i>N. Schulz, C. Silvestri Dobrovolny, D. Arrington, H. Prodduturu, J. Rupp and J. Hu</i>	
Development of a Motorcycle FE Model for Simulating Impacts into Roadside Safety Barriers	657
<i>Mario Mongiardini, Bill Walton, Raphael H. Grzebieta, Matthew McKay, Chris Menictas, Alexander Berg, and Peter Rücker</i>	
Upright Motorcycle Impacts Against Roadside Safety Barrier: Rider Injury Risks and Countermeasure Investigation Through FEA (Abstract only)	674
<i>Chiara Silvestri Dobrovolny, Antonio DeFranco, Nathan Schulz, and Roger P. Bligh</i>	

Improvement of Hybrid III 50th Percentile FE Model for Sliding Configuration Motorcyclist Impact	675
<i>Matteo Bernardini, Marco Mancini, Marco Anghileri, Michele Pittofrati, and Dario Guarino</i>	
Motorcycle Finite Element Computer Model to Assist with Roadside Safety Research Efforts (Abstract only)	686
<i>Nathan Schulz and Chiara Silvestri Dobrovolny</i>	
Investigation and Mitigation of Post Penetration into Floorpan of 1100C Small Cars	687
<i>Ronald Faller, Scott Rosenbaugh, Robert Bielenberg, Karla Lechtenberg, James Holloway, Cody Stolle, Jennifer Schmidt, John Reid, and Mojdeh Asadollahi-Pajouh</i>	
Recommended Updates to MASH for Testing of Cable Barrier Systems	705
<i>Scott K. Rosenbaugh, Ronald K. Faller, Roger P. Bligh, Robert W. Bielenberg, and Mario Mongiardini</i>	
Comparison of Human Occupant Kinematics in Laboratory Impact and Run-Off-Road Crash Configurations	718
<i>Rudolf Reichert, Cing-Dao (Steve) Kan, Dhafer Marzougui, and Kenneth Opiela</i>	
Investigation of Potential Mitigation of Driver Injury in Heavy Truck Frontal and Rollover Crashes (Abstract only)	733
<i>Nathan Schulz, Chiara Silvestri Dobrovolny, and D. Blower</i>	
Experience with Inclusion of Instrumented Anthropomorphic Test Devices in Roadside Safety Barrier Testing with Heavy Trucks (Abstract only)	734
<i>Chiara Silvestri Dobrovolny, Nathan Schulz, Roger P. Bligh, and D. Lance Bullard</i>	
Evaluation of a 31-inch W-Beam Guardrail for Placement on a 3H:1V Sloped Terrain through FEA (Abstract only)	735
<i>Nathan Schulz, Chiara Silvestri Dobrovolny, and D. Arrington</i>	
Development of Crash Modification Functions for the Safety Performance of Treatments on Rural Two-Lane Roads (Abstract only)	736
<i>Jiguang Zhao, Kim Kolody, Henry Brown, and Carlos Sun</i>	
Comparison of Verification and Validation of Crash Test and Simulation Results for Common Barriers	737
<i>Dhafer Marzougui, Cing-Dao (Steve) Kan, and Kenneth S. Opiela</i>	
Applying Finite Element Analysis to Assess the Crash Performance of Modified R350 TL4 Bridge Rail Design in Accordance with the Federal-Aid Reimbursement Eligibility Process (Abstract only)	764
<i>Chuck Plaxico</i>	
Roadside Safety Implications of Future Vehicle Designs (Abstract only)	765
<i>Dhafer Marzougui, Cing-Dao (Steve) Kan, Fadi Tahan, and Kenneth Opiela</i>	

Comparing Objective and Subjective Roadway Data Collection Methods Using Cost–Benefit Analysis for the Proposed Safety Countermeasures (Abstract only)	766
<i>Niloo Parvin</i>	
Performance Characteristics of Posts Embedded in Soil for Use in Computer Simulation	767
<i>Karla A. Lechtenberg, John D. Reid, and Ronald K. Faller</i>	
Impact Resistance of Guardrail Posts on Sloped Ground (Abstract only)	780
<i>Chung R. Song, Tewodros Y. Yosef, Ronald K. Faller, Mojdeh Pajouh, and Karla A. Lechtenberg</i>	
Behavior and Performance of Wood and Composite Blockouts Raised on Posts During Component Pendulum Impact Testing (Abstract only)	781
<i>Chiara Silvestri Dobrovolny, Nathan Schulz, Dusty Arrington, and Roger P. Bligh</i>	
Evaluation of Soil Conditions and Post Embedment Depth on Guardrail Post Performance (Abstract only)	782
<i>Ali O. Atahan, Murat Ornek, Murat Buyuk, and Ercan Epsileli</i>	
Development of the Australian and New Zealand Standard for Safety Barriers and Associated Devices	783
<i>Rod Troutbeck and Julian Chisnall</i>	
Evaluation of A MASH Test Level 4 Sound Wall Barrier Using Simulation (Abstract only)	794
<i>Nauman M. Sheikh</i>	
Evaluation of Head and Brain Injury Using Empirical and Analytical Predictors in Human Body Model (Abstract only)	795
<i>Davide Benetton, Benedetta Arosio, Marco Anghileri, Mario Mongiardini, and Garrett Mattos</i>	
Integrated Interior and Restraint Modeling for Occupant Risk Analysis	803
<i>Rudolf Reichert</i>	
Comparison of Hybrid III and Human Body Model in Head Injury Encountered in Pendulum Impact and Inverted Drop Tests	804
<i>Benedetta Arosio, Davide Benetton, Marco Anghileri, Mario Mongiardini, Garrett Mattos, and Raphael Gzerbieta</i>	
 VEHICLE TECHNOLOGIES AND SAFETY CONSIDERATIONS	
See Me Save Me: Improving the Safety of Cyclists (Abstract only)	819
<i>Harpreet Singh Dhunna</i>	
Heavy Vehicle Encroachment Trajectories	820
<i>Malcolm H. Ray, Christine E. Carrigan, and Chuck A. Plaxico</i>	

Intelligent Transportation System Technology Application for Notification of Vehicles with Right-of Way (Abstract only).....	831
<i>Chiara Silvestri Dobrovolny, Richard Zimmer, Hassan Charara, and Garrett Ackner</i>	

Advancements in Roadway Safety Features

Driving Speeds and Speed Tables *Slovenian Research*

MARKO RENČELJ

MATJAŽ ŠRAML

TOMAŽ TOLLAZZI

University of Maribor, Slovenia

It is especially in the last 20 years that traffic calming measures (all kind of devices, applications etc.) are also more and more frequent in Slovenia. The Slovenian Act about public roads defines measures and devices for traffic calming. According to our law the traffic calming devices are physical, light or other devices and obstructions that physically prevent the participants in road traffic to drive with inappropriate speed or they warn them to limit the speed on dangerous road sections.

In Slovenia we still have problems with speeding inside urban areas (settlements, cities). According to that there are still locations on our roads, where we need to reduce speeds of motor vehicles with physical measures. Based on foreign experience (Netherlands, Germany, Austria), we began to install traffic calming measures. Over those years, we have found that identical measures may not have the same results due to different mind-sets in different countries, also taking into account inconsistency of realization etc.

Speed tables are flat-topped speed humps that are often constructed with brick (or other textured materials) on the flat section. Speed tables are usually long enough for placing the entire pedestrian crossing. Speed tables are also good for locations where low speed is desired - but a somewhat smooth ride is needed.

In the article are shown analyzed results of our research, which was done in the last years. Main aim of our research was:

- Technical elements/dimensions of the speed tables: what is the correlation between dimensions of the speed tables—especially inclination of “ramps”—and driving speed over speed tables? For different types/layout of speed tables their dimensions was correlated with driving speeds, based on hidden speed measurements.
- Speeds between speed tables: in some cases it is necessary to place speed tables on longer longitudinal road sections. Each location is somehow specific; the question was, what is correlation, when we compare distance between two speed tables and driving speed in the middle? Again, hidden speed measurements was performed.

For hidden speed measurements we used laser measurement instrument Riegl LR90-235/P. All observed locations were inside urban areas on the road sections with similar vehicle traffic characteristics.

It is important to emphasize that comparison with some international standards/research results were also made. We established some deviate results, which are discussed and analyzed.

ADVANCEMENTS IN ROADWAY SAFETY FEATURES

Combating Roadway Departures

DICK ALBIN

FHWA Resource Center

CATHY SATTERFIELD

FHWA Office of Safety

Roadway departure (RwD) crashes account for more than half of the highway fatalities in the United States. Typically the most cost-effective treatments are those that deter drivers from leaving the roadway or crossing the center line. Improving these types of countermeasures and their application is one of the Federal Highway Administration (FHWA) RwD Team's objectives. Our overarching goal is to cutting roadway departure fatalities in half from nearly 19,000 in 2012 to less than 9,500 by 2030.

TAKING CURRENT COUNTERMEASURES TO THE NEXT LEVEL

Many proven treatment that keep drivers on the roadway can be enhanced to help meet crash reduction goals. For instance:

- While standard signs will always be important, in some locations added conspicuity or actuated signs can improve safety performance.
- Edge lines show benefits on low volume roads and innovative marking applications can bring the drivers attention to unexpected conditions.
- New rumbles strip designs are showing some promise to expand application potential.

Additionally, better data availability may provide more potential for knowing how these countermeasures are performing in various situations and where the greatest needs are.

THE CHANGING FACE OF COUNTERMEASURES WITH V2I TECHNOLOGIES

As new vehicle technologies are introduced, it is extremely important to evaluate how these will work with current safety treatments, what future treatments should look like, and how to deal with the transition period while we have a wide variety of vehicle capabilities on the roadway networks. We need to frame the research questions of the transition:

- How soon and how extensively will various technologies penetrate the fleet?
- Who is our design driver?
- Will there be different effects in urban, suburban, and rural areas?
- How do we transition from milled rumbles to something that works for vehicles with and without technologies?
- What are the limitations of these technologies

HURDLES TO IMPLEMENTATION

Perhaps as a new generation is ushered into the workforce, resistance to change will no longer be the biggest struggle in implementing new treatments or new applications of existing countermeasures. However cost, particularly unglamorous cost such as maintaining signs and pavement markings, are likely to continue to be an issue. We need to identify the hurdles and find ways to overcome them with more durable products and applications, such as inlaying our pavement markings so they are visible year round. Addressing friction concerns with retroreflective pavement markings would also open opportunities for more applications. Milled in rumble strips are very low maintenance, but continue to raise concerns with noise, bicycle accommodation, and pavement maintenance. And while we know adding shoulders or even a Safety Edge will improve the chances of safely recovering from a roadway departure, we need to address concerns with adding impermeable surface area.

The future holds much promise for more of our family, friends and neighbors arriving home safely from every trip, but there is much work ahead for those with vision to make it happen.

ADVANCEMENTS IN ROADWAY SAFETY FEATURES

Safety Impact of High-Friction Surface Treatment Installations In Pennsylvania

KIMBERLEY MUSEY

MONICA KARES

SERI PARK

GILLIAN KENNEDY

Villanova University

According to the National Highway Traffic Safety Administration (NHTSA), a total of 35,092 people died in motor vehicle crashes on the U.S. highway system in the year 2015, representing the largest annual% increase in nearly 50 years. Roadway departure crashes account for the majority of highway fatalities. To address this issue, transportation professionals have continued to investigate countermeasures to improve safety, such as High Friction Surface Treatments (HFSTs). HFSTs are pavement resurfacing systems applied in short sections to provide exceptional skid resistance. This technology has the potential to be an innovative and sustainable means of improving roadway safety.

This research seeks to review the performance of HFSTs from a safety and economic perspective through an analysis of installation projects in the state of Pennsylvania. Using data provided by the Pennsylvania Department of Transportation, it analyzes the extent of their effectiveness in reducing crash rates and crash severity through a before-after and benefit-cost study of 106 sites. The results indicate that the greatest reduction in crash number and severity, and the greatest return on investment occurred for intersections on horizontal curves in a rural environment.

Future study will involve the develop crash modification factors to quantify the expected crash reduction that can be expected at a particular location, as a function of various roadway features. The goal of this study is to enable DOTs to maximize return and to better anticipate the safety benefits of HFSTs prior to implementation.

INTRODUCTION AND BACKGROUND

Each year, thousands of drivers in the United States are involved in motor vehicle crashes (1). Roadway departure crashes are frequently severe and account for the majority of highway fatalities. These occur when a vehicle leaves the travelled way by crosses an edge line or center line. According to the Federal Highway Administration, there were 17,791 fatalities in 2014 as a result of roadway departure crashes, which was 54% of the traffic fatalities in the United States (2). Hence it is important to investigate cost efficient and sustainable methods of improving roadway safety in this regard.

Since the early 2000s, there has been an increase in state HFST installations projects as a potential safety countermeasure. Noteworthy practices according to the FHWA have been seen in the states of Kentucky, South Carolina, California, Florida, and New York, among many others. It is important, however, to analyze how these HFSTs are performing, and determine the

extent of their effectiveness in reducing crash rates and crash severity. It is also important to study the long-term benefits versus the costs.

This paper seeks to review the performance of HFSTs from a safety and economic perspective for roadway departure crashes through an analysis of HFST installation projects in the State of Pennsylvania. This study uses data provided by the Pennsylvania Department of Transportation (PennDOT) to perform a comprehensive before-after analysis and benefit-cost study of 106 sites. The findings serve as a proof of concept to show how DOTs can use crash data to determine the top locations types to invest in HFST projects for the maximum safety impact and best return on investment.

The results along with further statistical analysis will be used to develop a number of crash modification factors (e.g. for an urban, rural, intersection, segment, curve, or tangent facility) to calculate the expected crash reduction when deciding whether or not to proceed with a HFST project. Future study will also expand on this idea through the development of a safety performance function transportation professionals can use to quantify the average number of crashes per year they can expect at a location as a function of HFST installation, horizontal curvature, annual average daily traffic (AADT), and other geometric features. The goal of is to enable DOTs to better anticipate the safety benefits of HFSTs prior to implementing new projects. The findings would greatly benefit transportation agencies when developing projects and investing government funds, and most importantly meeting traffic safety goals.

RESEARCH OBJECTIVES

The objectives of this research are to:

- Conduct a comprehensive review and analysis of crash data to further explore the relationship of HFST installation, crash rates, and crash severity for projects in Pennsylvania;
- Perform a before-and after analysis of crash data
- Conduct a benefit-cost study of HFST installations
- Establish a basis for future research that includes: the development of a crash modification factor (CMF) of pavement friction factor along with other site specific features (e.g. degree of horizontal curvatures, rural vs urban environments, and other roadway features)

This paper is organized into major sections that include: a background and reviews of HFST; detailed crash data description and analysis methodology; resulting dataset findings; and the future direction of this research.

LITERATURE REVIEW

Pavement Friction

Friction factor can be defined as the amount of resistive force between a vehicle tires and the roadway. The amount of roadway friction on a roadway is generally quantified using some form of by what is known as a skid number. Pavement friction plays a very important role in driver safety. In general, the less friction that is available, the less a driver can control his vehicle and

remain on in their travel lane. Friction becomes a problem particularly under wet or slippery road conditions. Extreme speeds and distracted driving can also lead to roadway departure crashes in areas where friction demand is high. Therefore, friction plays a critical role in safe pavement and geometric roadway design.

High-Friction Surface Treatments

Horizontal curves, steep grades, and intersection approaches are all locations where drivers tend to brake excessively. As a result, the roadway tends to lose its friction more quickly than other locations. This reduction in pavement friction causes vehicles to skid, depart from the lane on curves, or rear-end leading vehicles when approaching an intersection. HFST are pavement treatments that can be applied at these spot locations, or locations where pavement friction was never adequate, in order to provide drivers with exceptional skid resistance (3). Greater pavement friction makes the loss of microtexture friction due to the wet weather less critical (4).

Calcined bauxite is the recommended aggregate for use in HFST applications due to their high resistance to polishing (5). Other materials that have also been evaluated for this purpose include flint, granite, and slags, which are all commercially available. The binder materials can include Bitumen-extended epoxy resins, epoxy resin, polyester-resin, polyurethane-resin, or acrylic-resin. The installation process can be done with either manual or machine automated mixing (6).

HFST have many strengths including its moderate cost and construction when compared to other alternatives, it does not add to the system of maintenance, and minimal impact on driver behavior because they do not typically recognize the difference in surfaces. It can therefore be a sustainable and cost-effective option to preventing roadway departure crashes and fatalities. HFSTs may even drain better than traditional paved surfaces, and may be applied systematically to problem locations.

Yet, while they clearly have a number of potential benefits, there are still some uncertainties regards to HFSTs. Due to its more recent implementation, there is still some uncertainty of its long-term durability. As seen through treatments implemented in Kansas, site preparation, uniformity, pavement condition at the time of construction, and construction quality all may have a large effect on its efficiency and durability, and whether or not the surfaces separate and create spalls and patching with use over time (7,8). In addition, HFSTs have a higher cost when compared to other pavements. Also, it is still unknown whether its specifications should be different depending on the variety of local features at various sites. There are also concerns as to whether or not their effectiveness will decrease over time (9).

Case Studies

Crash Reduction

HFST was first installed in Pennsylvania during the year 2007. The pilot program focused on a horizontal curve in which vehicles often slid and crashed into guiderail or opposing traffic. After HFST was applied, it was reported that “wet-pavement-related crashes at the spot dropped from 20 in the 10 years prior to the treatment to zero in the seven years since it has been installed” (3). Such positive results led the state of Pennsylvania to deploy several other projects, which

continue to also have success. In fact, PennDOT has reported a before/after total crash reduction of 100% for their signature HFST trial projects (10).

Pennsylvania, however, is not the only state to experience the benefits of HFSTs. As of July 2015, 40 States have applied HFST on at least one project site, and nine states have implemented HFST programs (10). In South Carolina, a one-mile section of US 25 in Greenville County was characterized by a rural and mountainous terrain, sharp horizontal and vertical curves, heavy truck traffic, 10,000 vehicles per day, and high speeds even in inclement weather. In 2008, HFST was applied for a total cost of \$1 million. Results showed that the wet crashes were reduced by 68% and total crashes by 56%. Other locations in South Carolina also experienced benefits. One study considered seven HFST project locations, and it was reported that South Carolina Department of Transportation (SCDOT) experienced an 81% reduction in wet crashes and 71% reduction in total crashes (11).

Similar positive outcomes have resulted in other states across the country. For example, the State of Kentucky installed HFST for the first time in 2009 at two trouble locations. “The two locations had 65 reported wet pavement crashes in the 3 years before the HFST treatment (average 21.7/year) and 15 (average 3.75/year) in the 4-year after period.” This led the state to develop an official HFST program that selects sites based on the Empirical Bayes methodology (12). In addition to the United States, HFST installations have been successful in reducing crashes for several decades around the world in areas such as New Zealand, Australia, and throughout Europe (14,15).

Benefit–Cost Ratio

The State of Florida conducted a study that sought to assess the effectiveness of HFST in reducing crashes on a number of roadway alignments based upon the benefit-cost ratio of previous installations. 23 HFST projects in Florida were identified by researchers. Each was analyzed based upon its bidding records, roadway geometry, and crash history. The cost of installing each project was based on the average HFST unit cost, and this value was scaled by the size of the application as obtained during the data collection phase. Savings were estimated based on the average cost per crash severity from the Florida DOT KABCO scale. “On average, HFST applications on tight curves reduced the total crash rate by 32% and the wet weather crash rate by 75%. The average BC ratio on tight curve sections was between 18 and 26. Wide curve and tangents sections had few accidents initially, and HFST had negligible impact” (13).

A recent before and after study from the SCDOT performed a similar analysis for a series of horizontal curves. The study revealed benefit-cost ratios of about 24 to 1. In contrast, the State of Kentucky placed HFST on 26 curves, and saw values from 6.2 to 1.9 at those locations. (14)

STUDY LOCATION AND DATA COLLECTION

This research utilized crash data provided by the Pennsylvania Department of Transportation. (PennDOT). The crash database includes crash data from 9 PennDOT Districts. A variety of sites were included from rural and urban facilities, intersections and segments, horizontal curves and tangents. The number of lanes ranged from two to six, and speed limits ranged from 15 mile-per-hour (mph) to over 55 mph. Some sites included features like rumble stripes, medians.

The original database contained a total of 3,322 crashes from the years 2003 through 2016. Each crash data entry recorded by PennDOT included detailed information on the crashes, including the county, state route, segment and offset where the crashes took place, the date and time of the crash, lighting, roadway surface conditions, weather, crash severity, environmental roadway factors, vehicle events, and driver actions. This information was crucial to analyze how each of these features correlated to the occurrence of crash events.

In addition to the crash database, PennDOT also provided a database of its HFST projects throughout the state, both planned and completed. As of March 2016, this included 140 locations where HFST projects were completed, and 60 that were planned or in construction. These projects are in nearly all counties in the state. In this database, each project site has a Multi-modal Project Management System (MPMS) number, district, county, state route, segment, offset, targeted crash type, actual/anticipated completion date, funding source, and amount of funding.

METHODOLOGY

This paper seeks to review the performance of HFSTs from a safety and economic perspective through an analysis of HFST installation projects in the state of Pennsylvania. Only projects with a completion date of 2015 or earlier were included in this study in order to ensure crash data after HFST installation is available to compare to the crash history prior to the installation. In addition, only locations where geometric and cost information can be found were included. This reduced the dataset to approximately 106 locations from the original 140 locations. These are marked with stars in Figure 1 along with a breakdown of various features.

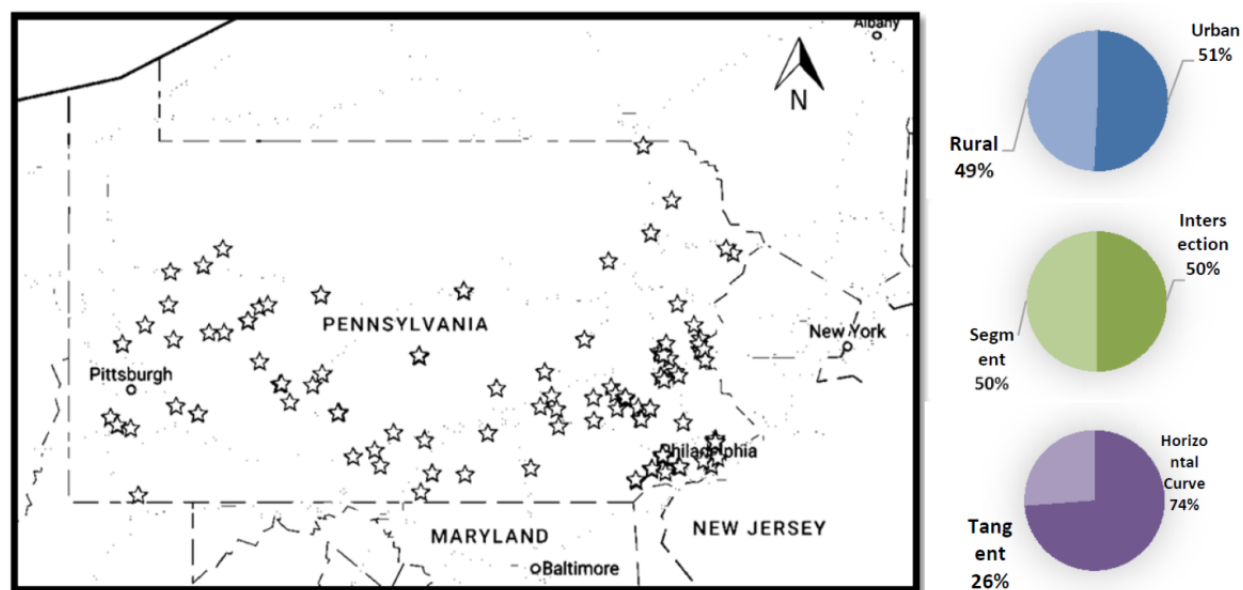


FIGURE 1 Study Site Locations

The first step of was the crash data compiling and database construction process. This involved collecting the crash records provided by PennDOT, followed by a review to the ensure accuracy of the data transfer. Since this research is focused on roadway departure crashes, the database was filtered to only consider the 2258 departure-related crashes. These included hit fixed object, head-on, sideswipe, and overturn/rollover crashes. Afterwards, a second database was constructed for the details regarding HFST projects throughout the state. This process involved the use of PennDOT's MPMS query, iTMS (Internet Traffic Monitoring System), ECMS (Engineering and Construction Management System), and Google Maps to obtain roadway features for each site. This information includes lane number, shoulder information, clearance zones, median type or other barriers, segment length, the presence of rumble strips, speed limit, AADT, rural/urban, functional classification, whether it was an intersection or segment, tangent or curve, and curve radius if applicable. During this step, each project site was assigned a unique site identification number.

After this data was also filtered and reviewed, steps 2 and 3 of this research involved the before and after analysis. This began by going through all each of the 2258 crashes, and correlating them to its respective site identification number based on the county, state route, segment, and offset. The site ID and the HFST installation completion date from the second database to determine whether the crash occurred before or after the HFST was installed, and then to calculate the number of years between these dates. As a result, the construction period for HFST was included in the before period; however, since it is not uncommon for the application to occur during the night, with lanes reopening for regular travel the next day, this likely did not have a major impact on the results. From here, two before-and-after analyses were performed, one limiting the crash data to the same number of years before and after the HFST installation, and one analysis where the data is converted to the average crashes per year based on the years of data available before and after installation. This is performed for each project site when the data is available.

Step 4 was a benefit-cost analysis. This analysis used the results of the two before-after analyses along with project cost information from ECMS and the MPMS Query. Costs were obtained by dividing total project cost proportionally to the site segment lengths within each project to determine the cost of each site. The benefits were determined based upon the reduction in crashes by severity levels.

The last step focuses on the development of Crash Modification Factors to determine the safety effect of HFST projects. A summary of this methodology is presented in Figure 2. It should be noted that step 5 is still under investigation and hence, this paper presents findings through step 4.

DATA ANALYSIS AND RESULTS

Before–After Analysis

As defined in the methodology portion of this report, the before-after analysis was divided into two comparisons. One analysis involved limiting crashes per site to include only those with the same before period of time before and after the HFST installation. The second comparison included all crash data that was converted to the average number of crashes per year before and after HFST installation. Both of these were to ensure that the comparison of crashes before and

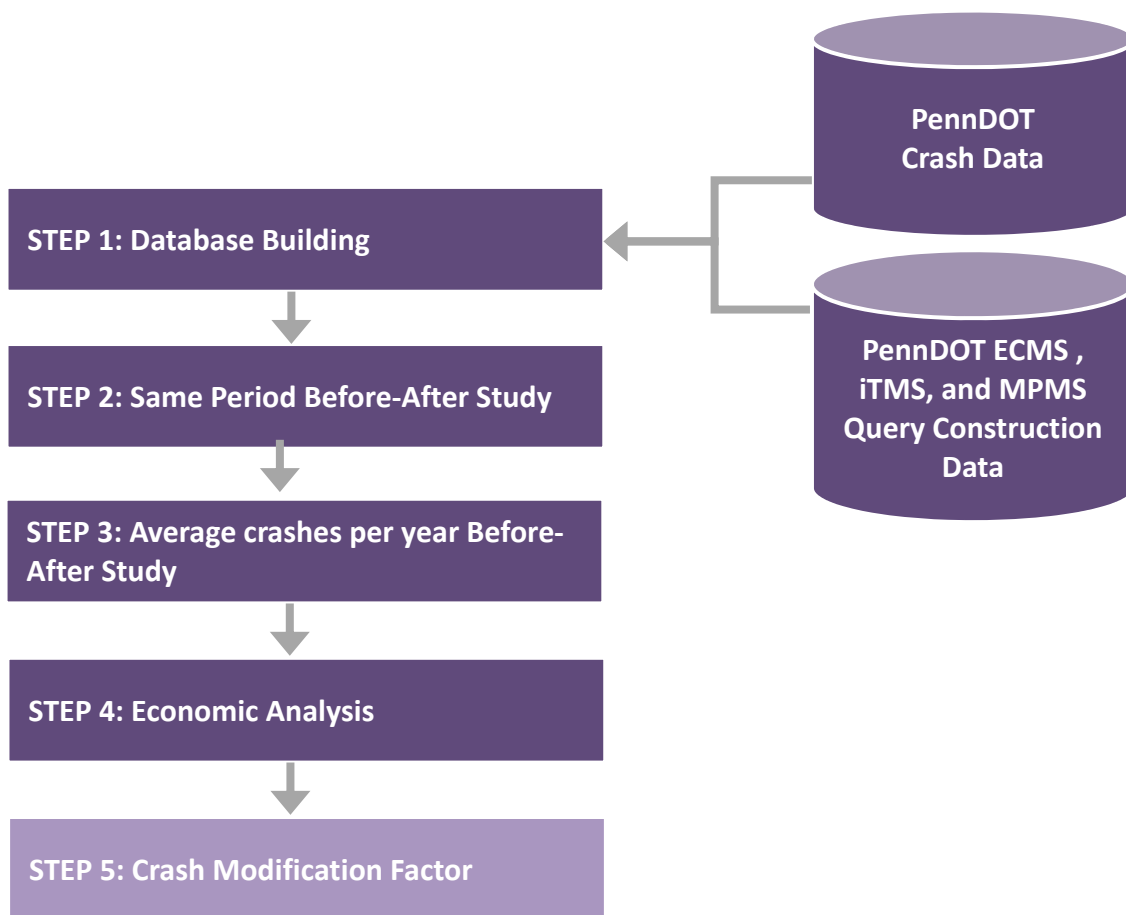


FIGURE 2 Research Process Flow Chart

after was fair. This section will describe the results of each investigation. It is important to note that the database provided by PennDOT did not indicate whether or not other improvements were made at these sites, which may have had an impact on the results of the analysis, but were out of the scope of this research investigation.

Total Data Analysis

The top portion of Table 1 shows the results of the simple before-after analysis. For this investigation crash data was limited to crashes within the same period before and after the HFST installation. For more recent projects, data was often limited by the available crash data after the project was completed. For example, if HFST was installed on January 1, 2013, a crash database ending in June 2016 would mean 3.5 years of “after” crash data. Therefore, the “before” crash data was limited to only include crashes 3.5 years prior to the January 2013 install. For the 106 sites, the periods used varied from less than a year to 4 years.

TABLE 1 Total Before-After Analysis (Simple and Average Departure Crashes Per Year)

Crash Severity	Before	After	Crash Reduction	% Reduction
Simple Before-After Analysis				
Fatal	5	0	-5	100
Major Injury	11	0	-11	100
Moderate Injury	24	0	-24	100
Minor Injury	72	0	-72	100
PDO	201	0	-201	100
Unknown Injury	31	0	-31	100
Total	344	0	-344	100.0
Before-After Analysis of Average Crashes Per Year				
Fatal	2.2	0.0	-2.2	100.0
Major Injury	7.7	3.8	-3.9	50.4
Moderate Injury	22.3	5.3	-17.0	76.3
Minor Injury	59.7	4.5	-55.2	92.5
PDO	147.8	29.5	-118.3	80.0
Unknown Injury	26.3	5.3	-21.0	79.7
Total	266.1	48.5	-217.6	81.8

As a result of the simple before-after analysis, the total percent reduction in crashes across all severity levels was 100%. Therefore, the installation of HFST was able to eliminate fatalities all injury levels, and property damage crashes by 100% at all of the 106 sites. This showed that HFST improved roadway safety by reducing both the number and the highest severity of departure crashes.

The bottom portion of Table 1 shows the before-after analysis for the average crashes per year data. As mentioned previously, the number of crashes before and after are divided by the total years of before and after crash data respectively. Therefore, the results are represented in average crashes per year. The total percent reduction in crashes across all severity levels was 81.8%. Once again, the installation of HFST was able to eliminate fatalities by 100% at all of the 106 sites. The severity level with the least percent crash reduction was major injury, however, installing HFST still reduced crashes here by 50.4%. Overall, the total data in both analyses showed that HFST improved roadway safety by reducing both the number and the highest severity of departure crashes.

Individual Site Analysis

After the analysis of the data as a whole, the sites were analyzed on an individual basis. First examined was in the framework of the simple before-after analysis. Of the 106 total sites, 64 were able to eliminate total departure crashes among all severity levels by 100%. 0 sites saw an increase in total departure crashes. Locations with the highest departure crash reductions were also investigated to identify any similarities between the geometric and operational features of these sites. From this examination, it is of note that 58% were in urban areas, 64% were intersection related crashes, and 89% were associated with a horizontal curve, with low and medium curvature sites experiencing the greatest reduction.

After the simple before-after analysis was the individual site investigation for the average departure crashes per year data. Of the 106 total sites, 74 were able to reduce total departure crashes among all severity levels by 100%. 8 sites actually saw an increase in one of their crash categories; however, the maximum increase was only by 2.13 average crashes per year, and the severity of crashes after installation were much lower with the majority being PDO crashes, a few minor injuries, and none of the crashes being fatal. Locations with the highest crash reductions were also investigated to identify any similarities between the geometric and operational features of these sites. From this examination, it is of note that 64% were in urban areas, 78% were intersection related crashes, and 98% were associated with a degree of horizontal curvature, with low curvature sites experiencing the greatest reduction.

Impact of Curvature

The next area that the dataset examined was the impact of horizontal curvature on departure crashes in locations where HSFT were considered. Examples of high, medium, and low curvature from the PennDOT installation sites can be found in Figure 3 below. These categories were defined based on the angle, θ , between the two legs of the curve along with Google imagery, which is a measure correlated to the deflection angle of a horizontal curve.

Table 2 shows the simple before-after analysis when the sites were broken down by curvature. For this dataset, all crash severities across all degrees of curvatures experienced 100% reduction in departure crashes, which was in line with the previous investigation. Therefore, HFST appear to be a good solution for improving the safety of this alignment.



FIGURE 3 Examples of Low ($\theta = 150-180^\circ$), Medium ($\theta = 120-150^\circ$), and High ($\theta = 0-120^\circ$) Curvature Roadway Sites

TABLE 2 Simple Before-After Analysis for Departure Crashes by Curvature

Crash Severity	Before	After	Reduction in Crashes	% Reduction
Low Curvature				
Death	3	0	3	100%
Major Injury	5	0	5	100%
Moderate Injury	8	0	8	100%
Minor Injury	35	0	35	100%
PDO	80	0	80	100%
Unknown Injury	11	0	11	100%
Total	3	0	3	100%
Medium Curvature				
Death	1	0	1	100%
Major Injury	3	0	3	100%
Moderate Injury	9	0	9	100%
Minor Injury	12	0	12	100%
PDO	52	0	52	100%
Unknown Injury	9	0	9	100%
Total	86	0	86	100%
High Curvature				
Death	0	0	0	N/A
Major Injury	3	0	3	100%
Moderate Injury	7	0	7	100%
Minor Injury	25	0	25	100%
PDO	60	0	60	100%
Unknown Injury	7	0	7	100%
Total	102	0	102	100%

Table 3 shows the same curvature investigation for the average departure crashes per year data. The same guidelines were used in defining curvature categories as in the previous simple before-after analysis. The greatest reduction in crashes, was seen by high curvature roadways, followed by low curvature. When considering crash severity, major injuries on low curvature was the only group to experience an increase in crash rates with 0.5 more departure crashes per year. However, HFST was able to reduce crashes overall, and fatalities were reduced by 100%. Therefore, the ability of HFST to eliminate fatalities until the end of the data collection period shows that such projects may be a good solution on all curvature roadways.

TABLE 3 Average Departure Crashes Per Year Before-After Analysis by Curvature

Crash Severity	Before	After	Reduction in Crashes	% Reduction
Low Curvature				
Death	1.2	0.0	1.2	100.0%
Major Injury	2.7	3.1	-0.5	-17.7%
Moderate Injury	6.6	1.7	4.9	74.1%
Minor Injury	17.9	1.4	16.6	92.3%
PDO	42.9	8.0	35.0	81.4%
Unknown Injury	9.1	0.3	8.8	96.8%
Total	80.5	14.5	66.0	82.0%
Medium Curvature				
Death	0.2	0.0	0.2	100.0%
Major Injury	2.5	0.0	2.5	100.0%
Moderate Injury	8.5	3.6	4.9	57.9%
Minor Injury	18.8	3.1	15.6	83.3%
PDO	50.1	12.9	37.2	74.3%
Unknown Injury	7.2	3.2	4.1	56.3%
Total	87.3	22.7	64.6	74.0%
High Curvature				
Death	0.5	0.0	0.5	100.0%
Major Injury	1.9	0.7	1.2	64.9%
Moderate Injury	5.6	0.0	5.6	100.0%
Minor Injury	16.6	0.0	16.6	100.0%
PDO	40.6	5.4	35.1	86.6%
Unknown Injury	5.9	1.6	4.4	73.5%
Total	71.2	7.7	63.5	89.2%

BENEFIT–COST RATIO

While a before-after analysis suggests practitioners the types of roadway facilities that experienced the greatest percent reduction in departure crashes, a benefit-cost analysis will indicate which types of locations will provide the greatest return on investment (ROI). A benefit cost ratio summarizes the overall value for money of a project or proposal. As shown in equation 1, the ratio is calculated by dividing the expected benefit of proceeding with a project by the costs.

$$B/C \text{ Ratio} = \frac{\text{Total Benefit from Crash Reduction}}{\text{Total Installation Costs}} \quad (1)$$

Having a B/C ratio greater than 1.0, indicates that the benefit outweighs the cost, and often provides evidence that the project is recommended to proceed. Based on this formula, the greater B/C Ratio, the better the argument that the project was successful and fulfilled its

objective. This is particularly important because limited project budgets, so transportation professionals must ensure that resources are used in the most efficient way possible.

For this analysis, the cost of the project (per site) was determined based on the material and construction costs to install the HFST. This information was provided by PennDOT. In general, HFSTs are considered to be an economical approach to roadway safety. When compared with transportation related construction projects with budgets in the million-dollar range, HFSTs cost between tens or hundreds of thousand dollars. For this dataset, the prices of installation per site ranged from about \$3,000 to \$500,000.

The benefit of installing HFST was measured based on the lives and injuries saved, which was measured in the reduction in departure crashes by severity. The following average cost associated with each injury level and are based on data provided by PennDOT from the years 2010 to 2014. These were multiplied by the reduction in departure crashes for each corresponding severity level, to calculate the total benefit that was derived from the project:

- Fatal = \$6,245,689.80
- Major Injury = \$1,365,629.20
- Moderate Injury = \$91,285.40
- Minor Injury = \$7,245.00
- Property Damage Only = \$2,898.00
- Unknown Injuries = \$7,245.00

For the B/C analysis, the average departure crashes per year data was used in order to define the average benefit cost ratio per year of installing HFSTs. The benefit-cost ratio for the combined cost and benefit of all projects was **2.85**. When the sites were examined individually, the median B/C ratio was **0.5** and the mean was **6.3**. The minimum B/C ratio observed was **-8.4**, and the maximum was at a value of **132.8**. 38% of the sites where HFST was installed resulted in an annual B/C ratio greater than 1.0. All of these results indicate that while individual projects may vary quite significantly, the overall value of deploying multiple HFST projects may provide desirable ROI costs.

The greatest returns on investment for this dataset were experienced by 2-lane roadways (which represented the majority of the project sites) with the following ranks and features:

1. **Site #18** – SR 2024, Urban, minor arterial, intersection, horizontal curve (low deflection)
2. **Site #22** – SR 0147, Rural, minor arterial, intersection, tangent
3. **Site #23** – SR 1001, Rural, minor arterial, segment, horizontal curve (high deflection angle)
4. **Site #33** – SR 0562, Urban, minor arterial, intersection, horizontal curve (low deflection angle)
5. **Site #15** – SR 4003, Rural, minor collector, segment, horizontal curve (med)

The least return on investment for this dataset also occurred on 2-lane roadways with the following ranks and features:

1. **Site #35** – SR 4030, Rural, major collector, intersection, horizontal curve (high deflection angle)
2. **Site #91** – SR 0352, Urban, minor arterial, intersection, tangent
3. **Site #62** – SR 0233, Rural, major collector, intersection, horizontal curve (high deflection angle)
4. **Site #58** – SR 0119, Rural, principal arterial, intersection, horizontal curve (medium deflection angle)
5. **Site #74** – SR 0164, Rural, minor arterial, intersection, horizontal curve (high deflection angle)

In terms of ROI, 3 of the top 5 sites were on rural roads, while only half of sites were located in this type of environment. Meanwhile, 3 of the top 5 sites were impacted by an intersection, which only represented 66% of all sites. Based on this information, it may be determined that PennDOT received the best return on investment at intersections in rural environments. Therefore, when taking cost into consideration, these results are in agreement with the two previous before-after analyses. In addition, 4 of the top 5 were at a horizontal curve. Although horizontal curves were represented in both the top and bottom ranked B/C ratios for the dataset, this may simply be due to the fact that curves represented 74% of HFST projects. Therefore, in line with the benefit cost analyses, it can be deduced that in addition to a rural intersection, horizontal curves also serve as critical locations for HFST. However, further investigation is necessary in order to identify the exact impact of specific deflection angles or even curve radius on the B/C ratio for this dataset.

CONCLUSIONS

This research involves a comprehensive review and analysis of PennDOT departure crash data to determine the efficiency of HFST projects throughout the state of Pennsylvania, and evaluate their ability to reduce not only roadway departure crash occurrences, but also crash severity. This was performed by means of two before-and after analyses, one in which the same departure crash history period was used before and after the HFST installation. The second averaged that data and therefore results were reported in average departure crashes per year. The two before-after analyses were conducted on a total of 106 sites. For this particular dataset, the HFST was able to reduce the number of departure crashes by at least 74.0% for each grouping of curve radius and each crash severity. Most importantly, fatalities at all sites were reduced by 100%. Sites with the greatest reduction in total departure crashes were urban environments, intersections, and horizontal curves.

The results of the benefit cost analysis showed very similar results in the selection of roadway facilities. However, comparing the individual sites indicated that while overall return on investment is high when deploying a large number of HFST projects throughout the state, the return on investment for individual projects may not show the same promising results.

Overall this paper shows that HFST installations throughout the state of Pennsylvania have been effective in their goal of reducing departure crash rates and severity. For this dataset, PennDOT received the greatest results at intersections involving horizontal curvature that are located in rural environments. Therefore, these may potentially be the types of facilities that

departments of transportation could target first in order to most efficiently improve roadway safety.

In the context of other case studies, as discussed in the literature review, it appears that the state of Pennsylvania experienced slightly greater crash reductions, and a much broader range of benefit cost ratios. However, an exact comparison is not possible due to the different research methodologies. This study focused on roadway departure crashes only while most other studies considered wet-road crashes and all crash types.

FUTURE RESEARCH

The next portion of this research will involve the use of empirical bayes analysis to account for potential regression to the mean and to support the development of crash modification factors that can help practitioners to predict the safety impact of installing HFST at a site in the future. The study can also be expanded to include a complete crash dataset, and any other HFST project sites that have been completed since output of this report. Afterwards, future research may include crash data and studies in other states and an analysis to determine the trend of crashes after HFST and determine if crash reductions persist or if a learning curve is present.

ACKNOWLEDGMENTS

The authors would like to acknowledge the PennDOT for providing the data which was used as a part of this research. The contents of this paper do not necessarily reflect the official views or policies of the State of Pennsylvania.

REFERENCES

1. National Highway Traffic Safety Administration. *2015 Motor Vehicle Crashes: Overview*. August 2016. US Department of Transportation. DOT HS 812 318. <https://crashstats.nhtsa.dot.gov/Api/Public/ViewPublication/812318><http://www-nrd.nhtsa.dot.gov/Pubs/812160.pdf>. Accessed July 24, 2015. October 31, 2016.
2. Federal Highway Administration. *Roadway Departure Safety*. August 2016. US Department of Transportation. http://safety.fhwa.dot.gov/roadway_dept/. Accessed October 23, 2016.
3. State Transportation Innovation Council, PennDOT. High Friction Surface Treatment. FHWA. http://www.dot.state.pa.us/public/pdf/STCTAC/STIC/HFS_FACT_SHEET.PDF. Accessed July 29, 2016.
4. Albin, R., V. Brinkly, J. Cheung, et al. Low-Cost Treatments for Horizontal Curve Safety 2016. Federal Highway Administration. FHWA-SA-15-084. January 2016. http://safety.fhwa.dot.gov/roadway_dept/horicurves/fhwasa15084/ch5.cfm#ch5a. Accessed July 29, 2016.
5. Julian, F. *High Friction Surface Treatments*. 2013. Everyday Counts 2: NACE Conference. <http://www.countyengineers.org/events/annualconf/Documents/2013%20Presentations/Hi%20Fric%20Treatments%20Julian.pdf>. Accessed May 2015.
6. Cheung, Joseph. Federal Highway Administration. *High Friction Surface Treatments*. USDOT. https://www.fhwa.dot.gov/everydaycounts/edctwo/2012/pdfs/fhwa-cai-14-019_faqs_hfst_mar2014_508.pdf. Accessed June 2015.

7. Meggers, D. Evaluation of High Friction Surface Locations in Kansas. Paper No. 15-0377 submitted for the 94th Annual Meeting *Transportation Research Board*, Kansas Department of Transportation, Topeka, KS, 2015, pp. 1.
8. Hall, J. W., Smith, K.L., Titus-Glover, L. *Guide-for-Pavement-Friction*. In National Cooperative Highway Research Program. Project 01-43, Transportation Research Board of the National Academies, Washington, D.C., 2009.http://onlinepubs.trb.org/onlinepubs/nchrp/nchrp_w108.pdf
9. Federal Highway Administration. Focus State Roadway Departure Safety Plans and High Friction Surface Treatments Peer Exchange. August 5-6, 2014. Document No. FHWA-SA-15-044. https://rspcb.safety.fhwa.dot.gov/p2p_reports/peer_report_AL_Aug2014.aspx. Accessed October 23, 2016.
10. Federal Highway Administration. *High Friction Surface Treatments (HFST)*. September 6, 2016. United States Department of Transportation. http://safety.fhwa.dot.gov/roadway_dept/pavement_friction/high_friction/. Accessed October 28, 2016.
11. Federal Highway Administration. South Carolina Case Study: A Cost-Effective and Time-Sensitive Safety Solution. FHWA-SA-15-056. http://safety.fhwa.dot.gov/roadway_dept/pavement_friction/case_studies_noteworthy_prac/sc/sc.pdf. Accessed October 23, 2016.
12. Federal Highway Administration. Case Study: Kentucky Transportation Cabinet's High Friction Surface Treatment and Field Installation Program. FHWA-SA-15-038. http://safety.fhwa.dot.gov/roadway_dept/pavement_friction/case_studies_noteworthy_prac/kytc/ky_hfst_15_038.pdf. Accessed October 23, 2016.
13. Wilson, B. T., Brimley, B. K., Mills, J., et al. Benefit–Cost Analysis of Florida High-Friction Surface Treatments. In *Transportation Research Record: Journal of the Transportation Research Board*, Volume 2550. DOI: 10.3141/2550-08. Transportation Research Board of the National Academies, Washington, D.C.
14. Federal Highway Administration. Frequently Asked Questions about High Friction Surface Treatments (HFST). https://www.fhwa.dot.gov/innovation/everydaycounts/edc-2/pdfs/fhwa-cai-14-019_faqs_hfst_mar2014_508.pdf. Accessed October 23, 2016.
15. Brimley, Brad, and Paul Carlson. "Using High Friction Surface Treatments to Improve Safety at Horizontal Curves." July 2012. *Texas Transportation Institute*. DBI Services, Web. 26 Feb. 2017. <<http://d2dtl5nnlpfr0r.cloudfront.net/tti.tamu.edu/documents/TTI-2012-8.pdf>>.

ADVANCEMENTS IN ROADWAY SAFETY FEATURES

High-Friction Surfacing Treatment

How a 45-Year-Old Process Has Been Reengineered into the Leading National Safety System Used by Highway Agencies to Reduce Fatalities and Serious Injuries

RICHARD JOHN BAKER
DBI Services, LLC

Through state and federal funding resources, highway agencies are increasingly specifying HFST as part of their safety campaigns. Through the mandatory federal safety audits state agencies are recording the positive results of implementing HFST statewide programs. HFST has become the standard safety treatment for many agencies, with continued educational presentations by the leaders in the industry more communities, cities, counties and private toll authorities are benefiting from integrating their own HFST programs.

Despite gains in safety, 2015 saw the largest percentage rise in motor vehicle deaths in the past 50 years, according to the National Safety Council. Cheaper gas and a stronger economy were likely key factors in the rise, the nonprofit group says.

The figures are estimates from the National Safety Council, which says it currently estimates that last year, “38,300 people were killed on U.S. roads, and 4.4 million were seriously injured,” meaning 2015 likely was the deadliest driving year since 2008

In 2013, there were approximately 5.6 million crashes reported across the nation, including 32,719 fatalities and over 2.3 million injuries.¹ More than half of the 2013 fatalities were roadway departure crashes.

Often, a small subset of the total highway network is responsible for a significant percentage of certain crash types. In 2008, for example, 28 percent of fatal crashes occurred on *horizontal curves*, yet horizontal curves make up only 5 percent of our Nation’s roadways. Compared to vehicles driving on a *tangent road section*, vehicles traversing horizontal curves require a greater lateral friction due to centrifugal forces.

A roadway must have an appropriate level of pavement friction to ensure that vehicles stay safely in their lane. Poor pavement conditions, especially wet pavement, have been identified as one of the major contributing factors in roadway departure (RwD) crashes. When a pavement surface is wet or polished from wear, the level of pavement friction is reduced which may lead to skidding or hydroplaning. A high friction surface treatment (HFST) is an ideal countermeasure for such locations because it significantly increases pavement friction and helps prevent drivers from losing control on severe curves.

Despite gains in safety, 2015 saw the largest percentage rise in motor vehicle deaths in the past 50 years, according to the National Safety Council. Cheaper gas and a stronger economy were likely key factors in the rise, the nonprofit group says.

The figures are estimates from the National Safety Council, which says it currently estimates that last year, “38,300 people were killed on U.S. roads, and 4.4 million were seriously injured,” meaning 2015 likely was the deadliest driving year since 2008.

A total of 40,200 people died on U.S. roads in 2016, the highest level in almost a decade, according to preliminary estimates from the National Safety Council (NSC).

The number of traffic fatalities last year represents a 6 percent increase over 2015 and a 14 percent increase over 2014 — the sharpest two-year escalation in more than 50 years, the safety group said.

The NSC draws its data from the states and the report could differ from final federal estimates. Still, safety advocates say the early data represents an alarming trend.

Maintaining the appropriate amount of pavement friction is critical for safe driving. Critical locations, such as sharp curves, steep grades, intersections, bridge decks, unique local environmental conditions, wet surfaces, and similar, make up a small portion of the Nation's highway miles. High friction surface treatment (HFST) is an EDC driven technology that targets these specific roadway segments to improve roadway safety.

- EDC Initiative
- HFST costs
- HFST as a safety countermeasure
- Research data
- Penn DOT's – "Like a Miracle" summary of effectiveness
- Construction process
- Materials
- Review real world projects
- FHWA EDC 11 low cost safety countermeasure 2012
- Dependent on project location, size and accessibility
- 36 states have HFST programs some with statewide multiple projects
- TTI and NCAT impute from long term durability and site location selection
- Penn DOT, after 7 years of testing and monitoring reported on dramatic crash reduction
- AASHTO and state materials development nationally
- Vendors innovation to drive better quality and long term durability
- NC, SC, PA and CA DOT's
- Pennsylvania Statistics

From 2010 to 2014 there were 615,947 reportable crashes with 6,323 fatalities (1.03%) and 16,701 major injuries (2.71%) in Pennsylvania. According to Pennsylvania's Crash Data Analysis Retrieval Tool (CDART) from 2010 to 2014, wet pavement crashes accounted for 104,733 or 17.0% of all reportable crashes. Because of the severity of this type of crash, they accounted for 14.89% of all fatalities.

To reduce the number of wet pavement crashes, PennDOT has installed a High Friction Surface Treatment (HFST) on two lane roads.

Candidate locations for installation are locations where:

- Drivers may brake excessively going around curves
- Drivers may brake excessively going down steep grades
- Drivers may brake excessively while approaching intersections

The road surface can become prematurely polished, reducing pavement friction and causing vehicles to skid when drivers brake. Wet road surfaces can also reduce pavement friction and cause skidding or hydroplaning. HFST uses high-quality, wear-resistant aggregates (such as bauxite) to provide increased friction on pavements. This helps to keep vehicles in their lane on slippery pavement around curves and allows drivers to stop. The epoxy-binder used to bond the aggregates together is designed to set quickly so there is minimal impact to the traveling public. HFST may be installed on two-lane roads with pavement widths of 20 feet or greater. They can also be applied on undivided multi-lane roads.

Pennsylvania's HFST Locations

Throughout Pennsylvania, approximately 27.55 mile (140 locations) of HFST has been implemented on state roadways. Of those, 1.18 miles (4.58%) were implemented between 2007 and 2012.

In an effort to gauge the effectiveness of applying the HFST, an analysis of crash data was performed for 15 locations consisting of approximately 1.18 miles of roadway with HFST installed between the dates of June 2007 and October 2012. To capture the long term effects of HFST, for the purpose of this report only the 15 locations that have been installed for three-years or longer will be included.

Benefit–Cost Analysis

This benefit/cost analysis was performed to ascertain whether or not a project's cost is justified by the cost saving benefit to society as a result of reduction in crashes and injuries. This information is based on the study of 15 locations in Northampton and Lehigh County. The average cost to install HFST is \$35.00 per square yard for all 15 locations.

PennDOT has estimated the economic loss due to reportable traffic crashes using the following average cost to society for the different categories below (in 2008 dollars).

Deaths	\$6,474,138
Major Injuries	\$1,412,675
Moderate Injuries	\$92,465
Minor Injuries	\$7,510
Property Damage Only	\$3,004
Unknown Injuries	\$7,510

Due to differences in installation dates, 1 location (Pilot) has 8-years before and after data, 14 locations have 3-years before and after data. For each location crash data was reduced to an average annual level then combined to give an annual crash reduction per location.

Important Characteristics of HFST for Quality and Longevity

Some quality issues are independent of the actual HFST installation. It is a function of the existing pavement condition. HFST will not improve the pavement structure although the crack sealing may help preserve the structure depending on the pavement condition at application. This is not the primary purpose but may be a side effect. Preparation of the pavement surface requires

Average Cost Benefit Table (15 locations)

	Crashes	Fatalities	Major	Moderate	Minor	PDO	Unknown Severity	Economic Savings Due to Reduction in Fatality/Injury
All 15 locations, annual reduction	49.13	.58	.79	2.13	13.04	30.71	13.92	\$5,361,406
Annual reduction per intersection	3.30	0.04	0.05	0.14	.87	2.05	.93	\$357,427.08

varying degrees of effort. The most extreme is shot blasting that should be done for all concrete surfaces. Most asphalt pavement just requires blowing dust and debris with high pressure air lances but a power sweeper before blowing could be required if the surface has heavy dirt or debris that has built up. Although an issue that is more common at intersections, oil leakage may need to be cleaned with detergents and allowed to dry thoroughly. All of this is to allow the polymer to make good contact with the pavement so to form a strong bond. Crack sealing may be required for moving cracks. Although the polymer would fill the cracks, this may not be desirable for the cracks that move. The polymer could pull away any weak material along the edge of the crack and open up the crack since the polymer is so much stronger than typical crack sealing material and it does not allow the compression that most crack sealers allow so that could cause the crack to rupture vertically if the crack moves enough in thermal expansion. Cracks that don't move (most small cracks) can be filled with the polymer but be aware this can affect the yield of the polymer resulting in less depth of polymer. Be aware that a roadway that is in marginal condition can be patched and treated but the life of the treatment may be determined by the life of the pavement structure. The project may not appear to be good quality but it may be the best that can be attained from that roadway in the current condition and this may not prove to be a cost effective solution. On the other hand, it may be needed to try and provide safety while the extra life is squeezed from the infrastructure before improvement. Only the owner agency can make that call.

- The most important is proper formulation of the polymer binder and correct ratio mix in the field. If this fails, nothing else works!
- The optimum viscosity of the binder which is determined by temperature and formulation
 1. Proper mixing can't occur if the components are not at the correct viscosity and this can be greatly enhanced by keeping the temperature of the components warm before blending. The higher the natural viscosity (at 70 degrees) of the components the more critical to have them heated even in slightly cool temperatures.
 2. When the polymer is at optimum viscosity, it makes better contact with all the surfaces it contacts such as the pavement and fully embraces the varied texture of the host pavement.
 3. Since the mixing of the components starts the chemical reaction of the polymer which starts a transition of the characteristics of the polymer, there is a phase that it is

ideal to introduce the aggregate to maximize the bond. In general, the quicker the better. The aggregate needs time to bond with the polymer when it is in the optimum viscosity phase as it is forming the cross links that provide the tensile strength that is the desired outcome. The later in this phase that the aggregate is introduced, the less of a bond will be formed. This is the cross linking phase and if the road surface is cool it begins to slow down the cross linking which ultimately effects the tensile strength. It is also this phase when the chemical reaction heats up the polymer which is the chemical reaction of the cross linking but this may not reach its potential or occur properly when the temperature is too cool and may fail at critical temperatures but this varies by polymer manufacturers. As the polymer continues to transition the material is more of a gel in the next phase and the initiation of new bonds has stopped while the bond that has been formed continues to mature. In this phase the aggregate bonds are still fragile and can be broken if disturbed by loading. This is phase where equipment and even walking on the new surface should not be allowed to minimize disturbing bonding which leads to unnecessary loss of aggregate. As this phase matures a set is eventually obtained that is often mistaken as being cured. Actual curing continues to occur for several days.

4. The proper thickness of the binder is important since it sets the embedment depth of the aggregate being applied. Since most pavements vary in texture the amount of polymer to get this depth correct varies. Anything like texture or numerous cracks need to be accounted for if they affect the polymer depth. If the depth is not correct, you may have the aggregate release the aggregate immediately or in short time if in a location with high friction demand (which creates the tensile load that drives the design). This depth can't be too shallow since it allows the aggregate to pullout and it can't be too deep or you sacrifice macro texture depth that addresses water flow and the deeper material can overstress the pavement during the weather cycle due to thermal stress since the polymer is stronger than the asphalt material.

5. Since Calcined Bauxite is required and the friction performance when proper quality control is followed by the aggregate supplier will likely outlast the other components of the system, the most likely way friction will be lost is through loss of particle. This happens as the binder gets harder over time and the bond to the aggregate is lost. While this process is a combination of the loads applied, the climatic exposure and the variation in the polymer formulation, it can also be because of a lower embedment of the aggregate. If the aggregate has a marginal embedment, it may not fail in the first few years. You may see spots of failure that are localized because of variation in the surface or variation of the installation that dipped below marginal binder depth. Marginal embedment depth will fail through aggregate loss in less time because there is less surface of the aggregate bonded to start with and as time of exposure and load weakens the bonds of the binder the overall cumulative bond is less in a shorter time.

6. While pavement smoothness is stressed in most DOT paving processes and it should be also stressed in HFST applications. The secret to attain HFST surface smoothness is timely aggregate distribution. If the aggregate is evenly and consistently distributed it will make a smoother surface. Some methods of aggregate distribution create piles of aggregate with the idea to be raked out smoothly. If the aggregate is quickly placed in its final location quickly while the polymer is in early stages of the liquid phase, then things are okay. This is critical because it maximizes the bond as mention before but also if the aggregate is allowed to stay in piles, a capillary effect can

occur that causes the polymer to rise in the aggregate and bond. End results when the material is swept, the surface appears to have waves in the surface creating a rough mega texture. These high spots can create localized excessive spot wear issues.

Improving Pavement Friction to Advance Roadway Safety on Horizontal Curves

Advancements in Roadway Safety Features

JOSEPH CHEUNG
FHWA Office of Safety

Roadway departure crashes account for more than half of the highway fatalities in the United States. The Federal Highway Administration (FHWA) Roadway Departure (RwD) Team developed a Strategic Plan to provide a common vision for research, policy, and implementation to address these crashes.

The three major efforts are: 1) Keep vehicles on the roadway, in their appropriate directional lane, 2) Reduce the potential for crashes when vehicles do leave the roadway or cross into opposing traffic lanes, and 3) Minimize the severity of crashes that do occur. High Friction Surface treatments in curves and other spot locations will address fatal crashes occurred on horizontal curves that are significantly overrepresented. Advancement of HFST is a game changer that will reduce RwD crashes other safety countermeasures cannot address and will continue to save lives for many years to come.

The presentation will include:

- The Technology
 - Background of High Friction Surface Treatments
 - What is High Friction Surface Treatments (HFST)? Background and how it is get started outside of the US and within.
 - Why is HFST important to the roadside safety community?
 - How is HFST installed? Will cover various methodologies from the use of manual operation to automated and mechanical installation.
 - Discussed where can HFST be placed to be most effective; at curves, ramps and intersections
- The Crash Reduction Outcomes and Benefits
 - Will cover crash reduction ability of HFST with several case studies including a HFST installation at an interchange ramp in Marquette, Wisconsin including a video and present dramatic crash reduction results (before HFST was installed, it experienced 219 crashes in 3 years. After HFST was applied, only 9 crashes within a 3 years period).
 - Will include other case studies on HFST installation that are noteworthy cover.
- Environmental Preservation
 - Discussion of the minimal impact of HFST in environmental sensitive areas such as National Parks and Historic locations with a case study of Caltrans opted to use HFST instead of reconstructing a curve that has been experiencing high crashes within a National Park with great results including safety issues resolved, millions of dollars saved, and did not endanger the environment.
- State of HFST Nationwide
 - EDC impact
 - Nationwide deployment

- **Conclusion**
 - **On-going Research is continuing in collecting additional data to develop Crash Modification Functions for application with the Highway Safety Manual and will help mainstream HFST for institutional application.**
 - **HFST Technology development**
 - **Why is HFST a game changer?**

A MASH TL-3 Compliant Short Radius System

AKRAM ABU-ODEH

ROGER BLIGH

Texas A&M Transportation Institute

CHRISTOPHER LINDSEY

WADE ODELL

Texas Department of Transportation

It is difficult if not physically unattainable to provide the required length of need barrier along a highway if it intersects private driveways and county roads. The presence of site constraints such as a bridge rail or a culvert along the highway may not allow the placement of a properly designed guardrail. In these cases, the alternatives are to relocate the site constraint if possible, shorten the guardrail length, or provide a curved guardrail design. The curved guardrail design is known as short radius or T-intersection depending on specifics of such constraints. Researchers and practitioners in the roadside safety area have been investigating the short radius issue for more than two decades. Subsequently, investigators conducted numerous crash tests for different short radius guardrail designs. None of those designs passed National Cooperative Highway Research Program (NCHRP) Report 350 TL-3 criteria. In 2009, the crash testing guidelines have been updated to the Manual for Assessing Safety Hardware (MASH). MASH test conditions have higher impact severity value for TL-3 tests than NCHRP Report 350. Satisfying such impact severity becomes even more challenging for any short radius system.

This paper presents a MASH TL-3 compliant short radius design that was successfully crash tested at Texas A&M Transportation (TTI). This short radius design utilizes a thrie-beam application through its perimeter as the basic element of containment. This thrie-beam is augmented with an energy absorption apparatus via sand barrels and tension carrying cable over the nose section. The research team used nonlinear finite element simulation to quantify the performance of several design concepts. Then, they simulated the most promising design concept with detailed modeling to finalize the prototype of the proposed short radius system. TTI proving ground staff constructed and tested successfully this short radius system per MASH TL-3 Tests conditions, namely tests 3-33, 3-32, 3-31 and 3-35.

Innovations in Roadside Safety Hardware and Features

Development of a Continuous Motorcycle Protection Barrier System Using Computer Simulation and Full-Scale Crash Testing

ALI O. ATAHAN

Istanbul Technical University

J. MARTEN HIEKMANN

PassCo Road Restraint Systems GmbH

JEFFREY HIMPE

JOSEPH MARRA

GDTech International

Road restraint systems are designed to minimize the undesirable effects of roadside accidents and improve safety of road users. These systems are utilized at either side or median section of roads to contain and redirect errant vehicles. Although restraint systems are mainly designed against car, truck and bus impacts there is an increasing pressure by the motorcycle industry to incorporate motorcycle protection systems into these systems.

In this paper development details of a new and versatile motorcycle barrier, CMPS, coupled with an existing vehicle barrier is presented. CMPS is intended to safely contain and redirect motorcyclists during a collision event. First, crash performance of CMPS design is evaluated by means of a three dimensional computer simulation program LS-DYNA. Then full-scale crash tests are used to verify the acceptability of CMPS design. Crash tests were performed at CSI proving ground facility using a motorcycle dummy in accordance with prEN 1317-8 specification.

Full-scale crash test results show that CMPS is able to successfully contain and redirect dummy with minimal injury risk on the dummy. Damage on the barrier is also minimal proving the robustness of the CMPS design. Based on the test findings and further review by the authorities the implementation of CMPS was recommended at highway system.

Relationship Between Roadside Hazard Rating and Crash Occurrence

JONATHAN S. WOOD

South Dakota State University

ERIC T. DONNELL

The Pennsylvania State University

When a vehicle departs from the roadway, the characteristics of the roadside influence the probability and severity of a crash. In the American Association of State Highway and Transportation Officials' (AASHTO) Highway Safety Manual (HSM), the characteristics of the roadside are codified using Roadside Hazard Ratings (RHR). The RHR is a 7-point scale that was developed more than 25 years ago to evaluate the safety performance of cross-sectional roadside design elements. While the HSM provides a function to determine a Crash Modification Factor (CMF) for the RHR, using a rating of 3 as the baseline (CMF = 1.0 for the baseline), no standard errors or confidence intervals are available for these CMFs, so the precision of the CMFs is not well known or understood. Aside from the CMFs found in the HSM, the Federal Highway Administration's CMF Clearinghouse does not contain any other CMFs for RHR. This study developed CMFs (with associated confidence intervals) for the 7-point RHR scale that is used in highway safety evaluations using a rating of 3 as a baseline value. Crash and roadway data from Pennsylvania for 21,340 two-lane road segments over an eight-year period (2005-2012), including RHRs ranging from 1 to 7, were used. A causal inference framework utilizing genetic matching in conjunction with random parameters negative binomial regression was used to develop the CMFs. It is expected that the results will be useful for supplementing the HSM RHR CMFs.

INTRODUCTION

The Federal Highway Administration (FHWA) defines a roadway departure crash as one in which a vehicle crosses the edgeline or centerline, or otherwise leaves the traveled way, and is involved in a multi- or single-vehicle collision (1). The most recent crash statistics in the United States (U.S.) estimate that over 20,000 fatalities occurred as a result of roadway departure crashes in the year 2015, which represents approximately 57 percent of traffic fatalities (2). Among the roadway departure fatalities, approximately 75 percent involve rollover events, collisions with trees, or crashes with other fixed objects off of the roadway. The remaining 25 percent of fatal roadway departure crashes are head-on collisions on undivided or divided highways. These statistics collectively indicate that the roadside, including the presence of fixed objects, hardware, or steep slopes, is a critical safety issue.

Zegeer et al. (3) developed a roadside hazard rating (RHR) scale for rural and urban highways to classify the potential frequency and severity of roadside hazards. The seven-point scale ranges from one for a roadside that is indicative of a clear, level roadside to seven for a roadside that has fixed objects or steep slopes close to the traveled way. This scale has been used

extensively by researchers evaluating roadway and roadside safety. In particular, the first edition of the American Association of State Highway and Transportation Officials' (AASHTO) Highway Safety Manual (4) includes a crash modification factor (CMF) for the RHR. In this context, a CMF is used to quantify the change in expected crash frequency when modifying a roadway segment, by either implementing a safety countermeasure or by modifying the physical features of the segment.

The CMF found in the HSM for the RHR on two-lane rural highways is as follows:

$$CMF_{RHR} = \frac{e^{(-0.6869+0.0668 \times RHR)}}{e^{(-0.4865)}} \quad (1)$$

where CMF_{RHR} is crash modification factor for RHR on two-lane rural highways; and RHR is roadside hazard rating (scale of 1 to 7)

If a RHR of 3 is assumed as the baseline (CMF is 1.0), modifying the roadside to a RHR of 1 is expected to reduce the expected total crash frequency on a two-lane rural highway by approximately 12.5 percent (CMF is 0.875). If the roadside is modified so that the RHR is 7, the expected total crash frequency is expected to be approximately 30.6 percent (CMF is 1.306) higher than the baseline case.

The RHR CMF for two-lane rural highways that is included in the first edition of the HSM is based on a combination of objective data and expert opinion. As such, the FHWA CMF Clearinghouse (5) does not offer a star quality rating.

The purpose of this study is to produce CMFs, with associated standard errors, for the RHR on two-lane rural highway segments using Pennsylvania data. A causal inference framework utilizing statistical matching (i.e., genetic matching) in conjunction with random parameters negative binomial regression analysis is used to develop the CMFs. The results of this analysis will be useful to engineers using RHR to predict crash frequencies and identifying hazardous roadside locations.

LITERATURE REVIEW

The RHR developed by Zegeer et al. (3) was based on a literature review and workshop among several highway safety professionals, who were shown many photos of roadside scenarios in rural and urban areas across 15 States. Both the frequency and severity of potential roadside crashes were assessed, resulting in the ordered seven-point scale.

Zegeer et al. (3) developed a database of approximately 4,785 two-lane rural highway miles with variable traffic volume, roadway, and roadside characteristics from seven states. Crash data were appended to these data. A statistical model to estimate the expected single-vehicle plus opposite-direction head-on, opposite-direction sideswipe, and same-direction sideswipe crashes per mile year was estimated, and is shown in equation 2:

$$AO/M/Y = 0.0019(ADT)^{0.8824}(0.8786)^W(0.9192)^{PA}(0.9316)^{UP}(1.2365)^H(0.8822)^{TER1}(1.3221)^{TER2} \quad (2)$$

where:

- $AO/M/Y$ = expected number of annual single-vehicle plus opposite-direction head-on, opposite-direction sideswipe, and same-direction sideswipe crashes per mile per year;
- ADT = average annual daily traffic (vehicles per day);
- W = lane width (feet);
- PA = average paved shoulder width (feet);
- UP = average unpaved shoulder width (feet);
- H = roadside hazard rating;
- $TER1$ = indicator variable for flat terrain (1 if flat; 0 otherwise); and
- $TER2$ = indicator variable for mountainous terrain (1 if mountainous; 0 otherwise).

The roadside hazard rating variable (H) in the model indicates that, as the RHR scale increases from 1 to 7, the expected number of target crashes increases. The authors' developed accident reduction factors associated with reducing the RHR, which are shown in Table 1.

TABLE 1 Accident Reduction Factors Associated with Reducing Roadside Hazard Rating (3)

Reduction in Roadside Hazard Rating	Reduction in Target or Related Crashes (%)
1	19
2	34
3	47
4	52
5	65

NOTE: An accident reduction factor (ARF) related to a crash modification factor (CMF) as follows:
 $ARF = 100 (1 - CMF)$.

In a separate analysis, Vogt and Bared (6) compiled a database of two-lane rural highway roadway inventory, traffic volume, and crash data from Minnesota and Washington. A statistical model of the expected number of non-intersection crashes per year was developed, and is shown in Equation 3 below:

$$N = EXPO \times \exp(0.6409 + 0.1388STATE - 0.0846LW - 0.0591SW + 0.0668RHR + 0.0084DD) \times (\sum WHi \times \exp(0.0450DEGi) \times (\sum WVj \times \exp(0.4652Vj) \times (\sum WGk \times \exp(0.1048GRk) \quad (3)$$

Where

- N = expected number of total crashes per year;
- $EXPO$ = traffic exposure in million vehicle-miles of travel;
- $STATE$ = indicator variable for state (1 if Washington; 0 if Minnesota);
- LW = lane width (feet);
- SW = average of left and right shoulder widths (feet);
- RHR = roadside hazard rating;
- DD = driveway density (driveways per mile);
- WHi = fraction of the segment occupied by the i th horizontal curve;

- DEGi = degree of curve (degrees per hundred feet of i th horizontal curve) that overlaps the segment;
- WVj = fraction of segment occupied by j th vertical curve;
- Vj = absolute change in grade (percent per 100 feet) of the j th vertical crest curve in segment;
- WGk = fraction of segment occupied by k th uniform vertical grade; and
- GRk = absolute grade (in percent) of k th uniform vertical grade in segment.

Based on equation 3, the association between the RHR and expected total crash frequency on two-lane rural road segments is positive. This indicates that roadsides with steep slopes, fixed objects within the clear zone, or the presence of roadside hardware is associated with higher expected crash frequencies relative to roadsides with flat slopes and no fixed objects or roadside hardware. In other words, the expected total crash frequency increases as the RHR increases from 1 to 7.

Harwood et al. (7) worked with an expert panel and, using the Vogt and Bared model shown in equation 3, developed a crash modification factor for RHR on two-lane rural highways, which is shown in equation 1. In this model, the baseline value is a RHR 3, which has a CMF equal to 1.0. A CMF less than 1.0 results for RHR values of 1 or 2, while a CMF greater than 1.0 results for RHR values greater than 3. The CMFs derived for RHR do not have a standard error, nor are they based on current statistical analysis methods. This research addresses this issue using a causal inference approach based on two-lane rural highway roadside and crash data from Pennsylvania.

METHODOLOGY

Causal inference approaches used in traffic safety research often include the application of propensity scores, matching, and potential outcomes. Propensity scores were not used in this paper. Rather, a method that optimizes matching (genetic matching) was used. Matching entities with similar characteristics (i.e., observed variables) improves the comparability of the treated and comparison groups, leading to a reduction in selection bias. Count regression methods are used to estimate the potential outcomes of a treatment (i.e., RHR) using the matched data.

Based on the theory and assumptions made in randomized experiments, causal inference methods have been developed to analyze non-randomized observational data. A particular set of assumptions that must be met in order for these methods to identify causal relationships have also been documented. The assumptions are as follows (8–13):

1. Stable Unit Treatment Value Assumption (SUTVA). SUTVA is the assumption that, when a treatment is applied to an entity, it does not affect the outcome for any other entity. This is the same assumption made for randomized experiments and should be qualitatively justified whenever possible. In the case of roadside hazard ratings (RHRs), the influence of the RHRs on one segment will likely have no impact or a negligible impact on the crash outcomes for other road segments.

2. Positivity. This is the assumption that the probability of receiving the treatment at any level is non-zero (i.e., all entities included in the analysis could potentially have received the

treatment). Given that all roads have roadsides, they could all potentially have had different RHRs. Thus, this assumption is met for the current study.

3. Unconfoundedness. The mechanism for treatment assignment is considered unconfounded if the treatment status (treated or untreated) is conditionally independent of the counterfactuals for a given set of covariates (i.e., ignorable treatment assignment). This assumption is untestable (14). It must be assumed that all confounding covariates are measured, available, and included in the analysis (i.e., no hidden bias).

Given that the above assumptions are met, the effects of the RHRs can be estimated using a combination of matching and regression methods. These methods, and how they are used in this research, are described below.

Matching Methods

Matching methods provide the opportunity to match similar treated and untreated observations, leading to the removal of correlation between the treatment and other observed variables that are correlated with the outcome (8, 14–20). Using matched data with regression to estimate treatment effects has also been used to account for any remaining selection bias and covariate imbalance after matching (12, 21). The methods used for matching and checking the quality of the matches used in this research are genetic matching and standardized bias, respectively.

Genetic matching is a sequential process (based on a genetic algorithm) that optimizes covariate balance by finding the best matches for each treated entity (22). This method does not require distributional assumptions about the covariates or the assignment mechanism (22). The genetic matching process minimizes imbalance across the covariates, thus optimizing covariate balance (23). This is accomplished by minimizing a general Mahalanobis distance (GMD), which is defined in equation 4 (23).

$$GMD(\bar{x}, \bar{y}, W) = \sqrt{(\bar{x} - \bar{y})^T \left(S^{-1/2} \right)^T S^{-1/2} W (\bar{x} - \bar{y})} \quad (4)$$

where

$(\bar{x} - \bar{y})$ = the matrix of the differences in values between groups x and y for the variables included in the matching;

S = the covariance matrix between x and y ;

$S^{-1/2}$ = the Cholesky decomposition of S (i.e., $S = S^{-1/2} \left(S^{-1/2} \right)^T$); and

W = a weighting matrix.

The iterative process of genetic matching uses Kolmogorov-Smirnov (K-S) statistics and standardized bias to measure covariate balance and works to minimize differences in the treated and untreated group variable distributions (23). The K-S test uses the maximum deviation (or distance) between the values in the distributions of the variable for the treated and untreated groups (24). Using this distance and the sample size, the significance of the differences between the treated and untreated groups are estimated and compared using p-values.

Standardized bias is also used to evaluate covariate balance. It is similar to a t-test, with a few minor differences. The standardized bias is estimated using equations 5 and 6 (25) for continuous and binary variables, respectively.

$$SB = \frac{100(\bar{x}_T - \bar{x}_C)}{\sqrt{\frac{(S_T^2 + S_C^2)}{2}}} \quad (5)$$

$$SB = \frac{100(\hat{P}_T - \hat{P}_C)}{\sqrt{\frac{\hat{P}(1-\hat{P}) + \hat{P}_C(1-\hat{P}_C)}{2}}} \quad (6)$$

Where

\bar{x}_T = the sample mean of the treated group for variable x;

\bar{x}_C = the sample mean of the comparison group for variable x;

S_T^2 = the sample variance of the treated group for variable x;

S_C^2 = the sample variance of the comparison group for variable x;

\hat{P}_T = the proportion of the treated group with a value of “1” for variable x; and

\hat{P}_C = the proportion of the comparison group with a value of “1” for variable x.

It should be noted that the values S_T^2 and S_C^2 should only be used from the full dataset prior to matching, even when evaluating the covariate balance for the matched data (18). If this is not done, the improvement in standardized bias could simply be the result of increased estimates of variance due to reduction in the overall sample size, leading to incorrect assessments of the effectiveness of the matching (18).

Comparisons of standardized bias for the propensity score and other covariates from before and after matching can provide an indication of the improvement in covariate balance due to matching on the propensity score. Some researchers have stated that a standardized bias with an absolute value of 20 or smaller indicates no statistical difference between the treated and comparison groups (i.e. they are equivalent) (22). However, others have used a threshold of 10 (25, 26).

A separate issue in matching is whether to allow replacement. Replacement occurs when a single, untreated entity is matched to more than one treated entity (8, 12). The untreated entity that is matched to more than one treated entity is then given a weight equal to the number of treated entities that it is matched to. Allowing replacement typically improves covariate balance, although it is at the cost of having a smaller percentage of the original comparison group in the matched dataset. As a general rule, replacement should be used when the treated group is larger than the comparison group or when required to improve covariate balance (22).

Random Parameters Regression

Unobserved heterogeneity and random parameters are concerns in safety evaluations that need to be considered when using count regression (potential outcomes). The most common regression method that accounts for unobserved heterogeneity in transportation safety is the random parameters negative binomial model (27, 28). The random parameters negative binomial log likelihood is shown in Equation 7 (29, 30).

$$LL = \sum_{\forall i} \ln \int_{\varphi_i} g(\varphi_i) P(n_i | \varphi_i) d\varphi_i \quad (7)$$

where

φ_i = the random distribution for coefficient i ;

$g(\)$ = the probability density function of φ_i ; and

$P(n_i | \varphi_i)$ is the probability density function for the negative binomial.

Given the nature of the random parameters negative binomial model, there is not a closed form solution to the log-likelihood function. Thus, it must be estimated using approximation methods. This is often accomplished using halton draw based simulation methods (31).

Sources of unobserved heterogeneity, which leads to random parameters, includes correlation of the parameter with unobserved variables, incorrect functional form, measurement error, true randomness of the treatment effect, or heterogeneity in the treatment itself (28, 32). For the case of roadside hazard ratings, there is an unobservable amount of heterogeneity in the differences between locations with the same roadside hazard rating values. Thus, even with matching, it is likely that crash modification factors (CMFs) for roadside hazard ratings will be random.

When the CMFs are estimated using regression analysis, the CMFs are based on indicator variables in the regression models. When this is done the CMFs are estimated using equation 8 (13). For the 95% confidence interval of the mean value of the CMF (i.e., used to establish statistical significance), equation 9 is used. For the 95% confidence interval for a random parameter CMF (i.e., the CMF varies across locations), equation 10 is used.

$$CMF = \exp(\beta_{Treated}) \quad (8)$$

$$CMF_{95\%,CI,mean} = \exp(\beta_{Treated} \pm 1.96 * SE_{Treatment}) \quad (9)$$

$$CMF_{95\%,CI,actual} = \exp(\beta_{Treated} \pm 1.96 * \sigma_{Treatment}) \quad (10)$$

where

CMF = the Crash Modification Factor for the treatment;

$\beta_{Treated}$ = the estimated coefficient for the treatment;

$SE_{Treatment}$ = the standard error of $\beta_{Treated}$ from the regression model; and

$\sigma_{Treatment}$ = the standard deviation of $\beta_{Treated}$ from the regression model.

If the CMF is random, the 95% confidence interval is a measure of the distribution of the CMFs across locations while the 95% confidence interval for the mean value of the CMF is a test of statistical significance for the mean CMF value when accounting for the random nature of the CMF. Thus, the 95% confidence interval for the mean value may not include a value of 1 (i.e., is statistically significant at the 95% confidence level) while the 95% confidence level for the random CMF does include a value of 1.

DATA

Data from Pennsylvania two-lane highways for the years 2005-2012 (inclusive) were used. The data included 21,340 road segments (1-3 digit routes) that are owned and maintained by PennDOT. Variable definitions and descriptive statistics are shown in Tables 2 and 3, respectively. The data used for this paper, and shown in Table 3, were collected for a previous project at Penn State University using various data sources including PennDOT data files, video photo logs, and Google Earth (33).

TABLE 2 Variable Descriptions

Variable	Variable Description
data_year	Year Identifier (2005–2012)
total_crash	Total Crash Count
Fatal_Injury	Total Fatal and Injury Crashes
ROR	Total Run-Off-Road Crashes
RHR = 1	1 = Roadside Hazard Rating is 1, 0 = Otherwise
RHR = 2	1 = Roadside Hazard Rating is 2, 0 = Otherwise
RHR = 3	1 = Roadside Hazard Rating is 3, 0 = Otherwise
RHR = 4	1 = Roadside Hazard Rating is 4, 0 = Otherwise
RHR = 5	1 = Roadside Hazard Rating is 5, 0 = Otherwise
RHR = 6	1 = Roadside Hazard Rating is 6, 0 = Otherwise
RHR = 7	1 = Roadside Hazard Rating is 7, 0 = Otherwise
LNAADT	The natural log of annual average daily traffic
LNLENGTH	The natural log of segment length (miles)
Curve Density	The number of horizontal curves per mile
Average Degree of Curve	The average Degree of Curve (degrees/100 ft)
Access Density	The number of access points per mile
Passing Zone	1 = Passing Zone Present, 0 = Otherwise
High Speed	Posted Speed 50 mph or Higher
Shoulder Rumble Strips	1 = Shoulder Rumble Strips Present, 0 = Otherwise

NOTE: RHR = 3 is the baseline condition for the CMF analysis (consistent with the HSM).

TABLE 3 Descriptive Statistics

Variable	Obs	Mean	Std. Dev.	Min	Max
total_crash	170,468	0.667	1.144	0	23
Fatal_Injury	170,468	0.362	0.751	0	15
ROR	170,468	0.295	0.626	0	13
LNAADT	170,468	7.701	0.964	4.304	10.264
LNLENGTH	170,468	-0.794	0.347	-5.799	0.389
Curve Density	170,468	2.299	2.506	0	42.581
Average Degree of Curve	170,468	3.804	6.068	0	194.551
Access Density	170,468	16.297	14.307	0	330
Variable	Obs	Percentage With Value of 1			
Passing Zone	170,468	0.2838			
High Speed	170,468	0.4542			
Shoulder Rumble Strips	170,468	0.0814			
RHR = 1	170,468	0.0009			
RHR = 2	170,468	0.0050			
RHR = 3	170,468	0.0512			
RHR = 4	170,468	0.2157			
RHR = 5	170,468	0.5312			
RHR = 6	170,468	0.1937			
RHR = 7	170,468	0.0022			
data_year = 2005	170,468	0.2500			
data_year = 2006	170,468	0.2500			
data_year = 2007	170,468	0.2500			
data_year = 2008	170,468	0.2500			
data_year = 2009	170,468	0.2500			
data_year = 2010	170,468	0.2500			
data_year = 2011	170,468	0.2500			
data_year = 2012	170,468	0.2500			

The crash variables include Total Crashes (which includes all types and severities of crashes), Fatal and Injury crashes, and Run-Off-Road crashes. Roadside hazard ratings were collected manually using road log video files and are based on a scale of 1-7 (a rating of 1 being a roadside that is free of fixed objects and contains recoverable slopes in an area that extends 30 feet or more from the outside edge of the traveled way; a rating of 7 being a non-traversable roadside due to slopes or fixed objects in the area less than 5 ft from the edge of the travelled way) that was developed in previous research (3). As indicated by the descriptive statistics in Table 3, RHRs of 1, 2, and 7 were rare in Pennsylvania, although there were a high proportion of other RHRs. The presence of a passing zone somewhere on the segment (for partial or full length of the segment) is indicated in the Passing Zone variable. Other variables related to horizontal alignment (i.e., curve density and average degree of curve), access density, posted speed, and shoulder rumble strips were also included, as shown in Table 2.

RESULTS AND DISCUSSION

Matching

Matching typically requires a comparison between a single treatment and a comparison group. For the analysis, it was determined that a baseline value of a RHR of 3 would be used as the “untreated” or baseline value, consistent with the HSM (4). Thus, all CMFs developed in this paper are for a baseline RHR outcome of 3.

Given the small sample sizes of RHRs 1, 2, and 7, the RHRs for 1 and 2 were combined. An analysis for RHR 6 alone was also compared to combined RHRs of 6 and 7, and the CMFs were nearly identical. Thus, the analysis results for combined categories of RHR for 1 and 2 and combined 6 and 7 are presented below.

Prior to matching, the standardized bias was as large as 54.48%. For all matched datasets, the absolute standardized bias values for all of the observed variables had values smaller than or equal to 5.26%, indicating that the matching was successful at removing the majority of selection bias for the observed variables. The K-S tests also indicated that there were no statistically significant differences in the data (i.e., p-values all larger than 0.50). Thus, the matching was determined to be effective at reducing selection bias. The standardized bias values for before and after matching for each of the analyses are shown in Table 4.

With the matching, none of the “treated” observations were lost (i.e., all were included in the matched datasets). When the number of observations with a RHR of 3 was larger than the number of “treated” observations (i.e., RHR of 1 and 2), replacement was not allowed. The resulting matched data for this case included all observations with RHRs of 1 and 2 with the same number of observations with a RHR of 3. For all other evaluations, replacement was allowed and all observations (treated and RHR of 3) were included in the matched datasets.

TABLE 4 Absolute Standardized Bias For Before and After Matching (%)

Absolute Standardized Bias (%)								
Variable	RHR 1&2 vs. RHR 3		RHR 4 vs. RHR 3		RHR 5 vs. RHR 3		RHR 6&7 vs. RHR 3	
	Before	After	Before	After	Before	After	Before	After
LNAADT	0.81	0.78	8.62	2.42	19.17	0.65	42.87	0.88
LNLENGTH	8.67	1.12	3.09	2.44	4.24	4.20	3.84	3.76
Curve Density	5.17	0.89	13.15	1.19	38.44	3.92	50.21	6.13
Average Degree of Curve	13.91	2.75	3.81	3.21	20.61	2.55	31.04	4.26
Access Density	20.46	1.22	8.92	4.02	7.53	2.21	7.46	4.15
Passing Zone	3.42	0.81	14.03	1.21	35.62	2.55	44.18	3.43
High Speed	10.51	0.28	11.39	0.22	30.88	0.41	54.48	5.26
Shoulder Rumble Strips	12.77	4.09	3.05	1.29	5.19	0.10	14.94	1.47

Regression analysis and CMFs

Using the matched data, regression analysis was applied to estimate CMFs for total crashes, fatal and injury crashes, and run-off-road crashes. To estimate the random parameters, 200 halton draws were used. This is consistent with previous research (30, 34, 35). As indicated in the discussion for matching, CMFs were developed for RHRs of 1 and 2 (combined), 4, 5, and 6 and 7 (combined). All of these CMFs used a baseline condition of RHR equal to 3. Also, as discussed in the methodology, random parameters negative binomial regression was used to estimate the regression models. These models are shown in Table 5. The parameters for access density, curve density, average degree of curve, the RHR's, and intercepts were all typically found to be random. In the case of the analysis for RHR's 1 and 2, access density and the average degree of curve were not random. Access density did not have a significant effect (statistically or practically, as the values were very close to 0) in the RHR 4 models (for all of the models) and the run-off-road models for the RHR3, RHR 5, and RHR 6 and 7 models. The CMFs based on the regression estimates are also shown in Table 5. The CMF for fatal and injury crashes was not random, while all other CMFs were. Also shown in Table 5 is the 95% error (i.e., based on the standard error and used to determine statistical significance) and the 95% confidence interval (based on the random parameters, indicating the range of the random CMFs). Estimates with an absolute value of the t-statistic equal to or greater than 1.96 is statistically significant at the 95% confidence level. The regression estimates for traffic volume and segment length are consistent with previous research (4, 11, 13, 32, 33, 36, 37). The regression estimates for passing zone presence indicates that segments with passing zones are expected to experience fewer crashes than segments without passing zones. This is likely due to the forgiving nature of the design of locations with passing zones and is consistent with previous studies (32, 38). The regression estimates for the high speed variable also indicated that segments with posted speed limits of 50 mph or higher have lower expected crash frequencies than roads with lower speed limits, which is consistent with published literature (11–13, 32, 37, 39). The finding that shoulder rumble strips are associated with fewer expected crashes is also not surprising as there is a significant amount of literature documenting CMFs for shoulder rumble strips with CMFs smaller than 1.0 (4, 40–44).

The findings that access density, curve density, and average degree of curve are random were expected. This is consistent with previous research (32). For the majority of the time, increased access density leads to higher crash frequencies. This is logical since the number of conflict points is increasing as access density increases. The findings that curve density and degree of curve are both associated with increases in expected crash frequency are also not surprising. Increasing the number of curves has been associated with higher expected crash frequencies previously (32, 37, 45). The degree of curve is a function of the inverse radius of curve. Thus, an increase in the degree of curve is correlated with smaller curve radii, meaning that larger values of degree of curve are associated with sharp horizontal curves. Thus, the association between increased degree of curve and increased crashes is consistent with expectations (32).

TABLE 5 Regression models for CMF development

Analysis	RHR 1 & 2 vs. RHR 3						RHR 4 vs. RHR 3					
Crash Type	Total		Fatal+Injury		Run-Off-Road		Total		Fatal+Injury		Run-Off-Road	
Variable	Coeff		t-stat		Coeff		t-stat		Coeff		t-stat	
Intercept	-7.81	-32.79	-8.78	-28.68	-6.18	-17.82	-6.47	-146.48	-6.91	-119.11	-4.91	-75.23
σ	-	-	0.12	4.17	0.47	15.95	0.35	89.50	0.39	73.31	0.45	75.53
LNAADT	0.93	33.31	0.97	26.52	0.64	17.86	0.78	157.49	0.76	117.03	0.50	67.49
LNLENGTH	0.88	14.12	0.73	11.99	1.03	8.39	0.64	62.08	0.62	45.23	0.88	49.45
Passing Zone	-	-	-0.20	-3.56	-0.19	-3.00	-0.17	-21.15	-0.17	-16.02	-0.12	-9.62
High Speed	-0.09	-2.08	-0.07	-1.14	-	-	-0.11	-14.55	-0.10	-9.71	-0.05	-4.58
Shoulder Rumble Strip	-0.14	-2.22	-0.10	-1.09	-0.11	-1.38	-0.18	-14.25	-0.17	-10.57	-0.23	-11.91
Access Density	0.01	6.62	0.01	6.12	0.01	5.37	0.01	23.49	0.01	17.78	-	-
σ	-	-	-	-	-	-	0.01	33.43	0.001	5.11	-	-
Curve Density	0.06	4.51	0.04	2.15	0.06	2.98	0.02	7.14	0.26	8.78	0.06	19.83
σ	0.12	13.52	0.25	24.32	-	-	0.08	49.28	0.07	32.82	0.05	23.40
Average Degree of Curve	0.06	9.32	0.06	6.68	0.07	8.40	0.01	18.14	0.01	10.29	0.01	11.79
σ	-	-	-	-	-	-	0.02	31.86	0.01	10.14	0.10	11.28
RHR = 1 or 2	-0.12	-2.79	0.02	0.39	-0.25	-4.28	-	-	-	-	-	-
σ	0.62	24.14	-	-	0.19	3.96	-	-	-	-	-	-
RHR = 4	-	-	-	-	-	-	0.05	5.47	0.03	2.60	0.07	4.87
σ	-	-	-	-	-	-	0.28	60.35	0.29	47.93	0.09	12.37
α	0.10	3.36	0.21	3.65	0.11	1.64	0.20	36.81	0.30	30.07	0.22	16.02
Log-Likelihood	-1853.85		-1346.09		-1152.71		-47162.57		-34420.16		-28675.13	
No. Segments	254		254		254		5,572		5,572		5,572	
CMF	0.889		1.021		0.777		1.055		1.034		1.076	
95% Error Lower Bound	0.819		0.921		0.692		1.035		1.008		1.045	
95% Error Upper Bound	0.966		1.132		0.872		1.076		1.060		1.109	
CMF 95% Lower Bound	0.265		-		0.534		0.615		0.583		0.905	
CMF 95% Upper Bound	2.981		-		1.129		1.810		1.835		1.280	

Continued on next page.

TABLE 5 (continued) Regression Models for CMF Development

Analysis	RHR 5 vs. RHR 3						RHR 6 & 7 vs. RHR 3					
Crash Type	Total		Fatal+Injury		Run-Off-Road		Total		Fatal+Injury		Run-Off-Road	
Variable	Coeff		t-stat		Coeff		t-stat		Coeff		t-stat	
Intercept	-6.00	-198.79	-6.44	-161.80	-4.78	-111.03	-6.05	-133.38	-6.33	-107.32	-5.33	-85.68
σ	0.33	118.05	0.43	118.67	0.44	110.69	0.38	83.08	0.39	62.71	0.42	62.29
LNAADT	0.73	217.57	0.71	160.74	0.50	104.20	0.73	137.23	0.69	100.90	0.56	78.55
LNLENGTH	0.70	96.70	0.71	70.63	0.94	82.14	0.65	51.98	0.69	39.94	0.92	53.17
Passing Zone	-0.16	-25.99	-0.18	-21.25	-0.15	-16.98	-0.19	-18.37	-0.20	-14.56	-0.16	-10.71
High Speed	-0.11	-19.70	-0.11	-14.70	-0.04	-4.83	-0.09	-9.11	-0.05	-3.49	-0.05	-3.61
Shoulder Rumble Strip	-0.12	-12.88	-0.13	-10.16	-0.15	-10.85	-0.15	-8.36	-0.15	-6.47	-0.14	-5.35
Access Density	0.01	31.33	0.01	25.97	-	-	0.01	23.51	0.01	22.43	-	-
σ	0.01	55.06	0.004	25.74	-	-	0.01	26.60	0.003	9.76	-	-
Curve Density	0.09	6.66	0.01	7.10	0.04	22.89	0.03	12.32	0.03	9.42	0.06	22.73
σ	0.06	64.05	0.05	44.63	0.05	40.32	0.04	32.48	0.05	25.13	0.03	18.63
Average Degree of Curve	0.01	29.69	0.01	18.63	0.01	22.04	0.01	17.71	0.01	12.36	0.01	15.03
σ	0.02	46.64	0.01	22.24	0.02	36.20	0.02	27.61	0.01	18.18	0.01	6.73
RHR = 5	0.05	5.00	0.03	2.37	0.14	9.94	-	-	-	-	-	-
σ	0.28	92.83	0.14	32.29	0.20	46.07	-	-	-	-	-	-
RHR = 6 or 7	-	-	-	-	-	-	0.03	2.92	-0.02	-1.03	0.12	6.66
σ	-	-	-	-	-	-	0.30	57.60	0.30	42.28	0.38	54.33
α	0.20	50.17	0.27	37.00	0.23	27.95	0.18	27.37	0.26	21.45	0.22	16.63
Log-Likelihood	-98552.47		-70418.81		-65289.94		-37240.76		-26562.24		-25284.51	
No. Segments	12,344		12,344		12,344		4,984		4,984		4,984	
CMF	1.046		1.029		1.152		1.036		0.984		1.122	
95% Error Lower Bound	1.028		1.005		1.120		1.012		0.955		1.085	
95% Error Upper Bound	1.065		1.054		1.185		1.060		1.015		1.161	
CMF 95% Lower Bound	0.608		0.788		0.774		0.576		0.546		0.538	
CMF 95% Upper Bound	1.800		1.343		1.715		1.863		1.773		2.343	

The CMF estimates for the RHR variables are noteworthy. The CMFs, with the associated 95% error range (based on the standard error and used for testing statistical significance) are shown in figure 1a. The CMFs with the 95% range for the random parameters are shown in Figure 1b. It was found that all RHR CMFs, with the exception of RHR 1 and 2 for fatal and injury crashes, were random due to unobserved heterogeneity. This is likely due to unobserved differences in the roadside across observations, as well as the impacts of human behavior, which is not directly accounted for in the models (28).

As shown in Table 5 and Figure 1a, all of the CMFs are statistically significant at the 95% confidence level, except for the fatal and injury CMFs for the combined RHRs of 1 and 2 and RHRs of 6 and 7. Since these two CMFs are not statistically significant, the CMF for RHRs of 1 and 2 is not random, and the range of the random CMF for RHRs of 6 and 7 is so large, there is no evidence that changing RHRs from 3 to 2, 1, 6, or 7 has any significant impact on fatal and injury crashes. This is likely due to the RHRs of 1-3 being forgiving enough not to impact fatal and injury crashes. Also, it is likely that RHRs of 6 and 7 impact driver behavior (e.g., driver speed), which could lead to the finding of no statistically significant association on these crashes.

Provided that all of the other CMFs are statistically significant, the signs of the mean values and the range of the random parameters are also of interest. In some cases, the percentage of the random parameters was nearly evenly distributed between CMFs less than and greater than a value of 1.0 (for fatal and injury crashes and RHR 5, 52.1% of the time the CMF values were

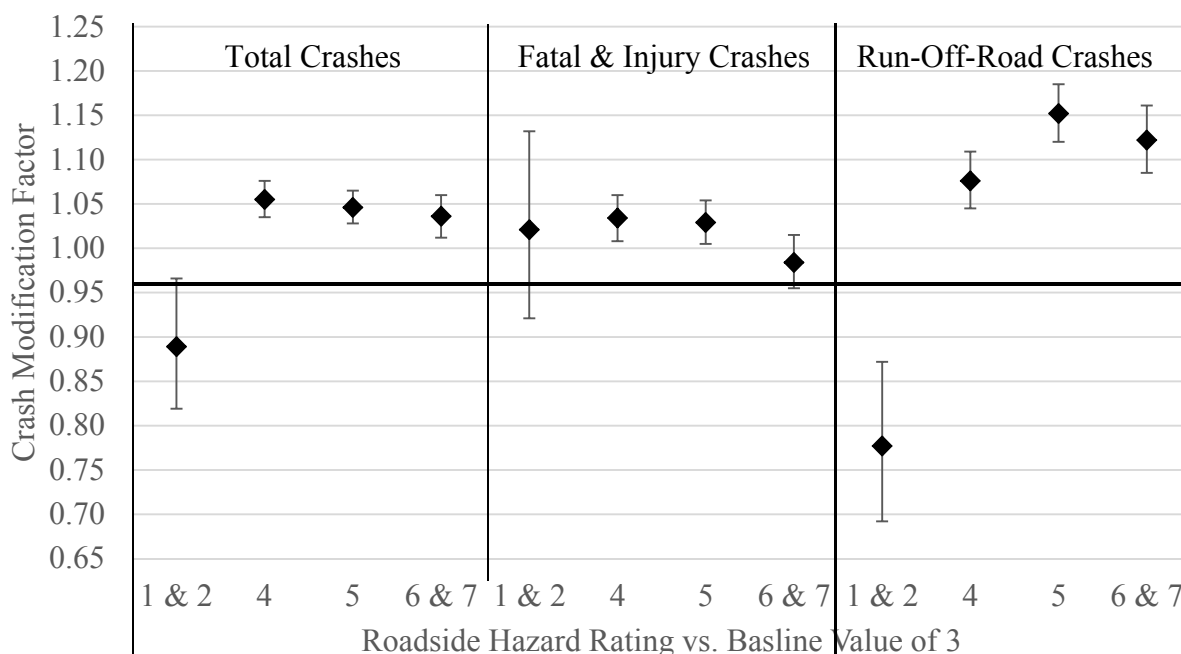


FIGURE 1a. CMFs and 95% error for tests of statistical significance.

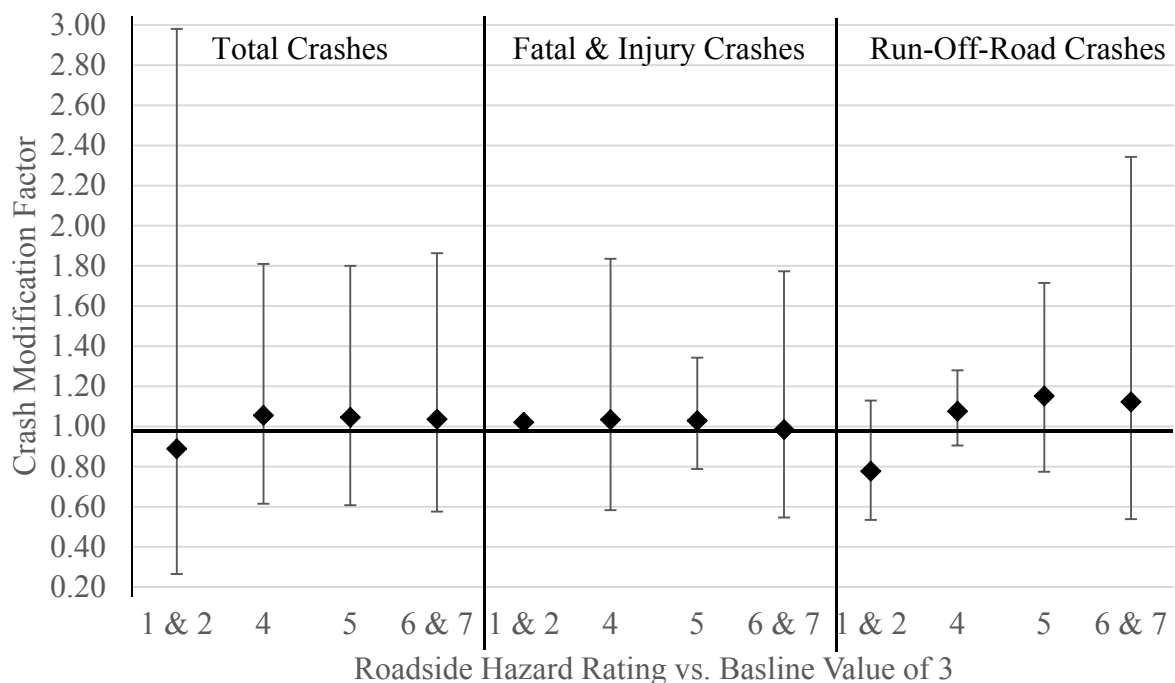


FIGURE 1b. CMFs and 95% range for random values.

greater than 1.0 and 47.9% of the time the values were less than 1.0). The CMF with the largest percentage of values on one side of the value of 1 was the run-off-road CMF for RHRs 1 and 2 (greater than a value of 1.0 79.8% of the time, and less than a value of 1.0 20.2% of the time). Thus, the actual CMFs experienced across locations can vary greatly, even when the CMFs are statistically significant.

It is also interesting to note the pattern of the mean values for the CMFs. For total and run-off-road crashes, the CMFs for RHRs of 1 and 2 indicate that crashes are lower than the baseline RHR equal to 3. This is consistent with the HSM (4). Also, the mean value for the CMFs for total and run-off-road crashes indicate that crashes increase when RHR is increased to a value larger than 3. However, it is interesting that the mean values of the CMFs are lower for total crashes as the RHR increases from 4 through 6 and 7. It is also notable that the CMF for run-off-road crashes is smaller for RHRs of 6 and 7 than for RHR of 5. However, it should also be noted that the range of the random CMFs increases for run-off-road crashes as the RHR increases from 4 to RHRs of 6 and 7. This is likely due to human factors and how drivers react to unforgiving roadsides.

When compared with the CMFs from the HSM (which only provides CMFs for total crashes), the findings are consistent with regards to higher RHRs being associated with higher expected crash frequencies, and lower RHRs being associated with lower expected crash frequencies. The magnitudes of the CMFs in this research are also consistent with the HSM CMFs for RHRs of 4 and lower. For RHRs of 5, 6, and 7, the HSM provides CMFs of 1.143, 1.222, and 1.306, respectively for total crashes. This research, however, produced CMF values of for RHRs 5, 6, and 7 of 1.046, 1.036, and 1.036, respectively for total crashes. However, the CMFs from the HSM are based on a function where the CMFs increase as a function of the

RHR. By estimating separate CMFs in this paper, the restriction of the functional relationship between CMFs and RHR is eliminated. Also, based on the magnitudes of the CMFs and the methodology used, along with the associated confidence intervals, the CMFs from this research are more informative and useful for crash prediction.

CONCLUSIONS AND RECOMMENDATIONS

This paper used data from 21,340 two-lane road segments in Pennsylvania, with associated RHRs and crash data (2005-2012), to estimate CMFs. Genetic matching was used to reduce selection bias and random parameters negative binomial regression was used to account for unobserved heterogeneity in the RHRs and other parameters. For matching and estimating the CMFs, a baseline value of $RHR = 3$ was used, consistent with the HSM (4). CMFs were developed for total crashes, fatal and injury crashes, and run-off-road crashes. Due to small sample sizes for RHRs of 1, 2, and 7, RHR categories 1 and 2 were combined into a single category, and RHRs of 6 and 7 were combined into another category for developing CMFs.

The results indicated that all CMFs, with the exception of fatal and injury crashes for RHRs 1 and 2 and RHRs of 6 and 7, were statistically significant at the 95% confidence level. Also, all CMFs, except for the RHR 1 and 2 for fatal and injury crashes, were found to be random (i.e., the CMFs varied across location). The randomness of the CMFs was also statistically significant at the 95% confidence level in all cases other than fatal and injury crashes for RHRs 1 and 2 and RHRs of 6 and 7. The mean values for the CMFs indicated that RHRs of 1 and 2 are associated with lower crash frequencies for total and run-off-road crashes. RHRs greater than 3 are associated with higher crash frequencies for total and run-off-road crashes. RHRs of 4 and 5 are associated with higher crash frequencies for fatal and injury crashes.

These findings are consistent with the HSM, although the magnitudes of the CMFs from the present study are smaller for RHRs of 5, 6, and 7 (4). Based on the CMFs developed in this paper, along with the 95% intervals (error and random parameter), the safety impacts of RHRs are better understood and predictions of the safety impacts of changing RHRs (including the associated uncertainties) are improved.

While the CMFs developed in this paper improve on the existing literature, there are limitations to the results. The largest limitation is the small sample sizes for RHRs 1, 2, and 7. Future research should develop CMFs for these RHRs using larger sample sizes and compare the results with the CMFs developed in this study. Also, since only data from Pennsylvania were used, data from other states should be used to develop CMFs for RHRs and compare them with the CMFs in this paper.

Future research should also further evaluate the benefits of estimating CMFs that are random, including application of the random CMFs, using both maximum simulated likelihood and Bayesian estimation methods.

REFERENCES

1. Federal Highway Administration (FHWA). Roadway Departure Safety. http://safety.fhwa.dot.gov/roadway_dept/. Accessed Oct. 18, 2016.
2. National Highway Traffic Safety Administration. NCSA Data Resource Website. <http://www-fars.nhtsa.dot.gov/QueryTool/QuerySection/Report.aspx>. Accessed Oct. 26, 2016.

3. Zeeger, C. V., D. W. Reinfurt, J. Hummer, L. Herf, and W. Hunter. Safety Effects of Cross-Section Design for Two-Lane Roads. *Federal Highway Administration*, Vol. Report No., No. 1, 1987.
4. AASHTO. *Highway Safety Manual*. American Association of State Highway and Transportation Officials, Washington, D.C., 2010.
5. Federal Highway Administration. CMF Clearinghouse. <http://www.cmfclearinghouse.org/>.
6. Vogt, A., and J. G. Bared. Accident Models for Two-Lane Rural Roads: Segments and Intersections. Report No. FHWA-RD-98-133. *Federal Highway Administration*, 1998.
7. Harwood, D. W., F. M. Council, E. Hauer, W. Hughes, and A. Vogt. Prediction of the Expected Safety Performance of Rural Two-Lane Highways. Report No. FHWA-RD-99-207. *Federal Highway Administration*, 2000.
8. Guo, C., and M. W. Fraser. *Propensity Score Analysis*. Sage Publications, Inc., Washington, D.C., 2010.
9. Sasidharan, L., and E. T. Donnell. Application of Propensity Scores and Potential Outcomes to Estimate Effectiveness of Traffic Safety Countermeasures: Exploratory Analysis Using Intersection Lighting Data. *Accident Analysis and Prevention*, Vol. 50, 2013, pp. 539–53.
10. Sasidharan, L., and E. T. Donnell. Propensity Scores-Potential Outcomes Framework to Incorporate Severity Probabilities in the Highway Safety Manual Crash Prediction Algorithm. *Accident Analysis and Prevention*, Vol. 71, 2014, pp. 183–93.
11. Wood, J. S., J. P. Gooch, and E. T. Donnell. Estimating the Safety Effects of Lane Widths on Urban Streets in Nebraska Using the Propensity Scores-Potential Outcomes Framework. *Accident Analysis and Prevention*, Vol. 82, 2015, pp. 180–191.
12. Wood, J. S., and E. T. Donnell. Safety Evaluation of Continuous Green T Intersections: A Propensity Scores-Genetic Matching-Potential Outcomes Approach. *Accident Analysis and Prevention*, Vol. 93, 2016, pp. 1–13.
13. Wood, J. S., E. T. Donnell, and R. J. Porter. Comparison of Safety Effect Estimates Obtained from Empirical Bayes Before-After Study, Propensity Scores-Potential Outcomes Framework, and Regression Model with Cross-Sectional Data. *Accident Analysis and Prevention*, Vol. 75, 2015, pp. 144–54.
14. Rosenbaum, P. R., and D. B. Rubin. The Central Role of the Propensity Score in Observational studies for Causal Effects. *Biometrika*, Vol. 70, No. 1, 1983, pp. 41–55.
15. Winship, C., and S. L. Morgan. The Estimation of Causal Effects from Observational Data. *Annual Review of Sociology*, Vol. 25, 1999, pp. 659–706.
16. Morgan, S. L., and C. Winship. *Counterfactuals and Causal Inference*. Cambridge University Press, 2014.
17. Ming, K., and P. R. Rosenbaum. Substantial Gains in Bias Reduction from Matching with a Variable Number of Controls. *Biometrics*, Vol. 56, No. 1, 2000, pp. 118–124.
18. Rosenbaum, P. R. *Design of Observational Studies*. Springer Science & Business Media, 2009.
19. Rosenbaum, P. R. *Observational Studies*. Springer Series in Statistics, New York, 2002.
20. Rosenbaum, P. R., and D. B. Rubin. The Bias Due to Incomplete Matching. *Biometrics*, Vol. 41, No. 1, 1985, pp. 103–116.
21. Rubin, D. B., and N. Thomas. Combining Propensity Score Matching with Additional Adjustments for Prognostic Covariates. *Journal of the American Statistical Association*, Vol. 95, No. 450, 2000, pp. 573–585.
22. Holmes, W. M. *Using Propensity Scores in Quasi-Experimental Designs*. SAGE Publications, 2013.
23. Diamond, A., and J. S. Sekhon. Genetic Matching for Estimating Causal Effects: A General Multivariate Matching Method for Achieving Balance in Observational Studies. *Review of Economics and Statistics*, Vol. 95, No. 3, 2013, pp. 932–945.
24. Haldar, A., and S. Mahadevan. *Probability, Reliability and Statistical Methods in Engineering Design*. John Wiley & Sons, Inc., New York, 2000.
25. Austin, P. C. Balance Diagnostics for Comparing the Distribution of Baseline Covariates Between Treatment Groups in Propensity-Score Matched Samples. *Statistics in Medicine*, Vol. 28, 2009, pp.

- 3083–3107.
26. Austin, P. C. An Introduction to Propensity Score Methods for Reducing the Effects of Confounding in Observational Studies. *Multivariate behavioral research*, Vol. 46, No. 3, 2011, pp. 399–424.
 27. Mannering, F. L., and C. R. Bhat. Analytic Methods in Accident Research: Methodological Frontier and Future Directions. *Analytic Methods in Accident Research*, Vol. 1, 2014, pp. 1–22.
 28. Mannering, F. L., V. N. Shankar, and C. R. Bhat. Unobserved Heterogeneity and the Statistical Analysis of Highway Accident Data. *Analytic Methods in Accident Research*, Vol. 11, 2016, pp. 1–16.
 29. Greene, W. H. *Econometric Analysis*. Prentice Hall, 2011.
 30. Anastasopoulos, P., and F. Mannering. A Note on Modeling Vehicle Accident Frequencies with Random-Parameters Count Models. *Accident Analysis and Prevention*, Vol. 41, No. 1, 2009, pp. 153–159.
 31. Greene, W. H. *Limdep Econometric Modeling Guide Version 9.0*. 2007.
 32. Wood, J. S., E. T. Donnell, and C. J. Fariss. A Method to Account for and Estimate Underreporting in Crash Frequency Research. *Accident Analysis and Prevention*, Vol. 95, 2016, pp. 57–66.
 33. Donnell, E. T., V. Gayah, and P. P. Jovanis. Safety Performance Functions: Final Report. *The Pennsylvania Department of Transportation Report No. FHWA-PA-2014-007-PSU WO 1*, 2014.
 34. Train, K. E. *Discrete Choice Methods with Simulation*. Cambridge University Press, 2009.
 35. Bhat, C. R. Simulation Estimation of Mixed Discrete Choice Models using Randomized and Scrambled Halton Sequences. *Transportation Research Part B*, Vol. 37, No. 9, 2003, pp. 837–855.
 36. Wood, J. S., and R. J. Porter. Safety Impacts of Design Exceptions on Nonfreeway Segments. *Transportation Research Record: Journal of the Transportation Research Board*, Vol. 2358, 2013, pp. 29–37.
 37. Butsick, A. J., P. P. Jovanis, and J. S. Wood. Modeling Safety Effects of Geometric Design Consistency on Two-Lane Rural Roads Using Mixed Effects Negative Binomial Regression. *Transportation Research Board 94th Annual Meeting*, Vol. 15-0797, 2015.
 38. Mayora, J. M. P., and L. R. Rubio. Relevant Variables for Crash Rate Prediction in Spains Two Lane Rural Roads. *Transportation Research Board 82nd Annual Meeting*, 2003.
 39. Malshkina, N., and F. Mannering. Emperical Assessment of the Impact of Highway Design Exceptions on the Frequency and Severity of Vehicle Accidents. *Accident Analysis and Prevention*, Vol. 42, No. 2, 2010, pp. 131–139.
 40. Torbic, D. J., J. M. Hutton, C. D. Bokenkroger, K. M. Bauer, D. W. Harwood, D. K. Gilmore, D. K. Dunn, J. J. Ronchetto, E. T. Donnell, H. J. Sommer III, P. Garvey, B. Persaud, and C. Lyon. *NCHRP Report 641: Guidance for the Design and Application of Shoulder and Centerline Rumble Strips*. 2009.
 41. Lyon, C., B. Persaud, and K. Eccles. Safety Evaluation of Centerline Plus Shoulder Rumble Strips. *Federal Highway Administration, Report FHWA-HRT-15-048*, 2015.
 42. Park, J., M. A. Abdel-Aty, and C. Lee. Exploration and Comparison of Crash Modification Factors for Multiple Treatments on Rural Multilane Roadways. *Accident Analysis and Prevention*, Vol. 70, 2014, pp. 167–177.
 43. Graham, J. L., D. W. Harwood, M. K. O’Laughlin, E. T. Donnell, and S. Brennan. NCHRP Report 794: Median Cross-Section Design for Rural Divided Highways. *Transportation Research Board of the National Academies*, 2014.
 44. Hanley, K. E., A. R. Gibby, and T. C. Ferrara. Analysis of Accident Reduction Factors on California State Highways. *Transportation Research Record: Journal of the Transportation Research Board*, Vol. No. 1717, 2000, pp. 37–45.
 45. Kweon, Y. J., and C. Oh. Identifying Promising Highway Segments for Safety Improvement Through Speed Management. *Transportation Research Record: Journal of the Transportation Research Board*, Vol. 2213, 2011, pp. 46–52.

Initial Investigation into Traversability of Rock Ditch Liners

MOJDEH ASADOLLAHI PAJOUH

JOHN D. REID

CODY S. STOLLE

RONALD K. FALLER

Midwest Roadside Safety Facility

University of Nebraska-Lincoln

ERIK EMERSON

Wisconsin Department of Transportation

Rock ditch liners were developed for areas susceptible to roadside erosion, such as silty soils in conjunction with steep grades. Rock ditch liners are common erosion control features which may be comprised of large and angular rocks. Current available guidance for installation of rock ditch liners generally has focused on rock gradation and sizing in an attempt to reduce safety concerns. However, the safe traversability of these features has not been studied.

Wisconsin DOT funded a research study in multiple phases to investigate the traversability of rock ditch liners that would eventually lead to development of guidelines for the safe implementation of these features. Vehicle stability was initially investigated using finite element analysis to simulate vehicular traversal over a rock ditch liner installed on level terrain. One full-scale vehicle test was conducted with a small passenger car (1100C) at speed of 50 mph traversing over a level-terrain, replica rock ditch liner to obtain physical data, calibrate vehicle models, and determine if wheel or suspension damage would occur. The small car experienced bouncing, but damage was limited to the tire deflation at the end of the event. After the finite element model was calibrated, further simulations were performed to identify critical scenarios for a vehicle traversing over a rock ditch liner installed on slopes. Simulation efforts consisted of both small car and pickup truck traversals on a 1V:3H fill slope at speeds of 30 and 45 mph. Vehicle stability and other safety concerns were investigated for the cases considered. From the simulation results, it was concluded that rock ditches filled with Type A riprap installed on fill slopes of 1V:3H or flatter are traversable for 1100C small cars and 2270P pickup trucks without rollover.

INTRODUCTION

For some roadside configurations, soil erosion due to water runoff is a significant concern. Erosion control features may be used to minimize the adverse effects of water runoff. Rock ditch liners are one example of an erosion control feature. Rock ditch liners are generally comprised of large and angular rocks. The geometric irregularities of rocks could pose a safety risk to motorist and errant vehicles. Little research has been performed to determine the traversability of these features. In general, rock ditches should be shaped to provide a reasonably smooth transition from the roadway to the front slope, ditch bottom, and through the back slope. Examples of rock-lined ditches are shown in Figure 1.



FIGURE 1 Rock ditch liners.

Two AASHTO road design manuals (1-2) provide general guidelines for some drainage devices (i.e., ditches, channels, and curbs) as well as for roadside slopes. AASHTO's Highway Drainage Manual states that grade-control structures, such as rock check dams, "are not recommended for use in roadside ditches unless they are located outside a safe recovery area or protected by guardrail or other appropriate safety barriers" (3). A guideline provided by the Federal Highway Administration (FHWA) briefly addresses the safety of side slopes, including riprap and ditch linings (4). Specifically, it denotes that rock ditch linings should be smooth, free of fixed objects, and free of snagging features so that a driver can regain control of the vehicle.

The Wisconsin Department of Transportation (WisDOT) funded a research study in two phases to determine the best practices of other DOTs in use of rock ditch liners, and to evaluate the traversability of these roadside hydraulic features (5). For the Phase I, the primary research objective was to evaluate the practices of other state DOTs regarding rock ditch liners, and to develop guidelines for the design and implementation of these features. The Phase II study focused on investigation of rock ditch liners through full-scale vehicle testing and computer simulation.

LITERATURE REVIEW

As no testing or computer simulation has been conducted to investigate the traversability of rock ditch liners, the key research studies that led to the current implementation practices of the drainage structures (such as slopes, drainage channels, ditches, and curbs) have been reviewed to provide insight into the behavior of vehicles traversing rock ditch liners (5).

In 1972, researchers at the Texas Transportation Institute (TTI) conducted a full-scale testing and computer simulation study of vehicle traversals on a 1V:3.5H fill slope with speeds ranging between 45.1 and 63.6 mph and angles ranging between 8.6 and 20.4 degrees (6). The researchers concluded that a vehicle can safely traverse a 1V:3.5H side slope with a flat bottom

ditch. In 1975, TTI researchers examined additional roadside slopes ranging from 1V:3H to 1V:10H at speeds of 40, 60, and 80 mph with encroachment angles of 7, 15, and 25 degrees through full-scale testing (7). No vehicle rollover occurred on any of the slope configurations with smooth surfaces. However, in simulation studies when coefficients of friction were changed and the slope was modeled with other obstacles, rollover occurred at speeds of 60 and 80 mph for an encroachment angle of 15 degrees. No rollovers occurred on slopes of 1V:5H or flatter.

In 1985, TTI researchers completed another testing and computer simulation effort to evaluate vehicles traversing 1V:3H fill slope using different vehicle types – a pickup truck, a Dodge van, and a small car at speed of 50 mph (8-9). Both pickup trucks and vans were able to return to the roadway, but the car encountered enough sideslip to reach the toe of the slope and ultimately rolled over. It was concluded that smooth, well-compacted slopes as steep as 1V:3H could be traversed safely, but small discontinuities along the slope would be highly likely to decrease the stability of the vehicle.

In 2002, Thomson and Valtonen conducted a study to examine the vehicle dynamics traversing a roadside V-shaped ditch. A 3.3-ft deep ditch was constructed with a 1V:3H front slope and a 1V:2H back slope, as shown in Figure 2 (10). A total of 16 full-scale tests were performed on this ditch configuration – fourteen tests with a 1,984-lb vehicle, and two tests with a 3,307-lb vehicle. The speeds ranged from 38.5 to 66.5 mph, while the encroachment angles ranged from 3 to 20 degrees. Three vehicle rollovers were observed with the 1,984-lb small car at the following conditions: 49 mph and 20 degrees; 66.5 mph and 19 degrees; and 51 mph and 11 degrees. In addition, the V-shaped ditch was evaluated with two different surface irregularities in the last two tests, as indicated in Figure 2. For test no. 15, the V-shaped ditch was modified into a U-shaped ditch by lining the bottom of the ditch with loose gravel. The test

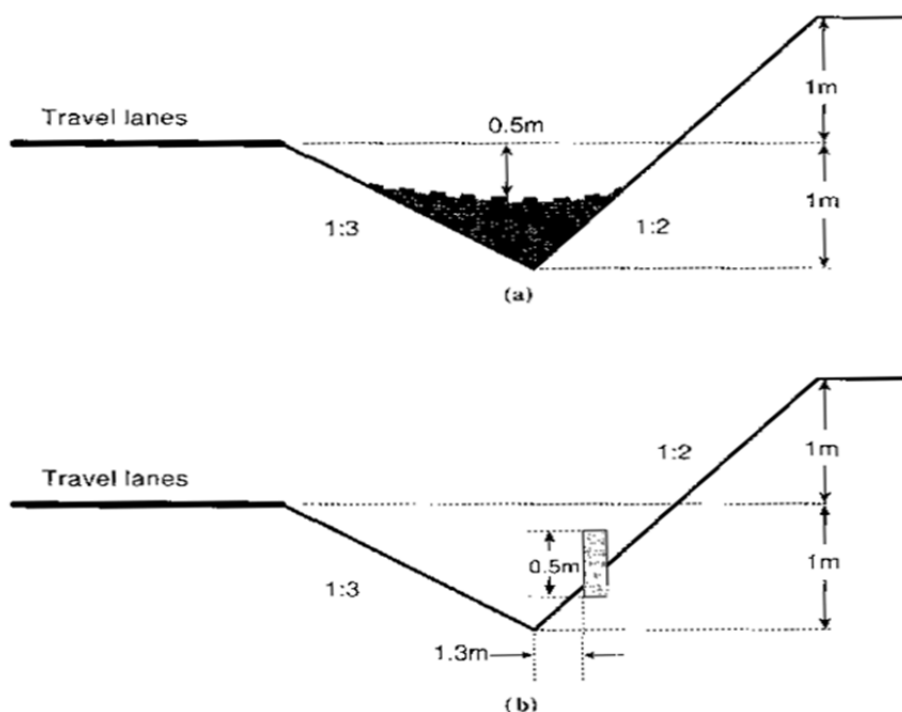


FIGURE 2 V-shaped ditch configurations:
(a) loose gravel and (b) longitudinal barrier (10).

vehicle, traveling at 60 mph and with a 10-degree encroachment angle, had no trouble traversing the configuration and climbing up the back slope. For test no. 16, a vertical barrier was installed near the toe of the back slope. In this case, the vehicle impacted at a speed of 62 mph and at a 10-degree encroachment angle, then it rolled over as it came into contact with the barrier on the back slope.

Later in 2008, the Midwest Roadside Safety Facility (MwRSF) completed a research study to investigate the safety performance of a pipe culvert grate system installed on 1V:3H fill slopes (11-12). Two full-scale vehicle crash tests were conducted on a grate system installed on a 1V:3H fill slope. The first crash test consisted of a 4,484-lb pickup truck traversing the slope at an angle of 25.4 degrees and a speed of 60.8 mph. During the test, the vehicle was able to completely traverse the grate system (13). The second test consisted of a 1,997-lb small car traversing the slope at an angle of 18.7 degrees and a speed of 61.3 mph. The vehicle was also able to completely traverse the grate system, and all evaluation criteria were met according to NCHRP Report No. 350. From this testing program, the researchers found that the standard grate system that was developed by TTI researchers in 1981 and later adopted by AASHTO was acceptable for use on 1V:3H or flatter fill slopes.

STATES PRACTICE

In addition to the basic FHWA guidelines, different State DOT procedures are available regarding the construction of rock ditch liners. These procedures are often open to significant engineering and construction judgment. The wide variance of characteristics associated with ditch geometries, soil characteristics, and water quantities from site to site make it very difficult to generate a standard set of design guidelines for ditch liners. Many state DOTs have recommended that rock ditch liners to be sufficiently entrenched within the soil ditch so that the final upper rock surface is approximately flush with the non-lined, adjacent soil terrain. The entrenchment depth or liner thickness is assumed to be equal to at least two times the average width of the D_{50} rocks contained therein. D_{50} denotes the particle diameter at 50% in the cumulative particle size distribution. In addition, a filter fabric should also be installed directly on the ground before any rock is placed to line the ditch surfaces. FHWA's HEC 15 (14) recommends gravel to be used to create a transition from soil to riprap. Therefore, consideration should also be given to lining the shoulder with gravel whenever a rock ditch liner is placed adjacent to a roadway. Given these design considerations, it is recommended that the side slopes of a trapezoidal ditch be no steeper than 1V:3H when constructed with a generally-smooth, rock lining surface.

Additional design criterion for rock ditch liners pertains to the size of rock or riprap, which is highly dependent on shape and size of the ditch as well as the expected runoff flows. First, the size of rock or riprap should provide adequate resistance to movement over a broad range of flow velocities. Second, the gradation of rock must allow for errant vehicles to safely traverse a ditch lined with compacted rocks or riprap within the soil surfaces. There are safety concerns regarding excessive rock exposure above the general upper plane of a ditch liner. Large exposed rocks may result in increased propensity for vehicular instabilities while traversing a rock-lined ditch.

Some common placement practices exercised by the state DOTs include: 1) stones should be placed in such a manner as to create a well-graded, flexible mass of stones with minimal voids

with an optional use of grout to fill the remaining voids; 2) the ditch terrain should be undercut, and the contours of the liner should match that of the existing grade to keep the liner free of any raised bumps or depressions; and 3) the liner should consist of stones that are angular in shape in order to create an interlocking mechanism when dumped or hand placed, thus reducing the possibility of deformation to any portion of the liner. A more detailed summary of the feature geometries presented by several state DOTs is listed in Table 1.

COMPUTER SIMULATION – INITIAL INVESTIGATION

A numerical study was initiated to investigate the stability of small cars traversing over a rock ditch liner installed on level terrain using computer simulation with the finite element program, LS-DYNA (29). For the preliminary investigation of the traversability of the rock ditch liner, a flat configuration (i.e., non-ditch) was selected to investigate vehicle bouncing and instability. As the modeled terrain was flat, an 1100C vehicle was deemed more critical than a 2270P pickup truck. Small cars have a lower profile, less suspension deflection, and a smaller tire size, which should result in more instability, bouncing, and roll angle displacement. The rock ditch liner was modeled with rigid shell elements with a maximum element size of 1 in., as shown in Figure 3.

TABLE 1 Sample State DOT Guidelines for Rock Ditch Liners

State DOT	Reference Manual	Predominant Rock Size (in.)	Minimum Thickness of Liner (in.)	Suggested Side Slope (V:H)
California	Roadside Management Toolbox (15)	4 - 6	6	-
Illinois	2007 Specifications, Division 200 & 1000 (16)	5 - 16	8	-
Iowa	2009 Specifications, Section 2507 & 4130 (17)	6 - 15	24	1:2
Kansas	Drainage, Section 12.7 (18)	4 - 12	12	1:6
Minnesota	2005 Specifications, Section 2511 & 3601 (19)	9 - 15	12	-
Missouri	2004 Specifications, Section 609 (20)	3 - 19	8	-
Nebraska	Drainage Design, Section 7 (21)	9 - 15	18	-
New York	Stormwater Facilities, Region 8 (22)	6	12	1:3
Ohio	2010 Specifications, Item 703 & 1100 (23)	6 - 18	12	-
South Dakota	Road Design, Chapter 11 (24)	-	-	-
Texas	2004 Specifications, Section 432 (25)	9 - 21	12	-
Virginia	2007 Specifications, Section 414 (26)	15 (max)	20	-
Wisconsin	2010 Specifications, Section 606 (27)	4 - 18	12	-
Wyoming	Standard Plans (28)	3	9	-

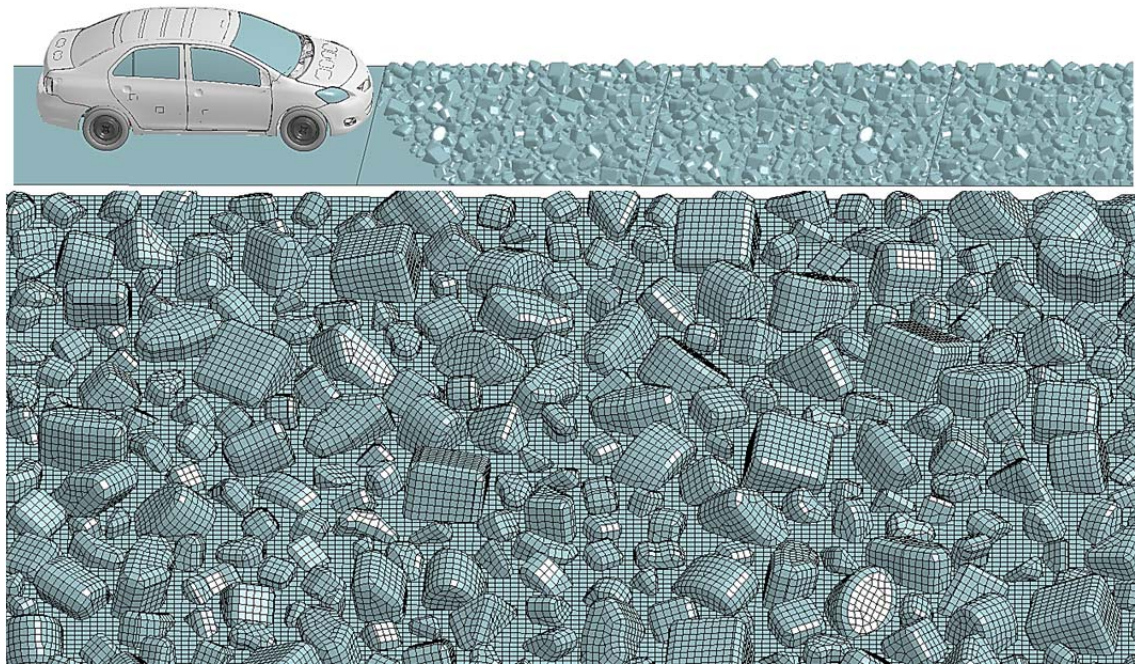


FIGURE 3 Simulated rip rap model on level terrain.

Rocks were modeled as geometric shapes (e.g., cubes, prisms, cylinders, and pyramids) with radiused edges for improved contact stability. The initial investigation of a Toyota Yaris model traversing over a ground ditch liner installed on level terrain at speed of 50 mph and an encroachment angle of 25 degrees suggested that the small vehicle could traverse the rocks placed on level terrain without snagging or rollover.

DESIGN DETAILS TEST RDL-1

A replica rock ditch liner was constructed to form a “flat ditch” (i.e., non-grade), for consistency with the computer simulation models and for ease of evaluating and calibrating vehicle motion while traversing the rocks, as shown in Figure 4. To ensure that the vehicle remained on the replica flat-ditch rock liner throughout the test, a 10-degree flare was added to the sides of the liner to account for any abrupt steering or partial redirection of the vehicle. Thus, the replica flat-ditch rock liner had a trapezoidal shape. The largest width and the length of the level terrain rock liner were 55 ft and 110 ft, respectively. Downstream from impact, the terrain was grassy, reasonably smooth, and free of all obstacles or hazards for a length of approximately 193 ft, to ensure that the vehicle would be able to successfully brake after reaching the end of the replica flat-ditch rock liner. Concrete barriers were placed downstream from the replica flat-ditch rock liner to contain the vehicle. The front edge of the replica flat-ditch rock liner was angled at 25 degrees to ensure that right- and left-front wheels did not make contact at the same time, to maximize roll behavior.

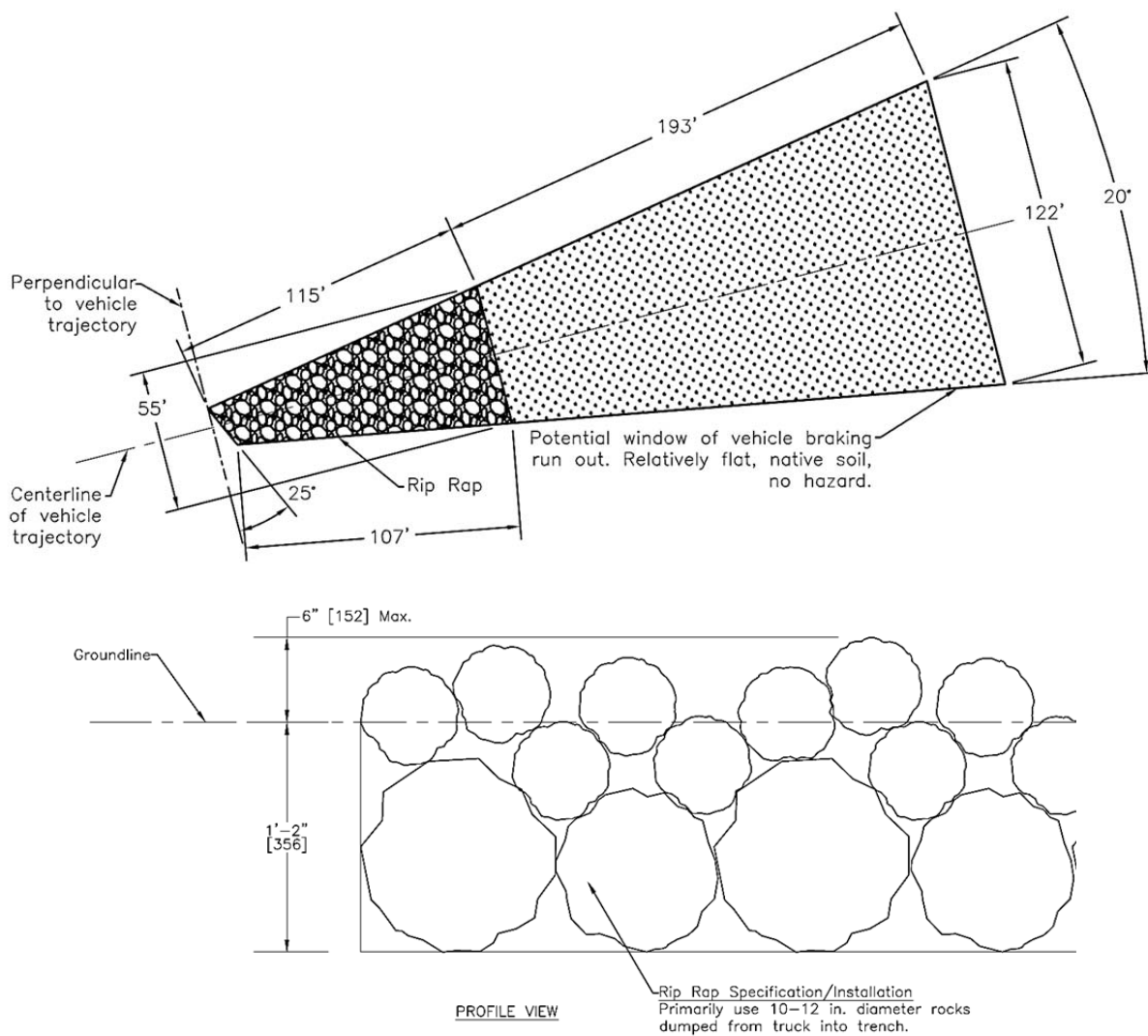


FIGURE 4 Test No. RDL-1 Installation and Rip Rap Detail

Accelerometers and linear displacement transducers rated for 20-g accelerations over 5-ms intervals were placed on the lower control arms of the front suspensions and the rear axle. The vehicle position was also tracked using high-speed digital video cameras.

After considering the common rock sizes reported by the state DOTs along with existing AASHTO guidelines for limiting the height of exposed elements above grade, the research team selected rock sizes ranging from 6 to 8 in. for the mean rock cross-sectional dimension. The mean, or 50th percentile, rock size is referred to as a D₅₀ specification. Likewise, the maximum rock size (i.e., D₁₀₀) ranged between 10 and 12 in. to be consistent with Type A Riprap. The rocks composing the liner were dumped into a 12-in. deep pit forming the trapezoidal shape of the “flat ditch”. No additional grading or smaller rocks were added to the top surface. Researchers believed this condition represented a “long-term” condition, in which smaller rocks may wash away or settle between the larger rocks, exposing only the largest rocks on the surface of the liner.

FULL-SCALE TEST RDL-1

The objective of the full-scale traversability test and the flat construction was to calibrate the vehicle model with all available data. As such, the only evaluation criterion for the test was that the vehicle did not roll over nor experience excessive deceleration; MASH limits of 20 g's were used to define acceleration limits. In test no. RDL-1, a 2,388-lb Toyota Yaris impacted the leading edge of the rock ditch liner at a speed of 51.7 mph and at angle of 25 degrees. Sequential photographs for the test, system installation and the vehicle damage are shown in Figure 5.

In test no. RDL-1, the 1100C vehicle traversed over the rock ditch liner with some bouncing. The vehicle damage was limited to the right front tire deflation and two contact marks, as shown in Figure 5. None of the rocks forming the ditch liner were damaged or displaced. Other minor damage consisted of scraping on front-passenger engine cradle leading edge, scraping on passenger floor pan, a slight dent on exhaust tube, and crushing of the oil pan. As there were no established criteria to evaluate the safety of the rock ditch liner, researchers evaluated the test results based on the vehicle relative stability and the vehicle damage. In test no. RDL-1, the passenger car could safely travel over the ditch with minimal bouncing and damage.

Immediately after the rear wheels contacted the leading edge of the replica non-grade, rock ditch liner, both rear linear displacement transducers fractured, and suspension deflection data could not be obtained. Front suspension accelerometer and displacement transducer data was analyzed and the magnitudes of deflection were used to investigate and partly calibrate model data. Due to the difficulty of representing the actual rock ditch liner surface in FEA, calibration efforts were limited to modifications of spring stiffnesses and damper properties.

INVESTIGATION ON CRITICAL IMPACT SCENARIOS

After the numerical model was validated against the full-scale test no. RDL-1, further computer simulations were performed to evaluate critical scenarios of vehicle traversing rock ditch liners on slopes. Parameters to be evaluated included: vehicle type, vehicle speed, and ditch side slope steepness. Simulation efforts consisted of both small car and pickup truck traversing a rock ditch



0.000 s



0.150 s



0.300 s



0.450 s

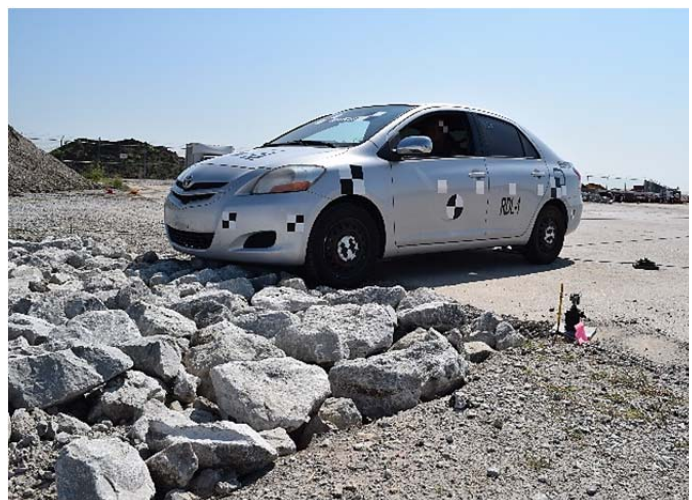


0.600 s

(a) Sequential Photos



(b) Rip Rap



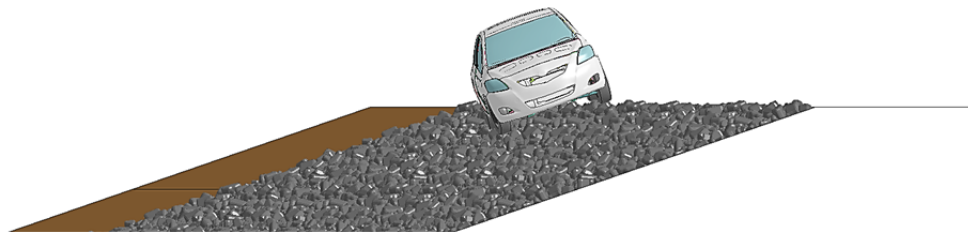
(c) Vehicle Prior Test



(d) Vehicle Damage

FIGURE 5 System and Vehicle Damage, Test No. RDL-1

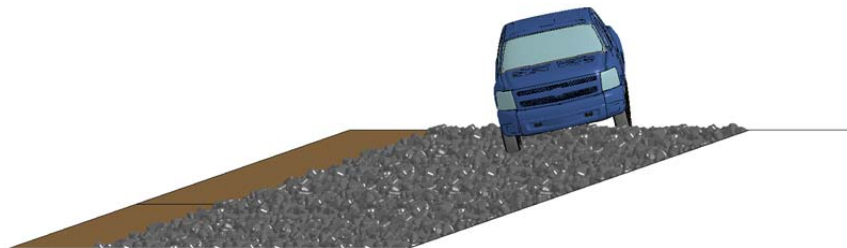
liner installed on a 1V:3H slopes at two speeds of 30 and 45 mph. At a relatively low speed, the tires of a vehicle traversing a non-uniform liner was deemed more likely to slip between the cracks of the liner, ultimately resulting in an increased propensity for the under-carriage of the vehicle to snag on a rock. Conversely, the suspension system of a vehicle traversing a rugged liner at a relatively high speed was more likely to become unstable. In these simulations, no snagging or rollover was observed, and the vehicles could safely traverse the rocks with minimal bouncing.



Toyota Yaris Traversing on 1V:3H Slope at 30 mph



Toyota Yaris Traversing on 1V:3H Slope at 45 mph



Silverado Pickup Truck Traversing on 1V:3H Slope at 30 mph



Silverado Pickup Truck Traversing on 1V:3H Slope at 45 mph

**FIGURE 6 Simulations of Vehicle Traversals over a 1:3 Slope,
at Angle of 15 Degrees – 0.7 s**

DISCUSSION

Phases I and II of this research effort were directed to determine the best installation practice for rock ditch liners and to start a detailed modeling effort for evaluating the safety of these liners. However, the current research does not yet constitute proof that the rock ditch liner will be a safely traversable feature. More investigation is needed to evaluate traversability under varying impact conditions, including:

- Different speeds and encroachment angles of the vehicle;
- Configurations in ditch and alternative slope profiles;
- Non-tracking and/or active steering input conditions; and
- Alternative vehicles, such as long sedans or low ground clearance trucks.

Further analysis may be warranted using computer simulation and full-scale testing. If these features are implemented, researchers recommend a detailed crash study in the location of the rock ditch liners to ensure that errant vehicles are not being exposed to undue risk from traversal conditions which have not yet been evaluated.

CONCLUSIONS AND RECOMMENDATIONS

Traversability of the rock ditch liners was evaluated using a combination of full-scale testing and computer simulation. An 1100C full-scale test was performed with a small passenger car traversing over a rock ditch on level terrain with speed of 51.7 mph and an angle of 25 degrees. In test no. RDL-1, the test vehicle traversed over the rock ditch liner with some bouncing, but did not displace or damage any of the rocks forming the ditch top surface. Also from the simulation results, rock ditches filled with smooth Type A riprap with a maximum slope of 1V:3H was determined to be traversable for small cars and pickup trucks without rollover. However, additional testing and simulation is recommended to verify the vehicle stability while traversing sloped-ditch liners.

Also, additional research should be conducted to develop a safety guideline that includes maximum side slope for a given speed, and maximum rock gradation, which assists engineers with configuring a safe roadside while minimizing roadside erosion. Further research is recommended to address the effects of ditch geometries and back side slope on traversing vehicle stability.

ACKNOWLEDGMENTS

The authors wish to acknowledge the Wisconsin Department of Transportation for sponsoring this project as well as the Departments of Transportation for the States of Illinois, Iowa, Kansas, Minnesota, Missouri, Nebraska, New York, Ohio, South Dakota, Texas, and Wyoming for providing resource materials. Acknowledgement is also given to MwRSF personnel for constructing the system and conducting the crash test.

REFERENCES

1. AASHTO, *A Policy on Geometric Design of Highways and Street*, Fifth Edition, American Association of State Highway and Transportation Officials, Washington, D.C., 2004.
2. AASHTO, *Roadside Design Guide*, Third Edition with Updated Chapter 6, American Association of State Highway and Transportation Officials, Washington, D.C., 2006.
3. AASHTO, *Highway Drainage Guidelines*, Fourth Edition, American Association of State Highway and Transportation Officials, Washington, D.C., 2007.
4. Federal Highway Administration, *Maintenance of Drainage Features for Safety – A Guide for Local Street and Highway Maintenance Personnel*, Report No. FHWA-SA-09-024, July 2009.
5. Jowza, E.R., Faller, R.K., Mongiardini, M., Sicking, D.L., Reid, J.D., *Crash Testing of Various Erosion Control Features – PHASE I: Preliminary Guidelines*, Transportation Research Report No. TRP-03-249-11, Midwest Roadside Safety Facility, University of Nebraska-Lincoln, November 28, 2011.
6. Ross, H. E., Jr., and E. R. Post. Full-Scale Embankment Tests and Comparisons with a Computer Simulation. *Transportation Research Record*, No. 488, 1974, pp. 53–63.
7. Weaver, G. D., E. L. Marquis, and R. M. Olson. *NCHRP Report No. 158: Selection of Safe Roadside Cross Sections*, 1975.
8. Buth, C.E. and Campise, W.L. *Performance Limits of Longitudinal Barrier Systems – Volume IV – Appendix C Details of Embankment Traversal Tests*, Texas Transportation Institute, Texas A&M University, College Station, FHWA Contract No. DTFH61-82-C-00051, May 1985.
9. Sicking, D.L., Buth, C.E., and Campise, W.L., *Performance Limits of Longitudinal Barrier Systems – Volume V – Appendix D Computer Simulations*, Texas Transportation Institute, Texas A&M University, College Station, FHWA Contract No. DTFH61-82-C-00051, May 1985.
10. Thomson, R., and J. Valtonen. Vehicle Impacts in V-Shaped Ditches. *Transportation Research Record*, No. 1797, 2002.
11. Polivka, K.A., Reid, J.D., Sicking, D.L., Faller, R.K., Bielenberg, R.W., and Rohde, J.R., Performance Evaluation of Safety Grates for Cross-Drainage Culverts. Transportation Research Report No. TRP-03-196-08, Midwest Roadside Safety Facility, University of Nebraska-Lincoln, October 23, 2008.
12. Sicking, D. L., R. W. Bielenberg, J. R. Rohde, J. D. Reid, R. K. Faller, and K. A. Polivka. Safety Grates for Cross-Drainage Culverts. *Transportation Research Record: Journal of the Transportation Research Board*, No. 2060, 2008.
13. Ross, H. E., D. L. Sicking, R. A. Zimmer, and J. D. Michie. *NCHRP Report 350: Recommended Procedures for the Safety Performance Evaluation of Highway Features*, 1993.
14. Federal Highway Administration, *Design of Roadside Channels with Flexible Linings*, Hydraulic Engineering Circular No. 15, Third Edition, Publication No. FHWA-NHI-05-114, National Highway Institute, HEC-15, September 2005.
15. California Department of Transportation (CALTRANS), *Caltrans Storm Water Quality Handbooks – Construction Site Best Management Practices Manual*, State of California, 2004.
16. Illinois Department of Transportation, *Highway Standards – Revision 212*, State of Illinois, 2011.
17. Iowa Department of Transportation, *Road Design Details – Division 4000*, State of Iowa, 2010.
18. Kansas Department of Transportation, *Standard Drawings – Landscape*, State of Kansas, 2009.
19. Minnesota Department of Transportation, *Standard Plan – Series 400*, State of Minnesota, 2006.
20. Missouri Department of Transportation, *Standard Plans for Highway Construction*, State of Missouri, 2009.
21. Nebraska Department of Roads, *Drainage and Erosion Control Manual*, State of Nebraska, 2006.
22. New York State Department of Transportation, *Standard Sheets (US Customary) – Group 209*, State of New York, 2010.
23. Ohio Department of Transportation, *Hydraulic Standard Construction Drawings*, State of Ohio, 2009.

24. South Dakota Department of Transportation, *Standard Plates – Section 734*, State of Ohio, 2001.
25. Texas Department of Transportation, *Roadway Standards (English)*, State of Texas, 1993.
26. Virginia Department of Transportation, *Road and Bridge Standards – Section 100*, State of Virginia, 2001.
27. Wisconsin Department of Transportation, *Roadway Standards – Section 606*, State of Wisconsin, 2011.
28. Wyoming Department of Transportation, *Standard Plans (dual units)*, State of Wyoming, 2004.
29. Hallquist, J.O. *LS-DYNA Keyword User's Manual*. Livermore, CA: Livermore Software Technology Corporation. 2007.

Development of Crashworthy Road Sign Post Using Energy-Absorbing Modules on the Sign Base Plate

DUKGEUN YUN

Korea Institute of Civil Engineering and Building Technology

MANGI KO

Kongju University

MINHYUNG NHO

Kongju University

JAEHONG PARK

Korea Institute of Civil Engineering and Building Technology

In order to mitigate passenger severity for the impact to the sign and lighting post on the road, the breakaway sign support was developed. The general mechanism of breakaway sign system is to mitigate the impact energy with separating the pole from the post base when vehicle impact the post. However, usually breakaway sign post is used at small size of the road sign due to prevent secondary accident. Moreover, generally the breakaway sign could be installed where the clear zone is exist on the roadside. Therefore the concept of passive safety columns with energy absorbing function was deployed in European countries.

In this study, passively safe column of new concept is developed. It consists of a column having a special base plate with a key of inversed T shape with Energy Absorbing Modules (EAM). The inversed T shape guide trough on base plate is inserted keeping the column stands against wind load, but moves in case of an impact. To enhance the resistance but absorb the impact energy, the compartment of the trough is filled with EAM made of circular steel tube stub, which absorbs part of the impact energy remaining after the vehicle and column completes their plastic impact.

In this system, energy dissipation takes place in two phases. In the first phase, it dissipates the impact energy by the linear momentum conservation principle while the plastic impact between the post and vehicle takes place, then, the second phase dissipation follows by the deformation of the energy absorbing modules embedded in the guide trough of the foundation. Energy dissipation mechanism is explained and simulations of impacts to the new column system are made using LS-DYNA program to investigate the vehicle response and occupant safety. The simulation results are used in tuning the dimension of the energy absorbing module for an impact of 0.9 ton–80 km/h with 0- to 15-degree impact angle. The simulation for the final design of the passively safe column shows its effectiveness to the proposed target impact of 0.9 ton–80 km/h.

Challenges in Developing Cost-Effective MASH TL4 Semi-Flexible Barriers

LEIGH BROWN

Valmont Highway Technology

This presentation will explore the challenges associated with the development of semi-flexible barriers to meet the new MASH TL4 standard. Semi-flexible barriers are traditionally steel w-beam or thrie-beam rails connected to strong or weak steel posts embedded into the ground. The presentation will cover the design elements and innovative mechanisms, of several systems, developed to enhance the crash testing performance of semi-flexible barriers to meet the new standard. The MASH TL4 standard has significantly increased the re-directive requirements of barriers over the NCHRP350 TL4 standard and this influence will be explored. The presentation will be in the format of a case study from initial design and concept testing through to full compliance testing.

New Zinc-Aluminum-Magnesium Metallic Coating for Guardrails

RICHARD A. CLAUSIUS
ArcelorMittal Global R&D

MICHAEL GREMLING
ArcelorMittal / CRM Group – AC&CS

This presentation will show the performance of a new Zn-Al-Mg (ZM) metallic coating with 3.5% Aluminum, 3.0% Magnesium and the balance Zinc called “Magnelis[®]”. This ZM continuous hot dip applied metallic coating offers corrosion performance that is different than conventional hot dip pure zinc galvanized (GI) coatings (at least 2 to 3 times better for equivalent coating thickness). Corrosion performance could be improved over GI coatings due to the sacrificial and barrier corrosion performance of the ZM coating, cut edge seal-healing characteristics, and ability to perform in a variety of corrosive environments including salt, alkaline, and a multitude of soils. In addition, this ZM coating is now being introduced for guardrails in Europe and South America, and when combined with higher strength steels, offers a new solution for performance based safety barriers guardrails with increased corrosion protection. This ZM coating is also suitable for other roadside applications such as gantries and posts, and a comparison of GI and ZM performance/attributes will be shown in the presentation.

New Thrie Beam Terminal End Shoe Connection

AKRAM ABU-ODEH

ROGER BLIGH

Texas A&M Transportation Institute

CHRISTOPHER LINDSEY

Texas Department of Transportation

Terminal thrie end shoes connect nested thrie beams to parapets or other bridge rail structure to provide a robust connectivity between a transition section and a rigid railing section. When connecting terminal end shoe to thrie beam transitions, the thrie section profile results in shifting of the connecting slots. This can result in slots misalignment, which makes installation and maintenance difficult. Multiple field adjustments are known to be used to fit the end shoe to the beam. Such methods include hammering drift pins to deform the metal, or torching or grinding away the interfering material, all of which may compromise the integrity of the rail element. TTI researchers embarked on simulation and pendulum testing activities to develop and evaluate a new end shoe connector. This presentation details the methodology and outcome of work performed to design this thrie end shoe connector that alleviate the construction issues listed earlier.

Attachment of a Combination Bridge Rail to Concrete Parapet Utilizing Epoxy Adhesive Anchors

ROBERT W. BIELENBERG

SCOTT ROSENBAUGH

RONALD K. FALLER

*Midwest Roadside Safety Facility
University of Nebraska-Lincoln*

The objective of this research was to develop and evaluate alternative epoxy adhesive anchorage systems for the BR27C combination bridge rail system. The BR27C combination bridge rail was originally designed and tested with a 24-in. tall by 10-in. wide vertical concrete parapet with a steel post and rail attached to the concrete parapet with a cast-in-place concrete anchorage. The Iowa Department of Transportation (IaDOT) desired an epoxy adhesive anchor design that would be easier to install on an updated version of the BR27C with a 12-in. wide vertical concrete parapet.

The research effort began with development of several proposed alternative anchorage concepts. The concepts were designed using a modified version of the ACI318-11 procedures for embedded anchor design with modifications for dynamic increase factors and the expected failure modes. A spread, four-anchor and an offset, two-anchor concept were selected as the preferred designs for evaluation. In addition to these two proposed configurations, the researchers evaluated a third option that had been previously installed on the US-20 bridge near Hardin, Iowa. Dynamic component testing was conducted on the original, cast-in-place anchorage as well as the three alternative anchorages using a simulated bridge rail parapet. All three of the alternative anchorages provided greater load capacity than the original cast-in-place design and were deemed acceptable surrogates. The offset, two-anchor design was deemed the best option due to its development of the highest peak load, the potential for reduced parapet damage, and improved ease of installation.

INTRODUCTION AND SCOPE

Combination bridge rails are commonly used by many state departments of transportation and often consist of a concrete parapet with an upper steel or aluminum railing system. In the past, these types of bridge rails have typically been designed with the posts attached to the concrete parapet using a cast-in-place anchorage system. While cast-in-place anchors have performed well, they have several disadvantages, including added complexity and issues with dimensional tolerances regarding their placement in the parapet.

Iowa Department of Transportation (IaDOT) was interested in investigating the use of epoxy adhesive anchorages for the attachment of the steel beam-and-post to the concrete parapet on the BR27C combination bridge rail system shown in Figure 1. In addition, IaDOT wished to evaluate an epoxy adhesive anchorage system for the BR27C previously used on an existing bridge on US-20 in Iowa. The alternative epoxy adhesive anchorages were to have equal or

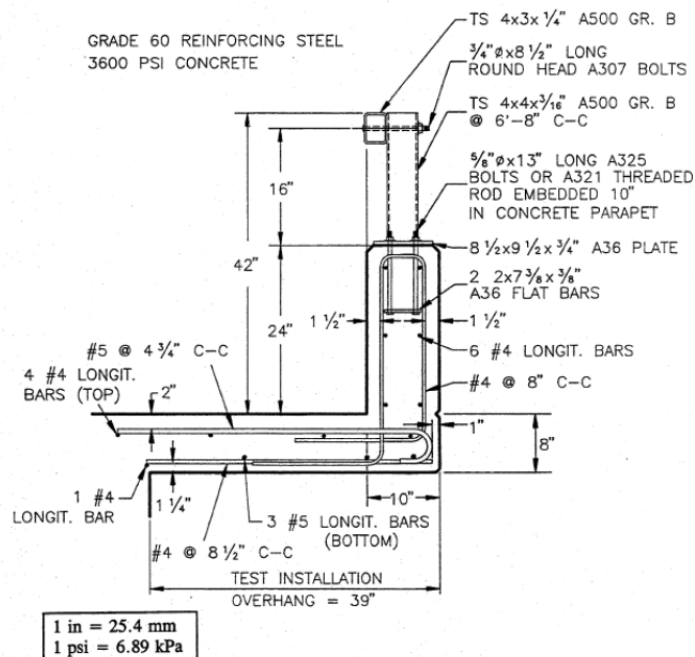


FIGURE 1 BR27C Design on concrete bridge deck and sidewalk.

greater capacity than the current cast-in-place anchorage, so that they could be used in new construction or as a retrofit to modify existing bridge railings.

Several alternative epoxy adhesive anchorage configurations were developed and IaDOT selected preferred systems for evaluation. Dynamic component testing was used to evaluate the selected epoxy adhesive anchorages and to demonstrate that their capacities were equal to or greater than the existing cast-in-place anchorage system. The capacity of the current cast-in-place anchorage had not been fully quantified with testing. Thus, one dynamic component test was performed on a bridge rail post using the original, cast-in-place anchorage configuration as a baseline. Comparisons of force levels, energy dissipated, and observed failure modes between the tests were used to verify that the proposed anchorages provided equal or greater capacities than the current anchorage, and that the alternative anchorages did not display undesirable failure modes.

BACKGROUND

IaDOT BR27C Combination Bridge Rail

The BR27C combination bridge rail design was originally developed and tested at the Texas A&M Transportation Institute in 1993 (1). The bridge rail design consisted of a 24-in. tall by 10-in. thick vertical concrete parapet, with the combination rail mounted on top of the parapet, as shown in Figure 1. Both the sidewalk- and bridge deck-mounted versions of the combination bridge rail were subjected to three full-scale crash tests according to Performance Level 2 (PL-2) of the AASHTO *Guide Specifications for Bridge Railings* (2). The three full-scale crash tests included:

1. Impact of an 1,800-lb small car at 60 mph and an angle of 20 degrees.
2. Impact of a 5,400-lb pickup truck at 60 mph and an angle of 20 degrees.
3. Impact of an 18,000-lb single unit truck at 50 mph and an angle of 15 degrees.

All six crash tests of the BR27C combination rail satisfied the AASHTO PL-2 criteria. Damage to the combination rail and parapet was limited. One of the single-unit truck tests did show detachment of the rail from the support posts, but most of the bridge rail damage was minor, and the combination rail posts remained attached to the parapet in all of the tests. Subsequent to the design and testing of the original BR27C combination bridge rail, the Federal Highway Administration (FHWA) released a memo regarding bridge railing designs (3) that listed the BR27C design as compliant with NCHRP Report No. 350 Test Level 4 (TL-4) (4).

As part of recent updates to their bridge rail designs, IaDOT has switched to a slightly wider concrete parapet design that is 24 in. tall by 12 in. thick. As such, the revised parapet design was used for the alternative epoxy adhesive anchor designs developed as part of this research.

Epoxy Anchorages for Roadside Barriers

Limited prior research has been conducted on the use of epoxy adhesive anchors for attachment of a beam-and-post railing system to the top of concrete parapets. In 2010, Texas A&M Transportation Institute (TTI) researchers conducted a study to develop two new retrofit combination steel and concrete bridge rail designs (5). This effort included the design of a retrofit epoxy anchorage design and pendulum testing of the anchorage system on a short section of concrete parapet in order to verify the capacity of the connection. Thus, the methodology of evaluating the alternative epoxy anchorage systems through dynamic component testing has been previously utilized.

MwRSF researchers also conducted a related study for the Wisconsin Department of Transportation involving epoxy adhesive anchors for attachment of concrete barriers to bridge decks (6). The objective of this research was to determine if epoxy adhesive anchors could be utilized to attach concrete barriers to bridge decks and to develop design procedures for implementing epoxy adhesive anchorages into concrete bridge railings. A series of 16 dynamic bogie tests and one static test were conducted to investigate the behavior of epoxy adhesive anchors under dynamic load.

Comparisons were made between the results from the component tests and analytical models for epoxy adhesive anchors. Both the cone and full uniform bond model (7-8) and ACI 318-11 (9) provided reasonable predictions for the failure mode of the epoxy adhesive anchors loaded in tension, but both methods were conservative for the prediction of capacity (i.e., underestimated strength). The shear testing results and findings were limited due to observation of only one failure mode (shear failure of the steel anchor) in the component tests. However, ACI 318-11 provided reasonable yet conservative estimates for shear capacity of the epoxy adhesive anchors. Dynamic increase factors for concrete breakout, steel fracture, and bond strength were proposed to improve the accuracy of the predicted of the anchor failure modes and capacities. Thus, it was recommended that the ACI 318-11 procedures be combined with the proposed dynamic increase factors for designing epoxy adhesive anchors.

EPOXY ANCHORAGE DESIGN

Design Methodology

Design of the epoxy adhesive anchorages began with determination of a design load for the post and baseplate of the BR27C combination rail. Because the exact impact loading of the BR27C rail during the original crash testing was unknown, it was assumed that the anchorage designs would need to develop the full-moment capacity of the bridge rail post. Designing the alternative anchorages to meet this load would ensure that the designs could develop the upper bound of the potential load imparted to the anchorage original anchorage.

The BR27C railing uses a HSS 4-in. x 4-in. x 3/16-in. A500 Grade B steel tube for the vertical support post attached to a 3/4-in. thick A36 steel baseplate. A500 Grade B steel has a minimum yield strength of 42 ksi. However, steel tube sections designed as A500 Grade B are regularly fabricated from higher-strength steel, occasionally up to the A500 Grade C minimum yield strength of 46 ksi. Assuming the potential for the higher-strength Grade C material and using the plastic section modulus of the tube (3.91 in.³) yielded a moment capacity for the post of 180 kip-in. This moment capacity was used for the design calculations of the alternative epoxy adhesive anchorages.

Based on the previous research on epoxy adhesive anchorages, it was proposed to design several potential alternatives for the BR27C combination rail anchorage using the analytical procedures developed during the Wisconsin study. IaDOT could select the alternative anchorage designs they found most desirable, and dynamic component testing would be performed to verify their capacity.

Full details of the design calculations for the proposed alternative anchorages are provided in the research report (10), but some comments on the basic design procedures should be noted. First, for concepts incorporating two rows of anchors, it was assumed the tensile loads to develop moment capacity would be supplied by the front anchors while the rear anchors would develop the shear loads. Anchorage concepts that used only a single row of bolts had to account for both tensile and shear loads in all anchors. The design calculations evaluated steel fracture, concrete breakout, and adhesive bond failure in tension. Shear calculations evaluated steel fracture, concrete breakout, and concrete pryout.

The calculations also accounted for reduction in anchor capacity due to the distance to the edge of the parapet and anchor spacing based on the area of influence for the concrete and bond failures. Anchorage area of influence defines a region of the concrete where the anchorage forces are distributed in order to develop load for both concrete breakout and bond strength. If these areas exceed the edge of the parapet or overlap among adjacent anchors, then the capacity of the anchor is reduced by the ratio of the unavailable area divided by the original assumed influence area. A simple example of area of influence for two anchors that exceed the concrete edge and interfere with adjacent anchors is shown in Figure 2. Note that for the simple two-anchor example, the purple area denotes where the area of influence exceeds beyond the parapet edges. The orange area indicates where the area of influence for anchors "A" and "B" overlap. In this area, only half of the overlapping area can be utilized by each anchor, so the anchor capacity must be reduced accordingly.

A final note should be made regarding an additional modification that was made to the ACI 318-11 calculations for this project. ACI 318-11 defines h_{eff} as the effective anchor embedment depth. Initial calculations for tensile concrete breakout capacity indicated that

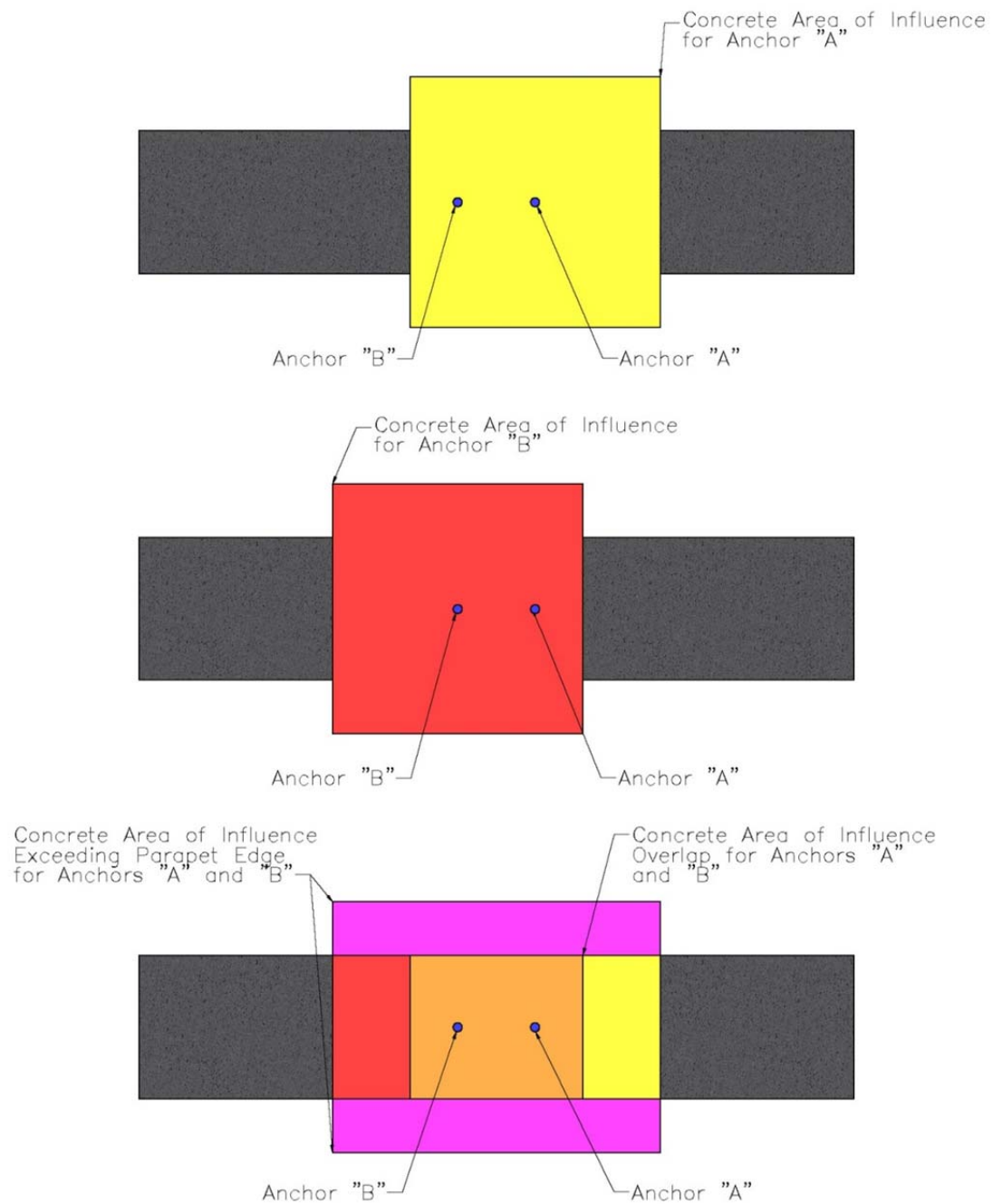


FIGURE 2 Concrete area of influence for two adjacent anchors on concrete parapet.

extremely large embedment depths would be required to provide the desired anchorage, due to the edge distance of the anchors to the side of the parapet. These calculations assume a concrete cone failure of the parapet that extends diagonally from the base of the anchor to the edges of the area of influence.

While this assumption may be true of large-area, unreinforced slabs, it was not believed to be accurate for a reinforced concrete parapet due to concrete confinement. A more reasonable form of the failure mode was believed to be a hybrid concrete cone and adhesive bond failure, as shown in Figure 3. In this type of failure mode, the concrete cone failure is prevented from extending to the base of the anchor by the longitudinal rebar. The hybrid failure assumption was extended to the ACI 318-11 calculations by assuming that the upper half of the anchor embedment contributed to the concrete breakout and the lower half of the embedment contributed to a bond failure. Thus, the calculations for the concrete breakout and bond strength were performed with one-half of the actual anchor embedment and then summed to determine the tensile anchor capacity.

All calculations for the alternative adhesive anchorages were performed assuming the use of an epoxy adhesive with a bond strength of 1,800 psi. The concrete compressive strength for the design calculations was assumed to be 4,000 psi.

Alternative Anchorage Concepts

Four primary concepts were developed and evaluated as part of the design effort, as shown in Figure 4. The four concepts varied the number, placement, and size of the anchors. All concepts were constrained to keep the anchors within the bounds of the longitudinal parapet reinforcement and have between $\frac{3}{4}$ in. and 1 in. of clearance from the reinforcement to ensure that they were not impacted during installation of the epoxy anchors. It was believed that all of the designs would develop the moment capacity of the post.

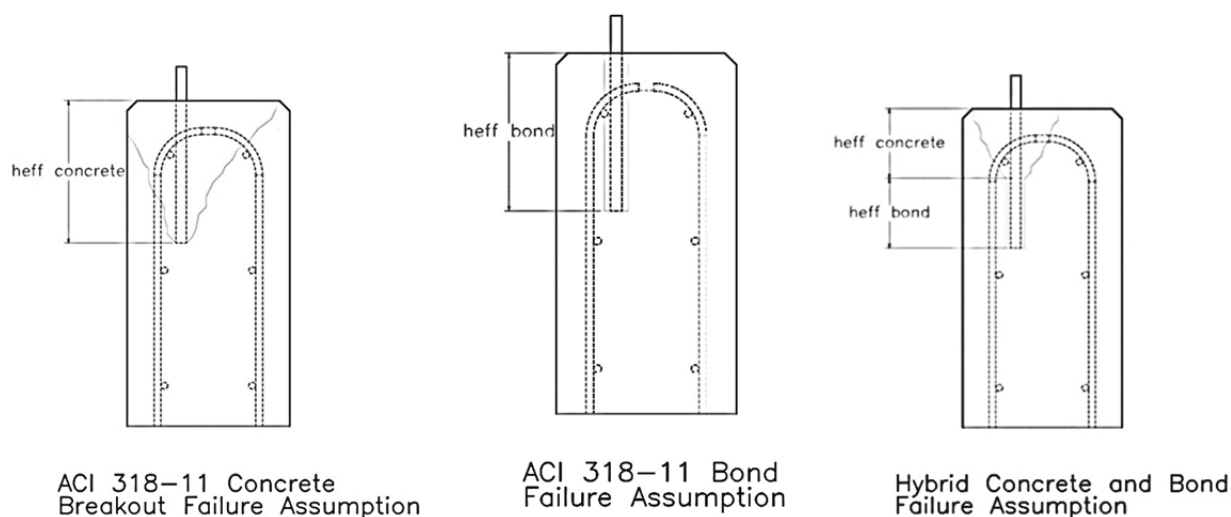


FIGURE 3 Comparison of ACI 318-11 concrete breakout and proposed hybrid failure assumptions.

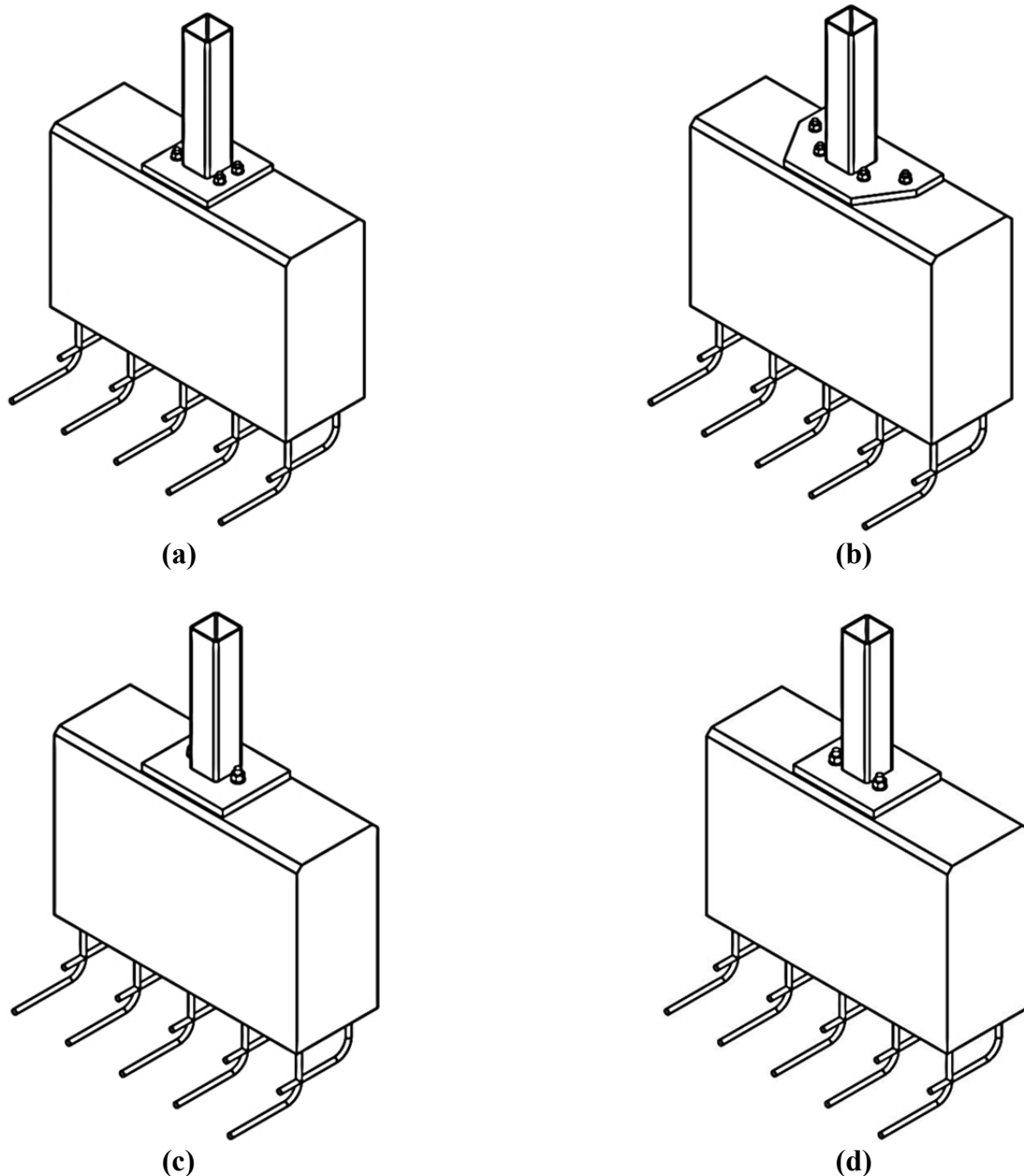


FIGURE 4 Alternative epoxy adhesive anchorage concepts: (a) square, four-anchor concept; (b) spread, four-bolt concept; (c) centered, two-anchor concept; and (d) offset, two-anchor concept.

Square, Four-Anchor Concept

The square, four-anchor concept used a rectangular anchor pattern of four rods on a square plate, as shown in Figure 4a. The four rods allowed for a design where the front rods develop the tensile loads and the back anchors accounted for the shear loads. This concept had a similar layout to the original, cast-in-place design. The anchor rods were 5/8 in. diameter and embedded 10 in. into the parapet. The main drawback of this concept was that the anchors were only 2.75 in. apart across the width of the parapet, which could make it difficult to install.

Spread, Four-Anchor Concept

The spread, four-anchor concept used the same anchor size and embedment depth, but it spread out the backside anchors to improve the anchor spacing for a four-anchor pattern, as shown in Figure 4b. Design calculations indicated that the increased spacing of the anchors satisfied the design loads and led to shear strength improvement over the four-bolt square anchorage concept.

Centered, Two-Anchor Concept

The centered, two-anchor concept used a linear anchor pattern of two anchor rods centered on a square baseplate, as shown in Figure 4c. This concept reduced the number of anchors but required increased anchor diameter and embedment depth due to combined shear and tension loading of the anchors. The concept used $\frac{3}{4}$ -in. diameter rods with a 12 in. embedment depth. Design calculations for this concept showed that the anchorage can develop both the shear and the tensile loads when determined individually. However, the ACI code recommends a reduction for combined loading, where the sum of the applied design load divided by the total capacity in both shear and tension must be less than 1.2. For this concept, that sum was calculated to be 1.44. However, neither the general anchor calculations nor the combined loading calculation in ACI 318-11 account for the reinforcing steel and its contributions to the anchorage capacity. As such, this design could potentially work under combined loads when including these other factors.

Offset, Two-Anchor Concept

This design was identical to the centered, two-anchor concept, except that the anchors were offset towards the front of the parapet to increase the shear capacity sufficiently to meet the combined loading requirement in the ACI code, as shown in Figure 4d. Thus, it was a more efficient design. If significant reverse bending loads are applied during an impact, this concept would have reduced capacity in that regard. However, reverse bending loads on the bridge rails and other barriers are typically lower than the primary impact loads, and concern for reverse bending overloading the anchorage was limited. In order to alleviate that concern, a smaller anchor could be placed on the backside of the post.

Selection of Preferred Alternative Anchorage Concepts for Evaluation

IaDOT representatives reviewed the four proposed alternative anchorage concepts and selected the spread, four-anchor and the offset, two-anchor concepts for evaluation through dynamic component testing. In addition to these two concepts, IaDOT also requested that the researchers conduct dynamic testing on a third option that had been previously installed on the US-20 bridge near Hardin, Iowa. IaDOT was interested in evaluating whether this specific configuration meets/exceeds the capacity of the FHWA-approved cast-in-place BR27C combination bridge rail, and they wished to verify its performance as constructed.

DYNAMIC COMPONENT TESTING

A series of four dynamic bogie tests were conducted; one on the original BR27C combination bridge rail post and cast-in-place anchorage to establish a baseline and three on alternative epoxy adhesive anchorage designs. The force versus deflection, energy dissipated versus deflection, and failure modes were documented for each test and compared against the baseline to verify that the proposed anchorages provided equal or greater capacity.

All four dynamic bogie tests were conducted on HSS 4-in. x 4-in. x 3/16-in. steel tubes with baseplates mounted on top of a reinforced concrete parapet. The concrete parapet layout and reinforcement was based on the parapet design used in the original full-scale crash testing of the BR27C combination bridge rail and the revised parapet design provided by IaDOT. As such, the parapet was 10 in. wide on one end and was then widened to 12 in. for the remainder of the parapet. The concrete used for the parapet was selected to be a 3,600-psi mix meeting IaDOT Class C-4 concrete specification consistent with the concrete strength of the parapet used in the original BR27C combination bridge rail crash testing. This concrete strength was lower than the 4,000 psi mix currently used by IaDOT and used in the design calculations, but it provided the best comparison with the original, as-tested BR27C system.

The posts, anchors, and baseplates used in the dynamic component tests were developed based on details of the BR27C combination bridge rail, the alternative anchorages developed previously and details provided by IaDOT for the US-20 bridge installation. Baseplates for the spread, four-anchor and the offset, two-anchor designs were 5/8-in. and 1-in. thick A36 steel plate, respectively, and were designed based on the anchorage system and moment capacity of the post. The original BR27C and US-20 bridge baseplates were 3/4-in. and 13/16-in. thick A36 steel plate, respectively. The original BR27C system was anchored with four, 5/8-in. diameter threaded rods cast into the concrete parapet with a washer plate to aid in development of the rods. The spread, four-anchor and the offset, two-anchor designs were anchored with four, 5/8-in. diameter threaded rods embedded 10 in. and two, 5/8-in. diameter threaded rods embedded 12 in., respectively. The US-20 design was anchored with four, 5/8-in. diameter threaded rods embedded 10 in. All anchor rods were ASTM A193 Grade B7 threaded rod. The two, new alternative anchor concepts were installed using Hilti RE-500 SD epoxy adhesive. The anchorage for the US-20 bridge was installed with Fastenal Pro-Poxy 300, per the IaDOT details.

The target impact conditions were a speed of 15 mph and an angle of 90 degrees, creating a lateral impact relative to the parapet. A rigid-frame bogie with a mass of 1,808 lb. was used to impact the posts. Target impact height for the testing was 17 in. above the top of the parapet on the post in order to produce a bending moment in the post and combined loading on the anchorage system similar to that provided during vehicle crash events.

Test No. IBP-1, Original BR27C Anchorage

During test no. IBP-1, the bogie impacted the post at a speed of 16.1 mph causing the post to deflect backward, as shown in Figure 5. During the test, shear cracks formed starting at the front anchors that propagated to the backside of the parapet. This concrete failure caused significant damage to the parapet but did not cause the yielding of the post. The post continued to rotate backwards, causing additional fracture and disengagement of the concrete parapet behind the post. The two front anchor rods on the post fractured in tension approximately 66 msec after impact, causing the loading of the bogie vehicle to drop to zero at a deflection of 13 in.

Damage to the system consisted of major damage to the concrete parapet and the cast-in-place anchorage, as shown in Figure 5. The concrete parapet displayed shear cracking along the top of the parapet and disengagement of a large section of concrete on the backside of the parapet. Lesser amounts of concrete were disengaged on the top and front sides of the parapet. The post and baseplate assembly were largely undamaged. The post and baseplate displayed minimal local deformations due to the impact. The threaded rod anchors on the front of the parapet fractured during the test, and the rear anchors were bent backward due to the rotation of the post.

A peak force of 22.9 kips was reached at a deflection of 1.5 in. prior to the concrete shear failure of the parapet. The post continued to develop load as the post deflected until the fracture of the front two anchor rods. The post assembly absorbed 146 kip-in. of energy.

Test No. IBP-2, Spread Four-Anchor Concept

During test no. IBP-2, the bogie impacted the post at a speed of 16.2 mph, causing the post to deflect backward, as shown in Figure 6. During the test, shear cracks formed starting at the rear anchors that propagated to the backside of the parapet and eventually disengaged a large section of the rear face of the parapet. At the same time, loading of the front two anchors caused cracking and concrete disengagement on the top-front of the parapet. The impact loads caused concrete shear failure and significant damage to the parapet but did not cause yielding of the post. As the post continued to rotate, all four anchor rods were pried from the parapet. The force on the bogie vehicle dropped to zero at a deflection of 11.9 in. as the bogie overrode the top of the post at approximately 156 msec after impact.

Damage to the system consisted primarily of damage to the concrete parapet, as shown in Figure 6. The concrete parapet displayed shear cracking along the top and disengagement of a large section of concrete on the backside. Lesser amounts of concrete were disengaged on the top and front sides of the parapet. The post and baseplate assembly were largely undamaged and displayed only minimal local deformations. The four threaded rod anchors were all disengaged from the parapet due to the fracture of the surrounding concrete.

A peak force of 24.9 kips was reached at a deflection of 1.4 in., prior to the disengagement of sections of the concrete parapet. The post continued to develop load as the post deflected until the disengagement of the anchor rods from the parapet. The post assembly absorbed 69.6 kip-in. of energy.

Test No. IBP-3, Offset Two-Anchor Concept

During test no. IBP-3, the bogie impacted the post at a speed of 16.3 mph, causing the post to deflect backward, as shown in Figure 7. During the test, shear cracks formed starting at the anchors and propagated to the backside of the parapet. As the bogie continued to load the post, the weld between the post and the baseplate fractured on the front-side of the post approximately 10 msec after impact. As the post continued to deflect, the weld between the post and the baseplate fractured along both sides of the post, allowing the post to rotate backward. The force on the bogie vehicle dropped to zero at a deflection of 2.7 in.. The post completely disengaged from the baseplate at approximately 112 msec.

Damage to the system consisted of damage to the concrete parapet and the weld between the post and the baseplate, as shown in Figure 7. The concrete parapet displayed shear cracking



FIGURE 5 Test No. IBP-1, Original BR27C anchorage: (a) sequential events; (b) pre-test; and (c) system damage.

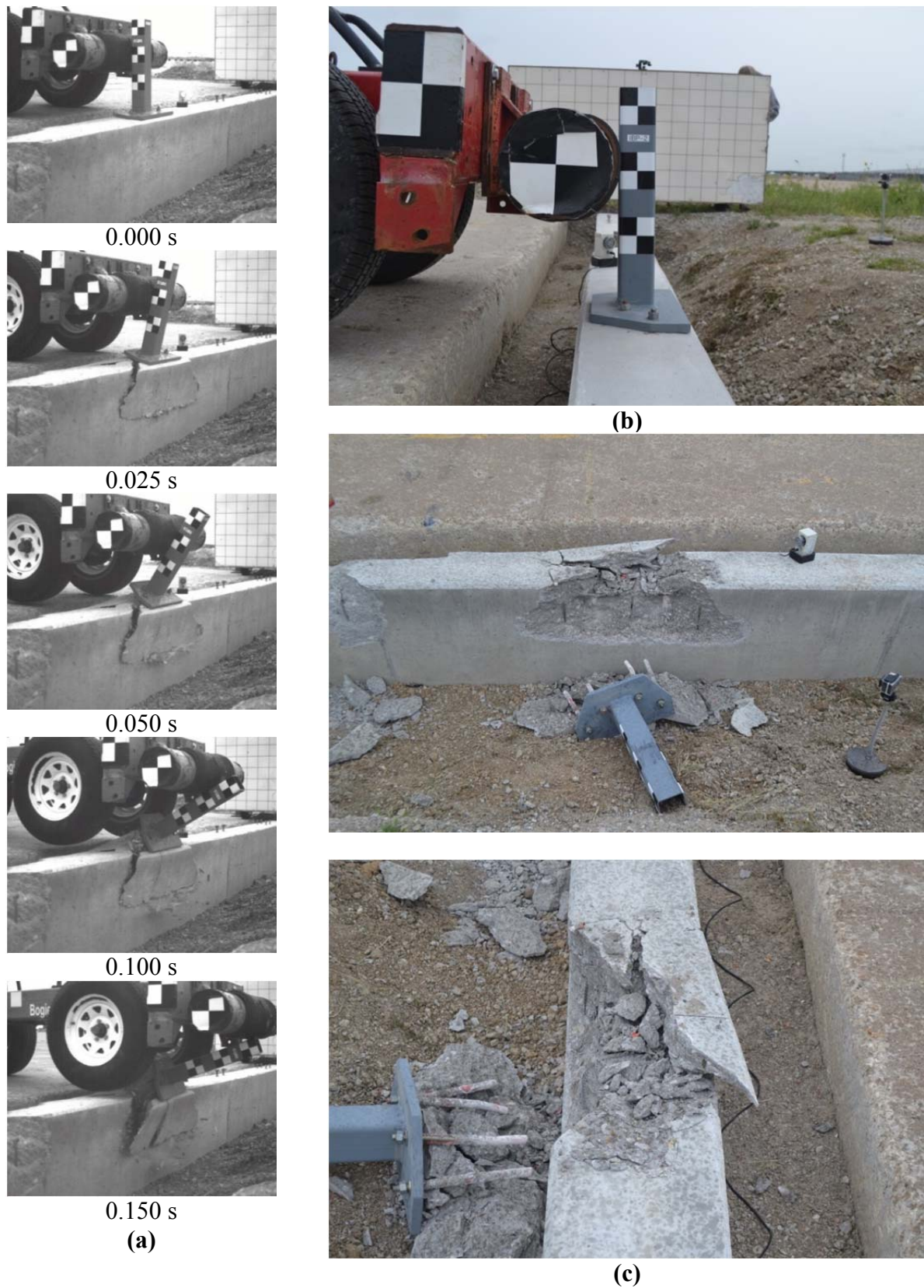


FIGURE 6 Test No. IBP-2, spread four-anchor concept: (a) sequential events; (b) pre-test; and (c) system damage.

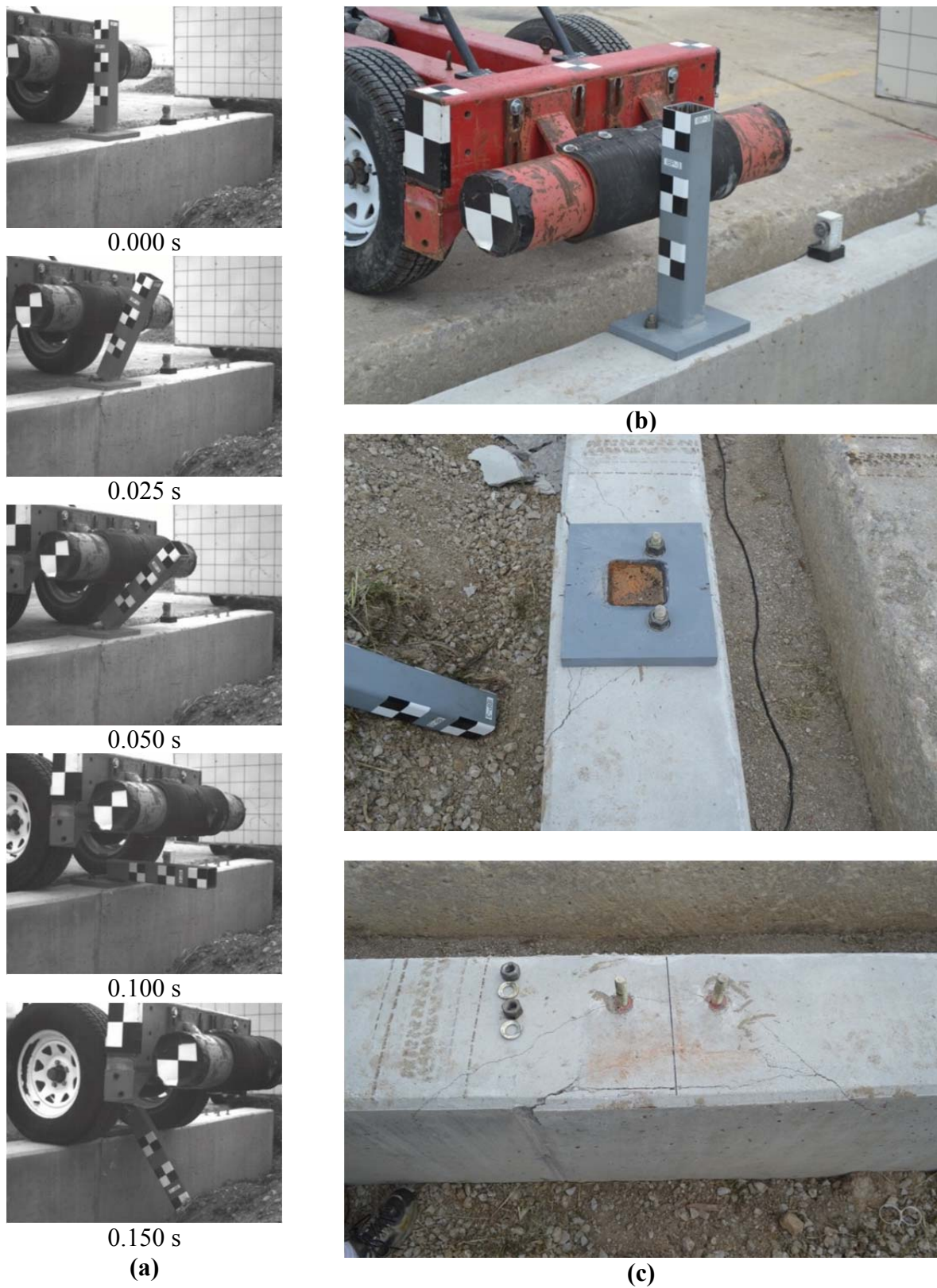


FIGURE 7 Test No. IBP-3, offset, two-anchor concept: (a) sequential events; (b) pre-test; and (c) system damage.

along the top of the parapet as well as some cracking of the top of the rear face of the parapet. No significant sections of concrete were disengaged from the parapet in this test. The post and baseplate assembly were not deformed, but the weld between them fractured and failed. The two threaded rod anchors remained embedded in the concrete.

A peak force of 28.3 kips was reached at a deflection of 1.4 in. The post continued to develop load as the post deflected until the fracture of the weld between the post and the baseplate. The post assembly absorbed 48.3 kip-in. of energy.

Test No. IBP-4, US-20 Bridge Anchorage

During test no. IBP-4, the bogie impacted the post at a speed of 15.4 mph, causing the post to deflect backward, as shown in Figure 8. During the test, the deflection of the post generated uplift of the front of the baseplate, which caused the front two threaded anchors to fail in tension approximately 12 msec after impact. The post continued to rotate backwards, causing shear cracks to form at the two back anchors and propagate towards the backside of the parapet. Concrete shear failure caused disengagement of a section of the back of the concrete parapet. The loading of the bogie vehicle dropped to zero at a deflection of 3.4 in. The bogie overrode the top of the post at approximately 166 msec.

Damage to the system consisted of damage to the concrete parapet and the anchor rods, as shown in Figure 8. The concrete parapet displayed cracking on the top and disengagement of a section of concrete on the backside. The post and baseplate assembly were largely undamaged and displayed minimal local deformations due to the impact. The threaded rod anchors on the front of the parapet fractured during the test, and the rear anchors were bent backward due to the rotation of the post.

A peak force of 23.2 kips was reached at a deflection of 1.4 in., prior to the fracture of the two front anchor rods. The post assembly absorbed 60.3 kip-in. of energy.

Discussion of Dynamic Component Tests

The dynamic component test results were reviewed to determine the feasibility of the alternative anchorage designs. The original, cast-in-place anchorage for the BR27C generated the lowest peak load of the four anchorages. The failure modes observed for this design were a combination of tensile failure of the front anchor rods and concrete shear breakout of the rear of the parapet. This level of damage was much higher than the damage observed in full-scale crash testing, which indicated that the damage and force levels developed in the component testing were significantly higher than the loading of the post and anchorage during full-scale testing. Thus, alternative anchorages that exceeded the peak force of the original cast-in-place anchorage should be considered acceptable.

The spread, four-anchor concept developed higher peak loads than the original cast-in-place anchorage. Higher peak loads were anticipated for the spread, four-anchor concept based on the increased anchor spacing, but testing found those gains to be minimal. Review of the failure of the anchorage showed that orienting the front and rear anchors for this design diagonal to one another may have allowed shear stresses and cracking to develop along the same plane for both the front and rear anchor simultaneously. This may have contributed to the lower-than-expected improvement in force level. However, the concept did possess improved capacity to the original cast-in-place anchorage and was considered an acceptable alternative.



FIGURE 8 Test No. IBP-4, US-20 Bridge Anchorage: (a) sequential events; (b) pre-test; and (c) system damage.

The offset, two-anchor concept developed the highest peak load of all of the tested designs. This design also exhibited less damage to the concrete parapet, as the increased offset from the rear face of the parapet increased the shear capacity of the anchorage over the other alternatives. The failure mode was rupture through the weld between the baseplate and the post. The weld used in the design was the same weld specification used on the BR27C post-base plate connect. This may suggest that a multiple pass weld is necessary for development of the full moment capacity of the post. Thus, it is the only design tested that did not result in failure of the anchorage itself. The offset, two-anchor concept was also considered to be an acceptable alternative anchorage.

The US-20 bridge anchorage displayed a peak force and failure modes that were similar to the original cast-in-place anchorage design. This was expected, as the two designs were similar in terms of the layout and anchor size. The US-20 bridge anchorage was considered to be an acceptable alternative anchorage.

All three of the alternative anchorage designs were considered to be acceptable alternatives to the original cast-in-place anchorage design. The peak force levels for the alternative anchorages indicated greater capacities than the original anchorage, and the damage levels observed in the dynamic component testing far exceeded the levels observed in full-scale crash tests. Of the three alternative designs, the two-bolt offset design was deemed the best option due to its potential to reduce parapet damage and improved ease of installation due to requiring only two anchors.

It should be noted that these results would change if the alternative epoxy anchorages were evaluated on the narrower, 10-in. wide parapet used with the original cast-in-place anchorage. It should also be noted that the four-bolt spread and two-bolt offset anchorages were designed to develop the full plastic moment capacity of the support post. However, the four-bolt spread anchorage was not capable of developing the capacity of the post due to concrete breakout in shear. This suggested that design calculations for concrete shear breakout may need further development when considering anchorage for dynamic impact on narrow parapets. The two-bolt offset design may have had the potential to develop the moment capacity, but the post-to-baseplate weld failed prior to reaching that load.

SUMMARY AND CONCLUSION

The objective of this research was to develop and evaluate alternative epoxy adhesive anchorage systems for the BR27C combination bridge rail system. The research effort began with development of several proposed alternative anchorage concepts. The concepts were designed using a modified version of the ACI 318-11 procedures for adhesive anchor design with modifications for dynamic increase factors and the expected failure modes. All of the concepts were designed to develop the full plastic moment capacity of the post. Four design concepts were developed, and IaDOT representatives selected a spread, four-anchor concept and an offset, two-anchor concept as the preferred designs for evaluation. IaDOT also requested that the researchers evaluate a third anchorage option that had been previously installed on the US-20 bridge near Hardin, IA.

In order to evaluate the performance of the proposed alternative anchorages, dynamic component testing was conducted on the original cast-in-place anchorage as well as the three alternative anchorages using a simulated bridge rail parapet. The test of the original cast-in-place

anchorage test no. IBP-1 was used as a baseline for comparison with the alternative designs. All three of the tested alternative anchorages provided greater load capacity than the original cast-in-place design and were deemed acceptable surrogates. Of the three alternative designs, a two-bolt offset design was deemed the best option due to its development of the highest peak loads, the potential for reduced parapet damage, and improved ease of installation. It was also noted that the alternative designs were developed and tested on a 12-in. (305-mm) wide version of the IaDOT concrete parapet. Thus, the alternative anchorages would not be recommended for use on the narrower parapet used with the original cast-in-place anchorage.

ACKNOWLEDGMENTS

The authors wish to acknowledge the Iowa Department of Transportation for sponsoring and providing guidance throughout the project.

REFERENCES

1. Buth, E.B., Hirsh, T.J., and Menges, W.L., *Testing of New Bridge Rail and Transition Designs, Volume VIII: Appendix G, BRs7C Bridge Railing*, FHWA-RD-93-065, Texas Transportation Institute, Texas A&M University, June 1997.
2. *Guide Specifications for Bridge Railings*, American Association of State Highway Transportation Officials, Washington, D.C., 1989.
3. Hatton, J.H., *Bridge Railing Design And Testing*, A Discussion with the AASHTO Subcommittee on Bridges and Structures Technical Committee (T-7) for Guardrail and Bridge Rail, Federal Highway Administration (FHWA), U.S. Department of Transportation, FHWA HNG-10, May 7, 1996.
4. Ross, H.E., Sicking, D.L., Zimmer, R.A., and Michie, J.D., *Recommended Procedures for the Safety Performance Evaluation of Highway Features*, NCHRP Report No. 350, Transportation Research Board, Washington, D.C., 1993.
5. Williams, W. and Boyd, C. "Design and Construction of Two New Retrofit Combination Steel and Concrete Bridge Rail Designs," *Transportation Research Record: Journal of the Transportation Research Board* 2251 (2011): 34-43.
6. Dickey, B.J., Faller, R.K., Rosenbaugh, S.K., Bielenberg, R.W., Lechtenberg, K.A., and Sicking, D.L., *Development of a Design Procedure for Concrete Traffic Barrier Attachments to Bridge Decks Utilizing Epoxy Concrete Anchors*, Report No. TRP 03-264-12, Midwest Roadside Safety Facility, UNL, November 26, 2012.
7. Collins, D.M., Klingner, R.E., Polyzois, D., *Load-Deflection Behavior of Cast-in-Place and Retrofit Concrete Anchors Subjected to Static, Fatigue, and Impact Tensile Loads*, Report No. FHWA/TX-89+1126-1, Center for Transportation Research, University of Texas, February 1989.
8. Cook, R.A., *Behavior of Chemically Bonded Anchors*, *Journal of Structural Engineering*, American Society of Civil Engineers, September, 1993.
9. ACI Committee 318, *Building Code Requirements for Structural Concrete (ACI 318-11) and Commentary*, Farmington Hills, MI, American Concrete Institute, August 2011.

10. Bielenberg, R.W., Reid, J.D., Rosenbaugh, S.K., Haase, A.J., and Faller, R.K., *Attachment of a Combination Bridge Rail to Concrete Parapet Utilizing Epoxy Adhesive Anchors*, Report to the Iowa Department of Transportation, TRP 03-325-15, Midwest Roadside Safety Facility, UNL, November 3, 2015.

Design and Evaluation of a Fascia-Mounted Bridge Rail for Steel Bridges on Local Roadways

CHUCK PLAXICO
Roadsafe LLC

Ohio generally uses steel bridge designs on its local road system. The bridge superstructure in these cases includes steel stringer beams which support a variety of deck types, including: concrete, timber, asphalt filled steel stay-in-place forms, and fiber reinforced composite. The bridge rail design that is currently used on these types of bridge structures is a side-mounted steel post-and-beam railing that mounts onto the steel fascia beam. The advantage of having a bridge rail design that mounts directly to steel fascia beams is that it gives local bridge owners the option of building steel bridges with lower-cost bridge decks, while avoiding having to build excess deck width to accommodate a top-mounted bridge railing anchorage. The design currently used in these cases has not been crash tested and is therefore not eligible for use on Federal Aid projects. Further, there are no alternative side-mount systems (deck mount designs) currently available for mounting to the various bridge deck types used on the local road system.

The objective of this project was to design a steel fascia beam mount for use with the side-mounted Illinois two-tube bridge rail. The Illinois design is classified as a Report 350 Test Level 4 barrier and is eligible for use on federal-aid projects. The modifications to the bridge rail system were limited to the post-mount design. That is, no changes were made to the bridge rail design regarding components located above the bridge deck surface. Additional consideration for the design included a release mechanism for the post-mount to ensure that excessive forces are not transferred to the bridge superstructure during high severity impacts (e.g., heavy truck impacts). For example, when post deflections reach critical limits the post will readily detach from the mount and avoid damage to the bridge superstructure.

The study involved a combination of finite element analysis (FEA) and pendulum impact testing. FEA was used in the development of the post-mount to ensure that the stiffness of the new design was equivalent to the original design. Pendulum testing was then used to confirm these results. Detailed finite element models of the bridge rail and the bridge superstructure were then developed and FEA was again used to simulate NCHRP Report 350 Test 4-12, as well as MASH Test Level 3 impact conditions on the bridge rail.

The results of the evaluation indicated that the design modifications met all structural capacity, occupant risk measures and vehicle stability criteria set forth in NCHRP Report 350. The modified post-mount design was shown through physical testing to provide equal or greater stiffness as the original post-mount and should therefore result in equivalent or better crash performance for the system when installed on steel bridges with fascia beams of size W14x30 and larger. The design modifications are further considered to be non-significant, regarding the changes to the original Report 350 TL4 design, since the effects of the changes were shown to be inconsequential to the performance of the system with respect to the baseline design. This system is eligible for use on federal-aid reimbursement projects and is currently being considered for implementation as an NCHRP Report 350 TL3 system.

MASH Equivalency of NCHRP 350-Approved Bridge Railings

WILLIAM WILLIAMS

Texas A&M Transportation Institute

An update to NCHRP Report 350 was developed under NCHRP Project 22-14(02), "Improvement of Procedures for the Safety-Performance Evaluation of Roadside Features." This document, Manual for Assessing Safety Hardware (MASH) published by AASHTO, contains revised criteria for safety-performance evaluation of virtually all roadside safety features. For example, MASH recommends testing with heavier light truck vehicles to better represent the current fleet of vehicles in the pickup/van/sport-utility vehicle class. Further, MASH increases the impact angle for most small car crash tests to the same angle as the light truck test conditions. These changes place greater safety-performance demands on many of the current roadside safety features.

AASHTO will soon be publishing an updated edition of the MASH document. Along with this, FHWA and AASHTO have adopted a revised joint implementation agreement that establishes dates for implementing MASH compliant safety hardware for new installations and full replacements on the NHS. Although some barrier testing was performed during the development of the updated criteria, many barrier systems and other roadside safety features have yet to be evaluated under MASH criteria. Therefore, evaluation of the remaining widely used roadside safety features using the safety-performance evaluation guidelines included in MASH is needed.

There are many types of non-proprietary bridge rails in use throughout the states and research is needed to determine which rails need to be retested to MASH criteria and which, if any, can be "grandfathered" based on evaluation under previous criteria. In 1997, FHWA provided a list of 74 bridge rails and their equivalent NCHRP 350 test levels based on testing performed under the earlier NCHRP Report 230 test levels and the performance levels contained in the AASHTO Specification for Bridge Rails. In 2000, FHWA provided guidance that allows for demonstrating that variations of a bridge rail design would not have to be crash tested if the basic geometry of a bridge rail has not been changed and the structural design of the rail is comparable to the rail that has been tested. With the pending approval and publication of an update to MASH and the recent adoption of a new joint AASHTO/FHWA implementation agreement, there is a need to review the current bridge rail systems and determine the level of evaluation required to demonstrate MASH compliance.

The objectives of this project are to prioritize metal, concrete, and combined metal and concrete bridge railings and determine the MASH equivalent test levels for these railings. In addition some individual types of bridge railings will be considered for submittal to FHWA for determination of Federal-aid reimbursement eligibility. Some railings will likely need to be retested in accordance with MASH criteria for FHWA eligibility. All barrier test levels will be considered for this project. However, TL-3, TL-4 and TL-5 bridge railings will be priority. This presentation will summarize the results from this project. This project will be for presentation only.

Ponderosa Pine Round Posts as Alternative to Rectangular SYP Posts in Retrofit G4(2W) Guardrail Systems

KARLA A. LECHTENBERG

RONALD K. FALLER

JOHN D. REID

SCOTT K. ROSENBAUGH

*Midwest Roadside Safety Facility
University of Nebraska–Lincoln*

DAVID E. KRETSCHMANN

*Forest Products Laboratory
U.S. Department of Agriculture—Forest Service*

Over the last several decades, the southwestern United States experienced numerous forest fires, prompting a need for more preventive techniques. In the 1960s, the U.S. Department of Agriculture - Forest Service began managing fuels by using controlled-burn techniques. However, due to both the lack of economic benefits and the high risk involved with controlled-burn methods, more cost-efficient methods were sought to remove the small-diameter forest thinnings. With such vast quantities of timber thinnings, local producers within the timber industry deemed it necessary to further explore the use of undamaged Ponderosa Pine (PP) material as posts in guardrail systems. Two W-beam guardrail systems were identified that may be compatible with PP posts: the U.S. standard G4(2W) guardrail system and the Arizona DOT (AzDOT) G4(2W) guardrail system. Therefore, research was undertaken to determine the appropriate dimensions (diameter and length) and embedment depth of round PP posts for use within these two strong-post, W-beam guardrail systems.

Dynamic component tests on rectangular SYP posts and round PP posts with diameters between 8 $\frac{3}{8}$ in. and 8 $\frac{3}{4}$ in. were performed to determine the appropriate diameter, length, and embedment depth for PP posts to be used as a surrogate for 6-in. x 8-in. rectangular Southern Yellow Pine (SYP) posts found in existing, strong-post, G4(2W) W-beam guardrail systems. In addition, one full-scale demonstration crash test was successfully performed according the Test Level 3 (TL-3) impact safety standards published in the National Cooperative Highway Research Program (NCHRP) Report No. 350 on a 175-ft long, G4(2W) guardrail system supported by 8 $\frac{1}{2}$ -in. diameter (ground line) by 64-in. long PP posts with a 35-in. embedment depth. A $\frac{3}{4}$ -ton Chevrolet pickup truck impacted at a speed of 60.7 mph and an angle of 24.8 degrees. The G4(2W) guardrail system with PP posts adequately contained and redirected the pickup truck and met the NCHRP 350 TL-3 safety performance criteria.

Based on dynamic component testing, a PP post with an 8 $\frac{1}{2}$ -in. diameter, a 35-in. embedment depth, and a 64-in. length was approved for use as a surrogate in existing Arizona G4(2W) guardrail systems. Similarly based on the dynamic component testing, a PP post with an 8 $\frac{3}{8}$ -in. diameter, a 36-in. embedment depth, and a 65-in. length was also approved for use as a surrogate in existing U.S. standard G4(2W) guardrail systems. The demonstration test offered confidence to State Departments of Transportation interested in using round PP posts to repair damaged strong-post, W-beam guardrail systems configured with 6-in. x 8-in. rectangular SYP posts.

INTRODUCTION

Over the last several decades, the southwestern United States (U.S.) experienced numerous forest fires, prompting a need for more preventive techniques. In 2000, President Bill Clinton initiated the creation of the National Fire Plan, which focused on four main goals: (1) improve prevention and suppression; (2) reduce hazardous fuels; (3) restore fire-adapted ecosystems; and (4) promote community assistance (1).

Historically, fuel management has been a commonly-used technique for fire protection. In the 1960s, the U.S. Department of Agriculture (USDA) - Forest Service began managing fuels by using controlled-burn techniques, which are generally effective (2). In order to remove the small-diameter forest thinnings (SDT) from a certain area, fires were started with containment. The thinnings, which could help fuel a fire in the future, consisted mostly of pine and fir species. However, due to both the lack of economic benefits and the high risk involved with controlled-burn methods, more cost-efficient methods were sought to remove the small-diameter forest thinnings.

Small-diameter trees can be used in a variety of ways, including lumber, structural roundwood, wood composites, wood fiber products, compost, mulch, and fuels (3). By removing the potential fuel and selling it as various products, the cost of SDT removal would hopefully be recovered. Therefore, more uses for small-diameter trees were recommended for development in order to increase the product potential (4).

In response to this need, researchers at the Midwest Roadside Safety Facility (MwRSF), in cooperation with the Forest Products Laboratory (FPL) and the Forest Service - USDA, (FS-USDA) developed an adaptation of the Midwest Guardrail System (MGS) that utilized SDT materials as timber posts (5, 6). The study determined appropriate sizes of Southern Yellow Pine (SYP), Douglas Fir (DF), and Ponderosa Pine (PP) round posts for use within the 31-in. (787-mm) tall corrugated W-beam system.

In recent years, several unexpected forest fires also harmed large forests of PP timber in the State of Arizona. With such vast quantities of timber thinnings, local producers within the timber industry deemed it necessary to further explore the use of undamaged PP material as posts in guardrail systems. Two additional W-beam guardrail systems were identified as systems that may be compatible with PP posts: the U.S. standard G4(2W) guardrail system and the Arizona DOT G4(2W) guardrail system. Although these W-beam guardrail systems utilize similar components to the wood post version of the MGS, differences in rail height and embedment depth exist between the three systems, as shown in Table 1. As a result, there may be different post performance requirements for each system. Therefore, further research was undertaken with a collaborative effort between the Arizona Timber Industry, MwRSF, and FPL-FS-USDA, to determine the appropriate dimensions (diameter and length) and embedment depth of round PP posts for use within these two strong-post, W-beam guardrail systems.

It is common knowledge that longitudinal barriers, or guardrail systems, fulfill several functions along highways and roadways, including to: (1) safely contain and redirect errant vehicles and prevent impacts with hazardous fixed objects or geometric features and (2) dissipate an errant vehicle's kinetic energy without imparting excessive risk to the occupants. The safety performance of strong-post, W-beam guardrail systems is highly dependent on the post-soil behavior of vertical posts. For wood posts, the post-soil behavior is controlled by post size and strength, embedment depth, load height, and soil compaction. Wood posts should possess

TABLE 1 Wood Post Options for W-beam Guardrail Systems

Guardrail System	Top Rail Height in. (mm)	Rectangular SYP Post Option			Round PP Post Option		
		Cross Section in. (mm)	Length in. (mm)	Embedment Depth in. (mm)	Diameter in. (mm)	Length in. (mm)	Embedment Depth in. (mm)
MGS	31 (787)	6 x 8 (152 x 203)	72 (1,829)	40 (1,016)	8 (203)	69 (1,753)	37 (940)
Arizona System G4(2W)	28 (711)	6 x 8 (152 x 203)	64 (1,626)	35 (889)	8½ (216)	64 (1,626)	35 (889)
U.S. System G4(2W)	27¾ (705)	6 x 8 (152 x 203)	72 (1,829)	43¼ (1,099)	8⅝ (219)	65 (1,651)	36 (914)

— Determined from Phase I project (7).

— Determined from Phase II project (8).

sufficient structural capacity, provide adequate lateral resistance, and exhibit reasonable energy dissipation characteristics during rotation in soil.

RESEARCH OBJECTIVE

The primary research objectives for the three-phase project was to determine the appropriate size and embedment depth for round PP posts in order to serve as a surrogate for standard 6-in. x 8-in. (152-mm x 203-mm) SYP posts used in both Arizona and U.S. crashworthy W-beam guardrail systems. The dynamic component testing program was conducted to determine an alternative round wood post for use in existing guardrail systems that have met or been grandfathered under the impact safety standards published in the National Cooperative Highway Research Program (NCHRP) Report No. 350 (9). In addition, the study would examine the post-soil behavior for PP round posts and SYP rectangular posts subjected to impact loading. Following a successful dynamic component testing program, MwRSF researchers would request eligibility from Federal Highway Administration (FHWA) regarding the surrogate use of PP post sizes within existing Arizona and U.S. standard G4(2W) W-beam guardrail systems based on dynamic bogie testing results. In addition, a demonstration crash test according to the Test Level 3 (TL-3) safety performance criteria set forth in the NCHRP Report No. 350 would be conducted on the retrofit G4(2W) W-beam guardrail system to further confirm the crashworthiness of the system. This study was performed by MwRSF in cooperation with the FPL-FS-USDA, the Arizona Log & Timberworks, and the Arizona State Forestry Division.

DYNAMIC COMPONENT TESTING

Phase I of the PP equivalency study incorporated 17 dynamic component tests on various wood posts - six were conducted on rectangular SYP posts and 11 tests were on round PP posts with diameters between 8⅝ in. and 8¾ in. (213 mm and 222 mm). Based on the results of these

component tests, an 8½-in. (216-mm) diameter PP post with a 35-in. (889-mm) embedment depth was found to provide strength and soil rotation resistance equivalent to the rectangular SYP post embedded 35 in. (889 mm) (7). Subsequently, this equivalent round PP post was recommended as a surrogate post for use in the Arizona G4(2W) W-beam guardrail system, as noted within Table 1.

Phase II of the PP equivalency study incorporated nine dynamic component tests on various wood posts – four were conducted on rectangular SYP posts and five tests were on round PP posts with diameters approximately between 8½ in. and 8-11/16 in. (216 mm and 221 mm). Based on the results of these component tests, an 8⅝-in. (219-mm) diameter PP post with a 36-in. (914-mm) embedment depth was found to provide strength and soil rotation resistance equivalent to the rectangular SYP post embedded 43¼ in. (1,099 mm) (8). Subsequently, this equivalent round PP post was recommended for use as a surrogate post for use in the U.S. standard G4(2W) W-beam guardrail system, as noted within Table 1. Within the Phase II study, enhanced grading criteria and materials specifications were compiled for the PP posts recommended for use in both Arizona and U.S. standard G4(2W) W-beam guardrail systems and are shown in Figure 1.

TEST REQUIREMENTS AND EVALUATION CRITERIA

Longitudinal barriers, such as W-beam guardrail systems, must satisfy impact safety standards in order to be declared eligible for federal reimbursement by the Federal Highway Administration (FHWA) for use on National Highway System (NHS). For retrofits of existing systems, these safety standards may consist of the guidelines and procedures published in NCHRP Report No. 350. According to TL-3 of NCHRP Report No. 350, longitudinal barrier systems must be subjected to two full-scale vehicle crash tests: (1) an 1,808-lb (820-kg) passenger car impacting at a speed of 62.1 mph (100.0 km/h) and at an angle of 25 degrees and (2) a 4,409-lb (2,000-kg) pickup truck impacting at a speed of 62.1 mph (100.0 km/h) and at an angle of 25 degrees. However, based on the success of prior small car testing on strong-post, W-beam guardrail systems, the 1,808-lb (820-kg) small car crash test was deemed unnecessary for this project (10-18). Details pertaining to the successful small car tests into strong-post guardrail systems can be found in the reference report (19).

The evaluation criteria for full-scale vehicle crash testing are based on three appraisal areas: (1) structural adequacy; (2) occupant risk; and (3) vehicle trajectory after collision. Criteria for structural adequacy are intended to evaluate the ability of the guardrail to contain and redirect impacting vehicles. In addition, controlled lateral deflection of the test article is acceptable. Occupant risk evaluates the degree of hazard to occupants in the impacting vehicle. Vehicle trajectory after collision is a measure of the potential of the vehicle to result in a secondary collision with other vehicles and/or fixed objects, thereby increasing the risk of injury to the occupants of the impacting vehicle and/or other vehicles. These three evaluation criteria are described in greater detail in NCHRP Report No. 350. Finally, the full-scale vehicle crash test was conducted and reported in accordance with the procedures provided in NCHRP Report No. 350.


SPECIFICATIONS		
<p>The Ponderosa Pine (PP) round post is for use in G4(2W) W-beam guardrail systems and shall be manufactured of material that conforms to the guidelines shown below.</p> <p>General: All posts shall meet the current quality requirements of the American National Standards Institute (ANSI) 05.1, Wood Poles, except as supplemented herein:</p> <p>Manufacture: All posts shall be smooth-shaved by machine. No ringing of the posts, as caused by improperly adjusted peeling machine, is permitted. All outer and inner bark shall be removed during the shaving process. All knots and knobs shall be trimmed smooth and flush with the surface of the posts. The use of peeler cores is prohibited. See the table on Sheet 1 for diameters and lengths.</p> <p>Groundline: The groundline, for the purpose of applying these restrictions of ANSI 05.1 that reference the groundline, shall be defined as being located 35" [889] and 36" [914] from the butt end of each post for PDE21 and PDE22, respectively.</p> <p>Size: The size of the posts shall be classified based on their diameter at the groundline and their length. The groundline diameter shall be specified by diameter in 1/8" [3] breaks. The length shall be specified in 1" [25] breaks. Dimension shall apply to fully seasoned posts. When measured between their extreme ends, the post shall be no shorter than the specified lengths but may be up to 3" [76] longer. See the table on Sheet 1 for minimum and maximum diameters.</p> <p>Scars: Scars are permitted in the middle third as defined in ANSI 05.1, provided that the depth of the trimmed scar is not more than 1" [25].</p> <p>Shape and Straightness: All PP timber posts shall be nominally round in cross section. A straight line drawn from the centerline of the top to the center of the butt of any post shall not deviate from the centerline of the post more than 1 1/4" [32] at any point. Posts shall be free from reverse bends.</p> <p>Splits, Checks, and Shakes: Splits or ring shakes are not permitted in the top two thirds of the post. Checks are not permitted in the top two thirds of the post if wider than one third of the diameter if dry and wider than three eighths of the diameter if not dry. Splits exceeding the diameter in length are not permitted in the bottom one third of the post. A shake or check is permitted in the bottom one third of the post as long as it is not wider than one half of the butt diameter. (Note - check size is determined as the average measured penetration over its length.)</p> <p>Knots: Knot diameter for Ponderosa Pine posts shall be limited to 3 1/2" [89] or smaller.</p> <p>Treatment: Treating - American Wood-Preservers' Association (AWPA) - Book of Standards (BOS) U1-05. Use category system UCS; user specification for treated wood; commodity specification B; Posts; Wood for Highway Construction must be met using the methods outlined in AWPA BOS T1-05 Section 8.2. Each treated post shall have a minimum sapwood depth of 3/4" [19], as determined by examination of the tops and butts of each post. Material that has been air dried or kiln dried shall be inspected for moisture content in accordance with AWPA standard M2 prior to treatment. Tests of representative pieces shall be conducted. The lot shall be considered acceptable when the average moisture content does not exceed 25 percent. Pieces exceeding 29 percent moisture content shall be rejected and removed from the lot.</p> <p>Decay: Allowed in knots only.</p> <p>Holes: Pin holes 1/16" [1] or less are not restricted.</p> <p>Slope of Grain: 1 in 10.</p> <p>Compression Wood: Not allowed in the outer 1" [25] or if exceeding one quarter of the radius.</p> <p>Ring Density: Ring density shall be at least 6 rings-per-inch, as measured over a 3" [76] distance.</p>		
ROUND POST FOR G4(2W) GUARDRAIL SYSTEM		
	PDE21-22	
	SHEET NO.	DATE:
	2 of 3	12/23/2014

FIGURE 1 Grading criteria for round PP posts.

ARIZONA G4(2W) W-BEAM GUARDRAIL WITH ROUND PP POSTS

System Details

Design details for the retrofit G4(2W) guardrail system with PP posts are shown in Figure 2. The installation for the guardrail system consisted of 175 ft (53.3 m) of standard 12-gauge (2.66-mm) W-beam supported by round PP wood posts. Photographs of the test installation are shown in Figure 3.

The barrier utilized standard 12-ft 6-in. (3.81-m) long 12-gauge (2.66-mm) W-beam rails. The W-beam guardrail was mounted with a top-rail height of 28 in. (711 mm) throughout the entire system. The rail splices were located at post locations. All lap-splice connections between the rail sections were configured with the upstream segment in front of the downstream segment to minimize the potential for vehicle snag at the splice during the crash test.

The rail was supported by twenty-nine guardrail posts spaced at 75 in. (1,905 mm) on center. All twenty-five PP posts were placed in a compacted coarse, crushed limestone material that met Grading B of AASHTO M147-65, as found in NCHRP Report No. 350. The posts were installed using MwRSF's installation procedures which comply with the 2009 *Manual for Assessing Safety Hardware* (MASH) specifications (20). Post nos. 3 through 27 consisted of a nominal 8½ in. (216 mm) diameter at groundline, a 64-in. (1,626-mm) length, and used a soil embedment depth of 35 in. (889 mm). A 6-in. wide x 8-in. deep x 14¼-in. long (152-mm x 203-mm x 362-mm) routed PP wood spacer blockout was used to block the rail away from the front face of each PP post.

The upstream and downstream ends of the guardrail installation were configured with a trailing-end anchorage system. This guardrail anchorage system was utilized to simulate the strength of other crashworthy end terminals. The anchorage system consisted of timber posts, foundation tubes, anchor cables, bearing plates, rail brackets, and channel struts, which closely resembled the hardware used in the Modified BCT system and now part of a crashworthy, downstream trailing end terminal (21-24). Post nos. 1, 2, 28, and 29 were breakaway cable terminal (BCT) timber posts that were inserted into 6-ft (1.8-m) long, steel foundation tubes.

Phase III Full-Scale Crash Testing – Test No. AZRP-1

For demonstration test no. AZRP-1, a 4,412-lb (2,001-kg) pickup truck impacted the modified Arizona G4(2W) W-beam guardrail system that was supported by 8½-in. (216-mm) nominal diameter PP posts at a speed of 60.7 mph (97.7 km/h) and an angle of 24.8 degrees. A summary of the test results and time-sequential photographs are shown in Figure 4. The critical impact point was determined to be 185 in. (4,699 mm) upstream from the centerline of post no. 15 which was selected using the CIP plots found in Section 3.4 of NCHRP Report No. 350 to maximize pocketing and the probability of wheel snag. The actual point of impact was 182¼ in. (4,629 mm) upstream from the centerline of post no. 15. At 0.342 sec after impact, the vehicle became parallel to the guardrail system with a speed of 33.3 mph (53.6 km/h). At 0.718 sec, the vehicle exited the guardrail at an angle of 21.3 degrees and at a speed of 25.5 mph (41.1 km/h). The vehicle was smoothly redirected. The exterior vehicle damage was moderate, as shown in Figure 5, and the interior occupant compartment deformations were below the previously-recognized NCHRP Report No. 350, with a maximum of 5½ in. (140 mm) in the wheel well and toe pan area. As shown in Figure 5, damage to the barrier was moderate, consisting mostly of

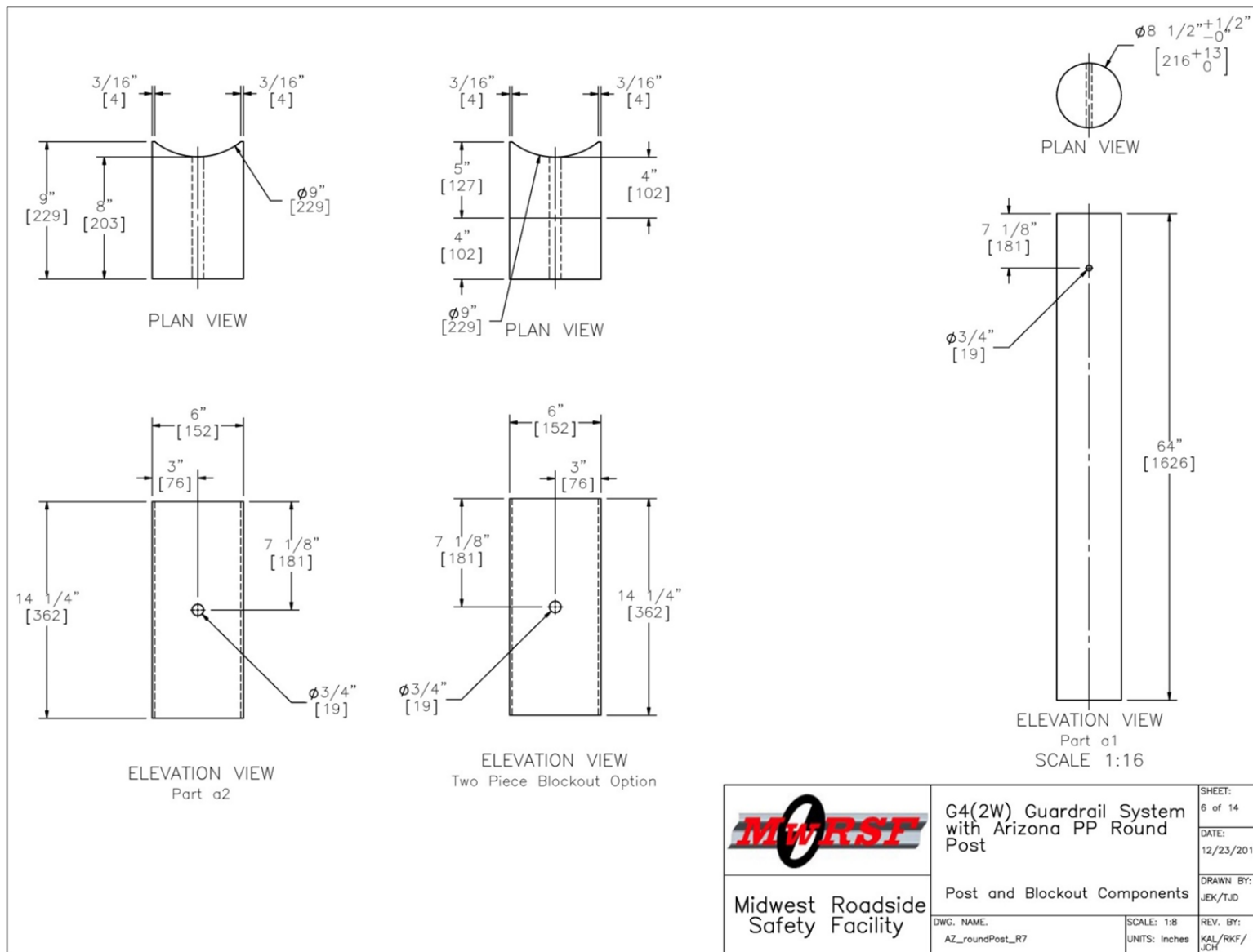


FIGURE 2 Round PP post details for Arizona G4(2W) guardrail system.



FIGURE 3 Arizona G4(2W) guardrail system with round PP posts.

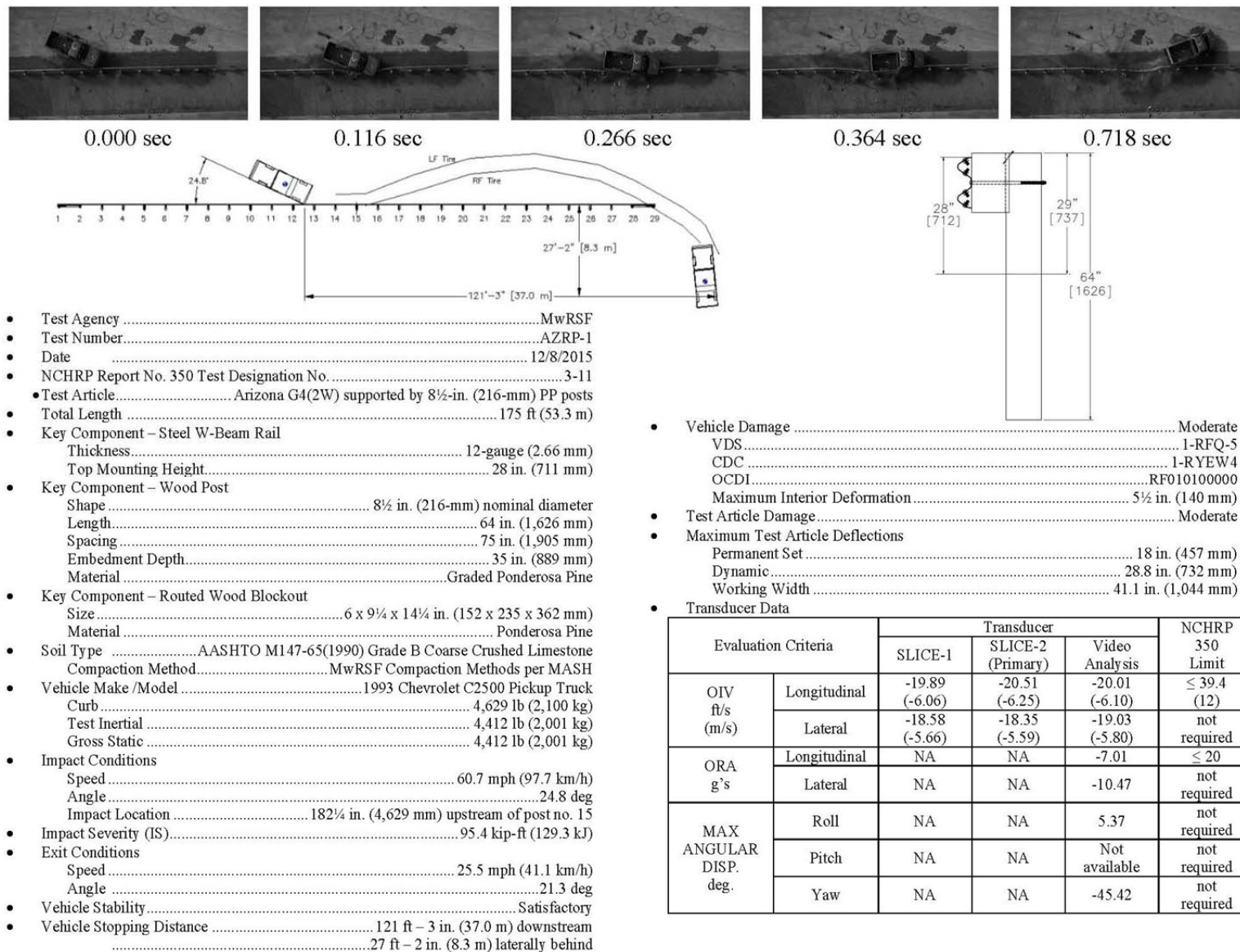


FIGURE 4 Summary of test results and sequential photographs, Test AZRP-1.



FIGURE 5 Vehicle damage and barrier damage, Test AZRP-1.

Deformed w-beam rail, disengaged w-beam rail from the posts, fractured wood posts, split wood blockouts displaced posts in the soil, and contact marks on a section of guardrail. The maximum lateral dynamic rail and post deflections were 28.8 in. (732 mm) at the rail between the midspan between post nos. 14 and 15 and 21.3 in. (541 mm) at post no. 14, respectively, as determined from high-speed digital video analysis. The working width of the system was 41.1 in. (1,044 mm), also determined from high-speed digital video analysis. The longitudinal occupant risk measures were below the required values, and the test vehicle showed no tendency to roll over. Therefore, test no. Azrp-1 was determined to be acceptable according to the tl-3 safety performance criteria found in nchrp report no. 350.

SUMMARY AND CONCLUSIONS

Round PP post alternatives for use as replacement posts in existing Arizona and U.S. standard G4(2W) W-beam guardrail systems were developed. An 8½-in. (216-mm) nominal diameter PP post with a 35-in. (889-mm) embedment depth and a 64-in. (1,626-mm) length was confirmed as a surrogate for use in existing Arizona G4(2W) guardrail systems based on dynamic component testing. Similarly, based on dynamic component testing, an 8⅝-in. (219-mm) nominal diameter PP post with a 36-in. (914-mm) embedment depth and a 65-in. (1,651-mm) length was found to be a surrogate in existing U.S. standard G4(2W) W-beam guardrail systems. The modified Arizona and modified U.S. standard G4(2W) guardrail systems with the specified PP posts are eligible for Federal reimbursement and are suitable for use on Federal-aid highways (25). The specific guardrail systems are those that have either met or been grandfathered under the impact safety standards published in the NCHRP Report No. 350.

A full-scale crash test was performed to further demonstrate the crashworthiness of the 28 in. (711 mm) tall Arizona G4(2W) W-beam guardrail system when supported by 8½-in. (216-mm) nominal diameter PP post with a 35-in. (889-mm) embedment depth and a 64-in. (1,626-mm) length. The demonstration test was conducted according to the TL-3 safety performance criteria published in NCHRP Report No. 350 and confirmed that the specified PP post as a suitable surrogate for use in existing Arizona G4(2W) W-beam guardrail systems.

Special attention should be directed toward the proper inspection of timber materials and emphasis for timber suppliers to follow the published PP round-post dimensions and grading criteria as shown in Figure 1. These measures should ensure that the PP posts are fabricated from suitable wood, have adequate strength, provide similar post-soil behavior to the rectangular SYP posts studied (7-8), and allow for G4(2W) guardrail systems to perform in an acceptable manner when using either round PP posts or rectangular SYP posts.

Federal, State, and local highway agencies could benefit from the use of surrogate, round PP posts to retrofit existing G4(2W) guardrail systems. Installation of the modified G4(2W) guardrail systems using round timber posts could: (1) continue to provide motorist safety along our nation's highways and roadways; (2) increase markets for wood products across the U.S. as well as in the State of Arizona; and (3) help to reduce the risk of devastating forest fires across the country.

DISCLAIMER

The contents of this report reflect the views of the authors who are responsible for the facts and the accuracy of the data presented herein. The contents do not necessarily reflect the official views or policies of the Forest Products Laboratory of the USDA - Forest Service, the Arizona Log & Timberworks, and the Arizona State Forestry Division. This report does not constitute a standard, specification, or regulation.

ACKNOWLEDGMENTS

The authors wish to acknowledge several sources that made a contribution to this project: (1) the Forest Products Laboratory of the USDA - Forest Service for sponsoring this research project; (2) the Arizona Log & Timberworks for sponsoring this research project and supplying the graded PP posts, blockouts, and material shipping; (3) the Arizona State Forestry Division for sponsoring this research project; (4) 2015 Wood Innovations Grant Program, USDA – Forest Service for additional research funding; and (5) MwRSF personnel for constructing the barriers and conducting the crash tests.

REFERENCES

1. *Collaborative Approach for Reducing Wildland Fire Risks to Communities and the Environment*, U.S. Department of Interior and U.S. Department of Agriculture, August 2001.
2. Gorte, R.W., *Forest Fires and Forest Health*, CRS Report 95-511, CRS Report for Congress. 14 July 1995. National Council for Science and the Environment, July 21, 2003.
3. LeVan-Green, S.L. and Livingston, J.M., *Uses for Small-Diameter and Low-Value Forest Thinnings*, Ecological Restoration, March 2003: 34-38.
4. Paun, D. and Jackson, G., *Potential for Expanding Small-Diameter Timber Market Assessing Use of Wood Posts in Highway Applications*, General Technical Report FPL-GTR-120, Department of Agriculture, Forest Service, Forest Products Laboratory, Madison, Wisconsin, 2000.
5. Hascall, J.A., Faller, R.K., Reid, J.D., Sicking, D.L., and Kretschmann, D.E., *Investigating the Use of Small-Diameter Softwood as Guardrail Posts (Dynamic Test Results)*, Final Report to the Forest Products Laboratory - U.S. Department of Agriculture, MwRSF Research Report No. TRP-03-179-07, Midwest Roadside Safety Facility, University of Nebraska-Lincoln, Lincoln, Nebraska, March 28, 2007.
6. Faller, R.K., Reid, J.D., Kretschmann, D.E., Hascall, J.A., and Sicking, D.L., *Midwest Guardrail System with Round Timber Posts*, Paper No. 09-0547, Transportation Research Record No. 2120, Journal of the Transportation Research Board, TRB AFB20 Committee on Roadside Safety Design, Transportation Research Board, Washington D.C., January 2009.
7. Price, C.W., Faller, R.K., Rosenbaugh, S.K., Lechtenberg, K.A., and Winkelbauer, B.J., *Phase I Ponderosa Pine Round Post Equivalency Study*, Final Report to the Forest Products Laboratory and Arizona Log & Timberworks, MwRSF Research Report No. TRP-03-287-13, Midwest Roadside Safety Facility, University of Nebraska-Lincoln, Lincoln, Nebraska, November 22, 2013.
8. Rosenbaugh, S.K., Faller, R.K., Winkelbauer, B.J., and Schmidt, T.L., *Phase II Ponderosa Pine Round Post Equivalency Study*, Final Report to the Forest Products Laboratory and Arizona Log & Timberworks, MwRSF Research Report No. TRP-03-315-14, Midwest Roadside Safety Facility, University of Nebraska-Lincoln, Lincoln, Nebraska, February 4, 2015.

9. Ross, H.E., Sicking, D.L., Zimmer, R.A., and Michie, J.D., *Recommended Procedures for the Safety Performance Evaluation of Highway Features*, National Cooperative Highway Research Program (NCHRP) Report 350, Transportation Research Board, Washington, D.C., 1993.
10. Michie, J.D., *Recommended Procedures for the Safety Performance Evaluation of Highway Appurtenances*, National Cooperative Highway Research Program (NCHRP) Report 230, Transportation Research Board, Washington, D.C., March 1981.
11. Bronstad, M.E., Michie, J.D., and Mayer, J.B., *Minicar Crash Test Evaluation of Longitudinal Traffic Barriers*, Transportation Research Record No. 1024, Transportation Research Board, National Research Council, Washington, D.C., 1985.
12. Sicking, D.L., Bligh, R.P., and Ross, H.E., Jr., *Optimization of Strong Post W-Beam Guardrail*, Research Report No. 1147-1F, Texas Transportation Institute, Texas A&M University, College Station, Texas, November 1988.
13. Stout, D., Hughes, W., and McGee, H., *Traffic Barriers on Curves, Curbs, and Slopes*, Report No. FHWA-RD-93-082, ENSCO, Inc., Springfield, Virginia, October 1993.
14. Brown, C.M., *Crash Test Between a Modified G4(1S) Guardrail System and a 1997 Geo Metro - Foil Test No. 99F003*, Contract No. DTFH61-99-F-001004, MiTech Incorporated, Silver Spring, Maryland, March 2000.
15. Bronstad, M.E., Michie, J.D., and Mayer, J.B., *Performance of Longitudinal Traffic Barriers*, National Cooperative Highway Research Program (NCHRP) Report No. 289, Transportation Research Board, National Research Council, Washington, D.C., June 1987.
16. Buth, C.E., Campise, W.L., Griffin, III, L.I., Love, M.L., and Sicking, D.L., *Performance Limits of Longitudinal Barrier Systems - Volume I - Summary Report*, Report No. FHWA/RD-86/153, Submitted to the Office of Safety and Traffic Operations, Federal Highway Administration, Performed by Texas Transportation Institute, May 1986.
17. Ivey, D.L., Robertson, R., and Buth, C.E., *Test and Evaluation of W-Beam and Thrie-Beam Guardrails*, Report No. FHWA/RD-82/071, Submitted to the Office of Research, Federal Highway Administration, Performed by Texas Transportation Institute, March 1986.
18. Ross, H.E., Jr., Perera, H.S., Sicking, D.L., and Bligh, R.P., *Roadside Safety Design for Small Vehicles*, National Cooperative Highway Research Program (NCHRP) Report No. 318, Transportation Research Board, Washington, D.C., May 1989.
19. Lechtenberg, K.A., Faller, R.K., Rosenbaugh, S.K., and Reid, J.D., *Phase III Demonstration of Ponderosa Pine Round Posts as Alternative to Rectangular SYP Posts in G4(2W) Guardrail Systems*, Final Report to the Arizona State Forestry Division, Forest Products Laboratory, and Arizona Log & Timberworks, Research Report No. TRP-03-329-15, Midwest Roadside Safety Facility, University of Nebraska-Lincoln, Lincoln, Nebraska, May 17, 2016.
20. *Manual for Assessing Safety Hardware (MASH)*, American Association of State Highway and Transportation Officials (AASHTO), Washington, D.C., 2009.
21. Mongiardini, M., Faller, R.K., Reid, J.D., Sicking, D.L., Stolle, C.S., and Lechtenberg, K.A., *Downstream Anchoring Requirements for the Midwest Guardrail System*, Research Report No. TRP-03-279-13, Midwest Roadside Safety Facility, University of Nebraska-Lincoln, Lincoln, Nebraska, October 28, 2013.
22. Mongiardini, M., Faller, R.K., Reid, J.D., and Sicking, D.L., *Dynamic Evaluation and Implementation Guidelines for a Non-Proprietary W-Beam Guardrail Trailing-End Terminal*, Paper No. 13-5277, Transportation Research Record No. 2377, Journal of the Transportation Research Board, TRB AFB20 Committee on Roadside Safety Design, Transportation Research Board, Washington D.C., January 2013, pages 61-73.
23. Stolle, C.S., Reid, J.D., Faller, R.K., and Mongiardini, M., *Dynamic Strength of a Modified W-Beam BCT Trailing-End Termination*, Paper No. IJCR 886R1, Manuscript ID 1009308, International Journal of Crashworthiness, Taylor & Francis, Vol. 20, Issue 3, Published online February 23, 2015, pages 301-315.

24. Griffith, M.S., Federal Highway Administration (FHWA). *Eligibility Letter HSST/B-256 for: Trailing-End Anchorage for 31" Tall Guardrail*, December 18, 2015.
25. Griffith, M.S., Federal Highway Administration (FHWA). *Eligibility Letter HSST/B-266 for: Modified U.S. Standard and Arizona G4(2W) W-beam Guardrail Systems with 8⁵/₈-in. and 8¹/₂-in. Nominal Diameter Ponderosa Pine Posts, respectively*, 2016.

A Synthesis of MASH-Tested 31-in. Tall, Nonproprietary, W-Beam Guardrail Systems

SCOTT K. ROSENBAUGH

RONALD K. FALLER

ROBERT W. BIELENBERG

Midwest Roadside Safety Facility

University of Nebraska-Lincoln

Since its initial development in the early 2000's, 31-in. tall W-beam guardrail has proven to be one of the most robust roadside barrier systems available today. Full-scale crash testing has been successfully conducted on numerous configurations of 31-in. W-beam guardrail installations including median and roadside systems, steel and timber post systems, 12-in. and 8-in. deep blockout systems, non-blocked systems, and systems placed on or adjacent to roadside slopes. Additionally, 31-in. W-beam systems have been developed for use in special applications such as bridge rails, long-span systems, and as culvert mounted installations.

This paper contains details and drawings encompassing a wide range of 31-in. tall W-beam guardrail configurations that have been developed and evaluated to MASH safety standards. The various configurations are discussed in terms of key components and performance characteristics, such as test level and working width. Finally, implementation guidance is provided for the proper selection, layout, and installation of the various 31-in. W-beam guardrail configurations.

INTRODUCTION

W-beam guardrail systems are some of the most popular and frequently used vehicle barrier systems. For over 50 years, these barrier systems have been redirecting errant vehicles and preventing impacts into roadside hazards. However, by the 1990's the increased size of the vehicle fleet was beginning to push the containment limits of the existing W-beam guardrail configurations. Multiple full-scale vehicle crash tests with heavy, high center-of-gravity passenger vehicles, such as pickup trucks and vans, resulted in rail ruptures and vehicle rollovers. Thus, W-beam guardrails needed to be updated to handle the larger vehicle fleet.

In the early 2000's, the Midwest Guardrail System (MGS) was developed through modifications to the existing G4(1S) W-beam guardrail system. These modifications included raising the height to the top of the rail to 31 in., a reduction in the post embedment depth to 40 in., and moving the rail splices from post locations to mid-spans (*I-2*). Additionally, the depth of the blockouts was increased to 12 in. to aid in the containment of taller vehicles and to reduce vehicle snag on the system posts. Details for the MGS are shown in Figure 1.

The MGS was originally developed and successfully crash tested to the Test Level 3 (TL-3) safety performance standards of NCHRP Report No. 350 (3). Since its inception, the MGS has proven to be a very robust barrier system as multiple variations and special applications of the MGS have been developed and successfully crash tested. Even with the adoption of a new crash testing standard, the *Manual for Assessing Safety Hardware* (MASH) (4), which utilizes larger

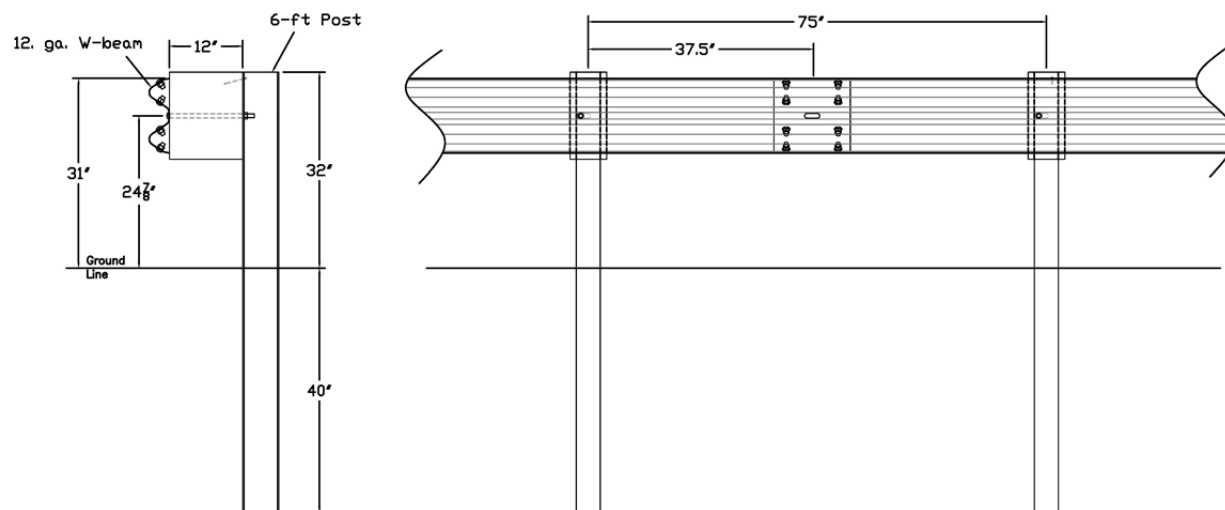


FIGURE 1 Characteristics of standard strong-post MGS, 31-in. tall W-beam guardrail.

vehicles and higher impact severities than NCHRP Report No. 350, the MGS and its variations have continued to provide crashworthy results.

The purpose of this paper is to provide a single resource documenting the numerous non-proprietary, 31-in. tall W-beam guardrail configurations and special applications. Details required for the proper installation of each system configuration are provided herein, including drawing sets, component details, performance levels, working widths, and installation guidance. Since AASHTO and FHWA established December 31, 2017 as the implementation date for W-beam guardrail installations to satisfy MASH safety standards (5), this paper is focused on only the MASH crash tested systems.

STRONG-POST SYSTEMS

Strong-post W-beam guardrail systems, which include both steel and timber posts, have been the most widely used guardrail systems for decades. Accordingly, both steel- and wood-post MGS systems have been successfully tested and evaluated to MASH TL-3 [6-10]. The steel post version of the MGS utilizes 6-ft long W6x9 or W6x8.5 posts, which have nearly identical flange widths and section depths and provide similar bending strengths. Thus, both post sections provide similar performance when used as a guardrail post. Timber post versions typically utilize 6-ft long rectangular posts measuring 6 in. wide and 8 in. deep nominally.

Both steel- and timber-post versions of the MGS utilize the same general system layout with 12-in. blockouts, a 75-in. post spacing, and rail splices located at mid-span, as shown in Figure 1. Aside from the posts, the only difference between the steel- and timber-post systems is the length of the 5/8-in. diameter guardrail bolt. Photos of both systems are shown in Figure 2.

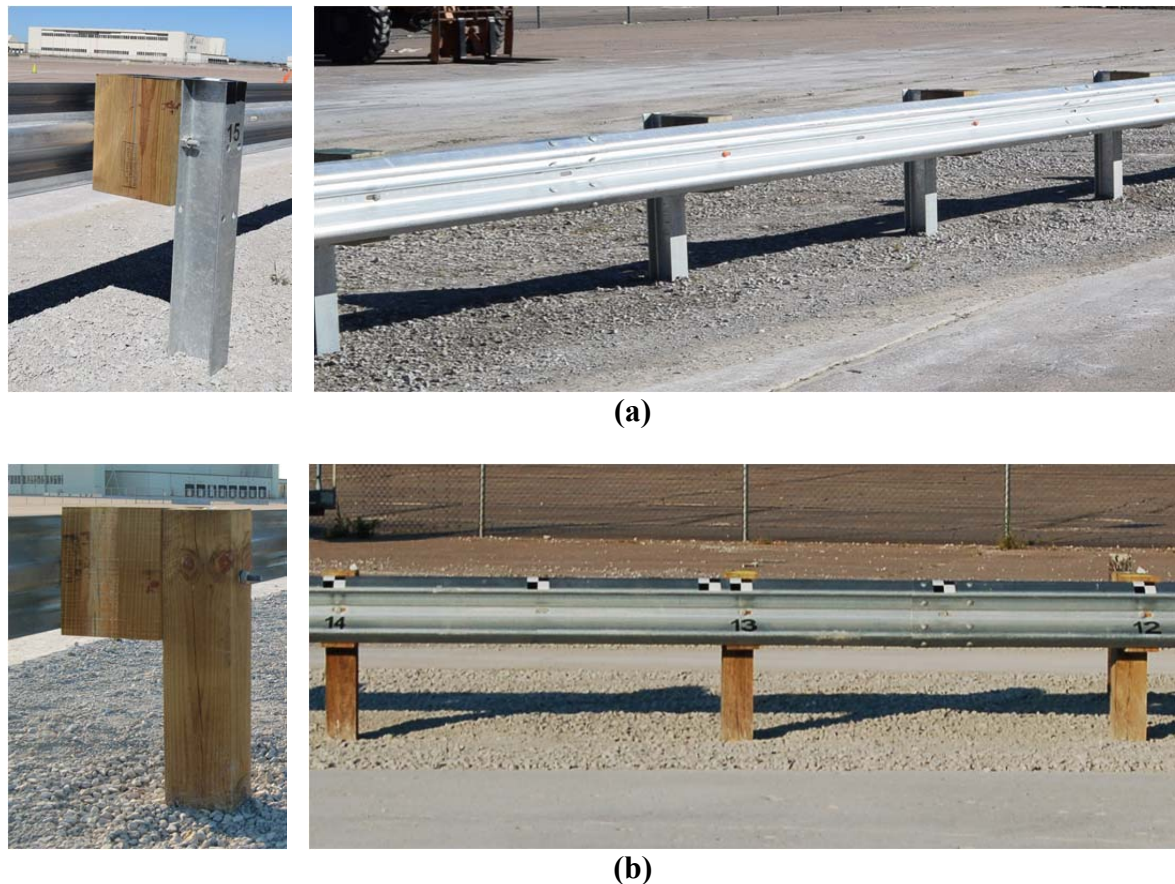


FIGURE 2 Strong-post MGS installations with (a) steel and (b) rectangular timber posts.

During full-scale crash testing, both the steel- and timber-post versions of the MGS performed similarly in terms of vehicle behavior, occupant ridedown accelerations (ORA), and occupant impact velocities (OIV), which were all well within the MASH limits. However, there are a few notable differences between the systems. Wood posts tend to fracture under extreme loading conditions while steel posts plastically deform and continue to apply a resistance force to the vehicle. Consequently, the working width for timber-post systems is slightly higher than that of the steel-post system, as shown in Table 1. Thus, the required clear distance behind the barrier, which should be free of all hazards, depends on the post type.

The timber species utilized for the posts also factor into the system performance. The MGS has been evaluated to MASH utilizing both Southern Yellow Pine (SYP) and White Pine (WP) rectangular timber posts. WP posts have roughly 37 percent less strength than SYP posts. This reduction in strength resulted in increases in the number of fractured posts, the deformed length of the guardrail system, and the system working width, as shown in Table 1. Therefore, it is recommended that rectangular timber posts only be made from timbers with strength greater than or equal to that of Select Structural WP unless further evaluation is performed.

TABLE 1 Comparison of Steel- and Timber-Post MGS

System	Steel-Post MGS	Timber-Post MGS	Timber-Post MGS
Posts	W6x8.5	6-in. x 8-in. SYP	6-in. x 8-in. WP
Reference	(6)	(8)	(10)
Performance Level	MASH TL-3	MASH TL-3	MASH TL-3
MASH 3-11 Results			
Working Width	48.6 in.	53.8 in.	58.4 in.
Contact Length	33.8 ft	34.3 ft	36.5 ft
No. Deflected Posts	6	6	7
No. Fractured Posts	—	4	5

BLOCKOUT VARIATIONS

The MGS was originally designed with 12-in. deep timber blockouts for two reasons: 1) to reduce the likelihood and severity of vehicle snag on guardrail posts and 2) to maintain rail height as the post deflects backward, making the system more likely to capture large vehicles. However, 31-in. tall W-beam guardrail has been successfully crash tested to MASH TL-3 standards while utilizing 8-in blockouts and in non-blocked configurations. All three blockout variations are shown in Figure 3.

The 31-in. W-beam guardrail system with 8-in blockouts differs from the standard MGS only in the depth of the blockout and length of the attachment bolt. This configuration was crash tested to MASH test designation 3-10 to evaluate any potential for the 1100C small car to snag on the guardrail posts. The test passed and resulted in vehicle and system behavior similar to that of the MGS with 12-in. blockouts (11). Thus, 8-in. blockouts can be utilized with either steel- or timber-post versions of the MGS.

The non-blocked MGS eliminated the timber blockout, but a 12-in. long segment of W-beam was placed between the rail and the post to prevent contact between the post flanges and the rail, which could initiate tearing of the rail. The non-blocked system was evaluated to MASH TL-3 and satisfied all safety criteria for both full-scale crash tests (12-13). The working width for the non-blocked system was measured to be 43.2 in.

During evaluation of the non-blocked system, the small car contacted the posts earlier in the impact event and caused the vehicle to be non-tracking, or side skidding, as it exited the system. Additionally, snag on the posts resulted in a longitudinal OIV value of 31.3 ft/s, which was more than double that of the MGS with 12-in. blockouts but still within the MASH limit of 40 ft/s. These differences illustrate the benefits of utilizing blockouts within a guardrail system. As such, the use of blockouts is recommended for guardrail installations whenever the roadside can accommodate the increased width. Additionally, the non-blocked system has not been evaluated with timber posts, which may further increase vehicle snag, vehicle decelerations, and the risk for vehicle instabilities. Therefore, it is not recommended to utilize a non-blocked system with timber posts until further analysis is performed.

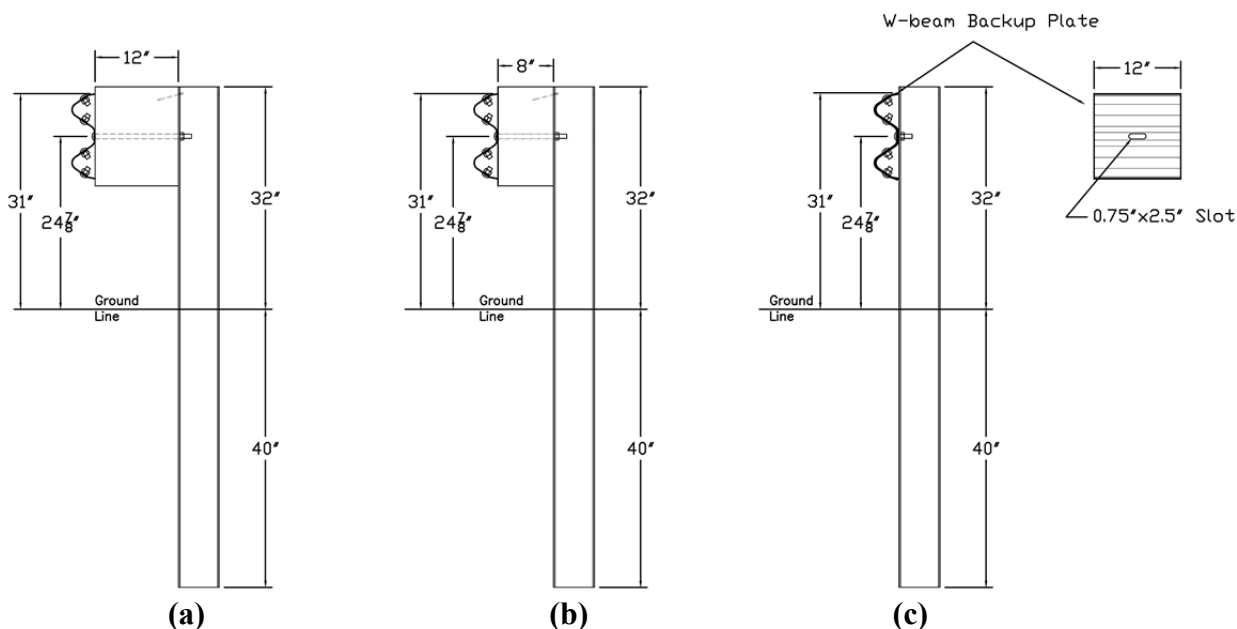


FIGURE 3 MGS details for (a) 12-in. blockouts, (b) 8-in. blockouts, and (c) non-blocked configurations.

MEDIAN BARRIER

A 31-in. W-beam median barrier was developed and successfully crash tested to MASH TL-3 safety criteria. The median system utilized 12-ga. W-beam guardrail, splices at mid-span locations, and 8-in. deep blockouts mounted on both sides of standard steel guardrail posts, as shown in Figure 4. Although the system deflections were similar to those of the standard roadside systems, the increased width of the median system resulted in a 55-in. working width (14).

Testing and evaluation of the median system was conducted with 8-in. blockouts, but 12-in. blockouts should provide similar system performance. During the small car test on the median system, a tear extended through two-thirds of the rail. Eliminating the blockouts could result in small increases to the rail loads and cause complete rupture of the rail. Additionally, vehicle snag on posts directly attached to two rail elements may result in excessive decelerations to the small car. Therefore, it is not recommended to install the median system in a non-blocked configuration without further analysis.

The median barrier system was evaluated on level terrain, and its performance on sloped terrain remains unknown. Thus, the median barrier system should only be installed in median with a slope of 10:1 or flatter until further evaluation is performed. Finally, the ends of the system need to be properly treated with a crashworthy median guardrail terminal capable of anchoring a dual-sided, W-beam system.

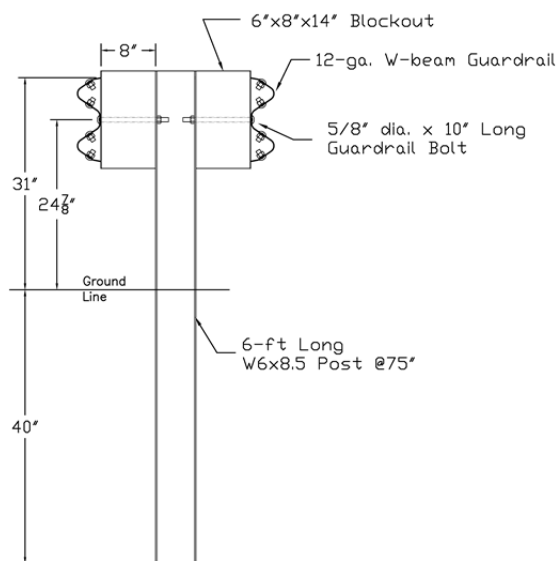


FIGURE 4 Details for 31-in. W-beam median barrier.

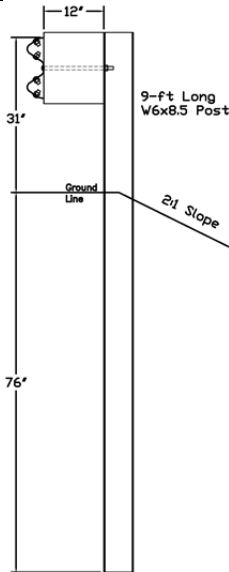
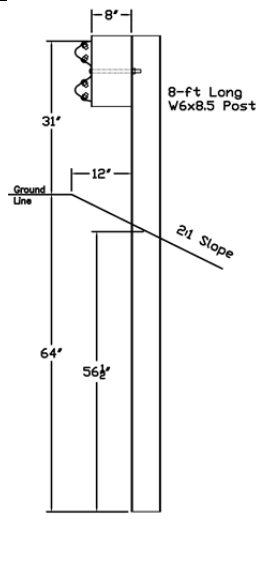
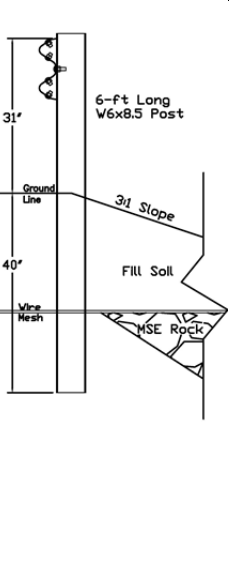
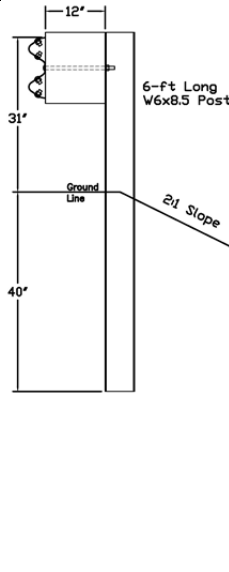
SYSTEMS INSTALLED NEAR SLOPES

The strength and stiffness of w-beam guardrail is heavily dependent on post-soil resistance forces. Placing the system on or adjacent to a slope reduces the amount of soil behind the post, lowers the post-soil resistance, and can negatively affect the performance of the system. Thus, it is recommended for guardrail posts to be installed with at least 2 ft of level terrain behind the system to ensure the system performs as initially developed and evaluated. However, there are instances where placing guardrail adjacent to slopes is necessary due to limited roadside widths.

To date, there have been four different W-beam guardrail configurations that have been successfully developed and crash tested to MASH TL-3 (15-20). Although all four systems utilized 31-in. tall w-beam rail, they had varying post lengths, blockouts, allowable slopes, and placements relative to the slope break point (SBP), as shown and detailed in Table 2. The system denoted as System C in Table 2 was developed specifically for use on top of Mechanically Stabilized Earth (MSE) walls. The posts were extended through the wire mesh utilized to anchor the MSE wall, effectively stiffening the system (18). Thus, System C requires installation within these MSE wall components in order to maintain the listed system performance, specifically the reduced working width. Placement on a standard fill slope would likely result in system deflections and working widths similar to System D.

System A was the first guardrail system developed for use adjacent to slopes and tested to MASH TL-3. It utilized 12-in. blockouts and 9-ft long posts centered on the SBP of a 2:1 slope. Dynamic testing of various posts located at the SBP of a 2:1 slope illustrated that 7.5-ft long 6-in. x 8-in. rectangular SYP timber posts would provide similar strength to the full-scale crash tested system (15). Full-scale testing of System B and additional dynamic post testing on slopes has since justified the use of 8-ft steel posts as well. Thus, both are listed as alternative post options for System A. Additionally, System C illustrated the crashworthiness of a non-blocked guardrail system on slopes, so both 8-in blockouts and non-blocked configurations of System A are listed as alternative options.

TABLE 2 Details for 31-in. W-Beam Guardrail on Slopes

System	A	B	C	D
Layout				
Reference	(15)	(17)	(18)	(20)
Performance Level	MASH TL-3	MASH TL-3	MASH TL-3	MASH TL-3
Full-Scale Tests	MASH 3-11	MASH 3-10 MASH 3-11	MASH 3-10 MASH 3-11	MASH 3-11
Post	9-ft W6x8.5	8-ft W6x8.5	6-ft W6x8.5	6-ft W6x8.5
Post Spacing	75 in.	75 in.	75 in.	75 in.
Blockout	12-in. Blockout	8-in. Blockout	Non-Blocked	12-in. Blockout
Slope	2:1	2:1	3:1	2:1
Post Locations	Centered on SBP	Centered 15 in. Down Slope	Centered on SBP	Centered on SBP
Working Width	62.4 in.	55.2 in.	45.2 in.	77.4 in.
Alternative Posts	8-ft W6x8.5 or 7.5-ft 6"x8" Timber*	-	-	6-ft 6"x8" Timber*
Alternative Blockouts	Non-Blocked or 8" Blockout	12-in. Blockout	-	Non-Blocked or 8" Blockout
Allowable Slopes	2:1 or Flatter	2:1 or Flatter	-	2:1 or Flatter

* Timber posts should have strength equal to or greater than SYP grade 1

System B is the only system to be developed and crash tested with the posts installed beyond the SBP. It utilized 8-in. blockouts and 8-ft long W6x8.5 posts centered 15 in. down a 2:1 slope (17). Thus, the face of the rail was located directly above the SBP. Due to a lack of dynamic testing on timber posts positioned beyond the SBP, which effectively increases the moment arm in the post from the center of the rail to the soil support and increases the possibility of post fracture, there have not been any timber posts identified as alternative posts for use with System B. Non-blocked guardrail located beyond the SBP has not yet been evaluated, but may affect the relative height of the W-beam rail as system deflects during impacts. Specifically, the rail may be pulled downward as the posts deflect backward, which increases the possibility of vehicle override. As such, System B is not recommended to be installed as a non-blocked installation without further analysis.

System D represents a standard strong post MGS installed at the SBP of a 2:1 slope (20). The system was tested with steel guardrail posts, but standard rectangular timber posts installed at the SBP should provide similar performance. Thus, the 6-ft long 6-in. x 8-in. SYP timber post is listed as an alternative post for System D. Additionally, based on the performance of System C, both 8-in blockouts and non-blocked were listed as alternative blockout options for System D.

Due to the shorter post length of System D, a significant increase in working width was observed. It is important to note that MASH requires guardrail systems to be tested within strong soils to evaluate critical loading to barrier components. If the system is installed in a weaker soil, the deflections and working width would increase even further and may eventually become excessive and lead to vehicle instability, loss of vehicle containment, or rail rupture. Thus, System D is only recommended to be utilized in strong soil conditions similar to the soil specified by MASH. Installations sites with weaker or sandy soils are encouraged to utilize Systems A or B.

During the full-scale testing of System A, a MASH 3-11 test was conducted on a system with a 27¾ in. top mounting height. The 2270P pickup overrode this lower-height guardrail, thus failing the test. Subsequently, it is recommended for all W-beam guardrails adjacent to slopes to be installed with a minimum rail height of 31-in. without further analysis. Additionally, guardrail systems have only been evaluated on slopes as steep as 2:1. Thus, these guardrail systems should be limited to slopes of 2:1 or flatter until further evaluation is performed.

Finally, the recommendations listed herein for W-beam guardrail placed on or adjacent to steep slopes are applicable only to guardrail length of need installations. Special guardrail applications such as long-span installations, omitted posts, roadway curbs, and guardrail stiffness transitions have not yet been designed or evaluated for use on slopes. As such, it is not recommended to install these specialized guardrail applications on or adjacent to steep slopes without further analysis. Similarly, guardrail end terminals require specific grading to function properly. It is recommended that guidance from the individual end terminal manufacturer be sought after and followed concerning placement on slopes.

GUARDRAIL WITH OMITTED POSTS

Occasionally within a guardrail installation, obstructions within the ground prevent the proper installation of a post. At these locations, it is often desired to omit the guardrail post leaving a 12.5-ft span between the posts adjacent to the obstruction. Subsequently, a steel post MGS installation with a single missing post was subjected to MASH test 3-11 to evaluate critical rail

loadings and possible vehicle instabilities. The system contained and redirected the vehicle with a working width of 50.1 in., and the system was determined to satisfy MASH TL-3 safety criteria (21).

The omission of a post effectively weakens the guardrail system and results in increased system deflections, rail loads, and vehicle pocketing. The omission of multiple posts within the contacted region of a guardrail installation system may lead to excessive displacements, loads, and/or pocketing that may ultimately lead to system failure. Therefore, until further evaluation is completed on multiple missing posts within a system, it is recommended that at least eight posts be installed between omitted posts to ensure proper system performance.

Since the performance of timber and steel posts are so similar, the same guidelines should be utilized for the omission of a post within a guardrail system for either post type. Additionally, utilization of either 8-in. or 12-in. blockouts are acceptable adjacent to the omitted post location. However, the increased deflections associated with an omitted post may be problematic for a non-blocked system due to the increased risk for rail rupture and exposure of the vehicle floor pan to contact with posts. Thus, it is not recommended to omit posts within a non-blocked system until further evaluation is conducted.

Finally, these guidelines on omitted post are only intended for standard, length-of-need installations. Specialized W-beam applications such as guardrail adjacent to slopes, guardrail stiffness transitions, guardrail in combination with roadway curbs, or guardrail end terminals are sensitive systems that may be negatively affected by a post omission. Thus, it is not recommended to omit posts within these specialized guardrail regions without further analysis.

MGS LONG SPAN GUARDRAIL

The MGS Long-Span guardrail system was developed to treat sites where an obstruction prevents multiple adjacent guardrail posts from being installed, such as a low-fill culvert or short bridge. The MGS Long Span system consists of a 25-ft unsupported span (equivalent of three omitted posts) with three timber Controlled Release Terminal (CRT) posts on each side (22-23), as shown in Figure 5. Because CRT posts were designed to breakaway when impacted, they help prevent excessive rail loads, pocketing, and vehicle snag during impacts to the unsupported span. Each CRT post utilizes a 12-in blockout, and standard strong-post MGS should be used adjacent to each end of the MGS Long Span. This system was successfully tested to the TL-3 safety criteria of MASH and the working width was determined to be 93.4 in.

The MGS Long Span was tested with the back of the CRT posts 9-in. in front of the outside face of a simulated culvert headwall, which resulted in the face of the guardrail being 32 in. from the edge of the culvert. These distances represent the recommended minimum lateral offsets required between the system and the outside edge of a culvert headwall or bridge deck without further analysis. Additionally, it is recommended it install the CRT posts with a minimum of 2 ft of level terrain behind the posts to ensure proper performance until further analysis is conducted.

Culvert headwalls may extend above the ground line and act a vertical roadway curb beneath barrier. Curbs of any type may create vehicle instabilities if placed in combination with the MGS Long Span. Thus, it is recommended that culvert headwalls extend no higher than 2 in. above the ground line.

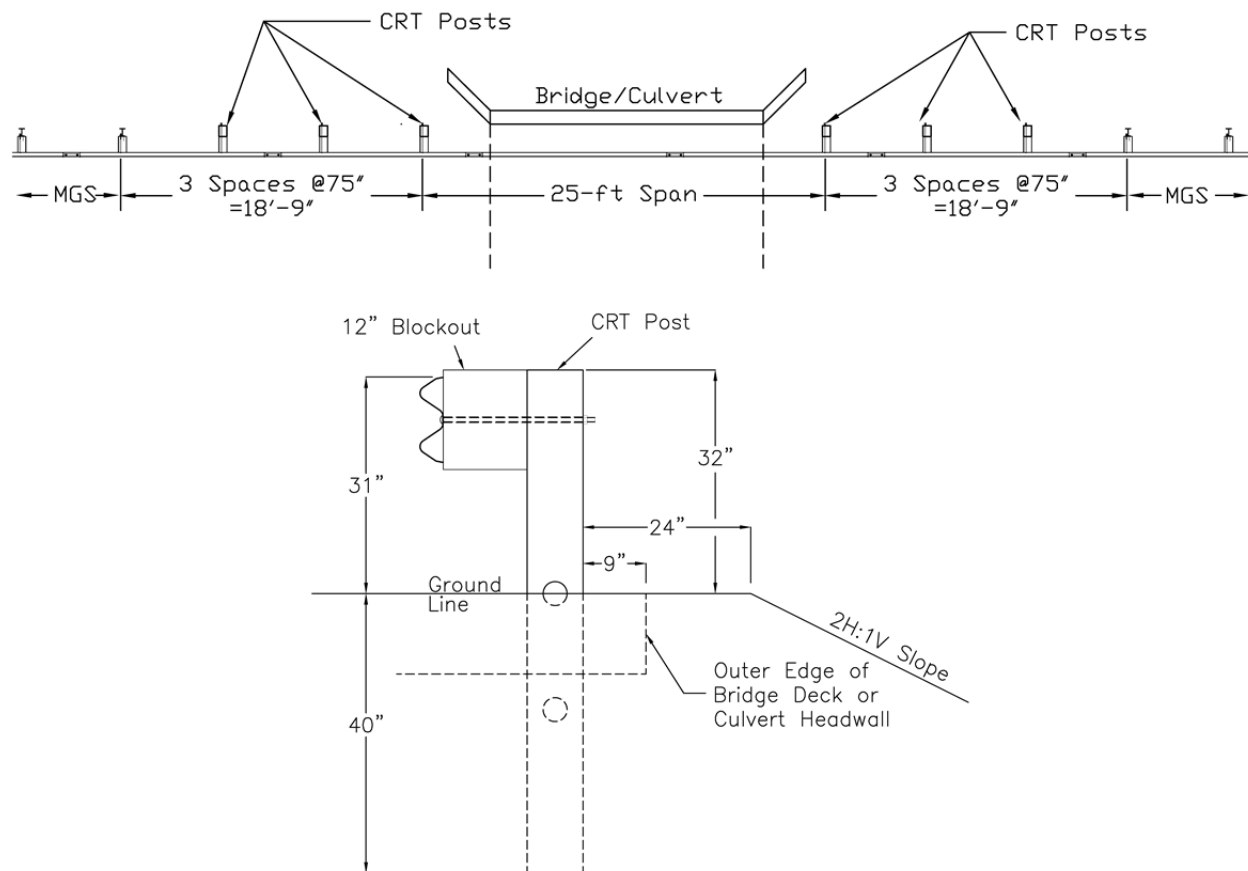


FIGURE 5 Details of the MGS long-span guardrail system.

As discussed previously, the increased rail height and blockout depth of the MGS over previous W-beam guardrail systems has led to a more robust barrier. With a working width of 93.4 in., these characteristics may be vital to the performance of the system. As such, it is recommended that the MGS Long Span be installed with a top rail height of 31 in. and a 12-in blockout until further analysis is performed. Additionally, it is not recommended to extend the unsupported length of the guardrail beyond 25 ft without further analysis as testing with a 31.25-ft unsupported span length has proven unsuccessful (24).

To ensure proper load distribution away from the MGS Long Span, it is recommended that at least 62.5 ft of guardrail, including the end anchorage, be installed both upstream and downstream from the CRT posts. The MGS adjacent to the three CRT posts may consist of any of the MASH TL-3 roadside configuration contained herein, unless otherwise noted.

END TERMINALS

Multiple 31-in. guardrail end terminals have been developed and successfully evaluated to MASH safety criteria. The majority of these terminals are proprietary, and, thus, are not discussed herein. However, two non-proprietary, trailing-end terminals have been developed for 31-in. tall W-beam guardrail. Both terminals were two post systems that utilize Breakaway Cable

Terminal (BCT) cable assemblies, bearing plates, and 6-in. x 8-in. x 72-in. long foundation tubes to anchor the W-beam. The two main differences between the two terminals were 1) the struts between the foundation tubes and 2) the size of the breakaway timber posts placed in the foundation tubes, as shown in Figure 6. One terminal utilized an 8½-in. x 5½-in. x 10 gauge channel strut and standard 5½-in. x 7½-in. BCT posts (25-26). The other terminal utilized dual C3x5 channels as the struts between foundation tubes and modified BCT posts measuring 5¼-in. x 7¼-in. (27).

Both terminals were successfully crash tested to MASH TL-3 safety criteria as trailing end terminals, meaning they should only be utilized on the downstream end of guardrail installations that are out of the clear zone of opposing lanes of traffic. The terminal utilizing standard BCT post was evaluated with a 2270P pickup, and the end of length-of-need point was determined to be the sixth post from the end of the installation. Due to the similarity of the terminal systems, this point could be the end of length-of-need for the modified BCT post terminal as well.

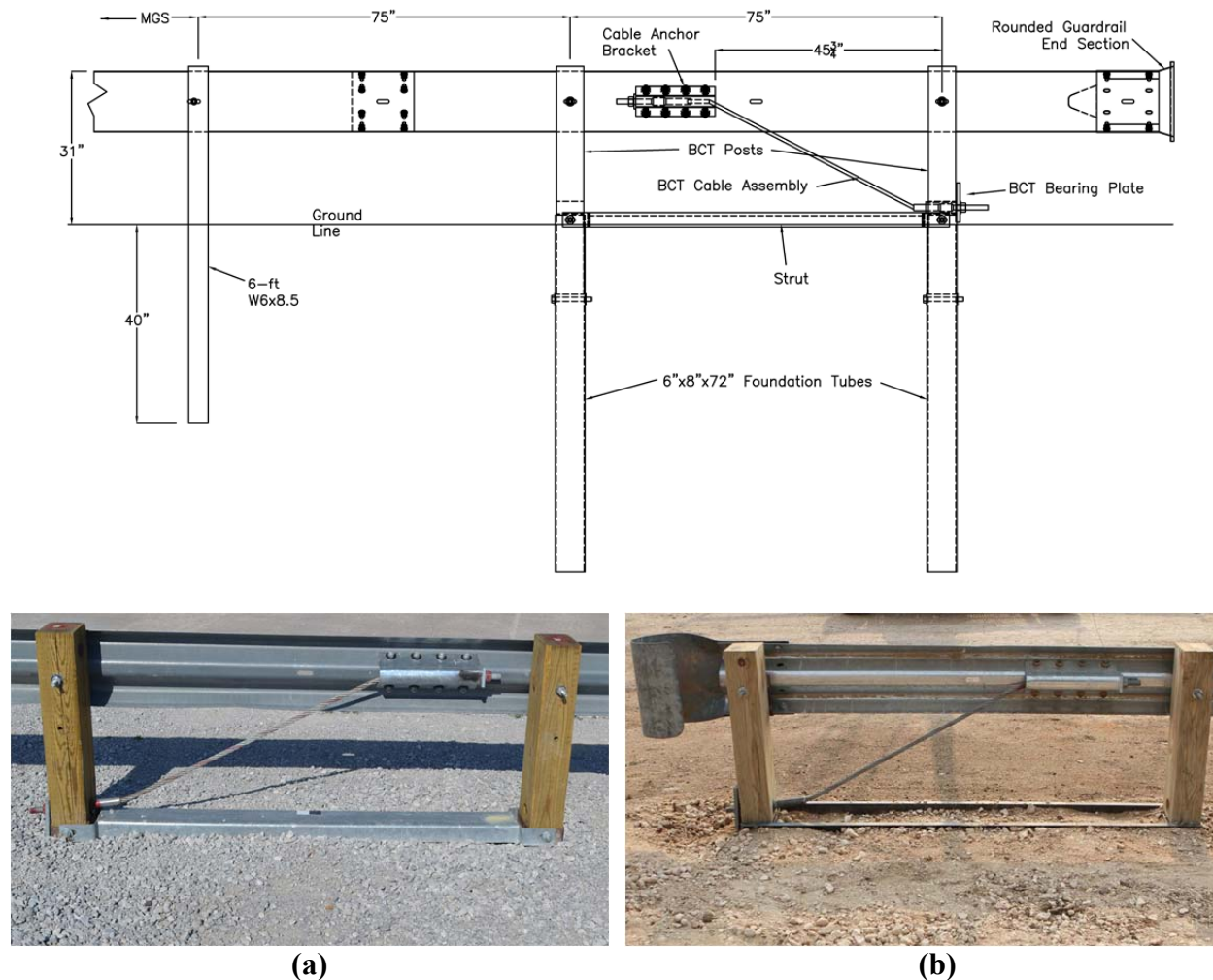


FIGURE 6 Details for the non-proprietary, trailing-end terminals with (a) BCT posts and a 10-gauge, bent-plate strut and (b) modified BCT posts and dual C3x5 struts.

Both terminals were crash tested in combination with a blocked, steel post 31-in. guardrail system. However, these trailing end terminals should be compatible with both steel or timber post systems, and blocked or non-blocked systems. As with most terminals, adequate grading (10:1 or flatter) is recommended around these terminals to ensure proper anchorage and vehicle stability while in contact with the system. Finally, the area behind the terminal should be clear of roadside hazards as these terminals are gating systems. Guidance on the recommended clear area behind the terminal was provided within one of the terminal testing reports (25).

WEAK POST BRIDGE RAILS

Two 31-in. W-beam bridge rails have been developed to MASH standards. Both bridge rails were comprised of non-blocked configurations supported by S3x5.7 weak-posts (28-32), as shown in Figure 7. Non-blocked guardrail maximizes the traversable width of the bridge, while the weak posts limit impact loads and the potential for deck damage. Both systems also utilized $\frac{5}{16}$ -in. diameter bolts and $1\frac{3}{4}$ -in. square washers to attach the rail to the posts.

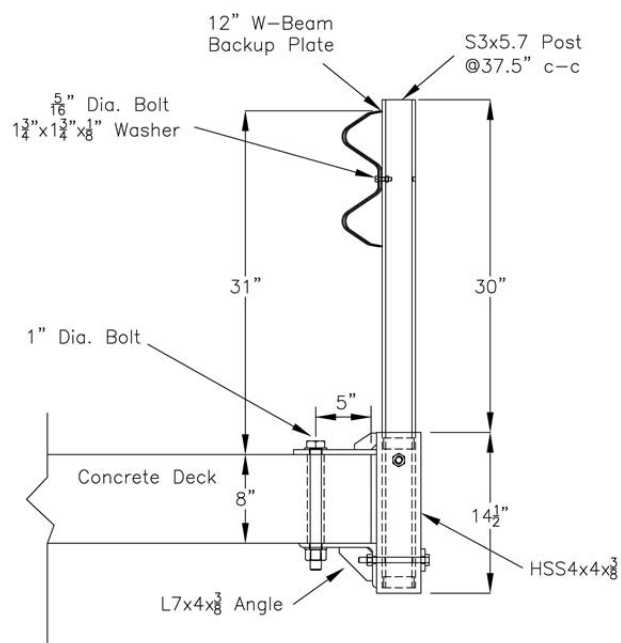
The weak-post MGS bridge rail utilized steel tube sockets mounted to the side of the bridge deck to support the S3x5.7 posts (28-29). The posts were spaced at 37.5 in. on center and had two $\frac{1}{4}$ -in. thick shim plates welded on the upstream and downstream sides of the post so that the post fit snugly in the socket. A $\frac{7}{16}$ -in. thick top mounting plate was welded to the front of the HSS4x4x $\frac{3}{8}$ sockets, and the assembly was attached to the deck with a 1-in. diameter bolt. The bottom of the socket was bolted to an L7x4x $\frac{3}{8}$ angle to provide support for reverse bending and longitudinal loads. This bridge rail utilized 12-in. long W-beam backup plates similar to the non-blocked version of the MGS. This system was successfully crash tested to MASH TL-3 and has a 53.2-in. working width.

The T631 bridge rail utilized a $\frac{5}{8}$ -in. thick baseplate, a $\frac{1}{4}$ -in. thick washer plate, and four $\frac{5}{8}$ -in. diameter bolts to mount the S3x5.7 posts to the top of the bridge deck (30-32). A $\frac{1}{2}$ -in. diameter shelf bolt was used to support the rail vertically. The T631 bridge rail can be configured with two different post spacings. A 75-in. post spacing was successfully tested and evaluated to MASH TL-2 with a 30.0-in. working width. A MASH 3-11 test was conducted on the 75-in. spacing, but the rail ruptured and the test failed. Reducing the post spacing to 37.5-in. resulted in the T631 being successfully tested and evaluated to MASH TL-3 with a 57.7-in working width.

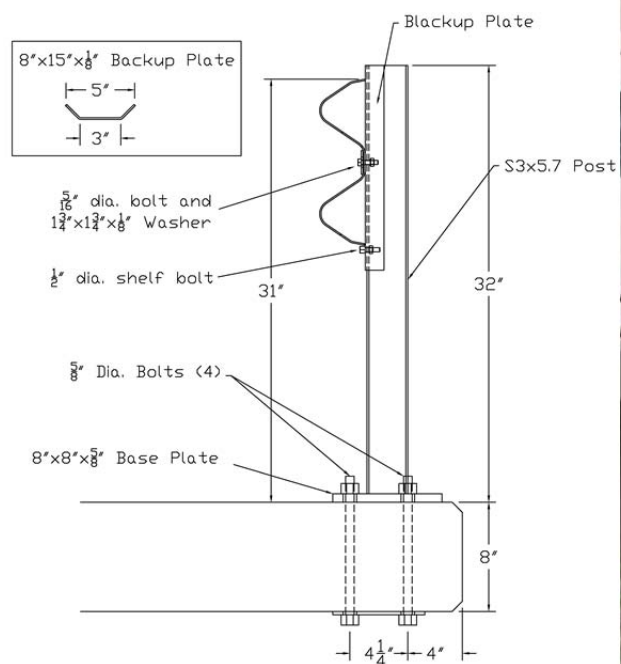
Because the working widths of these bridge rails are so similar to those of standard roadside MGS configurations, these bridge rails do not require guardrail stiffness transitions. The ends of the bridge rails attach directly to an adjacent MGS system utilizing a 75-in. spacing between the outermost bridge post and the adjacent MGS strong post. Additionally, the adjacent MGS may utilize any approved post and/or blockout combination. Guardrail installations utilizing 6-ft posts and placed adjacent to sloped terrain have working widths significantly higher than these weak-post bridge rails. Therefore, it is recommended to utilize either 8-ft or 9-ft posts in the adjacent guardrail installations when steep slopes are present.

GUARDRAIL ATTACHMENTS TO CULVERTS

Two 31-in. W-beam guardrail systems have been developed for attachment to low-fill culverts. The first system utilized the same posts, post spacing, guardrail bolts, backup plates, and sockets



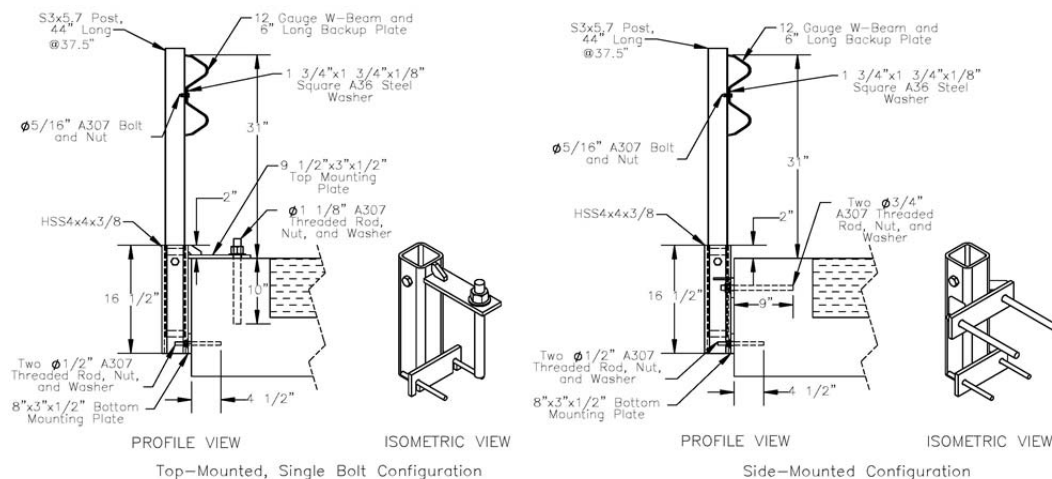
(a)



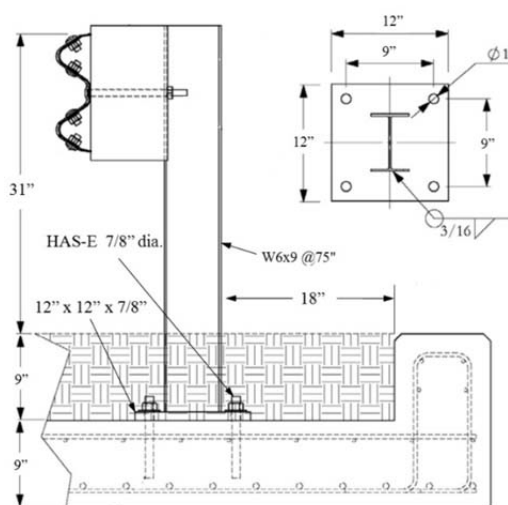
(b)

FIGURE 7 Details and photos of (a) the weak-post MGS Bridge Rail and (b) the T631 Bridge Rail

as the MGS bridge rail. However, the socket attachment hardware was modified to mount the socket to the outside face of culvert headwalls (33-34). Multiple attachment configurations were developed including a top mounted single bolt configuration, which was similar to the bridge rail, and a side mounted configuration, as shown in Figure 8. Both configurations utilized epoxy anchors so that the guardrail system could be attached to both new and existing culvert structures. Because the post and rail were identical to the weak-post MGS bridge rail, these culvert attachment configurations are crashworthy to MASH TL-3 and have the same installation guidance as the weak-post MGS bridge rail.



(a)



(b)



FIGURE 8 Details and photos of (a) side-mounted and (b) top-mounted guardrail systems attached to culverts.

The second system was a strong-post, top-mounted system, as shown in Figure 8. The W6x9 posts were spaced at 75 in. on center and were positioned 18 in. from the inside face of the headwall (35). The posts were welded to baseplates and mounted to the culvert slab with four epoxy anchors. The system requires a minimum soil fill depth of 9 inches. The system was successfully crash tested to MASH TL-3 and has a 49.2-in. working width. The system can be installed with either 8-in. or 12-in. blockouts, but it is not recommended to be installed non-blocked without further analysis. Finally, this system can be directly connected to the other 31-in. W-beam systems shown herein as long as adequate soil grading is provided behind the adjacent systems posts.

TL-2 SYSTEM

A TL-2 version of standard strong-post guardrail has been developed by doubling the post spacing to 12.5-ft. The system was comprised of 31-in. tall W-beam, standard 6-ft W6x8.5 posts, and 8-in. deep blockouts. The system was successfully tested and evaluated to MASH TL-2 and has a 44.3-in. working width (36). Either steel or timber strong-post are compatible with the TL-2 system. However, it is not recommended to install the TL-2 system on slopes, with omitted posts, or in a non-blocked configuration without further analysis.

FUTURE DEVELOPMENTS

Other MASH crashworthy, W-beam guardrail systems exist beyond the systems presented herein. Some are proprietary, some utilize different guardrail heights, and some were left out simply due to a lack of space in the paper (e.g., guardrail in mow strips and guardrail stiffness transitions). In addition, there are numerous 31-in. W-beam systems that were initially developed and evaluated under prior safety standards that have yet to be evaluated to MASH including:

- MGS with reduced post spacing
- MGS with curb
- MGS on approach slopes
- MGS with alternative timber species and round posts

The details and installation guidance provided for the various guardrail configurations herein incorporate all of the knowledge currently available on the testing and evaluation of 31-in. guardrail systems. However, it is recognized that the future will bring new developments, new systems, and new testing and evaluations on performance of W-beam guardrail. The guidance provided herein should be used in combination with any future knowledge to optimize the performance of W-beam guardrail systems.

ACKNOWLEDGMENTS

The authors wish to acknowledge several sources that made a contribution to this project: (1) TTI and MwRSF for conducting and documenting all of the full-scale crash tests referenced

herein, and (2) FHWA, NCHRP, and numerous State Departments of Transportation for sponsoring all of the research related to W-beam guardrail referenced herein.

REFERENCES

1. Polivka, K.A., et al., *Development of the Midwest Guardrail System (MGS) for Standard and Reduced Post Spacing and in Combination with Curbs*, Research Report No. TRP-03-193-04, Midwest Roadside Safety Facility, University of Nebraska-Lincoln, Lincoln, NE, September 1, 2004.
2. Sicking, D. L., J. D. Reid, and J. R. Rohde. Development of the Midwest Guardrail System, *Transportation Research Record: Journal of the Transportation Research Board*, No. 1797, 2002, pp. 44–52.
3. Ross Jr., H. E., D. L. Sicking, R. A. Zimmer, and J. D. Michie. *NCHRP Report 350: Recommended Procedures for the Safety Performance Evaluation of Highway Features*, 1993.
4. *Manual for Assessing Safety Hardware (MASH)*, AASHTO, Washington, D.C., 2009.
5. Everett, T, and Griffith, M, *AASHTO/FHWA Joint Implementation Agreement for MASH*, FHWA Memorandum, January 7, 2016.
6. Polivka, K.A., et al., *Performance Evaluation of the Midwest Guardrail System – Update to NCHRP 350 Test No. 3-11 with 28" C.G. Height (2214MG-2)*, Research Report No. TRP-03-171-06, Midwest Roadside Safety Facility, University of Nebraska-Lincoln, Lincoln, NE, October 11, 2006.
7. Polivka, K.A., et al., *Performance Evaluation of the Midwest Guardrail System – Update to NCHRP 350 Test No. 3-10 (2214MG-3)*, Research Report No. TRP-03-172-06, Midwest Roadside Safety Facility, University of Nebraska-Lincoln, Lincoln, NE, October 11, 2006.
8. Gutierrez, D.A., et al. *Midwest Guardrail System (MGS) with Southern Yellow Pine Posts*, Research Report No. TRP-03-272-13, Midwest Roadside Safety Facility, University of Nebraska-Lincoln, Lincoln, NE, September 4, 2013.
9. Stolle, C.J., et al., *Evaluation of the Midwest Guardrail System (MGS) with White Pine Wood Posts*, Research Report No. TRP-03-241-11, Midwest Roadside Safety Facility, University of Nebraska-Lincoln, Lincoln, NE, March 28, 2011.
10. Bielenberg, R.W., et al., Performance of the Midwest Guardrail System with Rectangular Wood Posts, *Transportation Research Record: Journal of the Transportation Research Board*, No. 2437, 2014, pp. 27–40.
11. Bligh, R.P., et al., MASH Test 3-10 on 31-in. W-Beam Guardrail with Standard Offset Blocks, Research Report No. 9-1002-4, Texas A&M Transportation Institute, College Station, TX, March 2011.
12. Schrum, K.D., et al., *Safety Performance Evaluation of the Non-Blocked Midwest Guardrail System (MGS)*, Research Report No. TRP-03-262-12, Midwest Roadside Safety Facility, University of Nebraska-Lincoln, Lincoln, NE, January 24, 2013.
13. Reid, J.D., et al. Midwest Guardrail System without Blockouts. *Transportation Research Record: Journal of the Transportation Research Board*, No. 2377, 2013, pp. 1–13.
14. Abu-Odeh, A.Y., et al., *Development and Evaluation of a MASH TL-3 31-in. W-beam Median Barrier*, Research Report No. 9-1002-12-8, Texas A&M Transportation Institute, College Station, TX, January 2014.
15. Wiebelhaus, M.J., et al., *Development and Evaluation of the Midwest Guardrail System (MGS) Placed Adjacent to A 2:1 Fill Slope*, Research Report No. TRP-03-185-10, Midwest Roadside Safety Facility, University of Nebraska-Lincoln, Lincoln, NE, February 24, 2010.
16. Polivka, K.A., et al., Midwest Guardrail System Adjacent to a 2:1 Slope, *Transportation Research Record: Journal of the Transportation Research Board*, No. 2060, 2008, pp. 74–83.

17. Abu-Odeh, A.Y., et al., *MASH TL-3 Testing and Evaluation of the W-beam Guardrail on Slope*, Test Report No. 405160-20, Texas A&M Transportation Institute, College Station, TX, March 2013.
18. McGee, M.D., et al., *Development of an Economical Guardrail System for Use on Wire-Faced, MSE Walls*, Research Report No. TRP-03-235-11, Midwest Roadside Safety Facility, University of Nebraska-Lincoln, Lincoln, NE, February 2012.
19. Lechtenberg, K.A., et al., Non-blocked Midwest Guardrail System for Wire-Faced Walls of Mechanically Stabilized Earth, *Transportation Research Record: Journal of the Transportation Research Board*, No. 2262, 2011, pp. 94–106.
20. Haase, A.J., et al., *Midwest Guardrail (MGS) with 6-ft Posts Adjacent to a 1V:2H Fill Slope*, Research Report No. TRP-03-320-16, Midwest Roadside Safety Facility, University of Nebraska-Lincoln, Lincoln, NE, August 22, 2016.
21. Lingenfelter, J. L., et al., *Midswest Guadrail System (MGS) with an Omitted Post*, Research Report No. TRP-03-326-16, Midwest Roadside Safety Facility, University of Nebraska-Lincoln, Lincoln, NE, February 22, 2016.
22. Bielenberg, R.W., et al., *Midwest Guardrail System for Long-Span Culvert Applications*, Report No. TRP-03-187-07, Midwest Roadside Safety Facility, University of Nebraska-Lincoln, Lincoln, NE, November 16, 2007.
23. Bielenberg, R.W., et al., Midwest Guardrail System for Long-Span Culvert Applications, *Transportation Research Record: Journal of the Transportation Research Board*, No. 2025, 2007, pp. 3–17.
24. Meyer, D.T., et al., *Increased Span Length ofr the MGS Long-Span Guardrail System Part II: Full-Scale Crash Testing*, DRAFT Report No. TRP-03-339-16, Midwest Roadside Safety Facility, University of Nebraska-Lincoln, Lincoln, NE, October 11, 2016.
25. Mongiardini, M., et al., *Downstream Anchoring Requirements for the Midwest Guardrail System*, Report No. TRP-03-279-13, Midwest Roadside Safety Facility, University of Nebraska-Lincoln, Lincoln, NE, October 28, 2013.
26. Mongiardini, M., et al., Dynamic Evaluation and Implementation Guidelines for a Nonproprietary W-Beam Guardrail Trailing-End Terminal, *Transportation Research Record: Journal of the Transportation Research Board*, No. 2377, 2013, pp. 61–73.
27. Arrington, D.R., et al., *MASH Test 3-37 of the TxDOT 31-Inch W-Beam Downstream Anchor Terminal*, Test Report No. 9-1002-6, Texas A&M Transportation Institute, College Station, TX, December 2011.
28. Thiele, J.C., et al., *Development of a Low-Cost, Energy-Absorbing Bridge Rail*, Report No. TRP-03-226-10, Midwest Roadside Safety Facility, University of Nebraska-Lincoln, Lincoln, NE, August 11, 2010.
29. Thiele, J.C., et al., Development of a Low-Cost, Energy-Absorbing Bridge Rail, *Transportation Research Record: Journal of the Transportation Research Board*, No. 2262, 2011, pp. 81–93.
30. Williams, W., F., et al., *Crash Test and Evaluation of the TxDOT T631 Bridge Rail*, Test Report No. 9-1002-12-10, Texas A&M Transportation Institute, College Station, TX, January 2012.
31. Williams, W., F., et al., *MASH TL-3 Crash Testing and Evaluation of the TxDOT T631 Bridge Rail*, Test Report No. 9-1002-12-12, Texas A&M Transportation Institute, College Station, TX, July 2016.
32. Williams, W., F., et al., Design and Full-Scale Testing of Low-Cost TxDOT Type T631 Bridge Rail for MASH Test Level 2 and 3 Applications, *Transportation Research Record: Journal of the Transportation Research Board*, No. 2521, 2015, pp. 117–127.
33. Schneider, A.J., et al., *Safety Performance Evaluation of Weak-Post, W-beam Guardrail Attached to Culvert*, Report No. TRP-03-277-14, Midwest Roadside Safety Facility, University of Nebraska-Lincoln, Lincoln, NE, February 12, 2014.

34. Rosenbaugh, S.K., et al., Weak-Post W-Beam Guardrail Attachment to Culvert Headwalls, *Transportation Research Record: Journal of the Transportation Research Board*, No. 2437, 2014, pp. 41–51.
35. Williams, W., F., et al., *MASH Test 3-11 of the W-Beam Guardrail on Low-Fill Box Culvert*, Test Report No. 405160-23-2, Texas A&M Transportation Institute, College Station, TX, January 2012.
36. Sheikh, N.M., et. al., MASH Test 2-11 of the 31-Inch W-Beam Guardrail with 12.5-ft Post Spacing, Test Report No. 602291-1, Texas A&M Transportation Institute, College Station, TX, August 2014.

Evaluation of Radar Speed Sign for Mobile Maintenance Operations

ALI JAFARNEJAD

JOHN GAMBATESE

Oregon State University

Road maintenance projects are often short-term and require working in proximity to the ongoing traffic. Due to the temporal and mobile nature of road maintenance projects, there are often fewer or less effective safety devices that can be implemented, resulting in the exposure of maintenance workers and moving traffic to greater risks, and the likelihood of crashes and fatalities. One way to mitigate these risks is to take advantage of speed reduction mechanisms throughout the work zone. A radar speed sign (RSS) is a traffic control device that measures the speed of oncoming vehicles and displays it to the drivers. Research shows that an RSS is a promising tool for positively affecting driver behavior in speed zones. The objectives of the study presented in this paper were to (1) evaluate the impacts of truck-mounted RSSs on vehicle speeds in maintenance work zones; and (2) determine the extent to which the RSSs apply to, and are appropriate for, typical mobile maintenance operations. In this regard, truck mounted RSSs are employed in four multi-lane maintenance work zones in the state of Oregon in the US. In each work zone, the vehicles' speed is collected with (treatment) and without (control) the RSS display operating. Descriptive statistics were used to summarize collected data, and a two-sample t-test was applied to each case study to compare the speed difference between control and treatment cases. The results of this study show that vehicles' speed is typically lower, and adjacent vehicles have lower speed variability, when the RSS is used. Furthermore, with the application of RSSs, the percentage of vehicles exceeding the speed limit reduces. Based on these findings, an RSS proves to be a promising device for controlling vehicle speed and making the work zones safer for both motorists and workers. Thus, using truck-mounted radar speed signs during mobile maintenance operations is recommended.

Compliance Crash Testing of the CA ST70 Side-Mounted Bridge Rail

VUE HER

California Department of Transportation

The California Department of Transportation (Caltrans) is faced with Right-of-Way issues and other limitations that impede placement of standard bridge rails mounted to the top of bridge decks. The Caltrans Division of Engineering Services and the Highway Safety Features New Products Committee, a committee comprised of representatives from several Divisions within Caltrans, recognizes that crash testing of a side mounted bridge rail that meets current MASH 2009 Test Level 4 (TL-4) rated guidelines is a high priority. The objective of this research project is to design and test a side mounted bridge rail that will meet the evaluation criteria of MASH 2009 TL-4 for longitudinal barriers. The design criteria for the side mounted bridge rail are as follows:

1. Must meet MASH 2009 Test Level 4 evaluation criteria
2. Low-Maintenance - minimal damage to bridge deck from TL-4 impact loading

The California ST-70 Side Mounted Bridge Rail was developed to meet this criteria. The all steel longitudinal barrier is 42 inches high and consists of four rails with posts every ten feet. It is mounted to the side of a bridge deck by five 1-1/4 inch high strength anchor rods. On each anchor rod, there are two disk springs stacked together totaling 10 per post. For testing, the end posts were rigidly mounted to the bridge deck and did not have disk springs. The disk springs have an outer and inner diameters of 5 and 1-1/2 inches. The disk springs allow the bridge rail to dampen some of the energy from impact, spreading the load to adjacent post and lessening damage to the bridge deck.

MASH 2009 TL-4 tests 4-10, 4-11, and 4-12 have been completed on the California ST-70 Side Mounted Bridge Rail. The barrier successfully redirected the 2270P, 1100C, and 10000s vehicles. The impact point for tests 4-11 and 4-10 was between posts 3 and 4. For test 4-11, the upper three sets of disc springs went into plastic deformation and required replacement. Test 4-10 did not have any disc springs that permanently deformed and thus, did not require any disc spring replacements. Other damage to the barrier for tests 4-11 and 4-10 were cosmetic and not structural. Impact point for test 4-12 was between posts 2 and 3. The upper disc springs for both posts went into plastic deformation. The lug nuts/studs on the 10000s vehicle dented the two inner rails during impact. It is suggested that the bridge rail disc springs and rail are promptly inspected after any significant impacts. All three crash tests passed the MASH 2009 safety evaluation criteria.

Development of MASH TL-5 Steel Median Safety Barrier

RICHARD A. CLAUSIUS
ArcelorMittal Global R&D

MICHAEL GREMLING
ArcelorMittal / CRM Group – AC&CS

This presentation will cover the successful development of a new MASH TL-5 rated steel median safety barrier from initial concept, optimization and final design using FEA Modeling of the barrier, soil, and vehicles required; and compare modeling and actual crash test results. This proprietary barrier was developed as an alternative to existing high containment median barrier technology for the North American Market and is the first MASH TL-5 approved steel median barrier. The barrier has the capability to contain and safely redirect a small car, quad cab pickup truck, and fully loaded tractor trailer truck. Modeling and optimization of the barrier design required selection of the proper high strength steel for top and bottom rails configurations and posts, development of a spacer and release system, and determination of optimally post and rail spacing along with optimal barrier height. As a result of significant modeling and simulation work using LS-Dyna and knowledge of steel properties by ArcelorMittal/CRM Group along with guidance from Gregory Industries on practicality of manufacturing components and barrier installation, an optimal TL-5 median barrier design was developed.

As a result, successful MASH crash testing of the barrier was completed by hitting the barrier at 62 mph (100 km/hr) and 25° with a 2,425 lb (1,100 kg) car and 5,000 lb (2270 kg) pickup truck, and at 50 mph (80 km/hr) and 15° with a 79,400 lb (36,000 kg) loaded tractor trailer truck. In all three cases the vehicles were safely contained and redirected without rollover and without excessive deceleration and no intrusion into the vehicle occupancy compartment. In addition, a review of the crash test simulations and actual crash tests showed very similar performance.

This project demonstrated good collaboration between the designer/steel supplier and guardrail fabricator in developing a successful barrier design that could meet the higher/more demanding test requirements of MASH, meet FHWA and USA standards, use steel products, be fabricated by the customer, and installed with conventional tooling and practices by a roadway crew.

INNOVATIONS IN ROADSIDE SAFETY HARDWARE AND FEATURES

Development of MASH TL-4 Safety Roller Barrier

FREDERICK MAUER
Gregory Industries

This presentation will cover the successful testing of a MASH TL-4 rated steel and plastic (PVC) median and roadside barrier. The Safety Roller Barrier has also been tested to EN13-17 H1&H2 and approved by Amstrads an Australian and New Zealand association of road agencies, Roads and Maritime Services in NSW Australia and the Korean government. This proprietary barrier was originally developed as an alternative to existing guardrails in Asia. The barrier has the capability to contain and safely redirect a small car, quad cab pickup truck, and box truck.

This is the first barrier of its type that utilizes a “PVC roller technology” which converts some of the typical impact energies associated with vehicle barrier impacts into rotational energy. This conversion process is done as the Safety Roller Barrier rollers rotate control plates. The rotational energy is reduced as the rollers rotate a series of “clutches” mechanisms on the control plates. This action correlates to safer and smoother return of vehicle after a collision.

As a result, successful MASH crash testing of the barrier was completed by hitting the barrier at 62 mph (100 km/hr) and 25° with a 2,425 lb (1,100 kg) car and 5,000 lb (2270 kg) pickup truck, and at 50 mph (80 km/hr) and 15° with a 22,046 lb (10,000 kg) box truck. In all three cases the vehicles were safely contained and redirected without rollover and without excessive deceleration.

Development of a New MASH Guardrail Terminal

JOHN C. DURKOS

Road Systems, Inc.

Many different technologies have been used for W-Beam guardrail terminals to meet the requirements of NCHRP Report 350, Test Level 3. Today's terminals must meet the more severe MASH (Manual for Assessing Safety Hardware) impact conditions for both a small car (2,420 lb. vs. 1800 lb. for NCHRP 350) and a pickup truck (5,000 lb. vs. 4400 lb. for NCHRP 350). This includes successfully passing the more critical shallow angle impacts at the end of the terminal and the increased angle for the Length-Of-Need redirection impact condition. In addition, MASH requires terminals to be tested with the small car at the highest allowable installation height and with the pickup truck at the lowest allowable installation height. As with NCHRP 350, MASH guardrail terminals are expected to be redirective/gating systems.

One of the technologies used for W-Beam guardrail terminals involves sequentially kinking the W-Beam when the terminal is impacted end-on. This technology has been used in over 300,000 NCHRP 350 installations and has proven to be very effective with an excellent field performance. Based on successful field performance, this technology has been tested to and has passed the new MASH criteria meeting Test Level 3. State DOTs will be challenged to manage new inventories of MASH products so the use of existing NCHRP 350 components in MASH products is very desirable.

Although the AASHTO/FHWA joint implementation agreement does not require W-Beam terminals to meet MASH until June 30, 2018, some states have already begun their implementation process requiring MASH terminals exclusively.

Worksite Safety Screens

EVAN COULSON

DANIEL CASSAR

Victorian Roads Corporation

Worksite Safety Screens or Anti-gawk/Anti-debris screens are commonly used in the Victorian and Australian construction industry. Screens are used at worksites to minimize visibility and help prevent distraction of construction activities to the travelling public and to protect workers in close proximity of passing traffic from flying debris. The intent of screens is twofold in that they aim to reduce distraction or prevent gawking from passing motorists and in turn reduce accidents and congestion associated with such as well as protect workers behind the barriers from debris coming from the roadway.

They are typically used on high speed roads or where temporary safety barriers are used on heavily trafficked roads including most major freeways and highways. The screens are usually attached to temporary work zone concrete or steel barrier systems because available working area is often restricted preventing screens from being independent of the barrier system. The construction industry demands safer worksites and one of the responses it has developed to this challenge are these products. Due to the demand to use them, industries desire to further improve and enhance safety at work sites suppliers have responded by providing new innovated treatments to address the challenge. However guidance had been limited up until now.

The barrier systems they are attached to are often not crash tested, to validate performance with the screen attached. VicRoads has attempted to provide guidance to industry, including expectations around the requirements for crash testing, to respond to industries need. However the benefits of worksite safety screens are often challenged due to lack of supporting evidence that they reduce gawking and in turn vehicle accidents or debris from entering the worksite. Their use and more so the benefit they provide is also challenged because the screens themselves could present a risk to workers if errant vehicle engagement with the screen creates "screen debris" which can enter the worksite, or affect road users. Because the use of these screens is unique to Victoria, this presentation presents an opportunity to challenge world's best practice in this area and will attempt to raise awareness of the pro's and con's of worksite safety screens to other road agencies, and how industry might respond to this need.

Study of an Innovative Type of Junction for Elements of Road Safety Barriers

SERGIO MARCO BASSI

DAVIDE BENETTON

ANDREA MILANESE

MARCO ANGHILERI

*La.S.T., Transport Safety Laboratory, Department of Aerospace Science & Technology
Politecnico di Milano*

MICHELE PITTOFRATI

Global Design Technology

In the field of road safety, a fundamental position is held by road restraint systems which increase traffic safety and reduce the consequences of a car accident.

The paper deals with the development of an innovative type of joint that can guarantee an effective behavior when used to connect components of road safety barriers.

Bolted junctions are the common method used to connect the components of road restraint systems. They have some critical aspects, in particular the bearing failure is important for thin elements like those used for road safety barriers.

The idea behind the new type of connection is that of overcoming limitations related to current bolted junctions, developing a joint specially designed to work under a traction load.

The research activity has been based on both experimental tests and numerical simulations with LS-Dyna FE solver.

Experimental tests have been carried out to evaluate the behavior of the new junction itself and to collect data to compare the numerical results with.

Numerical simulations have been used to verify the behavior of the new type of connection, for simplified configurations and for more complex and operative conditions.

The obtained results have shown a good numerical-experimental correlation in terms of force-displacement curves, deformations and failure mechanisms.

FE simulations regarding operative conditions (full scale simulation of a TB51 crash test) have shown the ability of the new connection to work under realistic impact loads.

INTRODUCTION

The problem of road traffic safety is of relevant importance because it involves many millions of people in the whole world. Statistics [1] show that injuries due to road accidents are the eighth leading cause of death globally, with more than 1.2 million people dying every year on roads and another 20-50 million sustaining non-fatal injuries. The costs that have to be supported to deal with the consequences of road crashes have been estimated to be in the order of billions of dollars.

In the field of road safety, a fundamental position is held by road restraint systems which increase traffic safety and reduce the consequences of a car accident deforming themselves while containing and redirecting a vehicle onto its carriageway.

Road barriers have been submitted to a remarkable transformation in the last few years,

with a rapid evolution in terms of effectiveness and performances thanks to the introduction of new Standards based on performance requirements (the European Standard EN 1317 is a suitable example [2]).

While many aspects of road barriers have been extensively modified and optimized to achieve the best possible global result for barriers as whole systems, the methodology used to connect components of barriers themselves has never been modified; the different components of a barrier are linked together with bolted connections.

When bolts are used to connect metal sheets or plates, a characteristic problem between the failure possibilities of a bolted connection is the bearing deformation of the holes of the elements, which is increasingly important with the reduction of the members' thicknesses. Beams and other components of road safety barriers have a characteristic thickness of around 3 mm, therefore they can be considered thin elements. A possible optimization of a road safety barrier, reducing the thickness of its components and improving the material characteristics can accentuate the bearing deformation. Moreover, if there is not any failure of the bolts, the behavior of the connection is not adjustable modifying the connection elements, i.e. the bolts themselves, but only acting on the material or on the characteristic dimensions of the metal sheets.

The research activity has been focused on studying and testing an innovative type of joint to be used on elements of road safety barriers, in particular for the connection between beams. The interest in studying the connection is due to the fact that junctions between elements of a barrier are of primary importance to guarantee the correct behaviour of the barrier itself, because a failure or an unacceptable performance in a main connection would cause a complete loss of effectiveness of the whole restraint system [3].

The idea behind the new connection method is that of overcoming limitations related to current bolted junctions, developing a joint specially designed to work under the typical loads acting on road barriers. Therefore, the objective is to develop a connection with a reliable behaviour, repeatable results and which can be easily designed to sustain the expected workloads.

The research work has been based on both experimental tests and numerical simulations.

Experimental tests have been carried out to evaluate the behavior of the new junction itself and to collect data to compare the numerical results with.

Numerical simulations have been performed to develop a reliable finite element (FE) model of the new connection, through the comparison with experimental outcomes, and to verify the behavior of the new connection in operative conditions.

NEW CONNECTION WORKING PRINCIPLE

The new connection studied in the research activity has been designed to properly work under tensile loads. The idea has been to develop a connection method which undergoes a tensile stress state when it is subjected to the typical loads of a road safety barrier, for example when there is the deformation of the beams of a barrier as a consequence of a vehicle impact.

The ability to convert impact loads into a tensile stress state is a positive aspect of the new junction because with such stress state it is possible to design the connection in an effective way, with characteristic dimensions and material precisely chosen to achieve the desired behavior.

The new connection is composed by two different elements, a flap and a hole, manufactured on the metal sheets to be joined together (Figure 1).



FIGURE 1 New connection, flap and hole.

To put the connection in operation condition, the flap has to be bent inside the hole; the bending of the flap is a process which requires the loading of the flap itself with a force normal to its surface, without any particular tool or technique. Then, with a relative displacement between the metal sheets, as when a vehicle hit a road safety barrier deforming its beams, the hole gets in contact with the flap applying a tensile load to the resistant area of the flap itself. The connection element is able to sustain the load until the failure of the resistant section of its geometry, therefore the stem of the flap. The workload of the junction can be accurately defined working on geometrical aspects, like width and thickness of the resistant section, and on the mechanical properties of the material.

A T-shape has been chosen as the initial geometry of the flap.

EXPERIMENTAL AND NUMERICAL ANALYSES

The design and the verification of the new connection have been done with different kind of both experimental tests and numerical simulations.

The behavior of a single connection element, i.e. one flap-hole couple, has been analyzed as the starting point of the research activity to verify the compliance of the obtained results with the expected outcome. Then, more connection elements have been put together, considering different configurations, to investigate the mutual interaction between them and to verify the ability of a multiple connection to work in an effective way.

The following step has been to introduce the flap junction in a splice section of a road safety barrier to evaluate from a numerical point of view the behavior of the new connection when used on a real barrier geometry and to identify a feasible configuration.

Finally, the ability of the flap connection to sustain the typical loads of a vehicle impact has been analyzed with a numerical analysis of an operative condition, the crash of a bus against a road safety barrier. The most stressed section of the barrier has been modelled in detail with the flap-hole couples as mean of connection.

Experimental Tests

Material Characterization Tests

Uniaxial tensile tests with dogbone specimens have been performed at the beginning of the activity to characterize the steel material of the metal sheets used in this research work. Two steels have been considered, a S235JR steel with a thickness of 3 mm (Figure 2) and a high strength steel with a thickness of 1.8 mm.

The experimental tests have been performed with a MTS 810 Material Testing System, with a test speed of 3 mm/min and a sampling frequency of 4 Hz.

Tests on Simplified Configurations

The second and main step of the experimental phase of the research activity has been the verification of the behavior of the new connection. A single flap junction has been tested at first, then different connection configurations considering multiple elements have been investigated to understand the behavior of the flap-hole system when many of them work together to sustain a load. A total of four simplified configurations has been analyzed (Figure 3):

- Single element connection;
- Two elements – in line connection;
- Two elements – side by side connection;
- Three elements – in line connection.

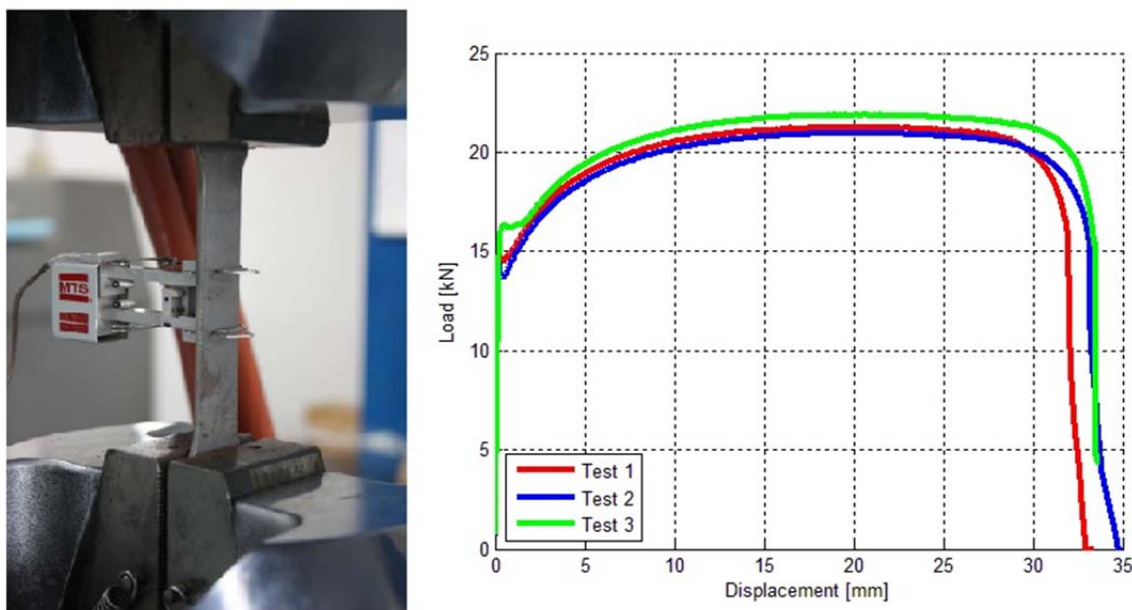


FIGURE 2 S235JR uniaxial tensile tests.

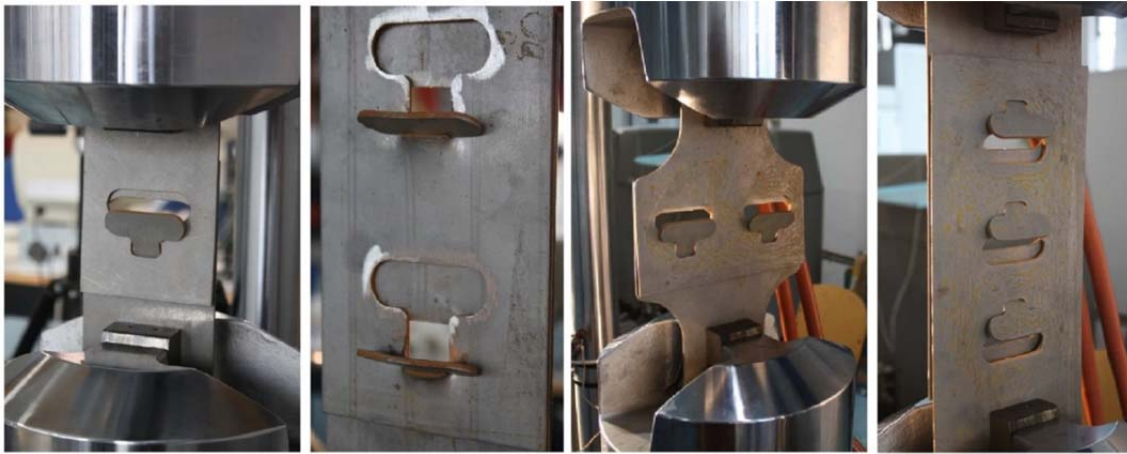


FIGURE 3 Tested configurations: single, double in line, double side by side, triple in line.

The tests on the simplified configurations have been performed with the same characteristics of the material characterization tests, therefore a test speed of 3 mm/min and a sampling frequency of 4 Hz. Also in this case a MTS 810 Material Testing System has been used. The test articles have been manufactured from a 3 mm sheet of S235JR steel, because such thickness and material are of common use for road safety barriers.

Three tensile tests have been performed for each configuration (Figure 4).

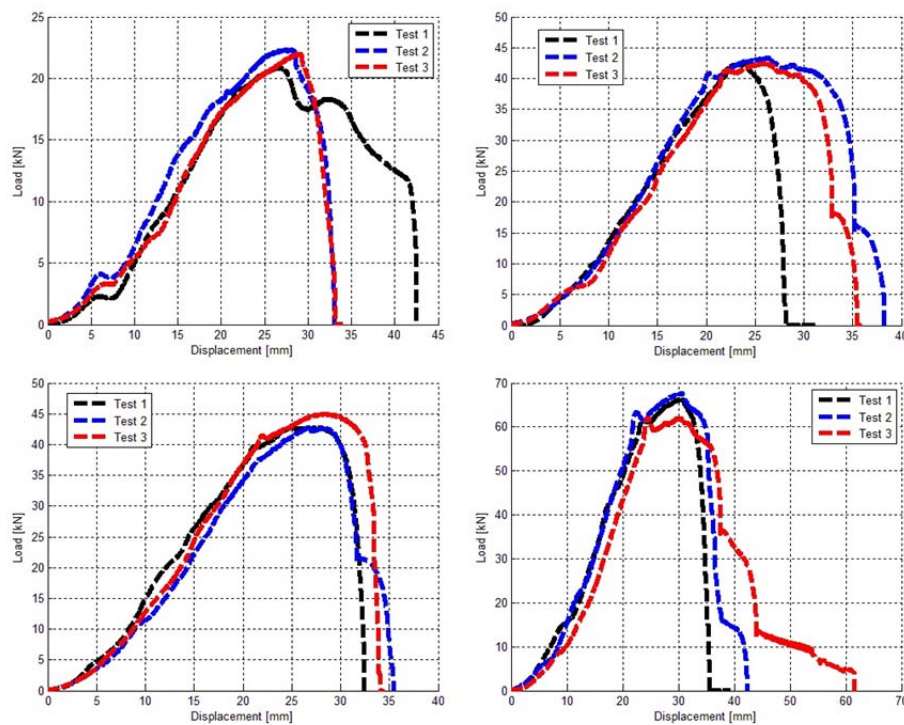


FIGURE 4 Simplified configurations test results (from top left clockwise): single, double in line, triple in line, double side by side.

From the experimental tests it is possible to observe the good repeatability of the results for each configuration, in particular in term of peak load. The results regarding the two elements in line and side by side configurations show that there are not significant differences in the mean values of peak force and elongation at failure, therefore the relative position between the flaps can be considered of negligible importance if the connection line is adequately designed and concentrations of stresses are avoided. Another important experimental outcome is that the workload of the connection is directly proportional with the number of flap, therefore a connection with three flaps is able to sustain a load around three times that of a single element connection while a two flaps connection doubles the single junction workload. The proportional increase of the peak force with the number of flap is a positive aspect of the new method of connection because it improves the predictability of the final workload of the whole junction, making the design process of a complex connection area more straightforward.

To verify the ability of the new kind of connection to work as expected also when lower thickness values are used, a comparison between two different configurations has been considered. The already discussed three elements in line connection made of a S235JR steel with a 3 mm thickness has been compared with a junction, again with three elements in line, made of a high strength steel (HSS) with a 1.8 mm thickness (material already investigated with tests on dogbone specimens).

As it is possible to observe from the load-displacement curves (Figure 5), the behavior of the new connection with high strength steel and a lower thickness is comparable with the previous results obtained with a S235JR steel and a thickness of 3 mm, in terms of absorbed energy, peak force and elongation at failure.

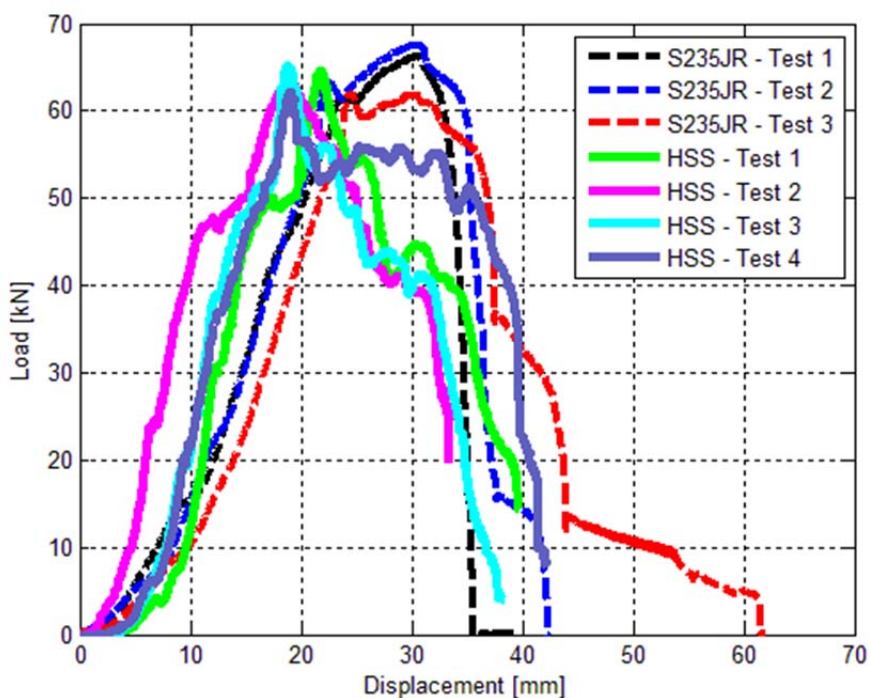


FIGURE 5 Comparison of tests results, triple in line, S235JR 3 mm, HSS 1.8 mm.

The good result in term of absorbed energy is a positive aspect because it shows the ability of the new connection to maintain a good absorption capability (important for components of road safety barriers) also when an optimization of the metal sheets is done, lowering their thickness and improving the mechanical characteristics of the material, while this is a critical point for bolted junctions due to the bearing problem. The positive outcome is also due to the fact that even lowering the thickness of the connected elements, the behavior of the new junction is still effective and dependent on the characteristic dimensions of the resistant section and on the mechanical properties of the material.

Numerical Simulations

Material Characterization Simulations

As for the experimental tests, also for the numerical activity the first step has been based on uniaxial tensile tests with dogbone specimens.

The tests performed experimentally have been reproduced developing a finite element model (with solid hexa elements) of the specimen with the objective of identifying all the parameters necessary to correctly reproduce the behavior of the metal material. Starting from the experimental results, a calibration procedure has been followed until a good correlation of the load-displacement curve has been obtained (Figure 6).

The material behavior has been taken into account not only in term of constitutive law but also regarding the dependency of the failure from the stress state. The influence of the state of stress on the failure has been considered through a failure algorithm based on the triaxiality factor [4], [5]. Moreover, the dependency of the results from the characteristic dimension of the elements of the mesh has been taken into account considering a regularization curve (Figure 6).

The calibration activity has been done for both the steel materials studied in this research activity, S235JR and HSS.

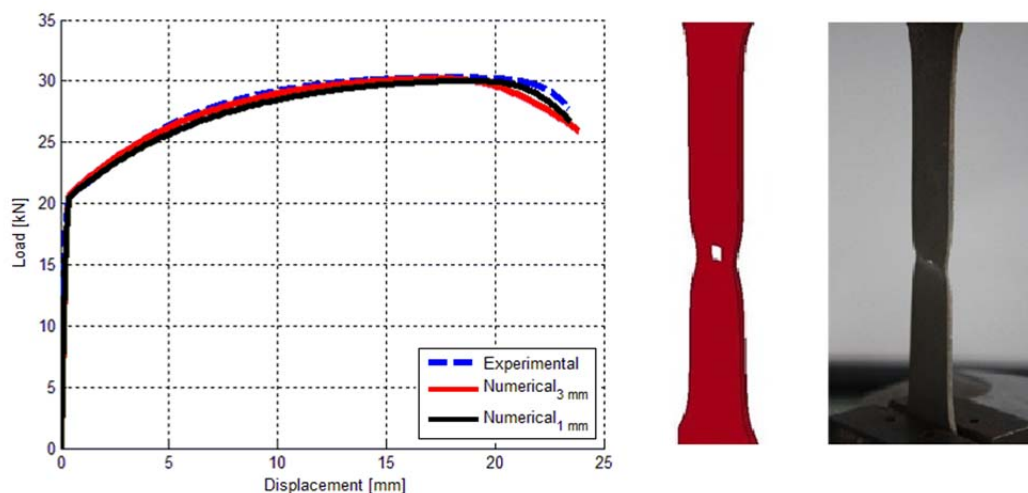


FIGURE 6 S235JR numerical-experimental correlation of uniaxial tensile tests.

Simulations on Simplified Configurations

The next step of the numerical phase has been the analysis of the behavior of the new connection considering the same simplified configurations previously tested. Therefore, a FE model of each configuration (single, double in line, double side by side and triple in line) has been developed, with solid hexa elements. A numerical-experimental correlation has been performed, comparing the simulation results with experimental ones for test articles with a thickness of 3 mm and S235JR material. The results of this process have been FE models of the connection configurations which have been considered validated.

The comparison between numerical and experimental outcomes has been qualitative and quantitative, qualitative in terms of behavior and failure modes (Figure 7), quantitative regarding the load-displacement curves (Figure 8).

The FE models considered validated have been then used to extend the experimental results, studying different aspects regarding the new connection method or investigating more complex cases.



FIGURE 7 S235JR numerical-experimental qualitative comparison of tests on simplified configurations.

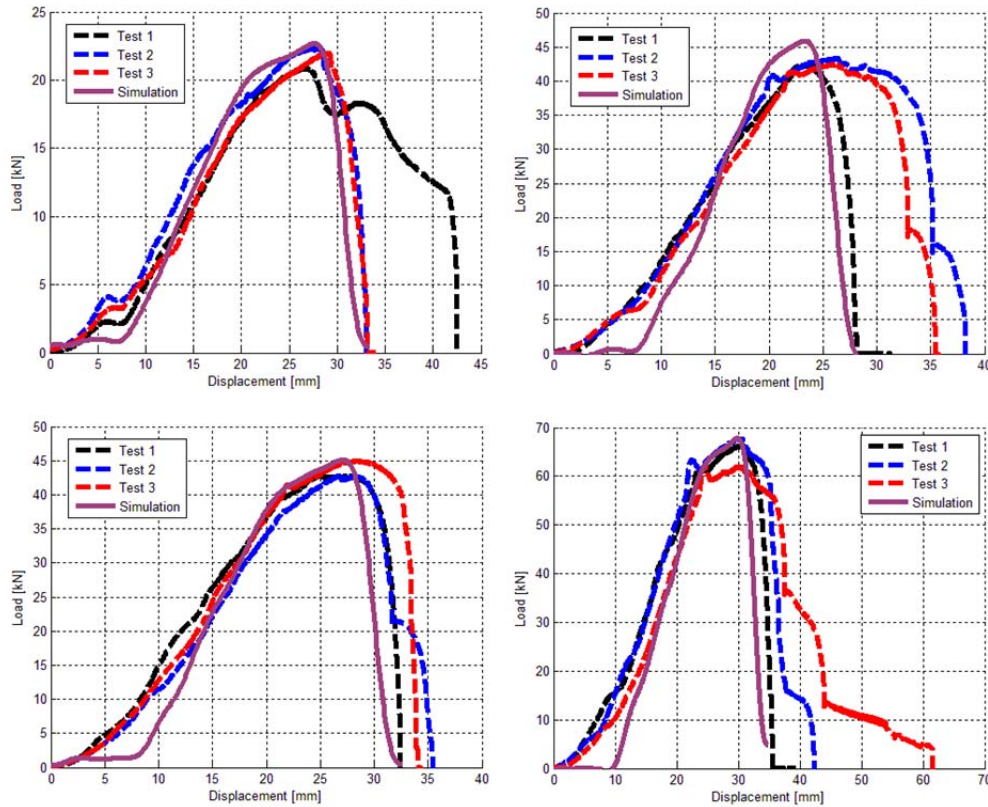


FIGURE 8 S235JR numerical-experimental quantitative comparison of tests on simplified configurations.

The influence of the initial bending required to put the flap connection in its operative condition has been preliminary evaluated with the validated FE models. Different values of deflection have been imposed as an initial condition for the tension phase (from 10 mm to 18 mm), in which the relative displacement between the metal sheets causes the contact between the hole and the flap. The outcome of this analysis is that the difference in the initial deflection of the flap produces a negligible influence on the global results of the simulation (peak force and elongation at failure) because there is not any change in the working principle of the flap-hole connection.

A preliminary optimization of the connection element has been performed evaluating different possible shapes other than the original T-shaped flap. As a result of this phase, a new circular geometry has been identified. Such geometry (Figure 9) has the same positive aspect of the original T-flap but its whole width is lower than the same dimension of the original connection, therefore increasing the efficiency of the junction in term of required space. This aspect is important when many flap-hole systems are used in a real complex junction, because a lower width gives the possibility to use more connection elements without compromising the ability of the whole junction to sustain the required load (critical due to the reduction of the overall resistant area).

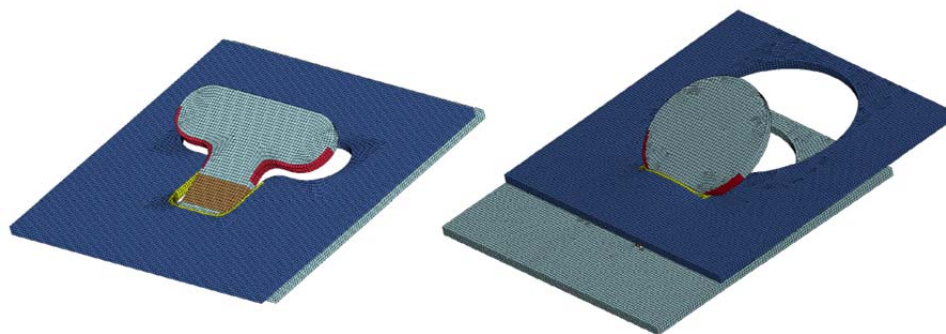


FIGURE 9 Original T-flap and new circular flap.

Simulations on Operative Conditions

The developed numerical models have been used to verify the behavior of the new connection method on real cases, like on a splice of a road safety barrier.

The flap-hole system has been used to connect two beams of a barrier, then a relative longitudinal displacement has been applied between them to load the connection section with a stress state similar to that of a crashed safety barrier. As a result, the ability of the new connection method to work effectively also when used on a real component has been verified, because the junction has shown the same positive results already obtained for the simplified configurations.

The same test has been performed also on a splice with a standard bolted connection and with the same characteristic dimensions of the splice with the flap-hole system. From the comparison between the two solutions, both with S235JR material and a thickness of 3 mm, it is possible to observe that the flap-hole system is able to sustain the same load of the bolted junction, without any undesired concentration of stresses (Figure 10).

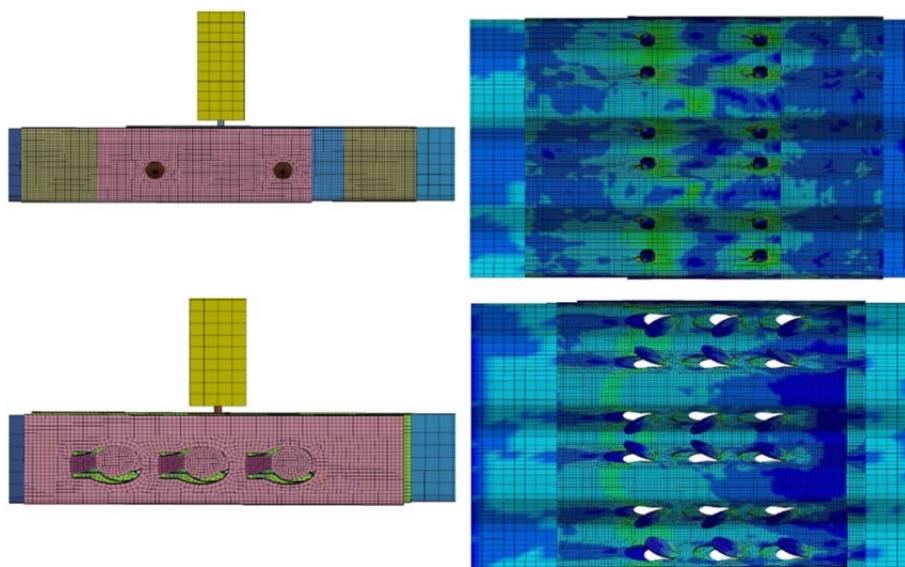


FIGURE 10 Comparison between a bolted connection and the new solution on a splice with Von Mises stresses fringe.

As previously reported, the advantage of the new connection is the possibility to adapt the whole junction resistance to different required workloads by only acting on characteristic dimensions and on the material. Numerical simulations on a splice with the flap-hole system have been performed analyzing the effects of different material and thickness. As previously obtained from experimental tests, even FE simulations have shown the ability of the new connection to maintain an expected behavior when different characteristics of the metal sheets are considered and to provide at the same time a good absorption capability (Figure 11).

The new connection method has been finally verified, through numerical analyses, when used on a road safety barrier in a crash test event.

A FE model of a homologated road safety barrier has been developed at the beginning of this work phase; the finite element model has been realized using shell elements. The road restraint system is characterized by a containment level H2, as indicated by the European Standard EN1317 [2]. The impact event conditions have been defined on the base of the EN1317 Standard as well (Table 1).

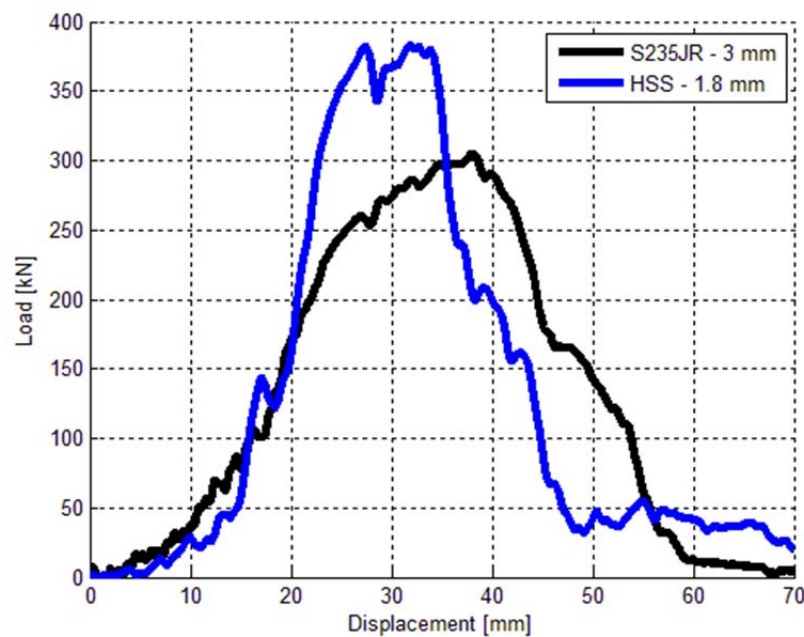


FIGURE 11 Comparison of simulations results, splice S235JR 3 mm, HSS 1.8 mm.

TABLE 1 Impact Conditions.

Test	Impact Speed (km/h)	Impact Angle (°)	Total Mass (kg)	Vehicle
TB51	70	20	13000	Bus

The numerical model has been used to reproduce the TB51 crash test performed for the homologation of the road restraint system. Such model has been tuned to obtain the same global results of the experimental test and at that point it has been considered able to reproduce the real crash event. With this validated numerical tool, the connection sections of the barrier have been analyzed to identify the most stressed junction line; this area has been then modified, introducing a detailed model of the flap-hole connections, discretized with solid hexa elements. As a comparison, the same procedure has been followed considering a standard bolted junction.

The crash tests performed have shown that the FE model with the detailed description of the bolted connection is able to correctly reproduce the real impact event, therefore confirming the accuracy of the simulations, while the numerical test with the detailed flap-hole connections has shown the ability of the innovative junction to be used effectively also on road safety barriers (Figure 12), sustaining the impact loads and with the expected qualitative behavior.

CONCLUSIONS

Road traffic safety is a problem of great importance due to its impact on costs and human lives. Road restraint systems are a fundamental aspect of the problem, because they increase traffic safety and reduce the consequences of a vehicle accident. In this research activity a particular and important part of road safety barriers has been studied, the means used to connect all the elements of the restraint system. A new method of connection has been proposed and investigated to evaluate its ability to work effectively when used on road safety barriers.

The activity on the new junction has been done with both experimental tests and numerical simulations.

The idea at the base of the proposed method is to use a connection element which works under a tensile stress state when in operative conditions on a road safety barrier. The junction is composed by a flap and a hole through which is the load path.

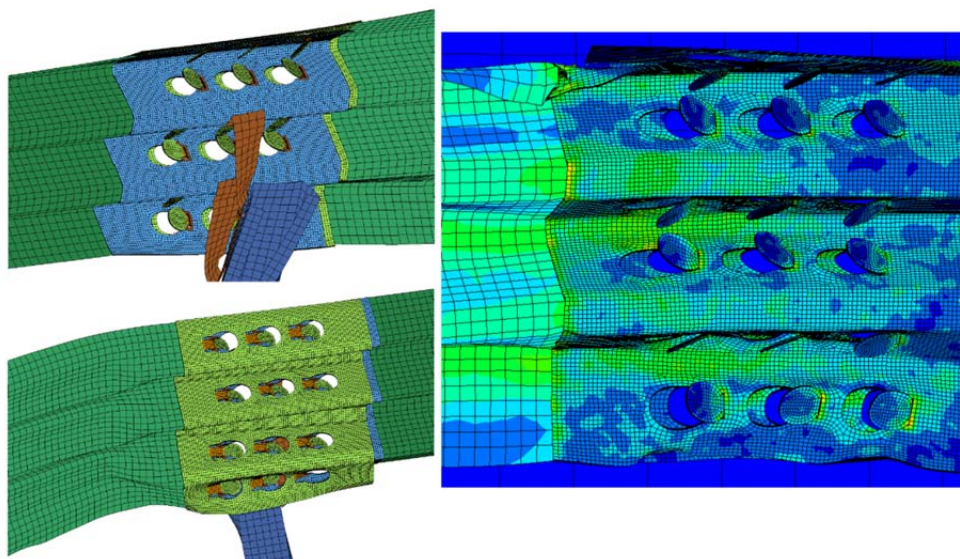


FIGURE 12 New connection on a road safety barrier, during a TB51 crash test, with Von Mises stresses fringe.

Experimental tests have been performed for the characterization of the materials used in the course of the activity, S235JR and a high strength steel, then for the evaluation of the behavior of the new connection when used on simplified configurations. Moreover, acquired data have been used for the validation of the numerical models.

Simulations have been done to develop a validated numerical model of the new connection, in terms of behavior and material characteristics, and to extend experimental results to more complex configurations and operative conditions.

The obtained results have shown that the proposed system is able to work under a tension load as expected, avoiding the bearing problem typical of bolted connections, even when a thickness value lower than standard 3 mm has been considered. Starting from an initial T-shape geometry, an optimized circular shape has been identified. At the end of the activity, with the validated numerical models, configurations with many connection elements working together have been analyzed with a positive outcome; the new junction has shown the ability to work in an effective way when used on a road safety barrier under impact loads.

It is suggested to investigate the ability of the new connection method to work in an effective way for other combinations of thicknesses and materials, to expand the available database and to identify possible limit values.

REFERENCES

1. World Health Organization. *Global status report on road safety 2013: supporting a decade of action*.
2. European Committee for Standardization. *European Standard EN 1317*, Road restraint systems, 2013.
3. Engstrand, K.E. Improvements to the weak-post W-beam guardrail. Master thesis. Worcester Polytechnic Institute, 2000.
4. Bao, Y. Wierzbicki, T. A comparative study on various ductile crack formation criteria. *Journal of Engineering Materials and Technology*, 126 (2004).
5. Lee, Y.W. Wierzbicki, T. Bao, Y. Calibration and evaluation of seven fracture models. *International Journal of Mechanical Sciences*, 47 (2005), pp. 719–743.

Length of Need for Free-Standing, F-Shape, Portable Concrete Barrier

ROBERT W. BIELENBERG

JOHN D. REID

RONALD K. FALLER

*Midwest Roadside Safety Facility
University of Nebraska-Lincoln*

PHIL TENHULZEN

Nebraska Department of Roads

Portable concrete barrier (PCB) systems are often used to redirect errant vehicles through a combination of inertial resistance, lateral friction loads, and tensile loads developed from the mass and friction of the barrier segments. State DOTs and other end users may wish to minimal length PCB installations to shield a hazard or work zone or limit the number of barriers required on the upstream and downstream ends to reduce overall system length. However, concerns with the performance of shorter PCB installations must be considered, including increased lateral deflections and working widths and barrier pocketing. Additionally, no impact testing has been performed near the upstream or downstream ends of the free-standing PCB system to determine the limits of the length of need of the system. These impacts may increase the potential for gating through the system, pocketing, rapid deceleration, and/or vehicle instability.

The objective of this research was to investigate and evaluate the safety performance of a previously developed F-shape PCB system to determine minimum system length and the number of barriers required for the beginning and end of the length of need. LS-DYNA simulation modeling was applied to determine potential beginning and end of length of need points on reduced system lengths to select a configuration for full-scale testing and evaluation of a minimum length PCB system. A 100 ft long PCB installation was selected, and full-scale crash testing was conducted at the beginning and end of length of need of the reduced length system. Test no. NELON-1 was conducted to MASH test designation 3-11 on the beginning of length of need of the 100 ft long PCB installation, and the vehicle was safely redirected. Test no. NELON-2 was conducted to MASH test designation 3-11 on the end of length of need of the 100 ft long PCB installation, but the test was deemed a failure as the vehicle demonstrated a roll angle in excess of 75 degrees. Review of the crash test results suggested that a nine barrier or 112.5-ft long PCB installation would perform acceptably.

INTRODUCTION

Portable concrete barrier (PCB) systems redirect errant vehicles through a combination of inertial resistance developed by acceleration of impacted barrier segments, lateral friction loads, and tensile loads developed from mass and friction of the upstream and downstream barrier segments. Historically, PCB designs have been evaluated and tested using 200-ft long system lengths. It has been assumed that this length of system provides vehicle redirection, resulting

system deflections, and working widths that are representative of longer PCB installations. Thus, recommendations for minimum PCB system lengths have generally been limited to this 200-ft, as-tested length in order to preserve the as-tested system deflections and impact performance. Additionally, guidance on the beginning and end of the length of need (LON) of these systems is typically given as a minimum of 100 ft (i.e., eight barrier segments of 12.5 ft long) in order to preserve performance similar to the existing crash tests. The length of need of a barrier is defined as the portion of a barrier system designed to contain and redirect an errant vehicle.

There are many instances where state DOTs wish to use shorter PCB installations to shield a hazard or work zone or limit the number of barriers required on the upstream and downstream ends to reduce overall system length. Shorter barrier lengths are associated with lower accident frequencies and provide improved cost and safety benefits as long as they retain their ability to safely contain and redirect errant vehicles. However, there are concerns with shorter PCB installations due to the reduction of upstream and downstream barrier mass and friction forces, including higher deflections and working width and the potential for barrier pocketing. Additionally, no impact testing has been performed near the upstream or downstream ends of free-standing PCB systems to determine the limits of the LON of the system. Impacts at or near the barriers at the ends of a free-standing barrier system maybe outside the LON. NCHRP Report No. 358 (1) provides guidance regarding minimum barrier lengths outside the LON, but these recommendations have not been evaluated through crash testing, and no guidance was given regarding minimum total system length. Impacts outside the LON may produce very different barrier performance than impacts near the center of the system, and the results may include the potential for gating of the vehicle through the system, pocketing, rapid deceleration, and/or vehicle instability.

MwRSF previously developed and full-scale vehicle crash tested a 12.5-ft long F-shape temporary concrete barrier system for use in both free-standing and tie-down applications. Full-scale crash testing of this barrier system was conducted under both the NCHRP Report No. 350 (2) and MASH (3) Test Level 3 (TL-3) safety requirements (4-5). During the MASH TL-3 full-scale crash test, test no. 2214TB-2, the F-shape PCB exhibited a dynamic deflection of 79.6 in. when impacting near the middle of a 16 barrier segment test system with an overall length of 200 ft.

There may be potential for shorter runs of free-standing F-shape PCB to safely redirect errant vehicles, but the limits of the system length have not yet been defined. In order to determine minimum system lengths and the required beginning and end of the LON for the free-standing F-shape PCB system, analysis of three main parameters must be considered. These include the number of barriers required on the upstream and downstream end of the system and the overall system length.

The objective of this research was to investigate and evaluate the previously developed F-shape PCB system in order to determine the minimum system length and the number of barriers required for the beginning and end of the LON. LS-DYNA computer simulation of the PCB system was conducted to provide guidance with respect to the potential minimum system length, number of barrier segments on the beginning and end of the LON, and critical impact points for evaluation with full-scale crash testing. The minimum system length was evaluated through full-scale crash testing of the minimum length system at the beginning and end of the LON according to the TL-3 criteria set forth in MASH.

SIMULATION ANALYSIS OF LON AND REDUCED SYSTEM LENGTHS

Evaluation of LON

In order to evaluate the performance of the F-shape PCB at the beginning and end of the LON and minimum system lengths, a model of the free-standing, F-shape PCB system based on previously developed PCB models (6-8) was used. This model correlated well with vehicle trajectory and barrier deflections when compared to test no. 2214TB-2 (5). Details for the baseline model can be found in the research report (9).

A series of simulations were run that impacted each barrier segment in a 16 barrier PCB system with the 2270P vehicle at 62 mph, an angle of 25 degrees, and at an impact point 4.3 ft upstream of the joint between the adjacent segments. This corresponded to the MASH TL-3 impact conditions for test designation no. 3-11. Due to computational instabilities with the truck model as it impacted the first barrier joint downstream of impact, some models were run with an impact point 12 in. to 24in. farther upstream in order to allow the simulations to run to completion. Barrier no. 16 was impacted midway along its length as there was no joint downstream of impact. Each simulation was analyzed to investigate a variety of parameters that would indicate the potential for safe vehicle redirection at that point along the length of the barrier system. These parameters included:

1. Vehicle redirection
2. Vehicle climb
3. Vehicle stability
4. Vehicle parallel time
5. Occupant risk
6. Barrier pocketing
7. Barrier displacement
8. Joint loads and pin deformation

Beginning of LON Simulations

Simulations impacting the first eight barrier segments of the 16 barrier, 200-ft long F-shape PCB system were compared to evaluate a potential beginning of LON point. Example sequential views comparing the behavior of the PCB system for all eight impact points at 800 msec after initial impact are shown in Figure 1. All of the impacts resulted in vehicle redirection due to the inertial resistance of the barriers supplying sufficient redirective forces necessary to prevent the vehicle from gating through the barrier. Similarly, the time required for the vehicle to parallel the barrier during the impacts, the occupant risk values, and the vehicle climb of the barrier were consistent through all eight impacts. Vehicle stability for all of the impacts was acceptable, but vehicle roll tended to increase as the impact point moved upstream.

Barrier motions and deflections were directly affected as the impact of the vehicle neared the upstream end of the system. Maximum lateral barrier deflections and maximum longitudinal displacement of the upstream end barrier are shown in Figure 2. Maximum lateral barrier deflections displayed only minor variations for impacts on the fifth through the eighth barriers in the PCB system. Impacts on the first four barriers of the system showed increasing lateral deflections as the impact approached the end of the system. This was a cause for concern due to

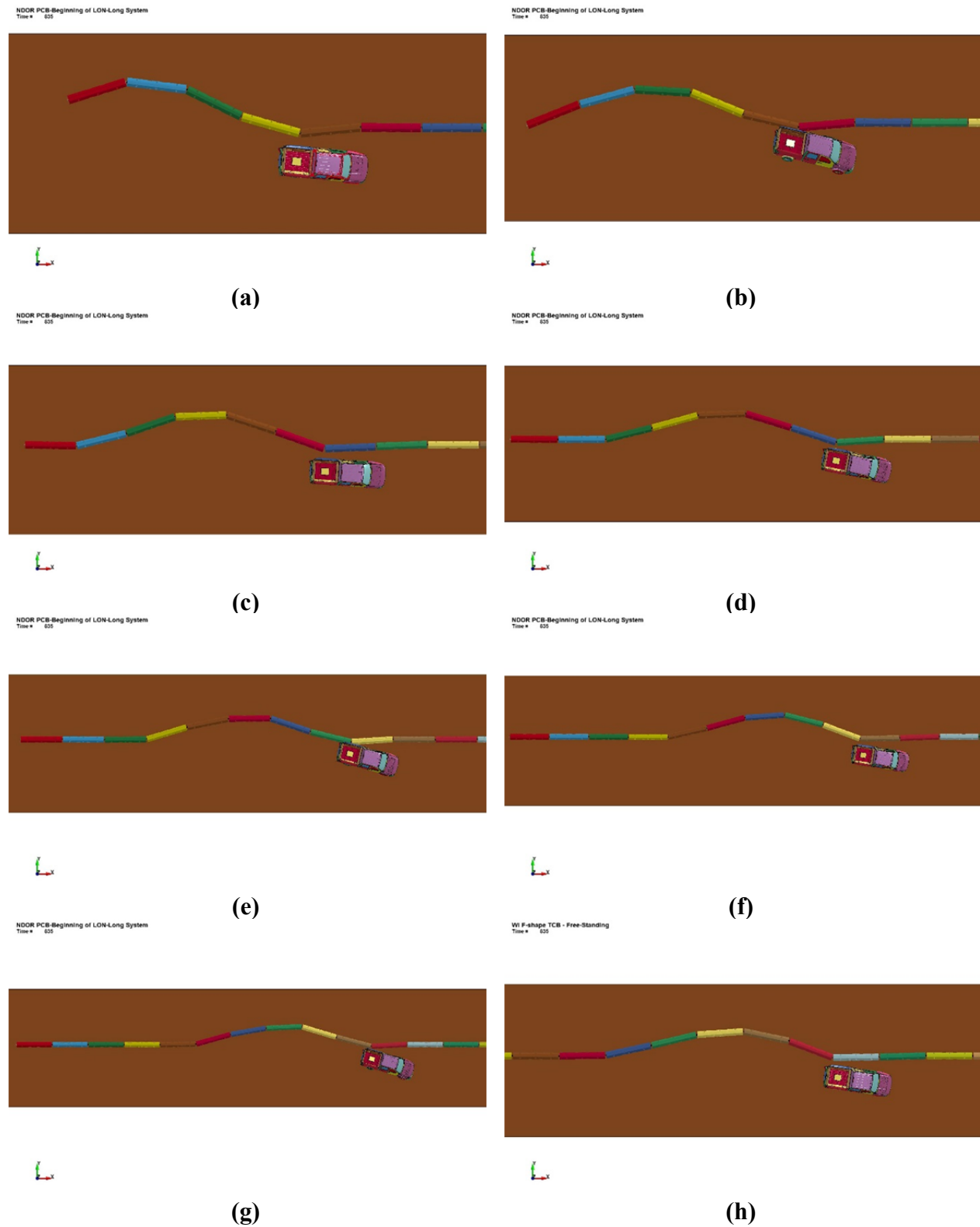
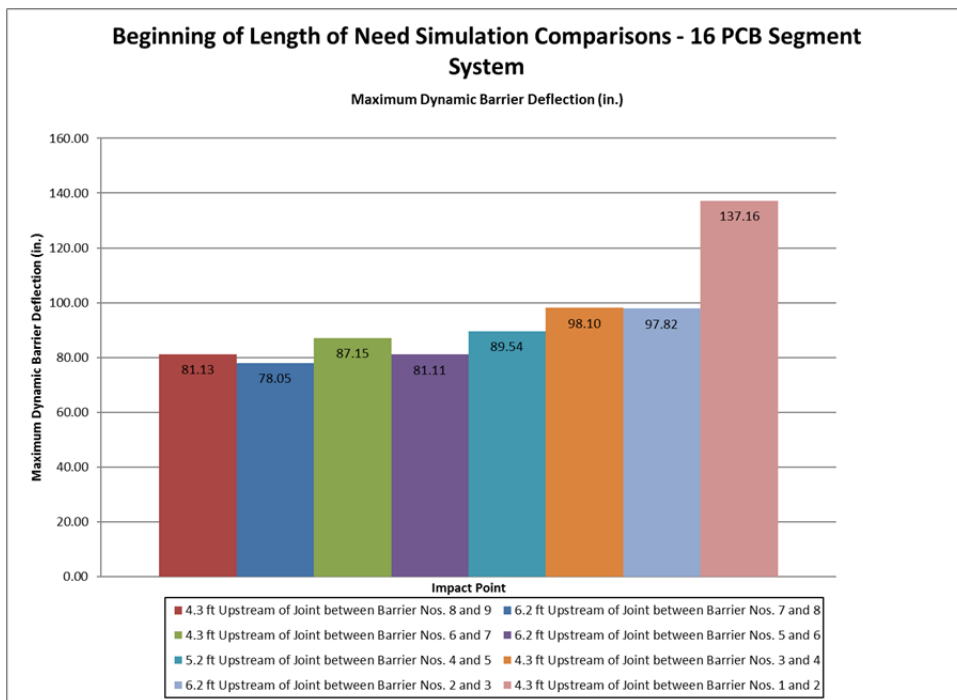
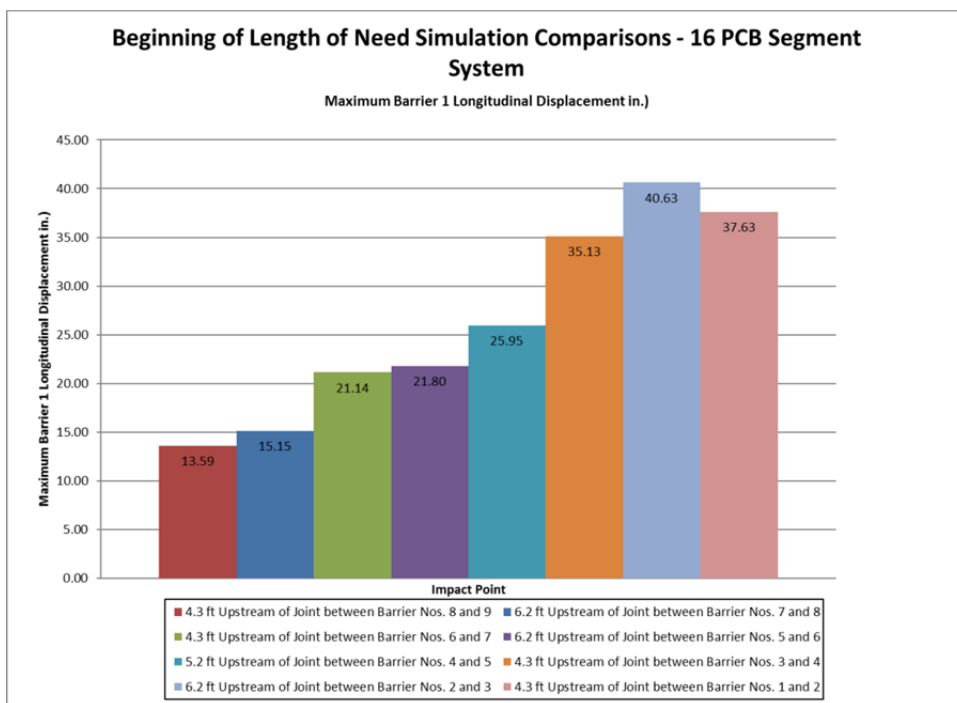


FIGURE 1 Simulation of beginning of LON for 16 Barrier PCB System, $t = 0.800$ s: (a) Barrier 1; (b) Barrier 2; (c) Barrier 3; (d) Barrier 4; (e) Barrier 5; (f) Barrier 6; (g) Barrier 7; and (h) Barrier 8



(a)



(b)

FIGURE 2 Beginning of LON Simulations, barrier displacements: (a) maximum lateral barrier deflection and (b) maximum longitudinal displacement of barrier No. 1

increased lateral deflections potentially affecting vehicle stability as well as requiring larger clear areas behind the barrier system.

Large longitudinal displacements of the barrier no. 1 were observed when impacting closer to the upstream end of the system, and potentially indicated that the barrier system was not providing sufficient tension upstream of the impact. Longitudinal displacements were less severe when impacting barrier nos. 4 through 8, but became larger when impacting the first three barriers of the system. The displacements observed for the impacts on the first three barriers were concerning as they effectively tripled the displacement of the end barrier observed for the baseline impact at the midspan of the system. Pocketing of the barrier ahead of the vehicle was not noted.

Finally, impacts near the upstream end of the system, particularly barrier nos. 1 through 3, produced high levels of deformation in the connecting pin between the barrier segments in the region where it was loaded by the barrier connection loops. This level of deformation was not observed in the baseline, midspan simulation nor was it observed in full-scale crash testing. Thus, the deformation of the pin indicated that the loading of the barrier joints was increasing for impacts near the end of the system.

Based on the concerns for increased deflections, vehicle stability, and joint loading, it was recommended that a minimum of three barrier segments be used to define the beginning of LON of the PCB system.

End of LON Simulations

Simulations impacting the last eight barrier segments of the 16 barrier, 200-ft (61-m) long F-shape PCB system were compared to evaluate a potential end of LON point. Example sequential views comparing the behavior of the PCB system for all eight impact points at 800 msec after initial impact are shown in Figure 3. Impacts on barrier nos. 9 through 14 resulted in vehicle redirection. Impact on barrier nos. 15 and 16 resulted in large deflections of the final barrier segment that represented more of a gating type behavior for the end of the system. Parallel times and occupant risk values were generally consistent for all of the impacts except barrier no. 16 due to the system gating. Vehicle stability for all of the impacts was acceptable, but vehicle roll and yaw tended to increase as the impact point moved downstream. Impacts on barrier nos. 12 through 15 displayed increased vehicle roll, while impacts on barrier nos. 15 and 16 yielded a significant increase in vehicle yaw. These increases potentially indicated a concern for vehicle stability.

Barrier motions and deflections were also affected as the impact of the vehicle neared the downstream end of the system. Maximum lateral barrier deflections and maximum longitudinal displacement of the upstream end barrier are shown in Figure 4. Maximum lateral barrier deflections were again increased for impacts on the last three barriers of the system. Longitudinal displacement of barrier no. 16 on the downstream end was most effected as the vehicle impacts approached the downstream end, especially when the vehicle impacting the last four barrier segments. Impact on barrier nos. 14 through 16 resulted in gating of the end of the barrier. Pocketing of the barrier ahead of the vehicle was not noted even with the increased barrier deflections.

Finally, impacts near the downstream end of the system, particularly barrier nos. 14 and 15, again produced high levels of deformation in the connecting pin adjacent to those barrier segments. The deformation of the pin indicated that the loading of the barrier joints was increasing for impacts near the end of the system.

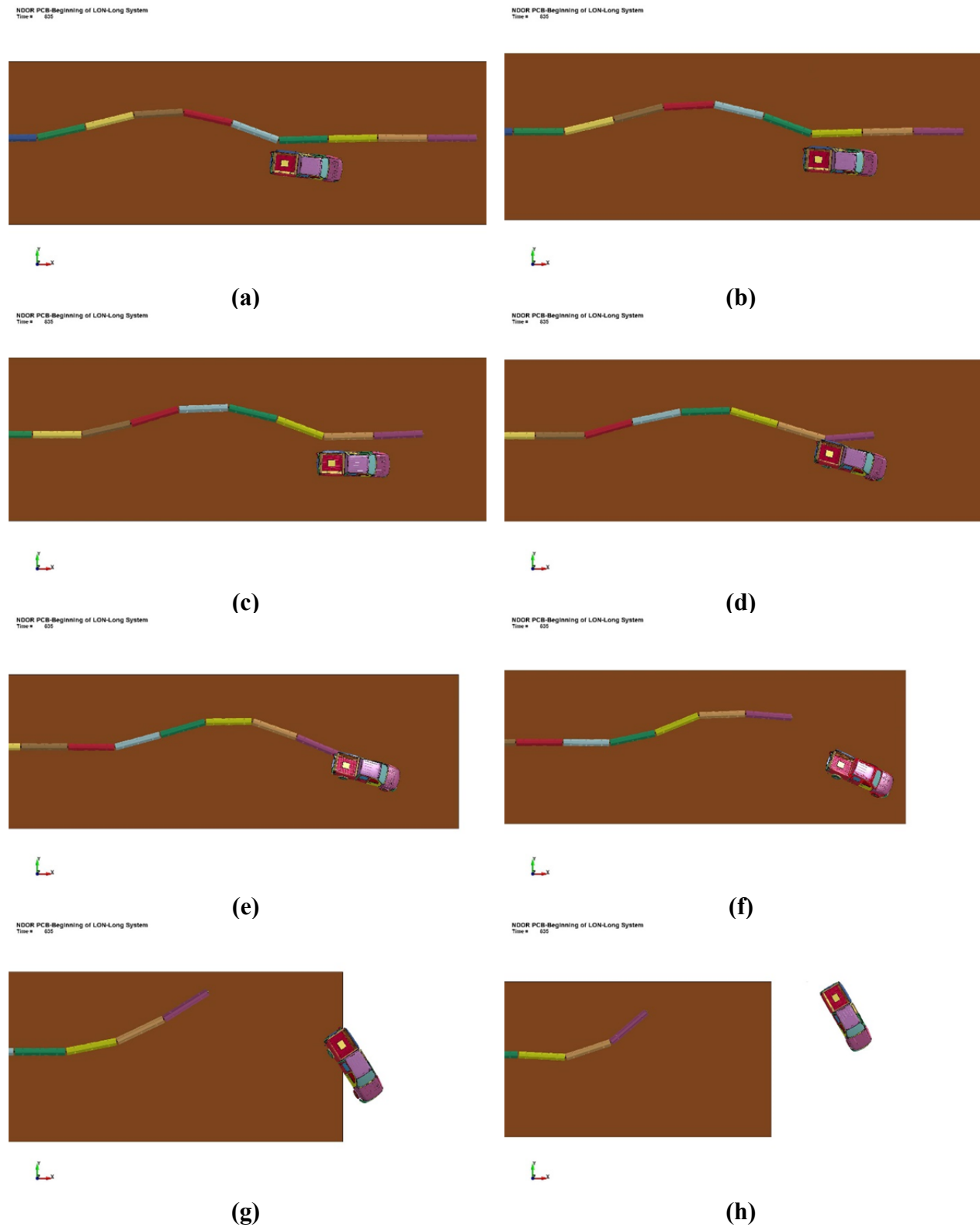
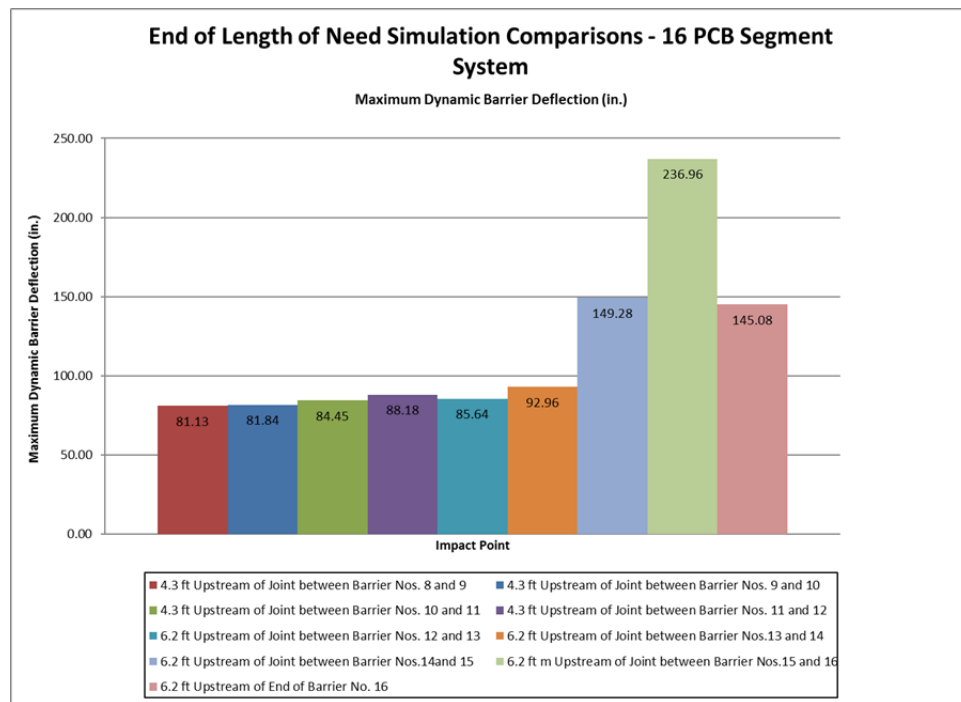
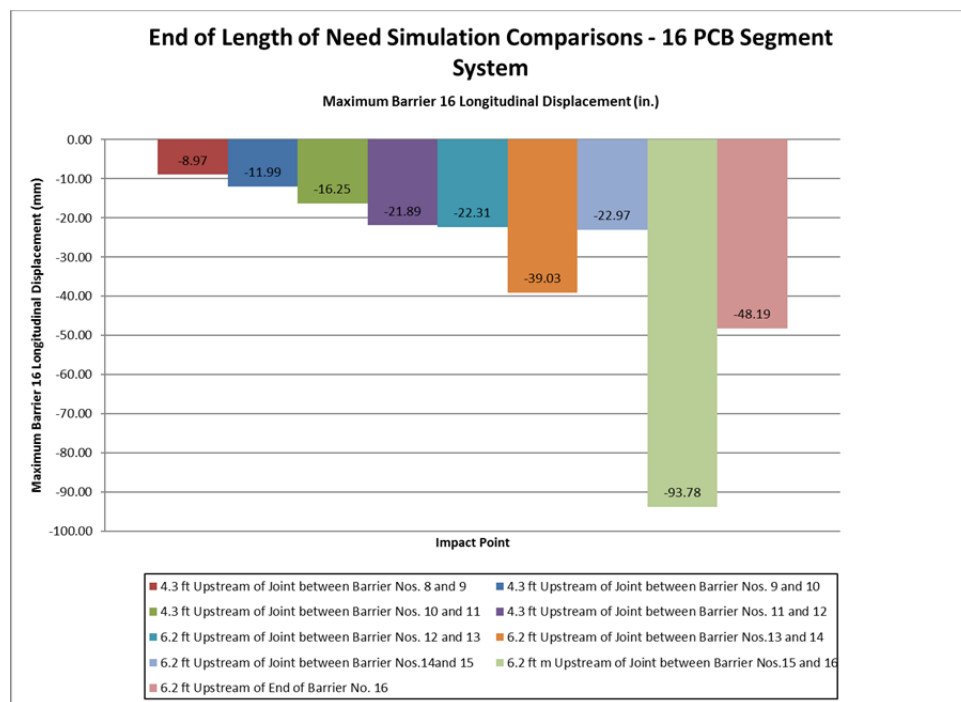


FIGURE 3 Simulation of End of LON for 16 Barrier PCB System, $t = 0.800$ s: (a) Barrier 9; (b) Barrier 10; (c) Barrier 11; (d) Barrier 12; (e) Barrier 13; (f) Barrier 14; (g) Barrier 15; and (h) Barrier 16.



(a)



(b)

FIGURE 4 End of LON Simulations, Barrier Displacements: (a) maximum lateral barrier deflection and (b) maximum longitudinal displacement of barrier No. 16

Based on the concerns for increased deflections, vehicle stability, and joint loading, it was recommended that a minimum of three barrier segments be used to define the end of LON of the PCB system.

Evaluation of Reduced System Lengths

Once beginning and end of LON locations were selected for the 16 barrier F-shape PCB system, the researchers turned to investigation of reduced system length. It was recognized that the overall performance of the barrier system, especially when impacted at the beginning and end of LON, could change if system length were minimized. Thus, simulation models were conducted on reduced length PCB systems to determine their potential to continue to perform safely and recommend a system length for full-scale crash testing and evaluation. Based on the previous analysis of the 16 barrier system, the researchers selected a seven barrier long system for investigation. This length would provide the recommended three barrier segments on each end of the system and a single barrier in the middle of the system to provide a finite redirective length.

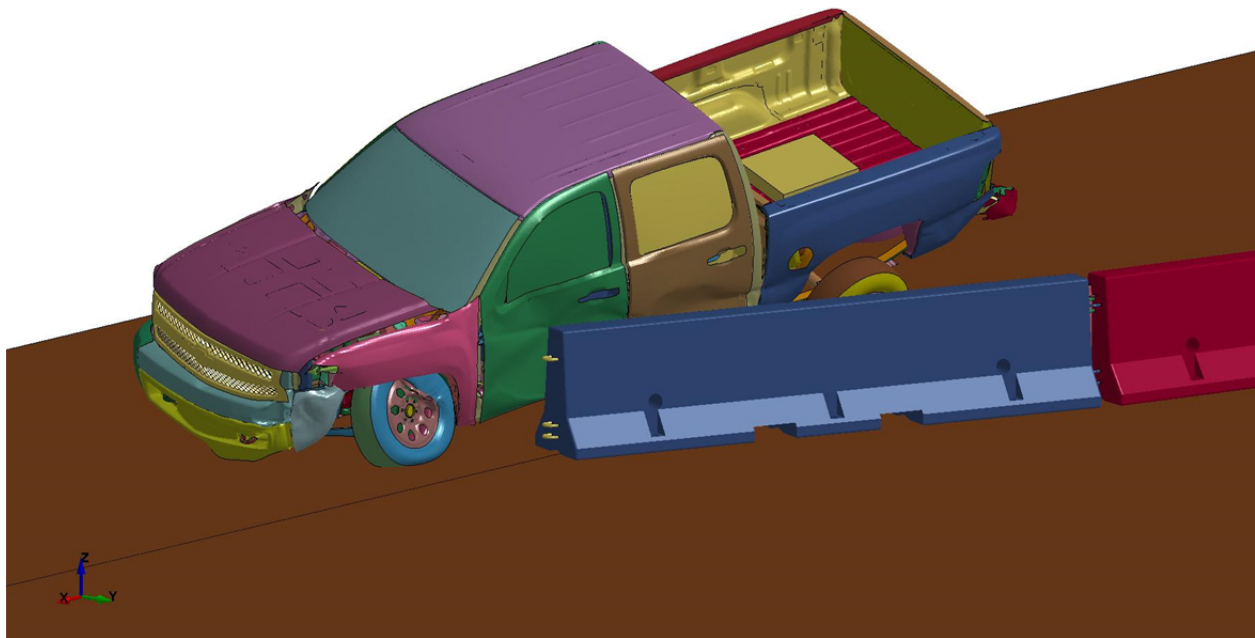
Seven Barrier F-Shape PCB System Simulations

Two simulations were conducted on a seven barrier F-shape PCB system with the 2270P vehicle under the MASH impact conditions for test designation no. 3-11. One simulation was run impacting 4.3 ft upstream of the joint between barrier nos. 3 and 4 to evaluate the beginning of LON for the reduced length system. A second simulation was run impacting 4.3 ft upstream of the joint between barrier nos. 4 and 5 to evaluate the end of LON for the reduced length system.

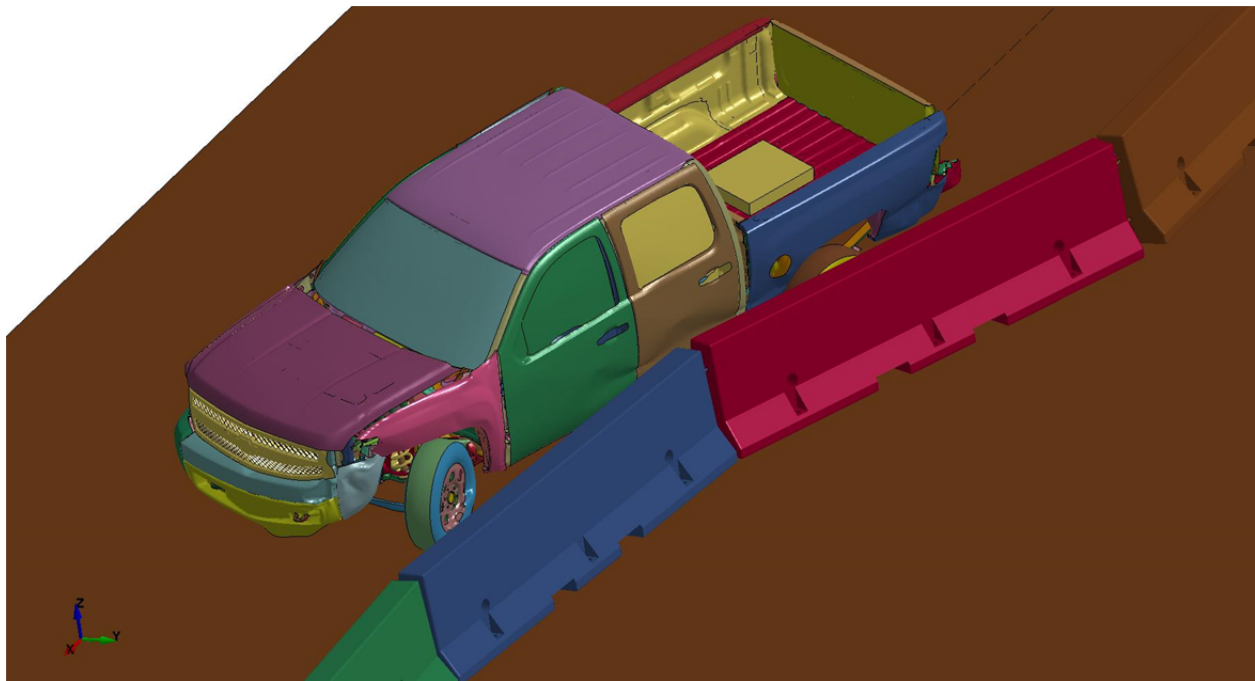
Simulation of the impact on the beginning of LON for the seven barrier system displayed acceptable barrier performance. The 2270P vehicle was safely and smoothly redirected with vehicle stability that compared well with the baseline model of the original 16 barrier long PCB system. Peak lateral barrier displacement was within 3 percent of those found in the standard length system when impacted at the beginning of LON. It was noted that a knee, an rotation of the barrier joint that extended a corner of the barrier segments laterally forward of the original position of the barrier segments, formed at the joint between barrier nos. 5 and 6 that impacted the left-rear door on the 2270P vehicle as the vehicle traversed the joint. The formation of a knee between the barrier segments that impacted the side of the vehicle was not observed in simulations of the full-length systems nor had it been noted in previous full-scale testing. The impact caused only moderate damage and did not affect vehicle stability or occupant risk values. Therefore, it was not believed to pose a serious degradation of the barrier performance, but it did indicate that the reduced length of the system was affecting the barrier behavior.

Simulation of the impact on the end of LON for the seven barrier long system raised potential concerns regarding the use of the shorter system length. The 2270P vehicle was redirected, and occupant risk values for the simulation were below the MASH limits. Peak lateral barrier deflections were again nearly identical to the standard length system simulation at the end of LON. However, there was concern regarding vehicle interaction with the PCBs as it reached the end of the system. At 0.630 sec after impact, the final barrier in the system rotated into the left-front door the vehicle as it proceeded past, as shown in Figure 5. The motion of the PCB segments downstream of impact in the reduced-length system was altered due to the reduced longitudinal resistance provided upstream of impact. This resulted in more pronounced rotation of the end barrier and caused the end of the barrier to impact the left-front door. The impact

NDOR PCB-Reduced Length-7 Barriers
Time = 655



(a)



(b)

FIGURE 5 End of LON simulations, PCB contact with side of 2270P vehicle: (a) 7 PCB system and (b) 8 PCB system.

caused significant damage to the door and raised concerns with respect to occupant compartment safety, occupant risk concerns, and potential degradation of vehicle stability. Thus, it was desired to mitigate impact of the end barrier segment on the vehicle.

Eight Barrier F-Shape PCB System Simulations

Based on the concerns with the door impact observed in the seven barrier PCB system simulations, the researchers conducted additional simulation models on an eight barrier long PCB system. Three PCB segments were used for the beginning of LON, four PCB segments were used for the end of LON, and a single barrier segment was placed between the regions to provide a finite redirective length. It was believed that the use of an additional PCB segment in the end of LON region would mitigate the door impact observed in the seven PCB system simulation. Simulation models were conducted on both the beginning and end of LON points similar to the seven barrier system.

Simulation of the impact on the beginning of LON for the eight barrier long system displayed similar results to those observed for the seven barrier system model. Simulation of the impact on the end of LON for the eight barrier long system displayed improved performance as compared to the seven barrier long system. The 2270P vehicle was redirected, and occupant risk values for the simulation were below the MASH limits. The use of an additional barrier on the end of the system mitigated the impact of the free-end of the final barrier segment with the side of the 2270P vehicle. However, it was noted that a knee formed at the joint between barrier nos. 6 and 7 that impacted the driver-side of the vehicle, as shown in Figure 5. The impact of the knee formed between these barrier segments posed less concern as the severity and damage associated with the vehicle contact with the knee appeared to be significantly less than observed with the rotation of the free end of the system into the door observed in the seven barrier PCB system simulation.

Based on these results, it was decided to proceed with full-scale crash testing evaluation of an eight barrier long F-shape PCB system under the MASH TL-3 criteria.

BARRIER DESIGN DETAILS

The test installations were comprised of eight 150-in. long, rebar reinforced, F-shape portable concrete barriers. The installation was identical for each full-scale crash test. The F-shape PCB segments were 150-in. long F-shape PCBs and constructed with a 5,000 psi compressive strength concrete. The barrier segments were 22½ in. wide at the base and 8 in. wide at the top. Each of the barrier segments were connected by 1¼ in. diameter A36 steel connection pins and connector plates placed between ¾ in. diameter, epoxy coated reinforcing bar loops extending from the end of the barrier sections. The connection loop bar material was A709 Grade 70 or A706 Grade 60 steel. All PCB segments were installed on the concrete tarmac at the MwRSF outdoor test facility.

FULL-SCALE CRASH TESTING

Two full-scale crash tests were selected to evaluate the reduced length, F-shape PCB system according to MASH TL-3. The first test, test no. NELON-1, consisted \ of MASH test designation no. 3-35 for evaluation of the beginning of length of need with a minimal system

length. The second test, test no. NELON-2, consisted of a modified version of MASH test designation no. 3-37 to assess the end of the length of need for the PCB system rather than maximize vehicle snag and instability on a terminal or crash cushion. This test involved an impact with a 2270P vehicle at a speed of 62 mph and an angle of 25 degrees on a critical impact point at the end of the LON. The critical impact points were selected based on the Table 2-6 of MASH and the beginning and end of LON locations determined through the LS-DYNA simulations. Thus, the impact point for test designation no. 3-35 would be 4.3 ft upstream of the joint between the third and fourth barrier segments, while the impact point for test designation no. 3-37 would be 4.3 ft upstream of the joint between the fourth and fifth barrier segments.

Test No. NELON-1

In test no. NELON-1, a 4,991-lb pickup truck impacted the portable concrete barrier system at a speed of 62.1 mph and at an angle of 24.8 degrees, as shown in Figure 6. Initial vehicle impact occurred $48\frac{11}{16}$ in. upstream of the centerline of the joint between barrier nos. 3 and 4. Following the initial impact, the vehicle was captured and began to be redirected by the barrier system. The vehicle became parallel to the barrier at 0.200 sec after impact. At approximately 0.460 sec, a knee formed at the joint between barrier nos. 5 and 6 impacted the left-front door causing deformation of the side of the vehicle that extended from the left-front door to the rear quarter panel. At 0.542 sec, the vehicle exited system. The vehicle came to rest 191 ft - 9 in downstream of the initial impact point and 9 ft - 8 in. in front of the front face of the barrier system.

Damage to the barrier system was moderate, as shown in Figure 6. Barrier system damage consisted of contact marks on the front face of the concrete barriers, spalling and gouging of the concrete, and concrete cracking and failure. Disengagement or fracturing off of the barrier toe was noted on the front and back of several barrier segments, and barrier no. 4 displayed vertical cracks that extended from the front to the back of the barrier segment. The length of vehicle contact along the barrier system was approximately 29 ft - 3 in. which spanned from 14 in. upstream of the targeted impact point to the downstream edge of barrier no. 5. The maximum lateral dynamic barrier deflection was 128.3 in., and the working width of the system was 150.8 in.

Exterior vehicle damage was moderate and was concentrated on the left-front corner and left side of the vehicle where the impact occurred, as shown in Figure 6. The interior occupant compartment deformations were minimal and did not violate the limits established in MASH. All occupant risk measures were below the required values, and vehicle stability was acceptable. Test no. NELON-1 was determined to be acceptable according to the MASH TL-3 safety performance criteria.

Test No. NELON-2

In test no. NELON-2, a 5,005-lb pickup truck impacted the portable concrete barrier system at a speed of 63.0 mph and at an angle of 24.5 degrees, as shown in Figure 7. Initial vehicle impact occurred $51\frac{3}{16}$ in. upstream of the centerline of the joint between barrier nos. 4 and 5. Following the initial impact, the vehicle was captured and redirected by the barrier system. At 0.190 sec after impact, the vehicle became parallel to the barrier. A knee formed at the joint between barrier segment nos. 6 and 7 that extended forward laterally from the original barrier line and

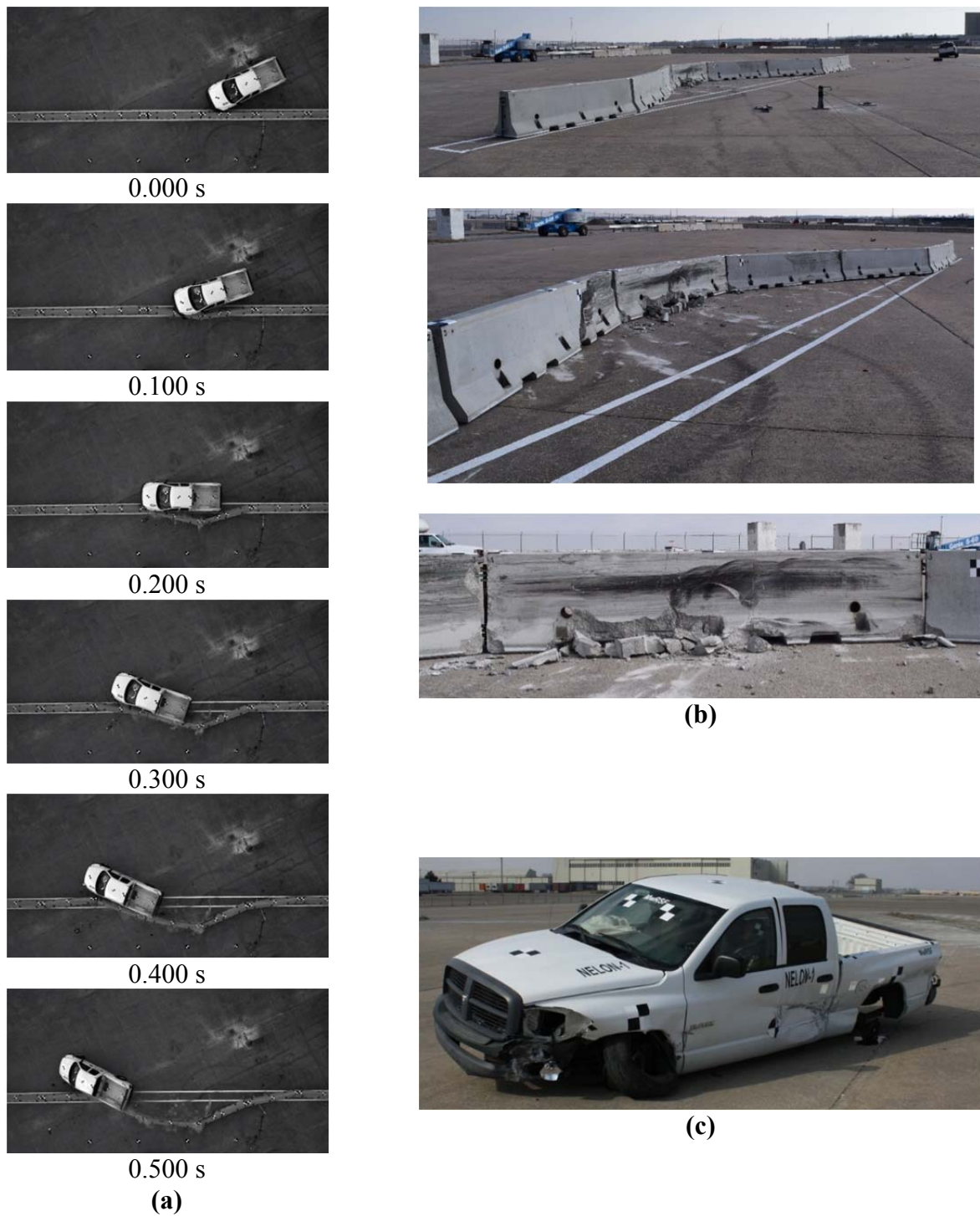


FIGURE 6 Sequential photographs and barrier and vehicle damage, Test No. NELON-1:
(a) sequential events; (b) barrier damage; and (c) vehicle damage



0.000 sec



0.100 sec



0.200 sec



0.300 sec



0.400 sec



0.500 sec

(a)



(b)



(c)

FIGURE 7 Sequential Photographs and Barrier and Vehicle Damage, Test No. NELON-2:
(a) sequential events; (b) barrier damage; and (c) vehicle damage

impacted the left-front door of the vehicle at approximately 0.390 sec after initial impact. The vehicle rolled onto the driver's side after it exited the system, before righting itself, and coming to a stop. Additionally, the left-front door became unlatched and opened as the vehicle was rolling towards the driver side and exiting the barrier. The vehicle came to rest 165 ft - 10 in downstream of the initial impact point and 28 ft - 11 in. in front of the front face of the barrier system.

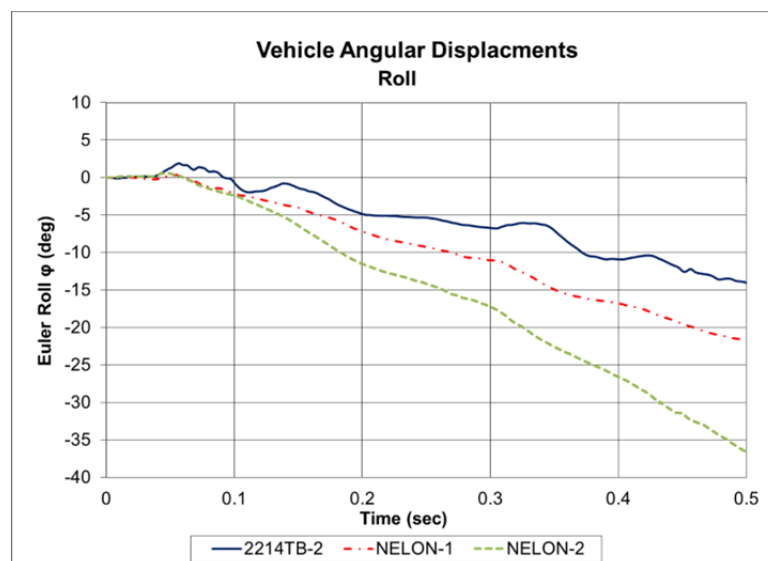
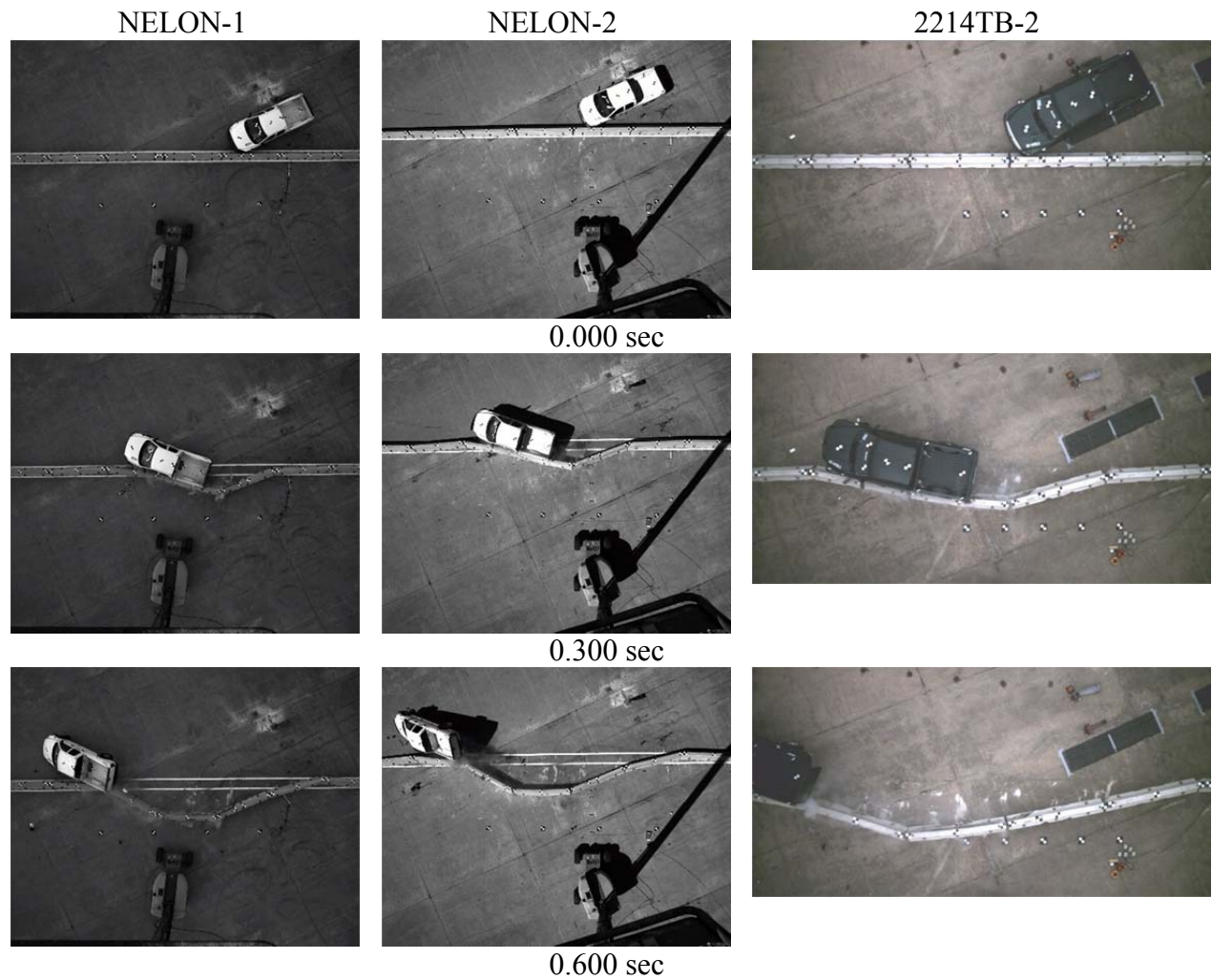
Damage to the barrier system was moderate, as shown in Figure 7. Barrier system damage consisted of contact marks on the front face of the concrete barriers, spalling and gouging of the concrete, and concrete cracking and failure. Disengagement of the barrier toe was again noted on the front and back of several barrier segments and barrier no. 5 displayed vertical cracks that extended from the front to the back of the barrier segment. The length of vehicle contact along the barrier system was approximately 30 ft – 2 in. which spanned from 18 in. downstream of the center target of barrier no. 4 extending to 9 in. downstream of the upstream edge of barrier no. 7. The maximum lateral dynamic barrier deflection was 127.8 in., and the working width of the system was 150.3 in.

Exterior vehicle damage was moderate and was concentrated on the left-front corner and left side of the vehicle where the impact occurred, as shown in Figure 7. Impact of the barrier knee on the left side of the vehicle caused deformation and gouging of the side of the vehicle that extended from the left-front door to the rear quarter panel. The interior occupant compartment deformations did not violate the limits established in MASH. All occupant risk measures were below the required values, but vehicle stability was unacceptable as the vehicle reached a peak roll angle of 82.3 degrees prior to righting itself. Additionally, the left-front door of the vehicle became unlatched and opened during the impact. While this behavior is not specifically outlined as violating the safety requirements in MASH, there was potential concern for exposure of the vehicle occupant due to the opening of the door. Test no. NELON-2 was determined to be unacceptable according to the TL-3 safety performance criteria found in MASH.

Discussion of Full-Scale Tests

The results of the two full-scale crash tests were reviewed to assess the performance of the reduced length F-shape PCB system when impacted at the beginning and end of LON. In test no. NELON-1 the 2270P vehicle impacted the beginning of LON on the eight barrier long F-shape PCB system and was safely redirected.

Test no. NELON-2 initially performed similarly to test no. NELON-1 as the vehicle was captured and redirected. However, the test was deemed unacceptable according to the MASH safety requirements due excessive roll after it exited the barrier system. Two potential factors may have contributed to the excess vehicle roll. First, the increased barrier deflections observed in test no. NELON-2 may have adversely affected the vehicle trajectory. Comparison of the barrier deflections and vehicle trajectories from test nos. NELON-1, NELON-2, and 2214TB-2 are shown in Figure 8. Review of these three tests showed that the reduced length system tests displayed higher deflections of the barrier segments near the impact of the vehicle and less gradual deflection of adjacent barrier segments as compared to the full-length PCB system. These differences were likely due to both the reduced upstream and downstream tensile forces developed by the shorter system and damage to the barrier structure and toes. Consequently, test nos. NELON-1 and NELON-2 exhibited higher exit angles of 12.3 degrees and 10.4 degrees, respectively, as compared to 7.9 degrees for test no. 2214TB-2. Similarly, comparison of vehicle

**FIGURE 8 PCB system comparison.**

roll angles during the first 0.500 sec of the vehicle redirection exhibited higher roll for the reduced length systems, as shown in Figure 8. Thus, it was believed that the effect of reduced system length on the PCB deflections contributed to the vehicle instability. A second factor that potentially contributed to the vehicle instability observed in test no. NELON-2 was the impact of the knee formed between barrier segment nos. 6 and 7 that impacted the left-front door at 0.390 sec after initial impact. The impact of the knee with the door may have further increased the instability of the vehicle.

While the results from test nos. NELON-1 and NELON-2 found that an eight barrier long PCB system was not adequate to safely redirect vehicles, it was believed that a nine barrier long system would be sufficient. A nine barrier system would be comprised of three PCB segments prior to the beginning of LON, one barrier segment for a finite redirective length, and five barrier segments following the end of the LON. Test no. NELON-1 demonstrated that three barrier segments prior to the beginning of LON was sufficient for an eight barrier long PCB system. The addition of a fifth barrier segment to the downstream end of the system provides the same number of downstream barriers for an impact at the end of LON as were utilized in NELON-1. It was expected that an impact on the end of length of need for a nine barrier long system would perform similarly to test no. NELON-1. Thus, it was recommended that the minimum system length for the free-standing F-shape PCB system be set a nine barrier segments.

SUMMARY AND RECOMMENDATIONS

This study consisted of analysis, full-scale crash testing, and evaluation of the length of need for a minimum length, free-standing, F-shaped PCB system. LS-DYNA computer simulation was the primary tool for analyzing the PCB system. A model of an F-shape PCB system was used to analyze and determine potential beginning and end of LON points for the barrier at its standard 16 barrier length. Next, analysis of a reduced length system was conducted to determine potential minimum system lengths. The simulation results determined that an eight barrier long F-shape PCB system three PCB segments prior to the beginning of LON, one PCB segment for the LON, and four PCB segments downstream of the end of LON had the potential to meet MASH TL-3 safety criteria.

Two full scale crash tests were performed to evaluate the selected beginning and end of LON and the reduced system length according to MASH TL-3 safety. Test no. NELON-1 evaluated the effectiveness of the beginning of LON with a minimal system length. The vehicle was safely captured and redirected with moderate damage to the barrier and the vehicle, and test no. NELON-1 was deemed acceptable based on the safety criteria for MASH test designation no. 3-35. Test no. NELON-2 assessed the end of the LON for the free-standing, PCB system with a minimal system length. The vehicle was successfully captured and redirected with moderate damage to the barrier and vehicle, but the vehicle's maximum roll exceeded the 75 degree limit established in MASH. Thus, test no. NELON-2 did not pass the safety requirements for MASH test designation no. 3-37.

Review of the results from both crash tests suggested that reduced length and impacts near the beginning and end of LON of the PCB system affected the performance of the barrier. Barrier deflections increased significantly, and the vehicle stability was reduced. However, the successful result from test no. NELON-1 led to the recommendation that a nine barrier long PCB system could meet the MASH TL-3 safety requirements. Thus, a minimum system length of nine barriers

was recommended with three barriers upstream of the beginning of LON and five barriers downstream of the end of LON. It should be noted that use of these reduced systems lengths requires consideration and accommodation of the associated increased barrier deflections.

This research indicated that PCB system lengths may be reduced significantly as compared with current guidance. However, evaluation of impacts between the beginning and end of LON and the ends of the system have not been evaluated. Computer simulation indicated that vehicle impacts outside the length of need may produce large barrier deflections, vehicle instability, increased barrier loading, and other hazards. Thus, research is needed to investigate the potential hazards associated with impacts outside the proposed length of need and to develop methods to safely terminate the PCB system in order to make effective use of reduced system lengths.

ACKNOWLEDGMENTS

The authors wish to acknowledge the Nebraska Department of Roads for sponsoring and providing guidance throughout the project.

REFERENCES

1. Ross, H. E., R. A. Krammes, D. L. Sicking, K. D. Tyer, and H. S. Perera. *NCHRP Report 358: Recommended Practices for the Use of Traffic Barrier and Control Treatments for Restricted Work Zones*, 1994.
2. Ross, H. E., D.L. Sicking, R. A. Zimmer, and J. D. Michie. *NCHRP Report 350: Recommended Procedures for the Safety Performance Evaluation of Highway Features*, 1993.
3. *Manual for Assessing Safety Hardware*. American Association of State Highway and Transportation Officials, Washington, D.C., 2009.
4. Faller, R.K., Rohde, J.R., Rosson, B.T., Smith, R.P., and Addink, K.H., *Development of a TL-3 F-Shape Temporary Concrete Median Barrier*, MwRSF Report No. TRP-03-64-96, Midwest Roadside Safety Facility, University of Nebraska-Lincoln, December 1996.
5. Polivka, K.A., Faller, R.K., Sicking, D.L., Rohde, J.R., Bielenberg, B.W., Reid, J.D., and Coon, B.A., *Performance Evaluation of the Free-Standing Temporary Barrier – Update to NCHRP 350 Test No. 3-11 with 28" C.G. Height (2214TB-2)*, MwRSF Report No. TRP-03-174-06, Midwest Roadside Safety Facility, University of Nebraska-Lincoln, October 2006.
6. Bielenberg, B.W., Faller, R.K., Rohde, J.R., Reid, J.D., Sicking, D.L., and Holloway, J.C., *Development of Tie-Down and Transition Systems for Temporary Concrete Barrier on Asphalt Road Surfaces*, Final Report to the Midwest States Regional Pooled Regional Pooled Fund Program, Transportation Research Report No. TRP 03 180 06, Midwest Roadside Safety Facility, University of Nebraska Lincoln, February 23, 2007.
7. Gutierrez, D.A., Bielenberg, R.W., Faller, R.K., Reid, J.D., and Lechtenberg, K.A., *Development of a Mash TL-3 Transition Between Guardrail and Portable Concrete Barriers*, Report No. TRP-03-300-14, Midwest Roadside Safety Facility, UNL, June 26, 2014.
8. Bielenberg, R.W., Quinn, T.E., Faller, R.K., Sicking, D.L., and Reid, J.D., *Development of a Retrofit, Low-Deflection, Temporary Concrete Barrier System*, Report No. TRP 03-295-14, Midwest Roadside Safety Facility, UNL, Lincoln, Nebraska, March 31, 2014.
9. Bielenberg, R.W., Meyer, D.T., Faller, R.K., and Reid, J.D., *Length of Need and Minimum System Length for F-Shape Portable Concrete Barrier*, Draft Report No. TRP-03-337-16, Midwest Roadside Safety Facility, UNL, Lincoln, Nebraska, November 2016.

INNOVATIONS IN ROADSIDE SAFETY HARDWARE AND FEATURES

A MASH TL-3 Compliant Short Radius System

AKRAM ABU-ODEH

Texas A&M Transportation Institute

WADE ODELL

Texas Department of Transportation

There is a growing need to place signs on median barrier as a way to relay vital traffic information to the traveling public. However, with the lack of MASH compliant sign mounting designs, state DOTs are limited to the Zone Of Intrusion (ZOI) guidelines to place such signs. The ZOI is derived from several NCHRP Report 350 tests and does not address the placement symmetry required for concrete median barriers (CMB) installation. In this presentation, four different sign mounting designs that are successfully crash tested according to MASH TL 3-11 are presented. These mounting designs concepts include rigid, movable, hinged based and plastic yielding based mechanisms. The research team recommend these designs to be placed on top of a 32-inch or taller CMB.

Development of a Precast Slim Temporary Concrete Safety Barrier STCSB 50 for Work Zone Applications

ALI O. ATAHAN

Istanbul Technical University

WOLFGANG GANSTER

THOMAS EDL

Delta Bloc International GmbH

TURAN ARSLAN

Uludag University

Selecting proper restraint systems for road work zone areas is essential in ensuring the safety of motorists and construction workers as well as preventing occurrence of severe accidents. Regulations surrounding these choices vary greatly with some countries leaving the discretion up to the managers while others mandate the use of barriers meeting specific requirements based on how they will be used. However, some nations have very detailed specifications including requirements for barriers to meet specified performances with respect to their application areas. Identifying performance criteria and making the right choices will determine how well authorities and traffic managers are able to provide safer environments for their workers.

Several different types of temporary protection barriers are available on the market. Today's barriers offer high performance, able to meet the requirements of work zone protection. These barriers are required to successfully pass crash test criteria in accordance with the European standard EN 1317. In particular, for the precast concrete barriers there are numerous crash tested solutions available for work zone areas.

Depending on how it will be used, a traffic manager can have many options to select the appropriate barrier from various design types and to define the necessary barrier height in order to provide the ideal protection. Naturally, a system with higher containment levels would be considered more suitable for heavy vehicle traffic conditions. However, slim barriers might be preferable in instances where they need to be placed very close to the work site or to separate contraflow traffic.

This paper summarizes performance requirements and development details of a precast slim temporary concrete safety barrier, STCSB 50, mainly utilized to guide the traffic flow and effectively divide lanes on motorways. Width of only 24 cm at the base and 12 cm throughout its height and 50 cm height makes STCSB 50 a very narrow and low profile work zone barrier. The design was crash tested according to EN 1317 requirements and its performance clearly demonstrated its robustness as a state of the art safety barrier for work zone applications. Its implementation is therefore recommended to protect both road users and construction site workers at work zone areas.

Roadside Safety Design and Hazard Mitigation

Development of a MASH TL-2 Crashworthy Pedestrian Railing System

**RONALD FALLER
KARLA LECHTENBERG
JENNIFER SCHMIDT
ANA GUAJARDO
ROBERT BIELENBERG
JOHN REID**

*Midwest Roadside Safety Facility
University of Nebraska-Lincoln*

ERIK EMERSON
Wisconsin Department of Transportation

In 2010, the National Highway Traffic Safety Administration (NHTSA) estimated that approximately 4,300 pedestrian fatalities occurred in the United States, with the highest risk for pedestrian injury occurring when crossing the street. When pedestrians choose a more direct path to cross a street at non-designated areas, driver expectations are violated and perception-reaction times are delayed, thus increasing pedestrian risks. In urban environments, pedestrian rails could be utilized to prevent dangerous excursions into nearby roadways as well as protect pedestrians from hazardous drop offs, such as near water crossings. Numerous pedestrian rails have been designed and implemented across the U.S. However, their crashworthiness has never been evaluated. The Wisconsin Department of Transportation funded a study to develop, test, and evaluate a crashworthy pedestrian railing system using the Test Level 2 (TL-2) impact safety criteria for longitudinal channelizers, as published in AASHTO's *Manual for Assessing Safety Hardware (MASH)*. Twenty-five preliminary railing concepts. Four concepts were advanced for final design and later subjected to dynamic bogie testing, evaluation, and re-design. The preferred railing was configured as a discrete panel system fabricated from aluminum rails, posts, base plates, and spindles, all welded together. The system consisted of 2-in. x 4-in. x 1/4-in. x 43-in. tall posts with three 2-in. x 2-in. x 1/8-in. rail components at heights of 42 in., 24¹⁵/₁₆ in., and 7⁷/₈ in. Two MASH TL-2 full-scale vehicle crash tests were conducted with small cars using test designation no. 2-90, but at impact angles of 25 and 0 degrees. Both tests successfully satisfied the MASH evaluation criteria for longitudinal channelizers. For the 0-degree impact condition, the maximum longitudinal occupant ride-down acceleration was near the acceptable limit. Thus, further modifications could be considered to reduce occupant ride-down accelerations for end-on impact events.

INTRODUCTION

The National Highway Traffic Safety Administration (NHTSA) estimated that approximately 4,300 pedestrian fatalities occurred in the United States in 2010 (1). Leaf and Preusser had estimated that only 5 percent of pedestrians would die when struck by a vehicle traveling at 20 mph or less, while fatality rates of 40, 80, and nearly 100 percent would occur for vehicles striking

pedestrians at 30, 40, and 50 mph or more, respectively (2). University of North Carolina researchers found that pedestrian fatalities may be related to transportation designs as well as human behaviors (3). Further, many pedestrian crashes occurred as a result of motorists and pedestrians not obeying traffic laws, not understanding safe driving practices, and not following safe walking behaviors (4).

Many intersections have marked crosswalks to provide increased pedestrian safety; since, the risk of pedestrian injury is highest when crossing the street. These marked areas also inform drivers to be mindful of nearby pedestrians. However, pedestrians may choose a more direct path to cross the street or even become distracted, thus entering the roadway at non-designation areas (i.e., locations without a marked crosswalk). Crossing at non-designated areas can increase the likelihood of a fatal or serious injury crash.

Rails are often placed adjacent to roadways to protect pedestrians from hazardous drop-offs, prevent dangerous excursions into the roadway, as well as provide access control. Several examples of pedestrian rail applications are shown in Figure 1 and include (1) busy streets where median fences deter pedestrians from crossing in non-designated locations, (2) median barrier retrofits to prevent pedestrians from crossing high-speed highways and freeways, and (3) sidewalks over culverts where rails separate pedestrians from hazardous drop-offs. In some cases, rails are installed to prevent pedestrians from entering areas beyond the right of way, as shown in Figure 2. Thus, the design and placement of pedestrian rails should carefully consider site-specific needs and requirements.

Although numerous pedestrian rails have been designed and implemented, their crashworthiness has never been evaluated using current impact safety standards. There are safety concerns for passengers of errant vehicles which strike non-crashworthy pedestrian rails. For example, vehicle-to-rail crashes could result in barrier elements penetrating the occupant compartment, excessive decelerations, and vehicle instabilities.

Serious failures, such as rails spearing through windshields, have been documented during real-world vehicle crashes into pedestrian rails (5). Therefore, a need existed to develop a crashworthy pedestrian railing system to meet current impact safety standards as well comply with the appropriate structural and geometric requirements published in existing design guidelines and standards.

RESEARCH OBJECTIVES AND PLAN

The research objective was to design a crashworthy pedestrian rail that would direct pedestrians away from various hazards (i.e., falling over drop-offs and crossing roads at non-designated areas) while not posing undue safety risk to motorists. The new pedestrian rail must meet the pedestrian rail standards contained in the American Association of State Highway and Transportation Officials (AASHTO) *Load and Resistance Factor Design (LRFD) Bridge Design Specifications* (6). The new pedestrian rail should also be configured in a manner such that it potentially may be modified to meet the design standards associated with the Americans with Disabilities Act (ADA) (7). Other pedestrian rail criteria from common codes should be reviewed and considered, such as the International Building Code (IBC) (8) and Occupational Safety and Health Administration (OSHA), Part 1910 (9). In addition, the pedestrian rail should be tested and evaluated using the Test Level 2 (TL-2) safety performance criteria for longitudinal channelizers, as published in the *AASHTO Manual for Assessing Safety Hardware (MASH)* (10).



FIGURE 1 Examples of Pedestrian Rails



FIGURE 2 Pedestrian Rail with Limited Escape Routes from Errant Vehicles.

The study objectives were met through the completion of several tasks. A review was conducted of existing pedestrian rails and fences that are used with State Departments of Transportation (DOTs) and available from various manufacturers. A survey was sent to and completed by several State DOTs to identify common locations and circumstances where crashworthy pedestrian rails may be warranted. A preliminary concept development effort was performed while investigating potential fabrication materials, such as aluminum, steel, wood, and polymers. Several design concepts were configured, and preferred concepts were selected for further refined and evaluation. Dynamic bogie tests were conducted on four design concepts to evaluate their dynamic performance. Design improvements were made, and two full-scale vehicle crash tests were performed on an aluminum railing system using MASH TL-2 impact conditions for longitudinal channelizers. The test results were analyzed and evaluated, while conclusions and recommendations were provided regarding the safety performance of a new pedestrian railing system. This paper provides a condensed summary of the research study, while additional details are provided by Lechtenberg et al (5).

DESIGN STANDARDS AND GUIDELINES

AASHTO LRFD Bridge Design Specifications

The AASHTO *LRFD Bridge Design Specifications* provided requirements for use in the design of a pedestrian rail (6). Pedestrian rail height should be a minimum of 42 in. above the walkway. A clear spacing shall apply to the lower 27 in. of the railing where a 6-in. diameter sphere cannot pass through the rail elements. The clear spacing in the upper section of the railing above 27 in. shall not allow an 8-in. diameter sphere to pass through the rail elements. Chain link or metal fabric fence should not have openings larger than 2 in.

Longitudinal railing elements must withstand a uniform live load of 50 lb/ft simultaneously applied both transversely and vertically, along with a concentrated live load of 200 lb applied at any point and in any direction on the longitudinal element, as shown in Figure 3. The posts are subjected to a concentrated live load, P_{LL} , defined in Equation 1. The concentrated live load P_{LL} shall be applied transversely at the center of gravity of the upper horizontal element. For a railing mounted taller than 5 ft, P_{LL} shall be applied at a point 5 ft above the walkway. Chain link or metal fabric fence shall be designed for a distributed live wind load of 15 lb/ft² applied perpendicular to the entire mesh surface.

$$P_{LL} = 200 + 50L \quad (1)$$

Where P_{LL} = post point live load (lb) and L = post spacing (ft).

American with Disabilities Act Design Criteria

A pedestrian rail must be accessible to all people, including those with disabilities. The *2010 ADA Standards for Accessible Design* sets forth handrail criteria (7). The handrail must be continuous along the full length of the walkway and not be obstructed on the top or sides. The handrail top gripping surface should be a minimum of 34 in. and a maximum of 38 in. vertically above the walking surface. There should be a minimum separation of 1½ in. between the back surface of the handrail and any adjacent surface. The handrail gripping surface for a circular cross section shall have minimum and maximum outside diameters of 1¼ in. and 2 in., respectively. Non-circular cross sections shall have minimum and maximum perimeters of 4 in. and 6¼ in., respectively, with the diagonal cross section length no greater than 2¼ in. If fittings are used, the handrail shall not rotate within them. When a vertical or horizontal force of 250 lb is applied on any point on the handrail, fasteners, mounting devices, or supporting structures, the allowable stresses shall not be exceeded.

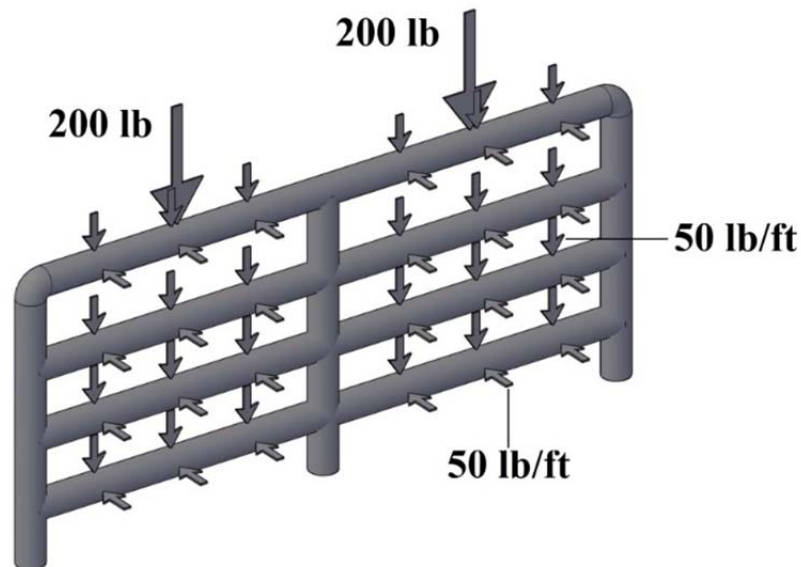


FIGURE 3 AASHTO Loading Criteria (Vertical 200-lb Point Load Shown)

International Building Code

The 2012 IBC (8) also contains handrail design criteria. Handrail criteria for continuity, height of gripping surfaces, separation distance between back of rail and adjacent surfaces, and sizes of circular cross sections, are identical those noted by the ADA. Non-circular cross sections shall have minimum and maximum surface perimeters of 4 in. and 6¼ in., respectively, with a cross-sectional dimension of at least 1 in. but no greater than 2¼ in. Edges shall have a minimum radius of 0.01 in. If fittings are used, the handrail shall not rotate within them. Handrails should be designed to resist a linear load of 50 lb/ft. Handrails should also be designed to resist a concentrated load of 200 lb applied in any direction at any point along the top. Intermediate rails, balusters, and panel fillers should be designed to resist a concentrated load of 50 lb.

Occupational Safety & Health Administration (OSHA)

Handrail design criteria is also contained in *Part 1910 – Occupational Safety & Health Administration Regulations (Standards – 29 CFR) (9)*. A standard railing shall consist of a top rail, intermediate rail, and posts, and it shall have a vertical height of 42 in., as measured between the upper surface of top rail to the ground. The top rail shall be smooth throughout the length of the railing. Pipe railings, posts, and top and intermediate railings shall have a nominal diameter of at least 1½ in. with posts spaced not more than 8 ft on center. The complete structure shall withstand a 200-lb load applied in any direction at any point on the top rail.

AASHTO MASH Longitudinal Channelizers

Longitudinal channelizers are intended to provide clear visual indication of the intended vehicle path through a construction or work zone. They are not intended to contain and redirect impacting vehicles, but rather a vehicle can traverse through and behind the system. Thus, the impact performance criterion for longitudinal channelizers is different from those used for longitudinal barriers. For MASH TL-2 longitudinal channelizers, two full-scale crash tests are recommended, test designation no. 2-90 with an 1100C vehicle and test designation no. 2-91 with a 2270P vehicle (10). For each vehicle type, the impact conditions consist of a speed of 44 mph and a critical impact angle ranging between 0 and 25 degrees, selected to maximize the risk of vehicle rollover and excessive vehicle decelerations.

REVIEW OF EXISTING SYSTEMS

At the onset of this study, researchers conducted a review of existing pedestrian rails that were used by State DOTs as well as commercially-available systems used by homeowners, businesses, and sporting venues. Several types of pedestrian rails were considered, including combination pedestrian rail and concrete parapet systems, plastic fences, wood fences, and metal rails. Combination concrete barriers are often used in combination with a metal rail or chain link fence to accommodate pedestrian safety in high-speed facilities, but those systems are associated with higher costs due to their ability to contain and redirect vehicles. Metal rails are typically fabricated with aluminum or steel materials for strength and ease of construction. Wood fences are often used for economic reasons. Numerous polymer fences are fabricated with polyvinyl chloride (PVC), high density polyethylene (HDPE), and fiber-reinforced polymers (FRP) to

provide aesthetics and corrosion resistance. Most combination pedestrian rail and concrete parapet systems have been crash tested and have met safety performance guidelines. However, plastic, wood, and metal fences or railings have not been crash tested. A summary of existing pedestrian rails can be found in Lechtenberg et al (5).

STATE DOT SURVEY – PEDESTRIAN RAIL NEEDS

A survey was conducted to identify the most common locations and circumstances where a crashworthy pedestrian rail would be warranted. The survey was sent to the Wisconsin DOT as well as members of the Midwest States Pooled Fund Program. Respondents were asked to evaluate pedestrian rail usefulness in various applications, including: (1) placement on top of culverts; (2) placement on top of retaining walls; (3) jaywalk prevention; (4) rail protection around private or public property; (5) bicycle or pedestrian path separation from roadway; (6) hazard protection for bicycle path traffic; (7) locations with raised sidewalks relative to surroundings; and (8) placement on bridges.

For the Pooled Fund member states, the first and second highest priority needs for a crashworthy pedestrian rail pertained to shielding hazardous drop-offs through its placement on top of culverts and on top of retaining walls. For the Wisconsin DOT, the highest-priority need for a crashworthy pedestrian rail pertained to its use in preventing urban/suburban pedestrian crossings at non-designated locations, such as jaywalking. Based on the survey results, the Wisconsin DOT prioritized the research study to focus on an application which prevents pedestrian crossings at non-designated locations.

INITIAL CONCEPT DEVELOPMENT

Preliminary Concepts

Following the system review and survey, researchers developed 25 concepts for a pedestrian rail (5). These concepts met the geometric requirements noted previously and the structural loading criteria when possible. Various materials were initially considered, which included steel, aluminum, PVC, wood, HDPE, and FRP, which were based on aesthetics, strength, weight, cost, and workability. The handrail, infill, and connections were not designed during the initial development effort.

Refined Concepts

Following a review, several preliminary concepts and fabrication materials were eliminated from consideration. FRP rail systems were eliminated due to material cost concerns. HDPE rail systems were eliminated due to concerns for lower material stiffness and strength, especially at elevated temperatures. Numerous concepts were eliminated due to concerns for aesthetics as well as feasibility of fabrication. Segmented systems were preferred over continuous systems to reduce barrier damage during impact events as well as to improve constructability and repair. Thus, only seven preliminary concepts were further refined, including: two modular aluminum concepts; one welded aluminum concept; two PVC concepts; and two wood concepts. System details are provided in Lechtenberg et al (5). Examples of the refined concepts are shown in Figure 4. Although some design guidance was provided with the concepts, final system details



(a)



(b)



(c)



(d)

FIGURE 4 Sample refined pedestrian rail concepts: (a) PVC; (b) wood; (c) modular aluminum; and (d) welded aluminum.

were not completed for each concept, such as the determination of welded or bolted connection details.

The refined concepts were submitted to the project sponsor for review and comment. Subsequently, the sponsor identified preferred concepts based on aesthetics, cost, installation, maintenance, and sight lines. Some concerns were raised with various concepts, including the possibility for a system to obstruct a driver's visual line of sight at critical locations, such as near intersections; the need to preservative treatment or routine maintenance of wood railing systems to prevent visual or structural degradation; additional fabrication costs associated with heat-treating welded aluminum components; and the potential for system components to fracture away from the railing panels and become projectile hazards to pedestrians or motorists. PVC-based concepts were eliminated due to lack of aesthetic appeal, difficulty with design and fabrication of post and rail connections, and instability of PVC rail segments. The wood-based concepts were eliminated due to the concerns for long-term durability, warping of the wood sections, and splinter hazards to pedestrians, vehicle occupants, and bystanders. After eliminating PVC-based and wood-based concepts, the modular and welded aluminum railing systems were recommended to be further pursued.

DESIGN LOADS – RAIL, POSTS, AND CONNECTIONS

For the initial concepts, simplified load cases were used to estimate longitudinal rails, vertical posts, and any infill components of a pedestrian rail. When a more complete analysis and design was required for the two types of aluminum systems, additional assumptions and load scenarios were used determine (1) rail members, (2) post members, (3) infill components, (4) post-to-rail connections, (5) post-to-base connections, (6) infill-to-rail connections, and (7) anchorage hardware. Details on the load scenarios can be found in Reference (5).

For rail components, the analysis and design was based on 60-in. long rails. Using the *AASHTO LRFD Bridge Design Specifications*, a 200-lb concentrated point load was applied at the ends, midspan locations, or anywhere between supports. The maximum shear and bending moment due to point loading on simply-supported beam was 200 lb and 3,000 lb-in. for end and midspan locations, respectively. A 50-lb/ft uniform load was applied across the entire rail. The maximum shear and rail bending moment due to uniform loading on a simply-supported beam was 125 lb and 1,876.5 lb-in. for end and midspan locations, respectively. The AASHTO criteria specifies that the two uniform loads must be applied vertically and transversely, but the concentrated load may be applied to the rail at any point and in any direction. The maximum shear and bending moment was determined from uniform loads in both transverse and vertical directions as well as the concentrated load acting in either vertical or transverse directions. Since it could be applied in either direction, a doubly-symmetric section would be most efficient for longitudinal rails. The maximum resultant shear force at the end of the rail was 348.2 lb. The combined bending moment resulting from the three separate loads acting on the longitudinal member were combined to determine a maximum bending stress in the cross section. For a doubly-symmetric section, the maximum rail bending moment on a simply-supported beam was determined as the sum of the maximum bending moments from the loads applied both vertically and transversely (i.e., two distributed loads plus a concentrated load at midspan), or 6,750 lb-in.

For rail components, the analysis and design was based on 60-in. long rails. Using the *AASHTO LRFD Bridge Design Specifications*, a 200-lb concentrated point load could be applied at the ends, midspan locations, or anywhere between supports. The maximum shear and

bending moment due to point loading on simply-supported beam was 200 lb and 3,000 lb-in. for end and midspan locations, respectively. A 50-lb/ft uniform load was applied across the entire rail. The maximum shear and rail bending moment due to uniform loading on a simply-supported beam was 125 lb and 1,876.5 lb-in. for end and midspan locations, respectively. The AASHTO criteria specifies that the two uniform loads must be applied vertically and transversely, but the concentrated load may be applied at any point and in any direction on the rail element. The maximum shear and bending moment was determined from uniform loads in both transverse and vertical directions as well as the concentrated load acting in either vertical or transverse directions. Since it could be applied in either direction, a doubly-symmetric section would be most efficient for longitudinal rails. The maximum resultant shear force at the end of the rail was 348.2 lb. The combined bending moment resulting from the three separate loads acting on the longitudinal member were combined to determine a maximum bending stress in the cross section. For a doubly-symmetric section, the maximum rail bending moment on a simply-supported beam was determined as the sum of the maximum bending moments from the loads applied both vertically and transversely (i.e., two distributed loads plus a concentrated load at midspan), or 6,750 lb-in.

For post components, the analysis and design was based on 60-in. long rails and 41-in. load height on posts. Using the AASHTO loads noted above, the maximum shear and bending moment in the cantilevered posts was 450 lb and 18,450 lb-in., respectively.

Other loading conditions were examined for use in designing infill regions, post-to-rail connections, post-to-base connections, and infill-to-rail connections, and base plate anchorages. The maximum shear and bending moments for designing these other components are contained in Reference (5).

SYSTEM DESIGN

The mechanical properties of aluminum can vary depending on alloy, shape, thickness, and existence of weld-affected zones. The process of welding aluminum at connections significantly reduces the material strength surrounding weld locations. While heat treatment can be used to regain most of the material strength in weld-affected zones, heat treatment was not desired. Thus, pedestrian rail concepts were to be designed using the lower weld-affected material strengths. A common aluminum alloy, 6061-T6, was selected for the pedestrian rail designs. The mechanical properties of non-welded 6061-T6 aluminum were provided in Table A.3.4 in the Aluminum Design Manual (ADM) (11). The mechanical properties of weld-affected 6061-T6 aluminum were provided in Table A.3.5 in the ADM.

As obtained from the ADM (11), LRFD design equations were used to configure most components used in the aluminum railing systems. The modular and welded aluminum concepts were further refined into four prototypes - one modular aluminum system and three welded aluminum systems, as shown in Figure 5. It should be noted that the modular system used commercially-available hardware from Hollaender's standard Speed-Rail® system (12). Complete design calculations and system drawings are not provided herein but can be found in Reference (5).



(a)



(b)



(c)



(d)

FIGURE 5 Four aluminum prototypes: (a) welded base; (b) socketed post; (c) modular system with round sections; and (d) welded base with full spindles.

DYNAMIC BOGIE TESTING

Dynamic bogie testing was utilized to evaluate the impact performance and system fracture for all four pedestrian rail prototypes. The rigid-frame bogie was configured with a front bumper positioned approximately 13 $\frac{5}{8}$ in. above the ground line. The bogie was not configured with a windshield, floorpan, or body panels. System evaluation considered trajectory of debris as well as potential for fractured components to deform and/or penetrate a hypothetical occupant compartment or windshield. Preferred system behaviors included: clean and consistent component fracture; no anchor damage; component trajectory away from windshield and undercarriage; limited to no vehicle instability; and no concerns for occupant risk.

Four test runs, or seven bogie tests, were conducted at 45 mph on four prototypes. Each prototype consisted of a two-panel system, which anchored to an existing concrete tarmac. Three prototypes were evaluated using two impact orientations in one test run, as shown in Figure 5(a) through 5(c). For the first device, the bogie impacted the spindle region on the first panel at 25 degrees. For second device, the bogie impacted the first panel at 0 degrees or end-on. For fourth test run, the prototype was only evaluated in the end-on orientation due to its similarity to two of the first three prototypes, as shown in Figure 5(d).

For the three square-tube, welded-aluminum prototypes, posts seemed to fracture or release from bases more consistently when directly welded to bases versus inserted into sockets that were welded to bases. For all four prototypes, minor deformations were observed in each base plate. Permanent deformations in base plates could likely be eliminated with increased plate thickness. Prototypes anchored with $\frac{3}{8}$ -in. diameter threaded rods exhibited slight permanent deformations in the fasteners, while prototypes anchored with $\frac{1}{2}$ -in. diameter threaded rods exhibited no visual permanent deformations in the fasteners.

For the systems depicted in Figure 5(a) through 5(c), the observed impact performance raised safety concerns when struck end-on. Specifically, the upper and middle horizontal rails had fractured or disengaged away from the posts, rode over the top of the bogie, and posed increased risk for windshield penetration and excessive deformation. The six bogie tests on these three prototypes had also indicated that end-on impact event were more critical than oblique impacts at 25 degrees. These three prototypes fractured away from the bases when impacted at 25 degrees and did not present concerns for penetration or excessive deformation to an impacting vehicle.

As shown in Figure 5(d), the middle rail was lowered to more closely align with the bumper heights of both pickup trucks and small cars and improve dynamic impact behavior. The change in position for the middle horizontal rail, along with (1) extending spindles from top rail to bottom rail, (2) passing spindles through the middle rail, (3) inserting rails into posts, and (4) increasing anchor size to $\frac{1}{2}$ in. diameter, greatly improved system behavior. Therefore, the welded aluminum prototype with posts welded to base plates and full spindles was recommended for further testing and evaluation.

TEST REQUIREMENTS AND EVALUATION CRITERIA

Longitudinal channelizing systems, or pedestrian rails, should be subjected to two full-scale vehicle crash tests using the MASH TL-2 guidelines. Test Designation No. 2-90 consists of a 2,425-lb passenger car (designated 1100C) impacting at 44 mph and a critical angle ranging

between 0 and 25 degrees. Test Designation No. 2-91 consists of a 5,000-lb pickup truck (designated 2270P) impacting at 44 mph and a critical angle ranging between 0 and 25 degrees. The critical angle should be selected to maximize risks for rollover or excessive decelerations. During discussions with FHWA, the 0-degree impact angle was deemed to likely provide greater risk for excessive decelerations, cause instabilities, as well as potentially result in excessive deformation and/or penetration to occupant compartment, including windshield. The 25-degree angle could cause instabilities as well as result in unacceptable damage to occupant compartment, including windshield. Thus, 0- and 25-degree angles were deemed critical, while other angles were deemed less critical.

Test no. 2-90 with a 1100C small car was also deemed critical due to concerns for excessive decelerations based on a smaller mass and instabilities while overriding components. The small car has lower hood, windshield, and floor pan heights. Thus, a small car versus a pickup truck is likely more susceptible to occupant compartment and windshield penetration and deformation under impacts with a pedestrian rail. Following discussions with FHWA, only 1100C small car tests were initially planned using test no. 2-90 at 0 and 25 degrees. If the results from either test indicated concerns for 2270P vehicles, then additional pickup truck testing would be considered.

MASH is unclear regarding centerline or quarter-point impacts on channelizers in end-on scenarios. Thus, centerline impact scenarios were selected to promote greater contact with panels, increasing risk for excessive decelerations. Although quarter-point impacts are often used to evaluate risks for rollover, it was deemed less critical for a channelizer system.

FINAL DETAILS – PEDESTRIAN RAIL

A 150-ft long pedestrian rail system was constructed using 26 aluminum panel sections. Complete system details are provided in Reference (5), while a simple schematic is shown in Figure 6.

Each panel utilized 2-in. x 4-in. x $\frac{1}{4}$ -in. by 43-in. tall aluminum posts with three 2-in. x 2-in. x $\frac{1}{8}$ -in. aluminum rail sections at heights of 42 in., $24\frac{15}{16}$ in., and $7\frac{7}{8}$ in. (2 in. plus $5\frac{7}{8}$ in. from ground to bottom of lower tube). Each rail end was inserted into a cutout in the posts and secured with a $\frac{1}{8}$ -in. fillet weld. Nine $\frac{1}{2}$ -in. x $\frac{1}{2}$ -in. x $32\frac{1}{8}$ -in. square spindles spanned between the top and bottom rails and passed through the middle rail. The aluminum spindles were attached with $\frac{1}{8}$ -in. fillet welds at each rail location. Each post was attached to a 3-in. x $7\frac{3}{4}$ -in. x $\frac{3}{8}$ -in. aluminum base plate with a $\frac{1}{4}$ -in. fillet weld. Each base plate had two $\frac{5}{8}$ -in. diameter holes spaced at $6\frac{1}{4}$ in. to accommodate two $\frac{1}{2}$ -in. diameter ASTM A193 Grade B7 threaded anchor rods with appropriate nuts and washers. Each rod was embedded 5 in. into the concrete using a chemical epoxy adhesive with a 1,450-psi minimum bond strength. All tubes, plates, and spindles conformed to 6061-T6 aluminum. The concrete foundation should have a minimum compressive strength of 2,500 psi and a minimum thickness of 7 in. The clear spacing between adjacent panel posts was $5\frac{1}{2}$ in.

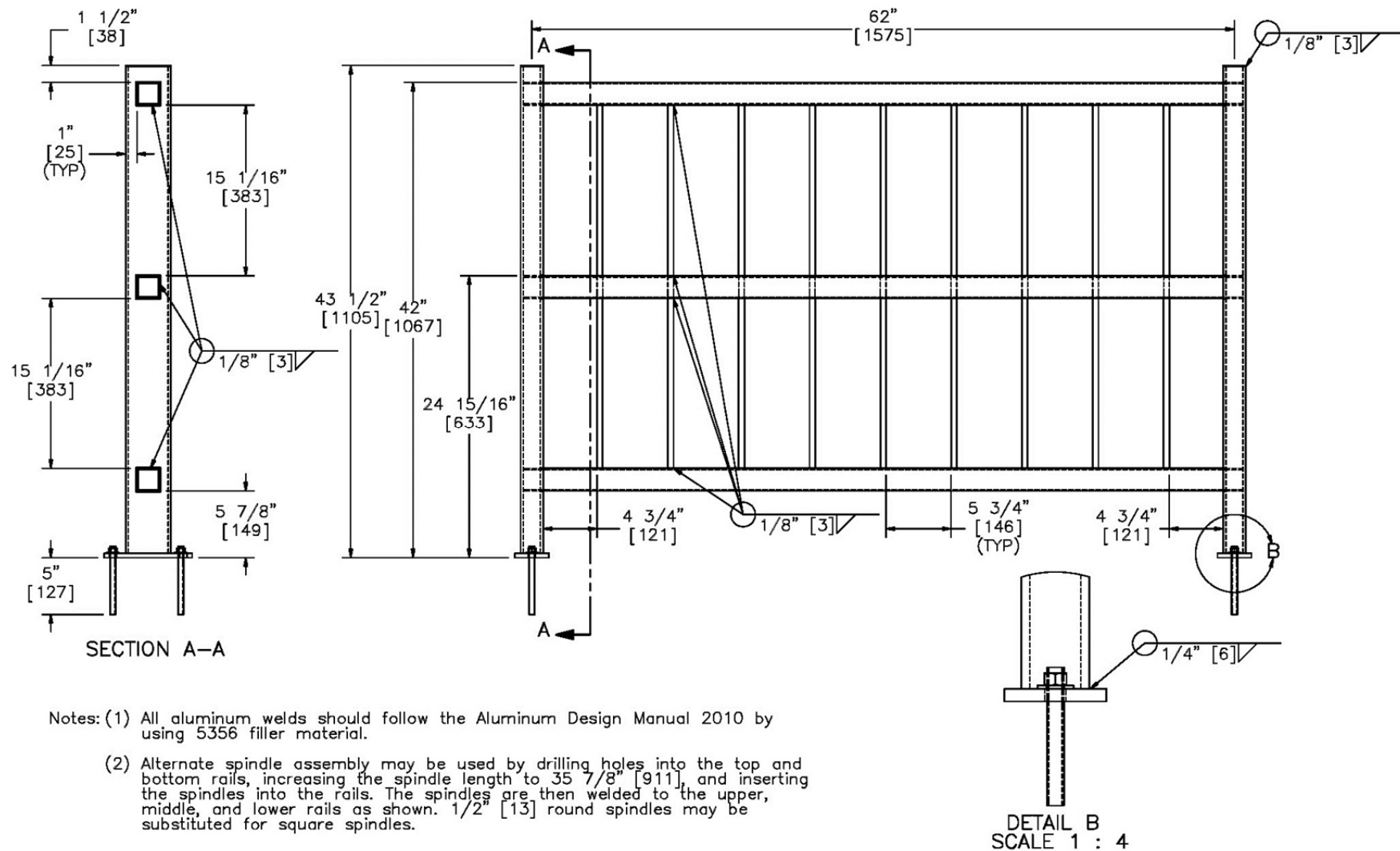


FIGURE 6 Schematic of aluminum pedestrian rail - final design.

FULL-SCALE CRASH TESTING

Test No. APR-1 (Test Designation No. 2-90 @ 25 Degrees)

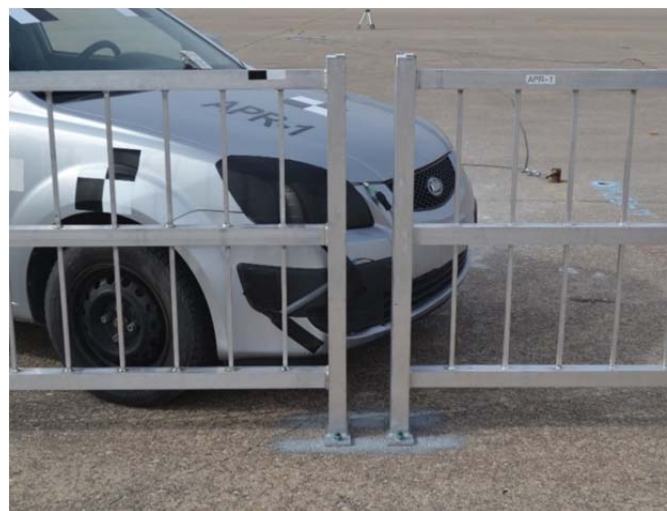
The 2,428-lb small car impacted the aluminum pedestrian rail at a speed of 45.2 mph and an angle of 25.1 degrees. The target impact location utilized the vehicle centerline aligned with the centerline of the downstream post of panel no. 12, which was selected to evaluate windshield damage from panels sliding up the hood and debris field. Actual vehicle contact occurred at the second spindle upstream from the downstream post in panel no. 11. The vehicle came to rest upright and 45.5 ft behind the centerline of panel no. 26. The pre-impact barrier system, impact location, system damage, and barrier damage are shown in Figure 7. Six panels were damaged, largely consisting of fractured welds between posts and base plates, fractured welds between posts and rails, and spindle disengagement from rails. No damage was observed in the vertical anchors. Vehicle damage was moderate, consisting of deformations in engine hood, front bumper, front quarter panels, and wheels, as well as fractured/disengaged headlights. The windshield was not damaged. The maximum occupant compartment deformation was ½ in. at the side front panel in front of A-pillar and side door above the seat. The occupant impact velocities (OIVs) were -19.08 fps and 3.89 fps in the longitudinal and lateral directions, respectively. The maximum 0.010-sec occupant ridedown accelerations (ORAs) were -1.85 g's and -3.33 g's in the longitudinal and lateral directions, respectively. The maximum roll angle was 10.61 degrees. The pedestrian rail allowed controlled penetration of the 1100C vehicle. Neither detached elements nor fragments showed potential for penetrating the occupant compartment or for presenting undue hazard to other traffic. Note, none of the pedestrian rail panels went over the hood, near the windshield, or underneath the vehicle. Deformations of, or intrusions into, the occupant compartment that could have caused serious injury did not occur. The OIVs and ORAs were within the suggested limits provided in MASH. The test vehicle remained upright during and after the collision. Vehicle roll, pitch, and yaw angular displacements were deemed acceptable. Test no. APR-1 was deemed acceptable under the MASH TL-2 safety performance criteria.

Test No. APR-2 (Test Designation No. 2-90 @ 0 Degrees)

The 2,437-lb small car impacted the aluminum pedestrian rail at a speed of 44.5 mph and an angle of 0 degrees. The target impact location utilized the vehicle centerline aligned with the centerline of the upstream post of panel no. 1, which was selected to evaluate the potential for windshield and roof damage, vehicle instability, occupant risk, and debris field. Actual vehicle contact occurred at the centerline of the upstream post of panel no. 1. The vehicle came to rest 15 ft – 11 in. upstream from the upstream post of panel no. 10 and parallel to the centerline of the system. The pre-impact barrier system, impact location, system damage, and barrier damage are shown in Figure 8. Ten panels were damaged, largely consisting of fractured welds between posts and base plates, fractured welds between posts and rails, and deformed spindles. No damage was observed in the vertical anchors. Vehicle damage was moderate, consisting of deformations in engine hood, front bumper, front quarter panels, and wheels, as well as fractured/disengaged headlights. The lower-right corner of the windshield was cracked. The maximum occupant compartment deformation was ¾ in. at the wheel well and toe pan. The occupant impact velocities (OIVs) were -21.69 fps and -1.19 fps in the longitudinal and lateral directions, respectively. The maximum 0.010-sec occupant ridedown accelerations (ORAs) were



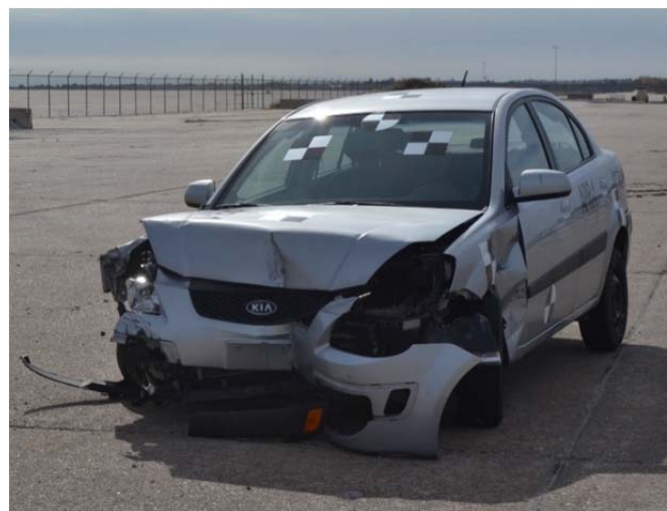
(a)



(b)



(c)



(d)

FIGURE 7 Test No. APR-1: (a) pre-impact barrier system; (b) impact location; (c) system damage; and (d) barrier damage.



(a)



(b)



(c)



(d)

FIGURE 8 Test APR-2: (a) pre-impact barrier system; (b) impact location; (c) system damage; and (d) barrier damage.

-19.41 g's and -3.87 g's in the longitudinal and lateral directions, respectively. The maximum roll angle was 8.63 degrees. The pedestrian rail allowed controlled penetration of the 1100C vehicle. Neither detached elements nor fragments showed potential for penetrating the occupant compartment or for presenting undue hazard to other traffic. Deformations of, or intrusions into, the occupant compartment that could have caused serious injury did not occur. The OIVs and ORAs were within the suggested limits provided in MASH. The test vehicle remained upright during and after the collision. Vehicle roll, pitch, and yaw angular displacements were deemed acceptable. Test no. APR-2 was deemed acceptable under the MASH TL-2 safety performance criteria.

SUMMARY, CONCLUSIONS, AND RECOMMENDATIONS

The primary objective was to develop a crashworthy pedestrian rail to protect pedestrians from roadside and median hazards while not posing undue safety risk to motorists. The new pedestrian rail met the AASHTO *LRFD Bridge Design Specifications* and the AASHTO MASH TL-2 safety performance evaluation criteria for longitudinal channelizers. Other design guidance was considered, including that provided by the ADA. A review was completed on existing pedestrian rail systems and commercially-available railings. A survey was performed to identify common locations and circumstances where crashworthy pedestrian rails may be warranted, which focused on prevention of road crossings at non-designated locations. Twenty-five pedestrian rail concepts were brainstormed, which included numerous materials. After multiple rounds of sponsor review, several concepts and material were eliminated. Four aluminum prototypes were further developed, including complete design details, fabricated, and subjected to dynamic bogie testing. From this evaluation, the preferred configuration was an aluminum prototype with posts welded to base plates, which included full spindles, repositioned middle rails, rails inserted into post cutouts, and ½ in. diameter anchor rods.

Two full-scale vehicle crash tests with 1100C vehicles (test designation no. 2-90) were conducted on the preferred pedestrian rail system using the MASH TL-2 safety performance criteria longitudinal channelizers. Test no. APR-1 occurred at 45.2 mph and 25.1 degrees, while test no. APR-2 occurred at 44.5 mph and 0 degrees. Both tests met the MASH TL-2 safety performance criteria for longitudinal channelizers. Following a review of the test results, test designation no. 2-91 was deemed not critical and not performed. Further discussions of the tests are provided by Lechtenberg et al (5).

The as-tested, prototype system did not include ADA-compliant handrails, which may be required for some roadside applications. As such, further design and crash testing may be required to investigate the use of ADA-compliant handrails. Initially, it was believed that the pedestrian rail system could be configured with segmented panels with gaps or as a continuous system. The researchers configured and tested a segmented panel system as it was believed to be easier to install. However, a continuous variation of this system is not recommended due to concerns for higher longitudinal ORAs when impacted end-on from loading simultaneously multiple posts. Although the pedestrian rail system met MASH requirements, further research on system modifications should be considered to improve safety performance, lower occupant risk measures, increase knowledge on crashworthiness of pedestrian rails, minimize debris, and incorporate ADA-compliant handrails.

ACKNOWLEDGMENTS

The authors wish to acknowledge the Wisconsin DOT for sponsoring this project as well as MwRSF personnel for constructing the barrier system and conducting component and full-scale crash tests.

DISCLAIMER STATEMENT

This paper was completed with funding from the Wisconsin DOT and the Federal Highway Administration, U.S. Department of Transportation. The contents of this paper reflect the views and opinions of the authors who are responsible for the facts and the accuracy of the data presented herein. The contents do not necessarily reflect the official views or policies of the Wisconsin DOT nor the Federal Highway Administration, U.S. Department of Transportation. This paper does not constitute a standard, specification, regulation, product endorsement, or an endorsement of manufacturers.

REFERENCES

1. *Traffic Safety Facts 2010 Data: Pedestrians*, United States Department of Transportation, National Highway Traffic Safety Administration, 2010.
2. Leaf, W.A. and Preusser, D.F., *Literature Review on Vehicle Travel Speeds and Pedestrian Injuries*, United States Department of Transportation, National Highway Traffic Safety Administration, October 1999.
3. Zegeer, C.V., Seiderman, C., Lagerwey, P., Cynecki, M., Ronkin, M., and Schneider, R., *Pedestrian Facilities Users Guide-Providing Safety and Mobility*, Report No. FHWA-RD-01-102, Submitted to the Office of Safety and Traffic Operations R&D, Federal Highway Administration, Performed by Highway Safety Research Center, University of North Carolina, March 2002.
4. Zegeer, C.V., Stewart, J.R., Huang, H.H., and Lagerwey, P.A., *Safety Effects of Marked vs. Unmarked Crosswalks at Uncontrolled Locations: Executive Summary and Recommended Guidelines*, Report No. FHWA-RD-01-075, Submitted by the Office of Safety Research and Development, Federal Highway Administration, Performed by Highway Safety Research Center, University of North Carolina, February 2002.
5. Lechtenberg, K.A., Schmidt, J.D., Faller, R.K., Guajardo, A.L., Bielenberg, R.W., and Reid, J.D., *Development of a Crashworthy Pedestrian Rail*, Final Report to the Wisconsin Department of Transportation, MwRSF Report No. TRP-03-321-15, Midwest Roadside Safety Facility, University of Nebraska-Lincoln, January 18, 2016.
6. *AASHTO Load and Resistance Factor Design (LRFD) Bridge Design Specifications*, American Association of State Highway and Transportation Officials (AASHTO), 2010.
7. *2010 ADA Standards for Accessible Design*, United States Department of Justice, September 2010.
8. *2012 International Building Code (IBC)*, International Code Council, Country Club Hills, Illinois, June 2011.
9. *Part 1910 – Occupational Safety and Health Standards (OSHA)*, United States Department of Labor, June 2012.
10. *Manual for Assessing Safety Hardware (MASH)*, American Association of State Highway and Transportation Officials (AASHTO), Washington, D.C., 2009.
11. *2010 Aluminum Design Manual*, The Aluminum Association, 2010.

12. *Speed-Rail, ADA Railing, Handrails, Panels & Pipe Fittings*, Hollaender Component Catalog, Hollaender Manufacturing Company, Cincinnati, Ohio, Website Link:
<<http://www.hollaender.com/?page=speedrail>>.

Vulnerable Road User Serious Injury Impacts into W-Beam Barriers

RAPHAEL GRZEBIETA

GEORGE RACHNITZER

MARIO MONGIARDINI

MIKE BAMBACH

*Transport and Road Safety Research Centre
University of New South Wales*

When motorcyclists, cyclist or pedestrians impact or fall onto unprotected guard rail barriers traditionally used to redirect cars and SUVs at road sides or in medians, the resulting injuries can potentially be quite severe and often life threatening. This is mainly because the interface between the vulnerable road user and such barriers is often hazardous in Australia, made up of thin steel profile sharp edges and posts with gaps that can catch and fracture/amputate limbs, and tear and cut human tissue. European road safety stakeholders recognizing this issue in regards to motorcyclists striking these barrier types introduced the European Standard EN 1317-8, where a specially developed anthropometric crash test device (ATD), i.e. crash test dummy, is propelled sliding head first into the barrier at a speed of 60 km/h and at an angle of 25 degree. Body impact kinematics (sliding as opposed to catching) and injury criteria for the head impact, and more recently for the thorax, are specified as performance requirements. The usual resulting countermeasure is the barrier is fitted with a rub rail along the bottom. This provides a safe interface against which the rider can be deflected in a sliding manner along the barrier without injury.

However, there are no tests for a motorcyclist impacting the barrier in an upright position despite the fatality data investigated by the authors showing that around 50% of motorcyclists strike the barrier upright and around half of these slide along the top of the barrier with consequential horrific injuries to the rider. Similarly there are no tests for either cyclists or pedestrians tripping and falling on top of such barriers. One of the Authors has been involved as experts in serious injury cases where either a cyclist or a pedestrian has fallen on top of a W-beam barrier which is constructed of C-section posts and block-outs. Because of the sharp thin-walled profile interface the victims have suffered serious life threatening cuts and injuries.

The objective of this presentation is to describe the mechanisms of injury for these vulnerable road users that have struck such unprotected W-beam barriers and to propose countermeasures which alleviate and reduce such injuries without reducing the barrier's capacity to safely redirect cars and SUVs. The circumstances of the event and the impact kinematics will be discussed and how the interface can be changed to be more forgiving to the vulnerable road user colliding with the barrier. The frequency of such events will also be discussed so that a perspective of the likelihood of such impacts occurring can be gained and how best it should be handled by road authorities and councils. For example, to keep infrastructure costs at a reasonable level, the Authors have recommended that rub-rails for W-beam barriers can be installed in motorcycle black spot areas such as mountainous curvy roads where there is a high frequency of motorcycle run-off-the-road crashes on curves. This is in contrast to installing rub rails on all W-beam barriers throughout the whole network.

Development of Guidance for Minimum Sign Area for Slipbase Sign Supports

ROGER BLIGH

CHIARA DOBROVOLNY

DUSTY ARRINGTON

Texas A&M Transportation Institute

This research establishes minimum sign area appropriate for slipbase sign support systems required to meet the impact performance criteria included in the Manual for Assessing Safety Hardware (MASH). Of particular interest to the performance of small sign supports is the windshield and roof crush criteria. Full-scale crash testing was performed with both the MASH 1100C passenger car and 2270P pickup truck at a speed of 62 mph. A passenger car test of an aluminum sign substrate with an area of 12 ft² mounted at 7 ft on a 10 gage support post with a triangular, omni-directional slip base failed to meet the MASH roof crush criteria. Subsequent testing with a 14 ft² sign panel met MASH criteria. Although the tests were performed on a triangular slipbase breakaway support system, the researchers recommend 14 ft² as the minimum sign area applicable for all types of frangible sign support connections when the sign panel and support post are released from the base and rotate as a rigid body after vehicle impact.

Consideration of Placement Criteria for Utility Poles to Minimize Crash Risk

CHRISTINE E. CARRIGAN

MALCOLM H. RAY

RoadSafe, LLC

Generally, the goal of roadside design is to minimize, in so far as practical, the chance of fatal or incapacitating injury crashes. Methods to quantify the risk reduction and make utility pole placement decisions have been problematic in the past. Traditionally, benefit-cost methods have been used in roadside safety to balance improvements to safety with implementation costs. The benefit-cost approach presents a significant challenge with respect to the consideration of utility poles because, although risks and costs are both measured in dollars, the risk reduction benefits and direct improvement costs do not accrue to the same entities. Crash cost reductions accrue to society in general as managed by road owners but the improvement costs are paid by the utilities. Using tools readily available to any engineer, this paper presents a method for establishing a baseline for risk based on existing crash performance and measuring the risk of different pole location alternatives such that engineers can identify which locations have higher than average risk, lower than average risk, and where the greatest risk reduction can be realized.

The primary advantage to the approach proposed is that it allows for utility companies to target their risk-reduction dollars on poles which represent the greatest risk. The poles which should be targeted can be quantified through a series of tables such as those presented. Implementation of this methodology will provide a scientific approach to pole location projects to ensure crash risk is explicitly considered and reduced where possible.

INTRODUCTION

The opening pages of AASHTO's *Roadside Design Guide* (RDG) are very clear that the *RDG* is intended to be used as a guide. The concepts, designs, and philosophies presented in the *RDG* "...cannot, and should not, be included in their totality on every single project." The guidelines presented in the *RDG* "...are mostly applicable to new construction or major reconstruction projects." (1) Generally, the goal of roadside design is to minimize, in so far as practical, the chance of fatal or incapacitating injury crashes on the roadside. While it may not be possible to minimize that risk to the level implied in the *RDG* while maintaining agreements for access with utility companies, it is still desirable to minimize the risk as far as practical.

Benefit-cost methods have been used in roadside safety for over 35 years to balance improvements to safety with implementation costs. Benefit-cost methods compare the risk reduction (i.e., reduction in crash costs) to the capital cost increase (i.e., cost of construction, repair and maintenance) for each viable alternative. While widely used, this approach presents a significant challenge with respect to the consideration of utility poles; although risks and costs are both measured in dollars, the risk reduction benefits and direct improvement costs do not

accrue to the same entities. Crash cost reductions accrue to society in general but the improvement costs are paid by the utilities. Separating the risk assessment from the benefit-cost assessment allows for the direct consideration of risk reduction across alternatives. Utilities generally operate on the right-of-way as a licensee of the State or local jurisdictions so it is the State or local government's responsibility to represent and protect the general public. Cost-benefit and risk assessment tools are readily available to the user in the third version of the Roadside Safety Analysis Program (RSAPv3).⁽²⁾ This paper quantifies the risk of varying utility pole spacing and offset and provides a rational basis for alternative pole placements which will reduce risk to vehicle occupants. This paper presents a quantitative approach for measuring the risk of different pole location alternatives such that engineers can identify where the greatest risk reduction can be realized.

RISK ANALYSIS

Before considering the problem of utility pole placement, it is useful to establish exactly what risk is in the field of roadside safety. Consider a very extreme example of a vehicle encroaching onto the roadside where there is a fifty percent probability of having a crash. There is then an equal fifty percent probability of not having a crash. The probability of an encroachment resulting in a crash is $p = 0.5$. Then define "crash" as the event of interest and let x equal the number of such events in n independent trials or encroachments, the probability of observing the event can be found using a binomial distribution. A popular example of events which can be modeled using a binomial distribution is a coin toss. If the coin is tossed one time ($n=1$), the probability that there will be one "heads" event ($x = 1$) is 0.5. If the coin is tossed twice ($n=2$), the probability that there will be two "heads" events ($x = 2$) is 0.25, etc. The same is true for roadside encroachments in our extreme example. If a vehicle encroaches onto the roadside one time ($n=1$), the probability there will be a crash in this extreme example is 0.5. If two vehicle encroach onto the roadside in two independent encroachment events ($n=2$), the probability that there will be two crashes is 0.25.

The probability of having a single encroachment resulting in a crash is generally much smaller than 0.5, however, the same principles apply when predicting how many crashes will occur based on how many encroachments have occurred. Each roadside design has a different probability of having a single encroachment result in a crash. Modeling that probability (p) for each alternative under consideration then allows for the consideration across all reasonable traffic volumes and resulting encroachments.

These concepts are used here to understand the risk utility pole placement alternatives present. The independent trials will be the vehicle encroachments which vary with traffic volume, roadway characteristics and segment length. The event of interest is a crash of a certain severity with a utility pole (x), the Cumulative Binomial Distribution (CBD) function is used to determine the probability of x or more crashes of a particular severity occurring for any design alternative.

Risk Assessment Procedures

The third version of the roadside safety analysis program (RSAPv3) ⁽²⁾ was used to model the cumulative distribution of crash costs over the life of each alternative. The severity of crashes are

most commonly measured using the police reported KABCO injury scale where a K injury represents a fatal injury, an A represents a incapacitating injury, a B represents a serious injury, a C represents a minor injury and an O represents a property damage only crash (i.e., PDO). Ray *et al.* defined the equivalent fatal crash cost ratio, EFCCR, for use in RSAPv3. (2) The EFCCR is simply the ratio between the crash cost of a particular crash divided by the cost of a fatal crash. These values were developed based on observed crash data. Essentially, the EFCCR values in the RSAPv3 database represent the average severity of a crash with that particular type of object divided by the cost of a fatal crash. Since the EFCCR is a dimensionless ratio it does not vary with time.

Crash data from police reports specify a discrete level of injury (e.g., KABCO) but, in fact, the actual crash cost for any specific crash varies along a continuous spectrum. RSAPv3 estimates crash costs on a continuous scale so it is necessary to map the continuous crash cost spectrum onto the discrete KABCO levels for this analysis. Table 1 shows recommended cut-off values for the various typical severity levels. (3) For example, while an EFCCR of 1 represents the average fatal crash severity, any crash with an EFCCR greater than 0.173 would be considered a fatal crash.

Take for example a utility pole located six feet from the edge of the travel lane of a two-lane undivided highway. The pole is on the outside of a horizontal curve with a 400-ft radius. Aside from the isolated pole, the clearzone is obstacle-free and traversable so there are no other hazards of concern. The traffic volume is 5,000 veh/day with 12% trucks. The pole is located within the clearzone as defined by the RDG so moving or shielding the pole would bring the site into conformance with the RDG guidelines. Does the pole in its present location, however, create sufficient risk such that it should be moved? The three alternatives that could be considered are:

1. Leave the utility pole where it is,
2. Move the pole to the inside of the curve or
3. Move the pole back to the edge of the clearzone.

The upper portion of the cumulative probability distribution of the crash severities in terms of EFCCRs are shown for these three utility pole alternatives in Figure 1. (3) The square marker in Figure 1 indicates that there is a 0.99 chance of a crash having an EFCCR (i.e., ratio of the crash cost to a fatal crash cost) less than 0.0160. As shown in Table 1 any EFCCR above 0.013 can be considered a fatal or incapacitating injury crash (i.e., K+A) so Figure 1 indicates that for the pole in its existing location there is a $1-0.99=0.01$ risk of observing a fatal or incapacitating injury crash.

TABLE 1 EFCCR Threshold for Each Identified Target Risk (3)

	K	A	B	C	PDO
EFCCR	1.0	0.07	0.01	0.007	0.0007
Risk of Fatal (K) Threshold	← $K > 0.173$				
Risk of K+A Threshold	← $K+A > 0.013$				
Risk of KABC Threshold	← $F+I > 0.001$				

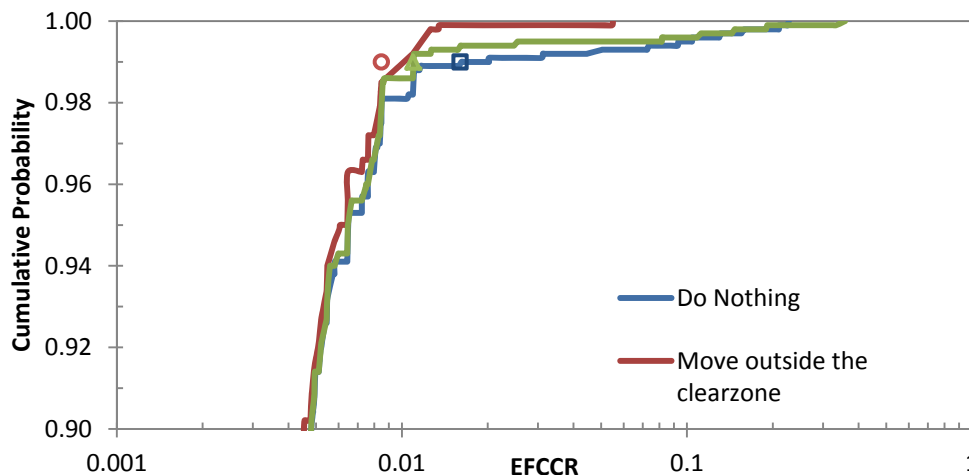


FIGURE 1 Cumulative probability distribution of EFCCR for utility pole alternatives.

Returning to the discussion of the risk assessment procedure, the independent trials are the vehicle encroachments (n). The event (x) is defined as a crash with a utility pole that has an EFCCR greater than the thresholds shown in Table 1. The cumulative binomial distribution function can be used to determine the probability of x crashes of a severity higher than the threshold occurring for any design alternative. This procedure allows for the calculation of expected risk, however, it does not establish what level or risk is acceptable. While it is desirable to eliminate all risk it is often impossible to do so; the best that can be accomplished is to minimize the level of risk to an acceptably low value.

Establishing Acceptable Risk Target

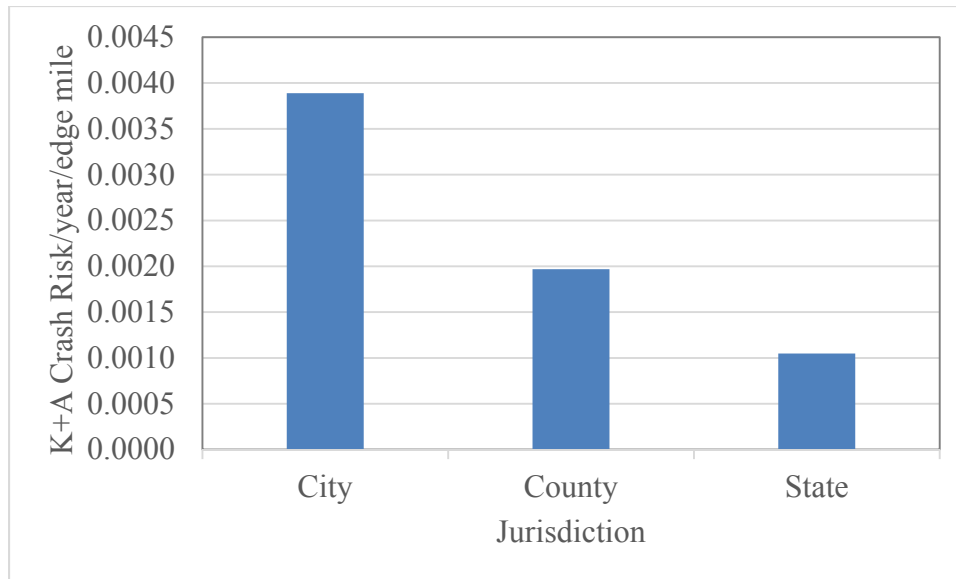
Establishing a risk target is a policy decision and could be done nationally, regionally or locally. To better understand the existing risk resulting from the current placement of utility poles, the risk of crashes with utility poles on roadways under the jurisdiction of the state, county and cities were examined in Washington State. The centerline miles of these three different highway jurisdictions were tabulated and converted to edge miles (see Table 2). Crash data from January 1, 2001 through December 31, 2014 were reviewed and tabulated for each jurisdiction type in Table 3. Additionally, crashes with utility poles per year per edge mile were summarized by jurisdiction type in Table 3. The risk of a fatal or incapacitating injury crash per year per mile is shown graphically for each jurisdiction in Figure 2. Figure 2 shows the existing risk of a fatal or incapacitating injury crash with a utility pole by roadway jurisdiction as follows:

- City: Incapacitating + Fatal Utility Pole crashes/mi/yr 0.0039 (1/256)
- County: Incapacitating + Fatal Utility Pole crashes/mi/yr 0.0020 (1/500)
- State: Incapacitating + Fatal Utility Pole crashes/mi/yr 0.0010 (1/1000)

Individual roads will experience a range of different risks; some will be higher and some will be lower than the average for these three roadway jurisdictions. These measures are offered as a benchmark to identify particular roads where the risk is higher than either the current or the acceptable risk.

TABLE 2 Centerline and Edge Miles by Highway Jurisdictions.

Jurisdiction	Centerline Miles			Edge Miles
	One-way Miles	Divided Miles	Undivided Miles	
State Highway	36.71	1,401.58	7,012.72	19,705.16
County Highway	1.98	0.00	14,379.94	28,763.83
City Highway	100.30	0.00	4,455.18	9,110.97

**FIGURE 2 Fatal and incapacitating (K+A) crash risk with utility poles for roadways in each jurisdiction type.**

Improvements by utility companies can now be focused on roadways where the risk at a particular site exceeds the average risk for roads in the appropriate jurisdiction. Under this proposed methodology, poles on roadways that already fall below the target risk (i.e., average existing risk) would not need improvements even if some of the roadway and roadside characteristics do not conform to the RDG. In these cases, it may be best to leave the existing situation as-is and spend safety dollars at another location where the target risk is exceeded. For situations where the system target risk cannot be obtained due to field conditions, the achievable level of risk can at least be documented and compared against the existing risk to ensure risk is reduced where possible.

The Cumulative Binomial Distribution function can be used to determine the probability of x crashes occurring for any design alternative with a knowledge of the independent trials (n) (i.e., vehicle encroachments which vary by traffic volume and length of the segment) and possible variations to the utility pole locations which will affect the number of crashes (p) and therefore the number of crashes (x) with a utility pole that have an EFCCR greater above the thresholds established in Table 1. The forgoing established risk goals provide the benchmark

TABLE 3 First or Second Object Struck Was a Utility Pole by Any Vehicle Type

	Dead on Arrival	Dead at Scene	Died in Hospital	Serious Injury	Evident Injury	Possible Injury	No Injury	Unknown
Crashes by Jurisdiction from January 1, 2001 through December 31, 2014								
City Street	5	55	32	404	1802	2035	6805	1482
County Road	12	132	49	600	2498	2341	7109	1358
State Route	5	57	21	206	875	900	2388	260
Miscellaneous	0	0	0	5	10	4	33	11
Sub-total	22	244	102	1215	5185	5280	16335	3111
Crashes/year	1.57	17.43	7.29	86.79	370.36	377.14	1166.79	222.21
Crashes/mile/year by Jurisdiction								
City Street	0.00004	0.00043	0.00025	0.00317	0.01413	0.01595	0.05335	0.01162
City K+A	0.0039							
County Road	0.00003	0.00033	0.00012	0.00149	0.00620	0.00581	0.01765	0.00337
County K+A	0.0020							
State Route	0.00002	0.00021	0.00008	0.00075	0.00317	0.00326	0.00866	0.00094
State K+A	0.0010							

needed to determine when a pole has an unreasonable risk and should be considered for relocation and when the existing pole can be left alone.

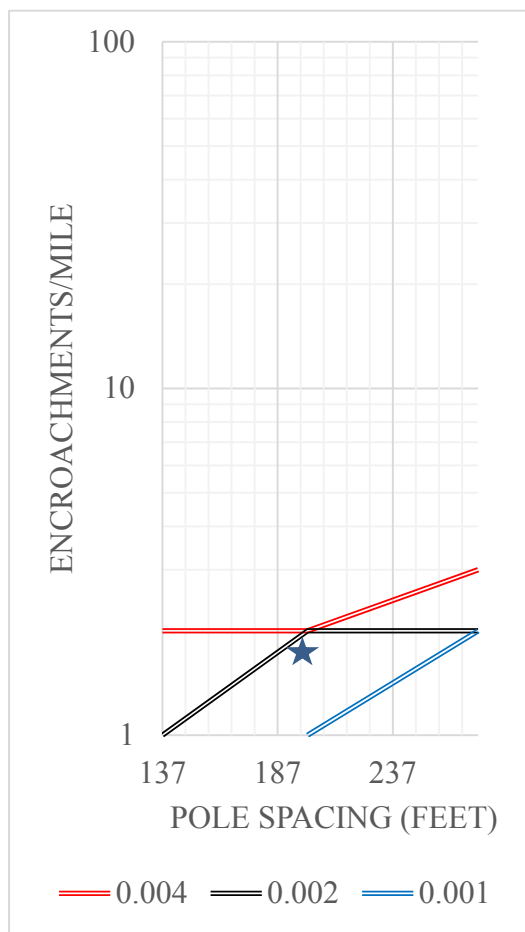
Example Utility Pole Line Risk Analysis

The probability of a utility pole being struck was considered for a variety of design alternatives using the third version of the Roadside Safety Analysis Program (RSAPv3). (2) An undivided roadway with a posted speed limit of 45 mph and 10% heavy vehicles was considered. The design alternatives considered were as follows:

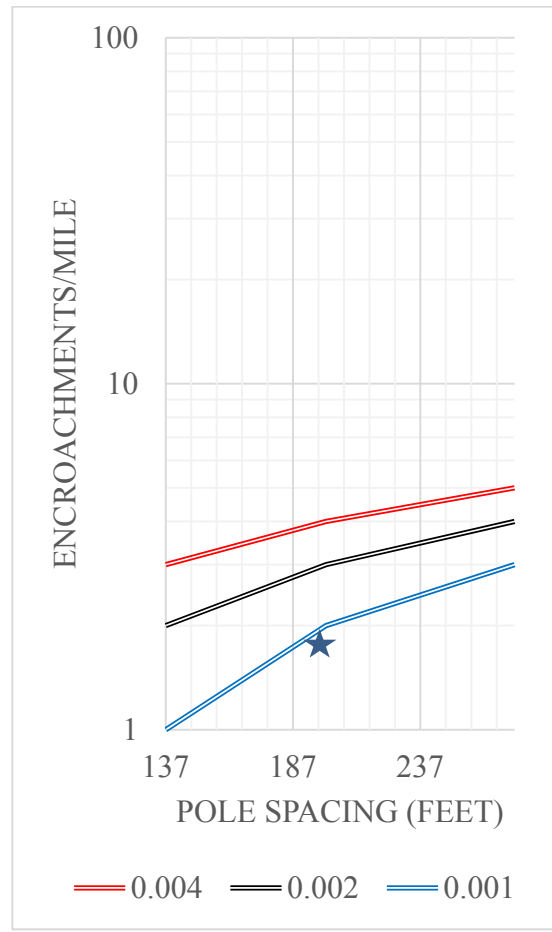
- Poles offset 5' from back of 6' shoulder; offset 20' from the travel way; or at the edge of the 30' clear zone for these three pole spacing options:
 - Spaced 137';
 - Increase the pole spacing by 50% to 200'; and
 - Double the pole spacing to 274'

The analysis resulted in a general figure which can be applied to any 45mph undivided roadway. The risk boundaries have been shown graphically for each existing risk threshold by jurisdiction discussed above (i.e., City=0.004, County=0.002, and State=0.001) in Figure 3. Figure 3 can be used two ways. One option is to use the figure to determine if the current location of a pole is above or below the statewide risk for that jurisdiction. The second option is to use the figure to determine the appropriate location for a new or relocated pole line to ensure the poles are located in such a way that the risk of a K+A crash with the poles will be below the statewide risk for that jurisdiction. Each of these uses are discussed below.

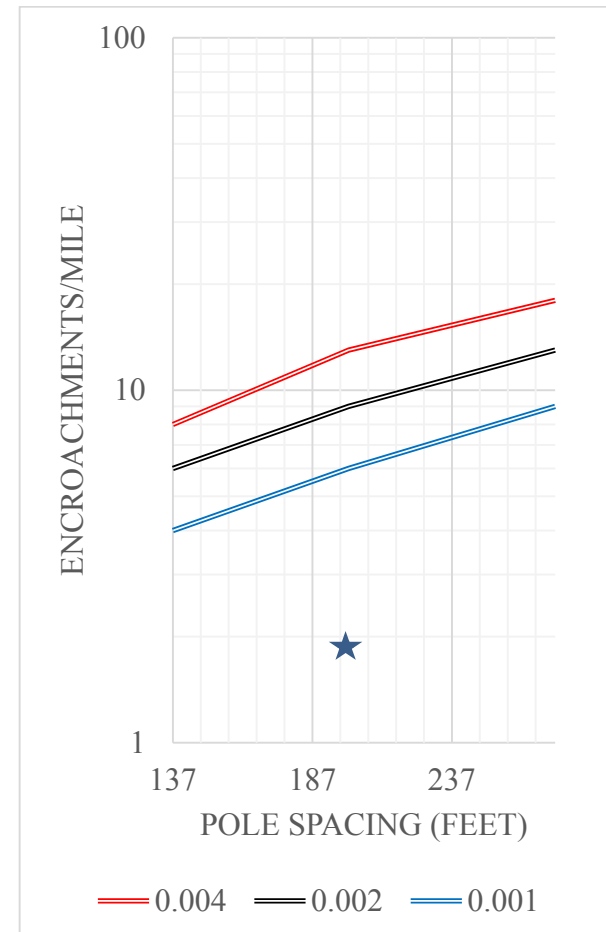
As an example, assume a line of poles are spaced 200 ft apart parallel to an undivided two-lane roadway on the State network with a speed limit of 45 mi/hr. The existing poles are 5 ft beyond a 6 ft shoulder so the distance from the edge of the travelled way to the poles is 11 ft. The traffic volume at this location is 10,000 vehicles/day and the road has a 6-degree horizontal curve which curves away from the poles when travelling on the side of the road next to the poles. The road is also on a 5% downgrade when travelling in the direction where the poles are next to the travel lane. First, the engineer would enter Figure 4 with the AADT of 10,000 vehicles/day and follow a line up to where it intersects the curve. This provides the estimate of the number of encroachments at this traffic volume if the road were straight and flat. There would be 0.93 encroachments/edge-mile/yr expected for a traffic volume of 10,000 vehicles/day. The horizontal curvature and grade will affect the number of encroachments so the engineer next would enter Figure 5a with the value of 6 degrees of curvature. Since the poles are on the outside of the curve (i.e., they curve away from the side of the road with the poles) the adjustment would be 1.56. Similarly, encroachments on a 5% downgrade should be adjusted by a factor of 1.28 as shown in Figure 5b. The total estimated number of annual encroachments, therefore, is $0.93 \cdot 1.28 \cdot 1.56 = 1.86$. On average 1.86 vehicles/edge-mile/year will leave the travelled way on this particular two-lane rural road with its 6 degree horizontal curve and 5% downgrade. Now the engineer can enter Figure 3 knowing (1) the estimated number of encroachments per edge-mile per year (i.e., 1.86) and (2) the pole offset (i.e., 11 ft from the travelled way) and (3) the pole spacing (i.e., 200 ft). The blue star in Figure 3a represents this point.



(a)



(b)



(c)

FIGURE 3 Bounds of K+A risk of utility poles crashes at a variety of pole spacing and offsets by vehicle encroachments: (a) poles 11 ft from traveled way; (b) poles 20 ft from traveled way; and (c) poles 30 ft from traveled way.

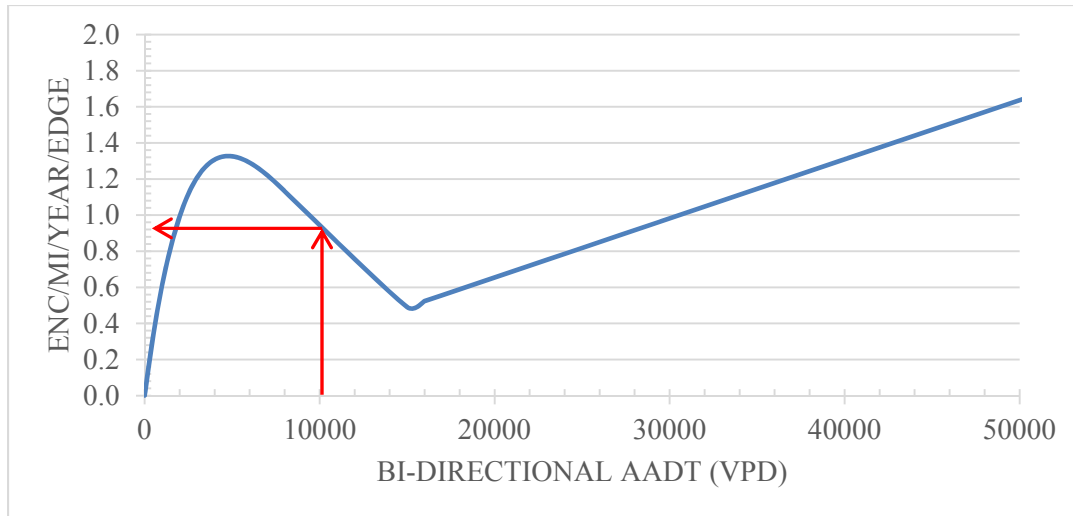


FIGURE 4 Expected number of encroachment per mile per year for an undivided two lane roadway (2).

This particular road is a State roadway and the average risk is represented in Figure 3a as a blue line. These particular site conditions plot above the blue risk line so this site does not fall below the State target of the average existing risk. Figure 3b shows the risk curves for a line of poles located 20 ft from the travelled way. The blue star again represents these particular field and traffic conditions and if the poles are located 20 ft from the travelled way, the point plots just below the Statewide average which would be acceptable. If the engineer wanted or could further reduce the risk, the offset could be increased to 30 ft from the travelled way as shown in Figure 3c.

This example shows that the existing utility pole risk can be quickly compared to the jurisdictional risk goal to determine if the site characteristics plot below or above the risk goal. This method also allows the engineer to quickly assess if changing the offset or spacing would reduce the risk to an acceptable level.

CONCLUSION

Existing crash data and mileage logs were reviewed to determine the current K+A risk of utility pole crashes by roadway jurisdiction. It was found that currently the jurisdictional risks for fatal and incapacitating crashes with utility poles are as follows:

- City K+A Utility Pole crashes/mi/yr 0.0039 (1/256)
- County K+A Utility Pole crashes/mi/yr 0.0020 (1/500)
- State K+A Utility Pole crashes/mi/yr 0.0010 (1/1000)

RSAPv3 was used to generate the K+A risk associated with some typical pole spacing and offsets. Risk boundaries were plotted to show the risks associated with each typical design evaluated. An example was used to demonstrate how this type of analysis can be used to either (1) determine if the current location of a pole line presents a risk which is above or below the

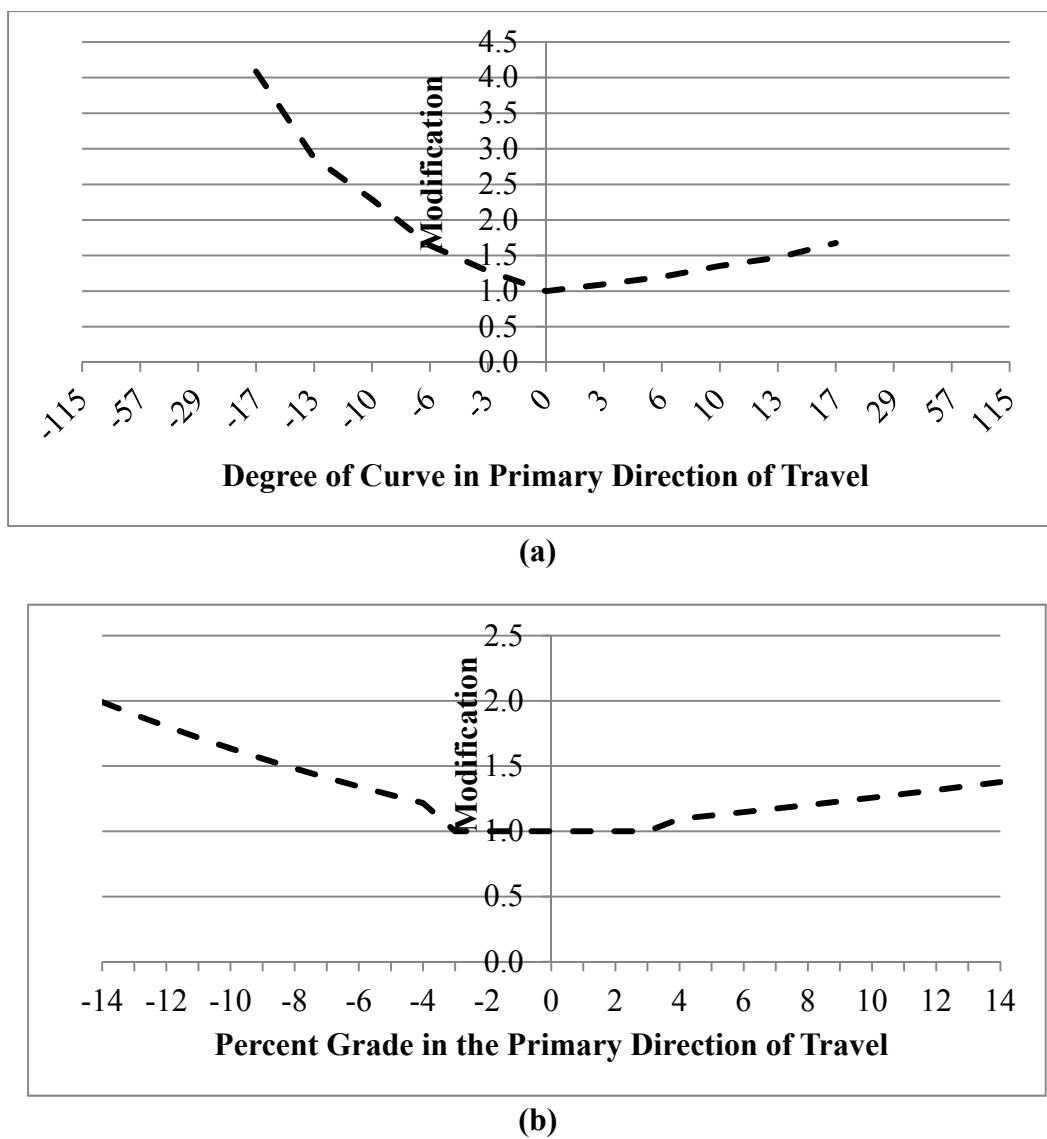


FIGURE 5 Undivided horizontal curve (top) and vertical grade (bottom) encroachment adjustment factors: (a) undivided horizontal curve encroachment adjustment factor and (b) undivided vertical grade encroachment adjustment factor (4).

statewide risk for that jurisdiction; or (2) determine the appropriate location for a pole line to ensure the poles are located in such a way that the risk of a K+A crash with the poles will be below the statewide risk for that jurisdiction.

The primary advantage to this approach is that it allows for utility companies to target their risk-reduction dollars on poles which are causing the greater risk. Similarly, this method allows the jurisdictions to more effectively manage risk on their roadway networks and target improvements to the neediest areas. The poles which should be targeted can be quantified through a series of tables such as that shown above, thereby removing the necessary step of analysis for every pole relocation project and saving time for both the utility companies and the departments of transportation. Implementation of this type of approach will necessitate

identifying typical pole placement for analysis and inclusion in a series of figures. Implementation of this approach will provide a scientific methodology to pole location projects to ensure crash risk is explicitly considered.

ACKNOWLEDGMENTS

The authors wish to acknowledge the thoughtful comments of the Washington Department of Transportation in the preparation of this paper. The authors also wish to thank the Washington Department of Transportation for providing the data for this analysis.

REFERENCES

- 1 American Association of State Highway and Transportation Officials, "Roadside Design Guide," Washington, D.C., 2011.
- 2 Ray, M. H., Carrigan, C. E., Plaxico, C. A., Johnson, T. O., "Engineer's Manual: Roadside Safety Analysis Program (RSAP) Update," <http://rsap.roadsafellc.com/RSAPv3EngineersManual.pdf>, Roadsafe LLC, Canton, ME, December 2012.
- 3 Ray, M. H. and Carrigan, C. E., "Using Risk Analysis to Minimize Adverse Consequences in Non-Standard Designs," Transportation Research Record, Transportation Research Board, Washington, D.C., (in press).
- 4 Carrigan, C.E. and Ray, M.H., "Proposed Horizontal Curve and Vertical Grade Encroachment Adjustment Factors," Transportation Research Record, Transportation Research Board, Washington, D.C., (in press).

ROADSIDE SAFETY DESIGN AND HAZARD MITIGATIONS

Utility Poles, Toleration, or Confrontation

DON L. IVEY
Scientific Inquiry, Inc.

C. PAUL SCOTT
Cardno, Inc.

Utility poles have resulted in about 1,000 fatalities every year for the past five years. One in every seventeen fatalities associated with roadway departures is due to a collision with these poles. This paper explores the reasons for fatalities associated with utility poles. There are many proven approaches to accomplish the goal of reducing exposure to rigid utility poles. State departments of transportation (DOTs), local highway agencies (HAs) and utility owners (UOs) have used these methods to varying extents. This paper illustrates the extent of the problem, the safety structures and analytical methods available to solve the problem, and the continuing effort to gain recognition of the problem.

INTRODUCTION

There are an estimated 1,000 fatalities and up to 30,000 serious injuries due to automobiles striking utility poles every year.

Table 1, from FHWA's Fatal Accident Reporting System documents these losses for 2015 and compares them with other objects struck within our highway right-of-way (ROW) (1).

TABLE 1 Fixed-Object Fatalities (2015)

Fixed Object Struck	Fatalities	% of Fixed Objects
Tree	3,514	47
Utility Pole	953	13
Traffic Barrier	609	8
Embankment	401	5
Ditch	252	3
Culvert	218	3
Bridge Pier	160	2
Fence	156	2
Building	141	2
Wall	127	2
Guardrail End	110	2
Sign Support	129	2
Other	728	10
Total	7,498	100

Utility poles and trees pose a similar hazard, but trees have sometimes been dealt with different than utility poles:

- Highway engineers have advocated the maintenance of a “clear zone” or a clear recovery area along our roadsides that statistically should work for 80% of vehicles leaving the roadway. (2,3)
- Highway engineers have tried to eliminate the rigid objects within the clear recovery area, and if the rigid object cannot be moved, it should be made
 - break-away, energy absorbing or shielded from vehicle impacts by a more collision tolerant structure. (4)
- It is estimated there are over 100 million rigid objects within highway ROWs that are utility poles. (5)
- An estimated 75,000 vehicle collisions with those utility poles every year. (6) (That is over 4 million utility pole collisions over the last 50 years, currently about 4 collisions every minute or one collision every 15 seconds).

Utility pole collisions account for about 13% of rigid obstacle collisions, which represents about 1000 collisions today, down from almost 2,000 in 1975.

Reasons for the reduction in utility pole collisions from 1975 to 1985 may be attributed to the overall the reduction in fatalities per 100 million vehicle miles—which is viewed as the result of implementing access-controlled freeways and Interstates.

In Figure 1, the estimated number of fatalities caused by utility pole collisions from 1965 until 2015 is estimated at 63,000. If the more recent ratio of 30,000 injuries per 1,000 fatalities holds, this would mean nearly 2 million injuries caused by utility poles over the same period.

Reasonably priced electrical power has affected the wellbeing and comfort of many in the 20th century. Timber utility poles have offered reasonably priced electrical power for the vast majority of Americans. The 100 million timber utility poles installed semi-permanently on highway ROWs are also carrying reasonably priced electrical power in developed countries.

The present system can be economically modified to reduce the human cost. To do this we must distinguish between poles that have been or may be subject to completely random collisions (reasonably exposed poles) and poles that for human, traffic or geometric reasons have a predictably higher than normal exposure. Those relatively rare poles, “Black Poles”, can be economically modified or moved to significantly reduce vehicle collisions. The problem is to recognize and implement a reasonably accurate way of identifying “Black Poles”.

It has been estimated that in the United States, no more than one-tenth of one percent (or about 100,000) of utility poles within highway ROWs are Black Poles. Modifying even some of these may appeal to utility owners and stockholders as doing so could allow for cost savings. See cost effectiveness section of SOAR No. 9 (5) and most recent report specific to New Jersey (8).

For the sake of comparison, State DOTs have replaced or added an estimated one million guardrail end treatments since the 1990s. (9) If the average cost of each marginally improved end treatment is \$1,000, the total cost nationwide comes to about \$1 billion dollars. The societal cost of deaths and injuries from less efficiently functioning Breakaway Cable Terminals and Turned Down end treatment terminals was relatively small compared to that of utility pole collisions. In the following section considers ways “Black Poles” can be identified and reasonably economic measures that could be used for their modification.

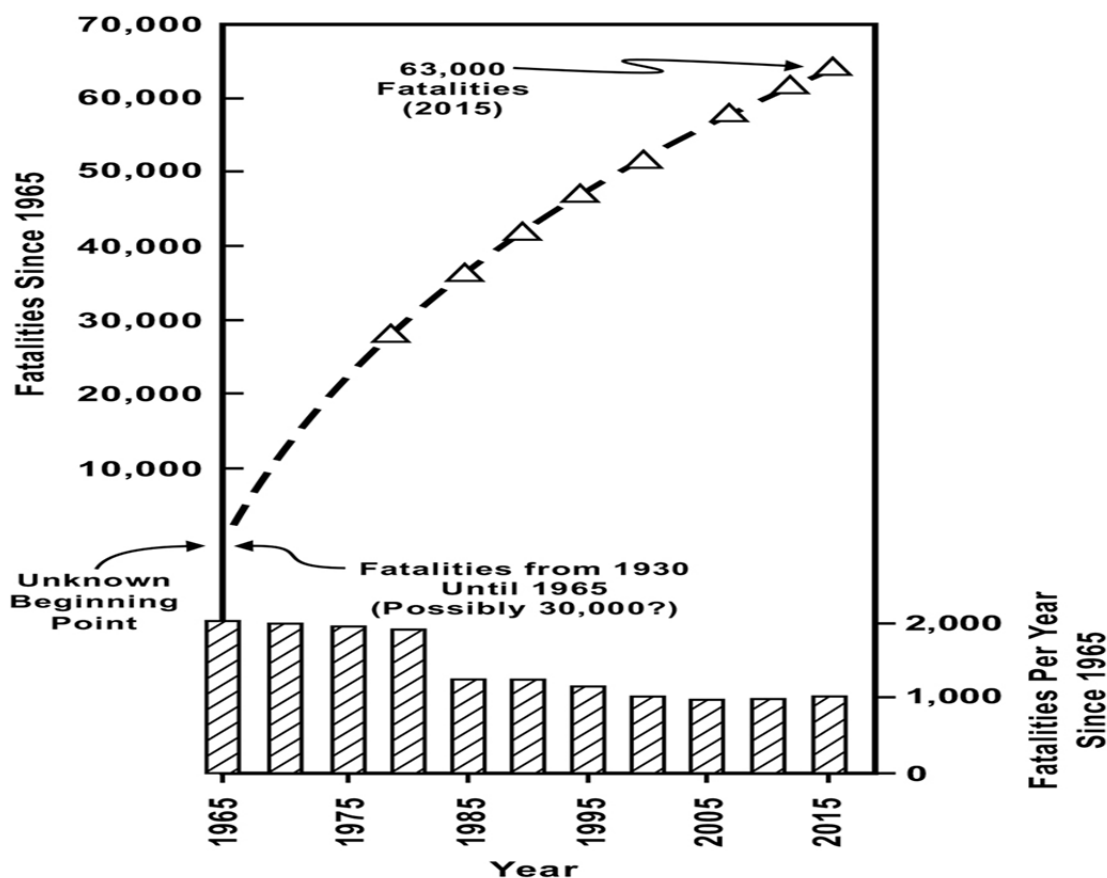


FIGURE 1 Total losses in life attributable to utility pole collisions since 1965.

IDENTIFYING BLACK POLES

We consider obvious violations of driver expectancy and probable collision trajectories. Exposure situations include the following: 1) Poles on the outside of curves, especially on curves where the advisory speed is less than the design speed of adjacent tangent sections; 2) Poles on the roadside immediately after, and in line with a lane termination; 3) Poles exposed to oncoming traffic in the zone where pavement narrows significantly; 4) Poles in the median of divided roadways; 5) Poles on traffic islands exposed to oncoming traffic; 6) Poles adjacent to reversed curves when the pole line moves from one side of the roadway to the other side; and 7) Poles in the critical quadrants of an intersection. See Figure 2.

Conflicts 1 through 5 are presented and discussed in SOAR No. 9 (5), pages 48- 51.

“Black Poles” are where collisions are occurring or can be predicted to occur. Note, however, that a single collision does not necessarily identify a Black Pole, but even a single event should constitute reason to consider that pole’s location. Figure 3 shows an easily identified Black Pole. The upper one is located in the clear zone, or zone of high traversal probability. The lower part of the figure shows poles simply too close to the traveled way.

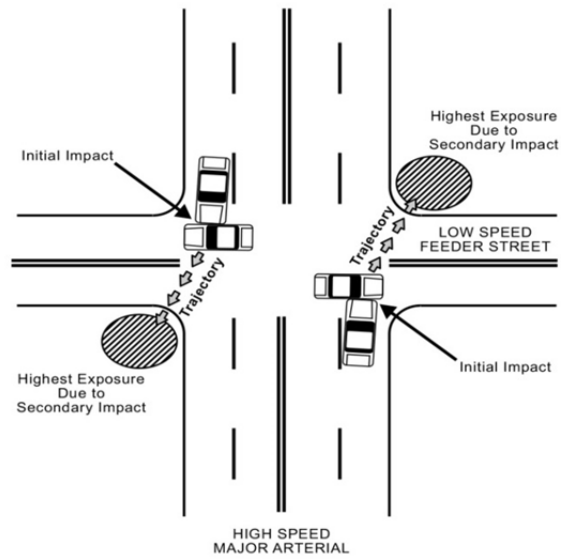


FIGURE 2 Intersection zones.



FIGURE 3 Black poles draw crowds, who then leave memorials.

Besides the geometric conflicts described, there are several methods that may be useful in determining crash probability locations. Each depends on setting up a Pole Exposure Record System or systematically determining the relative exposure within the utility system. Once exposure to collisions is determined as part of a comprehensive, prioritized, cost-effective, safety program, it is possible to use one or more of five different analytical methods to identify Black Poles. They are all related to either numeric frequency, collision rate, quality control, crash severity or a combination of those four characteristics. These approaches are described on page 54 of SOAR No. 9 (5) and are emphasized in the latest effort by Gabler et al (8) for New Jersey DOT and FHWA.

SOAR No.9, pages 18-21, gives a three-path approach to reducing utility pole fatalities consisting of Best Offense, Best Bet and Best Defense as summarized below:

- **Best Offense:** The best offense approach involves identifying where an over representative number of collisions are occurring, considering available countermeasures, prioritizing these poles for treatment, and implementing the improvements.
- **Best Bet:** The best bet approach involves prioritizing potentially hazardous poles and roadway sections (using statistical prediction algorithms) before an accident history develops and implementing appropriate improvements.
- **Best Defense:** The best defense approach complements the first two strategies. It involves striving to meet the recommendations of the *Roadside Design Guide (RDG)* (3). In the courthouse, a second legally damaging condition, behind a significant crash history, is failure to meet the recommendations of the *RDG*. This is true for state DOTs and Highway Agencies (HAs) and may become important for utility owners. (UOs)

The Best Offense requires the documentation of collisions to identify specific locations or segments of highways when an atypical number of collisions have and are occurring. This would be available from Police Accident Reports and the maintenance records of the Utility.

The Best Bet is an effort to identify where collisions are most likely to occur in the future. It requires a DOT or Utility to have knowledge of the roadway system, including utility positions within ROWs to identify where exposure to poles is most significant. There are predictive algorithms available for this that includes traffic density and speed, pole frequency and pole lateral placement.

The Best Defense also relies on knowledge of the highway and utility systems. It is almost as easy as identifying where ROW restrictions have resulted in poles too close to traffic movement. Where these ROW restrictions are in conflict with clear zone recommendations could be used to prioritize safety treatments.

COUNTER MEASURES

The Roadside Design Guide (3) contains the following options for the safe location and design of new utilities and the relocation of existing hazardously-located utility poles:

- Increase lateral pole offset.
- Increase pole spacing.
- Combine pole usage with multiple utilities (joint use).

- Place electric and telephone lines underground.

FHWA's Dwight Horne (retired) proposed a comprehensive set of solutions and countermeasures that can be used to address safety problems associated with hazardously-located utility poles (10). They are as follows:

- Keep vehicles on the roadway:
 - Use pavement markings and delineators.
 - Improve skid resistance and drainage.
 - Widen lanes.
 - Widen and pave shoulders.
 - Straighten curves.
- Change pole position or remove:
 - Move select poles.
 - Decrease number of poles through joint use.
 - Decrease pole density.
 - Increase lateral offset.
 - Increase spacing.
 - Locate poles where they are less likely to be struck (includes underground).
- Use safety devices:
 - Crash cushions.
 - Steel reinforced safety poles. (SRS Poles)
 - Guardrail.
 - Concrete barriers.
- Warn motorist of obstacles:
 - Pole delineation (reflective paint, sheeting, or delineation markers on poles).
 - Roadway lighting.
 - Warning signs.
 - Rumble strips.

Safety Devices

Crash Cushions

Crash cushions ranging from simple effective sand-filled barrels to the most sophisticated devices are appropriate to shield vehicles occupants from hazardously-located utility poles. At least seven approved designs are listed in the 4th edition of the Roadside Design Guide (3). Various crash cushions designs were first widely decimated in 1977 (4). These designs are approved for use by the FHWA on the National Highway System. The most cost effective crash cushions developed, where continuous collision recurrences are not expected, are sand-filled barrels. Figure 4 shows an installation in Lafayette, Louisiana where a Black Pole was in close proximity to traffic on a curve. Note how chevrons have also been used to better delineate the curve.

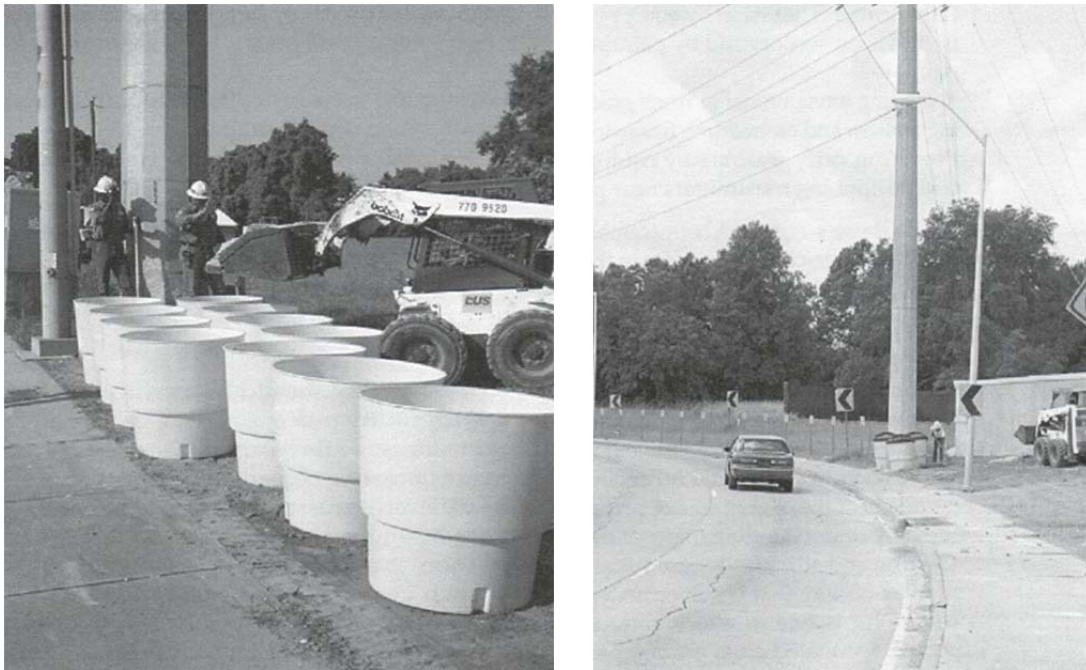


FIGURE 4 Installation of sand barrel crash cushion.

Steel Reinforced Safety Poles (SRS Poles)

The FHWA sponsored research in the early 1980s to develop an economical “yielding” timber utility pole that would increase the safety of passengers in impacting vehicles and satisfy the strength and durability requirements important to the utility industry. Consequently, in 1986 a slip-base design was developed (11) that met the stated requirements. That SRS Pole consisted of a slip base mechanism three inches above grade and an upper hinge consisting of a band and strap mechanism that allowed the bottom pole segment to yield and rotate clear of an impacting vehicle, the same mechanical function that tamed rigid sign supports on the Interstate system. That design was subjected to NCHRP 350 (12) testing and is now included in MASH (14).

Massachusetts Electric Cooperative and the New England Telephone Company installed 19 experimental SRS Poles in Massachusetts near Boston. (See Figure 5)

The FHWA provided technology application funds in 1989 for experimental installations of the SRS Poles in Kentucky where the Kentucky Utilities Company retrofitted 10 existing wooden poles in Lexington, and again in 1995 in Virginia where Delmarva Power installed five poles on the eastern shore.

The FHWA provided technology application funds in 1994 for experimental installations of the SRS Poles in Texas where the Texas Electric Company installed six poles on an urban arterial between Fort Worth and Dallas.

FHWA required evaluations of all these experimental poles for several years after installation. Results were as follows:



FIGURE 5 Steel reinforced safety pole (SRS pole).

- Massachusetts evaluated SRS Poles two years after installation. During that time, although the SRS Poles were exposed to wind, ice and snow, no pole problems resulted from these forces. An incident in Massachusetts in 1991 (Hurricane Bob) displayed the ability of the poles to resist wind loadings that toppled conventional poles. Poles in Massachusetts were hit five times during the evaluation period by errant vehicles. There were no serious injuries, no loss of utility service, no safety problems relative to linemen, and an average repair time of 90 minutes. In all these crashes, the SRS Poles were found by utility personnel to be safer, quicker and easier to repair than standard poles, primarily because the need to transfer or repair service lines was eliminated.

- Texas evaluated the SRS Poles three years after installation and reported only one crash, which occurred on March 13, 1995. In spite of a shoulder maintenance problem, the pole functioned during the collision and serious injuries did not occur. In the first three years after the SRS Poles were installed, there were several instances of high winds, including a hail storm that destroyed the roof and west wall of virtually every building that was not sheltered by trees or other buildings in this area of Ft. Worth and Arlington. Texas Electric Company engineers note that some wind gusts were as high as 80 mph and that some conventional poles were downed. The SRS Poles sustained no damage.

- Kentucky evaluated the modified SRS Poles two years after installation. It was reported that the poles performed well in high winds (up to 80 mph) and that maintenance costs consisted only of those necessary to straighten the upper segments of some poles.

- Virginia evaluated modified SRS Poles design two years after installation and reported there were no maintenance costs or problems. There were several instances of high winds without pole damage or even modest deformation.

Energy Absorbing Utility Poles

The Energy Absorbing Utility Pole (8) (Plastic reinforced with fiberglass) has now been successfully tested under the collision conditions of NCHRP 350. It is approved for use within highway rights-of-way by FHWA. This pole has been used to replace a number of atypically exposed wood poles in New Jersey with excellent overall results.

A comprehensive study of Energy Absorbing Utility Poles and Steel Reinforced Safety Poles (SRS Poles) was conducted for New Jersey DOT and reported in 2007 by Gabler et. al (8). Those authors found a variety of situations where both Energy Absorbing Poles and SRS Poles were cost effective and further reinforced many of the conclusions, and approaches to alleviate the human cost of “Black Poles”, that were presented in SOAR No. 9 (5).

Low Profile Barrier

The low-profile barrier (LPB) is simply a short portable concrete barrier (20 in. tall). It has been used extensively in construction zones in Texas (13). In segments as short as 12 feet, it can be placed to prevent vehicle entry into an area where a utility pole is within the needed clear zone. It is qualified under *NCHRP Report 350 Level 2* (12). In Des Moines, Iowa, a low-profile barrier was used in the median to shield drivers from trees as well as light poles.



FIGURE 6 Low profile portable concrete barrier.

Guardrail and Terminal

Short sections of guardrail with appropriate energy absorbing terminals are in use to provide safer vehicle impacts compared to impacting hazardously-located utility poles.

CONFRONTATION

There have been significant advances in roadside safety over the 10 years since the TRB report, SOAR No. 9 (5), was published. Total highway fatalities have dropped by about 20%; fixed object fatalities have dropped by almost 40%, but utility poles fatalities only dropped by 8%. Figure 1 also shows utility pole fatalities have hovered around 1,000 per year for the past ten years. Progress in reducing this number does not appear significant.

State DOTs, local HAs and UOs have two major reasons to be concerned about utility pole collisions: (a) the importance of improved safety for motorists and (b) the threat of litigation. Litigation is significant and is increasing. In a typical case, the defendants have a duty to provide a reasonably safe roadside. Breach of this duty could be installing or allowing a pole to be installed too close to the roadway or whether an obvious “Black Pole” was allowed to remain. Litigation experiences are documented in Appendix C of SOAR No. 9, pgs. 61 through 68. The courts have struggled to determine whether parties to the placement of a utility pole are indeed liable. Decisions rendered have been inconsistent. More frequently in recent years, the courts have ruled that a UO (and sometimes a state DOT or local HA) is liable to a motorist injured when his or her vehicle strikes a utility pole located too close to the roadway or in some other potentially hazardous location. However, recognizing it is not possible to expeditiously alleviate every such hazard, the courts traditionally have looked kindly on state DOTs, local HAs and UOs that demonstrate they are concerned about the problem of utility pole crashes and are addressing them in a positive manner by the development and implementation of utility pole crash reduction programs with documented results. See SOAR No. 9 Appendix A & B (5) pgs. 43 through 60.

Even though roadside safety programs and technologies are available to reduce utility pole crashes and the severity of such crashes, it is unclear the extent to which they are effective. In an effort to raise awareness and encourage responsiveness to the problem, members of the TRB Committees on Utilities (AFB70) and Roadside Safety Design (AFB20) have instigated development of a new Utility Task Group (UTG) to investigate the issue.

Initial objectives of the UTG are as follows:

- UTG Objective #1 – Organize a Utility Task Group (UTG) to address the utility pole crash problem, develop possible strategies for increasing awareness of the problem, and create a plan to implement these strategies.
- UTG Objective #2 -- Obtain critical information needed to raise awareness of the problem, such as but not limited to, identification of appropriate crash data, collection of location data showing where utility pole crashes occur, and identification of good practices being used by state DOTs, local HAs, and UOs.
- UTG Objective #3 – Identify the cause of state DOT's, local HA's, and UO's perceived reluctance to implement programs that address utility pole crashes, especially at locations where the poles are hazardously-located and crashes result in injuries or deaths.

- UTG Objective #4 – Develop an approach for state DOTs, local HAs and UOs that illustrates the advantages and cost-effectiveness of implementing system wide, carefully prioritized utility pole safety programs.
- UTG Objective #5 – Provide technical assistance to State DOTs, local HAs and UOs (when requested) to assist them in the development and/or implementation of utility pole safety programs.

CONCLUSIONS

In 2015, there were 943 fatalities related to motor vehicles leaving the roadway and crashing into utility poles. Those numbers were about the same as in the previous ten years. Utility companies own the poles involved in these crashes, but most of these poles are located on public road or street rights-of-way. It thus becomes a joint utility owner, state department of transportation, and local highway agency responsibility to take appropriate measures to reduce the hazard of these fixed obstacles.

A systematically applied program to identify Black Poles and an aggressive effort to remove or modify those Black Poles could result in the following:

1. Reduction in utility owner's maintenance costs.
2. Reduction in utility owner's litigation costs.
3. Increased safety for utility owner's maintenance workers.
4. Reduction in the fatalities and injuries associated with utility pole and collisions.
5. Public relations advantages will be achieved by the utility owner.

Proposed disadvantages for a utility owner implementing a well-planned roadside safety program have been carefully considered. See references 5, 6, 8, 10, and 11 in peer reviewed published documents.

The three-part plan for reducing utility pole fatalities developed and reported in SOAR No. 9 consists of the Best Offense approach (i.e. identifying where an over-represented number of collisions are occurring, considering available countermeasures, prioritizing for treatment, and implementing the improvements; the Best Bet approach (i.e., prioritizing potentially hazardous poles and roadway sections (using statistical prediction algorithms) before an accident history develops and implementing appropriate improvements; and the Best Defense approach (i.e., striving to meet the recommendations of the *Roadside Design Guide* (3).

BIBLIOGRAPHY

1. Insurance Institute for Highway Safety Web Site, Fatality Facts, <http://www.iihs.org/>
2. Yellow Book, *Design and Operational Practices Related to Highway Safety*, American Association of State Highway Officials, 1967 and 1974.
3. *Roadside Design Guide*, 4th Edition, American Association of State Highway and Transportation Officials, 2011.
4. *77 Barrier Guide, Guide for Selecting, Locating and Designing Traffic Barriers, AASHTO, 1977.

5. Utility Safety Task Group, TRB Committee AFB 70, Ivey, Don, L. and C. Paul Scott, et al, *Utilities and Roadside Safety*, TRB State of the Art Report 9, Transportation Research Board, 2004, www.TRB.org.
6. Hancock, Janell M. and Botkins, David, “2000 Vehicle Accidents Involving Utility Poles Last Year in Virginia”, Dominion Virginia Power, 2016, <http://www.dom.com>
7. Caro, Robert A., “The Path to Power (The Years of Lyndon Johnson, Volume 1), Amazon.com, 1990
8. Gabler, H. Clay et al, “Breakaway Utility Poles” Report No. FHWA-NJ-2007-018, December 2007, N Jersey Report
9. Ivey, Don L., M.E. Branstad and Lindsay I. Griffin, III, “Guardrail End Treatments in the 1990’s”. Transportation Research Record 1367, Washington D.C., January 1993.
10. Horne, D. A. Precedents for Action. In *Transportation Research Circular E-C030: Utility Safety: Mobilized for Action and State, City and Utility Initiatives in Roadside Safety*. Presentations from TRB Committee on Utilities (A2A07) from the 79th Annual Meeting of the Transportation Research Board, Washington, D.C., April 2001, pp. 7-10.
11. Ivey, Don L. and James R. Morgan, Timber Pole Safety by Design, Transportation Research Record 1084, 1986.
12. Ross, H.E., et al, Recommended Procedures for the Safety Performance Evaluation of Highway Features, NCHRP Report 350, 1993.
13. Guidry, T.R. and W. L. Beason, Development of a Low-Profile Portable Concrete Barrier Transportation Research Record 1367, 1992.
14. Manual for Assessing Safety Hardware AASHTO, 2009.

Making Roads (More) Motorcycle Friendly in New Zealand

Julian Chisnall

New Zealand Transport Agency

Motorcycling is seen by many in New Zealand as both a desirable recreational activity and an efficient means of transport, especially in response to rising fuel prices and increasing traffic congestion in major urban centres. Unfortunately, motorcyclists (and scooterists) are over-represented in New Zealand's crash statistics. As such, there is a need to improve motorcycle safety in New Zealand.

The "Safe System" recognises that people make mistakes and some crashes are inevitable. The collective aim of a safe system is to protect road users from crash forces by creating a more forgiving road system that reduces the price paid for human error. No one should pay for a mistake with their life or limb. The inherent vulnerability of motorcyclists to crash forces makes this a particularly pertinent challenge.

A Safe System for motorcycling requires roads and roadsides that are self-explaining, forgiving and help to manage conflicts. Equally important are appropriate travel speeds and for motorcyclists to be equipped with suitable levels of protection. A Safe System also requires skilled and responsible riders.

The "Making Roads Motorcycle Friendly" guide, produced by the author for the Motorcycle Safety Advisory Council, reflects not only international best practice for motorcyclist safety infrastructure, but also draws on findings from pilot projects, such as the Coromandel "Safer Rides" project. The information in the guide targets road owners, their consultants and maintenance contractors, and provides pragmatic and practical guidance about the impacts of their decisions and actions have on motorcyclist safety.

This presentation outlines the Safe System approach in a powered 2-wheel context and the resultant "Making Roads Motorcycle Friendly" guide.

To demonstrate the application and efficacy of the guide, the initial findings from "Safer Rides", a multi-agency safety project on a popular recreational motorcycle route, are presented. The project is a New Zealand first. Initiatives that prove effective on popular motorcycle routes around New Zealand are likely to be applicable in other countries.

ROADSIDE SAFETY DESIGN AND HAZARD MITIGATIONS

Design and Full-Scale Testing of Retrofit Bridge Rail for 24.8-mi Long Causeway Bridges Over Lake Pontchartrain, New Orleans, Louisiana

WILLIAM F. WILLIAMS
Texas Transportation Institute

The purpose of this project was to design and test a retrofit bridge rail for the Southbound Lake Pontchartrain Causeway Bridge in New Orleans, Louisiana. The southbound causeway bridge was constructed using a solid concrete parapet that is 25 inches high above the roadway surface. This height is not acceptable for MASH TL-4. This retrofit is needed to meet the strength and performance requirements of MASH TL-4. This retrofit design will also be considered for use on the northbound bridge later. The southbound bridge is approximately 24.8 miles in length and was constructed in the late 1950's. The northbound bridge is the same length and was constructed later in the 1960's. When the southbound bridge opened, it carried two-way traffic from New Orleans to the north shore of Lake Pontchartrain. The existing bridge railing consists of a 15-inch high concrete parapet mounted on top a 10 inches high by 28 inches wide concrete curb. Several retrofit options were developed for this project. A few retrofit designs were selected for full-scale testing. The purpose of the testing reported herein was to assess the performance of the Lake Pontchartrain Causeway Single Rail Bridge Rail Design Option A (25-inch tall concrete parapet, with steel posts and a single steel railing standing 14 inches above the parapet, atop a 10-inch curb, for a total height of 39 inches) according to the safety-performance evaluation guidelines included in AASHTO MASH Specifications (1). Three crash tests were required to evaluate the bridge rail's performance for Test Level 4 (TL-4) of MASH. These tests involved a 10000S vehicle (22,000-lb single unit truck), a 2270P vehicle (a 5000-lb (½-ton) Quad Cab Pickup), and a smaller 1100C vehicle (2420-lb small car). The Lake Pontchartrain Causeway 39-inch tall Option A single rail bridge rail design performed acceptably for MASH TL-4 criteria.

INTRODUCTION

The Greater New Orleans Expressway Commission desired to improve the railings on the Lake Pontchartrain Causeway Bridges, particularly the southbound lanes where 13 vehicles have gone over the side since 1994. The main focus of improvement has been on the southbound lanes, where the concrete bridge railing stands 25 inches above the roadway. An aluminum rail tops the concrete, but is not designed to resist vehicular impact. The concrete parapet on the northbound lane stands 31 inches above the roadway. Most of the vehicular accidents involved taller vehicles, such as pickups and SUVs.

The southbound causeway's bridge was built in the early 1950s. The bridge opened in 1956. The vehicle fleet since the 1950s has changed considerably. The taller and heavier vehicles of today have a greater propensity to go over the existing southbound bridge rail. Photos of the current bridge rail are shown in Figures 1 to 3. Details of the existing Bridge rail are shown in Figure 4.



FIGURE 1 Photo of southbound causeway bridge.



FIGURE 2 Photo of southbound causeway bridge rail.



FIGURE 3 Photo of southbound causeway bridge rail.

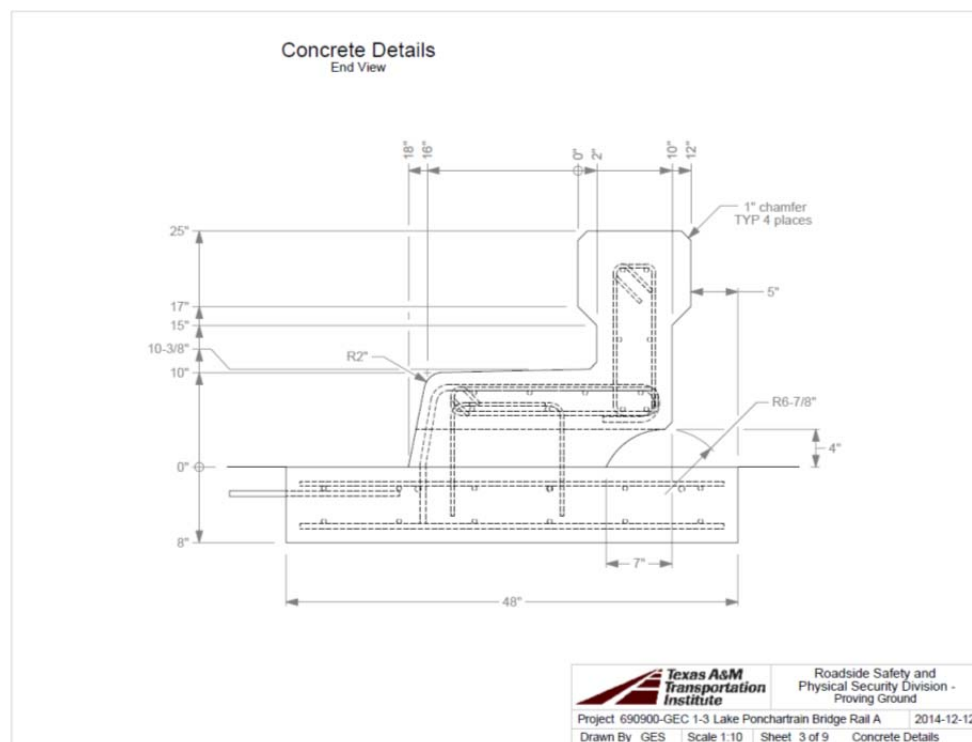


FIGURE 4 Details of concrete curb and parapet.
DESIGN AND STRENGTH ANALYSES OF RETROFIT OPTION A BRIDGE RAIL

Several retrofit options were developed for this project. A few were selected for analyses and full-scale static strength testing. Option A which consisted of a single steel post and tube rail section was selected as Option A. The steel posts were fabricated from steel plate and anchored to the top of the concrete parapet using $\frac{3}{4}$ -inch diameter HAS-e Rods anchored using Hilti RE500 Epoxy Anchoring System. The steel bridge rail element consisted of a HSS8x6x3/8 tube section. The steel tube section met the requirements of ASTM A500 Grade B Material. Details of Option A are shown in Figures 5 to 7.

Strength analyses and full-scale static strength testing was performed on Option A. The calculated post strength was approximately 28 kips. Full-scale static strength testing was performed on the actual bridge structure in New Orleans in July 2014. The average strength of the Option A post was approximately 27 kips. The post was designed to maximize the strength of the post anchorage in the concrete parapet. In addition the post anchorage was designed to minimize the interferences with existing reinforcing steel in the concrete parapet. Also, the post anchorage design minimized the post installation construction time. A photo of the full-scale testing of the post is shown in Figure 8.

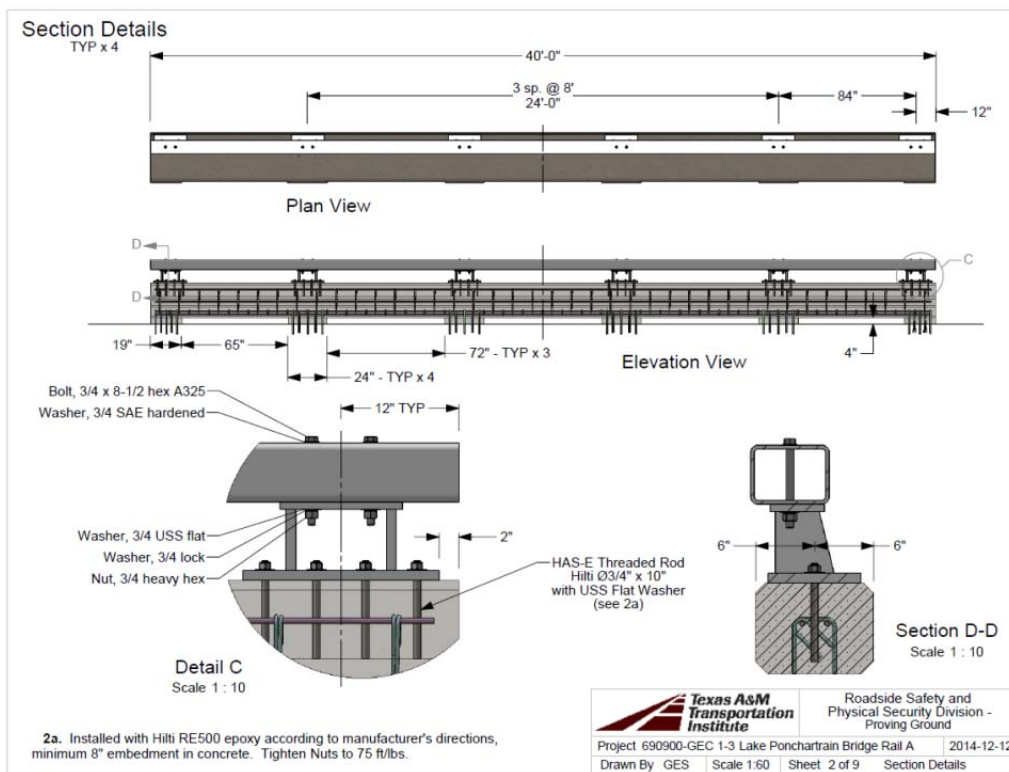


FIGURE 5 Details of Retrofit Option A.

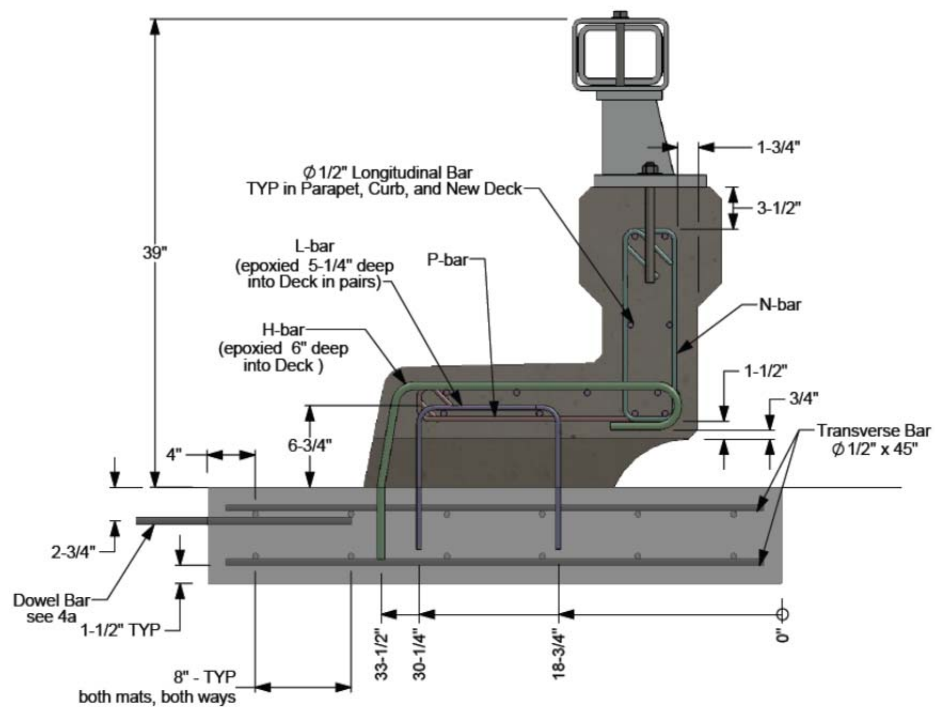


FIGURE 6 Rail section details of Retrofit Option A.

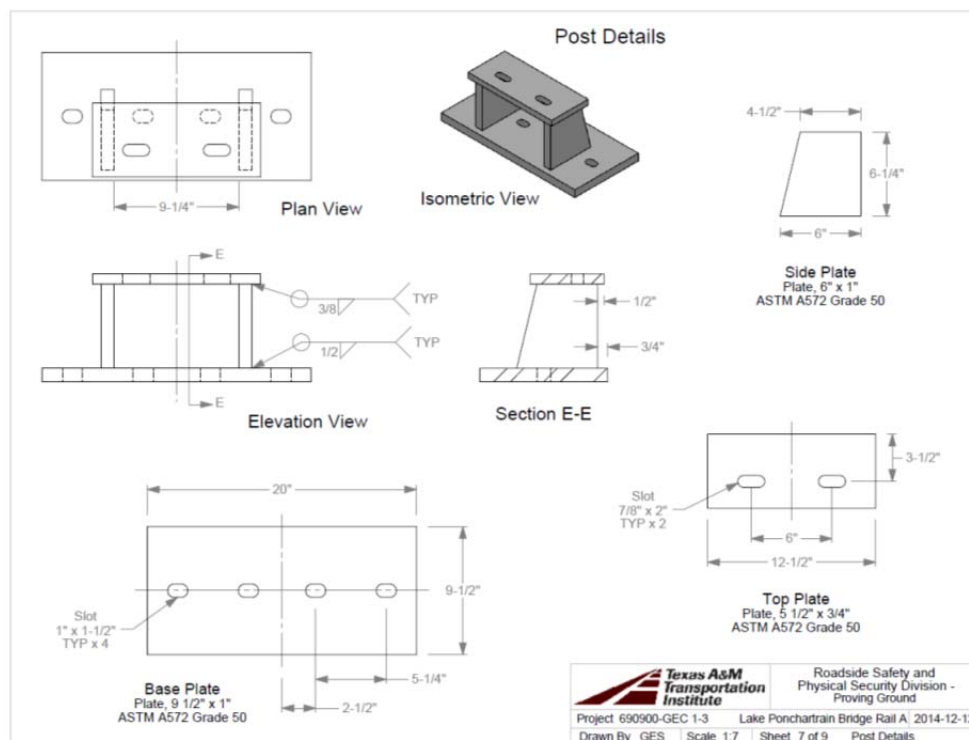


FIGURE 7 Details of steel post Retrofit Option A.



FIGURE 8 Photo of full-scale testing of steel post Retrofit Option A.

Strength analyses were performed on the retrofit Option A Design with respect to the American Association of State Highway and Transportation Officials (AASHTO) Load Resistance Factor Design (LRFD) Design Specifications (Section 13) (2). However, a higher lateral design load (target load) of approximately 80 kips was used in the analyses. Considering the strength of the existing concrete parapet and the new retrofit steel post and beam system, the calculate strength of the new retrofit rail system was approximately 85 kips @ 32 inches. The strength of the new design met the strength requirements for MASH Test Level 4 (80 kips at 30-inch height).

FULL-SCALE TEST INSTALLATION DETAILS

A full scale test installation for the Option A Lake Pontchartrain Causeway Single-Rail Bridge Rail was constructed for three full scale crash tests. The test installation was a 160-ft 6 $\frac{3}{4}$ -inch long single steel rail on a concrete parapet comprised of four 40-ft long rail segments with 2 $\frac{1}{4}$ -inch gaps at spliced expansion joints between each segment. The single bridge rail measured 39 inches in height above the bridge deck. The rail was anchored to the top of a 25-inch tall steel reinforced concrete curb and parapet that replicated the existing structure on the subject Lake Pontchartrain Causeway bridge deck. Additionally, the parapet had a 2 $\frac{1}{4}$ -inch wide expansion joint gap every 40 feet along the length of the installation, which coincided with the expansion splice between adjacent spliced rail segments.

Fabricated steel posts, 8 inches tall, supported the rail atop the parapet. Each post's base was a 20-inch long \times 9 $\frac{1}{2}$ -inch wide \times 1-inch thick plate containing four 1-inch wide \times 1 $\frac{1}{2}$ -inch long slots located on the longitudinal centerline and symmetrically centered about the lateral centerline at 2 $\frac{1}{2}$ inches and 7 $\frac{3}{4}$ inches. Each post's top was a 12 $\frac{1}{2}$ -inch long \times 5 $\frac{1}{2}$ -inch wide \times $\frac{3}{4}$ -inch thick

plate containing two $\frac{7}{8}$ -inch wide \times 2-inch long slots located $\frac{3}{4}$ -inch off of the longitudinal centerline and symmetrically centered about the lateral centerline at 3-inches. Two 1-inch thick side gusset plates, each tapered upward from 6 inches to $4\frac{1}{2}$ inches wide \times $6\frac{1}{4}$ inches tall and symmetrically located on $10\frac{1}{4}$ -inch centers, were welded to the base with a continuous $\frac{1}{2}$ -inch fillet weld, and to the top with a continuous $\frac{3}{8}$ -inch fillet weld such that the top plate holes were offset $2\frac{1}{2}$ inches to the traffic side relative to the base plate holes. The traffic-side face of the rail extended towards the traffic approximately $\frac{1}{2}$ inch beyond the traffic-side face of the parapet. All post material was ASTM A572 Grade 50.

The ends of each adjacent rail element, which were separated by a $2\frac{1}{2}$ -inch gap, were internally spliced (at three locations in the total installation) with a 38-inch long insert made from 7-inch \times 5-inch \times $\frac{1}{2}$ -inch thick wall hollow structural section (HSS) of ASTM A500 Grade B material. Two sets of two $\frac{7}{8}$ -inch diameter bolt holes were located on the 7-inch face's centerline and longitudinally spaced at 6 inches beginning 2 inches from one end of the HSS.

The rail elements were vertically bolted to each post with two $\frac{3}{4}$ -inch diameter \times 8-inch long ASTM A325hex bolts, SAE washers, flat washers, and heavy hex nuts (on the bottom of the post top). The posts were attached to the parapet with four Hilti $\frac{3}{4}$ -inch diameter \times 10-inch long HAS-E threaded rods, USS flat washers, and heavy hex nuts (on top of the base plate). The Hilti rods were secured a minimum of 8 inches deep in drilled holes in the parapet with Hilti RE500 epoxy anchoring system per Hilti instructions.

An exemplar curb and parapet was installed to match that of the Lake Pontchartrain Causeway Bridge. The curb was 28 inches wide \times 10 inches tall (nominal) with a 2-inch deep backwards sloping traffic side face ($2/10$, or 11.3 degrees) and a 2-inch radius shoulder. Each 40-ft curb section contained five 4-inch high water and debris drainage slots cast into the bottom of the curb at deck level. The top of the parapet extended 15 inches above the top of the curb for a height of 25 inches above the bridge deck. The parapet's upper section profile was a 12-inch wide \times 10-inch tall rectangle with 1-inch chamfers on the top edges. The upper section symmetrically reduced to an 8-inch wide by 5-inch tall web atop the curb via 2-inch tapers on the bottom edges. The upper face of the parapet was 18 inches from the traffic side of the curb.

Curb reinforcing steel consisted of eight $\frac{1}{2}$ -inch diameter longitudinal reinforcing bars (#4 rebar); four upper bars spaced on approximately 6-inch lateral centers with approximately 2 inches of concrete cover on top, and four lower bars spaced at approximated 8-inch, 8-inch, and 2-inch centers. For each section, these eight longitudinal bars were contained within #3 closed stirrups ('P'-bars) spaced at 12 inches.

Parapet reinforcing steel consisted of four $\frac{1}{2}$ -inch diameter longitudinal reinforcing bars (#4 rebar) spaced rectangular on approximately 7-inch on centers. For each section, these four parapet longitudinal bars, and three of the 'field' side curb longitudinal bars, were contained within 46 vertical 16-inch \times $4\frac{1}{2}$ -inch rectangular closed #3 stirrups ('N'-Bars). The 'N' bars were tied to the curb reinforcing steel prior to pouring the curb. Concrete cover was approximately $3\frac{1}{2}$ inches at the top of the parapet and $1\frac{3}{4}$ at the thinnest side section of the parapet. Details of the test installation are shown in Figures 9. Photos of the completed installation are shown in Figure 10.

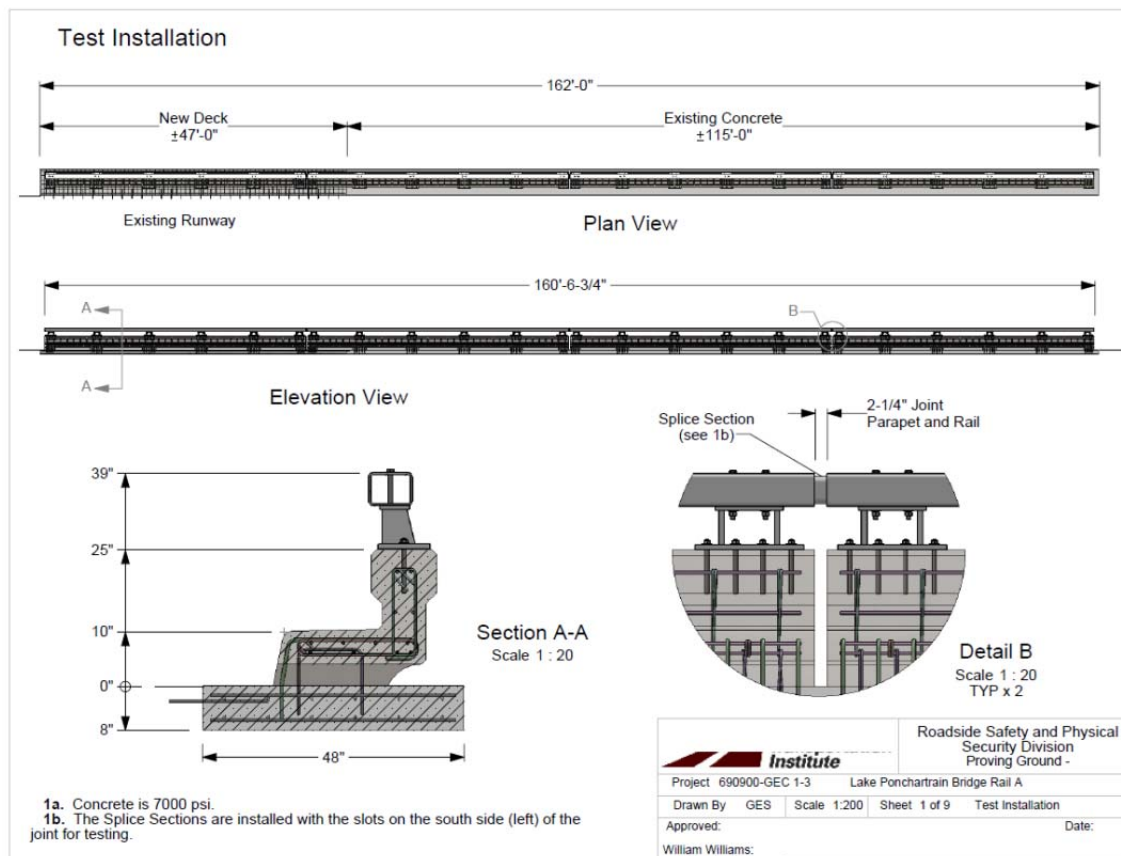


FIGURE 9 Details of the overall test installation.

FULL-SCALE MASH TL-4 CRASH TESTING OF RETROFIT BRIDGE RAIL

Full scale crash testing was performed on the retrofit bridge rail in accordance with MASH TL-4 specifications. The tests performed on the Option A Bridge rail design are as follows:

- **MASH Test 4-10** with a 2420-lb small passenger vehicle (1100C) impacting the critical impact point (CIP) of the length-of-need (LON) of the bridge rail while traveling at an impact speed and angle of 62 mi/h and 25 degrees. The purpose of this test is to evaluate the overall performance of the LON section, in general, and occupant risks, in particular.
- **MASH Test 4-11** with a 5000-lb pickup truck (2270P) impacting the CIP of the LON while traveling at an impact speed and angle of 62 mi/h and 25 degrees. The test is intended to evaluate strength of the section in containing and redirecting the 2270P vehicle.
- **MASH Test 4-12** with a 22,000-lb single-unit box-van truck (10000S) impacting the CIP of the LON while traveling at an impact speed and angle of 56 mi/h and 15 degrees. This test is intended to evaluate the strength of the LON in containing and redirecting the heavy test vehicle.



FIGURE 10 Photos of full scale test installation

All three tests were performed on the Lake Pontchartrain Causeway retrofit bridge rail. The target CIP for each test was determined according to the information provided in MASH, and are shown in Figure 11. All tests targeted joints in the rail and parapet.

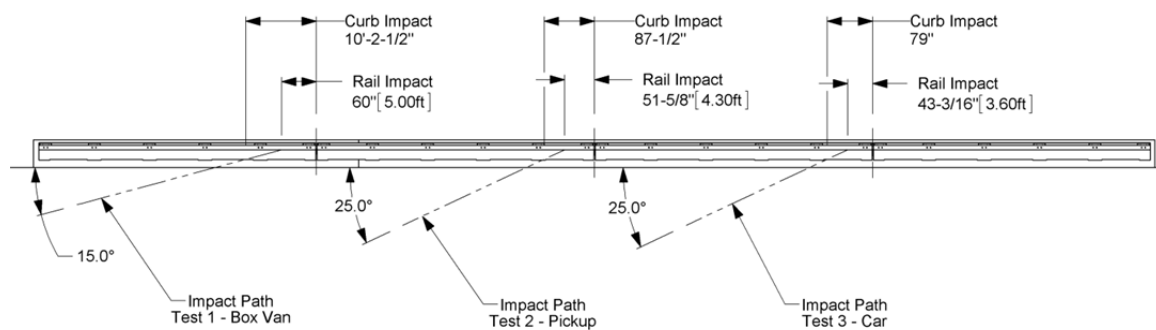


FIGURE 11 Critical impact points (locations) for full-scale crash tests.

MASH Test 4-12

MASH Test 4-12 was performed on December 12, 2014. MASH Test 4-12 involves a 10000S vehicle weighing 22,000 lbs. ± 660 lbs. and impacting the bridge rail at an impact speed of 56 mi/h ± 2.5 mi/h and an angle of 15 degrees ± 1.5 degrees. The target impact point on the curb was 10 ft. 2½ inches upstream of the joint between posts 6 and 7 and on the rail was 60 inches upstream of the joint between posts 6 and 7. Target impact severity (IS) was 154.5 kip/ft., and actual IS was 166.5 kip-ft. (+8%). Based on the results from the crash test, the Option A Retrofit Bridge Rail performed acceptably with respect to all the evaluation criteria in MASH Test Level 4-12 Specifications. Photos of the crash test before and after are shown in Figures 12 and 13. Photos of the test vehicle are shown in Figure 14.

MASH Test 4-11

MASH Test 4-11 was performed on December 15, 2014. MASH test 4-11 involves a 2270P vehicle weighing 5000 lbs. ± 100 lbs. and impacting the bridge rail at an impact speed of 62 mi/h ± 2.5 mi/h and an angle of 25 degrees ± 1.5 degrees. The target impact point on the curb was 87½ inches upstream of the joint between posts 12 and 13 and on the rail was 51⅝ inches



FIGURE 12 MASH Test 4-12 before test photos.



FIGURE 13 MASH Test 4-12 after test photos.



FIGURE 14 Photos of the MASH Test 4-12 test vehicle.

upstream of the joint between posts 12 and 13 (@ joint). Target IS was 115.5 kip/ft., and actual IS was 120.5 kip-ft. (+4%). Based on the results from the crash test, the Option A Retrofit Bridge Rail performed acceptably with respect to all the evaluation criteria in MASH Test Level 4-11 Specifications. Photos of the crash test before and after are shown in Figures 15 and 16. Photos of the test vehicle are shown in Figure 17.



FIGURE 15 MASH Test 4-11 before test photos.



FIGURE 16 MASH Test 4-11 after test photos.



FIGURE 17 Photos of the MASH Test 4-11 test vehicle.

MASH Test 4-10

MASH Test 4-10 was performed on December 16, 2014. MASH test 4-10 involves a 1100C vehicle weighing 2420 lbs. ± 55 lbs. and impacting the bridge rail at an impact speed of 62 mi/h ± 2.5 mi/h and an angle of 25 degrees ± 1.5 degrees. The target impact point on the curb was 79 inches upstream of the joint between posts 18 and 19, or on the rail at $43\frac{3}{16}$ inches upstream of the joint between posts 18 and 19. Target IS was 55.9 kip/ft., and actual IS was 54.6 kip-ft. (-2%). Based on the results from the crash test, the Option A Retrofit Bridge Rail performed acceptably with respect to all the evaluation criteria in MASH Test Level 4-10 Specifications. Photos of the crash test before and after are shown in Figures 18 and 19. Photos of the test vehicle are shown in Figure 20.



FIGURE 18 MASH Test 4-10 before test photos.



FIGURE 19 MASH Test 4-10 after test photos.



FIGURE 20 Photos of the MASH Test 4-10 test vehicle.

SUMMARY AND CONCLUSIONS

The Option A Retrofit Bridge Rail as presented herein met all the strength and safety performance criteria of MASH TL-4. The Greater New Orleans Expressway Commission is currently planning to construct the retrofit option on the Southbound Causeway Bridge over

Lake Pontchartrain in New Orleans, Louisiana. Another option Option B was also designed and successfully crash tested. Option B was a taller design and consisted of two rail elements.

REFERENCES

1. AASHTO, *Manual for Assessing Safety Hardware*, American Association of State Highway and Transportation Officials, Washington, D.C., 2009.
2. AASHTO LRFD Specifications, American Association of State Highway and Transportation Officials, Washington, D.C., 2010.

Safety Procedures for Emergency Responders When High-Tension Wire Rope Systems Are Involved with Run-Off-Road Accidents

DEAN C. ALBERSON

Texas A&M Transportation Institute (retired)

Texas DOT (Department of Transportation) has contracted with TTI (Texas A&M Transportation Institute) to develop a safety video to train emergency responders and TxDOT employees on the appropriate methods to release tension in High Tension Wire Rope Systems (HTWRS) when they have been impacted by an errant vehicle. In recent years, individuals responding to accidents have been injured when tension is inappropriately released on HTWRS. The video being produced will show the appropriate methods for releasing tension in various HTWRS through terminal release, disengagement of wire ropes from support posts, cutting of turnbuckles or a last option, cutting of wire ropes. This video will be available for wide distribution and will be of benefit to end users of HTWRS.

Design and Analysis of High-Energy-Absorbing Rock Fence

IRAJ H.P. MAMAGHANI
University of North Dakota

HIROSHI YOSHIDA
Be Safe Japan Ltd,

Rock fences have been widely designed and constructed in mountainous areas, where there is a high risk of rockfall to prevent the roads and highways against falling rocks. Rock fences are typically used to protect roadways, railtracks, power and pumping stations and residential or office buildings. They are also installed as roofing structures at tunnel exits and mounted underwater to protect turbine inlets from debris inflows.

Engineered solutions to rockfall problems have led to the development of new methods for stopping rocks, including high-tech rockfall barriers and fences. This paper is concerned with the design and analysis of a new high energy absorbing rock fence (HEARF) system. The developed HEARF system consists of: 1) Posts of concrete filled steel tubes reinforced by unbounded bars having high ductility and energy absorbing capacity; 2) Break or buffer devices installed on the posts to absorb energy through friction between cables and the holding device; 3) Cables spanning between the posts are further extended to adjacent spans with a constant length passing through the buffer devices; and 4) Stoppers which are installed at the cable ends.

The stopper limits the amount of slipping of the cable in the buffer device. That is, when the cable slipping exceeds a specified value in the buffer device, the stopper hits the buffer device and stops further slipping of the cable. The buffer device controls the tension force of the cable and prevents cutting the cable and destroying the device itself. Cables have a slipping mechanism with the tension kept constant up to a specified amount of slipping. Cables are allowed to slip inside the break device when they experience a predefined value of constant tension force.

The structural outlines and performance characteristics of the HEARF under impact of falling rock have been presented and discussed. A simple yet practically efficient analytical method for dynamic analysis of HEARF under impact of falling rock has been developed and verified against full size experiments.

INTRODUCTION

The transportation corridors in mountainous regions are subject to a range of rock slope movements in the form of rock falls, rock slides and rock avalanches that pose significant risks to road and rail traffic. For example, Figure 1 shows the road closed as a result of rock fall. Rock fences have been widely designed and constructed in mountainous areas where there is a high risk of rock fall to prevent the roads and highways against falling rocks. Rock fences are typically used to protect roadways, railtracks, power and pumping stations and residential or office buildings. They are also installed as roofing structures at tunnel exits and mounted underwater to protect turbine inlets from debris inflows. Figure 2 shows an example of a rock fence system constructed to prevent road and water reservoir from rock fall. As shown in this figure, there are two parallel sets of rock fences where there is a high risk of rock fall.

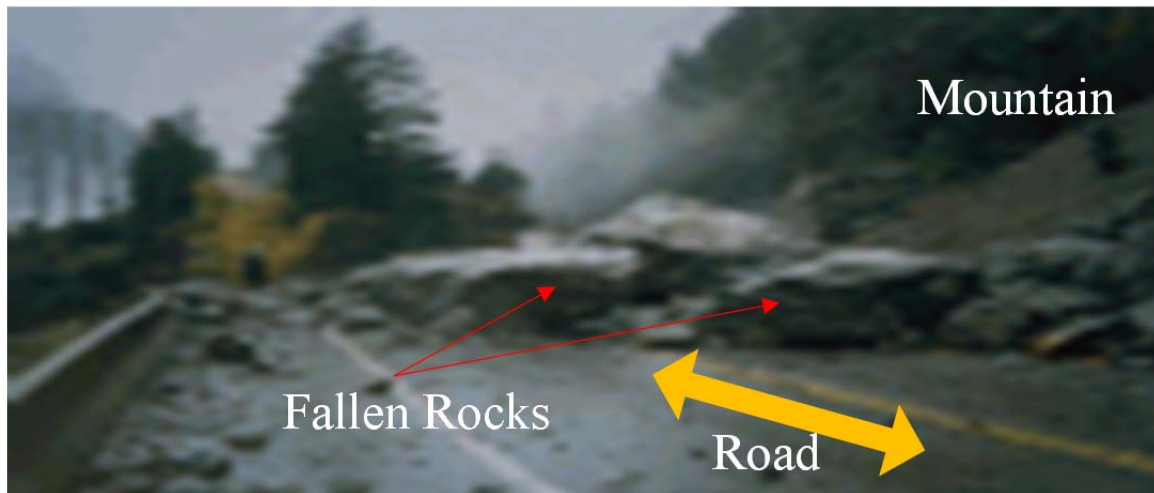


FIGURE 1 Road closed by rocks fallen from mountain.

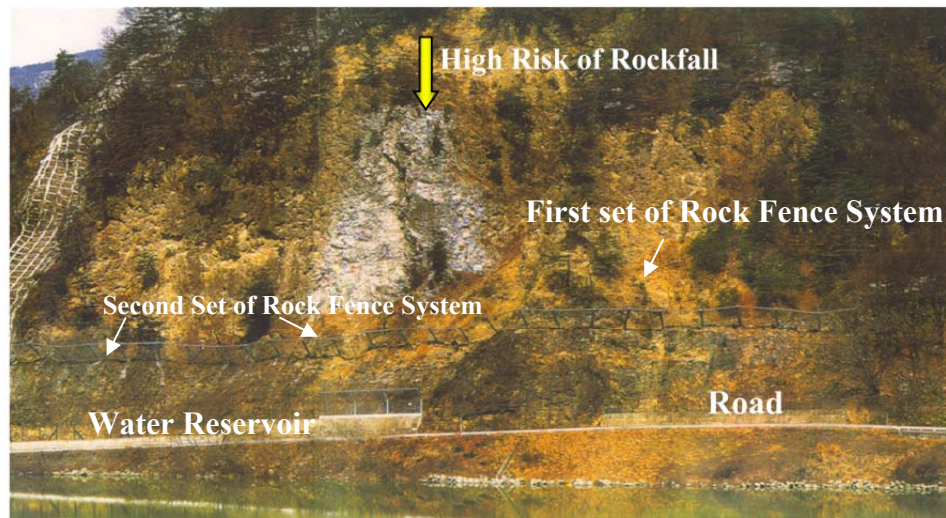


FIGURE 2 Rock fences to prevent road from rock falls.

Engineered solutions to rock fall problems have led to development of new methods for stopping rocks, including high-tech rock fall barriers and fences. This paper deals with the design concept and analysis of the high-energy absorbing rock fence (HEARF) system. The structural outlines and performance characteristics of the HEARF under impact of falling rock is presented and discussed. A simple, yet efficient and accurate numerical method for dynamic analysis of HEARF under impact of rock falls is proposed. This work is a part of an ongoing project for developing a practical design regulation for the HEARF systems (Mamaghani and Yoshida, 2000). The basic concept of the proposed method and algorithm of numerical analysis are briefly presented and discussed. A computer program is coded for the proposed method. It is used to carry out extensive numerical analyses of rock fences considering various parameters. The accuracy of the proposed method is verified by comparing the results from this method with those of the other numerical methods as well as the test results for various rock fences. It is

shown that the proposed method provides an efficient tool for researchers and practical engineers in analyzing and studying behavior of rock fences under impact of rock falls.

HIGH-ENERGY-ABSORBING ROCK FENCES (HEARF)

In this section, the structural outlines and performance characteristics of the HEARF under impact of falling rock are briefly reviewed and discussed.

Outline of the HEARF System

The HEARF system, as shown in Figure 3, consists of the following members:

- Posts composed of articulated steel, reinforced concrete or concrete-filled steel tubes reinforced by unbounded bars with high ductility and energy absorbing capacity;
- Steel cables spanning between the posts which are further extended to adjacent spans with a constant length passing through the buffer devices;
- Buffer devices (friction brake elements) installed on the posts as well as on the steel cables to absorb energy through friction between cables and the holding device;
- Stoppers which are installed at the cable ends;
- Anchoring and retaining steel cable ropes and corresponding buffer devices;
- Chains that connect steel cables used to prevent the passing through of a boulder between the cables and also to disperse the impact force acting on the cables; and
- Rock anchors.

Buffer devices absorb energy by means of friction between sliding steel cables and the holding device at a pre-specified cable tensile force. Three types of buffer devices are used, namely, the main buffer devices, the intermediate buffer devices and the end buffer devices,

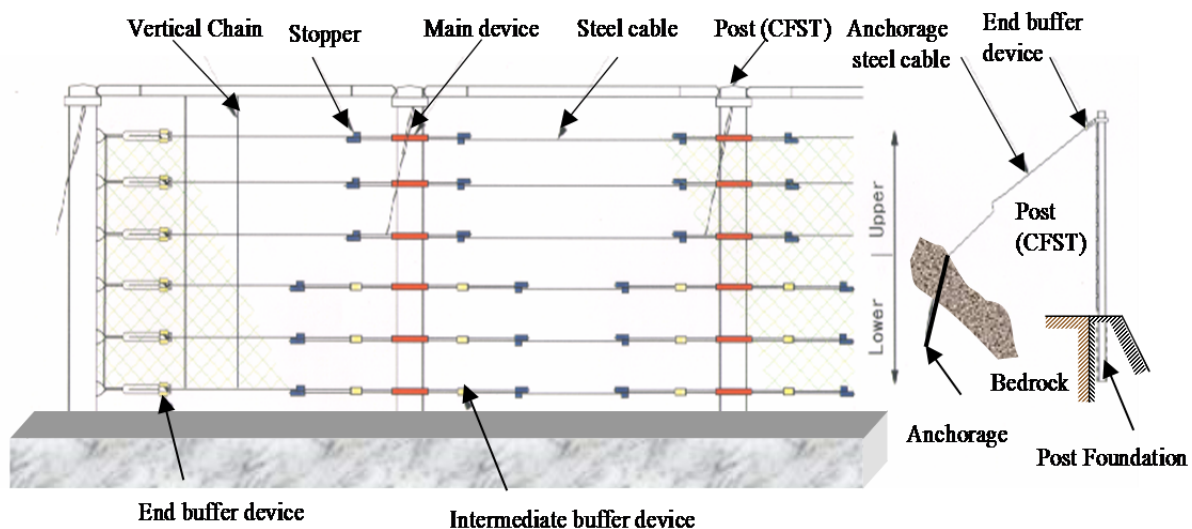


FIGURE 3 Structural outline of the HEARF system.

as shown in Figures 4(a) to 4(c). The stopper used in the HEARF system is shown in Figure 4(d). Steel cables are stretched between posts and are extended with a constant length passing through the main buffer devices set on the posts. The stoppers are installed at the end of steel cables, as shown in Figure 3. In cases when the supplied energy absorption capacity in the cables close to the mountain (where the contribution of the posts in energy absorption capacity is less) is not sufficient, only the main buffer devices are used. The complementary buffer devices (the intermediate buffer devices) are installed on the extended part of the steel cables between the posts and the stoppers, as shown in Figure 3. The upslope anchor support cables with the end buffer devices connect the posts head to the corresponding anchors fixed into the slope, as shown in Figure 3.

The ductility and energy absorption capacity of the posts are improved by using the concrete-filled steel tube reinforced with high strength steel bars. Cables are allowed to slip inside the break device when they experience a predefined value of constant tension force. The stopper limits the amount of slipping of the cable in the buffer device. That is, when the cable slipping in the buffer device reaches a specified value, the stoppers hit the buffer device and prevent further slipping of the cable. The buffer device controls the tension force of the cable, which in turn prevents cutting of the cable and destroying the device itself.

Performance of the HEARF System under Impact of Falling Rock

The performance of the HEARF system under impact of falling rock (boulder) depends on the location of the impact. As shown in Figure 5, three kinds of behavior for a boulder are expected when a boulder collides with: (1) the upper part of the fence between posts; (2) the lower part of the fence between posts; and (3) the posts. The HEARF systems should be designed to absorb the whole rock fall energy without collapse while the deformation of the structure remains within the allowable range in any case.

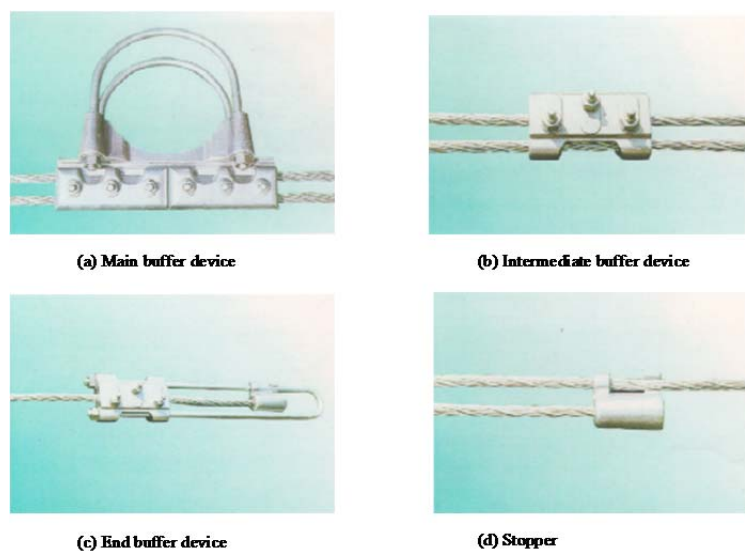


FIGURE 4 Buffer devices and stopper.

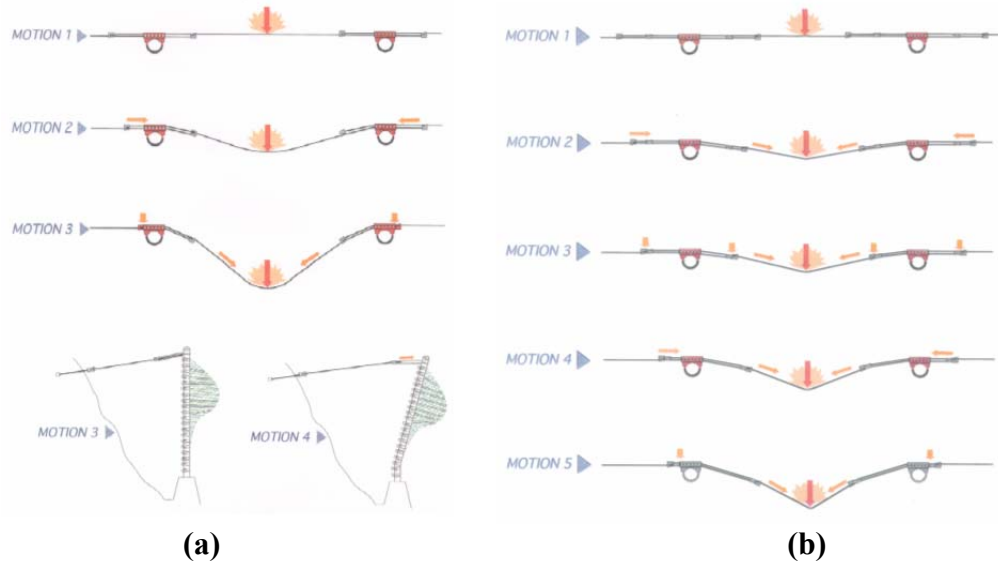


FIGURE 5 Behavior of HERF system under impact of rock fall (boulder): (a) boulder colliding with upper cables and (b) boulder colliding with lower cables.

Boulder Colliding with the Upper Part of the Fence Between Posts

When a boulder collides with the upper part of the fence between posts, steel cables stretch elastically when a boulder hits the fence. The cables slip in the buffer devices installed on the posts when tension force in the cables reaches a defined value. At this point, the posts are in the elastic range and the upslope anchor support cables do not slip in the end devices. When the amount of the slipping of a cable reaches a defined value (length of cable between main buffer device and stopper), the stopper installed at the end of the steel cable strikes to the main buffer device and the tension force of the cable increases.

A large bending moment acts at the fixed point of the posts at both sides of the span because of the increased tension force of the cables. Consequently the posts yield and experience large deformation, which in turn causes the upslope anchor support cables to slip because of the large displacement at the heads of the posts.

In this state, the part of the rock fall energy which was not absorbed by the slip of steel cables in the main buffer devices is absorbed by the plastic deformation of the posts and by the slip of the upslope anchor support cables in the end buffer devices. When the rock fall energy is larger than the absorbed energy by means of the slip of the cables between posts, the plastic deformation of the posts and the slip of the upslope anchor support cables, the steel horizontal cables of the adjacent spans slip and their corresponding posts suffer bending. In the design of HERF systems in general, the deformation of the cables and posts at the location of collision by a boulder is often limited within an allowable range.

Boulder Colliding with the Lower Part of the Fence Between Posts

The energy absorption by the plastic deformation of the posts and the slipping of the upslope anchor support cables cannot be expected as much when the boulder collides with the lower part of the fence between posts. However, because the posts do not suffer large deformation, a large

amount of slipping of the steel cables in the buffer devices installed on the posts is allowed. For this purpose, the extended length of steel cable is kept large and an intermediate buffer device is installed between the end stopper and the main buffer device.

In this case, the horizontal cables slip in the main buffer devices, while moving freely through the intermediate buffer devices, until the end stoppers collide with them. When the rock fall energy is larger than the energy absorbed till this moment, the steel cables further slip in the main buffer devices installed on the posts and in the two intermediate buffer devices installed on the cables of the adjacent spans until the whole energy is absorbed.

Boulder Colliding with the Posts

When a boulder collides directly with the posts, a large bending moment is generated at the base of the posts and thus the posts suffer plastic deformation. The tension force is simultaneously generated in the upslope anchor support cables and the horizontal steel cables. Those cables slip in the main buffer devices installed on the posts and the end buffer devices fixed at the ends of the upslope anchor support cables because of the increased tension forces. In this case, the rock fall energy is absorbed by the plastic deformation of the posts, the slipping of the upslope anchor support cables and the horizontal cables in the buffer devices. The difference when a boulder collides with the horizontal steel cables between the posts and when it collides directly with the post is that in the former case the posts begin the plastic deformation followed by the slip of the horizontal cables, while in the latter case the post suffers plastic deformation first.

PROPOSED NUMERICAL METHOD

In the proposed numerical method, beams and steel cables are modeled using three-dimensional beam and cable elements (with two nodes), respectively, as shown in Figure 6. The beam, cable, falling rock masses and externally applied loads are assumed as lumped at nodal points. The stress-strain relationship for cables and moment-curvature relationship for beams are assumed to be elastic perfectly plastic. In contrast to the usual finite element method, in the proposed method, dynamic response of the whole system is obtained through dynamic equilibrium of individual nodal points, beam elements and cable elements at a time step. This allows simplicity and yet efficiency of the numerical analysis procedures by eliminating the requirement for assemblage of global structural stiffness equations in the usual finite element method, in which ill condition of equations system might arise in the solution process.

Dynamics of Nodal Points

A nodal point of the rock fence is assumed as a particle of mass subjected to initial velocity (or acceleration) at a time step imposed upon from the impact of falling rock. Assuming that acceleration is constant in each time step, the fundamental equations of dynamics for kinematics of a nodal point rectilinear motion (in one dimension) for incremental velocity and displacement, respectively, read as:

$$v^{t+\Delta t} = v^t + a_{av}^t \Delta t ; \quad s^{t+\Delta t} = s^t + v^t \Delta t + a_{av}^t \Delta t^2 / 2 ; \quad a_{av}^t = (a^t + a^{t+\Delta t}) / 2 \quad (1)$$

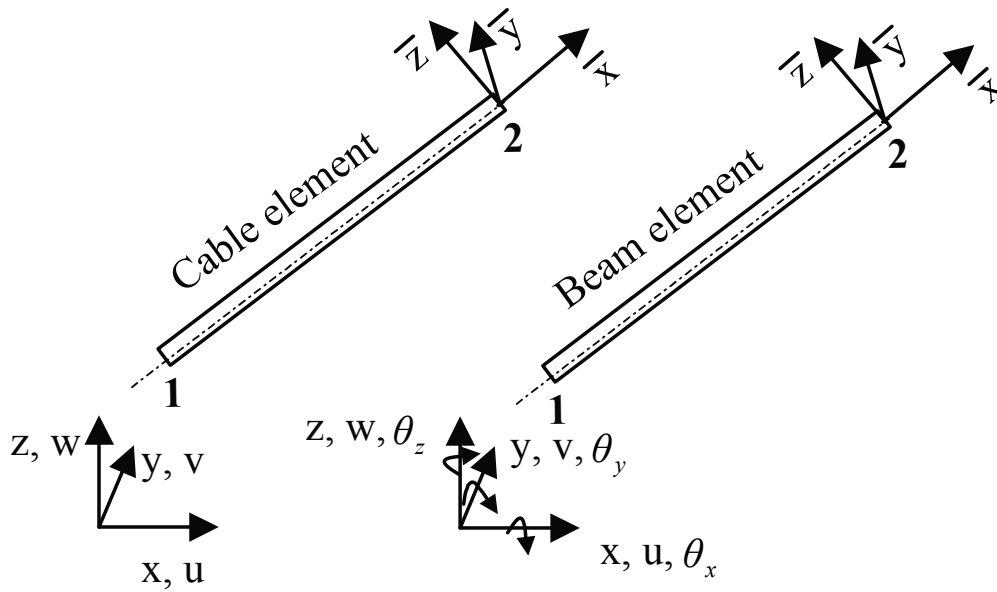


FIGURE 6 Cable and beam elements.

Here, s, v, a, t and Δt stand for the displacement, velocity, acceleration, time and time increment, respectively. Newton's second law of motion, $F^{t+\Delta t} = ma^{t+\Delta t}$, is applied to the equation of motion at a nodal point. Here, F and m stand for the nodal force and mass, respectively. It is worth noting that, the moment corresponding with the rotational degrees of freedoms at nodal points of beams is calculated using $M^{t+\Delta t} = I_m \alpha^{t+\Delta t}$; in which, I_m = mass moment of inertia and $\alpha^{t+\Delta t}$ = angular acceleration.

Cable and Beam Finite Elements

Cable finite elements are modeled using a cable element, having a total of six degrees of freedoms, oriented arbitrarily in a three-dimensional space, as shown in Figure 6. Cables are assumed to have an elastic perfectly plastic material with zero compression strength. Employing the energy method combined with coordinate transformation, the incremental stiffness equations of the cable element in an explicit form can be derived as:

$$\Delta \mathbf{X}^{t+\Delta t} = \mathbf{K}^t \Delta \mathbf{U}^{t+\Delta t}; \quad \mathbf{X} = \{X_1, Y_1, Z_1, X_2, Y_2, Z_2\}^T; \quad \mathbf{U} = \{u_1, v_1, w_1, u_2, v_2, w_2\}^T \quad (2)$$

where \mathbf{X} and \mathbf{U} denote nodal force and displacement vectors, respectively. The element stiffness matrix is given as:

$$\mathbf{K}^t = \mathbf{K}_1 + \mathbf{K}_2; \quad \mathbf{K}_1 = \frac{E^p A}{L} \begin{bmatrix} k_0 & -k_0 \\ -k_0 & k_0 \end{bmatrix}; \quad k_0 = \begin{bmatrix} l^2 & lm & ln \\ ml & m^2 & mn \\ nl & nm & n^2 \end{bmatrix}; \quad \mathbf{K}_2 = \frac{P^t}{L} \begin{bmatrix} k_1 & -k_1 \\ -k_1 & k_1 \end{bmatrix}; \quad k_1 = \begin{bmatrix} 1 & 0 & 0 \\ 0 & 1 & 0 \\ 0 & 0 & 1 \end{bmatrix} \quad (3)$$

in which E^p , A , L and P^t stand for the elastoplastic modulus of the material, cable cross sectional area, cable element length and cable force at the time t , respectively. l , m and n denote direction cosines of the local coordinate axis with respect to global coordinates at the time t . For the state of stress in elastic $E^p = E$ (E = modulus of elasticity) and for the state of stress in tensile plastic or compression $E^p = 0$. The cable force is obtained as:

$$P^t = X_2 l + Y_2 m + Z_2 n \quad (4)$$

Beams are modeled using the usual three-dimensional beam element, with a node at each end, having twelve degrees of freedoms, Figure 6. An elastic perfectly plastic moment curvature relationship is assumed for the beam elements.

Buffer Devices

Buffer devices absorb energy by means of friction between the sliding steel cable and the holding device at a pre-specified cable tensile force. The mechanism of buffer devices is modeled by means of stress-strain relationship for cable elements to which the buffer device is connected. That is, the cable element is allowed to slip (experience perfectly plastic deformation) under a prescribed cable tensile force obtained from the tests for a specific tightening torque of the buffer device nuts.

Procedure of Analysis

The procedure of analysis, for a time step $t + \Delta t$, is as follows:

Calculate each nodal point's velocity, incremental and total displacement vectors from the current acceleration vector using the dynamic equations of a nodal point.

For each element, calculate the incremental displacement vector $\Delta \mathbf{U}^{t+\Delta t}$ and stiffness matrix \mathbf{K}^t . Calculate the incremental force vector $\Delta \mathbf{X}^{t+\Delta t}$, by solving element stiffness equations, and the total force vector $\mathbf{X}^{t+\Delta t} = \mathbf{X}^t + \Delta \mathbf{X}^{t+\Delta t}$.

Calculate the force vector at each node using the element connectivity scheme as in the usual finite element method. Calculate cable force P^t for all cable elements.

Using the dynamic equations of a nodal point, calculate each nodal point acceleration vector as the input for the next step.

Update nodal coordinates.

Store the results for the nodal point's displacement, velocity and acceleration, cable force and etc.

NUMERICAL RESULTS

In this section the results for three typical examples analyzed by the proposed method will be presented and discussed.

Analysis of the Cable Net System

As the first example, Figure 7(a) shows the configuration of a three-dimensional cable net system subjected to initial velocity of -50cm/sec in the z -direction at the center of the net (node no. 11). The assumed steel cables have a cross sectional diameter of 1.28cm , Young's modulus of 206GPa and yield stress of 270MPa . Each node is assumed to have a lumped mass of $0.0204\text{kgf}\cdot\text{sec}^2/\text{cm}$. As shown in Figures 7(b) and 7(c), the results from proposed method compare well with those obtained using the commercial computer program NONSAP (Bathe et al. 1976).

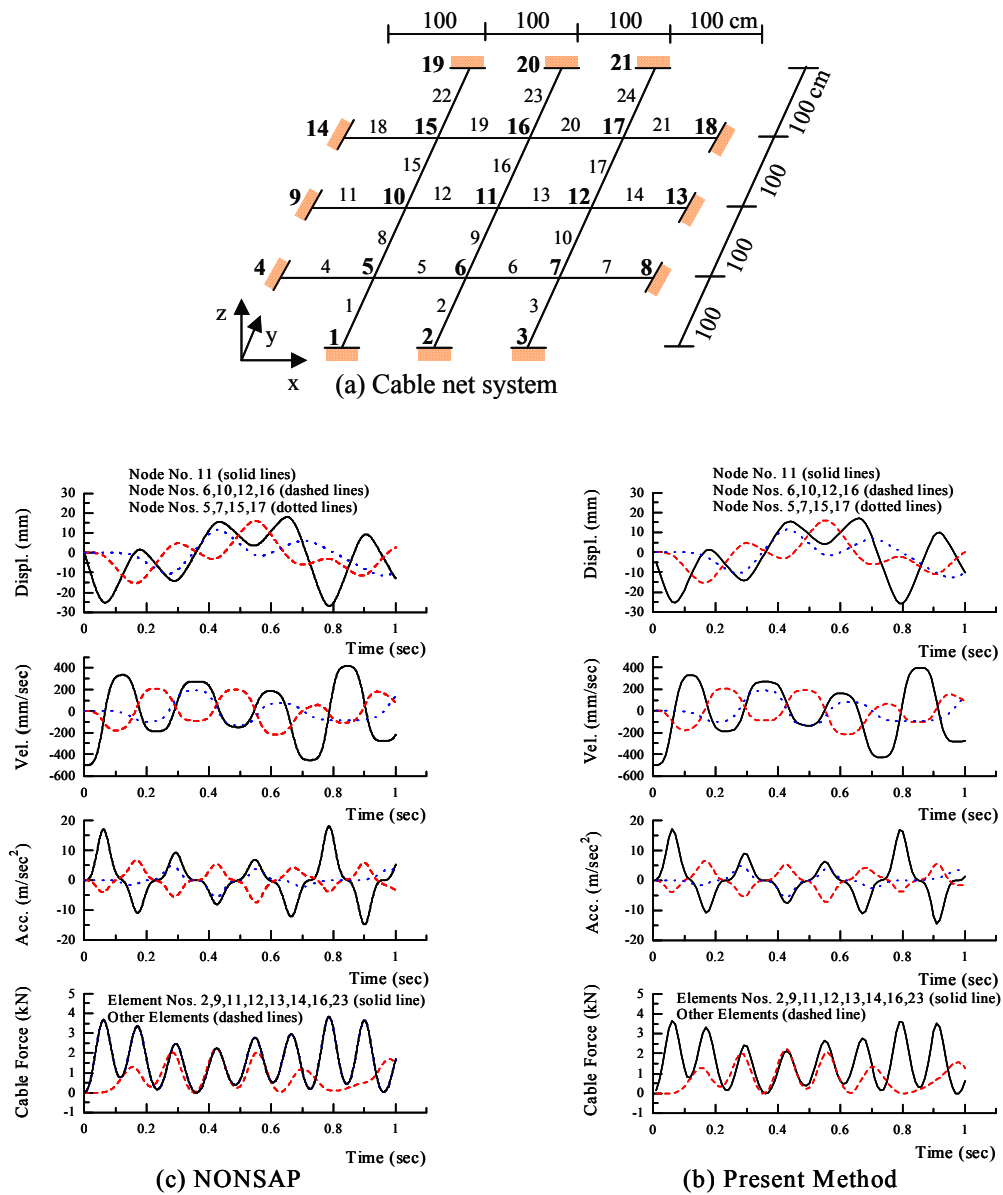


FIGURE 7 Analysis of the cable net system.

Analysis of the Rock Fence without Buffer Device

The second example is a three-dimensional single span rock fence, having the configuration shown in Figure 8(a). It is subjected to the impact of a spherical block at the center of the fence (node no. 13). The block has a diameter of 100cm, mass of $1.02\text{kgf}\cdot\text{sec}^2/\text{cm}$ and initial velocity of -100cm/sec at the onset of contact with the fence. The material for beams and cables is assumed to be structural steel with Young's modulus of 206GPa and yield stress of 270MPa.

The response of the fence is shown in Figure 8. The cable connecting node no. 3 to node no. 7 (cable elements 8, 13, 18, and 23), on which the block hits, suffers plastic deformation while the other cables and beams exhibit elastic behavior, Figures 8(b), 8(e) and 8(f). The block contacts node number 12 and 14 at the time $t = 0.22\text{sec}$ and $t = 0.25\text{sec}$, respectively, Figure 8(d). Thereafter the gap between deflections of the fence at these nodes with the central node (node number 13) remains constant (20cm), while the fence experiences permanent deflection of about -37cm at its center, Figures 8(c) and 8(d). The response of the fence is quite similar to those expected in actual fences under impact of rock fall.

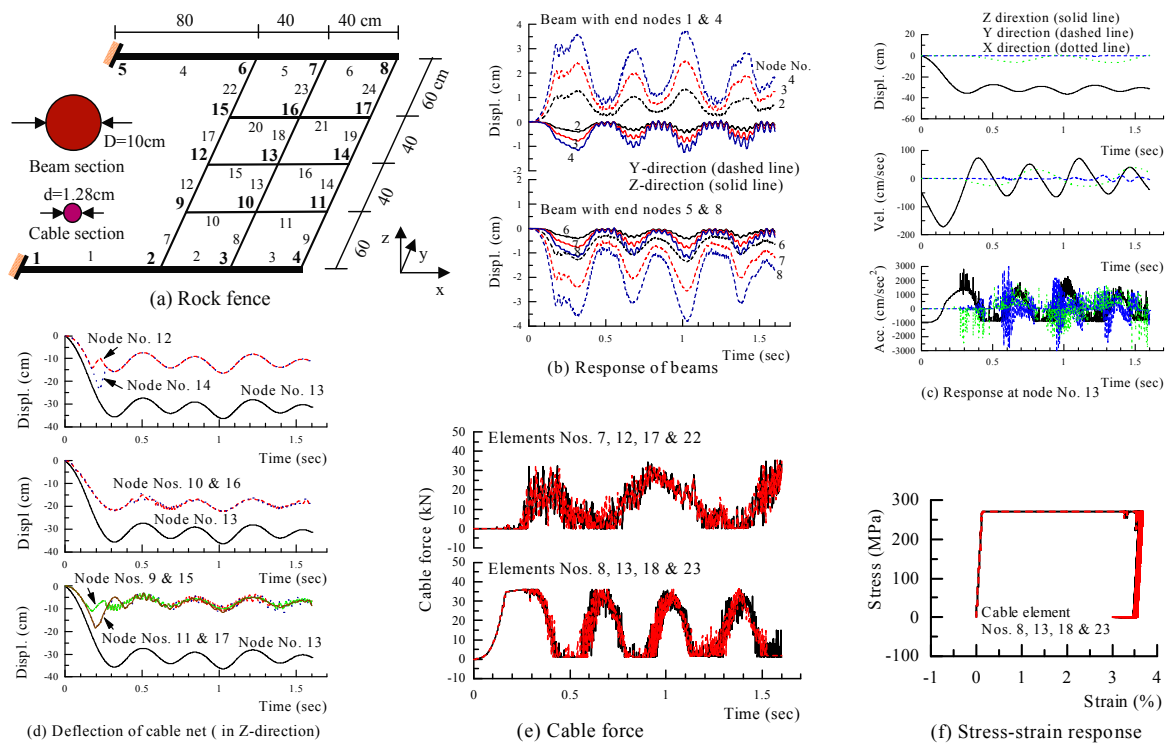


FIGURE 8 Analysis of the rock fence.

Analysis of the Rock Fence with Buffer Device

The conducted full-scale experiments on the HEARF systems are used to substantiate the proposed method. The details of experiments and the numerical method will be presented and discussed in the conference. Figure 9 compares typical results from the experiment and analysis using the proposed method for the impact acceleration versus time of a boulder of 29.4 kN freely dropped from the height of 10m on a HEARF system between posts near the mountain (as discussed in subsection 2.2). Figure 9 shows that a good correlation between the test results and numerical analysis is obtained indicating the accuracy of the proposed model.

CONCLUSIONS

This paper deals with the design concept and analysis of the high-energy absorbing rock fence (HEARF) system. The structural outlines and performance characteristics of the HEARF under impact of falling rock is presented and discussed. A numerical method for dynamic analysis of high-energy absorbing rock fences under impact of rock falls is proposed. The accuracy of the proposed method is verified by comparing the results from this method with those of the other models and full-scale experiments for various rock fences under impact of rock falls. The method is applied to study the behavior of HEARF systems concerning different parameters. The results for a few typical examples are presented and discussed. It has been concluded that the proposed method provides an efficient tool for researchers and practical engineers in analyzing and studying behavior of rock fences under impact of rock falls.

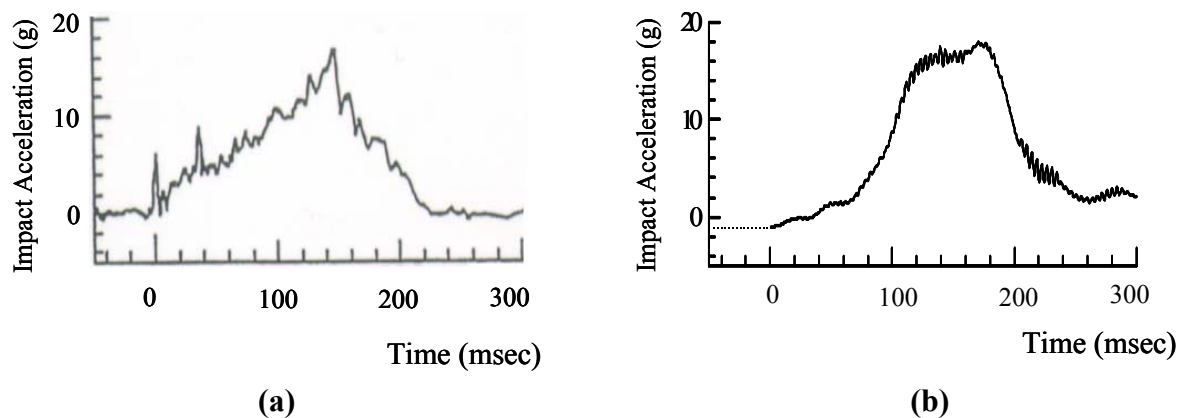


FIGURE 9 Comparison between test and analysis: acceleration of the boulder of weight 29.4 kN freely dropped on HEARF between posts (g = ground acceleration): (a) test and (b) proposed method.

REFERENCES

- Bathe, K.J., Wilson, E.L. and Iding, R.H. (1974), A Structural Analysis Program for Static and Dynamic Response of Nonlinear Systems (NONSAP), *Report No. UC SESM 74-3*, Department of Civil Engineering, University of California at Berkley, CA, USA.
- Mamaghani, Iraj H.P. and Yoshida, H. (2000), A Method for Dynamic Analysis of Rock Fences (Beam & cable net systems) under impact of rock falls. *Proc. of the second International Summer Symposium*, Japan Society of Civil Engineers (JSCE), Tokyo, Japan, July 28, pp. 27-40.

Design of Reinforced Expanded Polystyrene Styrofoam Covering Rock-Sheds Under Impact of Falling Rock

IRAJ H.P. MAMAGHANI
University of North Dakota

HIROSHI YOSHIDA
Be Safe Japan Ltd,

Rock falls constitute one of the most prevailing natural hazards in mountainous areas presenting a major hazard to infrastructures that are exposed to such phenomena. Rock sheds are usually built to reduce the risk of possible catastrophic events. Impact load by rock falls and the design of protection structures, such as rock-sheds, are important themes for researchers and engineers in civil engineering. When designing such structures, the safety of roads, railways and habitants in mountainous regions are our most important considerations. Designers and responsible organizations experience many problems with rock falls that should be considered, such as the risk, the selection from the measure works, design condition and required safety level of the structure.

This paper is concerned with the design of the reinforced expanded polystyrene styrofoam (R-EPS) under falling rock impact. The R-EPS is developed as an improved alternative buffer material to be placed on the roof of rock-sheds to absorb and distribute the impact of falling rock. First, based on the experimental data, the effects of some important parameters, such as reinforcement, thickness of styrofoam, weight and height of the falling rock on the buffer behavior and energy absorption capacity of the R-EPS subjected to impact of falling rock are discussed and evaluated. Then a design method, incorporating the design equations and design charts for the R-EPS is proposed and is substantiated using the experimental data. Finally, the practical application of the proposed method for design of R-EPS is presented and discussed.

This study is of extreme importance when the acceptance of rock fall risk is brought more and more into question after every major event. The results of this study will be useful to investigate the global standard of the design procedure of prevention structures, such as rock sheds against rock falls. The results of this research are also aimed to be useful for the scientific community and professional practicing civil engineers as well as for the decision-makers world-wide.

INTRODUCTION

With the rapid development of road and highway construction, rock suspending systems such as rock-sheds have also been widely designed and constructed all over the world. They have been constructed in mountainous areas where there is a high risk of rockfall to protect the roads and highways from falling rocks. Rock-sheds have often suffered severe damage and even full collapse caused by impact loads due to falling rocks. For example, the rock-shed shown in Fig. 1 was severely damaged and partially collapsed by a rockfall accident in Etizen, Japan, in July 1989 (Masuya, 1997). Therefore, strengthening existing rock-shed structures as well as developing a safe and economic design for new rock-sheds requires the development of a suitable and practical design method for such structures.



FIGURE 1 Failure of rock-shed caused by falling rock in Etizen, Japan, July 1989 (Masuya, 1997).

Materials such as general sand, macadam sand and mountain soil have been placed on rock-sheds to absorb the impulsive force of rockfall. So far, the buffer characteristics of these materials have been extensively studied by many researchers (Yoshida et al, 1987, Yoneda et al. 1993) and their buffer mechanisms and spread of impact force have been clarified to some degree. Moreover, examples in which old tires are used as a buffer material in steel rockfall barriers can easily be found all over the world. From the conducted experiments concerning the buffer characteristics of the sand materials and old tires, it has been determined that such materials have a limited buffer capacity against a large falling rock. For example, for a spherical falling rock, the maximum energy absorption capacity is obtained when the thickness of the sand layer on the rock-shed is almost the same as the diameter of the falling rock. That is, the buffer capacity of the sand will not increase by increasing the sand layer thickness beyond this level and a further increase in the thickness of the sand layer will only increase the dead load and consequently will lead to an increase in cost. Therefore the development of an effective buffer material to replace these materials has been highly desirable for a long time.

Recently, expanded polystyrene Styrofoam (EPS) has received more attention as a buffer material and the buffer characteristics of this material have been extensively investigated by many researchers (Yoshida, 1991; Yoshida et al., 1989). Some important features of this material, such as its light weight, smaller poisson's ratio, resistance to water and constructional simplicity, have proven that EPS is a good alternative as a buffer material. An extensive experimental study found that when a rock mass of spherical shape fell onto a shed roof covered by EPS, the EPS within the range of only 1.1 times of the falling rock's diameter was cut from the adjacent part of the Styrofoam and the falling rock energy was mainly absorbed by the compressed part of the Styrofoam (Yoshida, 1991; Mamaghani et al., 1999). However, in practice the actual shape of the rock mass is complex, and the section that penetrates into the styrofoam is generally smaller than the section of a sphere with an equivalent diameter. Therefore, the energy absorption capacity of the EPS is not so large. Thus, to obtain a larger buffer capacity it is necessary to install a thicker styrofoam on rock-sheds, increasing the cost.

As another alternative, a three-layer buffer system has been proposed (Mamaghani et al., 2000). In this system one layer of Styrofoam is installed on the shed roof and, as a second layer, a reinforced concrete slab with a fixed thickness is placed on it. The third layer is made of sand poured on the reinforced concrete slab. Although the impact force of falling rock is decreased by

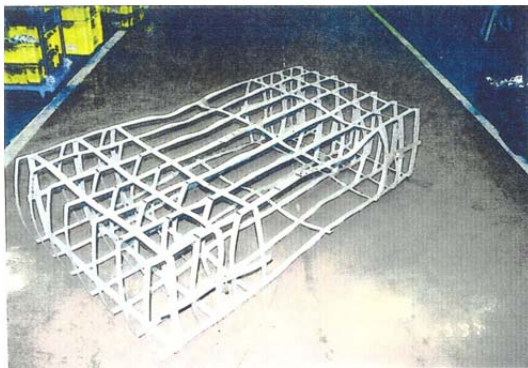
half using the three layer buffer system, the elucidation of its buffer mechanism is difficult. Specifically, it is believed that the energy absorption mechanism will be different between the cases of failure and non-failure of the reinforced concrete slab in the central layer. Moreover, the construction is not generally considered to be ideal. In addition, repair and maintenance, when the reinforced concrete slab is broken by rockfall, may not be easy. To improve the buffer capacity of EPS, reinforced expanded polystyrene Styrofoam (R-EPS) has been developed and its buffer mechanism has been investigated through an experimental study by the authors (Mamaghani et al., 1999).

The present paper is concerned with the buffer behavior and design of R-EPS under impact of falling rock. First, based on the experimental results, the effects of some important parameters, such as reinforcement, thickness of styrofoam, and weight and height of the falling rock on the buffer characteristics and energy absorption capacity of the R-EPS are briefly discussed and evaluated. Then a design method, incorporating the design equations and design charts, for the R-EPS is proposed and substantiated using the experimental data. Finally, the practical application of the proposed method for design of R-EPS is presented and discussed.

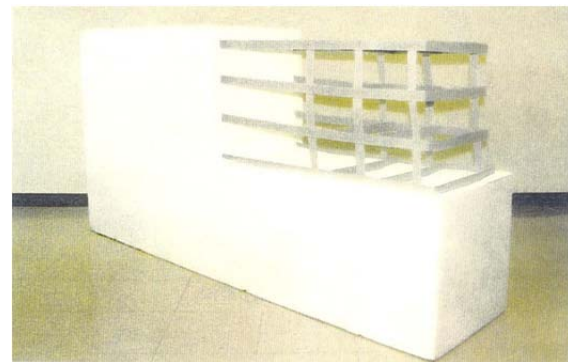
EXPERIMENTS

R-EPS blocks

As shown in Fig. 2, R-EPS blocks with a standard size of $2\text{m} \times 1\text{m} \times 0.5\text{m}$ were manufactured by inserting a reinforcement frame with loops of straps joined in the form of a basket in the foam furnace. The straps used have a width of 31.4mm and thickness of 0.97mm and are made of polypropylene (P.P.) with a tensile strength of 11.35kN. Fig. 3 shows the force-elongation response of the P.P. strap. No strength deterioration or shrinkage of the P.P. strap occurred due to heating during the foaming process.



(a)



(b)

FIGURE 2 R-EPS block: (a) reinforcement frame in the R-EPS block and (b) reinforcement frame.

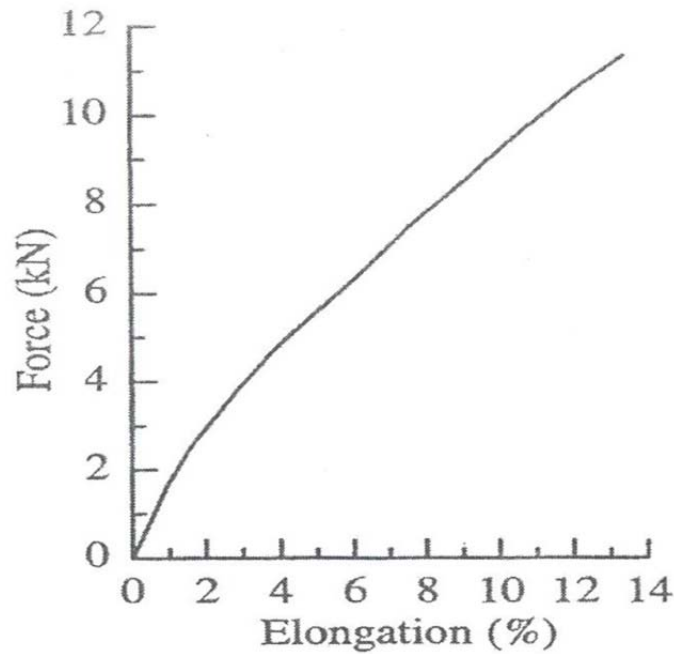


FIGURE 3 Force-elongation response of polypropylene strap.

Expanded Polystyrene Styrofoam

The Styrofoam used has a mass density of 20kg/m^3 . The stress-strain relationship of the Styrofoam is obtained from simple compression tests which were performed on two types of cylindrical specimens having a size (diameter-height) of 150mm-150mm and 100mm-200mm, respectively. The purpose of manufacturing two kinds of test specimens is to examine the influence of size on the stress-strain relation. The tests were carried out under two different speeds at 20mm/min and 500mm/min. The test results show that there is not a significant difference in the stress-strain response of Styrofoam. Fig. 4 shows the stress-strain response at the test speed of 500mm/min. The results in Fig. 4 show that the influence of the specimen size on the stress-strain response is negligible. The approximated stress-strain relation is shown in Fig. 4 with a dashed line. The region from the origin to the strain of 5 percent (c_5) is called the elastic region and the corresponding stress f_5 is 0.12 MPa. The ascendant of stress is extremely dull and linear as the strain increases beyond the (c_5) until the stress begins to increase rapidly when the strain reaches 60 percent (c_{60}); see Fig. 4. The stress at this stage is 0.30MPa (f_{60}). The stress increases sharply when the strain exceeds 70 percent (c_{70}) and reaches a maximum value of 0.70MPa (f_{80}) at a strain of 80 percent (c_{80}).

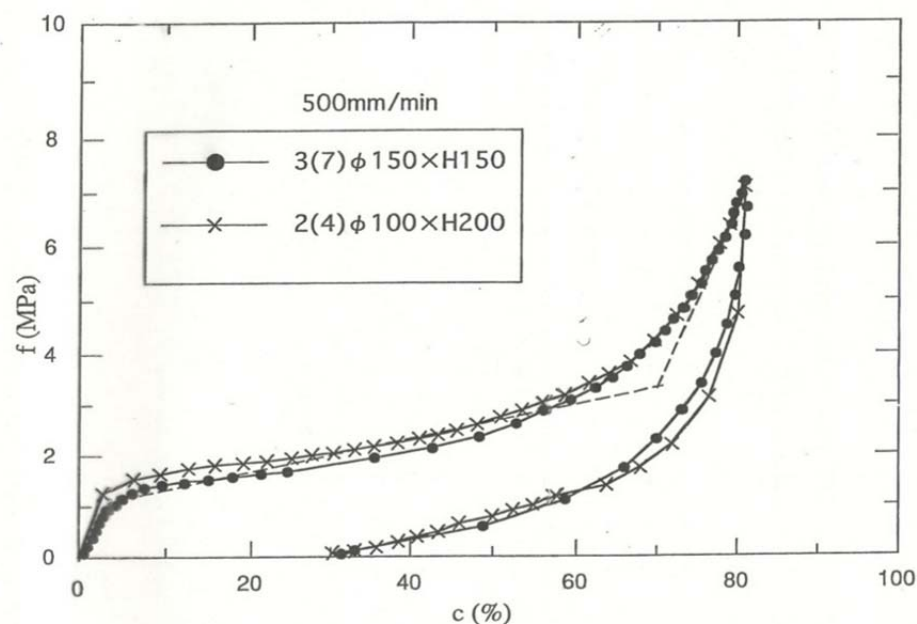


FIGURE 4 Stress-strain response of the EPS at the test speed of 500mm/min (Yoshida, 1991).

Testing Assembly

Fig. 5 shows the testing assembly for the cross-sectional layout of the experimental tank having Styrofoam of height $h = 2.5\text{m}$. An experimental tank with a section size of $5\text{m} \times 5\text{m}$ and L type retaining wall of height 2m was built on the reinforced concrete slab of $7\text{m} \times 7\text{m} \times 0.3\text{m}$ in length, width and thickness. A total of six load-cells, arranged at 30cm intervals from the falling position of the weight, were glued on the surface of the concrete slab as shown in Fig. 5(a). To have enough coherent, sand of 5cm thickness was spread evenly on the concrete slab. Styrofoam with layer shapes of A, B, C, D and E, as shown in Fig. 5(b), was laid in the experimental tank in the order indicated in Table 1 for the corresponding experiment, starting from the top. The gap that was not filled with styrofoam in the tank was filled with sand. Two weights of 10kN and 50kN were used in the experiments, as shown in Fig. 5(c)

Conducted Experiments

Table 1 shows a list of conducted experiments that were carried out to make comparisons between the response of general styrofoam and R-EPS under falling rock impact. In the test names in Table 1, "RP" indicates styrofoam reinforced by the P.P. straps and "GS" denotes the expanded polystyrene (general) styrofoam. The first, second and third numbers in the test names stand, respectively, for the number of styrofoam layers, weight of the falling mass (in kN) and the falling height (in meters) of the weight. The falling height of the weights are shown in Table 1; the symbols W, h and H stand for the weight, total thickness of styrofoam and falling height, respectively.

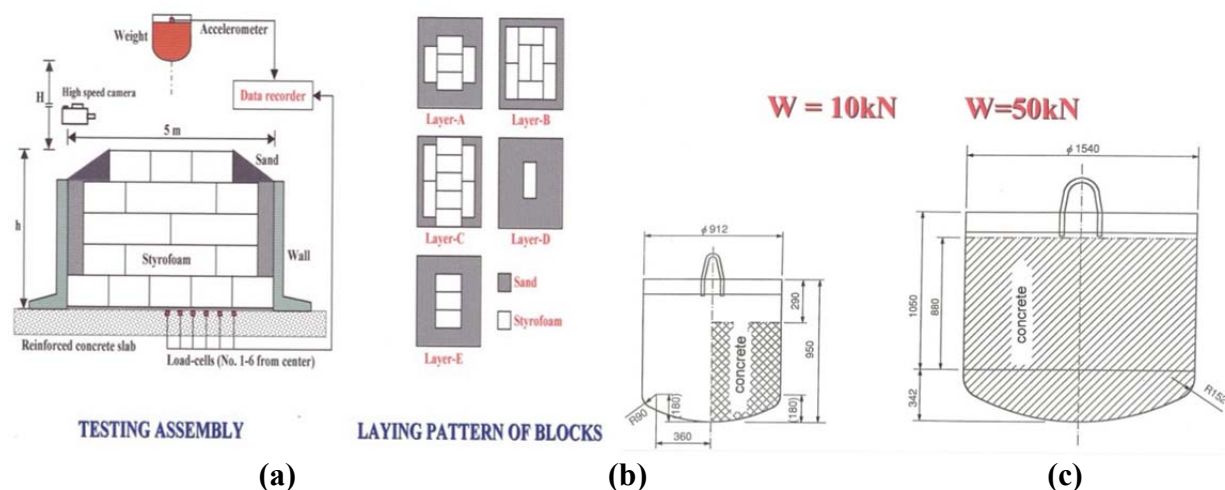


FIGURE 5 (a) Elevated section of testing assembly; (b) laying pattern of blocks; and (c) used weights.

TABLE 1 Conducted Experiments

Test Name	h(m)	W(kN)	H(m)	Layer Order from Top
RP-5-50-20	2.5	50	20	A+B+C+B+C
RP-4-50-20	2.0	50	20	A+B+C+B
RP-4-50-30	2.0	50	30	A+B+C+B
RP-3-50-15	1.5	50	15	A+B+C
RP-3-50-20	1.5	50	20	A+B+C
RP-2-10-20	1.0	10	20	D+E
RP-1-10-10	0.5	10	10	D
GS-5-50-20	2.5	50	20	A+B+C+B+C
GS-4-50-20	2.0	50	20	A+B+C+B
GS-3-10-20	1.5	10	20	A+B+C

Note: h = total thickness of styrofoam, W = weight, H = falling height.

EXPERIMENTAL RESULTS

Weight impact force and transmitted impact force

The weight impact force and the transmitted impact force concepts are used to evaluate the characteristics of the buffer material (styrofoam with and without reinforcement). The weight impact force is obtained by multiplying the mass and maximum acceleration (negative value) of the weight when it collides with the buffer material. The weight impact force spreads through the buffer material while the weight collides with and penetrates the buffer material. The transmitted impact force at the bottom of the buffer material caused by the falling rock, which acts directly on the structure, is obtained by integrating the transmitted impact pressure on the acting area.

The impact pressure, which is measured by six load-cells set at the bottom of the buffer material, is assumed to be distributed symmetrically about the falling point of the weight.

Buffer Response

The buffer response of the R-EPS and EPS under falling rock impact will be discussed in this section. The changes in weight impact force and transmitted impact force over time from the tests are shown in Fig. 6. This figure shows that when the thickness of the styrofoam is large enough compared with the energy of the falling rock, regardless of the presence of reinforcement, the weight impact force acts for a longer time, up to 300msec. The impact force starts to rise at 20msec and increases gradually until it reaches a maximum value at 100-150msec, at which point it decreases gradually and disappears. On the other hand, when the thickness of the styrofoam is small compared with the falling rock energy, the acting time of the weight impact force is short and the maximum value of the impact force is large.

As shown in Fig. 6, the transmitted impact force has almost the same shape as the weight impact force for the reinforced styrofoam. The transmitted impact force shows larger maximum values compared with the weight impact force. In the case of general styrofoam, though the transmitted impact force shows almost the same wave shape as the weight impact force, it decreases rapidly after reaching the maximum value as the styrofoam blocks were broken. In the case of reinforced Styrofoam, the shape of the transmitted impact force waves is extremely smooth and symmetric around the maximum value. Whereas in the case of general styrofoam without reinforcement, the transmitted impact force curve has a saw-tooth form and it is not symmetric. The experimental results show that the reinforced styrofoam does not break, deforms elastically, and restores its original state. Whereas the impact force wave of general styrofoam indicates that the Styrofoam suffers large deformation and breaks until it is completely collapsed.

Spread of Impact Pressure

As an example, for the RP-5-50-20 and GS-5-50-20 tests, Fig. 7 and Fig. 8, respectively, show the distribution and change over time of the transmitted impact pressure at the bottom of the buffer material measured using the load-cells. The impact pressure waves show a similar response to the weight impact force. The impact pressure corresponding to the general styrofoam without reinforcement concentrates on the center with a larger value (acts within a comparatively narrow range) and disappears in a short time, whereas the reinforced Styrofoam shows a comparatively small impact pressure distributed over a wide area and acting over a long time.

From the indicated impact pressure distribution of the reinforced Styrofoam, Fig. 7, and its variation over time, Fig. 8, it is clear that the impact pressure rises rapidly until the weight penetrates into the first layer of the styrofoam and then it increases gradually and reaches the maximum value by expanding within the wide range, also see Fig. 6 for the transmitted impact force. At this stage, the transmitted impact force is at its peak at the impact point and the impact pressure reduces and disappears with distance away from the impact point. The test results corresponding to the maximum weight impact forces, transmitted impact forces, and penetrations are summarized in Table 2.

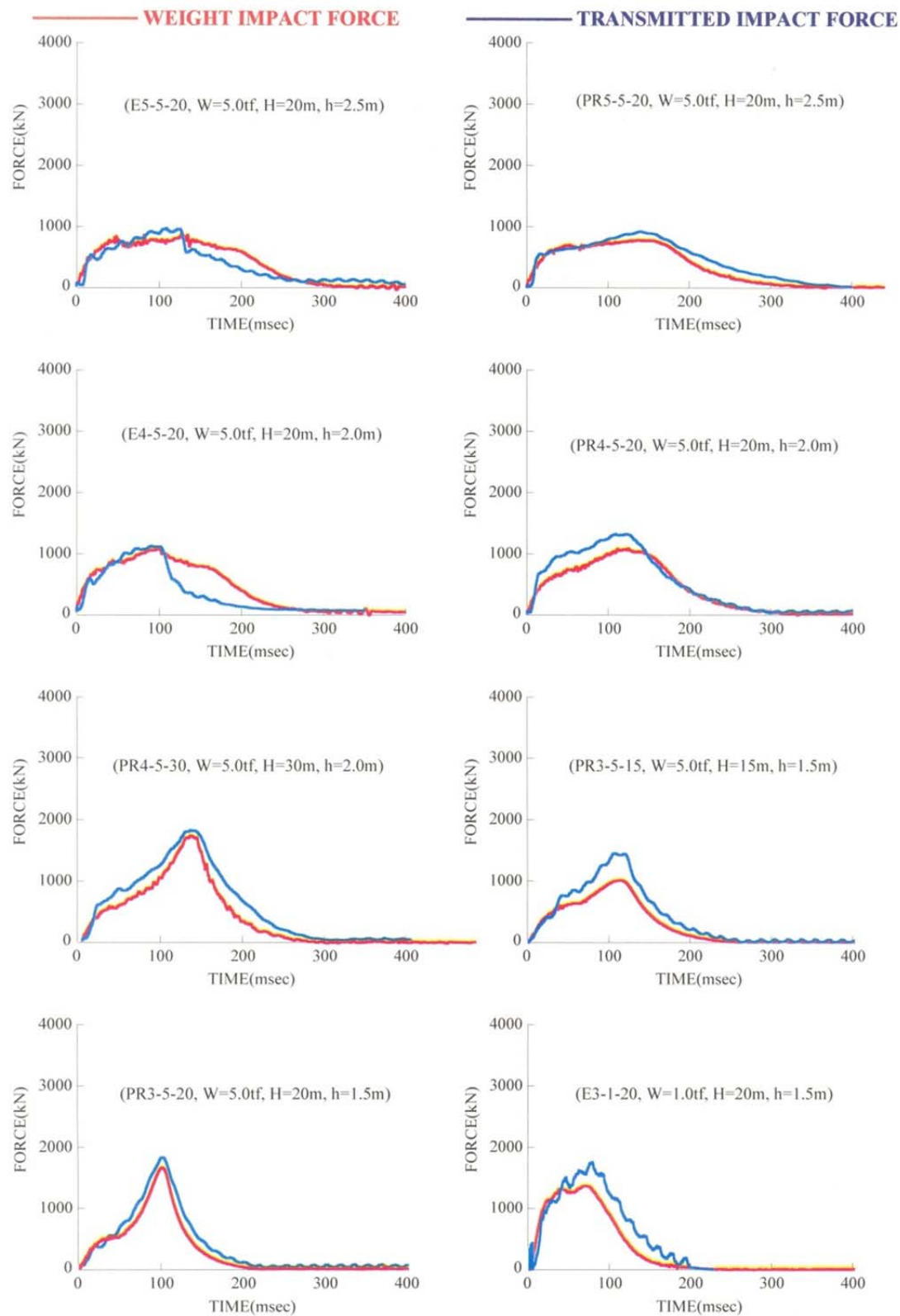


FIGURE 6 Weight impact force and transmitted impact force.

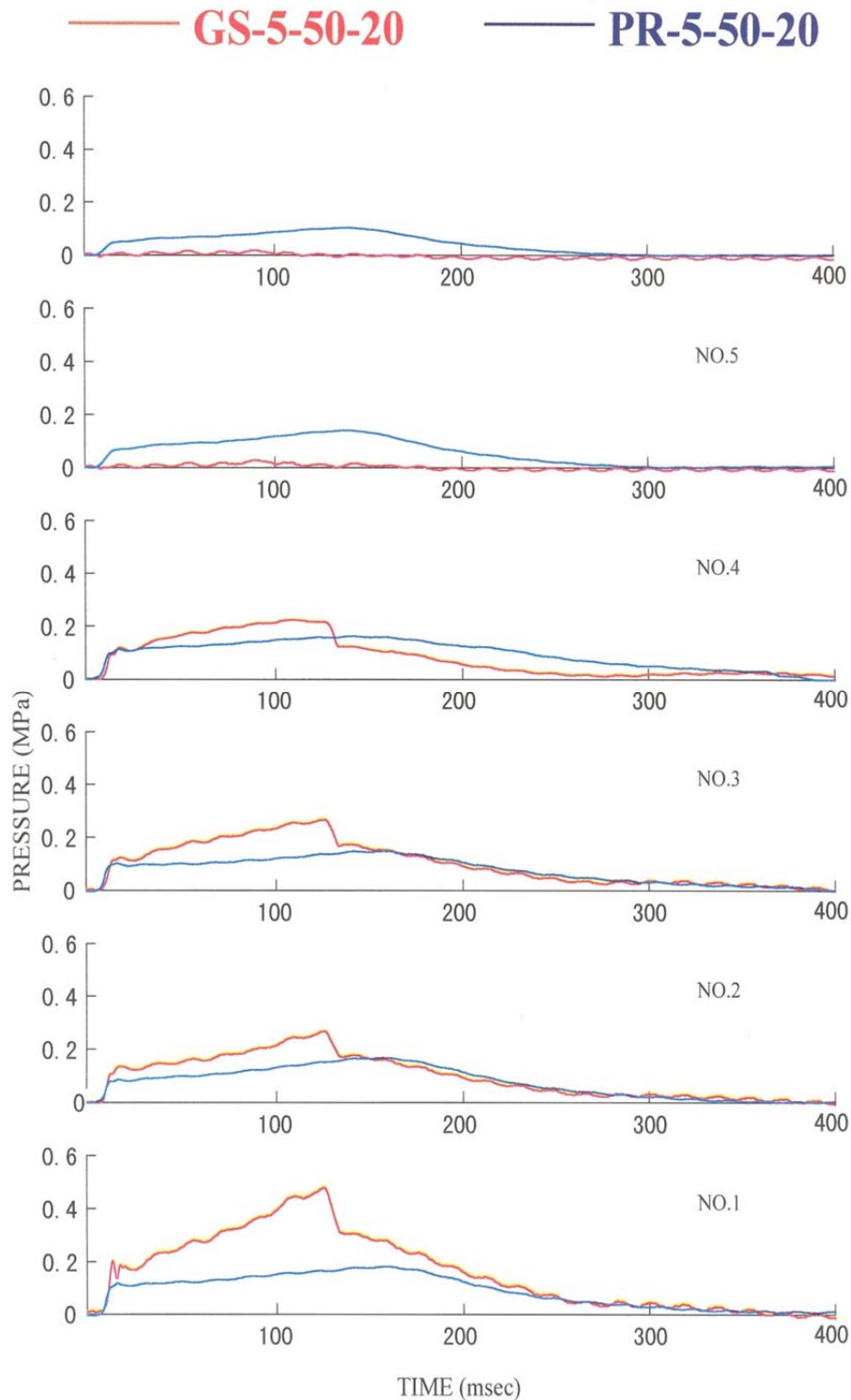


FIGURE 7 Impact pressure at monitoring points.

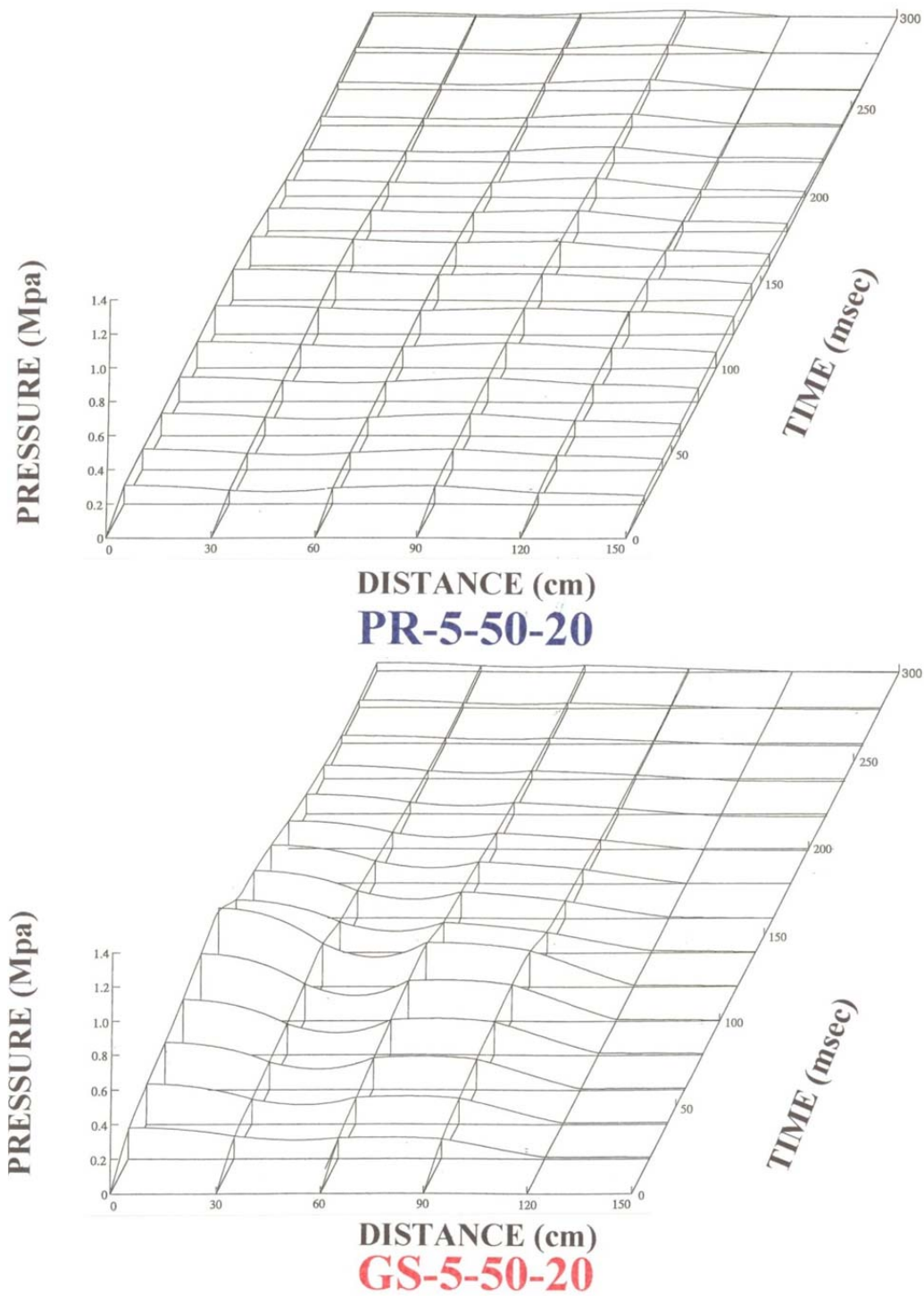


FIGURE 8 Impact pressure versus time and distance.

Table 2 Test Results

Test Name	M.W.F (kN)	M.T.F (kN)	M.P.(m)
RP-5-50-20	705	845	1.81
RP-4-50-20	985	1,210	1.64
RP-4-50-30	1,750	1850	1.84
RP-3-50-15	955	1365	1.21
RP-3-50-20	1615	1765	1.39
RP-2-10-20	400	610	0.84
RP-1-10-10	385	455	0.46
GS-5-50-20	790	970	1.76
GS-4-50-20	955	995	1.53
GS-3-10-20	255	325	1.05

Note: M.W.F = maximum weight impact force; M.T.F = maximum transmitted impact force; and M.P. = maximum penetration.

PRACTICAL APPLICATION

The thickness of styrofoam required when the falling rock weighing 50kN falls perpendicularly from height of 16m on the rock-shed designed for load of 1200kN will be calculated taking the main beam interval as 1.5m. As shown in Fig. 8, in the case of EPS with a thickness of 2.0m and a design load of 869kN, the strain exceeds 70 percent, which is considered dangerous. It is recommended that the maximum strain should not exceed 70 percent, in order to insure against shear failure and penetration into the styrofoam by the falling rock. Therefore, styrofoam thickness of 2.5m is required. However, in the case of R-EPS, even if the falling rock is slender and has a diameter less than the equivalent one, it is possible to allow the strain to reach up to 80 percent because one block behaves like one mass without suffering local shear failure. Therefore, a thickness of 1.5m for reinforced styrofoam is sufficient. In the case of a rock having a weight of 50kN falling perpendicularly from a height of 25m, the required thickness of styrofoam for the main beam interval of 1.5 m designed for a load of 800kN can be obtained from Figure 8. The charts in this figure indicate that the required thicknesses are 2.5m and 3.5m for reinforced styrofoam and general styrofoam, respectively.

CONCLUSIONS

Reinforced expanded polystyrene styrofoam (R-EPS) has been suggested as an improved alternative buffer material to be placed on the roof of rock-sheds to absorb and distribute the impact of falling rock. This extensive experimental study investigates the effects of some important parameters, such as reinforcement, thickness of styrofoam, and the weight and height of the falling rock on the buffer characteristics and energy absorption capacity of R-EPS. It was found that local failure of the styrofoam does not occur and the shape of the falling rock does not affect the buffer capacity of R-EPS. Therefore, the pressure that acts directly on the concrete slab beneath the R-EPS is distributed over a wide area due to improved R-EPS buffer characteristics owing to reinforcement. In summary, it is concluded that the use of R-EPS as a buffer material and the proposed design method can contribute to an efficient design by increasing the resistance of existing rock-sheds and the establishment of new rock-shed design regulation.

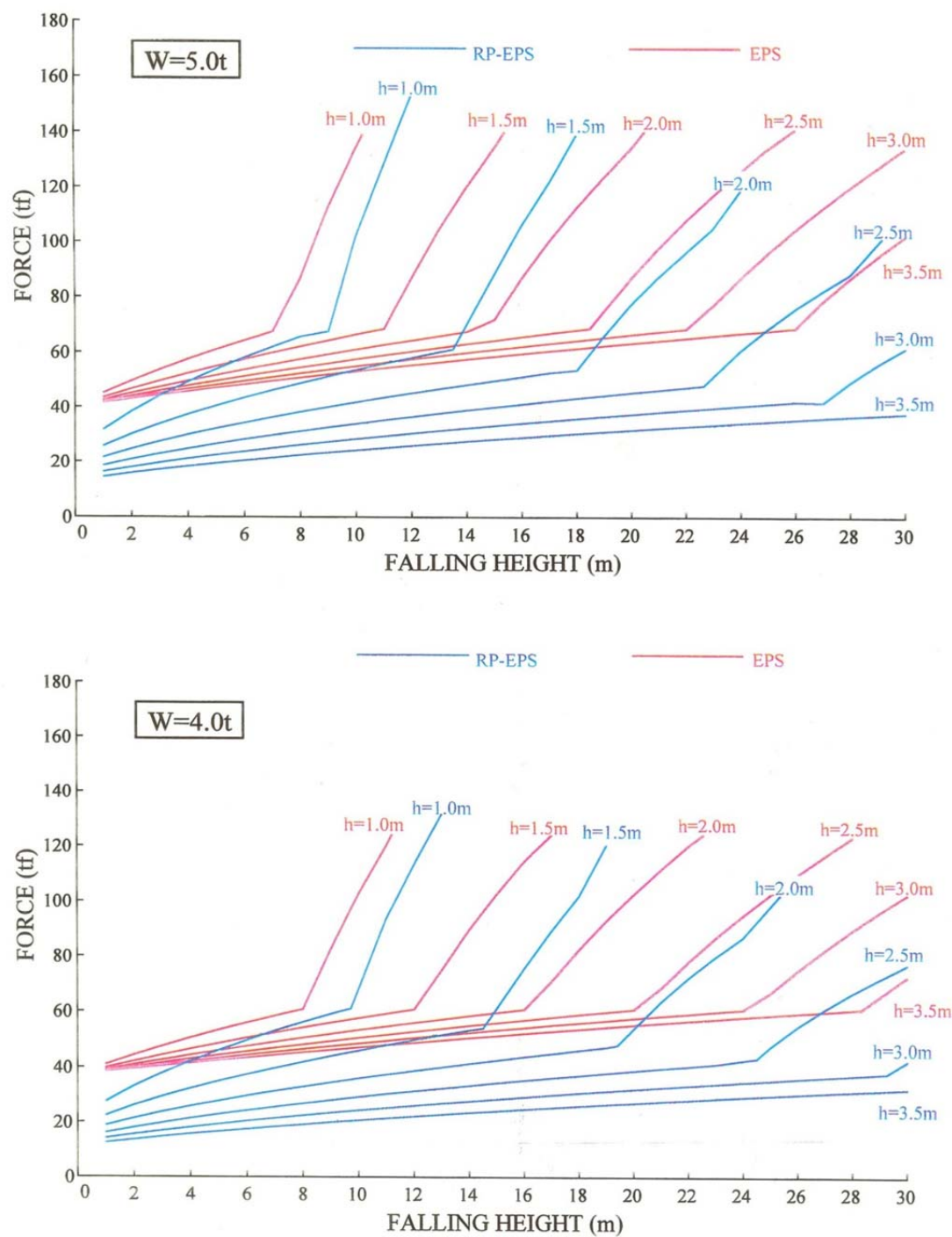


FIGURE 9 Practical application ($B=1.5$ m, $W=50$ kN).

REFERENCES

- Mamaghani, I.H.P., Yoshida, H., Obata, Y., 1999, Buffer characteristics of reinforced expanded polystyrene Styrofoam under falling rocks, *Proceeding of the first international summer symposium, JSCE*, pp. 85-88, Tokyo, Japan.
- Mamaghani, I.H.P., Yoshida, H., Obata, Y., 2000, Buffer behavior and design of reinforced expanded polystyrene Styrofoam under falling rock impact, *Journal of Structural Engineering*, JSCE, Vol. 46A, Japan.
- Masuya, H., 1997, Analysis of the impact behavior of a protective structure as a rock shed, *Journal of the Japan Society for Computational Engineering and Science (JSCEs)*, Vol.2, No.3, pp. 15-21.
- Yoshida, H., Masuya, M., Satou, M., Ihara, T., 1978, A database of rock falling tests and an estimation of impulsive loads by rockfall, *Journal of Structural Engineering*, JSCE, Vol.33A, pp. 571-583.
- Yoneda, Y., Washida, S., Koga, Y., Matsuba, M., Sato, A., 1993, Weight falling tests concerning falling rock impact force acting on rock-shed, *Proceedings of the 2nd Symposium on Impact Problems in Civil Engineering, JSCE*.
- Yoshida, H., Masuya, M., Fujii, T., Maegawa, K., 1989, Impulsive behavior of steel rock barriers under a falling rock, *Proceedings of JSCE*, No.409/VI-11, pp.75-84.
- Yoshida, H., 1991, An experimental study on shock absorbing effect of expanded polystyrene against falling rock, *Proceedings of JSCE*, No.427/VI-14, pp.143-152.

Feasibility of Predicting Light Vehicle Occupant Injury Disutility from Impacts with Road Safety Barriers

ANDREW BURBRIDGE

Queensland Government Department of Transport and Main Roads

ROD TROUTBECK

Queensland University of Technology

A procedure for predicting disutility associated with injury severity outcomes for occupants of vehicles impacting longitudinal road safety barriers is not well established. Roadside hazard management procedures use results from empirical studies of generic barrier types. Published literature suggests that the injury severity outcomes of vehicle-barrier interactions are more complex, and are a function of (among other things) impacting vehicle mass, impact speed and impact angle, and a road safety barrier system's stiffness (resistance to deflection).

Presented is an exploration of the feasibility of a structural model that could be used to predict occupant injury outcome disutility arising from tracking light passenger vehicle impacts with road safety barriers as a function of the impact configuration and stiffness of the road safety barrier system.

The study concludes that such a structural model is feasible subject to development of a satisfactory link between barrier stiffness and likelihood of impact configuration and injury outcomes. The use of Head Impact Criterion (HIC) as a proxy to link vehicle accelerations to injury outcome is considered to show promise.

Calibration of such a model would require reporting of the impacted barrier in terms of the factors that are expected to influence system stiffness as well as the configuration of impact (vehicle mass, impact speed and angle) and the geometric circumstances (cross-section, number of lanes, lateral offset). Other variables expected to contribute to occupant injury outcomes such as vehicle age and safety rating, number of occupants and mode of impact (tracking or non-tracking) should also be collected.

INTRODUCTION

Technical governance in Australia recognises three generic road safety barrier types discerned by stiffness. The Austroads Guide to Road Design Part 6 (1) describes road safety barriers as flexible, semi-rigid or rigid. Australian/New Zealand Standard AS/NZS 3845.1:2015 (2) adopts these same descriptions. The rigid classification includes concrete barriers and steel bridge rail barriers. Flexible barriers are typically wire rope (cable) barriers, while semi-rigid barriers include post-mounted steel rail systems.

With a few exceptions, published literature is generally similarly undiscerning. In the Australian context, Nilsson and Prior (3) report on the use of road safety barrier in New South Wales and compare wire rope safety barrier, steel guardrail and concrete barrier. Jurewicz et al (4) provide Fatal and Serious Injury (FSI) ratios for each of these three generic road safety barrier types, while the Australian National Risk Assessment Model (ANRAM) (5) provides risk factors for three generic barrier types, viz, 'concrete', 'metal' and 'wire rope'. Bambach, Mitchell and Mattos (6) compare outcomes for car drivers and motorcyclists in impacts with different roadside

objects, including wire rope, w-beam and concrete barriers. Internationally, Beaton and Field (7) provide definitions for flexible, semi-rigid and rigid barriers. Holdridge et al (8) present an analysis of the in-service performance of roadside hardware on the entire urban State Route system in Washington State, and include data for guardrail and concrete. Hu and Donnell (9) present a study of the severity of median barrier crashes from rural divided highways in North Carolina, and report outcomes in terms of cable, guardrail and concrete barrier. Chitturi et al (10) present analysis of all cross-median and median-barrier crashes in Wisconsin from 2001 to 2007 and report outcomes in terms of concrete, cable and guardrail. Zou et al (11) report on single-vehicle crashes on segments of the Indiana road network and discern barriers in terms of cable, guardrail and concrete. Karim et al (12) report on injury outcomes resulting from barrier collisions in Sweden, and report injury rates disaggregated by barrier type: w-beam, cable and concrete.

However, there is evidence that road safety barriers may not fit such discrete categories. Michie et al (13) conclude that “*vehicle acceleration and vehicle damage were somewhat higher for the relatively rigid G4 system than for the G2... system*”. Similarly, Ray and Weir (14) observe no difference between the performance of G1 cable and G2 weak-post w-beam guardrail or G1 and G4(1W) strong-post w-beam but that injuries were less common in collisions with a G1 guardrail than in collisions with G4(1W) strong-post w-beam. Martin et al (15) differentiate barrier types by (among other things) rail type, post type and post spacing. Soltani et al (16) present an analysis of semi-rigid barriers, discerning on the basis of deflection. Ray et al (17) distinguish in terms of aggressiveness between high-tension and low-tension cable (wire rope) barrier systems.

Published literature also suggests that barrier aggressiveness may be a function of the impact configuration and cross-sectional geometry. Michie et al (13) find that rigid barrier performs favourably when compared to semi-rigid systems in shallow angle (< 15 degrees) impacts, and that in tests where the barrier was repeatedly struck at 50 mph at 8 degrees “*no vehicle damage or driver injuries were observed*”. However in large angle (> 20 degrees) impacts, vehicle redirection is described as “*abrupt*”. This is consistent with Bronstad et al (18) who find that 15 degree impacts are not a discerning test for occupant risk, but that 20 degree impacts are a discerning test. Ydenius et al (19) report on observations from parametric testing that impact with concrete barrier at 80 km/h and 45 degrees was the most severe impact configuration in terms of all metrics employed, but “*at slight impact angles ($< 20^\circ$) the perpendicular forces on the barrier are relatively small, which most likely leads to a moderate vehicle crash severity*”. Sicking and Ross (20) show how severity index (as a vector to accident costs) from impacts into w-beam guardrail are predicted to vary as a function of impact speed and angle. Also Michie et al (13) find that vehicle mass is “*a most important parameter*” and that lighter vehicles are likely to experience more severe redirection. Doecke and Woolley (21) state “*ideally the barrier would be placed as close to the edge of road as practical to reduce the angle at which it may be struck*”. Burbridge and Troutbeck (22) likewise observe that occupant injury risk may be expected to increase with increasing barrier offset. In summary, occupant outcomes may be a function of the cross-sectional geometry, which influences the speed and angle of impacts that may occur. Burbridge and Troutbeck (23) conclude that “*occupant risk... is likely to be a function of the speed, mass and angle of the impact as well as the stiffness of the system*” and that “*it would be appropriate in empirical studies of in-service performance to report the detail of the barrier in terms of the factors that might be expected to influence stiffness of the system (for example post spacing, post type, rope configuration and tension) as well as the configuration of the impact (vehicle mass, impact speed and impact angle)*”.

Ray et al (17) present a methodology for calculating economic disutility in terms of

Equivalent Fatal Crash Cost Ratio (EFCCR). EFCCR is a dimensionless measure of the aggressiveness of a roadside object computed from crash data by dividing the average severity cost arising from all impacts (including allowance for unreported crashes) by the cost of a fatal crash. When EFCCR equals unity, the economic costs of a crash are equal to the value assigned to a fatality. In the Roadside Safety Analysis Program (RSAP) (17) the aggressiveness of different barrier types is defined in terms of EFCCR, based on empirical data from collected studies. The values reported by Ray et al (17) vary broadly and differently for different barrier types suggesting that there may be unexplained site, traffic, barrier or other variables that affect the computed values of EFCCR. As such, the transfer of a nominated value for EFCCR from one site to another may be inappropriate if, for example, the cross-sectional geometry or the traffic composition or the stiffness of the barrier is different to those on which the nominated EFCCR value is based.

Bonneson and Ivan (24) suggest that a structural modeling approach to estimating safety might be preferable to a statistical or empirical approach on the basis that *“it provides a framework for scientific advancement and a transparency to the interpretation of causal dependencies”*.

Gabauer and Gabler (25) describe efforts to correlate the occupant risk indicator Acceleration Severity Index (ASI) directly with occupant injury, finding that *“ASI, at least with respect to the preferred threshold, is a good indicator of occupant injury to belted and airbag-restrained occupants involved in frontal collisions”*, although the work does not have application across all injury strata.

In summary, a useful advancement would be to be able to predict ASI, and so to predict the full range of occupant injury outcomes for any vehicle-barrier impact. In the context of light vehicle occupant injury as a consequence of impact with a road safety barrier, published literature suggests that aspects such as cross-sectional geometry, traffic composition and barrier stiffness are relevant parameters in such a model. A structural modeling approach to the derivation of EFCCR may explain differences in values reported from empirical studies.

AIM

The aim of this study was through review of existing knowledge to consider the feasibility of developing a conceptual numerical procedure (in the form of a probabilistic causal model) that may be used to predict occupant injury disutility arising from light passenger vehicle impacts with road safety barriers. The objectives were as follows:

1. Explore prediction of ASI as a function of the impacting vehicle mass, impact speed and impact angle, and a road safety barrier system's resistance to deflection;
2. Explore development of a module that uses the computed ASI from the primary module to predict occupant injury outcomes via the proxy of the 15 millisecond Head Impact Criterion (HIC₁₅);
3. Explore development of a module that uses the derived HIC₁₅ to compute Effective Crash Cost Ratio (EFCCR).
4. Explore development of module that predicts occupant injury disutility as a function of crash configuration (in terms of mass, speed and angle) and barrier stiffness.

The paper is divided into four sections that respectively address each of these components.

PREDICTING ACCELERATION SEVERITY INDEX (ASI)

Acceleration Severity Index is a non-dimensional occupant severity indicator calculated from orthogonal time-averaged time-acceleration traces measured during crash testing at the centre of mass of the impacting vehicle. ASI is calculated using Equation 1 (25).

$$ASI = \max \left[\left(\frac{a_x}{\hat{a}_x} \right)^2 + \left(\frac{a_y}{\hat{a}_y} \right)^2 + \left(\frac{a_z}{\hat{a}_z} \right)^2 \right]^{\frac{1}{2}} \quad (1)$$

where $a_{x,y,z}$ are average component vehicle accelerations respectively in the longitudinal, lateral and vertical direction measured over a prescribed time interval (50 milliseconds), and $\hat{a}_{x,y,z}$ are corresponding threshold values for the respective component accelerations (25). The denominator values for the component threshold accelerations $\hat{a}_{x,y,z}$ as adopted in both the US and European test protocols are respectively $\hat{a}_x = 12g$, $\hat{a}_y = 9g$ and $\hat{a}_z = 10g$ (and g = acceleration due to gravity).

Burbridge and Troutbeck (23) investigate ASI values returned from full scale crash tests of longitudinal barriers conducted typically in accordance with NCHRP Report 350 (26). The results in Figure 1 are plots of ASI plotted against “flexibility” (the reciprocal of stiffness, computed as the ratio of recorded dynamic deflection divided by Impact Severity (calculated by Equation 2)) for a number of reported crash tests.

$$IS_{m,v,\theta} = 1/2000 m(v \cdot \sin \theta)^2 \quad (2)$$

where

IS = impact severity (kJ)
 m = vehicle mass (kg)
 v = vehicle speed (ms^{-1})
 θ = impact angle (degrees)

In panel (a) the results are disaggregated by barrier type, and in panel (b) the same results are disaggregated by nominal test conditions. Panel (b) suggests that there is a relationship between barrier flexibility and the ASI value recorded during crash testing, and moreover that ASI appears to be inversely proportional to barrier flexibility. The results for the nominal 8000 kg, 80 km/h, 15 degree tests for example indicate a distinct decay curve, as do the results from the two other nominal crash test configurations. The following observations are apparent:

- (i) ASI is highest for the lightest (kg) vehicle impacts (nominally 820 kg at 100 km/h and 20 degrees).
- (ii) ASI is lowest for the heaviest (kg) vehicle impacts (nominally 8 tonnes at 80 km/h and 15 degrees).

Notably the lowest values of ASI are also returned from impacts with the lowest impact speeds and highest for the highest impact speeds. Also, the effect of the flexibility (or stiffness) of the barrier is evident in the shape of the curve for each impact configuration. This is consistent

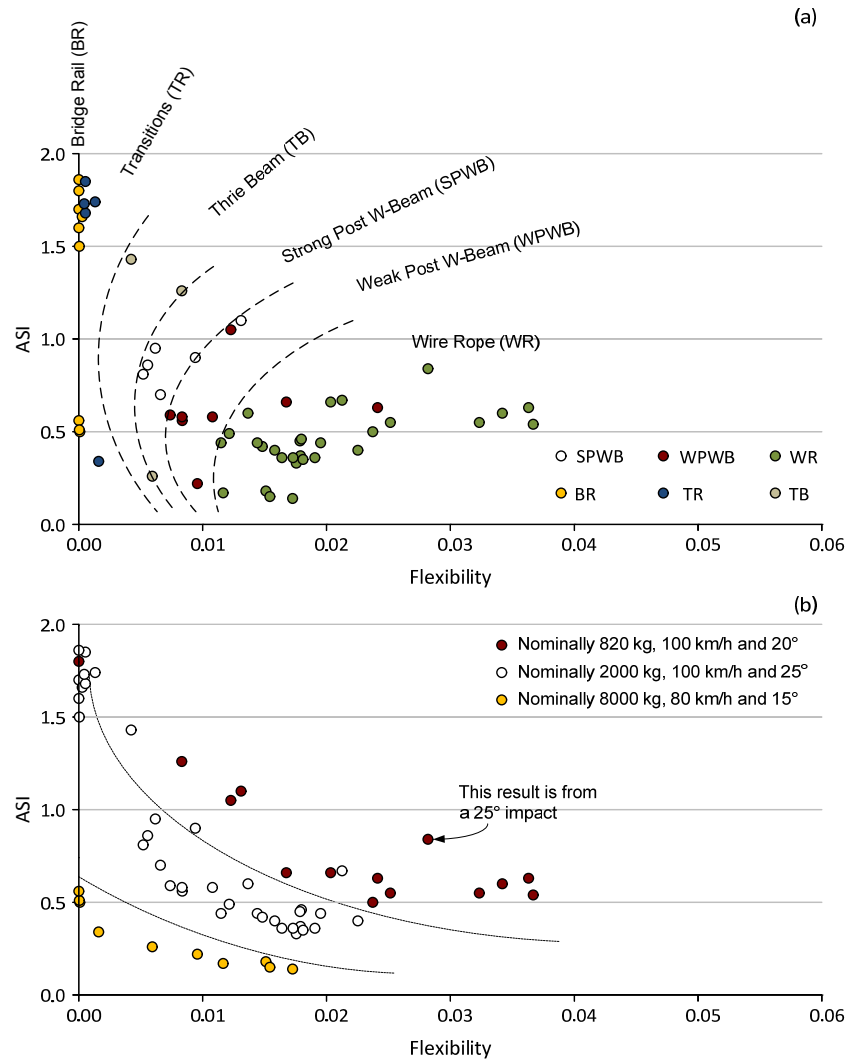


FIGURE 1 ASI v flexibility for 60 crash tests [adapted from Burbridge and Troutbeck (23)]: (a) depicts results disaggregated by barrier type and (b) depicts results disaggregated by nominal configuration of the crash test.

with Anghileri et al (27) who report a “*weak correlation between ... ASI and dynamic deflection*”. Burbridge and Troutbeck (23) make the following observations:

- (i) The shape of the ASI-flexibility curve is flattest for the lowest angle impact (15 degrees).
- (ii) The shape of the ASI-flexibility curve is steepest for the highest angle impact (25 degrees).

The authors hypothesize that occupant severity indicator ASI may be expected to increase as a function of:

- Decreasing vehicle mass

- Increasing impact speed
- Increasing impact angle
- Increasing barrier stiffness

The hypothesized function is represented in Equation 3. This equation is not solved here. If solved however, and it is reiterated that FIGURE 1b suggests that it may have a solution, then it may be possible to predict ASI if vehicle mass, impact speed, impact angle and barrier stiffness are known.

$$ASI = f(m, v, \theta, s) \quad (3)$$

PREDICTING HEAD IMPACT CRITERION (HIC) FROM ASI

Head Impact Criterion (HIC) is a quantitative indicator of head injury risk calculated using the results from data recorded at the centre of gravity of the head of an anthropomorphic test device (ATD)(an instrumented crash test dummy). HIC is calculated according to the expression in Equation 4:

$$HIC_{(t_2-t_1)} = \max_{t_2-t_1} \left\{ (t_2 - t_1) \left[\frac{1}{(t_2 - t_1)} \int_{t_1}^{t_2} a(t) dt \right]^{2.5} \right\} \quad (4)$$

where $a(t)$ is the acceleration of the head of the ATD in terms of the gravitational constant (g), t_1 and t_2 are any two arbitrary times during the acceleration pulse such that t_1 is earlier than t_2 by a predetermined interval, and $HIC_{(t_2-t_1)}$ is the Head Impact Criterion for a time interval reported in milliseconds. If the time interval t_2 minus t_1 is 15 milliseconds, then the expression returns the 15-millisecond Head Impact Criterion (HIC_{15}).

Several studies report on the possibility of a relationship between ASI and HIC. Naing et al (28) and Klootwijk and Hoogvelt (29) report a linear relationship between 36 millisecond HIC (HIC_{36}) and ASI, and claim that ASI is a reasonable predictor of injury in guardrail impacts. Sturt and Fell (30) report results for HIC_{36} and ASI in impacts with concrete step barrier, which are reported by Roque and Cardoso (31) as an exponential form, and which Roque and Cardoso contend underestimate occupant severity outcomes. Barrier comparison testing reported by Hammonds and Troutbeck (32) indicate similar results to those reported by Sturt and Fell for HIC_{36} measured in impacts with 810 mm high “F” shape barriers. Notably Hammonds and Troutbeck state that as the Hybrid III anthropomorphic test device (ATD) is designed for frontal impact testing, care should be taken with interpreting results as crash testing generates lateral forces that may not necessarily be reflected in the results of the ATD. Anghileri et al (27) caution similarly. Li et al (33) report a polynomial relationship between ASI and HIC_{15} for impacts with concrete New Jersey shape barrier, and an exponential relationship for impacts with w-beam barrier. The authors qualify that the observations should not be regarded as definitive and recommend that discrepancies observed between vehicle response criteria (e.g., ASI) and occupant responses (e.g., HIC) reinforce the need to use occupant responses directly in the evaluation of road safety barriers. Roque and Cardoso (31) also report the findings based on nine “*lateral crush tests*” conducted by Shojaati (34) as an exponential form although it is not explicit what time

interval is used in the calculation of HIC.

In summary, there is a body of work exploring the notion that some relationship between ASI and HIC exists, and that published literature suggests that this would likely be an exponential or power relationship. And so on the basis that HIC may offer a means to translate ASI to head injury there is evident value in pursuing a model that uses ASI to predict Head Impact Criterion.

PREDICTING OCCUPANT INJURY FROM HIC

It is worth acknowledging that Head Impact Criterion as a vector to occupant injury does attract some disquiet. Newman (35) presents a synthesis of literature pertaining to the use of HIC concluding that “*the use of HIC in automotive crash testing is fundamentally wrong*”. Among other things, Newman is concerned about the lack of any functional relationship “*between human head injury, cadaver and ATD head acceleration and time*”, and moreover that there is only a low correlation between HIC and head injury. This is consistent with Brell’s later observation that there is absence of a valid causal chain to explain correlation with test data (36).

But despite the criticism, the Head Impact Criterion does enjoy “*legislative imprimatur*” (36), and further, curves are developed which estimate head injury risk in frontal impacts in terms of the Abbreviated Injury Scale (AIS) (37) as a function of the 15 millisecond Head Impact Criterion (38). These curves, called the Expanded Prasad-Mertz curves are described by the general expression in Equation 5 (38) and are plotted here in Figure 2.

$$p(\text{injury} \geq \text{AIS } j) = \left[1 + e^{\left((\alpha_j + 200 / \text{HIC}_{15}) - \beta_j \times \text{HIC}_{15} \right)} \right]^{-1} \quad (5)$$

where

n = injury level, ranging from 1 to 6, and where injury level 6 represents a fatality.
 α_j, β_j = constants, values for which are provided in (38).

Hence, for any value of HIC_{15} , the probability of injury level “j” is calculated by Equation 6.

$$p(\text{injury} = \text{AIS } j) = p(\text{injury} \geq \text{AIS } j) - p(\text{injury} \geq \text{AIS } (j + 1)) \quad (6)$$

And since the probability of all injury outcomes (including no injury) is unity, the probability of a Property Damage Only (PDO) outcome is calculated by Equation 7.

$$p(\text{PDO}) = 1 - \sum_{j=1}^6 p(\text{injury} = \text{AIS } j) \quad (7)$$

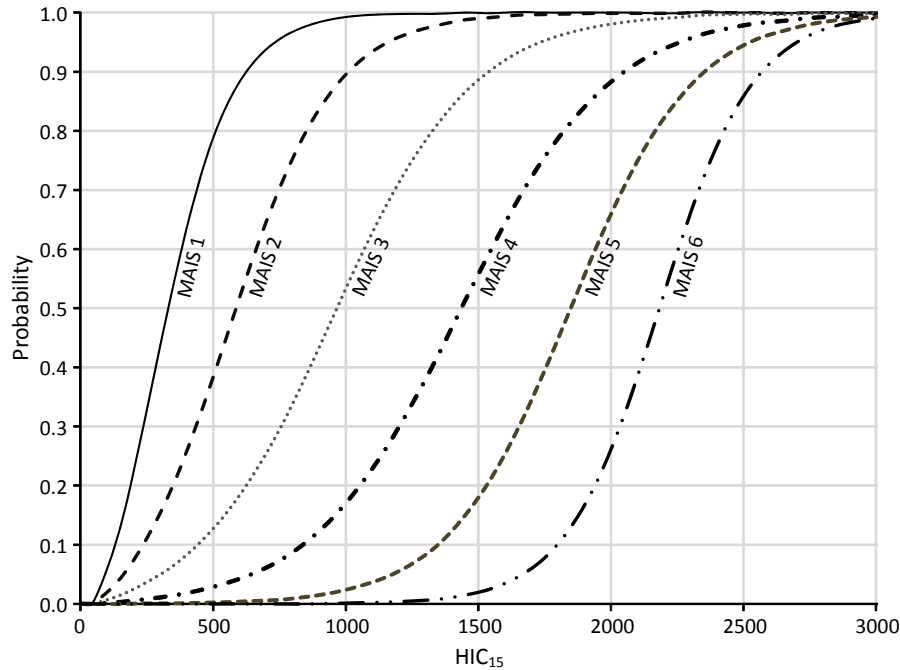


FIGURE 2 Expanded Prasad-Mertz curves (constructed from 38).

Translating Injury to an Economic Cost

Trottenberg and Rivkin (39) provide relative disutility factors (RDF) stratified by injury severity level in terms of the Abbreviated Injury Scale (AIS) (37). The factors are used to multiply the value of a statistical life to obtain the values of preventing such injuries. No value is assigned to a non-injurious outcome. However, a crash without injury does have economic consequence. Based on the summary of comprehensive unit costs from reported and unreported crashes published by Blincoc et al (40), the cost (in 2010 dollars) of a property damage only (PDO) outcome is \$3,862, which is 0.0004223 times the value of a fatality: \$9,145,998. Hence, for the purpose of this model, the value of a PDO outcome can be assigned a relative disutility factor of 0.0004223. These relative disutility factors are provided for each injury severity level in TABLE 1.

Since vehicle occupancy may be greater than one, actual disutility from a single crash event may exceed the disutility associated with one fatality. Hence, a factor (ϕ) representing vehicle occupancy is applied and the disutility value (DV) for any given value of HIC₁₅ is computed by Equation 8.

This assumption of a single value multiplier for vehicle occupancy may be simplistic for two reasons. First, in analysis of treatment costs associated with injuries due to vehicle impacts into fixed objects Bambach et al (6) observe that mean injury costs for passengers were “*greater for w-beam and wire rope barriers*” compared to mean injury costs for drivers. Second, the assumption is that occupancy is independent of other input parameters, whereas it may be (for example) that larger (heavier) vehicles have higher occupancy than smaller (lighter) vehicles. This deserves further exploration.

TABLE 1 Relative Disutility Values by Injury Level

Injury Level	Severity	Relative Disutility Factor (RDF)	Source
PDO	PDO	0.0004223	Derived from Blincoe et al (40)
AIS 1	Minor	0.003	Trottenberg and Rivkin (39)
AIS 2	Moderate	0.047	
AIS 3	Serious	0.105	
AIS 4	Severe	0.266	
AIS 5	Critical	0.593	
AIS 6	Unsurvivable	1.000	

$$DV_{HIC_{15}} = \phi \times \sum_{j=1}^6 \{p(AIS = j_{HIC_{15}}) \times (RDF_{AIS\ j})\} + p(PDO) \times 0.0004223 \quad (8)$$

Nevertheless, since disutility value is measured in terms of the proportional cost of a fatality, EFCCR = DV. So, for example, adopting an average vehicle occupancy (ϕ) of 1.25 persons per vehicle (based on Queensland (41)), the ceiling on relative disutility would be 1.25. Substituting EFCCR for disutility value at Equation 8, EFCCR as a function of HIC_{15} can be computed. Figure 3 shows computed EFCCR plotted against HIC_{15} by this method.

COMPUTING OCCUPANT INJURY DISUTILITY

Predicting barrier impact conditions

Roadway departure conditions are studied variously. Mak et al (42) report roadway departure conditions associated with serious ran-off road crashes, finding that roadway departure speeds are normally distributed, while roadway departure angle can be modeled using a gamma distribution fit to the square root of departure angle, and that departure angle and departure speed can be considered to be independent.

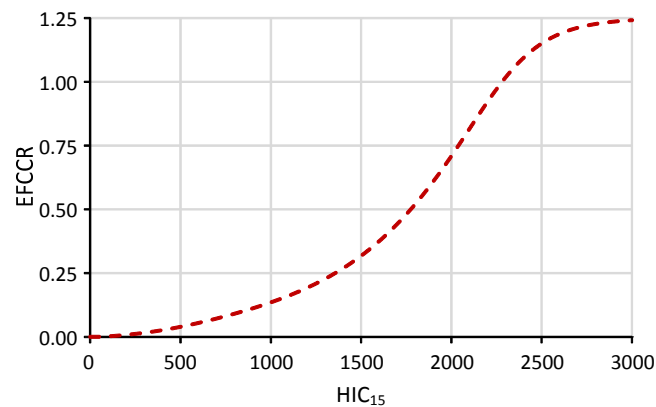


FIGURE 3 EFCCR v HIC_{15} . Note that an EFCCR value of 1.25 is a ceiling value based on an assumed vehicle occupancy of 1.25 [based on values for Queensland (41)].

Assuming that a road safety barrier exists at the point of roadway departure, lateral Impact Severity as a function of vehicle mass, speed and angle may be calculated (Equation 2), and assuming that mass and speed and angle are independent, the probability of that impact condition is given by Equation 9. Risk measured in terms of Impact Severity is the product of likelihood and consequence, and is the product of Equations 2 and 9 (Equation 10).

$$p(IS_{m,v,\theta}) = p(m) \times p(v) \times p(\theta) \quad (9)$$

$$Risk = p(IS_{m,v,\theta}) \times (IS_{m,v,\theta}) \quad (10)$$

The point-mass model may be used to calculate the maximum departure/impact angle that can be attained for any given vehicle speed for any cross-sectional geometry (lane configuration and shoulder width) and tyre-pavement friction (43). Maximum departure/impact angle is given by the expression in Equation 11 (adapted from (44)).

$$\theta_{max} = \arccos\left(1 - \frac{\mu g s}{v^2}\right) \quad (11)$$

where

- θ_{max} = limiting roadway departure angle (degrees)
- μ = coefficient of tyre-pavement friction
- g = gravitational constant g (ms^{-2})
- s = distance from vehicle centreline to road safety barrier (m)
- v = vehicle speed (ms^{-1})

The point-mass model can be used to “cap” departure conditions by eliminating those combinations of conditions that are unrealistic. For any combination of cross-section geometry (lane configuration), shoulder width and tyre-pavement friction, the combined probability distribution of speed and angle is truncated and then normalized so that the area under the combined probability surface has an aggregate value equal to unity.

Adoption of Equation 11 to implement a capped impact angle model excludes the possibility of a “double yaw” in which a vehicle departs initially to one side before recovering to leave the road on the opposite side (see Doecke and Woolley (21)). Equation 11 also assumes that the coefficient of friction is constant and by implication that the shoulder has the same friction as the trafficked pavement. As barrier is usually situated close to the trafficked pavement, this is not considered to be a significant issue.

Establishing Light Vehicle Mass-Frequency Distribution

Burbridge and Troutbeck (45) present an argument that vehicle registrations or sales are not necessarily representative of vehicle usage. Some vehicles or vehicle types may be used more or less frequently than others, and the prevalence of some vehicle variants or types may vary across a road network. As such, using registrations (or sales) may not represent true exposure. Further, in terms of barrier performance, the effective inertial mass of an impacting vehicle is almost certainly higher than the recorded tare mass. In-service vehicle payload, including restrained occupants,

cargo, fuel and fluids, and any after-sale modifications (e.g., bull bars, roof racks, toolboxes) may represent a significant additional contribution to the inertial mass during a barrier impact. A more realistic measure might be obtained from site-specific weigh-in-motion (WIM) data, as indicated by Burbidge and Troutbeck (22).

Calculating EFCCR

For a given barrier stiffness, relative occupant injury disutility in terms of EFCCR associated with any combination of vehicle mass, departure speed and departure angle is calculated by substituting the disutility value calculated in accordance with Equation 8 for the $IS_{m,v,\theta}$ term in Equation 10 for any combination of mass, speed and angle (see Equation 12).

$$EFCCR_{m,v,\theta} = p(IS_{m,v,\theta}) \times DV_{HIC_{15}(m,v,\theta)} \quad (12)$$

Total severity (also measured in terms of EFCCR) is then aggregated across all combinations of mass, speed and angle using the expression in Equation 13.

$$EFCCR = \sum_{m_{min}}^{m_{max}} \sum_{v=0}^{v_{max}} \sum_{\theta=0}^{\theta_{max}} EFCCR_{m,v,\theta} \quad (13)$$

1

DISCUSSION

The basis of the procedure is that the occupant risk indicator ASI as measured during crash testing can be predicted for any crash event and that occupant injury outcomes and hence economic disutility can be derived via the proxy of the head impact criterion (HIC). Some acknowledged limitations are introduced here.

Firstly, the model is incomplete in the sense that while ASI is hypothesized to be a function of impacting vehicle mass, speed and angle and barrier stiffness, the relationship is not solved.

Then, the ASI function (at Equation 3) assumes that all vehicles are equal, and does not allow for differential stiffness between vehicles. Further, given the same ASI, a vehicle with a higher safety rating might be expected to provide better occupant protection (e.g., airbags) than a vehicle with a lower safety rating. The point here is that the transformation from ASI to AIS is not likely to be identical for all vehicles.

Further points deserving attention are that road departure conditions may not be independent of mass, and that because full-scale crash test impacts (which are the basis of the model) are tracking frontal impacts, the model may not have immediate application to non-tracking or side impacts.

In terms of the translation of ASI to injury, the model is premised on occupant head injury being an indicator of whole of body injury. Viano and Arepally (46) suggest a weighted injury risk assessment for head, chest and femurs in the ratios 60:35:5. Schmitt et al (37) summarise the US Federal Motor Vehicle Safety Standards thresholds for head, neck, thorax and femur in frontal impacts and for head, thorax abdomen and pelvis in side-impacts. Eppinger et al (47) describe the frontal-impact combined thoracic index (CTI) as a combination of chest accelerations and chest deflections, and include injury probability curves for CTI values for strata on the Abbreviated

Injury Scale from AIS \geq 2 to AIS \geq 5. While Li et al (33) have made efforts to correlate maximum chest compression (MCC) with ASI (albeit with some reservation) a mechanism to translate vehicular accelerations to CTI is unknown. In this regard, the model would likely benefit from research undertaken in the field of Advanced Automatic Collision Notification (AACN), for example by Maika et al (48), wherein head injury is not the only injury considered.

This all deserves further exploration in any future development of the model. Nonetheless, in its current form, as a basis for a structural modeling approach to calculating light vehicle occupant injury disutility, the model might be adequate to explain variation in empirically determined values for barrier aggressiveness in tracking impacts.

Figure 4 shows for example EFCCR₆₅ (as described by Ray et al (17)) plotted against “flexibility” (the reciprocal of stiffness) for a selection of generic barrier types. Values of EFCCR₆₅ are taken from (17), while “flexibility” is approximated from Figure 1a. In summary, the range of injury outcomes is expected to be much broader for rigid barrier than for more flexible barriers, while greater lateral offset permits higher combinations of impact speed and angle, the consequences of which appear to be exacerbated by barrier stiffness. This is expected to explain the ranges of EFCCR₆₅ values presented in Figure 4.

It is suggested that re-analysis of the contributing empirical data would be useful to inform the model.

It is proposed that immediate further work required is as follows:

1. Solve Equation 2 so that ASI can be computed as a function of vehicle mass, impact speed, impact angle and barrier flexibility.
2. Investigate a functional relationship between ASI and AIS for all injury levels, whether via the proxy of HIC or not.

CONCLUSION

The aim of this study was to explore through review of existing knowledge the feasibility of developing a conceptual numerical procedure (in the form of a probabilistic causal model) that may be used to predict occupant injury disutility arising from light passenger vehicle impacts with road safety barriers.

The framework for such a model has been developed and presented. The key to the model is the link between barrier stiffness and likelihood of impact configuration and injury outcomes. The use of Head Impact Criterion (HIC) as an interim proxy to link ASI and AIS has been considered and shows promise, but linkages via proxies of other injury metrics would lead to a more complete model.

The work indicates that disutility in terms of the Equivalent Fatal Crash Cost Ratio may be predictable if the range of crash configurations are known.

It is concluded that a structural modeling approach is feasible. Calibration of such a model would require reporting of the impacted barrier in terms of the factors that are expected to influence system stiffness as well as the configuration of impact (vehicle mass, impact speed and angle) and the geometric circumstances (cross-section, number of lanes, lateral offset). Other variables expected to contribute to occupant injury outcomes such as vehicle age and safety rating, and number of occupants should also be collected.

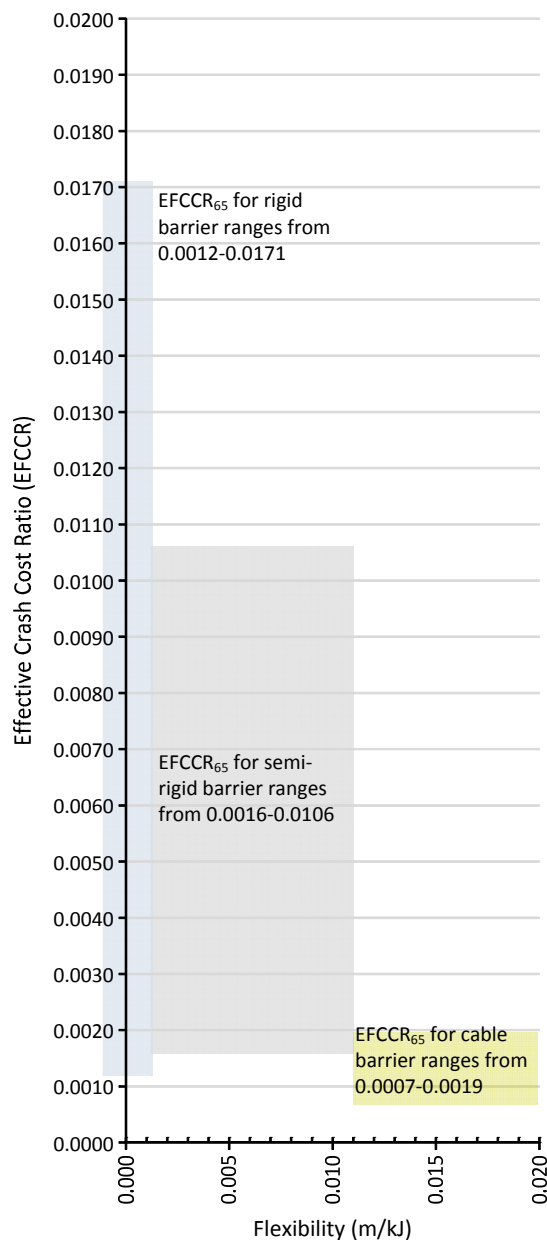


FIGURE 4 EFCCR ranges [from Ray et al (17)] for different generic barrier types. Note how the range of values diminishes with increasing barrier flexibility. This invites exploration/explanation.

REFERENCES

1. Austroads, Guide to Road Design, Part 6: Roadside Design, Safety and Barriers, 2009, Austroads: Sydney, NSW, Australia.
2. Standards Australia, AS/NZS 3845.1-2015 Road safety barrier systems, 2015, Standards Australia; Standards New Zealand: Strathfield, New South Wales, Australia; Wellington, New Zealand.

3. Nilsson, K. and N. Prior. Wire rope safety barriers and the Pacific Highway program: RTA research and investigations. Road Safety Research, Policing And Education Conference. 2004. Perth, WA, Australia.
4. Jurewicz, C., L. Steinmetz, C. Phillips, P. Cairney, G. Veith, and J. McLean. *Improving Roadside Safety: Summary Report*. Austroads, Sydney, NSW, 2014.
5. Jurewicz, C., L. Steinmetz, and B. Turner. *Australian National Risk Assessment Model*. Austroads, Sydney, NSW, 2014.
6. Bambach, M. R., R. J. Mitchell, and G. A. Mattos. Mean Injury Costs of Run-Off-Road Collisions with Fixed Objects: Passenger Vehicles and Motorcycles. *Journal of Transportation Safety & Security*, Vol. 7, No. 3, 2015, pp. 228–242. <https://doi.org/10.1080/19439962.2014.947395>.
7. Beaton, J. L., and R. N. Field. *Dynamic Full Scale Tests of Median Barriers*. State of California Department of Public Works, California, USA, 1959.
8. Holdridge, J. M., V. N. Shankar, and G. F. Ulfarsson. The crash severity impacts of fixed roadside objects. *Journal of Safety Research*, Vol. 36, No. 2, 2005, pp. 139–147. <https://doi.org/10.1016/j.jsr.2004.12.005>.
9. Hu, W., and E. T. Donnell. Median barrier crash severity: Some new insights. *Accident; Analysis and Prevention*, Vol. 42, No. 6, 2010, pp. 1697–1704. <https://doi.org/10.1016/j.aap.2010.04.009>.
10. Chitturi, M. V., A. W. Ooms, A. R. Bill, and D. A. Noyce. Injury outcomes and costs for cross-median and median barrier crashes. *Journal of Safety Research*, Vol. 42, No. 2, 2011, pp. 87–92. <https://doi.org/10.1016/j.jsr.2011.01.006>.
11. Zou, Y., A.P. Tarko, E. Chen, and M.A. Romero, Effectiveness of cable barriers, guardrails, and concrete barrier walls in reducing the risk of injury. *Accident Analysis and Prevention*, 2014. 72(-): p. 55-65. <https://doi.org/10.1016/j.aap.2014.06.013>.
12. Karim, H., R. Magnusson, and M. Wiklund, Assessment of Injury Rates Associated with Road Barrier Collision. *Procedia - Social and Behavioral Sciences*, 2012. 48(-): p. 52-63. <https://doi.org/10.1016/j.sbspro.2012.06.987>.
13. Michie, J. D., L. R. Calcote, and M. E. Bronstad. *NCHRP Report 115: Guardrail Performance and Design*, 1971.
14. Ray, M. H., and J. A. Weir. Unreported Collisions with Post-and-Beam Guardrails in Connecticut, Iowa, and North Carolina. *Transportation Research Record: Journal of the Transportation Research Board*, No. 1743, 2001, pp. 111–119.
15. Martin, J.-L., C. Mintsa-Eya, and C. Goubel, Long-term analysis of the impact of longitudinal barriers on motorway safety. *Accident Analysis and Prevention*, 2013. 59(-): p. 443-451. <https://doi.org/10.1016/j.aap.2013.06.024>.
16. Soltani, M., T. B. Moghaddam, M. R. Karim, and N. R. Sulong. The safety performance of guardrail systems: Review and analysis of crash tests data. *International Journal of Crashworthiness*, Vol. 18, No. 5, 2013, pp. 530–543. <https://doi.org/10.1080/13588265.2013.815020>.
17. Ray, M.H., C.E. Carrigan, C.A. Plaxico, S.-P. Miaou, and T.O. Johnson, NCHRP 22-27 Roadside Safety Analysis Program (RSAP) Update, 2012, RoadSafe LLC: Maine, USA.
18. Bronstad, M. E., J. D. Michie, and J. D. Mayer. *NCHRP Report 289: Performance of Longitudinal Traffic Barriers*, 1987.
19. Ydenius, A., A. Kullgren, and C. Tingvall. Development of a crashworthy system: interaction between car structural integrity, restraint systems and guardrails. 17th International Technical Conference on the Enhanced Safety of Vehicles. 2001. Amsterdam, Netherlands.

20. Sicking, D., and H. Ross Jr. Benefit–Cost Analysis of Roadside Safety Alternatives. *Transportation Research Record*, No. 1065, 1986, pp. 98–105.
21. Doecke, S. and J.E. Woolley. Further investigation into the effective use of clear zones and barriers in a safe system’s context on rural roads. Australasian Road Safety Research, Policing and Education Conference. 2011. Perth, WA, Australia.
22. Burbridge, A. and R. Troutbeck. Using weigh-in-motion data to predict the likelihood of exceeding the capacity of a road safety barrier. In 17th International Conference Road Safety On Five Continents (RS5C 2016). 2016. Rio de Janeiro, Brazil: VTI, Linköping, Sweden.
23. Burbridge, A. and R. Troutbeck. Decompartmentalising road safety barrier stiffness in the context of vehicle occupant risk. Australasian Road Safety Conference. 2016. Canberra, ACT, Australia.
24. Bonneson, J., and J. Ivan. *Transportation Research Circular E-C179: Theory, Explanation, and Prediction in Road Safety: Promising Directions*, 2013.
25. Gabauer, D., and H. C. Gabler. Evaluation of the Acceleration Severity Index Threshold Values Utilizing Event Data Recorder Technology. *Transportation Research Record: Journal of the Transportation Research Board*, No. 1904, 2005, pp. 37–45.
26. Ross, H. E., D. L. Sicking, R. A. Zimmer, and J. D. Michie. *NCHRP Report 350: Recommended Procedures for the Safety Performance Evaluation of Highway Features*, 1993.
27. Anghileri, M., M. Luminari, and G. Williams, ROBUST - Road Barrier Upgrade of Standards - Deliverable D.2.1. Analysis of test data from European laboratories, 2005: Milan, Italy.
28. Naing, C. L., J. Hill, R. Thomson, H. Fagerlind, M. Kelkka, C. Klootwijk, G. Dupre, and O. Bisson. Single-vehicle collisions in Europe: Analysis using real-world and crash-test data. *International Journal of Crashworthiness*, Vol. 13, No. 2, 2008, pp. 219–229.
<https://doi.org/10.1080/13588260701788583>.
29. Klootwijk, C.W. and R.H. Hoogvelt. Sensitivity of car with guardrail impacts with a multibody simulation tool. In 2nd International Conference on ESAR, Expert Symposium on Accident Research. 2012. Bergisch Gladbach, Germany: Wirtschaftsverlag NW.
30. Sturt, R., and C. Fell. The relationship of injury risk to accident severity in impacts with roadside barriers. *International Journal of Crashworthiness*, Vol. 14, No. 2, 2009, pp. 165–172.
<https://doi.org/10.1080/13588260802614365>.
31. Roque, C. and J.L. Cardoso, Investigating the relationship between run-off-the-road crash frequency and traffic flow through different functional forms. *Accident Analysis and Prevention*, 2014. 63(-): p. 121-132.
32. Hammonds, B.R. and R.J. Troutbeck. Crash test outcomes for three generic barrier types. 25th ARRB Conference – Shaping the future: linking research, policy and outcomes. 2012. Perth, WA, Australia.
33. Li, N., H. Fang, C. Zhang, M. Gutowski, E. Palta, and Q. Wang, A numerical study of occupant responses and injuries in vehicular crashes into roadside barriers based on finite element simulations. *Advances in Engineering Software*, 2015. 90(-): p. 22-40.
<https://doi.org/10.1016/j.advengsoft.2015.06.004>.
34. Shojaati, M. Correlation between injury risk and impact severity index ASI. 3rd Swiss Transport Research Conference. 2003. Monte Verità, Ascona, Switzerland.
35. Newman, J.A. Head injury criteria in automotive crash testing. In Stapp Car Crash Conference (24th). 1980. Troy, Michigan, USA: Society of Automotive Engineers, Warrendale, Pennsylvania, USA.
<https://doi.org/10.4271/801317>.

36. Brell, E. *Simplified Models of Vehicle Impact for Injury Mitigation*. Queensland University of Technology, Brisbane, Queensland, 2005.
37. Schmitt, K.-U., P. F. Niederer, D. S. Cronin, M. H. Muser, and F. Walz. *Trauma Biomechanics: An introduction to Injury Biomechanics*, 4th ed. Springer-Verlag, Berlin, Germany, 2014. <https://doi.org/10.1007/978-3-642-53920-6>.
38. US Department of Transportation National Highway Traffic Safety Administration, Actions to Reduce the Adverse Effects of Air Bags FMVSS No. 208, 1997: Washington, DC, USA.
39. Trottenberg, P., and R. S. Rivkin. *Guidance on Treatment of the Economic Value of a Statistical Life in U.S. Department of Transportation Analyses*. Washington, DC, 2013.
40. Blincoe, L., T. R. Miller, E. Zaloshnja, and B. A. Lawrence. *The economic and societal impact of motor vehicle crashes, 2010*. Revised, Washington, DC, 2015.
41. Transport and Infrastructure Council, National Guidelines for Transport System Management in Australia: Road Parameter Values (PV2), 2015, Commonwealth of Australia: Canberra, ACT, Australia.
42. Mak, K. K., D. L. Sicking, F. D. B. Albuquerque, and B. A. Coon. *NCHRP Report 665: Identification of Vehicular Impact Conditions Associated with Serious Ran-off-Road Crashes*, 2010.
43. Mak, K. and R. Bligh. Assessment of NCHRP Report 350 Test Conditions. *Transportation Research Record: Journal of the Transportation Research Board*, No. 1797, 2002, pp. 38–43.
44. Mak, K. K., and D. L. Sicking. *NCHRP Report 492 - Roadside Safety Analysis Program (RSAP)*. Engineer's Manual, Washington, DC, 2003.
45. Burbridge, A. and R. Troutbeck. A study of the mass-frequency distribution of the registered light vehicle fleet in Queensland. Australasian Road Safety Conference. 2016. Canberra, ACT, Australia.
46. Viano, D.C. and S. Arepally, Assessing the safety performance of occupant restraint systems. SAE Technical Paper 902328, 1990. <https://doi.org/10.4271/902328>.
47. Eppinger, R., E. Sun, F. Bandak, M. Haffner, N. Khaewpong, M. Maltese, S. Kuppa, T. Nguyen, E. Takhoumts, et al. *Development of Improved Injury Criteria for the Assessment of Advanced Automotive Restraint Systems - II*. National Highway Traffic Safety Administration, Washington, DC, 1999.
48. Maika, K., M. Yusuke, P. Jonas, and U. Sadayuki. Development of occupant injury prediction algorithms for advanced automatic collision notification by numerical crash reconstructions. In 23rd International Technical Conference on the Enhanced Safety of Vehicles. 2013. Seoul, Korea.

Modeling and Simulation of Vehicle Crashes on Curved, Superelevated Road Sections

DHAHER MARZOUGUI
CING-DAO (STEVE) KAN
STEFANO DOLCI
George Mason University

ALBERTO MORENA
Polytechnic University of Milan

KENNETH S. OPIELA
Transportation Consultant

Road curvature and surface slope are known to affect vehicle dynamics and influence trajectories. On curved roadway sections, this may mean that a vehicle leaves the road at a sharper angle, impacts the barrier at a less than ideal orientation, and/or be more prone to rollover. Consequently, impacts with roadside barriers are likely to involve different distributions and magnitudes of forces on the barrier as well as the vehicle and its occupants. The objective of this effort was to use modeling and simulation to analyze the safety performance of barriers when impacted by vehicles leaving the traveled way on curved, superelevated roadway sections. The intent was to develop a better understanding of the influence of roadway curvature, superelevation, and shoulder or roadside designs on vehicle trajectories leading to impacts with barriers to evaluate barrier designs and placement practices in these situations. The analyses considered two types of vehicles, six roadway curvature and superelevations conditions, and varying shoulder configurations. Simulations were conducted for three common types of longitudinal barriers and two barrier orientation options. This paper presents some of the simulation results that were performed for some of the situations analyzed relative to MASH requirements for large and small vehicles. Simulations efforts have been completed, but efforts continue to develop recommendations for improved design, selection, and placement of barriers on curved, superelevated roadway sections.

INTRODUCTION

Highways are comprised of tangent and curved roadway sections for which there are well established design criteria. Curved roadway sections on higher speed roads are generally constructed with superelevation to compensate for the centripetal forces exerted on the vehicles and to make it easier for the driver to control the vehicle through the curved section. There are well-developed guidelines for the design of curved superelevated roadway sections (CSRS) embodied in the AASHTO Policy for the Geometric Design of Highways (i.e., the Green Book) [1]. The same cannot be said for the design and installation of barriers for such sections of the road network. It is known that crashes occur proportionately more often on curves than tangent sections, but it is not clear whether (1) curvature and superelevation affect the likelihood of crashes, or (2) the effectiveness of various barriers and their placement on safety. Barriers are

often deployed on curved, superelevated roadway sections (CSRS) as a continuation of barriers on adjacent sections and/or to address situations created by the superelevated curve (i.e., the embankment needed to provide the superelevation slope). Guidance for the testing and deployment of barriers on CSRS is limited at best. The need exists for a better understanding of (1) the behavior of vehicles that as they leave the roadway in such situations, and (2) vehicle behavior influences the performance requirements for barriers in proximity to the CSRS.

Background

Road curvature and surface slope are known to affect vehicle dynamics and influence vehicle trajectories, orientation, and speed. On a CSRS, the vehicle is more likely to leave the road at a sharper angle, have an orientation that will not provide an ideal interface with a barrier, and surface effects may increase the propensity for rollovers. These can result in barrier impacts with greater forces that could result in a higher occupant risks and crash severity. The CSRS factors could lead to a less-than-ideal interface with the barrier which can increase vehicle instability, barrier climb, vehicle roll-over, or override. These are important concerns to efforts to enhance roadside safety, but here has been little past effort to analyze them. The underlying objective of this research was to determine if longitudinal barriers deployed on CSRS provide adequate safety and determine if improve practices were needed.

In initial stages of this research, vehicle dynamics analysis was employed to analyze the vehicle-to-barrier interface for various CSRS conditions. Vehicle dynamics analysis (VDA) has recently been used to provide new insights on the effects of a vehicle's suspension system on trajectories [2,3,4]. Trajectory data allows the interface of the vehicle with the barrier for various CSRS conditions to be analyzed. The combined effect of the superelevation of the roadway, the slope of the shoulder, and the side slope of the roadside for a vehicle leaving the roadway in a curve were used to explicitly analyzed using VDA tools to analyze barrier interface performance.

Guidelines for the testing and deployment of roadside safety barriers on sloped surfaces and curved sections has been limited. A review of the literature revealed only a few older efforts to address the safety of barriers on slopes or curves. Crash testing protocols for barriers have evolved to provide a "practical worst case" impact condition that is reproducible and comparable. Thus, barriers are typically tested under idealized impact conditions with the test barrier installed on a straight section having level approach terrain and the impacting vehicle is freewheeling with minimum roll and pitch effects. These protocols have evolved to provide important assessments that allow determination of whether safety hardware is "crashworthy." While crash testing protocols have evolved to include tests for a variety of angular impact conditions, one aspect that has not been addressed is the crashworthiness of barriers installed on CSRS. Consequently, the need exists to evaluate the performance of longitudinal barriers deployed along CSRS roadway sections to develop effective barrier designs and appropriate placement guidelines for such locations.

Advances in simulation technology, computer processing capabilities, the availability of detailed FE models, and increased success in using simulations to address safety questions led to the conclusion that it offered a viable means to assess impact performance under CSRS conditions.

Objective

The objective of this paper is to describe efforts to simulate the performance of longitudinal barriers when impacted by vehicles leaving the traveled way on curved, superelevated roadway sections. The intent was to develop a better understanding of the influence of various roadway curvatures, superelevation, and shoulder/roadside designs on the safety effectiveness of common longitudinal barriers used in these situations. This effort was focused on impacts occurring on the high side of CSRS for a cross section of six varying radii and superelevation conditions.

RESEARCH APPROACH

In this analysis, simulations were performed to assess the impact performance of three types of longitudinal barriers when impacted by vehicles leaving the roadway for different roadway curvatures and superelevation and with varying shoulder configurations. Simulations were conducted to replicate MASH Tests for longitudinal barriers [6]. This section describes simulation approach and the cases selected for analyses and the parameters describing them.

Simulation Analysis

The simulation efforts began using the findings of a broad analysis of vehicle dynamics analyses that focused strictly on the effects of speed, surface features, and vehicle type on the trajectory and orientations of a vehicle for vehicles departing the traveled way on curved, superelevated roadway sections. While there can be an unlimited number of vehicle trajectories and paths, these efforts focused on two types of vehicles on roads at speeds of 60 mph. The focus of the efforts were departures leaving the roadway towards the high side of the superelevated section under the assumption that upward vehicle trajectory would be more likely to result in vaulting or underride if a barrier impact occurred. The vehicle's path considered the curvature and superelevation rates for six categories of curves defined in the AASHTO Green Book. Varying shoulder widths and slopes were analyzed for each category. Three common barriers were analyzed assuming they were placed immediately adjacent to the outer edge of the shoulder.

The FE simulations were undertaken to investigate the performance (i.e., physics) of impacts with the barriers for varying curvature, superelevation, and shoulder configurations. The simulation analyses focused on the impact conditions prescribed in the Manual for Assessing Safety Hardware (MASH) as it represents to current standards for evaluation of barrier performance [5]. The number of runs varies for each barrier to focus on situations where performance issues were indicated by the VDA or other simulations suggested failing or marginal performance.

The intent of the research and these simulation studies was to answer or provide insights on a number of fundamental questions about barrier performance on CSRS. These include:

- Do barriers deployed on CSRS perform the same as barriers on tangent sections?
- What is the effect of curvature and superelevation on barrier performance?
- What is the effect of shoulder width and slope on barrier performance for various curvature and superelevation conditions?
- Are all barriers equally effective in deployments on CSRS?
- Is performance different by vehicle type?

- Does barrier orientation influence the performance on CSRS?

While certainly other questions may exist and there are details of performance that could be investigated in greater depth, the above were the primary topics. The focus was the efficacy of current practices, but where barrier performance is found to be inadequate, options to improve the barrier to meet requirements were considered.

In this research, several different possible conditions for road departures were considered. The following assumptions were made:

- Errant vehicles traversed a paved (firm) surface prior to impact.
- Vehicles are “tracking” as they reach the roadside (i.e. vehicle is moving in same direction as its longitudinal axis).
- Vehicle velocity was adjusted to reflect the effect of climbing the slope in the simulation.
- There are no driver inputs (e.g., steering, braking) that affect the vehicle trajectory.
- The road friction was identical in all runs using a friction coefficient of 0.9.
- There is a smooth transition between the pavement and shoulder and shoulder.

Other conditions related to these assumptions could be modeled, but were not at this stage.

Vehicle and Barrier Models

The simulations were conducted using vehicle FE models developed by the CCSA staff (under FHWA contracts) that meet the MASH Test Vehicle requirements. Detailed versions of these models were used to increase the accuracy of the results. These models have been extensively verified and validated as reported elsewhere [6,7,8,9,10]. They have proven stable in many simulation efforts by the staff and others. The details of these models are summarized in Table 1.

FE models of the types of barriers being studied were also modeled. Based on the state DOT survey and discussions with the Project Panel, three longitudinal roadside barriers were identified as candidates for this study to include the New Jersey concrete barrier (NJB), G41S w-beam guardrail, and Midwest Guardrail System (MGS). Brief descriptions of the models developed are summarized in Table 2. These FE models were adapted from models of these longitudinal barriers used in previous research. These barriers were modeled as a system the minimum test lengths and functional configurations. The model of the guardrail system has a total length of 53.3 m (175 ft) and it is anchored at both ends using a standard Breakaway Cable Terminal (BCT). The system consisted of 29 posts and 14 w-beam sections. The NJ barrier was modeled for a length of about 200 feet also. Vertical orientation of the barrier was either true vertical or perpendicular to the road surface.

Analysis Conditions:

The findings of the background research efforts, dialogue with the Project Panel, and VDA efforts suggested that the safety performance of longitudinal barriers when placed on curved, superelevated roadway sections is influenced by curvature, superelevation, shoulder features, side slopes, and barrier placement. A range of curved, superelevated roadway sections are

TABLE 1 Vehicle FE Models Representing MASH Test Vehicles



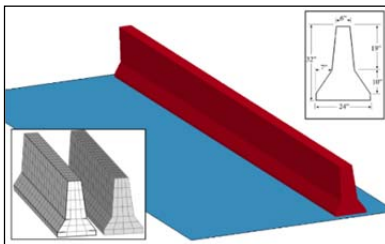
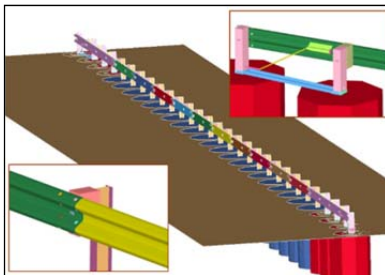
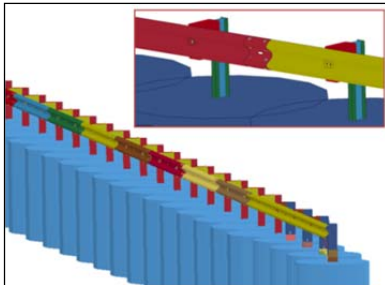
Description	Vehicle Image
2010 Toyota Yaris (1100C) Weight – 1,100 kg (2,420 lbs) CG 1004 mm rear, 569 mm high Model Parameters: Parts-771, Nodes- 998,218, Elements-974,348 Features: FD, CD, SD, IM Validations: FF, OF, MDB, SI, IP, SP, SC, ST, OT	
2007 Chevrolet Silverado Pick-up Truck (2270P) Weight – 2,270 kg (5,000 lb) CG 736mm (28.8 inches) Model Parameters: Parts-606, Nodes-261,892, Elements-251,241 Features: FD, CD, SD, IM Validations: FF, IP, SP, SC, ST, OT	

Table 2 FE Models Representing Typical Longitudinal Barriers Used on CSRS

Barrier Types & Features:	Model Images:
New Jersey Barrier: Top Height: 32 in [813 mm] Connections: Continuous	
G41S W-Beam Guardrail: Top Height: 27.75 inches [730 mm] Rail: Std 12-gauge W-beams Rail Length: 3.807 m (12.5 ft) Post: W150x12.6 (W6x9) steel posts Post Length: 1830 mm (72 in) Blockouts: 150 mm x 200 mm x 360 mm (6 in x 8 in x 14 in). Connections: Splices at posts	
MGS W-Beam Barrier: Top Height: 31 in [787 mm] Rail: Std 12-gauge W-beams Rail Length: 3.807m (12.5 ft) Post: W150x12.6 (W6x9) steel posts Post Length: 1830mm (72 in) Blockouts: 150 mm x 200 mm x 360 mm (6 in x 8 in x 14 in). Connections: Splices between posts.	

commonly found on the highway. These range from tight curves used on ramps to gentle sweeping curves. A total of six roadway curve conditions with different curvatures and superelevations were selected for this study based on the Green Book design superelevation tables. The analyses incorporated three superelevation rates (6, 8, and 12%). For each superelevation, two curvatures were selected representing the minimum radii at the 50 mph (80 km/hr) and 80 mph (130 km/hr) design speeds. These curvature/superelevation conditions were:

- 12% Superelevation – Radii 614 ft (187 m) and 2130 ft (649 m)
- 8% Superelevation – Radii 758 ft (231 m) and 2670 ft (814 m)
- 6% Superelevation – Radii 833 ft (254 m) and 3050 ft (930 m)

Variations in shoulder width and slope are also common, so the cases analyzed included three shoulder width: 4 ft (1.22 m), 8 ft (2.44 m), and 12 ft (3.66 m) widths and four shoulder angles: 0%, 3%, 6% and 8% (see Figure 1).

Impact Evaluations

The performance of the longitudinal barriers in the crash simulations were evaluated in accordance with the criteria presented in MASH. The barrier performance was evaluated based on three factors: structural adequacy, occupant risk, and post-impact vehicle trajectory for prescribed sets of impacts with vehicles of specific features. The simulations replicated MASH Test 3-10 for the small car (1100 kg test vehicle) and MASH Test 3-11 for the pick-up truck (2270 kg test vehicle) with impacts at 25 degrees and 100 km/hr (62 mph). The fundamental criterion for crashworthiness from these tests are noted in Table 3. These are intended to demonstrate that there is adequate structural integrity of the barrier, risks to occupants are

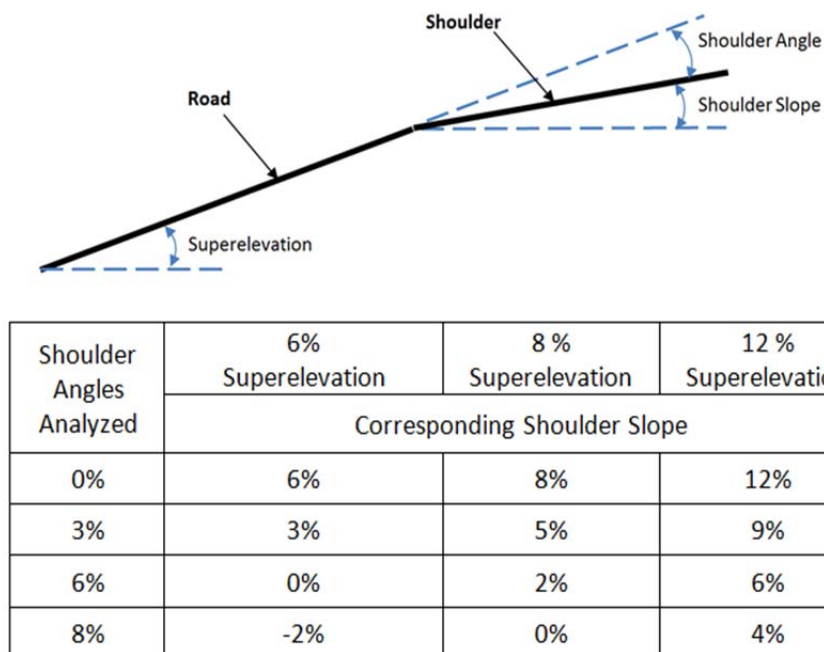


FIGURE 1 Shoulder slope conditions relative to the roadway surface analyzed.

TABLE 3 MASH Crashworthiness Evaluation Criteria for Simulation Analyses

Structural Adequacy	A - Test article should contain and redirect the vehicle; the vehicle should not penetrate, under-ride, or override the installation although controlled lateral deflection of the test article is acceptable.
Occupant Risk	D - Detached elements, fragments or other debris from the test article should not penetrate or show potential for penetrating the occupant compartment, or present an undue hazard to other traffic, pedestrians or personnel in a work
	F - The vehicle should remain upright during and after the collision although moderate roll, pitching and yawing are acceptable.
	H - The occupant impact velocity in the longitudinal direction should not exceed 40 ft/sec and the occupant ride-down acceleration in the longitudinal direction should not exceed 20 G's.
	I - Longitudinal & lateral occupant ridedown accelerations (ORA) should fall below the preferred value of 15.0 g, or at least below the maximum allowed value of 20.49 g.
Vehicle Trajectory	For redirective devices the vehicle shall exit within the prescribed box.

acceptable, and post-impact vehicle trajectories are acceptable. The primary difference reflected in the simulations is that the barrier is deployed on one of the CSRS configurations defined above and not on a tangent level surface as specified.

SIMULATION ANALYSIS RESULTS

Over 200 simulations were conducted in this research. Each of these took between 20 and 40 hours of CPU time to allow detailed analyses of crash events involving typical barriers on CSRS with varying features. Table 4 shows the distribution of the simulations conducted. Each simulation has been assigned a case number to facilitate discussions about specific runs and conveniently outline useful analyses and comparisons.

The number of runs in each cell is unequal for various reasons. A main reason was that when the VDA results indicated that there was a "poor interface" (when the simulation shows that the vehicle would impact the barrier at a significantly higher or lower level than it would when the barrier is placed on a flat surface), the need for FE simulations was less critical.

TABLE 4 Summary of Simulation Runs

Vehicle	New Jersey Barrier	G41S W-Beam Barrier		MGS Barrier
		27.75" Height	29" Height	
Small Car (1100C)	36 Runs (101-175) ^a	0 Runs	0 Runs	22 Runs (601-652) ^a
Pick-up (2270P)	50 runs (201-274) ^a	45 Runs (901-963) ^a	50 Runs (801-876) ^a	0 Runs

^a Case Numbers (000-000)

Since it was infeasible to simulate every CSRS condition under consideration given the amount of computing time that would be required, a reasoned selection process was followed. Selections were made considering:

- **New Jersey Barrier** – This classic, widely used concrete safety-shape barrier was a starting point since the sloping sides of the barrier profile have been attributed to vehicle vaulting and rollovers. The VDA analyses indicated that there would be no underride or override interface issues for the 1100C or 2270P vehicles. The panel, however, indicated the concern that the two-stage slopes of the barrier had been seen to cause small vehicle rollovers so these were simulated. The simulations included both the small car and the pick-up truck.
- **G41S W-Beam Barrier** – This widely used barrier was first accepted after the adoption of NCHRP 350 and it has been widely deployed. Its original design has a height at 27.75 inches. The VDA analyses indicated that there could be interface issues for the larger vehicle but no issues with the small car. FE Simulations with the Silverado into the G41S resulted in vaulting of the barrier for most cases. The simulations were rerun with the FHWA recommended 29” height. There were fewer cases of vaulting for the G4(1S) with 29-inch height. There were no cases where underride was indicated a problem.
- **MGS Barrier** – This newer w-beam barrier was designed to accommodate vehicles with higher centers of gravity with a rail height of 31 inches. This barrier was accepted by the FHWA in 2005. The VDA analyses indicated that there could be underride interface issues for the small car, so the focus of the simulations was on the 1100C vehicle. Based on VDA results and FE simulations with the 29-in G41S barrier, no simulations were performed for the MGS with pick-up vehicle.

For each simulation run, a summary sheet similar to that shown in Figure 2 was generated. It provides a pictorial view of vehicle behavior for a the specific CSRS situation. It documents the CSRS conditions including radius, superelevation rate, shoulder width and slope, barrier orientation, and speed and angle of impact. The diagram depicts the time sequence of vehicle and barrier interaction in the crash event. Below the diagram is the MASH evaluation summary which shows the key metrics generated by the simulation and whether the results passed or failed the criteria are noted.

Comparative Analyses

The simulation results permitted considerations of the influences of curvature, road profile, barrier vertical orientation, impact angle, impact speed, and combinations of these factors on safety performance. The findings provided the basis for formulating barrier design, selection, and installation guidelines. Multiple metrics were generated in the analysis, but all are not documented here. The following sections describe the findings from types of analyses that were undertaken.

Influence of Barrier Orientation

Figure 3 depicts typical results for situations with the same radius, superelevation, and shoulder configurations for the New Jersey concrete barrier but different barrier orientations. The barriers are installed with Normal and Vertical orientations. The first and second panels provide the

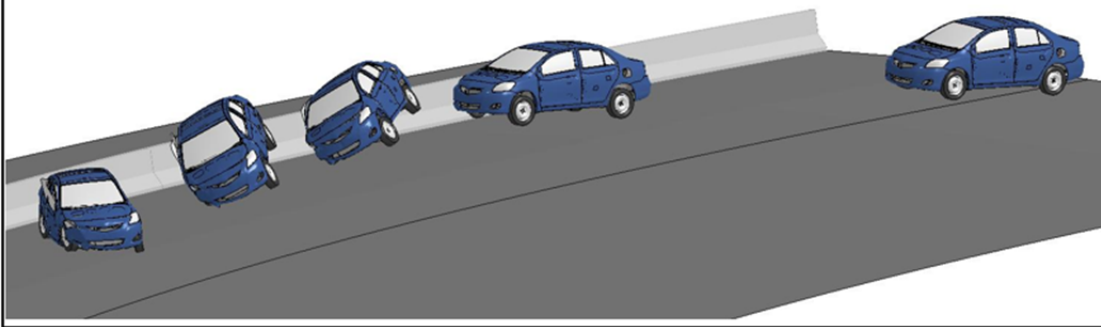
Toyota Yaris - New Jersey Concrete barrier						
Radius	Super	Shoulder Width	Shoulder Slope	Barrier Orient.	Speed	Angle
614 ft	12%	12 ft	6%	True Vertical	100 [kmh]	25 [deg]
						
Evaluation Criteria						
A	Test article should contain and redirect the vehicle; the vehicle should not penetrate, under-ride, or override the installation although controlled lateral deflection of the test article is acceptable.					Pass
D	Detached elements, fragments or other debris from the test article should not penetrate or show potential for penetrating the occupant compartment, or present an undue hazard to ...					Pass
F	The vehicle should remain upright during and after the collision. The maximum pitch & roll angles are not to exceed 75 degrees.			Max Roll (Deg)	35.11	Pass
				Max Pitch (Deg)	16.94	
H	Longitudinal & lateral occupant impact velocities (OIV) should fall below the preferred value of 30 ft/s (9.1 m/s), or at least below the maximum allowed value of 40 ft/s (12.2 m/s)			Vx (m/s)	-5.18	Pass
				Vy (m/s)	9.49	
I	Longitudinal & lateral occupant ridedown accelerations (ORA) should fall below the preferred value of 15.0 g, or at least below the maximum allowed value of 20.49 g			Ax (g)	-4.15	Pass
				Ay (g)	12.25	

FIGURE 2 Typical simulation analysis summary report.

MASH results and time sequence diagram for an 2270P vehicle impacting the barrier on a CSRS at 25 degrees and 100 km/hr for a tight curve with similar shoulder width conditions. It can be seen that the barrier impact event results in failure due to vehicle roll for the true vertical orientation case while the normal orientation case shows a pass. The MASH evaluation results reflect similar unacceptable degrees of maximum vehicle roll (91.77 deg, exceeding the MASH maximum 72 deg roll criterion) for the true-vertical orientation and acceptable (28.54 deg) roll angle for the normal orientation case. The values for Occupant Impact Velocity (OIV) and Occupant Ridedown Acceleration (ORA) in the longitudinal and lateral directions are similar for both vertical and normal orientation cases and are below the MASH maximum values. Similarly, panels 3 and 4 compare the impact event for the 2270P vehicle for the normal and vertical orientation with slight shoulder angle change. The results reflect similar patterns, but failures for the true-vertical orientation for both cases. These results suggest that, for these CSRS conditions with the NJ barrier, the normal orientation shows is better performance than the true-vertical. The true-vertical orientation also has a higher propensity for vehicle instability.

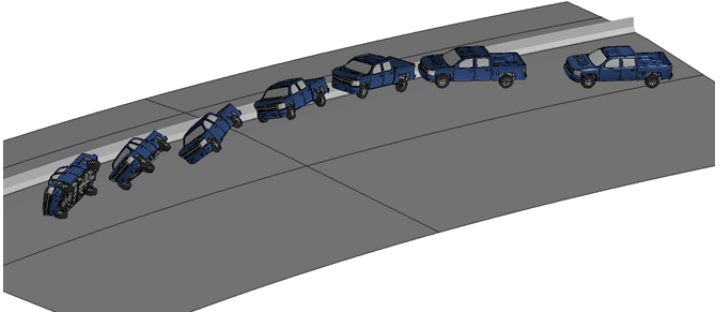
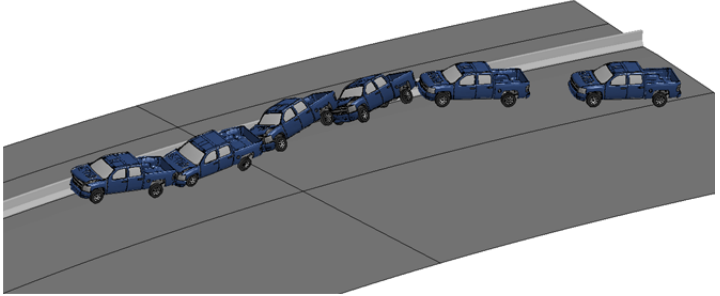
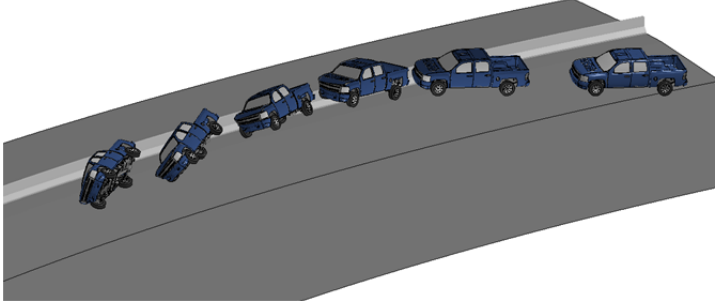
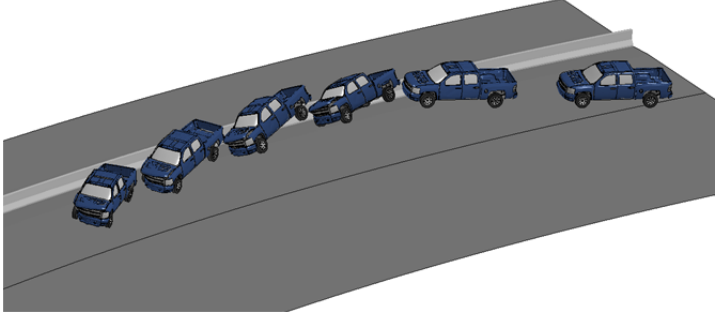
CSRS: Radius: 614 ft Superelevation: 12% Shoulder Width: 4 ft Shoulder Angle: 6% Barrier: New Jersey CSC Orientation: Normal or True Vertical Impact Speed & Angle: 100kmh/25°		
Parameters & Results	Case	Time Sequence View
CSRS: Radius 614, 12% super Vehicle: 2270P A – Containment (Pass) D – Detached Elements (Pass) F – Max Roll – 91.77 (Fail) Max Pitch – 61.09 (Fail) H – OIV – V _x - -4.67 (Pass) V _y – 7.61 (Pass) I – ORA – A _x –12.34 (Pass) A _y – 18.65 (Pass)	101 V	
CSRS: Radius 614, 12% super Vehicle: 2270P A – Containment (Pass) D – Detached Elements (Pass) F – Max Roll – 28.54 (Pass) Max Pitch – 23.38 (Pass) H – OIV – V _x - -5.29 (Pass) V _y – 8.15 (Pass) I – ORA – A _x –9.92 (Pass) A _y – 17.65 (Pass)	102 N	
CSRS: Radius: 614 ft Superelevation: 12% Shoulder Width: 4 ft Shoulder Angle: 8% Barrier: New Jersey CSC Orientation: Normal Impact Speed & Angle: 100kmh/25°		
CSRS: Radius 614, 12% super Vehicle: 2270P A – Containment (Pass) D – Detached Elements (Pass) F – Max Roll – 81.65 (Fail) Max Pitch – 55.67 (Fail) H – OIV – V _x - -4.73 (Pass) V _y – 7.65 (Pass) I – ORA – A _x - - 15.12 (Pass) A _y – -16.55 (Pass)	103 V	
CSRS: Radius 614, 12% super Vehicle: 2270P A – Containment (Pass) D – Detached Elements (Pass) F – Max Roll – 29.15 (Pass) Max Pitch – 26.25 (Pass) H – OIV – V _x - -5.47(Pass) V _y – 8.19 (Pass) I – ORA – A _x - -10.16 (Pass) A _y – 17.69 (Pass)	104 N	

FIGURE 3 Barrier orientation effects for similar CSRS conditions and vehicle size.

Influence of Curvature

Figure 4 depicts simulation results from two different radius conditions with similar shoulder configurations for the New Jersey barrier installed with a “Normal” orientation. The first and third panel provide the MASH results and time sequence diagram for an 1100C vehicle impacting the barrier on a CSRS at 25 degrees and 100 kmh. While there are some scaling differences in the diagrams, it can be seen that the barrier impact event results in similar performance for the 758 ft and 2670 ft curvatures. The MASH evaluation results also reflect similar degrees of maximum vehicle roll and pitch (e.g., roll 26.59 and 25.85 degrees and pitch 21.99 and 21.72 degrees). Similarly, the values for Occupant Impact Velocity (OIV) and Occupant Ridedown Acceleration (ORA) in the longitudinal and lateral directions are the same order of magnitude. Similarly, panels 2 and 4 compare the results for the 2270P vehicle. The results reflect comparable degrees of maximum vehicle roll and pitch (e.g., roll 33.66 and 35.84 degrees and pitch 35.84 and 31.6 degrees). The values for OIV and ORA for the longitudinal and lateral directions are also of similar order of magnitude. These results suggest that for these CSRS conditions with the NJ barrier, similar barrier performance was observed for these two curvatures.

Figure 5 depicts the results for two different radius conditions with similar shoulder configurations for the New Jersey barrier installed with a True Vertical orientation. The first and third panel provide the MASH results and time sequence diagram for an 1100C vehicle impacting the barrier on a CSRS at 25 degrees and 100 kmh. It can be observed that the barrier impact event resulted in different performance for 758 ft and 2670 ft curvatures. The MASH evaluation results reflect high vehicle roll and pitch for both curvatures (e.g., roll 53.93 and 70.93 degrees, and pitch 58.68 and 81.87), but only the impacts for the small car on the large radii curve exceeded allowable levels. Interestingly, the values for Occupant Impact Velocity (OIV) and Occupant Ridedown Acceleration (ORA) for the longitudinal and lateral directions are the same order of magnitude. Panels 2 and 4 compare the impact event for the 2270P vehicle. The results reflect similar degrees of maximum vehicle roll and pitch (e.g., roll 57.53 and 59.73 degrees and pitch 42.15 and 47.05 degrees) for the pick-up. The values for OIV and ORA for the longitudinal and lateral directions are the same order of magnitude. These results show a more pronounced roll effect due to the barrier orientation but not significant effect due to the difference in curvature.

Influence of Barrier Type

Figures 6, 7, and Figure 8 depict the different barriers analyzed for increasing curve radii and otherwise similar conditions. Since not all combinations of CSRS conditions were simulated, it is not possible to make impact comparisons across the three barrier types. It is useful to note that variation in the crash behaviors are apparent reflecting that the varying of CSRS parameters influences the vehicle-to-barrier interface and the performance of the barrier. It can be noted between these figures that the response for the small car and pick-up truck varied. For all cases, the Occupant Impact Velocity (OIV) and Occupant Ridedown Acceleration (ORA) values for the longitudinal and lateral directions are of similar order of magnitude and direction for the similar barrier type. This may suggest that current barriers can function effectively across a variety of CSRS conditions.

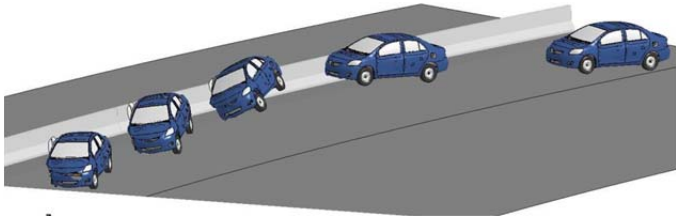
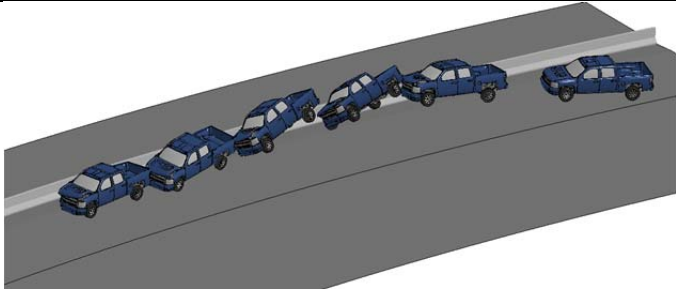
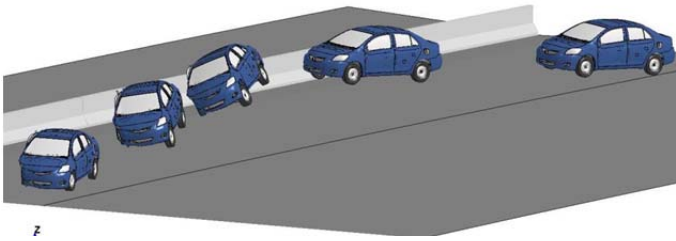
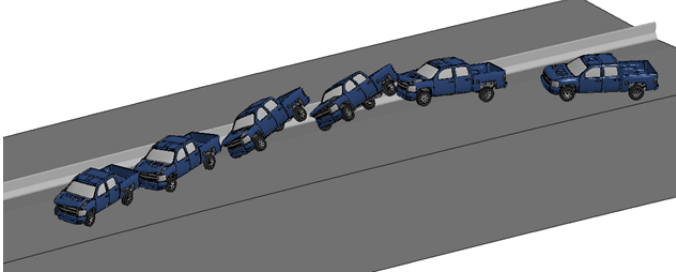
CSRS: Radius: 758 and 2670 ft Superelevation: 8%, Shoulder Width: 4 ft Shoulder Angle: 8% Barrier: New Jersey CSC Orientation: Normal Impact Speed & Angle: 100kmh/25°		
Parameters & Results	Case	Time Sequence View
CSRS: Radius 758, 8% super Vehicle : 1100C A – Containment (Pass) D – Detached Elements (Pass) F – Max Roll – 26.59 (Pass) Max Pitch – 21.99 (Pass) H – OIV – V _x - -5.47 (Pass) V _y – 9.76 (Pass) I – ORA – A _x – -3.19 (Pass) A _y – 14.23 (Pass)	224	
CSRS: Radius 758, 8% super Vehicle: 2270P A – Containment (Pass) D – Detached Elements (Pass) F – Max Roll – 33.66 (Pass) Max Pitch – 29.86 (Pass) H – OIV – V _x - -5.39 (Pass) V _y – 8.24 (Pass) I – ORA – A _x – -13.38 (Pass) A _y – 18.43 (Pass)	124	
CSRS: Radius: 2670 ft Superelevation: 8% Shoulder Width: 4 ft Shoulder Angle: 8% Barrier: New Jersey CSC Orientation: Normal Impact Speed & Angle: 100kmh/25°		
CSRS: Radius 2670, 8% super Vehicle : 1100C A – Containment (Pass) D – Detached Elements (Pass) F – Max Roll – 25.85 (Pass) Max Pitch – 21.72 (Pass) H – OIV – V _x - -5.49 (Pass) V _y – 9.72 (Pass) I – ORA – A _x – - 3.27 (Pass) A _y – -13.54 (Pass)	264	
CSRS: Radius 2670, 8% super Vehicle: 2270P A – Containment (Pass) D – Detached Elements (Pass) F – Max Roll – 35.84 (Pass) Max Pitch – 31.6 (Pass) H – OIV – V _x – -5.57 (Pass) V _y – 8.13 (Pass) I – ORA – A _x – -12.09 (Pass) A _y – 18.28 (Pass)	164	

FIGURE 4 Radius effects for NJ CSC barrier with normal orientation & vehicle size.

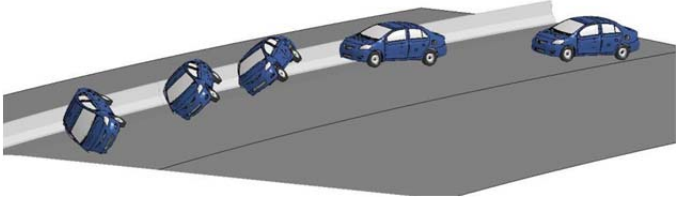
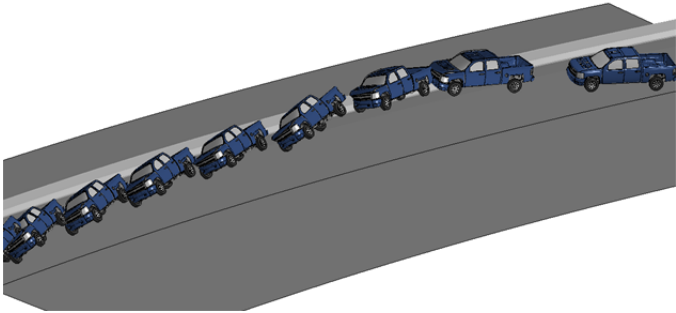
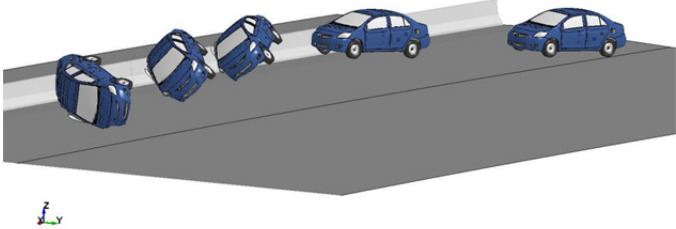
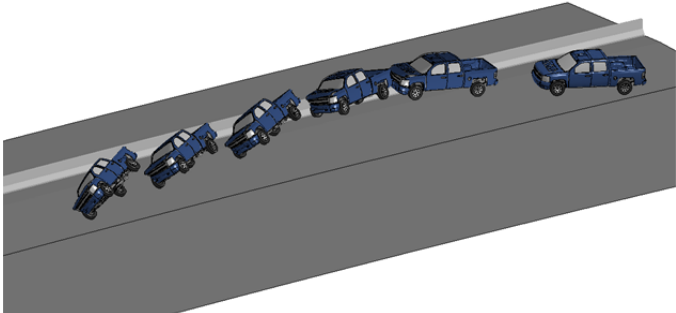
CSRS: Radius: 758 and 2670 ft Superelevation: 8% Shoulder Width: 4 ft Shoulder Angle: 8% Barrier: New Jersey CSC Orientation: True Vertical Impact Speed & Angle: 100kmh/25°		
Parameters & Results	Case	Time Sequence View
CSRS: Radius 758, 8% super Vehicle : 1100C A – Containment (Pass) D – Detached Elements (Pass) F – Max Roll – 53.93 (Pass) Max Pitch – 58.68 (Pass) H – OIV – Vx - -5.33 (Pass) Vy – 9.59 (Pass) I – ORA – Ax – -4.42 (Pass) Ay – 11.14 (Pass)	223	
CSRS: Radius 758, 8% super Vehicle: 2270P A – Containment (Pass) D – Detached Elements (Pass) F – Max Roll – 57.53 (Fail) Max Pitch – 42.15 (Fail) H – OIV – Vx - -4.75 (Pass) Vy – 7.89 (Pass) I – ORA – Ax – 10.47 (Pass) Ay – 17.64 (Pass)	123	
CSRS: Radius: 2670 ft Superelevation: 8% Shoulder Width: 4 ft Shoulder Angle: 8% Barrier: New Jersey CSC Orientation: True Vertical Impact Speed & Angle: 100kmh/25°		
CSRS: Radius 2670, 8% super Vehicle : 1100C A – Containment (Pass) D – Detached Elements (Pass) F – Max Roll – 70.93 (Fail) Max Pitch – 81.87 (Fail) H – OIV – Vx - -5.14 (Pass) Vy – 9.43 (Pass) I – ORA – Ax – - 4.44 (Pass) Ay – 10.41 (Pass)	263	
CSRS: Radius 2670, 8% super Vehicle: 2270P A – Containment (Pass) D – Detached Elements (Pass) F – Max Roll – 59.73 (Fail) Max Pitch – 47.05 Fail) H – OIV – Vx – -4.83(Pass) Vy – 7.95 (Pass) I – ORA – Ax – 9.71 (Pass) Ay – 18.12 (Pass)	163	

FIGURE 5 Radius and barrier orientation effects for CSRS conditions and vehicle size.

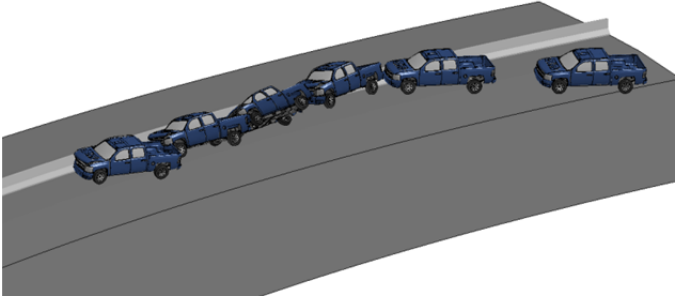
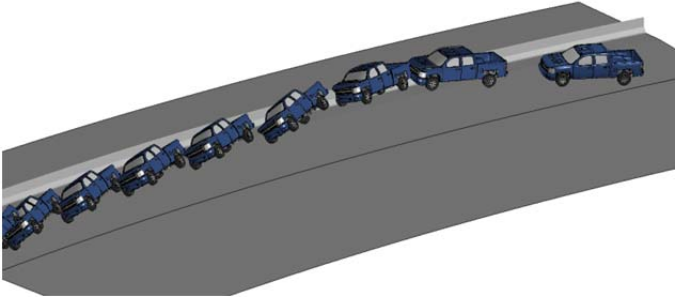
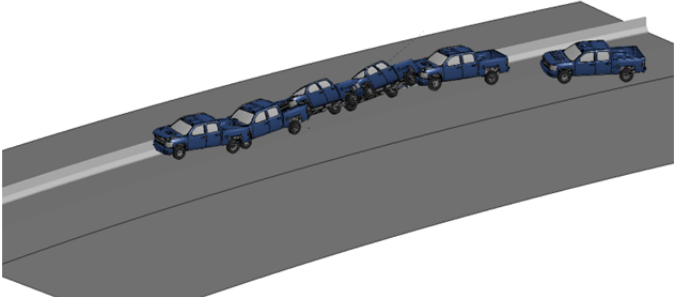
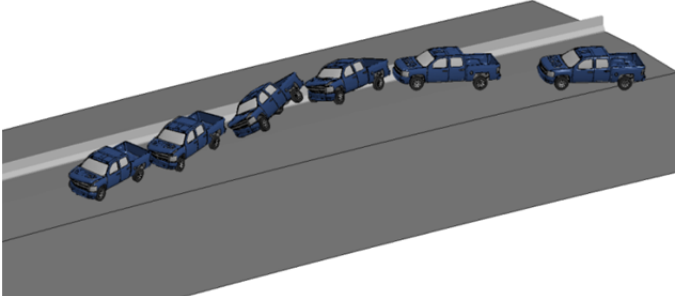
CSRS: Radius: 614 to 2130 ft Superelevation: variable Shoulder Width: 4 ft Shoulder Angle: 8% Barrier: New Jersey CSC Orientation: Vertical Impact Speed & Angle: 100kmh/25°		
Parameters & Results	Case	Time Sequence View
CSRS: Radius 614, 12% super Vehicle: 2270P A – Containment (Pass) D – Detached Elements (Pass) F – Max Roll – 54.42 (Pass) Max Pitch – 26.43 (Pass) H – OIV – V _x – -5.02 (Pass) V _y – 7.86 (Pass) I – ORA – A _x – -12.32 (Pass) A _y – 17.26 (Pass)	107	
CSRS: Radius 758, 8% super Vehicle: 2270P A – Containment (Pass) D – Detached Elements (Pass) F – Max Roll – 62.37 (Fail) Max Pitch – 25.18 (Fail) H – OIV – V _x – -5.05 (Pass) V _y – 7.97 (Pass) I – ORA – A _x – -14.75 (Pass) A _y – 17.22 (Pass)	125	
CSRS: Radius 833, 6% super Vehicle: 2270P A – Containment (Pass) D – Detached Elements (Pass) F – Max Roll – 49.51 (Pass) Max Pitch – 20.67 (Pass) H – OIV – V _x – -4.89 (Pass) V _y – 8.02 (Pass) I – ORA – A _x – -9.34 (Pass) A _y – -18.30 (Pass)	133	
CSRS: Radius 2130, 12% super Vehicle: 2270P A – Containment (Pass) D – Detached Elements (Pass) F – Max Roll – 34.13 (Pass) Max Pitch – 31.01 (Pass) H – OIV – V _x – -5.14 (Pass) V _y – 8.04 (Pass) I – ORA – A _x – -10.13 (Pass) A _y – 17.39 (Pass)	151	

FIGURE 6 Normal barrier orientation effects for CSRS conditions and vehicle size.

CSRS: Radius: 614 to 3050 ft Superelevation: variable Shoulder Width: 12 ft Shoulder Angle: 8% Barrier: MGS Orientation: Normal Impact Speed & Angle: 100kmh/25°		
Parameters & Results	Case	Time Sequence View
CSRS: Radius 614, 12% super Vehicle : 1100C A – Containment (Pass) D – Detached Elements (Pass) F – Max Roll – 5.23 (Pass) Max Pitch – 3.85 (Pass) H – OIV – V _x - -6.74 (Pass) V _y – 5.83 (Pass) I – ORA – A _x – -15.50 (Pass) A _y – 12.17 (Pass)	603 1100C	
CSRS: Radius 758, 8% super Vehicle : 1100C A – Containment (Pass) D – Detached Elements (Pass) F – Max Roll – 5.30 (Pass) Max Pitch – 4.52 (Pass) H – OIV – V _x - -6.78 (Pass) V _y – 5.88 (Pass) I – ORA – A _x – -17.26 (Pass) A _y – 10.98 (Pass)	611 1100C	
CSRS: Radius 853, 6% super Vehicle : 1100C A – Containment (Pass) D – Detached Elements (Pass) F – Max Roll – 5.23 (Pass) Max Pitch – 5.45 (Pass) H – OIV – V _x - -8.86 (Pass) V _y – 5.68 (Pass) I – ORA – A _x – - 12.42 (Pass) A _y – 10.45 (Pass)	627 1100C	
CSRS: Radius 2670, 8% super Vehicle : 1100C A – Containment (Pass) D – Detached Elements (Pass) F – Max Roll – 5.21 (Pass) Max Pitch – 3.23 (Pass) H – OIV – V _x - -6.88 (Pass) V _y – 5.71(Pass) I – ORA – A _x – -18.56 (Pass) A _y – 11.86 (Pass)	641 1100C	
CSRS: Radius 3050, 6% super Vehicle : 1100C A – Containment (Pass) D – Detached Elements (Pass) F – Max Roll – 5.30 (Pass) Max Pitch – 4.70 (Pass) H – OIV – V _x – -9.98 (Pass) V _y – 5.52 (Pass) I – ORA – A _x – -11.77 (Pass) A _y – 10.54 (Pass)	651 1100C	

FIGURE 7 Normal barrier orientation effects for CSRS conditions and vehicle size.

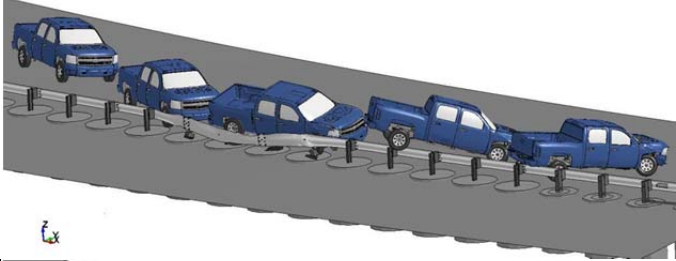
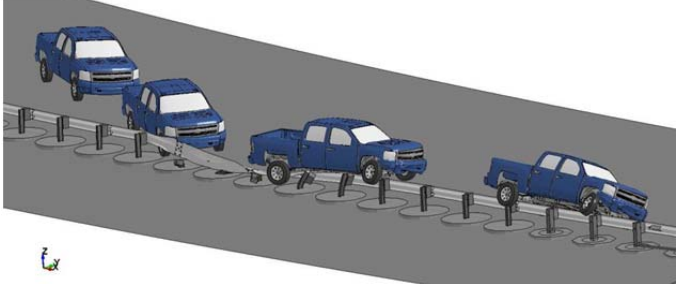
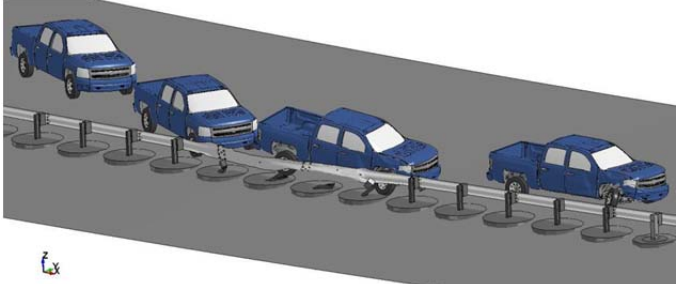
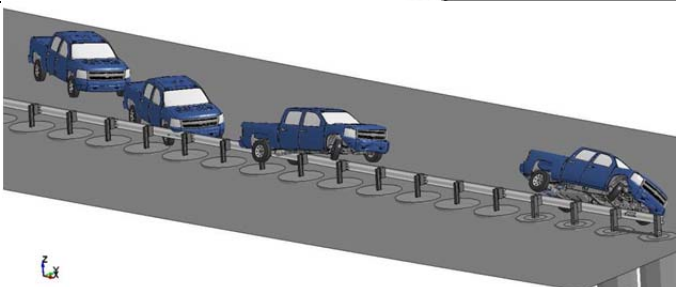
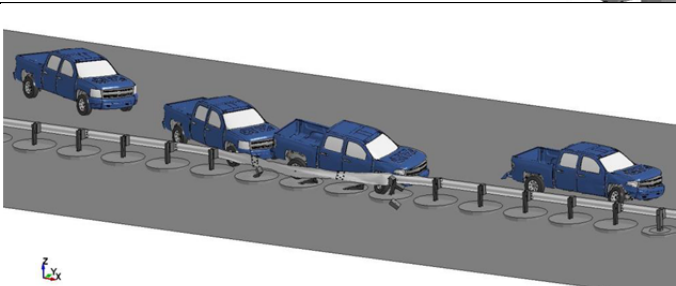
CSRS: Radius: 614 to 2670 ft Superelevation: various Shoulder Width: 8 ft Shoulder Angle: 6% Barrier: G41S (@ 29") Orientation: Normal Impact Speed & Angle: 100kmh/25°		
Parameters & Results	Case	Time Sequence View
CSRS: Radius 614, 12% super A – Containment (Pass) D – Detached Elements (Fail) F – Max Roll – 17.61 (Pass) Max Pitch – 12.04 (Pass)	305 2270P	
CSRS: Radius 758, 8% super MASH Evaluations: A – Containment (Fail) D – Detached Elements (Pass) F – Max Roll – 20.05 (Pass) Max Pitch – 17.96 (Pass)	175 315 2270P	
CSRS: Radius 833, 6% super MASH Evaluations: A – Containment (Pass) D – Detached Elements (Pass) F – Max Roll – 11.59 (Pass) Max Pitch – -7.51 (Pass)	329 2270P	
CSRS: Radius 2130, 12% super MASH Evaluations: A – Containment (Fail) D – Detached Elements (Pass) F – Max Roll – 33.84 (Pass) Max Pitch – 14.74 (Pass)	345 2270P	
CSRS: Radius 2670, 8% super MASH Evaluations: A – Containment (Pass) D – Detached Elements (Pass) F – Max Roll – 11.82 (Pass) Max Pitch – -6.35 (Pass)	355 2270P	

FIGURE 8 Normal barrier orientation effects for CSRS conditions and vehicle size.

These comparisons show that it is possible to analyze the performance differences across a range of CSRS conditions for typical barriers. It may also be possible to analytically define the influence patterns for safety performance, but that was not possible without simulation results for all combinations of factors. The final aspect of the simulation analysis generated summary tables to reflect the pass/fail patterns across the various CSRS conditions analyzed.

Performance Envelopes

A considerable amount of information was generated in the simulations. The crash outcomes were summarized in a series of tables for each barrier and MASH test condition across the range of conditions simulated. [Page limits prevent including a full set of these results here.] An example is reflected in Table 5.

It can be noted that in this stacked table all six of the superelevation and curve radii conditions are included as columns. The shoulder configuration factors (e.g., width and shoulder angle) are covered by the rows. Three barrier orientation features are also reflected in the vertical, namely true vertical, normal to the shoulder, or normal to the roadway. For each CSRS condition (i.e., curve radius and superelevation, shoulder width and shoulder angle), the results of the simulations for impacts with a specific type of barriers are provided. Some of these cells are marked with “*” to indicate that the outcomes were based upon expert judgement derived from the simulations and VDA analysis.

These summaries readily indicate the CSRS conditions where performance may be a concern. The insights that emerged from the performance tables included:

- Variations in barrier performance occur for the various conditions suggesting that the simulation models and approach reflect the physics of barrier impacts on CSRS.
- Varying barrier orientation influences the nature of the outcomes.
- Simulated failures occurred most often when shoulder angles were the largest. For these situations, the shoulder drops from the banked roadway surface.
- The NJ simulations noted large number of failures for ‘True Vertical’ installation.
- Impacts with the New Jersey barrier indicated that it can meet the crashworthiness requirements for all but the sharpest curve and greatest superelevation conditions.
- Performance under less severe CSRS and barrier placement conditions is incrementally improved. This might suggest that current applications of the concrete barrier are viable.
- Efforts to simulate G4(1S) W-beam barriers for the various conditions showed consistent results associated with barrier height. The 27.75-inch height barriers did not perform as well as those with greater heights.
- The simulations into G4(1S) barriers at 27.75 inches for CSRS applications showed a propensity for override, as the VDA results suggested. There were fewer cases of vaulting for the G4(1S) with 29-inch height. There were no cases where underride was indicated at a problem.
- Simulations of the MGS barrier (31-inch height) showed no propensity for underride issues with the small car.
- Additional simulations for F-shaped concrete barriers indicated improved performance over the NJ-shape.

TABLE 5 Sample Performance Table Based on Simulations**32" NJ Concrete Barrier Performance Table**

		Curvature/Superelevation (50 mph Design Speeds)								
		614 ft / 12%			758 ft / 8%			833 ft / 6%		
Shoulder Width	Shoulder Angle	FE True Vertical	FE I to Shoulder	FE I to Road	FE True Vertical	FE I to Shoulder	FE I to Road	FE True Vertical	FE I to Shoulder	FE I to Road
4 ft	0%	Pass*	Pass*	Pass*	Pass*	Pass*	Pass*	Pass*	Pass*	Pass*
	3%	Pass (111)	Pass*	Pass (112)	Pass*	Pass*	Pass*	Pass*	Pass*	Pass*
	6%	Fail (101)	Pass (113)	Pass (102)	Pass (121)	Pass*	Pass (122)	Pass*	Pass*	Pass*
	8%	Fail (103)	Pass (114)	Pass (104)	Fail (123)	Pass (129)	Pass (124)	Pass (131)	Pass*	Pass (132)
8 ft	0%	Pass*	Pass*	Pass*	Pass*	Pass*	Pass*	Pass*	Pass*	Pass*
	3%	Pass*	Pass*	Pass*	Pass*	Pass*	Pass*	Pass*	Pass*	Pass*
	6%	Fail (105)	Pass (115)	Pass (106)	Pass (127)	Pass*	Pass (128)	Pass*	Pass*	Pass*
	8%	Fail (107)	Pass (116)	Pass (108)	Fail (125)	Pass (130)	Fail (126)	Fail (233)	Pass*	Pass (134)
12 ft	0%	Pass*	Pass*	Pass*	Pass*	Pass*	Pass*	Pass*	Pass*	Pass*
	3%	Pass*	Pass*	Pass*	Pass*	Pass*	Pass*	Pass*	Pass*	Pass*
	6%	Pass (109)	Pass*	Pass (110)	Pass*	Pass*	Pass*	Pass*	Pass*	Pass*
	8%	Pass*	Pass*	Pass*	Pass*	Pass*	Pass*	Pass*	Pass*	Pass*
		Curvature/Superelevation (80 mph Design Speeds)								
		2130 ft / 12%			2670 ft / 8%			3050 ft / 6%		
Shoulder Width	Shoulder Angle	FE True Vertical	FE I to Shoulder	FE I to Road	FE True Vertical	FE I to Shoulder	FE I to Road	FE True Vertical	FE I to Shoulder	FE I to Road
4 ft	0%	Pass*	Pass*	Pass*	Pass*	Pass*	Pass*	Pass*	Pass*	Pass*
	3%	Pass*	Pass*	Pass*	Pass*	Pass*	Pass*	Pass*	Pass*	Pass*
	6%	Fail (145)	Pass (153)	Pass (146)	Fail (161)	Pass (165)	Pass (162)	Pass (171)	Pass*	Pass (172)
	8%	Fail (147)	Pass (154)	Pass (148)	Fail (163)	Fail (266)	Pass (164)	Pass (173)	Pass (175)	Fail (174)
8 ft	0%	Pass*	Pass*	Pass*	Pass*	Pass*	Pass*	Pass*	Pass*	Pass*
	3%	Pass*	Pass*	Pass*	Pass*	Pass*	Pass*	Pass*	Pass*	Pass*
	6%	Fail (245)	Pass (155)	Pass (150)	Pass*	Pass*	Pass*	Pass*	Pass*	Pass*
	8%	Fail (247)	Pass (156)	Fail (152)	Pass*	Pass*	Pass*	Pass*	Pass*	Pass*
12 ft	0%	Fail (249)	Pass (157)	Pass (142)	Pass*	Pass*	Pass*	Pass*	Pass*	Pass*
	3%	Pass (143)	Pass (158)	Pass (144)	Pass*	Pass*	Pass*	Pass*	Pass*	Pass*
	6%	Pass*	Pass*	Pass*	Pass*	Pass*	Pass*	Pass*	Pass*	Pass*
	8%	Pass*	Pass*	Pass*	Pass*	Pass*	Pass*	Pass*	Pass*	Pass*

It should be noted that simulation results provide a broad variety of other metrics not shown in the table. These would allow comparisons of vehicle damage, barrier deflections, rail stress concentrations, or other metrics. These provide the potential to represent results in the context of numerical measures that would a finer lever of comparisons.

Some simulations were planned to provide quantitatively based insights on the influence of roadway and barrier design elements on safety performance. In this effort, the results permitted considerations of the influences of curvature, road profile, barrier vertical orientation, impact angle, impact speed, and combinations of these on safety performance. There are many other conditions that need to be analyzed to provide support for engineering decisions and/or formulate barrier design and selection guidelines.

SUMMARY AND CONCLUSIONS

The efforts reported here described the successful simulation of the performance of longitudinal barriers when impacted by vehicles leaving the traveled way on curved, superelevated roadway

sections (CSRS). The intent was to develop a better understanding of the influence of various roadway curvatures, superelevation, and shoulder/roadside designs on the safety effectiveness of common longitudinal barriers used in these situations. This effort was focused on impacts occurring on CSRS for a cross section of six varying curve radii, superelevation, and shoulder conditions. Ultimately, more than 200 simulations were undertaken. These results found that in most cases the barriers met the MASH crashworthiness requirements. Where the simulations indicated the potential for failure, deeper analysis and additional simulations were undertaken to define the scope and causes. The results served as the major input to efforts to develop recommended guidance for the design, selection, and placement of barriers to be used on CSRS.

A tremendous amount of data and information was derived from the simulation efforts. The following general observations were made:

- The simulation models were adequate to reflect the differences in the features of CSRS and the associated shoulder conditions for impacts by two types of vehicles and three types of barriers.
- The simulation results were validated by using full-scale crash tests and the consistency of results across incremental changes in features. [Documented elsewhere]
- The New Jersey barrier provided sufficient containment and redirection of large and small impacting vehicles, but there were few cases where rollovers occurred when the barrier was installed in the true vertical orientation.
- The analysis of the G41S barrier was begun using the prescribed 27.75-inch height. Problems were noted in the early simulations with pattern of failures for most cases showing that the barrier would not adequately contain the large (pickup) vehicle.
- Based on FHWA recommendations, the height of the G4(1S) barrier be raised to 29 inches for further simulations. Simulation showed fewer cases of vaulting for the G4(1S) with 29-inch height. There were no cases where underride was indicated as a problem.
- The MGS analyses was conducted with a focus on potential underride issues. FE simulations of the MGS barrier (31-inch height) however showed no propensity for underride issues with the small car.
- The MGS barrier showed no indication of override issues in the VDA analyses, these were not confirmed using computer simulations but results from the 29 in G4(1S) finite element simulations supported these VDA results.
- The number of factors identified at the outset made for a very large analysis matrix making it hard to isolate individual effects. Further analyses of key combinations of factors may be useful to isolate the combined effects of shoulder width and slope for the six CSRS conditions.
- The Vehicle Dynamics Analyses helped to reduce the number of finite elements simulation runs needed.

During these efforts, the need for further research on this topic became apparent. These included:

- Additional simulation runs would be useful to expand the understanding of the relative differences in barrier performance for applications on CSRS. The additional analyses would include other metrics available from the simulation results.

- Since barriers need to function in crashes with all types of vehicles, provide a deeper look at the differences in metrics resulting from crashes at different speeds and angles or other vehicles.
- Perform additional simulations to isolate the influences of shoulder width and slope on the safety performance for sharp and gentle curves.
- For this research, the simulations provided useful fundamental understanding of the performance of barriers used on CSRS in a pass/fail context. The implications of this MASH (and its predecessors) approach for monitoring safety performance are well understood by highway engineers. It would be useful to consider more rigorous approach that uses simulated metrics to develop quantitative safety performance measures. The MASH testing protocols focus on several barrier metrics, but others are possible, including, deformations (barrier and post deflection, barrier component forces and stresses, vehicle accelerations at impact, and vehicle trajectory patterns while departing the traveled way on a CSRS.

The benefits of these additional efforts must be weighed in the context of providing needed insights or support for the recommendations that are to be developed. These will be discussed with the panel.

REFERENCES

1. American Association of State Highway and Transportation Officials, Policy for the Geometric Design of Streets & Highways, AASHTO, Washington, D.C., 2005. [check] AASHTO, Roadside Design Guide, published by the American Associations of State Highway & Transportation Officials, Washington, DC, 2006.
2. Marzougui, D., Kan, C.D.; and Opiela, K.S.; “Evaluation of the Influences of Cable Barrier Design and Placement on Vehicle to Barrier Interface,” NCAC Document 2008-W-001, The National Crash Analysis Center, The George Washington University, October 2008.
3. Marzougui, D., Kan, C.D.; and Opiela, K.S.; *Using Vehicle Dynamics Simulation as a Tool for Analyzing Cable Barrier Effectiveness* Report 2010-W-006 prepared for FHWA by the National Crash Analysis Center, George Washington University, August 2010.
4. Marzougui, D., Kan, C.D.; and Opiela, K.S.; *Analyzing the Effects of Cable Barriers Behind Curbs Using Computer Simulation* Report 2009-W-008 prepared for FHWA by the National Crash Analysis Center, George Washington University, November 2009.
5. AASHTO, Manual for Assessing of Safety Hardware (MASH), published by the American Associations of State Highway & Transportation Officials, Washington, DC, 2010.
6. NCAC, *Development & Validation of a FE Model of a 2010 Toyota Yaris Passenger Sedan (NCAC 2011-T-001)*; The George Washington University, Ashburn, VA May 2012.
7. NCAC, *Development & Validation of a Model of a 2007 Chevy Silverado Pick-up Truck (NCAC2009-T-005)*; The George Washington University, Ashburn, VA May 2012.
8. Marzougui, D.; et al; “Extended Validation of the Finite Element Model for the 2007 Chevrolet Silverado Pick-Up Truck (MASH 2270kg Vehicle); NCAC 2012-W-003, May 2012.
9. Marzougui, D.; et al, “Extended Validation of the Finite Element Model for the 2010 Toyota Yaris Sedan (MASH 1100kg Vehicle); NCAC 2012-W-005, May 2012.
10. AASHTO, Roadside Design Guide, published by the American Associations of State Highway & Transportation Officials, Washington, DC, 2006.
11. Ross H. E., Jr., D. L. Sicking, R. A. Zimmer, and J. D. Michie. *NCHRP Report 350: Recommended Procedures for the Safety Performance Evaluation of Highway Features*, 1993.

12. Hallquist, J.O.; LS-DYNA Theoretical Manual. Livermore Software Technology Corporation, Livermore, CA, USA, 1997.
13. Hallquist, J.O., "LS-DYNA Keyword User's Manual", Livermore Software Technology Corporation, 2006.

Commercial Motor Vehicle Safety Measures

JOHN C. DURKOS
Road Systems, Inc.

Over the past few years, newspaper headlines have publicized horrific Commercial Motor Vehicle (CMV) crashes having multiple fatalities. CMVs include large trucks and motor coaches. This problem has gained the attention of the US Congress. The Fixing America's Surface Transportation (FAST) Act signed December 2015 has a requirement to address CMV accidents. The Secretary of Transportation was required to produce a report to Congress by December 4, 2016 designed to improve the safety of CMVs. This included conducting a review of best practices with respect to the implementation of roadway safety infrastructure improvements that are cost effective and will reduce the number or severity of accidents involving CMVs.

Different treatments can address certain crash types. Roadside treatments such as high-visibility edge lines, barrier delineation, rumble stripes, and signage can provide information or alert CMV drivers that they are about to leave the lane and give them an opportunity to correct the error preventing a roadway departure crash. Mitigating treatments could include those that require redesigning the roadway or straightening curves although these types of treatments are more expensive and rarely used. Other roadside treatments intended to eliminate or reduce the vehicle impact should it run off the road include breakaway supports, removing/relocating/retrofitting fixed objects, and shielding the hazard using a high performance barrier.

There are various treatments and/or processes for developing appropriate mitigating measures for CMVs. Modifying standards and designs along with implementation guidelines can result in a significant difference preventing or minimizing the effects of crashes involving CMVs.

New Methodology for Analysis of Sand Barrel Arrays

ROBERT W. BIELENBERG.

RONALD K. FALLER

JOHN D. REID

Midwest Roadside Safety Facility

University of Nebraska-Lincoln

JOSEPH G. PUTJENTER

R&D Mechanical Engineer

Sand barrel crash cushion have been used for many years to provide staged energy absorption and shielding of rigid hazards such as the ends of concrete barriers. They are popular because they are relatively inexpensive and easy to install. Another benefit of sand barrel arrays is that they are can be configured and optimized for different impact scenarios or modified to shield wide or irregular hazards. The Roadside Design Guide outlines an inertial or momentum transfer method for analyzing head-on impacts where sand barrels are used to protect a narrow hazard. However, this analysis becomes considerably more complex and time consuming for non-standard configurations or angled impacts.

An improved method for analyzing complex sand barrel arrays was developed that accounts for barrels only partially struck by a vehicle and adjusts for a wide range of impact conditions. The method uses basic principles of momentum transfer, but considers the mass contribution of each impacted or partially-impacted barrel. Multiple methods for distributing mass between the impact events were considered and an optimal method was selected. The analysis method was implemented in a spreadsheet where sand barrel layout can be described in two-dimensional Cartesian coordinates describing the center position and mass of each barrier, and variable impact conditions can be input and analyzed. This improved sand barrel analysis procedure provides for efficient configuration of safe barrel arrays in a wide range of geometries and impact scenarios.

INTRODUCTION

Crash cushions are designed to protect an errant vehicle from impacting a fixed object by gradually decelerating the vehicle to a safe stop or by redirecting the vehicle away from the obstacle. Sand barrel arrays are crash cushion systems that have been used for many years to provide staged energy absorption and shielding of rigid hazards such as the ends of concrete barriers. These arrays are popular because they are relatively inexpensive and easy to install. Another benefit of sand barrel arrays is that they are can be configured and optimized for different encroachment speeds or modified to shield wide or irregular hazards. Thus, the arrays can be designed to provide safety performance ranging from narrow, short arrays for shielding rigid parapet end type hazards in low-speed areas to longer, wider arrays for shielding wide hazards in high-speed applications.

The AASHTO Roadside Design Guide (1) prescribes an inertial or momentum transfer method for analyzing head-on impacts where sand barrels are used to protect a narrow concrete barrier end or other hazard. As the vehicle travels through the system, each new contacted row of

barrels is considered a distinct impact event. However, in non-standard barrel configurations or angled impacts, some of the modules may only be partially impacted. This makes the analysis considerably more complex.

This paper describes a method developed for analyzing more complex sand barrel arrays that accounts for barrels only partially struck by a vehicle and adjusts for a wide range of impact conditions. The method uses basic principles of momentum transfer, but modifications to the method considered the discrete contributions of the mass of each impacted or partially impacted-barrel. Multiple methods for distributing mass between the impact events were considered and compared, and an optimal method was selected. Additionally, the analysis and mass distribution method were implemented into a spreadsheet program. The spreadsheet also allowed input of the sand barrel array in two-dimensional (2D) Cartesian coordinates and variable vehicle and impact conditions. This new and improved sand barrel analysis procedure provides for fast and easy determination of safe sand barrel arrays for a wide range of geometries and impact scenarios that were previously difficult to calculate.


BACKGROUND

Sand Barrel Attenuators

Four sand barrel crash cushions have been successfully evaluated to NCHRP Report No. 350 (2), as shown in Table 1. MASH evaluation of sand barrel attenuation systems has not been completed at this time. All current sand barrel crash cushions use some form of frangible, plastic barrel to contain a mass of sand. The mass of each barrel is prescribed in increments of 200 lb., 400 lb., 700 lb., 1,400 lb., and 2,100 lb. The height of the center of mass of the sand in the lighter barrels is generally raised to better align with the center of mass of the impacting vehicle through the use of some form of spacer/insert or variation in the barrel height.

The mass of the barrels typically increases within rows as the system approaches the hazard. This configuration provides a relatively safe deceleration rate for the vehicle until it slows to a safe velocity. Additionally the barrel array can be configured to shield various size hazards as well as account for a wide variation in expected encroachment speeds. Proper design of these types of systems requires the array configuration to account not only for head on impacts directly along the axis of the barrel array, but also should account safe vehicle gating or deceleration for angled and/or side impacts as well as consideration of reverse direction impacts. For example, the array should account for the so called “coffin corner” impact where the vehicle impacts along the side of the system at an angle and aligned with the end of the rigid hazard the array is shielding. However, design of sand barrel arrays to account for these types of impacts has been limited due to the difficulty associated with their analysis.

TABLE 1 NCHRP Report 350-Approved Sand Barrel Attenuators

Name	Image	Manufacturer	Test Level	Width	Length	Height	FHWA Approval Letter
			NCHRP 350				
Big Sandy		TraFFix Devices	TL-2, TL-3	Varies to fit site	VARIABLE (30 to 65 mph)	35"-47"	CC-52
CrashGard		Plastic Safety Systems	TL-2, TL-3	Varies to fit site	VARIABLE (25 to 70 mph)	53"	CC-97
Energite		Energy Absorption Systems, Inc.	TL-2, TL-3	Varies to fit site	VARIABLE (30 to 65 mph)	32"-36"	CC-29
Fitch		Energy Absorption Systems, Inc.	TL-2, TL-3	Varies to fit site	VARIABLE (30 to 65 mph)	33"	CC-28

Existing Sand Barrel Array Analysis Procedures

A method for analyzing and estimating the performance of sand barrel arrays in a head on impact is provided in the AASHTO *Roadside Design Guide*. A typical situation where a vehicle impacts the nose of an array with all of the barrels inside the path of the vehicle is shown in Figure 1. As the vehicle travels through the system, each new contacted barrel is considered a distinct impact event. When multiple barrels are contacted at the same time, the mass of the barrels is combined to form the same impact event.

Although other factors influence energy dissipation during an impact event, simple momentum transfer was the basis for predicting a system's performance. Using the conservation of momentum principle

where:

M_v	=	Mass of vehicle (lb)
M_1	=	Mass of sand in first contacted barrel (lb)
M_n	=	Mass of sand in the n th impacted container(s)
V_0	=	Original impact velocity (ft/s)
V_1	=	Velocity after first impact (ft/s)
V_n	=	Velocity after n th impact (ft/s)

$$M_v V_0 = M_v V_1 + M_1 V_1 \quad (1)$$

This equation can be rearranged such that:

$$V_1 = \frac{M_v V_0}{M_v + M_1} \quad (2)$$

The combined momentum of the vehicle and the sand after impact was assumed effectively equal to the momentum of the vehicle just before impact with the next barrel(s). This assumption implies that after the front of the vehicle has passed over the original location of the module, the sand has been completely dispersed and no longer contributes to absorbing the kinetic energy. Applying this in a sequential manner for each row of sand barrels impacted, the vehicle's speed after its n th impact is:

$$V_n = \frac{M_v V_{n-1}}{M_v + M_n} \quad (3)$$

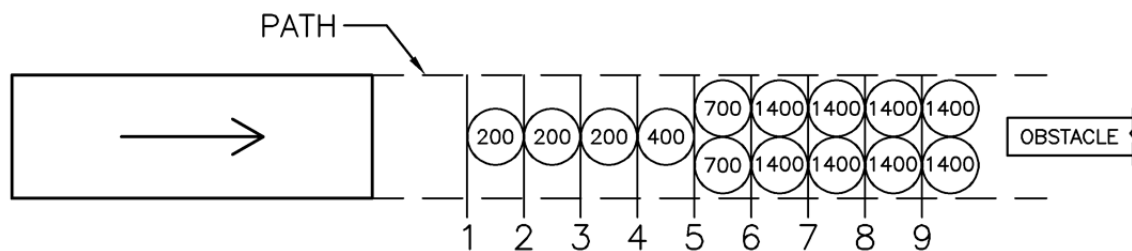


FIGURE 1 Standard Sand Barrel Crash Cushion Analysis.

For each row of sand barrels impacted, the deceleration distance is equal to the diameter of the barrel. The frangible plastic barrel breaks apart as it is struck by the vehicle. Frequently, the maximum deceleration in g's is desired for an estimate of the occupant risk from ridedown decelerations. The 1977 AASHTO *Guide for Selecting, Locating, and Designing Traffic Barriers* suggests a 12-g maximum average acceleration for crash cushions (3). This limit is considered common practice for designing sand barrel systems and was used in lieu of the MASH ridedown acceleration limit of 20.49 g's (4). Average acceleration is used in this analysis, because it is assumed that the velocity of the vehicle is immediately reduced after an impact with a barrel. This sudden drop in velocity would result in infinite, nonphysical accelerations that could not be used for assessing occupant risk. The average acceleration, a , and time between each impact event, t , can be calculated:

where:

l_n	=	Deceleration distance for n th impact (ft)
a_n	=	Deceleration for n th impact (ft/s ²)
g	=	Acceleration of gravity (32.174 ft/s ²)
G_n	=	Deceleration for n th impact (G's)
t	=	Duration of n th event (s)

$$a_n = \frac{v_{n-1}^2 - v_n^2}{2l_n} \quad (4)$$

$$G_n = \frac{a_n}{g} \quad (5)$$

$$t_n = \frac{v_{n-1} - v_n}{a_n} \quad (6)$$

Other important criteria include the theoretical Occupant Impact Velocity (OIV) and Occupant Ridedown Acceleration (ORA). These criteria represent the hypothetical velocity and acceleration of an unbelted occupant upon impact with an interior surface. These values can be estimated using the procedures outlined in MASH and the velocities and accelerations described above.

Theoretically, a vehicle will not be stopped using the conservation of momentum. For this reason, common practice is to design systems such that the velocity is reduced to below 10 mph after the last module has been impacted. Manufacturers often recommend placing another row of heavy barrels beyond the point at which the vehicle's velocity is reduced to less than 10 mph, although this is not required (1).

While the momentum transfer method detailed in the Roadside Design Guide is useful for analysis of narrow sand barrel arrays impacted head-on with the longitudinal axis of the array, analysis of non-standard or wide barrel configurations or angled impacts becomes more complex as the barrels in the array will be partially impacted and the barrel impacts will not align in easily discretized rows like those shown in Figure 1. Thus, a need existed for advanced analysis of more complex sand barrel array impacts that could account for the uneven distribution of impacted barrel masses.

ADVANCED INERTIAL BARRIER ANALYSIS

Basic Methodology

A method was developed for analyzing more complex sand barrel arrays that accounts for barrels only partially struck by a vehicle and adjusts for a wide array of impact conditions. The method used the same basic principles described previously, but modifications consider the discrete contributions of the mass of each impacted or partially impacted barrel.

Consider the wide, non-standard sand barrel array shown in Figure 2a. A 2270P vehicle, represented as a rectangle, impacts the barrels with an assumed linear trajectory. Although the shape for many commercially available modules varies, this analysis considers all barrels to be perfect cylinders with a diameter of 36 in. and spaced 6 in. apart.

The contribution of each impacted barrel to momentum transfer must be determined. Because sand barrels are made of frangible plastic, the vehicle breaks apart the barrel and accelerates the sand and barrel fragments in all directions. For partial impacts, only the mass inside of the vehicle's path is assumed to contribute to momentum transfer, as shown in Figure 2b.

Each impact with a barrel is considered a unique event, as shown in Figure 2c. The deceleration distance for each event is equal to either the distance between impact events or the length of contact with the barrel, whichever is less. The "length of contact" refers to the distance the vehicle interacts with the barrel. As shown in Figure 2d, the length of contact is equal to the diameter of the barrel when the center of a module is inside the vehicle's path (A and B). If the center of the module is outside of the path, then the length of contact is equal to the chord length of the split module (C).

The mass for impact event n is all of the mass that is located between impact n and impact $n+1$, as shown in Figure 2e. Thus, not all of a barrel's mass would necessarily contribute to energy absorption during the same impact event.

Mass Distribution

Multiple methods for distributing mass between the impact events were considered. The mass of each barrel that is inside the path of the vehicle can be determined algebraically for all barrels that are impacted or partially impacted. Between each impact event, there may be one or more barrels that are contributing to momentum transfer. The barrels are split between each impact event. The mass of each barrel segment can be directly determined using the area of each barrel segment, dividing it by the total area of the barrel that lies inside the vehicle's path, and then multiplying it by the mass of the barrel that lies inside the path.).

The first step in analyzing each impact event is to determine the amount of sand inside the vehicle's path:

where:

D	=	Diameter of sand barrel (ft)
X_t	=	Total area of sand barrel (ft ²)
X	=	Area of sand barrel inside of path (ft ²)
X_l	=	Area of circle with diameter equal to length of contact (ft ²)
K	=	Area of partially impacted sand barrel bisected by path (ft ²)

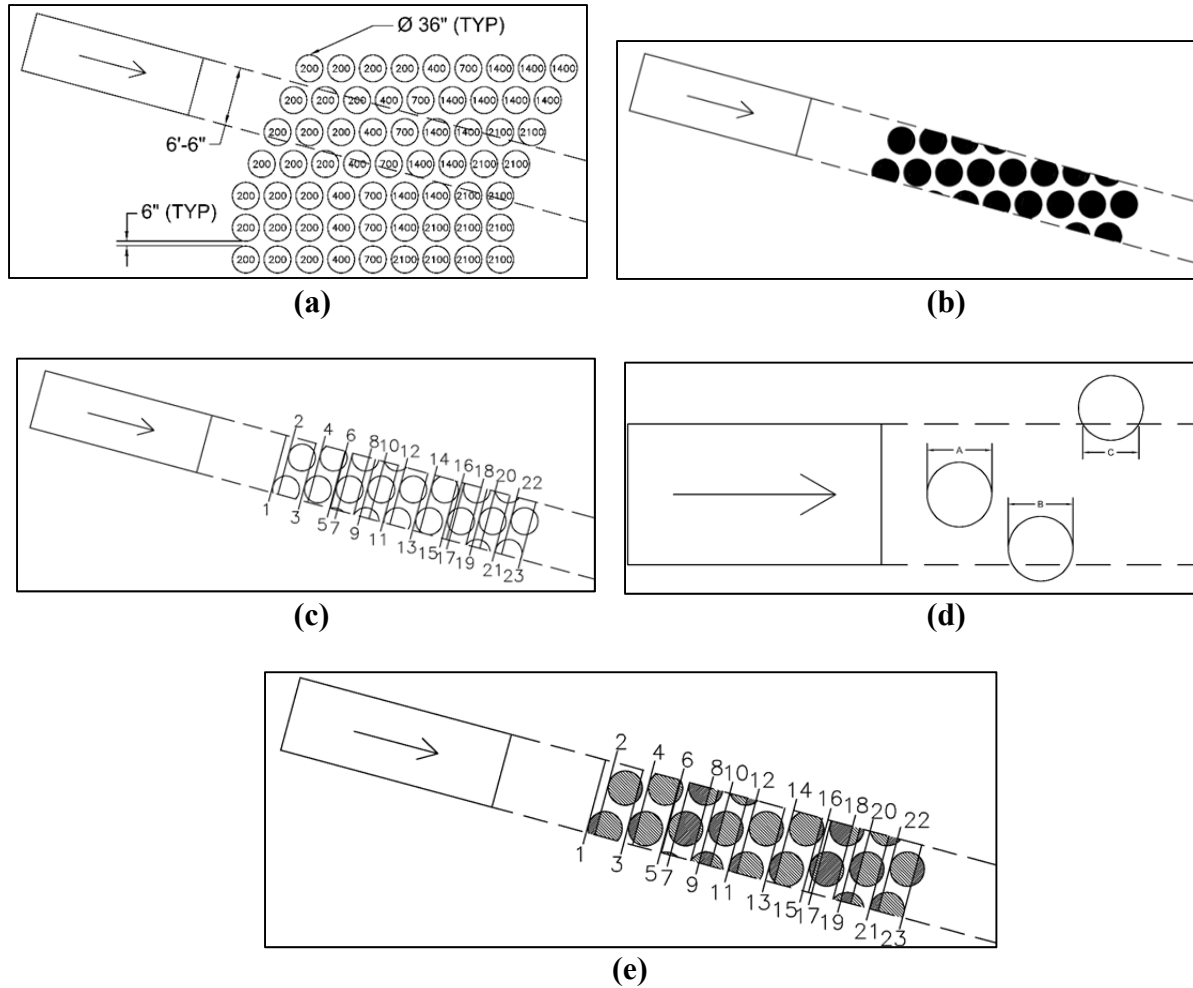


FIGURE 2 Vehicle impact on nonstandard sand barrel crash cushion: (a) angled impact on wide sand barrel array; (b) effective masses of each impacted barrel; (c) impact order and deceleration distance; (d) length of contact description; and (e) mass distribution between impact events.

K_b	=	Area segment defined by diameter equal to length of contact and width (ft ²)
h	=	Distance from path to center of sand barrel (ft)
c	=	Chord length of partially impacted sand barrel (ft)
b	=	Distance of bisection from circle edge (ft)
L_n	=	Distance from front of vehicle to impact point on barrel (ft)
M_{X_T}	=	Total mass of sand barrel X (lb)
M_X	=	Mass of sand barrel X contributing to momentum transfer (lb)
M_n	=	Mass at impact event n (lb)

For barrel area, X_T :

$$X_T = \frac{\pi D^2}{4} \quad (7)$$

The distance from the path to the center h can be used to determine K , the area of a bisected circle, as shown in Figure 3a. If the center of the module is inside the vehicle's path, $K = K_i$:

$$K_i = \frac{D^2}{4} \left(\pi - \cos^{-1} \left(\frac{2h}{D} \right) \right) + h \sqrt{\frac{D^2}{4} - h^2} \quad (8)$$

If the center of the module is outside the vehicle's path, the area of the barrel segment $K = K_o$:

$$K_o = \frac{D^2}{4} \cos^{-1} \left(\frac{2h}{D} \right) - h \sqrt{\frac{D^2}{4} - h^2} \quad (9)$$

And the chord length c is:

$$c = \sqrt{\frac{D^2}{4} - h^2} \quad (10)$$

The effective mass of the impacted sand barrel is thus:

$$\text{Full impact, entire barrel inside path: } M_X = M_{X_T} \quad (11)$$

$$\text{Partial Impact, center inside path: } M_X = \left(\frac{K_i}{X_t} \right) M_{X_T} \quad (12)$$

$$\text{Partial impact, center outside path: } M_X = \left(\frac{K_o}{X_t} \right) M_{X_T} \quad (13)$$

The mass calculations for the first seven impacts of the large sand barrel array example are shown in Figure 3b and depicted in the following equations. For this example, barrel A corresponded with impact event no. 1, barrel B with impact event no. 2, and so on. Area A refers to the area of barrel A that is inside the vehicle's path, while A_x refers to the area of the barrel between two impact events. Mass M_A was the mass of barrel A inside the vehicle's path, M_B , the mass of barrel B inside the vehicle's path, and so on. Mass M_1 was the sum of all sand barrel masses located between impact event no. 1 and 2, M_2 , the sum of all sand barrel masses between impact event no. 2 and 3, and so on.

$$M_1 = \left(\frac{A_1}{A} \right) M_A \quad (14)$$

$$M_2 = \left(\frac{B_1}{B} \right) M_B + \left(\frac{A_2}{A} \right) M_A \quad (15)$$

$$M_3 = \left(\frac{C_1}{C} \right) M_C + \left(\frac{B_2}{B} \right) M_B \quad (16)$$

$$M_4 = \left(\frac{D_1}{D} \right) M_D + \left(\frac{C_2}{C} \right) M_C \quad (17)$$

$$M_5 = \left(\frac{E_1}{E}\right) M_E + \left(\frac{E_2}{D}\right) M_D \quad (18)$$

$$M_6 = \left(\frac{F_1}{F}\right) M_F + \left(\frac{E_2}{E}\right) M_E + \left(\frac{D_3}{D}\right) M_D \quad (19)$$

$$M_7 = \left(\frac{G_1}{G}\right) M_G + \left(\frac{F_2}{F}\right) M_F + \left(\frac{E_3}{E}\right) M_E \quad (20)$$

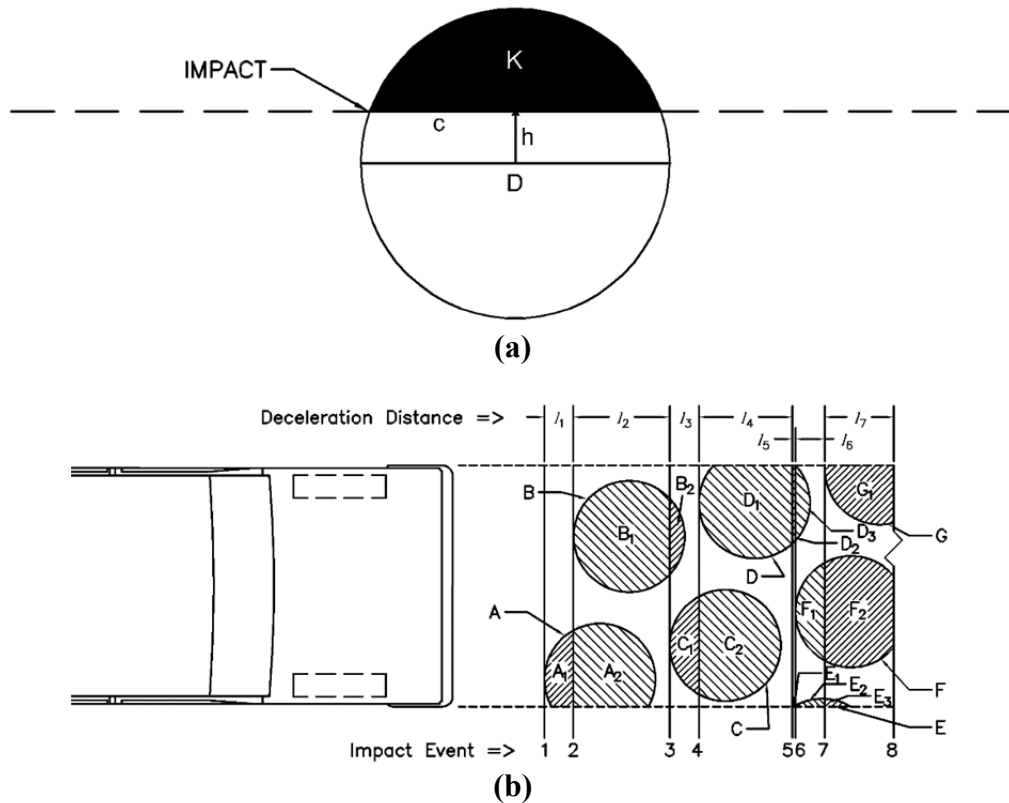


FIGURE 3 Sand barrel impact mass distribution: (a) detail of partially impacted sand barrel and (b) mass distribution between impact events.

Ideal Mass Distribution

Several approaches were considered for dealing with the discretized mass distribution of the mass as a vehicle proceeds through the barrel array. In an ideal mass distribution approach, the exact area for each split barrel segment would be calculated algebraically, which results in many calculations. A more efficient method for calculating the area would be to use a CAD program to determine the bisected areas. Whether the areas of the barrel segments are calculated algebraically or with CAD, the mass of each barrel segment can be determined using the area of each barrel segment, dividing it by the total area of the barrel that lies inside the vehicle's path,

and then multiplying it by the mass of the barrel that lies inside the path. Two different cases are geometrically represented in Figure 4, where segment area X_1 and X_2 are divided by area X to provide a ratio. The first case is where the individual sections are only split once. The scenario in Case 2 occurs when a section is taken out of the middle of the circle. Both of the cases shown in Figure 4 have a portion of the barrel that is outside of the path of the vehicle and does not contribute to the mass calculation.

Linear Mass Approximation

Although the exact area for each split barrel can be calculated algebraically or by using a CAD program for each instance, this task is often time-consuming. Instead of trying to calculate each individual area, a simpler method is to assume that the effective mass of each barrel is evenly distributed along the length of contact l with the barrel.

The location of the center of each barrel is known. Knowing the center position of the barrel relative to the impact events allows the masses to be split among the different impact events. A geometric representation of this approximation is shown in Figure 5. The hatched areas for Cases 1 and 2 represent a section of a barrel that is contributing to the mass at some impact event. In Case 1, the width of the first barrel section is divided by the overall length of contact to calculate the mass ratio. In Case 2, the width of the middle barrel segment is divided by the overall length of contact. The distance that the vehicle is in contact with the barrel is used instead

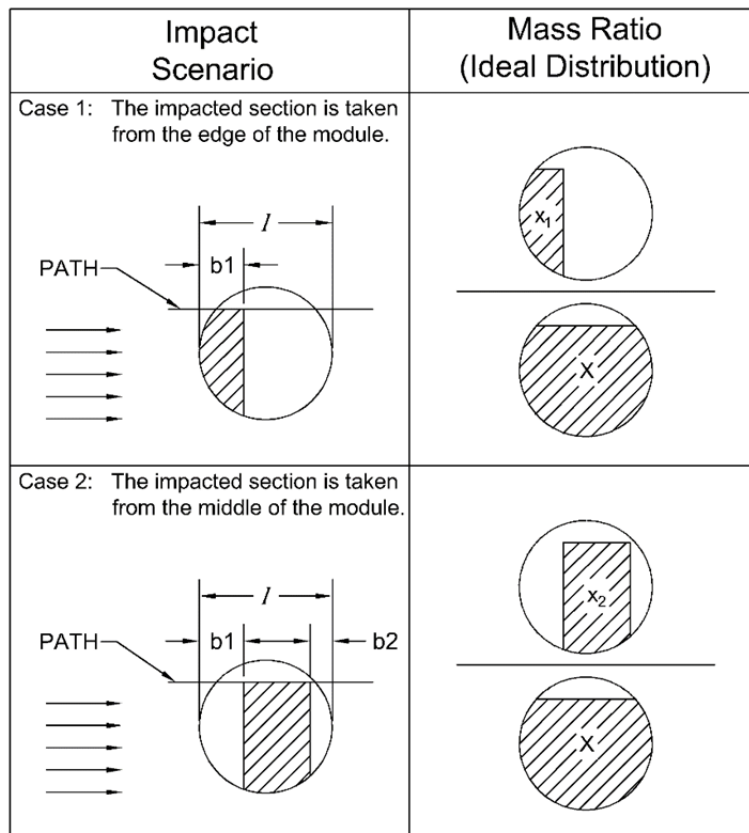


FIGURE 4 Ideal mass distribution.

of the diameter of the barrel in partial impacts where the center of the barrel is outside the vehicle's path.

If the vehicle passes through the entire barrel before the next barrel is struck:

$$\frac{L_{n+1} - L_n - l_n}{l_n} (M_n) \quad (21)$$

If barrel(s) $n+1$ are struck before the vehicle has passed completely over barrel n :

$$\frac{L_{n+1} - L_n}{l_n} (M_n) \quad (22)$$

The mass from previous barrels $n-u$ are included in the same fashion if:

$$(L_{n-u} + l_{n-u}) \geq L_N \quad (23)$$

Using this approximation method will overestimate the mass for small sections near the edge of the circle, resulting in larger-than-expected velocity drops and spikes in the average acceleration which exceed the 12-g limit.

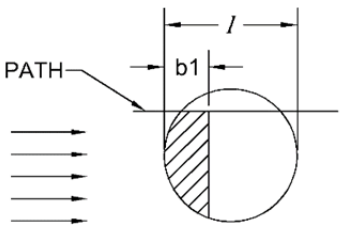
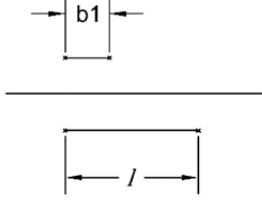
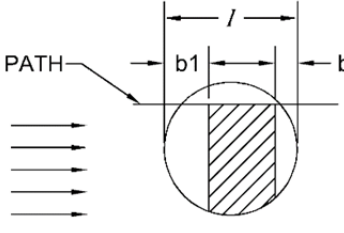
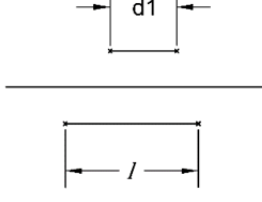
Impact Scenario	Mass Ratio (Linear Approx.)
<p>Case 1: The impacted section is taken from the edge of the module.</p> 	
<p>Case 2: The impacted section is taken from the middle of the module.</p> 	<p>$d1 = l - b1 - b2$</p> 

FIGURE 5 Linear mass distribution approximation.

Partial Area Approximation

Due to the potential errors in the linear mass distribution approximation, a more refined method was desired. The mass ratio can be approximated using the center position of the barrel relative to the impact events. The mass ratio of each cut section was estimated by dividing the area of the cut section by the area of a circle with a diameter equal to the deceleration distance l_n of the barrel, as geometrically shown in Figure 6.

The hatched areas for Cases 1 and 2 represent a section of a barrel that is contributing to the mass at some impact event. In Case 1, the width of the first barrel section and the length of contact were used to calculate the area K_{b1} . This area is then divided by the area of a circle equal to the length of contact of X_l and multiplied by the mass of the barrel inside the path of the vehicle. In Case 2, a section out of the middle of the barrel was needed. First, area X_2 is calculated by subtracting the areas to the left and right of the middle section. This area is then divided by the area of a circle equal to the length of contact of X_l and multiplied by the mass of the barrel inside the path of the vehicle. The overall length of contact is used, because for situations where the center of the barrel is outside the path of the vehicle, the length of contact is less than the diameter of the barrel.

For Case 1:

$$M_{X_1} = \frac{K_{b1}}{X_l} \cdot M_X \quad (24)$$

$$K_{b_n} = \frac{l_n^2}{4} \cos^{-1} \left(\frac{l_n - 2b_n}{l_n} \right) - \left(\frac{l_n}{2} - b_n \right) \cdot \sqrt{l_n \cdot b_n - b_n^2} \quad (25)$$

For Case 2:

$$M_{X_2} = \frac{X_l - K_{b1} - K_{b2}}{X_l} \cdot M_n \quad (26)$$

Comparison of Mass Distribution Methods

The large sand barrel array shown in Figure 2a was used to compare the different mass distribution techniques, as shown in Table 2. The areas of the segmented barrels were calculated using a 2D CAD program to determine the ideal mass distribution, while the linear approximation and partial areas approximation were incorporated into a spreadsheet program. All three techniques had the same total impacted mass. However, the partial areas distribution had an average absolute error of only 1.85 percent, and the linear method had an average absolute error of 17.12 percent. All three techniques for distributing masses provided identical results for the head-on impact shown in Figure 1.

The mass of a barrel must be mathematically split to allocate mass based on both the path of the vehicle and the impact of and adjacent creating a new impact event. To calculate the actual area of each split segment, there are many possible distribution scenarios that must be considered, as the barrel can be segmented based on two axes. Both the linear and partial areas methods calculate the mass distribution using one axis, drastically reducing the number of scenarios to calculate the mass distribution. The partial areas method provided simplified calculation and minimal error, thus it was selected for implementation into the sand barrel analysis procedure.

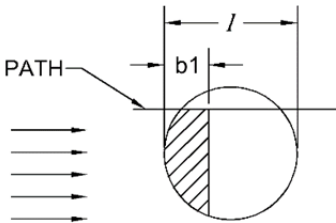
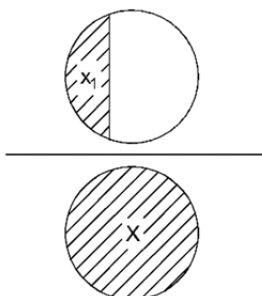
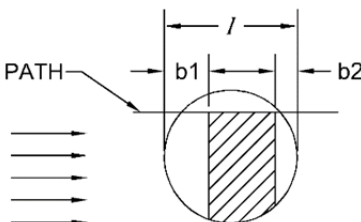
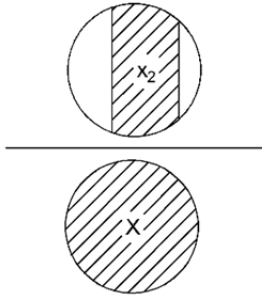
Impact Scenario	Mass Ratio (Partial Areas Approx.)
<p>Case 1: The impacted section is taken from the edge of the module.</p> 	
<p>Case 2: The impacted section is taken from the middle of the module.</p> 	

FIGURE 6 Partial areas mass distribution approximation.

Spreadsheet Program Implementation

Hand calculation sand barrel array impacts with the proposed method would be time-consuming and inefficient. A more practical way to apply this method was to implement it into a spreadsheet program. The sand barrel layout was input in 2D Cartesian coordinates describing the center position of each module with some mass. A vehicle and impact conditions were also needed. For the vehicle, four nodes were used to represent the corners of a vehicle model, as shown in Figure 7.

In Figure 8, the variables are defined as:

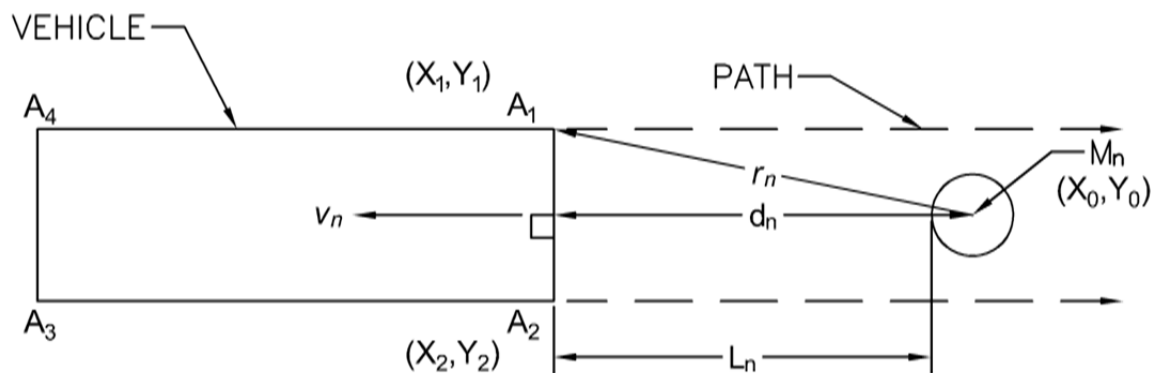
\vec{v}_n	=	Direction vector through center of vehicle
\vec{r}_n	=	Vector from center of barrel to point A ₁ on the front of vehicle
d_n	=	Distance from center of barrel to front of vehicle

Using this model, the distance, d_n , from the front of the vehicle to the center of a barrel can be used to determine the impact order. To find the distance from the vehicle to each barrel, a direction vector, \vec{v}_n , passing through the center of the sand barrel and perpendicular to the front of the vehicle, is created by the line between points A₁ and A₂:

$$\vec{v}_n = \begin{bmatrix} y_2 - y_1 \\ -(x_2 - x_1) \end{bmatrix} \quad (27)$$

TABLE 2 Mass Distribution Method Comparison

Impact Event	Ideal	Linear Approximation		Partial Areas Approximation	
	lb	Lb	Absolute Error	lb	Absolute Error
1	36.1	42.1	16.6%	33.5	7.2%
2	308.7	291.9	5.5%	311.3	0.8%
3	57.7	79.2	37.2%	57.7	0.0%
4	316.4	297.7	5.9%	318.5	0.7%
5	4.7	5.1	7.7%	4.4	6.6%
6	61.6	79.8	29.6%	59.7	3.0%
7	218.4	194.4	11.0%	218.7	0.2%
8	68.4	85.9	25.7%	70.5	3.2%
9	191.2	198.5	3.8%	187.7	1.8%
10	346.2	309.7	10.5%	346.0	0.0%
11	167.3	208.2	24.5%	160.0	4.3%
12	1038.6	984.8	5.2%	1047.0	0.8%
13	347.8	458.8	31.9%	346.6	0.3%
14	2324.6	2184.5	6.0%	2331.1	0.3%
15	259.9	406.6	56.5%	254.6	2.0%
16	145.0	139.8	3.6%	144.9	0.0%
17	1634.6	1468.6	10.2%	1641.2	0.4%
18	370.0	465.0	25.7%	384.5	3.9%
19	851.0	932.8	9.6%	825.8	3.0%
20	1971.2	1749.6	11.2%	1968.7	0.1%
21	628.0	786.2	25.2%	611.1	2.7%
22	2702.0	2561.0	5.2%	2726.8	0.9%
23	465.5	584.6	25.6%	464.2	0.3%
Total Impacted Mass:	14514.8	14514.8		14514.8	
Average Error:			17.12%		1.85%

**FIGURE 7 Simple vehicle model and sand barrel.**

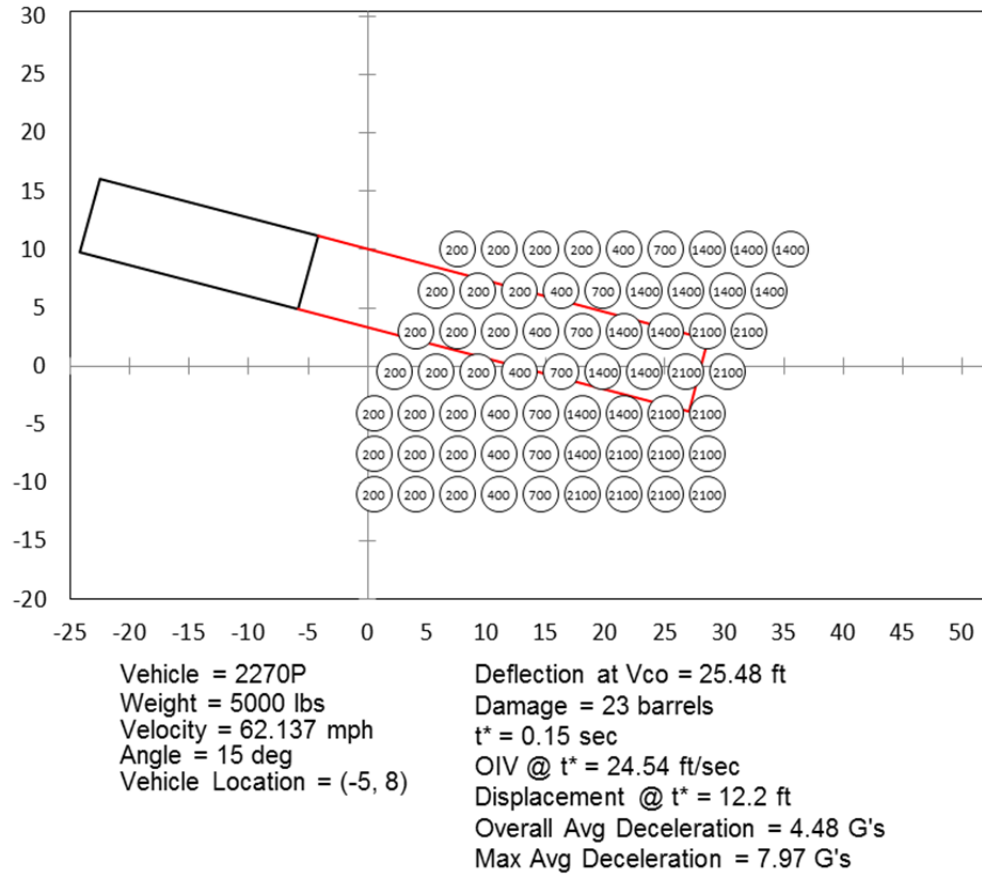


FIGURE 8 Sample calculation for angled impact on irregular barrel array.

Next, a vector is drawn from M_n to point A_1 :

$$\vec{r} = \begin{bmatrix} x_1 - x_0 \\ y_1 - y_0 \end{bmatrix} \quad (28)$$

Finally, the length of the projection of \vec{r} on to \vec{v} yields the distance from the center of the n th sand barrel to the front of the vehicle, d_n :

$$d_n = \frac{(x_1 - x_0)(y_2 - y_1) + (y_1 - y_0)(x_1 - x_2)}{\sqrt{(y_2 - y_1)^2 + (x_2 - x_1)^2}} \quad (29)$$

This process can then be used to find the distance to all of the modules in the system. The distance, L_n , to the front of the vehicle is:

$$L_n = d_n - \frac{c}{2} \quad (30)$$

When the center of a sand barrel is inside the path of the vehicle, the chord length is:

$$c = D \quad (31)$$

Similarly, the module's distance from the left and right sides of the vehicle's path can be determined using (A_4, A_1, M_n) and (A_3, A_2, M_n) , respectively. Calculating the distances from the left and right sides of the vehicle path would allow logic conditions to determine whether or not a module is in the path of the vehicle and if the barrel was fully impacted or partially impacted.

Sample Calculation for Angled Impact on Irregular Barrel Array

The sand barrel array shown in Figure 2a was used as a representative system to evaluate the spreadsheet procedure described in the previous section. With this program, each of the 36-in. diameter sand barrels had a unique mass and (x, y) coordinate, as shown in Figure 8. As noted previously, the partial areas mass distribution method was selected for use in analysis procedure and was implemented in the spreadsheet program. The spreadsheet was also setup to estimate average deceleration and OIV values during the impact.

Using the equations defined previously, the position of the vehicle relative to the barrels was used to determine the impact event order and the relative mass contribution of each impacted barrel. The impact event order and mass, as well as velocity calculation, average deceleration, and occupant impact velocity calculations, are presented in Table 3.

The duration and velocity of each event were used to determine the theoretical occupant impact time of 0.15 seconds. The OIV was 24.5 ft/s, which was below the 40 ft/s limit in MASH. The ORA based on average accelerations was 7.97 g's, which was below the 12-g average deceleration limit for sand barrel analysis. As noted previously, the vehicle was considered to be stopped after the velocity was reduced to less than 10 mph (14.67 ft/s).

This analysis verified that the partial areas approximation could be implemented into a spreadsheet program and that the relevant calculations could be made quickly. This spreadsheet program could be used to determine safe sand barrel arrays for a wide variety of installations and impact conditions.

SUMMARY AND CONCLUSIONS

Sand barrel crash cushion systems are a frequently used safety device due to their low-cost and flexibility. Existing analysis methods for sand barrel crash cushion arrays were developed primarily for head-on impact conditions where all of the sand barrels were impacted in evenly distributed rows. Analysis of non-standard barrel configurations was significantly more time consuming and complex due to calculation of the mass distribution for partially impacted barrels and irregular barrel spacing.

An improved methodology for the analysis of sand barrel arrays was developed based on the principles of momentum transfer that accounts for complex mass distributions of the impacted barrels. Several alternatives for calculating the mass distribution were proposed, including ideal, linear, and partial area mass distributions. Comparison of these alternatives found that the partial area mass distribution provided the best combination of accuracy and ease of computation.

TABLE 3 Inertial Barrier Example Calculations

Impact Order	Sand Weight Per Impact (lbs)	Initial Velocity V_{n-1} (ft/s)	Final Velocity V_n (ft/s)	Deceleration Distance (ft)	Impact Distance (ft)	Average Deceleration (gs)	Event Time (s)	OIV (ft/s)	OD (in.)
1	33.51	91.13	90.53	3.00	0.78	2.1832	0.0086	0.000	0.000
2	311.30	90.53	85.22	3.00	2.60	5.5818	0.0295	0.607	0.063
3	57.73	85.22	84.25	3.00	0.78	3.2654	0.0093	5.913	2.159
4	318.48	84.25	79.20	3.00	2.52	5.0913	0.0308	6.885	2.924
5	4.39	79.20	79.13	1.59	0.08	2.1597	0.0010	11.930	7.333
6	59.74	79.13	78.20	3.00	0.78	2.9122	0.0100	12.000	7.477
7	218.72	78.20	74.92	3.00	1.86	4.1995	0.0243	12.934	9.025
8	70.54	74.92	73.88	2.91	0.74	3.2610	0.0099	16.212	13.744
9	187.70	73.88	71.21	3.00	1.02	5.9307	0.0140	17.254	15.801
10	346.01	71.21	66.60	2.54	1.58	6.2470	0.0229	19.927	19.151
11	160.04	66.60	64.53	3.00	0.78	5.3656	0.0120	24.536*	25.902
12	1047.05	64.53	53.36	3.00	2.60	7.8851	0.0440	26.601	29.722
13	346.63	53.36	49.90	3.00	0.78	7.0760	0.0152	37.775	49.687
14	2331.07	49.90	34.03	3.00	2.60	7.9714	0.0619	41.235	57.206
15	254.62	34.03	32.38	3.00	0.49	3.4993	0.0146	57.101	99.597
16	144.93	32.38	31.47	0.46	0.30	3.0370	0.0093	58.750	109.923
17	1641.16	31.47	23.69	3.00	1.93	3.4601	0.0699	59.663	116.607
18	384.55	23.69	22.00	2.77	0.67	1.7955	0.0293	67.440	173.144
19	825.85	22.00	18.88	3.00	0.91	2.1879	0.0443	69.132	197.444
20	1968.74	18.88	13.55**	2.76	1.69	1.5905	0.1042	72.251	235.859
21	611.09	13.55	12.07**	3.00	0.78	0.7489	0.0612	77.586	332.917
22	2726.77	12.07	7.81**	3.00	2.18	0.6027	0.2197	79.061	391.015
23	464.16	7.81	7.15**	0.20	0.20	0.7730	0.0267	83.322	610.713
								83.985	637.607

* Occupant Impact Velocity

** Velocity 10 mph cutoff (14.67 ft/s)

The new sand barrel crash cushion analysis method was programed into a spreadsheet that allowed for simple and easy variation of the barrel array configuration and the vehicle impact conditions. Once the array and vehicle impact data are input, the spreadsheet determines peak average decelerations, estimated occupant risk values, the number of impacted barrels, and vehicle stopping distance. This updated procedure should allow end users to quickly and efficiently design sand barrel arrays to cover wide and/or non-standard hazards. Additionally, designers will be able to better design their barrel arrays to account for non-standard impacts, such as angled or reverse direction impacts, which are difficult to analyze using existing procedures.

ACKNOWLEDGMENTS

The authors wish to acknowledge the Nebraska Department of Roads for sponsoring this research as part of a larger research effort to develop treatments for intersecting roadways (5).

REFERENCES

1. *Roadside Design Guide*, American Association of State Highway and Transportation Officials (AASHTO), Issue 4, Washington, D.C., 2011.
2. Ross, H. E., D. L. Sicking, R. A. Zimmer, and J. D. Michie. *NCHRP Report No. 350: Recommended Procedures for the Safety Performance Evaluation of Highway Features*, 1993.
3. *Guide for Selecting, Locating, and Designing Traffic Barriers*, American Association of State Highway and Transportation Officials (AASHTO), Washington, D.C., 1977.
4. *Manual for Assessing Safety Hardware (MASH)*, American Association of State Highway and Transportation Officials (AASHTO), Washington, D.C., 2009.
5. Putjenter, J.G., Bielenberg, R.W., Faller, R.K., and Reid, J.D. *Conceptual Development of an Impact-Attenuation System for Intersecting Roadways*, Report No. TRP 03-312-15, Midwest Roadside Safety Facility, UNL, September 30, 2015.

Evaluation of Energy-Absorbing End Terminals Adjacent to Curbs

JENNIFER D. SCHMIDT

RONALD K. FALLER

ROBERT W. BIELENBERG

BROCK SCHRODER

Midwest Roadside Safety Facility⁴

University of Nebraska-Lincoln

ERIK EMERSON

Wisconsin Department of Transportation

Several guardrail end terminals have been developed to shield the end of a longitudinal barrier and function as a redirective barrier when struck along the side. The use of curbs in front of guardrail and end terminals, while undesirable, is often necessary due to restricted right-of-way, drainage considerations, access control, and other functions. Curbs can affect the interaction of errant vehicles with roadside barriers by affecting vehicle redirection and barrier loading. However the performance of energy-absorbing end terminals installed adjacent to curb and gutter is unknown. Little guidance is available to State Departments of Transportation (DOTs) who have installations where curbs are desired adjacent to energy-absorbing, guardrail end terminals. The objective of this research study was to investigate whether curb placement in front of guardrail end terminals significantly degrades system performance. A generic energy-absorbing, W-beam end terminal model was developed to represent existing, compression-based, terminal systems LS-DYNA computer simulation software. All of these systems include an impact head with a guide chute that is placed over the rail end, which dissipates a vehicle's kinetic energy when propelled downstream through changes to the rail shape. Impacts on the end of the terminal (test nos. 3-30, 3-31, 3-32, and 3-33) were evaluated according to NCHRP Report 350 and *Manual for Assessing Safety Hardware* (MASH) safety performance criteria. The simulations were compared to available crash tests data to ensure that the energy-absorbing, end terminal model accurately represented the performance of end terminals. Curbs that were 2 to 6 in. high with a sloped or vertical shape were offset 0 to 6 in. from the face of the Midwest Guardrail System (MGS) model. The performance of the system with and without curbs was compared, and general performance trends were identified.

INTRODUCTION

Several guardrail end terminals have been developed to shield the end of a longitudinal barrier and function as a redirective barrier when struck along the side. Several end terminal systems utilize an energy-absorbing mechanism to safely decelerate errant passenger vehicles that impact the end of the terminal. The FHWA resource charts identified seven energy-absorbing roadside end terminals for W-beam guardrail systems (1):

- 1) Flared Energy-Absorbing Terminal (FLEAT)
- 2) TREND 350 Flared
- 3) Sequential Kinking Terminal (SKT)
- 4) Extruder Terminal (ET-Plus)
- 5) SoftStop

- 6) X-Tension Guardrail End Terminal
- 7) X-Lite Terminal

All of these systems were installed on level terrain and tested at Test Level 3 (TL-3) of the NCHRP Report 350 (2) or the *Manual for Assessing Safety Hardware* (MASH) (3). However, the performance of these energy-absorbing end terminals may change if a curb is installed adjacent to the terminal, and little guidance is available to State Departments of Transportation (DOTs) who have installations where a curb is required adjacent to energy-absorbing end terminals.

Highway design policy typically discourages the use of 6- to 8-in. vertical curbs on high-speed roadways because of their potential to cause drivers to lose control in a crash (4). Curbs can also affect the interaction of errant vehicles with roadside barriers by affecting vehicle redirection and barrier loading. However, the use of curbs is often required because of restricted right-of-way, drainage considerations, access control, and other functions. Often, there is a need to offset the guardrail from the curb to reduce the propensity for snow plows to gouge and/or damage the W-beam rail sections or to allow for placement of sidewalks between the road and a barrier or other roadside features.

When curbs are required, the offset of the barrier from the curb has been shown to be critical in the performance of the system through modeling and crash testing. For example, when a 6-in. tall AASHTO Type B curb was placed 8 ft in advance of the Midwest Guardrail System (MGS) and tested MASH TL-3, the pickup truck became unstable and rolled over (5). Previous work with steel-post, nested W-beam guardrail has shown that a 4-in. high sloped curb with the toe of the curb placed flush or set out 1 in. from the front face of the guardrail is capable of meeting NCHRP Report No. 350 Test Level 3 (TL-3) safety requirements, and sloped curbs no higher than 4-in. tall should be used when speeds are above 52.8 mph (6-9). MASH TL-3 testing has demonstrated that the MGS can be used with a 6-in. tall, AASHTO Type B curb positioned 6 in. in front of the face of the guardrail element (10-11).

While curbs can be used adjacent to guardrail at small offsets, the use of curbs adjacent to energy-absorbing end terminals has not been evaluated. Therefore, the objective was to investigate whether curb placement in advance of W-beam, energy-absorbing end terminals significantly degrades terminal performance on high-speed roadways requiring MASH TL-3 guardrail. Suggestions were made about the placement of curbs and gutters installed adjacent to energy-absorbing guardrail end terminals.

METHODOLOGY

Several Midwest States Pooled Fund program member State DOTs were surveyed regarding their energy-absorbing end terminal installations. Based on the results of the survey, most State Departments of Transportation installed the ET-Plus, SKT, and FLEAT end terminal systems. These compression-based systems all involved an end terminal head that translates longitudinally along the end terminal rail upon impact and has an energy-absorbing mechanism that deflects guardrail laterally behind or in front of the guardrail system. Most State DOTs utilized 31-in. high guardrail. Tangent and flared end terminal systems were commonly used, and many tangent end terminals were installed with a 1:25 or 1:50 flare to

offset the impact head farther from the roadway, and, in cases where curbs are present, to allow for the anchorage posts to be installed behind a curb. Several State DOTs have at least a few curbs that were installed adjacent to energy-absorbing end terminal systems on high-speed roadways. The curbs were typically installed with the toe flush with the face of the rail or at a 6-in. offset. Most State DOTs used a constant-sloped curb, and two States use a vertical curb. The curb height may be up to 6 in., although 4-in. curbs were used most frequently.

Energy-absorbing W-beam guardrail end terminals, must satisfy impact safety standards in order to be declared eligible for federal reimbursement by the FHWA for use on the National Highway System. These devices should also be tested with geometric features, such as curbs, to fully understand the effect that curbs may have on end terminal performance. For new hardware, these safety standards consist of the guidelines and procedures published in MASH (3). According to TL-3 of MASH, end terminals must be subjected to nine full-scale vehicle crash tests:

1. 3-30 with a 2,425-lb small car, designated 1100C, impacting end of terminal at 62 mph and 0 degrees at a quarter-point offset
2. 3-31 with a 5,000-lb pickup truck, designated 2270P, impacting end of terminal at 62 mph and 0 degrees
3. 3-32 with a 1100C impacting end of terminal at 62 mph and 5/15 degrees
4. 3-33 with a 2270P impacting end of terminal at 62 mph and 5/15 degrees
5. 3-34 with a 1100C impacting critical impact point between gating and capturing behavior at 62 mph and 15 degrees
6. 3-35 with a 2270P impacting beginning of length of need at 62 mph and 25 degrees
7. 3-36 with a 2270P impacting at critical impact point with respect to the backup structure at 62 mph and 25 degrees
8. 3-37 with a 1100C and/or 2270P impacting in reverse direction at 62 mph and 25 degrees
9. 3-38 with a 3,300-lb sedan impacting end of terminal at 62 mph and 0 degrees

In lieu of conducting several full-scale crash tests to evaluate end terminal systems with curbs, a computer simulation effort was conducted and the results were evaluated with MASH evaluation criteria. Test nos. 3-30 through 3-33 involve impacts on the end of the system. Test nos. 3-34 through 3-37 involve impacts along the length of the system, which was not evaluated as the results of impacts along the length are expected to be similar to impacts along the length of W-beam guardrail with a curb, which was previously evaluated according to safety performance criteria. Test no. 3-38 is only recommended if a force vs. deflection analysis predicts that the terminal will not meet occupant impact velocity and ridedown acceleration, which is not expected to be the case, so this test was not evaluated.

Based on the results of the survey and with sponsor direction, a plan was devised for evaluation of energy-absorbing end terminal systems. Since several State DOTs install more than one type of system, a generic end terminal system that was representative of compression-based systems was developed rather than investigating a singular proprietary system or multiple systems.

END TERMINAL MODEL

Several end terminal systems involve an impact head that translates longitudinal along the end terminal system upon impact and has an energy-absorbing mechanism that deflects guardrail laterally behind or in front of the guardrail system, including the ET-2000, BEST (Beam Eating Steel Terminal), SKT, FLEAT, and ET-Plus. The ET-2000 and BEST were not included in the FHWA resource chart, but both have been crash tested and evaluated according to NCHRP Report 350 and are similar to the others. These five systems all had a 50-ft system length option, thus this length was selected for the design.

The representative end terminal model consisted of several components:

1. 50-ft long tangent end terminal system with 8 posts spaced at 6 ft – 3 in., consisting of
 - a. 2 breakaway cable terminal (BCT) wood posts and anchorage system similar to the MGS downstream anchorage (12);
 - b. 6 controlled release terminal (CRT) wood posts with blockouts embedded 40 in.;
 - c. 12-gauge W-beam guardrail sections
 - d. W-beam guardrail splices located every 12 ft – 6 in. at the midspans between post nos. 3 and 4, 5 and 6, and 7 and 8;
 - e. Impact head; and
 - f. Impact head support bracket attached to post no. 1;
2. 19 W6x9 steel posts with blockouts spaced at 6 ft – 3 in. embedded 40 in. for MGS, and 43¼ in. for G4(1S);
3. 2 BCT posts with the MGS downstream anchorage spaced at 6 ft – 3 in.;
4. 13-ft 6½-in. W-beam guardrail sections; and
5. W-beam guardrail splices located every 12 ft – 6 in. at the midspans between posts.

The dimensions of each system's impact head component varied and were averaged for the five systems, resulting in a representative system, as shown in Figure 1. Complete details of the system are provided by Schmidt, et al. (13). The impact head consisted of a 3/16-in. thick shell-element face plate, tapered head, and chute. The downstream end of the chute had a 180-degree, ½-in. diameter rounded corner to prevent contact problems from occurring when the chute impacted posts and blockouts. The interior of the chute had several rounded ¼-in. thick shell-element guide spacers merged to the chute to keep the W-beam rail centered vertically in the chute. A rectangular solid post breaker was attached to the chute to initiate fracture of post 1. The component interfaces were connected using merged nodes. The parts were modeled with a deformable steel material, with the exception of the chute, which was modeled with a rigid steel material.

The energy-absorbing mechanism in each of the end terminal systems varies greatly. Due to the variability between systems, the energy absorbing mechanism was not modeled for the generic end terminal system. However, the force to decelerate a vehicle is somewhat similar between end terminals. Coon previously determined the average force exerted during an impact with energy-absorbing end terminals ranged from 10.5 kips to 22.5 kips for the various systems (14-15). The average force range was determined by analyzing the rail deflection versus vehicle velocity and applying conservation of momentum during several full-scale crash tests. An average force that was representative of the forces produced by the energy absorbing

mechanisms was utilized for the simulations. While there was no determination whether higher or lower values in the force range would be more critical, a representative force in the middle of the range was desired. Thus, an average longitudinal and lateral force of 11.2 kips and 1.1 kips, respectively, was applied to the impact head at Node no. 1, as shown in Figure 1d, using the keyword *LOAD_MOTION_NODE. However, this applied force in the simulation only represented the energy-absorbing mechanism in the impact head whereas the average forces from full-scale crash testing included the energy-absorbing mechanism in the impact head plus post fracture, vehicle deformation, and other energies. Due to the modeling methodology used to simulate the energy-absorbing mechanism, the simulated guardrail will not be loaded in compression like an actual installation, so the guardrail buckling location in the simulations due to compression was not very accurate.

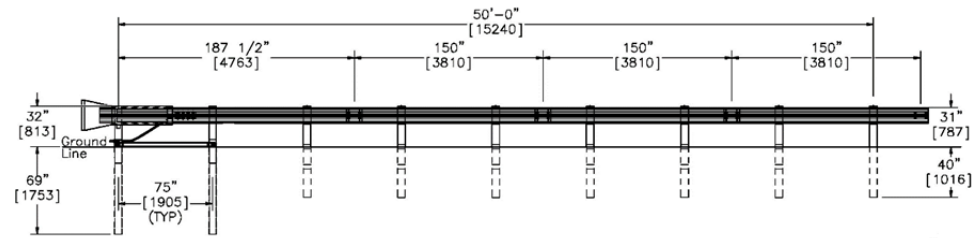
Since the internal structure of the impact head did not include the energy-absorbing mechanism, nine steel tubes connected the face plate and to an internal plate that spanned the height and width of the tapered impact head to add rigidity to the head. The internal plate was located longitudinally at 5¾ in. from the impact face plate, which was approximately where the W-beam would exit the side of the impact head. A rigid plate was merged to the internal plate, which included Node no. 1, where the end terminal force was applied. The total weight of the impact head was 220 lb.

All of the systems were tested with a 27¾-in. rail height and with wood posts spaced at 6 ft – 3 in installed in soil. Most also have steel post options, some which are proprietary, for the anchorage (post nos. 1 and 2) and/or the line posts (post no. 3 and downstream). The steel and wood post options were designed to be similar, so it was not necessary to evaluate each type. BCT wood posts and CRT wood posts were selected for the anchorage posts and the line posts, respectively, which had a calibrated failure region defined in the model.

End terminal system anchorages typically include a groundline strut to distribute loads between post nos. 1 and 2, steel soil tubes embedded in soil that contain the CRT posts, a cable anchor that spans between the bottom of post no. 1 and a cable anchor bracket attached to the W-beam. The cable anchor bracket disengages when impacted by the impact head, which releases tension in guardrail. Many of the anchorage parts are unique to each energy-absorbing end terminal system; however, they perform similarly. Therefore, the cable anchor bracket and posts utilized in the MGS downstream anchorage parts were incorporated into the simulation as a non-proprietary option (12). However, the downstream anchorage cable bracket does not disengage when impacted. Thus, the disengagement was simulated by deleting the part at the appropriate time using construction stages.

Most end terminals do not include a standard post-to-rail bolt at post no. 1. Rather, no bolt is present to allow the post to release easily, and a bracket is attached to the side of Post no. 1, which supports the impact head. This was replicated in the simulation with a rectangular support tied to the front face of post 1 that supported the impact head.

All of the systems utilized AASHTO M-180 W-beam guardrail. However, the length of each section and the location of rail splices varies by system. In general, the rail splices for 27¾-in. tall systems are located at post nos. 3, 5, 7, etc. For the 31-in. tall systems, most systems have rail splices located at the midspan between posts. However, the location of the first rail splice from the end of terminal varies by manufacturer. For example, different 31-in. tall systems may have the first rail splice located at post no. 3 or at the midspan between post nos. 3 and 4. The location of the rail splices may affect the performance of end terminals. When rail splices are located at posts, the rail becomes stiffer than when splices are located the midspans between

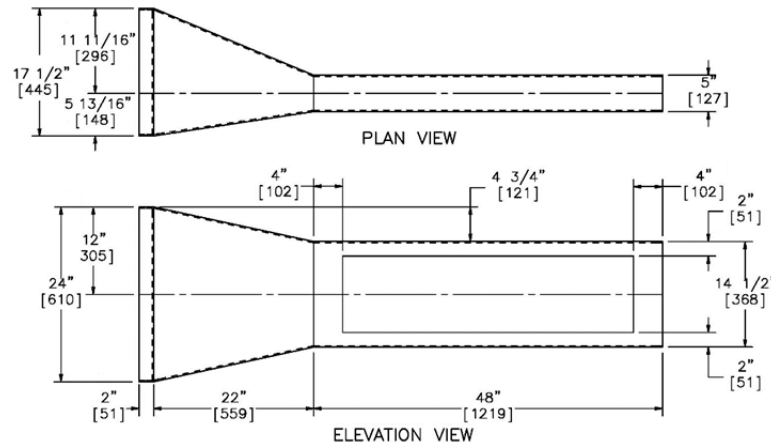


ELEVATION VIEW

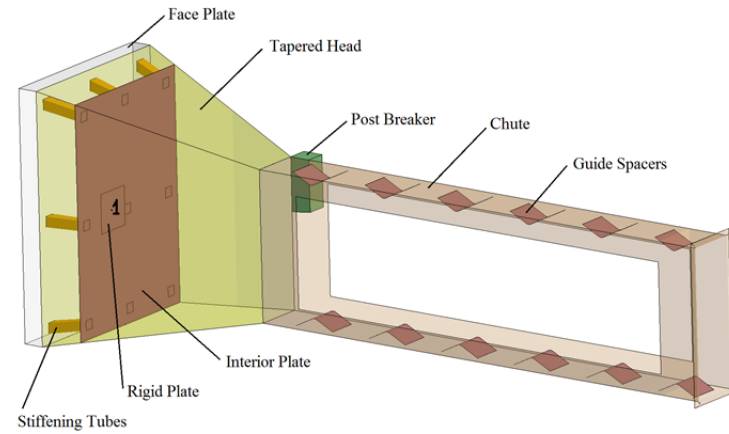
(a)



(b)



(c)



(d)

FIGURE 1 Representative end terminal, (a) representative end terminal: overall layout, (b) end terminal model layout: dimensions of impact head, (c) representative impact head: model layout, and (d) model impact head, parts shown transparent: model impact head.

posts, due to overlapping guardrails plies with splice bolts and the post bolt. In the model, the first rail splice was located at the midspan between post nos. 3 and 4. The splices were located at the midspans between posts in both the MGS and G4(1S) models.

The W-beam rail was modeled with no failure defined. In impacts on the end of end terminals, the W-beam rail may tear at the slots as the post-to-rail bolts release. However, no failure was defined in the W-beam guardrail material, so tearing could not occur. Without failure in the material, significant rail deformations occurred when the post bolt heads snagged on the rail elements. This led to instabilities in the simulations, especially with the impacts with the 2270P model where large rail deformations occurred. To account for the lack of guardrail material failure, parameters on the *CONTROL_SHELL card were activated to delete excessively distorted elements. The distorted element deletion modeling technique is not predicative of where actual tearing would occur in the rail but is used to overcome the lack of material failure.

Since the energy-absorbing mechanism was not modeling, the rail did not feed out the side of the impact head. Instead, construction stages were utilized to sequentially delete the rail at the point where it would have exited the impact head in a real impact for visualization purposes. No contact was defined between the vehicle models and the guardrail due to the model simplifications. Therefore, if the vehicle model lost contact with impact head and subsequently contacted the rail, the contact between the vehicle model and rail was not accurate.

BASELINE SIMULATIONS

The 175-ft long MGS LS-DYNA finite element analysis model previously developed and validated at MwRSF was modified to incorporate the end terminal system (16). Two variations of the 29-post long model were created:

1. 27³/₄-in. tall guardrail with posts with 8-in. deep blockouts representative of G4(1S) with an end terminal
2. 31-in. tall guardrail with posts with 12-in. deep blockouts representative of MGS with an end terminal

Four vehicle models were used to evaluate the end terminal. The NCHRP Report 350 820C vehicle was the Geo Metro small car. The NCHRP Report 350 2000P vehicle was the Chevrolet c2500 pickup truck. The MASH 1100C vehicle was the Toyota Yaris small car. The MASH 2270P vehicle was the Chevrolet Silverado pickup truck modified with a detailed tire model.

Eight different test designations from NCHRP Report 350 and MASH were simulated on the generic end terminal installed on MGS and G4(1S), as follows:

1. 820C (Geo) impacting end at 0 deg at quarter point offset (NCHRP Report 350 test no. 3-30)
2. 2000P (C2500) impacting end at 0 deg (NCHRP Report 350 test no. 3-31)
3. 820C (Geo) impacting end at 15 deg (NCHRP Report 350 test no. 3-32)
4. 2000P (C2500) impacting end at 15 deg (NCHRP Report 350 test no. 3-33)
5. 1100C (Yaris) impacting end at 0 deg at quarter point offset (MASH test no. 3-30)

6. 2270P (Silverado) impacting end at 0 deg (MASH test no. 3-31)
7. 1100C (Yaris) impacting end at 5/15 deg (MASH test no. 3-32)
8. 2270P (Silverado) impact end at 5/15 deg (MASH test no. 3-33)

NCHRP Report 350 and MASH test 3-30 were simulated at shallow (3/4 of the car towards the traffic-side) and deep (1/4 of the car towards the traffic-side) quarter point offsets. MASH tests 3-32 and 3-33 tests were simulated at both 5 and 15 degrees. Even though full-scale crash testing did not exist with all of these impact conditions, the simulations were conducted to provide more results for comparison.

Specific simulation results that were evaluated included interaction with the impact head, occupant risk measures, vehicle stability, guardrail feed length, average end terminal forces, and vehicle and system damage. The occupant risk measures included longitudinal and lateral occupant impact velocities (OIV) and occupant ridedown accelerations (ORA) that were calculated using acceleration data with a minimum 10,000 Hz frequency from the local c.g. node of the vehicle and then processed as defined in MASH. The average end terminal force was calculated based on the procedure established by Coon (14-15) for NCHRP Report 350 and MASH test 3-31.

The simulation results were compared to available 27¾ in. and 31 in. tall end terminal full-scale crash test data from the five compression-based terminals. The comparison of simulation and test results for NCHRP Report 350 test designation no. 3-31 is provided as an example in Figure 2. With the NCHRP Report 350 test designation 3-31 crash tests, the rail feed lengths with 31-in. tall guardrail were, on average, significantly greater than 27¾ in. tall guardrail. The simulations also showed an increase in feed length with rail height for 3-31 tests, although not as significant of a difference as seen in the crash tests. The average terminal force was calculated to be 17.5 kips, which was near the middle of the desired range of 10.5 to 22.5 kips.

The overall vehicle and system behavior and guardrail feed length were compared and calibrated to match NCHRP Report 350 test designations 3-30, 3-31, 3-32, and 3-33 crash tests. The rail feed lengths were similar to the crash tests in almost every simulation. The rail buckle locations was also very similar for NCHRP Report 350 3-32 and 3-33. The vehicle roll, pitch, and yaw were similar for all simulations and crash tests, except MASH 3-30, where the rail buckling was not accurate. Thus, yaw also differed. The lateral and longitudinal OIV and ORA in most of the simulations were below the limits established in NCHRP Report 350 or MASH. Two simulations, NCHRP Report 350 test 3-30 with 31-in. tall guardrail and MASH test 3-32 at a 5-degree impact angle with 27¾-in. tall guardrail exceeded the longitudinal ORA value of 20 g's. However, the high acceleration occurred when a post-to-rail bolt snagged as it tried to release. As discussed previously, rail release when impacted end-on has not been calibrated due to lack of modeling steel material tearing. In addition, all of the simulations tended to over predict occupant risk measures when compared to crash tests. Since none of the specific end terminals were modeled, the occupant risk values were not expected to compare with crash tests and were calculated to compare trends between simulations. Of note, very few crash tests were available with a 31 in. tall guardrail height. Overall, the comparisons were reasonably close. The complete results of the baseline simulations and comparisons to crash tests can be found in Schmidt, et al. (13).

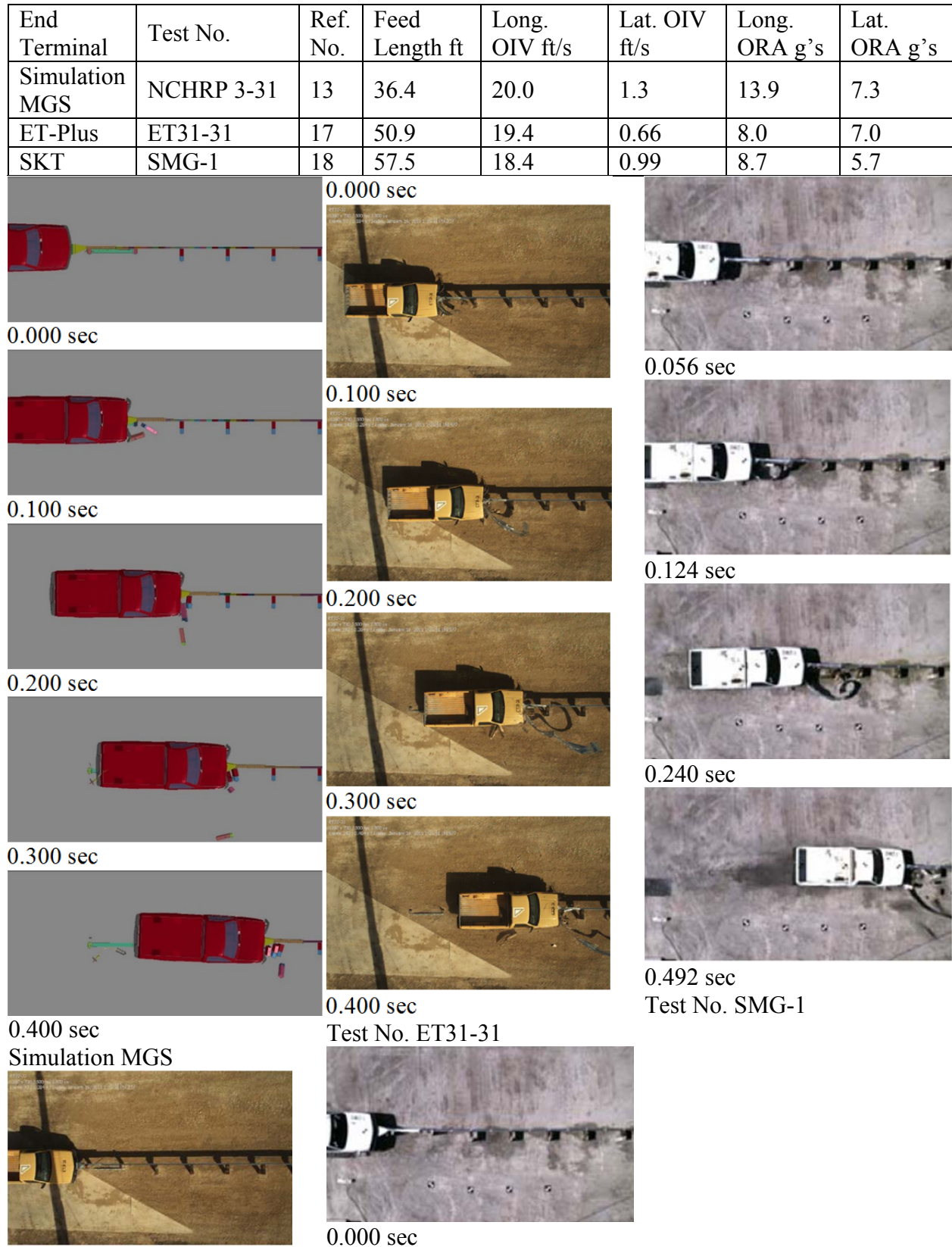


FIGURE 2 NCHRP Report 350 test no. 3-31 comparison with 31 in. tall guardrail.

SIMULATIONS WITH CURBS

After calibration of the model with several baseline tests, several curb configurations were incorporated into the model and simulated with MASH 3-30 (both deep and shallow quarter point offset), 3-31, 3-32 (both 5- and 15-degree impact angles), and 3-33 (both 5- and 15-degree impact angles) impact conditions. The configurations included 2-in., 4-in., and 6-in. tall sloped and vertical-shaped curbs with the toe offset 0 in. and 6 in. in front of the face of the guardrail. Thus, twelve curb configurations were simulated for each MASH test designation simulation.

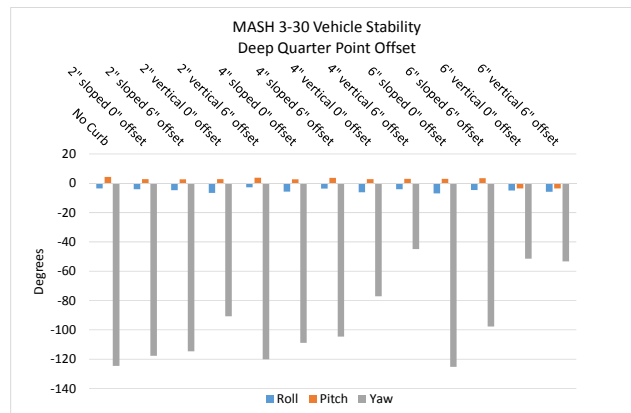
The curb was modelled as if it had soil backfill behind it, and the top rail height was 31 in. above the top of the curb. Although many guardrails are installed at small offsets with the height relative to the roadway surface or toe of the curb, the sponsor suggested that end terminals are commonly installed with the height relative to the top of the soil, so that the breakaway and groundline features remain at groundline.

The presence of curbs at a 0-in. or 6-in. offset did not affect test designation no. MASH 3-31. In these cases, the left-side of the pickup truck was on top of the curb and the right-side of the pickup truck was on the roadway, and the impact height on the impact head varied minimally from the baseline simulation. In the simulations of test designation no. MASH 3-30, the interaction with the impact head, occupant risk, feed lengths, roll, and pitch were minimally affected by the presence of curbs, due to the same reason as MASH 3-31. However, since the vehicle yaws due to the quarter-point impact location, the 4-in. and 6-in. tall vertical curbs noticeably affected vehicle yaw as the sidewall of the tires snagged on the curbs while the vehicle model was not tracking, as shown in Figure 3. The vertical curbs also affected the Yaris yaw in test designation MASH 3-32 at a 5-degree impact angle.

The vehicle and terminal performance was most similar to the baseline simulations with 2-in. tall curbs than 4-in. and 6-in. However, in MASH 3-32 with a 5-degree impact angle, high longitudinal ORAs occurred. The reason for these high longitudinal ORAs was that the post-to-rail bolt snagged significantly as it tried to release from posts 3 and 4. This happened in all MASH 3-32 5-degree simulations as the car pushed upwards on the impact head and guardrail due to the presence of sloped and vertical curbs. In the simulation with the 4-in. tall sloped curb, the rail buckled shortly after impact. Sequential photographs of the MASH 3-32 5-degree impact with no curb and 2-in. and 4-in. tall sloped curb simulations are shown in Figure 4. The maximum roll and pitch also increased and the feed lengths decreased with curbs. While the post-to-rail release was not calibrated, as mentioned previously, the slight uplift on the impact head and guardrail accentuated by the curb is likely to occur. However, it is unknown if it would affect the rail release without full-scale crash testing.

In MASH 3-32 with a 15-degree impact angle, the rails always buckled around post 3, and the feed lengths remained the same. The vehicle pitched in the opposite direction and the lateral and longitudinal ORA increased when curbs were present. However, much of the yaw and increased occupant risk values was believed to be due to the impact head nodes snagging in the bumper and hood and not releasing from the vehicle, which would not be expected in full-scale crash testing. While changing the contact definition improved this behavior, it was not remedied.

In MASH 3-33 with both the 5- and 15-degree impact angles, the pitch increased with increased curb heights. In MASH 3-33 with a 5-degree impact angle, the feed lengths decreased with 6-in. tall curbs. In MASH 3-33 with a 15-degree impact angle, the feed lengths were consistent with the rail buckling at post 2 or 3, both of which are likely to happen based on crash testing.



(a) Vehicle Stability

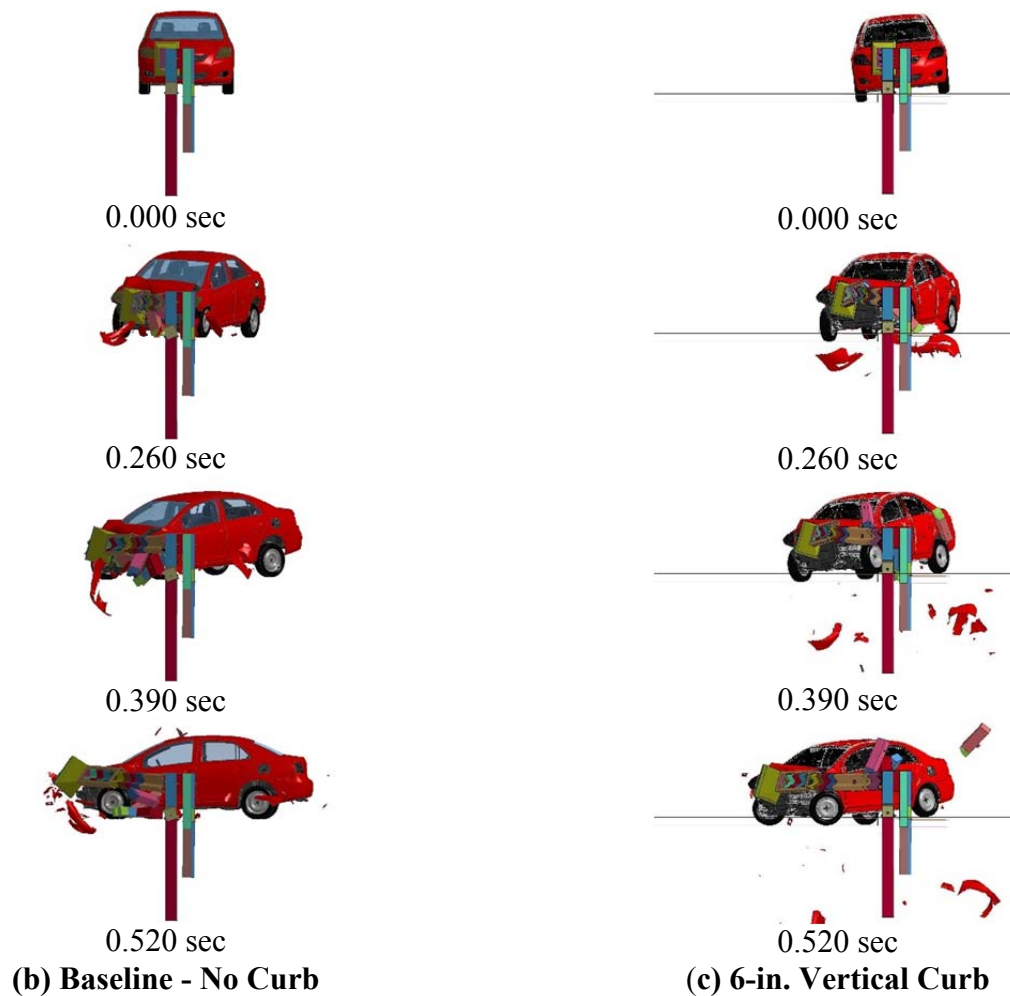


FIGURE 3 Test no. 3-30 at deep quarter point: (a) vehicle stability, (b) no curb, and (c) 6-in. vertical curb.

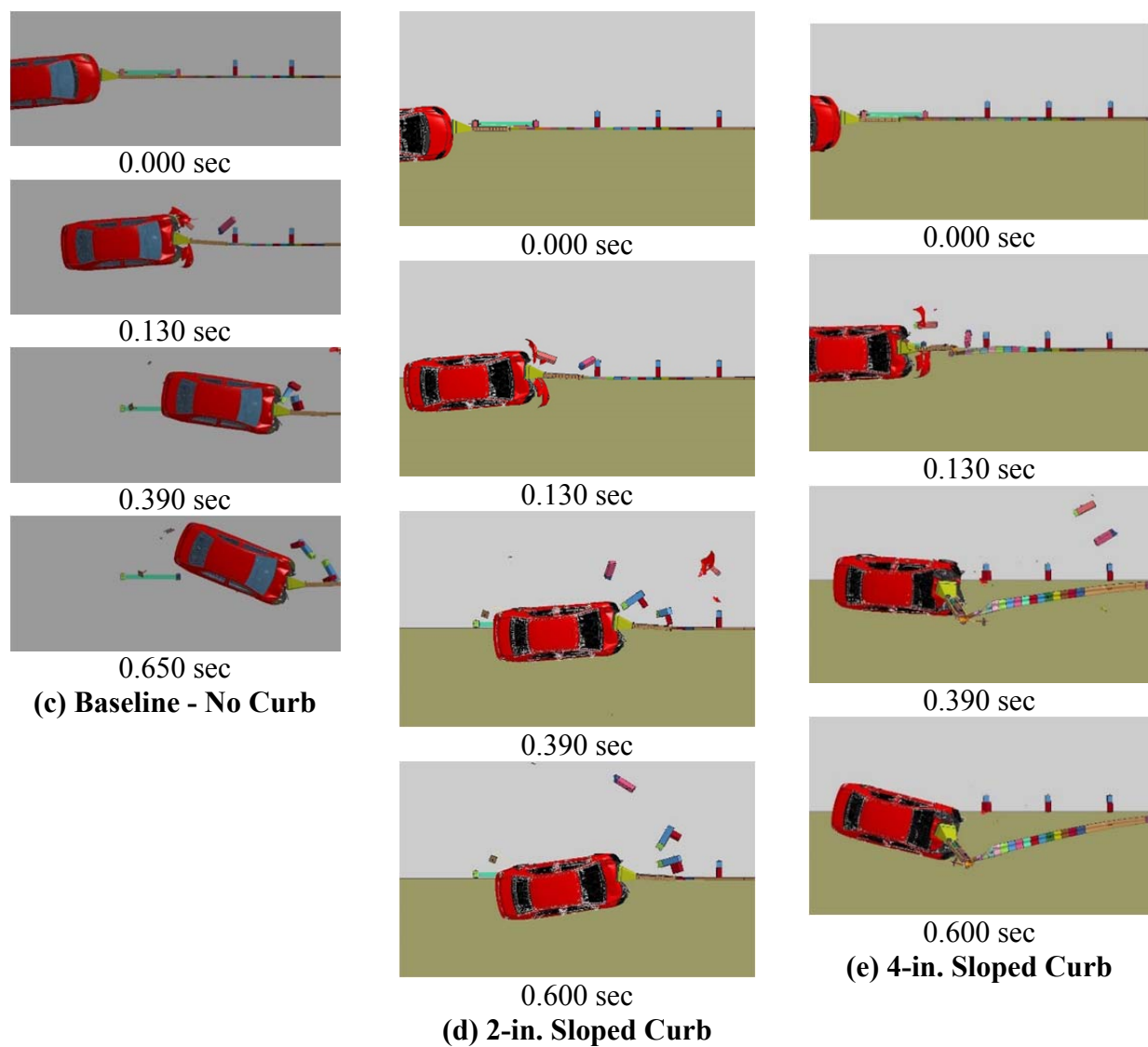
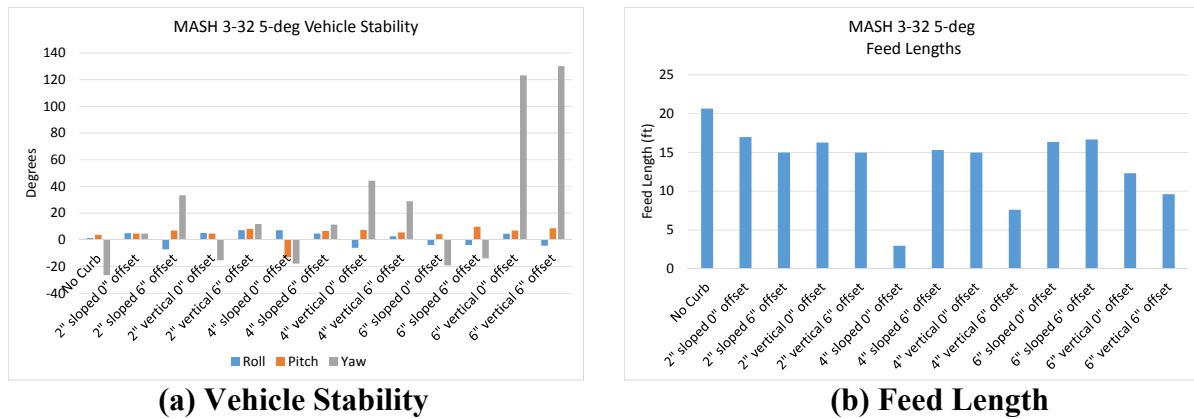


FIGURE 4 Test no. 3-32 at 5-degree impact angle, (a) vehicle stability, (b) feed length, (c) no curb, (d) 2-in. tall sloped curb, and (e) 4-in. tall sloped curb.

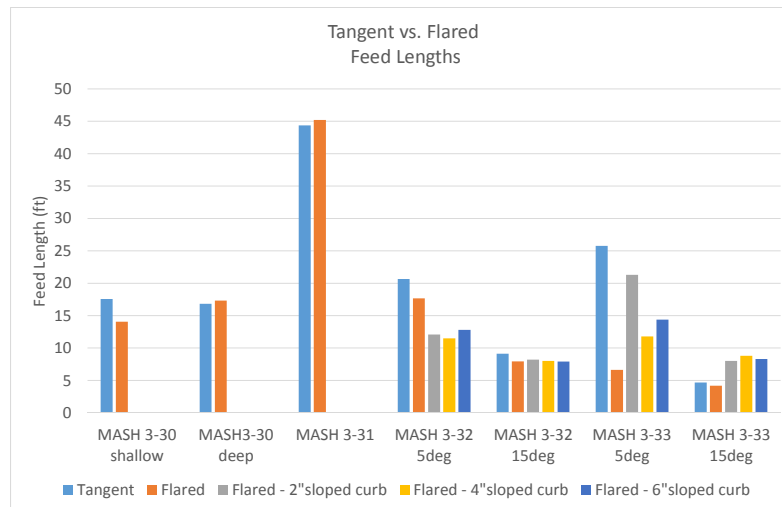
None of the simulations showed an inherent behavior that the system would fail MASH criteria, unless post-to-rail bolt release becomes hindered, especially at the shallow-angle impacts. However, this behavior cannot be fully evaluated with simulation. The lateral and longitudinal OIVs varied minimally in all of the simulations. The complete results of the simulations with curbs can be found in Schmidt, et al. (13).

SIMULATIONS WITH FLARED END TERMINAL

Since many State DOTs flare their tangent end terminals, the model was modified with a 1:25 flare rate with a 2-ft lateral offset. The seven impact conditions were simulated again without a curb. There were minimal changes in the barrier performance between the tangent and flared configurations. The most notable difference was the feed length was significantly less in test no. MASH 3-33 with a 5-degree impact angle when flared vs. tangent. The flared system buckled and gated more quickly than the tangent system, which led to the decreased feed lengths, as shown in Figure 5. However, there was no indication that this would negatively affect the system performance.

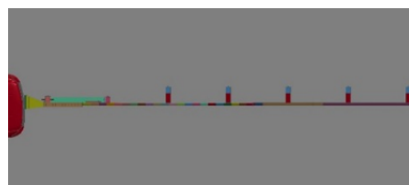
Three curb configurations (2-in., 4-in., and 6-in. tall sloped) were simulated at a 0-in. offset from the face of the tangent guardrail. Test nos. MASH 3-30 and MASH 3-31 were not simulated with curbs as the system would be expected to behave similar to the flared baseline simulations as the whole vehicle would be on top of the curb and may not interact with it at all until very late in the event. However, test nos. MASH 3-32 and MASH 3-33 at 5- and 15-degree impact angles were simulated. The Yaris and Silverado model suspension and steering was not believed to be correct as the tires turned significantly almost immediately after impacting the curbs, especially at a 5-degree impact angle. Because the curb was close to the impact head, the heading angle of the vehicle and vehicle impact with the impact head was still close to the targeted impact conditions for all 15-degree impact angles. However, some of the results at the 5-degree impact angles may not provide good comparisons as the centerline of the impact head was not at the centerline of the vehicle. The limitations with the vehicle model suspension and steering with curb impacts needs to be improved for future studies.

The lateral and longitudinal OIVs varied minimally in all of the simulations. The impact head nodes snagged on the Yaris hood and bumper, especially in the MASH 3-32 5- and 15-degree impacts, which caused the vehicle to yaw and decelerate quickly. The feed lengths remained the same or decreased with the presence of curbs. In general, the vehicle and terminal performance was not degraded significantly by the presence of a flared, tangent terminal with sloped curbs. The complete results of the simulations with flared end terminals can be found in Schmidt, et al. (13).



(a) Feed Lengths

(b)



0.000 sec



0.180 sec

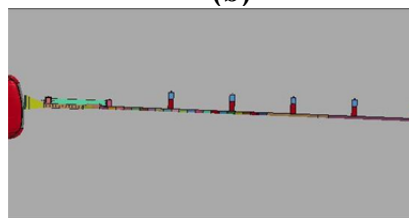


0.540 sec

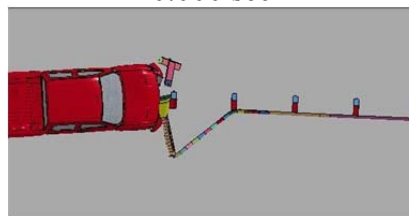


0.720 sec

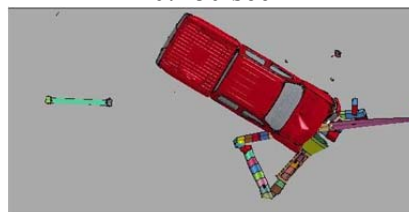
(b) Tangent



0.000 sec



0.180 sec

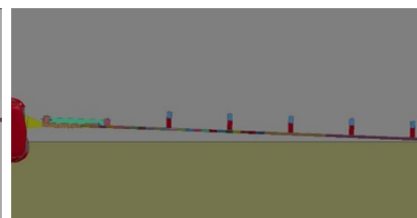


0.540 sec



0.720 sec

(c) Flared



0.000 sec



0.180 sec



0.540 sec



0.720 sec

(d) Flared, 4-in. Sloped Curb

FIGURE 5 Comparison of test no. 3-33 at 5 degrees – flared vs. tangent terminal, (a) feed lengths, (b) tangent, (c) flared, and (d) flared with 4-in. sloped curb.

CONCLUSIONS

An end terminal model was created to be representative of typical W-beam, compression-based energy-absorbing end terminals. Several simulations were conducted on tangent energy-absorbing end terminals attached to G4(1S) and MGS guardrail with and without curbs with impacts on the end of the terminal (NCHRP and MASH test designation nos. 3-30, 3-31, 3-32, and 3-33). The tangent end terminal was also flared at a 1:25 flare rate and evaluated with and without curbs. The curb configurations evaluated 2-in., 4-in., and 6-in. tall wedge and vertical-shaped curbs with the toe offset 0-in. and 6-in. in front of the face of the guardrail. All simulations were conducted with the curb extending in advance of and along the entire length of the end terminal.

Conclusions that were drawn from the study include;

1. Due to the small curb offsets, the vehicle interaction with the impact head was minimally affected by the curbs. However, larger curb offsets may have more of an effect on the vehicle trajectory and interaction with the impact head.
2. The presence of curbs affected the small car impacts the most. The 4-in. and 6-in. tall vertical curbs affected vehicle yaw in the small car impacts and the tires had a more difficult time traversing the curb, especially when the tires were non-tracking. The sloped curbs minimally affected vehicle yaw.
3. The flare affected the performance of the vehicle and end terminal the most in MASH 3-32 and 3-33 angled impacts.
4. The vehicle and terminal performance was most similar to the baseline simulations with 2-in. tall curbs than 4-in. and 6-in.

The computer simulations had several limitations for improvements of future similar studies, including:

1. Modeling one specific end terminal rather than a representative terminal and validating against crash tests specific to that system;
2. Calibrating and validating post-to-rail bolt release and tearing that may occur as the bolt releases in end terminal impacts;
3. Conducting a curb traversal study at shallow angles with the current MASH vehicles and calibrating the vehicle steering and suspension models.
4. Improving the contact between the impact head and vehicle models.

Due to the limitations with the computer simulation, it would be beneficial for full-scale crash testing be conducted on tangent and flared end terminals in conjunction with 4-in. tall or shorter sloped curbs, especially with MASH test designation nos. 3-30 and 3-32 where the curb significantly affected vehicle yaw and trajectory, to further evaluate the effects of curbs on end terminal performance. Additionally, further research may be required to evaluate impacts along the length of the end terminal. As noted previously, the height of the guardrail was relative to the top of the curb to keep breakaway features at groundline, whereas previous testing on the length-of-need of W-beam guardrail systems has been with a rail height relative to the roadway surface, or toe of the curb, at small curb offsets. Therefore, further consideration should be given to the rail height and/or the location of the breakaway features relative to groundline.

ACKNOWLEDGMENTS

The authors wish to acknowledge several sources that made a contribution to this project: (1) Wisconsin Department of Transportation and Erik Emerson for sponsoring the project and providing guidance; (2) Livermore Software Technology Corporation (LSTC) for LS-DYNA support; and (3) the Holland Computing Center at the University of Nebraska for the high-performance computing resources.

REFERENCES

1. Federal Highway Administration. *Roadside Terminals*. http://safety.fhwa.dot.gov/roadway_dept/policy_guide/road_hardware/resource_charts/roadsideterminals.pdf. October 2012. Accessed July 2014.
2. Ross, H.E., D.L. Sicking, R.A. Zimmer, and J.D. Michie. *NCHRP Report 350: Recommended Procedures for the Safety Performance Evaluation of Highway Features*, 1993.
3. *Manual for Assessing Safety Hardware*, AASHTO, Washington, D.C., 2016.
4. *A Policy on Geometric Design of Highways and Streets*. Fifth Edition, AASHTO, Washington, D.C., 2004.
5. Thiele, J.C., K.A. Lechtenberg, J.D. Reid, R.K. Faller, D.L. Sicking, and R.W. Bielenberg. *Performance Limits for 6-in. (152-mm) High Curbs Placed in Advance of the MGS Using MASH Vehicles Part II: Full-Scale Crash Testing*. Report No. TRP-03-221-09, Midwest Roadside Safety Facility, University of Nebraska-Lincoln, October 2009.
6. Polivka, K.A., R.K. Faller, D.L. Sicking, J.R. Rohde, J.D. Reid, and J.C. Holloway. *Guardrail and Guardrail Terminals Installed Over Curbs*. Report No. TRP-03-83-99, Midwest Roadside Safety Facility, University of Nebraska-Lincoln, March 2000.
7. Polivka, K.A., R.K. Faller, D.L. Sicking, J.R. Rohde, J.D. Reid, and J.C. Holloway. *Guardrail and Guardrail Terminals Installed Over Curbs – Phase II*. Report No. TRP-03-105-00, Midwest Roadside Safety Facility, University of Nebraska-Lincoln, November 2001.
8. Bullard, D.L. and W.L. Menges. *NCHRP Report 350 Test 3-11 on the G4(2W) Strong Post W-Beam Guardrail with 100 mm High Asphaltic Curb*. Report No. FHWA-RD-00, Federal Highway Administration, Washington, D.C., June 2000.
9. Plaxico, C. A., M. H. Ray, J. A. Wier, F. Orenge, P. Tiso, H. McGee, F. Council, and K. Eccles. *NCHRP Report 537: Recommended Guidelines for Curb and Curb-Barrier Installations*, 2005.
10. Polivka, K.A., R.K. Faller, D.L. Sicking, J.D. Reid, J.R. Rohde, J.C. Holloway, R.W. Bielenberg, and B.D. Kuipers. *Development of the Midwest Guardrail System (MGS) for Standard and Reduced Post Spacing and in Combination with Curbs*. Report No. TRP-03-139-04, Midwest Roadside Safety Facility, University of Nebraska-Lincoln, September 2004.
11. Faller, R. K., K. A. Polivka, B. D. Kuipers, R. W. Bielenberg, J. D. Reid, J. R. Rohde, and D. L. Sicking. Midwest Guardrail System for Standard and Special Applications. *Transportation Research Record: Journal of the Transportation Research Board*, No. 1890, 2004.
12. Mongiardini, M., R.K. Faller, J.D. Reid, D.L. Sicking, C.S. Stolle, and K.A. Lechtenberg. *Downstream Anchoring Requirements for the Midwest Guardrail System*. Report No. TRP-03-279-13, Midwest Roadside Safety Facility, University of Nebraska-Lincoln, October 28, 2013.
13. Schmidt, J.D., R.W. Bielenberg, and R.K. Faller. *Safety Investigation and Design Guidance for Curbs Near Energy-Absorbing End Terminals*. Draft Report No. 03-358-17, Midwest Roadside Safety Facility, University of Nebraska-Lincoln, October 2016.
14. Coon, B.A., and J.D. Reid. Reconstruction Techniques for Energy-Absorbing Guardrail End Terminals. *In Accident analysis and Prevention, Volume 38*, 2006, pp. 1-13.

15. Coon, B.A.. *Development of Crash Reconstruction Procedures for Roadside Safety Appurtenances*. Dissertation, University of Nebraska-Lincoln, 2003.
16. Hallquist, J.O. *LS-DYNA Keyword User's Manual, LS-DYNA R7.1*. Livermore Software Technology Corporation, Livermore, California, 2014.
17. Ferren, J. *Full-Scale Crash Evaluations of the ET Plus End Terminal with 4-inch Wide Guide Channel Installed with a Rail height of 31 Inches*, SwRI Document Number 18.20887.05.100FRO, Southwest Research Institute, San Antonio, Texas, February 2015.
18. Baxter, J.R., Federal Highway Administration. *Eligibility Letter No. HSA-10/CC-88 for Sequential Kinking Terminal*. To Kaddo Kothmann, Road Systems, Incorporated, March 8, 2005.

Flail-Space Model

A Review of the Lateral Impact Velocity for Thoracic Injuries

TANA C. TAN

RAPHAEL H. GRZEBIETA

Transport and Road Safety Research

ANDREW S. MCINTOSH

Monash Injury Research Institute

The flail-space model was introduced in 1981 and is currently used in the United States, Canadian, Australian and New Zealand road safety barrier and fixtures standards as a method of assessing vehicle occupant injury risk in certification crash tests when an instrumented anthropomorphic crash test dummy is not used. Instead, accelerations from a tri-axial accelerometer placed at the vehicle's centre of gravity are measured and compared to "preferred" and maximum acceleration threshold values for both the longitudinal and lateral directions. The acceleration data is then integrated to obtain impact velocity which is then compared to "preferred" and maximum impact velocity threshold values for both the longitudinal and lateral directions.

Previous studies have compared the longitudinal impact velocity component of the flail-space model with impact velocities from real world frontal crash data. However, the lateral velocity component has yet to be compared with impact velocities from any side impact tests or real world injury crash data. This study assesses the relationship between impact velocities from cadaveric lateral thoracic impact tests and injury severity, and relates this to the maximum and preferred lateral velocities as recommended in the flail-space model.

To perform the study, data from previous thoracic lateral impact cadaver tests were collated. This data included variables such as: impact velocity, cadaver age, cadaver mass, impact wall interface, impact test method and resultant Abbreviated Injury Scale level. Multiple logistic regression analysis was used to determine the significant variables in predicting AIS 3+ and AIS 4+ injuries. Single variable regression analysis was then performed to determine a relationship between lateral impact velocity and AIS 3+ and AIS 4+ injury level. From the results, the current flail-space model's preferred lateral occupant impact velocity used in the Manual for Assessing Safety Hardware standards was found to be high and a lower preferred threshold of 6.4 m s^{-1} is proposed.

Roadway Departure Data Collection and Analysis

Standardization of Roadside Safety ISPE Processes Using Data Dictionary for Pre- and Post-Crash Information

CHIARA SILVESTRI DOBROVOLNY

CHARLES STEVENS

ROGER P. BLIGH

MADILYN MENDOZA

CARLOS LEYVA

Texas A&M Transportation Institute

Roadside safety devices are installed along roadways with the intent to reduce occupant injury risk for errant vehicles. The performance of these devices is commonly evaluated through component and ultimately full-scale crash testing criteria detailed in the AASHTO Manual for Assessing Safety Hardware (MASH). These full-scale tests are conducted under ideal site conditions, representing only a fraction of the potential types of crashes and site conditions which motorists may experience in the field. In-Service Performance Evaluations (ISPE) are needed to gather realistic information about the field performance of these devices, with the understanding that real world crashes include a broad variety of impact vehicle types, impact speed and angle conditions, as well as field conditions.

The Texas A&M Transportation Institute Center for Transportation Safety funded a research study to investigate the possibility to standardize ISPE data across all safety hardware devices. Through this investigation, researchers have established common required information for standard safety hardware in-service evaluations. To facilitate the standardization of ISPE data, researchers developed a data dictionary including pre- and post-crash data categories. The pre-crash parent category includes standard data sets and attributes for inventory and installation child categories, while the post-crash parent category includes data sets and attributes for the device, roadway conditions and vehicle information child categories. Each child category data set was further developed to include a standardized data naming conventions, type of content, format, and data descriptions. The creation of the ISPE data dictionary will provide for creating standardized database structure and to help define the relationships between required ISPE data components. The ultimate vision of the ISPE data dictionary was conceived and should be utilized to aid in further standardization of roadside safety devices ISPE practices. Researcher then deployed the ISPE data dictionary on multiple well known ISPE methods and case studies found in literature to verify the ability of the data dictionary to serve as a universal tool for implementation as a state-of-the-practice reference tool.

A Study of Applying Mobile Mapping Result for Road Safety Audit on Rural Roads in Thailand

Chakree Bamrungwong
Preecha Soparat
Kawin Saiprasertkit
Nutvara Jantarathaneewat
Department of Rural Roads (DRR)

There are more than 1,000 accidents occurred on rural roads in Thailand per year. Deficient road geometry is one of the main causes that leads to the accidents. Department of Rural Roads, Ministry of Transport, Thailand, is aware that road safety audit, especially auditing of road geometry, is a primary measure to tackle this problem. However, due to abundant workloads the department has been carrying, only handful of its remaining staffs are assigned to handle a road safety audit task. In order to overcome human resource limitation, Department of Rural Roads has developed a system, called “Rural Road Network Management (RM) System”. The Mobile Mapping System (MMS) technology is applied to collect road asset data such as traffic signs, road markings, bridges and culverts, lighting post, etc. The collected asset data is complemented with geographic information, which accuracy is within 0.10 Meter tolerance. Moreover, the scenes of roads that MMS machine traveling on are also recorded in a movie format which can later be viewed in all spherical angles. All of collected data is stored in RM system database. MMS helps reduce fieldworks that previously had to be conducted by numbers of staffs because RM system can automatically detected risk spot on roads such as sharp curves, no-shoulder roads, intersections or junctions where there is no lighting equipment. After risk spots are located, the auditors can review the scene of road section again on RM system or in field. The developed system is proved to be cost effective option for road safety audit and can solve the human resource shortage problem of the Department of Rural Roads.

INTRODUCTION

Currently, there were accidents on rural road of Thailand more than 1,000 times per year. Road safety audit is the measurement that can reduce accident cause by road geometry, however, the numbers of road which belonged to department of rural road are exceeded the capability of our crews.

In year 2013, bureau of planning of Department of Rural Roads of Thailand has developing “Road Management System, RM. The mainly purpose of this system are to collect the road’s data and evaluating them. By importing the survey data to the software, image processing and assets evaluation were conducted and provided Geographic Information System (GIS). This system consist of information and location of assets on the road. Since user can locate and evaluate any asses in the system, it is possile to conduct Road Safety Audit without inspecting in field.

In addition, the system will detect list of risk spots on the road, then, user can sort the priority of road maintaining. Hence, road safety improvement will conduct in suitable sequence with effective measurement.

MOBILE MAPPING SYSTEM (MMS)

MMS data collection composed of vehicle, Ladybug3, Computer, GNSS and Inclinometer (Figure 1)

Vehicle

The vehicle is a compact passenger car. A rack is installed on the top of the vehicle for fixing a dual antenna.

Ladybug3

Two panoramic 360 video systems (Ladybug3) are installed on the roof. The first 360 video camera records picture of all assets surrounding. The second 360 video camera records images of the road surface, which shows the texture of the road for later evaluation. Computer is used for storing information and synchronizing all sensors.



FIGURE 1 Composites of MMS car.

GNSS

Both GNSS and IMU are used to record location. Global Positioning Navigation System (GNSS) receives location data from satellites. IMU determines location through the calculation of measured rotation and measured acceleration rate from six directions. GNSS and IMU are used together to increase the accuracy and to eliminate bad signal problems in the urban area and dense-forest area.

Inclinometer

Inclinometer is installed with one of the 360 video camera to optimize vertical visual output, and to determine location of assets.

Once all the equipments are installed, MMS will calibrate itself with its surrounding, in order to determine road assets location. The coordinate of a reference point will be manually measured. Utilizing both reference point location and recorded pictures, location of roadside assets can be.

The post-processing includes an image processing and post-processed GNSS Trajectory. The resulted video could be used to identify road asset objects and to measure their coordinate based on 3-D stereo measurement principle.

Road-side assets store in RM divided in to 13 categories. A certain quantity and quality could be evaluated or measured on the 360-video. Furthermore, the coordinate system was tied up to the national vertical reference system (Mean Sea Level: MSL).

User can access to all of the information via web application. The interface mainly divided into three section; panorama section, map section, and information of road section (Figure 2). In panorama section, user can use tools that provided in the system to evaluate asserts. Then, the characteristic of each assert will appear on information screen, which provided details such as coordination, type, and name of the road. Also, the data in the map will synchronize with any point that user click. It provided location of each asset on the map and the coordination.

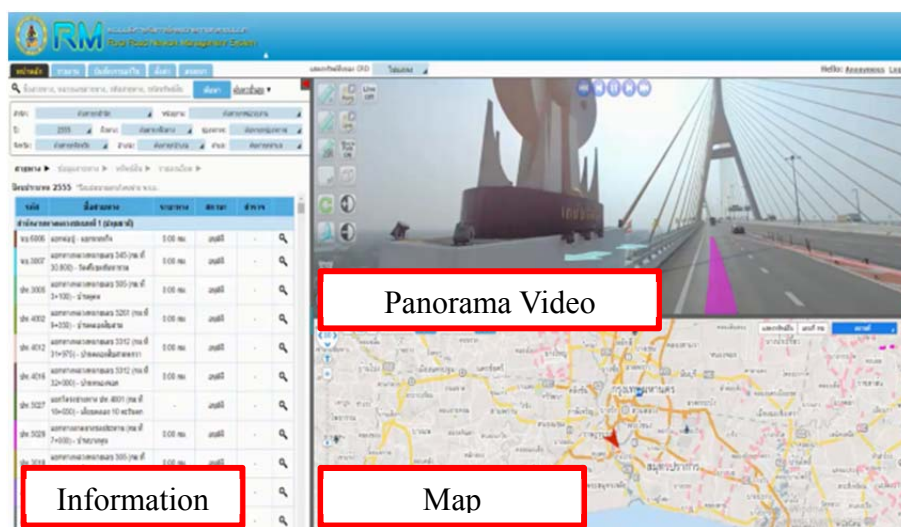


FIGURE 2 RM web application.

COLLECTED ASSETS IN THE SYSTEM

After finished the post-processing, user can obtained information and location of assets on the road which list as follow;

- Road Centerline (Figure 3)
- Location of Bridge (Figure 4)
- Traffic Light (Figure 5)
- Guardrail (Figure 6)
- Guide Post
- Pavilion on Roadside
- Kilometer Marker
- Road Sign (Figure 7)
- Road Marking on Pavement (Figure 8)
- Lighting (Figure 9)
- Right of Way (Figure 10)
- Intersection (Figure 11)
- Others; Footpath, Bicycle Lane, Pedestrian Crossing, Drainage Gutter.



FIGURE 3 Centerline.



FIGURE 4 Location of Bridge.

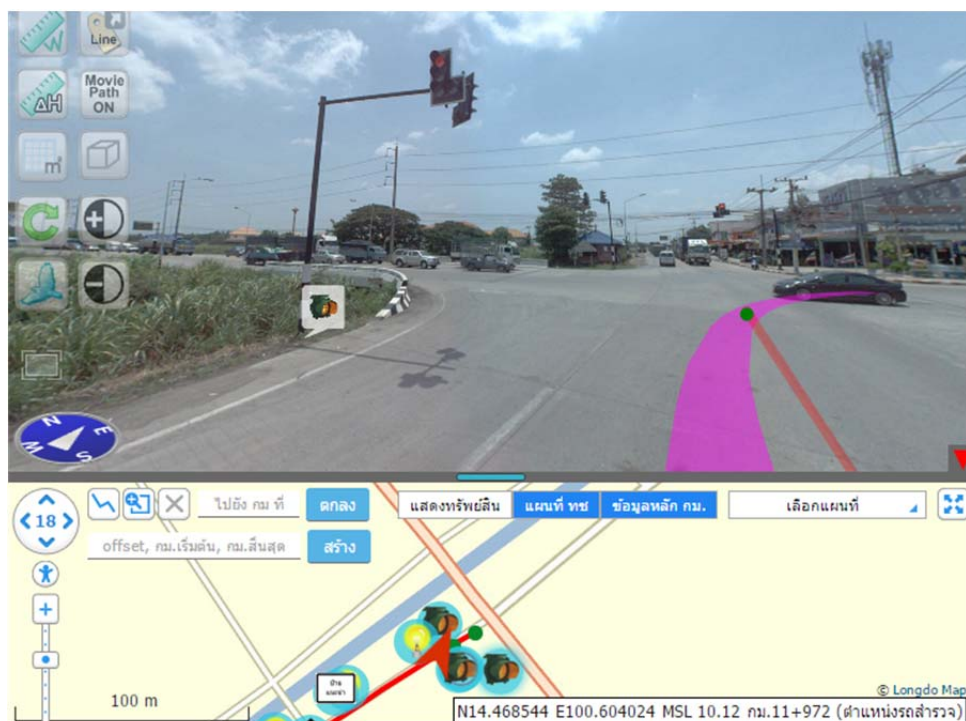


FIGURE 5 Traffic Light.



FIGURE 6 Guardrail.



FIGURE 7 Road sign.

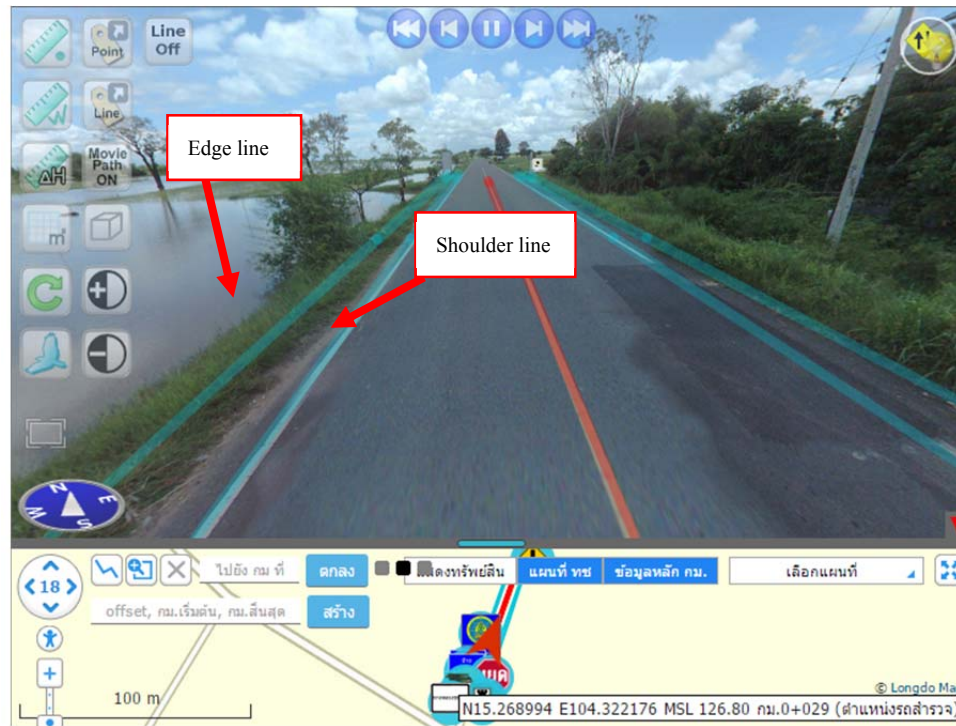


FIGURE 8 Road Marking.

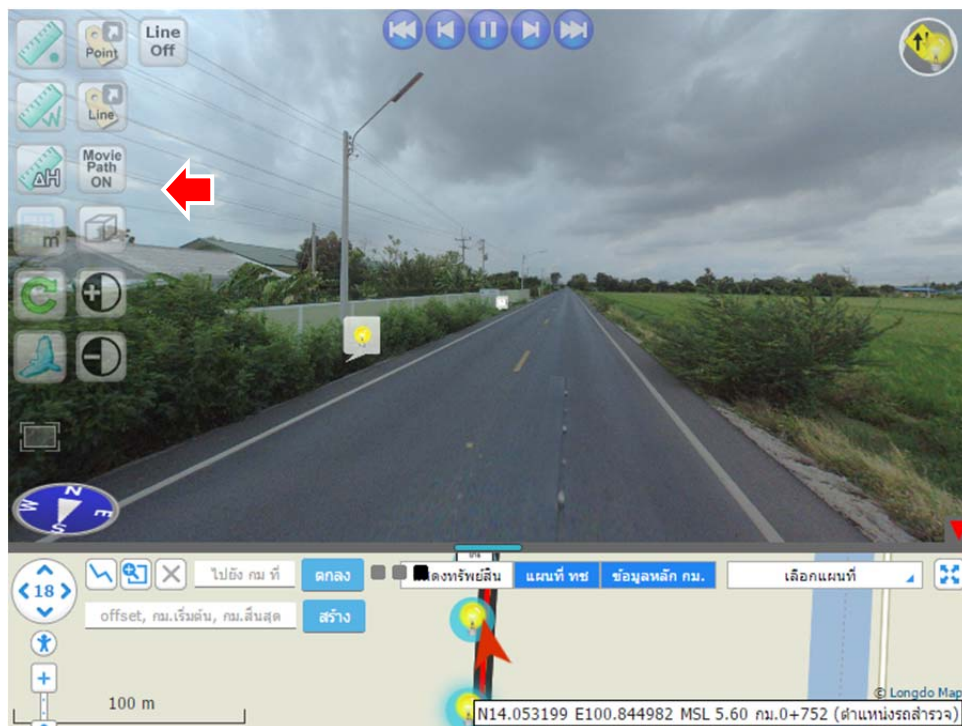


FIGURE 9 Lighting.

**FIGURE 10** Right of way.**FIGURE 11** Intersection.

To obtain coordination of each asset, click on the asset and the data will appear in information screen section. In addition, user can measure asset that are on panoramic video in both horizontal and vertical direction (Figure 12). For example, road width and pole height. The system provided Mean Sea Level chart, in which user can identify height of each point on the road.

APPLYING ROAD SAFETY AUDITING ON MMS

As aforementioned, the system will automatically detect risk spot on road by analyzing all of asset data together from coding. Here are some road safety audit topics that have successfully developed on this system;

Intersection (Road)

Since intersection signs are marked at intersection, the location of these intersections can be evaluated. After the system analyse the locations on map, it will check the lighting, which have been previously evaluated, weather it is located within radius of 30 m. around the point where interaction exist (Figure 13). If none, the system will report this intersection as risk spot.

Intersection (Rail)

Similar to intersection (Road) the system evaluate intersection between road and rail then marked as one type of the asset. User can obtained location of this type of intersection and manually check sufficiency of road equipment around the cross such as warning sign, bar and lighting through the system (Figure 14).

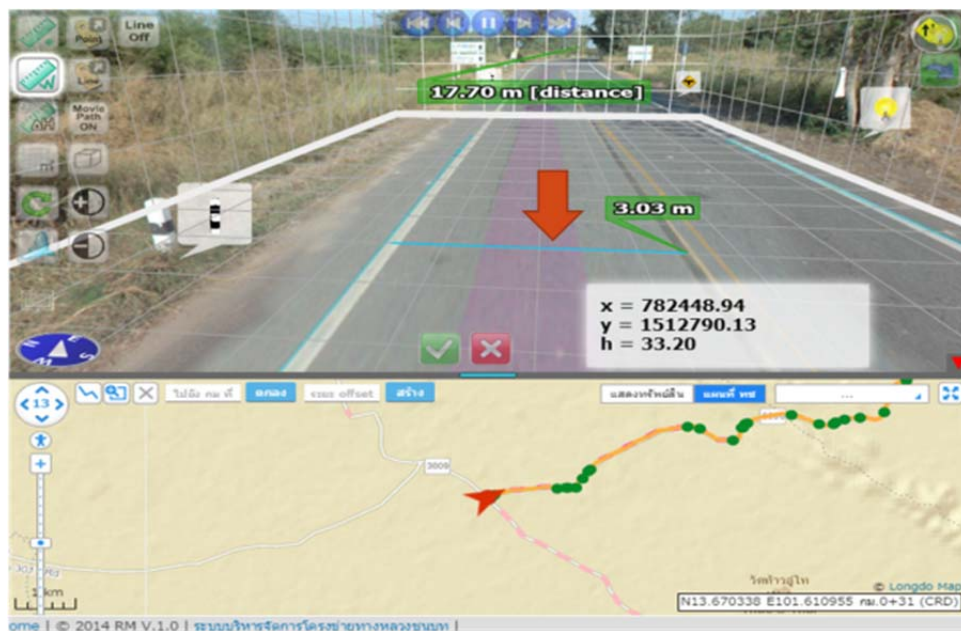
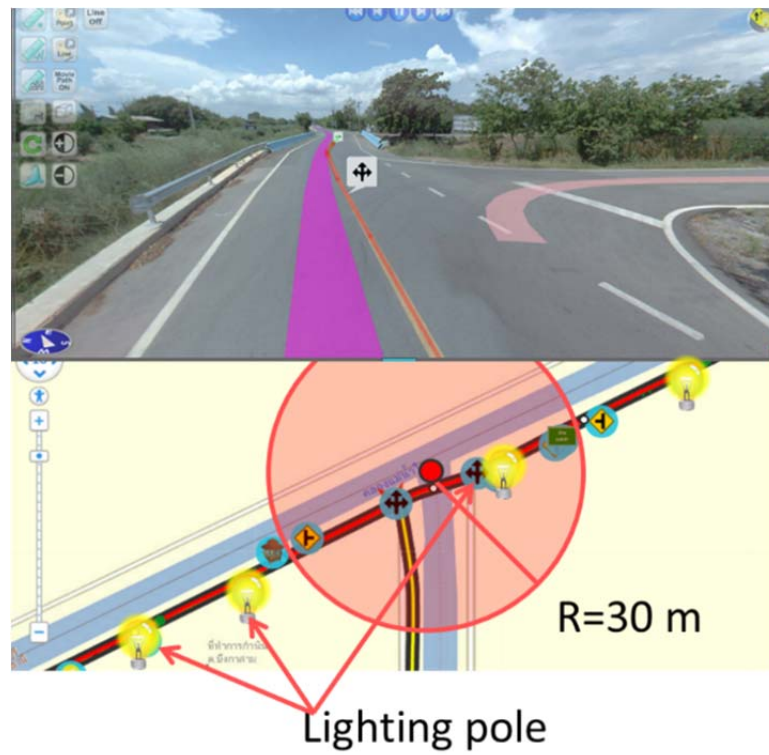


FIGURE 12 Measure asset in horizontal direction.

**FIGURE 13 Intersection (Road)****FIGURE 14 Intersection (Rail)**

Road Gradient

Since all the point that car had driven by, the recorded data consisted of horizontal and vertical data, therefore, gradient of road can be calculated. Based on standard of the department of Rural Roads of Thailand, alignment of the road which has slope more or less than 8% is regarded unsafe.

Dangerous Curve

Refer to ASSTHO, The formula for calculate curve radius is show below (1)

$$f = \frac{V^2}{127R} - 0.01e \quad (1)$$

Where

f = side friction factor,

V = Vehicle speed (km/hr),

R = Radius of curve (m)

e = Rate of roadway super

Side fiction factor is based on derived function from AASTHO table. By using speed at 60 kilometer per hour and side fiction factor as 0.15, then, the minimum radius of curve is 188 m. However, for increasing safety level, the department has set minimum radius at 200 m. instead.

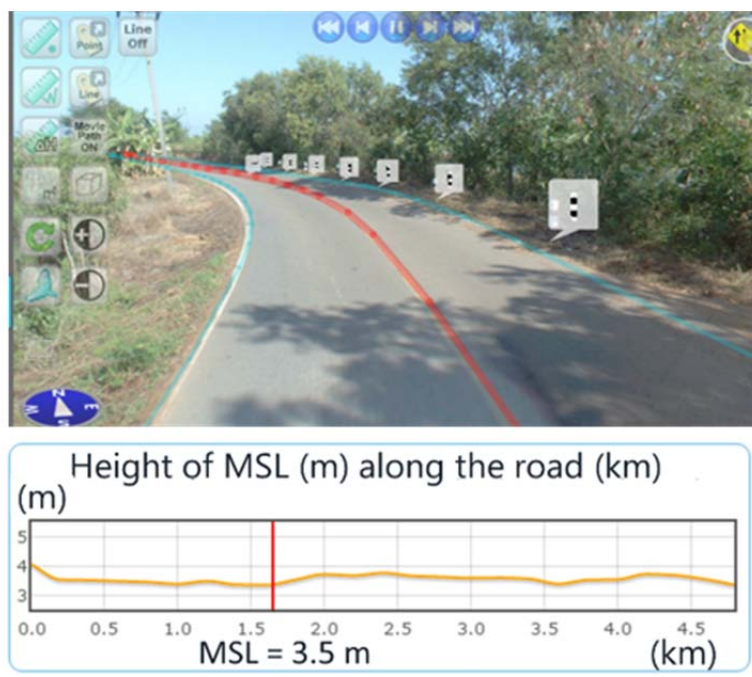


FIGURE 15 Mean sea level chart.

Curve on the road is obtained from centerline, which are generated by staffs clicking on the center of the road through the system, then, curve radius are calculated automatically. The system will query the portion that have curve radius less than 200 meters and regarded it as dangerous curve.

Curve that are regarded as dangerous will be assigned the speed limit by using the formula above. For the side fiction factor, the department has set at 0.14, therefore, each curve that is regarded as dangerous curve will be provided with speed limit.

Moreover, user can evaluate whether that curve has sufficient furniture for safety, such as, guard rail or guide post from the 360 panoramic view in the system by manually (Figure 16).

Vertical Sight Distance

Based on AASTHO-function, sight distance takes slope and speed as parameters and return sight distance as output. Since the system can calculate slope of the road and speed are set at 80 kilometer per hour, vertical sight distance can be calculated.

There are two main type of vertical curve; crest and sag. On a sag curve, slope at the start is negative, while, on a crest curve, slope at the start is positive. Curve type affects the criteria for safe-curve length consideration since the formulas differ between sag and crest bridges. The formulas are shown in below figure (Figure 17)



FIGURE 16 Dangerous curve that detected by RM.

Metric	US Customary
When S is less than L, $L = \frac{AS^2}{864}$	When S is less than L, $L = \frac{AS^2}{2800} \quad (3-47)$
When S is greater than L, $L = 2S - \frac{864}{A}$	When S is greater than L, $L = 2S - \frac{2800}{A} \quad (3-48)$

(a)

Metric	US Customary
When S is less than L, $L = \frac{AS^2}{200[0.6 + S(\tan 1^\circ)]}$	When S is less than L, $L = \frac{AS^2}{200[2.0 + S(\tan 1^\circ)]} \quad (3-49)$
or, $L = \frac{AS^2}{120 + 3.5S}$	or, $L = \frac{AS^2}{400 + 3.5S} \quad (3-50)$
When S is greater than L, $L = 2S - \frac{200[0.6 + S(\tan 1^\circ)]}{A}$	When S is greater than L, $L = 2S - \frac{200[2.0 + S(\tan 1^\circ)]}{A} \quad (3-51)$
or, $L = 2S - \left(\frac{120 + 3.5S}{A} \right)$	or, $L = 2S - \left(\frac{400 + 3.5S}{A} \right) \quad (3-52)$
where: L = length of sag vertical curve, m; S = light beam distance, m; A = algebraic difference in grades, percent	where: L = length of sag vertical curve, ft; S = light beam distance, ft; A = algebraic difference in grades, percent

(b)

FIGURE 17 (a) minimum length for crest curve and (b) minimum length for sag curve

POSTGIS was used for calculation. Diagram below shows the result of the final code (Figure 18). The data in result table consists of type of curve, curve length, and required length. Also, the code will evaluate whether this section is safe or not. Note that curve length is calculated from position of centerline that the staff had evaluated, same as methodology to determined curve shape as mention previously.

1	bridge_id	type	length	require	safe text	LAT	LONG
2	2034	down_sag	96.97	121	danger	14.1445	100.6192
3	2030	up_crest	32.39	94	danger	14.31985	100.7184
4	2031	up_crest	33.22	108	danger	14.32147	100.729
5	2030	up_crest	14.77	83	danger	14.3199	100.7182
6	81	up_crest	32.83	442	danger	13.49492	100.8551
7	82	up_crest	15.18	101	danger	13.51075	100.8589
8	84	up_crest	48.91	292	danger	13.52944	100.8718
9	88	up_crest	53.81	184	danger	13.53926	100.8727

FIGURE 18 Result form analysing sight distance

Road Without Shoulder

This system has evaluated the shoulder line and edge line along the road, which can acquire the width of road surface and the shoulder lane (Figure 19). The system will measure the space between 2 lines. In some case, width of road may narrow rapidly or shoulder lane may disappear, the system will report for which point are in this case as the dangerous lane and shoulder lane.

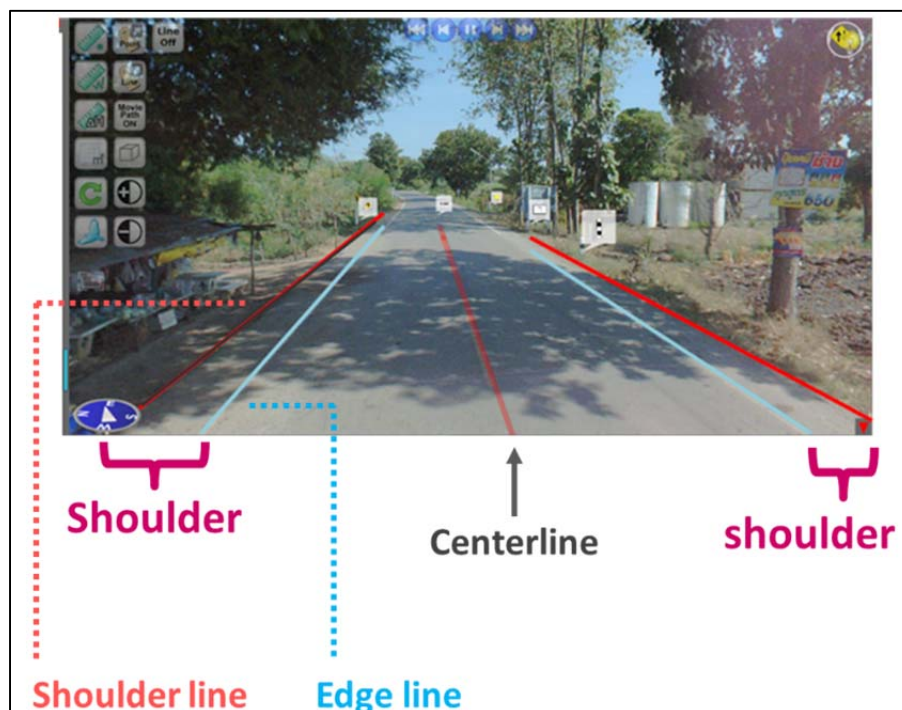


FIGURE 19 Road marking.

Bridge Width

Shoulder lane are sometime missing when the road is connect with the bridge and can lead to accident. Same as shoulder lane detecting function, the system will calculate space of shoulder lane on the bridges. Therefore, in case that shoulder lane are missing at the entrance of bridge, the system will report as dangerous bridge.

Otherwise, user can use measurement function that available in user interface function to determine and compare width of bridge and road manually.

USING MMS FOR ROAD SAFETY PLANNING

After analyse all of asserts in the system, user can obtain “Risk Spot List”. The risk spot list consist of various type as mention above. Since all of spots that are listed in risk spot are provided with coordination, user can plot the spots on the ArcGIS program (Figure 20).

Moreover, the department of rural road also recorded accident that occurred on the “Accident list”, which provided location and characteristic of accident. User can plot the accident spot on the ArcGIS program as well.

By combining two set of data, ArcGIS can detect location on risk spot list that located near accident spot within radius of 500 meters. Also, AADT volume has added to each of risk spot, which can use for prioritize planning of improving safety on road by list of black spot.

After all, we can divided each of risk spot into the planning of improving safety on road for 4 phase as follow (Figure 21);

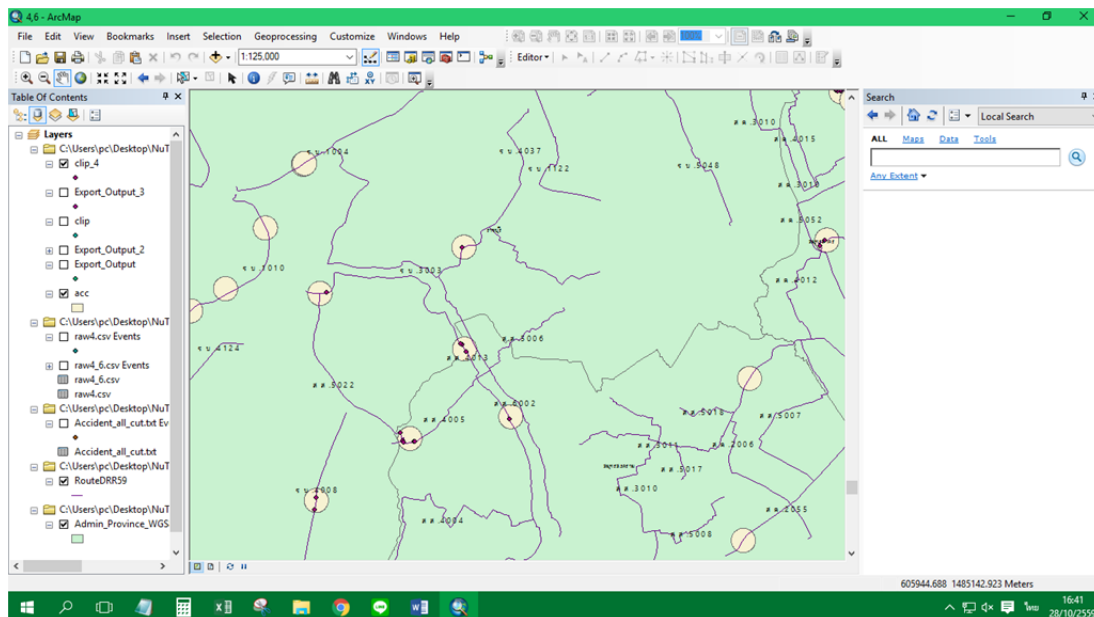


FIGURE 20 Plotting risk spot and accident spot on ArcGIS.

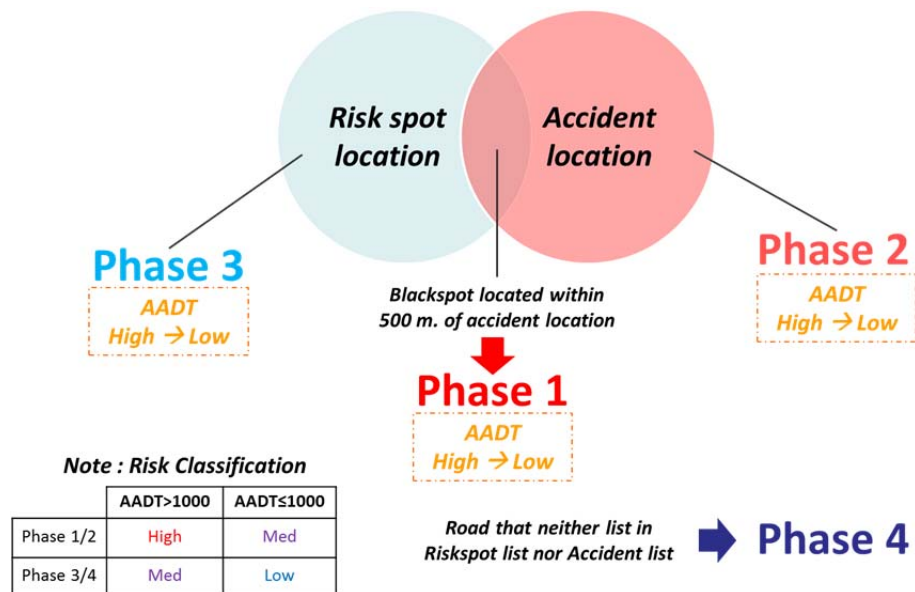


FIGURE 21 Using Venn – Euler Diagram for prioritize road safety improvement plans.

Moreover, we also do the risk classification by using AADT volume, which will improve the efficiency of prioritize planning of improving safety on road.

CONCLUSION

Applying road safety audit on MMS will decrease road accidents that caused by poor from geometry conditions. This method can not only reduce cost of road safety auditing, but it can also solve the human resource shortage problem. The road safety improvement plan that gain from the system can save time and increase the accuracy of data. Moreover, data in the system can be applied for other related works in the Department of Rural Roads such as flood preventing, road upgrading and road rehabilitation.

REFERENCES

1. Phisan Santitamnont. Mobile Mapping Applications for Data Collection and Evaluation of the Rural Road Assets. 2nd IRF Asia Regional Congress & Exhibition, October, 2016.

Testing and Analyses of Terrain Effects on Vehicle Trajectories and Kinematics

DHAIFER MARZOUGUI
CING-DAO (STEVE) KAN
KENNETH OPIELA
George Mason University

There has been limited effort over the past two or more decades to analyze the behavior of vehicles as they traverse sloped terrain. Recent concerns about cross-median crashes led to analyses of vehicle trajectories as they traverse medians of varying configurations. These analyses relied upon a well-developed set of tools for vehicle dynamics analyses (VDA). These tools provided plausible results related to understanding of vehicle-to-barrier interfaces for median barriers, but difficulties associated with measurement of vehicle position in testing limited the validation options. This paper addresses the need to assess the adequacy of these predicted effects using a more rigorous method for capturing vehicle trajectories in simulated medians. A series of forty-five full-scale tests were conducted at the FHWA Federal Outdoor Impact Lab (FOIL) to capture data that could be used to provide fresh insights on terrain effects on vehicle trajectories as well as provide a basis for validation of the VDA results. This paper describes the testing and provides the preliminary results and describes the difficulties encountered in attempting to get accurate digital trajectory traces for direct comparison to the VDA outputs. The use of a 3D motion analysis tool is described and the plans for the validation effort is outlined. The paper suggests means to capture data representing vehicle behavior on median sections in crash tests of barriers installed on slopes to assure validity of findings.

Evaluation of Safety Hardware Identification Methods Durability Using Crash Testing Opportunities

CHARLES R. STEVENS JR.

CHIARA SILVESTRI DOBROVOLNY

ROGER P. BLIGH

Texas A&M Transportation Institute

BEN ZOGHI

Texas A&M University Engineering Technology and Industrial Distribution Department

Building on current work in safety hardware identification methods, the Center for Transportation Safety at the Texas A&M Transportation Institute (TTI) funded an additional study of safety hardware identification methods and their durability during a crash event.

To accomplish an evaluation of tag durability, researchers completed an initial investigation of hardware identification methods to determine potential identification (ID) methods for crash testing. The investigation determined that researchers could deploy commercially available Radio Frequency Identification (RFID) technology. TTI worked with the Texas A&M University Department of Engineering Technology and Industrial Distribution to develop a methodology to propose to potential agencies scheduled to conduct crash testing during the summer of 2016. This methodology included having student technicians attach hardened RFID tags at key locations to steel longitudinal roadside safety hardware devices.

To simulate actual asset management and In-Service Performance Evaluations (ISPE) conditions, the testing methodology included pre-crash and post-crash data acquisition and input. For the pre-crash condition, researchers captured the identification number of the hardware ID method. For post-crash conditions researchers again captured, when possible, the identification number of the RFID, and verified readability. Researchers conducted post-crash readability in two distinct ways, first with a handheld reader and then again using mobile technologies from vehicle. Researchers completed an evaluation of the durability of two RFID tags including post-crash readability, attachment method, encasement materials, and placement.

INTRODUCTION

A rapidly emerging topic in the area of roadside safety hardware is asset management and the tracking and/or identification of roadside safety assets throughout their lifecycle. Safety hardware identification has become a national issue due to several incidents occurring over the past four years, when the absence of the ability to identify safety hardware proved to be a significant flaw in knowing what, who, and how devices were manufactured, installed, maintained and replaced. This inability became so significant that the United States Congress included a requirement in Section 1429 of the Fixing America's Surface Transportation Act for the Secretary of Transportation to study techniques that agencies can use to identify and document roadside safety hardware device including serial numbers, barcodes, and RFID (1).

BACKGROUND

The many benefits of a safety hardware identification program relies heavily on the successful deployment of an identification method. Identification methods, in simple terms, provide a user or system with an identification number or data key that when referenced to a database can provide the user with the ability to access and record information. Users would be able to access information by cloud-based infrastructure and/or through offline means. This ability would provide great benefit to manufacturers, installers, maintaining agencies and first responders for the tracking of a device through its lifecycle – from birth to death.

Developing the ability to access and record safety hardware information has many benefits outside of just tracking major milestone events (manufacture, installation, incident and replacement). Agencies can use the data key for standard asset management practices including the assessment of lifecycle and maintenance costs by a variety of variables. If included with ISPE efforts, agencies can begin to track which installation and system component combinations are statistically the safest when struck by a vehicle.

Ensuring that an identification method deployment will consistently provide this data key is vital to the success of any tracking system. It is extremely important to consider the durability of any potential method through the lifecycle of safety hardware devices. When considering the performance of a roadside safety system is most important at the time immediately after a vehicle strikes a roadside safety system, having the ability to access and record information about that system is vital. Therefore, it is necessary to investigate and understand the performance of identification methods and the ability to successfully read a data key during and after vehicle impact.

TTI Safety Center Project

In the spring of 2016, the Federal Highway Administration (FHWA) selected the TTI to perform research and evaluate hardware identification methods. During discussions with FHWA staff and the literature review task, researchers identified several knowledge gaps regarding identification tag durability including the ability to survive vehicle impact. TTI researchers, including experts from the Roadside Safety Division, approached the TTI Safety Center, whom provided research funding to evaluate tag performance during crash testing during the summer of 2016.

TECHNOLOGY OVERVIEW

Researchers considered three types of identification methods for crash durability evaluation including serial numbers, bar codes, and RFID. Researchers chose RFID tags for crash testing due to their ability to be read using mobile methods. A brief overview RFID technology is included below.

Radio Frequency Identification Tag (RFID)

RFID tag technology consists of two parts: an antenna for receiving and transmittal of a signal and an integrated semiconductor or microchip. An RFID system would incorporate a reader and software component. Passive tags do not require a power source and receive power from the

magnetic field generated by the reading device. Active RFID tags have their own internal battery which enables the tags to transmit data at a constant rate which results in the ability to read the tag at greater distances (2). Table 1 illustrates the different tags available and their characteristics. Researchers did not evaluate active RFID tags during the actual study.

RFID technology is not a new technology. The military and retail organizations have been using RFID for many years to track and identify assets and products. Potential users often question the technologies ability to operate effectively near water and metal. Research has proved to overcome these issues, with some RFID tags being able to turn the metal objects into antennas, increasing the range of the device. The primary problem with metal involves the reflection of energy away from the tag, detuning the tag antenna and decreasing readability. Research discovered that by placing spacers between the tag and the metal object, the metal object deflected less energy and in some cases directed more energy to the tag increasing range. Water absorbs energy and detunes the device. However, studies found that users could resolve the water problem by adjusting the antenna's impedance for proper tuning before installation (3).

Potential users often also question the durability of RFID tags to withstand roadside conditions. The perceptions that RFID tags are merely stickers can often result in such perceptions. However, RFID technologies and encasement options provide a wide range of applications. Ross et al investigated RFID technology durability for construction materials tracking in 2009 for the Georgia Department of Transportation. Researchers tested a variety of readers and transponders to test performance in water immersion, acid immersion, base immersion, pressurized water, freeze-thaw, and high temperatures. RFID tags were also placed in concrete cylinder samples and tested for readability. The research concluded that RFID tracking is a viable tracking technology and that the RFID tags performed well under a chemical immersion and temperature conditions. Researchers were able to consistently read tags within the acceptable constraints of locating construction sample (4). Investigation into the placement of RFID tags into truckloads of hot mix asphalt yielded similar results in a 2014 FHWA study (*Error! Bookmark not defined.*). Researchers used RFID tags to track truckloads of hot mix asphalt. RFID successfully provided researchers with the ability to track temperature in real-time and for the early detection of reflection cracking in overlays. In contrast, the study found that tracking in active Portland cement concrete was unsuccessful due to the high dielectric constant of the hydrated cement (5).

TABLE 1 RFID Technology Overview (3)

Frequency	Band	Mode	Range	Applications	Cost
120-150kHz	Low Frequency	Passive	1cm-10cm (0.5 in- 4in)	Animal tags	\$0.50-\$1
13.56Mhz	High Frequency	Passive	10cm-50cm (4in- 20in)	Door entry and smartcards	\$1 - \$5
433Mhz	Ultra-High Frequency	Active	1m-200m (3ft- 650ft)	Asset tagging and postal app.	\$4 - \$30
902-928Mhz	Ultra-High Frequency	Passive	50cm - 25m (20in- 80ft)	Retail apparel and asset tagging	\$0.10 to \$7
2.4-5.8Ghz	Microwave	Active	50cm - 25m (20in- 80ft)	Real-time location systems	\$5 - \$25

Despite the many recorded uses of RFID in construction, there is a significant knowledge gaps regarding their use on guardrails and other roadside hardware equipment.

PAPER OBJECTIVE

The objective of this paper is to focus primarily on the success and potential drawbacks of using RFID technology. The primary goal of these investigations were to assess the ability for researcher to install RFID technology and read identification numbers pre- and post-crash by both handheld and through mobile means.

STUDY METHODOLOGY

During the summer, researchers were able to gain permission to place RFID tags on a Texas Department of Transportation (TxDOT) picket bridge rail test installation and a 31-inch W-beam test installation. The primary goal of the investigation was to determine if tags would remain attached and remain readable to the test article after impact. To complete the evaluation, researchers developed a pre-crash and post-crash data collection plan to evaluate RFID tag readability. The team also developed a tag placement guide that sponsors reviewed and adjusted due to concerns of flying objects. Researchers attached each tag and read the tag pre-crash and post-crash.

Pre-Crash Tag Testing

Researchers read each tag using an ACC Systems (Figure 1) handheld reader prior to the full-scale crash test to ensure the tag was functioning properly.



FIGURE 1 ACC Systems Handheld Reader

Post-Crash Tag Testing (Handheld)

Researchers immediately investigated the ability of the RFID tags to withstand a vehicle collision by using the ACC Systems handheld to verify readability.

Post-Crash Tag Testing (Mobile)

In addition to reading each tag with a handheld reader, researchers also investigated the ability to read tags by mobile means using an instrumented vehicle (Figure 2). The instrumented vehicle made passes by the test article post-crash at 5, 10, 15, 20, and 25 feet (~1.5, 3, 4.5, 6, 7.5 meters) and at varying speeds of from 5 to 25 miles per hour (mph) [8 to 40 kilometers per hour (km/h)]. The vehicle also carried out these runs using three different antenna angles 90, 45, and 0 degree from the test article.

TXDOT PICKET STYLE BRIDGE RAILING TEST ARTICLE

TxDOT provided the team an opportunity to place RFID tags on a “Picket” style bridge railing (Figure 3) test article that is very similar to the standard 36-inch Type T1P currently in use (7).

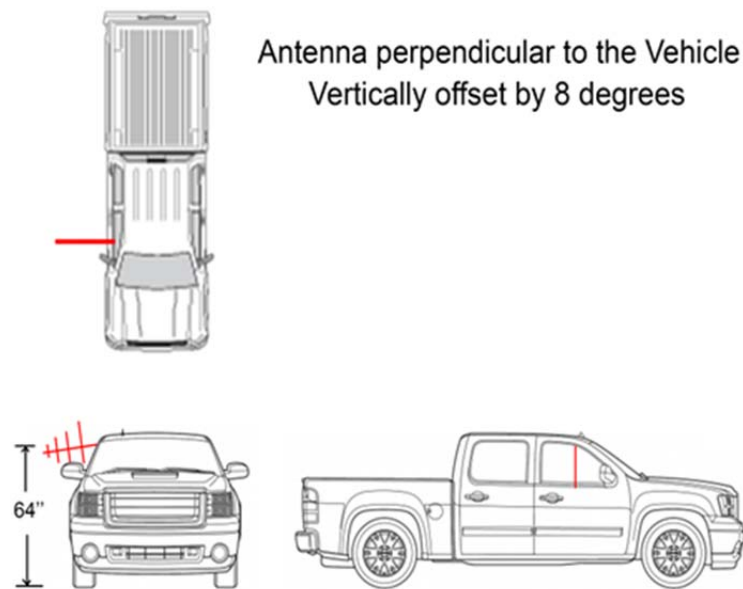


FIGURE 2 Example of Mobile RFID Unit with Vertical Antenna Orientation

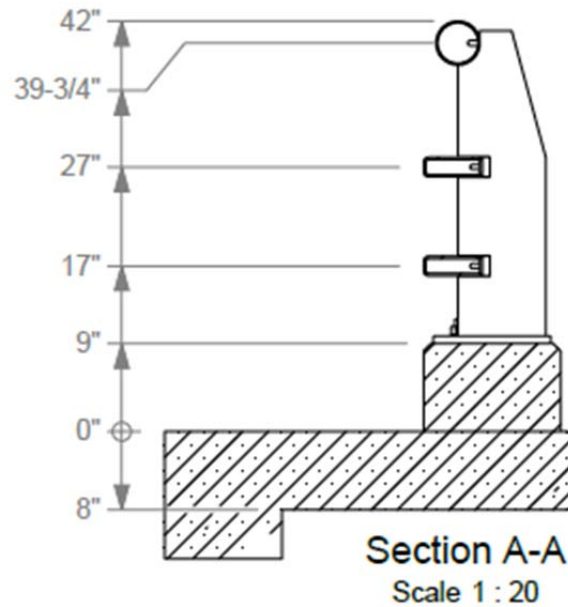


FIGURE 3 TxDOT Picket Style Bridge Railing

RFID Tag Specifications

For this full-scale crash test, the team used a TROI™ Pipe Riser RFID Tag (RS-102) (Figure 4). The manufacturer offers hardened tags for the applications in oil and gas, corrosive chemicals, construction, security, and industrial laundry (8). The RS-102 is an ultra-high frequency passive RFID tag operating in the 865 to 928 MHz frequency range. It can be installed on any metal surface. The tag has a rubber casing with a tensile strength of 2500 psi (17230 kpa) and passed drop tests of 25 or greater using 55lbs (18kg) to asphalt. Figure 5 shows the additional environmental specifications.

Tag Installation

A student from the Texas A&M University Engineering Technology and Industrial Distribution Department with students from the TTI Safety Center ATLAS Program attached 27 tags to the test article railing. Student prepared the surface by cleaning and sanding the area and attached the tags using a commercial polyurethane glue (Figure 6). The students under the supervision of researchers numbered each tag with a silver marker and placed them according to a predetermined installation plan (Figure 7).

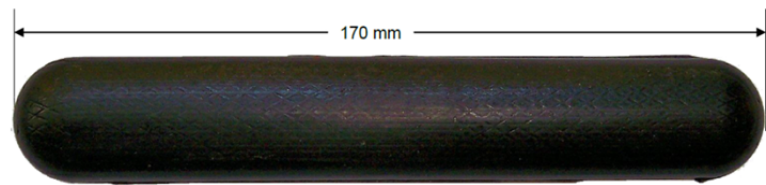


FIGURE 4 TROI™ Pipe Riser RFID Tag (RS-102) (Error! Bookmark not defined.)

Operating temperature	-50°C to +200°C* -50°F to +392 °F*
Temperature Cycling Test	85 deg C continuous for 30-days - with no negative affect 85 deg C / -25 deg C shock for 7 days - with no negative affect 125 deg C continuous for 7 days - with no negative affect 160 deg C continuous for 7 days - tag becomes brittle, but functions 200 deg C for 24 hours – with no negative affect
IP classification	IP69K EN 62262 IK-25 - Complete protection against dust - Protection against continuous immersion in water
Weather resistance	Excellent, including UV-resistance and sea water immersion
Pressure resistance	RFID tag tested to 30,000 PSI for 30 days
Chemical resistance	No physical or performance changes in: - Salt water - NaOH (depending on concentration) - Sulfuric acid (depending on concentration) - Motor oil (tested in 168 hour exposure) Generally good against: - Most solvents - Most acids and bases

FIGURE 5 TROI™ Pipe Riser RFID Tag (RS-102) Environmental Specifications (Error! Bookmark not defined.)



FIGURE 6 Adhered RS-102 Tags with ID Markings

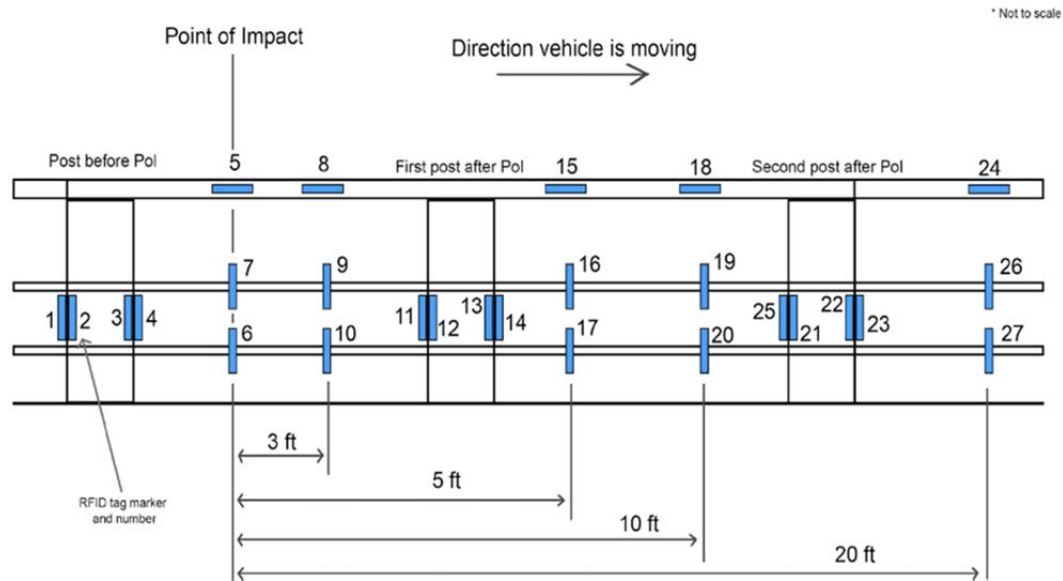


FIGURE 7 Tag Placement Diagram

Full Scale Crash Testing

The TxDOT 42-inch (1.06 meter) picket rail test article was subject to a full-scale crash test on July 13, 2016 using a pick-up truck according to the Manual for Assessing Safety Hardware (MASH) standards.

STRONG POST W-BEAM GUARDRAIL TEST ARTICLE

A private sponsor provided the team an opportunity to place RFID tags on the posts of a standard 31-inch Strong Post W-Beam (Figure 8) test article.



FIGURE 8 Strong Post W-Beam Test Article

RFID Tag Specifications

For this full-scale crash test, the team used TROI™ Bandable Rubber RFID Tag (RS-200) (Figure 9). The RS-200 is an ultra-high frequency passive RFID tag operating in the 865 to 928 MHz frequency range and can be installed on any metal surface (9). The tag has a rubber casing with a tensile strength of 2500 psi (17230 kpa) and passed drop tests of 25 or greater using 55lbs (18kg) to asphalt. The tags environmental specifications are almost the exact same as the RS-102 (Figure 5) with the exception of having a lower maximum operating temperature of 160 C/320 F.

Tag Installation

A student attached eight tags to the test article strong posts. A student again prepared the surface by cleaning and sanding the area and attached the tags using a commercial polyurethane glue (Figure 10). The students under the supervision of researchers numbered each tag with a silver marker and placed them according to a predetermined installation plan (Figure 11).

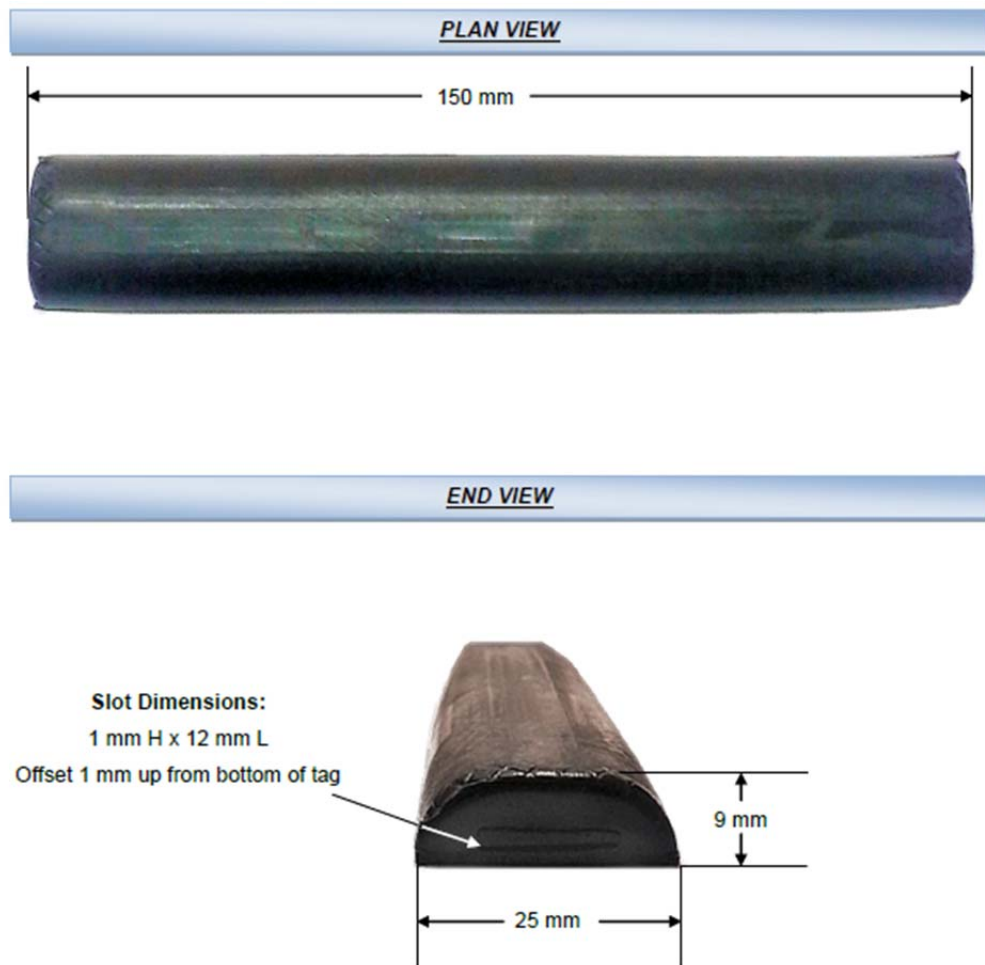


FIGURE 9 TROI™ Pipe Riser RFID Tag (RS-102)



FIGURE 10 Adhered RS-102 Tags with ID Markings

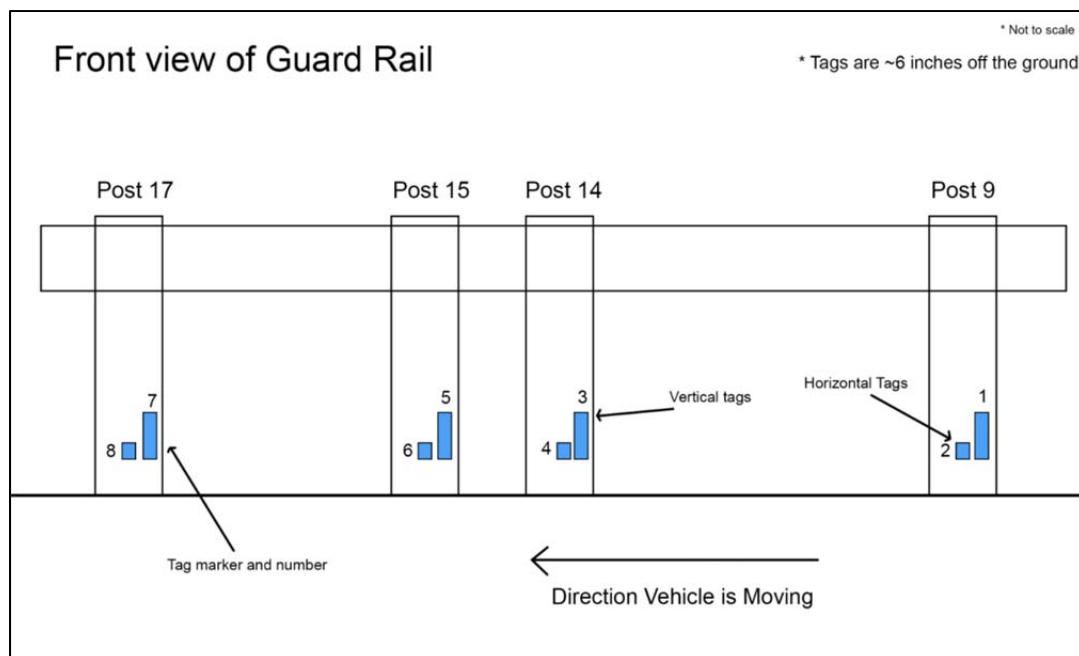


FIGURE 11 Tag Placement Diagram

Full Scale Crash Testing

The TxDOT 31-inch Strong Post W-Beam test article was subject to a full-scale crash test on July 18, 2016 using a pick-up truck according to MASH standards 3-11.

RESULTS

Researchers gathered all the data pre-crash and post-crash and compared. Researchers found that no RFID tag had detached from the 42-inch (1.06 meter) picket rail nor the 31-inch (0.787 meter) W-Beam test articles. Researchers were also able to read all RFID tags post-crash with the handheld reader (Figure 12).

Mobile Reading Results

Researchers also read RFID tags using a mobile approach. The mobile unit made multiple passes for antenna angle, speed, and distance from test article. For the “picket” style rail and RS-102 RFID tag, the mobile unit was able to pick up 52% of the 27 tags or 14 tags when the van approached with the antenna straight on in the direction of the vehicle and at a distance of five feet from the test article. Speeds did not appear to effect tag readability. At least one tag could be read up to 20 feet away while going 25 mph (40.2 km/h) (Table 2).

For the 31-inch Strong Post W-Beam mobile tag reading ability appeared to be less than the picket design. RFID tags could be read for up to 10 feet from the test article. Speed did not appear to impact readability as 25% of the eight tags could be read going 25 mph (40.2 km/h) from 10 feet away from the test article (Table 3).



FIGURE 12 Post-Crash RFID Still Intact

TABLE 2 Mobile RFID Readings for Picket Style Bridge Railing

Antenna Position		Distance feet (m)	Speed mph (km)				
Angle	Height inches (cm)		5 (8)	10 (16)	15 (24.1)	20 (32.2)	25 (40.2)
90	64 (162)	5 (1.5)	44%	44%	44%	44%	44%
45	64 (162)	5 (1.5)	7%	7%	7%	7%	7%
0	64 (162)	5 (1.5)	52%	52%	52%	52%	52%
90	64 (162)	10 (3)	41%	37%	30%	30%	30%
45	64 (162)	10 (3)	0%	0%	0%	0%	0%
0	64 (162)	10 (3)	15%	15%	15%	15%	15%
90	64 (162)	15 (4.5)	15%	11%	11%	11%	4%
45	64 (162)	15 (4.5)	0%	0%	0%	0%	0%
0	64 (162)	15 (4.5)	4%	4%	0%	0%	0%
90	64 (162)	20 (6)	4%	4%	4%	4%	4%
45	64 (162)	20 (6)	0%	0%	0%	0%	0%
0	64 (162)	20 (6)	0%	0%	0%	0%	0%

TABLE 3 Mobile RFID Readings for Strong Post W-Beam

Antenna Position		Distance feet (m)	Speed mph (km)				
Angle	Height inches (cm)		5 (8)	10 (16)	15 (24.1)	20 (32.2)	25 (40.2)
90	64 (162)	5 (1.5)	38%	38%	38%	38%	38%
45	64 (162)	5 (1.5)	75%	63%	63%	63%	50%
0	64 (162)	5 (1.5)	38%	0%	0%	0%	0%
90	18 (45.7)	5 (1.5)	13%	0%	0%	0%	0%
90	64 (162)	10 (3)	38%	38%	38%	38%	25%
45	64 (162)	10 (3)	13%	13%	13%	0%	0%
0	64 (162)	10 (3)	0%	0%	0%	0%	0%
90	18 (45.7)	10 (3)	0%	0%	0%	0%	0%

CONCLUSIONS AND RECOMMENDATIONS

In regards to withstanding vehicle impact and based on the findings of the two full scale crash tests, RFID tags are a viable option. All tags survived vehicle impact and researchers successfully read every tag with a handheld read post-crash. Researchers found varying success reading RFID tags using the mobile unit. Researchers had installed the tags differently on the test articles. The team had installed tags on the “picket” railing much closer and out front compared to the installed tags on the W-Beam test article being lower and concealed within the strong post. This greatly impacted mobile readability. Sponsors were very accommodating but did not want researchers to install the tags where a direct hit could take place. If the student would have been able to install the tags directly to the linear railing, mobile readability could have been significantly better.

However, based on the type of tag, crash test sponsors felt that the tags might cause flying objects during an incident potentially resulting in bodily harm. The manufacturer’s

specifications did not provide the weight of the tags, but researchers are confident the tag's weight did not exceed 4 ounces (0.11 kilograms). This sponsor request was not protested but could be revisited in the future. The tags tested are also bulky and noticeable, but the manufacturer could conceal tags with similar colors to avoid curiosity. Despite all the available products that could be custom designed to prevent curiosity, adhered tags are still possibly subject to vandalism. Tags do have the potential to be installed under sign sheeting, which may help prevent potential vandalism. However, understanding that hardened tags have a greater potential for unwanted removal should prompt investigation into mechanical fastening of the tags or even emersion within the concrete foundations of posts.

This area requires more research to better understand the identification technology options and more importantly installation option to reach an approach that will withstand the roadside environment, vehicle impact (flying objects), and potential vandalism.

ACKNOWLEDGMENTS

The authors acknowledge several sources that contributed to this project: The Texas A&M Transportation Safety Center for sponsoring the research, the assistance of Carlos Leyva, Madilyn Mendoza, Ghanshyam Bhutra, and William Ellison for diligent work effort in crash test preparation, and Thomas Lindheimer, Ph.D. for sharing his insights.

REFERENCES

1. http://transportation.house.gov/uploadedfiles/fastact_xml.pdf. Accessed October 27, 2016, Page 303.
2. Heimbecker, Chad. Swiftwater Solutions. Review of Identification Tag Technologies for Use in Roadside Hardware In-Service Performance Evaluation and Inventory Management Systems. April 30, 2015. White paper.
3. Roberti, M. About that Problem with Metal and Water. RFID Journal, 2012. <http://www.rfidjournal.com/articles/pdf?9841>. Accessed October 27, 2016.
4. Ross, W. A., S.E. Burns, P.Y. Wu and D.M. Jared. Radio Frequency Identification Tracking Technology Applied to Testing of Transportation Construction Materials. Transportation Research Record: Journal of the Transportation Research Board No. 2098, National Academy of Sciences, 2009, pp. 3-12.
5. Schwartz, C.W., J.S. Khan, G.H. Pfeiffer, and E. Mustafa. Radio Frequency Identification Applications in Pavements. Federal Highway Administration Report No. FHWA-HRT-14-061, University of Maryland, August 2014.
6. Zero to RFID in 60 Minutes Challenge? <https://www.linkedin.com/pulse/zero-rfid-60-minutes-andy-bridden>. Accessed October 27, 2016.
7. TxDOT Traffic Rail Standard Detail Type T1P. <http://ftp.dot.state.tx.us/pub/txdot-info/cmd/cserve/standard/bridge/r1stds35.pdf>. Accessed October 27, 2016.
8. TROI™ RS-102 Specification Sheet: http://troirfid.com/yahoo_site_admin/assets/docs/RS-102_Datasheet_updated_address.48130612.pdf Accessed October 27, 2016.
9. TROI™ RS-102 Specification Sheet: http://troirfid.com/yahoo_site_admin/assets/docs/RS-200_Datasheet_updated_address.48122919.pdf Accessed October 27, 2016.

Safety Evaluation of Safety Edge Treatment in Iowa

AMRITA GOSWAMY
SHAUNA L. HALLMARK
Iowa State University

MICHAEL PAWLOVICH
Iowa Department of Transportation

BO WANG
Ford Motor Company

A drop-off between the edge of the paved roadway and the adjacent ground proves to be a serious concern for vehicles that drift-off the roadway. Pavement edge drop off contribute to about 18% of rural ROR crashes with paved roadways and unpaved shoulders. Safety Edge is a design feature that creates a fillet (preferably 30 degrees) along the edge of the paved roadway which allows errant drivers to return safely to the roads.

The Safety Edge is a relatively low-cost countermeasure that can be applied during both asphalt and concrete paving operations. Safety Edge has been promoted to reduce the frequency and severity of rural roadway departure crashes. However, little information is available regarding the actual effectiveness of Safety Edge. Although the treatment only adds a small amount of additional material to a paving project, agencies are still interested in understanding the safety impacts in order to better justify programming of safety funds.

The safety impact of the Safety Edge on rural 2-lane roadways in Iowa was evaluated. A total of 659 treatments (418 miles) were constructed during the 2010 and 2011 construction season and 1031 control sites (662 miles) were identified and used to conduct before and after crash analyses. Safety Performance Functions (SPFs) were developed using negative binomial generalized linear models. The Empirical Bayes (EB) method was then used to develop crash modification factors (CMFs).

Eleven years (2004-2014) of non-intersection crashes were used in the study. Roadway and traffic data for corresponding eleven years was used in the study. Target crashes were identified as any crash related to run off the road (ROR) action. Results indicate a reduction of 8 to 16% depending on the type of crash. Not all of the results were statistically significant. This is likely due to sample size. Reduction in only the injury crashes was seen to be about 16.5%. Unknown injury and all property damage only crashes got reduced by about 20% each. For all of the three cases, the results were statistically significant at 95% confidence level. Crash reduction for target crashes ranged from 4% to 9% for the three different crash severity levels but were not statistically significant at 95% confidence level.

Investigating Effectiveness of Centerline Rumble Strips on Rural Two-Lane Roads in Louisiana with Empirical Bayes Method

M. ASHIFUR RAHMAN

XIAODUAN SUN

University of Louisiana at Lafayette

Louisiana rural two-lane highways possess a low geometric standard with very low AADT but more fatalities and fatal crashes compared to other type of roads. Over 20% of the fatal crashes occurred during 2006-2015 were cross-centerline crashes - mainly head on and opposite direction sideswipe crashes. To address the problem of drowsy, distracted, or inattentive drivers crossing the centerline, centerline rumble strips were installed on more than 2,100 miles of rural two-lane highways in Louisiana. About 90% of state maintained rural two-lane highways have AADT of less than 5,000, which has not been addressed by crash modification factor (CMF) documented in Highway Safety Manual.

By using at least three years of crash data for the before and after time periods, this study applied the Empirical Bayes (EB) method to estimate the CMF. Locally developed safety performance function was used as part of the estimation of safety effectiveness. The study revealed that estimated CMF from EB analysis on 2,140 miles is 0.809 with a very low standard deviation of 0.02%, which means there is a 19.1% expected total crash reduction in implementation of centerline rumble strips on rural two-lane highways.

Safety Impacts of the Safety Edge

SHAUNA L. HALLMARK

AMRITA GOSWAMY

Iowa State University

MICHAEL PAWLOVICH

Iowa Department of Transportation

BO WANG

Ford Motor Company

Around 56% of traffic fatalities in the US are due to roadway departures. In 2013, this represented 18,257 fatalities (FHWA 2014). One contributor to roadway departure crashes is the presence of pavement edge drop-off, which is a vertical elevation difference between two adjacent roadway surfaces. Edge drop-offs are potential safety hazards because significant vertical differences between surfaces can reduce vehicle stability and impede the driver's ability to handle their vehicle (Ivey et al. 1984). Pavement edge drop-off can also result in tire scrubbing where the tire sidewall is forced into the pavement edge, resulting in friction between the tire and pavement. When a driver compensates for scrubbing by increasing the steering angle and the right front tire finally remounts the pavement, a sudden loss in friction between the tire and the surface of the pavement edge occurs which can result in loss of control (Ivey et al. 1988).

The Safety Edge is a relatively low-cost countermeasure that can be applied during both asphalt and concrete paving operations. Safety Edge has been promoted to reduce the frequency and severity of rural roadway departure crashes. However, little information is available regarding the actual effectiveness of Safety Edge. Although the treatment only adds a small amount of additional material to a paving project, agencies are still interested in understanding the safety impacts in order to better justify programming of safety funds.

The safety impact of the Safety Edge on rural 2-lane roadways in Iowa was evaluated. A total of 659 treatments (418 miles) were constructed during the 2010 and 2011 construction season and 1031 control sites (662 miles) were identified and used to conduct before and after crash analyses. Safety Performance Functions (SPFs) were developed to predict before period crashes on control segments using negative binomial generalized linear models. An Empirical Bayes (EB) method was then used to develop crash modification factors (CMFs). Results indicate crashes are reduced by 8 to 16% depending on type of crash.

Safety Impacts of Centerline Rumble Strips in Georgia

MARISHA S. PENA

Georgia Institute of Technology

Vehicle crashes involving crossing over the roadway centerlines are among the most severe types of collisions nationwide. To address this issue, the Georgia Department of Transportation (GDOT) started implementing the construction of centerline rumble strips (CLRS) in rural locations across Georgia in 2005 and 2006. CLRS produce both an audible and tactile warning to alert drivers of impending lane departure into the lane of oncoming traffic. Currently, approximately 200 miles of CLRS have been installed by GDOT in the state of Georgia as a countermeasure for crossover crashes along rural two-lane undivided highways. This study evaluates the safety impacts of CLRS deployments in Georgia. The study analyzed approximately three years of before-and-after periods to evaluate the safety impacts associated with CLRS implementation of 10 treatment sites and a control group of comparison sites with similar traffic and physical characteristics. The study data set included approximately 2,000 crashes along over 125 miles CLRS treatment sites and 15,000 crashes along control group sites. The empirical Bayes method was used to develop a crash modification factor for CLRS, specific to rural two-lane undivided highways in Georgia.

High Tension Cable Barrier in the Median of a Freeway in Alberta, Canada

A Case Study of Two Successful Projects

**PAUL H. A. STEEL
MASOOD HASSAN
GERARD KENNEDY**
Tetra Tech Canada

BILL KENNY
Alberta Transportation

This paper presents the highlights of the design, construction, operation and maintenance, and safety and economic effectiveness of two high tension cable barrier (HTCB) projects in the median of Highway 2 in the province of Alberta, Canada. The projects were initiated by the provincial Department of Transportation (DOT), with a view to preventing cross-median crashes on this high traffic freeway. The design, construction-supervision, before-and-after safety evaluation, and benefit-cost analysis of the projects were undertaken by Tetra Tech.

The first project consisted of an 11km 3-cable HTCB installation (in 2007) in the depressed median (varying in width from 16m to 31m) of the six-lane divided Highway 2 within the City of Calgary (locally known as the Deerfoot Trail), carrying 154,000 AADT.

The second project consisted of a 135km 4-cable HTCB installation (in 2010) in the depressed median (varying in width from 14m to 18m, with varying sideslopes) of the mostly rural segment of the four-lane divided Highway 2 from Calgary northward, carrying 34,000 AADT.

The main findings of the paper are presented below.

- **Design Aspects.** Under a competitive bidding environment, the specifications should ensure that at least two suppliers are eligible to bid. Placing of the HTCB in the median, preferably near the shoulder, should ensure that the available deflection space exceeds the test deflection of the HTCB product installed; and if this condition cannot be met, the HTCB may need to be installed in the ditch or on both sides of the median.

- **Safety Effectiveness.** After HTCB installation, the percentage of fatal median related collisions was reduced from 4.4% to 0% on Deerfoot Trail, and from 2.1% to 0.5% on Highway 2.

- **Cost Effectiveness.** A rigorous benefit-cost analysis showed: for Deerfoot Trail, a benefit-cost ratio of 11.1 at the end of the design life of 20 years, with benefits exceeding costs in the first year after installation; and for Highway 2 a benefit-cost ratio of 4.58 at the end of the 20 year design life, with benefits exceeding costs in the second year after installation.

- **Innovative Construction Techniques.** The innovative and cost-saving techniques that the HTCB contractor utilized for the Highway 2 installation included: a vibratory post driver instead of the usual drop hammer; straight line production utilizing two customized truck-trailers each carrying 20 spools of cable instead of the usual four spools; a custom-built guide post attachment mounted on a mini-excavator; a customized post developed to maintain some tension in the system during splicing; and tensioning of cables with an electric winch instead of the usual block and tackle arrangement. An innovation that had some challenges was the use of precast concrete for the end-anchor foundations, with many

demonstrating movement beyond allowable tolerances, although not compromising the functionality of the HTCBB. One of the lessons from this experience is that in the future Alberta Transportation will require that concrete foundations be cast-in-place, or if driven steel, to be specified at a greater driven depth. Precast concrete foundations are no longer permitted.

- **Operational and Maintenance Experience.** The 11km Deerfoot Trail HTCBB experiences an average of 3.2 hits per month (or 0.3 hits per km per month) requiring repair. The maintenance contractors find repairing HTCBB not harder than other barrier types. Accumulated snow does cause occasional problems. Extra precautions are required to safeguard the safety of maintenance workers.

- **Training of First Responders.** Familiarization sessions were held with first responders to disseminate knowledge about vehicle extraction and cable-cutting if necessary.

- **Public Acceptance.** The reaction of the public and emergency responders to the HTCBB installations has been consistently positive.

The authors believe that the experience gained from the two Alberta Highway 2 projects would be of interest to highway jurisdictions around the world.

INTRODUCTION

This paper presents the highlights of the design, construction, operation and maintenance, and safety and economic effectiveness of two high tension cable barrier (HTCB) projects in the median of Highway 2 in the province of Alberta, Canada. An appreciable amount of literature dealing with various aspects of HTCB is available (e.g. References 1 and 2, which include additional bibliographies). The emphasis in this paper is on the experiences and innovative features of the Alberta HTCB projects that the authors believe would be of interest to other highway jurisdictions.

Figure 1 shows the location of the two HTCB projects on Highway 2 in Alberta. The first project consisted of an 11km section of 3-cable HTCB installation in 2007 in the depressed median (varying in width from 16m to 31m with median sideslopes of 6:1 or flatter) of the six-lane divided Highway 2 within the City of Calgary (locally known as Deerfoot Trail), carrying over 154,000 annual average daily traffic (AADT) with a posted speed limit of 100km/hr to 110km/hr.

The second project consisted of 135km of 4-cable HTCB installed in 2010 in the depressed median of 122km of four-lane divided, mostly rural, Highway 2 from Calgary northward. Note that 13km of highway had HTCB installed on both sides of the median. The median width varied over the project length up to 18m at its widest, with median sideslopes ranging from 6:1 to 4:1, and traffic volumes from 30,000 to 34,000 AADT with a posted speed limit of 110km/hr. This 122km project comprised a 118.5km section from north of Calgary to Red Deer, and a 3.5km section at Leduc, south of Edmonton.

The projects were initiated by Alberta (Department of) Transportation, which is responsible for all highways in the province. The design, construction-supervision, before-and-after safety evaluation, and benefit-cost analysis of the projects were undertaken by Tetra Tech. Certain aspects of these projects have been reported earlier (3 to 9); this paper summarizes items of interest from these references and presents additional unpublished material, thus depicting a reasonably complete picture of HTCBs in action. Note that all amounts mentioned are in Canadian dollars.

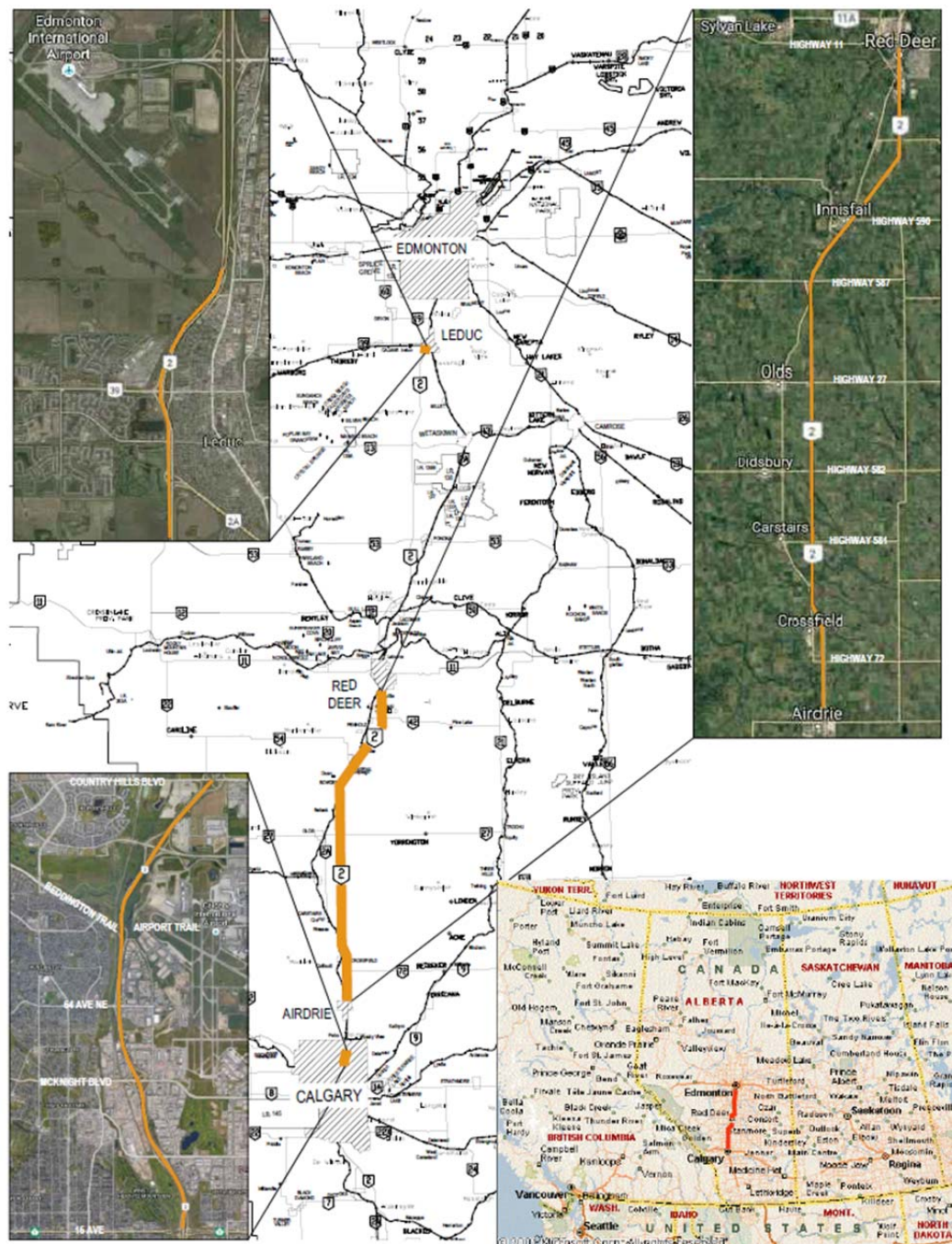


FIGURE 1 Location of the high tension median cable barrier projects on Highway 2 in Alberta, Canada.

PRE-ENGINEERING RESEARCH

Alberta Highway 2 projects were the pioneer HTCBB projects in Canada. A thorough background research was therefore considered necessary to obtain the latest information about HTCBBs elsewhere, particularly in the US.

Contact was initiated in 2006 and maintained throughout the planning and design of the Highway 2 projects with officials of the US Federal Highway Administration (FHWA), the Association of State Highway and Transportation Officials (AASHTO) and selective US DOTs.

To gain additional insights into the characteristics of the available HTCB systems, representatives of three HTCB suppliers with FHWA-accepted HTCB systems were invited to Calgary in March 2006 to make individual presentations about their respective cable barrier products to the staff from Alberta Transportation, Tetra Tech and the maintenance contractor for Deerfoot Trail.

SALIENT DESIGN FEATURES

The HTCB suppliers must get the crash impact tests of their proprietary barriers done by independent testing facilities at “Test Levels” defined by NCHRP Report 350 (10), which has been updated by the Manual for Assessing Safety Hardware (MASH) (11). Based on the test results, FHWA issues letters of acceptance indicating the maximum barrier deflection, post spacing and other conditions, guidelines and caveats under which the product can be used. FHWA also issues general guidelines regarding factors such as the placement of HTCB in the median.

Specifications Regarding Selection from the Available High Tension Cable Barriers

To comply with Alberta Transportation’s policy of competitive bidding, which required that at least two different HTCB systems were available to the bidding contractors, the following specifications were included in the tender for the Deerfoot Trail installation. References to the available HTCB suppliers and FHWA acceptance letters were included in the tender documents.

- NCHRP 350 Test Level 3 or Test Level 4 pre-stretched, post-tensioned cable system;
- 3-cable or 4-cable systems;
- Maximum test deflection of 2.4m (8ft);
- Maximum post spacing of 6.1m (20.0ft).

For the Highway 2 project the same specifications were used, except that Alberta Transportation stipulated a 4-cable system based on an indication in FHWA guidelines that a 4-cable system may stop a larger variety of vehicles.

Lateral Placement of Cable Barrier in the Median

The location of the cable barrier in the median must take into account many inter-related and potentially conflicting factors. The relevant factors, among others, considered for the Alberta projects were:

1. The FHWA guidelines regarding placement of HTCB in the median must be followed.
2. When only one median HTCB protects both directions of traffic, there must be sufficient deflection space to allow for the minimum test deflection plus as large a safety margin as the local conditions allow (the sum being the desired room for deflection) between the HTCB and the nearest median-side painted yellow shoulder line. This requirement would help keep a vehicle hitting the HTCB from the back after crossing the median from protruding into the median-side travel lane.

3. The above Point 2 about sufficient space also applies to hazards in the median such as bridge piers and overhead sign posts which do not have individual barrier(s) to protect a vehicle from hitting them.

4. Although the installation of the HTCB in the ditch centre would tend to satisfy both Point 1 and Point 2 above, the ditch soils are normally un-compacted, the ditches are subject to water accumulation, and there are catch basins or culvert outlets in the median. As a rule, therefore, HTCB installation at the top of the sideslope near the shoulder is preferred.

On the Deerfoot Trail, the HTCB was installed near the shoulder in the northbound direction. On the 122km of Highway 2, the median placement was as follows: HTCB was installed on the median slope near the shoulder on 66km in the northbound or southbound direction. However, the shoulder installation on another 56km could not satisfy the above conditions because of the median being too narrow or other local situations, and the HTCB was therefore placed at the centre of the ditch. On short sections totaling 13km, the placement conditions could not be satisfied by shoulder or ditch installation (because of the median narrowness or a local situation) and the HTCB was therefore installed on the shoulder in both directions.

Cable Run Length

End-anchors are the most expensive part of a HTCB system. Longer HTCB run lengths would reduce the number of end-anchors. However, the end-anchors hold the tension in a HTCB system. A vehicle collision with an end-anchor would release the tension in the entire segment, which would favour shorter run lengths.

For the Alberta projects, it was decided to divide the 11km of Deerfoot Trail HTCB into two segments of 8.5km and 2.5km. Although no hits with end-anchors were experienced with the Deerfoot Trail end-anchors, after additional consultations with FHWA it was decided to limit the HTCB segment length on Highway 2 to approximately 5km. The average segment length on Highway 2 turned out to be 2.5km (ranging from a few hundred metres to a little less than 5km), mainly because of natural breaks at bridges, overpasses and at-grade intersections.

BEFORE-AND-AFTER SAFETY EVALUATION

Alberta Transportation maintains a comprehensive Collision Information System, which classifies collision severity as fatal, major injury, minor injury and “property damage only”. From this database, median related collisions were analyzed to compare the before-HTCB and after-HTCB safety performance on Deerfoot Trail and Highway 2. The safety analysis was performed in terms of frequency and rate as well as by the Empirical Bayes method in AASHTO’s Highway Safety Manual (2010). A summary of the findings is presented below; details are available in References 4, 5 and 8.

Safety Evaluation of Deerfoot Trail

Median collision statistics for the before-HTCB period 2002 to 2006 (five years) were compared to the 32-month (May 2007 to December 2009) after-HTCB period.

A slight increase in the overall frequency of collisions was observed because of the increase in property damage only collisions, which is to be expected with any type of newly installed median

barrier, because some of the errant vehicles which previously might have recovered in the median and returned to the travelled way are now hitting the barrier simply because it is there.

After HTCBB installation, the proportion of median related fatal collisions dropped from 4.4% to 0% (the trend has endured: from 2007 to October 2016 there has been no median related fatal collision on Deerfoot Trail), and the percentage of median related injury collisions dropped from 21.1% to 11.8%. The frequency of severe (fatal and major injury) collisions dropped by 25% and the rate of severe (fatal and major injury) median related collisions per 100 million vehicle-km dropped by 40% after the installation of the HTCBB.

Application of Empirical Bayes method showed that the safety performance on Deerfoot Trail improved by 27.9% with respect to a reduction in severity (fatal and injury collisions) of median related collisions.

Safety Evaluation of Highway 2

Median related collision statistics for 63 months before-HTCBB were compared to the 18-month after-HTCBB period. Before HTCBB 2.1% were fatal collisions, and 34.5% injury collisions. The corresponding percentages after HTCBB were 0.5% fatal collisions and 10% injury collisions.

Application of Empirical Bayes method showed an overall 43.4% reduction in severity (fatal and injury collisions) of median related collisions after HTCBB.

A unique feature of the Highway 2 HTCBB analysis was the opportunity to examine the influence of HTCBB placement on the frequency of median related collisions. Table 1 shows the result of this analysis.

For “all collisions”, the rate is highest for locations with HTCBB on both shoulders. This is to be expected since the barrier is close to the lanes in both directions. Shoulder placement of the HTCBB has the next highest collision rate, and the ditch installations have the lowest rates, which is logical since it is furthest from the travel lanes and provides the largest area for recovery.

The collision rates by median width suggest that the rates for “all collisions” are similar but the “injury” rates are higher in locations with a narrower median.

The median sideslope on which a vehicle approaches the barrier can influence how a vehicle strikes the barrier and therefore the performance of the HTCBB. Not surprisingly, the collision rates for the 4:1 sideslopes (steepest) resulted in the highest rates when considering all categories of collision severity.

The results shown in Table 1 are interesting but tentative, and any generalization or extrapolation must await further research.

It should be noted that, although an analysis based on a longer after-HTCBB period has not yet been conducted for the Alberta HTCBB projects, there is little doubt that the positive safety effectiveness shown by the before and after analysis reported above should endure in the long term.

TABLE 1 Median-Related Collision Frequency and Rates by Placement, Median Width and Sideslope in the 18-month Period after HTCB Installation

Factor	Collision Counts			Segment Properties		Median-Related Collision Rates (Collisions/100 Million veh-km)		
	All Collisions	Injury	Fatal	Highway Length (km)	Daily Traffic (Weighted AADT)	All Collisions	Injury	Fatal
Barrier Location								
Both Shoulders	94	8	0	12.87	33,500	42.09	3.58	0.00
Ditch	267	29	1	55.92	29,950	30.78	3.34	0.12
Shoulder	238	23	2	53.17	29,510	29.28	2.83	0.25
Total	599*	50*	3	121.96				
Median Width								
<= 9.0 m	80	10	0	17.43	28,620	30.96	3.87	0.00
> 9.0 m	478	47	3	104.53	29,980	29.45	2.90	0.18
Total	558*	57*	3	121.96				
Median Sideslope								
4:1	136	13	1	15.21	33,260	52.28	4.96	0.38
5:1	313	30	1	73.16	29,950	27.66	2.64	0.09
6:1	150	16	1	33.59	30,060	28.87	3.06	0.19
Total	599*	59*	3	121.96				

* The anomalies in these numbers are attributed to certain parameters being absent in some collision reports, which made it difficult to assign particular collisions by median width, sideslope, or location.

BENEFIT-COST ANALYSIS

A rigorous benefit-cost analysis of the two projects was performed according to Alberta Transportation's benefit-cost guide which includes the monetary values of various collision types (the guide has since been update (12)). The analysis utilized the actual capital and annual operation and maintenance costs, the monetized reductions in median related collisions, and a design life of 20 years with no salvage value. The results of the benefit-cost analyses are summarized below; some details are provided in Reference 6.

Benefit-Cost Analysis of Deerfoot Trail Project

The capital construction cost of the 11km HTCB installation on Deerfoot Trail was \$946,000, or \$92,000 per HTCB-km (in 2007 Canadian dollars). The all-inclusive maintenance cost amounted to \$65,000 per year, or \$6,050/HTCB-km/year.

The analysis yielded a net present value (NPV) of \$18.5 million and a benefit-cost ratio of 11.1 at the end of the 20 year design life. The NPV-capital cost ratio was estimated to be 19.5 at the end of the design life. The benefit starts exceeding the cost in the first year after installation.

Benefit-Cost Analysis of Highway 2 Project

The capital construction cost of the 133km of HTCB installation on Highway 2 was \$7.5 million in 2010 Canadian dollars (amounting to \$56,100 per cable-km). This is much cheaper than the Deerfoot Trail capital construction cost of \$92,000 per cable-km in 2007 dollars. The unit cost reduction can be attributed to economies of scale and innovative installation techniques for the Highway 2 project. The total maintenance cost was \$504,500 per year, or \$3,790/HTCB-km/year.

For Highway 2, the analysis yielded a NPV of \$53.1 million and the benefit-cost ratio estimated 4.58 at the end of the 20 year design life. The NPV-capital cost ratio was estimated to be 7.11 at the end of the design life. The benefit starts exceeding the cost in the second year after installation.

INNOVATIVE CONSTRUCTION TECHNIQUES

The contractor for the Deerfoot Trail HTCB installation used poured concrete for line posts and end-anchor foundations, and routine methods for installing, posts, cables and tensioning the cables.

Summarised and illustrated below are several innovative techniques that the installing contractor developed for the Highway 2 HTCB installation; these helped reduce the cost and construction time as compared to the Deerfoot Trail installation. Details of the techniques and additional photos depicting technique are included in Reference 7.

Utilizing a Vibratory Post Driver (Photo 1)

Instead of the usual drop hammer, a vibratory post driver mounted on a mini excavator was used to install the driven steel post sockets. This allowed the contractor to install line posts at an average rate of one post every 1 to 2 minutes. In locations where soil conditions were challenging, either a backhoe mounted pneumatic driver or pre-drilling was required.



(a)



(b)

PHOTO 1 (a) Vibratory driver attached to mini-excavators installing a driven steel socket and (b) customized spool truck carrying 20 spools of cable barrier (approx. 12.0 linear km of cable or 2.5 km of 4-cable-barrier per truck).

Customized Spool Delivery Truck to Expedite Production (Photo 1)

Normally the delivery truck bringing the 1,000ft (303m) spools carries four spools. A customized truck and trailer for cable stringing work was employed. During installation, two trucks each carrying 20 spools carried approximately 12 linear-km of cable allowing approximately 5km of 4-cable barrier per day of production.

Special Guide-Post Attachment to Aid Cable Installation (Photo 2)

The contractor used a custom built attachment to assist workers with installation of the HTC.B. Mounted on a mini-excavator, the guide-post ensured cables were kept separated and untangled. This configuration also assisted workers by keeping the cable at a constant height above ground, thus reducing fatigue and potential worker injury from repetitive lifting motions at each line post, which is the usual procedure.



(a)



(b)



(c)

PHOTO 2 (a) Custom built cable-guide mini-excavator attachment maintaining cables at constant height to reduce worker fatigue from repetitive lifting motions; (b) Custom-post holding tension in system during splicing and installation of turnbuckles; and (c) Mini-excavator-mounted winch for use during tensioning and splicing work.

Special Tension-Holding Post (Photo 2)

Every 303m requires a splice in the cables by using a set of turnbuckles. In order to maintain consistent turnbuckle placement, a customized post was developed to maintain some tension in the system during splicing. At each splice, workers would pull cables taut using the mini-excavator-mounted winch; cables were then held in place, in tension, while the splice and turnbuckles were installed.

Tensioning of Cable with an Electric Winch (Photo 2)

Normally a block and tackle arrangement is used at the end-anchor to tension the barrier. For Highway 2 the contractor used a mini-excavator-mounted winch, which was parked in place at the end terminal. This method resulted in fewer setups per end terminal and allowed workers greater precision during tensioning.

Use of Driven Steel and Precast Concrete Foundations for End-Anchors (Photo 3)

For the Deerfoot Trail project, cast-in-place concrete foundations were specified for both the line post and end-anchor foundations. In its acceptance letters for HTCBB suppliers, FHWA permits either concrete or driven steel foundations for the line posts and end-anchors. For the Highway 2 project, the HTCBB design had specified either concrete or driven steel foundations for line posts and end-anchors. The contractor used driven steel for line post foundations on the entire length of the project.

Driven steel and precast concrete foundations are less expensive than cast-in-place concrete foundations. Of the 106 end-anchors and associated terminal posts, approximately 60% had driven steel foundations. As a cost-saving measure 35% of the end-anchors had precast concrete foundations. The remaining 5% had cast-in-place concrete foundations. The precast concrete foundation was a long solid vertical slab with a square cross section, which was lowered into a pre-drilled round hole and the four spaces between the sides of the square and the round hole were backfilled and compacted.

No significant foundation-related concerns were noted with the Deerfoot Trail post and end-anchor foundations, which were all built with cast-in-place concrete. Also, the line post driven steel foundations for the Highway 2 project were mostly problem-free. However, several deficiencies were noticed regarding the end-anchor foundations on Highway 2 during the initial one year warranty inspection.

The majority of the end-anchors, both precast concrete and driven steel, exhibited some movement. The distance of the movement varied from site to site and it is theorized that this may have been due to poor soil conditions, potentially inadequate compaction of the backfill material around the anchors, and/or insufficient depth of the driven steel end-anchors.

A follow up inspection carried out three years after installation found that much of the movement had either ceased or only increased nominally. The most recent follow up inspection, six years after installation, indicated that all movement of the majority of anchors has stopped. Of the 106 end-anchors installed, there are only a handful that will require remedial action.

It was concluded that movement of anchor foundations noticed on Highway 2 did not compromise the functionality of the HTCBB. One of the lessons from this experience is that Alberta Transportation now requires that end-anchor concrete foundations must be cast-in-place; and if



(a)



(b)



(c)

PHOTO 3 (a) Installing pre-cast concrete end-anchor foundation in bored hole; (b) Backfilling pre-cast concrete end-anchor foundation in bored hole; and (c) Installing driven steel anchor post using pneumatic driver.

driven steel, they should be specified at a greater depth than provided on some of the suppliers' standard details. Precast concrete foundations for end-anchors are no longer permitted.

The innovations described above enabled the installation of 133km of HTCBB on Highway 2 in 45 days compared to an estimated 150 days with conventional installation methods and the use of cast-in-place concrete foundations.

OPERATIONAL AND MAINTENANCE EXPERIENCE

After every hit to the HTCBB, repairs are carried out by the private contractor who has the maintenance contract for that particular section of the highway. The contractor keeps a record of all items for which payments are made, including traffic accommodation, inspection, supply and replacement of end-anchors, posts, hairpins, lockplates, re-tensioning of the cables, mowing/trimming around the posts and snow clearing.

The average maintenance and repair costs of the HTCBB (\$6,050/HTCBB-km/year for Deerfoot Trail, and \$3,790/HTCBB-km/year for Highway 2) have remained fairly constant except

for inflation. The main difference in the costs between the two projects is attributed to the level of traffic accommodation required to replace damaged components and re-tension the system on an urban freeway compared to a rural highway corridor. Much of the maintenance required for Deerfoot Trail is performed during off-peak times at night to minimize the impact to traffic, requiring a higher level of work zone protection and advanced notification.

The timing of HTCBB repairs has been established based on potential severity criteria with more severe hits (i.e. cables pinned to the ground or tension loss due to end terminal release) requiring repairs sooner than typical hits where cables remain at the correct height and tension.

Highway 2 HTCBB maintenance is under three separate contracts in three administrative regions of Alberta Transportation. The records for the 11km HTCBB on Deerfoot Trail HTCBB are reasonably complete for which the maintenance contractor recorded the following repair statistics for the 111 month period May 3, 2007 to September 4, 2016. Comparable statistics for Highway 2 are not available in a comprehensive form:

- No. of hits requiring repair: 359 (average of 3.2 hits per month, or 0.3 hits per km per month);
- No. of line posts replaced: 1,353 (average of 3.8 line posts per hit);
- No. of hairpins replaced: 1,718 (average of 4.8 hairpins per hit);
- No. of lockplates replaced: 1,821 (average of 5.1 lockplates per hit).

Over the 11 months, five of the 359 hits required replacement of more than 20 line posts. One of them involved a southbound city bus that crossed the median and hit the HTCBB from the back. Another two of these hits were by high speed pickup trucks with drivers apparently having fallen asleep -- in an interesting way, this helps illustrate the advantage of an HTCBB, which, having been hit, flexes and guides the vehicle along the cable barrier until the vehicles comes to a stop. If the same high-speed pickup truck had hit a solid barrier, it would probably have been deflected back into the traffic stream. It should be noted that no hits with or damage to the end-anchors were reported on the Deerfoot Trail.

The following summary of the lessons learned with respect to maintenance of HTCBB in Alberta would be of interest.

- Winter post replacement poses only minor problems as opposed to summer post replacement;
 - The Splicing of the cable, if needed, and re-tensioning is relatively simple after repairing of damage sections (the re-tensioning must be completed after any section is hit);
 - After a hit the barrier is still functional in most cases and will continue to do its job to a degree until repairs are completed (this holds true unless the cables are laying on the ground);
 - It appears the HTCBB can withstand many hits without compromising its strength or integrity;
 - The authors are unaware of any instance when the cable broke from anything other than being cut by first responders or others;
 - If an emergency arises requiring maintenance workers working in the driving lanes along the cable barrier on the shoulder, there escape route is eliminated or compromised greatly; workers can no longer just run into the ditch;

- In some cases, short-duration work that only took minutes and could be performed without traffic accommodation, now requires a full traffic control procedures, such as signs and flag persons.;
- An activity as routine as removing a road kill from the inside lane when the barrier is installed at the edge of asphalt can no longer be done from the inside lane. Workers must either drag the animal across the outside driving lane when traffic allows, (this causes great exposure and risk to maintenance workers) or drag the animal under the barrier and find a way to get inside the median to pick it up, (this cannot be done in the winter or wet weather) or use full traffic control;
- In some locations washing of the highway infrastructure is completed at night to limit the exposure of workers to the travelling public as there is no escape route on the inside travel lanes in some locations.
- The previous issue also applies to the activity of debris removal from the median. This can also only be done when weather and seasonal conditions permit. Maintenance workers are instructed not to lift objects over the barrier due to potential hazards of lifting on slopes or uneven ground. This process has added a lot of extra time to routine maintenance and operations;
- Narrow sections of median where the barrier is in the median ditch now forces mowing tractors onto the shoulder of the highway. In some cases traffic accommodation is now required;
- Some cases where the barrier transitions from the ditch bottom to the shoulder, mowing tractors are forced onto the shoulder of the highway. This leads to increased risk and large delays while waiting for gaps in traffic;
- Trimming of the grass along the length of the barrier exposes the contractors' workers to greater risk. At locations where the barrier is near the centre of the ditch of a narrow median with narrow shoulders, the workers are within arms-length of traffic travelling at highway speeds. Due to limited space, maintenance vehicles cannot be safely accommodated without the use of signage and a lane closure in order for the trimming to be completed safely;
- With the barrier on the shoulder it is no longer possible to push the snow further into the median. The snow now just builds against the barrier when ploughing is unable to throw the snow past the HTCB. This can be cause for further drifting and snow build up. In the spring, melting snow can be trapped and held on the shoulder of the highway due to the snow banks that have accumulated over the winter. Removal of the snow can only get so close to the barrier should it be needed;

In general, the introduction of the median HTCB there is a need to adjust and look at every activity at every location on a daily basis to ensure the safety of maintenance workers and the travelling public. Traffic accommodation can vary from a very simple strategy including a truck with an arrow board to a very complex strategy involving lane closures.

INFORMATION FOR FIRST RESPONDERS

To familiarize first responders (fire, ambulance, and police departments, and tow truck operators) with the characteristics of HTCB and best practices for dealing with HTCB collisions, three information sessions were held in Calgary, Red Deer and Leduc. A separate presentation was made to the Integrated Traffic Unit of the police for Highway 2.

The authors had surveyed the literature and contacted several US DOTs, and had prepared an overview of the characteristics of HTCB, a generic summary of vehicle handling, tension

release and cable cutting procedures that was provided to the first responders. A copy of an informative 10-minute video on HTCB obtained from the Michigan DOT was provided to the participants – this video titled ‘Cable Barrier for First Responders’ is available on YouTube at <http://www.youtube.com/watch?v=qSi4XkSHiFM>.

The following summarizes the guidelines regarding releasing cable tension to facilitate extraction of vehicles entangled in HTCB communicated to first responders:

- Remove hairpins and lockplates up and downstream of the crash site;
- Loosen the nearest turnbuckle(s); although turnbuckle designs may vary, simple tools like wrenches or crowbars are sufficient to loosen the turnbuckles; turnbuckles should not be loosened beyond a certain point, otherwise there is risk of the cable slipping out;
- Remove posts, or cut posts at grade (near the ground), on either side of the vehicle;
- Knock down/pushover the cable-release terminal at the end of the cable run; these can be long (up to 5km), and there may not be an end terminal in vicinity of the crash site. It should be remembered that this action, and cutting the cable, should be taken as a last resort because it will remove all tension from the entire cable run, and could allow a vehicle to cross the median.
- To extract the vehicle from the cable barrier, pull the vehicle out the same way it entered. In some cases, the part of vehicle entangled in the cables may need to be removed (preferred to cutting the cable). If the vehicle is lying on top of the cables, it may need to be lifted. In all cases, new posts should be installed and the cable tension checked as soon as possible.
- The cable should be cut only as a last resort. In this vein, it is interesting to note that the Michigan DOT requires first responders to obtain departmental permission before doing so. If the cable must be cut, it should preferably be cut at a turnbuckle between two upright posts.
- The repair of cut cables takes longer and is more expensive than replacing turnbuckles. A clear message was communicated to participants that cutting the cables will disable the entire cable run.

PUBLIC REACTION

The reaction of the public and emergency responders to the HTCB installations has been consistently positive. Perhaps the best testimonial is the experience of a driver within a few days after the installation of the high-tension median cable barrier on Deerfoot Trail:

“A Calgary man says the new post-and-cable barrier recently installed in the median along the north end of Deerfoot Trail saved his life. Earl Somerville was driving southbound on Deerfoot near 64th Avenue N.E. in the rain, when a hydroplaning pickup truck T-boned his SUV on the passenger side. The force of the impact sent his vehicle into the median and into the barrier. Somerville said “...it was gentle, like going into a cradle”. Without the barrier, he’s sure he would have ended up in the northbound lanes”. (*Calgary Herald*, May 7, 2007)

LESSONS LEARNED

The use of more forgiving barriers has been widely adopted by Alberta Transportation and bids for HTCB in contracts are more commonplace. To assist Alberta Transportation in developing its

guidance regarding the use and installation of HTCBB for median and roadside applications, Tetra Tech developed a standard specification for inclusion in construction contract project documentation to ensure consistent practices were being implemented. Input was sought from the engineering, operations and maintenance departments of Alberta Transportation as well as from the Consulting Engineers of Alberta and provincial roadbuilders' association.

Specific lessons learned as HTCBB continues to be installed along Alberta highways relative to adoption of the new specifications is summarized below:

1. HTCBB have been found to have many advantages when compared to traditional barrier systems where snow-drifting is a key concern. The accumulation of snow at HTCBB is considerably less than with other barrier types. This reduces the snow clearing effort required at barrier locations and also reduces the frequency of collisions in winter storm periods.

2. When collisions do occur, HTCBB can frequently provide protection for secondary hits. When repairs are required the effort and time needed to bring the system back to operational conditions is minimal compared to conventional systems.

3. The collision severity (based on frequency of fatalities and injuries) typically observed with HTCBB collisions is considerably less than at conventional barriers. This is due to the more forgiving nature of the barrier. Also, the incidence of vaulting, spearing and snagging is significantly reduced.

4. Most of the published testing and literature has been for HTCBB installation in the median. This results in restrictions on the slopes behind the barrier and for lateral placement on the slope. On undivided highways where impacts to the back of the HTCBB are not an issue, Alberta Transportation has been using HTCBB at the shoulder edge if the slope in front of the barrier would be steeper than 4:1. If the slope in front of the barrier is 4:1 or flatter, then a lateral offset is permitted based on the test approvals. By adopting this practice, Alberta Transportation is utilising HTCBB throughout a much larger network resulting in greater public safety and maintenance savings.

5. Alberta Transportation has experienced some operational difficulties as a result of the HTCBBs typically being taller than conventional barrier systems. This is due to wide loads and farm equipment overhanging the shoulders especially on narrow roads and thus impacting the cable barriers inadvertently. A solution has been to offset the barriers down the slope if the slopes and FHWA Guidelines allow or alternatively to use the smaller HTCBB products that are available on the market (only for locations where the width of road and slope steepness do not allow taller systems to be used).

CONCLUDING REMARKS

This paper has presented the highlights of the design, construction, operation and maintenance, and safety and economic effectiveness of two high tension cable barrier projects in the median of Highway 2 in the province of Alberta, Canada. A summary of the main points of the paper is presented in the Abstract at the beginning of this paper, and is therefore not repeated here.

The authors believe that the experience gained from the two Alberta Highway 2 projects would be of interest to highway jurisdictions around the world.

REFERENCES

1. Transportation Research Board. *NCHRP Synthesis of Practice 493: Practices for High-Tension Cable Barriers, A Synthesis of Highway Practice*, Transportation Research Board of the National Academies, Washington, D.C., 2016
2. Transportation Research Board, *NCHRP Report 711: Guidance for the Selection, Use, and Maintenance of Cable Barrier Systems*, Transportation Research Board of the National Academies, Washington, D.C., 2012
3. Hassan, M., McGregor, R., and Lahey, O. Design of a TL-4 median cable barrier For Deerfoot Trail, Calgary. Proceedings of the Transportation Association of Canada Annual Conference, Ottawa, Ontario, Canada, 2007.
4. McGregor, R., Hassan, M. and Lahey, O. *Safety Engineering for the High-Tension Median Cable Barrier on Deerfoot Trail, Calgary, Alberta*. Proceedings of the Canadian Multidisciplinary Road Safety Conference, 2008.
5. Churchill, A., McGregor, R., and Tay, R. *Speed and Collision Effects of the Median Cable Barrier on Deerfoot Trail, Calgary Alberta*. Proceedings of the Canadian Multidisciplinary Road Safety Conference, 2009.
6. Churchill, T., Barua, U., Hassan, M., Imran, M., and Kenny, B. Evaluation of safety and operational performance of high tension median cable barrier on Deerfoot Trail, Calgary, Alberta. Proceedings of the Transportation Association of Canada Annual Conference, Ottawa, Ontario, Canada, 2011.
7. Hassan, M., Rogers, C., Edgington, J., Damberger, M., Morison, C., Ngo, B., Kennedy, G., and McGregor, R. Construction of High Tension Median Cable Barrier in Alberta Highway 2: A Case Study of Cost-Effective Innovation. Proceedings of the Transportation Association of Canada Annual Conference, Ottawa, Ontario, Canada, 2011.
8. Churchill, T., Hassan, M., and Morison, C. Safety Performance of High Tension Cable Barrier in Alberta. Paper prepared for presentation at the 23rd Canadian Multi-disciplinary Road Safety Conference, Montréal, Québec. 2013
9. Churchill, T., Morison, M., and Wilkie, K. Operating and Maintaining Median High Tension Cable Barrier on Highway 2 in Alberta, Proceedings of the Transportation Association of Canada Annual Conference, Ottawa, Ontario, Canada, 2013
10. Ross, H., Sicking, D., Zimmer, R. and Michie, J. *National Cooperative Highway Research Program (NCHRP) Report 350: Recommended Procedures for the Safety Performance Evaluation of Highway Features*, Transportation Research Board of the National Academies, Washington, DC., 1993
11. Association of State Highway and Transportation Officials, *Manual for Assessing Safety Hardware (MASH)*, Washington, D.C., 2009.
12. Alberta Transportation. *Design Bulletin #86/2015, Benefit-Cost Model and User Guide*. Alberta Transportation, Edmonton, Alberta, Canada, 2015.
<http://www.transportation.alberta.ca/Content/docType233/Production/DB86.pdf>

An Analytical Framework of Systematic Screening of Roadway Departure Crashes on Rural Highways in Montana

MD. SHAFIUL AZAM

AgileAssets, Inc.

PATRICIA W. BURKE

Montana Department of Transportation

Roadway departure crash is the leading cause of highway crash related fatalities in Montana. Approximately, 64% of fatalities related to highway crash from 2010-2014 in Montana are related to single vehicle run-off the road crashes compared to the national average of 54%. The roadway departure crashes are more prevalent on rural than urban settings. Due to enormity of the problem a systemic analysis of roadway and low-cost treatment options across the entire roadway network is often a better option than providing expensive treatments on the pockets of networks that show excessive number of such crashes. This study shows an analytical framework to identify the roadway departure crashes on rural highways in Montana where low-cost safety countermeasures can be implemented. Montana uses roadway departure total and injury Safety Performance Functions (a.k.a. RD Total and RD Injury Model) in this screening. Network profiles are created on the predefined roadway segments by applying screening methods and segmenting criteria. The profile, composed of primary and secondary profiles, is then used in the systematic screening to identify the isolated locations as well as cluster of locations that show high propensity of roadway departure crash reduction by using the EB adjusted performance measures and level of service of safety (LOSS) as the criteria. A proactive screening methodology is also demonstrated using various types and degrees of geometric deficiencies and treatment strategies to assess the variability in cost and return on investment in different scenarios. The goal of this study is to identify and establish a consistent and standard method for Montana that can generate a safety work plan of roadway departure related treatments considering varying budgetary constraints.

INTRODUCTION

Roadway departure is the leading cause of fatality and serious injuries on roadways in the United States. In 2014, there were 17,791 fatalities related to roadway departure crashes; which is 54% of the total traffic fatalities [1]. In Montana the issue of roadway departure crash is even more pronounced. The percentage of fatalities due to roadway departure crashes in Montana was roughly 64%, based on an average percentage from 2010 to 2014. Other major contributing factors responsible for roadway crash fatalities and injuries in Montana are: lack of proper restraints (roughly 39%), careless driving (36%), alcohol involvement (35%) and speed (28%) based on the annual average of fatality injury counts from 2004-2013.

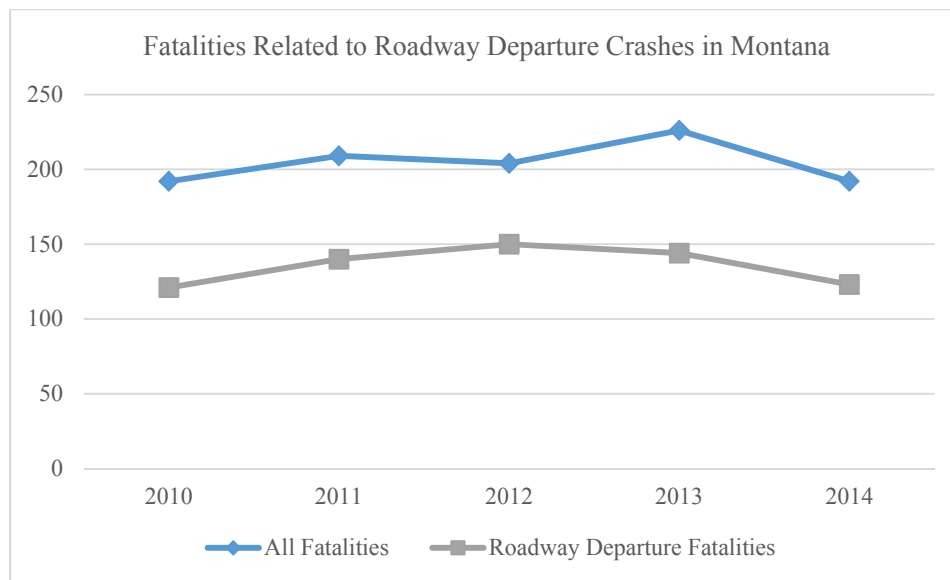


FIGURE 1 Roadway Departure Crash Trend in Montana

Rollover is the leading collision type responsible for most of the roadway departure crashes. The current trend of roadway departure crash (Figure 1) shows a gradual increase of fatalities up to 2012 following a declining pattern over the last few years. The roadway departure crash category in Montana considers single vehicle rollover or fixed object, multi-vehicle head-on as well as cross-median collision crashes resulting departure or impending departure of the vehicle.

This study shows an analytical framework to investigate and identify the roadway departure crashes on rural highways in Montana as well as a proactive screening approach to plan for long-term safety investments. The objective of this study is to highlight both the strategic objectives and analytical aspects of this issue and demonstrate case studies to reinforce the understanding of the framework.

STRATEGIC OBJECTIVES

The analytical framework for road departure crash identification in Montana considers the strategic vision and objectives of Montana and the Federal Highway Administration [1]. This is a bottom up approach meaning the vision and objectives of the country as a whole can reflect the state's vision and objectives, which eventually provides the building blocks for the analytical framework in Safety Management Systems.

Figure 2 shows the strategic pyramid for Roadway departure crash framework for Montana.

The FHWA's roadway departure strategic planning is a living document that primarily serves as a tool to provide long-term focus for the roadway departure team's efforts through data analysis [2]. There are primarily three areas of emphasis that FHWA recommended in their strategy: i) overturn/rollover crashes, ii) opposite direction crashes and iii) roadside trees and shrubs crushes, which is a type of fixed object crash. The primary vision of FHWA's strategic

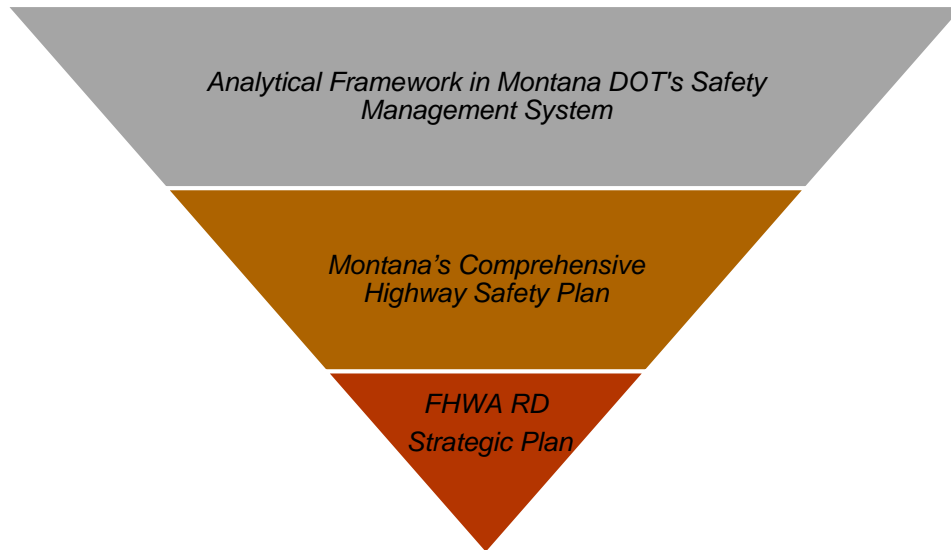


FIGURE 2 Roadway Departure Crash: The Strategic Pyramid

plan is to pursue a proactive approach that will lead toward zero deaths and serious injuries involving roadway departure crashes. The plan also suggested to reduce roadway departure fatalities nationwide by about 500 per year. By the goal in 2030, this translates to a reduction of fatalities by half, from the existing 17,000 per year to 8,500 per year.

The state of Montana has been taking initiatives to curb the roadway departure crash issue through agency's strategies and actions. Montana's Comprehensive Highway Safety Plan (CHSP) defines the emphasis areas, safety strategies, implementation steps along with implementation objectives [3]. The safety plan eventually formulated the basis for safety countermeasures in terms of engineering solutions, enforcement, education and media campaign. In MDT's CHSP the following strategies have been identified:

- Reduce and mitigate roadway departure crashes through data-driven problem identification and the use of best practices.
- Reduce and mitigate speed-related roadway departure and intersection crashes.
- Reduce roadway and intersection crashes through education.
- Explore and implement best practices to reduce certain behavioral factors responsible for road departure, such as distracted driving and fatigued driving.
- Improve the prosecution and adjudication of all roadway user violations.

In summary, Montana has primarily taken three (3) primary initiatives to deal with the roadway departure crashes (Figure 3):

- i) Establish an analytical framework to study and analyze the crash and infrastructure data for better decision making.
- ii) Implement both long and short-term engineering solutions.
- iii) Enforcement, media campaigning and education.

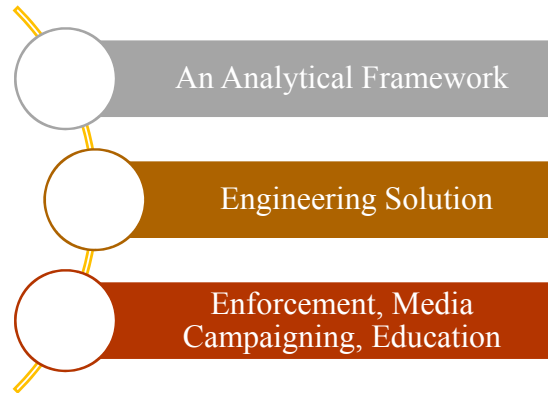


FIGURE 3 Road Departure Crash Strategies by Montana

ANALYTICAL FRAMEWORK

Montana announced “Vision Zero”, a multipronged initiative with the goal of eliminating deaths and injuries on Montana highways, in May 2014. Part of this Vision Zero goal is to reduce the number of fatalities and injuries at least by 50% by the year 2030. One of the major tasks to achieve this goal is to put a lot of emphasis on the roadway departure crashes. Montana’s Safety Information Management System (SIMS) provides the backbone of the analytical framework for the data-driven analysis. From the safety management perspective, we can consider the analytical framework having three major components as shown in Figure 4: i) Crash Data Driven Analysis, ii) Reactive Screening and Hotspots Identification, and iii) Proactive screening. Each of these processes can start from a different perspective but will eventually be targeted to composing the Safety program and associated safety projects.

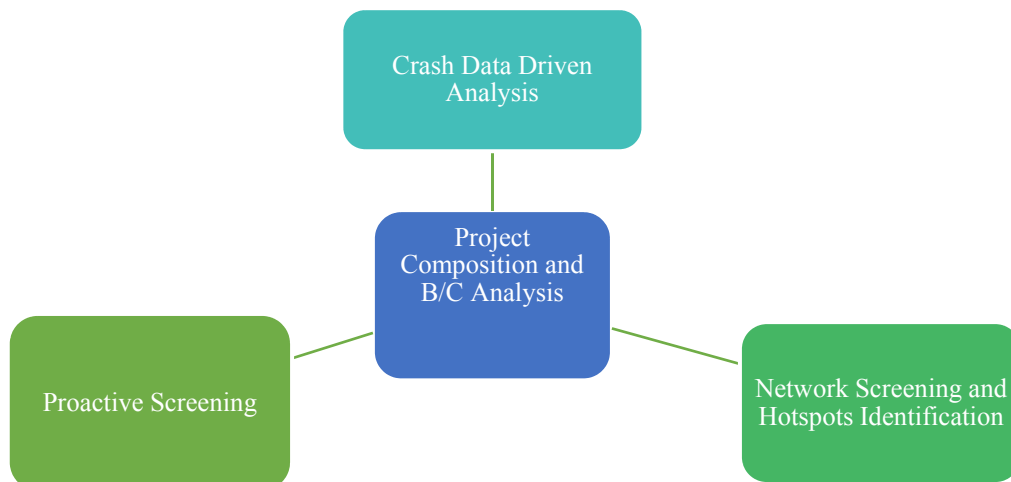


FIGURE 4 Analytical Framework: Major Components

Crash Data Driven Analysis

The most rudimentary analysis in any safety management system is querying or reporting crash data. Although, this seems to be quite a simple process, complexities may arise in dealing with numerous variables in crash data, each of which has its own significance. The process requires some expert judgement and knowledge base to precisely analyze the variables. The crash data driven analysis workflow, shown in Figure 5, comprises of three processes - query/reporting on crash data, identify behavioral factors and GIS based diagnosis.

To identify the risk factors for roadway departure crashes, Montana follows a simple identification checklist for the query/reporting:

- How many crash types to address?
- Criteria to use in selecting crash category by each roadway classification type or local versus statewide
- Infrastructure and/or behavioral

After the query is established based on the aforementioned checklist, it can lead to some additional in-depth analysis to identify any potential behavioral pattern. This step is followed by plotting the crashes on a GIS map to identify the location and spatial distribution of crashes. The identified behavioral pattern can be used to update the emphasis areas or highway safety plan.

A crash data driven analysis for roadway departure crash might require some hierarchical query to identify the behavioral pattern as shown in Figure 6. For example: the analytical search can start with collision type. In Montana four distinct types of crashes: rollover, fixed object, head-on and sideswipe opposite direction crashes are considered to be contributing to the roadway departure crashes. Therefore, this can be considered as the criterion for analysis. The second level of analysis might involve exploring the factors that can be related to the terrain or grade. For steep terrain, the contributing factors for crashes might require some engineering solution. However, for level terrain it is required to explore the behavioral pattern (e.g. cell phone use) to identify additional contributing factors.

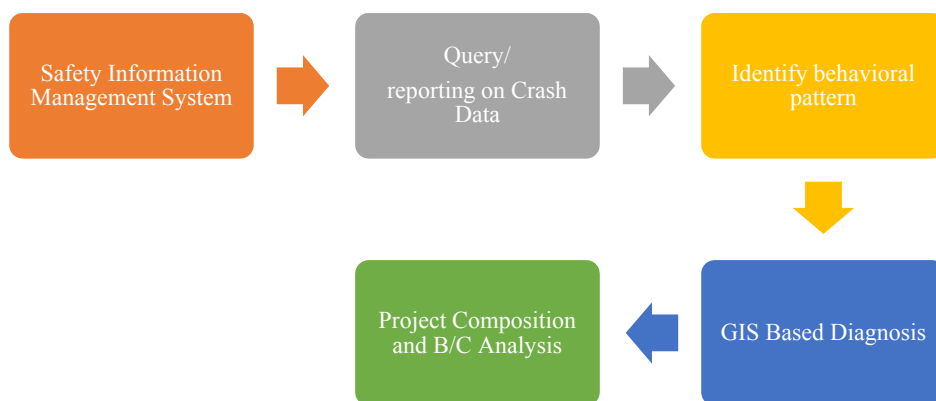


FIGURE 5 Workflow for Crash Data Driven Analysis

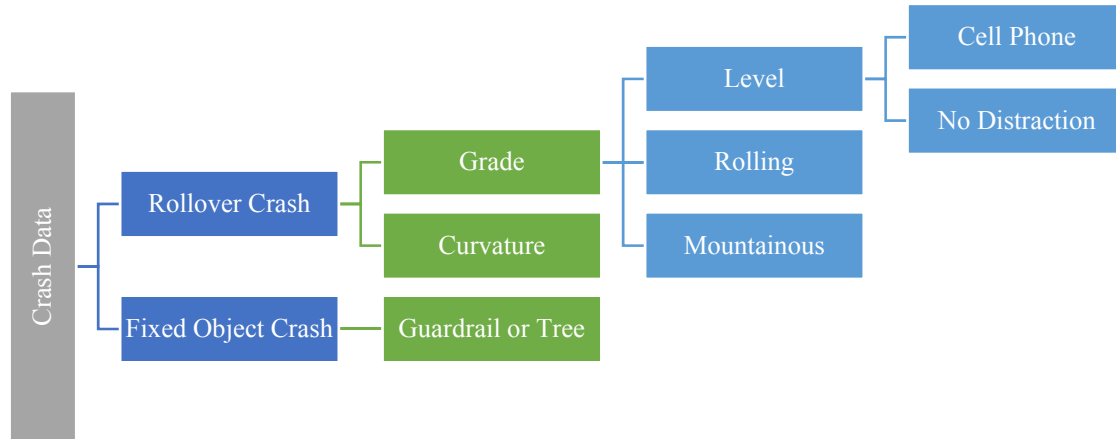


FIGURE 6 Crash Factor Identification Techniques

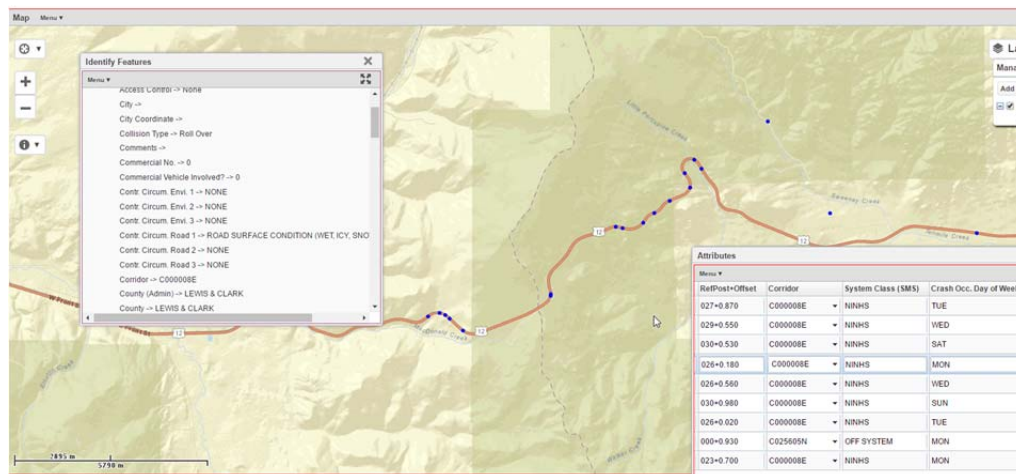


FIGURE 7 GIS Based Diagnosis

The next step in data driven analysis is a GIS based diagnosis. In this step, we need to locate the identified RD crashes to identify spatially any pattern. For example, the locations displayed in

Figure 7 are located to the west of the city of Helena in Montana along US-12. The roadway departure crashes seem to be concentrated in more circuitous parts of the roadway.

Network Screening and Hotspot Identification

The relatively structured analytical framework in Roadway Departure crash analysis is established for the network screening and hotspot techniques [5]. The workflow of this framework is shown in Figure 8. The first step in this process is to establish the required crash filter for roadway departure crash. As discussed earlier in the crash data driven analysis section,

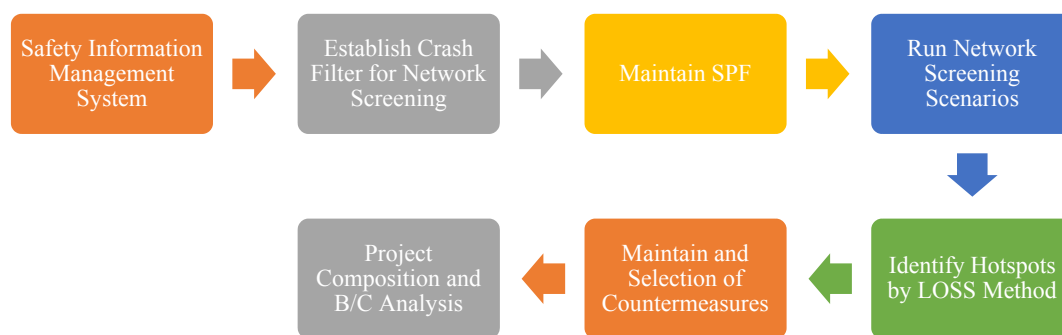


FIGURE 8 Workflow for Network Screening and Hotspot Identification

Montana has established the definition of a roadway departure crash as non-junction crashes that are either rollover, fixed object, head-on or a sideswipe opposite direction crash.

The Safety Performance Function (SPF) for a roadway departure crashes have also been established for Montana as part of the roadway departure safety implementation plan. The SPF's were developed and calibrated for nine roadway types. These nine roadway types are classified by: lane number, terrain type (rolling, flat, mountainous), rural vs. urban and access control (freeway vs non-freeway). SPFs have been developed for total crash model as well as for injury and road departure model (both injury and total) for Montana. These SPF's are then incorporated into the network screening process within SIMS.

The next process of identification is running the network screening using Level of Service of Safety (LOSS) as the performance metric. Montana uses empirical Bayes method to estimate the safety for any location. The EB-Adjusted performance metric is then used to estimate the Level of Services of Safety (LOSS) in order to evaluate the degree of safety for each roadway segment. At first, the condition of the roadway segments is evaluated by estimated crash rate using Safety Performance Functions (SPF). Since Montana highways generally exhibit low traffic volumes a sigmoidal function is adopted by the agency as the functional form for SPF. The general model form of a sigmoidal function is shown below:

$$E(y) = L \left(\beta_{min} + \frac{\beta_{max} (X^{\beta_0})}{X^{\beta_0} + \beta_1 \beta_0} \right) \quad (1)$$

Here, L = Length of the Segment (usually in miles)

β = Parameters to be estimated

X = Independent variable (i.e. AADT)

For almost all Montana specific SPFs, the independent variable is annual average daily traffic (AADT). The Level of Service of Safety (LOSS) can qualitatively and quantitatively describe the degree of safety of a roadway segment. It shows a method that a highway safety analyst can communicate the magnitude of a safety problem to other professionals and/or decision makers. It reflects how the roadway segment is performing with respect to the expected crash counts for similar roadway segments and annual average daily traffic (AADT). For

Montana, in order to define the upper and lower boundaries for LOSS, the 80th and 20th percentiles are defined using the Gamma Distribution Probability density function.

Suppose, the upper and lower estimates of LOSS are represented by μ_{lower} and μ_{upper} . Then, the various level of LOSS can be determined by the following rules.

$$\left. \begin{array}{l} \text{LOSS = I (if, } EB_{Est} \leq \mu_{lower} \text{)} \\ \text{LOSS = II (if, } \mu \geq EB_{Est} > \mu_{lower} \text{)} \\ \text{LOSS = III (if, } \mu_{upper} \geq EB_{Est} > \mu \text{)} \\ \text{LOSS = IV (if, } EB_{Est} > \mu_{upper} \text{)} \end{array} \right\} \quad (2)$$

Here, EB_{Est} = EB adjusted crash rate, μ = Estimated crash rate by SPF

A specific segment is identified as a hotspot when the estimated LOSS is IV. A schematic of SPF and Level of Services of Safety (LOSS) zones are shown in Figure 9 for rural undivided highways.

The next process in this framework is maintaining the treatment library. Montana has both long and short term treatment options for countermeasures that are entered in the treatment library. The short term treatment options are generally considered as interim solutions and include shoulder and centerline rumble strips, enhanced delineation, and signing. The long term options are considered more as a permanent solution and it includes shoulder widening, slope flattening, curve reconstruction, etc.

Finally, we can compose safety projects for the identified locations and run the B/C analysis to determine the economic justification of the projects. Multiple hotspots identified by screening can be considered in the safety project and each location can also have multiple treatments. A compound crash reduction factor is considered to estimate the treatment benefit. In general, the benefit is estimated as the present value of annual cost savings in terms of reduction of expected number of crashes per year. The cost is calculated as the present value of annual cash outflow over the service life of the investment.

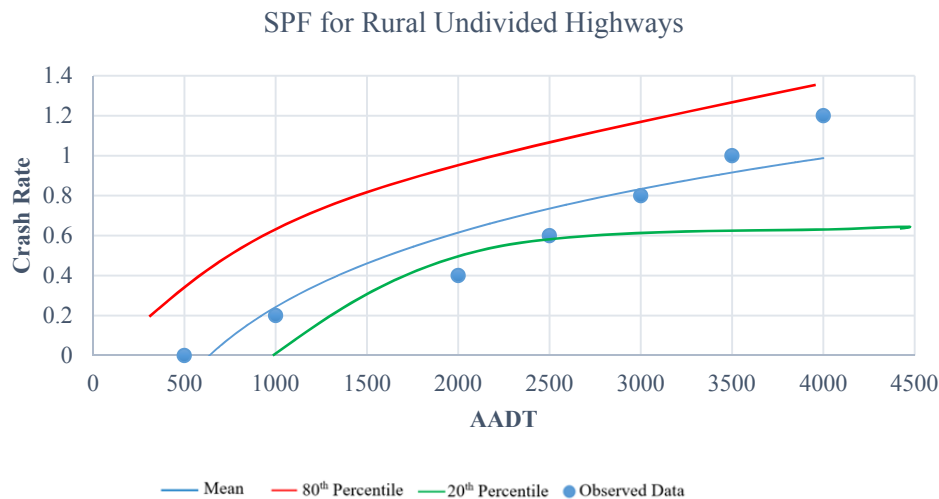


FIGURE 9 SPF and LOSS Zones for Rural Undivided Highways

Proactive Screening

Proactive screening enables MDT making a long term plan for future improvements for roadway departure or any specific type of crashes. The idea of having a proactive screening is to prevent manifestation of a specific pattern of crash occurrence (e.g. roadway departure). The workflow of the proactive screening process is shown in Figure 10. In order to conduct a proactive screening, the first step is to procure and maintain the inventory of roadways.

Montana, like many agencies, has been capturing and storing the Model Inventory Roadway Elements (MIRE) data [4] in the safety management system. One of the objectives is to gather the geometry attributes required for proactive screening. For example, the roadway departure related crash study requires some important attributes like shoulder type and width, highway grade, curvature, side slope, presence and type of rumble strips etc.

The decision matrix in proactive screening helps building a relationship between the roadway geometric deficiencies and the available treatment options for that. In general, each of the roadway deficiency can be labeled as “low”, “medium” or “high” category depending on the extent of the deviation each deficiency has from the standard value. The treatment for low severity is generally the least expensive. FIGURE 11 shows the conceptual framework of a proactive decision matrix for roadway width.

Here, W_r refers to the required width of the roadway and W_e refers to the existing width. The deviations from required (i.e. standard) width to existing widths on different segments are expressed by Δ_1 through Δ_3 .

Setting up network analysis for optimization involves preparing the network for analysis, defining necessary performance models, defining the objective function and constraints. For roadway departure crashes, the objective function for proactive screening could be solving one or more geometric deficiencies in the network that can reduce certain percentage of expected number of crashes using Crash Modification Factor (CMF). The constraints can be the budgetary limit for the agency. Optimization is the final step in the network analysis that generates a work plan for the long term safety program.

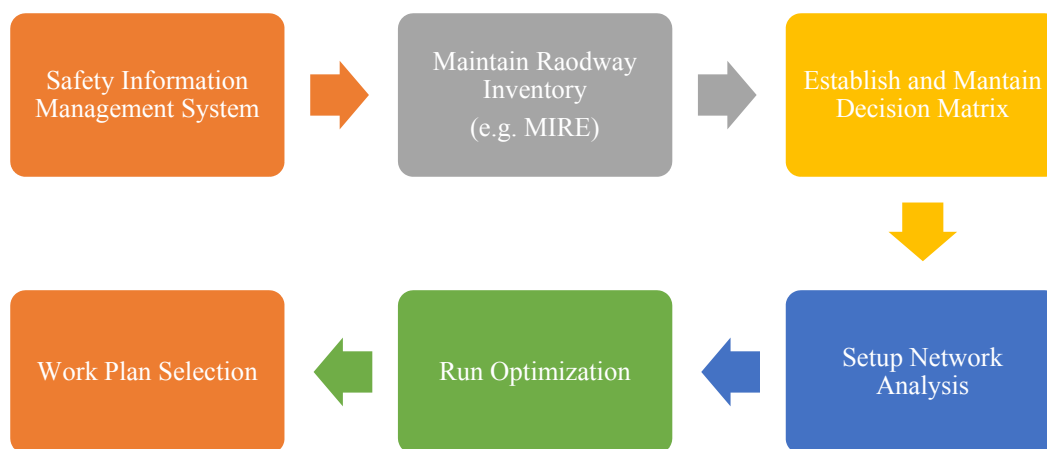


FIGURE 10 Workflow for Proactive Screening

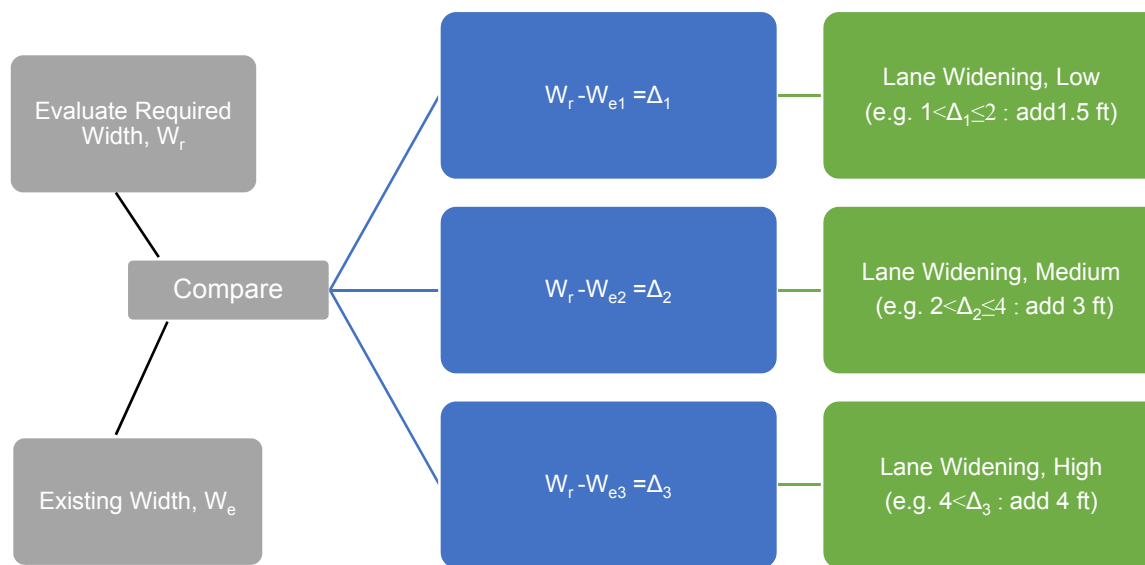


FIGURE 11 Conceptual Framework of a Proactive Decision Matrix

CASE STUDIES

This section presents a case study using the analytical framework of systematic screening of roadway departure crashes.

Analysis of Crashes related to Cell Phone Distractions

The example shows the utilization of a *crash data driven framework* in determining the behavioral pattern for roadway departure crashes. To identify the behavioral pattern of roadway departure crashes, an exploratory analysis or query on the total run of the road crashes needs to be considered similar to the identification rule shown in FIGURE 6. After this rule is applied it will narrow down the crashes that will require additional investigation to identify the behavioral factors.

Figure 12 shows the result of such an investigation. It shows the number of drivers in crashes using cell phones distributed over the top five Montana cities using crash data from 2010 thru 2014. If one carefully notices the percentage of total crashes for each city, the number is not significant. This means in Montana there are more cell phone related crashes in rural areas (often sparsely distributed throughout the state) than in urban concentrated areas.

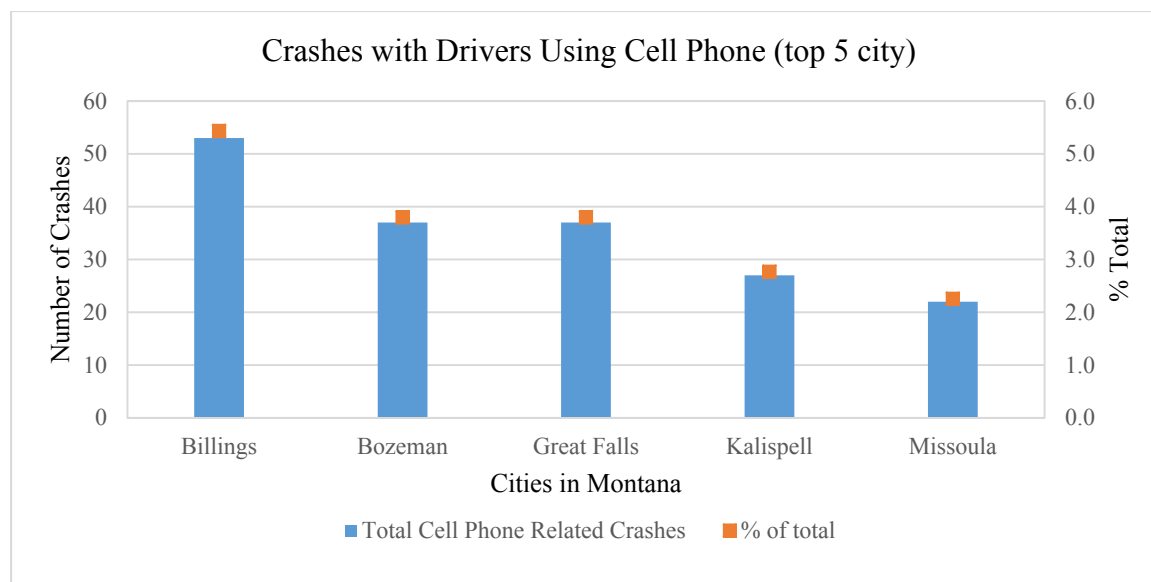


FIGURE 12 Number of Crashes with Drivers Using Cell Phone

However, considering the trend of crashes over the last few years (Figure 13) one would notice that there is a growing number of cell phone related crashes happening in urban areas and the rural/urban gap is gradually decreasing. Therefore, one may need to consider the distribution as well as the trend in formulating the strategies to be incorporated into a future safety plan to mitigate these challenges.

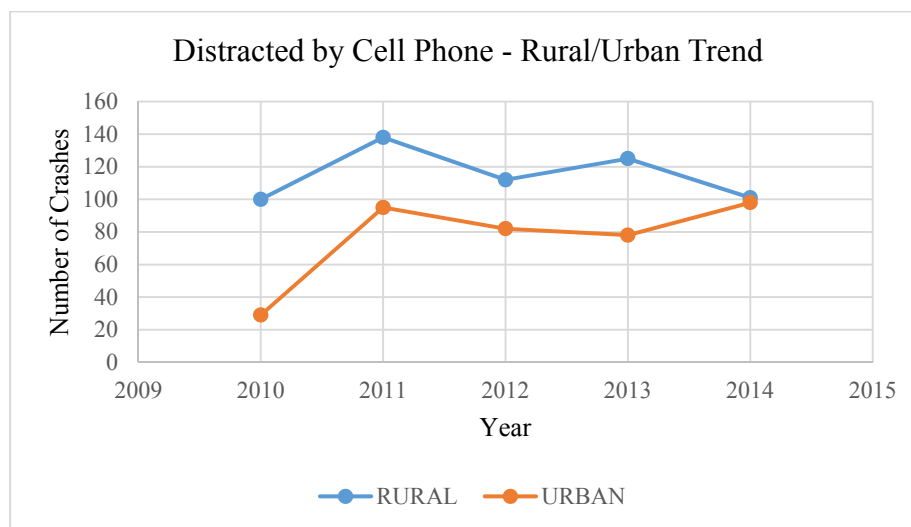


FIGURE 13 Roadway Departure Crashes by Cell Phone: Rural vs. Urban

Network-Level Funding Decisions

The analytical framework can help in making network level funding decisions for different jurisdictions. The distribution of high crash locations (i.e. LOSS IV) from the *screening of roadway departure crashes* for five financial districts for Montana from analysis period 2005-2014 is shown in

Figure 14. It shows that Missoula District had about 160 miles of roadways identified as hotspots with approximately 1800 roadway departure crashes. On the other hand, Glendive District had issues on about 8 miles of roadways having 90 roadway departure crashes.

The distribution can be considered as a tool to identify the issues in different jurisdictions. However, to properly assess the roadway conditions to make better funding decision a detailed *diagnosis* of roadway geometry and consideration of exposure (e.g. total mileages of roadway for each district) would be needed.

Identification of roadway and roadside deficiencies responsible for excessive number of roadway departure crashes can pinpoint the safety projects. Also, as part of systemic analysis proactive measures should be taken irrespective of the number of crashes on the roadways. Figure 15 shows the distribution of roadway and roadside deficiencies as established by the decision matrix for a roadway departure *proactive model*. In the context of budgetary limitations an agency level optimization would capture these deficiencies and generate a work plan for different jurisdictions.

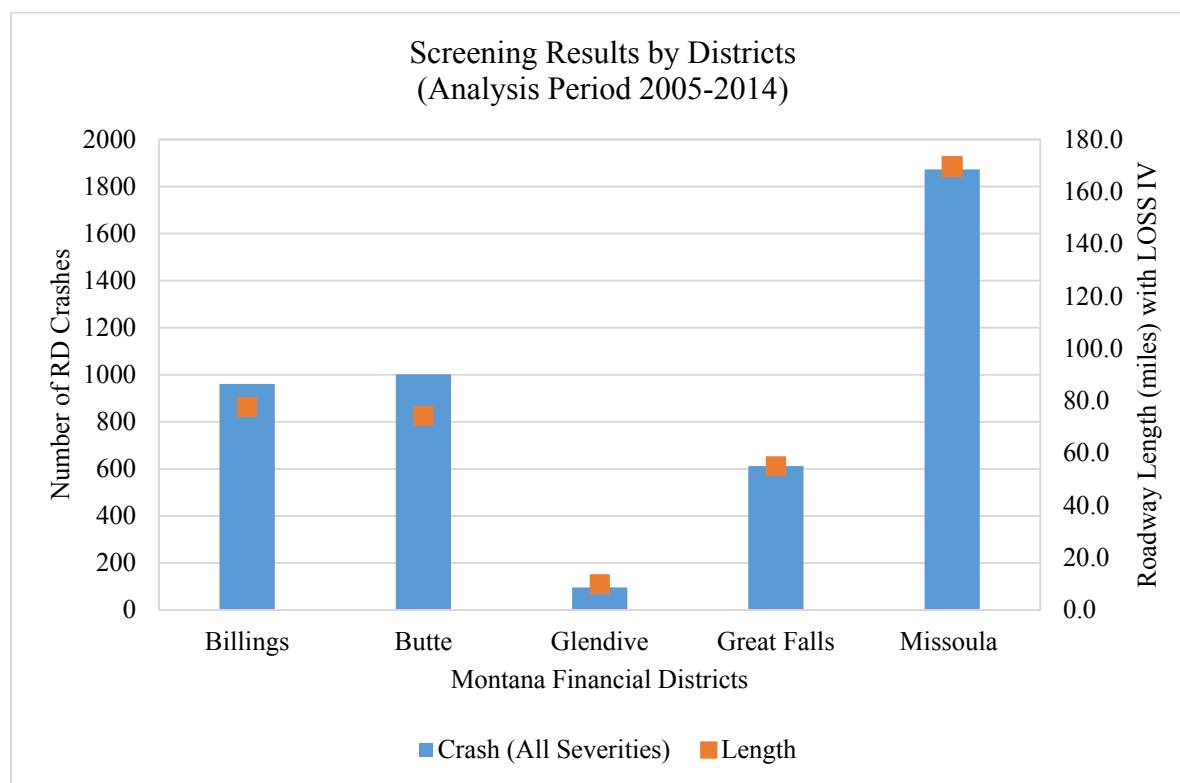


FIGURE 14 Network Screening Results by Districts

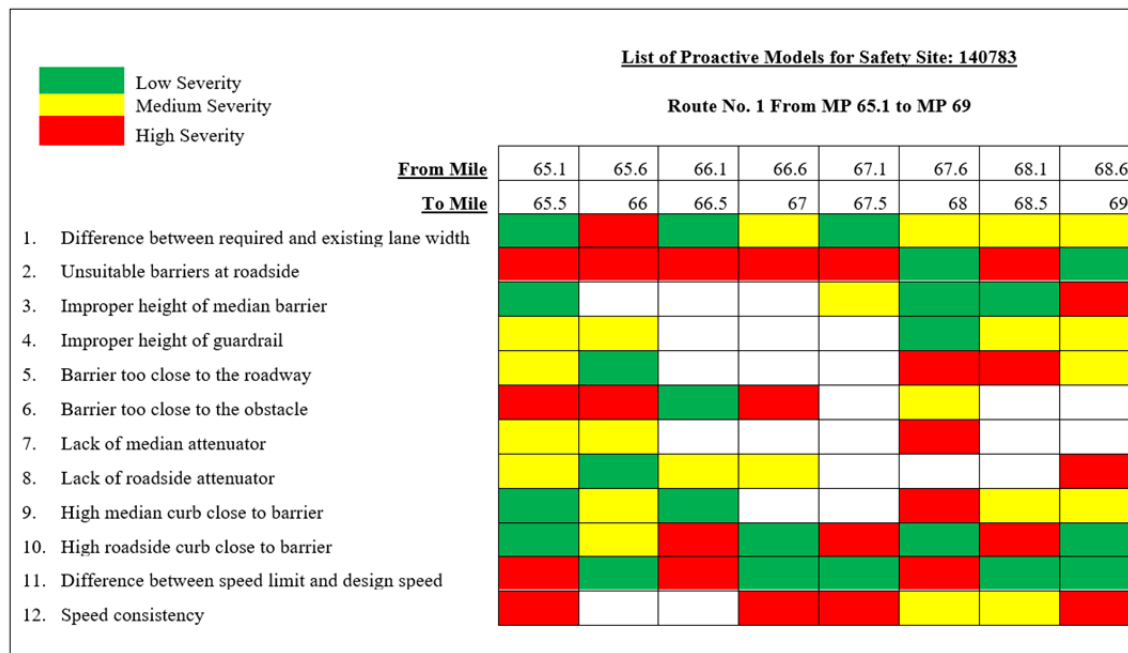


FIGURE 15 Proactive Screening Results

CONCLUSION

MDT's analytical framework in the Safety Information Management System helps MDT establish and/or confirm the goals, objectives and emphasis areas and strategies of the Highway Safety Plan. In addition, it assists the agency in utilizing its limited resources on roadway segments that will set the highest level of safety improvement. The framework consists of the crash data driven analysis, the network screening that has more structured processes and a proactive technique to support long term safety investment. Case studies show a wide variety of applications that can be prescribed by using the framework to mitigate the roadway departure crash related challenges. These include identifying the distribution and trend of driver's distractions – a leading cause of the roadway departure crash, and network screening and proactive analysis to support the funding distribution of roadway related projects and programs among different jurisdictions in the agency.

ACKNOWLEDGMENTS

The authors would like to acknowledge the Montana Department of Transportation (MDT) for allowing the Safety Information Management System (SIMS) data to be used in this study.

REFERENCES

1. FHWA. (2013). Retrieved from FHWA Roadway Departure Strategic Plan: http://safety.fhwa.dot.gov/roadway_dept/docs/rwd_strategic_plan_version2013.pdf
2. FHWA. (2016, August 1). Retrieved from Roadway Departure Study: http://safety.fhwa.dot.gov/roadway_dept/
3. MDT. (2015). *Comprehensive Highway Safety Plan*. Retrieved from Montana Official State Website: <http://www.mdt.mt.gov/visionzero/plans/chsp.shtml>
4. FHWA. (2010). *Model Inventory of Roadway Elements — MIRE, Version 1.0 Report No. FHWA-SA-10-018*. Washington: Federal Highway Administration Office of Safety.
5. Azam, S., Manepalli, U., Laumet, P. (2013), Network Safety Screening In The Context Of Agency Specific Screening Criteria, Transportation Research Board (TRB) Annual Meeting 2013, Paper No. 13-2887

Evaluation of Roadway Departure Characteristics Using SHRP 2 Naturalistic Driving Study and Road Information Database Data

Preliminary Results

NICOLE ONEYEAR

OMAR SMADI

SHAUNA HALLMARK

SKYLAR KNICKERBOCKER

Institute for Transportation at Iowa State University

Roadway departures make up 56% of roadway fatalities and 40% are speeding related as noted in a survey of FARS data (2010—2012). The majority of fatal roadway departure crashes (79.5%) occur in rural settings with 38.7% of fatal crashes on rural undivided two lane roads. Since an overwhelming number of fatal crashes are roadway departures, this is an emphasis area for the 45 US states in their Strategic Highway Safety Plans. Most highway agencies are pro-active in implementing a range of countermeasures to reduce road departures. However, agencies have only limited information about the effectiveness of some countermeasures. Analyses typically utilize crash studies which are not able to capture the effect of speed and distraction.

The Second Strategic Highway Research Program (SHRP 2) Naturalistic Driving Study (NDS), the largest naturalistic study done to date which includes over 30 million data miles and 5 million trips from 3,300 drivers aged 16 to 98, and Roadway Information Database (RID) which includes 12,500 centerline miles of mobile roadway data collected on the most traveled roads of the NDS. The NDS and RID data provides a unique opportunity to evaluate the relationship between driver and roadway characteristics in a manner not previously possible. These data provide a detailed record of driver and roadway characteristics during actual crashes/near-crashes as well as providing a snapshot of normal driving behavior.

This presentation will discuss preliminary results of a study which utilizes the SHRP 2 NDS and RID data to investigate the relationship between driver, roadway, and environmental characteristics and roadway departure risk utilizing appropriate crashes from the over 1,000 crash and near crashes that were coded as roadway departure related. The research will focus on assessing the impacts of specific roadway factors and countermeasures in order to provide agencies with better information about which countermeasures are effective and why. In addition to looking at their impact on crash risk, they will also be assessed for their impact on lane keeping and speed management. The study will also look at the role that speeding and driver characteristics such as engagement in secondary tasks have on roadway departure risk, which can be investigated in a manner not possible with traditional studies.

An Exploratory Analysis on Fatalities of Roadway Departure Crashes

MOUYID ISLAM

CH2M

Roadway departure is considered as a top priority emphasis area within the Strategic Highway Safety Plan by the American Association of State Highway and Transportation Officials. More of half of total fatalities and significant number of injuries as well as property-damage-only crashes are occurring annually because of roadway departure crashes. The economic losses due to roadway departure crashes are enormously high for the society. Realizing the gravity of this problem, safety professionals, highway designers, planners, and policy makers need to work collaboratively to reduce the frequency of fatalities on the national highways. Due to differences in geometry, traffic, environment and driving behavior, safety performance of these functional classes of roadways varies. With that mind, this study investigated the contributing factors that led to fatalities of roadway departure crashes in rural and urban functional classes based on the national crash and traffic database. This study explored a set of tobit models for rural and urban principal arterials, minor arterials, collectors, and local roads. Within the tobit modeling framework, fatalities per million vehicle-miles-traveled, as continuous variable (left censored at zero), was estimated by functional classes of roadway to recognize the variability in the design standards. As such, a data-driven approach for roadway departure crashes by functional classes of roadway unveils the complex interaction of traffic, traffic speed, roadway, temporal and environmental characteristics, driving behavior, and crash types. A proper understanding of the contributing factors resulting from the underlying data will provide a basis to formulate pragmatic countermeasures for state and local jurisdictions with a specific focus on a Strategic Highway Safety Plan.

INTRODUCTION

The American Association of State Highway Officials (AASHTO) in the United States (U.S.) (1) considers roadway departure (RwD) as a top priority emphasis area for any state within the Strategic Highway Safety Plan (SHSP). The underlying reason for top priority emphasis area is because when a vehicle crosses an edge line, a center line, or otherwise leaves the traveled way, it results in more than half of total fatalities occurring in different functional classes of roadways annually (2, 3). By magnitude, RwD accounts for 18,695 fatalities or 53.3% of the total traffic fatalities in 2015 (2). Besides, fatalities and serious injuries, RwD also accounts for lower injury levels and property-damage-only crashes that encompasses total comprehensive cost of US \$298 billion, indicating 36% of all societal harm (4). The Fatality Analysis Reporting System (FARS) indicates that on average, rural and urban roadways account for about 60% and 40% of total fatalities over last five years (2010 – 2014), respectively. Moreover, out of the fatalities, RwD fatal crash accounts for 65% and 35% on rural and urban roadways, respectively, based on the FHWA definition of roadway departure crashes in FARS database (5). In order to understand the contributing factors that lead to fatalities in these functional classes of roadways, a systematic quantitative approach and strategic plan needs to be formulated. With the vision of “Towards

Zero Deaths,” FHWA aims at reducing frequency and severity of RwD on any roadway with identified AASHTO’s SHSP (2) goals (i.e., Goal 15, Goal 16, and Goal 18 in AASHTO SHSP):

- Keeping vehicles on roadway
- Minimizing the consequences of leaving the road
- Reducing head-on and across median crashes

The quantitative approach followed in this study unveils the complex interaction of the roadway geometrics, road - environmental aspect, vehicular and driving behavior as well as the exposure (e.g., vehicle miles traveled (VMT)). Hence, these contributing factors studied in this paper will help understand the major problems of RwD and resulting fatalities by its roadway and area type where these factors vary for their differences in nature and magnitude of the effects. The main motivation of this study lies in the empirical evidence to analyze fatality rates per million VMT and understand the contributing that vary by functional classes of roadways in rural and urban areas. To avoid the dilemma of overestimation or underestimation of the effects of contributing factors from the combined database, separate models were estimated. These models shed light on the contributing factors where the safety performance of each of the functional classes of roadways varies between the area type (e.g., rural vs. urban) and within its functional classes in a given area type (e.g., rural principal arterial vs. rural collectors). In this paper, a set of tobit regression models on fatalities per million VMT were developed and estimated for respective major functional classes of roadways in rural and urban areas in the U.S. These estimated models investigated the unobserved heterogeneity in the respective functional classes in rural and urban areas because of the variability in contributing factors leading to RwD. This variability originates from the design standards and trade-off between mobility and accessibility aspect of roadways in rural and urban areas. The major effort of this paper contributes to the existing literature of road safety in the following:

- A full model on fatalities per million VMT for all RwD related factors covering rural and urban functional classes,
- A set of separate models (8) for all the following functional classes to understand the contributing factors for fatalities per million VMT:
 - rural and urban principal arterial,
 - rural and urban minor arterial,
 - rural and urban collector,
 - rural and urban local roads

In this analysis, the FARS crash data (2010 to 2014) was linked with exposure data (i.e., VMT and the length of roadways by functional classes) from the Highway Performance Monitoring System (HPMS). The marginal effect analysis from these estimated tobit models based on the linked data highlights the key contributing factors for major functional classes to support the safety professionals, planners, and policy makers at the state and local agencies. This analytical approach provides number of data-driven preventive strategies to reduce fatalities on the US highways. Very few studies have explored the contributing factors by major functional classes of roadways in rural and urban areas or might have analyzed one out of an entire set of functional classes (6, 7, 8, 9).

LITERATURE REVIEW

There are many safety studies focusing on models for crash frequency by severity levels or crash likelihood by severity levels. The most commonly used models in traffic safety are negative binomial and Poisson models (10 – 13), zero-inflated Poisson and zero-inflated negative binomial models (14 – 16), random parameter negative binomial models (17 – 19), Markov switching of crash occurrence (20), Bayesian statistics on negative binomial models (21), random parameter tobit models on crash rates (6, 22). However, the crash frequency, crash rates or rate of any severity levels by a set of functional classes of roadway in rural and urban areas have not been found in literature (23 – 30).

A study (6) demonstrated the tobit regression models on fatalities per million truck miles traveled and fatalities per ton-miles of freight. Tobit regression with fixed and random parameter framework was applied on large truck involved fatalities on national interstate system based on FARS and VMT database. The estimated models found important contributing factors related to crash mechanism, temporal, spatial, environmental, vehicle and human characteristics. Another study (22) also demonstrated crash rates based on Indiana interstate system with an interaction of pavement condition, roadway geometrics, and traffic characteristics. Another study (31) demonstrated the empirical evidence of splitting the negative binomial models into the subclasses of rural two-lane highways. This study found the contributing factors of lane width, shoulder width, pavement surface friction and pavement condition, horizontal and vertical alignment by severity levels. Based on the findings, this study recommended general safety improvements that include widening lanes and shoulder, enhancing pavement friction, and improving vertical and horizontal alignment.

EMPIRICAL SETTINGS

To illustrate the application of the fixed parameters tobit models, crash data were collected from the FARS from 2010 to 2014. FARS is a nation-wide crash census system where a set of files have been built documenting all qualifying fatal crashes that occurred within all the states in the US. The observation in the model is a fatal crash (A variable – *Fatals* includes the total number of fatalities in a fatal collision reported in the FARS database system) involving a motor vehicle with Rwd collision traveling on US roadways resulting in a fatality within 30 days of the collision. A variable in the vehicle dataset known as “Sequence of Events” (SOE) was filterer to select Ran Off Road– Right (63), Ran Off Road – Left (64), Cross Median (65), or Cross Center Line (68) to identify Rwd crashes. (32) Finally, crash and vehicle datasets are linked based on common and a unique identifier. (i.e., Crash IDs).

The VMT data from 2010 to 2014 were collected from the Highway Performance Monitoring System (33) data from FHWA travel reports (34). For model estimation, the VMT and length of roadway by functional class were aggregated from 2010 to 2014. Annual average daily traffic (AADT) is estimated based on the available VMT and roadway of respective functional class. In addition, rural interstates and principal arterial others are combined into rural principal arterial in the dataset. Rural major and rural minor collectors are combined as rural collector. Similarly, urban interstate, freeway, expressway and principal arterial others are combined as urban principal arterial.

Afterwards, the fatalities per million VMT for the full model and all the models by the four functional class of roadway for rural and urban roadways (i.e., total 8 models) were calculated as follows:

$$\text{Fatalities per million VMT} = \left[\frac{\text{Number of fatalities}}{\text{VMT}} \right] * 1,000,000 \quad (1)$$

Here, the VMT and length of roadway by functional class data was collected at the aggregate level for all state level by year of crashes. These data are very difficult to obtain at the disaggregated level (e.g., state level or segment level), and this is because they are not reported at the disaggregate level in the FARS nor HMPS database. Therefore, there are five years (i.e., 2010 to 2014) of VMT and length is available at the aggregate level by years in the national statistics. The crash database was linked with roadway and traffic data based on the linking variable (i.e., Crash IDs) by state and by year. The crash data was processed using the statistical software SAS and was utilized to estimate the fixed parameter tobit models with PROC QLIM procedure under censored regression framework (censored at zero) in SAS (35).

Table 1 presents the average in the respective data sample as descriptive statistics for key variables in separate models. These variables presented in Table 1 are found to be statistically significant in the estimated models. It is noteworthy that statistically significant variables in the models represent at least 8% of the respective sample size at minimum (average). This is considered important for stable computation in the model estimation process particularly to have adequate sample to estimate stable value of the co-efficient of variables (i.e., the betas). Among many key variables, some of them are found to be statistically significant across all the models. Traffic volume per lane, representing the level of exposure in the traffic, is such an important variable for these functional classes of roadways. Undivided two-way traffic is also another important variable with 68.5% in full sample, 42.1% in rural principal arterials, 90.5% in rural minor arterial, 92.9% in rural collector, 94.0% in rural local, 19.9% in urban principal arterial, 72.7% in urban minor arterial, and 76.9% in urban local data sample. Similarly, road alignment turning to the right of travel direction represents 16.2% in full sample, 16.3% in rural minor arterial, 19.6% in rural collector, and 14.0 % in urban principal arterial data sample. Rollover as the most harmful event represents 14.5% in full sample, 21.5% in rural principal arterial, 12.9% in rural minor arterial, 16.9% in rural collector, and 18.0% in rural local road data sample. Negotiating a curve prior to be involved in fatal crash represents 35.6% in full model, 26.0% in rural principal arterial, 39.5% in rural minor arterial, 47.9% in rural collector, 43.5% in rural local, 24.7% in urban principal arterial, 32.6% in urban minor arterial, and 40.1% in urban collector data sample. Single-vehicle crash running-off-the-road at left side of travel direction represents 29.7% in full sample, 26.7% in rural principal arterial, 24.8% in rural minor arterial, 32.6% in rural collector, and 27.7% in urban principal arterial data sample.

METHODOLOGICAL APPROACH

For this work, the standard tobit model is expressed (RwD fatal crash i) using a lower limit of zero (i.e., censored at zero) which is regarded as the condition in our analysis for zero fatalities per million VMT as (36):

TABLE 1 Descriptive Statistics (Average) of Key Variables of Models by Functional Class of Roadway

Key variables	Full Model	Rural Principal Arterial	Rural Minor Arterial	Rural Collector	Rural Local	Urban Principal Arterial	Urban Minor Arterial	Urban Collector	Urban Local
Fatalities per million VMT	20.108	24.831	21.215	21.228	20.449	15.574	17.260	17.752	16.391
Logarithm of traffic volume (AADT) per lane	12.773	12.66	12.726	12.730	12.833	12.809	12.836	12.932	12.891
Crash type (1 if single-vehicle departing at the right side of roadway, 0 otherwise)	0.387	-	0.342	-	0.435	-	-	-	-
Crash type (1 if single-vehicle departing at the left side of roadway, 0 otherwise)	0.297	0.267	0.248	0.326	-	0.277	-	-	-
Traffic way (1 if two-way traffic way is not divided, 0 otherwise)	0.685	0.421	0.929	-	0.949	0.199	0.727	-	0.769
Functional class of roadway (1 if it is Rural Principal Arterial Other, 0 otherwise)	0.123	-	-	-	-	-	-	-	-
Functional class of roadway (1 if it is Urban Principal Arterial Other, 0 otherwise)	0.077	-	-	-	-	-	-	-	-

Continued on next page.

TABLE 1 (continued) Descriptive Statistics (Average) of Key Variables of Models by Functional Class of Roadway

Key variables	Full Model	Rural Principal Arterial	Rural Minor Arterial	Rural Collector	Rural Local	Urban Principal Arterial	Urban Minor Arterial	Urban Collector	Urban Local
Light condition at the time of crash (1 if it is dark not lighted, 0 otherwise)	0.316	-	-	0.393	0.429	-	-	-	-
Number of occupants In the vehicle involved	1.611	1.819	1.494	1.506	1.587	1.663	1.514	1.523	1.565
Time of day (1 if it is between 2 pm to 7 pm, 0 otherwise)	0.297	-	-	-	-	-	-	-	-
Roadway alignment (1 if roadway alignment changes to the right side of travel direction prior to the critical pre-crash event, 0 otherwise)	0.162	-	0.163	0.196	-	0.140	-	-	-
Roadway alignment (1 if roadway alignment changes to the left side of travel direction prior to the critical pre-crash event, 0 otherwise)	-	-	-	-	-	0.118	-	0.177	-

Continued on next page.

Table 1 (continued) Descriptive Statistics (Average) of Key Variables of Models by Functional Class of Roadway

Key variables	Full Model	Rural Principal Arterial	Rural Minor Arterial	Rural Collector	Rural Local	Urban Principal Arterial	Urban Minor Arterial	Urban Collector	Urban Local
Average travel speed (1 if roadway section with speed limit is between 35 to 45 mph, 0 otherwise)	0.189	-	0.141	0.201	-	-	-	-	-
Average travel speed (1 if roadway section with speed limit is within 35 mph, 0 otherwise)	0.190	-	-	-	0.315	-	-	0.473	0.640
Roadway profile (1 if roadway profile is on Grade prior to the critical pre-crash event, 0 otherwise)	0.157	0.144	-	0.192	-	0.130	-	0.148	-
Month of year (1 if month is from December to February, 0 otherwise)	0.217	0.217	-	-	-	-	-	0.208	-
Month of year (1 if month is from June to September, 0 otherwise)	-	-	0.272	-	-	-	-	-	0.268
Weather condition at the time of crash (1 if weather condition is clear, 0 otherwise)	0.723	0.701	-	-	-	-	-	0.747	-

Continued on next page.

TABLE 1 (continued) Descriptive Statistics (Average) of Key Variables of Models by Functional Class of Roadway

Key variables	Full Model	Rural Principal Arterial	Rural Minor Arterial	Rural Collector	Rural Local	Urban Principal Arterial	Urban Minor Arterial	Urban Collector	Urban Local
Crash type (if multiple vehicle involved with head-on crashes, 0 otherwise)	-	0.102	0.154	0.079	-	-	-	-	-
Traffic way (1 if traffic way is two-way separated by positive median barrier, 0 otherwise)	0.117	0.206	-	-	-	-	-	-	-
Day of week (1 if fatal crashes happen on Wednesday, 0 otherwise)	0.117	-	-	-	-	-	-	-	-
Most harmful event (1 if most harmful event is rollover, 0 otherwise)	0.145	0.215	0.129	0.169	0.180	0.103	-	-	-
Relation of crashes to traffic way (1 if crash occurred outside of traffic way based on first harmful event, 0 otherwise)	0.313	-	0.319	-	0.408	-	-	-	-
Vehicle maneuver (1 if the driver is negotiating a curve prior to entering a crash situation, 0 otherwise)	0.356	0.260	0.395	0.479	0.435	0.247	0.326	0.401	-

Continued on next page.

TABLE 1 (continued) Descriptive Statistics (Average) of Key Variables of Models by Functional Class of Roadway

Key variables	Full Model	Rural Principal Arterial	Rural Minor Arterial	Rural Collector	Rural Local	Urban Principal Arterial	Urban Minor Arterial	Urban Collector	Urban Local
Total number of drivers with alcohol involvement	0.389	0.259	-	0.422	0.510	-	0.420	0.491	0.459
Traffic way (1 if one-way traffic way is divided, 0 otherwise)	-	0.334	-	-	-	0.246	-	-	-
Roadway profile (1 if road way is level, 0 otherwise)	-	0.671	0.626	-	-	-	-	-	-
Vehicle type (1 if motorcycle (or its derivatives) involved in the crashes, 0 otherwise)	-	0.089	-	-	-	-	-	-	-
Average travel speed (1 if roadway section with speed limit is between 55 to 65 mph, 0 otherwise)	-	0.261	-	-	-	0.286	-	-	-
First harmful event (1 if the first harmful event is crashing into a tree, 0 otherwise)	-	-	-	0.169	-	-	-	0.158	-
Day of week (1 if fatal crashes happen on Saturday, 0 otherwise)	-	-	-	-	0.222	-	-	-	-

Continued on next page.

TABLE 1 (continued) Descriptive Statistics (Average) of Key Variables of Models by Functional Class of Roadway

[illegible]

$$\begin{aligned}
Y_i^* &= \beta X_i + \varepsilon_i, \quad i = 1, 2, \dots, N \\
Y_i &= Y_i^* \quad \text{if } Y_i^* > 0 \\
Y_i &= 0 \quad \text{if } Y_i^* \leq 0
\end{aligned} \tag{2}$$

where

Y_i : is the dependent variable (fatalities per million VMT),
 X_i : is a vector of independent variables (e.g., human, roadway segment, vehicle, and crash mechanism characteristics),
 β : is a vector of estimable parameters,
 N : is the number of observations in the sample used in the model, and
 ε_i : is normally and independently distributed error term with zero mean and constant variance σ^2 .

For estimation procedures of the standard tobit model and marginal effects derivations the reader is referred to (22, 37 – 40).

The likelihood ratio test was conducted to justify the statistical significance of rural and urban roadway models separately from the full (i.e., combined) model. The null hypothesis is that the separate models are not statistically and significantly different from the combined model. The following likelihood ratio test was conducted to test the hypothesis (36):

$$\chi^2 = -2 * [LL_C(\beta^C) - LL_R(\beta^R) - LL_U(\beta^U)] \tag{3}$$

where

$LL_C(\beta^C)$ is loglikelihood at convergence of the combined model

(−386,624, degree of freedom, $n_T = 22$)

$LL_R(\beta^R)$ is loglikelihood at convergence of rural roadway model comprising 4 functional classes

(−243058, degree of freedom, $n_R = 53$)

$LL_U(\beta^U)$ is loglikelihood at convergence of urban roadway model comprising 4 functional classes

(−135,184, degree of freedom $n_U = 38$)

The test follows χ^2 distribution with degrees of freedom equal to the sum of rural and urban functional class models minus that of total model (combined of rural and urban functional class model). With 69 degrees of freedom and χ^2 value of 16,764, the test statistic indicates that we reject the null hypothesis. This leads to the fact that separate models (i.e., rural and urban functional class models) are statistically and significantly different from the combined model with P -value being less than 0.00001 (two-tailed P -value). Consequently, the test result indicates that significance of fatalities per million VMT should be modeled as rural and urban functional class models separately rather than a combined one.

To assess the degree of influence of specific variables, Table 2 to 10 illustrates the computed marginal effects for the fatalities per million VMT. Finding the marginal effect of an

TABLE 2 Model Estimates of Roadway Departure Fatal Crashes

Variables	Coeff.	t-stat	P-Value*	Marginal Effect
Constant	256.685	143.18	<0.0001	-
<i>Traffic/Exposure characteristics</i>				
Logarithm of traffic volume (AADT) per lane	-18.970	-136.96	<0.0001	-14.782
Number of occupants in the vehicle involved	1.303	25.17	<0.0001	1.016
<i>Roadway characteristics</i>				
Traffic way (1 if two-way traffic way is not divided, 0 otherwise)	2.191	10.15	<0.0001	1.708
Traffic way (1 if traffic way is two-way separated by positive median barrier, 0 otherwise)	-1.744	-5.78	<0.0001	-1.359
Roadway alignment (1 if roadway alignment changes to the right side of travel direction prior to the critical pre-crash event, 0 otherwise)	0.643	2.44	0.0148	0.501
Roadway profile (1 if roadway profile is on grade prior to the critical pre-crash event, 0 otherwise)	-1.949	-8.70	<0.0001	-1.520
Relation of crashes to traffic way (1 if crash occurred outside of traffic way based on first harmful event, 0 otherwise)	-0.685	-3.52	0.0004	-0.534
<i>Functional class</i>				
Functional class of roadway (1 if it is Rural Principal Arterial Other, 0 otherwise)	2.679	10.55	<0.0001	2.088
Functional class of roadway (1 if it is Urban Principal Arterial Other, 0 otherwise)	-2.932	-9.28	<0.0001	-2.285
<i>Traffic speed</i>				
Average travel speed (1 if roadway section with speed limit is between 35 to 45 mph, 0 otherwise)	-0.421	-1.92	0.0554	-0.328
Average travel speed (1 if roadway section with speed limit is within 35 mph, 0 otherwise)	3.334	14.87	<0.0001	2.598
<i>Temporal characteristics</i>				
Time of day (1 if it is between 2 pm to 7 pm, 0 otherwise)	0.630	3.40	0.0007	0.491
Day of week (1 if fatal crashes happen on Wednesday, 0 otherwise)	0.514	2.05	0.0399	0.401
Month of year (1 if month is from December to February, 0 otherwise)	-0.763	-3.86	0.0001	-0.595
<i>Environmental characteristics</i>				
Weather condition at the time of crash (1 if weather condition is clear, 0 otherwise)	-0.815	-4.47	<0.0001	-0.635
Light condition at the time of crash (1 if it is dark not lighted, 0 otherwise)	0.425	2.22	0.0264	0.331
<i>Human factors</i>				
Vehicle maneuver (1 if the driver is negotiating a curve prior to entering a crash situation, 0 otherwise)	2.032	9.78	<0.0001	1.584
Number of drivers with alcohol involvement	1.224	6.91	<0.0001	0.954

Continued on next page.

TABLE 2 (continued) Model Estimates of Roadway Departure Fatal Crashes

Variables	Coeff.	t-stat	P-Value*	Marginal Effect
<i>Crash type</i>				
Crash type (1 if single-vehicle departing at the right side of roadway, 0 otherwise)	0.826	3.50	0.0005	0.644
Crash type (1 if single-vehicle departing at the left side of roadway, 0 otherwise)	0.998	4.16	<0.0001	0.777
Crash type (if multiple vehicle involved with head-on crashes, 0 otherwise)	2.395	7.18	<0.0001	1.867
Most harmful event (1 if most harmful event is rollover, 0 otherwise)	3.101	13.19	<0.0001	2.416
Number of Observations	84,581			
Log Likelihood at zero, $LL(\mathbf{0})$	-396,031			
Log Likelihood at convergence, $LL(\beta)$	-386,624			
$X^2 = -2[LL(\mathbf{0}) - LL(\beta)]$	18,814			
Akaike Information Criteria	773,295			
Schwarz Criterion	773,519			

*The p-value is considered up to 0.10 indicating at 90% confidence that coefficient estimates are significantly different from zero.

TABLE 3 Model Estimates of Roadway Departure Fatal Crashes on Rural Principal Arterial

Variable Name	Coeff.	t-stat	P-Value*	Marginal Effect
Constant	360.527	83.16	<.0001	-
<i>Traffic/Exposure characteristics</i>				
Logarithm of traffic volume (AADT) per lane	-26.484	-83.57	<0.0001	-20.569
Number of occupants in the vehicle involved	1.822	15.43	<0.0001	1.415
<i>Roadway characteristics</i>				
Traffic way (1 if two-way traffic way is not divided, 0 otherwise)	2.162	1.93	0.0540	1.679
Traffic way (1 if one-way traffic way is divided, 0 otherwise)	-2.668	-2.33	0.0199	-2.072
Roadway profile (1 if road way is level, 0 otherwise)	-4.078	-7.19	<0.0001	-3.167
Roadway profile (1 if roadway profile is on grade prior to the critical pre-crash event, 0 otherwise)	-6.960	-9.36	<0.0001	-5.406
Traffic way (1 if traffic way is two-way separated by positive median barrier, 0 otherwise)	-4.753	-4.04	<.0001	-3.691
<i>Traffic speed</i>				
Average travel speed (1 if roadway section with speed limit is between 55 to 65 mph, 0 otherwise)	1.508	3.12	0.0018	1.171
<i>Temporal characteristics</i>				
Month of year (1 if month is from December to February, 0 otherwise)	-1.148	-2.21	0.0271	-0.891
<i>Environmental characteristics</i>				
Weather condition at the time of crash (1 if weather condition is clear, 0 otherwise)	-2.254	-4.80	<.0001	-1.751
<i>Human factors</i>				
Vehicle maneuver (1 if the driver is maneuvering while negotiating a curve prior to entering a crash situation, 0 otherwise)	3.093	6.05	<.0001	2.402
Number of drivers with alcohol involvement	1.606	3.29	0.0010	1.248
<i>Vehicle characteristics</i>				
Vehicle type (1 if motorcycle (or its derivatives) involved in the crashes, 0 otherwise)	1.722	2.24	0.0249	1.338
<i>Crash type</i>				
Crash type (1 if single-vehicle departing at the left side of roadway, 0 otherwise)	1.356	2.76	0.0058	1.053
Crash type (if multiple vehicle involved with head-on crashes, 0 otherwise)	2.739	3.71	0.0002	2.128
Most harmful event (1 if most harmful event is rollover, 0 otherwise)	2.839	5.29	<.0001	2.205
Number of Observation	16,344			
Log Likelihood at zero, $LL(0)$	-80,087			
Log Likelihood at convergence, $LL(\beta)$	-76,954			
$X^2 = -2[LL(0) - LL(\beta)]$	6,266			
Akaike Information Criteria	153,944			
Schwarz Criterion	154,083			

*The p-value is considered up to 0.10 indicating at 90% confidence that coefficient estimates are significantly different from zero.

TABLE 4 Model Estimates of Roadway Departure Fatal Crashes on Rural Minor Arterial

Variables	Coeff.	t-stat	P-Value*	Marginal Effect
Constant	324.999	63.39	<.0001	-
<i>Traffic/Exposure characteristics</i>				
Logarithm of traffic volume (AADT) per lane	-24.869	-62.15	<0.0001	-20.025
Number of occupants in the vehicle involved	2.720	13.12	<0.0001	2.191
<i>Roadway characteristics</i>				
Traffic way (1 if two-way traffic way is not divided, 0 otherwise)	4.955	5.88	<0.0001	3.989
Roadway profile (1 if road way is level, 0 otherwise)	1.577	3.50	0.0005	1.269
Roadway alignment (1 if roadway alignment changes to the right direction prior to the critical pre-crash event, 0 otherwise)	1.221	1.78	0.0747	0.983
Relation of crashes to traffic way (1 if crash occurred outside of traffic way based on first harmful event, 0 otherwise)	-1.279	-2.35	0.0187	-1.030
<i>Traffic speed</i>				
Average travel speed (1 if roadway section with speed limit is between 35 to 45 mph, 0 otherwise)	3.399	5.45	<0.0001	2.737
<i>Temporal characteristics</i>				
Month of year (1 if month is from June to September, 0 otherwise)	0.774	1.61	0.101	0.623
<i>Human factors</i>				
Vehicle maneuver (1 if the driver is maneuvering while negotiating a curve prior to entering a crash situation, 0 otherwise)	1.603	3.02	0.0026	1.290
Number of drivers with alcohol involvement	1.856	3.95	<0.0001	1.494
<i>Crash type</i>				
Crash type (1 if single-vehicle departing at the right side of roadway, 0 otherwise)	1.085	1.67	0.0940	0.873
Crash type (1 if single-vehicle departing at the left side of roadway, 0 otherwise)	1.474	2.19	0.0287	1.187
Crash type (1 if multiple vehicle involved with head-on crashes, 0 otherwise)	2.401	3.44	0.0006	1.933
Most harmful event (1 if most harmful event is rollover, 0 otherwise)	1.493	2.28	0.0228	1.202
Number of Observation	9,292			
Log Likelihood at zero, $LL(\mathbf{0})$	-43,032			
Log Likelihood at convergence, $LL(\mathbf{\beta})$	-41,306			
$X^2 = -2[LL(\mathbf{0}) - LL(\mathbf{\beta})]$	3,452			
Akaike Information Criteria	82,644			
Schwarz Criterion	82,758			

*The p-value is considered up to 0.10 indicating at 90% confidence that coefficient estimates are significantly different from zero.

TABLE 5 Model Estimates of Roadway Departure Fatal Crashes on Rural Collector

Variables	Coeff.	t-stat	P-Value*	Marginal Effect
Constant	357.155	86.34	<.0001	-
<i>Traffic/ Exposure characteristics</i>				
Logarithm of traffic volume (AADT) per lane	-26.632	-82.35	<0.0001	-21.575
Number of occupants in the vehicle involved	1.049	9.79	<0.0001	0.850
<i>Roadway characteristics</i>				
Roadway alignment (1 if roadway alignment changes to the right direction prior to the critical pre-crash event, 0 otherwise)	0.939	2.04	0.0416	0.761
Roadway profile (1 if roadway profile is on grade prior to the critical pre-crash event, 0 otherwise)	-2.254	-5.57	<0.0001	-1.826
<i>Traffic speed</i>				
Average travel speed (1 if roadway section with speed limit is between 35 to 45 mph, 0 otherwise)	1.171	2.96	0.0031	0.949
<i>Environmental characteristics</i>				
Light condition at the time of crash (1 if it is dark not lighted, 0 otherwise)	-0.692	-2.01	0.0449	-0.561
<i>Human factors</i>				
Vehicle maneuver (1 if the driver is maneuvering while negotiating a curve prior to entering a crash situation, 0 otherwise)	0.630	1.72	0.0846	0.511
Number of drivers with alcohol involvement	2.448	7.11	<0.0001	1.984
<i>Crash type</i>				
Crash type (1 if single-vehicle departing at the left side of roadway, 0 otherwise)	-0.858	-2.40	0.0163	-0.695
First harmful event (1 if the first harmful event is crashing into a tree, 0 otherwise)	1.608	3.64	0.0003	1.303
Collision type (1 if multiple vehicle involved with head-on crashes, 0 otherwise)	2.028	3.30	0.0010	1.643
Most harmful event (1 if most harmful event is rollover, 0 otherwise)	1.898	4.31	<0.0001	1.538
Number of Observation	16,758			
Log Likelihood at zero, $LL(0)$	-77,338			
Log Likelihood at convergence, $LL(\beta)$	-74,332			
$X^2 = -2[LL(0) - LL(\beta)]$	6,012			
Akaike Information Criteria	148,693			
Schwarz Criterion	148,801			

*The p-value is considered up to 0.10 indicating at 90% confidence that coefficient estimates are significantly different from zero.

TABLE 6 Model Estimates of Roadway Departure Fatal Crashes on Rural Local

Variables	Coeff.	t-stat	P-Value*	Marginal Effect
Constant	318.060	65.60	<0.0001	-
<i>Traffic/ Exposure characteristics</i>				
Logarithm of traffic volume (AADT) per lane	-23.694	-64.92	<0.0001	-18.755
Number of occupants in the vehicle involved	0.696	5.21	<0.0001	0.551
<i>Roadway characteristics</i>				
Traffic way (1 if two-way traffic way is not divided, 0 otherwise)	2.716	2.94	0.0033	2.150
Relation of crashes to traffic way (1 if crash occurred outside of traffic way based on first harmful event, 0 otherwise)	-2.179	-5.22	<0.0001	-1.725
<i>Traffic speed</i>				
Average travel speed (1 if roadway section with speed limit is within 35 mph, 0 otherwise)	4.835	11.10	<0.0001	3.827
<i>Temporal characteristics</i>				
Day of week (1 if fatal crashes happens on Saturday, 0 otherwise)	-1.193	-2.45	0.0142	-0.944
<i>Environmental characteristics</i>				
Light condition at the time of crash (1 if it is dark not lighted, 0 otherwise)	0.848	1.97	0.0485	0.671
<i>Human factors</i>				
Vehicle maneuver (1 if the driver is maneuvering while negotiating a curve prior to entering a crash situation, 0 otherwise)	1.701	4.15	<0.0001	1.347
Number of drivers with alcohol involvement	1.348	3.16	0.0016	1.067
<i>Crash type</i>				
Crash type (1 if single-vehicle departing at the right side of roadway, 0 otherwise)	0.727	1.77	0.0771	0.576
Most harmful event (1 if most harmful event is rollover, 0 otherwise)	1.609	3.04	0.0024	1.274
Number of Observation	11,272			
Log Likelihood at zero, $LL(\mathbf{0})$	-52,378			
Log Likelihood at convergence, $LL(\mathbf{\beta})$	-50,466			
$X^2 = -2[LL(\mathbf{0}) - LL(\mathbf{\beta})]$	3,824			
Akaike Information Criteria	100,957			
Schwarz Criterion	101,052			

*The p-value is considered up to 0.10 indicating at 90% confidence that coefficient estimates are significantly different from zero.

TABLE 7 Model Estimates of Roadway Departure Fatal Crashes on Urban Principal Arterial

Variables	Coeff.	t-stat	P-Value*	Marginal Effect
Intercept	92.796	25.46	<0.0001	-
<i>Traffic/ Exposure characteristics</i>				
Logarithm of traffic volume (AADT) per lane	-6.283	-22.50	<0.0001	-4.802
Number of occupants in the vehicle involved	0.584	5.91	<0.0001	0.447
<i>Roadway characteristics</i>				
Traffic way (1 if two-way traffic way is not divided, 0 otherwise)	3.966	6.76	<0.0001	3.031
Traffic way (1 if one way traffic way is divided, 0 otherwise)	2.122	3.79	0.0001	1.622
Traffic way (1 if traffic way is two-way separated by positive median barrier, 0 otherwise)	1.311	2.47	0.0134	1.002
Roadway alignment (1 if roadway alignment changes to the right direction prior to the critical pre-crash event, 0 otherwise)	1.444	1.70	0.0895	1.104
Roadway alignment (1 if roadway alignment changes to the left direction prior to the critical pre-crash event, 0 otherwise)	2.386	2.80	0.0052	1.824
Roadway profile (1 if roadway profile is on grade prior to the critical pre-crash event, 0 otherwise)	-1.420	-2.72	0.0065	-1.086
<i>Traffic speed</i>				
Average travel speed (1 if roadway section with speed limit is between 55 to 65 mph, 0 otherwise)	-2.361	-5.75	<0.0001	-1.805
<i>Human factors</i>				
Vehicle maneuver (1 if the driver is maneuvering while negotiating a curve prior to entering a crash situation, 0 otherwise)	2.162	2.75	0.0060	1.652
<i>Crash type</i>				
Crash type (1 if single-vehicle departing at the left side of roadway, 0 otherwise)	0.761	1.90	0.0575	0.582
Most harmful event (1 if most harmful event is rollover, 0 otherwise)	1.058	1.84	0.0661	0.8085
Number of Observation	14,895			
Log Likelihood at zero, $LL(0)$	-66,919			
Log Likelihood at convergence, $LL(\beta)$	-66,572			
$X^2 = -2[LL(0) - LL(\beta)]$	694			
Akaike Information Criteria	133,172			
Schwarz Criterion	133,279			

*The p-value is considered up to 0.10 indicating at 90% confidence that coefficient estimates are significantly different from zero.

TABLE 8 Model Estimates of Roadway Departure Fatal Crashes on Urban Minor Arterial

Variables	Coeff.	t-stat	P-Value*	Marginal Effect
Constant	145.499	24.71	<.0001	-
<i>Traffic/ Exposure characteristics</i>				
Logarithm of traffic volume (AADT) per lane	-10.523	-22.98	<0.0001	-8.405
Number of occupants in the vehicle involved	2.235	8.26	<0.0001	1.785
<i>Roadway characteristics</i>				
Traffic way (1 if two-way traffic way is not divided, 0 otherwise)	2.545	4.27	<0.0001	2.033
<i>Temporal characteristics</i>				
Time of Day (1 if it is between 8 pm to 11 pm, 0 otherwise)	2.257	3.21	0.0013	1.803
<i>Environmental characteristics</i>				
Light condition at the time of crash (1 if it is dark but lighted, 0 otherwise)	-1.348	-2.20	0.0279	-1.077
<i>Human factors</i>				
Vehicle maneuver (1 if the driver is maneuvering while negotiating a curve prior to entering a crash situation, 0 otherwise)	2.811	4.94	<0.0001	2.245
Number of drivers with alcohol involvement	1.609	2.88	0.0040	1.285
Number of Observation	5565			
Log Likelihood at zero, $LL(\mathbf{0})$	-24,737			
Log Likelihood at convergence, $LL(\mathbf{\beta})$	-24,433			
$X^2 = -2[LL(\mathbf{0}) - LL(\mathbf{\beta})]$	608			
Akaike Information Criteria	48,883			
Schwarz Criterion	48,943			

*The p-value is considered up to 0.10 indicating at 90% confidence that coefficient estimates are significantly different from zero.

TABLE 9 Model Estimates of Roadway Departure Fatal Crashes on Urban Collector

Variables	Coeff.	t-stat	P-Value*	Marginal Effect
Constant	121.080	9.75	<0.0001	-
<i>Traffic/ Exposure characteristics</i>				
Logarithm of traffic volume (AADT) per lane	-8.419	-8.81	<0.0001	-6.429
Number of occupants in the vehicle involved	2.950	6.47	<0.0001	2.253
<i>Roadway characteristics</i>				
Roadway alignment (1 if roadway alignment changes to the right direction prior to the critical pre-crash event, 0 otherwise)	5.277	3.85	0.0001	4.030
Roadway profile (1 if roadway profile is on grade prior to the critical pre-crash event, 0 otherwise)	-2.703	-2.07	0.0384	-2.064
<i>Traffic speed</i>				
Average travel speed (1 if roadway section with speed limit is within 35 mph, 0 otherwise)	2.074	2.25	0.0243	1.584
<i>Temporal characteristics</i>				
Time of day (1 if it is between 4 pm to 7 pm, 0 otherwise)	2.857	2.44	0.0149	2.183
Month of year (1 if month is from December to February, 0 otherwise)	-2.099	-1.86	0.0631	-1.603
<i>Environment characteristics</i>				
Weather condition at the time of crash (1 if weather condition is clear, 0 otherwise)	-2.569	-2.41	0.0158	-1.962
<i>Human factors</i>				
Vehicle maneuver (1 if the driver is maneuvering while negotiating a curve prior to entering a crash situation, 0 otherwise)	2.454	2.27	0.0231	1.874
Number of drivers with alcohol involvement	1.489	1.61	0.103	1.137
<i>Crash type</i>				
First harmful event (1 if the first harmful event is crashing into a tree, 0 otherwise)	-2.265	-1.81	0.0709	-1.730
Number of Observation	2,744			
Log Likelihood at zero, $LL(0)$	-12,694			
Log Likelihood at convergence, $LL(\beta)$	-12,607			
$X^2 = -2[LL(0) - LL(\beta)]$	174			
Akaike Information Criteria	25,240			
Schwarz Criterion	25,316			

*The p-value is considered up to 0.10 indicating at 90% confidence that coefficient estimates are significantly different from zero.

TABLE 10 Model Estimates of Roadway Departure Fatal Crashes on Urban Local Roads

Variables	Coeff.	t-stat	P-Value*	Marginal Effect
Constant	88.363	11.80	<0.0001	-
<i>Traffic/ Exposure characteristics</i>				
Logarithm of traffic volume (AADT) per lane	-6.513	-11.24	<0.0001	-4.742
Number of occupants in the vehicle involved	0.646	3.60	0.0003	0.471
<i>Roadway characteristics</i>				
Traffic way (1 if two-way traffic way is not divided, 0 otherwise)	6.993	8.81	<0.0001	5.093
<i>Traffic speed</i>				
Average travel speed (1 if roadway section with speed limit is within 35 mph, 0 otherwise)	4.370	6.35	<0.0001	3.182
<i>Temporal characteristics</i>				
Month of year (1 if month is from June to September, 0 otherwise)	1.439	1.97	0.0484	1.048
<i>Vehicle characteristics</i>				
Vehicle type (1 if passenger car (or its derivatives) involved in the crashes, 0 otherwise)	1.445	2.15	0.0312	1.052
<i>Human factors</i>				
Number of drivers with alcohol involvement	1.617	2.50	0.0125	1.178
<i>Crash type</i>				
First harmful event (1 if the first harmful event is crashing into roadside curb, 0 otherwise)	4.863	5.35	<0.0001	3.5414
Number of Observation	6,726			
Log Likelihood at zero, $LL(\mathbf{0})$	-31,710			
Log Likelihood at convergence, $LL(\beta)$	-31,562			
$X^2 = -2[LL(\mathbf{0}) - LL(\beta)]$	296			
Akaike Information Criteria	63,144			
Schwarz Criterion	63,212			

*The p-value is considered up to 0.10 indicating at 90% confidence that coefficient estimates are significantly different from zero.

independent variable on the expected value of a dependent variable for all cases, $E[Y]$ was calculated using the formula (36):

$$\partial E[Y]/(\partial X_i) = F(z) \times (\partial E[Y^*]/(\partial X_i)) + E[Y^*] \times (\partial F(z)/(\partial X_i)) \quad (4)$$

whereas

$F(z)$: is the cumulative normal distribution function, associated with the proportion of cases above the limit (in this case zero),

$E[Y^*]$: denotes the expected value for cases above zero,

$\frac{\partial E[Y^*]}{\partial X_i}$: denotes observations above zero, which indicate fatalities per million VMT (not censored),

$\frac{\partial F(z)}{\partial X_i}$: is the change in the cumulative probability of being above zero associated with an independent variable.

In the model estimation process, statistically significant variables were taken in the model by looking at the average in the respective data sample. At the same time, higher log-likelihood at convergence, lower AIC and Schwarz criterion were given importance in the model development process.

EMPIRICAL RESULTS AND DISCUSSIONS

The variables found statistically significant in full model were taken from 5 years (2010 – 2014) of RwD fatal crashes from FARS. Some of the key variables from the full model, were also found statistically significant in other functional class of roadway models. Thus, the key variables in different models for different functional class of roadway indicate the factors associated with a specific functional class of roadway.

Traffic/ Exposure Characteristics

As the traffic volume per lane increases, the frequency of fatalities per million VMT decreases across the models. This is an important exposure variable in the traffic. This is because the more vehicular interactions on any roadway, the RwD fatal crashes decrease (22). This is true for all the functional class of roadway. However, the effect of this variable is relatively more significant in rural roadways than urban roadways. Another important exposure variable is the number of occupants in the vehicles involved in the fatal crashes. A higher number of occupants in the vehicles leads to an increased number of fatalities per million VMT. A similar finding on exposure level in terms of occupants in the vehicle was found (41).

Roadway Characteristics

An undivided two-way roadway has higher impact on fatalities per million VMT than other roadway characteristics. The full model indicates an average impact of this particular variable considering rural and urban roadways. However, rural roadways have lower impact than urban

roadways. The marginal effect for rural roadway (i.e., rural principal arterial with 1.679, rural minor arterial with 3.989, and rural local roads with 2.15) is lower than that for urban roadways (urban principal arterial with 3.031, and urban minor arterial with 2.033, urban local with 5.093). This is because there is no barrier separating the opposing traffic and less driving alert compared to divided roadway facilities. Roadway alignment changes to the right side of travel direction (i.e., curve to the right of travel direction) as opposed to roadway alignment changes to the left side of travel direction, increases the fatalities per million VMT in the full model as well as the rural roadways, namely rural principal arterial, rural minor arterial, and rural collector. However, urban principal arterial has relatively higher on the left side of travel direction. But, urban collectors have higher fatalities per million VMT for road alignment changes to right direction compared to rural highways.

Functional Class

Functional class particularly rural roadways have higher fatalities per million VMT than urban roadways. It is quite evident from the full model that rural principal arterial (other) has higher marginal effect than the urban principal arterial (other) and their effect are opposite on the outcome of the model. In addition, it is quite clear from the intercept (constant) of the separate (11) models that rural highways have higher fatalities per million VMT than urban highways. This is because rural roadways have lower level of enforcement, wide landscape leading to higher speed, less traffic and lower level of driving attention relative to urban roadways. (42)

Traffic Speed

The speed limit on the roadway section with 35 to 45 mph has lower effects on fatalities per million VMT than other road sections of higher speed limit in the full model. However, the roadway section with 35 mph has higher effects on fatalities per million VMT in the full model. This indicates travel speed variability is higher in 35 mph roadway section compared to a higher speed limit. The roadway sections with 35 to 45 mph have higher fatalities per million VMT for rural minor arterial and rural collector roads. However, the roadway section within 35 mph has higher fatalities per million VMT on rural local roads. This clearly indicates the lower level of speed enforcement in rural local roadway sections combined with higher speed variability. However, roadway section with speed limit between 55 to 65 mph, has higher fatalities per million VMT in rural principal arterial than urban principal arterial. And, their effects on fatalities per million VMT are opposite.

Temporal Characteristics

The time between 2 pm to 7 pm has an increase number of fatalities per million VMT in full model as well as urban models. This is because of the after-lunch afternoon effect leads to inattentive driving (e.g., drowsy driving) and PM peak particularly in urban roadways – urban principal arterial, urban minor arterial, urban collector, and urban local road. A similar result was found in a study where afternoon is more likely to be resulting in fatal crashes in urban interstates (43). During the winter period (December to February), the fatalities per million VMT are lower in full model and urban collector roadway. This is because the drivers are more alert in the inclement weather with lower traveling speed. Naturally, summer months (June to

September) have higher effects on fatalities per million VMT on urban local roads and rural minor arterial because of higher level of exposure on the road (9).

Environmental Characteristics

Dark not lighted environment increases fatalities per million VMT in full model. And, this increase is reflected in rural local roads. Poor visibility causes drivers some level of difficulty in decision-making process to avoid crashes and severe consequences in fatal crashes. A similar result was found where likelihood of severe injury increases under dark condition (9). However, this effect decreases fatalities per million VMT on the rural collector. Clear weather condition decreases the fatalities per million VMT in rural principal arterial. This indicates better visibility and comfortable driving along the roadways.

Human Factors

Negotiating a curve (prior to be involved in fatal crashes as part of vehicle maneuvering) increases the fatalities per million VMT. This effect is reflected in full model as well as all the rural and urban roadways except urban local roads. This effect is relatively higher in urban minor arterial and urban collector than rural roadways. This could be because of inadequate road alignment signage (e.g., chevron, advance curve sign) or surface friction on the roadway section and part of attention level of the drivers. About 25% of total fatalities occurred on the curved section of roadways in the US (43). Furthermore, drivers' expectancy, speed advisory signs, speed selection along different parts of the horizontal curves (e.g., approach, curve discovery, entry and negotiation, and exit) highly affects the likelihood of increasing fatalities (44). In addition, as the drivers with alcohol involvement in the crashes increase, the fatalities per million VMT in rural and urban minor arterial roads. Drivers involved with alcohol become less reactive compared to the normal driving in terms of the cognitive decision making process in the critical driving situations like fatal crashes. A similar findings were found on rural roadways for roadway departure crashes resulting in higher likelihood of serious injury/ fatality (45, 46).

Vehicle Characteristics

Motorcycles (2-wheelers) involved in the fatal crashes on rural principal arterial increased fatalities per million VMT. This indicates the law enforcement levels on helmet usage and speed variability are probably major reasons in these functional classes. Furthermore, passenger car and its derivatives involved in the fatal crashes increase the fatalities per million VMT on urban local roads. This is because the passenger cars heavily travel urban local roads. Urban local roads do not have standard geometric features and less maintained roadway elements relative to urban principal arterials (e.g., freeway and expressways).

Crash Type

Single vehicle running-off-the-road at right and left side of roadway increases the fatalities per million VMT on rural principal and rural minor arterial. These effects were also observed in the full model. A similar result was found in study (9). Also, multiple vehicle head-on crashes increase the fatalities per million VMT on rural principal and rural minor arterial. Multi-vehicle

head-on crashes increase fatalities per million VMT on rural principal arterials (with marginal effect of 2.128), rural minor arterials (with marginal effect of 1.933), and rural collector roads (with marginal effect of 1.643). This is because of direct energy transferred between crash involved vehicles. Rollover crashes, as the most harmful event in the crash mechanism, lead to increase in fatalities per million VMT on rural principal arterials, rural minor arterials, rural collectors, rural local roads, and urban principal arterials. This mostly indicates the unsafe roadside design – shoulder edge, slope, fixed objects in close proximity of edge line and other related geometric elements. On urban local roads (in urban settings), crashing into roadside curb results in increase in fatalities per million VMT. Unsafe design of curb in urban settings in serious fatal crashes can result in more fatalities.

CONCLUSIONS AND FUTURE WORK

This study aimed at unveiling the contributing factors from developed full model on fatalities per million VMT. This paper highlights an important aspect of fatality rates normalized with traffic exposure (e.g., VMT) by functional class of roadways as opposed to annual frequency of crashes by functional class based on the predictive methodology of Highway Safety Manual. Moreover, this study developed and estimated separate models for rural and urban functional classes of roadways, particularly, principal arterials, minor arterials, collectors, and local roads. These eight developed separate models clearly demonstrated the importance of the contributing factors specific to the functional classes that should be analyzed and studied separately. The statistical significance demonstrated that the separate models are stronger in explaining and understanding the contributing factors. Separate models clearly provide more opportunities to study these factors related to geometry, traffic, environmental, temporal, and driving behavior, as well as traffic speed and crash characteristics specific to the functional class of roadways in rural and urban areas. The marginal effects show the impact of particular variables on the outcome – fatalities per million VMT. This provides a relationship between exposure and contributing factors by functional class of rural and urban roadways. Proper understanding of these factors and implementing strategic countermeasures paves the way “Towards Zero Deaths.” These factors clearly indicate the need to develop realistic strategic safety plan (for example, SHSP) tailored to roadway departure crashes where potential for safety improvements can be relatively higher compared to other emphasis areas. However, developing this strategic safety plan can be aligned with specific focus to functional class of roadways in rural and urban areas. In a very similar reason, the different states develop their own SHSP where roadway departure crashes are prioritized on top of all emphasis areas identified within the state specific crash experiences. It is noteworthy to understand the level of exposure for different functional class of roadways to implement the countermeasures based on the magnitude of their relative effects. A study (47) documented the effective low cost safety countermeasures focusing roadway departure crashes. Also, based on the recent increase in the fatalities in 2015 and 2016 (first 6 months comparative studies), it clearly indicates the importance of setting goals under the state SHSP to reduce fatalities and serious injuries resulting from roadway departure crashes (48). As such, the preventive strategies formulated based on the data-driven approach highlighted in this paper provides a realistic basis for the safety practitioners with a toolbox of cost effective countermeasures. And, pavement friction, safety edge at the shoulders, rumbles strips, horizontal

curve safety, clear zones and roadside design principals are some of the key countermeasures to consider to reduce the fatalities resulting from roadway departure crashes (2).

The heterogeneity involved with the combined dataset can be explained with the split dataset and separate model development process as conducted in this study. However, with regard to the heterogeneity involving the variation in observations in the dataset, random parameter tobit model helps to explain the contributing factors in better statistical power. In future, this study effort will extend to explore in estimating random parameter tobit models for all eight models to explain the heterogeneity involving varying observations by functional classes of roadways.

REFERENCES

1. AASHTO Strategic Highway Safety Plan, <http://safety.transportation.org/doc/Safety-StrategicHighwaySafetyPlan.pdf>, Accessed Feb 15, 2017.
2. Roadway Departure Crashes, Federal Highway Administration, http://safety.fhwa.dot.gov/roadway_dept/, Accessed Aug 12, 2016.
3. Federal Highway Administration Roadway Departure Crash Emphasis Areas. https://safety.fhwa.dot.gov/roadway_dept/strat_approach/brochure/roadwaydeparturebrochure.pdf, Accessed Feb 15, 2017
4. The Economic and Societal Impact of Motor Vehicle Crashes, 2010, <https://crashstats.nhtsa.dot.gov/Api/Public/ViewPublication/812013>, Accessed Feb 15, 2016.
5. Federal Highway Administration Memorandum on Roadway Departure Definition and Criteria, https://safety.fhwa.dot.gov/fas/docs/focus_area_data_mem.pdf Accessed Feb 15, 2017.
6. Islam, M.B. and S. Hernandez. Fatality Rates for Crashes Involving Heavy Vehicles on Highways: A Random Parameter Tobit Regression Approach. *Journal of Transportation Safety and Security*, Vol. 8, No. 3, 2016, pp. 247-265.
7. Islam, M.B. Multi-vehicle Crashes Involving Large Trucks: A Random Parameter Discrete Outcome Modeling Approach. *Journal of The Transportation Research Forum*, Vol. 54, No. 1, 2015, pp. 77-103.
8. Islam, M.B. and S. Hernandez. Modeling Injury Outcomes of Crashes involving Heavy Vehicles on Texas Highways. *Transportation Research Board: Journal of the Transportation Research Board*, Washington D.C., USA. TRR 2388, 2013, pp. 28-36.
9. Islam, M.B. and S. Hernandez, Large Truck Involved Crashes: An Exploratory Injury Severity Analysis. *Journal of Transportation Engineering. ASCE*. Vol. 139, No. 6, 2013, pp. 596-604.
10. Shankar, V. N., F. L. Mannering, and W. Barfield. Effect of Roadway Geometrics and Environmental Factors on Rural Accident Frequencies. *Accident Analysis and Prevention*, Vol. 27, No. 3, 1995, pp. 371–389.
11. Poch, M., and F. L. Mannering. Negative Binomial Analysis of Intersection Accident Frequencies, *Journal of Transportation Engineering*, Vol. 122, No. 2, 1996, pp. 105–113.
12. Abdel-Aty, M., and A. E. Radwan. Modeling Traffic Accident Occurrence and Involvement. *Accident Analysis and Prevention*, Vol. 32, No. 5, 2000, pp. 633–642.
13. Savolainen, P. T., and A. P. Tarko. Safety Impacts at Intersections on Curved Segments. In *Transportation Research Record: Journal of the Transportation Research Board*, No. 1908, Transportation Research Board of the National Academies, Washington, D.C., 2005, pp. 130–140.
14. Shankar, V. N., J. Milton, and F. L. Mannering. Modeling Accident Frequencies as Zero-Altered Probability Processes: An Empirical Inquiry. *Accident Analysis and Prevention* Vol. 29, No. 6, 1997, pp. 829–837.
15. Carson, J., and F. L. Mannering. The Effect of Ice Warning Signs on Accident Frequencies and Severities. *Accident Analysis and Prevention*, Vol. 33, No. 1, 2001, pp. 99–109.

16. Lee, J., and F. L. Mannering. Impact of Roadside Features on the Frequency and Severity of Run-Off-Roadway Accidents: An Empirical Analysis. *Accident Analysis and Prevention*, Vol. 34, No. 2, 2002, pp. 149–161.
17. Shankar, V. N., R. B. Albin, J. C. Milton, and F. L. Mannering. Evaluating Median Crossover Likelihoods with Clustered Accident Counts: An Empirical Inquiry Using the Random Effects Negative Binomial Model. In *Transportation Research Record 1635*, TRB, National Research Council, Washington, D.C., 1998, pp. 44–48.
18. Chin, H. C., and M. A. Quddus. Applying the Random Effect Negative Binomial Model to Examine Traffic Accident Occurrence at Signalized Intersections. *Accident Analysis and Prevention*, Vol. 35, No. 2, 2003, pp. 253–259.
19. Anastasopoulos, P. C., and F. L. Mannering. A Note on Modeling Vehicle Accident Frequencies with Random-Parameters Count Models. *Accident Analysis and Prevention*, Vol. 41, No. 1, 2009, pp. 153–159.
20. Malyshkina, N. V., and F. L. Mannering. Markov Switching Multinomial Logit Model: An Application to Accident-Injury Severities. *Accident Analysis and Prevention*, Vol. 41, No. 4, 2009, pp. 829–838.
21. Park, B. J., D. Lord, and J. D. Hart. Bias Properties of Bayesian Statistics in Finite Mixture of Negative Binomial Regression Models in Crash Data Analysis. *Accident Analysis and Prevention*, Vol. 42, No. 2, 2010, pp. 741–749.
22. Anastasopoulos, P. Ch., Tarko, A. P., and Mannering, F. L. Tobit analysis of vehicle accident rates on interstate highways. *Accident Analysis and Prevention*, Vol. 40, No. 2, 2008, pp. 768–775.
23. Patil, S., S. R. Geedipally, and D. Lord. Analysis of Crash Severities Using Nested Logit Model—Accounting for the Underreporting of Crashes. *Accident Analysis and Prevention*, Vol. 45, No. 1, 2012, pp. 646–653.
24. Golob, T., W. Recker, and J. Leonard. An Analysis of the Severity and Incident Duration of Truck-Involved Freeway Accidents. *Accident Analysis and Prevention*, Vol. 19, No. 5, 1987, pp. 375–396.
25. Islam, S., and F. L. Mannering. Driver Aging and Its Effect on Male and Female Single-Vehicle Accident Injuries: Some Additional Evidence. *Journal of Safety Research*, Vol. 37, No. 3, 2006, pp. 267–276.
26. Kim, J.-K., G. Ulfarsson, V. N. Shankar, and F. L. Mannering. A Note on Modeling Pedestrian Injury Severity in Motor Vehicle Crashes with the Mixed Logit Model. *Accident Analysis and Prevention*, Vol. 42, No. 6, 2010, pp. 1751–1758.
27. Moore, D. N., W. Schneider, P. T. Savolainen, and M. Farzaneh. Mixed Logit Analysis of Bicyclist Injury Severity Resulting from Motor Vehicle Crashes at Intersection and Non-Intersection Locations. *Accident Analysis and Prevention*, Vol. 43, No. 3, 2011, pp. 621–630.
28. Malyshkina, N. V., and F. L. Mannering. Empirical Assessment of the Impact of Highway Design Exceptions on the Frequency and Severity of Vehicle Accidents. *Accident Analysis and Prevention*, Vol. 42, No. 1, 2010, pp. 131–139.
29. Shankar, V. N., and F. L. Mannering. An Exploratory Multinomial Logit Analysis of Single-Vehicle Motorcycle Accident Severity. *Journal of Safety Research*, Vol. 27, No. 3, 1996, pp. 183–194.
30. Ulfarsson, G., and F. L. Mannering. Differences in Male and Female Injury Severities in Sport-Utility Vehicle, Minivan, Pickup and Passenger Car Accidents. *Accident Analysis and Prevention*, Vol. 36, No. 2, 2004, pp. 135–147.
31. Labi, S. Efficacies of roadway safety improvements across functional subclasses of rural two-lane highways. *Journal of Safety Research*, Vol. 42, No. 4, 2011, pp. 231–239.
32. Memorandum on Roadway Departure Definition and Criteria, https://safety.fhwa.dot.gov/fas/docs/focus_area_data_mem.pdf, Accessed on Jul 10, 2016.
33. Highway Performance Monitoring System, Annual Vehicle Miles. <http://www.fhwa.dot.gov/policyinformation/quickfinddata/qftravel.cfm>, Accessed Jul 15, 2016.

34. Highway Performance Monitoring System, Length by Functional Class.
<http://www.fhwa.dot.gov/policyinformation/statistics/2014/index.cfm#sec4>, Accessed Jul 28, 2016.
35. SAS 9.2 for windows. SAS Institute, Inc. Cary, N.C., 2009.
36. Washington, S.P., M. G. Karlaftis, and F.L. Mannering, *Statistical and Econometric Methods for Transportation Data Analysis*, 2nd Ed. Chapman & Hall/CRC, Boca Raton, FL. 2011.
37. Amemiya, T. Regression-analysis when dependent variable is truncated normal. *Econometrica*, Vol. 41, No. 6, 1973. pp. 997–1016.
38. Amemiya, T. *Advanced Econometrics*. Harvard University Press, Cambridge, MA. 1985.
39. McDonald, J. F., and R. A. Moffitt,. The uses of tobit analysis. *Journal of Review and Economics and Statistics*, Vol. 62, No. 2, 1980, pp. 318–321.
40. Roncek, D.W. Learning more from tobit coefficients: extending a comparative analysis of political protest. *Journal of American Sociology Review*, Vol. 57, No. 4, 1992, pp. 503–507.
41. Chang, Li-Yen, F.L. Mannering. Analysis of injury severity and vehicle occupancy in truck- and non-truck involved accidents. *Accident Analysis and Prevention*, Vol. 31, No. 5, 1999. pp.579–592
42. Islam, M.B. and S. Hernandez. Modeling Injury Outcomes of Crashes Involving Heavy Vehicles in Rural and Urban Settings in Texas. *93rd Annual Meeting of the Transportation Research Board*, Washington DC, 2014.
43. Horizontal Curve Safety, Federal Highway Administration Office of Safety
http://safety.fhwa.dot.gov/roadway_dept/horicurves/, Accessed Oct 15, 2016
44. Campbell, J. L., Lichty, M.G., Brown, J. I., Richard, C. M., Graving, J.S., Graham, J., O’Laughlin, M., Torbinc, D., and Harwood, D. National Cooperative Highway Research Program, Report 600, Human Factor Guidelines for Roadway Systems, Transportation Research Board of the National Academies, Washington, D.C., 2012. pp. 6-2.
45. Lee, J. and F.L. Mannering. Impact of roadside features on the frequency and severity of run-off-roadway accidents: an empirical analysis. *Accident Analysis and Prevention*, Vol. 34, No. 2, 2002. Pp. 149–161.
46. Xie. Y., K. Zhao, and N. Huynh, Analysis of driver injury severity in rural single-vehicle crashes. *Accident Analysis and Prevention*, Vol. 47, 2012, pp. 36 – 44.
47. Jalayer, M., H. Zhou, and C. Satterfield. Overview of Safety Countermeasures of Roadway Departure Crashes. *95th Annual Meeting of Transportation Research Board*, Washington DC, 2016.
48. National Safety Council, Motor Vehicle Fatality Estimates.
<http://www.nsc.org/Connect/NSCNewsReleases/Lists/Posts/Post.aspx?ID=134>, Accessed Oct 31, 2016.

ROADWAY DEPARTURE DATA COLLECTION AND ANALYSIS

Consideration of Roadside Features in the *Highway Safety Manual*

CHRISTINE E. CARRIGAN

MALCOLM H. RAY

RoadSafe LLC

This NCHRP project has developed new Rural and Urban Safety Performance Functions (SPFs) that predict the expected run-off-road (ROR) crash frequency across all road types. Additionally, this research has developed on-road and off-road crash modification functions (CMFs) which modify the predicted ROR crash frequency derived from the proposed roadside SPF for site-specific situations. Accomplishing these two major project objectives allows for (1) the coordination of the *Highway Safety Manual* (HSM) approach to roadside safety modeling using crash data with the *Roadside Design Guide* (RDG) approach using encroachment data; and (2) corridor-level comparison of roadside improvement alternatives using the HSM procedures and the IHSDM, a feature not currently available in the RDG. This presentation will include a summary of the developed SPFs and CMFs across all road types.

A New Method to Evaluate Roadside Safety for Rural Two-Lane Roads Based on Reliability Analysis

MOHAMMAD JALAYER

*Center for Advanced Infrastructure and Transportation
Rutgers, The State University of New Jersey*

HUAGUO ZHOU

Auburn University

The severity of roadway departure crashes mainly depends on the roadside features, including the sideslope, fixed-object density, offset from fixed objects, and shoulder width. Common engineering countermeasures to improve roadside safety include: cross section improvements, hazard removal or modification, and delineation. It is not always feasible to maintain an object-free and smooth roadside clear zone as recommended in design guidelines. Currently, clear zone width and sideslope are used to determine roadside hazard ratings (RHRs) to quantify the roadside safety of rural two-lane roadways on a seven-point pictorial scale. Since these two variables are continuous and can be treated as random, probabilistic analysis can be applied as an alternative method to address existing uncertainties. Specifically, using reliability analysis, it is possible to quantify roadside safety levels by treating the clear zone width and sideslope as two continuous, rather than discrete, variables.

The objective of this manuscript is to present a new approach for defining the reliability index for measuring roadside safety on rural two-lane roads. To evaluate the proposed approach, we gathered five years (2009-2013) of Illinois run-off-road (ROR) crash data and identified the roadside features (i.e., clear zone widths and sideslopes) of 4,500 300-ft roadway segments. Based on the obtained results, we confirm that reliability indices can serve as indicators to gauge safety levels, such that the greater the reliability index value, the lower the ROR crash rate.

Integrating Crash Severity in Roadside Safety Quantitative Analysis *Assessing Partial Proportional Odds Models*

CARLOS ROQUE

JOÃO LOURENÇO CARDOSO

*Laboratório Nacional de Engenharia Civil,
Departamento de Transportes. Núcleo de Planeamento, Tráfego e Segurança*

Robust knowledge of the underlying factors involved in run-off-road (ROR) crash occurrences and resulting injuries is a prerequisite for the development of sound methods to support roadside cost-efficient design and redesign and related asset management/road operations decisions. Over recent years, the understanding of ROR crashes on Portuguese roads has significantly increased due to roadside safety research carried out by the Laboratório Nacional de Engenharia Civil, emphasizing the importance of this type of crash in the overall interurban safety picture.

In this paper investigations of ROR crash injury severity on Portuguese freeways are reported, exploring the application of a partial proportional odds (PPO) model to study the contributors influencing ROR crash severities. The PPO model allows the covariates that do not meet the proportional odds assumption to have diverse effects at different severity levels.

This study is based on a detailed data set of ROR crashes that occurred on Portuguese freeways during the years 2009 and 2010.

Several variables in seasonal attributes, roadway and roadside attributes, crash characteristics and driver information were tested. Specifically, the use of the partial proportional formulation allows a superior identification of the varying effect of several variables on ROR crash injury severity. Furthermore it includes the effect of traversing ditches, which previously was masked when fitting the unordered framework models.

A comparison between the application of PPO models and mixed logit models for ROR crash severity evaluation is also included here. The study shows that the PPO model is a viable method for analyzing ROR crash severities.

INTRODUCTION

Robust knowledge of the underlying factors involved in run-off-road (ROR) crash occurrences and resulting injuries is a prerequisite for the development of sound methods to support roadside cost-efficient design and redesign and related asset management/road operations decisions. In Portugal, single-vehicle run-off-road (ROR) crashes result in ten thousand crashes with roadside features every year and account for approximately half of all freeway fatalities. Portuguese crash data (2007-2010) indicate that roadside geometry – including slopes, embankments, and ditches – contributes to more than half of all ROR accidents involving serious injury or death (1).

Over recent years, the understanding of ROR crashes on Portuguese roads has significantly increased due to roadside safety research carried out by the *Laboratório Nacional de Engenharia Civil*, emphasizing the importance of this type of crash in the overall interurban safety picture. This allowed the development of a computer-aided procedure for supporting cost-effective decisions with regard to roadside safety alternative interventions. As already described

in previous research by the authors, the procedure is based on cost–benefit analysis and makes extensive use of dedicated ROR crash prediction models (2, 3).

Currently, one limitation of this procedure is the non-consideration of the probability of different severity level outcomes conditioned on crash occurrence. This may impact crash cost estimations used when choosing amongst relevant alternatives. Hence, research towards the improvement of methods for considering crash severity has been carried out, attempting to integrate crash severity models in the said procedure in order to estimate the expected number of injuries at different severity levels and thus improve the estimation of ROR crash costs.

When studying crash severity injury outcomes, the most common study approaches may be grouped into unordered framework models and ordered framework models. The former includes, for example, the multinomial and mixed logit models already mentioned. Multinomial logit models are traditional discrete outcome models that consider three or more outcomes and do not explicitly consider the ordering that may be present in these outcomes. Mixed logit models are a more recent development for the analysis of discrete data that addresses the limitations of the multinomial logit (susceptibility to correlation of unobserved effects from one injury-severity level to the next) by allowing for heterogeneous effects and correlation in unobserved factors (4, 5).

The latter framework includes ordered probit or logit models, among others. In these models, the discrete injury severity levels are assumed to be associated with an underlying continuous latent variable (z) that is used as a basis for modeling the ordinal ranking of data. This unobserved variable is typically specified as a linear function for each crash observation, such that $z = \beta X + \varepsilon$, where X is a vector of variables determining the discrete ordering for each crash observation, β is a vector of unknown parameters to be estimated, and ε is a random disturbance term (4, 5). In this framework, crash injury severity outcomes are reported as an ordinal scale variable (such as no injury, minor injury, severe injury, and fatal injury). The ordered framework models explicitly recognize the inherent ordering within the outcome variable (as the severities become increasingly severe from no injury, to minor injury, to severe injury, to fatality) whilst in the non-ordered analyses it is completely ignored.

In a previous study, multinomial and mixed logit models were developed to explain ROR crash severity and detect unforgiving roadside contributors (6). The empirical findings showed the contribution of critical slopes and vehicle rollover towards increased probability of fatal injuries and highlighted the importance of introducing the “forgiving roadside” concept in Portuguese road design standards, namely to mitigate ROR crash severity on Portuguese freeways.

This study considers the ordered nature of crash injury severity. Thus, ordered framework models were used to examine the effect of various contributing factors to driver injury severity levels in ROR crashes on Portuguese freeways. These models represent the outcome process under consideration using a single latent propensity. Thus, the outcome probabilities are determined by partitioning the uni-dimensional propensity into as many categories as the outcome variable alternatives through a set of thresholds (7). However, it is important to keep in mind that these models are intrinsically case specific because they are limited to and constrained by the available data, which may be improved over time.

The main focus of this study is to investigate ROR crash injury severity, to study the contributors influencing ROR crash severities on freeways.

Accordingly, the modeling approach is mainly explanatory (based on past observations) rather than predictive (predicting new values for the future). Furthermore, a partial proportional

odds (PPO) models is used, a statistical technique not yet found in reported ROR crash research. In the literature several unordered framework models were found: the multinomial and mixed logit models (6, 8, 9, 10, 11), the nested logit models (11, 12, 13) and the latent class logit model (14). In addition, only two ordered framework models were found: ordered probit models, by Renski et al. (15) and Kockelman and Kweon (16).

The PPO model allows the covariates that meet the proportional odds assumption to affect different crash severity levels with the same magnitude. At the same time, the covariates that do not meet the proportional odds assumption can have diverse effects at different severity levels (17). Thus, this model ensures minimal complexity of the analysis framework while allowing some flexibility from the multinomial and mixed logit models.

A comparison between the application of PPO models and mixed logit models for ROR crash severity evaluation is also included here. In the final section, measures to be taken into consideration in supporting decisions on roadside safety design in Portugal are discussed based on the empirical findings.

METHODOLOGY

Crash severity models focus on the estimation of the probability of a crash resulting in one or more fatalities, severe injuries, minor injuries or property damage only (PDO) given the occurrence of the crash. Savolainen *et al.* (4) and Mannering and Bath (18) extensively reviewed the numerous methodological techniques applied in studying crash severity data. The most common options found in the literature when studying crash severity injuries can be grouped into unordered framework models (like multinomial logit (MNL), nested logit, probit and mixed logit models) and ordered framework models (including ordered probit or logit models, generalized ordered models and PPO models). In this paper, by focusing the attention on ordered models, the ordered nature of crash injury severity is favored, a characteristic that cannot be ignored completely.

Occasionally, it is more realistic to assume that the explanatory variables may vary across crashes; therefore, some researchers have used fixed parameters models (like Kockelman and Kweon (16)) others have used random parameters or mixed effects models (e.g. Roque et al. (6) and Wu et al. (11)). Random parameters models have the advantage of allowing the explanatory variables to take into account the individual differences among injury severity levels in different crashes.

In this study, two models were estimated. A PPO model was estimated using R (version 3.2.5) (19). “VGAM” (20) R package was used. The freeware BIOGEME software (21) was used for mixed logit model estimation.

Partial Proportional Odds Model

To Savolainen *et al.* (4) crash severity is ordinal in nature and recognizing this feature it is important to select the appropriate analysis tool, justifying the use of ordered framework models. In this study, driver injury severity is categorized into three levels of increasing severity and coded as: 1 = no injury, 2 = minor injury, 3 = severe or fatal injury.

On the one hand, traditional ordered logit models require data that adhere to the proportional odds assumption between different severity levels, i.e., the effect of an explanatory

variable will be uniform for all levels of the outcome variable (e.g., the deployment of an airbag may decrease the probability of a fatality and also increase the probability of no injury, or vice versa) (23). Imposing such restriction can lead to inconsistent parameter estimation (7). On the other hand, while mixed logit models completely ignore the sequential order of injury severity levels (in this case the deployment of an airbag may, e.g., decrease the probability of a fatality or increase the probability of no injury). In fact, in crash severity analysis, it is not logical to assume that the proportional odds assumption will be satisfied by all explanatory variables (in reality the deployment of an airbag may decrease the probability of both fatality and no injury (because the airbag itself may cause some minor injuries) nor to ignore the ordered nature of crash injury severity. The PPO model allows certain individual explanatory variables to affect each level of the response variable differently, while other independent predictors may adhere to the proportional odds assumption, if they are found not to violate this assumption based on relevant statistical tests (e.g., Wald test) (24, 25).

If j denotes the crash severity level (1 to 3) and J represents the number of severity levels (here $J = 3$), then the form of the PPO model is as follows (26):

$$\Pr(Y_i > j) = \frac{\exp[\alpha_j + (X_i\beta + T_i\gamma)]}{1 + \exp[\alpha_j + (X_i\beta + T_i\gamma)]}, j = 1, 2, \dots, J - 1 \quad (1)$$

where Y_i represents the observed severity for crash i ; plus, γ and β are the vectors of parameter estimations that do and do not violate the parallel line assumption, respectively. The corresponding vectors of explanatory variables that do and do not violate this assumption are T_i and X_i , respectively; and α_j is the cutoff term for the thresholds in the model.

In order to determine which predictor variables will belong to the subset q that rejects the proportional odds assumption, each variable was analyzed individually using a Wald test of proportional odds. This test takes the multinomial response variable and dichotomizes it based on cumulative probability, using $P(Y_i \geq j)$ and $P(Y_i < j)$ for each crash severity level j . This method determines whether the effect of a variable will remain the same across all “cuts” of j (17).

Special care must be exercised when interpreting the coefficients of intermediate categories in PPO models. The sign of β does not always determine the direction of the effect of the intermediate outcomes. Thus, marginal effects were used in this study for interpretation of the variables (27). The marginal effects estimated for an explanatory variable, measure how changes in the explanatory variable affect the outcome variable.

Mixed Logit Model

According to Train (5), a mixed logit model is derived from the multinomial logit model by allowing β_j to be random across i individuals in the severity function:

$$T_{ij} = \beta_{ij}X_{ij} + \varepsilon_{ij} \quad \text{with } \beta_i \sim f(\beta|\theta), \quad (2)$$

where β_j is a vector of coefficients to be estimated for outcome j , X_{ij} is a vector of exogenous (or explanatory) variables, θ are the parameters of the distribution of β_{ij} over the population, such as the mean and variance of β_{ij} and ε_{ij} is the error term that is independent and identically

distributed (*iid* extreme value property) and does not depend on underlying parameters or data characteristics.

As mentioned, the mixed logit is a generalization of the multinomial structure that allows the parameter vector β_j to vary across each driver or most severely injured occupant. The injury outcome-specific constants and each element of β_j may be either fixed or randomly distributed over all parameters with fixed means, allowing for heterogeneity in effects. A mixing distribution is introduced to the model formulation, resulting in injury severity probabilities as follows (5):

$$P_{ij} = \int \frac{e^{\beta_{ij} X_{ij}}}{\sum_x e^{\beta_{ix} X_{ix}}} f(\beta | \phi) d\beta \quad (3)$$

where $f(\beta | \phi)$ is a density function of β and ϕ is a vector of parameters which describe the density function, with all other terms conforming to previous definitions (30). The injury severity outcome probability is then simply a mixture of logits (5). The distribution is flexible in that β can also be fixed, and when all parameters are fixed the model reduces to the standard MNL formulation. In those instances, where β is allowed to vary, the model is in the open form, and the probability of an observation having a particular outcome can be calculated through integration (4).

In this particular case, the parameters vary across the roadway segment population according to a normal distribution (less well-fitting distributions were considered but discarded, such as the log-normal and uniform). Estimation can be done by solving the integral with Monte Carlo simulation. Efficiency has been increased using simulation with Halton draws, an efficient estimation technique for random parameters models (5, 22).

Goodness-of-Fit Statistics

The models' performance was evaluated using several well-known statistics: Pseudo R^2 measure $R^2 = 1 - (\ln L / \ln L_0)$; the McFadden adjusted- $R^2 = 1 - [(\ln L - p) / \ln L_0]$; Akaike's information criterion $AIC = -2 \ln L + 2p$; and Bayesian Information Criterion $BIC = -2 \ln L - p \cdot \ln n$. Where $\ln L$ and $\ln L_0$ are the log likelihood of the fitted and intercept-only models; p is the number of parameters used in each model; and n is the sample size.

Pseudo R^2 coincides with an interpretation of linear model R^2 (29). The McFadden adjusted- R^2 statistic was chosen to measure the explanatory power of the models fitted based on the sample data (27). AIC and BIC are two measures to evaluate and compare the quality of the models estimated.. AIC and BIC are estimated by considering simultaneously goodness of fit and complexity of the model (25). BIC is more appropriate for measuring goodness-of-fit for explanatory power; whilst AIC is more appropriate for measuring predictive accuracy (28) and hence predictive power.

DATA

In this study police reported ROR crashes that occurred on Portuguese freeways during a two-year period (2009 and 2010) are analyzed. Data were obtained from the national accident

database maintained by the National Road Safety Authority (ANSR) which manages the Portuguese road accidents database, a main source of evidence for this study. However, information on roadside features is lacking in that database. It was thus necessary to collect additional information from the original accident reports. This data was provided by the Guarda Nacional Republicana (GNR), which is a police force responsible for maintaining security and public order as well as protecting and defending the population and their property.

This dataset comprises 580 km of dual carriageway freeway segments situated in various regions across Portugal (Figure 1). All segments have full access control, two lanes per carriageway and paved shoulders (with widths of less than 2.5 m and 4.0 m for left and right shoulders, respectively). Access to and from the freeway is only possible through interchange ramps.

Only single-vehicle ROR crashes involving roadside features were used in this study.

Table 1 shows the variables that proved to be relevant for explaining crash severities and their observed distributions across different severity levels. Information related to ROR crashes including injury severity levels, seasonal attributes (winter, peak hour), roadside attributes (obstacles, barrier, ditch), roadway attributes (right curve), accident information (persons involved, right encroach, rollover, car, speed limit) and driver information (age, gender) was included in the models. The total frequency of crashes in different categories and the proportions of different injury severity levels for each category are also included in Table 1. In the case of continuous variables, the mean and standard deviation parameters are included. ROR crashes with missing information on the accident, driver or vehicle characteristics were removed before the statistical analysis, which resulted in a total of 764 crashes selected, out of 840 registered ROR crashes on dual carriageway roads. Correlation analyses were conducted for all independent variables considered in the study as a first step to identify correlated variables.



FIGURE 1 Google Street View still images of typical Portuguese freeway cross sections.

TABLE 1 Descriptive Statistics of the Significant Variables in the Models

Variable		Description	Total No. of Crashes	PDO (%)	Minor Injury (%)	Severe and Fatal Injury (%)
ROR crashes			764	16.4	76.7	6.9
Categorical variables						
Seasonal attributes						
	Winter	Winter (December, January or February)	225	19.6	74.7	5.8
	Peak hour	Evening period (18.00 to 20.00 pm)	33	12.1	72.7	15.2
Roadside attributes						
	Barrier	Collision with metallic safety barrier as first harmful event	313	19.2	73.5	7.3
	Ditch	Traversing/colliding with ditch as first harmful event	22	18.2	81.8	0.0
Roadway attributes						
	Right curve	Horizontal curve to the right (vs. straight segment or left curve)	94	10.6	85.1	4.3
Accident information						
	Right encroach	Leaving the road to the right side of the carriageway (vs. leaving the road to the left side of the carriageway)	422	13.5	79.1	7.3
	Rollover	Rollover	280	10.4	79.3	10.4
	Car	Passenger car involved	579	18.1	75.6	6.2
Driver information						
	Age	Driver under 32 years old	288	16.3	79.9	3.8
	Female	Gender (female=1)	282	8.9	86.5	4.6
Continuous variables			Mean	sd	Min	Max
Roadside attributes						
	Obstacles	Number of obstacles hit in a ROR crash	1.5	0.7	0	4
Roadway attributes						
	Speed limit	Segment speed limit	119.8	2.3	90	120
Accident information						
	Persons involved	Number of involved persons	1.6	0.9	1	7
	Speed limit	Segment speed limit	119.8	2.3	90	120

MODELING RESULTS

Partial proportional odds model

The first step in the development of the model was the examination of the parallel regression assumption to determine if the PPO model is the appropriate ordered-response model to use. As mentioned earlier, in this study, a Wald test was employed to examine if any variable violates the parallel regression assumption. The results of the Wald test demonstrated that only one variable (female) violated this assumption, hence justifying the development of the PPO model. PPO models with both logit and probit functions were fitted with this variable changing across equations while other variables were forced to have their effects meet the parallel-lines assumption. The PPO model with a logit function performed better than that with a probit function (AIC = 940.44 vs. 949.71; pseudo R^2 = 0.126 vs. 0.1171).

Only statistically significant explanatory variables were considered in the final specification model. A minimum confidence level of 85% was considered as criterion. Altogether, 13 parameters were calibrated, through which the potential effects of different factors related to the categories listed above were identified. It is important to point out that most parameters were statistically significant with *p-value* below 5% (i.e., confidence levels above 95%), with three exceptions where *p-values* ranged between 5% and 10% and one case where *p-values* went up to 15%. As previously mentioned, the aim of this paper was to detect unforgiving roadside contributors through a retrospective severity analysis of run-off-road crash data. Therefore, the models are used for explanatory purposes (within the range of values observed, only), where lower *p-values* are acceptable (27). The PPO model estimated for different crash injury severity levels is given in Table 2. The estimated PPO model had one beta coefficient for each variable, two gamma coefficients for the variable violating parallel-lines assumption, and three alpha coefficients reflecting the cut-off points. Insignificant parameter estimates are not included in Table 2.

Mixed Logit Model

The coefficients and standard errors for predictors in the mixed logit model developed for different injury severity levels are shown in Table 3.

Minor injury was set as the baseline severity level for the mixed logit model; the Alternative Specific Constant (ASC) was defined accordingly. To improve the numerical stability, the number of Halton draws to evaluate the log-likelihood function was 1000.

Comparison of Models

The same dataset was used to fit the two models, which were PPO and mixed logit, to make a comparison between their performances. The log-likelihood values at convergence, AIC and BIC values were used to compare the performance of the two models used in this study. AIC and BIC are both measures of unexplained variations in the data with a penalty for model complexity. Therefore, models with lower values provide a relatively better fit (31). FIGURE 2 shows such comparison based on the AIC and BIC values.

TABLE 2 PPO model for ROR crash injury severities in Portuguese freeways

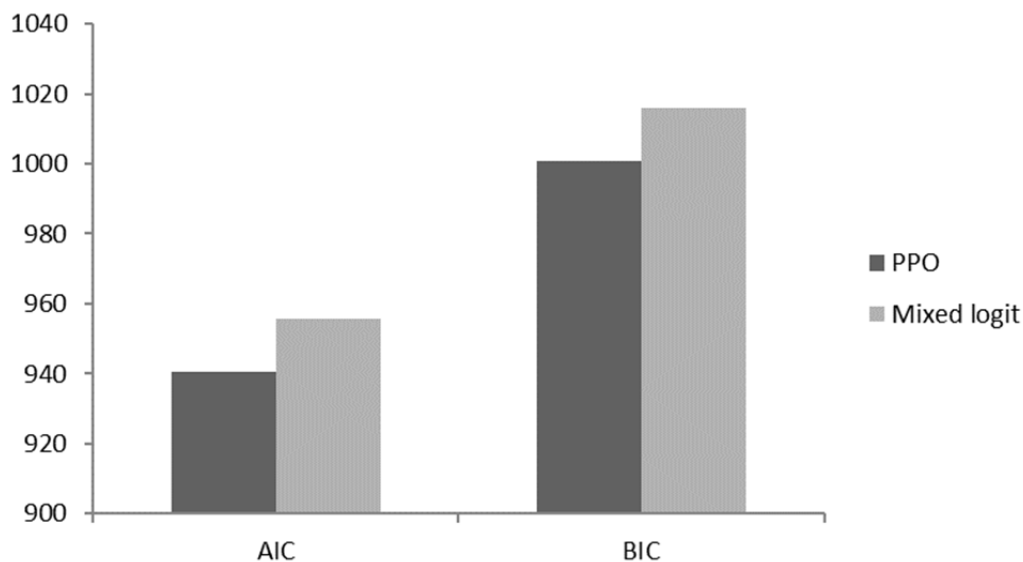
Variables	Coefficient	S.E.	z
Beta			
Winter	-0.4803	0.1975	0.0150
Peak hour	0.7240	0.4557	0.1121
Obstacles	0.3300	0.1274	0.0096
Ditch	-0.9270	0.5348	0.0830
Persons involved	-0.8220	0.1072	<0.001
Right encroachment	0.4175	0.1855	0.0244
Rollover	0.9298	0.1987	<0.001
Car	-0.3612	0.2156	0.0938
Age	-0.4628	0.1877	0.0137
Gamma_1			
Female	1.1045	0.254	<0.001
Gamma_2			
Female	-0.5920	0.3394	0.0811
Alpha			
Constant 1	2.3465	0.3456	<0.001
Constant 2	-1.9681	0.3513	<0.001
Summary statistics			
Number of observations		764	
Log likelihood at convergence		-457.222	
<i>Adjusted-p²</i>		0.101	
<i>Pseudo R²</i>		0.126	
<i>AIC</i>		940.443	
<i>Bayesian Information Criteria (BIC)</i>		1000.745	

Figure 2 shows that the PPO model has the lowest AIC and BIC values in this study, compared to mixed logit. This shows that the PPO model performed slightly better than the mixed logit model and it can be considered as a viable method in ROR crash injury severity modeling. Moreover, the results of the PPO model had plausible signs for all predictors, and the overall model fit was better than that of the mixed logit model. The McFadden's pseudo R-square of 0.126 is good considering the large amount of variance in the injury severity data. Based on the LL, AIC, and BIC, the PPO model provides a better fit than the mixed logit model in analyzing ROR crash injury severity data.

TABLE 3 Mixed Logit Model for ROR Crash Injury Severities in Portuguese Freeways

Severity level	Variables	Coefficient	t-test	p-value
PDO	Constant	6.890	11.06	<0.001
	Winter	0.502	1.85	0.06
	Barrier	0.428	1.67	0.09
	Right encroach	-0.738	-2.84	<0.001
	Car	0.683	2.04	0.04
	Persons involved	1.010	7.06	<0.001
<i>Std. dev. of parameter (Persons involved)</i>		0.905	2.37	0.02
Minor injury	Female	-0.884	-3.38	<0.001
	Night	-0.504	-2.08	0.04
	Right curve	0.646	1.66	0.10
	Age	-0.017	-2.08	0.04
Fatal and severe injury	Constant	14.600	3.73	<0.001
	Speed limit	-0.079	-2.40	0.02
	Rollover	0.646	1.59	0.11
	Persons involved	1.010	7.06	<0.001
Number of observations		764		
Log likelihood at convergence		-464.926		
<i>Adjusted-ρ^2</i>		0.429		
<i>Pseudo R^2</i>		0.446		
<i>AIC</i>		955.852		
<i>Bayesian Information Criteria (BIC)</i>		1016.153		

NOTE: The attribute *persons involved* was restricted to be equal across PDO and fatal and severe injury severity levels.

**FIGURE 2 Comparison of PPO and mixed logit models**

SUMMARY AND DISCUSSION

This paper describes the use of a PPO model to study the role of contributors influencing ROR crash severities on freeways and compared this model with a mixed logit model. The study was based on a two-year detailed infrastructure and accident dataset from Portuguese freeways (2009 and 2010). The crashes were categorized into three different levels based on driver's injury severity. Models were then estimated for the two methodological approaches (PPO and mixed logit models). Marginal effects of the PPO model were also computed to complement the analysis.

In all models, plausible signs were estimated for the coefficients of the variables. The PPO model performed the best out of the two models, based on log-likelihood at convergence, AIC and BIC values.

A PPO model allows the predictors that meet proportional odds assumption to take the same coefficient for all injury severity levels and other predictors to vary between injury severity levels, ensuring no potential loss in accuracy of prediction (25). The PPO models are clearly a viable method for modeling ROR crash injury severities.

Several variables in seasonal attributes, roadway and roadside attributes, crash characteristics and driver information were identified as significant predictors influencing the driver injury severity level in ROR crashes. The marginal effects of the parameters for PPO model provide valuable insight on the contribution factors for ROR crash injury severity. Table 4 shows the marginal effects and standard errors reported by the PPO model for different crash injury severity levels. Table 4 shows that, when involved in a ROR crash, the probability of occurrence of an occupant fatality or severe injury is higher for crashes: involving vehicle rollover; with vehicles leaving the road to the right side of the carriageway; and occurring at peak hours. Similarly, the probability of occurrence of severe injuries or fatalities in a ROR crash is lower: during winter; on ditches; with higher occupancy vehicles (higher number of persons involved); if passenger cars are involved; with younger population (below 32); and if female drivers are involved.

TABLE 4 Marginal Effects and Standard Errors for Different ROR Crash Injury Severity Levels

Variables	Crash injury severity					
	PDO		Minor injury		Severe injury + Fatal	
	M.E.	S.E.	M.E.	S.E.	M.E.	S.E.
Winter	0.0564	0.0329	-0.0276	0.0493	-0.0288	0.0219
Peak hour	-0.0850	0.0496	0.0416	0.0743	0.0434	0.0330
Obstacles	-0.0387	0.0226	0.019	0.0339	0.0198	0.0150
Ditch	0.1088	0.0635	-0.0533	0.0951	-0.0555	0.0423
Persons involved	0.0965	0.0563	-0.0472	0.0843	-0.0492	0.0375
Right encroach	-0.0490	0.0286	0.024	0.0428	0.025	0.019
Rollover	-0.1091	0.0637	0.0534	0.0954	0.0557	0.0424
Car	0.0424	0.0247	-0.0207	0.0371	-0.0216	0.0165
Age	0.0543	0.0317	-0.0266	0.0475	-0.0277	0.0211
Female	-0.1296	0.0757	0.1651	0.0632	-0.0355	0.027

These results are in line with several previous findings reported in the literature on ROR crash severity. This is the case for rollover and number of persons involved, which were found to increase the propensity for severe and fatal injury ROR crashes, just as in (6, 10, 14, 32) for rollover, and (6, 12) for the latter factor.

Female drivers were found to have lower probabilities of PDO, severe and fatal and injury ROR crashes. On the one hand this agrees with findings from Wu et al. (10) and Xie, et al. (14); on the other it partially differs from the results obtained by Schneider et al. (9), who found that female drivers are more likely to be injured in ROR crashes.

In addition to rollover and number of persons involved mentioned above, there are several factors for which this study found partly similar findings to those of previous research by the authors (6). These are the role of winter in ROR crashes, the involvement of vehicles leaving the road to the right side of the carriageway, the involvement of passenger cars and driver age.

This study also adds some new insight into the effect that some variables have on ROR crash severities for the case of freeways with “unforgiving” roadsides. Specifically, the use of the partial proportional formulation allows an improved identification of the varying effect that several variables have on ROR crash injury severity, and includes the effect of traversing ditches and the influence of the number of obstacles hit in a ROR crash, which were previously masked, when the unordered framework models were used.

In this study, the number of obstacles hit in a ROR crash was found to decrease the propensity for PDO ROR crashes. This is reasonable, as high kinetic energy may be involved in these crashes, more areas of a vehicle are damaged or more impacts are sustained in the same area of an errant vehicle. This study also shows that traversing a ditch tends to increase the chance of a PDO ROR crash. This appears sensible, as ditches on freeways are not especially “aggressive” (despite not being tolerant to errant vehicles, as well) and they are associated with cut embankments or carriageways leveled with the nearby terrain.

Findings from this type of studies are relevant for setting up preventing measures at the design stage and also in operation management. In the former case, one may expect that applying traversable ditches designs may improve considerably the safety of the road stretches where they are constructed. Additionally, it is more appropriate to improve embankment characteristics, rather than to address a few roadside obstacles. In the latter case, it may be hypothesized that enforcement should be stricter and more intense when cars are expected to carry less passengers (not in holiday periods) and outside of peak hour periods.

The procedure developed in SAFESIDE (described in (3)) does not fully take into consideration the probability of occurrence of crashes with different severity levels conditioned on crash occurrence. By estimating the probability of crash occurrence at different severity levels (using mixed logit models or PPO models), these crash severity models can be integrated in the said procedure, enabling the distribution of the estimated expected number of crashes by three severity levels and thus allowing the development of better crash cost calculations. Cost-benefit estimates tuned to the Portuguese freeway crash characteristics will positively support roadside safety decisions adapted to the country’s context and contribute to the progressive construction of an efficient safe traffic system.

ACKNOWLEDGMENTS

The authors would like to thank the *Guarda Nacional Republicana* for its cooperation in providing data on crashes and roadside characteristics used in this research.

REFERENCES

1. Roque, C., Cardoso, J.L. *Definição de Cenários Tipo para Acidentes envolvendo a Área Adjacente à Faixa de Rodagem*, 4º Relatório Safeside. (Run-off-road crash scenario evaluation. 4th Safeside report. – in Portuguese) Fundação para a Ciência e Tecnologia, Laboratório Nacional de Engenharia Civil, Lisboa 2012.
2. Roque, C., Cardoso, J.L. Investigating the relationship between run-off-the-road crash frequency and traffic flow through different functional forms, *Accident Analysis & Prevention* 63, 2014, pp. 121–132.
3. Roque, C., Cardoso, J.L. SAFESIDE: a computer-aided procedure for integrating benefits and costs in roadside safety intervention decision making, *Safety Science* 74, 2015, pp. 195–205.
4. Savolainen, P., Mannering, F., Lord, D., Quddus, M. The statistical analysis of highway crash-injury severities: a review and assessment of methodological alternatives. *Accident Analysis and Prevention* 43 (5), 2011, pp. 1666–1676.
5. Train, K. *Discrete Choice Methods with Simulation*. Cambridge University Press, New York, NY, 2009.
6. Roque, C., Moura, F., Cardoso, J.L. Detecting unforgiving roadside contributors through the severity analysis of ran-off-road crashes. *Accident Analysis & Prevention* 80, 2015, pp. 262–273.
7. Eluru, N., Yasmin, S. A note on generalized ordered outcome models. *Analytic Methods in Accident Research* 8, 2015, pp. 1–6.
8. Kim, J.K., Ulfarsson, G.F, Kim, S., Shankar, V.N. Driver-injury severity in single-vehicle crashes in California: a mixed logit analysis of heterogeneity due to age and gender. *Accident Analysis and Prevention* 50, 2013, pp. 1073–1081.
9. Schneider, W., Savolainen, P., Zimmerman, K. Driver injury severity resulting from single-vehicle crashes along horizontal curves on rural two-lane highways. *Transportation Research Record: Journal of the Transportation Research Board* 2102, 2009, pp. 85–92.
10. Wu, Q., Chen, F., Zhang, G., Liu, X. C., Wang, H., Bogus, S. M. Mixed logit model-based driver injury severity investigations in single- and multi-vehicle crashes on rural two-lane highways. *Accident Analysis and Prevention* 72, 2014, pp. 105–115.
11. Wu, Q., Zhang, G., Zhu, X., Liu, X.C., Tarefder, R.. Analysis of driver injury severity in single-vehicle crashes on rural and urban roadways. *Accident Analysis and Prevention*, 2016, pp. 94, 35–45.
12. Holdridge, J., Shankar, V., Ulfarsson, G. The crash severity impacts of fixed roadside objects. *Journal of Safety Research* 36 (2), 2005, pp. 139–147.
13. Lee, J., Mannering, F. Impact of roadside features on the frequency and severity of run-off-roadway accidents: an empirical analysis. *Accident Analysis and Prevention* 34, 2002, pp.149–161.
14. Xie, Y., Zhao, K., Huynh, N. Analysis of driver injury severity in rural single- vehicle crashes. *Accident Analysis and Prevention* 47, 2012, pp. 36–44.
15. Renski, H.,Khattak, A.,Council, F. Effect of speed limit increases on crash injury severity: analysis of single-vehicle crashes on North Carolina Interstate Highways. *Transportation Research Record* 1665, 1999, pp. 100–108.
16. Kockelman, K.M., Kweon, Y.J. Driver injury severity: an application of ordered probit models. *Accident Analysis and Prevention* 34 (3), 2002, pp. 313–321.
17. Mooradian, J., Ivan, J.N., Ravishanker, N., Hu, S. Analysis of driver and passenger crash injury severity using partial proportional odds models. *Accident Analysis & Prevention* 58, 2013, pp. 53–58.

18. Mannering, F.L., Bhat, C.R. Analytic methods in accident research: Methodological frontier and future directions. *Analytic Methods in Accident Research 1*, 2014, pp. 1–22.
19. R Development Core Team. R: A Language and Environment for Statistical Computing. *R Foundation for Statistical Computing*, Vienna, Austria, ISBN 3-900051-07-0 <http://www.R-project.org/>, 2011.
20. Yee, T.W. The VGAM package for categorical data analysis. *Journal of Statistical Software* 32 (10), 2010, 1–34.
21. Bierlaire, M. BIOGEME: A free package for the estimation of discrete choice models. *Proceedings of the 3rd Swiss Transportation Research Conference*, Ascona, Switzerland, 2003.
22. Bhat, C. Simulation estimation of mixed discrete choice models using randomized and scrambled Halton sequences. *Transportation Research Part B* 37(9), 2003, pp. 837–855.
23. Wang, X., Abdel-Aty, M. Analysis of left-turn crash injury severity by conflicting pattern using partial proportional odds models. *Accident Analysis and Prevention* 40 (8), 2008, pp. 1674–1682.
24. Pour-Rouholamina, M., Zhouba, H. Analysis of driver injury severity in wrong-way driving crashes on controlled-access highways. *Accident Analysis and Prevention* 94, 2016, pp. 80–88.
25. Sasidharan, L., Menendez, M. Partial proportional odds model – an alternate choice for analysing pedestrian crash injury severities. *Accident Analysis and Prevention* 72, 2014, pp. 330–340.
26. Williams, R. Generalized ordered logit/partial proportional odds models for ordinal dependent variables. *Stata J.* 6 (1), 2006, pp. 58–82.
27. Washington, S., Karlaftis, M., Mannering, F.L. *Statistical and Econometric Methods for Transportation Data Analysis*. Second Edition. Chapman and Hall/CRC. ISBN: 978-1-4200-8285-2.0, 2011.
28. Shmueli, G. To explain or to predict? *Statistical Science* 25 (3), 2010, pp. 289–310.
29. Cameron, A., Trivedi, P. *Regression Analysis of Count Data*. Cambridge University Press, Cambridge, England, 1998.
30. Milton, J.C., Shankar, V.N., Mannering, F.L. Highway accident severities and the mixed logit model: An exploratory empirical analysis. *Accident Analysis & Prevention* 40 (1), 2008, pp. 260–266.
31. Finch, W.H., Bolin, J.E., Kelley, K. *Multilevel Modeling Using R*. CRC Press, Florida, USA, 2014.
32. Hu, W., Donnell, E. T. Median barrier crash severity: some new insights. *Accident Analysis and Prevention* 42, 2010, pp. 1697–1704.

Estimate of Occupant Ejection and Occupant Head-Slap Prevalence in Real-World Longitudinal Barrier Crashes

DOUGLAS J. GABAUER

Bucknell University

Outside of limited crash testing experience and more limited real-world crash data, very little is known regarding the probability that an occupant's head is ejected out of a vehicle side window, i.e. head slap, in an impact with a traffic barrier. Similarly, a literature review revealed little information regarding occupant ejection specific to traffic barrier crashes. The purpose of this study was to estimate (1) the frequency of occupant ejection and head slap during impacts with traffic barriers and (2) determine characteristics typically associated with these events. Data included 1,367 real-world longitudinal barrier crashes with available vehicle damage, occupant injury, occupant injury source information, and traffic barrier information. The rate of occupant ejection in tow-away level single vehicle, single event barrier crashes was estimated to be 0.25 percent with an upper bound of 0.52 percent. These rates were found to be approximately three times higher than ejection rates for single event, two-vehicle crashes, primarily due to differences in full ejection rates. The results from this study reaffirm that barrier crashes involving ejection result in severe occupant injury and that side ejections dominate. A comparison of barrier ejection and non-ejection cases revealed that pickup trucks, older model year vehicles, and unbelted occupants were overrepresented in barrier ejection cases. Although the available data suggests that occupant head slap is rare, barrier height data was not available. Thus, this low rate may be attributed to relatively few barriers with heights exceeding 34.5 inches present in the data. Further study on the incidence of head slap on tall barriers is warranted.

INTRODUCTION

High speed oblique impacts with a longitudinal barrier increase both the probability that an occupant's head is ejected out of a side window and the likelihood of the occupant directly contacting the barrier or other nearby object. Often termed head slap, this direct contact scenario has a high potential for severe occupant injury. Previous research based on an analysis of full-scale crash tests has identified the extent of head ejection typical for impacts into rigid longitudinal barriers but very little is known regarding the incidence and crash characteristics associated with head ejection in real-world barrier crashes, especially in the US. Similarly, a review of previous literature revealed little information regarding occupant ejection specific to longitudinal barrier crashes.

The current US roadside hardware crash test procedures (1) recognize head slap and provide recommended guidance to document it in crash test scenarios where the risk of head slap exists. However, there is currently no occupant risk criteria associated with head slap. An improved understanding of the scope of this problem in real-world barrier crashes could provide either justification for the current documentation-level recommendations or impetus for the inclusion of specific head slap criteria within the occupant risk evaluation procedures. In addition, more information relative to the crash, vehicle, and barrier characteristics associated

with occupant ejection and/or head slap in real-world crashes could lead to improved countermeasures, either from a barrier design, barrier placement, or vehicle design perspective.

OBJECTIVE

The purpose of this study was to investigate real-world crashes to estimate (1) the frequency of occupant ejection and occupant head slap during impacts with longitudinal barriers and (2) determine characteristics typically associated with these events.

BACKGROUND

Full-Scale Crash Testing Criteria

Procedures for the conduct and evaluation of full-scale crash tests involving roadside safety hardware are detailed in the Manual for Assessing Safety Hardware (MASH) (1). Tests are evaluated based on three primary aspects: (1) the structural adequacy of the tested device, (2) the post-impact trajectory of the vehicle, and (3) the potential for occupant risk. MASH occupant risk assessment risk is based primarily on vehicle accelerations measured during the test, the deformation extent of the vehicle's occupant compartment, and observations regarding the potential for detached elements or crash debris to penetrate the occupant compartment. The use of an anthropomorphic test device (ATD), i.e. a crash test dummy, in these crash tests is optional but recommended in tests involving the small passenger car test vehicle. Generally, the use of an ATD in these tests is to document gross belted occupant motion and not used to directly assess occupant risk through the available ATD instrumentation.

While there is no MASH occupant risk criteria that specifically addresses head slap in longitudinal barrier crash tests, MASH does provide recommended guidance relative to this issue. The use of a 50th percentile ATD is recommended in tests where the potential for head slap exists; specifically, tests involving tall barriers (i.e., a height of 33 inches or more) or barriers that have luminaire and/or sign supports mounted to the barrier top (1). In these tests, MASH recommends an ATD in both the small passenger car and large pickup truck to be located in the front seat of the impact side of the vehicle and restrained with a lap and shoulder belt. MASH also recommends cameras positioned to allow documentation of ATD head motion during the test.

Previous Head Slap Crash Test Study Results and Insights

The primary source of data related to head slap has been from full-scale crash testing of longitudinal barriers, primarily rigid barriers or bridge rails. In Italy, Giavotto (2) conducted four full-scale crash tests of high containment level barriers and two sled tests to investigate differences in occupant risk for vehicles with tempered versus laminated side windows. The full-scale tests used a small passenger vehicle and included two tests with a precast NJ shape concrete barrier and two tests with a double rail metal beam barrier. All tests included instrumented ATDs to allow a detailed head injury risk comparison. The tests demonstrated that partial ejection of a belted occupant through a side window, especially tempered windows,

occurs in high speed oblique crashes with high containment barriers and presents significant occupant injury risk (2).

Early US crash test-based efforts involved altering the upper geometry of the barrier cross section to reduce head slap potential. Barriers designed with consideration for head slap included a steep single-slope concrete barrier developed by Rosenbaugh et al. (3) and an open concrete bridge rail developed by Polivka et al. (4). More recently, Rosenbaugh et al. (5) developed head ejection envelopes of belted occupants using available video data from full-scale crash tests involving primarily rigid barriers with non-mountable (i.e. vertical) faces. A total of eight small passenger car crash tests and three large pickup truck crash tests were used to develop the initial envelopes which were then adjusted for vehicle motion during the impact, occupant size, and vehicles not typically crash tested (e.g. midsize vehicles). The result was two head ejection envelopes, one for the 50th percentile male and one for the 95th percentile male, encompassing all possible occupant head positions to aid in developing rigid barriers with upper geometries that minimize head slap potential (5).

Based on full-scale crash testing experience, previous researchers have offered insights relative to head slap risk and possible countermeasures. Rosenbaugh et al. (5) noted that head slap is less likely with mountable, e.g. shapes such as the NJ or F-shape, rigid barriers due to the tendency of vehicles to climb the barriers. Likewise, semi-rigid and flexible barriers were noted to have reduced head slap risk due to lower lateral accelerations imparted to the vehicle during impact, barrier heights below the bottom of typical small passenger car side windows, and seldom having ancillary hardware attached (5). Giavotto (2) emphasizes that consideration must also be given to vehicle designs that could reduce head slap risk and suggests laminated glass side windows as a possible low-cost countermeasure.

Previous Crash Data Studies and Data Challenges

Compared to the crash testing based efforts, the identification of head slap in real-world crashes has been more limited. In addition to tests described above, Giavotto (2) collected real-world crash data for 12 months, from May 2001 to the end of April 2002, in three regions of Italy. A total of 399 crashes with occupant ejection were observed, 36 of which involved a longitudinal barrier impact. Two thirds of the crashes involving a barrier and ejection resulted in either fatal or serious/critical occupant injury. Of the 36 barrier crashes, the majority (58 percent) of fatal ejections and a large portion (40 percent) of the critical and serious injury ejections were through a side window. The reported barrier crash data, however, did not distinguish partial versus full ejection, include the distribution of the barrier types impacted, or distinguish between belted and unbelted occupants. No other previous studies investigating head slap using real-world crash data were found in the literature.

While there is a substantial existing literature pertaining to occupant ejection in vehicle crashes, very few studies were found specific to ejection in impacts with longitudinal barriers and/or roadside safety hardware devices. Viner et al. (6) does report ejection rates for fatal crashes involving roadside hardware by rollover occurrence and vehicle type. Based on 1988 Fatality Analysis Reporting System (FARS) data, occupants of pickup trucks impacting a roadside hardware device with no rollover were ejected approximately 33 percent of the time. If a rollover was present, this percentage increased to approximately 76 percent. For cars, ejection in non-rollover roadside hardware crashes was approximately 23 percent and approximately 66 percent for rollover roadside hardware crashes.

Previous researchers have also highlighted challenges associated with identifying head slap in real-world crashes. As any portion of the occupant's body protruding outside the vehicle during the crash event may return to a position inside the vehicle after the crash event, partial ejection of any type can be difficult to detect post-crash. Rosenbaugh et al. (5) cites this issue as well as a lack of a head slap specific data element present in police-reported crash data forms. Similarly, Giavotto (2) indicates that the estimates of ejection reported based on the collected crash data may be low as partial ejection may not always be evident after a crash. Despite difficulty obtaining real-world crash data pertaining to head slap, the availability of this data would be useful. Information on incidence of head slap by barrier type could affirm the assertions of Rosenbaugh et al. (5) regarding the decreased likelihood of head slap for impacts with mountable rigid barriers as well as semi-rigid and flexible barriers. Real-world head slap data could also inform decisions on the appropriateness of the current head slap guidelines present in MASH.

METHODOLOGY

The overall approach for this study was to use sampled in-depth crash data to estimate the frequency of occupant ejection and head-slap in tow-away level longitudinal barrier crashes. The in-depth crash data is used to overcome some of the limitations obtaining partial ejection data cited by previous research. All data processing and statistical analyses for this study were performed using SAS V9.4 (SAS Institute, Cary, NC).

Data Sources and Case Selection

In-depth crash data was selected from the National Automotive Sampling System (NASS) / Crashworthiness Data System (CDS). NASS/CDS provides detailed data on a randomly selected, representative sample of tow-away level crashes involving passenger cars, light trucks, vans and utility vehicles in the US (7). For approximately 5,000 crashes per year, specially trained NASS investigators collect detailed vehicle and crash scene information as well as interview crash victims and review pertinent medical records. The NASS/CDS data includes crash site and vehicle photographs as well as specific information on vehicle damage, occupant injuries, and occupant injury sources (7). This study used NASS/CDS data from 1997 through 2014, inclusive. Note that detailed photographs were not readily available for cases prior to 1997 and 2014 was the most recent data year available at the time of the study. Case selection criteria included single vehicle, single event crashes where the object impacted was a longitudinal barrier. These restrictions were used to ensure that any investigator-noted occupant ejection occurred during the impact with the barrier. Note NASS/CDS codes rollovers as an event so these criteria also exclude all cases involving rollover. For the purposes of this study, longitudinal barriers included w-beam guardrails (length of need, transition sections, and terminals), box beam barrier, concrete barrier, bridge rails and cable barrier.

Database Development

As the NASS/CDS does not contain detailed barrier data, scene photographs and scene diagrams for each suitable case were examined to ascertain variables of interest. Methodology for augmenting the existing NASS/CDS data with roadside specific barriers is similar to previous

procedures outlined by Gabauer and Gabler (9) and Gabauer (10). For each suitable NASS/CDS case, the following additional data was determined:

1. Barrier Type: An attempt was made to classify each barrier to the fullest extent possible based on the available scene photographs. This data was then used to classify the barrier by lateral stiffness into 3 categories: (1) flexible, (2) semi-rigid, and (3) rigid based on the Roadside Design Guide (11) classification scheme.
2. Impact Location Relative to Barrier: Based on the available scene diagram and photos, a determination was made as to whether the vehicle impacted the end of the barrier, the length of need (portion between the end terminals) or a transition section (portion joining two barriers of differing lateral stiffness).

Cases identified as not involving a longitudinal barrier or cases with no photographs of the impacted barrier were noted and excluded from further analysis. The additional data was imported into SAS as a barrier specific table so that it could be readily merged with the NASS/CDS tables.

Data Analysis

Quantification of Barrier Crash Ejection

The available NASS/CDS data was used to determine the characteristics of tow-away level longitudinal barrier crashes that involve either full or partial occupant ejection. These ejection crash characteristics were compared to the analogous characteristics for all available tow-away level longitudinal barrier crashes. Compared characteristics included vehicle type, model year, barrier type, barrier-relative impact location, occupant gender, occupant restraint use, airbag deployment, and occupant injury severity. Vehicle type was classified into passenger cars, vans, sport utility vehicles (SUV), and pickup trucks using the NASS/CDS “bodytype” variable. Model year was split into two categories, 10 or more years and less than 10 years, by comparing the crash year and the vehicle model year. Traditionally, NASS/CDS only collects detailed vehicle and occupant data for late model vehicles, e.g. less than 10 years old (7). Occupant injury severity was classified based on the Abbreviated Injury Severity (AIS) scale (12), which methodically rates injury on an integer scale from 0 to 6 based on threat to life. In NASS/CDS, each injury an occupant acquires is rated using this scale and the most severe of all the injuries is termed the maximum AIS (MAIS) score. The MAIS variable was used to classify injury as either severe (MAIS 3+) or no/minor/moderate injury (MAIS < 3). Characteristics specific to ejection cases included ejection area, door status, window status, and window type. Occupant ejection area was categorized as windshield, side, rear/roof, or unknown using the “ejectarea” variable. For the door/window status and window type, note that the data is presented only for the window/door associated with that particular occupant, e.g. for a driver, the vehicle left front door/window data is presented while for a right front passenger, data is presented for the right front door/window. As an additional benchmark, occupant ejection rates were computed for single event crashes involving two vehicles.

As NASS/CDS is a representative sample, the appropriate weighting factors were applied to the cases to provide national estimates of tow-away level crashes. Both raw and weighted case values are presented along with weighted value percentages and associated 95 percent

confidence bounds for the weighted percentages. The “surveylogistic” procedure within SAS was used to determine the confidence bounds while accounting for the first level stratification and clustering of the data. NASS/CDS case stratification is based on vehicle tow status, occupant injury level, and hospitalization (7). The first level clusters are represented by the primary sampling units located across the US. A more detailed description of the NASS/CDS sampling design methodology can be found in the Analytical User’s Manual (7).

Occupant-to-Barrier Contact Identification

To identify barrier crashes with head slap present or head slap potential, the NASS/CDS injury source and vehicle interior data was examined in more detail. For cases with medical record data available, NASS/CDS provides data on each injury that an occupant attains. This includes the severity of each injury, the injury source, as well as a metric to quantify the investigator confidence in the coded injury source (i.e. certain, probable, possible, unknown). For all previously identified barrier crash cases involving partial occupant ejection, the occupant injury data was examined. Head slap was noted if all of the following injury and injury source conditions held:

1. The occupant sustained one or more injuries to the head or face
2. The NASS/CDS investigator indicated an injury source of 598, “Other vehicle or object”
3. The NASS/CDS investigator confidence in the injury source was probable or certain

Based on data limitations suggested by previous research, it is expected that the identified cases of head slap will likely be small. As a means of providing additional head slap information, an effort was made to identify barrier crash cases where the potential for head slap existed. Cases with head slap potential were defined as a crash with no full occupant ejection, the occupant sustained one or more head or face injuries, and the associated side window sustained damage from occupant impact. The available NASS/CDS weighting factors were used to determine total number of head slap and head slap “potential” cases as a proportion of total occupants (with known injury information) involved in single vehicle single event barrier crashes.

RESULTS

The NASS/CDS case selection criteria led to an initial selection of 1481 single vehicle, single event barrier crashes. Close examination of each of these cases for database development (e.g. addition of barrier-related variables) led to the exclusion of 114 cases. This included cases with no available barrier photographs as well as cases involving an object other than a longitudinal traffic barrier, e.g. such as a planter, curb, or raised median. Table 1 summarizes the vehicle, roadway, barrier, and occupant characteristics for the remaining 1,367 suitable NASS/CDS cases. It is worth noting that NASS/CDS collects only limited data for the crash if the vehicle involved is more than 10 years old at the time of the crash; this is the primary reason for the relatively large portion of unknown values present in Table 1.

TABLE 1 Summary of Available Barrier Crashes (NASS/CDS 1997 -2014, inclusive)

Variable	Category	Raw	Weighted	Weighted %	95% CI for Weighted %
All	Crashes/Vehicles	1367	747,038	100	575,483 - 918,594*
Vehicle Characteristics					
Body Type	Passenger Car	951	505,875	67.7	62.0 – 73.4
	Van	62	23,609	3.2	1.9 - 4.4
	SUV	201	93,568	12.5	8.8 - 16.2
	Pickup Truck	153	123,986	16.6	11.6 – 21.6
Model Year	≥10 years (relative to crash year)	464	268,918	36.0	29.1 – 43.0
	< 10 years	903	478,121	64.0	57.1 - 70.9
Roadway and Barrier Characteristics					
Roadway Alignment	Tangent	821	389,458	52.1	44.9 – 59.4
	Curve	546	357,580	47.9	40.6 – 55.1
Relation to Junction	Non-Intersection/Junction	983	536,644	71.8	63.8 – 79.9
	Intersection/Junction	384	210,394	28.2	20.1 – 36.2
Barrier Type	Flexible	82	71,296	9.5	3.4 – 15.7
	Semi-Rigid	534	343,194	45.9	36.7 – 55.1
	Rigid	751	332,548	44.5	34.7 – 54.3
Impact Location	Length of Need	1,163	628,590	84.1	78.9 – 89.4
	End Terminal	189	109,689	14.7	9.5 – 19.9
	Transition	15	8,759	1.2	0.0 – 2.6
Occupant/Restraint Characteristics					
All	Occupants	2,039	1,045,491	100	792,075 – 1,298,908*
Gender	Male	1,112	580,229	55.5	49.9 – 61.1
	Female	890	417,232	39.9	35.9 – 43.9
	Unknown	37	48,030	4.6	1.3 – 7.9
Restraint Use	Belted	1,033	589,328	56.4	50.8 – 62.0
	Unbelted	423	125,178	12.0	9.1 – 14.9
	Unknown	583	330,986	31.6	26.4 – 37.0
Ejection	None	1,709	871,226	83.3	78.5 – 88.2
	Full Ejection	22	2,131	0.20	0.0 – 0.44
	Partial Ejection	12	483	0.05	0.0 – 0.08
	Unknown	296	171,651	16.4	11.6 – 21.2
Airbag Deployment	One or More Airbags Deployed	564	219,845	21.0	16.9 – 25.2
	No Airbags Deployed	449	298,342	28.5	22.4 – 34.7
	Not Available	543	266,290	25.5	19.0 – 31.9
	Missing/Unknown	483	261,014	25.0	20.3 – 29.7
Injury Severity	No/Minor/Moderate Injury (MAIS < 3)	1,437	789,898	75.6	70.6 – 80.5
	Severe/Fatal (MAIS 3+)	156	6,890	0.7	0.4 – 0.9
	Injured, Unknown Severity	116	32,757	3.1	1.7 – 4.6
	Unknown if Injured	330	215,946	20.6	16.1 – 25.2

*Denotes 95% confidence limits on weighted frequency.

Quantification of Barrier Crash Ejection

Table 2 provides a summary of the vehicle, barrier, and occupant characteristics for the single vehicle, single event barrier crashes involving any form of occupant ejection. The NASS/CDS weighted estimates have been provided for informational purposes but due to the limited number of raw cases (34 total), the confidence limits have not been included as many of these ranges include either zero or one hundred. Only a small portion (0.02 percent raw, 0.25 percent weighted) of occupants involved in tow-away level barrier crashes were either partially or fully ejected.

In terms of vehicle characteristics, both pickup trucks and older model year vehicles were overrepresented in barrier crashes involving ejection. Pickup trucks accounted for 62 percent of ejection cases but only 16 percent of all available barrier crashes. Older model year vehicles accounted for approximately two-thirds of barrier ejection crashes but approximately one-third of all available barrier crashes.

Comparing roadway characteristics between barrier crashes with and without ejection, horizontally curved sections as well as intersection/junction related crashes were overrepresented. Note that the NASS/CDS intersection designation includes entrance/exit ramps. Horizontally curved sections accounted for 71 percent of barrier crashes with ejection but only 48 percent of all barrier crashes. Intersection/junction locations accounted for 74 percent of the barrier ejection cases but only 28 percent of all barrier crashes. The weighted estimates suggest that rigid barrier types were involved in 58 percent of barrier ejection crashes. While semi-rigid and flexible barriers were underrepresented in ejection crashes, these barrier types together account for just over 40 percent of barrier ejection crashes.

The occupant characteristic distributions for barrier crashes with ejection also differed from the distributions for all barrier crashes. Based on the weighted estimates, females were overrepresented in ejection crashes, 57 percent of ejected occupants but 40 percent of all available barrier crash occupants. The vast majority of the ejected occupants were unbelted; nearly 90 percent compared to 12 percent for all barrier crashes. Ejected occupants also had a lower proportion of airbags available, approximately 30 percent, compared to all barrier crashes with approximately 50 percent of occupants airbag-restrained. Rates of severe occupant injury were also much greater for ejection crashes. Nearly 18 percent of barrier ejection crashes resulted in severe occupant injury compared to less than one percent for all occupants involved in a tow-away level barrier crash.

For barrier crashes involving ejection, the majority (56 percent raw and nearly 80 percent weighted) occurred through a side door or window. Of the 34 raw cases, only two noted a corresponding door had opened during the crash (19 either remained shut or were jammed shut and 13 had missing data). Of the 19 occupants ejected out the side of the vehicle, 10 had a closed window, 2 had the window partially open, 5 had the window fully open, and the remaining two had missing data. A total of 17 of these occupants had corresponding side windows that were identified as tempered while the remaining two had missing data.

Table 3 summarizes ejection status for NASS/CDS occupants involved in two-vehicle, single event crashes over the same time frame. The ejection rates for single event, vehicle-to-vehicle crashes were estimated to be 0.09 percent (0.005 percent raw) with an upper limit estimated to be 0.13 percent. For the single event barrier crashes, the ejection upper limit was estimated to be 0.52 percent. The ejection rate difference between these two crash types was larger for full ejection compared to partial ejection. The rates for partial ejection were estimate to

**TABLE 2 Summary of Barrier Crashes Involving Occupant Ejection
(NASS/CDS 1997 -2014, inclusive)**

Variable	Category	Raw	Weighted	Weighted %
Vehicle Characteristics				
Body Type	Passenger Car	23	930	35.5
	Van	2	28	1.1
	SUV	2	37	1.4
	Pickup Truck	7	1,620	62.0
Model Year	≥10 years (relative to crash year)	14	1,683	64.4
	< 10 years	20	931	35.6
Barrier Characteristics				
Roadway Alignment	Tangent	21	761	29.1
	Curve	546	1,218	70.9
Relation to Junction	Non-Intersection/Junction	19	689	26.3
	Intersection/Junction	15	1,926	73.7
Barrier Type	Flexible	1	89	3.4
	Semi-Rigid	18	1,007	38.5
	Rigid	15	1,518	58.1
Impact Location	Length of Need	25	2,111	80.8
	End Terminal	9	503	19.2
Occupant/Restraint Characteristics				
Gender	Male	24	1,123	43.0
	Female	10	1,491	57.0
Restraint Use	Belted	2	11	0.4
	Unbelted	27	2,331	89.2
	Unknown	5	271	10.4
Airbag Deployment	One or More Airbags Deployed	9	460	17.6
	No Airbags Deployed	6	290	11.1
	Not Available	15	1635	62.5
	Missing/Unknown	4	230	8.8
Injury Severity	No/Minor/Moderate Injury (MAIS < 3)	15	1,962	75.0
	Severe/Fatal (MAIS 3+)	15	465	17.8
	Injured, Unknown Severity	3	172	6.6
	Unknown if Injured	1	15	0.6
Ejection Area	Windshield	3	100	3.8
	Side (Front or Rear)	19	2,086	79.8
	Rear/Roof	2	21	0.8
	Unknown	10	407	15.6

**TABLE 3 Occupant Ejection in Single Event, Two-Vehicle Crashes
(NASS/CDS 1997 -2014, inclusive)**

Ejection Category	Raw	Weighted	Weighted %	95% CI for Weighted %
All Occupants	79,780	47,764,394	100	38,705,010 – 56,823,779*
None	58,776	31,820,246	66.6	64.6 – 68.7
Full Ejection	181	18,765	0.04	0.02 – 0.06
Partial Ejection	188	23,437	0.05	0.03 – 0.07
Unknown	2,635	15,901,947	33.3	31.2 – 35.3

*Denotes 95% confidence limits on weighted frequency.

be 0.05 percent in both crash types while full ejection rates were 0.04 percent for single event two-vehicle crashes and 0.20 percent for barrier crashes.

Occupant-to-Barrier Contact

Of the 2,039 occupants involved in a single vehicle, single event longitudinal barrier crash, 1,587 (68.7 percent) had detailed occupant injury data available. Of those with a reported number of injuries, 712 occupants (44.8 percent) had zero injuries recorded while 875 had one or more recorded injuries. Examination of the injury and injury source data for the 12 partial ejection cases revealed only a single occupant that met all three of the head slap conditions.

To verify additional cases were not present, the injury source data for all occupants with recorded injuries were examined further. The injury source code 598, “Other vehicle or object,” accounted for 66 injuries that were obtained by 11 different occupants in 11 different crashes (including the already identified head slap case). A closer examination of these 11 cases revealed that seven involved an impact with a strong post w-beam barrier, six of which were barrier end hits. Of the end impacts, five involved a portion of the w-beam barrier intruding into the vehicle occupant compartment and contacting the occupant and the sixth involved an upper extremity impacting the barrier through an open window. The single length of need impact with a strong post w-beam barrier resulted in full occupant ejection. None of these crashes exhibited characteristics typical of head slap. Of the four concrete barrier length of need impacts, one involved full occupant ejection while the remaining involved partial ejection. Two of the partial ejection cases involved only injury to occupant upper extremities. The lone remaining partial ejection case resulted in fatal occupant head injury, suggesting the presence of head slap (and had been previously identified above).

Using the criteria to identify cases with head slap potential resulted in an additional 5 occupants involved in a single event barrier crash. Data for the single head slap case and these additional head slap potential cases are summarized in Table 4. Although the only identified head slap case involved a concrete barrier, the other potential head slap cases involved metal beam barriers. All of the cases involved barrier length of need impacts. Two-thirds of identified cases involved passenger cars and half involved unbelted occupants. Based on the occupants available with recorded injury information (796,811 weighted occupants), head slap is estimated to occur in 0.003 percent of occupants involved in tow-away level barrier crashes. If the

TABLE 4 Vehicle, Barrier and Occupant Data for Head Slap and Head Slap Potential Cases (NASS/CDS 1997 -2014, inclusive)

Variable	Category	Raw	Weighted
All	Occupants	6	2,811
Head Slap Identification	Yes	1	23
	Possible	5	2,788
Barrier Type/Impact Location	Concrete/LON	1	23
	Strong Post W-Beam/LON	3	246
	Strong Post Thrie Beam/LON	1	2,452
	Box Beam/LON	1	90
Vehicle Type	Passenger Car	4	2,767
	Van	1	23
	Pickup Truck	1	20
Restraint Use	Belted	3	2,674
	Unbelted	3	136

definition of head slap is expanded to include those cases which demonstrate some potential for head slap, i.e. occupant head injury due to window impact, this proportion would be 0.35 percent of occupants involved in tow-away level barrier crashes.

DISCUSSION

Compared to single event crashes involving two vehicles, single event barrier impacts were found to have higher occupant ejection rates. The weighted estimates suggest the rates differ by nearly a factor of three, 0.09 percent for single event two-vehicle crashes compared to 0.25 percent for single event barrier crashes. Based on the 95 percent confidence limits, the rate of occupant ejection could be as high as 0.52 percent of all tow-away level single vehicle, single event barrier crashes. As expected, these values were much lower than those reported by Viner et al. (6) since the estimates are relative to all tow-away level barrier crashes, not just fatal barrier/roadside hardware crashes. Calculation of an analogous ejection rate using the Giavotto (2) data was not possible as the data was ejection specific and not barrier-crash specific, i.e. the total number of barrier crashes in the study period was not available/reported.

The results from this study reaffirm that barrier crashes involving ejection result in severe occupant injury and that side ejections dominate. For barrier crashes involving ejection, nearly half (44 percent) of the raw cases involved serious or fatal occupant injury. Although lower than the 66 percent fatal/serious reported by Giavotto (2), the rate is still roughly four times that for all available single vehicle, single event barrier crashes. Considering the available weighted estimates, the proportion of serious and fatal injuries for barrier-ejection crashes is nearly 18 times larger than for all available barrier crashes. The majority of the ejections (56 percent raw, 80 percent weighted) in barrier crashes were through a side window or door, reinforcing the findings of Giavotto (2). The available NASS/CDS glazing information for these side ejection cases suggested that all the side windows were tempered instead of laminated glass.

An examination of other characteristics of barrier-ejection crashes with all barrier crashes suggests vehicle type, barrier, roadway, and occupant differences. Similar to the findings of

Viner et al. (6), pickup trucks were found to be overrepresented in barrier ejection crashes. In addition, older model year vehicles, unbelted occupants, and to a lesser extent, rigid barriers and female occupants were overrepresented in ejection crashes. Despite an overrepresentation of rigid barrier types, flexible and semi-rigid barriers together accounted for approximately 40 percent of the observed barrier crash ejections.

Based on the available barrier crash data, occupant head slap is found to be extremely rare and estimated to occur in less than one hundredth of a percent of barrier crash exposed occupants with known injury information. The inclusion of occupants with identified head slap potential increases this percentage to 0.35 percent. Including only belted occupants, this percentage would remain essentially the same due to the low weighting values associated with the unbelted occupants. Although this suggests that barrier crash exposed occupants exhibiting the potential for head slap are relatively rare, barrier height data is not available in NASS/CDS. The low percentages reported herein could be in part due a relatively limited number of barriers in the data set that exceed a height of 34.5 inches. As previous research indicates, this type of partial ejection is difficult to identify suggesting that the estimates presented herein are likely lower estimates of head slap occurrence.

CONCLUSIONS

Using available in-depth crash data from 1,367 real-world tow-away level longitudinal barrier crashes, this study provides information on occupant ejection and head slap occurrence. The rate of occupant ejection in tow-away level single vehicle, single event barrier crashes was estimated to be 0.25 percent with an upper bound of 0.52 percent. These rates were found to be approximately three times higher than ejection rates for single event, two-vehicle crashes, primarily due to differences in full ejection rates. The results from this study reaffirm that barrier crashes involving ejection result in severe occupant injury and that side ejections dominate. A comparison of barrier ejection and non-ejection cases revealed that pickup trucks, older model year vehicles, and unbelted occupants were overrepresented in barrier ejection cases. Although the available data suggests that occupant head slap is rare, barrier height data was not available. Thus, this low rate may be attributed to relatively few barriers with heights exceeding 34.5 inches present in the data. Further study on the incidence of head slap on tall barriers is warranted.

REFERENCES

1. American Association of State Highway and Transportation Officials (AASHTO). Manual for Assessing Safety Hardware, 2009, 259 p.
2. Giavotto, V. Compatibility of Vehicles with Safety Barriers: Head Ejection through Side Windrows. In *Transportation Research Record 1890*, TRB, National Research Council, Washington, DC, 2004, pp. 71-78.
3. Rosenbaugh, S.K., Sicking, D.L., and R.K. Faller. Development of a TL-5 vertical-faced concrete median barrier incorporating head ejection criteria. Transportation Research Report No. TRP-03-194-07, Midwest Roadside Safety Facility, University of Nebraska, Lincoln, Lincoln, NE, 2007.
4. Polivka, K.A., Faller, R.K., Holloway, J.C., Rohde, J.R., and D.L. Sicking. Development, testing, and evaluation of NDOR's TL-5 aesthetic open concrete bridge rail. Transportation Research Report No.

- TRP-03-148-05, Midwest Roadside Safety Facility, University of Nebraska, Lincoln, Lincoln, NE, 2005.
5. Rosenbaugh, S.K., Faller, R.K. and D.L. Sicking. Head Ejection during Barrier Impacts. In *Journal of Transportation Engineering*, 2012, 138(1): 1-11.
 6. Viner, J.G., Council, F.M., and J.R. Stewart. Frequency and Severity of Crashes involving Roadside Safety Hardware by Vehicle Type. In *Transportation Research Record 1468*, TRB, National Research Council, Washington, DC, 1994, pp. 10-18.
 7. National Center for Statistics and Analysis (NCSA). National Automotive Sampling System / Crashworthiness Data System: 2014 Analytical User's Manual. DOT HS 812 198, Washington, DC: NHTSA, October 2015.
 8. Gabauer, D.J. and H.C. Gabler. Differential Rollover Risk in Vehicle-to-Traffic Barrier Collisions. *Ann Adv Automot Med.* 2009 Oct; 53: 131-40.
 9. Gabauer, D.J. Secondary collisions following a traffic barrier impact: frequency, factors, and occupant risk. *Ann Adv Automot Med.* 2010; 54: 223-32.
 10. American Association of State Highway and Transportation Officials (AASHTO). AASHTO Roadside Design Guide, 3rd edition, 2002, 344 p.
 11. Association for the Advancement of Automotive Medicine (1998) *The Abbreviated Injury Scale*, 1990 Revision, Update 98.

Comprehensive Analysis of Bridge-Related Crashes in New Jersey

MOHAMMAD JALAYER

HOOMAN PARVARDEH

*Center for Advanced Infrastructure and Transportation
Rutgers, The State University of New Jersey*

A roadway departure crash is defined by the Federal Highway Administration as “a crash in which a vehicle crosses an edge line, a centerline, or otherwise leaves the traveled way.” These crashes, involving run-off-road and cross-median/centerline head-on collisions, tend to be more severe than other crash types. According to a query of six years of crash data (2007-2012) from the Fatality Analysis Reporting System (FARS) database, an average of 57 percent of motor vehicle traffic fatalities occurred each year due to roadway departure crashes. Moreover, a total of 7,416 people perished in crashes involving fixed roadside objects in 2012, accounting for 22 percent of the total fatalities in the United States. Several previous studies have reported that the rural bridge-related crashes result in more fatalities, due to their being mostly fixed-object. As such, further in-depth investigation of this type of crashes is necessary.

Due to the lack of a comprehensive database which includes the bridge-related crashes and bridge characteristics, identifying the key factors contributing to this type of crashes on large or complex datasets, is a challenging task, which we address in this paper. We compiled and gathered five years’ (2011-2015) worth of crash data from the New Jersey crash database, and the characteristics of bridges from the Long-Term Bridge Performance (LTBP) Bridge Portal—a web-based application with advanced visualization and analysis tools. Following identifying the bridge-related crashes, we use a logistic regression model to identify the significant confounding factors to the severity of these crashes. Based on the obtained results, this study determines the effect of the various identified variables and recommends several safety countermeasures (e.g., signage, friction treatments, and barrier) to prevent or mitigate the frequency and severity of bridge-related crashes in New Jersey.

Comprehensive Analysis of Run-Off-Road Crashes in New Jersey

MOHAMMAD JALAYER

MICHAEL O'CONNELL

*Center for Advanced Infrastructure and Transportation
Rutgers, The State University of New Jersey*

Reducing roadway departure crashes is among the safety emphasis areas and strategies identified in the *2015 New Jersey Strategic Highway Safety Plan*. Based on a query of five years of crash data (2008-2012) from the New Jersey crash database, an average of 47 percent of motor vehicle traffic fatalities occurred each year due to roadway departure crashes. These crashes, comprising run-off-road and cross-median/centerline head-on collisions, tend to be more severe than other crash types. The contributing circumstances for roadway departure events include driver inattention due to fatigue or distraction, and traveling too fast on a curve. A variety of roadway and roadside geometric design features, such as lane and shoulder widths, also play a significant role.

Given the fact that run-off-road crashes accounted for most of the roadway departure crashes in New Jersey, the factors contributing to this type of crash must be identified to implement effective safety countermeasures, which we address in this paper. Given the large and complex datasets, identifying the key factors contributing to crashes is a very challenging task. This paper identifies the significant confounding factors for run-off-road crashes using multiple correspondence analysis to determine the dataset structure. Five years (2011-2015) worth of crash data was obtained from the New Jersey crash database. The study results provide engineers and policymakers with useful insight into run-off-road crashes for the development of effective safety countermeasures.

Evaluating the Relevancy of Current Crash Test Guidelines for Roadside Safety Barriers on High-Speed Roads

CONNIE XAVIER
DOMINIQUE LORD
Texas A&M University

CHIARA SILVESTRI DOBROVOLNY
ROGER BLIGH
Texas A&M Transportation Institute

Current crash test guidelines are contained in the Manual for Assessing Safety Hardware (MASH), which defines 62 mph being the 85th percentile impact speed for high speed roads. A crash data analysis of high speed roads in Texas with posted speed limits of 70, 75, 80, and 85 mph was performed to investigate whether MASH's current test guidelines are applicable for roadside safety appurtenances placed on roads with posted speed limits greater than 75 mph. A representative sample of real-world, single-vehicle, run-off-road crashes involving longitudinal barriers as the first harmful event was extracted from TxDOT's CRIS database. Specific data was compiled with respect to vehicle information including injury severity. The relevancy of current longitudinal roadside safety barriers designed for 62 mph oblique impacts is examined by determining whether or not injury severity has increased for real-world vehicle crashes that occurred on higher speed roads, among other factors. At the 5% significance level, the fatal and incapacitating injury severity percentage was not statistically different between 70 mph and ≥ 80 mph for years 2010 – 2013. However, the combined crash data for all four years did show an increase and statistical significance between the percentages at the 5% level. Now that speed limits have generally increased, this preliminary study shows the need for further research into determining impact speeds with updated data to better support the call for revision of MASH impact criteria on posted speed limit roads of ≥ 80 mph.

INTRODUCTION

Just recently, Texas opened a highway with an 85 mph posted speed limit, which is the highest in the United States (1). In fact, maximum speed limits have been increasing across the nation. Most of the states in the nation have a maximum speed limit of 70 mph or higher (2). With the implementation of these speed limits, design requirements of roadside safety barriers might change, and this possibility needs to be investigated. Ensuring that the barriers on high speed roads are tested at impact conditions representative of real-world data is crucial to maintaining safety. Highways with posted speeds over 70 mph were defined as “high speed” roads for this project.

Due to the high cost associated with detailed data collection and in-depth crash investigation and reconstruction to determine impact conditions for single vehicle ran-off-road crashes, few studies of this type have been performed. The analyses performed under the Texas Department of Transportation (TxDOT) Project 0-5544 used older crash data (3). Since completion of that project, a new database of reconstructed ran-off-road crashes was developed

under NCHRP Project 17-22 (4). This newer database better reflects current operating conditions, posted speed limits, and vehicle fleet characteristics. The Project 0-5544 analyses were based on design speed not posted speed limit. The 17-22 data was segregated by posted speed and is believed to be more applicable to evaluation of roadside hardware on roadways with posted speeds of 75 mph and higher. The findings of 17-22 were used in the development of NCHRP Report 665 (5). A surprising observation in 17-22 was that “highways with 60 to 65 mph speed limits had higher impact speeds than roadways with 70 to 75 mph speed limits” (4). However, through theoretical modeling, NCHRP 665 noted that the trend in variation in mean departure velocities was correlated with speed limit (5). Therefore, increases in injury severities at higher posted speed limits could be evidence of the need for further investigation of impact speeds on very high speed roads.

The current “guidelines for the crash testing of both permanent and temporary highway safety features and recommended evaluation criteria to assess test results” are outlined in the Manual for Assessing Safety Hardware (MASH) (6). This report also defines different test levels based on the type of impact conditions and employed test vehicle. Test Level 3 (TL-3) is the basic test level that specifies both the passenger cars and pickup trucks impacting at an angle of 25 degrees and a speed of 62 mph (6). This impact speed was derived from crash data collected on roads with design speeds up to 75 mph from the 17-22 study (4). This impact speed and angle combination happens to represent “approximately the 92.5 percentile of real-world crashes” (6). The highest impact speed used for testing (62 mph) has not changed since the previous guideline, NCHRP Report 350, dated 1993 and is currently in use for all roads with a 70 or greater mph posted speed limit (7). Fitzpatrick et al. (3) evaluated the criteria for high design speed roads up to 100 mph based on Report 350 and found that the impact angle of 25 degrees does “not vary significantly with functional class.” Therefore, the focus of this project was to examine whether or not the testing impact speed should be raised for roadways with posted speed limits higher than 70 mph.

There have been tests performed, both computer-simulated and real-life, involving higher speed impacts against barriers that have passed MASH TL-3 specifications. Sheikh et al. (8) performed computer simulations to evaluate roadside safety hardware for high speed applications and found issues as the impact speed increased. Bligh et al. (9) performed full-scale crash tests against a bridge rail and guardrail at 85 mph and found stability concerns associated with the bridge rail, while the guardrail did not successfully contain and redirect the vehicle. Although it has been shown that there are structural integrity concerns associated with higher speed impacts, there might not be a reason to increase the testing impact speed of roadside safety barriers if drivers are not actually impacting at very high speeds. Unfortunately, information about the impact speed of the vehicle during a crash incident is not provided in crash databases. Information about the actual impact speed of the crash can only be obtained through the reconstruction of crashes and looking at police reports which is time-consuming and requires special training. Therefore, to more quickly determine whether current roadside safety barriers are acceptable for use on high speed roads, this study sought to investigate how high speed roads (70, 75, \geq 80 mph) influence the severity of injuries, since it has been shown that very high impact speeds with the barrier can cause structural integrity concerns.

To accomplish the study objective, crash statistics were examined for the state of Texas. Since Texas is home to some of the highest speed limits in the nation, examining crash data for Texas provided the opportunity to compare crash severity statistics for roads with posted speed limits up to 85 mph. Crash data was provided from the TxDOT Crash Records Information

System (CRIS) database. The crash data were filtered to include 2010-2013, single-vehicle and single occupant run-off-road crashes happened on all types of highways with a posted speed limit of and greater than 70 mph. Crashes were selected with the first harmful event being a roadside safety barrier (median barrier, concrete traffic barrier, guardrail, retaining wall, bridge rail). Crash latitude and longitude were provided, as well as injury severity description. Since the 85 mph speed limit was implemented in 2012, an analysis performed on more recent years would include more data on crashes on higher speed limit roads. Before 2010, many of TxDOT's CRIS crash data entries had missing information. In order to ensure that the same information could be compared across the years, years 2010 and beyond were analyzed. The analysis only focused on single occupant (driver) crashes to simplify injury classification. With the CRIS database including only a total of fourteen crashes happened on 85 mph posted speed limit roads in the year 2013, the search was expanded to include multiple vehicles with multiple occupants. However, since this search only brought up three additional crashes, it was determined that the 'single occupant' restriction did not substantially limit the available data.

One drawback with the crash data was that it did not provide information on the most harmful event. Although a collision with a barrier was the first harmful event, it is unknown whether or not the vehicle also impacted an additional object which might have caused the reported injuries. However, it is known that the injuries were not due to a crash with another motor vehicle because the data were filtered to include crashes with only one motor vehicle. Although the occupant injuries may have not been caused by an impact with the longitudinal barrier (e.g., a vehicle could have rolled over after hitting the barrier, which led to the fatality), the purpose of the barrier should have been to safely contain and redirect the vehicle and keep it from colliding with other objects beyond the barrier. Consequently, a high injury severity could be interpreted as barrier failure to safely redirect the vehicle and may suggest that the impact speed was higher than the 62 mph value the barrier was initially designed for. However, within the scope of this analysis, no investigation has been and will be carried on the orientation of impact against the longitudinal barrier. Information on the impacting angle is not included in the CRIS database and might be available only through police reports for specific crashes. Time and budget constraints of this project would not allow such an in-depth investigation of the crashes.

CHARACTERISTICS OF DATA

Data Collection Process

Crash data were extracted from TxDOT's CRIS database by a staff at the Texas A&M Transportation Institute who was cleared by the Texas A&M Institutional Review Board (IRB) to review such information. CRIS is a "statewide automated database for all reported motor vehicle traffic crashes received by TxDOT" (10). The records are kept for the past five calendar years plus the current calendar year. Examining crash data from Texas provides insight on the structural integrity of longitudinal barriers on high speed roads without having to examine crash data from all the states. First, a request to use the crash data was sent in to TxDOT. Once approved, the staff described above was able to extract the data from CRIS based on the requested categories.

Several variables were used to extract the data. The "crash date" included years 2010-2013. Before 2010, there was an inconsistency on what types of data were recorded. The "crash

speed limit” included all types of roadways with a posted speed limit of and greater than 70 mph, the “first harmful event” was set as a fixed object, and the “object struck” was against a specific type of longitudinal barrier (median barrier, guardrail, retaining wall, bridge rail, concrete traffic barrier). The “crash severity” variable included categories such as unknown, not injured or property damage only (PDO or O), possible injury (injury type C), non-incapacitating (injury type B), incapacitating injury (injury type A), and fatal (injury type K). “Person count” was set to one to ensure that only single occupant run-off road crashes were included to make it easier to classify the injuries, and the “manner of collision group” was set to one motor vehicle. These two extra constraints did not greatly limit our received data as only three extra crashes were reported on 85 mph in 2013 when the data included multiple occupants and multiple vehicles. Variables involving location of the crash were also extracted. These variables included the “roadway system” the crash happened on, the “crash longitude and latitude”, the “city”, the “county”, and the “crash control section”. Specifics about the road where the crash occurred were also extracted. This information included the “roadbed width” and the “total paved width”. The “crash contributing factor list” gave the cause of the crash. After receiving all of the data under these different variables, specific variables that would provide the best insight to the scope of this project were chosen.

Summary of Characteristics of Data

After compiling the data, it was observed that only 2013 had reported crashes on 85 mph posted speed limit roads, so all subsequent data collection combined crashes that happened on 80 and 85 mph roads into one ≥ 80 mph category to better compare across the years. Most crashes were found to occur against guardrails and median barriers which could be attributed to their higher frequency in the distribution of barriers on highways. Crash severity across the speed limit categories will only be compared for crashes occurring on state highways and interstates since these were among the few roadway types to have reported crashes on the ≥ 80 mph category and are the more common types of highways. An analysis of ≥ 80 mph road barrier crashes showed that most crashes occur in Hudspeth and Reeves counties.

CRASH SEVERITY ANALYSIS

Data Collection

The crash data were filtered to only include those crashes occurring along interstates and state highways in order to better access the injury severity level across all years for the 70 mph, 75 mph, and greater than or equal to 80 mph speed limits. Interstates and state highways had among the highest number of total reported crashes and reported crashes on ≥ 80 mph posted speed limit roads. Consequently, a crash data analysis of the crashes occurring along these types of roads would give the best representation of changes in injury severity level for all speed limit categories.

The injury severity of each crash was classified according to the KABCO scale, which is used by police officers to categorize the injuries of a victim at a crash scene. These categories include fatal (K), incapacitating injury (A), non-incapacitating injury (B), possible injury (C), and property damage only (O), as originally described above. The injury severity level of the

person involved in the crash is decided upon by the police officer at the crash scene. The injury severity level reported in the CRIS database is based on the police officer's report. Without access to the police reports filled out at the crash scene, knowledge of exactly what type of injuries fit into each of the categories was not attained. For this study, a reported fatal or incapacitating injury was assumed to be an obvious severe injury that resulted from the crash with the barrier.






Mapping Crash Data

All following maps of Texas only plot crashes occurring along state highways and interstates using ArcMap 10.2. Figures 1-3 show plots of crashes on state highways and interstates color-coded by injury severity level. The crashes listed with a crash severity level of 'unknown' were not plotted. The legend for the color scale of the pins is shown in Table 1. The corresponding KABCO injury severity letter classification is also given. For this project, severe injuries were considered for any crashes with a K or A classification.

Different symbols were chosen to plot the data to better show the differences in injury severity. The highway numbers are indicated next to the highway in red. Figure 1 shows a sequence of plots with crashes occurring on 70 mph posted speed limit state highways and interstates, color-coded by injury severity level, for all four years. From the figure, it can be observed that one particular curved section of road of I-20 in the middle of Texas constantly reported to have a large number of crashes every year between 2010 and 2012. The reason it is not seen in the last picture of Figure 1 could be because the speed limit was raised on that section of highway. 2012 was likely the year the speed limit changed. This can be seen by comparing the crashes on I-20 between Figures 1 and 2 in 2012 and 2013. Additionally, it can be observed that all of the fatal and incapacitating injuries are scattered throughout the state. The number of fatal and incapacitating injuries appears to be the greatest in 2011, with I-20 showing the most fatal injuries.

Figure 2 shows a sequence of plots with crashes occurring on 75 mph posted speed limit state highways and interstates, color-coded by injury severity level, for all four years. From the figure, it can be observed that the number of crashes significantly increased between 2011 and 2012. This could be due to the number of new freeways with a 75 mph posted limit.

TABLE 1 Injury Severity Color Scale Legend

Color	Injury Severity	KABCO Scale
	Fatal	K
	Incapacitating Injury	A
	Non-Incapacitating Injury	B
	Possible Injury	C
	Property Damage Only	O

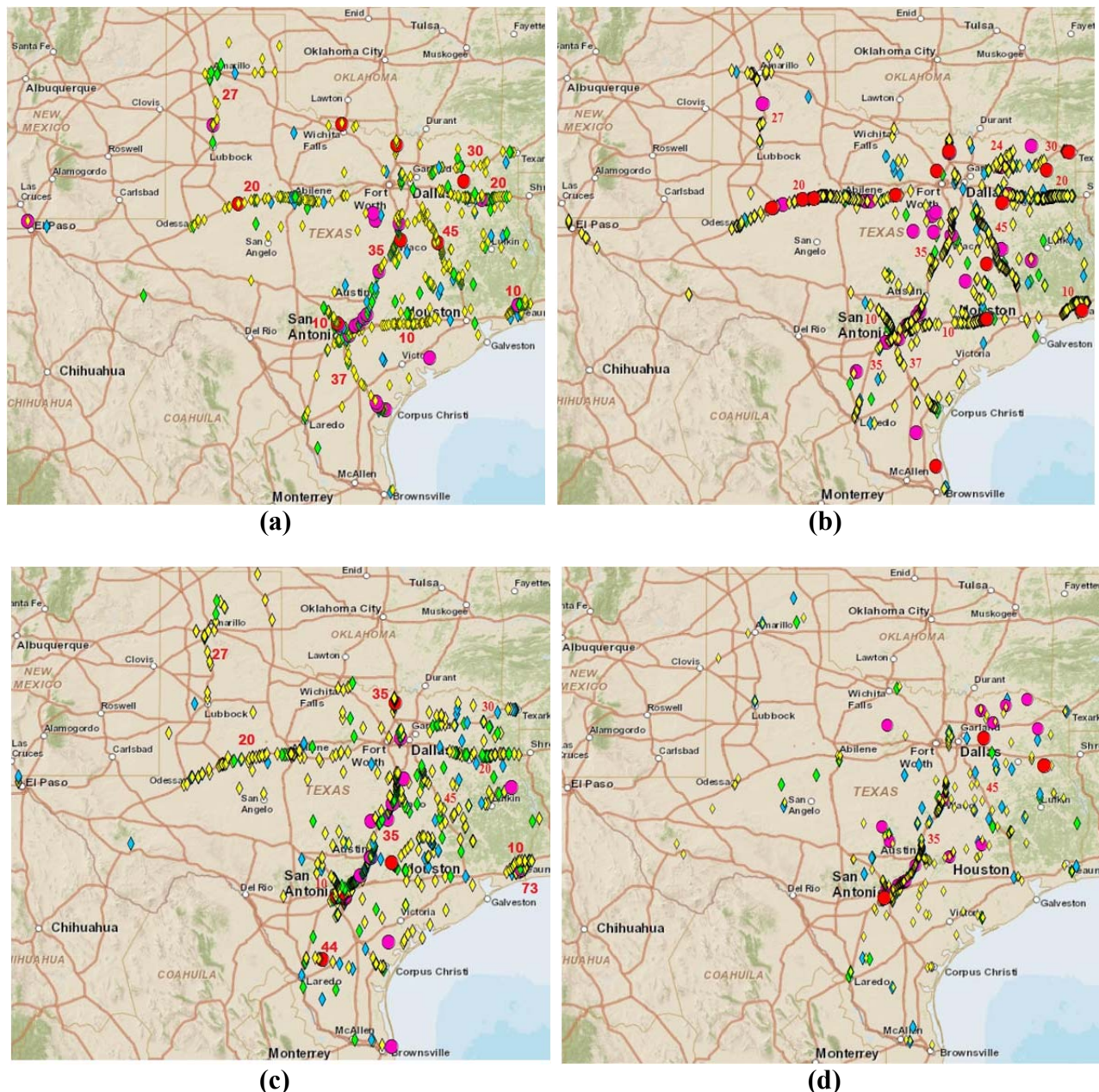


FIGURE 1 Plotted crashes by injury severity on 70 mph state highways and interstates: (a) 2010; (b) 2011; (c) 2012; and (d) 2013.

Additionally, it can be observed as the number of 75 mph posted speed limit reported road crashes increased, the number of fatal and incapacitating injuries also increased. 2013 shows the most number of reported fatal crashes. However, these crashes are not concentrated in one particular spot. I-20, I-45, and I-10 are shown to be problem areas for K and A injuries in both 2012 and 2013.

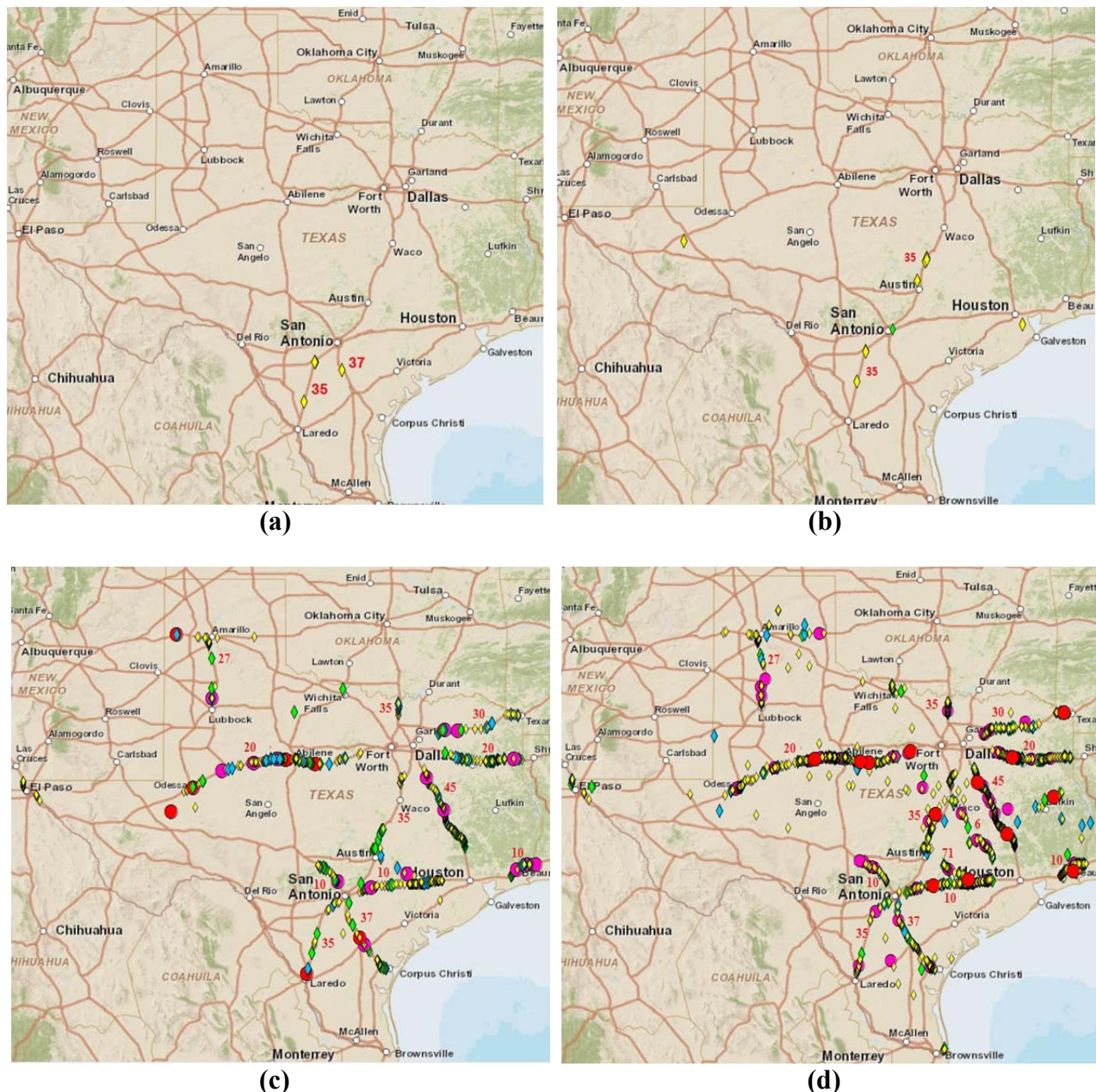


FIGURE 2 Plotted crashes by injury severity on 75 mph state highways and interstates: (a) 2010 (b) 2011 (c) 2012 (d) 2013.

Figure 3 shows a sequence of plots with crashes occurring on ≥ 80 mph posted speed limit state highways and interstates, color-coded by injury severity, for all four years. From the figure, it can be observed that the frequency of crashes greatly increased from 2010 to 2013 for the same highways. Highway 130 in Austin is the only road in Texas with an 85 mph speed limit. Crashes for this road can be seen in 2012 and 2013. The crashes shown in 2012 for this road were for an 80 mph posted speed limit, and the crashes in 2013 were on an 85 mph posted speed limit. There was an increase in crashes for 130 between those years following an increase in speed limit. Additionally, it can be observed that more fatal and incapacitating injuries were

reported in 2012 and 2013 than in 2010 and 2011. There was a great jump in the number of reported crashes between 2010 and 2013. This could be the result of speed limits being raised to 80 mph. State Highway (SH) 130 is the freeway with the 85 mph posted speed limit in 2013, but it only reported not injured or possible injury severity level crashes.

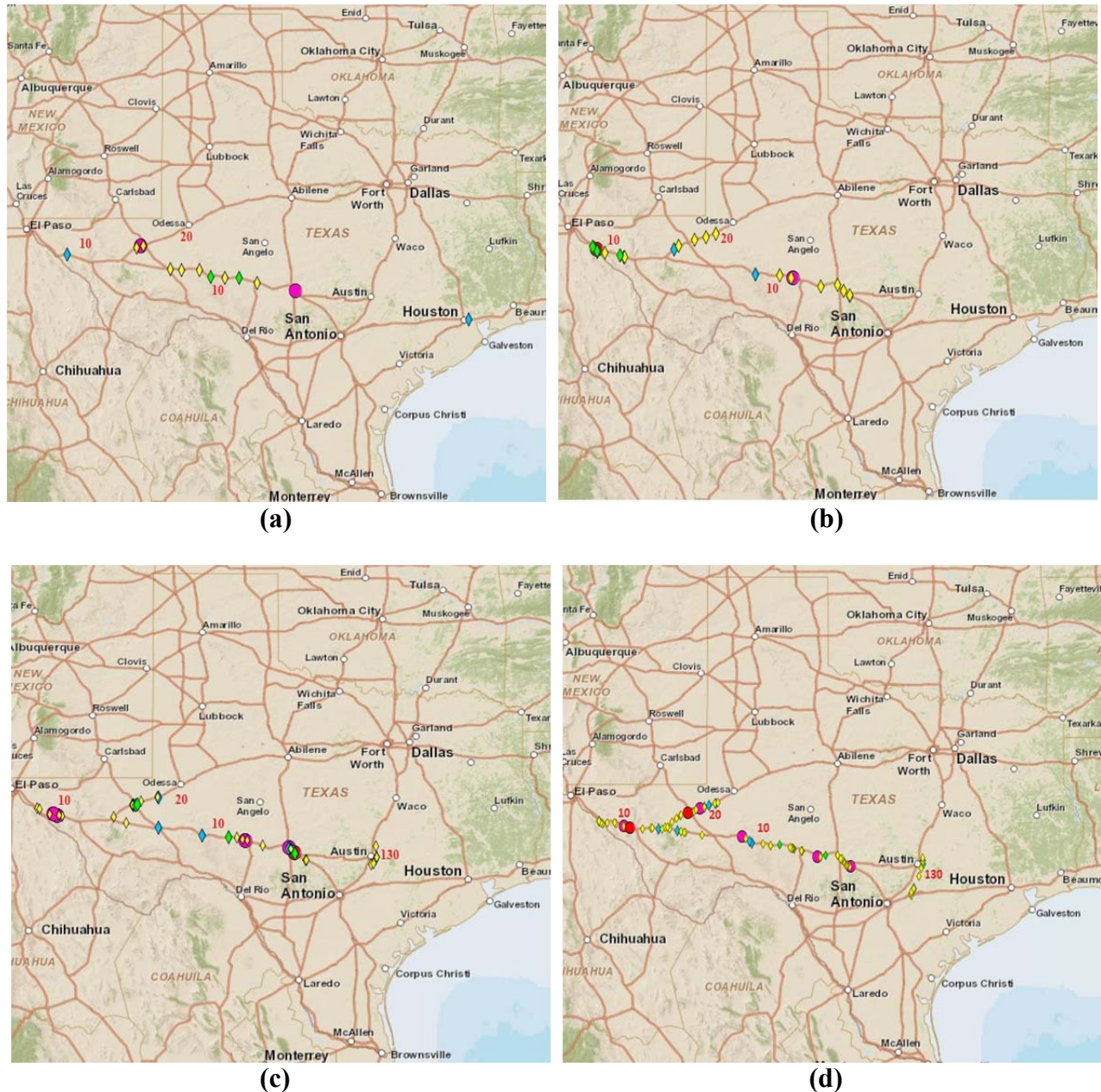


FIGURE 3 Plotted crashes by injury severity on ≥ 80 mph state highways and interstates:
(a) 2010 (b) 2011 (c) 2012 (d) 2013.

Crash Injury Severity Percentages

To quantify the numbers of crashes in each injury severity level for all speed limits, Table 2 shows the number of crashes on state highways and interstates for each type of injury severity based on the KABCO scale. Not many fatal crashes were reported for ≥ 80 mph posted speed limit roads because roads with the 85 mph posted speed limit had only opened in 2012. It should be pointed out that SH130 was designed with higher design standards than all existing interstates (11).

To observe the changes across all speed limits, the percentages for the injury severity levels were obtained. Table 3 shows the percentages of each type of injury severity based on the KABCO scale for crashes on state highways and interstates. The percentages are respect to the total number of crashes for that speed limit in a specific year, without the unknowns, to reduce the variability in the percentage. Since both fatal and incapacitating injuries were assumed to be a 'severe injury' and the ≥ 80 mph posted speed limit roads had only recently opened and therefore would not represent an accurate percentage of severe injuries, K and A listed crashes were combined into a single category (K+A). Possible injuries were chosen to be included in the total because of the possibility that they could have been an injury.

Table 3 shows that the K+A percentage category increases from 70 mph to ≥ 80 mph posted speed limit roads. This is consistent for all years. Although 0% of crashes were reported to have a fatal or incapacitating injury in 2010 or 2011 on 75 mph roads, there was a greater than 12% increase in the K+A percentage between 70 mph and ≥ 80 mph in 2010 and a greater than 4% increase in 2011. Years 2012 and 2013 did report crashes with a K or A injury severity level on 75 mph roads and showed an increase in those severity levels as the posted speed limit increased. Along with an increase in the percentage of K+A category, there was a decrease in the percentage of PDO crashes on 70 mph roads to ≥ 80 mph roads for years 2010-2012, suggesting that more crashes resulted in more severe injuries.

TABLE 2 Number of Crashes on State Highways and Interstates by Injury Severity

Speed Limit (mph):	2010			2011			2012			2013		
	70	75	≥ 80	70	75	≥ 80	70	75	≥ 80	70	75	≥ 80
K	7	0	0	13	0	1	7	7	1	3	13	2
A	20	0	2	27	0	1	15	17	4	18	49	5
B	80	0	2	104	0	5	120	72	9	80	109	11
C	117	0	2	134	1	3	125	75	4	69	145	5
O	680	4	7	679	16	13	585	653	27	369	1218	78
Unknown	14	0	1	17	0	0	29	16	0	33	39	1
Total	918	4	14	974	17	23	881	840	45	572	1573	102
Total (no unknowns)	904	4	13	957	17	23	852	824	45	539	1534	101

TABLE 3 Percentage of Crashes on State Highways and Interstates by Injury Severity

Speed Limit (mph):	2010			2011			2012			2013		
	70	75	≥80	70	75	≥80	70	75	≥80	70	75	≥80
K+A (%)	2.99	0	15.38	4.18	0	8.70	2.58	2.91	11.11	3.90	4.04	6.93
B (%)	8.85	0	15.38	10.87	0	21.74	14.08	8.74	20.00	14.84	7.11	10.89
C (%)	12.94	0	15.38	14.00	5.88	13.04	14.67	9.10	8.89	12.80	9.45	4.95
O (%)	75.22	100	53.85	70.95	94.12	56.52	68.66	79.25	60	68.46	79.40	77.23
Total (%)	100	100	100	100	100	100	100	100	100	100	100	100

Table 4 combines the K, A, B, C, and O reported crashes for all four years in each speed limit category. Percentages were found with respect to the total number of crashes in each speed limit category. The K+A percentages increase as the posted speed limit increases.

Statistical Analysis

Although it was shown that the fatal and incapacitating injury severity percentages increased as the posted speed limit increased from 70 mph to ≥ 80 mph, the ranges of the means of the two percentages may overlap, indicating that the two percentages are not statistically different. In order to determine statistical significance for the K+A percentages, a 95% confidence interval was performed to determine significance at the 5% level. A confidence level provides a range of values that are likely to contain the true proportion of fatal and incapacitating injuries. In other words, if the analysis was reproduced 100 times, it would be expected that the mean values lie outside the 95% boundaries 5% of the time. The higher the percentage of the confidence interval, the more likely the true value will be assumed to be located within the estimated interval. The following equation was used in computing the confidence interval:

TABLE 4 Percentages of Crashes on State Highways and Interstates by Injury Severity for Combined 2010–2013 Data

Speed Limit (mph):	70	75	≥80
K (%)	0.92	0.84	2.20
A (%)	2.46	2.77	6.59
K + A (%)	3.38	3.61	8.79
B (%)	11.81	7.61	14.84
C (%)	13.68	9.29	7.69
O (%)	71.13	79.49	68.68
Total (%)	100	100	100

$$\hat{p} \pm Z_{\alpha/2} \sqrt{\frac{\hat{p}\hat{q}}{n}} \quad (1)$$

\hat{p} = proportion of incapacitating and fatal injuries out of the total number of injuries

$$\hat{q} = 1 - \hat{p}$$

$$Z_{\alpha/2} = 1.96$$

n = total number of crashes with reported injuries for that particular year and speed limit

Table 5 provides the results of the computed confidence intervals for the 70 mph and ≥ 80 mph posted speed limit roads for all years as well as for the combined data. The true proportion of fatal and incapacitating injuries is estimated to be within the provided ranges. From the table, it was found that the K+A percentages between the 70 mph and ≥ 80 mph were not statistically different at the 5% significance level since the ranges for these two proportions overlap. However, the combined data did show significance at the 5% level. The range was higher for the ≥ 80 mph proportion of K+A crashes than for the 70 mph. This indicates that there was an increase in severity as the posted speed limit increased. The reason for the different result for the combined data could be attributed to having a higher sample size.

Summary

The plots of the crashes on maps using ArcMap 10.2 showed that the fatal and incapacitating injuries are not concentrated in one particular area, but certain highways reported these more severe injuries consistently for consecutive years. The data for each year shows that the K+A percentage increases as the posted speed limit increases from 70 mph to ≥ 80 mph, suggesting that higher speed limits lead to more severe injuries. The K+A percentage for the combined data showed an increase across all three speed limit categories. However, the K+A percentages between the 70 mph and ≥ 80 mph were not statistically different at the 5% significance level. This was consistent for every year. The K+A percentages for the combined 2010-2013 data showed significance at the 5% level between 70 mph and ≥ 80 mph posted speed limit roads. This difference in results could be that the combined data had a higher sample number and could give a better representation of the percentages. Therefore, data for more years as they become available need to be investigated to obtain a larger sample size. The increase in injury severity for those roadways with posted speed limit equal to or higher than 80 mph could be attributed to

TABLE 5 95% Confidence Intervals for Fatal and Incapacitating Injury Proportions

	70 mph	≥ 80 mph
2010	[0.019, 0.041]	[-0.042, 0.350]
2011	[0.029, 0.054]	[-0.028, 0.202]
2012	[0.015, 0.036]	[0.019, 0.203]
2013	[0.023, 0.055]	[0.020, 0.119]
2010-2013	[0.028, 0.040]	[0.047, 0.129]

a structural or impact energy absorption inadequacy of the roadside safety barrier(s) placed on these high speed roads. These barriers are full-scale crash tested at a much lower testing speed according to current standards. Highways with a posted speed limit over 80 mph showed increased injury severity during barrier impacts. Therefore, further study to determine impact conditions on highways over 75 mph not investigated under NCHRP 665 could be warranted.

CONCLUSIONS AND FURTHER WORK

In this research, data were extracted through TxDOT's CRIS crash database. Characteristics of these data were examined. Injury severity levels were compared for single-vehicle and single-occupant ROR crashes occurring against longitudinal barriers on state highways and interstates between 2010 and 2013. Injury severity levels were compared for the speed limit categories of 70 mph, 75 mph, and ≥ 80 mph. Plots of the crashes for each year and each speed limit category with the KABCO injury severity scale classification were done using ArcMap 10.2. The percentage of crashes in each severity level for each speed limit category and year were found and compared. The fatal and incapacitating injuries were combined to provide more robust results. A 95% confidence interval was performed to determine statistical significance between the 70 mph and ≥ 80 mph K+A severity percentages for all years. The key study results showed the following:

- Plots of crashes showed that the fatal and incapacitating injuries are not concentrated in one particular area, but some highways experienced more severe injuries consistently for consecutive years.
- The K+A injury severity percentages increased as the posted speed limit increased from 70 mph to ≥ 80 mph.
- The K+A percentages between the 70 mph and ≥ 80 mph were not statistically different at the 5% significance level. This was consistent for every year and was attributed to the small sample size issue.
- The K+A percentages for the combined 2010-2013 data showed significance at the 5% level between 70 mph and ≥ 80 mph posted speed limit roads.
- Since the combined data showed a statistically significant difference, it was concluded that there is a possibility that the severity of injuries increases as the posted speed limit increases. However, due to time and budget constraints, actual impact speeds were not determined in this study. Therefore, no conclusion can be drawn between injury severity and impact speed. This was meant as a preliminary study to show the need for further investigation of the relevancy of current crash test criteria.

Further Work

Further work should include a detailed review of the original police report. Police reports provide more insight into factors that were involved in the crash, which are not reported in the electronic version. For example, police sketches of the crash scene could provide information on the manner at which the vehicle impacted the barrier. Similarly, the sketches can also show where the barriers were hit (e.g., end treatment, barrier proper), and whether or not the vehicle was redirected into the traffic. Vehicles that impacted on its side tend to result in more severe

injuries than vehicles that impacted at an angle, since vehicles are usually better designed to dissipate energy in front-end collisions than broadside collisions. Data could be examined for more years as they become available. Since the first 85 mph road opened in 2012, examining data for more years would make the study of 85 mph roads more robust with a larger sample size. With more data to analyze, the injury severity with respect to the exact type of roadside barrier could be examined. For roadways with a change in speed limit, speed data collected prior to and after the change in speed limit would provide more insight on speed distribution changes. Future work is also needed to develop a baseline to compare the trend in injury severities of lower speed ranges (less than 70 mph) to higher speed ranges. In addition, the reconstruction of crashes could be performed to find the impact speed of the vehicle against the barrier. Future studies could use the information from these resources to make a more conclusive statement about a need for review of the testing impact speed condition required for evaluation of those roadside barriers to be placed on high speed roads (≥ 80 mph).

ACKNOWLEDGMENTS

This study was initially conducted by the lead author as part of the Undergraduate Research Scholars Program at Texas A&M University. Their help and support were greatly appreciated

REFERENCES

1. P. LeBeau. "Fastest Road in America: 85 MPH and We May Be Going Even Faster." CNBC. 23 Oct. 2012. Web. 21 Aug. 2014. <<http://www.cnbc.com/id/49520151#>>.
2. "Speed." Highway Safety Research & Communications. Insurance Institute for Highway Safety, 1 Mar. 2015. Web. 31 Mar. 2015. <<http://www.iihs.org/iihs/topics/laws/speedlimits/mapmaxspeedonruralinterstates?topicName=Speed>>.
3. Fitzpatrick, K., Zimmerman, K. H., Bligh, R.P., Chrysler, S. T., and B. C. Blaschke. *Criteria for High Design Speed Facilities*. FHWA/TX-07/0-5544-1, Texas Transportation Institute, College Station, Texas, 2007.
4. Mak, K. K., Sicking, D. L., de Albuquerque, F. D. B., and B. A. Coon. *Identification of Vehicular Impact Conditions Associated with Serious Ran-Off-Road-Crashes*. Final Report on NCHRP Project 17-22. Midwest Roadside Safety Facility, University of Nebraska-Lincoln, 2009.
5. Mak, K. K., D. L. Sicking, and B. A. Coon. *NCHRP Report 665: Identification of Vehicular Impact Conditions Associated with Serious Ran-off Road Crashes*. Transportation Research Board of the National Academies, Washington, D.C., 2010.
6. AASHTO, *Manual for Assessing Safety Hardware*. American Association of State Highway and Transportation Officials, Washington, D. C., 2009.
7. Ross, H. E., Sicking, D. L., Zimmer, R. A., and J. D. Michie. *Recommended Procedures for the Safety Performance Evaluation, NCHRP Report 350*. National Academy Press, National Cooperative Highway Research Program, Washington, D. C. 1993.
8. Sheikh, N., Ferdous, R., Bligh, R., and A. Abu-Odeh. *Analysis of Roadside Safety Devices For Use On Very High-Speed Roadways*. FHWA/TX-09/0-6071-1, Texas Transportation Institute, College Station, Texas, 2009.
9. Blight, R., Sheikh, N., Abu-Odeh, A., and W. Menges. *Evaluation of Barriers for Very High Speed Roadways*. FHWA/TX-10/0-6071-2, Texas Transportation Institute Proving Ground, Bryan, Texas, 2010.

10. "Crash Data Analysis and Statistics." Texas Department of Transportation. Web. 26 Jan. 2015.
<<http://www.txdot.gov/inside-tdot/division/traffic/crash-statistics.html>>.
11. *Mobility Corridor (5 R) Design Criteria*. Roadway Design Manual, 2014.

Design Impact Conditions for Testing and Evaluation of Longitudinal Safety Barriers for Use on High-Speed Roadways

ROGER BLIGH

CHIARA DOBROVOLNY

NAUMAN SHEIKH

Texas A&M Transportation Institute

Roadside safety longitudinal barriers installed on high speed roadways are currently tested and evaluated at a design impact speed of 62 mph. For economic reasons, many existing barrier systems are optimized for the current design impact conditions and may have little or no factor of safety for accommodating more severe impacts. It is becoming more common for states to establish higher posted speeds on rural interstates and freeways. New or modified barrier designs may be required to maintain the desired level of safety for motorists traveling on highways with higher posted speed limits.

This paper suggests design impact requirements that can be considered for use in testing and evaluating roadside safety features intended for use on roadways with high posted speeds. The objectives of this study were to use existing crash data to analyze the distribution of impact conditions associated with run-off-road crashes for a variety of highway classes and posted speed limits.

A critical element needed to help guide the design of roadside safety hardware for use on high speed roadways is the establishment of appropriate design impact requirements. These requirements are described by a crash test matrix with a prescribed set of impact conditions defined in terms of vehicle type, vehicle mass, impact speed, and impact angle. Historically, design impact conditions for testing and evaluation of roadside barrier systems has been derived from analysis of real-world impact conditions associated with roadway departure crashes. Determination of impact conditions for single vehicle ran-off-road crashes requires in-depth investigation and reconstruction of detailed crash data. Police-level crash data do not provide sufficient detail for this purpose.

Due to the high cost associated with detailed data collection and in-depth crash investigation and reconstruction, few studies of this type have been performed. A database for run-off-road crashes funded through NCHRP Project 17-22 was obtained by the researchers, and the impact speed distributions associated with run-off-road crashes were reanalyzed. Normal distributions were fit to the data and the 85th percentile impact speed was determined for each category of posted speed limit. The 85th percentile impact speeds for roadways with 45, 50-55, 60-65, and 70-75 mph posted speed limits were found to be 55, 56.5, 64.3, and 61.6 mph, respectively. The researchers used linear regression of the 85th percentile impact speed values to extrapolate the impact speed for highway segments with 80 and 85 mph posted speed limits.

Because reconstructed ran-off-road crash data does not exist for trucks, a different approach was needed to determine an appropriate design impact speed the 10,000S single unit truck, which is a design vehicle for MASH Test Level 4 (TL-4). The researchers used an impact severity ratio between TL-3 and TL-4 crash test conditions to develop a recommended design impact speed for the SUT design vehicle.

Impact angle was found to be independent of posted speed and, therefore, current impact angles in MASH are recommended for testing of longitudinal safety barriers for use on high speed roadways. Similarly, the MASH design vehicles are suggested.

ROADWAY DEPARTURE DATA COLLECTION AND ANALYSIS

Roadside Barrier Issues *Lessons Learned from NTSB Accident Investigations*

DONALD F. KAROL
National Transportation Safety Board

The National Transportation Safety Board is an independent Federal agency dedicated to promoting transportation safety. Established in 1967, the agency is mandated by Congress to investigate transportation accidents, determine the probable causes of the accidents, issue safety recommendations, study transportation safety issues, and evaluate the safety effectiveness of government agencies involved in transportation. Throughout the agency's 50 year history, the NTSB has investigated a large number of highway roadway departure crashes in which the adequacy or lack of roadside barriers played a significant contributing role in the causation of the accident.

The presentation will review some of the lessons learned from our crash investigations and recommendations made by the NTSB to improve safety. In addition to providing specific catastrophic highway crash examples, the presentation will highlight the need for improved guidance and warrants for high performance barriers (median, bridge railing, roadside) to better contain or redirect heavy vehicles (trucks and buses) to prevent future crashes.

The SHRP 2 Roadway Information Database *A Template for Data Collection*

OMAR SMADI
NEAL HAWKINS
ZACHARY HANS
Iowa State University

The presentation will discuss the development, population, and implementation of the SHRP 2 Roadway Information Database (RID) which was created to support the SHRP 2 Safety program and the Naturalistic Driving Study (NDS). The RID includes very detailed information for over 25,000 miles of roads in 6 study sites (FL (Tampa area), IN (Bloomington and Indianapolis), NC (Raleigh/Durham area), NY (Buffalo area), PA (State College), and WA (Seattle area) with a comprehensive quality assurance process with minimum accuracy requirements collected using mobile data collection equipment. The attributes collected include:

- **Horizontal curvature:**
 - Radius
 - Length
 - Point of curvature (PC)
 - Point of tangency (PT)
 - Direction of curve (left or right based on driving direction)
- **Grade**
- **Cross-slope/Superelevation**
- **Lanes: number, width, and type (turn, passing, acceleration, car pool, etc.)**
- **Shoulder type/curb (and paved width, if it exists)**
- **All Manual on Uniform Traffic Control Devices (MUTCD) signs**
- **Guardrails/Barriers**
- **Intersection: location, number of approaches, and control (uncontrolled, all-way stop, two-way stop, yield, signalized, roundabout). Ramp termini were considered intersections.**
 - **Median presence: type (depressed, raised, flush, barrier)**
 - **Rumble strip presence: location (centerline, edgeline, shoulder)**
 - **Lighting presence**

In addition to the mobile data collected, roadway data from existing public resources (e.g., Highway Performance Monitoring System [HPMS] data and comprehensive data items available from state transportation agencies) and a list of supplemental data items were acquired and included in the RID. The supplemental data items included a number of other roadway variables that are critical to further characterizing a roadway or analyzing the operation of that roadway segment. The term “supplemental” refers to any data item that characterizes a roadway segment that is not included as part of the mobile data collection undertaken by SHRP 2 or existing roadway data being acquired from transportation agencies within the six NDS sites. These supplemental items included crash histories, traffic, weather, work zones, changes to infrastructure, aerial imagery, Federal Railroad Administration (FRA) grade crossings, safety enforcement laws, and active safety campaigns. The existing and supplemental data that were acquired are estimated to cover about 200,000 centerline miles within the six NDS sites. All the data in the RID have a geospatial relationship and is part of a GIS dataset.

ROADWAY DEPARTURE DATA COLLECTION AND ANALYSIS

The Use of Corporate Crash Data to Assist Companies Improve Road Infrastructure for Workplace Fleet and Road Safety

KEITH SIMMONS

KND Consulting Pty Ltd and Transport and Road Safety Research Centre

GEORGE RECHNITZER

George Rechnitzer and Associates Pty Ltd and Transport and Road Safety Research Centre

RAPHAEL GRZEBIETA

Transport and Road Safety Research Centre

This paper demonstrates how analysis of three company's crash data, has been used to help identify the key risk collision types and circumstances, and formed a basis for subsequent in-depth investigations and analyses, leading to development of appropriate road treatment options and to improve road safety in their respective workplaces. The methodology was developed and applied by the authors, in separate major reviews of roads where large, dissimilar company vehicle fleets operate in dissimilar environments, in Laos, Chile and Indonesia.

In each case, interpretation of available data was required, in order to code it into common crash and injury mechanisms, or identify crash locations by locality or road type. With analysed data, together with associated in-depth investigations and analyses, the priority road infrastructure issues become evident and appropriate treatment options can thus be developed.

Such crash data analyses formed an important part of much larger, systematic road safety reviews for the companies using the five pillars of the Safe System approach. Safety improvements and risk reduction strategies developed as recommendations recognised the level of development in the particular country and the pragmatic limitations that could be applied to the road environment, in the short, medium and long term.

The key message for industry is the importance of maintaining quality road safety related incident records, so data can be used to identify crash trends and appropriate road infrastructure treatments developed, to reduce crashes, associated trauma and property / productivity losses affecting their people and their business.

INTRODUCTION

Most road safety researchers are familiar with using government based, police reported, mass crash and casualty data to conduct road safety research, in order to address common or specific crash and injury mechanisms. Output from such analysis can be used to identify priority locations or zones for road and roadside treatments. They can also be used for administrative behavioural campaigns as well as to improve vehicle safety standards.

On private property and/or company roads, such as those associated with mine sites or plantations, crashes are often not reported to authorities unless they involve serious injury or death. In these circumstances, the only available crash data are the records the company keeps for their own purposes (such as detailed incident investigations for fleet or plant management),

or to comply with local Workplace Health and Safety (WHS) regulations or corporate WHS policy.

When crashes do occur in these “private” environments, as they inevitably will, they are normally investigated internally and reported upon in accordance with corporate procedures. Depending on the maturity of the corporate system for managing workplace safety, these crash reports may generate only local or immediate treatments or reactions, rather than comprehensive and long term road safety improvements to the network as a whole.

The authors have developed and successfully applied a methodology to undertake detailed analysis of private company road safety related data, in three separate major reviews of road safety where large, dissimilar corporate vehicle fleets operate in dissimilar environments, in Laos, Chile and Indonesia. The three reviews are summarised here as case studies and demonstrate how analysis of available corporate safety data can identify improvements to roadside infrastructure or other treatments to address major road safety trends.

The key "take home" message for industry is the importance of maintaining quality road related incident records, so that the data can be used to help identify real world road safety trends within their organisation. Appropriate road infrastructure treatments can then be developed that will reduce casualty crashes and associated trauma and property, productivity, liability, and insurance losses affecting both their people and their business.

BACKGROUND

The road safety reviews follow the Safe System Approach that is now adopted in many countries including Australia and New Zealand and worldwide by the World Health Organisation and World Bank (2,3,4,5)

Each of the three major international companies discussed in the following three case studies contracted the authors following a trigger event, where a serious road safety incident led to a corporate decision to obtain expert road safety advice, seeking to reduce the overall road safety risks in their operations. These trigger events are not discussed in any detail in the case studies, suffice to say, they are included in the data analysed. This commitment by each company to improving safety for all employees and the public using such roads, is worthy of special acknowledgement. Business as usual was considered unacceptable by all company executives and employees.

CASE STUDY 1. MINING OPERATION – CENTRAL LAOS

Case Study 1 is of a company who operate two large mines in central Laos highlands. Company A, has their corporate headquarters and main personnel base in the Capital, Vientiane. Most of the nearly 5000 Lao employees are transported to and from the mine site by bus and work a 20 days on, 8 days off roster cycle.

On-site base camp facilities accommodate these personnel. The mine sites are about 200kms from Vientiane, or about 4 hrs travel. Some local villagers are employed by the mine or their sub-contractors. These employees either self transport from their village to and from the mine base camp each day (mostly by motorcycle) or are transported by their employer. All personnel are transported from the base camp, to and from the mine operational areas on a daily

basis. The monthly travel demand (passenger exposure) is approximately 196,000 passenger kilometres per month. Almost all travel is on public roads, with around 80% undertaken on sealed roads and 20 % on gravel. Just under half the journeys and all the gravel roads are in mountainous terrain, with monsoonal rainfall and associated road condition and climate problems.

Company A originally engaged the authors to assess the crashworthiness of their passenger carrying vehicle fleet, in order to make recommendations for improving safety for passenger transport operations.

Visits to the mine sites were undertaken during 2013, to assess the current risks to safety for passengers being transported in mine and contractor vehicles. Subsequent analysis of the corporate data provided, along with observations made during the visit, led to recommendations being made across all the key road safety elements of Safer Roads, Safer Vehicles, Safer People, Safer Speeds and Post-Crash Response.

At the time of the review, regular management reporting of vehicle and road safety performance data occurred. However, the summarised results focussed on gross numbers of events by outcome severity (e.g. number of recorded events vs number of lost time injuries and property damage incidents) and included summaries of key behaviours of personnel (e.g. incorrect procedures, drugs and alcohol, policy breaches, poor maintenance, fatigue etc).

Management, as with many organisations, lacked an appreciation of the Safe System approach to Road Safety. This statement is not made as a criticism of the company or its management. A truism is that: “*You don’t know what you don’t know*”, and this was the situation in Mining Company A at that time. As a result of this, the only systematic analysis of crash data made was of ‘time of day’ and ‘shift pattern (night vs day / shift start – finish)’ as fatigue was quite well understood. Serious incidents were being investigated using an Incident Cause Assessment Method (ICAM) developed by J. Reason (1) (ICAM is a systematic method of determining root causes of events or incidents common in the mining industry). Few investigation results had been incorporated into broader roadside treatments, training standards or fleet/equipment specifications.

The results of the systematic analysis of Company A’s 2012 safety data undertaken by the authors showed that a large number of incidents being reported were near-miss events¹, such as failure to wear seatbelts, etc. While this is a very important part of a comprehensive and systematic approach to safety improvement, the raw numbers told little of what crashes were actually occurring. Accordingly, the actual crash data were further coded and analysed as shown in Figure 1. The fleet travels around 23.5 million km per year.

In addition to the available crash data, the authors undertook detailed field inspections and information gathering with management and personnel at all levels. This included detailed examinations of vehicles, roads and roadside safety infrastructure, driver training and safe driving policies and procedures, travel speeds, first response and more. Only an overview of some of the key road infrastructure findings are presented here.

Roads and roadside infrastructure often lacked early warning signage, bridges and culverts were often unprotected by guard rails. Where guard rails were installed, they were sometimes discontinuous, often with fishtail end terminals or even no end terminal and no rub rails, significantly increasing crash severity risk for motorcycle riders and other vulnerable road users that were the predominant road user type in Laos. There was limited or no delineation at roadsides and curves (Figure 2).

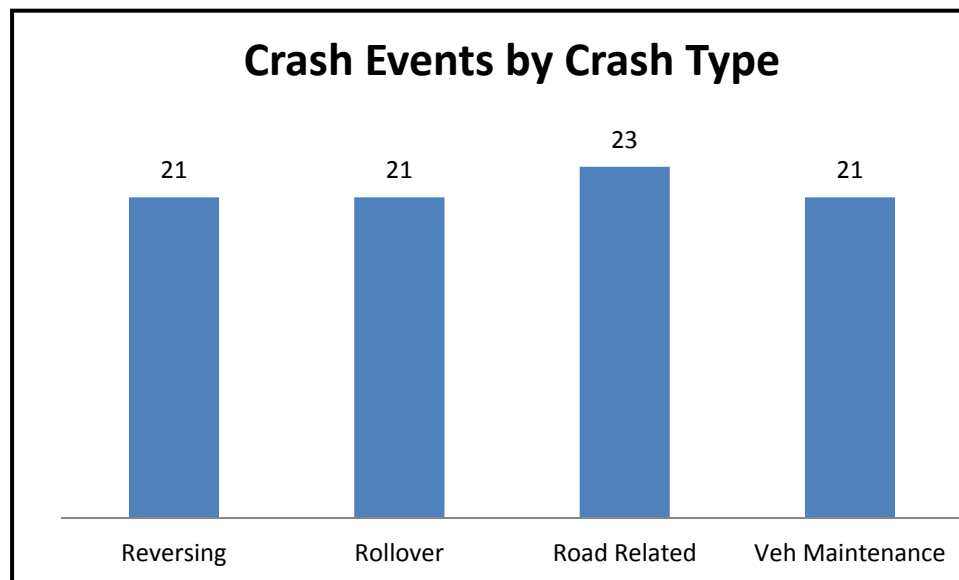


FIGURE 1 Summary of crash events by crash type.



FIGURE 2 Example of discontinuous, open W beam steel barrier with no end treatments.

Major recommendations to improve road safety for Company A that followed from this review included Safer Vehicles, Safer People, Safer Speeds and Post-Crash Response. Only the Safer Road (Infrastructure related) recommendations are included here.

Safer Roads

- Progressive improvement in route delineation and signage, including early warning;
- Road side barriers to be installed at high risk locations. All roadside barriers to have energy absorbing end terminals appropriate to the road user demography;
- Consideration be given to adopting improved barrier design which reduces severe injury risk (compared to the open W beam style in use) for collisions involving motorcycles, which are the predominate vehicle transport mode in Laos.

CASE STUDY 2. MINING OPERATION IN CHILE

Case Study 2 is of a large company operating a copper mine in Chile.

Background

Company B has an operational base at a major port city located on the Pacific coast, within reach of the mine site and the source of much of the mine labour, who are bussed to and from the mine daily. Shifts generally operate Monday to Friday, with maintenance occurring on weekends. The subject mine is accessed via a sealed road, approximately 135 kilometres long, that was built and is privately owned by Company B. This route has been adopted as part of the Chilean public road network under a licensing agreement between Company B and the Chilean Government.

Route Details

The route carries around 4100 vehicles (all classes) per day and up to 5000 per day at peak times. The first 60 kms or so rises progressively to 850 metres and the second section (~75 kms) rises steeply, by more than another 2250 metres, with an even steeper, very curvy section of around 15 kms length, about half way along the steep section, where the route traverses an escarpment. The route has a maximum speed limit of 100 km/h for light vehicles and 90 km/h for heavy vehicles. Wire rope barrier and other physical two-way separation methods are not suitable on the route, as the largest mine haul trucks traverse the route, straddling the entire sealed two lane surface.

Route Safety Review

The Authors were contracted to undertake a route safety review of the route connecting the port city to the mine site. A visit to the area was undertaken during the second half of 2015, to assess the current road safety risks for all route users. Subsequent analysis of the corporate data provided, along with observations made during the visit, led to recommendations being made across all the key road safety elements of Safer Roads, Vehicles, People, Speeds and Post-Crash Response.

Controls and Crash Data

Company B have implemented a number of controls on the route to address speeding and fatigue (including altitude related health effects). The route is least two lanes (bi-directional) with additional lanes in selected locations. In the previous five years, the route had experienced 67

serious crashes, resulting in 14 fatalities and 106 serious injuries. The route crash and injury rate was considered unacceptably high by Company B.

Company B maintains very good crash records as part of its corporate safety recording and reporting protocols. Records included crash date, time, location and direction of travel, an estimate of crash cause (in recent years), details of vehicle(s) involved (including ownership or mine being serviced), details of injuries suffered and a record of response time by first responders. To allow analysis, data were translated from Spanish to English, then coded into common vehicle or crash types, crash causes and injury severity.

Crash Data Analysis

The first analysis made, was to understand when crashes were occurring and which vehicles were involved. This provided useful opportunities to immediately prioritise road safety enforcement activity around major risk times.

The data were then analysed with respect to the section of route where crashes occur. The upper section had consistently more than twice the number of crashes than the lower section of the route.

The data were analysed to identify the type of crash for each vehicle type, by route section for 2011 to 2015 as seen in Figure 3.

The results showed light vehicles were significantly over-represented in rollover crashes in the lower section with 53% LCV² and sedan (Taxi) ~27% of crashes (LCV are 42% and Sedan 2% of average daily traffic respectively). A combination of speed and fatigue is exacerbated by poor delineation and lack of sealed shoulder and cleared zones on this road section.

Trucks were over-represented (~46%) in rollover crashes in the upper section. LCV were also significantly represented in rollover crashes in the upper section of the route, with 29% of

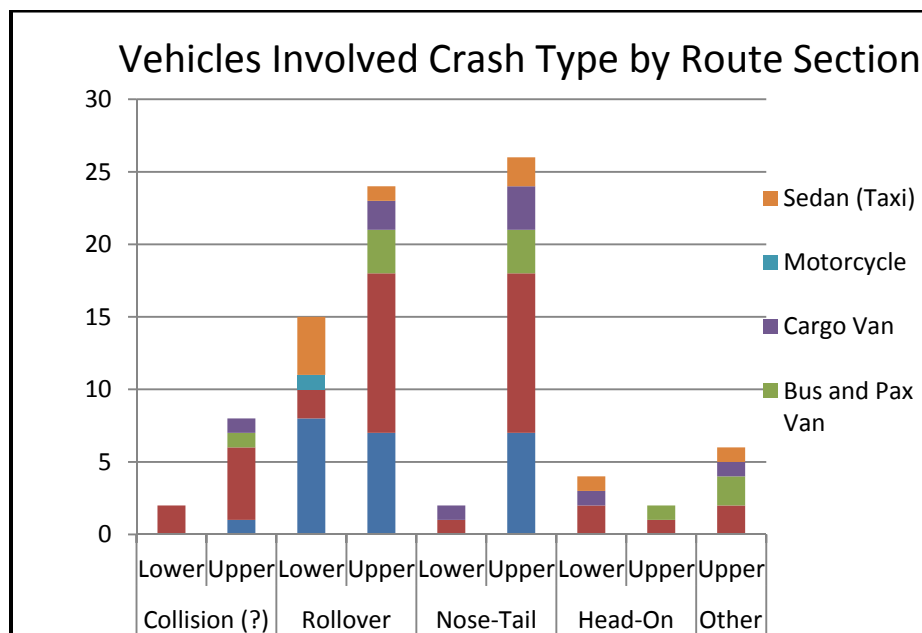


FIGURE 3 Crashes segregated into crash type and route section.³

rollover crashes. This suggested the speed limits (overall and truck advisory limit) on the curved section of the route is too high for vehicles with lower static stability or rollover resistance.

Trucks were also significantly over-represented in multi-vehicle collisions (~63% of collision type crashes in the upper section but only 30% of vehicle traffic), suggesting truck speeds are too high for road conditions.

Trucks were also significantly over-represented in nose-tail crashes in the upper route section, ~44% of all vehicles involved (Trucks represent 30% of all vehicle traffic). LCVs are also over-represented in nose-tail crashes in the upper route section, with 28% involvement. This suggests the overall speed limit is too high for the sight distances available and relative travel speeds of heavy vehicles in the steep sections.

Downhill speed (and brake failure) of trucks appeared an issue in regards to rollover, requiring reduced speeds and appropriate downhill descent control for the steep, curvy section.

The steeper Curved Zone was analysed separately, as seen in Figure 4, as many of the crashes occurred within that route segment. The analysis showed that trucks were significantly over-represented in crashes in the Curved Zone, (~88% of rollover crashes occurring in the downhill direction). Brake failures also occurred in this region, suggesting a separate heavy vehicle speed limit in the downhill direction (with associated 'Engage Low Gear' zone) would significantly reduce the rate of rollover and brake failure related crashes occurring.

Trucks heading uphill are significantly over-represented in nose-tail crashes, (not always the causal vehicle), with 50% of involvements. This suggests following vehicles cannot correctly estimate the speed of the slow moving trucks, or see them too late for the available stopping distance (stopping distance = reaction distance plus braking distance). While overtaking lanes are provided in parts of the uphill direction of the Curved Zone, lowering the speed limit for all vehicles in the uphill direction of the Curved Zone would reduce frequency of this particular crash type in this zone. Requiring forward collision warning devices on all vehicles that access the route would also help reduce the nose-tail crash risk, but only if travel speeds were appropriate to the stopping distances.

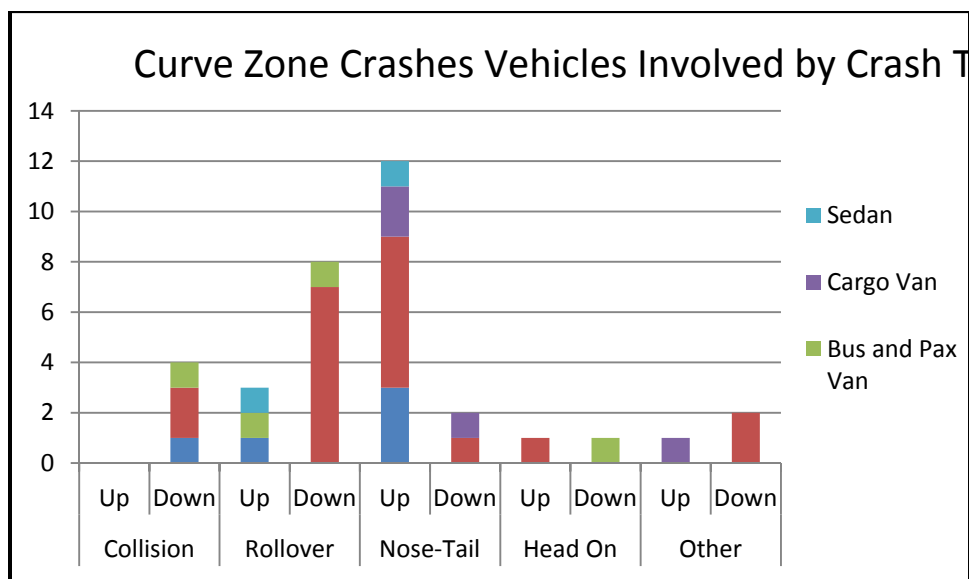


FIGURE 4 Crashes along the steep, curved section of route

Injury severity for the common crash types was analysed by route segment for the available data.

Rollover caused 10 of the 14 fatalities, with all 10 occurring in the upper section of the route. 45 injured persons also resulted from rollover crashes in the upper section of the route, accounting for ~78% of all rollover injured persons. Rollover crashes caused 58 of the total 106 injured persons recorded (~55%). Rollover crashes caused ~57% of all fatalities and injured persons recorded in the period.

Nose-Tail crashes were the second most injurious crash type, with 4 fatalities and 27 injured persons resulting from nose-tail crashes in the upper section of the route and none in the lower section. This strongly suggested maximum travel speeds are too high for the sight distances, relative to heavy vehicle travel speeds and vehicle stopping distances.

This analysis was confirmed by detailed analysis of the Curved Zone crashes, as seen in Figure 5.

In addition to the data analysis, a large number of observations were made in order to provide recommendations to improve route safety. Some of those observations included the following:

- Curve signs identified the beginning but not radius or extent of a horizontal curve. No curve advisory speeds were displayed for heavy vehicles (Figure 6).
- Many significant obstacles, such as rock walls in cuttings, were unprotected by appropriate barriers and not highlighted by day/night visible markings or reflectors. Approaches to obstacles presented ramps that can cause corkscrew rollover of errant vehicles
- Where W beam barriers were installed, turned down ends present ramps to errant vehicles, increasing risk of both rollover and barrier breach.
- Tactile centre and edge line markings installed in short lengths at limited locations, often installed as a response to a crash at that location.

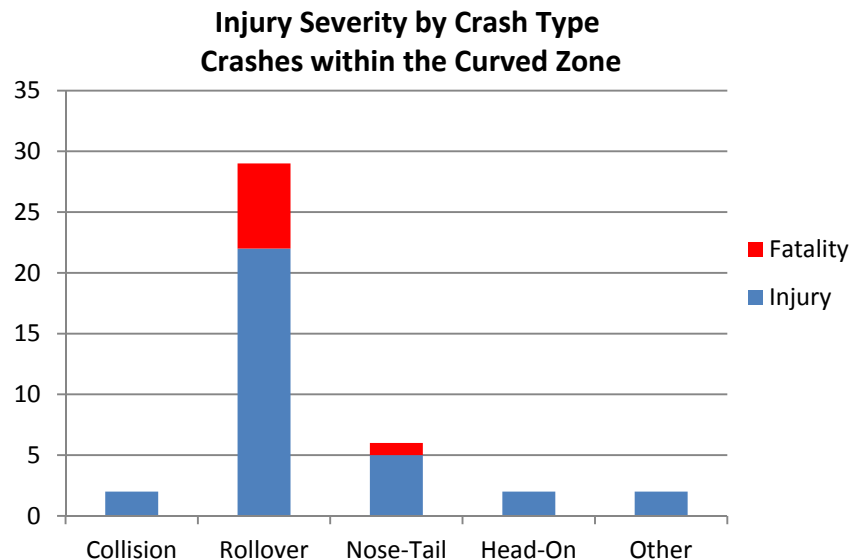


FIGURE 5 Injury severity by crash type crashes within the Curved Zone



FIGURE 6 Curved zone: poor side delineation, unprotected obstacle and minimal sight distance

- Large sections of the route had poor centreline or poor / no edge line marking, with crumbling outer edges, no compacted or sealed shoulder and no, or only limited, cleared zones.
- Pavement in some critical areas was glazed, with low co-efficient of friction.

There were many examples of sub-optimal roadside treatments identified during the review, that were considered likely to increase risk of crashes, or severity of crashes (or both). In addition, driver training, safe driving rules and enforcement, vehicle safety standards and speeds and more were all subjected to review. The observations and analysed crash data were considered in terms of the Safe System and a large number of improvement recommendations were made to Company B, separated by the following priorities:

- Urgent (simple and rapid, low cost and high impact treatments),
- Medium (within existing resources, medium cost and impact), and
- Long Term (more complex and costly treatments, although with medium to high potential for safety improvements).

Listed below are a road infrastructure subset of the 84 major recommendations made.

Urgent Treatments

- Speed Reductions. A range of speed reductions were recommended related to road conditions, including lack of sealed or compacted shoulder, limited delineation, poor curve advisory signage, roadside obstacles, barrier condition and more.
- Speed limits near work zones be reduced to 40 km/h until appropriate Manual for Assessing Safety Hardware (MASH) TL3 barriers can be introduced.

- **Dust, sand and Fog.** Establish “dust, sand and fog zones” are areas where these conditions are likely to reduce visibility considerably, and at no notice. In these zones, drivers must immediately reduce speed to 40 km/h when entering the obscuring cloud and activate hazard warning lamps. Training and reminder signage along these zones is required.
- **Signage.** Increase density of speed zone signage, install curve alignment markers and improve delineation at curves, provide heavy vehicle warning speeds for sharp curves wherever appropriate. Where differential speed limits apply, both to be clearly displayed and identified.
- **Delineation.** Improve centre and side line marking along the length of the route. Provide sideline tactile markings (rumble strips) along sidelines for all high speed (80 km/h or more) sections of the route. Install roadside delineation guide posts (RDG) along the route.

Medium Term Treatments.

- **Delineation.** Install ‘cats eyes’ (Raised Reflective Pavement Markers, RRPMS) along the entire route for both centreline and edgeline marking and also install reflectors on rock walls in cuttings and/or install hazard markers to visually highlight the rock walls through cuttings as a road hazard.
- **Signage.** Word signage be progressively replaced by pictogram signs. Early warning of speed zone changes be posted ahead of new speed zone. Complex locations or dangerous areas be de-cluttered, to reduce driver workload and to ensure attention is not drawn away from road itself.
- **People.** Drivers to be inducted to the route. Induction to include speed limits, route hazards and downhill descent control techniques for heavy vehicle drivers.

Longer Term Treatments.

(Intended to lower crash rates and allow increased maximum speed limits)

- **Surface Friction.** Test surface friction in high crash areas and consider High Friction Surface Treatment (HFST) where necessary. Extend HFST to high risk curves when funding permits.
- **Shoulder Width.** Seal shoulders to minimum 1.5 metres, to gain maximum road safety benefit, seal shoulders to 3 metres if funding permits.
- **2 + 1 Lane design.** Implement alternating 2 + 1 lane design in the curved zone. The Curved Zone should be progressively developed into continuous dual carriageway.
- **Batter slopes.** Batter slopes of road sides should be gently sloping and tapered where possible. Where this is not possible, aggressive batters and obstacles should be protected by appropriate barrier technologies.
- **Clear Zones and Run-off Areas.** Establish roadside clear zones and run-off areas to a minimum 12 metres (up to 30 metres) where possible, to reduce rollover crash risk for errant vehicles.
- **Barriers.** Replace existing barrier sloping end treatments or fan type end terminals with appropriate energy absorbing end terminal treatments. Extend barriers to ensure approaches do not create increased risks to road users

CASE STUDY 3. PALM OIL PLANTATION IN REMOTE INDONESIA

Case Study 3 is of a company operating a palm oil plantation in a remote part of Indonesia.

Background

Company C operates a large plantation consisting of a number of both contiguous and separated company owned estates of palm trees, as well as a number of private (locally) owned estates. The plantation includes three palm oil crushing mills. Traditional Dayak native enclaves have not been disturbed and their villages are dotted throughout the estates as well as other, more modern villages which are connected by public roads. The plantation occupies more than 25,000 Ha and includes over 2,000 km of privately built roads (all classes) with around 2,000 intersections. Around 3,500 vehicles are associated with the plantation, with more than 3,000 of these being motorcycles. More than 100 trucks, 120 items of plant, 70 Light Vehicles and 30 Heavy Tankers make up the fleet. Around 3,100 workers are moved around the estates by Company C each day. Apart from plantation traffic, local village traffic (as well as native villagers) utilise the plantation road network.

Road Network Details

The entire road network of the plantation is unsealed gravel, with a uniform maximum speed limit of 50 km/h. Road standards range from major through roads, collector roads (used for transportation of palm bunches to the mills) and access roads (minor tracks that allow access within the estates). The plantation has its own road safety enforcement team, who conduct speed enforcement (radar gun) and traffic stops to perform random breath testing and vehicle registration and safety checks. The local villagers appear to submit to this routine, even though their speeding and alcohol use cannot be enforced by Company C.

Roads are maintained by three road maintenance crews, each allocated to the major Estates within the plantation. There is no centralised control of road design standards or maintenance condition, although significant infrastructure tasks (such as a major bridge over a large river) are coordinated and delivered by the parent company.

Route Safety Review

The Authors were contracted to undertake review of road safety for Company C in 2016. A visit to the plantation was undertaken early 2016, to assess the current road safety risks for all road users. Subsequent analysis of the corporate data that was provided, along with observations made during the visit, led to recommendations across all the key road safety elements of Safer Roads, Vehicles, Safer People, Safer Speeds and Post-Crash Response.

Controls and Crash Data

Company C have worked hard to improve the standard of road safety within their operations to well above indigenous and national performance levels. Despite this effort, a number of crashes continue to occur, and unfortunately, some with catastrophic consequences. However, the speed

limit throughout the plantation was 50 km/h and travels speeds often well below this, which likely resulted in the severity of most of crashes being low.

Company C had maintained very good injury data (recorded by the medical team), although some desirable crash information were lacking in their protocols. Despite this, the data was able to be used to produce meaningful analysis that can support road safety treatment decision making. The original records were in Bahasa (Indonesian) and were translated into English. The trends highlighted by the data analysis are quite obvious and provide a sound basis to establish priority of effort to improve road safety.

Coded crash data were analysed to determine both underlying crash causation factors and to identify injury risk.

Crash Data Analysis

The first analysis made, was to understand what crashes were occurring and which vehicles were involved, as seen in Figure 7.

Motorcycles were by far the most significant crash involved vehicle (81% of all crashes). Truck (10%), Light Vehicle (2%), Pedestrian (1%), Bicycle (1%) and “unknown” crash involvements (5%).

“Fall From” Motorcycle (for whatever reason) was the most common crash type, 78% of all motorcycle crashes causing injury. Collisions with other vehicles (11%), Impact Other Object (3%) and Entanglement (1%). Motorcycle incidents where the crash type was unknown (7%).

Truck Rollover was the most frequent (39% of truck crashes). Collisions involving Trucks (22%) and Entanglements (11%). Run-Overs involving trucks (11%). Contact injury, Impact Other Object and Fire (5.5% each).

Light Vehicles were reported involved in 4 crashes, including one each Run Over, Contact Injury, Impact Other Object and an Entanglement.

Of the people injured in motorcycle crashes, ~1% were Fatal crashes, ~26% Serious Injuries and ~73% Minor Injuries.

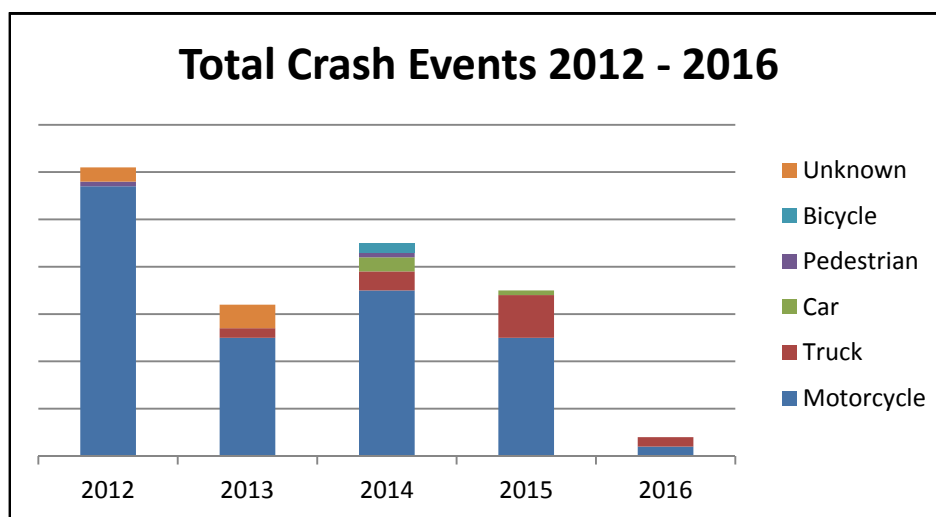


FIGURE 7 Total crash events 2012–2016

Of the other injury crash events, 12% were Serious Injury Truck crashes, 6% Minor Injury Truck crashes and 35% Truck crashes with no injuries (property damage only). 3% Light Vehicle Serious Injury and 3% Light Vehicle Minor Injury crashes, 6% Pedestrian Serious Injury crashes, 6% Bicycle Minor Injury crashes. 15% Unknown Serious Injury and 9% Unknown Minor Injury crashes.

Motorcycle crashes were the most common crash type, therefore it was important to understand the injuries occurring. Of the persons injured as a result of Motorcycle crashes, Fall From motorcycle caused the most injuries to different body parts (number of body regions injured). Lower limbs were the most frequently injured body region (43%), followed by Head/Face and Hands both presented in 36%. Feet injuries (31%), upper limb injuries (18%), injuries to the torso (shoulder to thigh) (15%) and chest / abdominal injuries (5%). (Note: most casualties received injuries to more than one body region). Thus, treatments that could reduce fall from motorcycle crashes, or reduce lower limb, face, hand and feet injuries when those crashes occurred, would have the most significant benefit to the plantation workforce and community.

Most truck rollovers occurred as a result of unstable ground, resulting in near-stationary tip-over events. Keeping trucks away from unstable soil, especially when tipping, was identified as important.

In addition to the data analysis, a large number of observations were made in order to provide recommendations to improve road user safety. Some of those observations included road design and water management, as seen in Figure 8.

In addition, a number of culverts and other roadside hazards or constriction points had W Beam barriers installed with simple fan end terminals. These present a significant hazard to the most common road user – the motorcyclist, at even low impact speeds.



FIGURE 8 Road where water is not drained either across (by use of a pipe culvert) or away from the roadside, but is left to pool on the road surface. Vehicle traffic will destroy the road at this location.

The observations and analysed crash data were considered in terms of the Safe System approach to Road Safety. A large number of improvement recommendations were made to Company C across all elements of the Safe System. The following were key road infrastructure recommendations :

Safer Roads.

Road design and construction. Establish a road design office, with a roads engineer appointed to oversee road design and maintenance, especially drainage management.

- Bridges and Culverts. Audit bridges and culverts to establish an asset database. Regularly inspect drainage channels and ensure free flow of waters.
- Signage. Standardise roadside signage with international (ISO) standard designs and placement.
- Delineation. Improve delineation by use of reflective markers placed on guide posts, or attached to trees along estate roadsides.
- Barriers. Repair or replace barriers that are deemed ineffective or dangerous. Fan tail end treatments replaced with energy absorbing, motorcycle friendly options, such as gated end terminals. Rub rails be installed on W beam barriers.
- Roundabouts. Roundabout centre ring size be increased and outer kerbs brought in, to force vehicles to circulate, instead of cutting corners. Approaches signposted with vehicle directions (keep left/right as appropriate).
- One Way Network. Establish a one-way network for heavy vehicles, to keep heavy vehicles centred (away from drains and unstable soil) and minimise crash and run-off road risks when passing head on.

DISCUSSION OF COMMERCIAL CRASH DATA ANALYSIS

In each case, a large amount of interpretation of the available data was required, in order to code it into common crash and injury types, or to identify crash locations by locality or road type. The results may contain minor errors based on these interpretations, but overall the priority road infrastructure issues became clearly evident and together with the associated in-depth investigations and analyses, appropriate treatment options were developed and offered to the respective companies for consideration.

The crash data analysis formed an important part of much larger, systematic road safety reviews using the five pillars of the Safe System Approach. Detailed background research, management and staff interviews, in-depth studies, personal site observations, review of crash investigation reports and more formed part of the information gathering and analysis phase for each project. The identified areas for safety improvements and the risk reduction strategies developed as recommendations recognised the level of development in the particular country, national driver / rider behaviours and the pragmatic limitations of what could be applied to the road environment, in the short, medium and long term.

The analysis and recommendations made in client reports were fully referenced to relevant current research, International Standards, Codes of Practice or best-practice policy documents.

CONCLUSIONS

This paper provides an example of using available crash information that is maintained by a company, often for purposes other than road safety, to identify the different crash types and injury outcomes involving their vehicles and on different parts of their corporate road network. Such analysis can help identify the key risk collision types and circumstances, and form a basis, together with detailed in-depth investigations, to recommended appropriate treatment options for each major road safety concern.

ACKNOWLEDGMENTS

The companies in the case studies are gratefully and respectfully acknowledged by the authors. No criticism of any of them is intended in our observations, analysis and recommendations. As stated earlier, “*You don’t know what you don’t know*”, and in each case, these companies sought outside, expert advice, to help them address their road safety concerns. For that, they are each to be commended for their commitment to the health, safety and wellbeing of their employees and the public.

REFERENCES

1. Reason J.; Managing the Risks of Organizational Accidents; Allgate Publishing; 1997
2. Mooren, L, Grzebieta, R., Job, S., (2011) Safe System – Comparisons of this Approach in Australia, Proc. Australasian College of Road Safety Conference
3. “A Safe System: Making it Happen!” Melbourne 1-2 September 2011.
4. Rechnitzer G. and Grzebieta R.H., Crashworthy Systems – a paradigm shift in road safety design, Transport Engineering in Australia, IEAust, Vol.5, No.2, Dec. 1999, (also presented and in proceedings of “Aus Top Tec” Topical Technical Symposia, Society of Automotive Engineers Australia, Melbourne, Aug 1999).
5. Grzebieta R.H. and Rechnitzer G., *Crashworthy Systems – a paradigm shift in road safety design (part II)*, Transport Engineering in Australia, IEAust, Vol. 7, Nos. 1&2, Dec 2001.
6. George Rechnitzer and Associates Confidential Report to Company A: Review of Personnel Transport Vehicles for Mining Company A, Laos; 11 November 2013
7. George Rechnitzer and Associates Confidential Report to Company B: Road Safety Route Review for the Antofagasta to Mine Area road transport route; 1 January 2016
8. George Rechnitzer and Associates Confidential Report to Company C: Reducing Vehicle Operation and Road Safety Risks for Operations in Indonesia; 2 November 2016.

NOTES

1. A “near miss event” has been taken to be one that has potential to cause harm, especially if circumstances had been different. An example is failure to wear seat belt, which becomes problematic if a crash occurs, or a “near crash”, which would have been a crash but for a small margin. Near miss events are reported in corporate safety reporting systems and analysed as part of good safety management practices.

2. LCV means Light Commercial Vehicle. Typically a single or dual cab utility such as Ford Ranger, Toyota HiLux (Tacoma), Nissan Navara (Titan) etc
3. In Figure 3, Collisions(?) refers to vehicle to vehicle crashes that are not head-on or nose-tail (typically side impact).

Monitoring and Predicting Traffic Safety in Slovenia

PETER LIPAR

University of Ljubljana

For the main urban roads the spots with a high accident rate are identified on the annual basis. After the implementation of the measures the spots with a high accident rate are monitored to define the effectiveness of implemented measures. The main aim is to define how much the implemented measures contributed to the improvement of road safety. By using relevant methods for predicting road safety road planners and designers would acquire the necessary data about the predicted condition of road safety on existent and planned traffic routes. Consequently, relevant measures could be predicted to prevent a bigger number of road accidents.

Based on the methodology of assessing the effectiveness of the measures, for each identified spot with a high accident rate the effect of the implemented measure on road safety was calculated as well as the crash reduction factors according to individual groups of measures.

On the basis of the conducted researches a methodology was developed that shows the effects of individual measures on the elimination of a spot with a high accident rate and shows the possible consequences in case the suggested measures are not implemented.

Regarding roadway departures the measures had following results on traffic safety:

- Speed limits: reduction up to 45%
- Speed limits with additional signalization (chevrons): reduction up to 65%
- Guard rails: reduction up to 45%
- Improving skid resistance (resurfacing): reduction up to 45%

All the measures implemented had a positive effect on road safety. After implementing the short-term measures (additional traffic signs, reduction in speed limit, rumble strips, guardrails) the number of accidents fell from on average by 40% while implementing the long-term measures (resurfacing, roundabouts, signal control intersections, turn lanes) they fell an average of more than 50%.

Further, a methodology was developed in order to predict road safety on the existent as well as the planned roads. The main aim of the new methodology is to identify potential spots with a high accident rate already in the phase of planning the changes on existent road network or a new traffic route in order to predict the measures for ensuring higher road safety.

The methodology is defined according to the guidelines of international research and is partly adapted to the Slovenian regulations and road conditions. The developed methodology is appropriate for two-lane roads outside settlements and in smaller settlements. These are the roads where the majority of spots with a high accident rate are located as well as the majority of newly constructed two-lane roads.

The core aim of the new methodology is to examine different project solutions for predicted traffic volumes that affect the probability of an event occurrence.

ROADWAY DEPARTURE DATA COLLECTION AND ANALYSIS

Identifying Roadway Risk Factors in Pennsylvania's Delaware Valley Region

KIMBERLEY MUSEY

SERI PARK

Villanova University

PATRICK MCTISH

Michael Baker International

There are many types of risk factors associated with roads when it comes to vehicle crashes. These risks can range from the design of the road to the current weather or illumination. Each presents a unique hazard and/or obstacle for vehicles to overcome. Renovation or refurbishment projects on all types of roadways are designed to improve safety through the minimization of risk to users of the roadways. The Federal Highway Administration defines the systemic approach to safety as “*implemented improvements based on high-risk roadway features correlated with specific severe crash types*” (1). This study uses 4-year crash data, provided by the Pennsylvania Department of Transportation, to identify potential contributing factors on interstates and state roads associated with single-vehicle run-off-the-road crashes. It identified a number of roadway features and characteristics that were correlated with the occurrence of fatalities and major injuries. These correlations can be used to identify roadway risk factors, prioritize future renovation or refurbishment projects, and help transportation engineers identify the patterns to avoid in the design of new roadways.

Based on both the interstate and 2-lane highway sites, the most frequent occurring contributing factor for crashes was the lack of illumination on roadways for both fatal and major injuries. Improvements addressing these factors would especially be helpful for Interstate 95 and Route 0001, which experienced the most occurrences of no illumination for interstates and 2-lane highways, respectively. The results of this research could help to indicate roadway risk factors for transportation users, allow planners and designers to design safer roads in the future.

INTRODUCTION

Through its programming, the Federal Highway Administration (FHWA) has been taking a more systemic approach to improving roadway safety that focuses on risk rather than exact locations. Potential contributing factors to crashes include roadway and intersection features such as the number of lanes, lane width, shoulder width/type, presence of lighting, median width/type, and intersection traffic control device. Other contributing factors include traffic volume, such as average daily traffic volumes, and other features, such as posted speed limit or operating speed, presence of nearby railroad crossings, and adjacent land use type. By looking at its crash history, states can identify factors that are overrepresented in run-off-road crashes, conduct further research of these factors and their potential to be “risk factors” for roadways, and be proactive to fix problems wherever these risk features exist (2).

Using crash data from 2011, 2012, 2013, and 2014 provided by the Pennsylvania Department of Transportation (PennDOT), the focus of this research is on the five Pennsylvania counties located within the Delaware Valley (Bucks County, Chester County, Delaware County, Montgomery County, and Philadelphia County). The fields in PennDOT's crash database that was provided included roadway functional classification, speed limit, roadway geometric features, etc. These five counties are serviced by PennDOT District 6 and contain both rural and urban areas, including the City of Philadelphia. A network of interstate roads runs through these counties, such as Interstates 76, 95, and 476, where high speeds and movements occur. This wide array of road networks and facility types brings an opportunity to view different types of risk factors, which will be identified and could possibly be correlated with the occurrence of fatalities and major injuries.

RESEARCH OBJECTIVES

The objective of this study is to:

- Conduct a comprehensive review and analysis of PennDOT crash data;
- Determine the contributing features for single-vehicle run-off-road crashes on Pennsylvania District 6 roadways, which are associated with a large portion of fatalities and serious injuries; and
- Identify overrepresentation of certain characteristics or features that can be identified as roadway "risk factors," and should be prioritized when addressing roadway safety.

LITERATURE REVIEW

Contributing factors for wrong-way fatal and injury-related crashes on freeways were identified and investigated in Illinois using causal tables and a Haddon matrix. Factors identified included drivers' age, drivers' condition, crash causes, vehicle types, vehicle maneuvers, roadway conditions, weather, and wrong-way entry points. Crashes with multiple contributing factors had the different factors weighted and ranked. Additionally, a significance test was used to analyze the statistical significance of each factor. The results of this analysis showed that the top contributing factors included alcohol impairment, darkness (illumination), and driver's age and skill (3). Illinois also incorporated an analysis technique to assist with the implementation of SafetyAnalyst. For this technique, safety performance functions for state routes and intersections within the state were developed using the Empirical Bayes method for safety improvement projects. The safety performance functions were then used to calculate a potential for safety improvement, which is the difference between the corrected crash frequency and the expected crash experience, for all locations. Using safety performance functions has significantly reduced the number of fatalities in Illinois (4).

The Systemic Safety Project Selection Tool is a proactive measure used to better identify and treat roadway problem areas. This tool was created by FHWA and provides a step-by-step process for conducting systemic safety planning. Additionally, this tool also provides considerations for determining the balance between spot and systemic safety improvements and provides analytical techniques for quantifying the benefits of a systemic safety program. Three

elements are included, which are selecting locations and countermeasures, achieving a balance between systemic and traditional safety investments, and evaluating the effectiveness of the systemic approach. The benefits of this tool include the identification of a problem based on a system-wide analysis of the data and risk factors, focusing on low-cost countermeasures, and identifying and prioritizing problem locations (1).

The Kentucky Transportation Cabinet (KYTC) applied the Systemic Safety Project Selection Tool to a local road system in five counties, which included Boyle, Bourbon, Franklin, Mercer, and Montgomery. The focus crash type selected was roadway departure crashes on horizontal curves, with the focus facility type being rural county roads. The KYTC produced a list of potential risk factors from information presented in the *Highway Safety Manual*, with five factors representing roadway attributes. These factors were horizontal curve density, lane width, shoulder type, shoulder width, and posted speed limit. Threshold values were determined and the number of factors present was tallied for each road segment. 90 of the 92 segments analyzed had at least three risk factors present, and 83 of those 90 had the same three risk factors (lane width, shoulder width, and speed limit). Curve density and shoulder type were the determining factors for scores greater than three. The risk ratings were compared to the crash data, and fatal, serious injury, and severe crash rates were found to increase with the number of risk factors present for the segments (5).

The Thurston County Public Works Department also used the *Systemic Safety Project Selection Tool* to produce benefits of proactive safety planning. The focus crash type selected was roadway departure crashes on horizontal curves and the focus facility type selected was signed curves on arterial and collector roadways. These were selected because 81% of the severe curve crashes occurred on arterial and collector roads. Collecting crash data from 2006-2010, Thurston County created a spreadsheet to link the road, intersection, and curve data with crash data to identify risk factors. 19 risk factors were selected and an analysis was performed to identify 9 risk factors for use in screening and prioritizing problem locations. Identified risk factors included roadway class, presence of an intersection, presence of a vertical curve, consecutive horizontal curves, and presence of a visual trap. Based on these identified risk factors, selected countermeasures included additional use of traffic signs, pavement markings, shoulder rumble strips, and roadside improvements (6). The state of New York used this tool to deploy low-cost countermeasures by identifying sites with high crash risk, as opposed to areas with a history of severe crashes. To this end, the New York Department of Transportation (NYSDOT) gathered crash data from 2007-2011 and selected lane departure crashes as the focus crash type because it was the most reoccurring type of crash in the state. The focus facility type selected was two-lane, undivided rural state highways with posted speed limit equal or greater than 55 mph. Risk factors were selected and the proportion of locations where location characteristics existed were compared with the percentage of severe crashes that occurred at similar locations. The three risk factors identified were traffic volume between 3,000 and 5,999 annual average daily traffic (AADT), curve radii between 100 and 300 feet, and shoulder width between one and three feet (7).

The basis of this research is in line with the FHWA's current Every Day Counts (EDC) program. EDC is a state-based model that seeks to "identify and rapidly deploy proven but underutilized innovations to shorten the project delivery process, enhance roadway safety, reduce congestion and improve environmental sustainability" (8). EDC3 focuses on two main analysis areas, one of which systematically screens roadways for features that have been correlated to

severe crashes and are therefore classified as high-risk. One identified, these roadway systems can be treated with lower cost treatments, even over wide areas.

Outside of the United States, England is also exploring factors that affect vehicle crashes. A study was performed in England that explored factors affecting vehicle accident severity. Comparing and contrasting the factors affecting the severity of hard shoulder and main carriageway accidents, a logistic regression model was developed. The factors examined included crash and vehicle characteristics, traffic and environment conditions, and behavioral factors. The results of this analysis identified the factors positively affecting crash severity were the number of vehicles involved in the crash, peak-hour traffic time, and low visibility. The presence of vehicles carrying heavy goods and driver fatigue were also factors present. This research hopes to bring awareness to fatigue when driving, especially among drivers carrying heavy goods (9).

RESEARCH METHODOLOGY

The crash data used for this study was provided by PennDOT. The PennDOT database contains a wide assortment of information regarding the details of a crash, including the latitude and longitude, crash type, crash severity, crash cause, environmental conditions, etc. The crash data for this research was filtered to only include single vehicle run-off-road crashes since this was the focus of the paper. These were identified based on the provided crash type information.

For this study, prime factors are defined as any attribute, characteristic or exposure that may have contributed to the likelihood of a run-off-road crash occurrence. Risk factors may be associated with features of the roadway, the environment, or the driver itself. In its crash database, PennDOT flags certain features that may have been associated with each crash. Therefore, although many different items contribute to crashes, these were the contributing factors selected for analysis in this research. The features with the highest occurrences for fatal and major injury crashes were considered to be contributing factors to crashes in PA District 6, and potential risk factors.

For this analysis, four interstates and four two-lane highways were selected from the five counties to compare to each other. The roadways were ultimately chosen because they experienced the most number of crashes during the selected time period. In addition to comparing the total fatal and major injury crashes for each site, an analysis on the top two contributing factors associated with fatal and major injury crashes was performed to consider the impact risk factors had on single-vehicle run-off-road crashes.

STUDY SITES

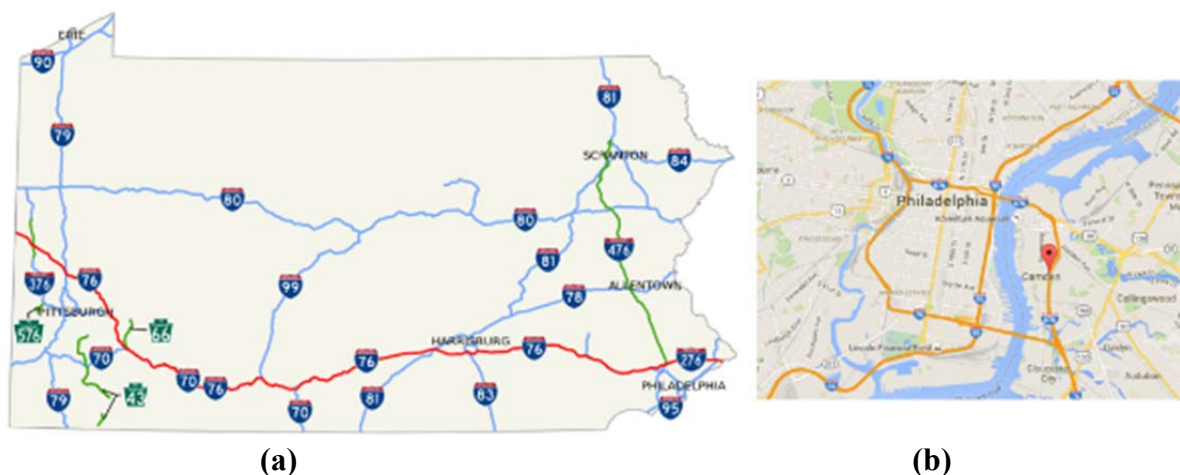
Interstate Study Sites

The four interstates selected were Interstates 76, 95, 476, and 676 (Figure 1). Table 1 compares the roadway characteristics to one another. All four interstates have a lane width of 12 feet and a large right lateral clearance. For Interstate 76, this right lateral clearance averages about 10 feet, with Interstates 95 and 476 averaging a slightly larger shoulder of 11 feet.

TABLE 1 Study Site Description

	Interstates				State Routes			
	76	95	476	676	0001	0013	0202	0611
Lane Width (ft)	12.0	12.0	12.0	12.0	12.0	11.0	11.0	12.0
Clearance (ft)	10.0	11.0	11.0	—*	11.0	4.0	0.0	0.0

*Data not provided

**FIGURE 1 Locations of Interstates (a) I-76, I-95, I-476, and (b) I-676.**

As mentioned previously, the crash data used to analyze state routes was obtained from PennDOT. For the year 2012, however, the crash data did not include information on the prime factor or cause of each crash. Therefore, for the year 2012 data is only included when analyzing total fatalities or major injuries. It is not included for analysis involving the prime factor analysis of crash cause or type. As a result of the crash history from the years 2011, 2013, and 2014, the top prime factors involved with run-off-road fatalities on interstates were due to drivers being affected by their physical condition and driving too fast for conditions, while the top two prime factors for major injuries were driving too fast for conditions and careless passing or lane change. Only fatalities and major injuries were considered for this study due to the severity of the crashes. This presents more of a need to address the risk factors.

State Route Study Sites

The four highways selected were Routes 0001, 0013, 0202, and 0611 (Figure 2). The four highways had more variable road characteristics than the interstates, with Route 0001 having a lane width of 12 feet, Routes 0013 and 0202 with a lane width of 11 feet, and Route 0611 with a lane width of 10 feet. The right lateral clearances for these highways were 11 feet for Route 0001, 4 feet for Route 0202, and no shoulders for Routes 0013 and 0611. The highways with no

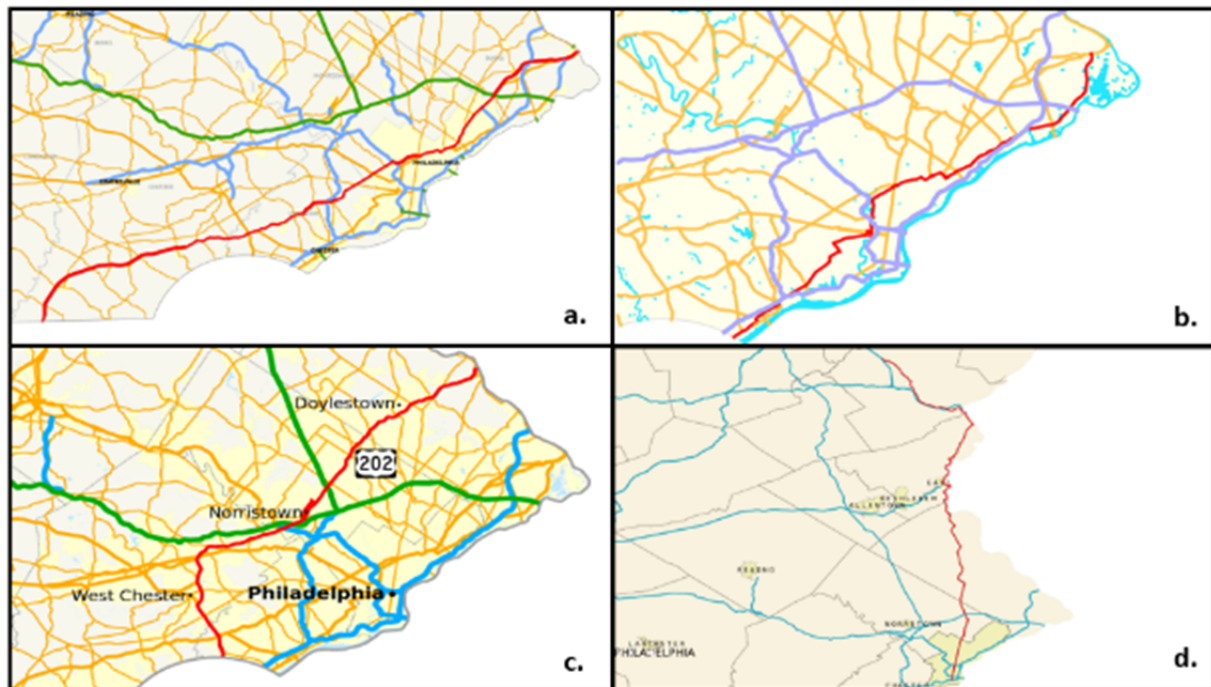


FIGURE 2 Locations of (a) US Route 0001, (b) US Route 0013, (c) US Route 0202, and (d) PA Route 0611 in Pennsylvania

right lateral clearances (Routes 0013 and 0611) ran through the city of Philadelphia, where urban development often limits clear zones. This information is summarized in Table 1.

Similar to interstates, the crash data obtained from PennDOT did not include information on the prime factor or cause of each crash for the year 2012. Therefore, 2012 data is only included when analyzing total fatalities. Its crashes are not included for analysis involving the prime factor analysis of crash cause or type. As a result of the crash history from the years 2011, 2013, and 2014, the top two prime factors associated with run-off-road fatalities on state routes were due to drivers being affected by their physical condition and other improper driving actions, while the top two prime factors for major injuries were drivers affected by their physical condition followed by unknown driver actions.

RESULTS

Interstates

For total fatal crashes and for fatal crashes caused when drivers are affected by a physical condition or are driving too fast, the most frequently occurring contributing factor on the interstates was a lack of illumination on the roadway, with 13 fatal crashes experiencing this risk factor. For total fatalities, each crash averaged 1.83 contributing factors (includes year 2012), while drivers affected by physical condition and driving too fast for conditions fatalities averaged 2.50 and 2.00 contributing factors, respectively (excludes year 2012). To calculate the average number of contributing factors per study site, the total number of risk factors present at

each individual site were summed up and divided by the total number of study sites (Equation 1). This average shows the approximate number of contributing factors present at each study site.

Average Contributing Factors Per Site

$$= \frac{\sum_{i=1}^n \text{Contributing Factors per Site}}{\text{Number of Sites}} \quad (\text{Equation 1})$$

Where $i = 1, 2, 3 \dots$ denotes individual contributing factors

The breakdown of contributing factors per interstate can be seen in Table 2 below. Based on the table, I-95 had the most contributing factors involved for fatal crashes, with the most frequent contributing factor being a lack of illumination, followed closely by curved roads. This table also shows how prevalent the lack of illumination contributing factor is among all four sites, along with the curved road contributing factor.

For major injury crashes on the interstate sites, the results were almost the same, which can be seen in Table 3. All three major injury crash scenarios (total, driving too fast, and careless passing), had the most frequent occurring contributing factor being the lack of illumination on the roadway, with 38 major injury crashes experiencing this contributing factor (excludes year 2012). For total major injuries, each crash averaged 1.44 contributing factors (includes year 2012), while driving too fast for conditions and careless passing/lane change fatalities averaged 1.50 and 1.23 contributing factors, respectively (excludes year 2012). These averages are lower

TABLE 2 Interstate Fatality Contributing Factor Site Breakdown

Contributing Factors	Total Fatalities				Affected by Physical Condition (Fatalities)*				Driving Too Fast for Conditions (Fatalities)*			
	I-76	I-95	I-476	I-676	I-76	I-95	I-476	I-676	I-76	I-95	I-476	I-676
Curved Road	1	6	3			1	2			2		
Shoulder Related												
Cross Median												
Hit Barrier	2	4	2		1		1			2		
Illumination Dark	3	7	3		1	1	2			2		
Speeding		5	2				1			1		
Wet Road		2								1		
Icy Road		1										
Cell Phone Use		1										
Total	6	26	10	---	2	2	6	---	---	8	---	---

*Excludes year 2012 crash data

Shaded boxes indicate no fatal crashes observed for contributing factor

TABLE 3 Interstate Major Injury Contributing Factor Site Breakdown

Contributing Factors	Total Major Injuries				Driving Too Fast for Conditions (Major Injuries)*				Careless Passing or Lane Change (Major Injuries)*			
	I-76	I-95	I-476	I-676	I-76	I-95	I-476	I-676	I-76	I-95	I-476	I-676
Curved Road	6	13	1	1	3	4		1				
Shoulder Related												
Cross Median												
Hit Barrier	7	20	2	2	3	4		2		5		
Illumination Dark	7	27	3	1	2	4		1		6	1	
Speeding		4				2				1		
Wet Road	3	6	1		1	3				2	1	
Icy Road		3	1									
Cell Phone Use												
Total	23	73	8	4	9	17	---	4	---	14	2	---

*Excludes year 2012 crash data

Shaded boxes indicate no fatal crashes observed for contributing factor

than the ones for fatal crashes, which indicate that the presence of additional contributing factors can increase the crash severity. Based on Table 3, I-95 was the site that had the most contributing factors involved for major injury crashes, with the most frequent contributing factor being the lack of illumination. The other three sites had much fewer major injury crashes and fewer contributing factors in comparison.

2-Lane Highways

For all three fatal crash scenarios (total, drivers affected by physical condition, and other improper driver action), the most frequent occurring contributing factor was also the lack of illumination on the roadway, with 20 fatal crashes experiencing this contributing factor. For total fatalities, each crash averaged 1.07 contributing factors (includes year 2012), while drivers affected by physical condition and other improper driver action fatalities averaged 0.70 and 0.40 contributing factors, respectively (excludes year 2012). These averages are much lower than those of the interstate sites, even though the 2-lane highway sites experienced more crashes. The breakdown of contributing factors per interstate can be seen in Table 4 below. Based on the table, Route 0001 had the most contributing factors involved for fatal crashes, with the most frequent contributing factor being the lack of illumination.

For major injury crashes on the interstate sites, the results were almost the same, which can be seen in Table 5. All three major injury crash scenarios (total, drivers affected by physical condition, and unknown driver action), had the most frequent occurring contributing factor being the lack of illumination on the roadway, with 34 major injury crashes experiencing this contributing factor. For total major injuries, each crash averaged 1.17 contributing factors (includes year 2012), while drivers affected by physical condition and unknown driver action major injuries averaged 1.54 and 1.00 contributing factors, respectively (excludes year 2012). These averages are higher than the ones for fatal crashes. Based on Table 5, Route 0001 again

TABLE 4 2-Lane Highway Fatality Contributing Factor Site Breakdown

Contributing Factors	Total Fatalities				Affected by Physical Condition (Fatalities)*				Other Improper Driver Actions (Fatalities)*			
	001	0013	0202	0611	001	0013	0202	0611	001	0013	0202	0611
Curved Road	1	2	2	2				1				
Shoulder Related												
Cross Median				1								
Hit Barrier	2	1								1		
Illumination Dark	13	4	1	2	4		1			1		
Speeding	4	1	2	2				1				
Wet Road	3											
Icy Road	1											
Cell Phone Use												
Total	24	8	5	7	4	---	1	2	---	2	---	---

*Excludes year 2012 crash data

Shaded boxes indicate no fatal crashes observed for contributing factor

was the site that had the most contributing factors involved for major injury crashes, with the most frequent contributing factor being the lack of illumination.

CONCLUSIONS

Based on both the interstate and 2-lane highway sites, the most frequent occurring contributing factor for run-off-road crashes was the lack of illumination on roadways for both fatal and major injuries. While further research is necessary to determine if this is an overrepresentation and therefore a “risk factor,” a potential way to address to this issue would be the implementation of more lights in high crash locations on interstates and major two-lane highways if the cost is reasonable. A low-cost solution to address illumination issues would be the implementation of raised pavement markers or retroreflective road paint. These low-cost solutions would better outline the road surface to make it easier for drivers to see at night in low-visibility areas. As opposed to actual lights, raised pavement markers and new road paint are much cheaper and require less maintenance, allowing improvement in more areas. In snow removal areas where raised pavement markers are not feasible, retroflective paint may provide another alternative. These improvements would especially be helpful for Interstate 95 and Route 0001, which experienced the most occurrences of no illumination for interstates and 2-lane highways, respectively. The two most frequent prime factors for interstate roads were affected by physical

TABLE 5 2-Lane Highway Major Injury Contributing Factor Site Breakdown

Contributing Factors	Total Major Injuries				Affected by Physical Condition (Major Injuries)*				Unknown Driver Actions (Major Injuries)*			
	001	0013	0202	0611	001	0013	0202	0611	001	0013	0202	0611
Curved Road	10	1	4	2	3		4					
Shoulder Related												
Cross Median												
Hit Barrier	2		2	2			1		1			
Illumination Dark	17	6	7	4	4		4		3	1		
Speeding	5	2	2	2			1					
Wet Road	3	4	3	1	1		2		2	2		
Icy Road	2		1	1								
Cell Phone Use												
Total	39	13	19	12	8	---	12	---	6	3	---	---

*Excludes year 2012 crash data

Shaded boxes indicate no fatal crashes observed for contributing factor

condition and driving too fast for conditions for fatal crashes, and driving too fast for conditions and careless passing or lane change for major injury crashes. The two most frequent crash types for 2-lane highways were drivers affected by physical condition and other improper driving actions for fatal crashes, and affected by physical condition and unknown driver actions for major injuries.

For future studies, the prime factors could be analyzed based on their overrepresentation in the database to identify potential risk factors that could apply to not just the examined locations, but all roadways. The systemic safety analysis process could be completed by identifying the specific sections of these roadways that would be at greater risk for fatal or serious injury crash based on the presence of these identified prime factors.

In addition to these topics, more study sites can be included to see the impact contributing factors present on additional roads in the Delaware Valley region in regards to run-off-road crashes. It would be interesting to compare the results by county to see the impact in smaller regions, such as the city of Philadelphia or the outlying suburbs. The impact of clear zone and its condition on reducing run-off-the-road crashes, as well as the role of delineation treatments. Additionally, more research can be put into further investigating the crash severities, taking into account minor injuries and property damage only crashes. While these severities are less damaging than fatalities or major injuries, they are more plentiful. Identifying contributing factors for these injury levels can still improve roadway safety.

ACKNOWLEDGMENTS

The authors would like to acknowledge PennDOT for providing the data which was used as a part of this research. The contents of this paper do not necessarily reflect the official views or policies of the state of the university.

REFERENCES

1. A Systemic Approach to Safety-Using Contributing to Drive Action. Federal Highway Administration Office of Safety. <http://safety.fhwa.dot.gov/systemic/> Accessed April 1, 2016.
2. Potential Contributing Factors. Federal Highway Administration. http://safety.fhwa.dot.gov/systemic/pdf/FHWA_SystemicApproach_PotentialContributingFactors.pdf Accessed April 4, 2016.
3. Zhou, H., J. Zhao, M.R. Gahrooei, and P.A. Tobias. Identification of Contributing Factors for Wrong-Way Crashes on Freeways in Illinois. *Journal of Transportation Safety & Security*, Vol. 8, No. 2, 2016, pp. 97-112.
4. Nance, R. *Illinois Develops SPFs for All State Routes and Intersections*. Publication FHWA-SA-11-02. FHWA, U.S. Department of Transportation, 2011.
5. Lovell, T. Kentucky Transportation Cabinet Applies Systemic Safety Project Selection Tool on Behalf of Local Agencies. Federal Highway Administration. <http://safety.fhwa.dot.gov/systemic/ky.htm> Accessed April 1, 2016.
6. Davis, S. Thurston County, Washington, Public Works Department Applies Systemic Safety Project Selection Tool. Federal Highway Administration. <http://safety.fhwa.dot.gov/systemic/tc.htm> Accessed April 3, 2016.
7. Doyle, R. New York State Department of Transportation Applies Systemic Planning Process to Lane Departure Crashes on State Highway System. Federal Highway Administration. <http://safety.fhwa.dot.gov/systemic/ny.htm> Accessed April 3, 2016.
8. Data-Driven Safety Analysis. Federal Highway Administration. <http://www.fhwa.dot.gov/innovation/everydaycounts/edc-3/ddsa.cfm>. Accessed July 29, 2016.
9. Michalaki, P., M.A. Quddus, D. Pitfield, and A. Huetson. *Exploring the Factors Affecting Motorway Accident Severity in England using the Generalised Ordered Logistic Regression Model*, Journal of Safety Research, 2015.

Benchmarking the Risks of Roadside Hazards

CHRISTINE E. CARRIGAN

MALCOLM H. RAY

RoadSafe LLC

There are indeterminate circumstances, realistic or not, where the countless roadside objects and terrain are a hazard to passing motorists. “Hazard” and “risk,” however, mean something very different in scientific jargon. The assessment of the risks these roadside objects and terrain present under real-life conditions is more relevant to policy establishment than the mere presence of roadside hazards.

Consider an individual parked in the shoulder of a two-lane rural road, adjacent to a steep slope which leads to a lake at the bottom to illustrate the difference. When the individual is simply parked looking down at the lake, the steep slope is a hazard, but there is no risk of injury. When an individual drives off the road and interacts with the slope, the slope is still a hazard and there is now a risk of injury.

Policy or regulatory agencies quantify “risk” by studying the probability of interaction with the hazard and the conditions where interaction actually results in injury. It has long been recognized, and was recently restated by Geoffrey Kabat, a cancer epidemiologist at the Albert Einstein College of Medicine that studying hazards absent of the risk “...bears no immediate relation to anything in the real world.”

The probability of leaving the roadway, $P(\text{enc})$, and the probability of interacting with a hazard, $P(\text{cr})$, are independent of the risk of observing an injury with a hazard, R_i . $P(\text{enc})$ and $P(\text{cr})$ are well documented in the roadside safety literature. This research quantifies R_i values for a number of roadside hazards. The data used to quantify risk were collected from a variety of data sources. These risk values can be used as benchmark values by policy or regulatory agencies when establishing risk-based guidance.

Safety Policy, Guidelines, Programs, and Strategies

Challenges and Opportunities for Improving the SAFESIDE Procedure for Cost-Benefit Assessment of Roadside Safety Intervention Alternatives

JOÃO LOURENÇO CARDOSO

CARLOS ROQUE

Laboratório Nacional de Engenharia Civil, Departamento de Transportes

Single-vehicle crashes involving impacts with roadside obstacles or vehicle rollover are a major source of traffic fatalities and permanent disabilities. Modern road safety intervention frameworks are based on the belief that permanent disabilities are unacceptable and that human frailty must be considered in road infrastructure design (Vision Zero). Roads and roadsides should be able to accommodate human errors, and forgiving in the event a driver loses control of his/her vehicle (Sustainable Safety). This new road safety paradigm assigns strong responsibilities to road agencies, urging them to take opportunities for road safety improvement throughout the whole infrastructure life cycle, instead of pushing safety decisions and responsibilities mainly to road users.

This paper refers to the method for assessing the influence of roadside characteristics in road safety developed at the *Laboratório Nacional de Engenharia Civil* to support decisions concerning the design of new roads and the redesign and maintenance of operating roads. This procedure sets the framework for the application of cost-benefit analysis to the design of roadside features, including the selection and installation of road restraint systems and support structures complying with European standards.

Specific software tools were developed, providing a user-friendly interface, and a suitable platform for incorporating new knowledge into the procedure and for adapting it to developments in construction and maintenance costs.

A description of the procedure is made, with an abridged presentation of supporting outcomes resulting from the analysis of traffic and detailed accident data registered on Portuguese roads and the observation of in-service performance of installed equipment.

INTRODUCTION

Single-vehicle crashes, involving running off the roadway and impacts with roadside obstacles or vehicle rollover are a major source of traffic fatalities, severe injuries and permanent disabilities. In Portugal, run-off-road injury crashes (RORIC) represented 33% of the number of accidents and 40% of the registered number of deaths in 2010-2014. At the international level, crash data confirm the importance of this problem: for example, European Transport Safety Council's data for 25 European countries show that single vehicle accidents accounted for 30% of the road fatalities registered in the period 2010-2014 (1). According to the World Health Organization, non-crash-protective roadside objects are a main risk factor influencing crash severity (2). Past studies demonstrated that roadside characteristics have an important influence on the severity of a significant fraction of RORIC crashes involving serious injury or death and that roadside geometry has a leading role in the rollover of errant vehicles (3, 4). In fact, estimates in the USA show that 83% of the single-vehicle rollovers occurred after the vehicle left the roadway and that roadside features initiated 95% of rollovers in single-vehicle crashes (5). The analysis of factors

influencing the severity of over 750 RORIC that occurred in Portuguese dual carriageway roads showed the contribution of critical slopes and vehicle rollover towards fatal injuries, as well as the importance of protecting errant vehicles from dangerous obstacles, particularly in horizontal curves, as these are linked with fatalities (6).

Current road safety intervention frameworks are based on the belief that permanent disabilities are unacceptable and that human frailty must be considered in road infrastructure design (*Vision Zero*). Therefore, roads and roadsides should be able to accommodate human errors, and forgiving in the event a driver loses control of his/her vehicle (*Sustainable Safety*). This recent road safety paradigm also assigns stronger responsibilities to road agencies, urging them to take opportunities for road safety improvement throughout the whole infrastructure life cycle, instead of pushing safety decisions and responsibility mainly to road users. According to this safe system approach, road transport accidents are not a major issue provided that no serious or fatal injuries occur resulting in loss of life or permanent disability (7).

In some countries, this new road safety paradigm led to a major shift in roadside safety interventions. Protecting the traffic from roadside obstacles is the current emphasis, rather than saving the integrity of telephone and electricity poles from errant vehicles. Also, minimizing the area of occupancy of a road (taking advantage of the geotechnical characteristics of soil materials) is no longer the sole criterion to define embankment slope values. Currently, the capacity to recover vehicle control in roadside incursions is also a major feature to consider in road design. Liability issues, reputation and ethics are strong motivations for incorporating roadside safety at the design and operation stages (8). However, lower public funding, increased share of private investment in road infrastructures, and non-transferability to road users of all mitigation costs may hinder the implementation of roadside safety interventions. This phenomenon is aggravated by the fact that disadvantages of road safety intervention scenarios (investment costs and work-zone level of service degradation) are immediate and certain, whilst the disadvantages of non-intervention (accident and permanent disability occurrence) are uncertain and delayed.

In the USA, clear zones were created since the early 1970s to increase the likelihood that a roadway departure results in a safe recovery rather than in a crash, and to mitigate the severity of crashes that do occur (9). Under this policy, roadside hazards within the clear zone are either eliminated or moved away. When hazards cannot be removed nor relocated, a determination needs to be made if a safety device (e.g., guardrail or crash cushion) is warranted to protect occupants from the roadside obstacle. This principle has guided the development of design policies to the present day, such as the fourth edition of American Association of State Highway and Transportation Officials' (AASHTO) Roadside Design Guide (10). Decision support tools for this type of choice were provided to designers, including benefit/cost analysis, for site examination, such as ROADSIDE (11) and RSAP-Roadside Safety Analysis Program (12, 13).

In Europe, efforts by the Conference of European Directors of Roads lead to the development of manuals for roadside safety (14) and the formulation of recommendations concerning the application of road restraint systems (15).

In Portugal, run-off-the-road (ROR) crashes were recently studied in detail, through a roadside safety research project named SAFESIDE - 'safe (road) side'. This research ran from 2007 to 2011. New methods for roadside design and maintenance of Portuguese interurban roads were developed and it contributed to the adoption and application of the "forgiving roadside" and "clear zone" concepts, as well as the relevant European technical standards, namely CEN-EN 1317 and CEN-EN 12767, which were not yet used in the country. For this purpose two design

guideline manuals were developed at *Laboratório Nacional de Engenharia Civil* (LNEC, the National Laboratory for Civil Engineering) at the request of the Portuguese road administration (16, 17), and a computer aided procedure (18) was prepared, for the evaluation of alternative roadside configurations (at the design level) or interventions (at the maintenance/operation level).

The main reasons for developing a new particular procedure were the uncertainty concerning the similarity of Portuguese and North American ROR scenarios, the absence of Portuguese encroachment frequency data, the requirement to fit the national ROR crash risk characteristics and the specificity of the Portuguese road construction industry. Two approaches have been followed to model the relationship between roadway and roadside features and RORIC risk: The encroachment-based method used in RSAP and the crash-based method used in the Portuguese procedure. The former uses a series of conditional probabilities for each event in the sequence that lead to a run-off-the-road crash following the encroachment of an errant vehicle on the roadside. The latter is based on the adjustment of generalized linear regression models to estimate RORIC frequencies, using exposure and relevant highway and roadside parameters as covariates (19). Our procedure was the first crash-based reported method specifically developed for evaluating roadside safety alternatives.

This paper refers to the method for assessing the influence of roadside characteristics in road safety developed at LNEC to support decisions concerning the design of new roads and the redesign and maintenance of operating roads. The procedure follows Portuguese roadside design standards developed at LNEC, and sets the framework for the application of cost-benefit analysis to support decisions concerning roadside features, including the selection and installation of road restraint systems and support structures complying with the aforementioned European standards.

Specific software tools were developed (named SAFESIDE), that provide a user-friendly interface and a suitable platform for incorporating existing knowledge (e.g., expected crash frequency models) and upcoming knowledge (e.g., the effectiveness roadside safety measures) into the procedure (18, 19). Furthermore, it is possible to adapt the procedure to future developments in construction and maintenance costs. SAFESIDE may also be applied in diverse contexts.

A description of the procedure is made, with an abridged presentation of supporting outcomes, resulting from the analysis of traffic and detailed accident data registered on Portuguese roads, as well as the observation of in-service performance of installed equipment. The practical implications of using a modified Ricker non-monotonous functional form in the crash prediction module are discussed, through real-world examples. Also mentioned are the challenges and opportunities for improved ROR scenario simulation presented by image evidence of vehicle encroachment angles currently available at public warehouses and in some agencies' road inventories.

GENERAL DESCRIPTION OF THE *SAFESIDE* PROCEDURE

In this section a summary description is presented of the *SAFESIDE* procedure for the assessment of alternative roadside safety interventions in the road infrastructure.

Basically, the method allows to simulate the effect on road safety outcomes (expressed as frequency of accidents and their consequences, as well as the corresponding estimated costs) of alternative scenarios for roadside characteristics. It may be applied at the design stage of new

roads or the redesign of existing ones (when designers must decide on removing dangerous obstacles, reducing the likelihood that such obstacles will be hit, reducing the severity of consequences of hitting those obstacles, or shielding the traffic through road restraint systems). The procedure may also be used at the operation stage, to help maintenance and roadside asset management decisions, including the selection of the functional characteristics required for restraint systems.

Basically, road infrastructure safety interventions comprise five stages: identification of high risk sites where corrective measures will likely be efficient; site analysis to assess the relations between road environment characteristics and safety risks at those sites; the selection and design of promising safety interventions; the execution of the selected corrective measures; and the monitoring of safety developments and the assessment of effects. Figure 1 depicts graphically those stages, highlighting the general structure of the *SAFESIDE* procedure (blue area), which is carried out using a computer application especially developed to that task.

Three sources of relevant data are used, requiring the fusion of data from three different administrative bodies: the road operator, responsible for managing its road asset inventory and traffic census; the National Road Safety Authority, providing aggregated injury crash data for the identification of high risk sites; and the police (GNR), delivering the detailed accident data required for the analysis of each relevant site.

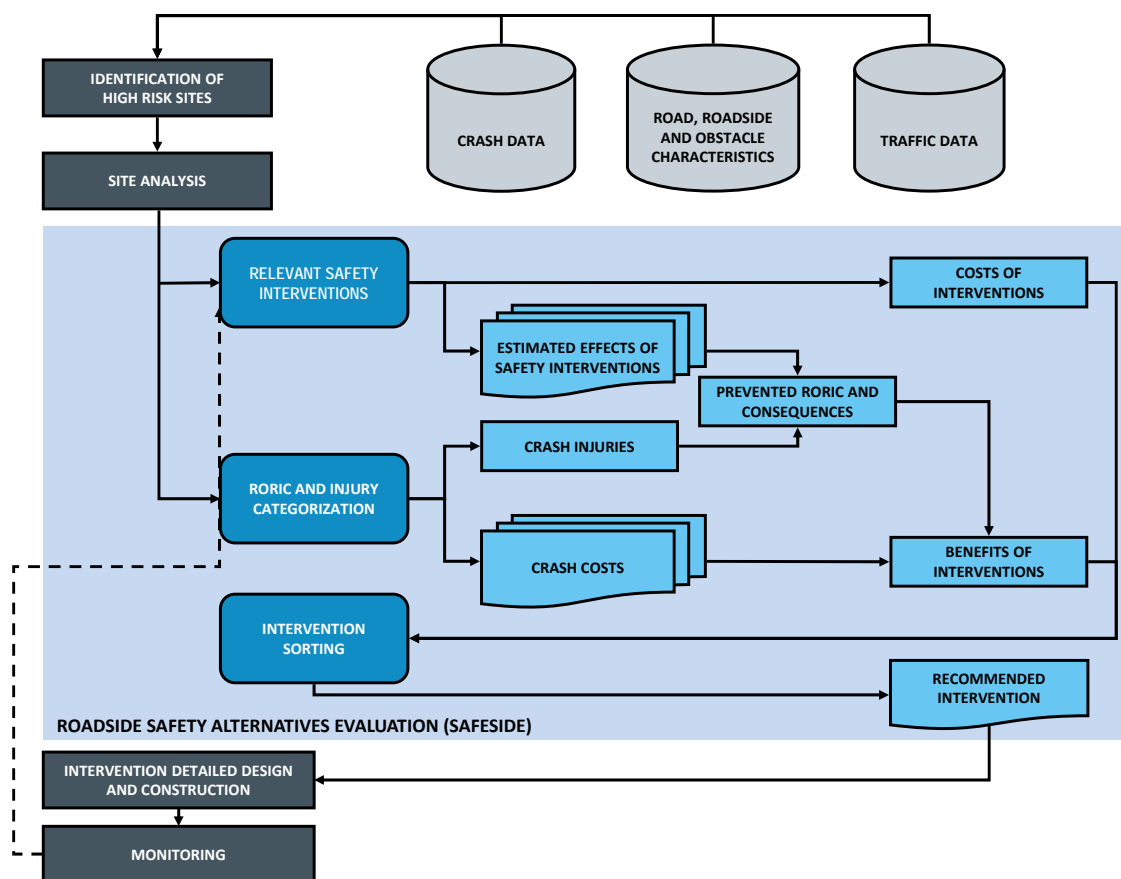


FIGURE 1 Integration of the roadside safety evaluation procedure (*SAFESIDE*) in infrastructure safety management

Merging these data sources is achieved through geographic and time tags embedded in each appropriate data base. Road designation and milepost are used for roadway characteristics, AADT and crashes. Date and hour of occurrence are registered for each road crash; traffic volume is reported per year and road characteristics modifications are reported per year and month.

Identification of high risk sites to analyze is made using the difference between the theoretically expected RORIC frequency at a site (calculated with relevant accident prediction models) and the expected number of accidents (estimated combining accident prediction models and observed RORIC frequencies), using the empirical Bayes method. For link sites, 250 m single carriageway road segments and 500 m dual carriageway road segments are used; four years of RORIC data are used.

Once the safety assessment of a site is completed and it has been confirmed as having an abnormally high RORIC risk, relevant infrastructure safety interventions are identified by means of designing alternative roadside scenarios and evaluating the corresponding effects on the site's road safety. To this end, fitting corrective interventions are selected from a built-in list and a summary of the most important characteristics of the RORIC occurred at the site are introduced by the user. This last component includes the breakdown of accidents by relevant typologies (for quantification of the target accidents and costs of each intervention). Each corrective measure defined in the built-in list has several attributes, such as the specific effectiveness for each type of target accident (i.e., the net effect on the frequency of each type of target RORIC), the respective cost of construction, as well as the maintenance cost during its useful working life. The number of RORIC that may be prevented by a safety intervention (a corrective measure or a combination of measures) is calculated by the product of the target RORIC frequency by the corrective measure effectiveness.

Selection of the most appropriate infrastructure intervention from a set of fitting alternatives involves four steps:

1. Assess the average number of victims (by injury severity class) that may be spared with the application of each fitting infrastructure intervention;
2. Evaluate the benefits' net present value, multiplying the monetary cost of each victim class by the average number of spared victims in that class, across all classes of severity;
3. Estimate the net present value of construction and maintenance costs of each safety intervention at stake;
4. Compute the benefit-cost ratio of each safety intervention under examination, including the "do nothing" alternative, and sort them according to the calculated values.

The ranking produced with this procedure allows identifying the most efficient corrective interventions for a given road segment. Additionally, a sensitivity analysis may be carried out to find critical variables (those with most impact on the safety intervention financial performance) in the cost-benefit analysis. The variables under consideration in the sensitivity analysis are the following: investment costs, annual operation and maintenance costs, average crash costs, AADT, length of road segment, safety effects of each intervention, discount rate, and residual value of the investment.

The supporting software was built with a modular structure, to enable easy upgrading, resulting from future improvements in roadside safety knowledge on the Portuguese context. This structure also enables an easy adaptation of the procedure to road contexts different from

Portuguese highways. For instance, the crash prediction models and the method for estimating crash costs of the safety module may be fitted and adjusted to other countries' road crash data.

Safety Interventions Module

The main characteristics of the road scheme are setup in the safety interventions module: the first year of operation, the lifetime horizon and the discount rate to be used, as well as the definition of the alternative safety interventions. Each safety intervention is defined as a combination of corrective measures, which may be selected from the list of predefined ones or added as new ones.

The safety interventions module contains a pre-defined set of 49 roadside safety measures and their implementation costs and safety effects. Safety measures are implemented to decrease the damage caused by road crashes: therefore, these safety effects are preferably expressed as changes in the number of fatalities, serious injuries, slight injuries, and property damage, to both vehicles and roadside objects.

At this stage, values for the default safety effects were mostly obtained from reference literature (e.g. 20, 21 and 22), only too few Portuguese values being available – e.g. CMFs for type of medium on dual carriageway roads and for shoulder width (19). In these knowledge sources, most listed safety measures have their effects described as changes in injury crash frequencies (the total number of crashes, the number of RORIC or both).

Calculating the safety effect of a single measure safety intervention is straightforward. However, when several measures are combined in a safety intervention, their effects are not absolutely independent. Measures that have large effects (such as speed reducing measures) are likely to also influence risk factors that are targeted by other measures, thus reducing their likely effects. To account for this, Elvik's "*method of common residuals*" is applied to calculate the effect of these complex interventions (23). The term *residual* corresponds to the number of occurrences not prevented by a safety measure. This method for estimating the combined effects of several road safety measures fits closely the reported findings of assessments made to the effects of several treatments introduced simultaneously at the same location (23).

The costs associated with each road safety measure are composed of investment costs and the annual costs of operation and maintenance. The user selects the set of measures to be analyzed, enters their costs on an individual basis for each intervention, and *SAFESIDE* converts the implementation costs to their present values. A survey was carried out to assess typical costs of engineering roadside safety measures in Portugal, to define reasonable default values for the pre-defined safety measures.

Even for pre-defined measures, parameters may be changed to fit the application context. For example, the cost of flattening an existing slope is heavily dependent on the ground conditions and available filling material, thus being very much dependent on the spatial setting of the implemented measure. Furthermore, safety effects may also be updated, as new results from before-after studies on Portuguese roads are obtained.

Crash Module

Crash prediction models (CPM) are used to estimate the expected number of crashes (four year periods), based on the assumption that road crashes are negative-binomially distributed. The number of RORIC and the total number of injury accidents are expressed as a function of traffic

volume (AADT) and the segment length. Based on crash data, the segment length was assumed to have a non-linear relation with the crash occurrence. Thus, the segment length is considered to be a covariate rather than considered as an offset. Separate equations were fitted for single and dual carriageway roads; these were further divided in two-lane carriageway roads and three or more lanes per carriageway roads.

CPM for the total number of injury crashes have the traditional multiplicative, monotonically increasing, functional form (see F1SCar curve in FIGURE 2), with the mean expected number of crashes per reference time period for segment i (λ_i) calculated by the following type of equation:

$$\lambda_i = \beta_0 \times AADT_i^{\beta_1} \times L_i^{\beta_3} \quad (1)$$

where

$AADT_i$ = Average Annual Daily Traffic in segment i ,

L_i = Length (in kilometers) of segment i – usually not more than 250 m for single carriageway and not more than 500 m for dual carriageway roads,

β_0 = intercept (to be estimated),

β_1 = coefficient associated with AADT (to be estimated),

β_3 = coefficient associated with L (to be estimated).

For RORIC, a different, non-monotonically increasing, functional form was adopted, which is more adapted to the logic variation of the crash frequency with changes in traffic, i.e., as traffic volume increases, after a certain point the number of opportunities for an injury departure diminishes – being null at congestion. The adopted modified Ricker model has an inverted “U-Shaped” curve (see the F2SCar curve in FIGURE 2), with the crash frequency increasing with AADT up to a critical value and then decreasing as AADT continues to increase, as depicted in FIGURE 2. The equations for RORIC have the following form (24):

$$\lambda_i = \beta_0 \times AADT_i^{\beta_1} \times e^{\beta_2 \times \frac{AADT_i}{10000}} \times L_i^{\beta_3} \quad (2)$$

Where the variables and parameter designations are the same as in equation (1), except for, β_2 = coefficient associated with $e^{AADT/10000}$ (to be estimated).

Models were developed for over 16 900 km of roads, using data from the four year period 2010-2014. Selected roadway data are presented in Table 1, for single carriageway and dual carriageway (two lanes per carriageway) highways,

Selected model parameters are presented in TABLE 2, where α corresponds to the dispersion parameter. A more detailed description of the developed models may be found in referenced published documents (19, 24).

CPM for dual carriageway roads with three or more lanes per carriageway have the traditional functional form because AADT values in the existing Portuguese segments are not sufficiently high to reach the point where crash frequencies start decreasing with the increase in AADT.

TABLE 1 Descriptive statistics of independent variables and crash data for road segments

Road category	Variable	Minimum	Maximum	Mean (Std. dev.)	Total
Single carriageway	Segment length (kilometers)	0.17	62.67	13.47 (8.70)	8189.21
	ADT (vehicles/day)	283	47900	6927.82 (6700.03)	-
	Total injury crashes	0	332	41.69 (46.16)	25350
	ROR injury crashes	0	129	11.07(11.54)	6733
Dual carriageway (2×2 lanes)	Segment length (kilometers)	0.31	33.28	5.66 (5.52)	4913.32
	ADT (vehicles/day)	1056	104778	16838.37 (17192.60)	-
	Total injury crashes	0	138	12.63 (15.74)	10967
	ROR injury crashes	0	76	5.86 (7.48)	5085

TABLE 2 Crash prediction models: selected statistics

Road category	Crash type	$\ln(\beta_0)$	β_1	β_2	β_3	α
Single carriageway	Total	-6.0436	0.874	-	0.882	0.379
	RORIC	-6.4682	0.811	-0.454	0.905	0.365
Dual carriageway (2×2 lanes)	Total	-7.4514	0.919	-	0.767	0.343
	RORIC	-9.9360	1.161	-0.410	0.847	0.411
Dual carriageway (2×3 or more lanes)	Total	-9.6593	1.146	-	0.894	0.405
	RORIC	-8.0796	0.880	-	1.035	0.449

The expected crash frequency in road segments under analysis is calculated using the CPMs mentioned in TABLE 2. When past accident frequencies are available for existing road segments being analyzed, the empirical Bayes method (25) may be used in SAFESIDE, to improve this estimation; in these cases, the software user is given the opportunity to enter crash data for the previous four-year period.

For the purpose of benefit-cost ratio estimations, it is assumed that the interventions affect in the same way the AADT developments over time and that there is no variation in the AADT resulting from the intervention. Thus, the number of crashes prevented by a safety intervention is estimated multiplying the average number of expected accidents by the crash modification factor of the analyzed safety intervention, through its whole useful life.

Accident costs are the sum of five main items: medical costs; loss of production; costs of property damage; administrative costs; and economic valuation of lost quality of life (21). Currently, there are no updated reference official values for crash costs in Portugal that might be used in roadside safety benefit-cost analysis, the last true research effort having been done in a

1995 update of values obtained in the late 1980's with 1987 data. Henceforth, the reference values used in the procedure are based on HEATCO European project (26) calculations, corresponding to benefits from casualties avoided. Correction factors for unreported crashes are also based on results from HEATCO (26).

Crash costs are calculated separately for total accidents and RORIC, in single and in dual carriageway roads. This is done multiplying the following three parts:

- The average number of participants in a crash, by type and severity level of injured victims, np_{tg} ;
- The costs of crashes for each severity level, $cost_g$;
- The respective correction factor for the number of unreported road crashes per crash severity level, cfu_g .

Then, the costs are summed up to obtain C_t^c , the crash cost for each type of crash. The following equation is used:

$$C_t^c = \sum_g (np_{tg} \times cost_g \times cfu_g) \quad (3)$$

Where t is crash type (RORIC in single or dual carriageway, total number of injury crashes in single or dual carriageway) and g is the injury severity level (fatal, severe and slight).

Police reports consider three levels of injury severity: fatality at the crash scene or during transport to hospital; severe injury, corresponding to victim's admission to hospital as in-patient (during 24 hours or more); slight injury, corresponding to treatment at the crash site or in hospital as an out-patient.

For each type of crash and road category, the corresponding costs are summed up to obtain the resultant value, as presented in Table 3. These average values are used in comparisons between different alternatives.

Ranking Module

The roadside safety evaluation model generates a benefit-cost ratio for each alternative road safety intervention under consideration. The implementation costs are entered and the software calculates the benefits for each alternative. This is done multiplying the estimated number of prevented crashes by their costs.

TABLE 3 Average Crash Costs, in Euros (2010 prices)

Road category	Crash type	Cost
Single carriageway	Total	108 617
	RORIC	96 157
Dual carriageway	Total	83 321
	RORIC	80 814

Following the calculation of the costs and benefits for each alternative intervention, the incremental benefit-cost ratios between each pair of safety alternatives (i and j) are then calculated using equation 3.

$$BCR_{ij} = \frac{B_i - B_j}{C_i - C_j} \quad (4)$$

Where BCR_{ij} is the Benefit-Cost Ratio of alternative i with respect to alternative j ; B_i and B_j are the net present value of the future benefits of alternatives i and j ; and C_i and C_j correspond to the net present value of future costs of alternatives i and j .

In addition, a sensitivity analysis may be performed by varying one variable at a time and determining the effect of that change on the net present value of each intervention. The following variables may be considered in the sensitivity analysis: investment costs, annual costs of operation and maintenance, average crash costs per crash, AADT, segment length, safety effects of each intervention, discount rate, and residual value of the investment. An absolute variation of 10% around the best estimate is used, except for the discount rate (which takes a 1% absolute variation) and the residual value of the investment (which is removed when the analysis of this variable is carried out). The general criterion adopted for the choice of the critical variables is to consider those variables or parameters with an elasticity that is unity or greater. This means that for these variables an absolute variation of 1% around the best estimate originates a corresponding variation of not less than 1% (one percentage point) in the net present value.

A detailed example of the application of SAFESIDE to a Portuguese road is presented in reference 19.

DISCUSSION AND FUTURE DEVELOPMENTS

Impact of the crash prediction model functional form

Using the modified Ricker non-monotonous functional form to estimate the “normal” expected RORIC frequency in a road class has some practical consequences that need to be highlighted.

Figure 2 presents the estimated number of RORIC in single (a) and dual (b) carriageway roads, as a function of AADT, as estimated using the traditional CPM’s functional form (F1) and the modified Ricker CPM functional form (F2). Curves for single carriageway roads refer to 250 m segments and those for dual carriageway roads refer to 500 m long segments. These are the values typically used for detecting high risk sites on those two types of road.

As expected, F1 curves show an increasing trend in the number of RORIC, with a rise in AADT values. The F2 curves show a different configuration: the number of RORIC and AADT values increase jointly up to a critical AADT value, which is an inflection point; afterwards, the number of RORIC drops as AADT values continue to rise. The critical value for single carriageway roads is roughly 16 000 vehicles per day; for dual carriageways it is 23 750 vehicles per day. For equal values of AADT up to the critical value, F2 estimated numbers of RORIC are slightly greater (up to +21%) than those estimated by F1. For AADT values greater than the critical value, the figures estimated by F2 are increasingly lower than those estimated by F1. At the top end of the CPM AADT validity spectrum, F1 estimates are more than twice those from F2 for single carriageway roads, and more than six times greater for dual carriageway roads.

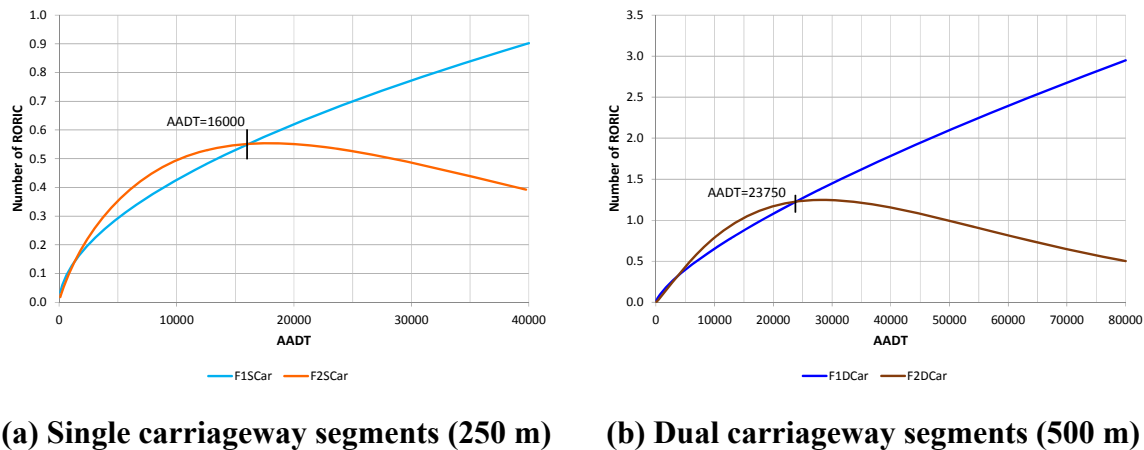


FIGURE 2 Comparison between estimated number of RORIC (4 years periods) with monotonic (F1) and non-monotonic forms (F2)

Therefore, the CPM traditional functional form grossly overestimates the “normal” expected number of RORIC on road segments with high AADT. This has implications for the identification of high risk sites and for the estimation of the benefits anticipated with road safety interventions.

When state of the art methods are applied to a given road class, high risk sites may be detected using a ratio (between the expected number of crashes at a site and the “normal” expected number of crashes on that road class) as a threshold. In this case, estimating “normal” RORIC frequencies as higher than they should be leads to selecting a lower number of detected sites that deserve further investigation. This biased selection affects especially those segments with higher AADT and moderate crash frequencies.

On the other hand, the valuation of benefits from road safety interventions with F1 type CPM is overestimated, as the basis for the safety level in the “before” situation is an overrated RORIC frequency estimation.

A practical example of the relevance of these two issues is presented below, using data from 3200 kilometers of Portuguese dual carriageway roads, mostly motorways, divided in 6521 segments. Less than 10% of these roads have AADT greater than 23750 vehicles per day. Crash data for the 2010–2014 four years period were used, totaling 3519 police registered RORIC.

The expected number of RORIC in each road segment was estimated by means of the empirical Bayes method, using the number of observed RORIC in the period and the CPM for this type of road. The CPMs for dual carriageway presented by Roque and Cardoso (24) in a previous paper were used in this comparison. Estimate F1 refers to the traditional functional form; estimate F2 refers to the modified Ricker model.

The “normal” number of RORICS in each segment was calculated by application of the corresponding CPM (F1 and F2) for this type of road.

High risk segments (HR) were detected using as criterion the ratio between the expected number of RORICS in a segment ($\lambda_i|x_i$) and the “normal” number of RORICS (λ_i) for this road category:

$$(\lambda_i | x_i) > a \times (\lambda_i) \quad (5)$$

Where a is the threshold value.

In this example, three values were adopted, to assess the sensibility to its parameter. The results obtained are presented in TABLE 4.

As expected, with model F2 more segments are labeled as potentially HR and the percentage of segments with AADT greater than 23 750 vehicles per day is also higher than in the case of model F1. The subset of RORIC potentially amenable for treatment is greater with F2 than F1. Furthermore, the application of F2 CPM in the estimation of the expected number of RORIC in the sites selected using F1 results in fewer numbers of RORIC than when F1 CPM is applied. This is an interesting result as it happens despite the fact that, for AADT bellow the critical value the F1 CPM calculates higher RORIC estimates than F2. These conclusions are applicable for all three tested threshold values.

In summary, overall the modified Ricker model provides more HR segments as promising sites for roadside safety improvement and a lower number of expected accidents to prevent, than the traditional multiplicative CPM. The roadside safety interventions' efficiency assessment is improved.

Integration in road safety management systems and further developments

As mentioned, the SAFESIDE procedure is currently used by road operators, both at the design stage and as an aiding tool for improving the road safety level at accident black spots and high risk sites.

Work towards its inclusion in infrastructure road safety management procedures and asset management policy unveiled new opportunities for improving ROR scenarios definition, resulting from image evidence of vehicle encroachment angles currently available at agencies' road inventories and even public warehouses (27). Vast amounts of images are produced and stored, namely by both pavement surface and road marking assessment systems, which are

TABLE 4 Comparison of practical application of traditional and modified Ricker functional forms in the detection of dual carriageway high risk segments

CPM type	High risk threshold ratio	+2	+3	+4
Modified Ricker (F2)	Number of HR sites	149	33	16
	HR sites with AADT > 23 750	44%	64%	63%
	Total expected RORIC – $\Sigma(\lambda_i x_i)$, using F2	420	147	90
Traditional multiplicative (F1)	Number of HR sites	131	24	10
	HR sites with AADT > 23 750	32%	38%	20%
	Total expected RORIC – $\Sigma(\lambda_i x_i)$, using F1	361	107	60
	Total expected RORIC – $\Sigma(\lambda_i x_i)$, using F2	275	89	43

available for off-line automatic processing by artificial vision algorithms. In this way, evidence of road departures may be detected and further processing allows for extraction of relevant parameters. These inventories and image warehouses (Figure 3) have the potential for facilitating the acquisition of improved understanding on the relations between features of common departure scenarios, road category and geometric design characteristics.

Within the scope of the integration of SAFESIDE in the Portuguese road administration infrastructure safety management system, it is envisioned to explore the joint analysis of RORIC crash frequency and severity, through multivariate models that accommodate the correlation of unobserved factors among crash counts by severity levels. This is now possible, due to the recent fusion of police and hospital data, achieved with the implementation of the 30 days fatality definition since 2010. Improved departure scenarios and enhanced modelling of RORIC severity outcomes are the envisioned immediate developments for SAFESIDE.

ACKNOWLEDGMENTS

The authors would like to thank the *Guarda Nacional Republicana* (GNR) for its cooperation in providing data on crashes and roadside characteristics used in this research.



FIGURE 3 Google Street View image with carriageway departure skid marks and evidence of restraint system substitution

REFERENCES

1. Adminaité, D., Jost, G., Stipdonk, H., Ward, H. *Ranking EU progress on road safety. 10th road safety performance index report*. European Transport Safety Council, Bruxelles, 2016.
2. Mohan, D., Tiwari, G., Khayesi, M., Nafukho, F.M. (2006). Road traffic injury prevention training manual. World Health Organization
3. Viner, J.G. .Risk of Rollover in Ran-Off-Road Crashes. *Transportation Research Record 1500*, 1995.
4. Sicking, D. L., Mak, K. K. *Improving roadside safety by computer simulation*. In *Transportation in the New Millennium: State of the Art and Future Directions*, Perspectives from Transportation Research Board Standing. TRB, 2001.
5. NHTSA. *Initiatives to address the mitigation of vehicle rollover*. National Highway Traffic Safety Administration, 2003.
6. Roque, C., Moura, F., Cardoso, J.L. Detecting unforgiving roadside contributors through the severity analysis of ran-off-road crashes. *Accident Analysis & Prevention 80*, 2015, pp. 262–273. DOI: <http://dx.doi.org/10.1016/j.aap.2015.02.012>.
7. ITF. Zero Road Deaths and Serious Injuries: Leading a Paradigm Shift to a Safe System, OECD Publishing, Paris, 2016. <http://dx.doi.org/10.1787/9789282108055-en>.
8. Hale, A., Kirwan, B., Kjellén, U. Safe by design: where are we now? *Safety Science 45*, 2007, pp. 305–327. DOI: <http://dx.doi.org/10.1016/j.ssci.2006.08.007>.
9. Donnell, E. T., Mason Jr., J. M. Predicting the frequency of median barrier crashes on Pennsylvania interstate highways, *Accident Analysis & Prevention 38 (3)*, 2006, pp. 590-599
10. AASHTO. *Roadside Design Guide*, fourth ed.. American Association of State Highway and Transportation Officials, 2011.
11. Mak, K.K., Sicking, D.L., Zimmerman, K. Roadside Safety Analysis Program: A Cost-Effectiveness Analysis Procedure. *Transportation Research Record No. 1647*, 1998, pp. 67-74.
12. Mak, K.K., Sicking, D.L. *Roadside Safety Analysis Program (RSAP), Engineer's Manual*, National Cooperative Highway Research Program Report 492. Transportation Research Board, Washington D.C., 2003.
13. Ray, M.H., Carrigan, C.E., Plaxico, C.A., Miaou, S.P., Olaf Johnson, T. *NCHRP 22-27 Roadside Safety Analysis Program (RSAP) Update*. RoadSafe LLC, Final report: RSAP. Version 3.0.0, 2012.
14. La Torre, F., Erginbas, C., Williams, G., Thomson, R., Hemmings, G., Stefan, C.. *Guideline for the selection of the most appropriate Roadside Vehicle Restraint System*. Deliverable of SAVeRS-Selection of Appropriate Vehicle Restraint Systems, 2015.
15. La Torre, F. (2012). Forgiving roadsides design guide. CEDR report 2013/09, Paris, France
16. Roque, C.; Cardoso, J.L. *Sistemas de retenção rodoviários. Manual de aplicação*. ('Road restraint systems. Guidelines for their selection and installation', in Portuguese) Study to the *Instituto de Infra-estruturas Rodoviárias, I.P.* Report LNEC 382/2010, Lisboa, 2010. (<http://www.imtt.pt/sites/IMTT/Portugues/InfraestruturasRodoviaras/InovacaoNormalizacao/Divulgao%20Tcnica/SistemasRetencaoRodoviaros.pdf>).
17. Roque, C.; Cardoso, J.L. *Área Adjacente à Faixa de Rodagem. Manual sobre aspectos de segurança* ('Roadside. Manual for safe design', in Portuguese). Study to the *Instituto de Infra-estruturas Rodoviárias, I.P.* Report LNEC 199/2011, Lisboa, 2011. (<http://www.imtt.pt/sites/IMTT/Portugues/InfraestruturasRodoviaras/InovacaoNormalizacao/Divulgao%20Tcnica/Manual+sobre+Aspectos+Seguran%C3%A7a+AAFR-SEC.pdf>).
18. Roque, C.; Cardoso, J.L. *Procedimento de avaliação de alternativas de intervenção / Procedure for evaluating safety interventions. 5th SAFESIDE Report* (In Portuguese). Fundação para a Ciência e Tecnologia, LNEC, Lisboa, 2012.
19. Roque, C., Cardoso, J.L. SAFESIDE: A computer-aided procedure for integrating benefits and

- costs in roadside safety intervention decision making, *Safety Science*, Volume 74, 2015, pp. 195-205, ISSN 0925-7535, <http://dx.doi.org/10.1016/j.ssci.2015.01.001>.
20. AASHTO. *Highway Safety Manual*. American Association of State Highway and Transportation Officials, 2010.
 21. Elvik, R.; Høye, A.; Vaa, T. and Sørensen, M.. *The Handbook of Road Safety Measures*. Second Edition. Emerald, Bingley, 2009. ISBN: 978-1-84855-250-0.
 22. FHWA. *Toolbox of Countermeasures and Their Potential Effectiveness for Roadway Departure Crashes*. Publication N°. FHWA-SA-07-013. U.S. Department of Transportation. Federal Highway Administration, Washington, D.C., 2008.
 23. Elvik R. Road safety management by objectives: A critical analysis of the Norwegian approach. *Accident Analysis and Prevention* 40, 2008, pp.1115–1122.
 24. Roque, C., Cardoso, J.L. Investigating the relationship between run-off-the-road crash frequency and traffic flow through different functional forms. *Accident Analysis & Prevention*, 63, 2014, pp.121-132. <http://dx.doi.org/10.1016/j.aap.2013.10.034>.
 25. Hauer, E. *Observational Before–After Studies in Road Safety*. Pergamon, Oxford, UK, 1997. ISBN 0-08-043 053 8.
 26. HEATCO. *D5 - Developing Harmonised European Approaches for Transport Costing and Project Assessment*, Deliverable 5 - Proposal for Harmonised Guidelines, February, 2006.
 27. Roque, C.; Cardoso, J.L. *Integrating large samples of errant vehicles encroachment angles from google street view in a roadside safety assessment framework*. 5th International Symposium on Highway Geometric Design, Vancouver, Canada, 2015.

Road Safety Audit and Proposal for Corridor Extension Plan *Case Study Barapullah Corridor, New Delhi, India*

NAMIT KUMAR
MUKESH KUMAR
RITES Ltd.

Delhi, the Capital of India, has become an important centre for international events and is home to over 7 million vehicles, including 2 million cars and an equal number of motorcycles. Also, the large number of signalized intersections in the city has led to excessive travel time and fuel consumption leading to a loss of almost 420 million man-hours every month while commuting between home and office through public transport, due to the traffic congestion and road accidents.

Barapullah elevated corridor having a length of about 4.4 km (Phase-I) was constructed and used as an exclusive corridor for the sports personnel between the Games village to the Jawahar Lal Nehru (JLN) Stadium in New Delhi during Commonwealth Games, 2010 and was taken as the case study for this project. The corridor was opened to public post Commonwealth Games in October 2010 and aimed to provide an efficient connectivity to the commuters passing through busy Lala Lajpat Rai road and Mathura road connecting the Ring road.

This study focuses on Road Safety Audit (RSA) for Post-opening Stage of the Barapullah elevated corridor which is a vital tool for safety management system alongside the proposal to extend the corridor for east – west connectivity to ease the traffic flow in Delhi. The main objective is to identify potential safety problems and to suggest measures to mitigate them. RSA is a vital tool of safety management system and makes it necessary for the corridor to be safety conscious when planning, designing, constructing, maintaining and operating road & traffic systems.

The RSA for Post-opening Stage conducted on the Barapullah corridor confirm the issues of lack of traffic control devices and markings on the corridor. The survey data assessed for the Spot speed analysis illustrates a lower rate of lane utilization of the corridor for movement in both directions. While moving from Sarai Kale Khan towards JLN Stadium, theoretical frequency in the normal distribution curve computes to 40.7% for a speed of 40 km/h, while theoretical frequency in the reverse direction computes to 40.32% for a speed of 50 km/h. The cumulative frequency curve illustrates the peak at a speed of 55 km/h in both directions of traffic. Thus, the survey result exemplifies the movement of low traffic volume at high speed on the corridor due to its limited connectivity. Hence, to increase the lane utilization, augmentation of the corridor is required at both approaches to enlarge the east – west connectivity in the city.

Seeking the issue, an extension of Barapullah corridor towards Mayur Vihar in the east and Karol Bagh & Janakpuri in the west was proposed as an elevated corridor. It was designed to entice traffic for achieving lane utilization and to provide direct access from east to west of the city via the proposed route. This will also effect in providing an analogous corridor to the Ring road in the city and reduce the excessive traffic volume on it. After proposing the extensions to the Barapullah corridor in east and west directions, it was analyzed that the travel time for commuters will reduce from 60 mins to 25 mins, saving about 35 mins respectively.

INTRODUCTION

India is a rapidly growing developing country of South Asia in terms of urbanization and economic growth. There were about 9,391 towns/cities and 31% of urbanization in 2011 which is estimated to grow up to 50% by 2039 as per Census of India, 2011. Urban India presently contributes 63% of India's Gross Domestic Product (GDP) and it has estimated to grow up to 75% by 2021 (Barclays Equity Research Report 2014).

Congestion causes a severe crisis on road as the traffic in a city grows rapidly in developing countries like India. Steep rise in vehicular growth in most of the cities in India have been due to accelerated economic development in the country resulting in severe traffic congestion and haphazard movement on the road network. The rapid growth of large cities is primarily due to the growth in the population coupled with the increase in urbanization, representing a serious challenge in terms of development of adequate infrastructure facilities. Travel demand has risen sharply, exceeding the available supply in transportation infrastructure and services. All the Indian cities, irrespective of their sizes and forms, are suffering from severe traffic and transportation problems. Transport infrastructure of these cities has not grown commensurate with its demand. As a result of the rapid growth in motorization, most of the cities are suffocated with severe traffic congestion along with significant rise in the road traffic accidents.

As per the Ministry of Road Transport and Highways (MoRTH), the numbers of motorized Vehicles have increased from 21 million in 1991 to 142 million in 2011 in India, registering nearly 10% increase every year. The over-concentration of vehicles, notably in metropolitan cities, is one of the major problems in the cities. According to the Basic Road Statistics 2011, the urban street length went up from 123,120 km in 1981 to 411,840 km in 2011 viz an increase by 3.35 times. Vehicles per million population have expanded by 219% while urban streets for every million of vehicles have expanded by just 124%, in the most recent decade. The street space for vehicles has diminished (from 0.18 km for each vehicle to 0.01 for every vehicle) in the most recent couple of decades, resulting in high level of congestion in all urban areas.

Delhi, the Capital of India, the largest democracy of the world, has become an important centre for international events thus desiring a continued and sustained effort to maintain the transport system most effective, direct and fast at internationally acceptable standards.

Delhi is located at 28.61°N 77.23°E, and lies in Northern India. It borders the Indian states of Haryana on the north, west and south and Uttar Pradesh (UP) to the east. The total area of the National Capital Territory of Delhi is 1483 km². It has a length of 51.9 km (32 miles) and a width of 48.48 km (30 miles). Due to rapid pace of urbanization, landscape of Delhi has undergone a shift from majority of rural areas into urban. Delhi is rapidly urbanized in last three decades from 685.34 km² in year 1991, 924.68 km² in year 2001 to 1113.65 km² in year 2011.

Delhi is home to over 7 million vehicles, including 2 million cars and an equal number of motorcycles. Based on existing situations and trend Delhi will grow by more than 22 million people and over 8 million vehicles by 2021. Thus, there is an imbalance between the demand & supply. An estimated 1,200 vehicles are added to its roads each day. The urban road system of Delhi has historically emerged on a ring and radial pattern. The total length of roads is around 29,000 km, which has increased almost three times since 1971-72 comprising of ring and radial pattern. These radial and ring roads serve as major arterials, which carries bulk share of traffic in the city. During morning and evening peak hours, 55 to 60% of the major arterials have travel

speeds less than 30 km/h, while even in off peak hours, 40 to 45% of major arterials have travel speeds less than 30 km/h. The overall capture of public transport services in the city is only 60% of the total trips, of which, the metro currently accounts for 15%. The large number of signalized intersections in the city has led to excessive travel time and fuel consumption due to the traffic congestion leading to a loss of almost 420 million man-hours every month while commuting between home and office through public transport. The road network of Delhi has increased from 32,131 lane-km in 2007-08 to 33,198 lane-km and additional 62 km flyovers in 2014-15.

Due to this vast urbanization, Delhi has significantly relied on its transport infrastructure. Delhi has developed a highly efficient transport system with the introduction of Delhi Metro, which is undergoing a rapid modernization and expansion. The people of Delhi lose a large number of man-hours while commuting by road due to traffic congestion. Therefore, the efforts to improve the ring and radial roads in Delhi were directed towards capacity augmentation, segregation of pedestrians and vehicular traffic, strengthening of roads, flyovers, spot improvements of junctions etc. With a significant increase in the vehicle ownership levels of the city, Ring Road, Arterial Roads and Outer Ring Road are congested for most of the hours of the day and there is an established need to divert the vehicular traffic by providing additional length of the road.

Accordingly, in line with the sustained development of Delhi, Delhi Government provided fast and reliable access along Barapullah Nala connecting south eastern and south western part of the city, the Barapullah elevated corridor. It was constructed and was used as an exclusive corridor for the sports personnel between the Games village and Jawahar Lal Nehru (JLN) Stadium during Common Wealth Games, 2010. The project aimed to provide an efficient connectivity to the commuters passing through busy Lala Lajpat Rai road & Mathura road and connecting Ring road. The elevated corridor of about 4.4 km starts from Sarai Kale Khan to Jawahar Lal Nehru Stadium in phase – I and extends further from JLN stadium to INA market in Phase-II which is under construction and in Phase-III it stretches from Sarai Kale Khan to Mayur Vihar.

The major issues on Delhi's road network are:

- Rapidly increasing number of vehicles on the network
- Narrow roads, poorly designed road & intersections, encroachment on roads and haphazard on-street parking
- Chronic congestion on ring road
- Heterogeneous traffic, old (poorly maintained) vehicles
- Lack of facilities for pedestrian, pedestrian crossing, poor maintenance of foot over bridge, and footpath
- High rate of road accidents especially among the pedestrian and motorized vehicles

Along with the above issues, Road safety is a major concern in India where 0.5 million accidents occurred in 2011, injuring 0.5 million people and claiming lives of 0.14 million people, according to a report by the Ministry of Road Transport and Highways. Road fatality rates in India are probably among the highest and out of 1.25 million deaths worldwide every year, 8-10 percent of all road deaths are in India. Road safety is a multidisciplinary multi sector problem and is now recognized as a major socio economic concern. It refers to methods and measures for reducing the risk of a person using the road network being killed or seriously injured. Road users include pedestrians, cyclists, motorists, passengers of public transport, mainly buses. A large

number of accidents are caused by driver errors. The purpose of road safety strategies focus upon the reduction in the occurrence of an accident and the prevention of serious injury and fatalities. The most effective way of improving road safety is to have the key agencies in each country collaborate and implement a coordinated action plan and to carry out road safety audits at different stages of construction.

The subsequent paragraph's of the paper focuses on the need for road safety, features of road safety audit conducted on the Barapullah corridor Phase-I, corridor extension plan of Barapullah corridor towards east and west directions and conclusion.

NEED AND OBJECTIVES

There are numerous grade-separated infrastructure built on Ring road to de-congest it. In spite of diverse efforts, major areas of South Delhi viz. Maharani Bagh, Ashram, Lajpat Nagar & South Extension still remains clogged. As per National Capital Region Planning Board Report (NCRPB), the projected traffic is estimated at about 400,000 PCU/day by 2021 (Passenger Car Units (PCU)). The section from Ring road – Bhairon Marg and Mathura road ROB experiences traffic of about 117,900 PCU/Day and 110,000 PCU/Day during peak hour. The Barapullah elevated corridor was constructed as an analogous road to the Ring road to provide access from Common Wealth Games Village to Jawaharlal Nehru Stadium.

The increasing number of road fatalities is a pointer towards improvements required to enhance the safe design and construction of roads. Road safety is an issue of immense human importance which affects people socially and economically. An urban road safety management strategy and road safety audit thus is necessary which focuses on reducing the number and severity of road accidents within the context of development and transport goals of local authority.

Given the impression of Ring road running to its capacity and traffic speeds hindered, there is a need to intend the extension of Barapullah elevated corridor towards Mayur Vihar in East and Dhaula Kuan in the west to decongest the Ring road along with Road Safety Audit of the existing Barapullah elevated corridor.

The major objectives of the Study are:

1. To conduct road safety audit of Barapullah Elevated Corridor Phase-1
2. To propose an extension for providing east – west connectivity in Delhi (India) to reduce congestion and to save travel time

STUDY AREA

Barapullah drain, close to Humayun's Tomb with an average width of 70 meters, covers an area of 9.60 ha. This drain collects the discharge of other internal, peripheral and trunk drains to further discharge its contents- 125,000 KLD (Kilo Litres per Day) of domestic sewage into the Yamuna river. The Barapullah elevated corridor of 4.4 km from Sarai Kale Khan to Jawahar Lal Nehru Stadium (as shown in Figure 1) was constructed over the drain over a period of 20 months in September 2010 at a cost of INR 5000 million by DSC Limited. The Barapullah elevated corridor was meant to provide unhindered access from Common Wealth Games Village to



FIGURE 1 Barapullah Elevated Corridor Phase-I

Jawaharlal Nehru Stadium to about 10,000 athletes and was opened to public after Common Wealth Games in October 2010. The areas along the BarapullahNalla include INA, Seva Nagar, JLN Stadium, CGO complex, Jangpura, Nizammuddin, Siddhartha Extension and Sarai Kale Khan Village. It is reported to cater to about 60,000 vehicles/day. This corridor was built to cut down travel time and decongest Ashram Chowk, Bhairon Road, Lajpat Nagar, Ring Road and South Extension and also promises direct travel as compared to Delhi metro.

The long corridor from Ring Road (Sarai Kale Khan) to Aurobindo Marg (Delhi Haat) is planned to be constructed in different phases. Phase-I from Sarai Kale Khan to JLN stadium. Phase-II of the project extends the elevation of stretch from JLN stadium till Aurobindo Marg near INA market. Phase-III of the project extends the road towards Mayur Vihar. The slip roads connecting with the Lala Lajpat Rai Marg, just next to Jungpura, benefits the motorists heading towards Lajpat Nagar, Defence Colony, Greater Kailash and South Extension areas and reduces the pressure on Maharani Bagh and Ashram stretch of Ring Road, which witnesses bumper-to-bumper traffic in the peak hours. The Figure 2 shows the Barapullah Bridge and site appreciation images of the existing Barapullah corridor Phase-I.

ROAD SAFETY AUDIT

Road Safety Audit (RSA) is a systematic procedure that brings traffic safety knowledge into the road planning and design process to prevent accidents. It is a systematic and formal safety performance examination of a road project. The aim of safety audit is to ensure that all new road schemes and major existing roads are subjected to Road Safety Audit so that the roads can operate as safely as possible. RSA helps in implementing speed measures, minimize risk and severity of accidents, improve the level of awareness of safe design practices involved in planning, design, construction, maintenance and operation of roads. Road safety audit can be done in various stages:



FIGURE 2 Site Appreciation of Barapullah Elevated Corridor

- Planning/ feasibility stage
- Preliminary design stage
- Detailed design stage
- Construction phase
- Post opening stage, existing roads

The main aim of road safety audit is to ensure that all new road schemes operate as safely as practicable. Specific aims of RSA are:

- To minimize the risk of accidents likely to occur/occurring on the project facility and to minimize their severity.
- To minimize the risk of accidents likely to occur/occurring on adjacent roads i.e., to avoid creating accidents elsewhere on the adjoining of road network.
- To recognize the importance of safety in road design to meet the needs and perceptions of all types of road users; and to achieve a balance between needs of different road user types where they may be in conflict with one another.
- To reduce long-term costs of a project facility, bearing in mind that unsafe designs may be expensive or even impossible to correct at a later stage.
- To increase awareness about safe design practices among all those involved in the planning, design, construction and maintenance of roads. Road safety audits assess the operation of a road, focusing on road safety as it affects the users of the road. These users include

pedestrians, cyclists, motorcyclists, truck/bus drivers, on-road public transport users, etc. The outcome of a road safety audit is the identification of any road safety deficiencies and formulation of recommendations aimed at removing or reducing those deficiencies.

NECESSITY OF ROAD SAFETY AUDIT

- **Compliance with standards does not guarantee safety** – although conformity with standards and guidance is helpful for safety, there will be many situations that are not covered by the standards – and sometimes a number of individual elements, all designed to standard, may, when combined, be unsafe;
- **Safety can be unduly compromised in the trade-off** between conflicting requirements - it Can be difficult for highway designers to produce a design that meets all the project objectives, and sometimes safety is neglected;
- **Lack of knowledge of crash causation** - highway designers may not have the necessary Understanding of human-vehicle-road interactions to be able to detect potential safety problems.

DOCUMENTS USED FOR AUDIT

- i. IRC:SP: 88-2010 (Manual on Road Safety Audit)
- ii. IRC:35-1997 (Code of practice for Road Markings)
- iii. IRC:67-2012 (Code of practice for Road Signs)
- iv. Other relevant IRC, IS and BS Codes as applicable

ROAD SAFETY OF BARAPULLAH ELEVATED CORRIDOR PHASE-I

Audit Coverage

As per the National Highway Authority of India (NHAI), it is mandatory to conduct safety audit for all stages for the National Highways only. Since, there are no such guidelines available for the safety audit of urban roads in India, therefore, the IRC code of practice viz. IRC:SP:88-2010 was referred to audit the Barapullah elevated corridor. According to IRC:SP:88-2010 it was recommended to conduct Post Opening stage audit (Stage-6) on existing roads. The checklist for audit covers the elements of present condition of the road after opening for public use as well as any hazardous conditions that may have been created during its lifetime such as inappropriate road marking, location of signage's in line of sight or deterioration of road conditions as well as traffic conditions, etc. Post Opening stage audit is important to check the location and visibility of marking and other traffic control devices.

Audit Findings and Recommendations

Since, it an existing six lane divided elevated corridor, an overall examination is carried out to audit the safety measures with respect to the applicable IRC codes of practice. The audit findings are as follows:

- Types of Signages placed as per applicable guidelines
- Informatory Signage at few located are not visible due to obstacles
- Road markings are as per guidelines
- Continuous guard is provided
- Sight distance at curved section are complied as per guidelines
- Undulated road surface leads to bad driving comfort
- Consistent width of carriageway available
- Well placed traffic control devices
- Crash barrier at few location is damaged

SPOT SPEED ANALYSIS

The table 1 below explains the theoretical frequency and figure-3 illustrates the normal distribution curve while moving from Sarai Kale Khan towards JLN Stadium.

CORRIDOR EXTENSION PLAN

The extension of Barapullah corridor Phase-I towards East and West Delhi is being proposed to increase the utilization of Barapullah corridor and also to provide direct connectivity from Mayur Vihar and NOIDA towards Dhaula Kuan and Karol Bagh via the proposed route. The proposal in both the directions aims to reduce the travel time of commuters by almost half of the present.

TABLE 1 Frequency Analysis

Upper Speed limit (in km/h)	Theoretical frequency (in %)	Observed frequency (O)
20	2.62	0
30	17.71	15
40	40.7	59
50	30.59	12
60	7.76	14
Total	99.38	100

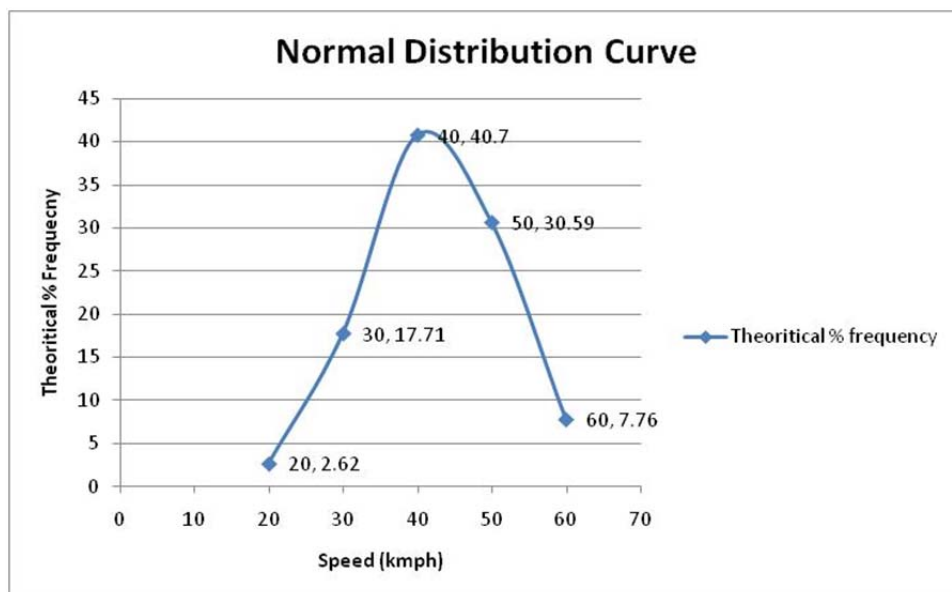


FIGURE 3 Bell curve analysis.

Proposal Towards East Delhi

The figure-4 exhibits the connectivity of Barapullah Corridor towards East Delhi (Mayur Vihar, Lakshmi Nagar, Geeta Colony, etc.) and NOIDA. A two lane (7m) two way link road has been proposed from the existing Barapullah corridor to the Delhi - NOIDA Direct (DND) expressway. The proposed links are 0.62 km in length and are proposed at a height of 6.5m. The alignment consists of 2 simple curves in each link, 511.29m and 218.27m from Barapullah corridor towards DND and 408.30m and 556.60m in the vice-versa direction. The ramps in the proposed links have a slope of 1:33 and also consist of lamp posts at distance of 30m each along with the road markings and signages.

Proposal Towards West Delhi

The figure-5 demonstrates the connectivity from Barapullah Corridor towards West Delhi in the Upper Ridge area providing connectivity to Dhaula Kuan and Karol Bagh. A six lane divided carriage way of 7.4 kms in length and at a height of 6.5m has been proposed. The alignment consists of six simple curves as shown in table-2.

The extended section of Barapullah towards Dhaula Kuan covers major residential and commercial zones of West Delhi. The extended alignment in the west direction originates from JLN stadium and covers INA Colony, Lakshmi Bai Nagar, Chanakyapuri etc.

TABLE 2 Details of Simple Curves

Chainage (in m)	Location	Type of Section		Type of Land Use (in 100m Strip)	
		Straight (in m)	Curve (in m)	Left	Right
0-1000	Delhi drain – Najafkhan's Tomb (along the Railway line)	786	214	Residential (INA Colony)	Residential (Lodhi Colony)
1000-2000	Najafkhan's Tomb - Lakshmi Bai Nagar (along the Railway line)	1000	0	Residential (Lakshmi Bai Nagar)	Airport
2000-3000	Chanakyapuri - Nehru Park (along the drain line)	855	145	Residential (Chanakyapuri)	Airport
3000-4000	Nehru Park – KautalayaMarg (along the drain line)	675	325	Commercial (Hotel Ashoka)	Residential/ Commercial
4000-5000	Karnataka House – NyayaMarg (along Embassy Area)	624	376	Residential/ Public (Embassy area)	Residential/ Public (Embassy area)
5000-6000	NyayaMarg - Sardar Patel Marg (along Embassy Area)	510	490	Residential/ Public (Embassy area)	Forest area
6000-7000	Sardar Patel Marg – Ridge area	650	350	Forest area	Forest area
7000-7500	Ridge area	500	0	Forest area	Forest area

CONCLUSION

The RSA for Post-opening Stage conducted on the Barapullah corridor conform the safety measures adopted irrespective of qualitative values for the vulnerable road users. The survey data assessed for the Spot speed analysis illustrates lower rate of lane utilization of the corridor for movement in both the directions. While moving from Sarai Kale Khan towards JLN Stadium, theoretical frequency in the normal distribution curve computes to 40.7% for a speed of 40 km/h, while theoretical frequency in the reverse direction computes to 40.32% for a speed of 50 km/h. The cumulative frequency curve illustrates the peak at a speed of 55 km/h in both directions of traffic. Thus, the survey result exemplifies the movement of low traffic volume at high speed on the corridor due to its limited connectivity. Hence, to increase the lane utilization; augmentation of the corridor is required at both approaches to enlarge the east – west connectivity in the city. Presently, the time taken to travel from Mayur Vihar on the east and Karol Bagh & Janakpuri on the west of the city, a distance of about 15 Km is 60 mins (approximately).

Seeking the issue, an extension of Barapullah corridor towards Mayur Vihar in the east and Karol Bagh & Dhaura Kuan in the west was proposed as an elevated corridor. It was designed to entice traffic for achieving lane utilization and to provide direct access from east to west directions of the city via the proposed route. This will also effect in providing an analogous corridor to the Ring road in the city and reduce the excessive traffic volume on it. Also, since

heavy commercial vehicles like trucks are not allowed on the corridor making it safe for the 2-wheelers and 4-wheelers to travel on the corridor. After proposing the extensions to the Barapullah corridor in east and west directions, it was analyzed that the travel time for commuters will reduce from 60 mins to 25 mins, saving about 35 mins respectively.

The proposed East-West connectivity of Delhi through Barapullah corridor shall also come as a relief to tourists who travel to nearby tourist destinations such as Agra, Mathura, Vrindavan, Meerut, etc. from hotels around Connaught Place, Karol Bagh and Sardar Patel Marg, etc.

REFERENCES

1. ADB (June, 2003), Road Safety Audit for Road Projects: An Operational Toolkit, Asian Development Bank, Manila. ‘
2. “Road Safety Audit in India”, L. Ajit Kumar, Santosh A. Jalihal, Frischmann Prabhu (India) Pvt. Ltd., Mumbai, 2011 in International Seminar on National Road Development Strategies & Road Safety on Improved Highways, School of Planning and Architecture, New Delhi, India, 14-19 March 2011.
3. SPA (2002) , Pedestrian Behaviour and Road safety : Case Study Delhi, unpublished thesis, Department of Transport Planning, School of Planning and Architecture, Delhi.
4. SPA (2005), Design Stage Road Safety Audit: Case Study – IT Expressway Corridor, Chennai, unpublished thesis, Department of Transport Planning, School of Planning and Architecture, Delhi.

Roadside Safety Hardware Framework Concept for Enhanced In-Service Performance Evaluation and Asset Management Practices

CHARLES R. STEVENS JR.

Texas A&M Transportation Institute

Developing a common framework for roadside safety hardware can provide a reference to aid planning, defining and evaluating the success of roadside safety devices. To accomplish this the Texas A&M Transportation Institute Center for Transportation Safety funded an investigation of common institutional interactions, in-service performance evaluation practices (ISPE), safety hardware asset management practices (and identification methods), and the general life cycle of safety hardware. From this study of literature and talking to experts from industry and academia, researchers developed a multi-level conceptual framework including an institutional level, information level, and systems level.

The high level institutional level will aid in formalizing the known roles of institutions, policies, funding mechanisms and processes as required for effective manufacturing, testing, installation and maintenance.

The information level framework will define necessary information standards, its flow from collection to terminus, and the particular data analysis components necessary to validate effectiveness in manufacturing, installation and maintenance including and pre- and post-crash performance.

The systems level will create the foundation for the development of universal standard roadside safety hardware “packages”, which can provide for a common naming convention and aid in, technology transfer and training opportunities (installation), in-service performance evaluation standards and asset management practices. Among the many areas this standardization could be useful; one particular area with the most potential is with the advancement and trending practice of hardware identification for asset management, monitoring and tracking.

The vision of a common framework affords the roadside safety practice area with a flexible tool for documenting and understanding institutional relationships, data needs and processes, and universal roadside safety hardware “packages”. This potential concept paper or presentation will discuss the relationships between the three layers and provide an example for each layer for discussion and further development.

Safe System Assessments of Roadside Safety Projects

JAMIE ROBERTSON

KENN BEER

Safe System Solutions Pty Ltd

DANIEL CASSAR

Victorian Roads Corporation

Safe System principles are an accepted part of road safety strategies in Victoria, Australia. The underpinnings are that humans are fallible and will inevitably make mistakes when driving, riding, or walking. Nevertheless, road trauma is not inevitable. No one should be killed or seriously injured on our roads. Consequently, to prevent serious trauma, the road system must be forgiving, so that collision forces do not exceed limits that the human body can tolerate. At a national level, the Australian Government has committed to the Safe System.

In recent years, translating the agreed philosophical aspirations of the Safe System into practical application has been challenging. Also, assessing a project's alignment with Safe System principles has caused much debate and consternation.

A key change in thinking has been that a hazard free and driveable roadside (clear zone) is less likely to reduce the likelihood of fatal or serious injuries when compared to shielding the entire roadside with continuous safety barrier treatments. This paper examines the concept of a "Safe System compliant" roadside and reflects on the site-specific constraints that have influenced the use of safety barriers in the projects assessed.

In February 2016, Austroads (the association of Australian and New Zealand Road Transport and Traffic Authorities) published *AP-R509-16 Safe System Assessment Framework* to provide guidance in assessing a project's alignment with the principles of the Safe System approach.

This paper reviews the application of this framework draws on case studies of three significantly different roadside safety projects which have sought to incorporate Safe System principles.

INTRODUCTION

The Safe System/Towards Zero

The Safe System road safety vision is internationally regarded as the most appropriate path to dramatically reduce road trauma (Figure 1). Sometimes referred to as Towards Zero or Vision Zero, because it seeks to reduce fatalities and serious injuries to zero, it is based on the successful and ambitious road safety visions of Sweden and the Netherlands, which are consistently the best performing road safety countries. The Safe System/Towards Zero vision has been embraced by the TRB with the adoption of the Vision Towards Zero Deaths subcommittee, with the aim to provide "transportation safety management systems that result in zero fatalities and serious injuries on the nation's roadways" (1).

Safe System principles are an accepted part of road safety strategies in Victoria, Australia. The underpinnings are that fallible humans will inevitably make mistakes when driving, riding, or



FIGURE 1 The Safe System/Towards Zero.

walking. Nevertheless, road trauma is not inevitable. No one should be killed or seriously injured on our roads. Consequently, to prevent serious trauma, the whole road system must be forgiving, so that collision forces do not exceed limits that the human body can tolerate. At a national level, the Australian Government has committed to the Safe System.

The Safe System consists of four core interrelated components: safer roads, safer speeds, safer vehicles and safer people. A fifth component is also emerging in the area of post-crash response. It is a well-known principle that has been philosophically adopted by road authorities such as VicRoads (state of Victoria road agency). Translating the principles into practice has been challenging – because application of the principles requires thinking and innovation outside normal practice and current infrastructure guidelines. Safe System Assessment is one tool being used by road authorities, including VicRoads, to translate Safe System principles into practice.

A Safe System Assessment is the formal safety examination of a road-related project, program or initiative such as:

- A road investment project, whether at feasibility, design or pre-opening stage;
- An existing road, intersection or length;
- A community road safety program or funding application; or
- A road transport policy or strategy.

The aim of a Safe System Assessment is to help road agencies and practitioners methodically consider Safe System objectives in road infrastructure projects. The Austroads Safe System Assessment Framework (2) is useful in assessing how closely road design and operation

align with the Safe System objectives, and in identifying elements that would need to be modified to achieve closer alignment with objectives. Road safety treatments are classified into four categories:

1. **Primary Treatment:** Road planning, design and management consideration that virtually eliminates the potential of fatal or serious injuries occurring in association with the foreseeable crash types (eg. continuous flexible barriers at an appropriate setback from traffic lanes).
2. **Step Towards:** Road planning, design and management considerations that improve the overall level of safety associated with foreseeable crash types, but not expected to virtually eliminate the potential of fatal or serious injuries occurring. When applied to an existing road environment, they improve the ability for a Primary Treatment to be implemented in the future (eg. a wide central painted median of adequate width to allow future application of safety barrier).
3. **Supporting Treatments:** Road planning, design and management considerations that improve the overall level of safety associated with foreseeable crash types, but not expected to virtually eliminate the potential of fatal or serious injuries occurring. When applied to an existing road environment, they do not change the ability for a primary treatment to be installed in the future (eg. audio-tactile edge lines on a high-speed road).
4. **Non-Safe System Treatment:** Road planning, design and management considerations that are not expected to achieve an overall improvement in the level of safety associated with foreseeable crash types occurring, or when applied to an existing road environment, they reduce the ability for a primary treatment to be installed in the future (eg. conventional at-grade intersections with potential for transverse vehicle impacts).

Safe System Assessments distinctly go beyond the work of a Road Safety Audit at the early stage of a project. A Road Safety Audit qualitatively estimates and reports on potential road safety issues against current standards and guidelines but only identifies opportunities for improvements in safety in this 'limited' perspective, however a Safe System Assessment measures compliance with Safe System principles which can, and does, push outcomes to a higher level – while at the same time considering realistic constraints.

VicRoads has worked with Safe System Solutions Pty Ltd to undertake a number of Safe System Assessments of infrastructure projects the results of which will be described in this paper.

ASSESSMENT METHODOLOGY

The Safe System Assessment methodology involves identifying the key crash types that result in death and serious injury, and using a risk assessment approach to identify elements that might contribute to fatal or serious injury outcomes. These key crash types are run-off-road, head-on, intersection, other (including rear end) and vulnerable road user (pedestrian, cyclist and motorcyclist) crashes. Slightly different to traditional risk (likelihood x severity), the risk elements considered include road user exposure to risk (e.g. traffic volumes), likelihood of a crash, and the likely severity outcome in the event of a crash. The framework includes consideration of all elements of the system, including an assessment of issues relating to the road and travel speeds, road user issues, vehicle-related issues and post-crash care.

Exposure, likelihood and severity are defined in the Austroads Safe System Assessment

Framework (2) as follows:

1. **Road user exposure:** this refers to which road users, in what numbers and for how long are using the road and are thus exposed to a potential crash. The measures of exposure include: AADT, side-road traffic volumes, number of motorcycles, cyclists and pedestrians crossing or walking along the road, length of the road, area and length of time.
2. **Crash likelihood:** groups of factors affecting the probability of a crash occurring. They can be elements which moderate opportunity for conflict (e.g. number of conflict points, offset to roadside hazards, and separation between opposing traffic). They can also include elements of road user behaviour and/or road environment. Typically, these are the elements which moderate road user error rates. This includes issues such as level of intersection control (e.g. priority/signals/movement ban), speed, sight distance, geometric alignment, driver guidance and warning, and maintenance (change in practice; implications of timing).
3. **Crash severity:** groups of factors affecting the probability of severe injury outcomes should a crash occur. Typically, these factors are associated with the amount of kinetic energy and its transfer in the crash, e.g. impact speeds and angles, severity of roadside hazards.

A score of between zero and is determined for each of the three elements described above, with zero representing full alignment with the Safe System vision for that component of a given crash type and four representing significant misalignment with Safe System conditions. This is done for each of the seven key crash types and the product of the three scores provides the total score for that key crash type. The lower the score the better, and the aim is to achieve a total score of zero for each crash type (by achieving a score of zero for at least one of the three elements).

By way of example, a high-volume high-speed roadway with poor horizontal and vertical alignments and many hazards located near the roadway might receive a score of 4 (exposure) x 4 (likelihood) x 4 (severity) = 64 for run-off-road crashes. The same road might score $0 \times 4 \times 4 = 0$ for pedestrian crashes if the subject section is not utilised by pedestrians.

The sum of the total scores for each crash type provides the overall score for the project or proposal.

WHAT IS A SAFE SYSTEM ROADSIDE?

Road design should incorporate the Safe System approach, which ensures that the needs of all road users are considered in all aspects of the design process. The objectives of new and existing road projects should be carefully considered to achieve the desired balance between competing objectives such as operation, the level of traffic service provided, safety, whole-of-life costs, flexibility for future upgrading or rehabilitation, and environmental impact. These objectives may include:

- strategic fit with relevant government policies, strategies and plans
- the nature and magnitude of transport demand
- road safety to reduce death and serious injury to all road users
- community views and expectations
- travel times and costs
- freight costs

- public transport provision
- provision for cyclists and pedestrians
- environmental impacts

A Safe System roadside is one where the risk of death or serious injury in the event of a crash is virtually eliminated. This requires consideration of not only traditional hazards including fixed objects and non-driveable embankments but the entire roadside environment. To eliminate death and serious injury, research (4) suggests that the provision of a “clear zone” (i.e. an unobstructed, traversable roadside area that allows a driver to stop safely, or regain control of a vehicle that has left the roadway) alone is generally not sufficient, as possibilities such as the following remain:

- Errant vehicles may impact hazards located beyond the clear zone
- Vehicles may spin, flip or roll over due to driver overcorrection or a flat roadside that is not well compacted

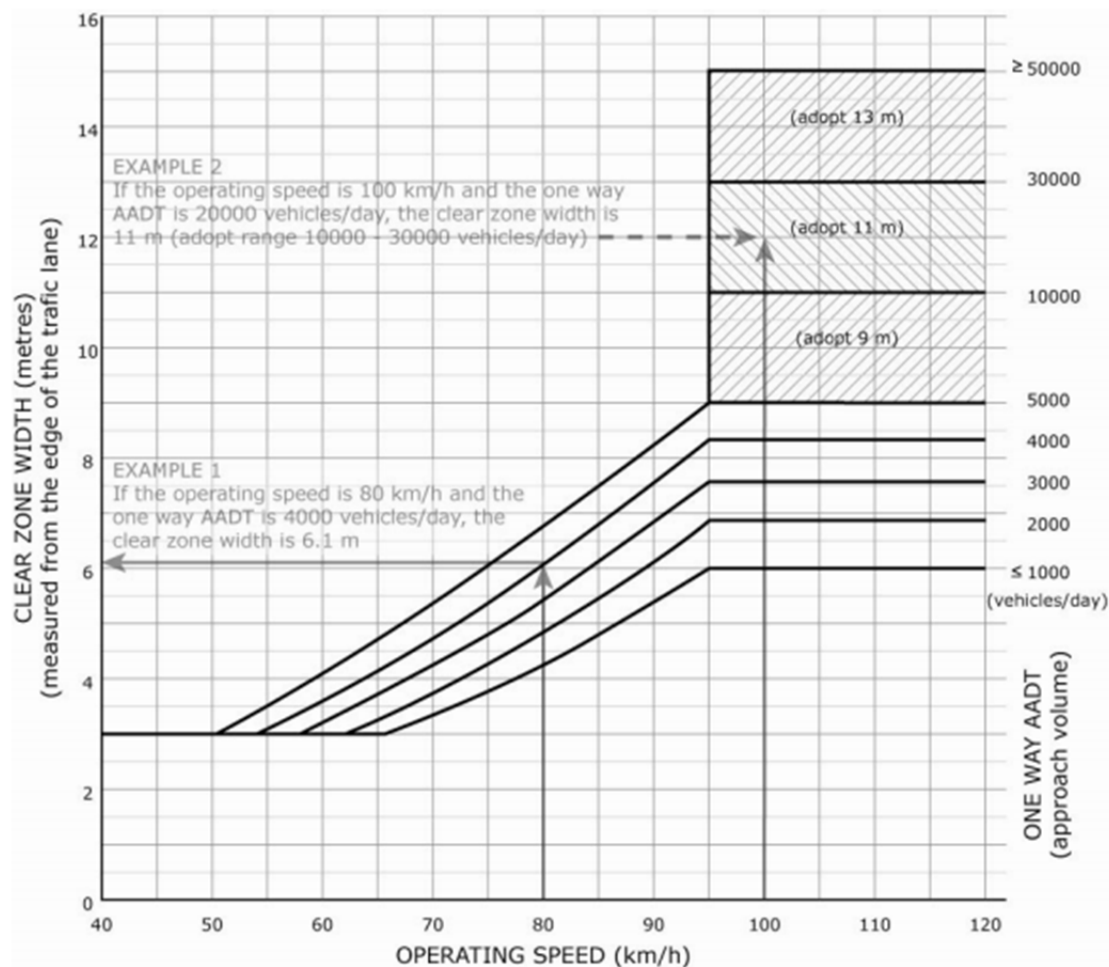


FIGURE 2 Basic clear zone widths on straights (5)

- Vehicles may be redirected back into traffic by embankments or due to driver overcorrection

In Victoria a clear zone of up to fifteen metres is recommended on a straight section of road (refer Figure 2). In-depth crash investigations in South Australia determined typical dynamics of vehicles in single vehicle run-off-road crashes, with a particular focus on the lateral departure distance and the departure angle of the vehicle. (3)

The relationship between the speed of the vehicle and its lateral distance from the edge of the road throughout the departure event was investigated. The merit of barrier was assessed by determining the barrier normal velocity at differing barrier offsets. Initial analyses showed that in crashes where no fixed object was struck, all vehicles travelled well beyond the traditional nine metre clear zone, with several travelling over 20 metres laterally. Simulations suggest that adequate clear zones to ensure non-injurious impact speeds can not be provided in most situations. Roadside barriers in combination with narrower clear zones may provide the most cost effective way to treat rural roadsides to achieve a Safe System.(3)

As a result of this research (3) and other research conducted in Australia, the concept of a ‘clear zone’ has changed dramatically with the acceptance of Safe System principles. Table 1 below shows the lateral distance from the edge of the road that if not free of hazards is likely to experience fatal or serious injury crashes. It is also important to note that the surface of this ‘clear zone’ must be traversable and well compacted so that the yawing car’s tyre does not gouge deep enough to flip the car.

Because in many situations the clear zone distances of Table 1 cannot be implemented, another recognised Safe System approach for protecting vehicle occupants from roadside hazards is to use an appropriate frangible roadside barrier that does not pose an additional roadside hazard. Also, the Safe System approach looks to proactively treat the road environment where possible. Thus, full shielding of the roadside with an appropriate roadside barrier at an appropriate offset from the edge of the roadway is generally the preferred approach, even if there is not a crash cluster.

Preferred Safety Barrier Systems

Flexible safety barrier systems are the most forgiving for vehicle occupants and are the preferred choice for continuous roadside barriers (5). Flexible systems include Wire Rope Safety Barrier (WRSB) and a number of newer weak post W-beam systems. VicRoads presently accepts WRSB

TABLE 1 Summary of clear zone distances (metres) for better alignment with Safe System principles (4) for different speeds and perception and reaction times (PRT)

Speed (km/h)	110		100		80		60		50	
PRT (sec)	1.2	2.5	1.2	2.5	1.2	2.5	1.2	2.5	1.2	2.5
clear zone distances for Safe System compliance (m)										
100% chance of death	27	37	19	30	6.8	15	5	11	4	9
50km/h impact speed	37	48	30	40	18	25	7	14	4	9
Safe System	40	50	33	42	20	27	10	16	7	11

systems that meet NCHRP 350 Test Level 4 (i.e. capable of containing an 8 tonne truck) and weak post W-beam systems that meet MASH Test Level 3. Whilst WRSB has been the traditional choice, weak post W-beam systems offer comparable safety performance and offer some advantages over WRSB such as reduced deflection in some cases, protection for motorcyclists by adding an additional under-rail or top-cover rail, and reduced ongoing maintenance costs, and so may be a more appropriate choice in some situations.

The use of continuous lengths of semi-rigid or rigid barrier systems (as opposed to flexible systems with frangible supports) does not offer good alignment with Safe System principles. Although they meet crash testing requirements, these more rigid systems are not as forgiving on vehicle occupants as flexible system, and their use should be limited to situations where the use of flexible barrier systems is not feasible (5). Common examples include geometrically constrained locations and locations where preventing vehicles from penetrating the barrier is of paramount importance (for example at a structure over a railway).

Barriers should be located at a suitable distance from the edge of the road to allow vehicles to safely pull over in emergency situations, provide a recovery area for errant vehicles (including motorcycles) and minimise nuisance impacts.

The adoption of barrier offsets less than the prescribed minimums should only be considered where a documented risk assessment has been undertaken. This should not be necessary at greenfield sites (i.e. one with no development as yet) but may be justifiable at already developed brownfield sites where significant constraints exist.

CASE STUDIES

Three projects were assessed using a Safe System Assessment methodology. While there were many other aspects to the Safe System Assessment that are not documented herein (such as intersections and carriageway crash considerations), the following descriptions focus on the roadside aspects of the Safe System Assessment.

Drysdale Bypass

The Drysdale Bypass is a Victorian Government commitment to provide an alternative route for road users around the town of Drysdale. It is expected to be completed by 2020 at a cost of \$109 million.

The bypass route is approximately six kilometres long and will follow a ‘greenfield’ alignment from Jetty Road to north of Whitcombes Road. It will include a separate off-road bicycle path on the same alignment. The intended speed limit is 80 km/h and 12,000 vehicles per day are forecast to use the road in the year 2046.

TABLE 2 Safety barrier offsets relative to road edge lines (4)

	Desirable	Minimum
Outer verges	4.0m	3.0m
Medians	3.0-4.0m	1.0m

Following a Safe System Review by three qualified Road Safety Auditors (7), a number of Safe System features have been incorporated into the design of Figure 3, including the use of a WRSB on the outer verges and in the median as well as the provision for roundabouts at several key intersections.

This project demonstrates a strong alignment with Safe System principles. Key features include:

- Provision of continuous flexible barriers (exceptions being intersections and accesses)
- Provision of shoulders for broken down vehicles
- Intersection treatments which limit conflict points, impact angles and crash forces (i.e. roundabouts)

Being a greenfield project, there are few constraints on the design of the roadway which hinder the provision of Safe System infrastructure.

The project has been assessed as having a score of 12/64 for run-off-road crashes and 12/64 for head on crashes.

Yan Yean Road Duplication

Yan Yean Road is an arterial road that provides an important link between Epping/Mill Park/South Morang and the Greensborough/Diamond Creek area. Yan Yean Road also services a corridor to the north of Kurrak Road providing access to the Doreen area.

The proposed duplication is of the 3.9km length from Diamond Creek Road to Kurrak Road. It is in hilly terrain and the existing road alignment is significantly sub-standard.

There has been steady growth in the traffic volume along Yan Yean road with two way volumes reaching 18,400 vehicles per day in 2013, with 880 being commercial vehicles (6). Yan Yean Road is classified as a Bus Priority Route and a Traffic Route.

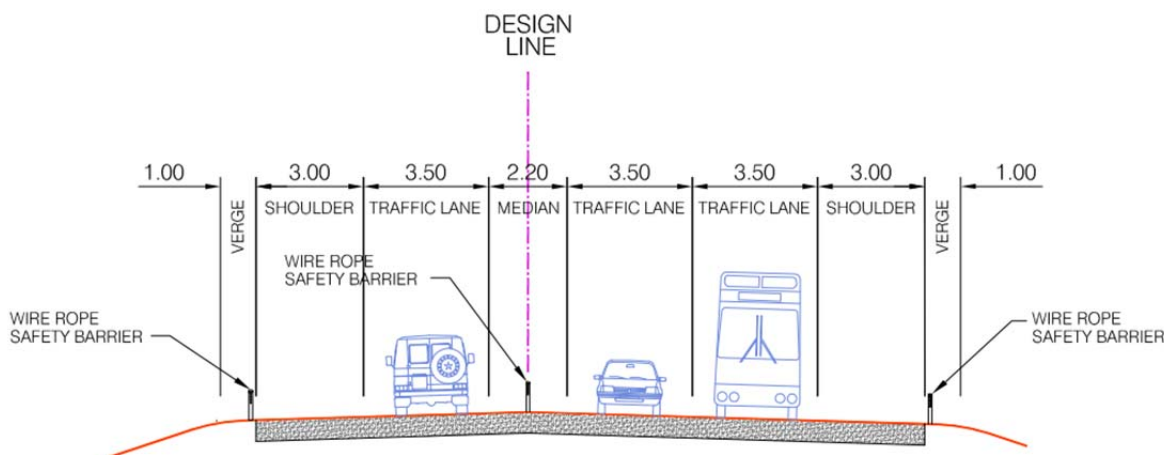


FIGURE 3 Typical cross section – Drysdale Bypass (7)

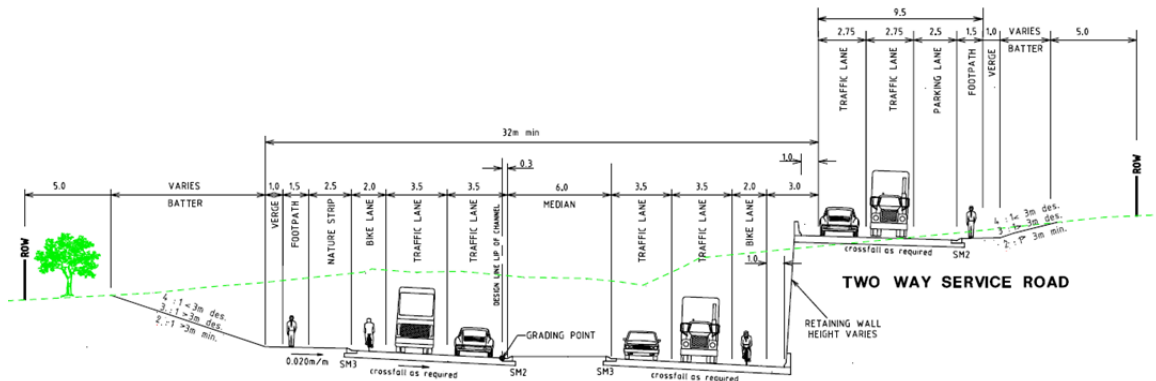


FIGURE 4 Typical cross section – Yan Yean Road Duplication (8)

The project proposal demonstrated low alignment with Safe System principles. Key shortcomings included:

- Clear Zone theory incorporated into the design, which will not result in zero death and serious injury
- Potential for head-on crashes and run-off-road crashes due to the hilly and winding alignment
- Vulnerable road users (pedestrians and cyclists) exposed to high speed traffic (80 km/h)

Key recommendations to improve alignment with Safe System principles included:

- Install flexible safety barriers (weak post W-Beam) in the median and on the outer verges
- Physically separate pedestrians and cyclists from traffic
- Various improvements to proposed intersections, crossings and other conflict points

The unfavorable horizontal and vertical alignment of the existing roadway as shown in Figure 4 together with the constraints imposed by surrounding land development are significant barriers to achieving Safe System compliant roadsides as part of this project.

The project has been assessed as having a score of 36/64 for run-off-road crashes and 36/64 for head on crashes.

Rushworth-Tatura Road (9)

Rushworth-Tatura Road is a slightly undulating 3.6 km long high-speed (100 km/h speed limit) rural road with heavily treed roadsides, unsealed shoulders and carrying 1,260 vehicle per day on average. It has 2.7 m northbound and 3.0 m southbound lane widths. Over the past 5 years there have been four serious injury crashes, and one other injury crash on this short stretch of road. A project was recently developed to address a history of run-off-road crashes, focussing on the identification of high risk locations based on clear zone theory and protecting road users from roadside hazards (i.e. trees) using barriers. The project was developed in accordance with current

guidelines and in the same way as other similar projects.

This project has varying alignment with Safe System principles

- Some areas shielded and some not (based on assessment of risk and other considerations)
- Closely spaced access points limit the continuity of barriers
- A mix of flexible barriers and semi-rigid barriers has been used (due to closeness of tree hazards)
- Some compromises have been made with respect to desirable safety barrier design, such as allowing trees to be located within the barrier deflection zone
- The likelihood of head-on crashes remains unchanged

The design of safety barrier treatments for this project was heavily influenced by a strong desire to retain significant native vegetation location close to the roadway. This, together with the narrow road cross section and frequency of access points led to the use of a guard fence, a vastly different barrier implementation strategy than the flexible barrier that would be the case in a less constrained situation.

The project has been assessed as having a score of 16/64 for run-off-road crashes and 24/64 for head on crashes.

CONCLUSION

The three case studies illustrate that a Safe System Assessment is a process, rather than a set of rigid prescriptive tools. Experience has shown that site-specific constraints can heavily influence design elements including roadside design, especially in retrofit and brownfield situations, and present significant challenges for road agencies committed to the Safe System philosophy.

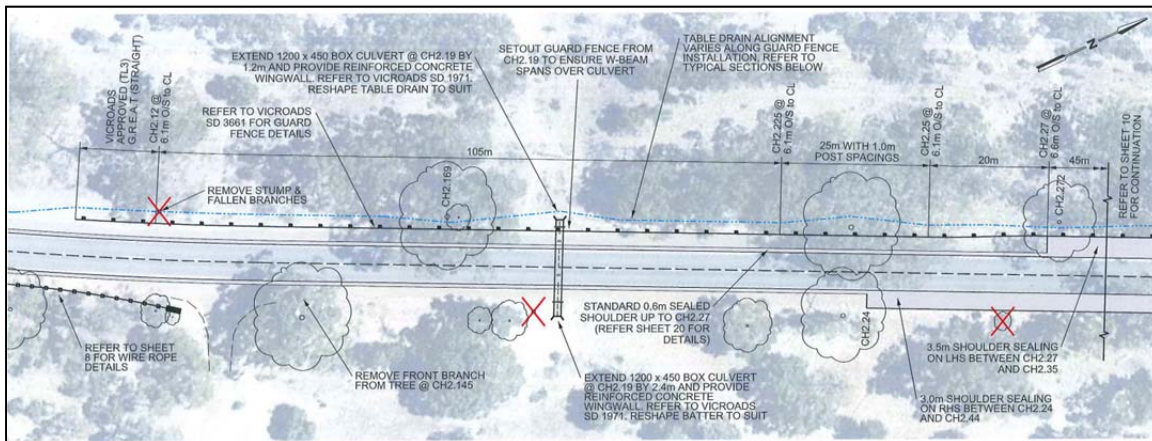


FIGURE 5 Typical safety barrier treatment – Rushworth-Tatura Road

Though research (4) supports the provision of continuous, flexible safety barriers as the preferred way to achieve Safe System compliant roadsides the Australian experience is too short to determine whether their application will accord with research. However, it is particularly evident in the Rushworth-Tatura Road situation that site-specific issues determine the design elements because in this case the desire to preserve native trees made it impossible completely to align the project with Safe System principles. The concept of a “Safe System roadside” continues to evolve as research continues, new and improved safety barrier products enter the market, and practitioners adjust to incorporating Safe System principles into designs.

Safe System Assessments are proving to be a valuable tool to identify and quantify a project’s alignment with Safe System principles, in a structured and consistent way, and taking into account realistic constraints at the site. When undertaken at an early stage of a project, this process has encouraged alternative thinking and solutions with the potential to raise safety outcomes to a higher level.

REFERENCES

1. ANB10(9) <https://sites.google.com/site/trbsubcommitteeanb109/> 2015.
2. Turner, B., C. Jurewicz, K. Pratt, B. Corben, and J. Woolley. *Safe System Assessment Framework*. Publication AP-R509-16. Austroads Ltd., Sydney, Australia, 2016.
3. Doecke S. and J. Woolley. *Effective use of clear zones and barriers in a Safe System’s context*. Presented at Australasian Road Safety Research, Policing and Education Conference, Canberra, Australian Capital Territory, 2010.
4. Moon W. and P. Mihailidis. *Outcome Based Management of Roadside Hazards*. Australasian Road Safety Conference, 2013. Based on Candappa et al, *Outcome-based Clear Zone Guidelines*. Monash University Accident Research Centre, 2008.
5. VicRoads. *VicRoads Supplement to Austroads Guide to Road Design Part 6 – Roadside Design, Safety & Barriers*. Rev. 2.0 – July 2011.
https://www.vicroads.vic.gov.au/~/_/media/files/technicaldocumentchapters/standards-and-supplements/vicroadssupplementtoagrdpart6roaddesignsafetybarriers.pdf?la=en. Accessed October 27, 2016.
6. VicRoads Traffic Volume Information July 2014.
<https://www.vicroads.vic.gov.au/traffic-and-road-use/road-network-and-performance/road-use-and-performance>
7. Safe System Solutions Pty Ltd., Safe System Review – Drysdale Bypass, Report SSS20150818LB1 to VicRoads South Western Projects.
8. Safe System Solutions Pty Ltd., Safe System Audit – Proposed Duplication of Yan Yean Road, Report SSS20150717KB1 to VicRoads Metropolitan Projects - Western.
9. Safe System Solutions Pty Ltd., Rushworth-Tatura Road: Project Case Study – Context Sensitive Design, Report SSS2015104KB1.8 to VicRoads Northern Region

Utilizing the Safe System Approach to Meet the Challenge of the Decade of Action

MICHAEL DREZNES

International Road Federation

The Safe System Approach recognizes that the human body has a limited tolerance of violent forces, and that when crash energies exceed this tolerance, death or serious injury will be a probable outcome. It also accepts the fact that crashes on a the road will continue to occur as long as human beings are driving the vehicles. The Safe System Approach emphasizes the use of “Forgiving Roads,” vehicles designed to withstand impacts as well as appropriate speed limits to reduce the horrendous consequences of the inevitable mistakes made by road users.

The Safe System Approach challenges the traditional theory that drivers are responsible for the majority of crashes and therefore enforcement and education can reduce the carnage on the roads. While it recognizes the importance of education and enforcement, the Safe System Approach transfers the responsibility to engineers for the proper design of roads using proven best practices and state of the art technologies and concepts to make the roads safer for all road users.

Safe System Approach countermeasures aim either to prevent a crash from occurring or to reduce the severity of the crash. Some of these road related countermeasures could include properly designed and tested longitudinal barriers along the center and sides of roads to prevent run-off-road and head-on crashes or roundabouts designed to reduce possible impact speeds and to reduce the number of crash conflict points. Vehicle related countermeasures could include in-vehicle crash-avoidance technologies, ranging from alcohol and seatbelt interlocks to various crash-warning devices, to automated vehicle control in pre-crash circumstances (for example, Electronic Stability Control) or crumple zones to absorb crash energies as well as improvements to seat belts and air bags to provide improved occupant protection. An excellent example of the potential of these countermeasures would be Volvo’s recent campaign that states “No One Will Die in a Volvo by 2020.”

Finally speed related countermeasures could include reduced speed limits particularly where high numbers of vulnerable road users can be expected (for example, shopping areas and school zones) and along high-risk road sections where no apparent or immediate engineering solutions can be implemented. Road authorities who adopt the Safe System Approach have made the conscious decision not to accept road trauma as a fact of life. They challenge the engineering profession to strive for zero deaths and serious injuries on their roads, and they accept the fact that although crashes will always occur, no one needs to die as a result of a crash.

Taxonomy of Roadside Safety Hardware

T. OLAF JOHNSON
MALCOLM H. RAY
RoadSafe, LLC

In 1995, the AASHTO-AGC-ARTBA Joint Committee Subcommittee on New Highway Materials published the Task Force 13 report, A Guide to Standardized Highway Barrier Hardware, with the goal of standardizing proprietary and non-proprietary hardware and hardware systems. This printed guide used unique “designators” for each system and component to alleviate confusion between similar products. These designators consist of three letters that describe what type of system or component it is, followed by a unique number. The first letter is the Category, the second stands for the Function, and the third stands for the Type. The Task Force 13 online guides are an already established and continually updated resource that is free and accessible to all DOTs, maintenance divisions, and the general public. The increased adoption of these guides as an industry standard reference has the potential to both reduce installation and maintenance errors, as well as improve hardware inventory asset control.

INTRODUCTION

Maintenance crews that repair or replace existing roadside inventory are currently reliant on experience or maintenance division specific guidelines to follow to correctly repair or replace this hardware. These guidelines are not uniform and can vary between maintenance divisions or state DOTs, which can lead to inconsistencies between areas and improper repair or installation. This, in turn, can lead to liability concerns for DOTs and city/county/state maintenance divisions.

A possible solution to these problems can be found in a set of online guides to hardware systems and components that is maintained by the Task Force 13. From their website:

Task Force 13 develops, recommends, and promotes standards and specifications for bridge and road hardware used by highway and transportation agencies on the nation's roadways. Task Force 13 is a committee of concerned and experienced representatives from industry, academia, and state and federal transportation departments. Task Force 13 serves the Joint AASHTO-AGC-ARTBA Subcommittee on New Highway Materials and Technologies, whose mission is to develop guide specifications for new materials and technologies identified for use in highway construction projects.(1)

The online guide website consists of six different guides: Bridge Rail Systems, Transition Systems, Sign Support Systems, Luminaire Support Systems, Barrier Hardware Systems, and Components. The guides are set up to complement and reference each other. As an example, a user can begin with a particular bridge rail that their DOT has on a bridge and locate it in the online guide. The guide will then tell the user which transition systems are compatible with it and what components are included in each system. Each system and its components are identified by unique designators, which eliminates the problem of uncertainty in compatibility with repair/replace parts lists and procedures. The universal adoption of these designators by

DOTs and maintenance agencies, along with the use of the information on the website, would reduce confusion about what parts and systems are intended by designers, installers and manufacturers located in different parts of the country.

BACKGROUND

In 1995, the AASHTO-AGC-ARTBA Joint Committee Subcommittee on New Highway Materials published the Task Force 13 report, A Guide to Standardized Highway Barrier Hardware, with the goal of standardizing proprietary and non-proprietary hardware and hardware systems. This printed guide used unique “designators” to identify each system and component to alleviate confusion between similar products. These designators consist of three letters that describe what type of system or component it is, followed by a unique number. The first letter is the category, the second stands for the function, and the third stands for the type. As an example, a guardrail button-head bolt has the designator prefix of “FBB”, which stands for “Fastener” category, “Bolt/Screw” function, and “Button Head Bolt” type, respectively.

Since the printing of the 1995 guide, the guide has been transferred to the Internet and has evolved into an interactive cross-referencing system. On the page for each system or component is the most current standard drawing, a photograph of the system, FHWA acceptance letter, and any pertinent documents for that system. The 4th edition of the Roadside Design Guide refers to the online guides as a depository of roadside hardware information and references the online guides in section 5.1.2:

The AASHTO-Associated General Contractors of America (AGC)-American Road and Transportation Builders Association (ARTBA) Joint Committee Task Force 13 report, A Guide to Standardized Highway Barrier Hardware is a depository of engineering drawings for a multitude of guardrail components and systems. Each system is given a unique designation used to catalog the different systems and variations of each system. A web site has been established for each supported system, and is available at <http://www.aashtotf13.org>. (2)

A link to the online guides can be found in the website at <http://www.aashtotf13.org/Links.php>, however, the direct link is: <http://guides.roadsafellc.com/>. Once at the guides homepage, a navigation menu on the left of the page provides links to each of the six guides, as well as links to manufacturers and contacts, and an “about” page that gives the guides history, useful external links, and a way to contact the support team.

METHODS

The user starts at the homepage and selects the type of system or component of interest and clicks on the link to bring them to its guide. From there, users have the option to browse the guide or search for a specific system/component based on several criteria. Figure 1 shows the search page for the Barrier Hardware Guide.

Search Barrier Hardware

General System Type	Any ▾
Specific System Type	Any ▾
Test Specification	Any Test Specification ▾
Test Level	Any Test Level ▾
Rail Type	Any Rail Type ▾
System Height	Any Height ▾
Aesthetic	Any ▾
Manufacturer	Any Manufacturer ▾
Review Status	Any Approval ▾
<input type="button" value="Search"/>	

FIGURE 1 Barrier hardware guide search page.

As previously mentioned, each system in the guide is identified with a unique “designator”. The designators consist of five sections: Category, Function, Type, Sequence #, and Option. The possible entries for each of these sections vary according to which guide a system or component belongs to. The Category section tells if a designator is a system or some type of component. The Function section describes what kind of system or component it is. The Type section gives information about the material the system is made of, what systems a transition is compatible with, or more specific information about the system/component. The Sequence # and Option are assigned numerically and alphabetically, respectively, in the order in which a designator request has been received.

Designator Tree for Bridge Rails, Transitions, Sign Supports, and Luminares

Table 1 shows the designator tree for bridge rails, transitions, sign supports, and luminaires. These are complete systems, and have “S” in the Category field to indicate this. The Function tells which of these systems a designator is describing. The Type describes different properties of the systems, which varies depending on the system being described. For bridge rails, Type generally describes the dominant material the system is made from. For transitions, Type indicates which bridge rail and/or guardrail systems the transition is compatible with. For sign supports and luminaires, Type describes the type of connection to the base. The sequence number is an arbitrary two-digit number that identifies a particular bridge rail. The Option is an alphabetic character a through e corresponding to various options or versions of particular systems.

TABLE 1 Designator Tree for Bridge Rails, Transitions, Sign Supports, and Luminaires

Category	Function	Type
S = System	B = Bridge Rail	A = Aluminum
		B = Steel Tube
		C = Concrete
		D = Wood
		O = Other Steel
		T = Steel Thrie Beam
		W = Steel W-Beam
	T = Transition	B = Guardrail to Bridge Rail
		C = Cable to BCT End Terminal
		G = Guardrail to Guardrail
	S = Sign Support	C = Coupling
		F = Fracturing/Frangible
		M = Mailbox Supports
		P = Splice
		S = Slipbase
	L = Luminaire	C = Coupling
		H = Shoe
		J = Breakaway Joint
		S = Slip
		T = Transformer

Designator Tree for Barrier Hardware

Table 2 shows the designator tree for barrier hardware systems. As all the entries are complete systems, the Category is “S”. The Function describes whether the barrier is a crash cushion, end treatment/terminal/anchor, guardrail/median barrier, or a work zone system. Type varies for each of the Functions, as shown in Table 2. The sequence number is an arbitrary two-digit number that identifies a particular barrier hardware system. The Option is an optional alphabetic character corresponding to various options or versions of particular systems.

Designator Tree for Components

Currently, the designators for components are the only designators that are not assigned to systems. The Components guide is comprised of a large collection of individual parts to both proprietary and non-proprietary systems. It includes fasteners, luminaire parts, posts, and rails. Each of these categories is shown in Table 3 through Table 6. All of the components in Table 3 through Table 6 are in the same “Components” guide, but they have been separated here for size reasons.

TABLE 2 Designator Tree for Barrier Hardware Systems

Category	Function	Type
S = System	C = Crash Cushion	I = Independent
		T = Thrie-Beam
	E = End Treatment / Terminal / Anchor	B = Box
		C = Cable
		D = Wood
		R = Rigid
		W = W-Beam
	G = Guardrail / Median Barrier	M = Median Barrier
		R = Roadside Barrier
	W = Work Zone	C = Concrete
		M = Miscellaneous

TABLE 3 Designator Tree for Component Luminaires

Category	Function	Type
L = Luminaire	A = Arm	C = Cross
		D = Davit
		M = Mast
		N = Tenon
		T = Truss
	B = Frangible Base	C = Coupling
		H = Shoebase
		J = Breakaway Joint
		S = Slipbase
		T = Transformer
	P = Pole	A = Aluminum

TABLE 4 Designator Tree for Component Fasteners

Category	Function	Type
F = Fastener	B = Bolt	B = Button Head Bolt
		C = Carriage Bolt
		H = Hook Bolt
		L = Lag Screw
		S = Cap Screw
		T = Toggle Bolt
		X = Hex
	C = Cable	A = Anchor
		C = Cable Clip
	L = Plate	S = Slipbase
	M = Miscellaneous Fastener	A = Anchor
		C = Coupling
		M = Miscellaneous
		W = Work Zone
	N = Nut	S = Square Nut
		X = Hex
	P = Plate	A = Anchor
		B = Bearing Plate
		C = Clamp Plate
		P = Post Fitting
	R = Rod / Bar	H = Hooked Anchor Stud
		J = J-Hook Anchor Stud
		S = Straight Anchor Stud
	W = Washer	C = Circular
		R = Rectangular

TABLE 5 Designator Tree for Component Posts

Category	Function	Type
P = Post	A = Aluminum	B = Bearing Plate
		F = Foundation
	D = Wood	B = Blockout / Bracket
		E = Soil Embedded
		F = Foundation
	F = Flanged Channel	E = Soil Embedded
		P = Post Fitting
		P = Post
	L = Plate	S = Soil Plate
	O = Concrete	F = Foundation
	S = S-Section	E = Soil Embedded
	T = Tube	C = Composite
		E = Soil Embedded
		F = Foundation
		P = Post
	W = W-Section	B = Blockout / Bracket
		E = Soil Embedded
		F = Foundation
	W = Wide-Flanged Steel	F = Foundation

Example

As an example, in the Barrier Hardware guide a system with the designator “SGM02” (See Table 2) is a: System – Guardrail / Median Barrier – Median Barrier. It is the second such system listed in the guide as indicated by the number 02. Clicking on the designator link brings the user to the information page for that system, as seen in Figure 2.

At the bottom of the information webpage, the user sees a table where they can access the standard drawing, other documents, an image gallery, and a list of components used in this particular system. Also listed are any transitions compatible with the system. All components and compatible transitions are clickable hyperlinks that bring the user to the information webpage for those components/transitions. The interconnectivity between the different system and component guides allows users to quickly find all components used in a particular system, as well as which transitions they are compatible with, reducing the possibility for system maintenance errors. As an added benefit, the information webpages for components list all of the systems the components are used in, which aids in maintenance inventory management.

TABLE 6 Designator Tree for Component Rails

Category	Function	Type
R = Rail	A = Aluminum	E = End Section
		M = Main Member
		S = Splice
	B = Box	M = Main Member
		S = Splice
	C = Cable	E = End Section
		M = Main Member
	E = Plate	E = End Section
		R = Rub Rail
	L = Channel	R = Rub Rail
	O = Concrete	M = Main Member
	P = Pipe	X = Spacer / Expansion
	T = Thrie-Beam	B = Backup Plate
		E = End Section
		M = Main Member
	W = W-Beam	B = Backup Plate
		E = End Section
		M = Main Member
		T = Transition

Weak-Post W-Beam Median Barrier (SGM02)

Review Status:	Review Complete
Test Specification:	Report 350
Test Level:	TL-2
Manufacturer:	Non-Proprietary
Aesthetic:	No
Rail Type:	W-Beam
General System Type:	Guardrail / Median Barrier
Specific System Type:	Median Barrier
System Height:	30" [762mm] < H ≤ 33" [838mm]
Contact:	William P. Longstreet (Click for details)
Last Updated:	June 29, 2016
FHWA Eligibility Letters:	Letter b64



Drawings	Other Documents	Images	Components	Compatible Transitions
<ul style="list-style-type: none"> sgm02.pdf 	No files found.	<ul style="list-style-type: none"> Thumbnail Gallery 	<ul style="list-style-type: none"> RWM02a-b - 2-Space W-Beam Guardrail PSE03 - Weak-Post Guardrail Post & Welded Soil Plate FWR01 - Square Guardrail Washer FBX06a-24 - Class 4.6 Hex Bolt and Nut FBF01-05 - Guardrail Bolt and Recessed Nut 	<ul style="list-style-type: none"> None

FIGURE 2 Information webpage for barrier hardware system SGM02.

CONCLUSIONS

For roadside safety hardware to function properly, the systems must be installed and maintained properly. Maintenance crews that repair or replace existing roadside inventory are currently reliant on experience or maintenance division specific guidelines to follow to correctly repair or replace this hardware. These guidelines are not uniform and can vary between maintenance divisions or state DOTs, which can lead to inconsistencies between areas and improper repair or installation. The Task Force 13 online guides are an already established and continually updated resource that is free and accessible to all DOTs, maintenance divisions, and the general public, and the increased adoption of these guides as an industry standard reference has the potential to both reduce installation and maintenance errors, as well as improve hardware inventory asset control.

ACKNOWLEDGMENTS

The online system and component guides are maintained by Roadsafte, LLC with a support contract provided by Task Force 13.

REFERENCES

1. Task Force 13 website, <http://www.aashtotf13.org/>, accessed online on 1 November, 2016.
2. Roadside Design Guide, 4th Edition 2011, American Association of State Highway and Transportation Officials, 444 North Capitol Street, NW, Suite 249, Washington, D.C. 20001.

Protecting the Most Vulnerable *Which Safety Measures Generate Public Support for Paratransit and Bus Transportation?*

ISABELLA GUAJARDO

University of Pennsylvania, Perelman School of Medicine

Policymakers must weigh the costs and benefits of safety strategies for public transportation like paratransit vehicles and buses. Not only do officials want to protect vulnerable passengers, they also want the public to approve and support their actions. **Methods:** But what does the public support? And to what extent? A survey was administered to a random cross section of American adults, including paratransit users and the relatives, friends and guardians of paratransit users to find out. Z-tests and Pearson's r correlations were analyzed. All p-values < .001. Approximately half (55%) of respondents were female, with an average age of 33 (s=9.7). Approximately 24% of respondents were paratransit users.

RESULTS: Among many other intriguing results, the data showed: **Individual Safety Strategies** Participants ranked three distinct safety strategies on a 1 to 10 Likert-type scale of how safe the strategy would make them feel, from lowest (1) to highest (10). The strategies were collision avoidance technology, safety cameras that record g-force incidents like sharp braking or sudden swerving, and hiring a transit operator who rewards good drivers with incentives like gift certificates and raffles. The three strategies were considered a good investment by 90% (collision avoidance technology), 98% (safety cameras), and 95% (incentivized drivers) of respondents. If their county adopted the three strategies, the decision would receive strong approval/ approval/disapproval/strong disapproval from 53%/40%/7%/0% (collision avoidance technology), 55%/43%/3%/0% (safety cameras), and 48%/50%/3%/0% (incentivized drivers) of respondents.

Respondents stated that they would feel approximately 47% safer riding on a vehicle with collision avoidance technology, 46% safer riding on a vehicle with safety cameras, and 42% safer riding on a vehicle with an incentivized driver. **Strong Support for Using Multiple Safety Strategies** Participants stated that they would feel approximately 63% safer riding on a vehicle that used all three safety strategies. Paratransit users stated that they would feel 60% more comfortable on such a vehicle. Relatives, friends and guardians of paratransit users stated they would feel 65% more comfortable if their loved one rode on such a vehicle. Participants believe, on average, that a county should willing to pay an 89% premium on top of basic transportation costs for safety. Approximately 96% of participants stated that a company that is five times safer than the industry average should be paid more than average. Participants felt this premium should be, on average, 58%. Participants stated that a company that is 20 times safer than average should be paid a premium of 68%, on average. Participants' views take the approximate form $y=6.75-6.75e^{(-.39*x)}$, meaning respondents most highly value being two to three times safer than average. Almost all respondents stated that buses should have the same safety as paratransit vehicles (75%) or even more (23%). Views were consistent across ages and between sexes, with no strong outlying correlations.

CONCLUSIONS: These results safety areas where policymakers can invest in order to both help the public and receive public support for their efforts.

Safety Countermeasures for Roadway Departure Crashes *An Overview*

MOHAMMAD JALAYER

*Center for Advanced Infrastructure and Transportation
Rutgers, The State University of New Jersey*

HUAGUO ZHOU

Auburn University

A roadway departure (RwD) crash occurs when a vehicle leaves the traveled way by crossing an edgeline or a centerline. These crashes, comprising of run-off-road and cross-median/cross-centerline head-on collisions, tend to be more severe than other crash types. In 2013, RwD crashes accounted for 56 percent of all motor vehicle traffic fatalities. Inattention or fatigue, an avoidance maneuver, or traveling too fast are the common reasons a driver may leave the travel lane. Roadway and roadside geometric design features (e.g., lane and shoulder widths, horizontal curvatures, sideslope, and clear zones) play a significant role in whether human error results in a crash. To achieve the Federal Highway Administration's *Toward Zero Deaths* vision, many safety countermeasures have recently been implemented by state departments of transportation and local agencies to mitigate RwD crashes.

In this paper, an investigation of 14 real-world case studies has provided an overview of current safety countermeasures practices for RwD crashes. These case study examples fall into three major categories: signs (i.e., chevrons, dynamic curve warning systems, and advance curve warning and advisory speed signs), pavement safety (i.e., high friction surface treatments, raised pavement markers, edge line pavement markings, safety edge, centerline rumble strips, and shoulder rumble strips), and roadside design (i.e., cable barrier, guardrail, breakaway supports for signs and lighting, clear zone improvements, and shoulder widening). The results of this study identify pavement safety as the most effective countermeasure for reducing RwD crash frequency and severity.

Initial Developments Supporting a Roadside Tree Removal Marketing Campaign

CODY S. STOLLE
KARLA A. LECHTENBERG
RONALD K. FALLER
TAE EUN (ALEXIS) YIM
University of Nebraska-Lincoln

Roadside tree crashes have been the most deadly of all run-off-road, fixed-object crash types since the 1970s, when records were first kept detailing causes of run-off-road fatalities. Despite more than 3,500 fatalities every year associated with roadside tree crashes, state DOTs often encountered resistance to removing trees and requiring minimum lateral offset planting guidelines, as many groups opposed tree removal. The Midwest Roadside Safety Facility (MwRSF) is conducting an ongoing research study to evaluate historical tree crash data, tree litigation, and brainstorm or create new safety marketing campaigns to assist DOTs with positively and proactively preventing roadside tree crashes, and preliminary results are shown here. A five-year, 12-state crash data set involving more than 400,000 tree and utility pole crashes was analyzed, revealing that annual comprehensive costs due to tree crashes likely exceed \$58 billion dollars in the U.S. Thus, each state loses an average of \$1 billion annually, on average. The general public is adversely affected by roadside tree planting which results in car crashes, road closures and delays, maintenance and trimming costs including replacement when infected with disease or insects, litigation from tree-related incidents, and risks for pedestrians. To improve road safety and reduce the societal cost burden associated with trees, researchers must develop safety programs and campaigns to empower advocacy groups and citizens to take action using emotional and logical motivations. Partnerships with external agencies may be critical before change can be expected.

INTRODUCTION

In the 1970s, the National Highway Traffic Safety Administration (NHTSA) created the Fatal Accident Reporting System (FARS), which tracked causes of fatal crashes in the United States, including run-off-road (ROR) crashes. Every year since records were kept, trees were the most common and deadly of the fatal fixed-object ROR crash types [1-2]. Tree crashes are responsible for nearly half of the total ROR fixed-object crash fatalities each year, and utility poles are consistently either the second or third most common cause of ROR fixed-object fatalities. An example of a distribution of fatal ROR fixed-object crashes for 2013 is shown in Figure 1. Trees and utility poles have caused approximately 3,500 and 900 fatalities, respectively, each year since the 1970s. Since this problem was first identified in 1979, nearly 160,000 people have died in crashes involving either trees or utility poles in the United States alone.

Using guidance from the Roadside Design Guide [3], safety treatments for roadside trees and utility poles are generally limited to (a) removal, (b) establishing placement guidelines near to or outside of the clear zone, (c) shielding, or (d) delineating the trees. Tree removal efforts often face resistance from the general public (and most commonly, environmental groups), and

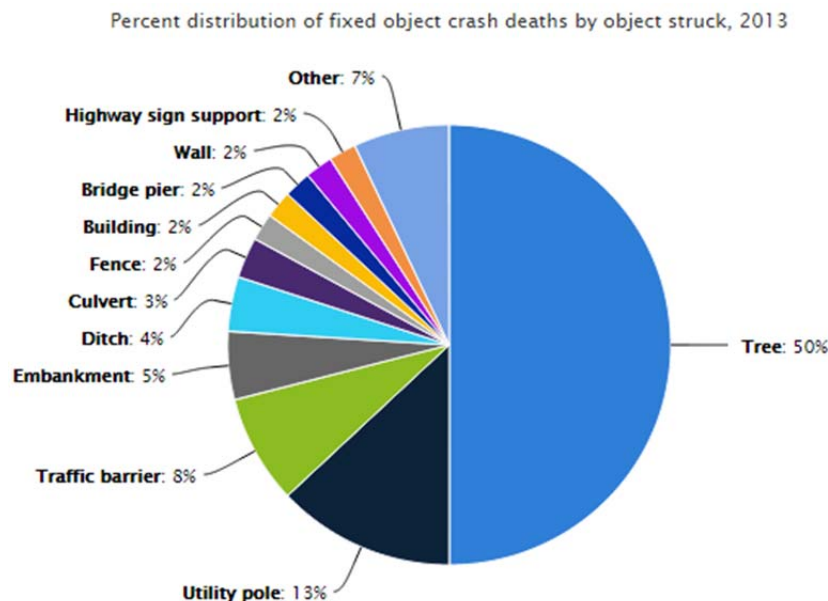


FIGURE 1 Deaths in fixed object crashes by object struck in 2013 [1].

often state Departments of Transportation (DOTs) are not consulted for best practices regarding tree offsets from the road before trees are planted. Likewise, completely removing utility poles may not be practical. Utility poles are often installed and maintained by utility companies and not cities, counties, or DOTs.

Shielding all trees and utility poles with guardrail is impractical due to their frequency, spacing density, proximity to the road, the cost of installing and maintaining guardrail, and the perception that guardrail could adversely affect roadside aesthetics. Delineation is only effective at increasing driver awareness and is unlikely to prevent run-off-road crashes unrelated to driver distraction. In order for state DOTs to see a substantive decrease in fatal tree and utility pole crashes, it is necessary to generate broad support to remove trees and develop strict guidelines for roadside tree maintenance and minimum installation offsets for installing new trees and utility poles.

Therefore, the Midwest States Pooled Fund Program funded a research study at the Midwest Roadside Safety Facility (MwRSF) to (a) conduct a literature review and crash study supporting tree removal marketing efforts and (b) develop preliminary ideas for the content and means of distribution of the roadside tree safety campaign. The objective of this research is to maximize the effectiveness of DOT safety marketing campaigns at a minimum cost and to provide a blueprint for conducting similar campaigns in the future. Information will also be useful for agencies interested in crafting communication strategies supporting project-level outreach activities and program efforts.

CRASH DATA INVESTIGATION

To provide the background and support for tree removal, researchers investigated available literature regarding tree crashes and liability associated with State DOTs regarding trees. The

information in the following sections is intended to provide factual content for the marketing campaigns.

Literature Review

Impacts with trees account for approximately half of all fixed-object ROR fatal crashes each year, as shown in Figure 1 [1]. According to FARS, tree crashes typically accounted for more than 3,500 fatalities and up to 3,000 fatal crashes annually [2, 4]. Tree crashes have been shown to be more severe than most other fixed-object types [5]. Thus, in the last four decades years since FARS was established, the United States has suffered approximately 140,000 fatalities caused by run-off-road crashes involving trees, and another 18,000 fatalities associated with utility poles. Because the number of references for tree crash statistics are overwhelming, researchers provided a few examples of findings from the literature review:

- A study evaluating a 60-mile segment of state route SR-3 in Washington determined that trees were tied for the 3rd most common roadside fixed object crash type (42 crashes) [6-7]. Trees also had one of the largest average roadside offsets along that stretch of road (1.54 m from the shoulder for isolated trees and 1.32 m from the shoulder for clusters of trees). Only utility poles had a larger average offset from the shoulder of 1.92 m. Seven of the 42 tree crashes were severe (i.e., fatal or disabling injuries). Findings were more severe than a previous study determined that 7.7% of all Washington state tree or stump crashes were severe (i.e., fatal or disabling injuries) between 1993 and 1996 [8].
- Ray, Troxel, and Carney determined that side impacts with fixed objects, such as trees, cost the U.S. an estimated \$2.5 billion in crash costs annually [9]. Trees and utility poles were the most common side-impact fixed-objects involved in ROR crashes. Impacts with trees were responsible for 48% of all side-impact fatalities, but only 25% of all fixed-object crashes. Half of all side impacts involving a tree result in injury or fatality.
- Zeigler conducted a study of tree crashes in Michigan between 1978 and 1985 and determined that tree crashes were much more likely to occur adjacent to curved roads, and that 77% of all curved road tree crashes occurred on the outside of the curve [10]. More recently, NCHRP Report No. 500 noted that 90% of tree crash fatalities occurred on two-lane roads, and that 8% of all fatal crashes in the U.S. in 1999 involved trees [11].
- A research study of trees planted in curb-lined medians adjacent to California highways indicated that tree crash rates were significant and contributed to severe crashes [12]. Increased hazard offsets, associated with wider medians, did not strongly affect crash rates or crash severities involving trees.
- Nonfatal crashes with trees are also a significant problem in the U.S. In 2001, 141 thousand of 229 billion household vehicle trips in the U.S. resulted in tree crashes [13]. Thus, on average, a tree crash occurred in every one out of 1.62 million trips. Drivers who took an average of 2 trips per day, every day in 2001, had a 1 in 2,200 chance of impacting a roadside tree in 2001.

Roadside trees and their associated crash risks have also been well-established internationally. Some examples of international findings are presented below.

- Thailand has seen an increasing number of fatal traffic crashes in the last two decades, and ROR crashes constitute approximately 45% of all fatal crashes [14]. Nearly 1/3 of all tree crashes in Thailand result in fatal or disabling injuries.
- A study reviewing fatal single-vehicle crashes in Victoria, Australia determined that trees were struck in 75% of the crashes [15]. Approximately half (53%) of fatal tree crashes and more than a third (36%) of fatal utility pole crashes occurred on the roadside of the opposing travel lanes (i.e., the right-hand side). Fatal tree crashes were more common adjacent to rural roads and were typically located between 3 m and 10 m (10 ft and 33 ft) from the side of the road. A separate study of South Australian crashes found that roadside hazards contributed to 40% of all fatal crashes, 39% of all fatal injuries, and 38% of all hospitalizations in South Australia between 1985 and 1996 [16]. Approximately 90% of all fatal crashes involved a hazard located within 9 m (30 ft) from the roadway, and over 50% were within 3 m (10 ft) from the roadway. Trees alone accounted for 23% of all roadside deaths, and 17% of all serious injuries.

Due to space and page limitations, interested readers are encouraged to refer to Reference [17] for more resources and literature review regarding tree crash studies.

Tree Litigation and State DOT Liability

Historically, many lawsuits have been levied regarding roadside trees, generating a large volume of case law. Roadside tree crash and non-crash injury histories have been discussed at length by Vance [18]. Historically, outcomes of case law regarding vehicular impact with trees which were still standing, in the process of falling, or having previously fallen favored the defendants (governmental agencies such as DOTs, counties, and cities) when at least one of the following conditions was met:

- The road on which the crash occurred was rural, invoking the “rural-urban distinction” in which rural roads are not held to similar expectations of routine maintenance and inspection [18];
- Maintenance of the government-owned property (e.g., street, right-of-way, sidewalk, etc.) did not directly contribute to, nor was the cause of, the crash or injury outcomes;
- The tree was located outside of the right-of-way or on private property;
- Reasonable maintenance procedures would not have detected defects in a tree or limb which fell; or
- Trees or limbs which fell during adverse weather events did not show signs of distress, disease, or damage.

A summary of some relevant tree liability cases which the plaintiff was awarded and not awarded are shown in Tables 1a and 1b, respectively, but the list is not comprehensive.

Many of the lawsuits which were successfully levied against the state were awarded based on the premise of negligence. These cases included events when an agency was notified of an issue regarding a tree (e.g., tree fallen in roadway, diseased or dead tree adjacent to roadway, etc.) and failed to act, or when proper maintenance procedures (e.g., mowing and pruning) around critical locations, such as at intersections, were not followed which allowed trees to obscure traffic control devices (e.g., stop signs). Because legal opinions and rulings often depend

TABLE 1a Example Lawsuits Involving Trees in which Plaintiff Was Awarded

Case Title	Events Precipitating Lawsuit	Judgment
<i>Trees were Primary Contributor</i>		
Edgett v. State of New York (1959)	Tree limbs hanging over roadway constituted a hazard	State failed to properly inspect and maintain tree
Harris v. Vil of E. Hills (1977)	Rotted tree limb fell through vehicle roof, paralyzing victim	Village failed to properly inspect and maintain tree
Jezek v. City of Midland (1980)	Tree posed obstruction to driver's line of sight, causing crash	City failed to maintain line of sight at intersection
Julian v. State of New York (1946)	Tree limb fell in front of vehicle on highway, causing collision, injuries	State failed to properly inspect and maintain tree
Lewis v. State of Louisiana, DOTD (1994)	Dead tree fell over onto highway causing crash, injury	State failed to properly inspect and maintain tree
Marsh v. SCDHPT (1989)	Tree fell onto vehicle driven by plaintiff, causing injury	State failed to properly inspect and maintain tree
Patton v. Department of Transportation (1996)	Tree limb fell onto moving vehicle, causing fatality	State failed to properly inspect and maintain tree
Sanchez v. Clark County (1988)	Overhanging tree limbs obscured oncoming traffic from view, causing crash and fatality	County failed to maintain line of sight at intersection
Sanker v. Town of Orleans (1989)	Limb overhanging roadway was struck by motorcyclist, causing fatality	Town was negligent in failing to prune tree branches to ensure safe travel
Texas Dept. of Transp. v. Olson (1998)	Vehicle ran stop sign and struck motorcyclist, who was obscured by tree at intersection	DOT was negligent to maintain line of sight at intersection and properly place stop sign
Texas Dept. of Transp. v. Pate (2005)	Tractor-trailer impacted and killed occupants of vehicle obscured from sight by tree overgrowth at intersection	DOT failed to ensure visibility of traffic control device
Twomey v. Commonwealth (2005)	Vehicle ran stop sign causing crash and fatality, due to tree growth at sign location	Commonwealth failed to ensure visibility of traffic control device
Wilson v. State, Through Dept. of Highways (1978)	Tree fell and was an obstruction on highway, causing crash and injury	DOH failed to maintain tree and placed public at risk during maintenance of roadside trees
<i>Trees were Secondary Contributor</i>		
Harris v. State of Louisiana (2008)	Vehicle lost control when traversing pavement edge drop-off, and vehicle crashed into tree, causing fatality	Pavement edge drop-off was major cause of crash and DOTD was negligent to provide proper maintenance for roadway
Peterson v. Transportation Dep't (1986)	Vehicle lost control due to pavement edge drop-off and crashed into tree, causing injury	DOT failed to properly maintain roadway

on historical precedent to determine whether to award a plaintiff and the degree of culpability of the defendant, modern cases still use results of cases which were decided many decades ago.

However, the significance of the historical case law may be reduced in the future, because many of the lawsuits were decided in the prior to the completion of the modern highway and interstate system, installation of federal transportation guidance, and creation of transportation groups including NHTSA, FHWA, and AASHTO (American Association of State Highway Transportation Officials). In 1956, U.S. President Eisenhower signed the *Federal-Aid Highway Act of 1956*, which first awarded federal funding for a nationwide, continuous network

TABLE 1b Example Lawsuits Involving Trees in which Plaintiff Was Not Awarded

Case Title	Events Precipitating Lawsuit	Judgment
Carr v. City of Lansing (2003)	Trees obscured stop sign causing crash and fatality	Unclear definition of highway and uncertain duties to maintain signage did not warrant award of damages
Carver v. Salt River Valley Water Users Association (1969)	Rotted tree fell, harming pedestrian	Defendant failed to prove the Association's responsibility to inspect and maintain tree
Cline v. Dunlora South, LLC (2012)	Tree fell on vehicle, causing injury	Private landowner is not responsible for injuries to travelers adjacent to property on roadway
Commonwealth v. Callebs (1964)	Tree fell during storm, crushing car and causing fatality	Commonwealth would be excessively burdened to inspect and maintain trees in wooded area
Jessop v. Department of Transportation (2011)	Tree hanging over roadway impacted by vehicle causing crash, injury	Ohio DOT was not responsible for inspection nor maintenance of tree causing injury and no notice was given to the state indicating imminent risk to public
McGinn v. City of Omaha (1984)	Tree fell on vehicle during storm, causing paralysis	Defendant failed to prove that proper inspection and maintenance of the tree would have prevented injury
Miller v. Department of Transportation (2008)	Fallen tree on roadway caused crash	Plaintiff failed to establish that fallen tree could not be adequately observed within a safe stopping distance or that ODOT had been given sufficient notice of tree and failed to respond
Pietz v. City of Oskaloosa (1958)	During strong winds, park tree fell on stationary vehicle, causing injury	Court determined that routine, sufficient inspection unlikely to identify tree rot, and that the strong winds at the time of the crash did not constitute a lack of sufficient maintenance by city
Porta v. State, State Board (1970)	Hurricane caused tree to fall, causing fatal crash	Defendants were not responsible for failing to maintain roadways during or immediately after weather disaster
Roman v. Stamford (1989)	Rotted tree fell on vehicle, causing injury	City was not responsible for the maintenance of tree on park property
Thompson v. State of Louisiana (1996)	Tree fell across highway, causing crash and injuries	Fallen tree was outside of DOT's right-of-way maintenance responsibility, and fallen tree was considered a temporary condition, not defect, since DOT was not notified in advance of condition
Walker v. Dept. of Transp. & Development, Office of Highways (1984)	Tree fell across highway during ice storm, causing fatal crash	Tree was located on railroad company property and did not show signs of distress, rot, or defect which would have warranted maintenance, and DOT did not have responsibility to remove tree within 1 hour of falling on roadway
Luceri v. County of Orange (2004)	Tree fell on roadway, causing crash and fatality	Plaintiff failed to demonstrate that the County was negligent in maintenance of tree or that the county was given sufficient notice to remove tree blocking roadway
Tinao v. City of New York (1985)	Vehicle ran off road and struck roadside tree, resulting in fatality	Tree location on shoulder was not the result of City's negligence
Hensley v. Montgomery County (1975)	A rotted limb of a tree located within the clear zone fell and penetrated the occupant compartment of a moving car, resulting in severe injury	Neither the property owner nor County were found to be negligent, owing to the principle philosophy of "natural conditions" and onerous duty of inspection
Kinne v. State (1959)	Plaintiff was forced to take evasive maneuver to avoid vehicle driving wrong way in lane and struck tree located 3 ft from roadway	State was not found to be negligent for allowing tree to be located adjacent to the roadway. Court affirmed that it was the prerogative of the state to use roadside land for whatever purposes it sees fit.

of roadways which previously did not exist [19-21]. Construction in the continental United States began immediately in 1956, and the original design of the highway system was completed in 1991. Additional construction, maintenance, and improvements continue to today. Furthermore, the U.S. Department of Defense (DOD) designated portions of state highways and interstate routes as part of the National Highway System (NHS), a high-mobility transportation network which could provide emergency high-flow transportation in the event of national need [22-23]. Likewise, AASHTO published the first de facto standard in roadside safety standardization, the *Roadside Design Guide*, in 1988 [24] and a fourth revision was released in 2011 [3]. As of 2016, these recommendations and practices have been widely accepted and implemented by every state in the U.S. Vance's review of tree case law preceded all of these developments [18]. Therefore, future litigation regarding roadside trees may be altered by modern safety developments.

Much of the available tree-related case law is from before the 1970s, but other tree-related problems became apparent later. Trees have been observed to disrupt and damage curb, gutter, road, sidewalk, and stormwater systems, costing millions to replace and sometimes contributing to congestion and flooding [25]. The burden of tree maintenance and the liability associated with inadequate maintenance has been transferred to transportation departments, including cities, counties, and states in recent years [26]. Unevenness in sidewalks has also been identified as a property-owner liability [e.g., 27-28]. Tree foliage decreases urban roadway lighting effectiveness by blocking street lights, as well as obscuring pedestrians, including children, from the line of sight of drivers, which can decrease a driver's reaction time and increase the risk of vehicle-pedestrian collisions [25]. State DOTs in disaster-affected areas noted that fallen trees constitute a significant safety risk by obstructing travel, complicating rescues, and are hazards to cleanup and utility crews. The State DOT anecdotal evidence is supported by a large number of lawsuits levied against the states with claims regarding adverse weather and fallen trees, as noted in Tables 1a and 1b.

Investigation of State DOT Tree and Utility Pole Crashes

Researchers at MwRSF received data from State DOTs to further explore the factors contributing to severe tree and utility pole crashes and the best means of using those factors for safety

TABLE 2 Summary of Tree and Utility Pole Crash Data Provided by State DOTs

State DOT	Crash Data Years	Number of Crashes	A+K Crashes	A+K Percentage
Illinois	2009-2013	42,048	3,913	9.3%
Indiana	2010-2014	25,039	788	3.1%
Kansas	2010-2014	49,352	382 (Fatal only)	0.8% (Fatal only)
New Hampshire	2009-2013	11,284	520	4.6%
New Jersey	2009-2013	59,540	1,586	2.7%
North Carolina	2010-2014	53,696	2,659	5.0%
Ohio	2010-2014	91,072	1,160 (Fatal only)	1.3% (Fatal only)
Oregon	2009-2013	7,062	286 (Fatal only)	4.0% (Fatal only)
South Dakota	2010-2014	1,943	147	7.6%
Utah	2010-2014	8,662	408	4.7%
Washington	2009-2014	30,470	1,789	5.9%
Wisconsin	2010-2014	20,690	365 (Fatal only)	1.8% (Fatal only)
Total	2009-2014	400,858	> 14,003	~5.4%

campaign purposes. Utility poles and trees have many similarities in terms of rigidity, offset from the roadway, and size, and thus were lumped together for a more complete analysis.

Due to the significant volume of data collected, it was impossible to manually sort the data to extract only crashes in which tree and/or utility pole impacts were the most harmful. In other words, researchers were unable to remove or reject crashes in which a tree impact was incidental (e.g., scraping, minor sideswipe, low-speed impact at end of crash sequence, etc.). However, most of the contributing state DOTs sorted crashes by most harmful event (MHE), and thus the dataset primarily consisted of tree or utility pole crashes as MHE. Thus, the following evaluation of the tree crash data was intended for overview purposes only.

Crashes were sorted by injury level whenever possibly, using the KABCO scale:

- “K” injury: fatality in which one or more occupant died within the reporting period after a crash (typically 30 days);
- “A” injury: severe injury consisting of broken limbs, stupor or coma, severe abrasions, amputations, or dislocations, and other injuries requiring hospitalization;
- “B” injury: apparent injury consisting primarily of deeper abrasions, bruises, soreness, and minor confusion which did not require hospitalization;
- “C” injury: possible or minor injury consisting mainly of light abrasions, bumps, mild soreness, and bruising; and
- “O” (non-injury): property damage-only (PDO).

Some states did not tabulate injury data using the KABCO scale, instead indicating highest injury scale with a singular “injury” field. No attempt was made to determine which, if any, of these crashes should be listed as “A”-injury, and for purposes of analysis, were included only with the “B” and “C”-injury crash statistics. Thus, the actual severe crash percentage for all states may be underreported. Note that states which did not provide KABCO injury levels had more fatal crashes and a higher fatal crash percentage than states which did provide KABCO data, on average.

Crash data was sorted by severity and the time of day, and plotted on a radial (i.e., radar) chart, as shown in Figure 2. Property damage-only (PDO) and minor-injury (i.e., non-incapacitating) crashes had similar trends, with the majority of crashes occurring between 6 am and 10 am, as well as between 2 and 6 pm. Fatal and severe crashes peaked around 4:00 pm, during the afternoon commute, as well as at 2:00 am. Results indicate that the evening “rush hour” traffic during the afternoon commute home from employment was more commonly associated with severe crash outcomes than the morning commute, which may be due to fatigue and/or sunlight at dusk blinding drivers. Nonetheless, most fatalities occurred during early morning hours and are likely related to either impairment (e.g., alcohol) or drowsiness.

Injuries were also plotted by vehicle type when data was available, as shown in Figure 3. Passenger cars and light trucks (i.e., pickup trucks, SUVs, and vans) accounted for approximately 60% and 37% of all crashes, respectively, and large trucks (e.g., single-unit trucks, buses, tractor-trailers) and motorcycles accounted for 2.1% and 0.7% of crashes, respectively. The severe crash percentage (“A”+“K” injuries divided by total injuries) was approximately the same for passenger cars, light trucks, and large trucks. In contrast, “A”+“K” injuries occurred in 41% of police-reported motorcycle crashes, and motorcyclists constituted 7% of all fatal tree crashes. Police-reported crashes involving motorcyclists are likely to be

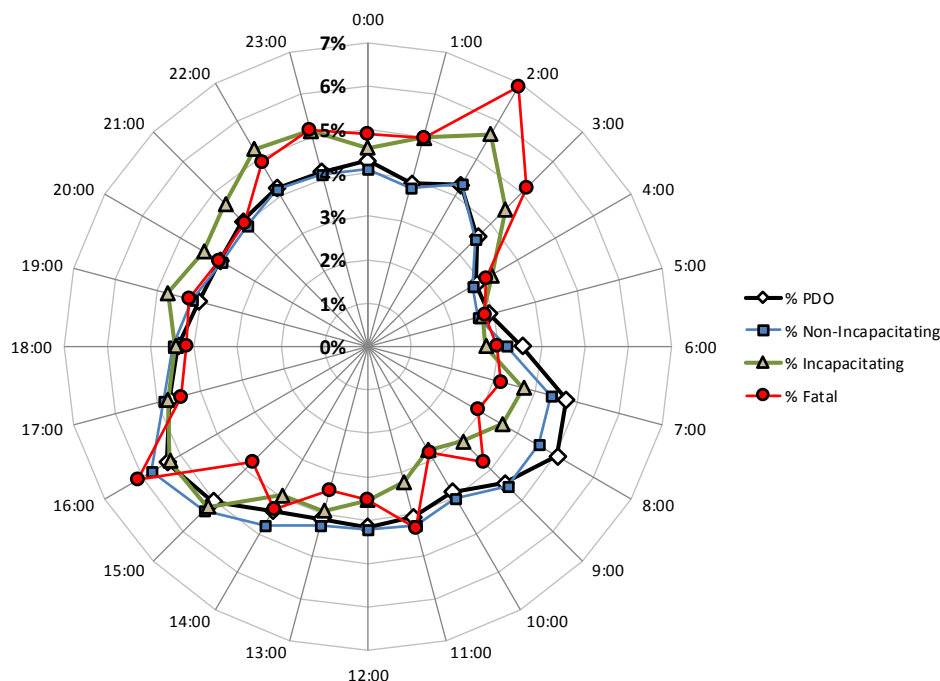
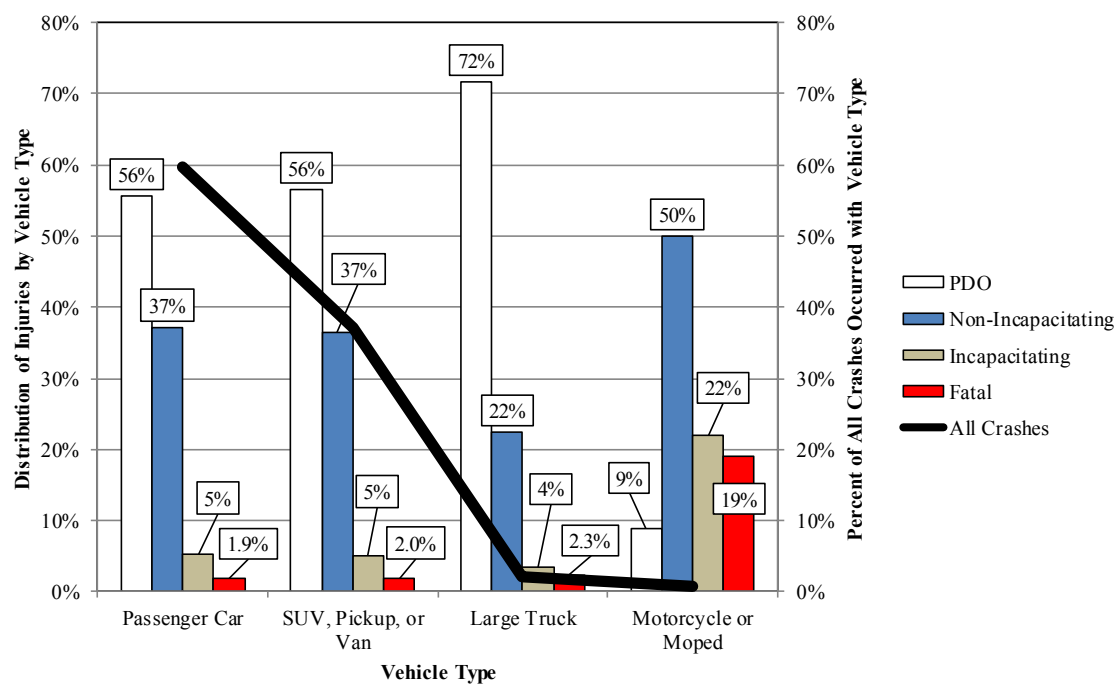


FIGURE 2 Time of crash distribution based on injury type.

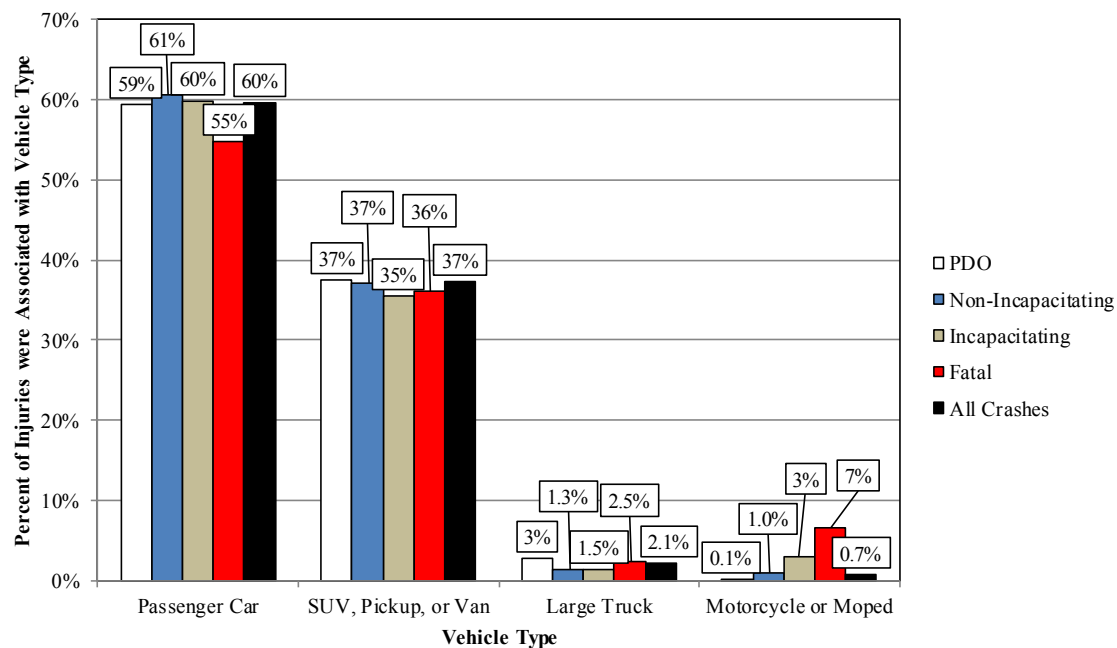
disproportionately severe because motorcyclists do not have safety mechanisms nor an additional energy-absorbing structure like a vehicle frame to protect the motorcyclist during impact. No attempt was made to include unreported crashes with any vehicle type, as these crashes are likely to be predominantly low-severity (PDO or “C”-injury).

Severe crashes were segregated by road characteristics, as shown in Figure 4a. Curved roads accounted for approximately 31% of all crashes and nearly 44% of all fatal crashes involving trees and utility poles. Unfortunately, crashes occur at elevated rates on curves; a study conducted by NHTSA in 2009 indicated that ROR crashes accounted for approximately 62% and 90% of all police-reported crashes on straight and curved roads, respectively [29]. Thus, the increased severity and number of crashes associated with curved roads involving trees and utility poles suggest that safety treatments adjacent to roadway curves could have a very high cost-effectiveness.

Not surprisingly, urban roads were associated with less fatalities than rural roads, as shown in Figure 4b, likely because urban roads typically use lower posted speed limits (PSL). Crash rates and average injury severity may be higher on higher-PSL urban roads. Nonetheless, urban roads still accounted for 36% of severe tree and utility crashes, and 42% of all tree and utility pole crashes. Based on the available data, it is estimated that a total of more than 5,000 severe crashes occurred in urban areas for the twelve contributing states over a five-year period. Thus, an average of 84 severe tree and utility pole (mostly tree) crashes occur in urban areas for each state, each year. Recall that because some states did not provide “A”-injury data, the number of average annual severe tree and utility pole crashes is likely to be underreported.

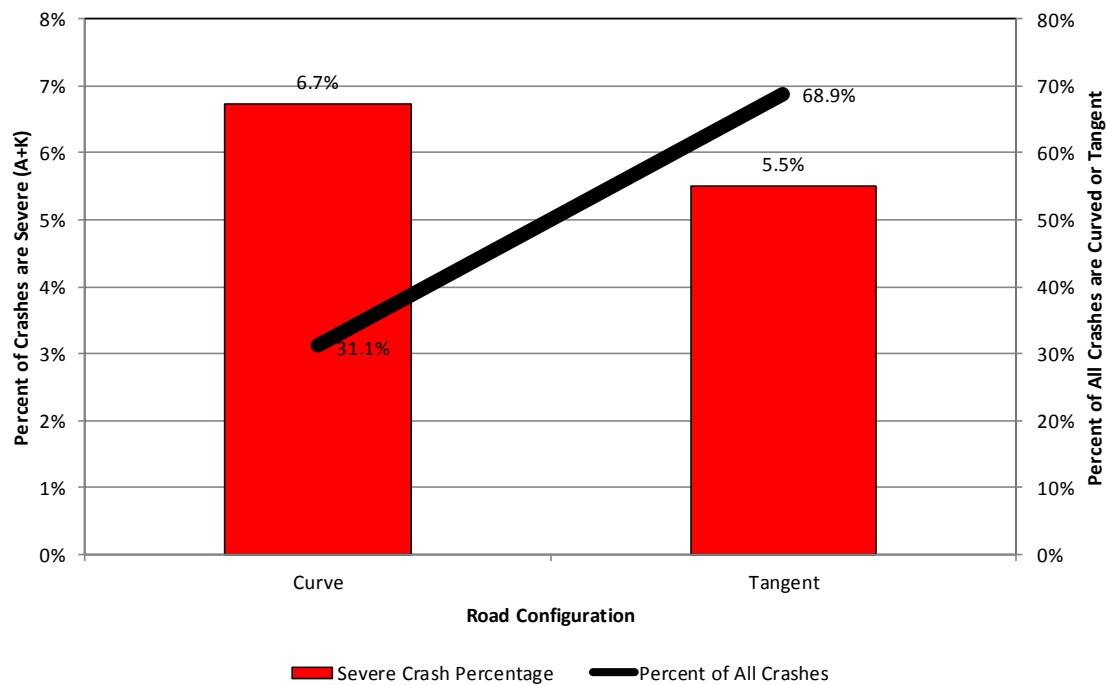


(a)

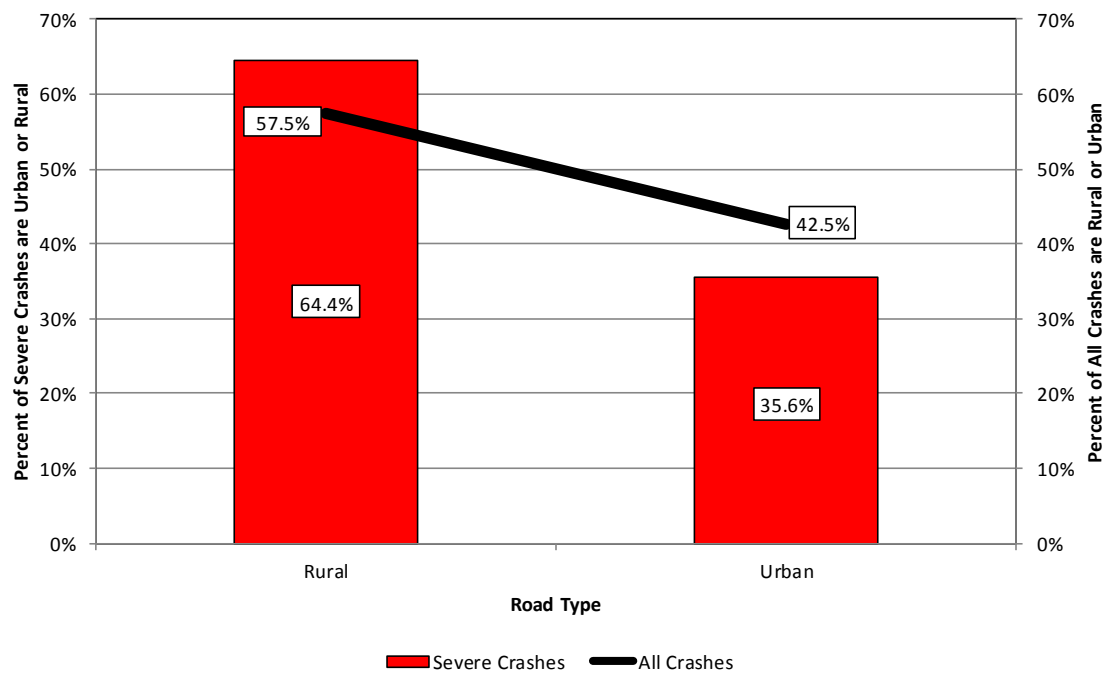


(b)

FIGURE 3 Injuries by vehicle type: (a) Injury distribution by vehicle type; and (b) the percent of crash injuries which occurred in conjunction with each vehicle type.



(a)



(b)

FIGURE 4 Severe (A+K) injury risk by roadway type: (a) Curved and tangent roads; and (b) rural and urban roads.

Annual Tree and Utility Pole Crash Costs

While characteristics of tree and utility pole crashes can assist state DOTs to prioritize treatments, costs and likelihood of fatalities are equally important to assist with marketing purposes. Researchers attempted to determine the comprehensive crash cost for tree and utility pole crashes for the data provided by State DOTs and then determined an average annual cost per state, annual nationwide cost, and total state and nationwide cost for the study period.

Only data between 2010 and 2013 was analyzed because all states provided data for those calendar years. The 2012 FHWA's Value of a Statistical Life (VSL) was used to estimate the fatal crash cost of the tree and utility pole crashes for each state [30]. While nonfatal crashes also are associated with crash costs, determination of the appropriate comprehensive costs by KABCO scale are inexact. The 2011, 2013, and 2015 memoranda published by FHWA regarding the VSL estimates do not denote injuries by KABCO scale, but rather by modified AIS injury levels [30-32]. Means of determining approximate costs for KABCO injury scales vary widely [e.g., 33-34]. State DOTs may use crash cost tables unique to the respective state for determining the economic loss from motor vehicle crashes. Although many different scales could be used to translate AIS injury scale factors to the KABCO injuries, MwRSF researchers selected the TIGER Grant Benefit-Cost Analysis (BCA) Resource Guide, Table 4 [30, 33] for differentiating costs because all TIGER grant applications must denote expected crash cost reductions using this same format. Results of the crash cost analysis are shown in Tables 3a and 3b.

TABLE 3a Estimated Annual Fatal Crash Costs Using 2012 VSL and TIGER Grant BCA Resource Guide, All State Data [30, 33]

			Crash Cost Per State, Per Year by KABCO Injury Level ^(1,2) (Millions of Dollars)					
Year	No. Crashes	No. Fatal Crashes	K	A	B	C	O	Injured, Unk ⁽³⁾
2010	81,566	1,119	848.6	62.7	70.0	108.4	12.8	168.8
2011	78,012	1,054	799.3	61.5	65.5	105.3	12.2	164.4
2012	76,144	1,067	809.1	62.6	62.0	106.8	11.7	163.7
2013	77,239	1,046	793.2	58.6	58.1	102.8	12.3	153.3
Annual Average			\$812.6M	\$61.3M	\$63.9M	\$42.5M	\$12.3M	\$162.5M
Average Annual Total Cost Per State DOT								\$1.06B
Average Annual Nationwide Total Cost								\$58.26B
Estimated Total Nationwide Cost for 2009-2014 Study Period								\$349.6B

(1) KABCO injury costs estimated using 2013 FHWA Memo regarding VSL and the Tiger Grant BCA appendix [30, 33]

(2) Unless otherwise noted, numbers are in millions of U.S. dollars. "M" denotes millions of U.S. dollars. "B" denotes billions of U.S. dollars.

(3) Injury cost distribution for Unknown injury applicable for data from Kansas, Ohio, Oregon, and Wisconsin, which did not differentiate between injury levels A, B, or C.

TABLE 3b Estimated Annual Fatal Crash Costs Using 2012 VSL and TIGER Grant BCA Resource Guide, Excluding States Without Injury Severity Differentiation [30, 33]

			Crash Cost Per State, Per Year by KABCO Injury Level ⁽¹⁾ (Millions of Dollars)				
Year	No. Crashes	No. Fatal Crashes	K	A	B	C	O
2010	81,566	1,119	716.6	94.0	105.0	63.9	11.1
2011	78,012	1,054	712.1	92.2	98.3	61.8	10.1
2012	76,144	1,067	705.3	93.8	93.0	64.6	10.0
2013	77,239	1,046	732.6	87.9	87.1	64.7	10.5
Annual Average			\$716.6M	\$92.0M	\$95.9M	\$63.7M	\$10.4M
Average Annual Total Cost Per State DOT							\$0.98B
Average Annual Nationwide Total Cost							\$48.9B
Estimated Total Nationwide Cost for 2009-2014 Study Period							\$293.6B

(1) KABCO injury costs estimated using 2013 FHWA Memo regarding VSL and the Tiger Grant BCA appendix [30, 33]

When all state data was tabulated and states which did not differentiate between non-fatal injuries were included in the dataset (as shown in TABLE 3a), the average annual, per-state fatal and all tree and utility pole crash costs were \$812.6 million and \$1.17 billion, respectively. The total, combined fatal crash cost between 2010 and 2013 for the 12 states participating in this study was \$39.0 billion. By extrapolation, the nationwide annual tree and utility pole fatal crash cost and total cost between 2010 and 2013 would therefore be \$40.6 billion and \$162.5 billion, respectively. The surveyed state data compares very well with the annual national fatal crash cost of \$40.0 billion (average of 3,500 fatal tree crashes and 900 fatal utility pole crashes annually [1]). When only state data with full KABCO injury differentiation were used, overall estimated crash costs declined, as shown in TABLE 3b, but this was believed to be strongly correlated with an overall reduction in the number of deaths in those states.

SAFETY-RELATED MARKETING CAMPAIGNS

While the crash data was useful for determining the factual basis for a successful marketing campaign, research was still required to identify what methods, techniques, and approaches for the campaigns would be the most successful. Researchers conducted a literature review of marketing campaigns, identified characteristics of those campaigns with the best likelihood of success, and drafted example ideas using those techniques and the background data to provide initial ideas for state DOTs.

Marketing Research

Modern marketing campaigns typically use a combination of three principle elements: logic and/or facts; emotion (e.g., audience empathy, humor, shock); and a sense of societal obligation, ethics, or morals. These foundations resemble the historical *logos*, *pathos*, and *ethos*, respectively, of Aristotle's *Rhetoric*.

Historically, transportation safety campaigns which utilized a mix of emotional and factual appeals were more effective than campaigns with only factual appeal [35, 36]. A meta-analysis of 67 studies in 12 countries noted that the effectiveness of transportation safety campaigns increased by 50% when emotional and rational arguments were paired (15% reduction in crashes), vs. when only rational arguments were used (10% reduction in crashes) [37]. Studies have shown that specific and simple messages suggesting desirable behavior with positive motivation can be the most effective way of conveying messages [38, 39].

Although the use of positive emotional reinforcement, such as humor and inspiration, have been linked to successful campaigns and public behavior changes [39], the effectiveness of negative emotional appeals to change behaviors is unclear [36, 40-42]. The examination the effectiveness of fear appeals is still inconclusive, although many research studies have been conducted to clarify its efficiency [36]. The extent to which the audience reacts to a fear arousal approach cannot be quantified, and thus an optimum level of fear arousal cannot be identified [35, 43]. Moreover, long-term exposure to fear appeals may desensitize the audience to the message.

Overall, women are more likely to react to fear appeals by positively changing behaviors than men [44]. Lewis, Watson and White postulated that women tend to process and react to negative information more than men [45, 42]. On the other hand, males will respond more favorably to positive emotional appeals than females [46, 42].

Social psychologists offered theoretical explanations of the differences between genders with positive and negative appeals emotion [40-42, 47]. According to theories of information processing based on a selectivity hypothesis, most positive emotional appeals are tied to centric themes of advertisements, and males, which selectively or sequentially process cues, are more prone to focusing on the primary message and react to it. In contrast, negative emotional appeals generate feelings of consequence and possible outcome based on maintaining negative behaviors, and females are more apt to identify, relate, and react to those appeals. Nonetheless, fear appeals must also provide a message indicating what reaction is desired. Advertisements which invoked fear, coupled with a recommendation (such as safer driving habits) were much more effective than advertisements which only stimulated feelings of fear, shock or grief without additional recommendations [48].

Safety Campaign Design

The means of communicating a message in media channels (e.g., newspaper, television, radio, word-of-mouth, etc.) may have limited effectiveness without contributions from law enforcement, educational outreach, and new technologies, as shown in Figure 5 [36, 49-52]. Delaney noted that the combination of public relations and law enforcement lead to significant reductions in crashes and behavioral improvements Australia and New Zealand [35]. Reductions in fatalities were not sustained when educational, informational, and public marketing approaches were conducted independently of each other. When mass media alone is used to promote a message, very little effect was observed, whereas more integrated campaigns had much higher rates of success [49-50].

For instance, a hospital-led youth helmet advocacy promotion campaign in UK utilized trusted professionals to engage in educational outreach to young males, which resulted in a nearly 200% increase in helmet use by 11 to 15 year-olds (from 11% to 31%) in five years [53].

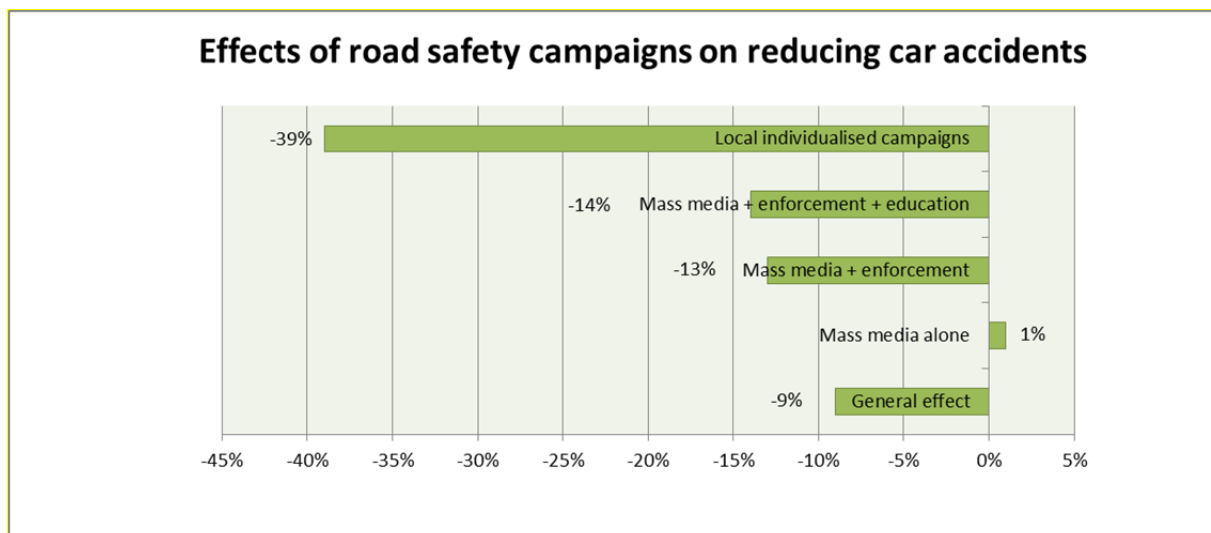


FIGURE 5 The effects of road safety campaigns on reducing car accidents [49, 50]. State Survey

As a result, cycle related head injuries for individuals less than or equal to 16 years old fell from 112 per to 60 per 100,000 total population in the campaign area.

In order to determine how best to present the need for safety improvements at the DOT level, a survey was sent to representatives of all 50 U.S. states to determine what marketing techniques and tree removal projects were attempted, if any, and to determine the relative success of those efforts. Of the 50 states surveyed, 25 State DOTs responded. A brief summary of the survey results are shown in Table 4.

TABLE 4 Summary of State Survey Results: Tree Removal Projects and Public Advertising Projects

Question	Yes	No	Did Not Answer
Has your State DOT or government agency utilized marketing campaigns (Ads, lobbying, brochures, etc.) to either raise public awareness of safety risks, including roadside trees or garner public support for safety treatments for hazards, particularly roadside trees, such as removal, relocation, or shielding?	1	23	1
Has your State DOT or government agency funded any safety improvement projects that have included roadside tree removal or relocation?	15	6	4
Does your State DOT or government agency utilize specific maintenance practices (i.e., mowing, trimming, removal, etc.) for addressing roadside trees located within the clear zone?	19	2	4
Has your State DOT or government agency conducted any crash data analysis studies to investigate safety risks involving roadside trees and/or utility poles (i.e., telephone and power)?	15	6	4

Only one state which responded to the survey (NDOR) noted conducting a targeted marketing campaign to raise public awareness and/or support for tree removal projects. However, fifteen of the responding states indicated that tree removal was conducted as part of a safety improvement project, but nearly all states indicated that this is typically conducted during roadway rehabilitation and rarely a stand-alone safety improvement. Nineteen of the responding states indicated that standard practices were in place to prevent new tree growth adjacent to major roadways, mostly through routine mowing and annual tree maintenance projects. Lastly, fifteen states indicated that annual or biennial crash data studies are used to determine statewide safety priorities, though four states indicated that trees were a specific focus group. Nearly all states noted that when a specific corridor was identified as a “black spot” with multiple fatal crashes, and the crash cause was found to be a tree or utility pole, that action was subsequently taken to remove the fixed object responsible for those crashes.

Examples of Marketing Campaign Strategies

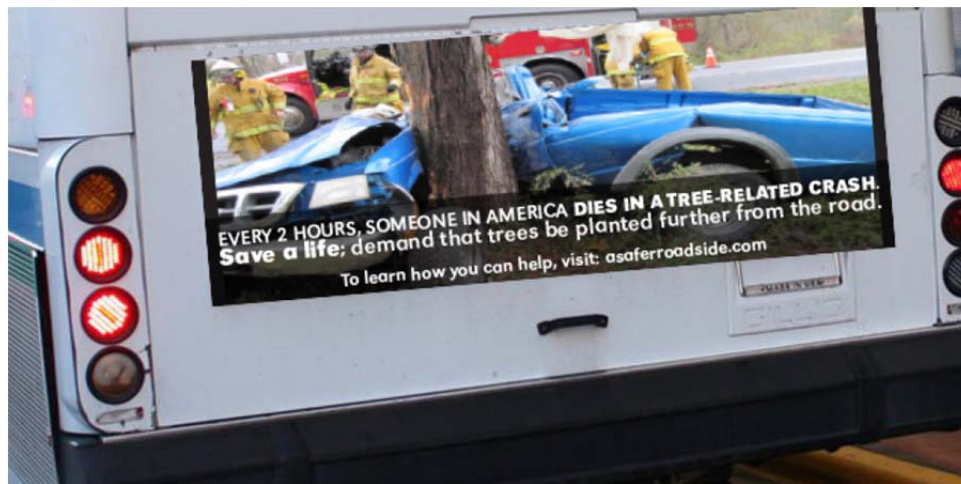
Effective safety campaigns, which are similar to effective marketing campaigns, motivate people to take action – such as supporting the work of a jurisdiction (e.g., removing trees) or contacting local authorities, such as stakeholders or transportation agencies and staff, or banding similarly disaffected people together to lobby for safer solutions. MwRSF researchers evaluated marketing campaign approaches, audiences, and means of conveying messages, especially as they pertained to roadside safety messages, to determine what approaches may have the best likelihood of success. While this phase of the research is ongoing, initial visual designs were generated and drafts were shown to the Midwest States Pooled Fund program for review. Some examples of initial marketing advertisements are shown in Figure 6.

Researchers also identified various groups of people to target, messages which could resonate with those groups, and means by which to convey those messages. Example results are shown in Table 5.

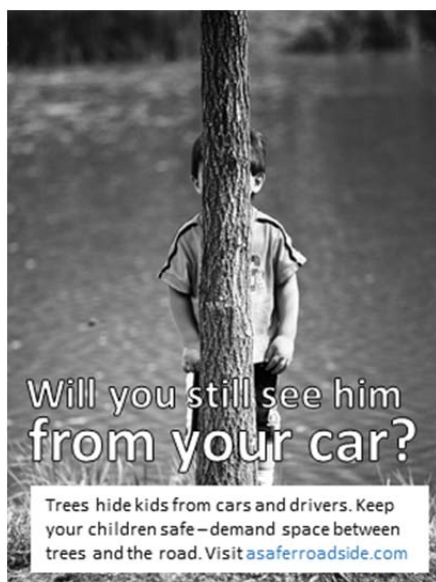
Although positive emotional elements have been shown to invoke more change with male audiences, fear appeals are the predominant technique and the easiest to apply for most safety campaigns. Thus, campaigns may be more successful if the recommended action to the listener is focused toward proactive protection (such as for a relative, e.g., child) as a positive reinforcement, rather than focusing primarily on the negative consequences of the crashes themselves. In addition, partnering with unlikely sources, such as the Arbor Day Foundation, may increase the receptiveness of the public to the DOT’s safety campaign, accomplishing a safety goal while simultaneously encouraging a broader goal of providing greener roadsides. Other groups, such as motorcycle advocacy groups, could similarly lobby on behalf of safer tree guidelines, increasing the base appeal of a campaign and its outreach.

Preliminary designs are presented in this paper. Additional research is in progress at the Midwest Roadside Safety Facility to develop and provide example advertisement and marketing strategies to the contributing members of the Midwest States Regional Pooled Fund Program [17].

Lastly, it is important to note that for some locations, removing or relocating trees or utility poles may be impossible or too politically sensitive to accomplish. In these locations, the safety campaign approaches described here could be utilized for separate but related safety



(a)



(b)

FIGURE 6 Some preliminary examples of outdoor, visual marketing advertisements: (a) Bus advertisement; and (b) billboards. (Note, image taken from [54]. The safety website is still under development and the final web address is not shown.)

TABLE 5 Examples of Outreach Target Groups, Marketing Methods, and Outreach

Target Group	Why:	Methods:	Example Themes/Slogans:
General Public	Broad need Could inspire individuals to take action Likely to resonate with families, friends of fatal crash victims	Billboards (low benefit per-person, high exposure) Radio/TV slots Mailers, advocacy websites News stories, newspaper articles, press releases Denote public share of crash costs on utility bills, tax forms, etc.	“Don’t Leave the Wrong Impression” “Room to Breathe” “Better for Trees, Better for Everyone” “End the Roadside Death Penalty” (#RoadsideDeathPenalty) “Beware: Deadly Falling Tree Limbs” #Widowmakers (in reference to colloquial name for dead or decayed branches which can fall from trees)
Parents	May have children who are young drivers Trees on residential and urban streets can hide children (pedestrians)	Radio/TV slots Billboards Mailers, advocacy websites News stories, newspaper articles, press releases Informational meetings at schools or city council meetings	“Hide and Seek” (e.g., chalk outline of pedestrian on the ground next to street tree) “What’s hiding behind the tree?” #ProtectYoungDrivers #GiveThemRoom or #RoomtoBreathe (in reference to new drivers needing roadside space)
Taxpayers	Crash costs hurt tax rates, emergency service costs Tree maintenance, repair, and removal are taxpayer costs Tree growth can damage utilities, storm sewers, roads, etc. requiring costly repairs	Billboards (low benefit per-person, high exposure) Radio/TV slots Mailers, advocacy websites News stories, newspaper articles, press releases Denote public share of crash costs on utility bills, tax forms, etc.	“Beautiful, Costly, Deadly” (in reference to roadside tree aesthetics projects) “That Tree will Cost You” (in reference to maintenance, crash, and install costs) “Who pays for a crash? You do”
Environmental Groups	Likely to be opponents to most tree removal efforts Co-opting support from these groups could greatly improve success for safety projects	Mailers, PSAs, websites Attending and speaking at group meetings Public events to raise money for removing trees and replanting further from roads	“Move the Tree, Save the Tree” “Trees and Cars Don’t Mix” “(Open Roads &) Breathe Easy” (in reference to oxygenating properties of trees but coupled with safer roadsides) “Greener, Safer, Better” #CarsareTreeKillers or #MoveItSaveIt #Greenshield (in reference to guardrail installations around tree clusters)

efforts, including means to reduce run-off-road crash events (e.g., reduced speeds) or to improve driver safety (e.g., seat belt usage). The messaging and safety campaign material will be sensitive to the PSL, type of roadway (urban or rural), and the proposed safety treatment (e.g., removal vs. shielding).

CONCLUSIONS

Despite more than 3,500 fatalities every year associated with roadside tree crashes, state DOTs often encountered resistance to removing trees and requiring minimum lateral offset planting guidelines, as many groups opposed tree removal. MwRSF is conducting a research study to evaluate historical tree crash data, tree litigation, and brainstorm or create new safety marketing campaigns to assist DOTs with positively and proactively preventing roadside tree crashes. A five-year, 12-state crash data set involving more than 400,000 tree and utility pole crashes was analyzed, revealing that annual comprehensive costs due to tree crashes likely exceed \$58 billion dollars in the U.S. Thus, each state loses an average of \$1 billion annually, on average. The general public is adversely affected by roadside tree planting which results in car crashes, road closures and delays, maintenance and trimming costs including replacement when infected with disease or insects, litigation from tree-related incidents, and risks for pedestrians.

The burden of tree maintenance traditionally falls to the property owners, whether private citizens, local authorities (e.g., urban government), or transportation agencies (e.g., DOT). All agencies and local authorities suffer a backlog of potentially useful safety treatments and improvements, thus it is important to emphasize the need and potential benefits that roadside tree safety treatments could provide. Crafting strategies for detecting and managing risk is imperative to safety campaigns and should be emphasized to both the campaign officials and to those targeted for action.

With a shifting litigious climate, it is in the best interest of the motoring public and the DOTs to quickly take action to safely treat roadside trees, promote guidelines for tree planting policy which balances aesthetics and safety, and to generate political strategies for combating negative perceptions of tree treatments and removal before encountering an impending rush of litigation. Although most calls to action are based on fear appeals, marketing campaigns should invoke positive emotions or whenever possible. Outreach and partnerships, combined with targeted messaging, may be critical for safety campaigns moving forward. Collaborating with groups which traditionally oppose tree removal to work together to form safer guidelines for tree installation and protection may reduce opposition and improve the likelihood of successfully, safely treating roadside trees.

ACKNOWLEDGMENTS

The authors would like to thank the Midwest States Regional Pooled Fund Program, consisting of Illinois, Indiana, Iowa, Kansas, Minnesota, Missouri, Nebraska, New Jersey, Ohio, South Dakota, Wisconsin, and Wyoming Departments of Transportation for sponsoring this project. In addition, the authors would like to acknowledge several State DOTs for providing crash data and support during the crash analysis phase of the project: Illinois; Indiana; Iowa; Kansas; New

Hampshire; New Jersey; North Carolina; Ohio; Oregon; South Dakota; Utah; Washington; and Wisconsin.

DISCLAIMER

The views of the authors are theirs alone and may not reflect the views and standards of the sponsoring or participating State DOTs, FHWA, NHTSA, nor USDOT. This paper does not constitute an endorsement of manufacturers, standard, nor specification.

REFERENCES

1. *Roadway and environment: Fatality Facts*, Insurance Institute for Highway Safety, Highway Loss Data Institute. <<http://www.iihs.org/iihs/topics/t/roadway-and-environment/fatalityfacts/fixed-object-crashes/2009>>
2. *Fatal Accident Reporting System (FARS) Encyclopedia*, National Highway Transportation Safety Administration (NHTSA), 2016. <http://www-fars.nhtsa.dot.gov/Main/index.aspx>
3. *Roadside Design Guide – 4th Edition*, American Association of State Highway and Transportation Officials (AASHTO), Washington, D.C., 2011.
4. Viner, J.G., “Harmful Events in Crashes”, *Accident Analysis and Prevention*, Vol 25 No. 2, 1993, pp. 139-145.
5. *Motor Vehicle Collisions with Trees Along Highways, Roads, and Streets: An Assessment*, NTSB Report No. NTSB-HSS-81-1, NTIS Report No. HS-032 489, Special Study by the National Transportation Safety Board, Alexandria, Virginia, May 1981.
6. Lee, J., and Mannering, F., “Impact of roadside features on the frequency and severity of run-off-roadway accidents: an empirical analysis”, *Accident Analysis and Prevention*, Vol 34, 2002, pp. 149-161.
7. Lee, J., and Mannering, F., *Analysis of Roadside Accident Frequency and Severity and Roadside Safety Management*, Final Report to the Washington State Transportation Commission, Washington State Transportation Center (TRAC), University of Washington, Seattle, December 1999.
8. Holdridge, J.M., Shankar, V.N., and Ulfarsson, G.F., “The crash severity impacts of fixed roadside objects”, *Journal of Safety Research*, Vol 36, 2005, pp. 139-147.
9. Ray, M.H., Troxel, L.A., and Carney III, J.F., “Characteristics of Fixed-Roadside-Object Side-Impact Accidents”, *Journal of Transportation Engineering*, Vol 117 Iss 3, May 1991, pp. 281-297.
10. Zeigler, A.J., “Risk of Vehicle-Tree Accidents and Management of Roadside Trees”, *Journal of the Transportation Research Board No. 1127*, Washington, D.C., 1988, pp. 37-43.
11. Neuman, T.R., Pfefer, R. Slack, K.L., Lacy, K., and Zegeer, C., *A Guide for Addressing Collisions with Trees in Hazardous Locations*, NCHRP Report No. 500 Volume 3, Washington, D.C., 2003.
12. Sullivan, E.C., *Safety of Median Trees with Narrow Clearances on Urban Conventional Highways*, Final Report to the State of California Department of Transportation: Traffic Operations Program, Cal Poly State University, San Luis Obispo, California, March 2004.
13. Dixon, K.K., and Wolf, K.L., “Benefits and Risks of Urban Roadside Landscape: Finding a Livable, Balanced Response”, *3rd Urban Street Symposium*, Seattle, Washington, June 24-27, 2007.
14. Somchainuck, O., Taneerananon, P., and Jaritngam, S., “An In-Depth Investigation of Roadside Crashes on Thai National Highways”, *Engineering Journal*, Vol 17 Iss 2, April, 2013.
15. Haworth, N., Vulcan, P., Bowland, L., and Pronk, N., *Fatal Single Vehicle Crashes Study: Summary Report*, Report No. 122, Accident Research Centre, Monash University, September 1997.

16. Kloeden, C.N., McLean, A.J., Baldock, M.R.J., and Cockington, A.J.T., *Severe and Fatal Car Crashes Due to Roadside Hazards*, Final Report to the Motor Accident Commission, MHMRC Road Accident Research Unit of University of Adelaide, Adelaide, South Australia, May 1999.
17. Vargas, C.M., Poulas, A.C., Tan, J., Yim, A., Schroder, B.D., Faller, R.K., Lechtenberg, K.A., and Stolle, C.S., *Marketing Approaches for Addressing Roadside Trees*, Draft Report in Progress.
18. Vance, J.C., Liability of State for Injury or Damage Occurring in Motor Vehicle Accident Caused by Trees, Shrubbery, or Other Vegetative Obstruction Located in Right-of-Way or Growing on Adjacent Private Property, Selected Study in Highway Law, Transportation Research Board, Washington, D.C., June, 1988, pp. 1966-N89 to 1966-N122.
19. *Federal-Aid Highway Act of 1956*, U.S. Government public law no. 627, June 29, 1956.
<https://www.gpo.gov/fdsys/pkg/STATUTE-70/pdf/STATUTE-70-Pg374.pdf>
20. "History of the Interstate System", Federal Highway Administration, Updated July 12, 2016.
<http://www.fhwa.dot.gov/interstate/history.cfm>
21. Weingroff, R.F., "The Year of the Interstate", *Public Roads*, Federal Highway Administration, Document No. FHWA-HRT-2006-002, Volume 69 No. 4, January/February 2006.
22. *National Highway System Designation Act of 1995*, U.S. Government public law no. 104-59, November 28, 1995.
<https://www.congress.gov/104/plaws/publ59/PLAW-104publ59.pdf>
23. "National Highway System Designation Act: Guidance", Federal Highway Administration.
<http://www.fhwa.dot.gov/legregs/guidance.html>
24. *Roadside Design Guide*, American Association of State Highway and Transportation Officials (AASHTO), Washington, D.C., 1989.
25. Albin, R., and Mauthner, J., *Roadside Landscaping and Safety*, Federal Highway Administration and Florida Department of Transportation, May 15, 2014. (Webinar)
26. Mortimer, M.J., and Kane, B., "Hazard tree liability in the United States: Uncertain risks for owners and professionals", *Urban Forestry & Urban Greening*, Vol. 2, 2004, pp. 159-165.
27. *Sidewalk and Street Tree Maintenance*, City of Placentia Public Works Department, Placentia, California. <http://www.placentia.org/index.aspx?nid=475>
28. *Sidewalk and Street Tree Maintenance*, Public Works Agency Transportation Department, Ventura, California, 2015.
http://pwportal.ventura.org/td/Residents/Streets_and_Transportation/FAQs_and_Citizen_Brochures/Brochure_SidewalkandStreetTreeMaintenance.pdf
29. *Factors Related to Fatal Single-Vehicle Run-off-Road Crashes*, National Highway Traffic Safety Administration, Report No. DOT HS 811 232, 2009.
30. Guidance on the Treatment of the Economic Value of a Statistical Life in U.S. Department of Transportation Analyses, Federal Highway Administration, 2013.
31. Treatment of the Economic Value of a Statistical Life in Departmental Analyses – 2011 Interim Adjustment, Federal Highway Administration, 2011.
32. Guidance on the Treatment of the Economic Value of a Statistical Life in U.S. Department of Transportation Analyses – 2015 Adjustment, Federal Highway Administration, 2015.
33. *TIGER Benefit-Cost Analysis (BCA) Resource Guide*, U.S. Department of Transportation, March 2015. <http://www.dot.gov/tiger/guidance>
34. *Estimating the Cost of Unintentional Injuries, 2012*, National Safety Council, Itaska, Illinois, February 2014.
35. Delaney, A., Lough, B., Whelan, M., and Cameron, M., *A review of mass media campaigns in road safety*, 2004.
36. Wundersitz, H., Hutchinson, T.P., and Woolley, J.E., "Best practice in road safety mass media campaigns: A literature review", *Social Psychology*, 2010
37. Phillips, R.O., Ulleberg, P., and Vaa, T., "Meta-analysis of the effect of road safety campaigns on accidents", *Accident Analysis & Prevention*, Vol 43 Issue 3, 2011, pp. 1204-1218.
38. Smith, K., The Design and Evaluation of Road Safety Publicity Campaigns.

39. Henley, N., Donovan, R.J., Moorhead, H., "Appealing to positive motivations and emotions in social marketing: Example of a positive parenting campaign", *Social Marketing Quarterly*, 1998.
40. Lewis, I., Watson, B., Tay, R., and White, K.M., "The role of fear appeals in improving driver safety: A review of the effectiveness of fear-arousing (threat) appeals in road safety advertising", *International Journal of Behavioral Consultation and Therapy*, Vol 3 No. 2, 2007, 203-222.
41. Lewis, I.M., Watson, B.C., and White, K.M., "What do we really know about designing and evaluating road safety advertising? : current knowledge and future challenges " In *Proceedings of 2009 Australasian Road Safety Research Policing and Education Conference: Smarter, Safer Directions*, Sydney, 2009.
42. Lewis, I.B., Watson, B.C., and White, K.M., "Response efficacy: the key to minimizing rejection and maximizing acceptance of emotion-based anti-speeding messages", *Accident Analysis & Prevention*, Vol 42 Issue 2, 2010, pp. 459-467.
43. Donovan, R., Henley, N., Jalleh, G., and Slater, C., *Road safety advertising: An empirical study and literature review*, 1995.
44. Goldenbeld, C., Twisk, D., and Houwing, S., "Effects of persuasive communication and group discussions on acceptability of anti-speeding policies for male and female drivers", *Transportation Research Part F: Traffic Psychology and Behaviour*, 2008.
45. Lewis, I., Watson, B., and Tay, R., "Examining the effectiveness of physical threats in road safety advertising: The role of the third-person effect, gender, and age Research", *Part F: Traffic Psychology and Behaviour*, 2007.
46. Fisher, R.J., L Dubé "Gender differences in responses to emotional advertising: A social desirability perspective" *Journal of Consumer Research*, 2005.
47. Dube, L., and Morgan, M.S., "Trend effects and gender differences in retrospective judgments of consumption emotions", *Journal of Consumer Research*, Vol 23 No. 2, 1996, pp. 156-162.
48. Elliott, B.J., "The psychology of fear appeals re-visited" Retrieved on June, 2003.
<<http://acrs.org.au/files/arsrpe/RS030056.pdf>>
49. Elvik, R., Vaa, T., Erke, A., and Sorensen, M., *The handbook of road safety measures*, 2009.
50. Hoekstra, T., Wegman, F., "Improving the effectiveness of road safety campaigns: Current and new practices", *IATSS Research*, 2011.
51. Elder, R.W., Shults, R.A., Sleet, D.A., Nichols, J.L., Thompson, R.S., and Rajab, W., "Effectiveness of mass media campaigns for reducing drinking and driving and alcohol-involved crashes: A systematic review", *American Journal of Preventive Medicine*, Vol 27 Issue 1, 2004, pp. 57-65.
52. McGuinness, K., Arney, F., Chessell, S., and Salveron, M., *Community Education and Social Marketing Literature Review*, Centre for Child Development and Education, Menzies School of Health Research On behalf of the Caring for Kids Consortium.
53. Lee, A.J., Mann, N.P., and Takriti, R., "A hospital led promotion campaign aimed to increase bicycle helmet wearing among children aged 11-15 living in West Berkshire 1992-98", *Injury Prevention*, Vol 6, 2000, pp. 151-153.
54. Image taken from: "Hiding in Plain Sight – or – I know, Let's Call a Meeting!". <http://schoolhouse-consulting.com/hiding-in-plain-sight-or-i-know-lets-call-a-meeting/>

Retrospective Look at 1998 Strategies to Improve Roadside Safety

Mission 2: Build and Maintain Information Resources and Analysis Procedures

KENNETH S. OPIELA

*Center for Collision Safety and Analysis
George Mason University*

In 1998, the national Cooperative Highway Research Program (NCHRP) published the results of four years of efforts involving a broad cross-section of safety professionals aimed at identifying a comprehensive set of “strategies” for improving roadside safety. As the 20 year anniversary of this effort approaches, it is interesting and potentially useful to retrospectively consider the viability of the missions, goals, objectives, and action items that were outlined as strategies. The detailed version of the strategies included more than 600 specific mission, goal, objective, and action items. These were recently “revisited” in an effort to outline a comprehensive analysis of current roadside safety efforts. This paper summarizes the findings of that effort related to Mission 2 - “Build and Maintain the Information Resources and Analysis Procedures.” Under all Missions, there were Goals, Objectives, and Action Items defined. These focused upon the information resources and analysis tools/procedures needed to understand, design, evaluate, monitor, and react to roadside safety issues from varying perspectives under changing conditions. The comprehensive set of Action Items that were developed by a broad cross section of knowledgeable professionals were believed to represent most of the efforts necessary to successfully address roadside safety and hence provide a useful benchmark to assessing the efforts of an organization and possibly indicate areas where a more effort was needed.

The Mission 2 strategies outlined in 1998 are reviewed in the context of attention on them, the effects of changes in highways, vehicles, and traffic, and the influences of technology, practice and policy that have occurred over the last 20 years. This paper attempts to highlight the progress, unresolved issues, and/or aspects receiving limited attention. For example, under Mission 2, Goal 2.4 “On-going programs to conduct safety analyses and identify hazardous roadside locations” includes three Objectives, namely “2.4.1- Identify hazardous or potentially hazardous roadside locations,” “2.4.2 – Analyze problem locations to determine the primary causes of crashes,” and “2.4.3 - Select alternative treatments using cost-effectiveness techniques.” Fourteen Action Items were identified for these objectives to reflect the fundamental aspects where improvements were considered possible. This paper examines the status of efforts related to each group of Action Items previously formulated. Progress and constraints relative to them are cited. The objective of this reassessment was to find evidence to support continuation of approaches that have worked, determine the potentials for modified actions, and/or consider the value of aspects that have received limited attention or new ones.

This retrospective analysis was considered useful towards measuring progress, revisiting aspects not addressed relative to persistent problems, and setting new research priorities considering technological advances relative to roadside safety. Such updates are necessary not only for updating specific strategic plans, but for assessing effectiveness, reflecting on emerging issues, evaluating threats to success, noting the effects of changing conditions, and redefining roles for transportation agencies and parties involved in safety.

INTRODUCTION

There has been a long commitment in the United States to improve all aspects of highway safety. While efforts to improve roadside safety originated in the early years of the automobile, it might be argued that a major impetus on roadside safety began in 1960 with the Stonex's paper "Roadside Design for Safety"[1]. Prior to that little attention was given to safety of the roadside and run-off-the-road accidents were attributed to "the nut behind the wheel." His paper identified common roadside hazards such as unprotected bridge abutments, blunt guardrail ends, rigid supports for street lights and signs, trees and utility poles, steep side slopes, and unsafe ditch cross sections. Solutions to these problems have evolved since then, but problems still exist.

Although catastrophic accidents involving airliners, ships and trains receive a great deal of media attention, almost all transportation fatalities occur on highways. Traffic deaths, usually occur one or two at a time dispersed across the nation every day, and hence they do not receive widespread attention. The cumulative annual toll in the 1990's was more than 40,000 deaths and more than 3.5 million injuries [2,3]. The safety of U.S. highways had improved since the 1950's as a result of efforts on many fronts. For example, the number of highway fatalities has declined from a peak of over 53,000 in 1969 to slightly less than 42,000 in 1993. In 1996, after concerted efforts to enhance highway safety, there remained serious concerns that the number of annual fatalities and injuries was still too large. Available data at the time indicated that:

- On an average day in 1996, over 110 people were killed and over 6,000 persons sustained disabling injuries in crashes on U.S. highways.
- Roadside crashes accounted for one-third of the total fatalities implying more than 14,000 people killed and almost 1,000,000 people injured in roadside crashes in the U.S [4].
- Roadside crashes were estimated to cost society \$80 billion per year in medical costs, worker losses, property damages, and emergency services. These annual societal costs were more than three times the annual governmental expenditures on highways in the U.S. [5].
- Crashes with trees accounted for about 10% of the national fatalities (Approx. 3,500 fatalities) with 90,000 severe injuries, and approximately 19% of the estimated roadside losses.
- Crashes with utility poles accounted for about 5% of the national fatalities (Approx. 1,500 fatalities) with 110,000 severe injuries and about 14% of the estimated roadside losses are attributed to such crashes.
- Rollovers, the most severe type of roadside crashes, occurred in only 15% of them, but were responsible for more than 25% of all roadside fatalities.

These facts provided a strong impetus to take a comprehensive look at roadside safety as a major source of injury, death, and economic loss and define new options to address it.

A continued focus on the roadside is warranted as the proportion of crashes attributed to the roadside has remained fairly constant over the past two decades. Figure 1 shows the trends based upon FARS data from 1994 to 2015 for fatalities and fatal crashes and the primary subsets of roadside crashes, namely fixed object and overturns, as tracking similar trends. It can be noted that there was a major decrease in fatal crashes and fatalities over this period as indicated by the red and blue lines (see legend). While this is a positive effect, the reasons for the decreases have not been fully explained. It can also be noted that the lower green and purple lines (see legend) reflect fixed object and overturn crashes that might be considered prime surrogates of roadside safety problems. These track the same downward trend in overall fatalities, but don't show the

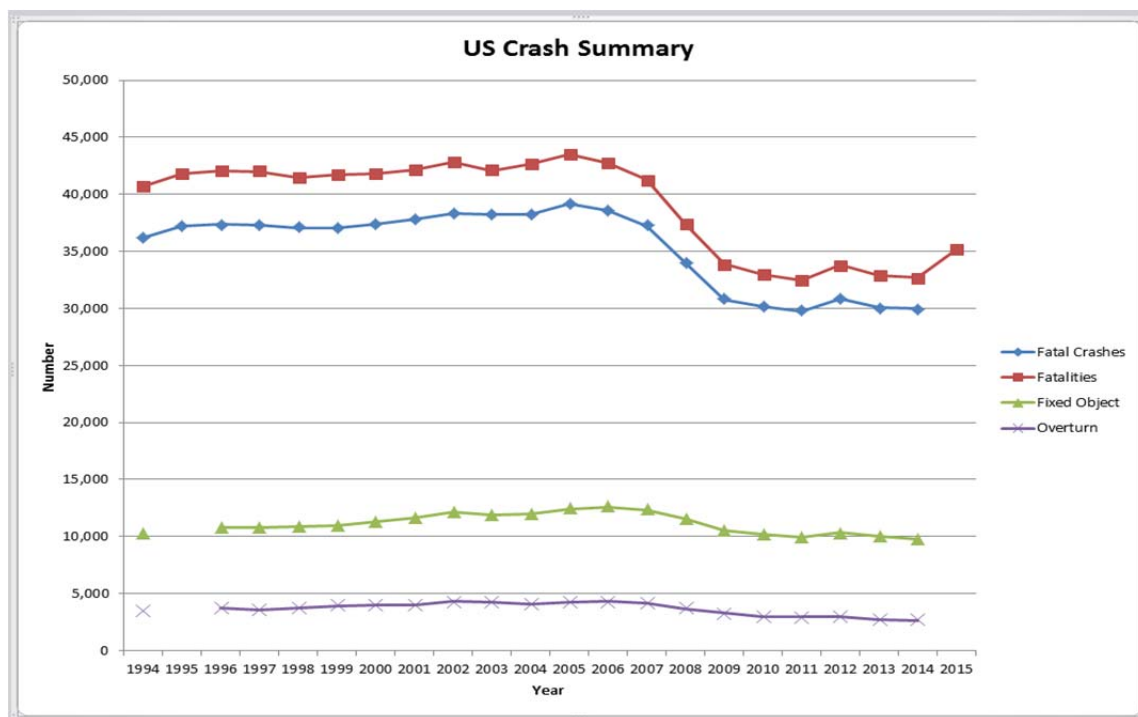


FIGURE 1 U.S. Total Traffic Fatalities and Fixed Object and Overturn Fatalities

same degree of decrease. This might be interpreted to suggest that the roadside safety problem has not been as effectively addressed. This provides an impetus for asking why. Further, the upturn reflected in the preliminary 2015 data suggests that there is a need to revisit overall safety efforts.

Developing Strategies to Improve Roadside Safety

The need to address the roadside safety problem was recognized by The American Association of State Highway & Transportation Officials (AASHTO), and NCHRP Project 17-13 “Strategies for Improving Roadside Safety” was initiated in 1995 to recommend a strategic, multi-faceted, multi-organizational approach to improving roadside safety. The initial objective of this project was to develop a consensus plan for future research activities in roadside safety. The plan was intended to identify the gaps in current knowledge and define the scope and priorities for research activities believed necessary to address them. It became apparent that focusing strictly on research needs would not be sufficient to address the problem nor would it appropriately direct activities toward all the sectors and agents able to contribute towards mitigating the problems. Consequently, a comprehensive approach was pursued to define all strategies that could address the problem. This led to involvement of highway designers, vehicle manufacturers, roadside safety hardware developers, law enforcement personnel, safety advocates, academics, and others. In this effort, attempts were made to assess the efficacy of emerging technologies for addressing roadside safety problems and research needs.

Under NCHRP Project 17-13, a panel of sixteen prominent safety professionals was formed to direct a “strategic planning approach” to provide a comprehensive, multi-disciplinary overview of options to improve highway safety in general and roadside safety in particular. The

Project Panel did not have the authority to recommend a Strategic Plan, but aimed to formulate strategies to address roadside safety problems. They choose to follow a strategic planning approach to develop and organize the strategies. The strategies were formulated and refined in

professionally facilitated discussions to develop the vision, missions, goals, and objectives. They reviewed safety strategic plans generated by various groups and noted various procedures to develop the strategies. Their strategic agenda was subsequently refined at several open meetings that included many diverse groups and persons interested in highway safety. Through these meetings the fundamental missions and goals did not change, but the goals, objectives, action items were expanded and reorganized repeatedly into an integrated list of action items to improve roadside safety.

The resulting strategic agenda was structured into missions, goals, objectives, and actions addressing the driver, vehicle, and roadway elements. The following definitions apply:

- Mission - A broad functional area that joins related goals in critical areas.
- Goal - A statement of desired outcomes under each mission.
- Objective - Specific measurable aspect of a goal used to determine the degree of change.
- Action - Activities that can be undertaken by one or more entities to satisfy an objective.
- Research - Investigations needed to define the relationships between factors, compiled critical data, and/or develop technology and procedures to create, evaluate, and implement solutions.

The “strategic planning” efforts began with the identification of a broad-based set of current and emerging roadside safety issues. It was recognized that issues overlap and other issues were likely to emerge in the coming years. During the efforts, it was recognized that highway safety encompasses a very broad range of organizations including State and Federal Departments of Transportation, law enforcement agencies, emergency services providers, citizen action groups, automobile manufacturers, insurance providers, and professional groups. Each of these groups has its own specific areas of expertise and concern which sometimes complement each other and at other times may work against each other. The primary purpose of a strategic agenda was to provide a framework for all the different groups to coordinate actions towards improving roadside safety.

Vision and Missions for Improved Roadside Safety

The distinguished panel of experts charged with the task of identifying ways to improve roadside safety started with discussions of roadside issues and expression of concepts to address them [6]. Through their deliberations, they formulated a vision –

“A highway system where drivers rarely leave the road; but when they do, the vehicle and roadside work together to protect vehicle occupants and pedestrians from serious harm.”

To achieve this vision, the experts outlined five basic missions for transportation agencies and its partners. These were:

- **Mission 1 - Increase the awareness of roadside safety and support for it.** Roadside safety cannot be enhanced until the public, decision makers, and other groups see it as a problem. Significant improvements to roadside safety will require a coordinated effort of transportation agencies, manufacturers, departments of motor vehicles, advocacy groups, and others. Additional funding at the federal, state, and local levels is needed to implement critical improvements and upgrade processes for safety management. Coalitions of government, industry, and civic partners should be formed to promote improved roadside safety.

- **Mission 2 - Build and maintain information resources and analysis procedures to support continued improvements in roadside safety.** A better understanding of the driver-vehicle-roadway relationship in roadside crashes is needed so that cost-effective remedies can be identified. Improved roadside and roadway inventory systems and better crash data are needed to provide highway designers, safety analysts, decision makers, and researchers with much-needed information. State-of-the-art computer analysis techniques can be used to monitor changing conditions and their influence on roadside crashes, provide better information to decisions makers, and/or simulate crash events. Safety audits, safety management systems, and other techniques can assure that efforts to improve roadside safety are most effective.

- **Mission 3 - Keep vehicles from leaving the roadway.** Roadside crashes occur when vehicles leave the roadway, as the result of driver error, vehicle failure, highway conditions, traffic situations, or environmental factors. Improved highway designs and better control of traffic operations can minimize the occurrence of events that lead to loss of vehicle control and roadside encroachment. Similarly, improved maintenance of highways and vehicles and innovative vehicle-based systems can help keep drivers on the road. Education, altered insurance regulations, and traffic law enforcement can promote appropriate driver behavior important to staying on the road.

- **Mission 4 - Keep vehicles from overturning or striking objects on the roadside when they do leave the roadway.** The chances for severe injury or death increase greatly when an errant vehicle overturns or hits a fixed object. Utility poles, trees, steep side slopes, drainage facilities, and roadside hardware are potential hazards found along the roadside. The slopes and configurations of ditches on the roadside should be designed to reduce the chances of rollover. Hazardous fixed objects should be held to a minimum and protected if they must remain. Vehicles should be designed to increase stability in run-off-the-road situations and driver needed to be educated about the proper actions in such situations.

- **Mission 5 - Minimize injuries and fatalities when overturns occur or objects are struck in the roadside.** When a vehicle rolls or strikes a fixed object, the risk of injuries can be reduced if the occupants are wearing seat belts and the vehicle has airbags and the vehicle has been designed to be crashworthy. Crash severity can also be reduced by better roadside hardware designs that absorb greater amounts of impact energy assuming that these devices are properly selected, installed, and maintained. Better emergency response after highway crashes can also contribute to reducing the number of fatalities.

These Missions were initially expanded by the Panel to include a preliminary set of twenty-five Goals. The panel's Goals were subsequently reviewed, discussed, expanded, and reorganized in a series of meetings involving many other professionals over the first two years of the project. The consensus Missions and Goals are summarized in Table 1. Each of the goals was subsequently taken to the next level of detail by defining more than 600 specific Objectives and Action Items. It was estimated that more than 4 person years of effort were involved in formulation of strategies to improve roadside safety following the strategic planning process.

TABLE 1 Missions and Goals Associated with Strategies for Improving Roadside Safety

Missions	Goals
1 - Increase the awareness of roadside safety and support for it.	1-A network of partners. 2-Greater public awareness of the importance of roadside safety. 3-Increased emphasis by partners and better communication between them. 4-Sufficient fiscal resources to address critical needs. 5-Programs to disseminate roadside safety information. 6-Integration of roadside safety into SMS. 7-On-going process for updating the plan.
2 - Build and maintain information resources and analysis procedures.	1-Improved roadway & roadside inventory data systems. 2-Comprehensive roadway safety information resources. 3-Effective tools and methods for safety analyses. 4-On-going programs to monitor roadside safety.
3 - Keep vehicles from leaving the roadway.	1-Improved highway designs and standards. 2-Improved traffic operating environments. 3-Improved vehicle-based systems to keep driver on the road. 4-Improved driver performance & behavior. 5-Sufficient levels of highway & vehicle maintenance.
4 - Keep vehicles from overturning or striking objects on the roadside when they do leave the roadway.	1-Improved roadway design to reduce vehicle overturning. 2-Improved vehicle designs to increase stability. 3-Reduced numbers of hazardous objects on the roadside. 4-Improved driver performance in run-off-the-road situations
5 - Minimize injuries and fatalities when overturns occur or objects are struck in the roadside.	1-Improved roadside safety hardware. 2-Improved vehicle-roadside compatibility & crashworthiness. 3-Proper selection, design, installation, and maintenance of roadside features. 4-Improved emergency team response. 5-Increased seat belt use and effectiveness.

There have been projects and initiatives that have followed the impetus of the 1998 efforts to implement elements by federal, state, local, and industry (private sector) players. These include the formulation of the AASHTO Highway Safety Strategic Plan [11], NCHRP Project 17-18 “Implementation of the AASHTO Highway Safety Strategic Plan [12-20], FHWA Roadmaps, and specific plans generated by the states and various organizations. NCHRP Project 17-18 was the most extensive implementation effort that led to a series of documents that highlighted “proven” and “promising” actions to enhance roadside safety in a few areas. These, while useful, reflected the state-of-the-art when developed and did not provide much guidance for other options. They were also focused on single factors and not coordinated, sustainable efforts. It is believed that the original efforts offered further potential to focus attention across a broader set of critical elements of roadside safety beyond the Mission and Goal levels. Thus, this effort attempted to take a deeper look at “Action Items” embodied in the “Strategies to Improve Roadside Safety.”

Mission 2 Retrospective

The retrospective look was initialized in an effort to propose on a project to develop a strategic plan for an organization involved on roadside safety. The strategies described in the 1998 effort were viewed as providing a deep set of specific elements across a broad range of disciplines that could contribute to improving roadside safety. The action items were viewed to offer a yardstick on progress and/or a source of new opportunities to be considered towards improving roadside safety. While the proposal was not successful, the effort stimulated a curiosity about the viability of the ideas documented in 1998 and whether the strategies could be useful to guiding new efforts. An unfunded effort was begun to step through the all Action Items for Mission 2. Each Action Item was reviewed in the context of known research and development efforts and/or the advancement of new programs, guidance, or policy. Given the breadth of the topics, it was difficult to review all areas equally and in great depth. Much of the information available reflected national level efforts and initiatives. Clearly, there may have been noteworthy efforts at state, regional, and local levels that have not been noted. Tabular summaries were created to summarize the findings of the efforts for each Objective by Action Item.

Table 2 summarizes the Goals and Objectives under Mission 2 as evolved from the NCHRP 17-13 project efforts as published in “Strategies to Improve Roadside Safety” [with a little editing of the titles to keep the tables short]. It can be noted that it includes four Goals and fourteen Objectives. These are believed to have reflected a comprehensive picture of the aspects and thinking circa 1996-1998. There was no effort at the time to set priorities for these elements nor did the participants have the authority to mandate implementation of any or all of these strategies.

In this effort, a tabular summary was created for each Objective under Mission 2, but the number and detail of them prevents full inclusion in this paper. Instead the “retrospective review” focuses on four selected “Objectives” from the fourteen related to Mission 2, Goal 2 (see shaded Objectives in table above). A table listing the Action Items for each Objective is provided that cites the accomplishments and constraints that were identified in the review. The reviews attempt to cite known efforts to advance a particular Action Item, reflect on-going efforts, or cases where there is limited attention. In addition, constraints and uncertainties are noted reflecting external influences, changing policies, modified priorities.

The nature of such a review or assessment makes it hard to apply any formal measurement or rating system to the process. The assessments focus on “progress” and “constraints” for each Action Item. The Progress column includes notes about efforts, programs, reports, or other initiatives related to the Action Item. The Constraints column notes particular aspects or threats that have been limited Progress in development or implementation efforts associated with the Action Item. For example, an Objective under Mission 2 was to “increase the use of modeling and simulation for analyzing roadside crashes and evaluating hardware to mitigate problems.”

The Progress column notes that there have been strides in (1) developing a large array of vehicle and hardware models, (2) the capabilities of simulation software to address more complex problems, and (3) the increased number of studies that have utilized this technology to cost-effectively address difficult roadside safety problems. The Constraints note that there are limited numbers of persons with the expertise to use simulation tools and that virtually no state transportation agencies have the capabilities in-house. The assessment notes useful progress, but

TABLE 2 Mission 2 Goal and Objective Elements

Mission 2 - Build and Maintain Information Resources and Analysis Procedures	
Goal 2.1 - Improved roadside and roadway inventory systems based on a common location referencing system.	
	Objective 2.1.1 - Establish a common location referencing system to integrate all databases.
	Objective 2.1.2 - Improve roadway/roadside inventory databases
	Objective 2.1.3 - Improve traffic operations data.
Goal 2.2 - Sufficient roadside safety information resources including accident databases, in-service evaluations, funding sources, research results, educational programs, and other information related to roadside safety.	
	Objective 2.2.1 - Create a framework for cooperative agreements to develop needed information resources.
	Objective 2.2.2 - Improve highway accident databases.
	Objective 2.2.3 - Monitor the effectiveness of roadside treatments to increase performance information.
Goal 2.3 - State-of-the-art methodologies and tools for analyses of crashes and simulations of roadside accidents and crash tests.	
	Objective 2.3.1 - Improve the understanding of fundamental relationships between safety & roadside features.
	Objective 2.3.2 - Develop a database on vehicle dynamics in roadside crashes.
	Objective 2.3.3 - Develop finite element analyses techniques to model vehicle-roadside safety device interactions.
	Objective 2.3.4 - Utilize vehicle dynamics models to investigate rollover issues and pre- and post-impact scenarios.
	Objective 2.3.5 - Examine Federal Motor Vehicle Safety Standards for link to roadside appurtenance performance.
Goal 2.4 - On-going programs to conduct safety analyses and identify hazardous roadside locations.	
	Objective 2.4.1 - Identify hazardous or potentially hazardous roadside locations.
	Objective 2.4.2 - Analyze problem roadside locations to determine the causes of crashes.
	Objective 2.4.3 - Select alternative treatments using cost-effectiveness techniques.

limited use of this analytic tool for project specific design, deployment, and maintenance needs. Such assessments are provided for the four objectives in the following sections.

Review of Objective 2.1.2. Improve Roadway/Roadside Inventory Databases

Table 3 provides a summary of the assessment of the Action Items under the Objective 2.1.2. It notes that there has been increased recognition of the need for up-to-date, accurate inventories of roadway features and the elements that are placed on the roadside. The MMIRE effort outlined a minimum set of inventory requirements considered important for safety analyses [21]. These did not however put sufficient emphasis on roadside hardware and other features important for assessing “roadside safety.” MMIRE provided recommendations that were not supported by FHWA requirements for implementation, so while it was a step in the right direction it didn’t fulfill the need. The lack of viable roadway data has limited the usefulness of data resources like HSIS. It offers linked safety, inventory, and traffic data for seven states, but only one state includes curvature data, making it difficult to do meaningful research into the effects of curvature on crashes or the relative performance of longitudinal barriers installed on curves.

TABLE 3 Review of Objective 2.1.2 Action Items.

Objective 2.1.2. Improve roadway/roadside inventory databases. Action 2.1.2.1 - Develop comprehensive model roadway/roadside inventory databases for use by highway agencies. Action 2.1.2.2 - Provide incentives for state and local highway agencies to create (or enhance) roadway inventory databases. Action 2.1.2.3 - Expand the HSIS system to include more roadside data. Action 2.1.2.4 - Create/improve/maintain databases on construction zones. Action 2.1.2.5 - Create/improve/maintain databases on roadside maintenance activities (e.g., guardrails & crash cushions).		
Item	Progress	Constraints
2.1.2.1	The FHWA promoted the development of MMIRE as a recommended model or standard for road inventories. It was not required, so it is not clear the extent to which states have adopted it. The intent of MMIRE is to standardize the data items and definitions for road databases to permit comparisons across states.	There will be a time lag in getting the new data requirements in place and data captured. This will even take longer as it is a recommendation and not a requirement. I have not seen a critical review of the MMIRE factors and their adequacy for roadside safety efforts.
	FHWA developed the Digital Highway Measurement System (DHMS) using off-the-shelf components and demonstrated the applications of emerging technologies to capture needed inventory data.	These efforts demonstrated that the capabilities exist, and these were demonstrated with other systems to compare features & functionality, but the DHMS effort ended with implementation support.
	LIDAR and RFID technologies have been applied for highway inventory purposes & road scanning and inventory services are commercially available. Others have discussed and tested means to capture additional information related to "hardware health."	Only a few states have allocated the resources needed to undertake inventories and they do not all capture the same data or fully identify roadside features.
2.1.2.2	MMIRE provides an incentive in so far as it outlines the data needed, but it is only a recommendation. Stronger incentives were used to standardize traffic standards or require that ANSI standards be applied to PCRs.	There was no specific funding or support provided as an incentive for following the MMIRE recommendations. Many agencies manage to meet basic needs without needing to follow a national model.
	Recent barrier performance issues have led to new FHWA upgrade requirements for certain barriers over a short time frame that has states actively updating or creating new, more specific inventories for critical devices.	Discussions at recent national roadside meeting noted that agencies do not know how many and the condition of the cited barriers in their state. many have embarked on "quick" inventories to estimate budget needs to meet the FHWA upgrade requirements.
2.1.2.3	HSIS is a federally maintained linked crash, traffic, and inventory database for seven states. It has provided the basis for a number of useful research efforts related to roadside safety.	HSIS has been continued and modified, but the fundamental problem of non-conforming data elements has always limited the scope of research that was possible across states.
	The SHRP2 NDS data set has been a major focus of effort at FHWA in recent years. It offers extremely detailed data about crash events that may be useful in getting new insights about roadside crashes	The SHRP2 data, however, only represents a snapshot of crashes over three years in six states. It does not provide the continuous sources of data that is needed to monitor in-service performance.
2.1.2.4	Many agencies have begun maintaining on-line databases for deployed work zones to support traffic monitoring & traffic routing applications.	These vary in coverage of the highway system, duration of the WZ, and have not been linked to crashes reported for the locations and WZ times.
	23 CFR part 630 Subpart J noted the need for work zone data capture to support better monitoring of safety and driver behavior, although it did not specify the data items.	The FHWA did not however mandate that WZ data be collected, set minimal data requirements, nor establish a repository for WZ data to support analysis under revisions to the CFR.

Continued on next page.

TABLE 3 (continued) Review of Objective 2.1.2 Action Items.

Objective 2.1.2. Improve roadway/roadside inventory databases. Action 2.1.2.1 - Develop comprehensive model roadway/roadside inventory databases for use by highway agencies. Action 2.1.2.2 - Provide incentives for state and local highway agencies to create (or enhance) roadway inventory databases. Action 2.1.2.3 - Expand the HSIS system to include more roadside data. Action 2.1.2.4 - Create/improve/maintain databases on construction zones. Action 2.1.2.5 - Create/improve/maintain databases on roadside maintenance activities (e.g., guardrails & crash cushions).		
Item	Progress	Constraints
	The WZ clearinghouse at TTI maintains WZ data from any agency willing to contribute data.	The data has limited detail, temporal, and regional coverage.
2.1.2.5	There have been grand efforts initiated to gather and link data representing elements of the WZ environment to support various DOT purposes.	The last major FHWA research effort that attempted to develop a better understanding of the effects of WZ treatments failed due to poor quality control in capturing data for more than 300 WZs.
	The NCHRP Report 350 and MASH documents recommended the use ISPEs to maintain a continuous link to the crashworthiness testing protocols and real world performance.	Hardware inventories and maintenance data are critical to generating ISPEs, but many agencies continue to use traditional practices to manage their roadside hardware.

Recent roadside safety issues have highlighted the fact that the safety performance (or lack thereof) cannot be monitored because most agencies cannot identify the specific barriers deployed at given locations on their highway network or the data is not detailed enough to determine when it was installed and/or maintained. There are many reasons why this may be the case across DOTs, but it has limited the opportunities to undertake in-service performance evaluations as recommended in NCHRP 350 and MASH [22,23]. The lack of detailed inventory data also limits the use of performance-based design and maintenance practices within the agencies. Technologies have been developed that facilitate undertaking inventories including digital imagery, GPS locating, RFID tagging, and even impact monitors that can alert the appropriate response teams. There have not been federal mandates for the deployment of such technologies due to their costs and the perception that it may put agencies under greater risk of tort liabilities.

Digital technologies such as LIDAR, DHMS, and GIS have demonstrated that tools are available to create inventories and maintain them. Several states have embarked to undertake the field studies and build databases, but such efforts require a significant long term commitment by the agency. For example, the Arizona DOT was working on a highly complex inventory of that included everything from roadside barriers to underground wiring for traffic control systems. The premise was that these systems share the roadway environment and changes to any subset might influence others and they are all important to achieving high safety goals. It is not clear whether the system reached full implementation and is in use today. In the absence of a formal inventory, it may be more critical to implement improved crash reporting to link crashes to specific features for analysis purposes, as well as to trigger effective maintenance actions. This process is complicated by the many types of roadside hardware and the difficulty in properly identifying it after it has been impacted.

The recommendation to add more roadside data to the HSIS had been considered to have validity, but since the states that voluntarily provide the linked databases that support this system, the objective has not been met. It may be possible to find other states that can be added

to the HSIS states, but it is not clear whether there has been support for the idea. Considerable emphasis has been placed on the NDS approach used in the SHRP2 Program to capture insights on safety. While this has usefulness to enrich the insights about roadside crashes, it is not a continuous source of data and it may not provide sufficient cases of actual road departure or roadside crashes.

Objective 2.1.2.4 addressed the need to improve and maintain databases on construction zones. It has been noted that many agencies post information announcing both long and short term work zones to help drivers avoid them. Such systems were initiated for traffic management purposes, but there are not known efforts to link this information to crash reports. PCRs do not uniformly address crashes in WZs and typically the features of a WZ (e.g., lane closures, active work close to the roadway, or speed limits) may not be appropriately reflected (e.g., they are changed often to support work activities). Recent changes to Subpart J of 23 CFR 650 did not require agencies or contractors to capture data on WZ crashes in the context of this objective. This implies that this objective has not been addressed to the intent that was outlined in 1998.

Review of Objective 2.2.2 - Improve Highway Accident Databases

Table 4 provides a summary of the assessment of the Action Items under the Objective 2.2.2. There were many Action Items generated for this critical aspect of roadside safety. Since the mid-1990s there have been efforts to improve the quality of reported crash data. NHTSA's CADRE, MMUCC, and CODES provided useful standardization of the basic data captured the crash scene, but as there are limits on the time that can be devoted to any aspect, elements associated with roadside features only don't meet needs [25]. A subsequent effort focused on the role of technologies to support these efforts [26].

Technological advances now provide greater accuracy relative to the location of crashes, but that may not be compatible with the location data for roadside hardware. A compatible degree of accuracy is needed to correlate a crash to a specific hardware item. On-vehicle technology logged in EDR represent an area that was suggested in the strategies, but access to the data is limited and it generally does not provide visual or locational data of any object hit. Information on the speed, driver reactions, and impact forces can be derived. The SHRP2 NDS effort demonstrated that digital imagery could address these limitations, but it only did so for a small number of cases. Technology also can address hardware identification needs. This could be addressed with RFID tags attached to major hardware elements or even bar code or other device labeling schemes. These have been proposed and demonstrated, but they have not seen widespread implementation.

Some Action Items under this object may be misplaced or difficult. For example, "including threshold data" is something that having the database would allow, as long as the needed data has been captured. Similarly, developing a database of "unreported crashes" while ideally useful may be impractical to deliver. Under a NCHRP project video images of concrete barriers were captured and scanned against previous images of the same barrier to record evidence of new "hits" in scuff marks or damage [27,28]. This was a tedious process that would not be practical for a DOTs entire network. Similarly, attempting to get vehicle trajectory for crashes would be difficult. Such data is captured for serious crashes and VDA tools are commonly used by investigators to determine vehicle tracking, yaw, pitch, and roll, loading and other measures that can help explain the reasons for the crash and its outcomes. Crash reconstruction methods allow the systematic analyses of these aspects. The use of computers in

the field to record crash information has increased. Agencies use “smart reporting” schemes to facilitate the entry of data based upon the type of crash. This has meant that the crash data can be uploaded to state files more expeditiously and accurately. There are some agencies linking digital images of the crash to the reports, but this is not required, so limited. There has not been known efforts to provide “apps” to agencies to automatically provide periodic reports for “locations of concern,” trigger warnings” for crash specific devices or other factors, and linkages to other factors that influence the potentials for crashes (e.g., traffic volumes, mix, and speeds).

The Action Items suggest monitoring citizen reports on near misses or observations of poor driver compliance that may be indicators of future crashes. The wise safety engineer will take note of such inputs, but there have not been formal efforts to do so. Highway safety strategic plan efforts in the states have opened more dialogue with citizens [29]. Similarly, there has not been much effort working with the insurance companies to get insights about roadside crashes. The IIHS does support a data base and conducts crashes for general analysis as well as to certify vehicle safety. NHTSA has undertaken detailed studies under its NASS and CDS programs. The “longitudinal barrier study” (LBS) conducted in the 1990’s provide useful insights, but most of the studies have focused on vehicle-oriented safety aspects. FHWA and NCHRP have attempted to develop a comprehensive database for run-off-the-road crashes. Multiple efforts have struggled to capture the needed data and the varying types of crashes and conditions have limited the sample size. NCHRP Project 17-45 has worked to obtain NHTSA’s cooperation. The last Action Items relate to enhancing the linkages between the police and engineers to jointly address highway safety issues. Many professional groups have undertaken efforts to promote the sharing of knowledge and collaboration. A mutual understanding by the involved parties has been shown to improve the effectiveness of the processes. Turnover of personnel, the number of crashes, and manpower constraints have limited these efforts in many cases.

In summary, the 1998 effort seemed to “boldly” offer a breadth of possible efforts to enhance the nature and usefulness of crash data in the interest in of improving highway safety. There has been limited emphasis and federal leadership on many of these aspects. Given the technologies developed to support ITS, cell phones, and “big data” schemes, it might seem that more could have been accomplished.

The Action Items under this Objective have all seem considerable attention and important progress has been made. There is, however, a limited number of persons have solid credentials for undertaking simulation analyses. This expertise is very limited in the DOTs and consequently, there is less application of these tools to address routine issues within the DOTs. The tools can provide a wealth of data for vehicle to barrier impacts and the software allows the impacts to be shown from varying perspectives. DOTs or their agents cannot do independent, comparative analyses of proprietary barriers because models of these barriers are not available.

TABLE 4 Review of Objective 2.2.2 Actions Items

Objective 2.2.2 - Improve highway accident databases. Action 2.2.2.1 - Incorporate the goals and actions of the "National Agenda for Improving Highway Information Systems." Action 2.2.2.2 - Establish standardized data requirements to facilitate national performance comparisons(e.g., NGA, CADRE). Action 2.2.2.3 - Improve identification of accident location by investigating officers (e.g., using on-board locational devices). Action 2.2.2.4 - Include data related to sequence of events and/or most harmful event on accident reports. Action 2.2.2.5 - Improve accuracy/consistency of roadside object definitions for police use. Action 2.2.2.6 - Work with the NSC Traffic Records Division & law enforcement to include key roadside data on PCRs. Action 2.2.2.7 - Include "threshold" data in databases so that comparisons can be made across jurisdictions and time. Action 2.2.2.8 - Develop a database of unreported roadside impacts to support research on impact severity . Action 2.2.2.9 - Obtain improved data on vehicle trajectories in roadside crashes to support simulation studies & B/C models. Action 2.2.2.10 - Capture and monitor information from citizen reports. Action 2.2.2.11 - Request generic information from insurance companies on PDO crashes. Action 2.2.2.12 - Explore feasibility of in-depth accident databases for specific roadside issues. Action 2.2.2.13 - Develop "smart computers" to automate data collection efforts and location accuracy. Action 2.2.2.14 - Improve feedback/coordination between engineers and police. Action 2.2.2.15 - Identify "successes" from good police accident reports & communicate these to law enforcement leaders.		
Item	Progress	Constraints
2.2.2.1	These items developed in the 1990's certainly warranted considerations, but it is not clear whether it was done.	After 20 years, it is likely that these recommendations need to be revisited.
	The evolving "big data" interest may provide useful tools and resources for roadside safety.	The fundamental needs are at the State level, but a national approach would be better to support conformity that will provide a better basis for policy, design guides, and crashworthiness standards.
2.2.2.2	MMUCC has replaced CADRE as the crash data standard with a series of improvements.	MMUCC is a recommendation, so not all agencies have adopted its requirements. Thus, national conformity has not been achieved to support research that could support better design, selections, and evaluations of roadside hardware.
2.2.2.3	The prevalence of GPS technology makes it possible to get far better location data for crashes. These have been embodied in the accident reporting software used by police in some agencies.	There are accuracy issues that might lead to erroneous locating. The accuracy needs to be consistent with the systems used to locate other features.
2.2.2.4	Event Data Recorders are found in most vehicles as part of the systems to activate airbags. These provide seven seconds of pre-impact data for crashes leading to airbag deployment. There have been studies using this data.	The EDRs vary considerably from the 8-10 suppliers. The data elements are not necessarily the same and the data is not preserved for less severe crashes.
	On-board crash notification systems provided on some vehicles (GM On-Star) offer similar potentials to provide pre-impact data.	Privacy and legal concern have limited access to the data.
	The NDS study has captured a wealth of data for privately-owned vehicles (of all types) driven by random members of the population in six states. Some of these vehicles were instrumented with devices to record vehicle movements as well as videos of traffic and road conditions.	A number of efforts are underway to "mine" this data to determine influences on driver behaviors that lead to crashes. The instrumentation on some of the vehicles will allow correlations to factors such as speed, road friction, and steering/braking.

Continued on next page.

TABLE 4 (continued) Review of Objective 2.2.2 Actions Items

Objective 2.2.2 - Improve highway accident databases. Action 2.2.2.1 - Incorporate the goals and actions of the "National Agenda for Improving Highway Information Systems." Action 2.2.2.2 - Establish standardized data requirements to facilitate national performance comparisons(e.g., NGA, CADRE). Action 2.2.2.3 - Improve identification of accident location by investigating officers (e.g., using on-board locational devices). Action 2.2.2.4 - Include data related to sequence of events and/or most harmful event on accident reports. Action 2.2.2.5 - Improve accuracy/consistency of roadside object definitions for police use. Action 2.2.2.6 - Work with the NSC Traffic Records Division & law enforcement to include key roadside data on PCRs. Action 2.2.2.7 - Include "threshold" data in databases so that comparisons can be made across jurisdictions and time. Action 2.2.2.8 - Develop a database of unreported roadside impacts to support research on impact severity . Action 2.2.2.9 - Obtain improved data on vehicle trajectories in roadside crashes to support simulation studies & B/C models. Action 2.2.2.10 - Capture and monitor information from citizen reports. Action 2.2.2.11 - Request generic information from insurance companies on PDO crashes. Action 2.2.2.12 - Explore feasibility of in-depth accident databases for specific roadside issues. Action 2.2.2.13 - Develop "smart computers" to automate data collection efforts and location accuracy. Action 2.2.2.14 - Improve feedback/coordination between engineers and police. Action 2.2.2.15 - Identify "successes" from good police accident reports & communicate these to law enforcement leaders.		
Item	Progress	Constraints
2.2.2.5	It would be extremely useful to have better information about the roadside hardware hit to understand in-service performance.	It is often not easy to identify the types of hardware after they have been hit. It has been suggested that all hardware be labeled (in varying degrees) and that information included on the police accident report. Digital pictures of crash scenes would be a very useful adjunct.
2.2.2.6	MMUCC and other efforts have aimed to provide better data for roadside safety analyses. Involved parties have contributed towards improving information resources.	Better characterization of crashes and the influences of the roadside are needed to make the next quantum leap in regular roadside safety assessments.
2.2.2.7	Threshold values for the number and severity of crashes by type is useful as a benchmark to determine whether a location has an "unusual" crash history. The best benchmarks would be based upon similar conditions in the same locale.	Agencies need to establish crash histories (and other data) for all locations to monitor the effects of changing conditions. Theoretically, this could be automatically generated as part of periodic reports by location.
2.2.2.8	There have been research efforts that used various means to capture data on unreported crashes. One effort took periodic side video scans of median barriers to allow comparisons of evidence of minor impacts. Maintenance systems in some states record the nature of damage to devices that provides the potential for in-service evaluations of devices.	These approaches while useful are time consuming even with technological supports. These may be useful for in-service evaluations for new devices.
2.2.2.9	The NDS offers some potential to demonstrate means to capture such data that would be very useful in roadside research.	These approaches while useful are time consuming even with technological supports. These may be useful for in-service evaluations for new devices.
2.2.2.10	Police and advocacy groups have provided call centers for the reporting of PDO crashes as agencies when agencies have cutback there police response to minor crashes.	These do not provide uniform coverage and consequently, the reporting of PDO crashes does not occur. Its role as an index of potentials more serious safety problems has been lost in some communities.

Continued on next page.

TABLE 4 (continued) Review of Objective 2.2.2 Actions Items

Objective 2.2.2 - Improve highway accident databases. Action 2.2.2.1 - Incorporate the goals and actions of the "National Agenda for Improving Highway Information Systems." Action 2.2.2.2 - Establish standardized data requirements to facilitate national performance comparisons(e.g., NGA, CADRE). Action 2.2.2.3 - Improve identification of accident location by investigating officers (e.g., using on-board locational devices). Action 2.2.2.4 - Include data related to sequence of events and/or most harmful event on accident reports. Action 2.2.2.5 - Improve accuracy/consistency of roadside object definitions for police use. Action 2.2.2.6 - Work with the NSC Traffic Records Division & law enforcement to include key roadside data on PCRs. Action 2.2.2.7 - Include "threshold" data in databases so that comparisons can be made across jurisdictions and time. Action 2.2.2.8 - Develop a database of unreported roadside impacts to support research on impact severity . Action 2.2.2.9 - Obtain improved data on vehicle trajectories in roadside crashes to support simulation studies & B/C models. Action 2.2.2.10 - Capture and monitor information from citizen reports. Action 2.2.2.11 - Request generic information from insurance companies on PDO crashes. Action 2.2.2.12 - Explore feasibility of in-depth accident databases for specific roadside issues. Action 2.2.2.13 - Develop "smart computers" to automate data collection efforts and location accuracy. Action 2.2.2.14 - Improve feedback/coordination between engineers and police. Action 2.2.2.15 - Identify "successes" from good police accident reports & communicate these to law enforcement leaders.		
Item	Progress	Constraints
2.2.2.11	The IIHS provides some data from the crash claims to the industry, but these only provide limited insights.	Privacy issues, the differences in the processes used to review claims, and regional differences in costs, limit the usefulness of data from these sources.
	Getting PDO crash data from insurance companies is possible. In Canada, where insurance companies work with the states it can be readily done.	Given insurance coverage is provided by many firms it would be difficult to track down all the data. Further, given the role of the insurance firms, the nature of the data would likely be different than a PCR.
2.2.2.12	In-depth studies have been conducted to focus on specific situations or treatments. Sometimes this is done to evaluate the effectiveness of a new type of hardware. NHTSA undertook the Longitudinal Barrier Study under its NASS program.	These efforts have not occurred often, despite the fact that they could be. It might be easier if the crash reporting process was computerized, where certain types of crashes could trigger additional questions over a period of time to build a deeper data base.
2.2.2.13	Technology has evolved to simplify crash reporting at all levels. These range from crash notification systems (e.g. On-Star) to cell phone apps for crash claims.	See notes above.
2.2.2.14	Effective programs to encourage the interaction between safety engineers, police, and maintenance staff in Oakland County, MI revealed that there was not a clear understanding of the importance of crash data. Once all understood how it was used by the others, there was greater effort towards accuracy and completeness.	It is not clear whether similar efforts have been undertaken in other areas.
2.2.2.15	Success have been reported, used as examples in training programs, and reflected in procedural manuals.	It is critical that there be a basis for continuity in safety efforts that assures that such successes are promoted over time and continued through staff turnover in the various participating agencies.

Review of Objective 2.3.3 - Develop and utilize finite element analyses techniques to model vehicle-roadside safety device interactions

Table 5 provides a summary of the assessment of the Action Items under the Object 2.1.2. It notes that there has been considerable progress in this area. In the mid-1990's there were just three of four finite element models (FEM) of vehicles available for safety analyses. They reflected the Test Vehicles associated with NCHRP Report 350. Today an array of almost 20 vehicles is easily downloadable. These models have evolved in the level of detail and degrees of validation. FE models of the MASH 1100C, 1500S, and 2270P vehicles are available in course and fine mesh versions. The array of vehicle models includes other passenger vehicles, single unit trucks, and tractor-trailer combinations [30-34]. The models developed over the past ten years have been validated for analysis of a full range of impacts. The models also include functional representations of suspension and steering systems to allow analyses of impacts on sloped surfaces.

Similarly, FE models of basic roadside hardware have been developed. These range from various concrete safety shapes, various types of guardrails, transition sections, end-terminals, sign and luminaire supports, and ancillary hardware like mailboxes. Models for cable barriers were developed to support the interests in them. Most of the publicly available barrier models are for non-proprietary versions. Proprietary hardware models have also been developed for the development and evaluation of innovative designs. These models have been used in multiple studies for varying purposes and under varying conditions. For example, simulation was used to evaluate the influence of cable barrier effectiveness when placed on sloped surfaces in medians of varying configurations. A current study evaluated the safety performance of longitudinal barriers on curved, superelevated roadway sections. The results were validated by crash tests using a consensus verification and validation procedure developed under an NCHRP project. It is believed that rarely does a crash test occur before it has been simulated to understand varying failure modes [35-40].

Efforts continue to develop the models and the related information to support simulation analyses. FHWA contracted for efforts to develop new wood and soils models to enhance the range of barrier features that can be analyzed. Efforts continue to develop representative models for new metals and composites that are being used in new vehicles and barriers. Simulation allows considerations of options that might not be considered otherwise. A recent NHTSA effort analyzed the crashworthiness of a pickup truck with a composite frame to reduce its weight by more than 15%. The effort demonstrated that the vehicle could meet the New Car Assessment Program's (NCAP) crashworthiness requirements. Similarly, efforts were undertaken to analyze the effects on the crashworthiness of common longitudinal barriers when impacted by typical vehicles that had been reduced in weight. It was noted that some approaches to reducing weight led to higher occupant risks. FHWA sponsored efforts to develop a tire model for the vehicles that would better reflect impact behavior.

The simulation technology has been used by NHTSA to evaluate prospective new test protocols for its NCAP program, as well as a variety of occupant risk issues. The recent FE vehicle models have fully modeled interiors including all restraint and air bag systems. These features of the models allow occupant risk metrics to be derived from the simulation efforts.

The last Action Item called for establishing a Forum for communicating findings and simulation approaches to address roadside safety issues. Over the last 12 years ten forums were presented under FHWA and TRB support involving groups from 16 to 110 persons.

TABLE 5 Review of Objective 2.3.3 Actions Items

Objective 2.3.3 - Develop & use finite element analyses techniques to model vehicle-roadside safety device interactions.		
Action 2.3.3.1 - Develop vehicle models of standard test vehicles.		
Action 2.3.3.2 - Obtain vehicle models from vehicle manufacturers or manufacturer trade associations.		
Action 2.3.3.3 - Develop models of widely-used roadside hardware.		
Action 2.3.3.4 - Develop material failure models for timber.		
Action 2.3.3.5 - Develop material models & modeling techniques for analyzing reinforced concrete roadside hardware.		
Action 2.3.3.6 - Develop material behavior models for soils that include the effects of compaction, moisture content, & type.		
Action 2.3.3.7 - Develop modeling techniques to account for the effects of rolling tires and vehicle suspension systems.		
Action 2.3.3.8 - Develop validation techniques for roadside hardware and vehicle models.		
Action 2.3.3.9 - Use FEA to analyze test repeatability & sensitivity of hardware to installation and maintenance errors.		
Action 2.3.3.10 - Use finite element analysis to explore the effects of airbags on vehicle occupants in roadside collisions.		
Action 2.3.3.11 - Utilize available occupant models to estimate severity of injury in simulated crashes and crash tests.		
Action 2.3.3.12 - Examine the effects of various vehicle improvements in protecting occupants in off-road rollovers.		
Action 2.3.3.13 - Explore the expected performance of roadside hardware in impacts with future generations of vehicles.		
Action 2.3.3.14 - Establish a forum for communication between vehicle and roadside hardware modelers.		
Item	Progress	Constraints
2.3.3.1	An array of sixteen vehicle FE models has been developed for FHWA/NHTSA and is available for free download to support simulation analysis. These cover NCHRP 350 and MASH test vehicles. Coarse and fine mesh versions have been developed for many to allow use on less powerful computers.	A broader array of vehicles would be useful to analyze specific crashes and or considered crashworthiness evaluations for limited production vehicles (e.g., Smart Car).
2.3.3.2	There has never been success in getting FE vehicle models from the auto industry, even after vehicles went out of production. There have been occasions where vehicle models were temporarily share by industry for specific studies.	There is limited funding for the creation of new models, but the reverse engineering process has been enhanced to reduce the costs of developing more detailed models at lower costs.
2.3.3.3	The FHWA has supported efforts to develop and apply FE models for most types of non-proprietary roadside hardware. These are available for free download.	These basic barrier models provide a good starting point for simulation analysis, but modifications of the models or creation on new models is often necessary to reflect specific barrier features. Further effort is needed to educate engineers about the simulation results and how they were derived to increase confidence in the results.
	Other models have been developed and are often available from other sources. The European models can be requested.	
2.3.3.4	FHWA sponsored research and delivered a report on wood modeling.	These basic models provide a good starting point for simulation analysis, but modifications of the models or creation on new models is often necessary to reflect specific features or conditions.
	Testing over the years has involved tests of wood components of barrier systems. Data is available and new standard materials models have been included in LS Dyna.	

Continued on next page.

TABLE 5 (continued) Review of Objective 2.3.3 Actions Items

Objective 2.3.3 - Develop & use finite element analyses techniques to model vehicle-roadside safety device interactions.		
Action 2.3.3.1 - Develop vehicle models of standard test vehicles.		
Action 2.3.3.2 - Obtain vehicle models from vehicle manufacturers or manufacturer trade associations.		
Action 2.3.3.3 - Develop models of widely-used roadside hardware.		
Action 2.3.3.4 - Develop material failure models for timber.		
Action 2.3.3.5 - Develop material models & modeling techniques for analyzing reinforced concrete roadside hardware.		
Action 2.3.3.6 - Develop material behavior models for soils that include the effects of compaction, moisture content, & type.		
Action 2.3.3.7 - Develop modeling techniques to account for the effects of rolling tires and vehicle suspension systems.		
Action 2.3.3.8 - Develop validation techniques for roadside hardware and vehicle models.		
Action 2.3.3.9 - Use FEA to analyze test repeatability & sensitivity of hardware to installation and maintenance errors.		
Action 2.3.3.10 - Use finite element analysis to explore the effects of airbags on vehicle occupants in roadside collisions.		
Action 2.3.3.11 - Utilize available occupant models to estimate severity of injury in simulated crashes and crash tests.		
Action 2.3.3.12 - Examine the effects of various vehicle improvements in protecting occupants in off-road rollovers.		
Action 2.3.3.13 - Explore the expected performance of roadside hardware in impacts with future generations of vehicles.		
Action 2.3.3.14 - Establish a forum for communication between vehicle and roadside hardware modelers.		
Item	Progress	Constraints
2.3.3.5	FHWA sponsored research and delivered a report on concrete modeling.	These basic models provide a good starting point for simulation analysis, but modifications of the models or creation on new models is often necessary to reflect specific features or conditions.
	Testing over the years has involved tests of concrete components of barrier systems that can be requested, found in published reports, or included in LS Dyna.	
2.3.3.6	FHWA sponsored research and delivered a report on soils modeling.	These basic models provide a good starting point for simulation analysis, but modifications of the models or creation on new models is often necessary to reflect specific features or conditions.
	Testing over the years has involved tests of soils for barrier systems that can be requested, found in published reports, or included in LS Dyna.	
2.3.3.7	FHWA sponsored research on tire modeling that led to better representation of tire behavior and influence on crash outcomes. The Virginia Tech tire research center has focused on very detailed tire modeling efforts to support the industry.	The added details for tires in simulation models increases the required computer run times. Schemes need to be defined for when the increase detail is necessary. Further research is still needed.
	Similarly, FHWA and others have undertaken research to develop better suspension models and assess vehicle dynamics effects in crashes.	VDA tools provide a fast means to analyze vehicle effects of terrain and their subsequent influence on barrier interface. This capability needs to be used more often.
2.3.3.8	NCHRP 22-24 developed a verification and validation procedure for comparing simulation and test results. The procedure provides tabular and statistical comparisons that lead to pass/fail metrics. The FHWA recognized the value of this procedure as a means to assess eligibility of previously tested hardware [35].	The procedure has been in use for about five years, but there has not been a critical assessment of the sensitivity of the results.

Continued on next page.

TABLE 5 (continued) Review of Objective 2.3.3 Actions Items

Objective 2.3.3 - Develop & use finite element analyses techniques to model vehicle-roadside safety device interactions.		
<p>Action 2.3.3.1 - Develop vehicle models of standard test vehicles.</p> <p>Action 2.3.3.2 - Obtain vehicle models from vehicle manufacturers or manufacturer trade associations.</p> <p>Action 2.3.3.3 - Develop models of widely-used roadside hardware.</p> <p>Action 2.3.3.4 - Develop material failure models for timber.</p> <p>Action 2.3.3.5 - Develop material models & modeling techniques for analyzing reinforced concrete roadside hardware.</p> <p>Action 2.3.3.6 - Develop material behavior models for soils that include the effects of compaction, moisture content, & type.</p> <p>Action 2.3.3.7 - Develop modeling techniques to account for the effects of rolling tires and vehicle suspension systems.</p> <p>Action 2.3.3.8 - Develop validation techniques for roadside hardware and vehicle models.</p> <p>Action 2.3.3.9 - Use FEA to analyze test repeatability & sensitivity of hardware to installation and maintenance errors.</p> <p>Action 2.3.3.10 - Use finite element analysis to explore the effects of airbags on vehicle occupants in roadside collisions.</p> <p>Action 2.3.3.11 - Utilize available occupant models to estimate severity of injury in simulated crashes and crash tests.</p> <p>Action 2.3.3.12 - Examine the effects of various vehicle improvements in protecting occupants in off-road rollovers.</p> <p>Action 2.3.3.13 - Explore the expected performance of roadside hardware in impacts with future generations of vehicles.</p> <p>Action 2.3.3.14 - Establish a forum for communication between vehicle and roadside hardware modelers.</p>		
Item	Progress	Constraints
2.3.3.9	The increase numbers of tests and simulations has generally indicated that the process has improved considerably. There have been numerous vehicle-to-barrier impacts analyzed over a wide range of conditions. These have provided useful results about the viability of the devices.	Increased efforts to analyze the sensitivity of the simulation and test results would provide greater confidence in the results and lay the ground work for understanding the range of conditions under which the design meets crashworthiness requirements. There are numerous variations possible, so it would be infeasible to address all.
2.3.3.10	Research has developed airbag models for occupant risk analysis in NCAP tests. These have been integrated to allow considerations of all occupant safety systems across a wide range of crashes.	Restraints are not considered in barrier crashworthiness evaluations. Efforts should be initiated to assess the sensitivity of their influence on occupant risk metrics.
2.3.3.11	Occupant risk simulations have contributed greatly to advancing occupant safety systems (i.e., restraints & airbags). These have been undertaken in considerable detail for the auto industry, but could be applied for hardware evaluations.	Analysis of hardware crashes with varying degrees of safety systems and combinations of occupants would provide insights to potential problems. be
2.3.3.12	The FHWA is continuing studies of rollover crashes. Initial efforts indicated that barriers can play a role in initiating rollovers. Since the severity is more highly related to the manner in which the occupant is tossed about in rollovers it will be important to simulate occupants.	Including occupants increases the complexity of the simulations and the duration of computer processing time. Models need to be carefully formulated to avoid computational errors as the crash events are longer in duration.

Continued on next page.

TABLE 5 (continued) Review of Objective 2.3.3 Actions Items

Objective 2.3.3 - Develop & use finite element analyses techniques to model vehicle-roadside safety device interactions.		
Action 2.3.3.1 - Develop vehicle models of standard test vehicles.		
Action 2.3.3.2 - Obtain vehicle models from vehicle manufacturers or manufacturer trade associations.		
Action 2.3.3.3 - Develop models of widely-used roadside hardware.		
Action 2.3.3.4 - Develop material failure models for timber.		
Action 2.3.3.5 - Develop material models & modeling techniques for analyzing reinforced concrete roadside hardware.		
Action 2.3.3.6 - Develop material behavior models for soils that include the effects of compaction, moisture content, & type.		
Action 2.3.3.7 - Develop modeling techniques to account for the effects of rolling tires and vehicle suspension systems.		
Action 2.3.3.8 - Develop validation techniques for roadside hardware and vehicle models.		
Action 2.3.3.9 - Use FEA to analyze test repeatability & sensitivity of hardware to installation and maintenance errors.		
Action 2.3.3.10 - Use finite element analysis to explore the effects of airbags on vehicle occupants in roadside collisions.		
Action 2.3.3.11 - Utilize available occupant models to estimate severity of injury in simulated crashes and crash tests.		
Action 2.3.3.12 - Examine the effects of various vehicle improvements in protecting occupants in off-road rollovers.		
Action 2.3.3.13 - Explore the expected performance of roadside hardware in impacts with future generations of vehicles.		
Action 2.3.3.14 - Establish a forum for communication between vehicle and roadside hardware modelers.		
Item	Progress	Constraints
2.3.3.1 3	The FHWA and NHTSA have undertaken studies of the potential influences of the future vehicle design changes on barrier crashworthiness. A recent study analyzed angular impacts for various types of “modified” vehicles for angular impacts into concrete barriers. The modifications the vehicle models reflected changes to component materials to reduce weight.	Potentially there can be many variations in vehicle design and the interactions with barriers may vary. These simulations can help to determine where problems may occur.
2.3.3.1 4	The FHWA restarted the forums that had occurred in the early 1990’s. These have included persons from academia, vehicle & hardware industries, and public agencies. Sharing of simulation techniques & knowledge acquired has been a hallmark of these gatherings. TRB has provided support for such forums.	Support needs to be continued and efforts made to document the offerings at these forums to meet the simulation and modeling needs of others.

Review of Objective 2.4.2 Analyze problem roadside locations to determine the causes of crashes

Table 6 provides a summary of the assessment of the Action Items under the Objective 2.1.2. It was noted that there has been significant progress relative to this Objective. There have been numerous efforts to develop causal models related to all types of crashes, including roadside crashes. These have been possible over the last 20 years as a result of the freater availability of crash data and computers. A major impetus was the effort to develop a Highway Safety Manual. The analytic approach that underlies the HSM is Bayesian statistical analyses that relies onSPFs. These link various roadway, traffic, and environmental features to the probability of a crash. The first version of the HSM that emerged about eight years ago, was not fully developed for

addressing roadside safety issues. Since then several research efforts have been initiated that will soon be added to the HSM. This is expected to provide a major enhancement in the understanding of the factors influencing roadside safety. The HSM with these elements will improve efforts by highway agencies to analyze, address, and monitor roadside safety. These methods are supplanting the HSIP, HSES, and HSE procedures promoted by the FHWA in the early nineties. It will be important to track the implementation of these methods and their success in addressing safety problems.

Under Objective 3.4.3, improvements in collision diagramming was considered important. Collision diagrams offer a visual perspective of crashes on a highway section or at an intersection. They allow patterns of crashes to be readily seen, but only if it is possible to effectively portray the road section being analyzed and accurately locate the crash. Often crash data does not provide adequate lane position, trajectory, and features data for accurate plotting. There have been software tools developed to facilitate generating collision diagrams. The IHSDM has been developed as another tool for crash analyses, but with a focus on road sections [43,44]. It includes several different reports and graphics that provide useful information related to monitoring and analyzing highway safety that are useful to roadside analyses. It is however limited to two-lane roads.

Action Item 2.4.2.3 calls for developing improved diagnostic tools. There are examples of such tools that have emerged over the last 20 years. Other tools have emerged to provide additional useful information. For example, CarSim allows animations of specific types of vehicles traversing medians or side slopes. There are also tools that are focused on benefit-cost analyses for roadside crashes like RSAP and RSAP2 that can be useful in determine the likelihood of crashes. These are covered in other parts of the strategies.

Road Safety Audits have become more common over the last 15 years. They are encouraged by the FHWA, International Road Federation (IRF), and others. They are undertaken in different ways and depth. In some cases, there are semi-structured drive throughs aimed at noting evidence of safety problems or potentials for them. The observers are trained to look for varying types of evidence in the process (e.g., skid marks, damages trees, barriers, or fences, poor pavement, barriers needing repair or replacement, compromised sight lines). These can be prioritized in the development of an improvement plan. These efforts might be supplemented by other studies to determine traffic levels, pavement friction, turning movements, or traffic speeds. In some cases, the audit is conducted just before a new or improved section of road is opened to make sure that everything is in place and the information provided to the driver is adequate.

It is hard to judge the extent of effort relative to this Objective as it is generally addresses efforts at the lower echelons of highway agencies. Products and tools are noted to exist from advertisements or demonstrations at conferences. The real contribution to roadside safety is hard to judge, but progress is apparent.

TABLE 6 Review of Objective 2.4.2 Actions Items

Objective 2.4.2 - Analyze problem roadside locations to determine the causes of crashes. Action 2.4.2.1 - Develop causal models to study the effects of road, traffic, vehicles, environment, & drivers on crashes. Action 2.4.2.2 - Upgrade collision diagramming procedures to provide better information on roadside accidents. Action 2.4.2.3 - Develop improved diagnostic techniques (e.g., use of tort claims data and diagnostic teams). Action 2.4.2.4 - Increase the use of road safety audits (RSA).		
Item	Progress	Constraints
2.4.2.1	IHSDM has been developed and is in use by several states for analyzing the safety effects of two-lane highway design features. This software provides a number of useful metrics or graphs to analyzing links and intersections.	This software is only operational for two-lane roads, although efforts have been underway to develop the capabilities to analyze 4-lane roads. Some functions originally planned for this tool never were completed (e.g., cost effectiveness analysis).
	The FHWA HSES procedures provided a comprehensive approach to analyzing hazardous locations considering various factors.	These were traditional tools that have not been updated, but might be candidates for new laptop applications.
	The HSM has led to the development of many new models aimed at correlating various causal factors to crashes in safety performance functions. These support new tools to evaluate safety treatment needs and options.	The HSM has been under development for more than a decade and is still not in widespread use. The viability of SPFs still needs to be ascertained and improved versions implemented.
2.4.2.2	A number of collision diagramming tools have been developed and are commercially available. These provide useful diagrams that are helpful in identifying predominant crash patterns by location.	Variations in the nature of crash & inventory data maintained by agencies make it difficult to develop a generic software tool with appropriate details. The number of crashes sometimes poses difficulties.
	IHSDM provides useful crash diagrams for intersections and segments that are coordinated with other graphics.	The use of these options requires detailed data from multiple sources, which may not all be available. Accurate location of the crash is often difficult making the accuracy of the diagrams questionable.
	Aerial and ground level views of the road system are readily available on the web and provide a source of specific features data and a backdrop for collision diagrams.	The views need to be captured more frequently for effective correlations to crashes in a given period. Crash data needs to include lane position data for the collision diagrams to be most effective. Roadside hardware may be apparent, but not identifiable.
2.4.2.3	RSAP tools provide crash probability & cost effectiveness metrics that can be useful in diagnostic efforts. This tool emerged in the 1990's & has been updated.	The tool focuses on road segments and requires a fair amount of data. It has not been integrated into global tools & is based on dated encroachment data.
	Technology has made it possible to have more data and digital imagery available to investigate crashes and sites. FARS data has been expanded to include GPS locations for crashes where available.	There has been little known effort to routinely capture digital images as part of PCR. GPS data needs to provide sufficient accuracy to allow effective correlation among features at crash sites,

Continued on next page.

TABLE 6 (continued) Review of Objective 2.4.2 Actions Items

Objective 2.4.2 - Analyze problem roadside locations to determine the causes of crashes.		
Action 2.4.2.1 - Develop causal models to study the effects of road, traffic, vehicles, environment, & drivers on crashes.		
Action 2.4.2.2 - Upgrade collision diagramming procedures to provide better information on roadside accidents.		
Action 2.4.2.3 - Develop improved diagnostic techniques (e.g., use of tort claims data and diagnostic teams).		
Action 2.4.2.4 - Increase the use of road safety audits (RSA).		
Item	Progress	Constraints
	There exists a strong cadre of crash reconstruction experts who can analyze site and vehicle damage to explain the causes of a crash. Reconstruction is typically undertaken for fatal or unusual crashes. This expertise or related tools could be provided to DOT staff.	Reconstruction requires significant expertise that is not typically available to highway agencies. There has not been tools developed that allow this process to be more readily used by DOT and law enforcement staff to be interpret crash scene evidence or reports.
	Crash simulation has evolved to the point where it can very effectively replicate any crash.	Again, highly specialized expertise is needed to simulate a crash assuming that the appropriate FE models are available.
2.4.2.4	The FHWA, IRF, and others have promoted the use of RSAs for various applications ranging from pre-opening reviews to system level condition assessments.	RSAs are manpower intensive and require well-trained assessors to effectively identify safety issues. It is not clear whether anyone has attempted this process using digital imagery or other technologies. Processes for tracking safety changes over time are lacking.
	RSA programs are undertaken by agencies to assess the safety conditions for an entire area or road corridor. These provide a structured approach to determining where safety needs to be enhanced and it allows comparisons of safety effectiveness across areas.	RSA assessments are labor intensive and offer only limited detail. Follow-up studies are needed for locations with high hazard rankings.

SUMMARY AND CONCLUSIONS

The efforts under NCHRP Project 17-18 identified a broad set of possible efforts and a more coordinated approach to improving roadside safety. The strategies forged in the effort represented the contributions of more than 100 professionals at 11 meetings over three years (an estimated 4 person-years of time). The efforts were considered to have provided the impetus for the development of the AASHTO Safety Strategic Plan [ref] which directly incorporated many of the strategies. Further efforts to translate the items into actions continued at varying paces at the Federal, state, local, and organizational levels.

NCHRP Project 17-18 supported the implementation of the strategies in a number of guideline reports for practitioners [ref]. It outlined efforts that could be undertaken with a focus on proven solutions and several new approaches deemed to have potentials. These were undertaken by many agencies, but there was no significant new support for roadside safety efforts. Some of these actions have been supported by FHWA initiatives that were widely undertaken by the states, including:

- Install shoulder rumble strips to alert drivers
- Strategically remove or shield trees or utility poles close to the roadway
- Use public service announcements & citizen initiatives to increase awareness

- Improve safety management systems
- Implement proactive highway maintenance programs
- Improve driver education programs
- Increase speed enforcement at locations with known roadside safety problems
- Promote development of innovative technologies to keep vehicles on the road
- Improve the proficiency of persons responsible for roadside safety
- Improve vehicle design to increase compatibility with roadside hardware
- Improve hardware design

There was a strong consensus that these could lead to reductions in the deaths and injuries related to roadside crashes.

Continued effort to address roadside safety issues is needed, particularly to assure that all perspectives are considered and that the most cost-effective options are selected. A great deal has been accomplished in improving the effectiveness of roadside safety hardware during the past several decades. The always-changing vehicle fleet and highway environment do not allow the roadside safety community the luxury of complacency. Significant challenges remain ahead to improve roadside safety. These challenges can only be met by openly discussing difficult issues as they emerge and focusing the myriad of options in a coordinated fashion by all those interested in improving roadside safety. Further, there are new needs resulting from changes in drivers (age and behavior), vehicles, roadways, and the environment. These include:

- Changing vehicle fleet characteristics and increasing variance in vehicle size and weight.
- Growing volumes of traffic across all periods of the day.
- Growing demands by non-vehicle users of the highway.
- Continued growth of urbanized areas and limits on right-of-way availability
- Deterioration of the infrastructure.
- Increased costs associated with construction, repair, and maintenance of highways.
- Aging driver population.
- Increased competition for government resources.
- Resistance to highway improvements for environmental reasons.

Further, it must be remembered that the roadside safety problem is distributed over the almost 4 million miles of public roads in the U.S. These aspects coupled with agency limits on monetary and staff resources, inadequate crash and inventory data, and the general uncertainties related to crashes pose a major challenge.

General Observations:

Revisiting the “strategies” after twenty years was a tedious effort. It revealed that some of the basic difficulties encountered then still exist and noted that some fundamental issues still remain, but important progress was noted. The following observations were made:

- The overall number of highway fatalities has decreased, but the reasons are not fully known. The relative proportion of roadside crashes remains about the same. New types of crashes are however occurring because of other new technologies (e.g., texting).
- Assessing the effectiveness of most action items is difficult because the crash and operational data still do not provide all the detail needed for micro-level analyses to isolate their relative contribution to the safety problem.
- Resource constraints limit the attention on all aspects and more critically the failure to undertake essential feedback loops like “in-service performance evaluations” effect decision-making.
- The 1998 strategies provided a very comprehensive overview of options that could be useful to enhancing roadside safety. They were systematically isolated in the decomposition of goals and objectives, but efforts to create appropriate linkages in new projects and programs did not occur.
- There has been significant technological progress over the last twenty years and these new technologies offer the potential to play important roles in enhancing roadside and highway safety.
- Efforts to fully describe and translate the action items defined in the 1998 strategies into new or updates programs and policies did not occur. Primary and secondary responsibilities were not formally identified. This retrospective found that there were redundancies across some of the action items and missing details.
- The persons that worked to develop the strategies were limited by the inability to parse crash data to the levels of detail that would have allowed the relative degree of safety impact to be understood and priorities for efforts set. Crash data has not yet evolved sufficiently to allow the relative contributions to be understood.
- There have been federal initiatives aimed at improving roadside safety, but nothing that addresses an entire goal. There is evidence of efforts at the state level, but the full scope and effectiveness of these are harder to follow.
- Follow-up efforts to the 1998 strategies led to the AASHTO Highway Safety Strategic Plan that covered a broader array of topics addressed by DOTs. NCHRP Project 17-18 was undertaken to facilitate state implementation of the plan.
- New crashworthiness requirements for roadside hardware were developed and implemented in 2009 and 2016. These are intended to bring the safety requirements into conformity with the vehicles using and the current nature of crashes.
- A novel, large scale data collection under the Naturalistic Driving Study (NDS) gathered a massive, highly detailed “snapshot” of driver behaviors and in many cases correlations to conflicts and crashes. The NDS will reveal new insights on roadside safety as researchers mine the data, but only to a limited extent for actual crashes.
- New barriers continue to be developed and demonstrated. Research efforts have focused on some long term roadside safety problems with innovative solutions.
- New issues have arisen with some roadside hardware that are leading to new policies for the in-service evaluations that have long been overlooked.
- Vehicle-based technological advances have provided significant advances towards improved roadside safety through event data recorders, electronic stability controls, collision avoidance, lane tracking, and other such systems. These, however, vary in there features and have not been fully deployed to the vehicles operating on U.S. highways.

The following list describes some of the significant advancements and important shortcomings under each of the four goals under Mission 2 over the last 20 years derived from this effort. The aspects of the 1998 strategies that have not received much attention are also noted.

- Goal 1 – “Improved roadside and roadway inventory systems based upon a common location reference system.”
 - Location referencing technologies have advanced significantly using GPS. Standardized schemes to relate the various elements of a highway network to their names and features data provide new means to locate crashes relative to the roadway alignment, hardware locations, and roadside conditions.
 - Despite these advances, there have only been limited efforts to undertake new analyses of the influences of the roadway and roadside features to crash propensity. There may, however, be interoperability issues in the implementation of these technologies.
 - Digital technologies have enhanced the ability to capture aerial or street level views of the road with GPS coordinates. These images are generally available for many developed areas, but as in the past, the images may not have been taken often enough to provide a historical record of conditions close in time to when crashes have occurred.
- Goal 2 – “Sufficient roadside safety information resources.”
 - Crash data standards have been updated and supplemented to provide new data (e.g., CADRE, MMUCC) as well as improvements to Federal sources. For example, GPS location references for crashes is now available for over half of the FARS cases. It is not clear when all crash reports will have a GPS location codes or when accident location displays will more accurately reflect crash locations on collision diagrams and other summaries.
 - Similarly, there have been recommendations developed for highway inventories that are necessary to relate crash propensity to specific features (e.g., MMIRE). These are, however, recommendations that haven’t been widely implemented.
 - Vehicle on-board technologies to provide electronic stability control, support lane tracking, provide collision avoidance, and automatic stopping have been deployed to address many safety problems. While these technologies are an important step towards improved highway safety, they are not uniform in their operations or performance and certainly not on all vehicles. It will take a considerable amount time for these technologies to change the needs for providing roadside safety hardware.
- Goal 3 – “State-of-the-art methodologies and tools for analyses and simulations of roadside crashes and tests.”
 - Vehicle Dynamics Analysis (VDA) tools have been applied to many run-off-the-road scenarios to provide an understanding of the trajectory of the vehicle as it negotiates the shoulder and side slopes. This has provided a solid basis for understanding vehicle-to-barrier interfaces.
 - Finite Element (FE) simulations can now be conducted for a larger array of crashes involving many different types of vehicles. The FE models have become far more detailed allowing the influences of small changes to more reliably modeled.
 - Truck models have been developed to allow crashes involving them to be studied.
 - Simulations are widely used to analyze crashworthiness tests before full-scale test begins. Barrier designs are improved in the process and fewer tests fail.

- Many roadside crashes types have been simulated and the effectiveness of various barrier designs, including minor changes, successfully analyzed. Since analyses address typical deployment conditions, there are unintended effects where the deployment conditions vary.
- Goal 4 – “On-going programs to conduct safety analyses and identify hazardous roadside locations.”
 - An underlying purpose of the HSM is to proscribe methodologies to monitor highway safety. The roadside aspects have not evolved to offer any specific monitoring tools.
 - Advances in computer technology have made it possible in most states to get crash data more readily allowing regular monitoring following traditional approaches. Privacy concerns limit access to the full details about a crash.
 - Tools like the IHSDM provide means to monitor changing conditions for the two-lane subset of the road network. There has not been much change in the amounts of data available to allow new analytical metrics to be used in the monitor process.
 - Road Safety Audits have advanced, but while these are useful for general awareness of roadside hazards, they may not be sufficient to recognize the effects of changing conditions.

It is obvious that continued efforts are necessary.

Closure

The review of this single mission of the 1998 Strategies was a tedious effort that is believed to have value in various forms. These include:

- At the action item level basic needs are identified. These serve as a basis for assessing new approaches or efforts. On-going efforts to update these items would enhance that effort and potentially increase their effectiveness.
- Some of the action items could have been consolidated into more specific statements. An update would be appropriate to reflect advancements.
- Action items were developed for planning, design, construction, operations, maintenance, administrative, enforcement, and driver licensing functions of DOTs. In addition, the strategies provide a basis for identifying roles for vehicle designer, roadside hardware manufacturers, and other related disciplines. It is useful to consider these associations and how they may have changed in assessing linkages between action items.
- The decomposition of the strategies aids in revealing areas where synergy can be achieved through the coordination of actions. It is also possible to isolate all actions that can be directed to specific problems for program development purposes.
- The strategies also permit interaction analysis to provide the foundations for the establishment of coalitions, linking of activities, and finding places where multiple purposes can be achieved.
- Many of the problems that remain are the difficult ones that have defied solution for many years. Maintaining the current level of safety in the face of increased travel demand, lighter vehicles, new adverse drive behaviors, and strained public resources will require bold

strategies that coordinate the efforts of all agencies involved and maximizes the effectiveness of future research and development efforts.

- A comprehensive review of the strategies to improve roadside safety can lead to the identification of areas where new research was needed.
- There is a need to address areas of uncertainty about roadside crashes to support a new generation of risk-based assessments for roadside safety improvement options.
- Similarly, an assessment of the impacts of emerging technologies and the options to develop the next generation of roadside hardware is needed.
- Opportunities for vehicle design changes and other of technology transfer policy alternatives should be weighed.

There is surely more examples of efforts to improve roadside safety that could be found in discussions with state and local agencies, but that was outside the scope of this effort.

REFERENCES:

1. K.A. Stonex, "Roadside Design for Safety," Highway Research Board Proceedings, Vol. 33, 1960.
2. NHTSA, Traffic Safety Facts -- 1992, Report DOT-HS-808-022, National Highway Traffic Safety Administration, Washington, D.C., March 1994.
3. E. C. Cerrelli, 1994 Traffic Crashes, Injuries and Fatalities -- Preliminary Report, Report DOT-HS-808-222, National Highway Traffic Safety Administration, Washington, D.C., March 1995.
4. Carney *et al*, Roadside Safety Issues, Transportation Research Circular 436, Transportation Research Board, Washington, D.C., 1995.
5. Carney *et al*, Roadside Safety Issues Revisited, Transportation Research Circular 436, Transportation Research Board, Washington, D.C., 1996.
6. Transportation Research Board, Strategies for Improving Roadside Safety, NCHRP Research Results Digest 220, Transportation Research Board, Washington, D.C., 1997.
7. Strategic Plan for Improving Roadside Safety. NCHRP Research Results Digest, Transportation Research Board, Issue 256, 2001, 3 p.
8. McGinnis, R G. Strategic Plan for Improving Roadside Safety. NCHRP Web Document, National Cooperative Highway Research Program; McGinnis, Richard G., Issue 33, 2001, 113 p.
9. Opiela, K. Information and Decision Support Needs For Highway Safety. Proceedings Of The Conference Road Safety on Three Continents In Pretoria, South Africa, 20-22 September 2000 (VTI Konferens 15A), Swedish National Road and Transport Research Institute (VTI), Issue 15A, 2001
10. Opiela, K S; McGinnis, R M. Strategies For Improving Roadside Safety. Crossroads 2000, Iowa State University, Ames, 1998, p. 19-21
11. AASHTO Strategic Plan 2009-2013. American Association of State Highway and Transportation Officials, 2009, 4p
12. Kochevar, Ken; Warden, Randy. California's Strategic Highway Safety Plan. Tech Transfer, 2008, p. 4-7
13. Antonucci, Nicholas D; Hardy, Kelly K; Bryden, James E; Neuman, Timothy R; Pfefer, Ronald; Slack, Kevin. Guidance for Implementation of the AASHTO Strategic Highway Safety Plan. Volume 17: A Guide for Reducing Work Zone Collisions. NCHRP Report, Issue 500, 2005, 180p
14. AASHTO Strategic Highway Safety Plan: A Comprehensive Plan To Substantially Reduce Vehicle-Related Fatalities And Injuries On The Nation's Highways (Revised). American Association of State Highway & Transportation Officials, 2005, 40 p.
15. Knipling, R R; Waller, P; Peck, R C; Pfefer, R; Neuman, T R; Slack, K L; Hardy, K K. Guidance For Implementation Of The Aashto Strategic Highway Safety Plan. Volume 13: A Guide For Reducing

- Collisions Involving Heavy Trucks. NCHRP Report, Transportation Research Board; CH2M HILL, Issue 500, 2004, 125 p.
16. Lacy, K; Srinivasan, R; Zegeer, C V; Pfefer, R; Neuman, T R; Slack, K L; Hardy, K K. Guidance For Implementation Of The AASHTO Strategic Highway Safety Plan. Volume 8: A Guide For Reducing Collisions Involving Utility Poles. NCHRP Report, Transportation Research Board; CH2M HILL, Issue 500, 2004, 80 p.
 17. Torbic, D J; Harwood, D W; Gilmore, D K; Pfefer, R; Neuman, T R; Slack, K L; Hardy, K K. Guidance For Implementation Of The AASHTO Strategic Highway Safety Plan. Volume 7: A Guide For Reducing Collisions On Horizontal Curves. NCHRP Report, Transportation Research Board; CH2M HILL, Issue 500, 2004, 97 p.
 18. Neuman, T R; Pfefer, R; Slack, K L; Hardy, K K; Council, F; McGee, H; Prothe, L; Eccles, K. Guidance For Implementation Of The AASHTO Strategic Highway Safety Plan. Volume 6: A Guide For Addressing Run-Off-Road Collisions. NCHRP Report, Transportation Research Board; CH2M HILL, Issue 500, 2003, 111 p.
 19. Neuman, T R; Pfefer, R; Slack, K L; Hardy, K K; McGee, H; Prothe, L; Eccles, K; Council, F. Guidance For Implementation Of The AASHTO Strategic Highway Safety Plan. Volume 4: A Guide For Addressing Head-On Collisions. NCHRP Report, Transportation Research Board; CH2M HILL, Issue 500, 2003, 82 p.
 20. Neuman, T R; Pfefer, R; Slack, K L; Hardy, K K; Lacy, K; Zegeer, C. GUIDANCE FOR Implementation of the AASHTO Strategic Highway Safety Plan. Volume 3: A Guide For Addressing Collisions With Trees In Hazardous Locations. NCHRP Report, Transportation Research Board; CH2M HILL, Issue 500, 2003, 76 p.
 21. Harkey, David L., Carter, Daniel L., White, Bryon, Council, Forrest M., Model Minimum Inventory of Roadway Elements—MMIRE, Vanasse Hangen Brustlin, Incorporated, FHWA, McLean, VA 22101.
 22. Ross HE, Jr, Sicking DL, Zimmer RA, Michie JD, Recommended Procedures for the Safety Performance Evaluation of Highway Features,” National Cooperative Highway Research Program Report 350. Transportation Research Board, National Research Council, Washington, D.C., 1993.
 23. American Association of State Highway and Transportation Officials, “Manual for Assessment of Safety Hardware”, American Associations of State Highway & Transportation Officials (AASHTO), Washington, DC, 2009.
 24. Strategic Directions on Roadway Departure Crashes: Supporting the Decade of Action. Summaries of a Workshop July 29-August 2, 2012, Irvine, California. Transportation Research E-Circular, Issue E-C175, 2013, 116p
 25. Delucia, B.H. et al, Crash Records Systems, NCHRP Synthesis 350, Transportation Research Board, Washington, DC. 2005.
 26. Ogle, J.H., Technologies for Improving Safety Data, NCHRP Synthesis 367, Transportation Research Board, Washington, DC. 2007.
 27. Ray, M H; Weir, J; Hopp, J. IN-SERVICE PERFORMANCE OF TRAFFIC BARRIERS. NCHRP Report, Transportation Research Board; Worcester Polytechnic Institute, Issue 490, 2003, 199 p.
 28. Fitzpatrick Jr, M S; Hancock, K L; Ray, M H. VIDEOLOG ASSESSMENT OF VEHICLE COLLISION FREQUENCY WITH CONCRETE MEDIAN BARRIERS ON AN URBAN HIGHWAY IN CONNECTICUT. Transportation Research Record, Transportation Research Board, Issue 1690, 1999, p. 59-67.
 29. Strategic Highway Safety Plans - A Champion’s Guidebook to Saving Lives, Second Edition. Cambridge Systematics, Inc.; Federal Highway Administration, 2013, 40p
 30. Hallquist, J.O.; LS-DYNA Theoretical Manual. Livermore Software Technology Corporation, Livermore, CA, USA, 1997
 31. Bolarinwa, E.; Mahadeviah, U.; Marzougui, D.; Opiela, K.S.; “The Development of an Enhanced Finite Element Tire Model for Roadside Hardware Assessment;” Institute of Mechanical Engineers. Publication pending, England, 2012.

32. Plaxico, Chuck; Kennedy, James; Simonovic, Srdjan; Zisi, Nikola. Enhanced Finite Element Analysis Crash Model of Tractor-Trailers (Phase A). National Transportation Research Center, Incorporated; Research and Innovative Technology Administration, 2007, 120p
33. Reid, J D; Boesch, D A; Bielenberg, R W. Detailed Tire Modeling for Crash Applications. International Journal of Crashworthiness, Volume 12, Issue 5, 2007, pp 521-529
34. Marzougui, Dhafer; Samaha, Randa Radwan; Nix, Lilly; Kan, Cing-Dao (Steve). Extended Validation of the Finite Element Model for the 2010 Toyota Yaris Passenger Sedan (MASH 1100kg Vehicle). Transportation Research Board 92nd Annual Meeting, Transportation Research Board, 2013, 19p
35. Ray, M.L., et al; "Guidelines for Verification and Validation of Crash Simulations Used in Roadside Safety Applications," NCHRP Project 22-24, Transportation Research Board, Washington, DC, 2010.
36. Marzougui, Dhafer; Tahan, Fadi; Opiela, Kenneth S; Kan, Cing-Dao (Steve); Arispe, Eduardo. Analysis of the Sensitivity of Bridge Rail Face Slope on Crashworthiness Performance. Transportation Research Board 94th Annual Meeting, Transportation Research Board, 2015, 19p
37. Marzougui, Dhafer; Mohan, Pradeep; Kan, Cing-Dao; Opiela, Kenneth S. Evaluation of Rail Height Effects of the Safety Performance of W-Beam Barriers. National Crash Analysis Center; Federal Highway Administration, 2007, 21p
38. Marzougui, Dhafer; Mohan, Pradeep; Mahadevaiah, Umashankar; Kan, Steve. Performance Evaluation of Low-Tension, Three-Strand Cable Median Barriers on Sloped Terrains. National Crash Analysis Center; Federal Highway Administration, 2007, 42p
39. Kim, Taewung; Bollapragada, Varun; Kerrigan, Jason; Crandall, Jeff; Clauser, Mark. Effects of Types of Vehicles and Maneuvers on Vehicle Kinematics during Steering-Induced Soil-Trip Rollovers. 23rd International Technical Conference on the Enhanced Safety of Vehicles (ESV), National Highway Traffic Safety Administration, 2013, 11p
40. Marzougui, Dhafer; Mohan, Pradeep; Kan, Cing-Dao; Opiela, Kenneth S. Evaluation of Rail Height Effects of the Safety Performance of W-Beam Barriers. National Crash Analysis Center; Federal Highway Administration, 2007, 21p
41. Gettman, D; Head, L. Surrogate Safety Measures From Traffic Simulation Models. Transportation Research Record, Transportation Research Board, Issue 1840, 2003, p. 104-115.
42. AASHTO-AGC-ARTBA Task Force 45, *Asset Management Data Collection Guide*, American Association of State Highway and Transportation Officials, Washington, D.C., 2006, 35 pp.
43. Harwood, D W; Mason, J M; Graham, Jerry L. CONCEPTUAL PLAN FOR AN INTERACTIVE HIGHWAY SAFETY DESIGN MODEL. Midwest Research Institute, 1994, 136 p.
44. Donnell, E.T.; Gross, F.; Stodart, B.P.; Opiela, K.S.; "Appraisal of the Interactive Highway Safety Design Model's Crash Prediction and Design Consistency Modules: Case Studies from Pennsylvania," Journal of Transportation Engineering, Volume: 135, Issue 2; American Society of Civil Engineers, Reston, VA 2009.
45. Harwood, D W; Mason, J M; Graham, Jerry L. CONCEPTUAL PLAN FOR AN INTERACTIVE HIGHWAY SAFETY DESIGN MODEL. Midwest Research Institute, 1994, 136 p.
46. AASHTO, Roadside Design Guide, published by the American Associations of State Highway & Transportation Officials, Washington, DC, 2006.
47. Cambridge Systematics, Inc.; PB Consult, Inc.; Texas Transportation Institute, *NCHRP Report 551: Performance Measures and Targets for Transportation Asset Management*, Transportation Research Board, National Research Council, Washington, D.C., 2006.

Organizations

- ANSI – American National Standards Institute
- GAO – Government Accounting Office
- IRF – International Road Federation

- NSC – National Safety Council
- NTSB – National Transportation Safety Board
- TCRS – Technical Committee on Roadside Safety
- TTI – Texas Transportation Institute

Programs

- CADRE – Critical Automated Data Reporting Elements
- CE – Cost Effectiveness
- CFR – Code of Federal Regulations
- CODES – Crash Outcomes Data Evaluation System
- DHMS – Digital Highway Measurement System
- EDR – Event Data Recorders
- ESC – Electronic Stability Control
- FARS – Fatal Accident Reporting System
- FEM – Finite Element Model
- FMVSS – Federal Motor Vehicle Safety Standards
- GIS – Geographic Information System
- GPS – Global Positioning System
- HSIS – Highway Safety Information System
- HSE – Highway Safety Evaluation
- HSIP – Highway Safety Improvement Program
- HSES – Highway Safety Engineering Studies
- HSM – Highway Safety Manual
- IHSDM – Interactive Highway Safety Design Model
- ISO – International Standards Organization
- ISPE – In-Service Performance Evaluation
- ITS _ Intelligent Transportation Systems
- LBS – Longitudinal Barrier Study
- LIDAR – Light Detection & Ranging
- LRS – Location Referencing System
- LSDyna – Livermore Software Dynamic Analysis Program
- MMIRE – Model Minimum Inventory of Roadway Elements
- MMUCC – Model Minimum Uniform Crash C??
- NASS – National Accident Sampling System
- NCAP – New Car Assessment Program
- NDS – Naturalistic Driving Survey
- PCR – Police Crash Report
- PDO – Property Damage Only Crash
- RFID – Radio Frequency IDentification
- RSAP – Roadside Safety Analysis Program
- RSA – Road Safety Audits
- SHRP2 – Strategic Highway Research Program 2
- SPF – Safety Performance Function

- VDA – Vehicle Dynamics Analysis
- WZ – Work Zones
- V&V – Verification & Validation

Traffic Stopped Ahead

Everything You Wanted to Know About Work Zone Queue Warning Systems

JOSEPH “JOE” JEFFREY

Road-Tech Safety Services, Inc.

26% of work zone fatalities come as a result of end of queue crashes. Today we have the tools to reduce those fatalities significantly. They are supplied by several different vendors and contractors. And they are inexpensive and proven to work.

This presentation will provide a detailed explanation of queue warning systems including system components, operation, maintenance and other considerations. We will look at recent study results proving the benefits of these systems. We will discuss several secondary benefits such as satisfying federal work zone performance measurement requirements and tort risk mitigation. We will cover many new and innovative contracting methods in use today and look at the evolution of specifications for work zone ITS systems. And finally we will briefly discuss other related technologies including dynamic merge systems and variable speed limit systems.

Other benefits:

- Work zone safety data collection and possibly analysis.
- Tort risk mitigation.
- Speed reduction.
- Enforcement in sense that data will show when officers should be present and enforcing posted limits.
- Maybe SHSP too – if you have reduction of work zone fatalities or crashes as a goal, this will get you there quickly.
- Automated, real-time reporting to traffic management centers and traffic data contractors.

Queue warning systems work. They are proven. They are easy to use. Here is everything you need to know to get started in work zone queue warning systems, including new and innovative contracting methods.

Reducing the Incidence of Impaired Driving Through Globally Effective Countermeasures

DANIELLE COMEAU

Alcohol Countermeasure Systems Corp.

FELIX J.E. COMEAU

DENISE CONNERTY

Alcohol Countermeasure Systems Corp.

Road traffic fatalities will be the fifth leading cause of death by 2030. In Colombia, the fatality rate is 5.9 per 10,000 registered vehicles and 12.8 per 100,000 inhabitants. This means that a driver in Colombia is approximately three times more likely to die in a traffic accident, than a driver in Spain, and four times more than a driver in England¹. According to the WHO 2013 Global Status Report on Road Safety, in approximately 9% of all accidents, impairment was the evident cause². These statistics are alarming, although many countries and community organizations are finding effective measures to reduce the number of fatalities caused by traffic accidents.

Specifically, Bloomberg Philanthropies is committed to reducing the number of road traffic fatalities and injuries around the world through their Global Road Safety Initiative. Bloomberg Philanthropies expects that this improvement will come from providing police forces with increased resources and support from municipal and state governments, health care providers and community leaders. These resources include, hiring more police officers, using the latest technology, better training and promotion of their activities, including making the officers more visible.

Despite stricter impaired driving legislation in South America, there are a number of contributing factors that weaken enforcement practices and make it less likely to change driver behavior. In our presentation, we will expand upon Bloomberg's approach, and relate it to constructive measures that are being implemented in other countries such as Canada, USA and Australia, whereby utilizing proven impaired driving detection resulting in reduced recidivism rates.

Our presentation will demonstrate that South American countries can increase impaired driving detection with the use of random and frequent road sobriety checkpoints, and employing the latest commercially available technology, which provide greater accuracy and reach a wider breadth of impaired drivers. These countries can also reduce recidivism rates for those drivers convicted of driving while impaired, via implementation of behavior modification programs, and by the deployment of alcohol interlocks and oral saliva testing. Alcohol interlocks when properly implemented reduce recidivism by an average of 64%³, and allow participants to be constructive members of their societies.

With strong legislation, and public education, all levels of transportation governance can tackle the challenges posed by impaired driving, particularly in areas of enforcement and intervention. The resulting benefits will relieve stress on health care providers, and the impact that impaired driving has on families. The measures that will be noted in our presentation have proven to be effective in many countries around the world in reducing the incidence and costs associated with impaired driving.

NOTES:

1. **El Banco Mundial, Los accidentes de tránsito son la segunda causa de muerte violenta en Colombia, 2013, <http://www.bancomundial.org/es/news/feature/2013/10/28/los-accidentes-de-transito-son-la-segunda-causa-de-muerte-violenta-en-colombia> [Consulted: Thursday July 29 2015]**
2. **World Health Organization, Global Status Report on Road Safety, 2013, http://www.who.int/violence_injury_prevention/road_safety_status/2013/en/ [Consulted: Tuesday, 24 July 2015]**
3. **Vanlaar, Ward. "Drinking and Driving: Countermeasures that work." Simposio de Accidentalidad Vial y Alcohol, Bogota, Colombia. 19 November 2013**

Selection and Placement Guidelines for Test Level 2 Through Test Level 5 Median Barriers

CHRISTINE E. CARRIGAN

MALCOLM H. RAY

RoadSafe LLC

There has been interest in the roadside safety community for several decades in developing selection and placement guidance for the multiple test levels of median barriers. The variety of median widths and terrains combined with evolving testing specifications and lack of conclusive data on median cross over crashes have been past obstacles to success. The currently ongoing implementation of the Manual for Assessing Safety Hardware (MASH) combined with new data collection efforts and the availability of new analysis tools have overcome some of the primary obstacles to developing median barrier guidance.

The objective of this NCHRP research is to develop, in a format suitable for consideration and possible adoption by AASHTO, proposed guidelines for the selection and placement of MASH Test Levels 2 through 5 (TL2-TL5) median barriers. The guidelines will be based on traffic volume and mix, roadway and median geometry, median barrier placement, in-service performance, cost benefit, risk analysis, and barrier type (i.e., shape, material, rigidity, etc.). The guidelines will be suitable for use by government transportation agencies at the state and local level. It is anticipated that the results will be integrated into an updated edition of the AASHTO Roadside Design Guide (RDG).

A risk-based approach to the guideline develops has been used, where the frequency and severity of crashes with and without median barriers are estimated and the risk of observing an incapacitating or fatal injury crash calculated. The third version of the Roadside Safety Analysis Program (RSAPv3) was developed to perform cost-benefit analysis and expanded during the NCHRP 22-12(03) effort to document the risk-analyses which is the basis of the cost-benefit analysis. RSAPv3 is the best available tool for the conduct of this research and will be used in the development of these guidelines. This presentation will summarize the work completed to date. Draft guidelines are anticipated at the time of this meeting.

Establishing a National Accreditation Scheme for Road Safety Barrier Industry

DANIEL CASSAR

Victorian Roads Corporation (VicRoads)

Design, installation and maintenance practices are often the missing link in realizing the full potential of road authorities' investments in road safety. As new systems are developed, improved and accepted for use by road authorities, the challenge for designers, installers and maintainers to remain informed and keep abreast of safety hardware performance and installation/maintenance requirements is challenging. The often complex nature of many of the systems developed also presents as a challenge for industry to build and retain skills to ensure hardware performance is optimized.

Installers and suppliers of hardware approached road authorities 5+ years ago to raise concerns for the design, installation and maintenance practices being used by the road safety barrier industry.

Some states in Australia were finding that road safety hardware was not being installed in accordance with supplier requirements and in some cases representing more of a hazard to road users as performance would likely be compromised. Over that 5 year period Australian road authorities engaged with the entire industry to understand the issue and work collaboratively on a solution. This presentation looks to inform the world of Australia's recent move to establish a national industry accreditation scheme that will require designers, installers and maintainers of road safety hardware to be adequately trained and accredited. The presentation will share the journey starting from when road authorities began engaging with industry on this issue, investigating the problem and how it arrived at a nationally workable solution to help overcome the issue. Having hardware designed, installed and maintained to the best possible standard that ensures it is fit for purpose, is a vital piece of the Safe System puzzle.

Progress Toward a National Harmonization of Training and Accreditation Schemes for Roadside Safety Barriers in Australia and New Zealand

Changing Work Practices for the Benefit of All

PAUL HANSEN

*Working Party for National Training and Accreditation
in the Roadside Safety Barrier Industry in Australia and New Zealand*

There is a desire in Australasia for nationally harmonized standards and work practices in the roadside safety barrier construction industry. Since 2005 proprietary roadside safety barriers have been assessed and recommended for use made by a national panel of engineers selected from each SRA (state road authority) and from the New Zealand Transit Authority. This committee is known as the Austroads Safety Barrier Assessment Panel or ASBAP. This is an orderly system that then allows each SRA a range of approved proprietary products to use locally. This orderly product range is slightly complicated by the non-proprietary products that each individual SRA still endorses for use within its domain. The concern for the SRA engineers is the quality of workmanship in the construction of the roadside barriers. The concern for the Contractor is the needless costs of duplicating services, registrations and pre-qualifications with each individual SRA. Both parties are concerned that the industry works in an environment often with few controls, an environment that allows “cowboys” to thrive and where substandard workmanship is not uncommon. This low regulated construction environment is in stark contrast to the regulations imposed on manufacturers for the provision of safety barrier product.

It is in the interests of both government and industry that the situation be rectified. An industry working party was formed and recommended the UK model for national harmonization for training in the roadside safety barrier industry and an on-going accreditation system is adopted. Adoption of the UK system, being from a country of similar culture and legal processes and similar barrier products and road vehicles was considered the wisest recommendation.

This presentation is both an overview and update to related papers presented at the AFB(20) conference in Melbourne in March 2014 by Daniel Cassar (“Roadside Barrier Installation and Maintenance Issues : the Need for Quality Control”) and Paul Hansen (“Sector Schemes: What Are They and How Should They Be Used in Australia?”). Both these papers are in the *Transportation Research Circular E-C215* dated November 2016.

Advances in Winter Maintenance Practices to Improve Roadside Safety

DAVID L. BERGNER

Monte Vista Associates, LLC

Roadside safety efforts generally focus on reducing or eliminating the impact of vehicles with off-pavement structures, objects, vegetation and topographical features. What has been overlooked is the value of snow and ice control practices in mitigating the surface conditions that contribute to uncontrolled vehicle roadway departures. The primary goal of local and state transportation agencies following winter storms is to regain a near-normal level of safety and mobility as quickly and reasonably possible. Pavement friction is vital for drivers to maintain control of vehicles; just a very thin coating of snow or ice substantially reduces the ability of even prudent drivers to safely move, steer and brake.

Recent advances in weather forecasting, pavement condition sensing, anti-icing materials, vehicles, plows, spreaders, plowing techniques and application methods have greatly improved the ability of transportation agencies to achieve desired Levels of Service efficiently, effectively and within reasonable times. In addition, agencies are revising their plans, policies and procedures to better deal with a trend toward more extreme winter weather, stricter environmental regulations, expanding safety mandates, increasing litigation, heightened public expectations and constrained budgets. Many agencies are modifying existing Levels of Service often resulting in less than “ideal” but still acceptable pavement conditions. For example, lower-volume roads and streets may no longer be completely cleared but still passable. This paper will discuss methods and practices that can prevent, reduce or mitigate roadside crashes before, during and following winter storms.

INTRODUCTION

Winter weather is challenging for both drivers and the transportation agencies responsible for maintaining highways, roads and streets. According to the Federal Highway Administration (FHWA), over 70% of the U.S. road system is in areas that receive at least five inches of snow annually (1). Most of the U.S. population lives in these same regions. Other regions, particularly the Southeast, occasionally experience light snow and ice storms. About 24% of all vehicle collisions are due to snowy or icy roadways, 15% happen during snow or sleet (1). Many of these crashes involve run-off roadway (ROR) vehicles that strike barriers, structures, buildings, walls, poles, posts, fences, railings, culverts, trees, medians, embankments and vehicles that are also off the road. In the United States, collisions with fixed objects and non-collisions account for 19% of all reported crashes; yet they result in 44% of all fatal crashes according to the National Highway Traffic Safety Administration (2).

ROR crashes occur on all roadway types, with a significant percentage on two-lane rural highways. The causes are varied and include avoiding a vehicle, object, or animal in the travel lane; inattentive driving due to distraction, fatigue, sleep, or drugs; the effects of weather on pavement conditions; and traveling too fast through a curve. (3) More to the point, average monthly snowfall exceeding 4 in. and interactions between snow depths and horizontal curves were found to have a statistically significant effect on roadside crash frequency probabilities.

Furthermore, the contribution of weather and related interactions to the likelihood of roadside crash frequencies was approximately 19%. (4).

Roadside safety has focused mostly on the design geometrics of roadways (for example, gradients, alignment, lane widths and markings); the type and placement of roadside hardware and structures (i.e., guardrails, light poles, sign posts, retaining walls); adjacent natural features, such as trees and rock outcrops, and driver ability and behavior. However, what has been overlooked is how winter weather operations (snow and ice control) can substantially mitigate conditions that contribute to many road departure related crashes.

The goal of transportation agencies is to restore safety and mobility as effectively and efficiently within a reasonable time following the cessation of winter storms. Before and during these storms, the agencies strive to keep the roadways passable for prudent drivers operating properly equipped vehicles, thus reducing the potential for roadway departures. Winter maintenance has evolved considerably in the past several decades due to advancements in technology, weather forecasting and reporting, equipment, materials and the science and art of plowing and material applications. Likewise, training has substantially improved as the operations have become more complex. This paper will examine how municipal, county, state and other transportation agencies attempt to meet that goal.

THE IMPACT OF WINTER WEATHER ON THE U.S. ROAD SYSTEM

Obviously, winter weather is hazardous for motorists. Statistics from FHWA (1) help illustrate the prevalence and danger of snowy, icy roads:

- Over 70 percent of the nation's roads are in snowy regions, those which receive more than five inches average snowfall annually.
- Nearly 70 percent of the U.S. population lives in these snowy regions.
- Over 1,300 people are killed and more than 116,800 people are injured in vehicle crashes on snowy, slushy or icy pavement annually.
- Every year, nearly 900 people are killed and nearly 76,000 people are injured in vehicle crashes during snowfall or sleet.
- Each year, 24 percent of weather-related vehicle crashes occur on snowy, slushy or icy pavement and 15 percent happen during snowfall or sleet.
- Freeway speeds are reduced by 3 to 13 percent in light snow and by 5 to 40 percent in heavy snow.
- Average speeds on arterial roads decline by 30 to 40 percent on snowy or slushy pavement.

Though there is an extensive amount of research concerning accidents during winter storms, a literature review, including the Transportation Research Board's TRID, ResearchGate and ScienceDirect, did not discover any studies with precise numbers of RORs directly attributable to wintry roads. While it is evident that timely and appropriate snow and ice control measures can reduce accidents, the actual correlation with ROR is difficult to determine. In fact, "Although a large number of studies have attempted to draw conclusions about factors contributing to road departures, most rely on crash data which is a second hand and incomplete picture of the events leading to the crash." (5)



FIGURE 1 Multi-vehicle ROR crash on snowy interstate highway.

CHALLENGES FOR TRANSPORTATION AGENCIES

Winter weather has become more severe in the last 10-15 years; unprecedented snow storms have pummeled the Northeast, New England, Midwest, Mid-Atlantic, Great Plains and even the Southeast. Atlanta, GA and Charlotte, NC for example so rarely experienced snow or ice that they were woefully unprepared for even a three-inch storm that paralyzed that region. Agencies in the traditional “Snow Belt” dealt with more storms and deeper accumulations. While accurately identifying future weather trends can be problematic, recent events indicate that transportation agencies need to be better prepared to deal with more extreme winter weather.

Already faced with budget reductions, increased retirements, difficulty in recruiting and retaining new employees, aging infrastructure, obsolete equipment, stricter environmental mandates and higher demands and expectations from the public, transportation agencies must seek innovative ways to deliver efficient and effective snow and ice control. Furthermore, according to the FHWA, winter road maintenance accounts for roughly 20-percent of state Department of Transportation (DOT) maintenance budgets, a strong indication of the high importance placed on the value of timely snow and ice control. As transportation agencies improve winter operations, the efforts will also help mitigate the probability of ROR. As noted in a NHTSA report, “ROR events were found to occur most frequently, on a per-mile basis, in low-friction conditions and snow or ice increased the likelihood by seven times that of dry conditions.” (6)

However, it is also important to recognize that snow and ice and control may adversely affect existing roadside safety features. For example:

- Snow and ice, before plowing and material applications are effective, can cover lane lines, edge lines, raised pavement markers and rumble strips. These devices guide drivers in the right direction and, in the case of rumble strips, warn of impending roadway run-off.

- Plowing can remove or destroy raised pavement markers; plowing and spreading abrasive materials wear down pavement markings.
- Heavy, wet snow cast by plows can obscure warning signs. Plows may also knock down signs and pole-mounted warning beacons.
- Snow plows wear down special friction surfaces.
- Dry abrasives, like sand, on bare pavement can cause a loss of traction.
- Liquid deicers can create slickness under certain conditions.
- Deeper piles of plowed snow can hide roadside objects such as posts, railings, hydrants, drainage structures, boulders and even abandoned or wrecked vehicles.
- Snow plowed against guardrails and overpass railings can create “ramps” that project errant vehicles up and over.
- Piled snow on the shoulder or curb can melt and then refreeze overnight on the pavement creating icy patches that contribute to vehicle run-offs.

The Transportation Research Board, AASHTO, Pacific Northwest Snowfighters, Clear Roads Consortium, Aurora, FHWA, several state DOTs and universities have completed a substantial amount of research, on equipment, plowing, materials, application methods and environmental monitoring. Additionally, training program managers, supervisors and operators on new methods and practices is a continuing effort; incorporating understanding of the effects on roadside safety needs to be emphasized.

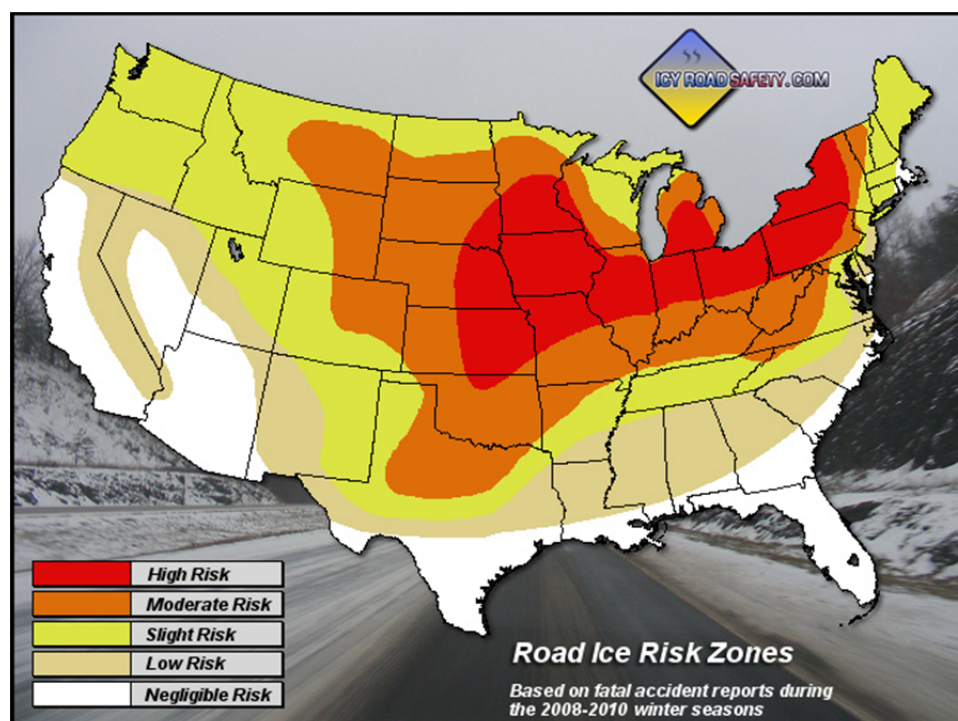


FIGURE 2 Map of U.S. Icy Road Risk Zones (7)

SNOW AND ICE CONTROL STRATEGIES

The principal concept of winter weather road operations is to prevent, as much as feasibly possible, the bonding of snow and ice to the pavement. Once that occurs, removing snow and ice becomes considerably more difficult. The main strategies in snow and ice control are preventive, reactive and remedial:

- Anti-icing---application of mainly liquid materials prior to a winter weather event to prevent bonding.
- De-icing---application of solid (predominantly rock salt) and/or liquid chemicals to melt snow and ice that has already bonded.
- Traction improvement ---application of granular abrasives, commonly sand, as a temporary remedy for very slick surfaces, particularly on steep grades and horizontal curves.
- Mechanical removal of packed snow and ice--- use of serrated plow blades, spiked rotators or hammers to break up thick ice.
- Hauling---removing excessive accumulations of plowed snow from certain locations such as congested areas, intersections, interchanges, bridge/ overpass decks, and critical access points.
- Snow fences--- temporary and permanent structures or plantings that hinder snow from blowing onto the roadway.
- Avalanche sheds---structures cover the mountain roadway and divert the avalanche.
- Closures--- Road closures are an extreme measure but necessary when a winter storm overwhelms an agency's ability to keep the roadway minimally safe and navigable.

Anti-icing is not practical for all winter storms; certain conditions must be present for it to work but it has proven to be very effective, especially for preventing black ice. Anti-icing chemicals are applied by sprayer trucks up to several days before an expected snow or ice event. Fixed automated spray systems (FAST) are installed on bridges and overpasses susceptible to early freezing.



FIGURE 3 Pre-storm anti-icing operation.

De-icing, applying melting chemicals after snow or ice has accumulated, has long been the most common approach to snow and ice control. Typically, solid and /or liquid materials are applied as a truck is plowing snow. The materials work well at milder pavement and air temperatures; however, severe to extreme cold greatly inhibits their efficacy. This is a more acute problem when materials are applied on packed snow and ice.

Abrasives are still widely used with or without rock salt and liquid deicers. Abrasives alone do not have any melting properties. Many agencies are greatly reducing or eliminating use of sand due to environmental considerations such as air-borne particulate limits and infiltration of water bodies. It is also widely recognized that any traction improvement is very short-lived; the abrasives become pulverized by traffic or embedded below the surface of packed snow or ice.

Plowing obviously clears snow, slush and loose ice from the pavement and is the primary strategy for quickly achieving bare pavement. Plow technology has rapidly advanced; the size, shape and composition of plows and blades increases the capability to remove more snow on one pass and decrease down-time to repair or replace blades. This aids prevention of ROR by substantially improving pavement friction. Serrated, or toothed, blades can break thick packed snow or ice but there is the potential for pavement damage. A few DOTs use special “ice breakers” for the more difficult accumulations; these devices use reciprocal or vibrating action to pound and break up packed ice.

In areas that normally experience deep snows, huge blowers are used to propel snow farther back from the roadway in rural areas.

Hauling is necessary when accumulated snow obscures driver visibility, encroaches into travel lanes and shoulders or is too deep for normal plowing to remove. It is an intensive post-storm operation and is used predominantly in dense urban areas. The snow must be loaded onto trucks and then transported to designated “snow farms” for disposal. As a limited alternative, excessive snow is dumped into a melter and the water discharged into storm sewers.

Snow fences are typically used in open rural areas subject to frequent prevailing winds such as the Great Plains and certain western mountain locations. The structures may be temporary and installed only for the winter season or permanent. Many are wood and metal but some are dense windbreaks of trees and large shrubs. Regardless of type, the purpose is to prevent snow blowing from adjacent fields onto the roadways causing large drifts. This contributes to roadside safety by providing clearer, drier pavements which reduces the potential for ROR.

Closing roads is sometimes necessary due to extreme winter conditions. Permanent “snow” gates and signage are used in the Great Plains and mountainous areas that normally experience frequent heavy snowfalls. Portable signs and barricades are also used. Restricting vehicles from travelling on closed roads is certainly effective in preventing ROR.

PLOWING EQUIPMENT AND TACTICS

Plowing immediately removes snow, slush and, in some cases, ice from the pavement. During a storm the snow is typically pushed to the shoulder or curb; on narrow two-lane roads with no shoulders the snow goes into the adjacent drainage ditch. Achieving bare pavement certainly reduces the potential for accidents, including ROR, but do some plowing techniques have a negative effect on roadside safety?

Plowed snow piled against guardrails, median barriers and railings can create “ramping” of errant vehicles. Wing plows, mounted either on the right, left or both sides, increase the capability of a truck to clear shoulders on the same pass for the travel lanes. Wing plows are also useful for “benching” to cut down the height of snow alongside the roadway and improve driver visibility of roadside objects. Trailer-mounted tow plows with material spreaders are a recent innovation that allows one truck with a front plow to also plow and treat one or two adjacent lanes.

Studies are being conducted as to best practices for plowing diverse interchanges and intersections. However, many ROR occur on rural two-lane roads with acute horizontal curves. In suburban and rural areas, objects close to the pavement edge are occasionally knocked down by snow plows. This includes road signs, particularly curve and steep slope warning signs, delineators and object markers. Also, the signs and markers can be covered by heavy snow cast by plowing. If these devices are missing or obscured, the probability of ROR may increase, especially for drivers unfamiliar with the area. Research is needed to determine how changes in plowing techniques can lessen the potential risk of ROR.

LEVELS OF SERVICE

The core of winter weather road operations is the provision of Levels of Service (LOS). Highways, roads and streets are classified by each jurisdiction according to criteria that includes traffic volumes, capacity and function. Typical classifications are expressway or limited access highway, major arterial, minor arterial, collector, residential, service road. These classifications influence the priority rankings for maintenance operations. The higher the priority the more resources will be directed towards a particular segment. Obviously, a national highway route and major arterial in a metropolitan area will have a higher priority than a two-lane collector street in a residential neighborhood. Priority ranking systems vary; some jurisdictions use alphabetical or numerical designations, others a color code or a descriptive term. Regardless of the nomenclature, each ranking has a defined LOS. A top priority LOS, for example, will usually strive for bare pavement on all lanes and shoulders soon after the end of a storm. It will also call for continual plowing and material application during the storm to keep the pavement as clear as reasonably possible under prevailing conditions. A lower priority, for instance a low-volume two-lane rural highway, may have as its LOS bare pavement only in the wheel tracks. Even lower on the priority scale, say a residential street, a LOS that provides just a bladed surface may be adequate. The assignment of priority ranking and concomitant LOS may also be influenced by proximity or linkage to critical transportation, medical, police, fire, governmental, commercial, industrial and educational facilities and nodes. What bearing does LOS have on roadside safety? Unarguably, a higher LOS provides a better pavement surface thus reducing the potential for ROR. However, a general LOS may not take into account specific road segments or locations that pose a greater risk of ROR. That can be addressed in route planning.

IMPACT ON ROADSIDE SAFETY DUE TO CHANGES IN LOS

Transportation agencies have for years struggled to fully provide services and functions. Funding has long been inadequate to meet the demands caused by growth and obsolete infrastructure.

This affects funds for winter weather road operations as well. Faced with budget cutbacks, program managers look to conserve critical resources of personnel time, equipment use and materials. A significant amount of overtime is incurred during winter operations as storms often occur outside regular working hours.

Likewise, vehicles and equipment accumulate considerable equipment engine-hours and miles leading to increased maintenance, repair and fuel expenditures. Material usage can vary depending upon the specific conditions of each storm; suffice it to say that a prolonged, severe event will require substantial amounts of material. To contain costs-of-operation during a winter season, a transportation agency may have to adjust LOSs; reducing plowing and treatment of roads may increase the potential for wrecks and ROR. Any adjustments must therefore take into consideration the effect on safety as 17% of weather -related crashes occur during snow or sleet, 13% occur on icy pavement and 14% take place on snowy or slushy pavement based on ten-year averages from 2005 to 2014 analyzed by Booz Allen Hamilton. (8) Agencies need to finely balance limited resources with the duty to maintain safety and mobility on the roadways.

ROUTES

The next step is to configure efficient routes. Lane-miles/ kilometers, cycle-times, traffic patterns, distance from road maintenance facilities, material application rates and number, types and capacities of snow control equipment are major factors in determining the routes. Generally, a higher priority route will have shorter cycle-times, the interval it takes to make one complete pass or circuit plowing or spreading. Again, the question; how does this impact roadside safety? Simply stated, the quicker that a truck can reach its start point and the faster it can complete the route then the better the road conditions. Many routes have not been updated for years or have had only slight revisions. Few have been reconfigured based on optimizing for highest efficiency. Route optimization has become more prevalent for scheduled, routine functions but has not been used much for snow control.



FIGURE 4 Extra material applied at hazardous curve.

On any route, there are known “trouble spots” such as steep grades, curves, elevated structures, open areas susceptible to snow drifting and locations where seeps or melt-water often freezes on the roadway. Pre-season “dry-runs” familiarize the plow operators with those locations; operators can also observe changes that may have occurred since the last season that could be new ROR spots. Operations managers and supervisors can then determine appropriate treatments for these chronic hazardous locations.

WEATHER FORECASTS AND CONDITIONS REPORTING

Weather forecasting has substantially advanced in recent years. Transportation agencies rely upon public and private weather services for precise information to better plan, prepare and execute snow and ice control. Additionally, Road Weather Information Systems (RWIS) at strategic locations provide real-time data such as air temperature, amount and type of precipitation, visibility, dew point, relative humidity, wind speed and direction, pavement temperature, subsurface temperature, surface condition (dry, wet, frozen), pavement salinity and freezing point of the road surface. RWIS stations mounted at known high -risk road locations can alert program managers when conditions deteriorate and prompt, specific treatment is needed at those sites.

Many plow trucks and supervisors’ vehicles are now equipped with air and pavement surface temperature sensors. Some also have sensors that detect surface moisture and salinity (from road salt applications). Sensors are being developed that can measure the thickness of ice or snow on the pavement. More plow trucks are now equipped with AVL (Automatic Vehicle Locator). In addition to precisely indicating a truck’s location, an AVL device can record travel direction and speed, position of the plow(s) and operation mode of the material spreader(s). Once again, the question: how does this mitigate ROR? By reporting in real-time what was done and at what time by the plow truck, supervisors can better assess if plowing and material applications are being effective in those high-risk locations and thus whether adjustments are needed. As noted by Thordasonn and Olafsson: “Preventive treatment of the road is important to reduce the risk of ice forming on the road. The use of advanced systems in weather forecasting and monitoring along with staff education and improved procedures is expected to improve the winter traffic safety.” (9)

COMMUNICATIONS, INTRA and INTER-AGENCY

Another important element is good communication between operators in the field and supervisors and dispatchers. Two-way radios are the most common system though cell phones and mobile computers are increasingly used. Regardless of the method, the key point is to provide information about road conditions. How does this improve roadside safety? Notifying a truck operator of a hazardous location on the assigned route ensures that he /she will deploy extra material or plowing to mitigate the risks of ROR. Conversely, an operator can promptly advise the control office of adverse conditions observed while in the field. In certain cases, the particular location may be under the purview of another agency or jurisdiction, for example, a shared boundary road or major arterial. Or, a municipal agency truck may transit over a road segment that belongs to the state DOT.

ADVANCED VEHICLE TECHNOLOGY

Automated Vehicles/ Connected Vehicles (AV/CV) technology is here to some degree and will dramatically increase in the near future. How will this aid roadside safety during winter weather operations? Automated vehicles rely for guidance on being able to “read the road” by identifying the presence, proximity and type of certain pavement features such as lane and edge markings, crosswalks and stop bars, RPMs and roadside devices such as delineators, object markers, signs, guardrails and longitudinal barriers. What effect snow and ice accumulations will have is a concern though the AV developers believe that the technology will surmount this. Ford, for example is testing vehicles that use LIDAR and “extremely detailed 3d maps” with cameras and radar to precisely read the road. (10)

But can the technology detect the presence of packed snow and ice on the road? More to the point, can it determine degree of slickness? Many problems still need to be addressed before self-driving vehicles are totally reliable in winter weather. Meanwhile, the technology can be used to assist drivers in safely navigating snowy roads.

INTELLIGENT TRANSPORTATION SYSTEMS (ITS)

ITS is widely used in traffic management and control systems; video vehicle detection, CCTV to monitor actual traffic conditions, advanced signal controllers, fiber-optic interconnections, electronic tolling and weigh-in-motion provide for more responsive, adaptable, efficient and safer movement of traffic. Winter road operations control is trending towards co-location with Traffic Management Centers (TMC) to share technology and information. Winter weather conditions can change suddenly and dramatically; managers and supervisors can adjust operations quicker and more effectively when they have access to real-time traffic information combined with the data from telematics on-board the plow trucks.

PUBLIC INFORMATION

Educating, informing and alerting the public are key elements in reducing risk of ROR on winter roads. Regardless of the efforts of transportation agencies to keep the roadways open and safe, motorists have a major responsibility to curtail unnecessary travel, drive carefully for the conditions and watch for hazardous situations. Transportation agencies rely upon local radio and television stations to disseminate timely information as to weather and traffic conditions. Agency and social media websites, mass e-mails and texts are other ways to inform the public. Highway Advisory Radio (HAR) and Dynamic Message Signs (both portable and stationary) alert motorists of conditions ahead. For example, the Icelandic Road and Coastal Administration has an ambitious vision for the ongoing deployment of information technology for the benefits of winter road accessibility and safety. (9)



FIGURE 5 DMS advisory of icy conditions; note vehicles on left shoulder.

ROAD WEATHER RESEARCH AND TRAINING

The Quebec Ministry of Transportation developed a nine-module training program to improve winter response capabilities of operators and managers and enhance skills and knowledge for using climatological data received from remote weather stations. The American Association of State Highway Transportation Officials (AASHTO) developed a computer-based training regimen that includes information on weather. American Public Works Association (APWA) developed its Winter Maintenance Supervisor certificate class. The Clear Roads Consortium is also developing a winter maintenance training course with separate levels for operator, supervisor and agency officials. Aurora, Clear Roads, AASHTO, the Transportation Research Board and the FHWA individually and collectively sponsor research on a myriad of winter road maintenance issues. Additional research is conducted by various state DOTs, colleges and University Transportation Centers. Though much of it has examined increasing safety and mobility, little if any information specifically pertains to ROR mitigation. Nonetheless, it is evident that better training of operators, supervisors and managers on understanding how meteorological conditions, material applications and plowing techniques can significantly reduce the potential for ROR.

PLANNING AND POLICY

Winter road operations is truly a year-round program; as soon as one season ends, planning and preparation for the next season begins. The interval is only six months or less depending upon the locale and much has to be accomplished in that time. Part of the process involves a review of the past season and a critical, objective assessment of what worked well and what needs improvement. Typically, planning has concentrated on equipment repair, replacement and upgrades; material re-stocking; route revisions and staffing requirements. Analyzing traffic accident records has been of little if any concern to maintenance managers; they have viewed that as a function of traffic engineers. That mindset needs to change and maintenance operations staff and traffic engineers need to communicate and collaborate on identifying causes of wrecks, including ROR, during winter conditions. As noted by Liu and Subramanian, “among the crashes

that occurred in adverse weather conditions, 75.5% were ROR crashes.” (11). Approximately 12% of that total is due to snow and ice covered roadways.

Do specific sites or segments need special treatment with materials? Is extra warning signage or beacons needed to alert drivers? Can the road geometrics or pavement be improved to reduce ROR? Are there locations that operators and supervisors have observed as being hazardous though not identified as such by engineers due to insufficient accident data? Perhaps measures such as installation of guard rails, removal of large rocks, relocation of poles and posts farther back from the roadway and clearing trees and bushes in the right-of-way can be easily implemented. But, no matter how much the agency does, some motorists will disregard warnings and observable conditions.

Lastly, the agency’s written winter operations policy should clearly identify what roadways it is responsible for maintaining (and note those within or adjacent to the boundaries that are the responsibility of other entities); state the goals and objectives; explain the priority classifications of the roadways; detail the Levels of Service to be provided; outline the general strategies and tactics of snow and ice control; describe the concept of operations and list the equipment and facilities utilized. It is very important to include a disclaimer that, despite the agency’s full effort, any winter storm may overwhelm its capability to provide more than very minimal LOS. Winter weather road operations plans and manuals are public documents; agencies must avoid statements that commit themselves to unrealistic expectations. When accidents, including ROR, occur on wintry roads, victims’ attorneys and insurance companies will look to the “deep pockets” of government agencies. Having a sound policy and plan has proven to be very effective in defending against litigation.



FIGURE 6 Plow trucks, too, can slide off icy roads

CONCLUSIONS

Highway agencies spend millions of dollars to ensure safe and efficient winter travel. However, the effectiveness of winter-weather maintenance practices on safety and mobility are somewhat difficult to quantify. (12). While the actual rate of Run-off Road accidents due to winter conditions is indeterminate, it can be reasonably assumed that snow and ice on the pavement are a major contributory factor.

Achieving clear, dry pavement, particularly on hills and curves, will certainly reduce the potential for ROR. Improved weather forecasting, advanced technology for monitoring environmental conditions, broader use of anti-icing strategies, better understanding of the use and application of various de-icing materials, newer equipment and vehicles that increase productivity and efficiency of snow control, and more training of operators in proper plowing techniques and material applications all contribute to mitigating hazardous road situations. Local and state agencies have incorporated these technologies and practices to varying degrees and the trend will expand as program managers become more knowledgeable about these innovations. However, budgetary constraints may hinder the pace of and breadth of adaptation.

It is suggested that during annual planning for winter weather operations Maintenance, Engineering and Law Enforcement examine where RORs tend to occur more often and what additional measures could be implemented to lessen risk. Transportation agencies do not have unlimited resources; special tactics could help at those locations having a higher risk of ROR. Further research could determine the actual percentage of ROR directly due to slick winter roads and how snow and ice control operations could be improved to substantially reduce those occurrences.

REFERENCES

1. FHWA Road Weather Management Program, Snow and Ice, http://www.ops.fhwa.dot.gov/weather/weather_events/snow_ice.htm. Accessed September 23, 2016.
2. Holdridge, J.M., V. N. Shankar and G. F. Ulfarsson. The Crash Severity Impacts of Fixed Roadside Objects. *Journal of Safety Research*, Vol. 36, 2005, pp.139-147.
3. Run-off Road Collisions, Descriptions of Strategies, http://safety.transportation.org/htmlguides/RORcrashes/description_of_strat.htm. Accessed February, 21, 2017.
4. Shankar, V., S. Chavanan, S. Sittikariva, M. Shyu, N. Juvva and J. Milton, Marginal Impacts of Design, Traffic, Weather and Related Interactions on Roadside Crashes. Transportation Research Record: Journal of the Transportation Research Board vol.1897, January, 2004.
5. "Use of SHRP2 NDS Data to Evaluate Roadway Departure Characteristics," TRB Research in Progress, Iowa State University Institute for Transportation Studies.
6. McLaughlin, S., J. M. Hankey, S.G. Klauer, and T.A. Dingus. *Contributing Factors to Run-Off-Road Crashes and Near-Crashes* DOT HS 811 079 National Highway Traffic Safety Administration, January, 2009 <https://www.nhtsa.gov/sites/nhtsa.dot.gov/files/811079.pdf>.
7. <http://icyroadsafety.com/fatalitystats.shtml>. Accessed February 22, 2017.
8. How Do Weather Events Impact Roads? FHWA Road Weather Management Program. Accessed February 15, 2017. https://ops.fhwa.dot.gov/weather/q1_roadimpact.htm.
9. Thordarson, S. and B. Olafsson, *Weather induced road accidents, winter maintenance and user information*. Transport Research Arena Europe, 2008.
10. Huynh, T. Can a Self-driving Car Handle Winter? *Techradar*, March 10, 2016

1. <http://www.techradar.com/news/car-tech/can-a-self-driving-car-handle-winter-snoooooo-problem-1316700>. Accessed September 15, 2016
11. Edwards, C., N. Morris and M. Manser. A Pilot Study on Mitigating Run-Off-Road Crashes, Intelligent Transportation Systems Institute, Center for Transportation Studies University of Minnesota, July, 2015.
12. Hans, Z., N. Hawkins, K. Gkritza, M. Shaheed and I. Nienanya, Safety and Mobility Impacts of Winter Weather – Phase 3, Center for Transportation Research and Education, Iowa State University, September, 2014.

Guidelines for Shielding Bridge Piers

MALCOLM H. RAY
CHRISTINE E. CARRIGAN
CHUCK A. PLAXICO
RoadSafe LLC

This NCHRP project has multiple objectives, including to develop (1) risk-based guidelines for new and existing structures that quantify when bridge piers should be investigated for vehicular collision forces per AASHTO LRFD Bridge Design Specifications or be shielded with a longitudinal barrier considering as a minimum: site condition, traffic, bridge design configurations, geometry of the roadway section passing beneath a bridge, operations characteristics, and benefit/cost and (2) guidelines for barrier selection, length-of-need, and placement for shielding bridge piers and protecting the traveling public.

Changes to the *AASHTO LRFD Bridge Design Specification* and/or the *Roadside Design Guide* may be necessary to implement the results of this research. A review of the current and pending publication of both documents was conducted to determine where modifications or additions may be necessary. This presentation will summarize the possible changes to these publications and present the draft guidelines. The draft guidelines are more detailed and more substantiated for the treatment of bridge piers, both for the protection of the bridge structure as well as protection of motorists.

Handling an Instant Hazard

ERIC HEMPHILL

North Texas Tollway Authority

The typical roadway departure crash is thought of as leaving the roadway and striking a permanent fixed object. However, at the North Texas Tollway Authority (NTTA), a regional tollway authority covering the Dallas/Fort Worth Metroplex, we also realize the importance of handling stalled, stranded, and disabled vehicles to reduce the probability of crashes. The typical stranded motorist is typically only feet from the edge line of traffic moving at 70 miles per hour and it only takes a moment to cause a severe crash. Therefore, the NTTA has invested in cameras able to detect stranded motorists, a 24x7 courtesy patrol to respond to assist them, tow trucks to remove them, and a 24x7 traffic management/dispatch center to monitor it all.

The Safety Operations Center (SOC) is the backbone of roadway safety for the NTTA. The SOC is staffed to monitor the nearly 2,000 cameras throughout the roadway system, dispatch Roadside Safety Services (courtesy patrol), dispatch State Troopers, and handle various alarms generated by monitors throughout the system 24x7.

The cameras along the NTTA system are capable of “learning” their environment and can detect a stalled vehicle. If the camera detects something it sends an alert to the Safety Operations Center for a specialist to evaluate the situation. If it is determined it is an accident the appropriate fire, ems, and first responders can be notified, often before the first 911 call is received. However, if it is determined it is a disabled vehicle a courtesy patrol unit is dispatched to assist. The content analytic cameras have allowed the NTTA to assist over 24,000 motorists in 2015. The ultimate goal is to remove the hazard prior to being struck by another motorist.

In addition to the content analysis, the SOC monitors alerts for wrong way drivers. The NTTA has programmed all of the tolling points on the system to detect activation by a driver going the wrong direction. Once detected and alert is sent to the SOC indicating the location of the wrong way driver, which allows the dispatching of police prior to getting any 911 calls. The process has allowed NTTA to be able to intercept wrong way drivers prior to them causing crashes.

The NTTA is also testing the use of our roadway cameras to automatically detect wrong way drivers on the system, similar to their ability to detect stalled vehicles. The additional detection method will provide further coverage for wrong way drivers on the system.

The technology of the SOC is in place to reduce crashes and create a safe roadway and address the "instant hazards" created by stranded motorists and wrong way drivers.

Simulation, Testing, and Evaluation Methods

MGS Dynamic Deflections and Working Widths at Lower Speeds

MOJDEH ASADOLLAHI PAJOUH

NICHOLAS A. WEILAND

CODY S. STOLLE

JOHN D. REID

RONALD K. FALLER

Midwest Roadside Safety Facility

University of Nebraska-Lincoln

The Midwest Guardrail System (MGS) has been full-scale crash tested in many configurations, including installations on or adjacent to slopes, embedded into wire-faced mechanically-stabilized earth walls, with different shapes and species of wood posts, with and without blockouts, for culvert and bridge applications, and at high flare rates. The barrier is very versatile, and State DOTs have expressed an interest in using it adjacent to lower-speed and/or lower-service level roadways. On many urban and lower-speed roads, lateral working widths may be more limited because of bicyclist and pedestrian considerations, limited right of way, traffic control structures, or obstructions which have close proximity to the roadway. In addition, guardrail is itself a hazard, and larger lateral offsets could reduce guardrail collision frequencies. Accurate dynamic deflections and working widths of the MGS when impacted at lower speeds are necessary to determine safe and cost-effective placement of guardrail adjacent to shielded hazards within working width. To determine the maximum dynamic deflection and working width of the MGS system at TL-1 and TL-2 impact conditions of MASH, an LS-DYNA computer simulation effort was performed. This investigation included a calibration effort against physical crash test using a simulated 2007 Chevrolet Silverado impacting both a tangent MGS and an MGS in combination with a 6-in. tall, AASHTO Type B curb, both supported by posts at a 6-ft 3-in. spacing. The calibrated model was then used to simulate lower impact speeds of 31 mph (TL-1) and 44 mph (TL-2) and a 25-degree impact angle at five locations along the barrier. The maximum dynamic deflections and working widths were identified at different design speeds for the MGS on level terrain both with and without blockouts as well as with and without blockouts. A 10 to 15 in. decrease in the maximum dynamic deflection and working width was observed for each decrease in test level. The MGS installed in combination with a curb reduced both dynamic deflections and working widths by more than 15%, which was relatively constant for all speeds considered.

INTRODUCTION

The Midwest Guardrail System (MGS) has demonstrated excellent performance under a variety of crash tests with MASH Test Level 3 impact conditions (1, 2). The standard MGS utilizes W-beam rail with a 31-in. top rail mounting height, W6x9 steel posts, 75-in. post spacing, 12-in. deep blockouts, and rail splices located at the midspan between posts. In test no. 2214MG-2, a 5,000-lb pickup truck impacted the steel-post MGS with a 31-in. top rail height, installed in standard soil and with standard post spacing, at an impact speed of 62.9 mph and at an angle of 25.5 degrees (1). In test no. 2214MG-3, a 2,588-lb small car impacted the steel post MGS with a 32-in. top rail height at an impact speed of 60.8 mph and at an angle of 25.4 degrees (1). In both tests, the barrier safely contained and redirected the vehicles. Moreover, the MGS has been full-

scale crash tested in many configurations, including installations on and adjacent to slopes (4, 5), with different types of wood posts (6, 7), with and without blockouts (8, 9), for culvert and bridge applications (9–11), and in combination with curbs, transitions, and high flare rates (12, 13).

Many State Departments of Transportation have adopted the MGS as the standard W-beam guardrail for all TL-1 (impact speed of 31 mph), TL-2 (impact speed of 44 mph), and T-L3 (impact speed of 62 mph) applications, as the rail deflections and working widths are lower for the lower design requirements. Maximum dynamic deflection of the system is a measure of the maximum distance any individual component in the system deflected when compared to its undeflected position. Working width is defined as the farthest distance the barrier or vehicle extended laterally during impact, as measured from the original, undeformed front face of the guardrail. Working widths are always greater than or equal to dynamic deflections. The TL-3 version of the MGS could be installed for the TL-2 and TL-1 applications. However, it is often difficult to account for TL-3 deflections or working widths for the MGS in lower-speed urban and transitional areas due to bicyclist and pedestrian considerations, limited right of way, traffic control structures, and obstructions within proximity of roadway. It may be feasible to install these systems farther away from the roadway and closer to the front face of hazard along lower-speed roads. Rural transitions to urban areas are common locations where TL-3 MGS may be installed in along lower-speed roads with reduced hazard clearance. Thus, it is critical to determine accurate dynamic deflections and working widths of the MGS when impacted at lower speeds, which assures the safe placement of guardrail and reduces the likelihood of vehicle impact with a shielded hazard within the clear zone. Also, some modifications to the MGS, such as reduced blockout depth or non-blocked options, may result in reduced clearances in limited offset installations. These modifications may be highly beneficial at lower speeds as the likelihood of vehicle snagging on posts decreases as impact speed decreases.

In this study, validated numerical models of vehicle impacts into the MGS were compared to crash test results. Subsequently, these models were utilized to simulate impacts with the MGS installed on level terrain at various locations and with and without a 6-in. tall, AASHTO Type B curb using MASH TL-1, TL-2, and TL-3 test conditions. The maximum dynamic deflections and working widths were identified.

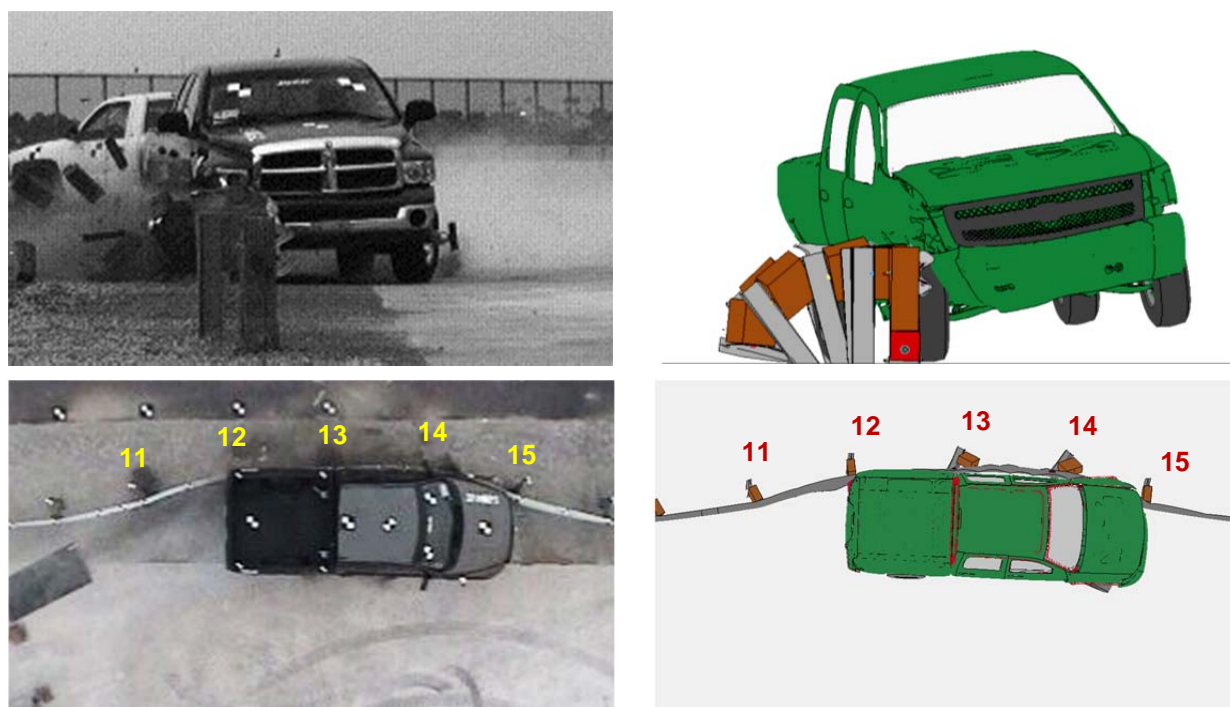
MGS AT TL-1 AND TL-2 IMPACT CONDITIONS

A baseline model of a 29-post, 175-ft long MGS was validated with test no. 2214MG-2 using NCHRP W179 procedures for verification and validation of computer simulations (1, 14). The full V&V comparison is reported in Asadollahi Pajouh et al. (15). The LS-DYNA (16) simulation consisted of a 2270P pickup truck impacting the MGS with a 6-ft 3-in. post spacing at an impact speed of 62 mph and at an angle of 25 degrees corresponding to TL-3 impact conditions. A summary of the results from numerical simulation and test no. 2214MG-2 and a comparison between the actual and finite element simulation of test no. 2214MG-2 are shown in Table 1 and Figure 1, respectively.

Note that considering widely varying soil conditions, it is impossible to predict the accurate dynamic deflection and working width without knowing the in situ strength and

TABLE 1 Summary of Crash Test No. 2214MG-2 and Simulation Results

Evaluation Parameters	Max. Dynamic Deflection m (ft)	Length Contact m (ft)	Max. Roll Angle (degrees)	Max. Pitch Angle (degrees)	Max. Yaw Angle (degrees)	Long. ORA (g's)	Lateral ORA (g's)	Long. OIV ft/s (m/s)	Lateral OIV ft/s (m/s)
Test No. 2214MG-2	1.11 (3.64)	10.3 (33.8)	4.81°	1.84°	45.74°	8.23	6.93	4.67 (15.32)	4.76 (15.61)
Simulation	0.98 (3.21)	9 (29.5)	11.67°	3.17°	46.21°	11.16	9.05	4.43 (14.53)	4.99 (16.37)

**FIGURE 1 Sequential Images, Test No. 2214MG-2 (left) and Simulation (right)**

stiffness soil properties. Other complicating factors, such as asphalt overlays or posts embedded in soil tubes or concrete, further affect vehicle-to-barrier impact dynamics. Since the objectives of this study were to estimate working widths for lower-speed impacts and establish minimum offsets for the fixed objects, weaker soil models with reduced strength and stiffness properties were used to generate conservative results. Therefore, stronger soils in real-world conditions may result in reduced barrier deflections as compared to those shown in this analysis.

The validated baseline model was modified to simulate impacts with the MGS at speeds of 44 mph and 31 mph corresponding to MASH TL-2, and TL-1, respectively. Several impact locations were investigated at each test level to evaluate their effect on maximum dynamic deflections and working widths. In the simulations, impact locations were staggered by $\frac{1}{4}$ -post spacing increments, starting at the mid-span between post nos. 11 and 12, and terminating at the mid-span between post nos. 12 and 13. The results summarized in Table 2 demonstrate the influence of impact location on the barrier deflections.

TABLE 2 Barrier Deflections and Working Widths

Test Level 1 - 31 mph (50 km/h)			
Impact Location	Maximum Dynamic Deflection (in.)	Working Width (in.)	Max. Working Width Component
11½	16.6	35.3	Post no. 12
11¾	15.6	37.0	Post no. 13
12	15.1	37.6	Post no. 13
12¼	15.7	37.3	Post no. 13
12½	15.9	35.2	Post no. 13
Test Level 2 - 44 mph (70 km/h)			
Impact Location	Maximum Dynamic Deflection (in.)	Working Width (in.)	Max. Working Width Component
11½	24.0	48.5	Post no. 13
11¾	25.0	49.3	Post no. 13
12	24.5	46.5	Post no. 13
12¼	24.4	47.6	Post no. 14
12½	24.1	48.3	Post no. 14
Test Level 3 - 62 mph (100 km/h)			
Impact Location	Maximum Dynamic Deflection (in.)	Working Width (in.)	Max. Working Width Component
11½	37.5	58.1	Post no. 13
11¾	38.0	60.2	Post no. 14
12	36.6	59.6	Post no. 14
12¼	39.3	59.3	Post no. 14
12½	37.7	58.7	Post no. 14

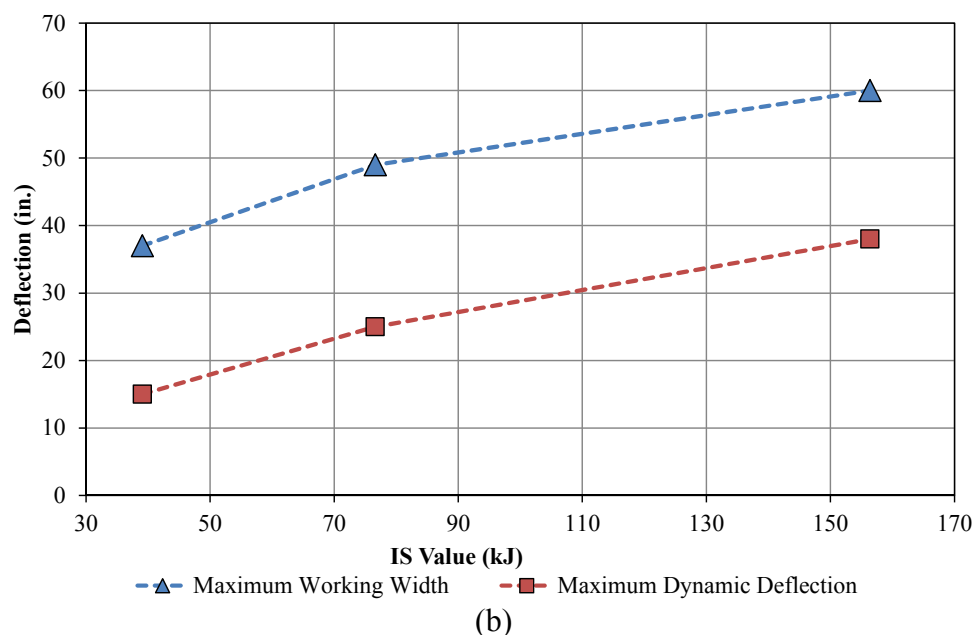
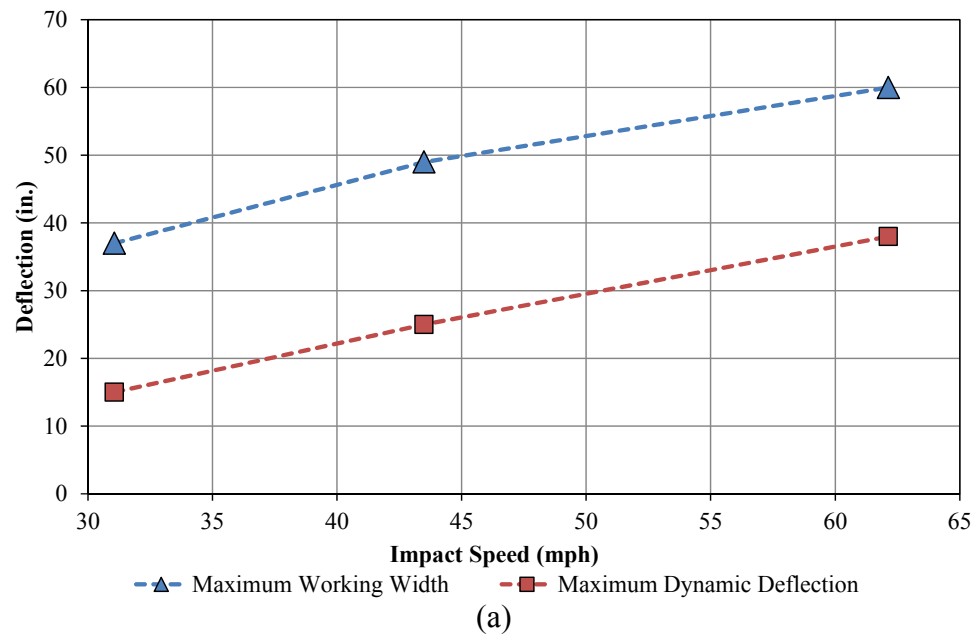
For each test level, maximum dynamic deflections and working widths were very similar, within less than 6% difference, regardless of impact location. The maximum dynamic deflections and working widths occurred at the mid-span upstream from post no. 12 for TL-1 impact conditions, ¼-span upstream from post no. 12 for TL-2 impact conditions, and ¼-span downstream from post no. 12 for TL-3 impact conditions.

It was observed that the post-soil behavior exhibited similar load and deflection characteristics to weak or native soils. Thus, the simulated working widths were believed to be conservative. Simulated working widths were associated with post or blockout deflections, whereas full-scale test working widths were more commonly associated with rail or vehicle displacements. However, the posts tended to rotate further than what was observed in full-scale crash tests, and engaged the rail for a longer period of time, more energy was absorbed by the posts' soil rotations, and the dynamic deflections of the rail and impacting vehicle were lower than observed in the full-scale testing.

Maximum barrier deflections and working widths in simulations at three test levels were compared, as shown in Table 3 and in Figure 2. The working widths increased by 12.2 in. from TL-1 to TL-2 and 11.0 in. from TL-2 to TL-3. At all three test levels, deflected posts were the elements with the greatest working width. It appears that the correlation between maximum dynamic deflection and working width is approximately linear at an impact angle of 25 degrees.

TABLE 3 Simulated Barrier Deflections and Working Widths - Test Levels 1, 2, and 3

Test Level	Impact Velocity (mph)	MASH IS Value (kip-in.)	Maximum Dynamic Deflection (in.)	Working Width (in.)	Vehicle/System Component
1	31	28.7	15.6	37.0	Post no. 13
2	44	57.8	25.0	49.3	Post no. 13
3	62	114.8	38.0	60.2	Post no. 14

**FIGURE 2 Working width and dynamic Deflection a) Versus impact speed
b) Versus IS value.**

MGS INSTALLED IN COMBINATION WITH CURB

In many situations, such as urban and suburban arterials, collectors, and local roads, guardrail may be installed in combination with a curb or a drainage structure. Vehicle instabilities have been observed with some curb-guardrail installation configurations (17, 18). In test no. NPG-5, the MGS was successfully full-scale crash tested with the rail face located 6 in. behind the front face of a curb, consistent with the AASHTO Type B curb (19, 20). A second configuration, consisting of an MGS-to-thrie beam transition with a wedge-shaped curb was also successfully full-scale crash tested (12). Many of the curb-guardrail installations on urban and suburban roads occur in combination with TL-2 or TL-1 design level roadways, which can be characterized by lower posted speed limits, more discrete hazards, and closer hazard proximities to the roadway. In test no. NPG-5, 72-in. long posts were embedded 46 in. into soil behind the curb, such that the top guardrail mounting height was 31 in., as measured above the roadway. The MGS in combination with the curb was impacted by a 4,389-lb 2000P pickup truck at speed of 60.1 mph and at angle of 24.8 degrees. The 2000P test vehicle was successfully redirected with a maximum dynamic deflection of 43.1 in. and a maximum working width of 49.6 in.

A baseline simulation of the Chevrolet Silverado 2270P pickup truck impacting a 175-ft long MGS was modified to simulate impacts on a guardrail located 6 in. behind the front face of a 6-in. tall AASHTO Type B curb. The simulation was validated against test no. NPG-5, which was successfully crash tested according to the TL-3 test conditions in NCHRP Report No. 350 involving and involved an MGS placed 6 in. behind a curb (19–21). The vehicle model utilized for the simulation of test no. NPG-5 was slightly different from the testing vehicle in terms of mass and geometry. However, the main objective of this study was to have comparable dynamic deflections and working widths between the simulation and the test. A summary of the results from numerical simulation and test no. NPG-5 and a comparison between the guardrail performance in terms of deflection obtained from the test and simulation are shown in Table 4 and Figure 3, respectively. As shown in Table 4, the dynamic deflection and working width of the MGS in the simulation and test reasonably compare; thus, this simulation was used for further investigation of the MGS performance at lower speeds.

TABLE 4 Summary of Simulation and Test No. NPG-5 Results

Comparison	Working Width (in.)	Dynamic Deflection (in.)	IS Value (kJ)	Posts Deflected	Post Disengaged from Rail	End Anchorage Permanent Set (in.)
Simulation	48.8	33.4	156	6	3	Negligible
Test No. NPG-5	49.6	38.4	126	7	5	1.5

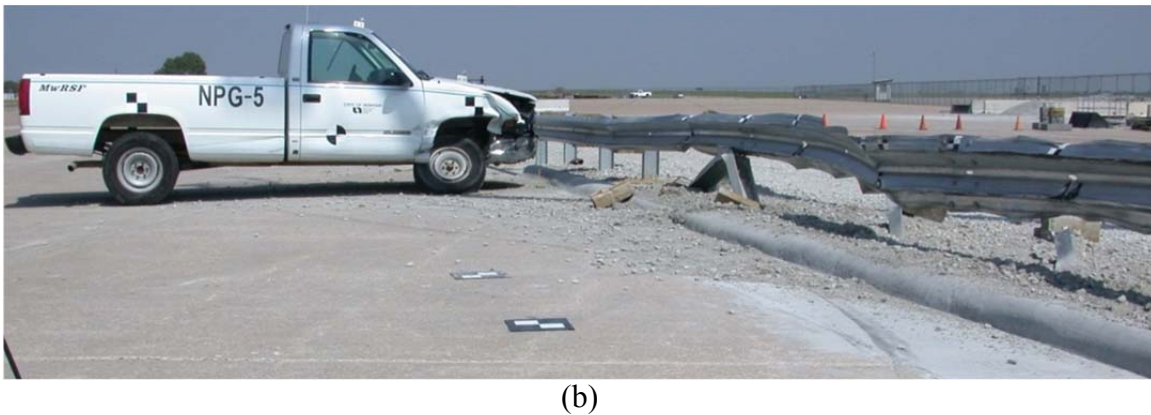
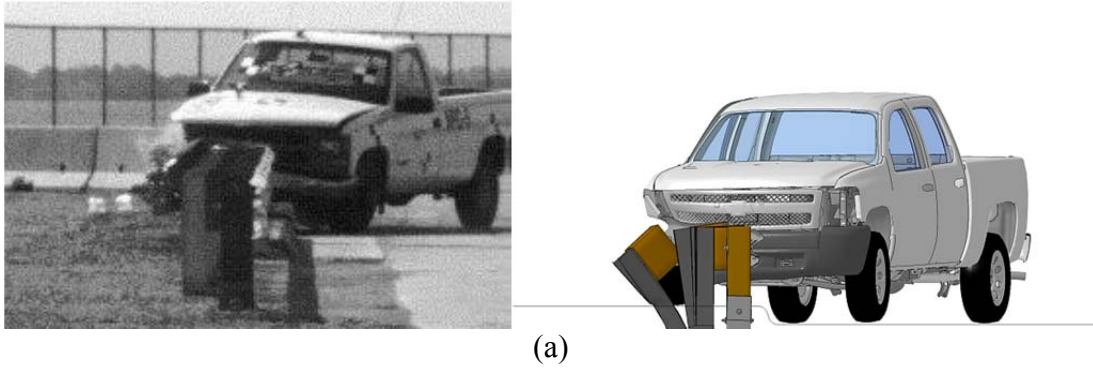


FIGURE 3 a) Sequential images, Test No. NPG-5 (left) and simulation (right) and b) System damage.

MASH testing has resulted in similar, and at times, lower dynamic deflections and working widths than observed in tests conducted in accordance with NCHRP Report No. 350, despite a 13.5 percent increase in energy at impact (i.e., IS value). It is believed that the soil may have been weaker than often used in full-scale crash testing in this test, and a comparison with the 2270P simulation was reasonable. Another major difference between the test and simulation results consisted of wheel geometry. The vehicle utilized during test no. NPG-5 had a stiffer suspension (i.e., $\frac{3}{4}$ -ton vehicle vs. $\frac{1}{2}$ -ton vehicle in the model) and increased gap between the wheel and fender, which allowed the guardrail to protrude behind the wheel during redirection. As the rail protruded behind the wheel, it lifted the vehicle's impact side upward. This rolling moment and the truck's lower roll moment of inertia as compared to the 2270P vehicle resulted in a higher roll angle displacement. The truck remained engaged with the rail for a longer amount of time than observed for the 2270P simulated vehicle. The right-front wheel of the simulated truck was not restricted and rebounded more smoothly and quickly. The simulated and full-scale crash test results for working widths were nearly identical. Thus, the simulations were considered calibrated, and the researchers proceeded with the simulations for impacts at lower speeds.

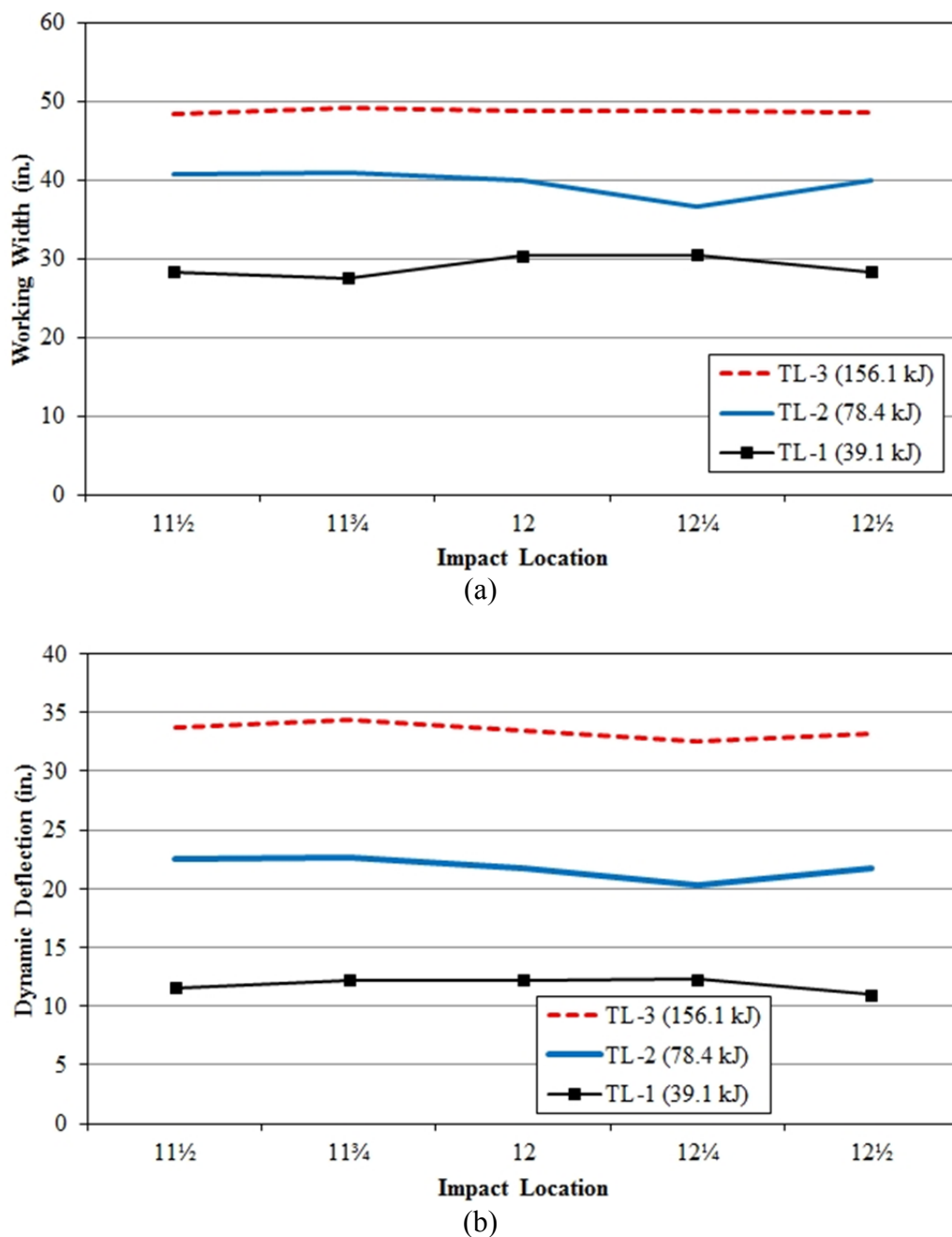
Similar to the level-terrain cases, several impact locations were simulated at each test level to investigate the working width of the MGS installed 6 in. behind a 6-in. tall AASHTO Type B curb. A total of five impacts were simulated for each speed, at quarter-post spacing starting at the mid-span between post nos. 11 and 12, and terminating at the mid-span between

post nos. 12 and 13. Barrier deflections and working widths were compared for impacts at TL-1, TL-2, and TL-3 conditions, as shown in Table 5. Maximum working widths were relatively constant regardless of impact location. For all impact conditions, the maximum dynamic deflection occurred at approximately the $\frac{1}{4}$ -post span upstream from post no. 12.

The trend of maximum dynamic deflection was similar for TL-2 and TL-3 impacts, as shown in Figure 4. The maximum dynamic deflections were at least 15 in. less than the maximum working widths. In all simulations, barrier deflections, barrier exit times, longitudinal exit displacements, vehicle roll and pitch angles, and the number of posts damaged increased with increased impact speed. For all impact conditions, vehicles were smoothly redirected with no instabilities. Vehicle damage was limited for impacts at TL-1 and TL-2 impact conditions, and barrier permanent sets were minimal.

TABLE 5 Barrier Deflections and Working Widths

Test Level 1 - 31 mph (50 km/h)			
Impact Location	Maximum Dynamic Deflection in. (mm)	Working Width in. (mm)	Max Working Width Component
11½	11.6 (295)	28.4 (722)	Post no. 12
11¾	12.2 (311)	27.6 (701)	Post no. 13
12	12.2 (310)	30.4 (772)	Post no. 13
12¼	12.3 (313)	30.5 (775)	Post no. 13
12½	11.0 (279)	28.3 (720)	Post no. 13
Test Level 2 - 44 mph (70 km/h)			
Impact Location	Maximum Dynamic Deflection in. (mm)	Working Width in. (mm)	Max Working Width Component
11½	22.5 (571)	40.7 (1033)	Post no. 13
11¾	22.7 (576)	40.9 (1038)	Post no. 13
12	21.7 (551)	39.9 (1013)	Post no. 13
12¼	20.3 (517)	36.7 (931)	Post no. 14
12½	21.8 (553)	40.0 (1015)	Post no. 14
Test Level 3 - 62 mph (100 km/h)			
Impact Location	Maximum Dynamic Deflection in. (mm)	Working Width in. (mm)	Max Working Width Component
11½	33.7 (856)	48.5 (1232)	Post no. 13
11¾	34.4 (873)	49.2 (1250)	Post no. 13
12	33.3 (847)	48.8 (1240)	Post no. 14
12¼	32.6 (829)	48.9 (1243)	Post no. 14
12½	33.2 (844)	48.7 (1238)	Post no. 14



**FIGURE 4 a) Working widths and
b) Dynamic deflection for MGS in combination with curb.**

ALTERNATIVE APPLICATIONS FOR MGS WITH LOWER IMPACT SPEEDS

Study results were examined to identify modifications that could increase the versatility of the MGS for lower-speed roadways. Several modifications were considered for a variety of reasons: elimination of the blockout; modified post spacing; and varying configurations with curbs. A

non-blocked version of the MGS was successfully tested on level terrain at MASH TL-3 impact conditions (8, 9). Given the successful performance of the system at TL-3 conditions, it is reasonable to assume that the system will also perform acceptably at TL-2 and TL-1 conditions. The working width of the non-blocked MGS recorded during the test was 43.2 in. Numerical efforts with lower speeds were made to estimate the effective working width of a system on level terrain without blockouts when impacted with MASH TL-1 and TL-2 impact conditions. The results are shown in Table 6. The depth of the post and the rail thickness were added to the simulated dynamic deflection to estimate the conservative values for the associated working widths. At TL-1 impact conditions, the maximum dynamic deflections were typically between 11 and 12 in. for the MGS installed in combination with curbs, and were as high as 16.6 in. without curbs. For these low deflections, it may be reasonable to reduce the depth of the blockout to 4 or 8 in. to reduce the cost of the barrier and its associated working width. Full-scale crash testing is recommended before installing a non-blocked MGS in combination with 4-in. and 6-in. tall AASHTO Type B curbs.

Decreased post spacing has been tested on level terrain for the MGS with blockouts. A quarter-post spacing, MGS was successfully full-scale crash tested according to NCHRP Report No. 350 [19]. Reducing the post spacing from 6 ft - 3 in. to 18¾ in. resulted in a 35% reduction in working width, from 57.2 in. to 36.7 in. If the trend is considered approximately linear, a half-post spacing would reduce deflections by approximately 18%. These reductions would be applicable for the MGS with 12-in. deep blockouts and would likely be successful with 8-in. deep blockouts as well. The performance of 8-in. and 12-in. deep blockouts has been shown to be similar under MASH TL-3 impact conditions. Thus it is reasonable to believe that 8-in. deep blockouts would have successful performance under lower-speed impacts [23]. Shallower blockouts or non-blocked systems may require further analysis with full-scale crash testing and/or simulation.

In some urban locations, clear zone may come at a premium expense. It may be cost effective to install guardrail in these locations, but space requirements may be impractical due to shy line and hazard offsets, particularly for rigid, unmovable hazards. Reducing speed limits to accommodate existing working width recommendations may not be practical in all applications. For these unique and difficult scenarios, typical recommendations for guardrail offsets – maintaining a hazard-free envelope defined by the working width – may be impractical. Special considerations may be required for these situations including the MGS installation in combination with curbs taller than 6 in.

TABLE 6 Estimated Working Width Envelopes for Non-Blocked MGS

Design Speed (mph)	IS Value (kJ)	Dynamic Deflection, MGS with Blockouts (in.)	Recommended Working Width Non-Block MGS (in.)	Working Width Test No. MGSNB-1 Non-Block MGS (in.)
31	38.9	16.6	25.9	-
44	78.4	25.0	34.3	-
62	155.6	39.3	48.6	43.2 [8]

If lateral offsets between guardrail and hazards are reduced, there is a possibility that the impacting vehicle will engage or interact with the shielded hazard. However, the statistical likelihood of (1) impact in critical locations with (2) IS values at or above the design condition is small. States must determine if the benefits associated with closer guardrail-to-hazard offset and increased guardrail offset from the road outweigh the potential consequences of a vehicle engaging a hazard while being redirected by the rail. In a recent study at MwRSF, safety of the breakaway luminaire poles installed with an offset from the MGS was evaluated. The MGS offset 20-in. from a light pole was successfully crash tested using a 2270P pickup truck and 1100C passenger car according to MASH TL-3 impact conditions (22).

SUMMARY AND CONCLUSIONS

The performance of the MGS, the dynamic deflection, and working width of the barrier have been examined at TL-3 impact conditions. However, little is known about the dynamic deflection and working width of the MGS when impacted at lower speeds. In this study, models of the MGS installed on level terrain and in combination with curbs were simulated using the non-linear FEA program LS-DYNA consistent with MASH TL-3, TL-2, and TL-1 impact conditions to investigate dynamic deflections and working widths at lower speeds and at alternative impact locations. Maximum dynamic rail and post deflections and the extension of the pickup truck over the top of rail are provided shown in Table 7, which compared well with the TL-3 full-scale test results. If dynamic deflections and working widths must be less than those suggested in this report, stiffer barrier constructions (i.e., half- or quarter-post spacing, or thrie beam) are preferable to relying on an unsaturated, compacted, MASH strong soil.

TABLE 7 Suggested Working Width Envelopes for Guardrail

Design Speed (mph)	Minimum Working Width Envelope by Guardrail Configuration (in.)			
	Level Terrain with Blockouts	6 in. Behind Curb with Blockouts	Level Terrain without Blockouts	6 in. Behind Curb without Blockouts
31	37.6	30.5	25.9	Recommend Testing
44	49.3	40.9	34.3	Recommend Testing
62	60.2 (simulation) 60.3 (full-scale)	49.6 (simulation)	48.6 (simulation) 49.6 (full-scale)	Recommend Testing

ACKNOWLEDGMENTS

The authors wish to acknowledge the Wisconsin Department of Transportation for sponsoring this project as well as the Departments of Transportation for the States of Illinois, Iowa, Kansas, Minnesota, Missouri, Nebraska, New York, Ohio, South Dakota, Texas, and Wyoming for providing resource materials. Acknowledgement is also given to MwRSF personnel for constructing the system and conducting the crash test.

REFERENCES

1. Polivka, K.A., Faller, R.K., Sicking, D. L., Rohde, J.R., Bielenberg, R.W., Reid, J.D., *Performance Evaluation of the Midwest Guardrail System – Update to NCHRP 350 Test No. 3-11 with 28" C.G. Height (2214MG-2)*, Final Report to the National Cooperative Highway Research Program, MwRSF Research Report No. TRP-03-171-06, Project No. NCHRP 22-14(2), Midwest Roadside Safety Facility, Nebraska Transportation Center, University of Nebraska-Lincoln, Lincoln, Nebraska, October 2006.
2. Polivka, K.A., Faller, R.K., Sicking, D. L., Rohde, J.R., Bielenberg, R.W., Reid, J.D., *Performance Evaluation of the Midwest Guardrail System – Update to NCHRP 350 Test No. 3-10 (2214MG-3)*, Final Report to the National Cooperative Highway Research Program, MwRSF Research Report No. TRP-03-172-06, Project No. NCHRP 22-14(2), Midwest Roadside Safety Facility, Nebraska Transportation Center, University of Nebraska-Lincoln, Lincoln, Nebraska, October 2006.
3. *Manual for Assessing Safety Hardware (MASH)*, American Association of State Highway and Transportation Officials (AASHTO), Washington, D.C., 2009.
4. Johnson, E.A., Lechtenberg, K.A., Reid, J.D., Sicking, D.L., Faller, R.K., Bielenberg, R.W., and Rohde, J.R., *Approach Slope for Midwest Guardrail System*, Final Report to the Midwest States' Regional Pooled Fund Program, MwRSF Research Report No. TRP-03-188-08, Midwest Roadside Safety Facility, University of Nebraska-Lincoln, December 2008.
5. Wiebelhaus, M.J., Lechtenberg, K.A., Faller, R.K., Sicking, D.L., Bielenberg, B.W., Reid, J.D., and Rohde, J.R., *Development and Evaluation of the Midwest Guardrail System (MGS) Placed Adjacent to a 2:1 Fill Slope*, Final Report to the Midwest States Regional Pooled Fund Program, MwRSF Research Report No. TRP-03-185-10, Midwest Roadside Safety Facility, University of Nebraska-Lincoln, February 2010.
6. Stolle, C.J., Lechtenberg, K.A., Faller, R.K., Rosenbaugh, S.K., Sicking, D.L., Reid, J.D., *Evaluation of the Midwest Guardrail System (MGS) with White Pine Wood Posts*, Final Report to Wisconsin Department of Transportation, MwRSF Research Report No. TRP- 03-241-11, Midwest Roadside Safety Facility, University of Nebraska-Lincoln, March 2011.
7. Faller, R.K., Polivka, K.A., Kuipers, B.D., Bielenberg, R.W., Reid, J.D., Rohde, J.R., and Sicking, D.L., *Midwest Guardrail System for Standard and Special Applications*, Journal of the Transportation Research Board, Transportation Research Record No. 1890, Washington, D.C., January 2004, pp. 19-33.
8. Reid, J.D., Faller, R.K., Bielenberg, R.W., and Lechtenberg, K.A., *Midwest Guardrail System Without Blockouts*, Paper No. 13-0418, Journal of the Transportation Research Board, Transportation Research Record No. 2377, Washington D.C., 2013, pp 1-13.
9. Schrum, K.D., Lechtenberg, K.A., Bielenberg, R.W., Rosenbaugh, S.K., Faller, R.K., Reid, J.D., and Sicking, D.L., *Safety Performance Evaluation of the Non-Blocked Midwest Guardrail System (MGS)*, Final Report to the Midwest States Regional Pooled Fund Program, MwRSF Research Report No. TRP-03-262-12, Midwest Roadside Safety Facility, University of Nebraska-Lincoln, January 2013.

10. Rosenbaugh, S.K., Faller, R.K., Lechtenberg, K.A., and Bielenberg, R.W., *Weak-Post, W-Beam Guardrail Attachment to Culvert Headwalls*, Journal of the Transportation Research Board, Paper No. 14-3930, February 2014.
11. Bielenberg, R.W., Faller, R.K., Sicking, D.L., Rohde, J.R., and Reid, J.D., *Midwest Guardrail System for Long-Span Culvert Applications*, Journal of the Transportation Research Board, Transportation Research Record No. 2025, Washington, D.C., 2007, pp. 3-17.
12. Polivka, K.A., Coon, B.A., Sicking, D.L., Faller, R.K., Bielenberg, R.W., Rohde, J.R., and Reid, J.D., *Midwest Guardrail System W-Beam-to-Thrie-Beam Transition*, Journal of the Transportation Research Board, Transportation Research Record No. 2025, Washington, D.C., 2007, pp. 45-50.
13. Stolle, C.S., Polivka, K.A., Reid, J.D., Faller, R.K., Sicking, D.L., Bielenberg, R.W., and Rohde, J.R., *Evaluation of Critical Flare Rates for the Midwest Guardrail System (MGS)*, Final Report to the Midwest States Regional Pooled Fund Program, MwRSF Research Report No. TRP-03-191-08, Midwest Roadside Safety Facility, University of Nebraska-Lincoln, Lincoln, Nebraska, July 2008.
14. Ray, M.H., Plaxico, C.A., and Anghileri, M., *Procedures for the Verification and Validation of Computer Simulations Used for Roadside Safety Applications*, NCHRP Web-Only Report No. 179, NCHRP Project No. 22-24, March 2010.
15. Asadollahi Pajouh, M., Bielenberg, R.W., Schmidt, J., Lingenfelter, J.L., Faller, R.K., and Reid, J.D., *Placement of Breakaway Light Poles Located Directly behind Barrier*, Report to the Illinois Tollway, Transportation Report No. TRP-03-361-17, Midwest Roadside Safety Facility, University of Nebraska-Lincoln, Lincoln, Nebraska, 2017.
16. Hallquist, J.O. *LS-DYNA Keyword User's Manual*. Livermore, CA: Livermore Software Technology Corporation. 2007.
17. Zhu, L., Faller, R.K., Reid, J.D., Sicking, D.L., Bielenberg, R.W., Lechtenberg, K.A., and Benner, C., *Performance Limits for 152-mm (6-in.) High Curbs Placed in Advance of the MGS Using MASH-08 Vehicles, Part I: Vehicle Curb Testing and LS-DYNA Analysis*, Final Report to the Midwest States Regional Pooled Fund Program, MwRSF Research Report No. TRP-03-205-09, Midwest Roadside Safety Facility, Nebraska Transportation Center, University of Nebraska-Lincoln, Lincoln, Nebraska, May 2009.
18. Thiele, J.C., Lechtenberg, K.A., Reid, J.D., Faller, R.K., Sicking, D.L., and Bielenberg, R.W., *Performance Limits for 152-mm (6-in.) High Curbs Placed in Advance of the MGS Using MASH-08 Vehicles, Part II: Full-Scale Crash Testing*, Final Report to the Midwest States Regional Pooled Fund Program, MwRSF Research Report No. TRP-03-221-09, Midwest Roadside Safety Facility, Nebraska Transportation Center, University of Nebraska-Lincoln, Lincoln, Nebraska, October 2009.
19. Faller, R.K., Polivka, K.A., Kuipers, B.D., Bielenberg, R.W., Reid, J.D., Rohde, J.R., and Sicking, D.L., *Midwest Guardrail System for Standard and Special Applications*, Journal of the Transportation Research Board, Transportation Research Record No. 1890, Washington, D.C., January 2004, pp. 19-33.
20. *A Policy on Geometric Design of Highways and Streets*, American Association of State Highway Transportation Officials, 6th Edition, Washington, D.C., 201.
21. Ross, H.E., Sicking, D.L., Zimmer, R.A., and Michie, J.D., *Recommended Procedures for the Safety Performance Evaluation of Highway Features*, National Cooperative Highway Research Program (NCHRP) Report 350, Transportation Research Board, Washington, D.C., 1993.
22. Asadollahi Pajouh, M., Bielenberg W.R., Schmidt J., Reid, J.D., and Faller, R.K. "Safe Placement of Luminaire Poles behind Midwest Guardrail System under MASH TL-3." Draft Report to Illinois Tollway, MwRSF Research Report, UNL.
23. Dobrovolny, C.S., White, K.M., and Bligh, R.P., *Synthesis of System/Vehicle Interaction Similarities/Dissimilarities with 12-Inch vs 8-Inch Blockouts with 31-Inch Mounting Height, Mid-Span Splices*, Research Program Report No. 601621, Texas Transportation Institute, Texas A&M University, College Station, Texas, July 2014.

Development and Validation of the Surrogate Vehicle Used in Testing Protective Devices at Low Speed

DEAN C. ALBERSON
MICHAEL S. BRACKIN
WANDA L. MENGES

Texas A&M Transportation Institute Proving Ground

ASTM F3016-14 *Standard Test Method for Surrogate Testing of Vehicle Impact Protective Devices at Low Speeds* was developed to assess the effectiveness of low speed bollards and streetfurniture when impacted by an errant vehicle. Some data indicates that up to 500 people are killed each year in storefronts, sidewalk cafes and general businesses where vehicles and pedestrians are comingled. The leading cause of the accidents is pedal error and occurs predominantly with older drivers. Prior to the development of this standard, business owners would sometimes employ pipes or other types of devices to provide separation and “protection” of pedestrians. Often these devices were woefully inadequate and demonstrated performance was needed. TTI, working in conjunction with ASTM and other concerned individuals developed F3016 and also developed the prototype surrogate vehicle used in this standard. TTI proposes to show the development and validation of the surrogate vehicle used in F3016.

INTRODUCTION

In an effort to reduce the number of vehicle-into-building impacts, city and county governments have begun to create legislation requiring the use of protective devices, such as bollards, that are capable of arresting an impacting vehicle. In an effort to establish uniform testing guidelines, a standard test method was developed to quantify the dynamic performance of a protective device. This standard test method was developed by ASTM International (ASTM) under *ATSM F3016-14, Standard Test Method for Surrogate Testing of Vehicle Impact Protective Devices at Low Speeds (1)*.

The tests reported herein were performed to develop and validate a full-scale surrogate vehicle for use in the testing of low-speed protective devices (2, 3). A full-scale crash test of Dodge ½ ton Quad Cab Pickup into and instrumented bollard was used as a baseline test. Subsequently a number of tests were done on the proposed surrogate test vehicle with a staged honeycomb nose. This paper discusses the findings of these projects and how the frontal force-deformation response of the new surrogate test vehicle accurately represents *ASTM F3016-14* criteria.

TEST ARTICLE DESIGN AND CONSTRUCTION

One full-scale crash test with a Dodge 1/2 Ton Quad Cab Pickup and four full-scale crash tests with a surrogate test vehicle were performed. All tests involved the new vehicles impacting a

simulated fixed bollard affixed to an instrumented pier. The support for the simulated fixed bollard consisted of a 36-inch diameter instrumented semi-rigid pier supported by a braced column load frame and foundation system. The frame column was diagonally braced to a shorter vertical support anchored into the foundation. Two instrumented transducer links (load cells) were connected to the pier and supported by the load frame. These load cells were used to measure the force of the impacting vehicle. These load cells were independently attached to the support column. An attachment was used to simulate an impact with a semi-rigid 10-inch nominal diameter bollard, as shown in Figure 1. The bollard attachment bolted directly to and transferred the load to the instrumented rigid pier. The bollard attachment fit to the instrumented pier via a curved plate. The plate was 1 inch thick, and the inner face was curved with an 18-inch radius. The straight line distance between the inner edges at the ends of the plate was 18 inches, and the plate was 72 inches tall. A 0.875-inch diameter hole was located at each of the four corners of the plate, and was drilled so that the centers of the holes were 2 inches from either edge.

TEST VEHICLES

A 2005 Dodge Ram 1500 pickup truck was used for the first full-scale crash test. Test inertia weight of the vehicle was 5017 lb, and its gross static weight was 5017 lb. The height to the lower edge of the vehicle front bumper was 13.5 inches, and the height to the upper edge of the front bumper was 26.0 inches. The height to the center of gravity was 28.12 inches. The test vehicle had been used in a previous crash test with minimal structural damage, and is shown in Figure 2. 11



FIGURE 1 Instrumented pier and simulated bollard.



FIGURE 2 Dodge 1/2 ton quad cab pickup.

The surrogate test vehicle prescribed by *ASTM F3016-14* is modeled after a 2270P pickup truck as prescribed in the American Association of State Highway and Transportation Officials (AASHTO) *Manual for Assessing Safety and Hardware (MASH)* (4). This vehicle represents the 94th percentile in terms of vehicle weight for all passenger vehicles sold in 2002 and has similar weights and center of gravity as large sport utility vehicles (SUV) and is shown in Figure 3 below.

MEASURED LOAD

Load cells were used to measure the force applied to the simulated bollard by the pickup. Figure 4 shows the raw force measured by each load cell. Using these data and engineering statics, a resultant force applied to the simulated bollard can be calculated. Figure 5 shows this resultant force.



FIGURE 3 Surrogate test vehicle.

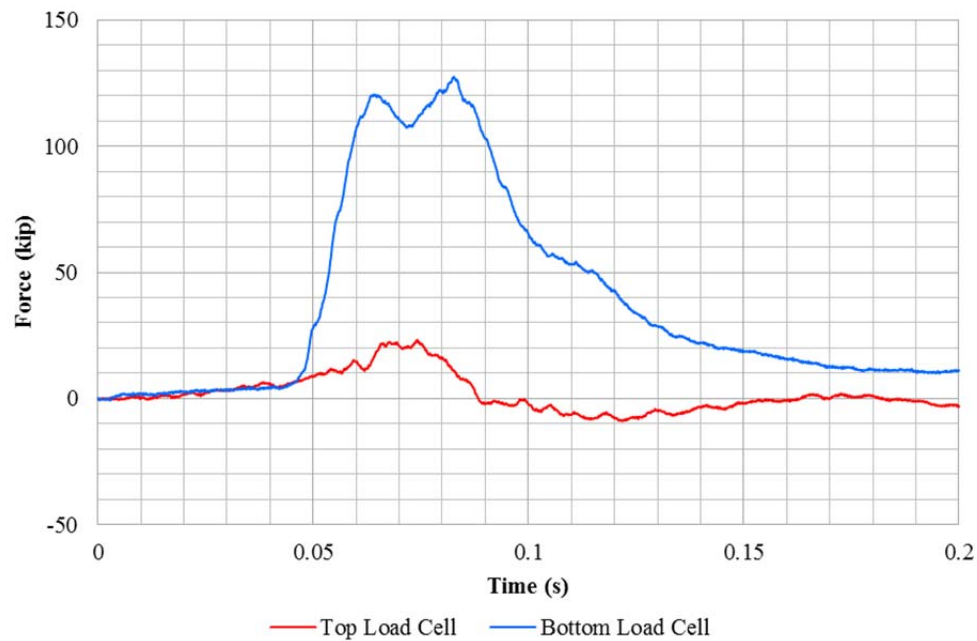


FIGURE 4 Force measured by top and bottom load cells during test no. 194001-USD1.

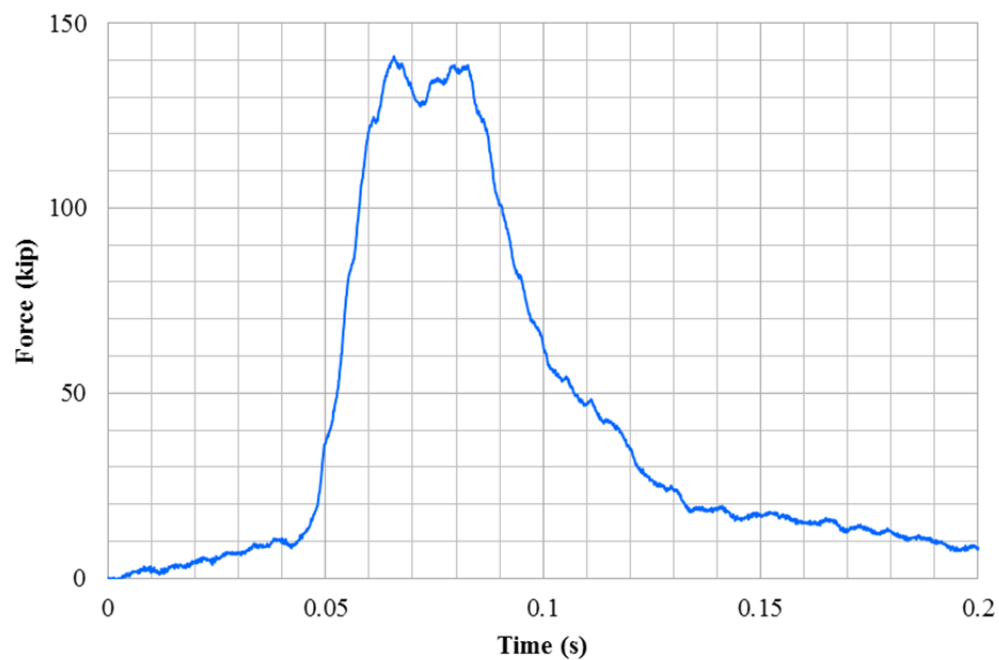


FIGURE 5 Resultant force measured from load cells during test no. 194001-USD1.

Aluminum honeycomb material has been widely accepted for use in roadside safety testing since the early 1980s and is a readily available material. Table 1 is a chart of commonly used material specifications for pendulum testing performed under National Cooperative

Highway Research Program (NCHRP) Report 350 “*Recommended Procedures for the Safety Performance Evaluation of Highway Features*”(5).

From the material specifications shown in Table 1, modules can be sized to achieve the desired force characteristics. This analysis is shown in Table 5. A linear force can be achieved, in lieu of a step-wise force, by cutting the honeycomb’s sides at an angle (measured from vertical) rather than square. Modules with angled sides are shown below in red. Dimensions such as the height, width, and cut angle were then rounded to a reasonable number that may be cut on typical cutting equipment. Figure 6 shows these data compared to the idealized surrogate test vehicle stiffness presented in *ASTM F3016 -14* for a 30 mph impact.

The force-deformation response or stiffness of the surrogate test vehicle was developed from the previous full-scale crash with the 2005 ½ ton Dodge Quad Cab pickup. *ASTM F3016-14* does not limit any test facility to just one method for achieving the required stiffness. Rather, *ASTM F3016-14* states:

TABLE 1 Material Specifications for Pendulum Testing under NCHRP Report 350

Color	Crush (lb/inch ²)	Specs	Thickness (inch)
Red	25	3/8-5052-.007N-1.0	2.25
Green	130	3/16-5052-.001N-3.1	3.25
Orange	230	1/4-5052-.002N-4.3	3.25
Yellow	390	3/16-5052-.002N-5.7	3.25

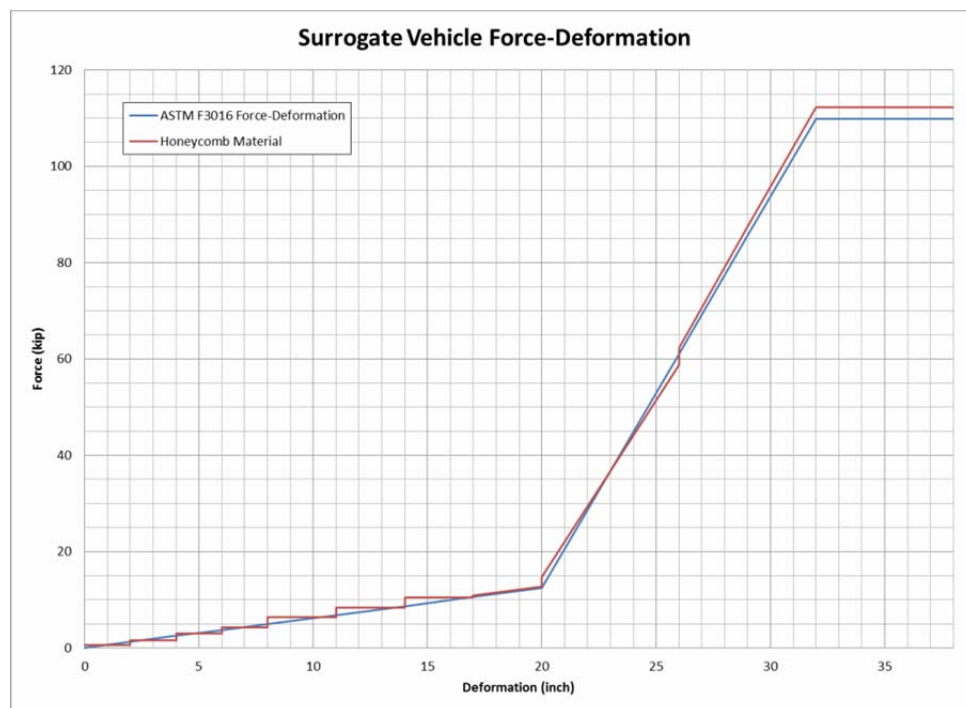


FIGURE 6 Idealized vehicle stiffness using aluminum honeycomb.

“A method shall be used to replicate the measured MASH 2270P test vehicle crush as the impactor nose displaces. The required stiffness rate is provided in Table 3. Common methods to replicate vehicle crush, while not exclusive, are the use of crushable aluminum honeycomb or linear-elastic springs. The impactor nose shall have zero stored energy before impact and no elastic rebound after the impact.”

The required stiffness of the surrogate test vehicle, as prescribed in *ASTM F3016-14*, is shown below in Table 2.

TEST DESIGNATION AND ACTUAL TEST CONDITIONS

According to *ASTM F3016-14*, protective devices can be rated according to one of three impact speed ratings when tested with a surrogate test vehicle, as shown in Table 1. The test conditions establish a range for penetration performance ratings, which may be used to identify appropriate penetration performance for specific needs of the end user. Actual vehicle weight and speed must be within a permissible range to receive the specific impact condition designation. The impact speed ratings are shown in the last column of Table 3, as taken from *ASTM F3016-14*. 24

The overall dimensions and weight of the surrogate test vehicle and fabrication drawings for the surrogate test vehicle and honeycomb modules used for the tests are available with ASTM F3016-14 document. Table 4 lists the module size and force characteristics.

TABLE 2 Impactor Nose Stiffness

	<19 inches	19-31 inches	>31 inches
Rate	620 lb/inch	8125 lb/inch	110,000 lb (constant)

TABLE 3 Impact Speed Ratings According to *ASTM F3016-14*

Surrogate Test Vehicle Weight, lb	Nominal Minimum Test Velocity mi/h	Permissible Speed Range, mi/h	Impact Speed Rating
5000 ±110	10 20 30	9.0-18.9 19.0-27.4 27.5-32.5	S10 S20 S30

TABLE 4 Module Size/Force Characteristics

Module	Displacement (inch)	Force (lb)	Crush (lb/inch ²)	Areqd (inch ²)	AreqdAvg (inch ²)	Amodule (inch ²)	Height (inch)	Width (inch)	Cut Angle from Vertical (degrees)	
1	0	0	25	0.0	24.8	25	5	5		
	2	1240	25	49.6		25	5	5		
2	2	1240	25	49.6	74.4	64	8	8		
	4	2480	25	99.2		64	8	8		
3	4	2480	25	99.2	124.0	121	11	11		
	6	3720	25	148.8		121	11	11		
4	6	3720	25	148.8	17.6	169	13	13		
	8	4960	25	198.4		169	13	13		
5	8	4960	130	38.2	45.3	49	7	7		
	11	6820	130	52.5		49	7	7		
6	11	6820	130	52.5	59.6	64	8	8		
	14	8680	130	66.8		64	8	8		
7	14	8680	130	66.8	73.9	81	9	9		
	17	10540	130	81.1		81	9	9		
8	17	10540	130	81.1		84	14	6	9.46	10
	20	12400	130	95.4		98	14	7		
9	20	12400	230	53.9		64	16	4	45	45
	23	36775	230	159.9		160	16	10		
10	23	36775	230	159.9		160	16	10	45	45
	26	61150	230	265.9		256	16	16		
11	26	61150	390	156.8		160	16	10	33.69	34
	29	85525	390	281.8		224	16	14		
12	29	85525	390	219.3		224	16	14	33.69	34
	32	109900	390	281.8		288	16	18		
13	32	109900	390	281.8		288	16	18		
	35	109900	390	281.8		288	16	18		
14	35	109900	390	281.8		288	16	18		
	38	109900	390	281.8		288	16	18		

SURROGATE TEST VEHICLE VALIDATION TEST NO. 690900-BV3 (ASTM F3016-14 Test S30)

Brief Test Description

The surrogate test vehicle, traveling at an impact speed of 30.1 mi/h, contacted the simulated bollard with the centerline of the surrogate test vehicle nose aligned with the centerline of the simulated bollard. The surrogate test vehicle stopped forward motion at 0.108 s. The surrogate test vehicle then began to yaw counterclockwise, the bumper separated from the surrogate test vehicle, and the honeycomb fell out of the nose.

Surrogate Test Vehicle Damage

Maximum dynamic crush of the surrogate test vehicle nose was 45.6 inches. Maximum residual crush could not be measured as the surrogate test vehicle nose and honeycomb separated from the surrogate test vehicle. Figure 7 shows the surrogate test vehicle nose before and after the test. The connection between the bumper and the two pipes was ruptured during the test.

Occupant Risk Values

Data from the accelerometer, located at the surrogate test vehicle center of gravity, were digitized for evaluation of occupant risk. In the longitudinal direction, the OIV was 44.3 ft/s at 0.123 s, the highest 0.010-s occupant RDA was 1.7 g from 0.148 to 0.158 s, and the maximum 0.050-s average acceleration was -22.5 g between 0.057 and 0.107 s. In the lateral direction, the OIV was 6.2 ft/s at 0.123 s, the highest 0.010-s occupant RDA was 3.2 g from 0.200 to 0.210 s, and the maximum 0.050-s average was -4.3 g between 0.066 and 0.116 s. THIV was 49.4 km/h or 13.7 m/s at 0.123 s; PHD was 3.2 g between 0.200 and 0.210 s; and ASI was 2.03 between 0.082 and 0.132 s.



FIGURE 7 Surrogate test vehicle before and after test no. 690900-BV3:
(a) before and (b) after.

Figure 8 shows the surrogate test vehicle's acceleration during Test No. 690900-BV3. Figure 9 shows the measured stiffness curve for the surrogate test vehicle compared to the required stiffness curve set forth in *ASTM F3016-14*. Figure 10 provides a summary of pertinent data from the test.

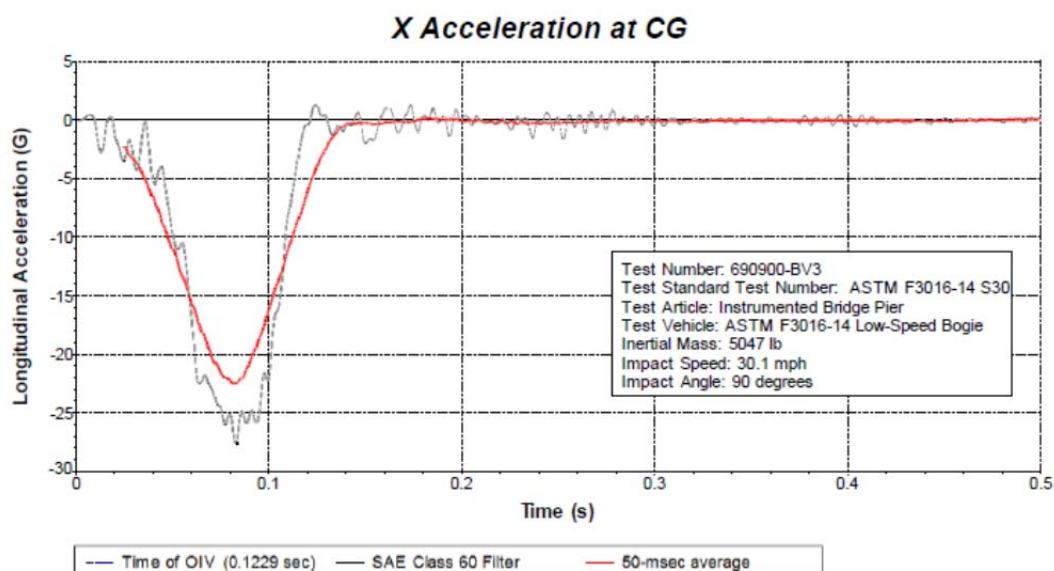


FIGURE 8 Longitudinal acceleration trace for *ASTM F3016-14* S30 test (690900-BV3).

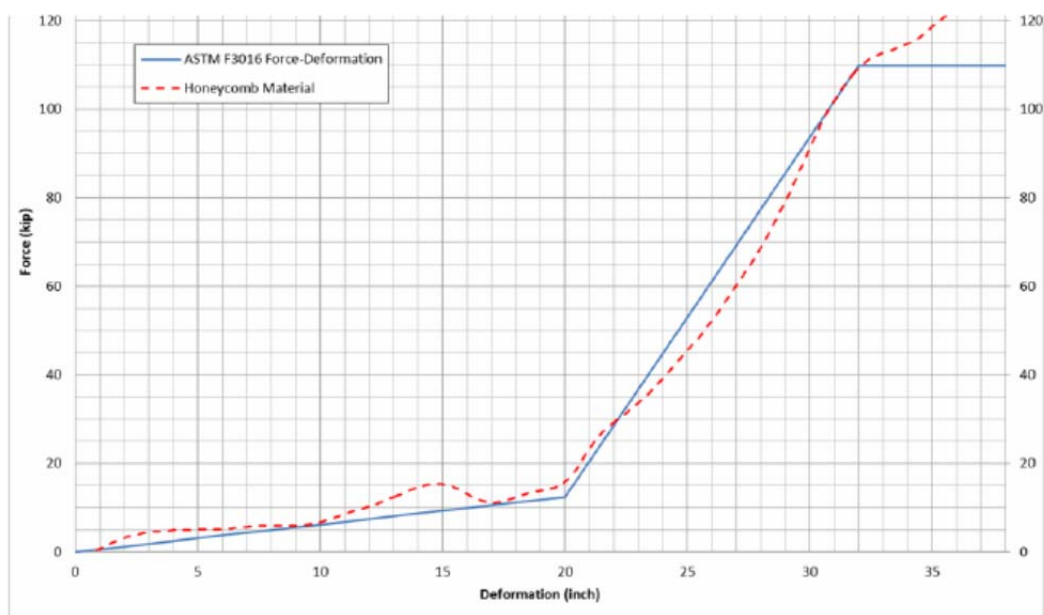


FIGURE 9 Comparison of required stiffness of surrogate vehicle to measured stiffness for *ASTM F3016-14* test S30 (690900-BV3).

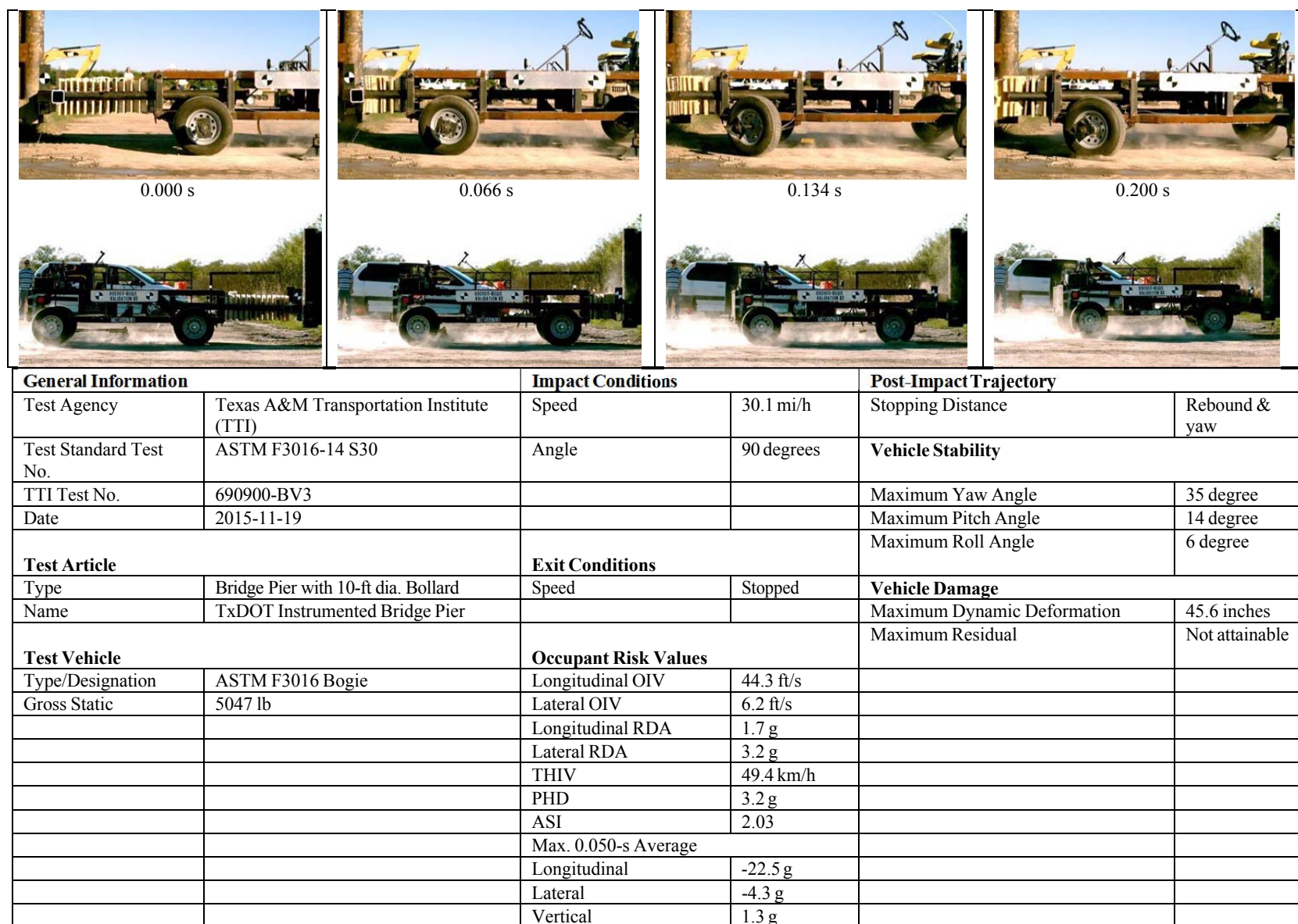


FIGURE 10 Summary of results for *ASTM F3016-14* test S30 on the instrumented pier.

SUMMARY AND CONCLUSIONS

The original test with the ½ Ton Quad Cab Pickup provided the crush characteristics subsequently used to develop the prototype honeycomb nose used in the surrogate vehicle testing. The subsequent full-scale crash test with the surrogate vehicle and honeycomb showed good correlation to the tested pickup crush and force characteristics. This surrogate vehicle and honeycomb configuration has been adopted in the current ASTM F3016 testing standard.

The final configuration of honeycomb modules is provided in Table 5 and Figure 11 below.

TABLE 5 Specifications for Honeycomb Modules

#	SPECIFICATION	CRUSH	HEIGHT	WIDTH	THICKNESS
1	1.0 3/8 .007N 5052 MIL-C-7438G	25 lb/inch ²	5 inch	5 inch	2 inch
2	1.0 3/8 .007N 5052 MIL-C-7438G	25 lb/inch ²	8 inch	8 inch	2 inch
3	1.0 3/8 .007N 5052 MIL-C-7438G	25 lb/inch ²	11 inch	11 inch	2 inch
4	1.0 3/8 .007N 5052 MIL-C-7438G	25 lb/inch ²	13 inch	13 inch	2 inch
5	3.1 3/16 .001N 5052 MIL-C-7438G	130 lb/inch ²	7 inch	7 inch	3 inch
6	3.1 3/16 .001N 5052 MIL-C-7438G	130 lb/inch ²	8 inch	8 inch	3 inch
7	3.1 3/16 .001N 5052 MIL-C-7438G	130 lb/inch ²	9 inch	9 inch	3 inch
8	3.1 3/16 .001N 5052 MIL-C-7438G	130 lb/inch ²	14 inch	See Figure 17.	3 inch
9	4.3 1/4 .002N 5052 MIL-C-7438G	230 lb/inch ²	16 inch	See Figure 17.	3 inch
10	4.3 1/4 .002N 5052 MIL-C-7438G	230 lb/inch ²	16 inch	See Figure 17.	3 inch
11	5.7 3/16 .002N 5052 MIL-C-7438G	390 lb/inch ²	16 inch	See Figure 17.	3 inch
12	5.7 3/16 .002N 5052 MIL-C-7438G	390 lb/inch ²	16 inch	See Figure 17.	3 inch
13	5.7 3/16 .002N 5052 MIL-C-7438G	390 lb/inch ²	16 inch	18 inch	3 inch
14	5.7 3/16 .002N 5052 MIL-C-7438G	390 lb/inch ²	16 inch	18 inch	3 inch
15	5.7 3/16 .002N 5052 MIL-C-7438G	390 lb/inch ²	16 inch	18 inch	3 inch

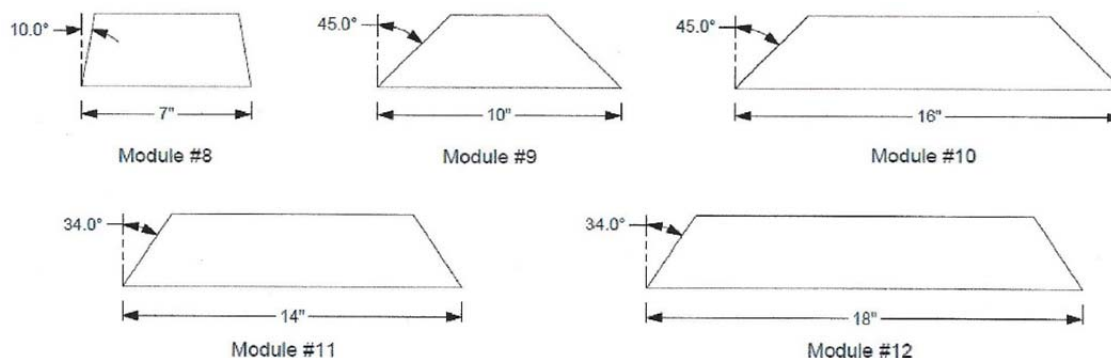


FIGURE 11 Geometry for honeycomb modules 8 through 12.

REFERENCES

1. ASTM. Standard Test Method for Surrogate Testing of Vehicle Impact Protective Devices at Low Speeds,” ASTM Designation: F3016-14, American Standards for Testing Materials International, West Conshohocken, PA, August 2014.
2. M.S. Brackin, W.L. Menges, *Technical Memorandum 194001-USD1*, Texas A&M Transportation Institute, College Station, Texas, 2014.
3. M.S. Brackin, W.L. Menges, *Technical Memorandum 690900-BV1-4*, “ASTM F3016-14 Bogie Validation”, Texas A&M Transportation Institute, College Station, Texas, 2016.
4. AASHTO. *Manual for Assessing Roadside Safety Hardware*. American Association of State Highway and Transportation Officials, Washington, D.C., 2009.
5. H.E. Ross, Jr., D.L. Sicking, R.A. Zimmer, and J.D. Michie, *Recommended Procedures for the Safety Performance Evaluation of Highway Features*, National Cooperative Highway Research Program Report 350, Transportation Research Board, National Research Council, Washington, D.C., 1993.

Correlation Between Roadside Safety Hardware and Vehicle Safety Standards Evaluation Criteria

N. SCHULZ

C. SILVESTRI DOBROVOLNY

D. ARRINGTON

H. PRODDUTURU

J. RUPP

J. HU

Texas A&M Transportation Institute

The Manual for Assessing Safety Hardware (MASH) defines crash tests to assess the impact performance of highway safety features in frontal and oblique impact events. The evaluation criteria defined by MASH depends on the structural adequacy, occupant injury and post-impact vehicle trajectory. Within MASH, the risk of injury to the occupant is assessed based on a “flail-space” model that estimates the average deceleration that an unrestrained occupant would experience when contacting the vehicle interior in a MASH crash test and uses the parameter as a surrogate for injury risk. However, this model has become a limitation with the increase in use of seatbelts and airbags in vehicles today. Therefore, there is potential for increasing the maximum limits dictated in MASH for occupant risk evaluation.

A frontal full-scale vehicle impact was performed with inclusion of an instrumented anthropomorphic test device (ATD). The scope of this study was to investigate the performance of the Flail Space Model in a full scale crash test compared to the instrumented ATD recorded forces which can more accurately predict the occupant response during a collision event.

Results obtained through this research will be considered for better correlation between vehicle accelerations and occupant injury. This becomes extremely important for designing and evaluating barrier systems that must fit within geometrical site constraints, which do not provide adequate length to redirect test vehicles according to MASH conservative evaluation criteria.

Development of a Motorcycle FE Model for Simulating Impacts into Roadside Safety Barriers

MARIO MONGIARDINI

BILL WALTON

RAPHAEL H. GRZEBIETA

Transport and Road Safety—University of New South Wales

MATTHEW MCKAY

Murrumbidgee Irrigation

CHRIS MENICTAS

School of Mechanical and Manufacturing Engineering—University of New South Wales

ALEXANDER BERG

PETER RÜCKER

DEKRA Automobil GmbH, Accident Research & Crash Test Center

Recent studies have identified roadside safety barriers as a cause of severe injuries and fatalities for motorcyclists. Roadside safety barrier have traditionally been designed with limited consideration for motorcyclist safety since the primary focus was on the safety of occupants of enclosed vehicles. Computer simulations of full-scale crashes between motorcyclists and road barriers would provide valuable support to improve the limited knowledge of the interaction between motorcyclists and barriers during a crash as well as assess any proposed design countermeasure to reduce serious injuries and fatalities.

This study aimed to develop a Finite Element (FE) model of a sport-touring motorcycle that may be used to investigate in detail the characteristics of upright impacts between motorcyclists and different types of roadside safety barriers. Verification and validation was performed on the critical components of the developed motorcycle model, such as the steering system and the front/rear suspensions. Validation against a full-scale crash test involving a concrete safety barrier was also performed to assess the overall response of the modeled motorcycle in combination with an ATD model during a crash. The promising results obtained using the developed motorcycle FE model provided an initial level of confidence for using it in future applications aimed at investigating crash scenarios involving roadside safety barriers and motorcycles.

INTRODUCTION

Motorcycle crashes into roadside safety barriers

In Australia, motorcycles account for 4.4% of total vehicle registrations, yet approximately 17% of all motor vehicle fatalities involve motorcyclists. Such statistics, which are similar for most other countries, clearly indicate the higher risks to which motorcyclists are subjected compared to other road users. Recent studies in both Australia and USA have identified roadside safety barriers as a possible cause of severe injuries and fatalities for motorcyclists (1-4).

Roadside safety barriers can effectively protect motorists from impacting fixed objects and various hazards located along the side of the road and are designed to reduce the potential for serious injuries when impacted by an errant vehicle (5). However, their design has traditionally had limited consideration for motorcyclist safety since primary focus was on the safety of vehicle occupants, which are by far the category with the largest representation of all the road users seriously injured and killed. Nonetheless, based on the safe-system approach for a safer road transport system, which has been adopted in many countries worldwide, impacts into roadside safety barriers should become a forgiving event for all road users, including motorcyclists. Further, recent consideration for motorcyclists safety in the design of roadside safety hardware has started to grow due to the concerning increasing percentage of motorcyclist fatalities relative to the total number of road deaths (6,7).

Motorcyclist crashes into roadside safety barriers can be classified in two main typologies, depending on the rider posture at impact: (a) motorcyclist riding into the barrier at an upright riding position or (b) rider sliding into the barrier after being already separated from the motorcycle. Likely, different injury mechanisms may be associated with each of these two rider postures. Previous analyses indicated that either of the two mentioned crash postures appear to be equally distributed in real-world crashes between motorcyclists and roadside safety barriers in Australia and New Zealand as well as in Europe (2,8). However, it is predicted that the effectiveness of recently introduced active systems for improving motorcycle stability during critical maneuvers, such as the Motorcycle Active Braking System (MABS), would likely shift the majority of those motorcycle crashes that are still unavoidable to occur in an upright riding position once these new technologies would reach full market penetration (9,10). Thus, it is likely that also the majority of motorcyclist crashes into roadside safety barriers in the future will mainly occur while the rider is straddling the motorcycle in an upright riding position.

So far, standard testing procedures for assessing the safety performance of roadside safety barriers in a crash involving a motorcyclist have been developed exclusively in Europe. The majority of these standard testing procedures, which are either European or national standards, have been focused solely on the case of a rider sliding on the road after it has already been separated from the motorcycle (11-13). The only exception is a crash test protocol developed by the German Federal Highway Research Institute, BAST, which considers an impact of an upright motorcyclist into the tested barrier (14,15). Therefore, only a limited number of non-standardized full-scale crash tests have been performed so far to investigate the performance of a motorcyclist crashing into various types of roadside safety barriers in an upright riding posture (8,10).

Computer simulations of full-scale crashes would provide a valuable support to improving the limited knowledge regarding the interaction between motorcyclists and roadside safety barriers, especially for the case of an upright crash posture. Further, simulations may also support engineers in assessing any future proposed design countermeasure to reduce the injury risks associated with motorcyclist crashes into barriers. Most of the existing numerical models of motorcycles have been developed to assess the rider kinematics and dynamics during crashes into another vehicle (16,17). Such scenario does not require specific modeling of the motorcycle kinematics, especially in terms of suspension behavior. Limited modeling efforts have been performed to specifically simulate impacts of motorcyclists into road safety barriers in an upright riding position. As an example, simplified multibody models of a motorcycle and rider were previously used to perform a basic analysis of a rider head-on impact into a deformable guardrail (18) or angled impacts into wire-rope and concrete safety barriers (8). Further, a Finite Element

(FE) approach would be preferred to model the motorcyclist deformable body and thus simulate more realistically any loads applied to the rider during an impact into a barrier. The only motorcycle FE model that was developed to assess the interaction between motorcyclists and road safety barriers was based on a simplified moped-style motorcycle. That model was used as a bullet vehicle (without a rider model) in simulations aimed to perform a preliminary assessment of a novel design of a motorcycle-friendly barrier (19).

Objective and methods

This study aimed to develop a FE model of a motorcycle that may be used to investigate in detail the impact characteristics between motorcyclists and different types of roadside safety barriers when impacting in an upright riding posture. Since a previous study identified that touring motorcycle riders have a higher tendency to collide with barriers in an upright posture (1), a sport-touring motorcycle was selected as the most appropriate two-wheel vehicle to be modeled.

Initially, the geometry of each relevant component of a sport-touring motorcycle was digitally acquired using a three-dimensional scanner. The motorcycle FE model was then developed and the proper functionality of critical modeled components such as the steering system and the front/rear suspensions was verified. Finally, the model was validated against experimental tests with the motorcycle traversing various sloped obstacles as well as against a previously performed full-scale crash test into a concrete safety barrier.

MOTORCYCLE FE MODEL

Model development

The model was developed for use with the non-linear FE solver LS-DYNA, which is highly suitable to simulate impact events (20). It replicated in detail the geometry and mass of a 2008 Suzuki GSX-650F motorcycle, which is well representative of modern sport-touring motorcycles with the rider sitting in an upright posture. Both the actual motorcycle and the developed FE model are shown in Figure 1.

The major motorcycle structural components as well as any other non-structural parts that may interact with a road safety barrier and the rider during a crash and, thus potentially affect their kinematics and dynamics, were explicitly modeled. The geometry of the selected components of the actual motorcycle was initially digitized using a 3D laser scanner and the obtained surfaces were then used as a basis to create the FE mesh. Most components were modeled using shell elements with the exception of a few bulky parts, such as the engine, the radiator, and the brake calipers, which were modeled using solid elements. The motorcycle truss frame served as the main structure, with all the other modeled components connected to it using rigid links of various types, depending on the specific degrees of freedom of the actual connection.

Both the front and rear suspensions were modeled in detail. The paired upper and lower forks of the front suspensions were explicitly modeled using shell elements. A cylindrical-type kinematical joint was defined between each pair of upper and lower forks to allow the suspension to either compress or extend. The upper and lower forks were then connected by separate discrete spring and damper elements, which modeled the coil spring and the damper of



FIGURE 1 Suzuki GSX-650F motorcycle – actual motorcycle and FE model.

the actual front suspension, respectively. Each of the two triple clamps that connect the two upper forks in the actual front suspension was approximated as a rigid constraint between the modeled upper forks.

The swingarm of the rear suspension system was explicitly modeled using shell elements. A kinematical joint was used to model the actual hinge between the swingarm and the frame. The rear suspension cushion-lever-rod assembly was then modeled using two dummy elements connected through a series of rigid kinematical joints that replicated the kinematics of the actual assembly, as shown in Figure 2.

The end of the cushion lever that is connected to the shock absorber was modeled as a rigid element, A, which was hinged relatively to the frame at a position equivalent to the pivot location in the actual cushion lever. The ends of the two parallel cushion rods that are connected to the swingarm were modeled using another rigid element, B, which was hinged relatively to element A at a location corresponding to the rods' actual hinge to the cushion lever. Finally, the center of the element B was hinged relatively to the swingarm. The spring-shock-absorber assembly of the actual rear suspension was modeled using a parallel combination of discrete spring and damper elements, which were defined between element A and an appropriate location of the frame.

The stiffness of the coil springs that are located inside each fork of the front suspension and in the rear suspension assembly was measured through compression tests conducted by a specialized laboratory. The force-velocity characteristic curve of the damper of the rear suspension was measured as well. Unfortunately, the damping curve for the front-suspension

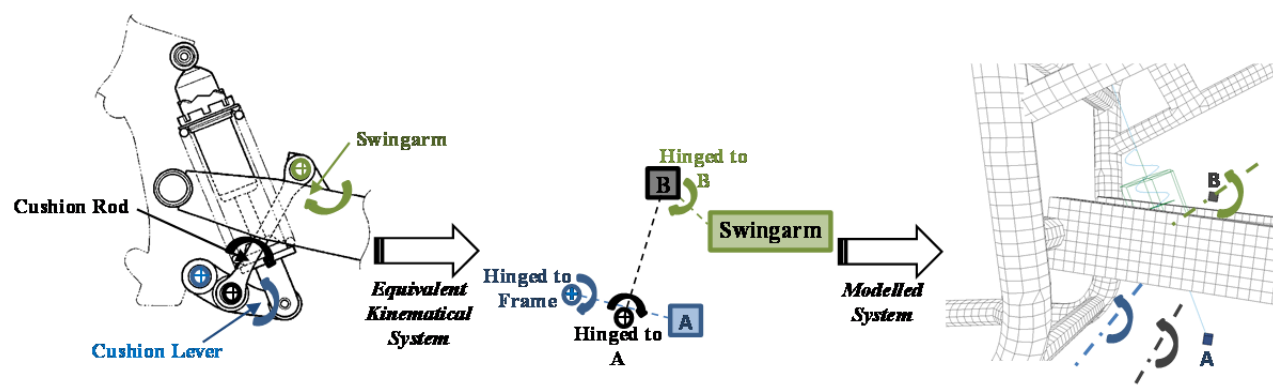


FIGURE 2 Cushion-lever-rod assembly: actual system (Left), equivalent kinematical system (Center), FE modeled system (Right).

forks could not be measured due to a dimensional limitation of the testing machine. The geometry of the developed model was based on the standing motorcycle when balanced under gravity. Thus, to account for the weight of the motorcycle, appropriate pre-compression values were assigned to the discrete spring elements used to model the front and rear suspensions. For both front and rear suspensions, two additional discrete elements acting as a compression and an extension stopper, respectively, were also modeled.

Both the rim and the tire of the front and rear wheels were modeled using shell elements, whereas solid elements were used for the wheel hubs. For each tire, an LS-DYNA airbag definition was used to assign the internal pressure within the volume enclosed by the tire and the rim circumferential surface. Finally, all the other components of the motorcycle that could interact with the rider or the road safety barrier during a crash such as front and rear brake discs and calipers, fairings, radiator, handlebar, fuel tank, seat, engine case, foot pegs, and exhaust were explicitly modeled as well.

The location of the actual motorcycle center of gravity along the longitudinal and vertical directions was experimentally measured before the motorcycle was disassembled. In order to match the location of the motorcycle center of gravity, lumped-mass elements were added to the motorcycle model to compensate for any other non-relevant components that were not explicitly modeled as well as for the various fluids.

Model verification

Front and rear suspensions

An initial verification of the proper kinematics of both front and rear suspensions was carried out. To facilitate the verification of both suspension systems up to their compression limit, their stiffness and damping were zeroed while the motorcycle model was left free to settle under the effect of gravity onto a rigid surface. Also, to prevent the motorcycle model from tilting on either side, its frame was constrained in the vertical plane. The simulated displacement of both the front and rear suspensions is shown in Figure 3(a). Both suspensions replicated the expected kinematics while the motorcycle settled under gravity and eventually reached a stop at the defined limit displacement equal to 130 mm (5.1 in.) and 38 mm (1.5 in.) for the front and the rear suspensions, respectively.

The overall dynamic response of the front and rear suspensions was also verified by simulating the response of the motorcycle model when riding over a 100-mm high bump at 20 km/h. A 75-kg (165-lb) lumped mass was added to the motorcycle center of gravity to model the mass of the rider. Both modeled suspensions proved to be capable of simulating the typical dynamic behavior expected when traversing a bump, as shown in Figure 3(b). The front and rear suspensions compressed allowing the respective tire to maintain constant contact with the bump and the bike to remain stable while traversing the bump.

Steering

The proper kinematics of the steering system was verified for rotations in both directions over the maximum steering range. The motorcycle frame was fully constrained and a steering torque was induced by applying a 50-N (11-lbf) force at the most forward location of the front-wheel rim. A plot of the wheel rotation along the steering axis for the case of a right turn is shown in

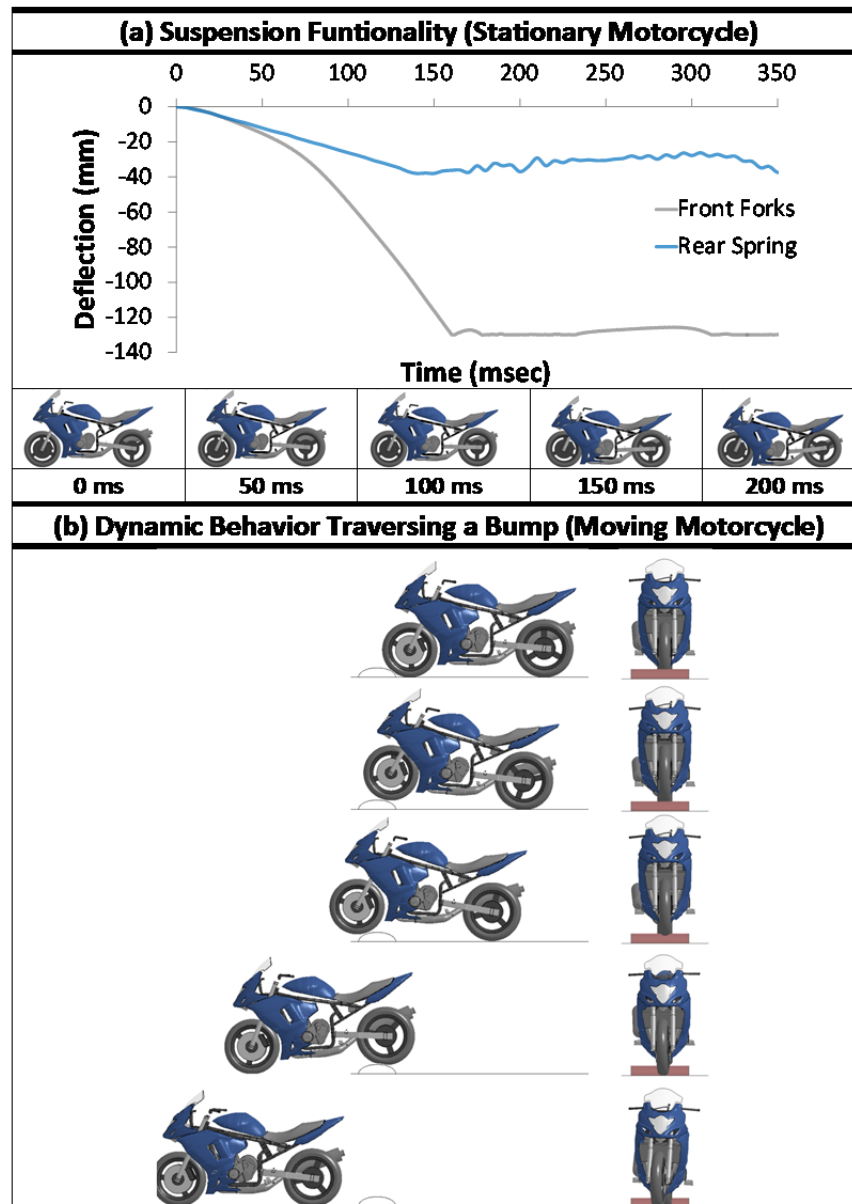


FIGURE 3 Suspension verification – behavior with stationary and moving motorcycle.

Figure 4(a). The front wheel steered properly and came to a stop at the desired maximum angle of 32 degrees.

The functionality of the steering to turn the motorcycle model when it is travelling was also verified. In this case, a gradual rotation of the steering was imposed while the motorcycle model was travelling along a straight trajectory at an initial speed of 30 km/h (18.6 mph) on a flat rigid surface. Upon application of a steering input, the motorcycle model, which was initially leaning on its left side by 30 degrees, gradually transitioned its trajectory along a curve path and started to lean towards the external side of the curve due to the centrifugal force, as shown in the sequence in Figure 4(b). The motorcycle kept leaning to the external side of the curve, until its right side eventually impacted the ground surface at completion of a quarter turn.

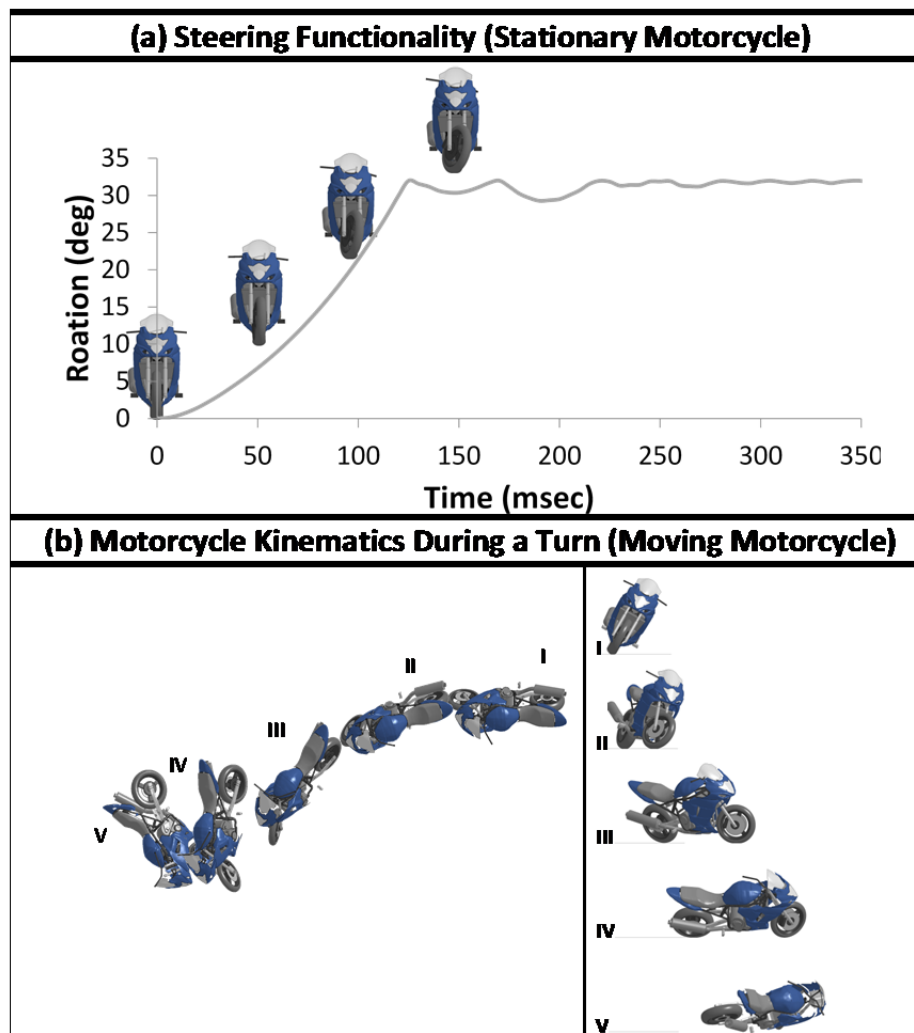


FIGURE 4 Steering verification – behavior with stationary and moving motorcycle.

MODEL VALIDATION

Motorcycle response to sloped obstacles

During a crash into a road barrier with the motorcyclist riding in an upright position, the motorcycle front wheel is likely to be the first component to impact. For crashes into a safety-shape barrier, the front wheel of the upright motorcycle will initially impact the protruding slope at the bottom of the barrier. This slope, which is shallower than the barrier upper slope, is designed to mitigate the vehicle deceleration at the beginning of the impact by initially compressing the suspension of the impacting front wheel and inducing a subsequent vehicle lift so that part of its kinetic energy is converted into gravitational potential energy. Since a lift of the vehicle would facilitate its redirection, it is important that the motorcycle model could accurately predict this critical initial interaction between the front wheel and the bottom slope of a safety-shape barrier. Thus, the model was validated against experimental tests specifically performed to

assess the kinematics of the motorcycle and the front suspensions during an impulsive event involving slopes.

Setup of experimental and simulated slope tests

A series of experimental tests were conducted with the actual Suzuki motorcycle traversing various sloped obstacles. In these tests, a rider maneuvered the motorcycle over 200-mm (7.9-in) high sloped obstacles at initial nominal speeds varying between 15 km/h (9.3 mph) and 20 km/h (12.4 mph). The details of each tested configuration are shown in the test matrix in Table 1. Two levels of slope steepness were tested, equal to 20 deg and 45 deg. For the case with a 20-deg slope, both a 90-deg (i.e., head-on) and a 45-deg approach angle were tested; whereas in the case with a 45-deg slope only a 90-deg approach could be safely tested by the rider. In all tests, the displacement of the front suspension right fork and the rear suspension swingarm were measured using string potentiometers. For repeatability purpose, each scenario was tested a minimum of three times.

The plots of the measured displacements for all the tests are shown in Figure 5. Note that, in the tests with a head-on approach, the motorcycle front suspension underwent some undesired oscillation due to smooth irregularities of the pavement along the approach path to the ramp. Gradually increasing initial segments indicated by the dashed lines in the relevant graphs show how those curves would have been without the initial pre-compression that was caused by those undesired oscillations.

Experimental and simulated kinematics of the motorcycle and suspension system

As an example, the simulated and experimental motorcycle kinematics for the case with a 20-deg slope and 45-deg approach direction is compared in Figure 6. The motorcycle kinematics simulated using the developed FE model coupled with the ATD was in most part in good

TABLE 1 Experimental Tests with Sloped Obstacles

			Impact Speed * (km/h) [mph]	Ramp Angle (deg)	Approach Angle (deg)
Test No.	20° Slope	20/90-1	20.1 [12.5]	20	90
		20/90-2	20.6 [12.8]		
		20/90-3	19.7 [12.2]		
		20/45-1	14.4 [8.9]	20	45
		20/45-2	18.0 [11.2]		
		20/45-3	18.2 [11.3]		
		20/45-4	19.3 [12.0]		
	45° Slope	45/90-1	15.6 [9.7]	45	90
		45/90-2	17.0 [10.6]		
		45/90-3	17.9 [11.1]		

* Speed determined at time front suspension begins compressing upon contact w/ ramp

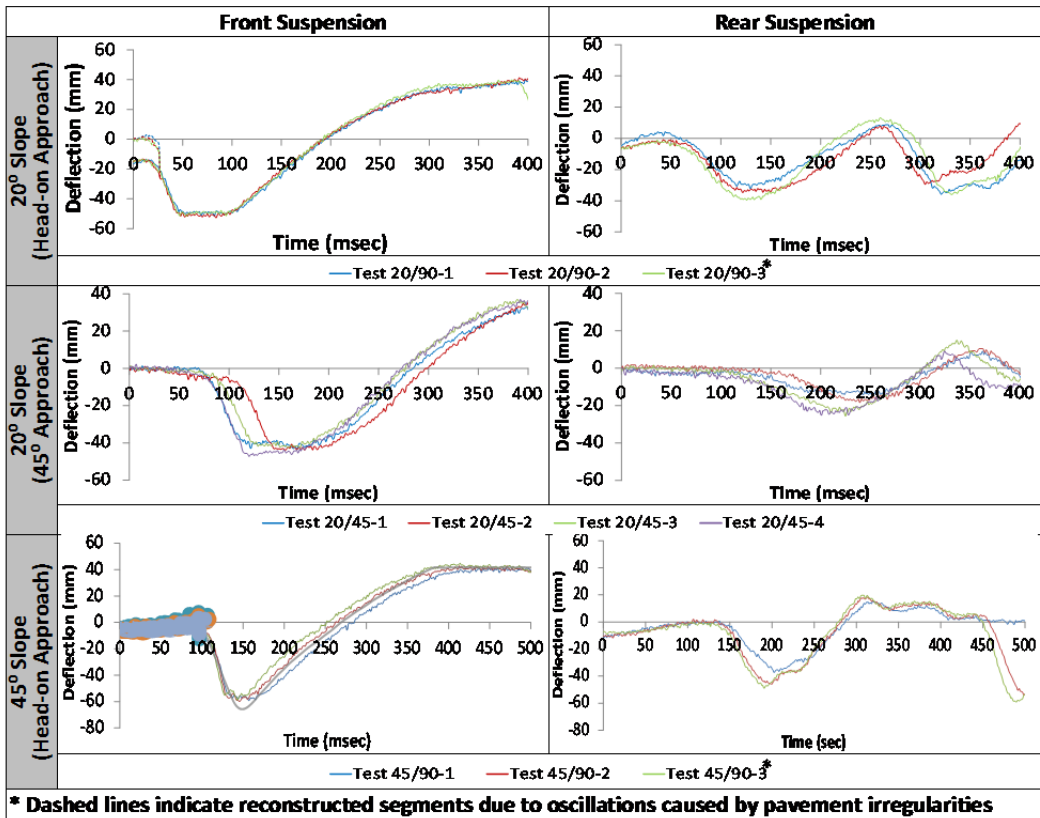


FIGURE 5 Slope tests - displacement of front forks and rear swing arm for repeated tests.



FIGURE 6 Slope tests - simulated and experimental motorcycle kinematics with 20-deg slope at 45-deg approach angle (Test 20/45-3).

agreement with what observed during the experimental test. The simulated motorcycle pitching when traversing the slope as well as the dynamic behavior of both front and rear suspensions closely matched the test. A comparison of the experimental and the simulated deflection of the front and rear suspensions for all the three simulated scenarios is shown in Figure 7.

In general, the simulated compression of the front suspensions was in good correlation with the experimental measurements for all the three tested scenarios. However, a fair correlation was only obtained for the rear suspension (i.e., the simulated deflection of the rear swingarm). The rear suspension underwent two distinct compression peaks. The initial compression peak was caused by the motorcycle pitching up when the front wheel rode over the ramp; whereas the subsequent compression peak occurred when the rear wheel climbed over the ramp. In both cases, the simulated compression of the rear suspension occurred earlier than in the experimental tests and was also smaller in magnitude. Both these aspects of the rear suspension response could be significantly influenced by the timing and intensity of the rider body movements. During the tests, the human rider instinctively pro-actively readjusted his body in order to stabilize the motorcycle. The simplified movements that were imposed to the ATD model in the simulations could not entirely replicate such complex adaptive response of the human rider. Detailed modeling of an active rider would be a major effort per se and was not part of this research scope. Since the major focus of this validation activity was that of assessing the response of the motorcycle front suspension, the fair simulated response for the rear suspension was not considered as a major issue.

A quantitative comparison between the experimental and the simulated response of the front and rear suspensions was also assessed using the Sprague&Geers (SG) and the Anova metrics that are proposed in the National Cooperative Highway Research Project (NCHRP) Report 179 (21) for the verification and validation of numerical models in the field of roadside safety. The values of these comparison metrics, which were calculated using the RSVVP software (22), are shown in Figure 7.

The SG metric components were within the proposed acceptance scores for any of the three simulated test scenarios. However, the Anova metrics were larger than the proposed limits. For two of the three considered scenarios, in the case of the front suspensions the average of the normalized residuals was slightly larger than the suggested 5% limit. For the case of the rear suspension system, the values of the Anova metrics further exceeded the acceptance criteria. In general, both the SG and the Anova metrics indicated that the simulated response of the front suspension system was in better agreement with the experimental results than in the case of the rear suspension.

Full-scale crash into a safety-shape barrier

The developed motorcycle FE model coupled with the ATD FE model was used to simulate a previous crash test involving an upright motorcycle impacting into a concrete safety barrier. The accuracy of the simulated interactions between the motorcycle, ATD and barrier model was assessed.

Setup of experimental and simulated crash test

The crash test was conducted at DEKRA using a sport-touring motorcycle and a Hybrid III ATD (23). The test involved an impact between a Kawasaki ER-5 Twister and an 810-mm (32-in) tall

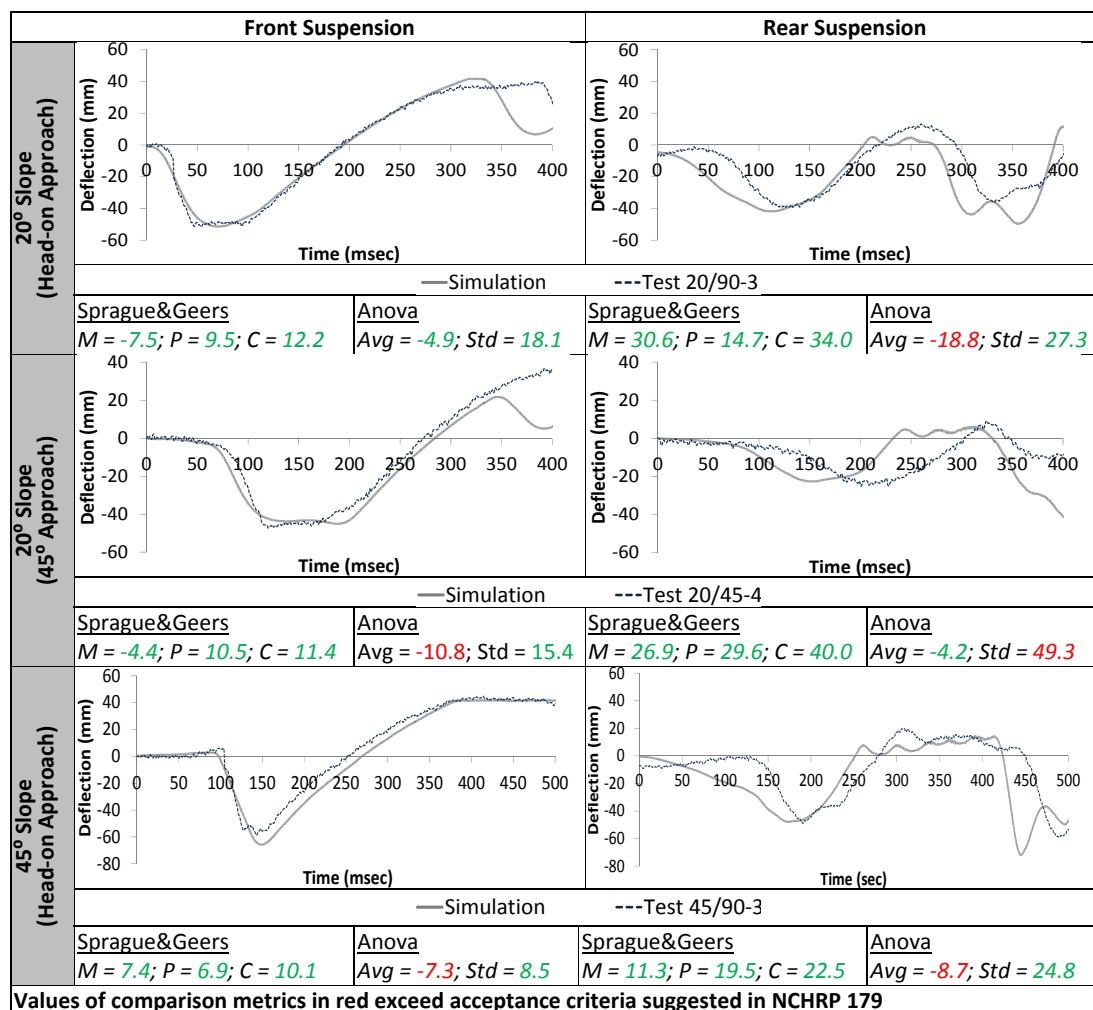


FIGURE 7 Slope tests -simulated and experimental displacement of front/rear suspensions.

New-Jersey concrete barrier at initial impact speed and angle of 58.5 km/h (36.4 mph) and 12 degrees, respectively.

A comparison of the main specifications for the Kawasaki ER-5 and the modelled Suzuki GSX-F650 is provided in Table 2.

Although the tested Kawasaki ER-5 and the Suzuki GSX-F650 were generally similar, their designs were characterized by some intrinsic differences. The Kawasaki ER-5 was slightly smaller than the modelled motorcycle and, consequently, it was also about 41 kg (90 lb) lighter. Given the intrinsic geometrical differences in the design of the two motorcycles, the mass of the modelled Suzuki motorcycle was not reduced to limit any undesired consequent changes to its moments of inertia.

The ATD FE model previously used for simulating the slope tests was seated on the motorcycle model with an initial posture similar to that of the actual ATD at the beginning of the crash test. A model of the New-Jersey shape barrier was assembled to replicate the tested barrier curved configuration, which was reconstructed from an analysis of the images available in the test report.

TABLE 2 Specifications of Motorcycle used in Experimental and Simulated Crash Test

		1998 Kawasaki ER-5	2008 Suzuki GSX-F650
Dimensions	Length (mm) [in]	2,070 [81.5]	2,130 [83.9]
	Width (mm) [in]	730 [28.7]	760 [29.9]
	Max Height (mm) [in]	1,070 [42.1]	1,225 [48.2]
	Seat Height (mm) [in]	800 [31.5]	760 [29.9]
	Wheelbase (mm) [in]	1,430 [56.3]	1,470 [57.9]
	Ground Clearance (mm) [in]	125 [4.9]	130 [5.1]
Tires	Front Tire	110/70-H17	120/70-ZR17
	Rear Tire	130/70-17	160/60-ZR17
Mass	Weight* (kg) [lb]	197* [434]	238 [524]
* Weight of test vehicle including instrumentation			

Experimental and simulated kinematics of motorcycle and ATD

A visual comparison of the simulated and experimental kinematics of both the motorcycle and the ATD for each major critical event that occurred during the crash test is shown in Figure 8. Initially, the motorcycle front wheel hit the barrier bottom slope with a consequent compression of the front suspension. Immediately after this first impact, the front wheel started to climb over the slope, thus inducing the motorcycle to pitch up. Subsequently, the deceleration due to the friction between the sliding upright motorcycle and the barrier upper slope caused the rear wheel to also lift off the ground. The motorcycle deceleration also caused the ATD to be displaced both forward and sideways towards the barrier. When the motorcycle rolled toward the barrier and impacted its top edge, the ATD leaned over the barrier with its right leg being crushed between the motorcycle and the barrier surface. The impact of the motorcycle exhaust against the barrier then caused the rear wheel to be pushed away from the barrier, while the front suspension right fork kept sliding along the barrier edge. Consequently, the ATD separated completely from the motorcycle and become airborne over the barrier. The ATD right leg impacted back onto the barrier top surface and kept sliding along it until the ATD fell completely off the back of the barrier.

In general, the FE model proved to be capable of replicating the motorcycle and ATD behavior in a reliable manner. Also the simulated ATD kinematics compared generally well against that of the actual ATD during the test; however, some differences between the simulated and experimental ATD kinematics could be noticed as well. In the simulation, the ATD separated from the motorcycle earlier than in the test and it was also thrown slightly higher over the edge of the barrier. Both these two minor differences between the simulated and experimental ATD kinematics could be potentially caused by some intrinsic geometrical and inertial differences between the tested and modeled motorcycle (i.e., Kawasaki ER-5 Twister versus a modeled Suzuki GSX-650F). Also, the motorcyclist protective clothing (i.e., jacket, pants, boots, and gloves) worn by the ATD in the experimental test likely contributed to make its response slightly stiffer. The lack of this protective garment in the modeled ATD may have then allowed for the faster ATD simulated response compared to the experimental test.

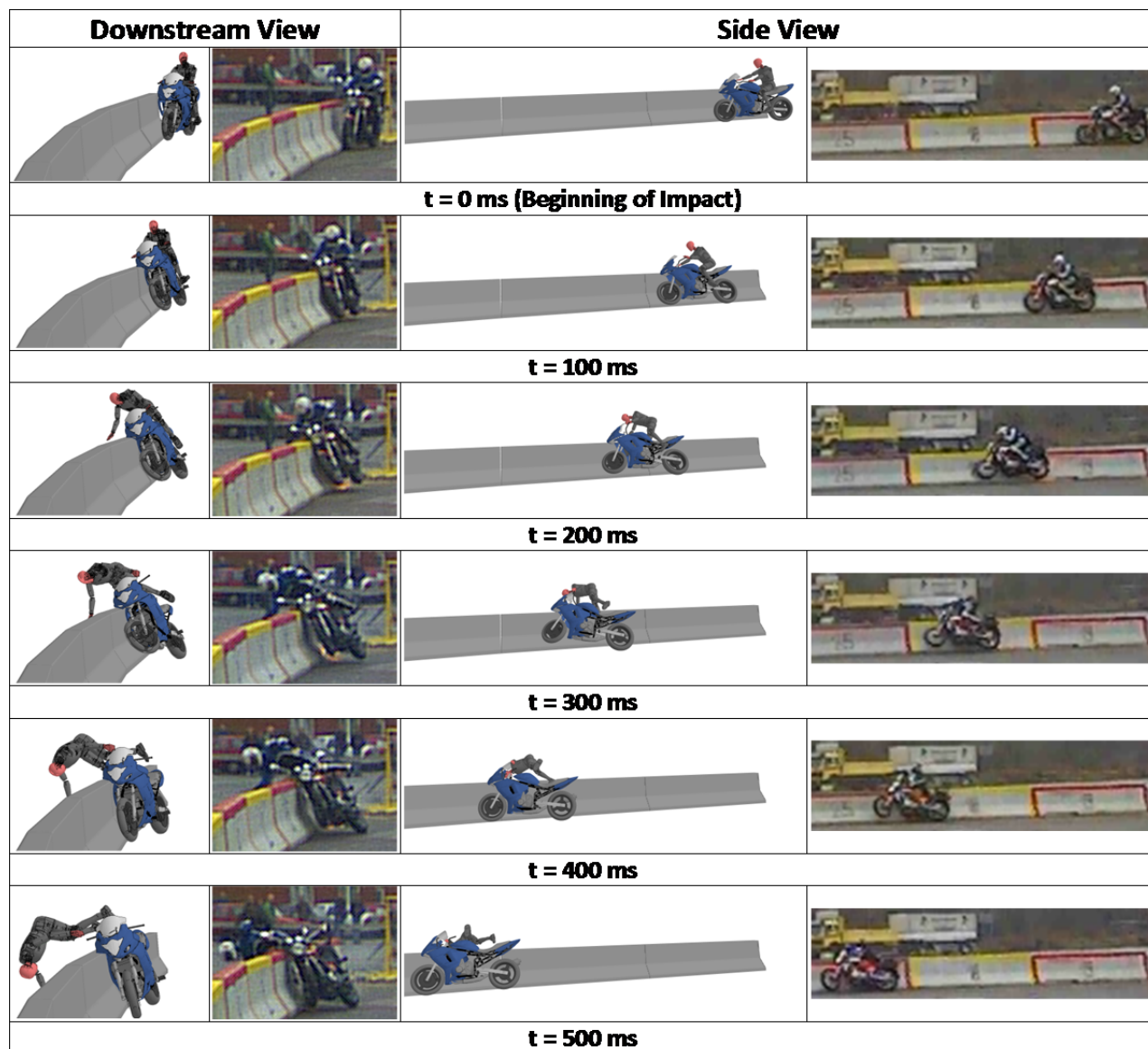


FIGURE 8 Crash into New-Jersey safety barrier – simulation and experimental test.

A qualitative and quantitative comparison of the simulated and experimental motorcycle resultant accelerations that were measured at the top of the steering column and under the seat is shown in Figure 9. The simulated peak accelerations at both bike locations matched within a reasonable tolerance the corresponding experimental peak values.

Overall, the simulated resultant acceleration at the steering column was in good correlation with the experimental acceleration, as also indicated by the value of the SG metric components. Only the anova average slightly exceeded the suggested 5% acceptance criterion.

However, the predicted acceleration at the seat location was larger than the experimental acceleration both at the beginning of the impact and between 250 ms and 400 ms. This resulted in the M and C components of the SG metric for the seat resultant acceleration to exceed the acceptance criteria suggested in NCHRP Report 179. The mentioned differences in the simulated and experimental resultant acceleration at the seat location may have been caused by intrinsic

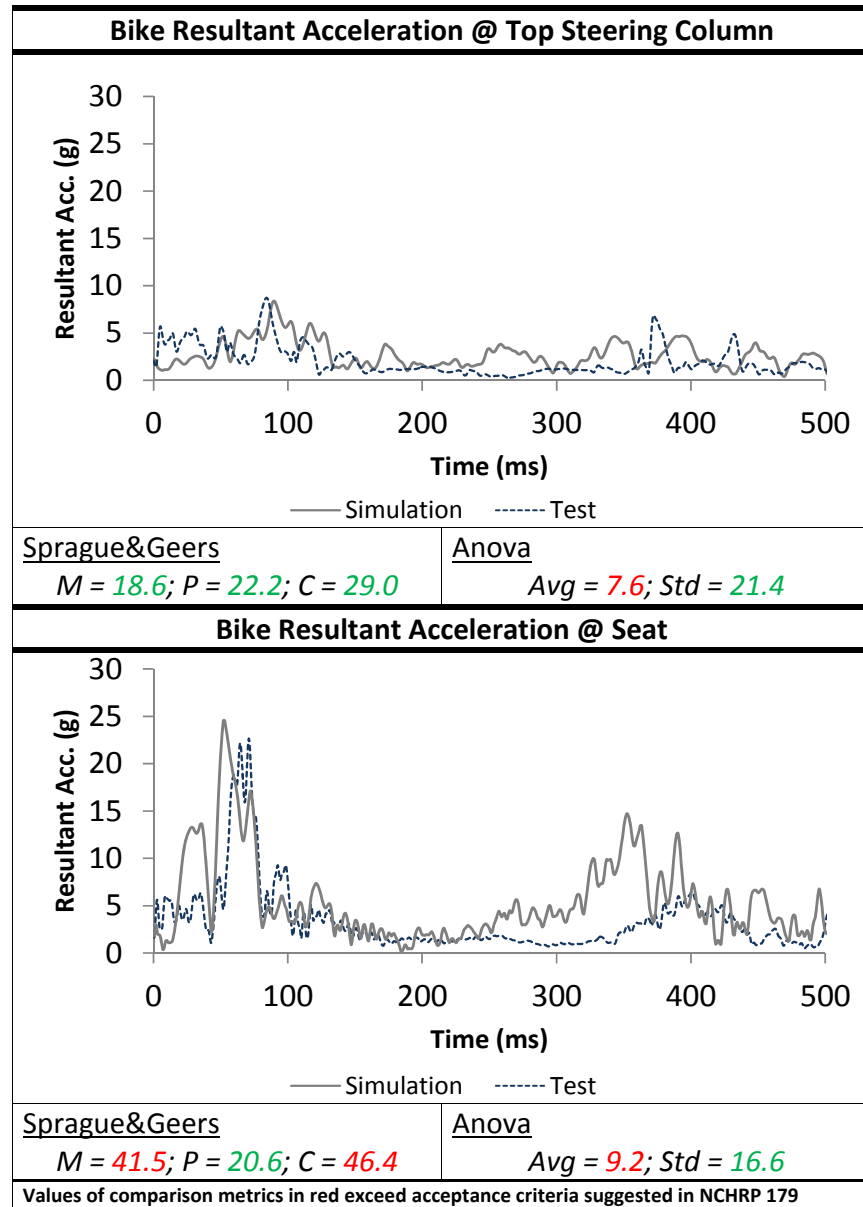


FIGURE 9 Crash into New-Jersey safety barrier - simulated and experimental motorcycle resultant accelerations.

geometrical differences between the modelled Suzuki motorcycle and the tested Kawasaki ER-5. Ultimately, these geometrical dissimilarities may have caused some localized, but relevant, differences between the simulated interaction of the motorcycle model with the front and top surface of the safety barrier and the actual test.

DISCUSSION AND CONCLUSIONS

A detailed FE model of a Suzuki GSX-650F sport-touring motorcycle was developed for simulating upright impacts into roadside safety barriers when coupled with a model of a straddling ATD. Initially, modelled features that are relevant for simulating an impact into a roadside safety barrier, such as steering and suspension kinematics, were verified. Validation of the model was then carried out against experimental tests involving slope obstacles as well as a crash test into a concrete safety barrier.

Overall, the simulated response of the developed motorcycle model showed a promising level of confidence for future applications aimed at simulating a variety of crash scenarios involving roadside safety barriers. The motorcycle model proved to be capable of replicating in a reliable manner the kinematic response of a sport-touring motorcycle when traversing sloped obstacles as well as in a full-scale crash into a curved concrete barrier. The simulated resultant acceleration at the motorcycle steering column was in good correlation with the experimental acceleration measured in the full-scale crash test. Localized differences between the simulated and the experimental acceleration measured at the seat location were likely caused by inherent geometrical differences between the modeled and the tested motorcycles. Further, the simulated kinematics of the ATD model that was coupled with the motorcycle replicated the general behavior of the actual ATD during the full-scale crash test into the barrier. This motorcycle FE model will provide researchers with a useful tool to improve the understanding of the interaction of motorcyclists during upright collisions into roadside safety barriers, allowing to complement the limited real-world crash data currently available.

Future work should consider validating the predicted ATD dynamic loading during a full-scale crash test. Validation of the model for crashes into semi-rigid and flexible roadside safety barriers, such as guardrails and cable barriers, may be considered as well.

ACKNOWLEDGMENTS

The authors kindly thank the staff at the Crashlab testing facility of the Roads and Maritime Services of New South Wales for providing the testing instrumentation used in the experimental tests for the validation of the FE model suspension system. Acknowledgments go also to Mr. Cameron Peacock for manufacturing the wooden structures and helping with the execution of the tests. Finally, the authors would like to also thank DEKRA for providing the results of the experimental full-scale crash test with the concrete barrier. All the simulations were run on the Linux computational cluster Katana from the Faculty of Science at UNSW Australia.

REFERENCES

1. Bambach, M.R., R.H. Grzebieta, and A.S. McIntosh. Injury Typology of Fatal Motorcycle Collisions with Roadside Barriers in Australia and New Zealand. *Accident Analysis & Prevention*, No. 49, 2012, pp. 253–260.
2. Jama, H.H., R.H. Grzebieta, R. Friswell, and A.S. McIntosh. Characteristics of Fatal Motorcycle Crashes into Roadside Safety Barriers in Australia and New Zealand. *Accident Analysis & Prevention*, No. 43, 2011, pp. 652–660.

3. Daniello, A. and H.C. Gabler. Fatality Risk in Motorcycle Collisions with Roadside Objects in the United States. *Accident Analysis & Prevention*, No. 43, 2011, pp. 1167-1170.
4. Gabler, H.C. *The risk of fatality in motorcycle crashes with roadside barriers*. In Proceedings of the 20th International Conference on Enhanced Safety of Vehicles (ESV), Lyons, France, 2007.
5. Elvik, R. The Safety Value of Guardrails and Crash Cushions: A Meta-Analysis of Evidence from Evaluation Studies. *Accident Analysis & Prevention*, Vol. 27, 1995, No. 4, pp. 523-549.
6. EuroRap. *Barriers to Change: Designing Safe Roads for Motorcyclists*. European Road Assessment Program, Publication Number 01/08, Basingstoke Hampshire, UK, 2008.
7. European Union Road Federation (ERF). *Discussion Paper: Road Infrastructure Safety of Powered Two-Wheelers*. Discussion Paper, Brussels, Belgium, February 2009.
8. Berg, F.A., P. Rücker, M. Gartner, J. König, R. Grzebieta, and R. Zou. *Motorcycle Impact into Roadside Barriers – Real-World Accidents Studies, Crash Tests and Simulations Carried out in Germany and Australia*. In Proceedings of the 19th International Conference on the ESV, Washington, USA, 2005.
9. Rizzi, M., J. Strandroth, J. Holst, and C. Tingvall. Does the Improved Stability Offered by Motorcycle Antilock Brakes (ABS) Make Sliding Crashes Less Common? In-Depth Analysis of Fatal Crashes Involving Motorcycles Fitted with ABS. *Traffic Injury Prevention*, Vol. 17, No. 6, 2016, pp. 625-632.
10. Rizzi, M. *Towards a Safe System Approach to Prevent Health Loss among Motorcyclists - The Importance of Motorcycle Stability as a Condition for Integrated Safety*. Thesis for the degree of doctor of philosophy in Machine and Vehicle Systems, Chalmers University, Gothenburg, Sweden, 2016.
11. Centre Europeen de Normalisation (CEN). *Road Restraint Systems - Part 8: Motorcycle Road Restraint Systems which Reduce the Impact Severity of Motorcyclist Collisions with Safety Barriers*. CEN/TS 1317-8, 2012.
12. Spanish Association for Standardization and Certification (AENOR). *Evaluation of Performance of the Protection Systems for Motorcyclists on Safety Barriers and Parapets*. Spanish Standards UNE 135900-1/2, 2008.
13. Bloch J. and M. Page. *Evaluation Procedures of Motorcyclist Roadside Protection Devices*. In Proceedings of the 16th International Road Federation World Meeting, Lisbon, Portugal, 2010.
14. Bürkle, H., and A. Berg. *Anprallversuche mit Motorrädern an Passiven Schutzeinrichtungen [Crash Tests with Motorcycles into Safety Barriers]*. Report by the Federal Highway Research Institute (BASt), Traffic Engineering Report V 90, 2001.
15. Klöckner, R., and M. Zedler., *Anprallversuche an Motorradfahrerfreundlichen Schutzeinrichtungen [Crash Tests of Motorcycle Safety Barriers]*. Report by the Federal Highway Research Institute (BASt), Traffic Engineering Report V 193, 2010.
16. Chawla, A., S. Mukherjee, D. Mohan, D. Bose, P. Rawat, T. Nakatani, and M. Sakurai. FE Simulations of Motorcycle—Car Frontal Crashes, Validations and Observations. *International Journal of Crashworthiness*, Vol. 10, No. 4, 2005, pp. 319-326.
17. Barbani, D., N. Baldanzini, and M. Pierini. Development and Validation of an FE model for Motorcycle—Car Crash Test Simulations. *International Journal of Crashworthiness*, Vol. 19, No. 3, 2014, pp. 244-263.
18. Ibitoye, A.B., A.M.S. Hamouda, S.V. Wong, and R.S.R. Umar. Simulation of Motorcycle Crashes with W-Beam Guardrail: Injury Patterns and Analysis. *Proceedings of the Institution of Mechanical Engineers*, Vol. H8, No. 223, 2009, pp. 1033-40.
19. Tan, K.S., W. Tan, and S.V. Wong. Design of Motorcyclist-Friendly Guardrail Using Finite Element Analysis. *International Journal of Crashworthiness*, Vol. 13, No. 5, 2008, pp. 567-577.
20. *LS-DYNA - Keyword User's Manual LS-DYNA R8.0*. Livermore Software Technology Corporation (LSTC), Livermore, CA, Mar. 2015.
21. Ray, M.H., M. Mongiardini, C.A. Plaxico, and M. Anghileri. *Procedures for Verification and Validation of Computer Simulations Used for Roadside Safety Applications*. National Cooperative

- Highway Research Program (NCHRP) Web-Only Document 179, National Academy of Sciences, Washington DC, 2011.
22. Mongiardini, M. and M.H. Ray. *Roadside Safety Verification and Validation Program (RSVVP) - User's Manual*. Worcester Polytechnic Institute, MA, USA, Rev 1.4, Dec. 2009.
 23. DEKRA. Anprall-Versuche mit Motorrädern an Passiven Schutzeinrichtungen [Crash Tests of Motorcycles into a Passive Safety Barrier: Upright-Propelled 1998 Kawasaki ER-5 Twister Against a 0.81-m Tall Unilateral Concrete Barrier]. Report of Test SH 99.06, Department of Accident Research/Crash Centre, 1999.

Upright Motorcycle Impacts Against Roadside Safety Barrier

Rider Injury Risks and Countermeasure Investigation Through FEA

CHIARA SILVESTRI DOBROVOLNY

ANTONIO DEFranco

NATHAN SCHULZ

ROGER P. BLIGH

Texas A&M Transportation Institute

Over the past years, extensive research efforts were made to improve roadside safety hardware to reduce injury to occupants of passenger vehicles and heavy trucks. Although some European Countries lead significant research to address motorcycle riders' safety when impacting roadside safety devices in sliding position, still very limited investigation has been conducted to address motorcycle riders' safety when impacting roadside hardware in an upright position. When compared to vehicle crashes, motorcycle accidents can lead to a high risk of severe injury for the rider due to the vulnerability of the rider who is fully exposed when impacting the roadside safety barrier.

National standards exist for consideration when assessing roadside safety hardware impacted by passenger vehicles and trucks; full-scale crash testing are required to be conducted to evaluate the crashworthiness of such roadside safety hardware and occupant risk values obtained during impacts with vehicles. Currently, no standards have been developed requiring crash testing of upright motorcycles impacting roadside safety barriers. Therefore, roadside barriers might be ideal to contain and safely re-direct vehicles, but they are currently not designed to be forgiving when impacted by upright motorcycles riders.

There is a need to improve motorcyclist safety by designing and evaluating a more motorcycle-forgiving concept of roadside safety barrier, which could either prevent or limit riders' injury severity during impact.

Within this research study, finite element computer simulations were developed to identify interaction and injury risk associated with a rider impacting in an upright position a commonly deployed type of combination rail safety system. Computer simulations were then utilized to assist with the design and evaluation of a proposed countermeasure for the same combination rail system for upright rider impact.

Although a full-scale crash test is ultimately recommended to verify the proposed "motorcycle-friendly" barrier concept while still comply with national standard assessing roadside safety hardware, preliminary simulations suggest that the proposed design reduces the rider injury risk by limiting the interaction between the ATD (rider) and the barrier system.

Improvement of Hybrid III 50th Percentile Finite Element Model for Sliding Configuration Motorcyclist Impact

MATTEO BERNARDINI

MARCO MANCINI

MARCO ANGHILERI

*LaST, Transport Safety Laboratory, Department of Aerospace Science & Technology
Politecnico di Milano*

MICHELE PITTOFRATI

Global Design Technology (GDTech)

DARIO GUARINO

Global Design Technology (GDTech)

Roadside safety barriers used to restraint impacting vehicles are characterized by exposed elements which represent an excessive hazard for impacting motorcyclists, even if they are well protected by regular suit and helmet.

To face the problem of a barrier that is not biker friendly, a numerical study was carried out with the aim of predicting the motorcyclist behaviour during impacts and of improving the design of roadside safety barriers. To represent the two-wheeler rider during a head front impact against a roadside protection system, the numerical model of a Hybrid III Anthropomorphic Test Device (ATD) was used. The numerical model of the ATD, as it is, seems to fail in reproducing the direct impact of a motorcyclist against a roadside safety barrier. Hence, an adaptation process was conducted on the Hybrid III Finite Element (FE) model. The most important actions were conducted on the ATD's head and on the numerical model of a full-face helmet. The main modifications were related to geometries, material parameters and contact definitions. The results obtained from the numerical simulations realized with the LS-DYNA nonlinear finite element software were compared with experimental tests.

A first calibration was conducted on the head-helmet assembly using a series of drop tests. The head of the Hybrid II, instrumented with uniaxial accelerometers in the three main directions, was used to perform tests of free fall from defined heights to the ground, with and without a helmet. The acceleration data were used as reference for the calibration of numerical head and helmet models.

The FE model of the head, modified in the calibration process, was used in a whole ATD model of to numerically reproduce different impact scenarios: impacts of motorcycles against a concrete new-jersey and against a steel Continuous Motorcyclist Protection System (CMPS) were simulated and compared with available crash-test data.

INTRODUCTION

The World Health Organization states that the traffic crashes make 1.25 million deaths each year [1]. The report attributes half of these figures to crashes involving vulnerable road users as pedestrian, cyclist and motorcyclist. Road safety for Powered Two-Wheeler (PTW) riders, for long time neglected, receive nowadays a call for attention. To reduce the risk of death and injuries from

motorcyclist road traffics impact, an effective intervention is represented by the design of safer infrastructures also referred to as *biker-friendly*.

This is the real problem for motorcyclists with the common safety barriers that usually are placed at the sides of the roads: they are incompatibles with the relative softness of a human body. Commonly, roadside barriers use structurally-stiff steel elements and are designed for impacts with passenger vehicles. However, these barriers with discrete posts and sharp edges may not be compatible with motorcyclists, which are more compliant, flexible, and fragile than vehicle counterparts. A sliding motorcyclist, even wearing appropriate suit and helmet, has low chance to survive to a high-speed impact with the post of the barrier, and a high chance to undergo to severe injuries at lower speeds.

It's possible to distinguish two main groups for protection structures:

- Discontinuous Motorcycle Protection Systems (DMPS), placed around potentially aggressive elements at the side of the road with the purpose of reducing the severity of a direct impact;
- Continuous Motorcycle Protection Systems (CMPS), along a barrier, with the aim of reducing the severity of an impact with posts or anchorages and retaining and redirecting the rider.

The regulation kept as reference for the development of this work is the EN 1317-8 [2], a part of a comprehensive testing standard for assessing the safety performances of the vehicle restraint systems.

The biomechanical indices for assessing the impact severity of a PTW rider against a motorcyclist protection system were evaluated thanks to experimental tests, carried out with a Hybrid III ATD, and numerical simulations, with its numerical counterpart. The data acquired for the evaluation of the biomechanical indices were the accelerations in the ATD head (Head Injury Criterion, HIC) and the forces and moments at the load cell between the head and the neck.

The aim of this work was to improve the FE model of an anthropomorphic test device to make it produce realistic results during a headfirst impact simulation against a roadside safety barrier. Hence, it should be used during the design process of motorcyclist protections systems, reducing testing costs and improving the optimization of such protections.

Starting from the numerical ATD model commonly used in car crash tests and pedestrian involved accidents, the objective was to simulate a sliding configuration impact obtaining the same severity levels of real tests performed with different barriers.

As a first step of the work, the helmet role and its interaction with the ATD head were investigated to calibrate their numerical model. Once this result was reached, the head model was integrated into the complete ATD model and several full-scale simulations were carried out.

METHODOLOGY

Experimental Tests

The experimental activity consisted in several drop tests conducted isolating the Hybrid II head from the whole body and letting it falls freely, with and without the helmet. The scenarios analysed varied with respect to the falling height and the initial orientation of the head, both in absolute

orientation with respect to the ground and in relative position between head and helmet. All the drop tests were executed on a planar surface.

The ATD head was hung upside down, from the holes that allows its connection with the rest of the body, and the falling height was taken from the lowest part of the device till the ground. A quick release mechanism gave the start to every drop test and to the data acquisition.

The initial heights selected were 100 mm, 150 mm and 200 mm. The rise of the falling height led to an increase in the maximum acceleration value.

The maximum acceleration peak and the head injury criterion were computed for each head impact (Table 1). The mean peak of acceleration and the mean HIC were used as a comparison to verify the results obtained with the numerical simulations.

The same procedure was followed to perform experimental drop of the head of the ATD with the helmet worn (Figure 2). The head was hung upside down with the same trigger mechanism used for the head drop tests. The head protection used for the drop tests campaign was a city road full face helmet (Figure 1). The protective helmet was constituted by an outer shell in thermoplastic resin material and a protective expanded polystyrene (EPS) closed cell foam as inner layer. As the protection attached documentation asserts, the helmets are designed to comply the United Nations ESE R22.05 [3] homologation standard, also applicable in all European countries.

In Table 3 are reported the results obtained for Hybrid II head with the helmet worn. As expected the higher the initial height, the higher the acceleration peak reached.

To evaluate the response of the head and helmet behavior with small wearing differences, a campaign of drop tests was conducted. The initial height was fixed at 450mm. The following small wearing variations were introduced:

- Rotation around frontal axis (x);
- Rotation around transverse axis (y)
- Tension on the safety strap

The acceleration curves of the experimental drop tests are reported in Figure 2

TABLE 1 Acceleration peaks and HIC values obtained in experimental Hybrid II head drop tests.

Initial Height [mm]	Acceleration peak [g]	HIC
100	169.07 ± 18.93	229.95 ± 53.67
150	227.39 ± 15.94	422.34 ± 49.5
200	305.45 ± 10.62	767.02 ± 31.89

TABLE 2 Geometric properties of the helmet.

	Helmet
Head circumference [mm]	570-590
Weight [Kg]	1.4±0.05
Max longitudinal dimension [mm]	325±0.5
Max lateral dimension [mm]	242±0.5



FIGURE 1 Helmet drop test configuration.

TABLE 3 Acceleration peaks and HIC values obtained in experimental Hybrid II head and helmet drop tests.

Initial Height [mm]	Acceleration peak [g]	HIC
150	35.34 ± 2.52	41.16 ± 5.08
300	51.13 ± 4.48	97.95 ± 22.43
450	73.4 ± 2.52	170.99 ± 1.22

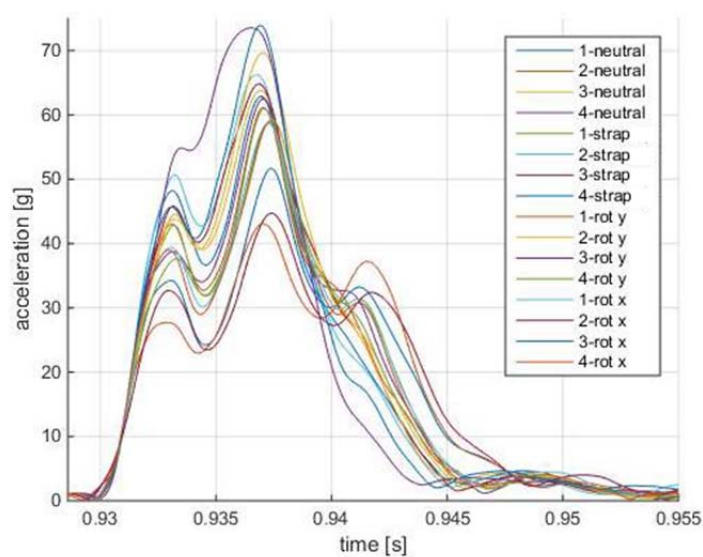


FIGURE 2 Hybrid II head and helmets drop test acceleration curves.

The results shown a significant scatter between the acceleration curves.

The same test setup was used for Hybrid III head with and without helmet. To have a comparison between the head behavior of Hybrid II and Hybrid III, drop tests were conducted: without helmet with 150 mm initial height (Table 4) and with helmet at 450 mm initial height (Table 5).

Numerical Simulations

Simulations were performed using the non-linear explicit FE solver LS-DYNA and LS-PrePost for the pre and post processing procedures.

Head and helmet model calibration

Severe problems were identified in the contact behavior between the head skin and the inner helmet parts. The mesh geometry and the size of the elements of the two parts of interest were not comparable. To overcome the problem, the mesh elements of the skin and, as a consequence, of the skull were splitted in four.

**TABLE 4 Acceleration peaks and HIC values
obtained in experimental Hybrid III head drop test.**

Initial Height [mm]	Acceleration peak [g]	HIC
150	130.14 ± 2.81	199.6 ± 7.09

**TABLE 5 Acceleration peaks and HIC values
obtained in experimental Hybrid III head and helmet drop test.**

Initial Height [mm]	Acceleration peak [g]	HIC
450	52.31 ± 3.81	87.37 ± 18.32

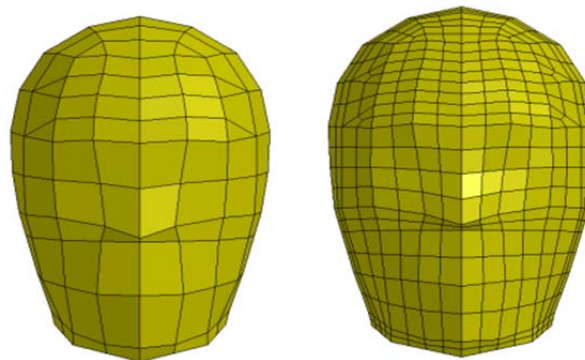


FIGURE 3 Mesh refinement for the FE head model.

The material properties of the head skin were modified as well. The effect of a variation of the terms that define the shear relaxation behaviour into the viscoelastic card (skin material) was inspected for each element, till obtaining a set of parameters that allowed a satisfying correlation between acceleration-time history and the resulted HIC value.

The FE model of the full-face helmet can be subdivided in three main parts. The outer layer of the helmet was modelled by shell elements that share their nodes with the inner layer part modelled by solids. In the lower part of the helmet the safety strap was modelled as a shell that came in contact with the chin of the ATD. The safety strap was connected, on its ends, to the outer shell by two beam modelled as cords (Figure 4). Since the head mesh was modified to better represent the ATD behavior, the coupling between head and helmet elements was checked.

During the first simulations, the head showed an excessive moving capability inside the helmet. Two main modifications were applied on the helmet model:

- the gap due to the different shapes of the head and the inner layer of the helmet was reduced filling the empty space with solid elements (Figure 4);
- the two beam elements that modelled the safety strap were converted in cable formulation to define an axial tensioning force.

An optimization process on the 450 mm drop simulation was set with the objective to fit the numerical and the experimental acceleration time history. The variables of LS-OPT in this process were Young modulus, tensile stress cut-off and damping of the helmet inner foam. The optimization process led to the definition of a calibrated model for the full-face helmet.

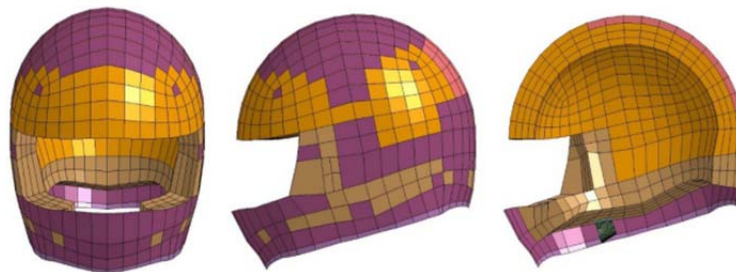


FIGURE 4 FE model of full-face helmet.

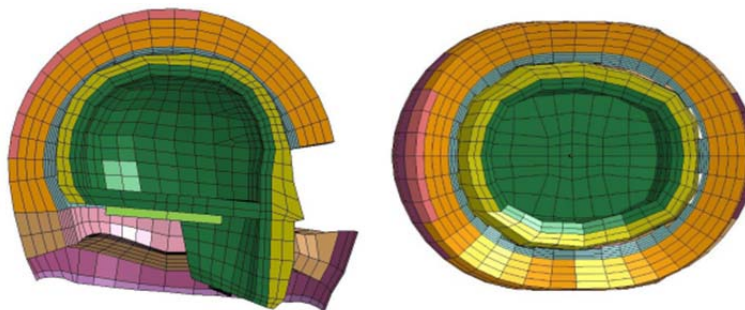


FIGURE 1 Inner layer of the FE model of the helmet.



FIGURE 6 Head and helmet drop test, experimental (left) and numerical (right).

Experimental-numerical comparison

A first comparison was made between the HIC values of numerical and experimental drop tests without helmet (Table 8). In Table 9 the data obtained with the optimized model are summarized, compared with the experimental mean values.

The comparison of the numeric and experimental accelerations was also performed by means of the comparison metric values of “Road Safety Verification and Validation Program” (RSVVP) (Figure 7) [4].

TABLE 8 HIC comparison between experimental and numerical head drops.

Height [mm]	Test	HIC
150	Experimental	199.6 ± 7.09
	Numerical	230.9

TABLE 9 HIC comparison between experimental and numerical head and helmet drops.

Height [mm]	Test	HIC
150	Experimental	40.35 ± 4.27
	Numerical	42.56
300	Experimental	101.58 ± 18.82
	Numerical	107.6
450	Experimental	171.24 ± 0.98
	Numerical	176.9
600	Experimental	236.65 ± 56.68
	Numerical	246.3

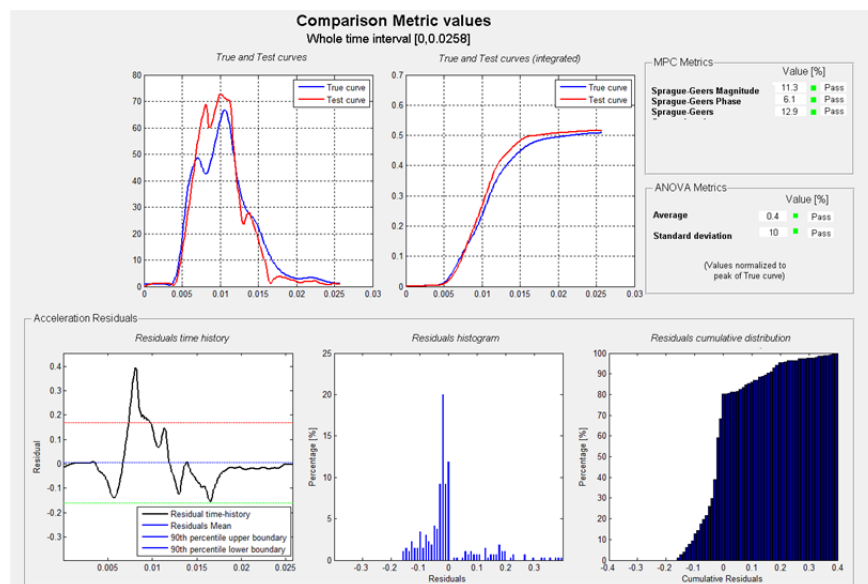


FIGURE 7 RSVVP Comparison metric values.

Full-scale test

Due to verify the global behavior of the complete numerical ATD, the calibrated head was introduced in the Hybrid III model.

The qualitative comparison of the whole dummy behavior was analyzed looking at the available data of three full scale tests:

- New Jersey concrete barrier impact;
- Steel barrier post centered impact;
- Steel barrier midspan impact.

The numerical and experimental HIC values were compared to evaluate the ATD head response during real scenarios (Table 9). In Figure 8 and Figure 9 some frames of the experimental and numerical tests are shown. They depict a qualitative comparison of an impact against a concrete New Jersey barrier and a steel barrier, respectively.

TABLE 9 Full scale Test - Numerical/Experimental HIC comparison.

	HIC Experimental	HIC Numerical
Concrete Barrier	1289	1174
Steel Barrier – Post Centered	317	308
Steel Barrier – Mid Span	267	227

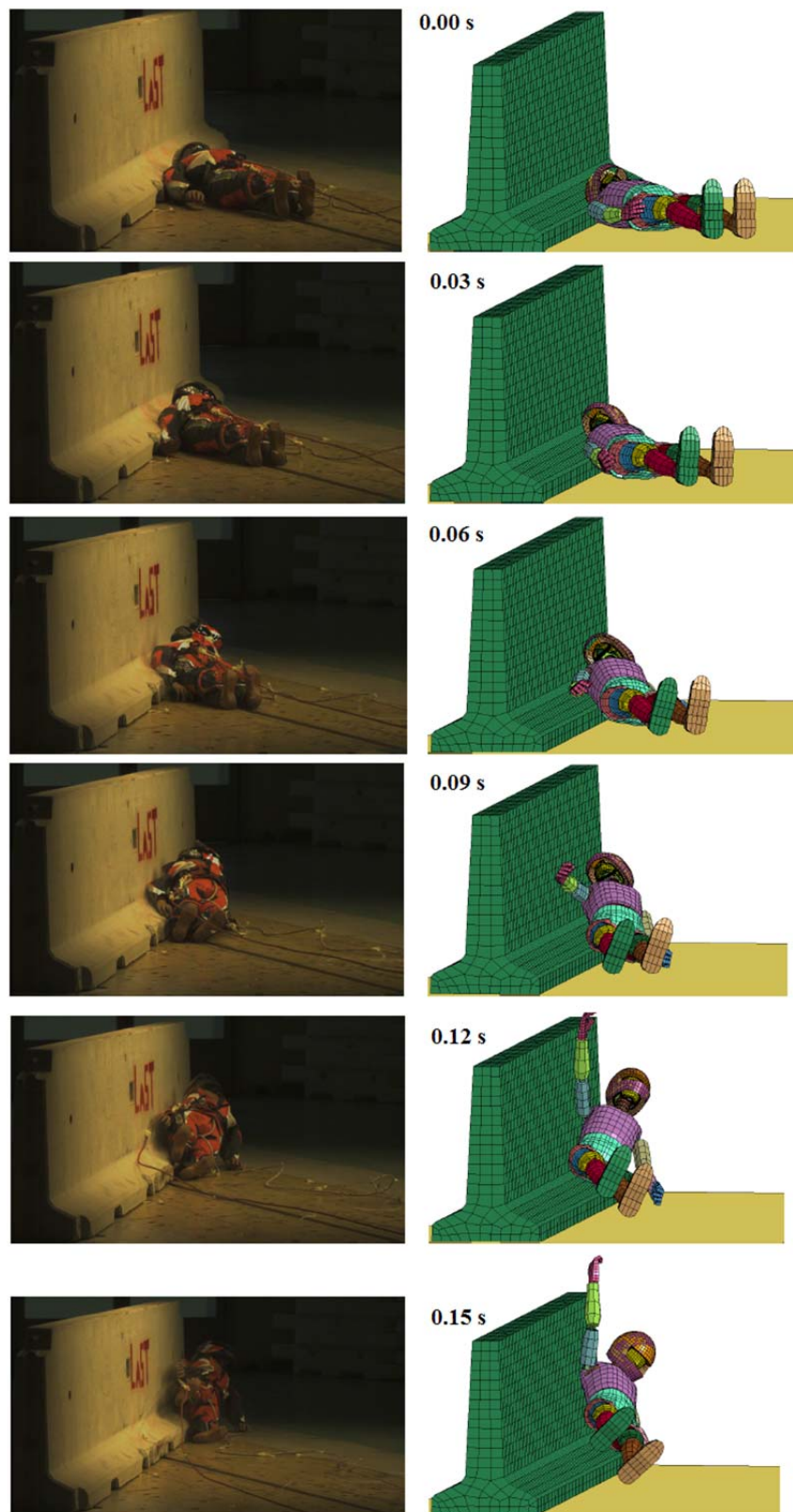


FIGURE 8 Concrete Barrier – Global comparison.

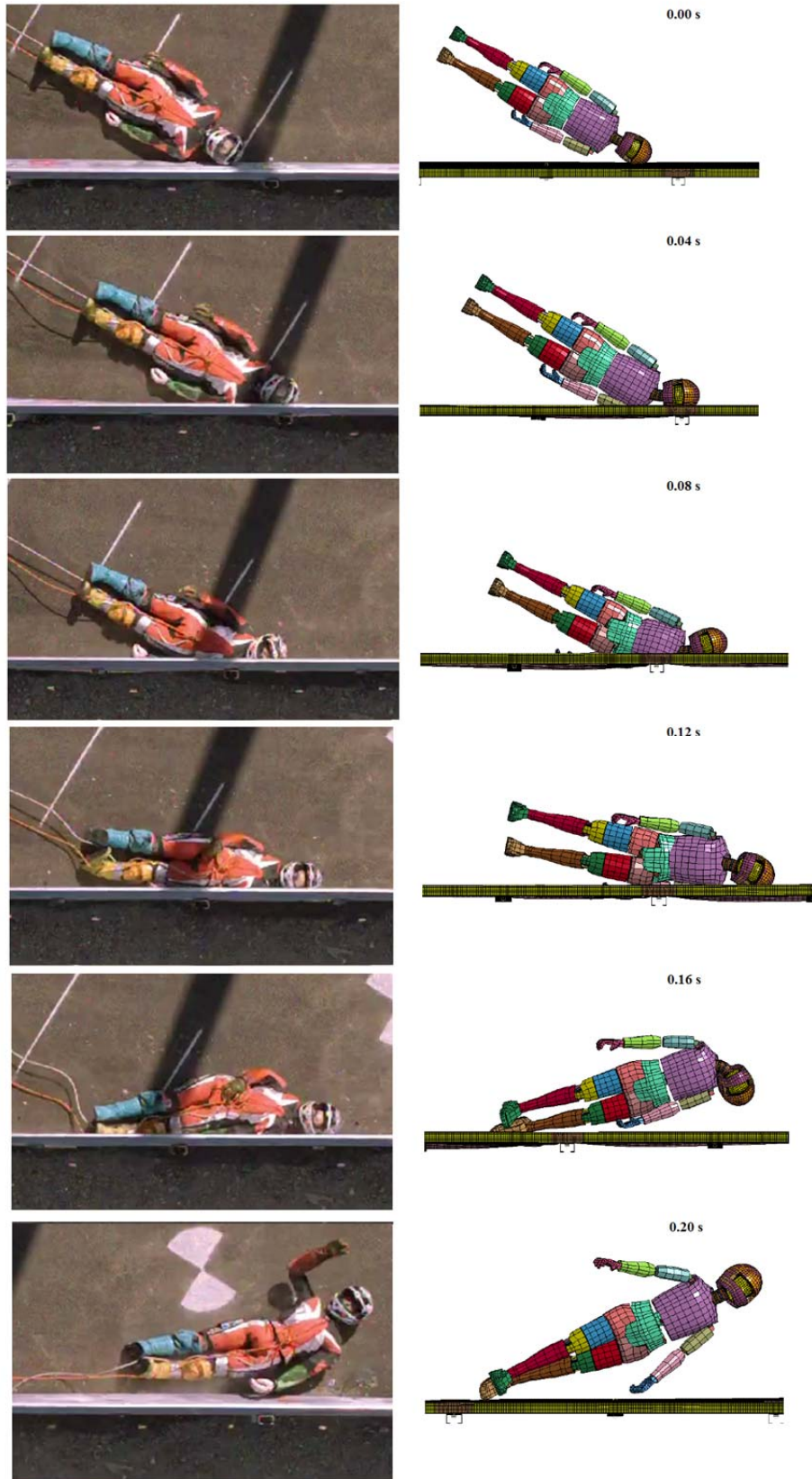


FIGURE 9 Steel Barrier - Post Centered – Global comparison.

CONCLUSIONS

This activity has been conducted on Hybrid II and Hybrid III head with and without helmet. The comparison of the drop test results shown different behavior of the ATD heads. This discrepancy can be ascribed to different skin thickness of the two dummies.

The test campaign conducted on the Hybrid II head with helmet shown a significant scatter in terms of acceleration and HIC values considering small differences in term of reciprocal position of head and helmet. The significant differences experienced with Hybrid II and Hybrid III head without helmet resulted mitigated considering the same drop-test with helmet. The calibration procedure applied to the head with helmet FE model shown good results comparing numerical-experimental acceleration curves and HIC.

The obtained model was tested on full scale simulations to verify its global behavior. The full scale FE simulations shown an acceptable correlation between experimental and numerical results in terms of global behavior and acceleration peak.

REFERENCES

1. WORLD HEALTH ORGANIZATION, Global Status Report on Road Safety, May 2016, <http://www.who.int/mediacentre/factsheets/fs358/en/>
2. UNI EN 1317-8 "Road restraint systems - part 8: motorcycle road restraint system which reduce the impact severity of motorcyclist collision with safety barriers.", 12 July 2012.
3. ESE R22.05 "Uniform Provision Concerning the Approval of Protective Helmets and of their Visors for Drivers and Passengers of Motor Cycles and Mopeds", 24 September 2002.
4. Mario Mongiardini, Malcolm H. Ray. Roadside Safety and Verification and Validation Program (RSVVP), User's Manual. Dec 2009 (Rev 1.4)

Motorcycle Finite Element Computer Model to Assist with Roadside Safety Research Efforts

NATHAN SCHULZ

CHIARA SILVESTRI DOBROVOLNY

Texas A&M Transportation Institute

Over the past years, extensive research efforts have been made to improve roadside safety hardware to reduce injury to occupants of four wheel vehicles and heavy trucks. In comparison, limited research has been conducted to address the safety of motorcycle riders when impacting roadside safety hardware. The vulnerability of motorcycle riders can lead to a high risk of injury for the rider, especially when impacting roadside barriers. In real-world motorcycle crashes there is a wide range of impacts against other vehicles and barriers. Reproducing these different motorcycle crash scenarios through physical crash testing can be considerably costly and time consuming. Computer simulations are a great tool to address the wide range of impacts in real world motorcycle crashes because they are significantly cheaper and quicker than performing full scale crash tests. Motorcycle simulation models have been developed since the 1970's and have improved in detail and complexity over the years. However, there is still a need to develop detailed motorcycle models that are geometrically accurate and can accurately predict motorcycle response behavior. The researchers have developed a Finite Element (FE) computer model of a motorcycle through reverse engineering. This model can be used to investigate impact scenarios involving motorcycles. To validate the accuracy of the model, measurements of the motorcycle computer model such as mass, geometry, etc, were compared to measurements of the physical motorcycle.

Investigation and Mitigation of Post Penetration into Floor Pan of 1100C Small Cars

RONALD FALLER

SCOTT ROSENBAUGH

ROBERT BIELENBERG

KARLA LECHTENBERG

JAMES HOLLOWAY

CODY STOLLE

JENNIFER SCHMIDT

JOHN REID

MOJDEH ASADOLLAHI-PAJOUH

Midwest Roadside Safety Facility

University of Nebraska-Lincoln

The Midwest Roadside Safety Facility conducted research to develop a Test Level 3 cable barrier system for use in sloped medians using MASH 2009 and MASH 2016 safety criteria. Several small car crash tests (test designation no. 3-10) were performed to evaluate cable barrier systems installed on level terrain. Although most safety performance criteria were met, several floor pan tears were observed as small cars traversed over the tops of steel posts. The cable barrier systems failed to provide acceptable safety performance with 1100C vehicles due to post penetration into the occupant compartment. Numerous concepts were brainstormed to mitigate floor pan tearing and post penetration, including: incorporating alternative fabrication methods to eliminate sharp corners and free edges with the addition of corner radii, edge hemming, and edge rounding; post weakening with holes or slots to reduce weak-axis bending strength and upward rebound force against undercarriage; adding post caps or edge protectors; and selecting a closed-section post. A dynamic bogie testing program was used to investigate the effectiveness of design modifications. An existing, steel-framed, bogie vehicle was modified to incorporate a steel sheet floor pan that was representative of a Kia Rio small car. Baseline dynamic component testing revealed that the top of posts would tear and crease the simulated floor pan, which reasonably matched the damage observed in actual full-scale crash tests with small cars. The bogie vehicle with simulated floor pan demonstrated its usefulness in evaluating post modifications. Post treatments with corner radius and edge rounding did not prevent floor pan penetration when combined with the existing prototype line post. Post weakening with various hole and slot patterns were evaluated and showed promise for mitigating floor pan penetrations. Post caps or edge protectors were shown to mitigate concerns for floor pan penetration in the bogie testing with surrogate floor pan. For comparison purposes, component testing was also performed on other common weak posts. Three additional 1100C small car tests were performed on design modifications. One crash test was performed on a four-cable, median barrier system with radii on the upper free edges, which resulted in floor pan tearing and post penetration. A second crash test was performed on a four-cable, median barrier system supported by weakened steel posts using two 3/4-in. diameter holes at the ground line. This test revealed improved performance, although tearing occurred during the third vehicle-to-barrier contact event. Another crash test was performed on a four-cable, median barrier system supported by weakened steel posts and an upper post cap system. This test demonstrated that weakening holes and an upper post cap prevented floor pan penetration, although excessive A-pillar deformation was observed.

INTRODUCTION

History

The Midwest Roadside Safety Facility (MwRSF) and the Midwest States Pooled Fund Program began to develop a non-proprietary, high-tension, four-cable, barrier system for use in median ditches with 1V:4H side slopes. The cable barrier system was intended to meet the Test Level 3 (TL-3) impact safety criteria published in the American Association of State Highway and Transportation Officials (AASHTO's) *Manual for Assessing Safety Hardware* (MASH) (1) as well as the revised test matrices for evaluating cable barrier systems, eventually contained in the MASH Update (2). The initial full-scale vehicle crash testing program revealed several design concerns in the prototype barrier system, including compromised vehicle capture while traveling through median V-ditches and excessive occupant compartment deformations (3-6). These safety concerns led to continued barrier development to improve the performance of the high-tension, cable median barrier system.

Several design changes were made to improve system performance and satisfy the MASH TL-3 safety requirements for four-cable, median barrier systems (1-2). First, the top cable attachment was modified to alleviate vehicle override concerns when the barrier was placed down the front slope of a depressed median during test no. 4CMB-5 (4). A new top cable configuration was incorporated to allow the upper cable to reside within a V-notch cut into the top of the post and retained with a brass keeper rod. Component testing demonstrated quick cable release during impacts with posts, thus preventing cables from being pulled down and allowing vehicle override (7-9). A new post was developed to reduce the lateral stiffness and strength of line posts following test no. 4CMBLT-1, which resulted in a crushed A-pillar (5). The Midwest Weak Post (MWP) was developed with a reduced lateral bending capacity, approximately one-half of the strong-axis bending strength of S3x5.7 posts (10). Cable tension was lowered from 4,200 lb at 100 degrees Fahrenheit to 2,500 lb at 100 degrees Fahrenheit to decrease risks for occupant compartment penetration and A-pillar crush (7). In addition, a new bolted-tabbed bracket was developed to optimize cable-to-post release loads, which provided one-third of the vertical release load of the previous clips and sufficient lateral strength to allow MWPs to yield (7).

Initially, the cable barrier system was developed for placement anywhere within a 1V:4H median V-ditch. After initial development and testing, the sponsors redirected the development effort to consider barrier placement anywhere within a 1V:6H V-ditch. The cable heights were adjusted to reflect the changes to vehicle trajectories through sloped medians (8). The center height of the top cable was reduced from 45 in. to 40 in., and the vertical cable spacing was reduced from 10½ in. to 8¾ in. The barrier system would be investigated using post spacing ranging between 8 ft and 16 ft. The modified four-cable, median barrier system is depicted in Figure 1, including the MWP's cross-sectional geometry. The MWP was fabricated with 7-gauge thick, ASTM A1011 HSLA Grade 50 steel with an unfolded width of 7¹/₁₆ in.

The modified cable barrier system was evaluated using full-scale crash testing under MASH (1-2). Three full-scale vehicle crash tests were initially performed using test matrices associated with barrier placement anywhere within a 1V:6H median V-ditch (11).

Test no. MWP-1 was conducted using MASH test designation no. 3-17, which utilized a 1500A passenger car impacting the barrier with 16-ft post spacing and positioned at the slope break point. This test vehicle was contained and redirected by the barrier, and the test was deemed acceptable. Test no. MWP-2 was conducted using MASH test designation no. 3-11,

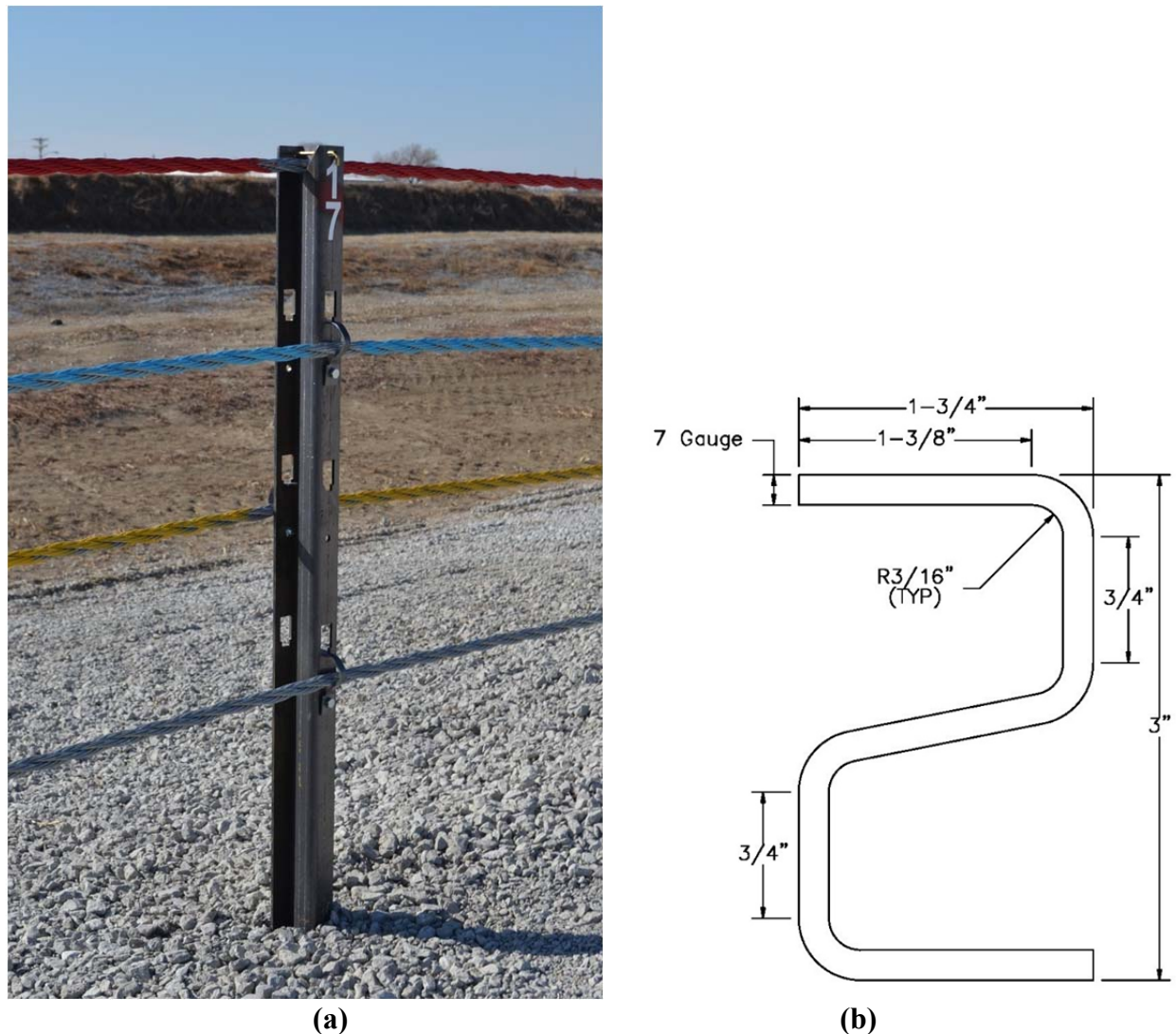


FIGURE 1 Modified Four-Cable, Median Barrier System with 40-in. Top Cable [Test No. MWP-1]: (a) Alternating Cables and (b) Cross-Sectional Geometry at Base.

which utilized a 2270P pickup truck impacting the barrier with a 16-ft post spacing and positioned on level terrain. This vehicle was contained and redirected by the barrier, and the test was deemed acceptable. Test no. MWP-3 was also conducted with a 2270P pickup truck using MASH test designation no. 3-11. For this test, the post spacing was reduced from 16 ft to 8 ft. After initial vehicle capture, three cables were eventually overridden. Subsequently, the vehicle rolled, and the test was deemed unacceptable.

For test no. MWP-3, several factors likely contributed to loss of vehicle capture. In test no. MWP-3, cable no. 3 was pushed down by a support post and later disengaged from the vehicle, thus compromising vehicle capture. It was believed that cable no. 4, or the top cable, needed to interlock into the vehicle to contribute with capture and redirection.

Previous research on vehicle trajectories traversing 1V:6H median ditches (8) indicated that the top cable could be lowered and still be effective in capturing a 2270P pickup truck when projected over and above the front slope. Thus, the center height of the top cable was reduced

from 40 in. to 38 in. to improve vehicle capture in test designation no. 3-11. The vertical cable spacing was reduced from $8\frac{3}{4}$ in. to $7\frac{1}{2}$ in. to improve vehicle capture and reduce concerns for vehicle penetration between cables. With a reduced cable spacing, the center height of the bottom cable was raised from $13\frac{1}{2}$ in. to $15\frac{1}{2}$ in., which was deemed sufficient to capture sedans with narrow front profiles and prevent barrier underride.

There were concerns that the 8-ft post spacing may have negatively affected cable interlock with the vehicle, potentially contributing to cables being pulled down and loss of vehicle capture. The post spacing was increased from 8 ft to 10 ft to improve vehicle capture but limit barrier deflections. The modified four-cable, median barrier system with an upper cable height of 38 in. and adjacent to a 2270P vehicle is depicted in Figure 2.

The modified cable barrier system was evaluated using full-scale crash testing (I-2). Two full-scale crash tests were performed on the revised system (I2). Test no. MWP-4 was conducted using MASH test designation no. 3-11, which utilized a 2270P pickup truck impacting the barrier system installed on level terrain and posts spaced on 10 ft centers. This test vehicle was contained and redirected by the barrier, and the test was deemed acceptable.

Test no. MWP-6 was conducted using MASH test designation no. 3-10, which utilized a 1100C passenger car impacting the barrier with an 8-ft post spacing and positioned on level terrain. The vehicle was safely contained and redirected. However, several steel posts contacted, cut, and penetrated the vehicle's floor pan, and the test was deemed unacceptable. The contact marks, floor pan tears, and post penetration occurred as posts were overridden and free edges of flanges scraped the undercarriage. Left- and right-side flanges of posts contacted and deformed the floor pan. Free edges on deformed posts and floor pan tears in 1100C vehicle are depicted in Figure 3. Following test no. MWP-6, there existed a need to prevent floor pan tearing and post penetration during 1100C tests into four-cable, median barrier systems supported by steel posts.



FIGURE 2 Modified Four-Cable, Median Barrier System with 38-in. Top Cable and 2270P Pickup Truck – Test No. MWP-4.

RESEARCH OBJECTIVE

The primary research objective was to brainstorm, design, and implement modifications to mitigate floor pan tearing and post penetration into 1100C small passenger cars when impacting four-cable, median barrier systems supported by steel posts. Design modifications would be incorporated into a revised cable barrier system for testing and evaluation under the MASH TL-3 impact safety guidelines (*I-2*). If necessary, dynamic component testing would be used to aid in investigating the effectiveness of design modifications.

MITIGATION OF FLOOR PAN PENETRATION

Several design modifications were brainstormed to mitigate floor pan tearing and line post penetration into 1100C small passenger cars (*I2*). These modifications included:

1. reducing weak-axis bending capacity of post to decrease upward force exerted on floor pan, possibly achieved by placement of weakening holes, reduction in material thickness, or alteration to post's cross-sectional geometry;
2. removing sharp corners at top of post with placement of various radii;
3. treating post edges with edge rounding or hemming;
4. adding edge or corner protectors to shield the upper portion of the post;
5. adding caps to cover entire end of post; and
6. developing new post section without free edges.

A change to the post's cross-sectional geometry and a reduction in the post's weak-axis, bending capacity were deemed viable options. However, these options would likely require moderate to significant investigation. The treatment of the sheet metal edges through rounding or hemming was also considered. Edge rounding was initially deemed too costly, while edge hemming was deemed impractical for the existing post dimensions, shape, sheet thickness (7 gauge), slot locations, and cable-to-post attachment hardware. Edge or corner protectors were believed to be an effective option to shield free edges. However, concerns for placement, retention, and cost made edge protectors initially less attractive. A post cap was initially deemed to be a significant modification, requiring substantial investigation to properly release of the upper cable during impact events. A new post section without free edges was deemed highly effective, but this option required significant research and development. The placement of radii at the sharp, upper corners of the post was deemed viable to reduce stress concentration imparted to floor pan, thus eliminating tears. Corner radii were believed to be the simplest to implement into the MWP. Thus, a $\frac{5}{8}$ -in. radius was added to the top free edges of the MWP and a $\frac{1}{4}$ -in. radius was added to the top corners of the V-notch. This design modification was recommended for further crash testing and evaluation under MASH TL-3 impact safety guidelines.

TEST REQUIREMENTS AND EVALUATION CRITERIA

Longitudinal barriers (i.e., cable median barriers) must satisfy impact safety standards to be declared eligible for federal reimbursement by the Federal Highway Administration (FHWA) for



(a)



(b)



(c)

FIGURE 3 Test No. MWP-6 (1100C Vehicle): (a) Free Edges on Deformed Posts; (b) Passenger-Side Floor Pan Tear; and (c) Driver-Side Floor Pan Tear.

use on the National Highway System (NHS). For new hardware, these safety standards consist of the guidelines and procedures published in MASH (*I-2*). Per the proposed MASH testing matrix for cable barriers placed anywhere within median V-ditches, eight full-scale vehicle crash tests must be successfully conducted. For systems with variable post spacing, test designation no. 3-11 must be conducted with the narrowest and widest post spacing to establish the working width limits, thus increasing the required number of crash tests from eight to nine. Although the impact speed and angle are consistent for all nine tests, the critical location of the barrier system within the median ditch is dependent upon the specific crash test and slope of the ditch. For the investigation to mitigate floor pan penetration reported herein, all full-scale crash tests conformed to test designation no. 3-10, which consisted of a 2,425-lb passenger car (1100C) impacting at a speed of 62 mph and an angle of 25 degrees with the barrier installed on level terrain.

TEST DESIGNATION NO. 3-10 - CRASH TEST MWP-7 - CORNER RADII

Following test no. MWP-6, the line posts, spaced on 8 ft centers, were modified to include two different corner radii, as depicted in Figure 4(a). Each sharp corner of a free edge incorporated a $\frac{5}{8}$ -in. radius, while each bent corner forming the V-notch in the center of the post incorporated a $\frac{1}{4}$ -in. radius. Complete design details are provided by Kohtz et al (*12*).

Test no. MWP-7 was conducted with a 2,557-lb small car (1100C) at a speed of 63.9 mph and an angle of 25.7 degrees. The target impact location was at a midspan location, or 4 ft upstream from a post. Moderate barrier damage was observed, consisting of disengaged cables as well as deformed and/or fractured posts, brackets, and brass rods. At its final resting position, the vehicle remained in contact with the cables. Cable no. 3 was beneath the vehicle, cable no. 2 was on the impact side of the vehicle, and cable nos. 1 and 4 were on the non-impact side of the vehicle. Vehicle damage was moderate and primarily located on the left-front and right-front corners of the vehicle. The front bumper, left headlight, left side mirror, left fender, right-front door handle, and rear antennae were disengaged. Deformations and contact marks were observed on various regions of the vehicle. Barrier damage, floor pan damage, and vehicle damage are shown in Figures 4(b) through 4(d). During the test, the small car was captured and redirected by cable no. 2. The A-pillar was slightly deformed as the vehicle underrode cable nos. 3 and 4. The vehicle remained stable throughout the impact event. As the vehicle overrode line posts, the floor pan was gouged, cut, and penetrated due to post-to-undercarriage contact. Four separate tears were observed. The maximum occupant compartment deformation was 1.2 in. at the floor pan and transmission tunnel. The occupant impact velocities (OIVs) were -15.45 fps and 12.03 fps in the longitudinal and lateral directions, respectively. The maximum 0.010-sec occupant ridedown accelerations (ORAs) were -10.29 g's and 6.78 g's in the longitudinal and lateral directions, respectively. The maximum roll angle was 5.3 degrees. All occupant risk criteria were below the recommended MASH limits. The test vehicle remained upright during and after the collision. Vehicle roll, pitch, and yaw angular displacements were deemed acceptable. Test no. MWP-7 was deemed unacceptable under the MASH TL-3 safety performance criteria. A detailed discussion of the test results is provided by Kohtz et al (*12*).

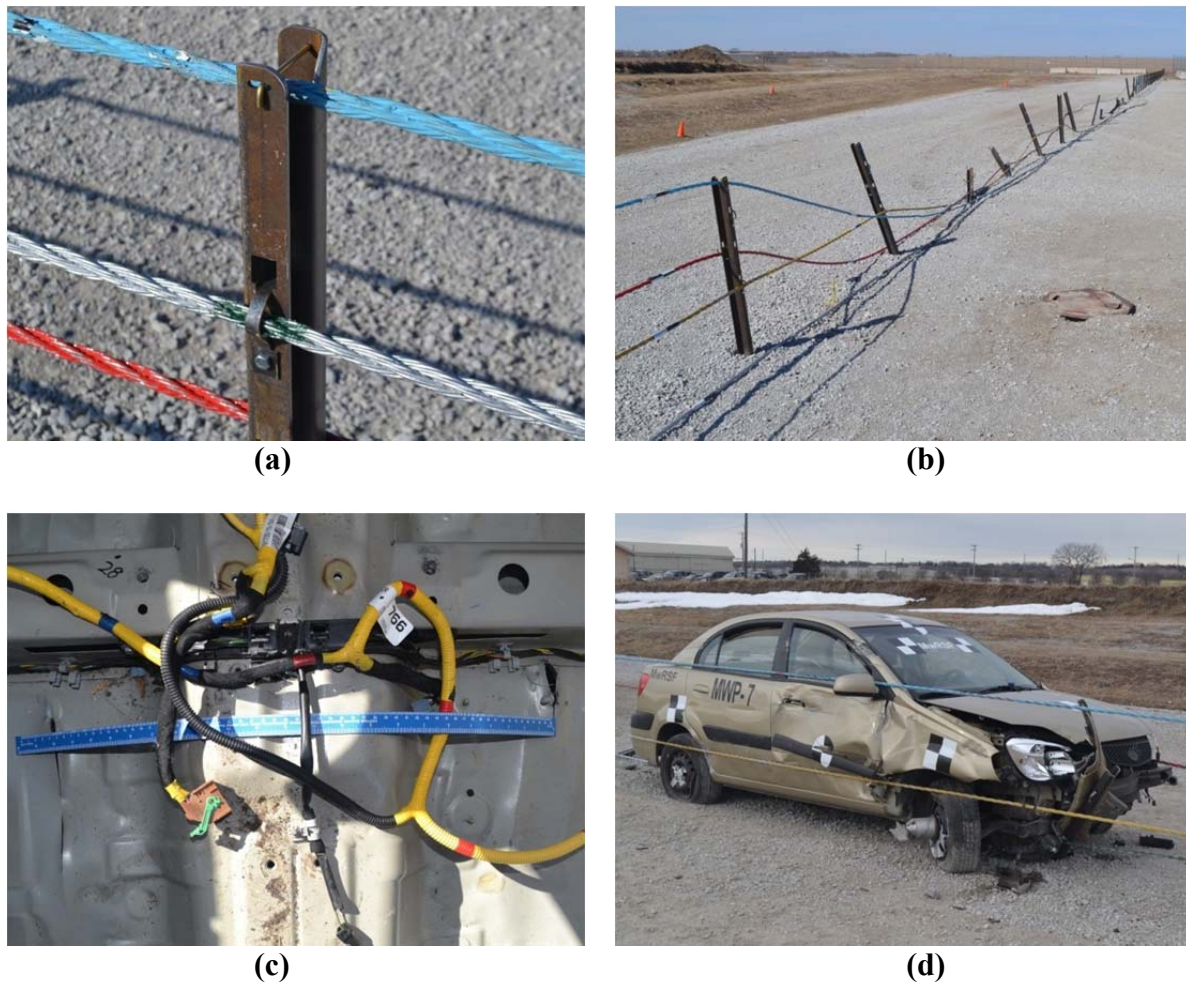


FIGURE 4 Test No. MWP-7: (a) Corner Radii Treatment; (b) Barrier Damage; (c) Floor Pan Tears; and (d) Vehicle Damage.

PHASE I DYNAMIC BOGIE TESTING

During test no. MWP-7, floor pan tearing and post penetration was observed, even with posts treated with edge radii. Thus, it was deemed necessary to further investigate post modifications to mitigate the undesired behavior.

This effort began with the development of a new component testing apparatus to simulate a small car overriding cable barrier support posts. Through a combination of field measurements and static coupon testing, a 24-gauge thick, ASTM A653 steel sheet approximately represented the thickness and tensile strength of Kia Rio floor pans. A Kia Rio vehicle satisfies the MASH vehicle requirements for an 1100C small car. Subsequently, this steel sheet material was mounted to the underside of a rigid-frame, bogie vehicle at the same height as the floor pan of the Kia Rio, or approximately 8 in. above the ground. The modified bogie vehicle with simulated floor pan was utilized to impact and override various post configurations, including a two-post configuration spaced 8 ft apart with a slight lateral offset from one another, as depicted in Figure 5(a). The target impact speed for the bogie was 25 mph. Further information on the test protocol, schematics of design modifications, and detailed results and findings are provided in Reference (13).

Baseline testing was conducted on the MWP with edge radii to investigate whether floor pan tearing could be predicted. For the baseline tests, creasing and tearing was observed in the simulated floor pan, as shown in Figure 5(b), which resembled the floor pan damage found in test no. MWP-7. Thus, dynamic bogie testing with a surrogate floor pan was deemed appropriate for investigating the effectiveness of design modifications to the MWPs in mitigating floor pan tearing and penetrations.

Based on sponsor interest, two dynamic bogie floor pan tests were also conducted on S3x5.7 steel posts, which are commonly used in low-tension, cable barrier systems and other weak-post barrier systems. From this testing, S3x5.7 posts resulted in nearly twice as many floor pan tears as observed with the MWPs. In addition, S3x5.7 posts caused larger tears than those observed in tests on the MWPs, likely due to a greater weak-axis bending strength for S3x5.7 posts as compared to the MWPs. This initial testing suggested that floor pan tearing may potentially occur with other weak-post guardrail systems with free or exposed edges on support posts.

Next, dynamic bogie testing was conducted to evaluate the effectiveness of three design modifications to the MWPs to mitigate floor pan tearing and post penetration. First, MWPs were treated with a simulated Standard AISI No. 1 Round Edge on each free edge. This edge treatment resulted in similar floor pan tearing to that observed in the baseline bogie testing of MWPs. Edge rounding did not adequately reduce the stress concentrations that led to tearing. Thus, edge rounding was eliminated from further consideration.

Second, MWPs were treated with bent steel plates, which covered the free edges. Dynamic bogie testing on free edges treated with steel plate edge protectors resulted in contact marks and creasing of the floor pan but without tearing or post penetration. Due to a fabrication error, a sharp corner on the continuous/bent side of the post allowed floor pan tearing on a non-treated bent corner. Although simulated steel edge protectors had prevented tearing and post penetration, this concept initially was not desired due to concerns for fabrication, installation, and the number of parts required to modify the MWPs. Thus, no further development or testing of the edge protector concept was performed in the initial investigation.

The third design modification involved post weakening with strategically-placed material reductions at ground line, which was explored through numerous dynamic component tests. Three different post weakening patterns near the ground line were investigated, including: (1) one $\frac{3}{4}$ -in. diameter hole placed in each short web segment for a total of two holes; (2) three $\frac{3}{8}$ -in. diameter holes placed in each short web segment for a total of six holes; and (3) one $\frac{3}{8}$ -in. wide x $1\frac{1}{8}$ -in. long slot placed in each short web segment for a total of two slots. When the modified MWPs were impacted with the bogie vehicle, the weakened regions near holes or slots began to rupture, thus reducing the post section modulus and ability to elastically rebound upward to contact the undercarriage. For posts modified with three smaller holes or one slot in each short web segment, no post-to-undercarriage contact was observed in bogie testing with the simulated floor pan. This finding was also observed for impact angles at 0 and 25 degrees. For MWPs weakened with one $\frac{3}{4}$ -in. diameter hole in each short web segment, the weakened region still began to rupture but less than observed for the other two weakening patterns, as shown in Figure 5(c). Thus, these modified MWPs retained enough elastic stiffness to rebound upward to contact the simulated floor pan. As shown in Figure 5(d), the MWPs with one $\frac{3}{4}$ -in. diameter hole in each short web segment imparted contact marks and creases in the simulated floor pan, but it did not cause floor pan tearing or post penetration when impacted 0, 25, and -25 degrees. Thus, all three post weakening concepts showed a propensity to mitigate vehicle floor pan tearing and post penetration.

Prior to implementing a weakening concept into existing posts, further dynamic bogie testing was performed to determine and compare the strong-axis, bending capacity of standard and weakened MWPs. Six dynamic bogie tests were conducted on posts oriented at an angle of 90 degrees (i.e., strong-axis bending). For each weakening concept, two posts were tested and evaluated. Each impacted post hinged at the ground line. However, MWPs that were weakened with either one $\frac{3}{8}$ -in. wide x $1\frac{1}{8}$ -in. slot or three $\frac{3}{8}$ -in. diameter holes in each short web segment experienced significant tearing through the cross section. The post's front flange completely ruptured in all four tests. When compared to unmodified MWPs, the average resistive forces over 20 in. deflection at the impact height for weakened MWPs with either three $\frac{3}{8}$ -in. holes or one $\frac{3}{8}$ -in. wide x $1\frac{1}{8}$ -in. slot in each short web segment were reduced by approximately 30 percent and 44 percent, respectively. For MWPs weakened with one $\frac{3}{4}$ -in. diameter hole in each short web segment, no tearing was observed in the cross section near ground line. When compared to unmodified MWPs, the average resistive force over 20 in. deflection at impact height for weakened posts with one $\frac{3}{4}$ -in. diameter hole in each short web segment was reduced by approximately 10 percent.

Based on an evaluation of test results for various design modifications, researchers recommended that the MWPs be modified with one $\frac{3}{4}$ -in. diameter hole at the ground line in each short web segment to mitigate floor pan tearing and post penetration. This option was selected due to its limited effect on the post's strength in strong-axis bending and anticipated minor effect on lateral barrier deflections. This design modification was recommended for further crash testing and evaluation under MASH TL-3 impact safety guidelines.

TEST DESIGNATION NO. 3-10 - CRASH TEST MWP-8 – WEAKENING HOLES

The four-cable, median barrier system was modified following the unacceptable results observed in test no. MWP-7. Dynamic component testing was used to investigate the effectiveness of various treatments. The line posts, spaced on 8 ft centers, were modified to include two $\frac{3}{4}$ -in. diameter holes in the web at the ground line, as shown in Figure 6(a). The corner radii on free edges were retained. Complete design details are provided by Hartwell et al (14).

Test no. MWP-8 was conducted with a 2,583-lb small car (1100C) at a speed of 63.0 mph and an angle of 25.7 degrees. The target impact point was at a midspan location, or 4 ft upstream from a post. Moderate barrier damage was observed, consisting of disengaged cables as well as deformed and/or fractured posts, brackets, and brass rods. At its final resting position, the vehicle remained in contact with the cables. Cable nos. 2 and 3 were beneath the vehicle, while cable nos. 1 and 4 were on the non-impact side of the vehicle. Vehicle damage was moderate and primarily located on the left-front and right-front corners of the vehicle. The front bumper, left and right headlights, left and right side mirrors, left and right fenders, were damaged. Deformations and contact marks were observed on various regions of the vehicle. Post no. 50 penetration marks, floor pan damage, and vehicle damage are shown in Figures 6(b) through 6(d). During the test, the small car was captured and redirected by cable no. 2. The vehicle remained stable throughout the impact event. No floor pan tearing or post penetration occurred during initial contact and exit from barrier. As the vehicle re-contacted the barrier farther downstream and overrode several line posts, the floor pan was gouged, cut, and penetrated due to post-to-undercarriage contact, specifically with post no. 50. Two separate tears were observed. The maximum occupant compartment deformation was 0.5 in. at the floor pan and transmission

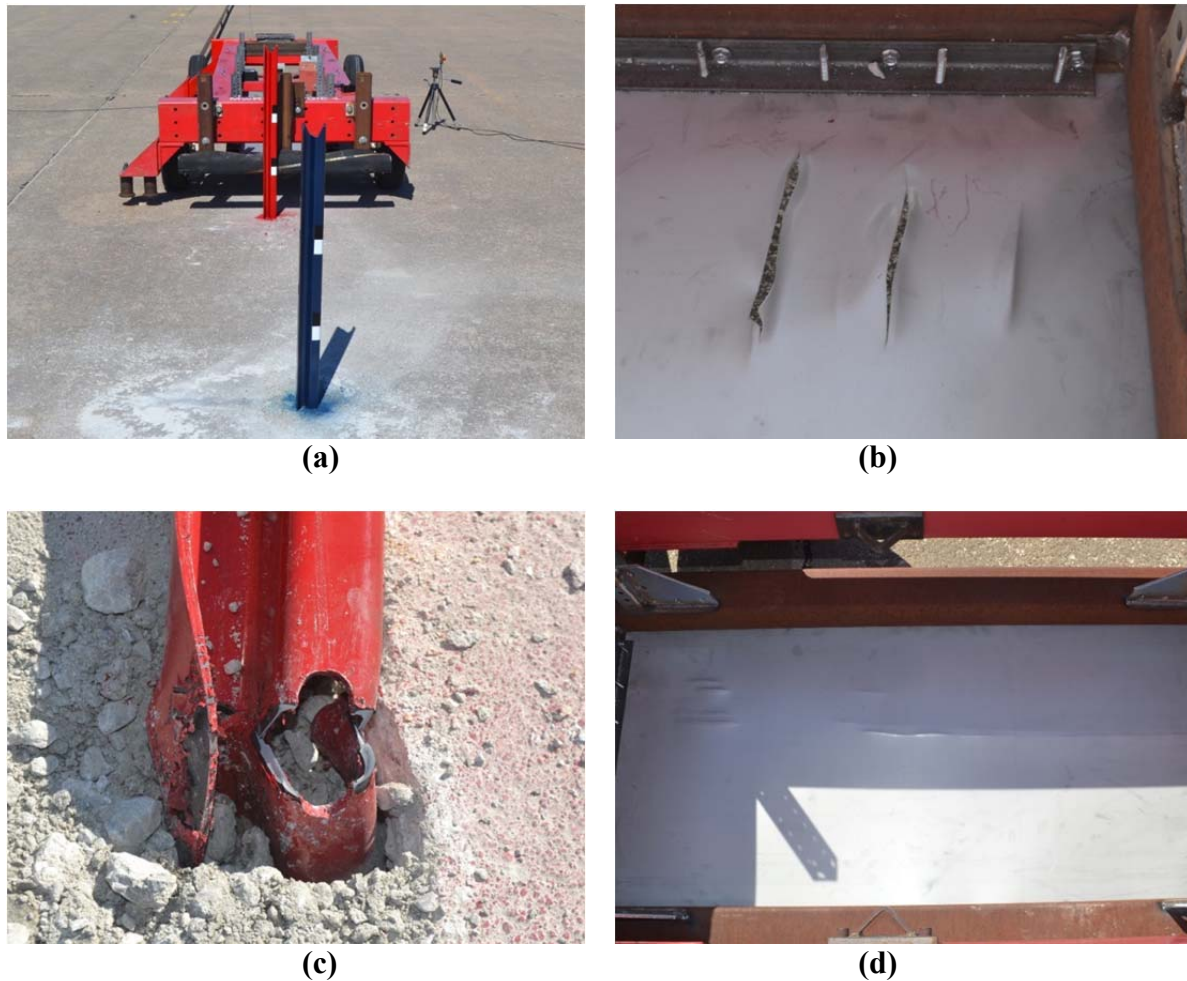


FIGURE 5 Phase I Dynamic Bogie Testing: (a) Two-Post Setup; (b) Baseline Post Floor Pan Tearing; (c) Partial Post Fracture – $\frac{3}{4}$ -in. Hole; and (d) Contact Marks and Gouging in MWP with $\frac{3}{4}$ -in. Hole.

tunnel. The occupant impact velocities (OIVs) were -13.35 fps and 11.91 fps in the longitudinal and lateral directions, respectively. The maximum 0.010-sec occupant ridedown accelerations (ORAs) were -6.54 g's and -5.87 g's in the longitudinal and lateral directions, respectively. The maximum roll angle was -55.1 degrees. All occupant risk criteria were below the recommended MASH limits. The test vehicle remained upright during and after the collision. Vehicle roll, pitch, and yaw angular displacements were deemed acceptable. Test no. MWP-8 was deemed unacceptable under the MASH TL-3 safety performance criteria. A detailed discussion of the test results is provided by Hartwell et al (14).

PHASE II DYNAMIC BOGIE TESTING

During test no. MWP-8, floor pan tearing and post penetration did not occur during the initial vehicle impact and exit away from the modified cable barrier system with weakened MWPs. The vehicle re-contacted the barrier system farther downstream, and the lower cables remained attached to several posts, which prevented posts from easily bending over. Floor pan tearing and

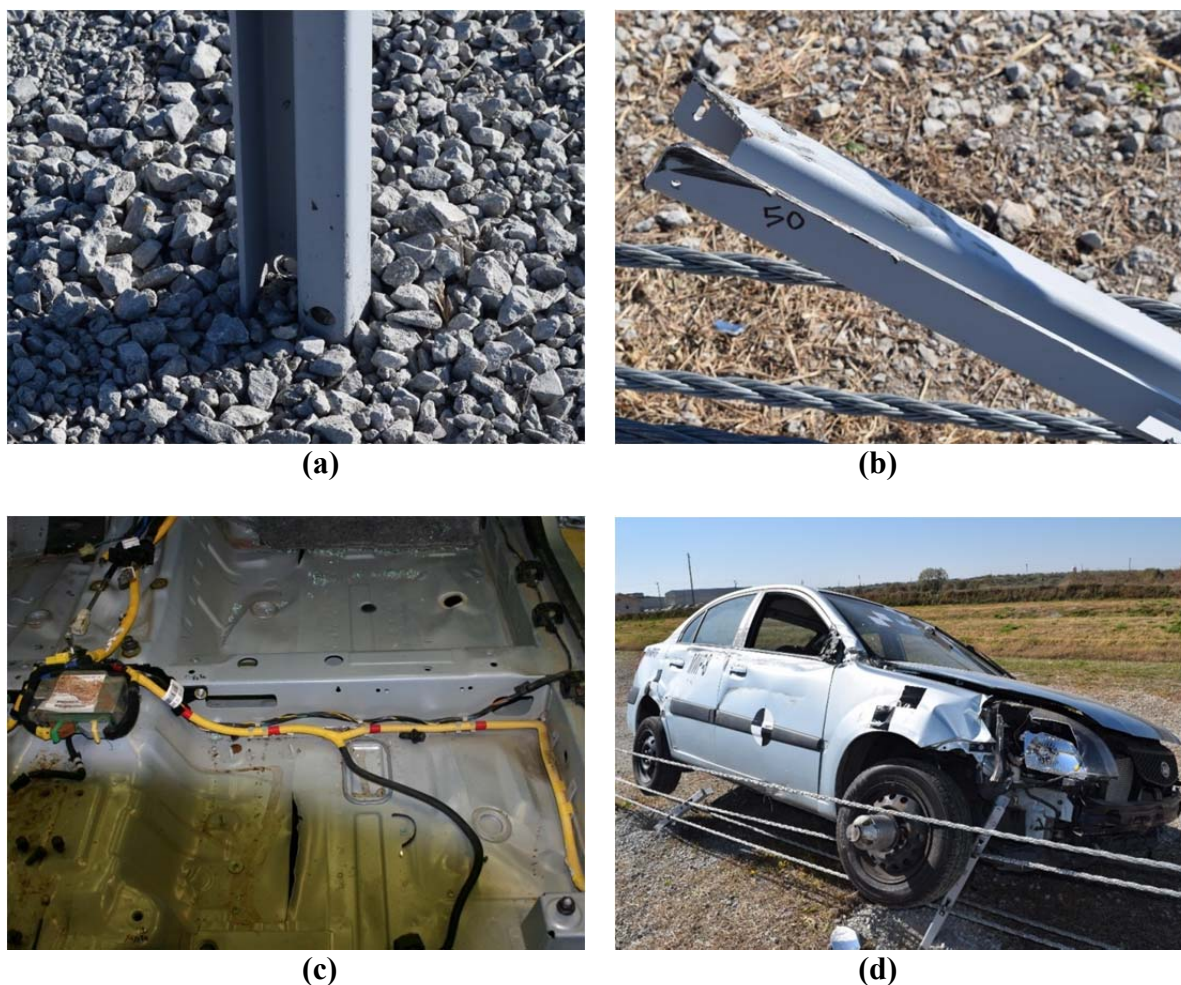


FIGURE 6 Test No. MWP-8: (a) Weakening Holes; (b) Post No. 50 Penetration Marks; (c) Floor Pan Tears; and (d) Vehicle Damage.

post penetration still occurred, even with $\frac{3}{4}$ -in. diameter ground line holes placed in the short web segments. Thus, further investigation was necessary to explore other post modifications, including the initial ideas for treating free edges with edge protectors or caps.

Dynamic bogie testing was utilized to evaluate the effectiveness of prototype cap systems for mitigating floor pan tearing and post penetration during contact by free edges. The bogie testing setup consisted of a two-post configuration spaced 8 ft apart with a slight lateral offset from one another, as depicted in Figure 7(a). The target impact speed for the bogie was 25 mph, while impact angles were largely 0 degrees except for limited testing at -25 degrees. Further information on the test protocol, schematics of design modifications, and detailed results and findings are being compiled in a draft research report (15).

Several single-part cap systems (i.e., tube sections) were explored. However, the sizes of available tubes were incompatible with the MWP geometry and were believed to increase concerns for vehicle snag on a poorly-fitting, single-part cap system. Thus, a two-part cap system was configured for attachment to the top of MWPs, as depicted in Figures 7(b) and 7(c). For this concept, the existing V-notch at the top of the MWP was removed and replaced with the formed parts, creating V-notch for the upper cable and brass rod. Both top free edges of the MWP were

modified to include the removal of a $\frac{1}{8}$ -in. x $4\frac{3}{8}$ -in. strip of steel to enhance fit on the post and reduce snag concerns. Each folded part (i.e., U-shape) was fabricated with 7-gauge steel sheet conforming to ASTM A1011 HSLA Grade 50. The two U-shaped parts were attached to the top of the post using a single bolt and nut. A $\frac{1}{2}$ -in. diameter x 4-in. long ASTM A449 or A325 hex-head bolt was selected for use in the final design. In the component testing program, the two-part cap system was retained to the post, as shown in Figure 7(d), which mitigated floor pan tearing and post penetration. This design modification was recommended for further crash testing and evaluation under MASH TL-3 impact safety guidelines.

TEST DESIGNATION NO. 3-10 - CRASH TEST MWP-9 – POST CAP

The four-cable, median barrier system was modified following the unacceptable results observed in test no. MWP-8. Dynamic component testing was again used to investigate the effectiveness of an upper post cap to mitigate floor pan tearing and post penetration. Thus, the line posts,

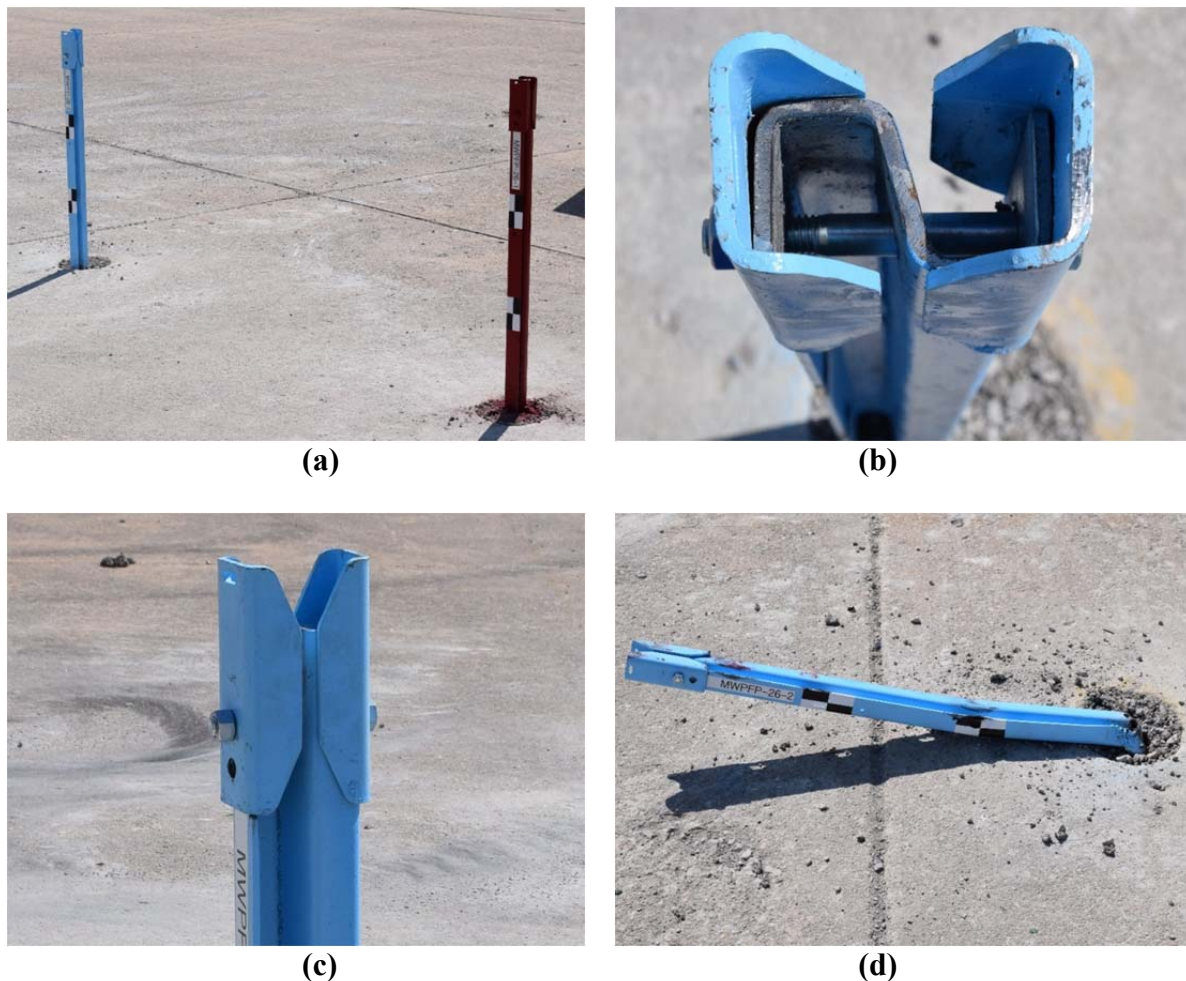


FIGURE 7 Phase II Dynamic Bogie Testing: (a) Two-Post Setup; (b) Two-Part Cap – Top View; (c) Two-Part Cap – Side View; and (d) Damaged Post with Cap System.

spaced on 8 ft centers, were modified to include a two-part post cap along with the two $\frac{3}{4}$ -in. diameter holes in the web at the ground line, as shown in Figure 8(a). Complete design details are provided by Lechtenberg et al (16).

Test no. MWP-9 was conducted with a 2,594-lb small car (1100C) at a speed of 63.1 mph and an angle of approximately 25.3 degrees. The target impact location was at a midspan location, or 4 ft upstream from a post. Moderate barrier damage was observed, consisting of disengaged cables as well as deformed and/or fractured posts, brackets, and brass rods. At its final resting position, the vehicle remained in contact with the cables. Cable nos. 1 and 3 were beneath the vehicle, while cable nos. 2 and 4 were on the impact side and non-impact side of the vehicle, respectively. Vehicle damage was largely moderate, primarily located on the front, left side, and right side of the vehicle. The front bumper, left and right headlights, left and right side mirrors, and left and right side panels were damaged. The left-side A-, B-, and C-pillars were gouged and deformed. More significant deformation occurred to the left-front A-pillar where cable nos. 3 and 4 deformed and locked into the support member during vehicle redirection. The front windshield was fractured on the drivers-side due to cable-contact and crushing of the A-pillar. The left side windows were shattered as well. Deformations, contact marks, creasing, and cutting of outer sheet metal cutting were observed around various body panels. Typical post damage, a retained two-part cap, and vehicle damage, including A-pillar, are shown in Figures 8(b) through 8(d). During the test, the small car was captured and redirected by cable nos. 2, 3, and 4. The vehicle remained stable throughout the impact event. No floor pan tearing or post penetration was observed during initial contact and exit from barrier. As the vehicle re-contacted the barrier farther downstream and overrode several line posts, no floor pan tearing or post penetration was observed. The maximum occupant compartment deformation was 3.4 in. at the left-side A-pillar in the lateral direction. The occupant impact velocities (OIVs) were -15.22 fps and 13.07 fps in the longitudinal and lateral directions, respectively. The maximum 0.010-sec occupant ridedown accelerations (ORAs) were -5.53 g's and -7.26 g's in the longitudinal and lateral directions, respectively. The maximum roll angle was 5.4 degrees. All occupant risk criteria were below the recommended MASH limits. The test vehicle remained upright during and after the collision. Vehicle roll, pitch, and yaw angular displacements were deemed acceptable. Although floor pan tearing and post penetration was mitigated, test no. MWP-9 was deemed unacceptable under the updated MASH TL-3 safety performance criteria due to excessive lateral deformation of the left-side A-pillar. A detailed discussion of the test results is provided by Lechtenberg et al (16).

SUMMARY, CONCLUSIONS, AND RECOMMENDATIONS

The primary objective was to investigate design modifications to mitigate floor pan tearing and post penetration into 1100C small passenger cars when impacting four-cable, median barrier systems supported by steel posts. Four full-scale vehicle crash tests (test designation no. 3-10) were performed with 1100C small passenger cars on prototype four-cable, median barrier systems under the TL-3 impact safety standards published in MASH 2009 (1) and the MASH Update (2). Test no. MWP-6 was conducted on a barrier system configured with MWPs spaced on 8 ft centers with cables vertically spaced at $7\frac{1}{2}$ in. and center heights for top and bottom cables of 38 in. and $15\frac{1}{2}$ in., respectively. During test no. MWP-6, free edges located at the top of overridden steel posts contacted and tore the floor pan, and penetrated the vehicle. All other

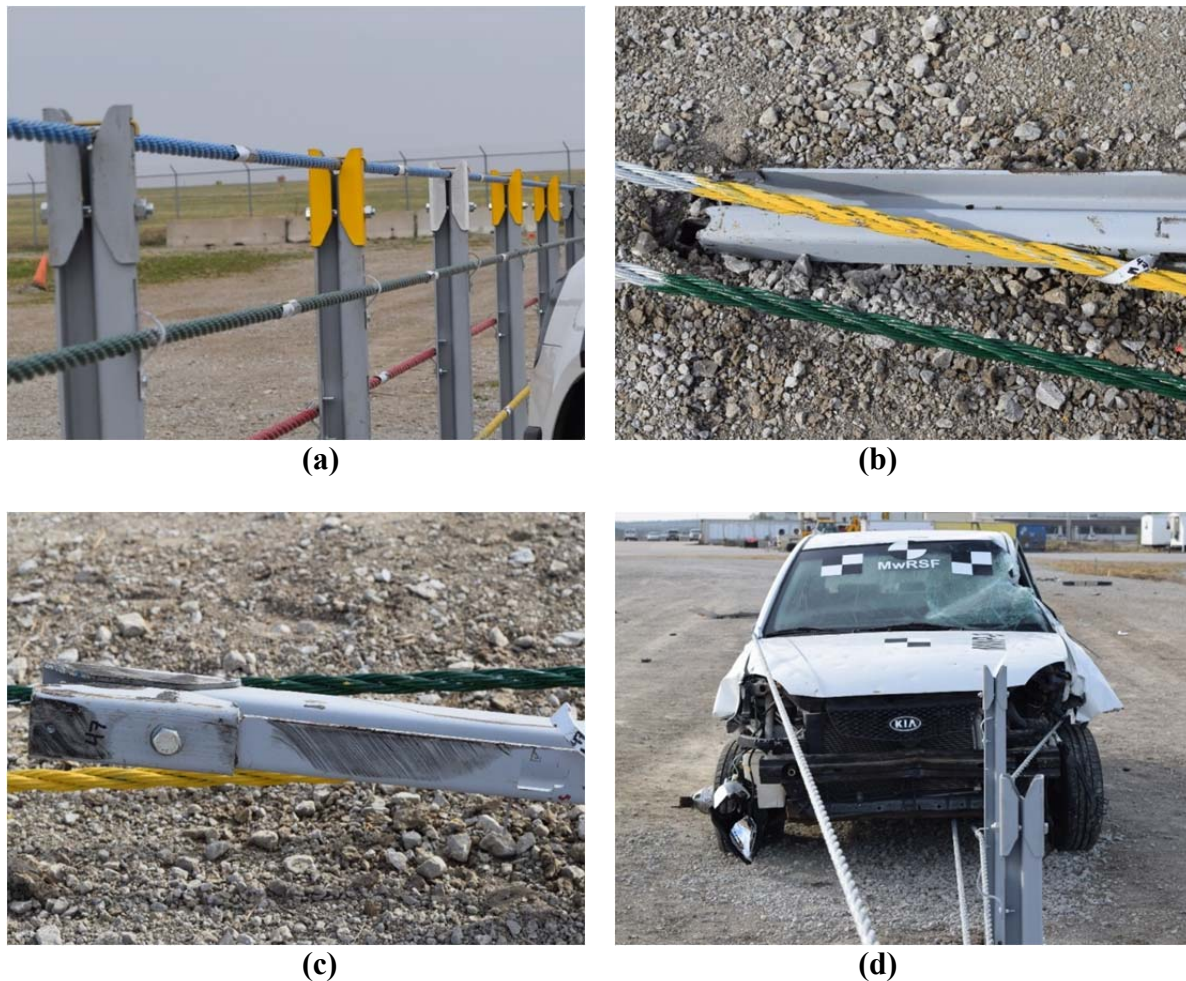


FIGURE 8 Test No. MWP-9: (a) Two-Part Cap System; (b) Partial Fracture at $\frac{3}{4}$ -in. Hole and Retained Cable No. 1; (c) Retained Cap with Contact Marks; and (d) Vehicle Damage.

safety performance criteria were met. Test no. MWP-6 was deemed unacceptable under the MASH TL-3 safety performance criteria.

Several design modifications were brainstormed to mitigate floor pan tearing and post penetration. These modifications included: (1) reducing weak-axis bending capacity of post to decrease upward force on floor pan with placement of weakening holes, reduction in material thickness, or changes cross-sectional geometry; (2) removing sharp corners at top of post with use of radii; (3) treating posts with edge rounding or hemming; (4) adding edge protectors to shield upper post region; (5) adding caps to cover end of post; and (6) selecting post without free edges. The placement of radii at the sharp, upper corners of post was selected to reduce stress concentration imparted to floor pan to eliminate tears. A $\frac{5}{8}$ -in. radius was added to the top free edges, and a $\frac{1}{4}$ -in. radius was added to the top corners of the V-notch.

Test no. MWP-7 was performed on the same system that was used in test no. MWP-6, except each upper corner of post incorporated a radius to eliminate sharp corners. During testing, steel posts were overridden, and free edges with radii tore the floor pan and penetrated the vehicle. All other safety performance criteria were met. Test no. MWP-7 was deemed unacceptable under the MASH TL-3 safety performance criteria.

A dynamic bogie testing program was initiated to further investigate design modifications. A bogie vehicle was configured with a surrogate floor pan to replicate Kia Rio 1100C small cars. Numerous post modifications were investigated, including edge rounding, edge protectors, and post weakening. From this effort, ground line weakening eliminated floor pan tearing and post penetration. Thus, post weakening was selected, consisting of one $\frac{3}{4}$ -in. diameter hole at the ground line in each short web segment. The modified MWP's contained radii at the top free edges and ground line weakening holes. Test no. MWP-8 was performed on the same system that was used in test nos. MWP-6 and MWP-7, except one $\frac{3}{4}$ -in. diameter hole was placed in each short web segment at ground line. For this test, neither floor pan tearing nor post penetration occurred during initial contact and exit from barrier. As the vehicle re-contacted and overrode the barrier farther downstream, the floor pan was torn and penetrated. All other safety performance criteria were met. Test no. MWP-8 was deemed unacceptable under the MASH TL-3 safety performance criteria.

A dynamic bogie testing program was again used to investigate design modifications, specifically the treatment of free edges with folded plate or caps. A two-part cap eliminated floor pan tearing and post penetration and deemed effective during later vehicle impacts into barrier when weakened posts do not easily bend over. The modified MWP's contained a two-part cap and ground line weakening holes. Test no. MWP-9 was performed on the same system that was used in test nos. MWP-6 through MWP-8, except for a few differences. First, the V-notch was removed from the top of the MWP, and a two-part cap was attached to the top of the posts. However, the new two-part cap system integrated a V-notch between the parts, which formed a slot for the upper cable. For this test, floor pan tearing and post penetration were not observed. The left-side A-pillar was laterally deformed 3.4 in., greater than the 3-in. limit. All other safety performance criteria were met. Although floor pan tearing and post penetration was eliminated with the two-part cap system and ground line weakening holes, test no. MWP-9 was deemed unacceptable under the updated MASH TL-3 safety performance criteria.

After incorporating several design modifications and conducting 1100C small car tests, floor pan tearing and post penetration was mitigated. With the number of changes, the benefits for using the folded MWP's may arguably have been lost, including ease of fabrication and economy. Thus, it may be beneficial to investigate a closed-section, rectangular tube or a rolled post that eliminates free edges. Test no. MWP-9 was captured by three cables, nos. 2, 3, and 4. The top two cables located at 30½ in. and 38 in. became interlocked with the left-side A-pillar. Further research is recommended to improve barrier performance and cable-to-post release with tall cable heights when subjected to 1100C impacts under test designation no. 3-10.

ACKNOWLEDGMENTS

The authors wish to acknowledge the Midwest States Pooled Fund Program for sponsoring this project as well as MwRSF personnel for constructing the prototype components and barrier systems as well as conducting dynamic component tests and full-scale crash tests.

DISCLAIMER

This paper was completed with funding from the Midwest States Pooled Fund Program and the Federal Highway Administration, U.S. Department of Transportation. The contents of this paper reflect the views and opinions of the authors who are responsible for the facts and the accuracy of the data presented herein. The contents do not necessarily reflect the official views or policies of the Midwest States Pooled Fund Program or the Federal Highway Administration, U.S. Department of Transportation. This paper does not constitute a standard, specification, regulation, product endorsement, or an endorsement of manufacturers.

REFERENCES

1. *Manual for Assessing Safety Hardware (MASH)*, American Association of State Highway and Transportation Officials (AASHTO), Washington, D.C., 2009.
2. *Manual for Assessing Safety Hardware (MASH) Update*, American Association of State Highway and Transportation Officials (AASHTO), Washington, D.C., Expected in 2016.
3. Johnson, E.A., Sicking, D.L., Faller, R.K., Lechtenberg, K.A., Rohde, J.R., Bielenberg, R.W., Reid, J.D., and Rosenbaugh, S.K., *Phase I Development of a Non-Proprietary, Four-Cable, High-Tension Median Barrier*, Final Report to Midwest States Pooled Fund Program, Transportation Research Report No. TRP-03-213-11, Midwest Roadside Safety Facility, University of Nebraska-Lincoln, December 28, 2011.
4. Schmidt, J.D., Sicking, D.L., Faller, R.K., Lechtenberg, K.A., Bielenberg, R.W., Reid, J.D., and Rosenbaugh, S.K., *Phase II Development of a Non-Proprietary, Four-Cable, High-Tension Median Barrier*, Final Report to Midwest States Pooled Fund Program, Transportation Research Report No. TRP-03-253-12, Midwest Roadside Safety Facility, University of Nebraska-Lincoln, March 21, 2012.
5. Kampschneider, L.R., Homan, D. H., Lechtenberg, K.A., Faller, R.K., Bielenberg, R.W., Sicking, D.L., Reid, J.D., and Rosenbaugh, S.K., *Evaluation of a Non-Proprietary, High-Tension, 4-Cable Median Barrier on Level Terrain*, Final Report to Midwest States Pooled Fund Program, Transportation Research Report No. TRP-03-258-12, Midwest Roadside Safety Facility, University of Nebraska-Lincoln, November 29, 2012.
6. Bligh, R.P. and Menges, W.L., *MASH TL-3 Testing and Evaluation of the Midwest Cable Median Barrier System*, Draft Report to National Cooperative Highway Research Program (NCHRP), Transportation Research Board, NCHRP Project No. 22-14(04), Test Report No. RF 47830-1, Texas A&M Transportation Institute, Texas A&M University, December 2011.
7. Bateman, R.J., Faller, R.K., Bielenberg, R.W., Sicking, D.L., Reid, J.D., Stolle, C.S., Lechtenberg, K.A., and Rosenbaugh, S.K., *Design of Cable-to-Post Attachments for use in Non-Proprietary, High-Tension, Cable Median Barrier*, Final Report to Midwest States Pooled Fund Program, Transportation Research Report No. TRP-03-285-13, Midwest Roadside Safety Facility, University of Nebraska-Lincoln, August 29, 2013.
8. Mongiardini, M., Faller, R.K., Rosenbaugh, S.K., and Reid, J.D., *Test Matrices for Evaluating Cable Median Barriers Placed in V-Ditches*, Final Report to Midwest States Pooled Fund Program, Transportation Research Report No. TRP-03-265-12, Midwest Roadside Safety Facility, University of Nebraska-Lincoln, July 13, 2012.
9. Rosenbaugh, S.K., Bielenberg, R.W., Humphrey, B.M., Faller, R.K., Reid, J.D., and Lechtenberg, K.A., *Cable-to-Post Attachments for Use in Non-Proprietary, High-Tension, Cable Median Barrier, Phase II*, Final Report to Midwest States Pooled Fund Program, Transportation Research Report No. TRP-03-313-15, Midwest Roadside Safety Facility, University of Nebraska-Lincoln, June 2, 2015.
10. Bielenberg, R.W., Schmidt, T.L., Faller, R.K., Lechtenberg, K.A., Rosenbaugh, S.K., Reid, J.D., and Sicking, D.L., *Design of an Improved Post for Use in a Non-Proprietary, High-Tension, Cable*

- Median Barrier*, Final Report to Midwest States Pooled Fund Program, Transportation Research Report No. TRP-03-286-14, Midwest Roadside Safety Facility, University of Nebraska-Lincoln, May 7, 2015.
11. Bielenberg, R.W., Rosenbaugh, S.K., Faller, R.K., Humphrey, B.M., Schmidt, T.L., Lechtenberg, K.A., and Reid, J.D., *MASH Test Nos. 3-17 and 3-11 on a Non-Proprietary Cable Median Barrier*, Final Report to Midwest States Pooled Fund Program, Transportation Research Report No. TRP-03-303-15, Midwest Roadside Safety Facility, University of Nebraska-Lincoln, November 3, 2015.
 12. Kohtz, J.E., Bielenberg, R.W., Rosenbaugh, S.K., Faller, R.K., Lechtenberg, K.A., and Reid, J.D., *MASH Test Nos. 3-11 and 3-10 on a Non-Proprietary Cable Median Barrier*, Report to Midwest States Pooled Fund Program, Transportation Research Report No. TRP-03-327-16, Midwest Roadside Safety Facility, University of Nebraska-Lincoln, January 21, 2016.
 13. Rosenbaugh, S.K., Hartwell, J.A., Bielenberg, R.W., Faller, R.K., Holloway, J.C., and Lechtenberg, K.A., *Evaluation of Floor Pan Tearing and Cable Splices for Cable Barrier Systems*, Draft Report to Midwest States Pooled Fund Program, Transportation Research Report No. TRP-03-324-16, Midwest Roadside Safety Facility, University of Nebraska-Lincoln, In Progress, 2017.
 14. Hartwell, J.A., Bielenberg, R.W., Rosenbaugh, S.K., Faller, R.K., Lechtenberg, K.A., and Reid, J.D., *MASH Test No. 3-10 on a Non-Proprietary, High-Tension Cable Median Barrier for Use in 6H:1V V-Ditch*, Draft Report to Midwest States Pooled Fund Program, Transportation Research Report No. TRP-03-331-16, Midwest Roadside Safety Facility, University of Nebraska-Lincoln, In Progress, 2017.
 15. Lechtenberg, K.A., Rosenbaugh, S.K., Bielenberg, R.W., Faller, R.K., Schmidt, J.D., Stolle, C.S., Holloway, J.C., and Pajouh, M.A., *Phase II Evaluation of Floor Pan Tearing for Cable Barrier Systems*, Draft Report to Midwest States Pooled Fund Program, Transportation Research Report No. TRP-03-359-17, Midwest Roadside Safety Facility, University of Nebraska-Lincoln, In Progress, 2017.
 16. Lechtenberg, K.A., Bielenberg, R.W., Rosenbaugh, S.K., Faller, R.K., and Reid, J.D., *MASH Test No. 3-10 (MWP-9) on a Non-Proprietary, High-Tension Cable Median Barrier for Use in 6H:1V V-Ditch*, Draft Report to Midwest States Pooled Fund Program, Transportation Research Report No. TRP-03-360-17, Midwest Roadside Safety Facility, University of Nebraska-Lincoln, In Progress, 2017.

Recommended Updates to MASH for the Testing of Cable Barrier Systems

SCOTT K. ROSENBAUGH

RONALD K. FALLER

ROBERT W. BIELENBERG

*Midwest Roadside Safety Facility
University of Nebraska–Lincoln*

ROGER P. BLIGH

*Texas A&M Transportation Institute
Texas A&M University*

MARIO MONGIARDINI

*Transport and Road Safety
University of New South Wales*

Cable barriers are unique vehicle barrier systems in terms of their function and intended use. Instead of utilizing a singular rail element like typical W-beam, thrie-beam or box beam guardrail systems, cable barriers utilize a number of longitudinal cables spaced vertically along the height of the barrier in which to capture and redirect errant vehicles. Thus, the interactions between vehicles and cable barriers is significantly different from that standard guardrail. Additionally, cable barriers are commonly utilized on sloped roadsides and within depressed medians, and system performance can be greatly affected if the impact vehicle is traversing across sloped terrain. However, despite these unique features, the testing and evaluation of cable barrier devices has largely remained identical to the evaluation of other longitudinal barrier systems.

After studying the behavior and performance characteristics of cable barriers, recommendations were made to improve the testing criteria of cable barriers. Critical system orientations and configurations were identified in order to test the actual worst case scenario impacts into these barriers. Further, additional crash tests were recommended for inclusion into the testing matrix for cable barriers intended for use on sloped terrain and in median ditches. The additional tests were developed to ensure cable barriers are robust enough to remain crashworthy within the various terrain in which they are commonly installed.

INTRODUCTION

Cable barriers are a relatively new type of vehicle barrier system compared to other roadside safety barriers such as W-beam guardrail or concrete barriers. Due to limited performance knowledge of these systems, the evaluation of cable barrier systems have largely consisted of the same full-scale testing matrix as other longitudinal barrier systems. Current safety standards found in the 2009 edition of the *Manual for Assessing Safety Hardware* (MASH) (1) require all longitudinal barrier systems be evaluated through oblique impacts to the system from both a small car and a pickup truck. The specific impact conditions for MASH Test Level 3 (TL-3) are

shown in Table 1. Higher performance criteria (e.g., TL-4 or TL-5) call for larger and heavier trucks, but cable barrier systems are seldom designed or utilized to capture and redirect heavy trucks. Thus, most cable barrier systems are designed and evaluated to satisfy TL-3 safety criteria.

MASH does specify a few test conditions unique for cable systems. Recognizing that the performance of flexible barriers can be sensitive to installation length, cable barriers are required to be evaluated with minimum system lengths of 600 ft, compared to only 175 ft for W-beam guardrail systems. Additionally, MASH identifies critical impact points unique to cable barriers, as listed in Table 1. The critical impact point (CIP) for small cars is mid-span between adjacent posts in order to maximize the potential for penetration through the system, while the CIP for pickup trucks is 12 in. upstream from a post. Vehicle impacts at post locations will often result in the post pushing down any cables located on the backside of the post, making it more likely for the vehicle to override the system. Thus, impacting just upstream of a post represents a worst-case-scenario for vehicle containment.

Unfortunately, MASH 2009 specifies little else in terms of evaluating cable barrier systems even though their performance and intended use differs greatly from other guardrail systems. Cable systems are more flexible than W-beam or thrie-beam systems, thereby allowing higher system deflections and working widths. Further, vehicles impacting cable barriers tend to remain in contact with the system longer and impact more system posts than vehicles impacting semi-rigid guardrail systems. These characteristics should be considered when testing and evaluating cable barrier systems. Additionally, cable barriers are commonly utilized in depressed roadway medians as opposed to on level terrain. System performance can be greatly affected if the impacting vehicle is traversing across sloped terrain. However, MASH 2009 does not require cable barriers to be tested and evaluated on sloped terrain.

This paper takes a closer look at the performance of cable barrier systems and the mechanisms that make them unique from other vehicle barrier systems. A combination of data from real-world accident reports, full-scale testing, and simulation analysis was utilized to identify trends and inherent weaknesses in cable barriers. Finally, recommendations were made concerning the future testing and evaluation of cable barrier systems

TABLE 1 MASH TL-3 Crash Test Conditions for Longitudinal Barriers

Test Article	Test Designation No.	Test Vehicle	Vehicle Weight (lb)	Impact Conditions		Critical Impact Point
				Speed (mph)	Angle, (deg.)	
Longitudinal Barrier	3-10	1100C	2,425	62	25	Mid-Span (Between Posts)
	3-11	2270P	5,000	62	25	12-in. Upstream of a Post

CRITICAL VEHICLE SELECTION

MASH requires longitudinal barrier systems to be tested and evaluated through impacts with two different passenger vehicles, the 1100C small car and the 2270P pickup truck. The 2,420-lb small car was selected to represent the 2nd percentile lightest passenger vehicle, while the 5,000-lb pickup truck represents the 90th percentile heaviest passenger vehicle. Barrier systems that safely contain and redirect vehicles representing both the lower and upper ends of passenger vehicle sizes are assumed to be crashworthy for all vehicles in between.

Unfortunately, recent studies of vehicle impacts into cable barriers have indicated that system failures are associated more with mid-size and heavy sedans than any other vehicle types. Specifically, sedans were found to be the vehicle type most likely to penetrate through a cable barrier system (2-3). Sedans typically have narrow front profiles similar to those of 1100C small cars, which can be difficult for cable barriers to capture. However, due to their increased mass, sedans have more momentum and require higher redirective forces from a barrier system. This combination of narrow profile and increased inertia results in a vehicle that is harder to capture and more likely to penetrate through a cable barrier. Therefore, cable barriers should be subjected to impacts from sedans to evaluate the potential for vehicle penetration through the system.

MASH already has a mid-size sedan as one of its standard vehicles, the 3,300-lb 1500A sedan. This vehicle standard was originally designated for use in evaluating crash cushions and terminals. Fortunately, it falls in line with the vehicle type and weight associated with a high propensity for penetrating cable barriers. Thus, it is recommended that impacts from a 1500A vehicle be included in MASH evaluations of cable barrier systems. Evaluation with the 1500A should be conducted in a manner which maximizes the risk of vehicle penetration. Thus, the initial impact point should be at a mid-span location. Further, if the barrier is intended for use on sloped terrain (discussed more in the following section), the barrier should be placed at a position relative to the slope break point such that the front bumper impacts between adjacent cables with the largest vertical spacing, which maximizes the risk of penetration.

This new test recommendation is meant as an addition to the testing matrix and testing with the 1100C and 2270P should remain part of the evaluation of cable barriers. Small cars are more susceptible to vehicle instabilities and occupant compartment damage, while heavy pickups impart critical loads to the system components and cause higher deflections.

CRITICAL BARRIER PLACEMENT IN MEDIAN DITCHES

Cable barriers are often desired for placement on roadside slopes or within depressed medians. Vehicles traversing over sloped terrain can easily become airborne and be subjected to significant angular displacements. These changes to the vehicle height and orientation result in significantly different impact conditions for barriers installed on sloped terrain as compared to barriers installed on level terrain. Further, differences in impact conditions can greatly affect barrier performance. Therefore, cable median barriers should be evaluated on sloped terrain representative of the installation sites in which they are desired for use.

The most common usages of cable barriers on sloped terrain are within depressed medians. As such, a number of studies have been conducted to analyze the behavior of vehicles traveling through median ditches and to aid in the identification of critical barrier placements (4-

10). These studies utilized a combination of vehicle dynamics and computer simulations to track the location of the front bumper as the vehicle traversed across the median ditch. Many vehicle trajectories were created incorporating various vehicle types, impact conditions, a median geometries. Example bumper trajectories from five vehicles traversing through a median V-ditch are shown in Figure 1.

Although the individual trajectories varied depending on the specific vehicle type, impact conditions, and ditch geometry, three distinct areas of concern appeared in all of the simulations. First, the vehicles reached a peak height relative to the surface of the ditch as they were airborne over the front slope of the depressed median. The location of this phenomenon on the front slope is denoted as region A in Figure 1. As the vehicles return to the ground, the suspension is compressed and the vehicles reached a minimum height relative to the ditch, which is denoted as region B in Figure 1. Finally, the compressed suspension caused the vehicles to rebound or spring back upward. This rebounding effect, typically off of the back slope of the ditch, was typically accompanied with rapid changes to the vehicle pitch and roll orientations as well. The area in which the vehicle has significant height and angular displacements is denoted as region C in Figure 1.

As stated previously, vehicle trajectories and behaviors are dependent upon vehicle type, impact speeds, and ditch geometries. It would be unreasonable to evaluate a barrier system at each possible configuration of these variables, so worst case scenarios had to be identified for use in testing and evaluation. A full-scale crash test utilizing the 1500A vehicle to evaluate the risk of vehicle penetration has already been recommended herein. Thus, it was recommended that evaluation of cable median barriers placed in median ditches should utilize the typical MASH vehicles, the 1100C and 2270P, which have already been classified as critical representative vehicles.

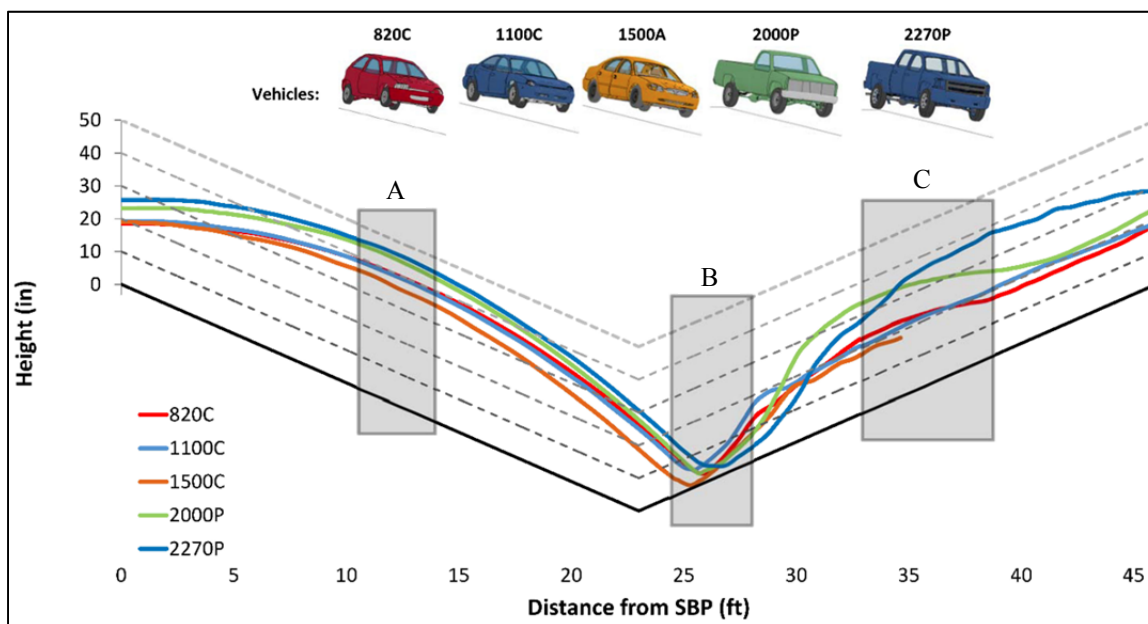


FIGURE 1 Bumper heights as vehicles traverse through a median V-ditch with highlighted regions indicating locations of concern.

Increasing the speed and angle in which the vehicle entered the median ditch resulted in more extreme values for the bumper height as the vehicle traversed the ditch (i.e., the maximum heights increased and the minimum heights decreased). Thus, higher speeds and angles were more critical, just as they are for typical longitudinal barrier performance. Therefore, it was recommended to utilize the same vehicle speed and angle prescribed by MASH when evaluating cable barriers in ditches, which were designed to represent a 97th percentile worst case impact. For TL-3 criteria, these correspond to 62 mph and 25 degrees, respectively. However, after contacting the ground within a ditch, the vehicle's speed and heading angle are often altered. If the barrier were located on the back side of the ditch, it is unlikely that the vehicle will impact the barrier under the same conditions in which it entered. Further, the changes to the speed and heading angle while traversing a median ditch are not easily predicted due to variance in soil strength, vehicle inertia, and suspension stiffness. Thus, it is recommended that the prescribed impact conditions be obtained just prior to the vehicle entering the median ditch.

Depressed medians can be formed in a wide variety of geometries characterized by general shape, width, depth, and side slopes. A review of cable median barrier installations within the United States found the most common median shape was V-shaped followed by flat bottom or trapezoidal shaped (6). Simulations of vehicles traversing these median shapes demonstrated that the more severe terrain change found at the bottom of a V-ditch resulted in greater deviations to the vehicle trajectory (10). Thus, it is recommended to test cable median barriers in V-ditches as the worst case scenario. Demonstration of barrier performance within a V-ditch should allow for use in different shaped medians of similar side slopes.

Studies have also been conducted to evaluate the critical side slope and width for V-ditches (4-6). As expected, steeper slopes resulted in increased vertical and angular displacements of the traversing vehicle. The most common side slope for median ditches has been 6:1, but roadway agencies desire and utilize 4:1 slopes as well (6). Thus, it was desired to utilize 4:1 side slopes when evaluating cable barriers in median ditches. However, due to the significant differences in vehicle behavior between traversing 6:1 and 4:1 V-ditches, some designers were not in favor of pushing beyond a 6:1 side slope. Thus, it was recommended to develop testing conditions for V-ditches with both 4:1 and 6:1 side slopes.

Multiple analyses have shown that the critical width of the V-ditch is dependent on the side slope. In general, the worst case for minimum bumper height and maximum rebound affects occurs when the airborne vehicle contacts the back side slope near the bottom of the ditch. Different slopes and their associated depths will result in different critical widths. Therefore, it is recommended to utilize the critical ditch widths of 30-ft and 46-ft when evaluating cable barriers intended for use in 6:1 and 4:1 V-ditches, respectively (4).

As shown in Figure 1, three different regions of concern had already been identified for barriers placed within median ditches. With the identification of the critical vehicles, impact conditions, and ditch geometries, additional analysis was conducted to determine the exact locations for critical barrier placement within median V-ditches. Region A had denoted were the vehicle would reach a maximum height above the surface of the V-ditch. Any airborne vehicle impacting a barrier system would be at risk for vehicle instabilities and possible rollover. In addition, airborne vehicles at their maximum trajectory height would be at risk to override the barrier. With these concerns in mind, it is recommended that impacts with both the 1100C and the 2270P vehicles be evaluated with the barrier located at the critical distances of 12 ft and 9 ft from the front slope break point (SBP) for 4:1 and 6:1 V-ditches, respectively.

Region B denoted where vehicles would impact the back slope of the barrier causing the suspension to compress and the vehicles to obtain their minimum height above the ground. It is at this location that a vehicle is at the greatest risk for penetrating the barrier by underriding the longitudinal cable elements. The front end of a small car is narrower and more likely to penetrate under a cable barrier than a pickup truck, so only the small car was determined to be critical to the evaluation of barrier underride. Because both critical ditch configurations cause the airborne vehicle to impact the back slope just beyond the bottom of the ditch, the critical location for minimum bumper height of the small car was identified as 4-ft up the back slope for both ditch configurations. Thus, it is recommended to conduct an 1100C impact into a median barrier located 4 ft up the back slope for both 4:1 and 6:1 V-ditches.

Region C denoted the area in which vehicles would rebound off the back slope, possibly become airborne again, and see rapid pitch and roll angular displacements. A number of full-scale tests have been conducted on various vehicles traversing through V-ditches that illustrate these vehicle behaviors (11). However, only one MASH crash test has been conducted with the vehicle traversing a V-ditch and impacting a cable barrier near the back SBP. During this test, the 1100C vehicle rebounded off the back slope of a 4:1 V-ditch and nearly overrode the 45-in. tall cable barrier (12). Until more full-scale crash testing has been conducted on under these conditions, testing and evaluations with both vehicle types is recommended to evaluate the performance of cable barriers on the back side of median ditches. Critical barrier placements for these recommended tests were selected as the location in which the front bumper reached its maximum height. For 4:1 V-ditches, this corresponded to 4 ft and 8 ft from the back SBP for the 1100C and 2270P vehicles, respectively. For 6:1 V-ditches, the critical barrier placements were 1 ft from the back SBP and at the back SBP, respectively.

The roadside safety industry has been discussing these recommended additional tests for cable barriers placed within depressed medians for years. As such, all six of the tests recommended herein have been assigned likely test designation numbers for use when they are implemented into the next version of MASH. Table 2 contains the complete testing matrix recommended for the evaluation of cable median barriers intended for use anywhere within 4:1 median V-ditches. The two original tests required by MASH for longitudinal barrier systems have remained part of the recommended test matrix to evaluate working width with the 2270P and vehicle stability and occupant compartment deformation with the 1100C. The critical barrier placements for these tests is also illustrated in Figure 2 for clarification purposes. Similarly, Table 3 contains the recommended testing matrix for evaluating cable median barriers intended for use anywhere within 6:1 median V-ditches. It is anticipated that a barrier system that passes all of the tests within one of these recommended test matrices will be crashworthy within any median ditch with shallower slopes. Thus, a barrier that satisfied the 4:1 V-ditch testing matrix may not be required to be tested within a 6:1 ditch.

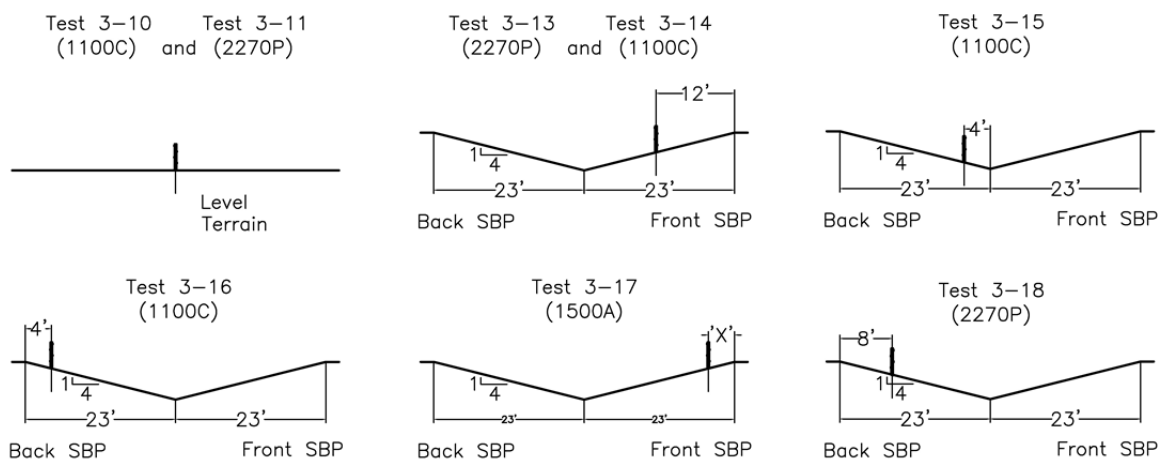
As opposed to placing a cable barrier anywhere within a median ditch, many designers have limited the placement of cable barriers to between 0 ft and 4 ft from the SBP. The evaluation of such barrier systems should be adjusted to reflect this placement limitation. Recommended tests 3-13 and 3-14 remain critical to evaluate vehicle capture and stability when the barrier is on sloped terrain. However, the critical barrier placement should be shifted to 4 ft from the front SBP to match the placement window. This applies for either of the ditch configurations. The rest of the test matrices can remain the same (with a few side notes). Barriers placed 4 ft from the back SBP within medians wider than 24 ft would not reside in regions of the ditch where underride is likely. Thus, test 3-15 would not be necessary to evaluate barrier

**TABLE 2 Recommended TL-3 Test Matrix for Median Barriers
Located Anywhere within 4:1 V-Ditches**

MASH Test No.	Vehicle Type	V-Ditch Width	Barrier Location	Critical Impact Point	Critical Evaluation Factors
3-10	1100C	NA	Level Terrain	Mid-Span Location	Vehicle Stability, Occupant Compartment Deformation, and Penetration
3-11	2270P	NA	Level Terrain	1 ft Upstream from Post	Working Width and Vehicle Stability
*3-13	2270P	46 ft	Front Slope: 12 ft from Front SBP	1 ft Upstream from Post	Vehicle Stability and Override
*3-14	1100C	46 ft	Front Slope: 12 ft from Front SBP	Mid-Span Location	Vehicle Stability and Override/Penetration
*3-15	1100C	46 ft	Back Slope: 4 ft from Ditch Bottom	Mid-Span Location	Underride and Occupant Compartment Deformation
*3-16	1100C	46 ft	Back Slope: 4 ft from Back SBP	Mid-Span Location	Vehicle Stability and Rebound Override/Penetration
*3-17	1500A	46 ft	Front Slope: **Variable	Mid-Span Location	Penetration and Occupant Compartment Deformation
*3-18	2270P	46 ft	Back Slope: 8 ft from Back SBP	1 ft Upstream from Post	Rebound Override and Vehicle Stability

* Test not specified in MASH 2009 but recommended for future evaluations

** Location dependent upon specific barrier configuration and cable heights



**FIGURE 2 Critical Median Barrier Locations within
4:1 V-Ditches, Impacts from Right Side.**

**TABLE 3 Recommended TL-3 Test Matrix for Cable Median
Barrier Located Anywhere within 6:1 V-Ditches**

MASH Test No.	Vehicle Type	V-Ditch Width	Barrier Location	Critical Impact Point	Critical Evaluation Factors
3-10	1100C	NA	Level Terrain	Mid-Span Location	Vehicle Stability, Occupant Compartment Deformation, and Penetration
3-11	2270P	NA	Level Terrain	1 ft Upstream from Post	Working Width and Vehicle Stability
*3-13	2270P	30 ft	Front Slope: 9 ft from Front SBP	1 ft Upstream from Post	Vehicle Stability and Override
*3-14	1100C	30 ft	Front Slope: 9 ft from Front SBP	Mid-Span Location	Vehicle Stability and Override/Penetration
*3-15	1100C	30 ft	Back Slope: 4 ft from Ditch Bottom	Mid-Span Location	Underride and Occupant Compartment Deformation
*3-16	1100C	30 ft	Back Slope: 1 ft from Back SBP	Mid-Span Location	Vehicle Stability and Rebound Override/Penetration
*3-17	1500A	30 ft	Front Slope: **Variable	Mid-Span Location	Penetration and Occupant Compartment Deformation
*3-18	2270P	30 ft	Back Slope: Back SBP	1 ft Upstream from Post	Rebound Override and Vehicle Stability

* Test not specified in MASH 2009 but recommended for future evaluations

** Location dependent upon specific barrier configuration and cable heights

performance. Additionally, test 3-18 would still be considered critical for barriers offset 4 ft from the back SBP in 4:1 ditches with a slightly reduced width. However, instead of requiring the construction of two different ditches, the testing facility can utilize the same 46 ft wide ditch and conservatively test at the originally specified location, 8 ft from the back SBP.

Finally, some median locations call for dual barrier systems, one located along each side, to prevent vehicles from entering the median and impacting hazards therein. Cable median barriers intended for such use would not be subjected to impacts from the opposing side of the median. Thus, only tests 3-10, 3-11, 3-13, 3-14, and 3-17 would be recommended for evaluating cable barriers intended for use as a dual barrier system. The same testing requirement would apply for cable barriers intended for use on sloped roadsides.

CRITICAL BARRIER ORIENTATION

Cable barriers typically utilize three or more longitudinal cable elements in which to capture and redirect errant vehicles. Since median barriers can be impacted on either side of the system, the

side of the post in which the cables are attached may differ between the individual cables or may vary from post to post if weaving is incorporated. This is a characteristic unique to cable median barriers and it can have a drastic effect in the performance of the system

Cables located on the back side of the post have the propensity to be pushed down by the post as it rotates backward. Subsequently, these cables are prevented from capturing the vehicle and the risk of vehicle override is maximized. Examples of this behavior are shown in Figure 3. This behavior is the reason that MASH requires test 3-11 with the 2270P pickup truck to be conducted with the initial impact point located 12 in. upstream from a post.

Due to their location between opposing lanes of traffic, cable median barriers must be crashworthy for impacts on either side of the system. Thus, it is recommended that cable median barriers be evaluated in a critical orientation with the primary capture cable located on the back side of the posts. For barrier designs that incorporate weaving of the cables around adjacent posts, the primary capture cable should be located on the back side of the first post downstream of impact.

In addition to the potential for vehicle override during pickup truck impacts, this barrier orientation may also be critical for small car and sedan impacts as well. Cables located on the backside of a post must rely on the strength of the cable-to-post attachment hardware to provide the lateral restraint forces necessary to redirect the vehicle, while cables located on the front of a post can bear directly against the post. Orienting a barrier such that the capture cables are located on the back side of the post will critically load the cable attachment hardware and may result in increased system deflections and working widths. Therefore, it is recommended that cable barriers be oriented with the primary capture cable located on the back side of posts for all evaluation tests required by MASH.

Vehicles impacting cable barriers are typically captured and redirected by cables located between the front bumper and the headlight. However, cables located near the lower end of this window have an increased propensity to be forced downward and eventually overridden as they interact with a rotating front tire. Thus, the primary capture cable is identified as the highest cable located between the mid-height of the front bumper and the mid-height of the headlight. This capture window is shown in Figure 4 for both small cars and pickup trucks. If no cable is located within this critical region, the next cable above the critical region should be considered the primary capture cable. When the barrier is located on sloped terrain or within a median ditch, it is recommended to determine the height change of the vehicle relative to the ground line utilizing either analytical methods or existing simulated trajectories (4).

CRITICAL POST SPACING

Cable barrier systems are often developed to accommodate a range of acceptable post spacings. Although testing a barrier system at only a single post spacing will not determine the crashworthiness of the system at other post spacings, it is impractical to conduct the MASH crash testing matrix, including the additional tests recommended herein, at each post-spacing alternative intended for use with the barrier. Therefore, a critical post spacing should be utilized during each of the full-scale crash tests.

It is recommended that the critical post spacing be determined based on critical evaluation factors for a specific test. In general, the narrowest intended post spacing should be utilized for tests where vehicle stability is critical since interactions with more posts will likely



Top cable on back side of post



3rd cable on back side of post



Top cable pushed down by post



3rd cable pushed down by post



Tire overrode top cable



Tire overrode 1st and 3rd cable



Vehicle overrode barrier



Vehicle redirected by 2nd and 4th cables

FIGURE 3 Examples of vehicles overriding cables located on the backside of the support posts.

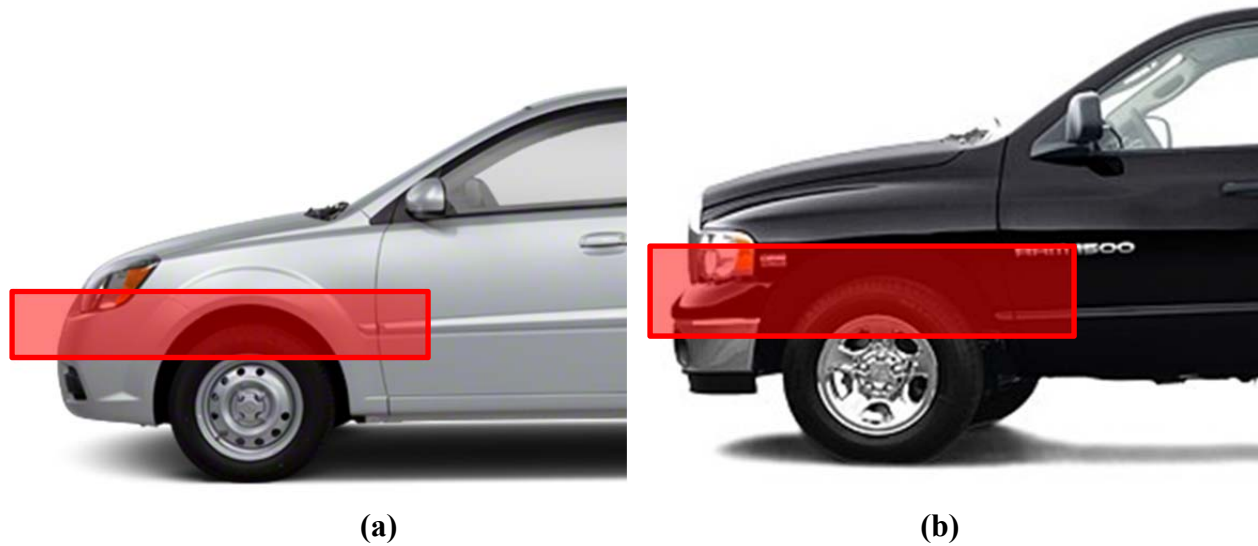


FIGURE 4 Critical capture region for (a) small cars and (b) pickup trucks.

maximize vehicle instabilities. In contrast, the widest intended post spacing should be utilized for tests where vehicle capture is deemed critical to minimize the support to the cables and maximize the changes of vehicle penetration, override, or underride. Table 4 lists the recommended post spacing for each MASH test, including all additional tests recommended herein. Note, it is recommended to conduct MASH test 3-11 utilizing both the narrowest and the widest post spacing in order to determine the working width of the system for both post-spacing configurations. Thus, a variable-post spacing system would require a total of nine tests to complete the testing matrix.

CONCLUSIONS AND RECOMMENDATIONS

Cable barriers are unique from other vehicle barrier systems in terms of components, function, and intended use. As such, the testing matrices utilized to evaluate cable barriers need to be uniquely tailored to match their performance demands. The additional crash tests introduced herein were developed to ensure cable barriers are robust enough to remain crashworthy under the strenuous circumstances in which they are commonly installed. Therefore, it is recommended to include these testing matrices and barrier configuration requirements within the next update to MASH.

Although this paper focused entirely on cable barriers, some of the testing recommendations may be applicable to the evaluation of future systems or systems placed within median ditches. For example, the recommended barrier placements to evaluate override and underride potential may apply to W-beam guardrail placed within depressed medians. It is recognized that various barrier types behave differently depending on their materials and configurations, so the testing recommendations presented herein should not be universally applied to all new barrier types. However, similar processes and methodologies could be utilized to identify critical placements, orientations, vehicles, and full-scale tests for the evaluation of future barriers.

TABLE 4 Recommended Critical Post Spacing for Evaluation of Cable Barriers

MASH Test No.	Vehicle	Barrier Position	Critical Evaluation Factors	Post Spacing
3-10	1100C	Level Terrain	Vehicle Stability, Occupant Compartment Deformation, and Penetration	Narrowest
3-11	2270P	Level Terrain	Working Width and Vehicle Stability	Both
*3-13	2270P	Ditch Front Slope	Vehicle Stability and Override	Narrowest
*3-14-	1100C	Ditch Front Slope	Vehicle Stability and Override/Penetration	Narrowest
*3-15-	1100C	Ditch Back Slope	Underride and Occupant Compartment Deformation	Widest
*3-16	1100C	Ditch Back Slope	Vehicle Stability and Rebound Override/Penetration	Narrowest
*3-17	1500A	Ditch Front Slope	Penetration and Occupant Compartment Deformation	Widest
*3-18	2270P	Ditch Back Slope	Rebound Override and Vehicle Stability	Widest

* Test not specified in MASH 2009 but recommended for future evaluations

REFERENCES

1. *Manual for Assessing Safety Hardware (MASH)*, American Association of State Highway and Transportation Officials (AASHTO), Washington, D.C., 2009.
2. Stolle, C.S., *Cable Median Barrier Failure Analysis and Remediation*. PhD Dissertation. University of Nebraska-Lincoln, Lincoln, Nebraska, December 2012.
3. Stolle, C.S., and D.L. Sicking, *Cable Barrier Failure Analysis and Prevention*, Research Report No. TRP-03-275-12, Midwest Roadside Safety Facility, University of Nebraska-Lincoln, Lincoln, NE, December 17, 2012.
4. Mongiardini, M., R.L. Faller, S.K. Rosenbaugh., and J.D. Reid, *Test Matrices for Evaluating Cable Median Barriers Placed in V-Ditches*, Research Report No. TRP-03-265-12, Midwest Roadside Safety Facility, University of Nebraska-Lincoln, Lincoln, NE, July 13, 2012.
5. Haque, F., and N.S. Sheikh, *Vehicle Dynamics Analysis of MASH Pickup and Small Car Traversal Through Symmetric V-Ditch*, Texas A&M Transportation Institute, Texas A&M University, College Station, TX, September 2013.
6. Marzougui, D., U. Mahadevaiah, F. Tahan, C.D. Kan, R. McGinnis, and R. Powers, *Development of Guidance for the Selection, Use, and Maintenance of Cable Barrier Systems*, National Cooperative Highway Research Program (NCHRP) Report No. 711, Transportation Research Board of the National Academies, Washington D.C., 2012.
7. Marzougui, D., C.D. Kan, and K.S. Opiela, *Further Considerations for Effective Median Barrier Lateral Placement for Varying Highway Cross Sections*, Journal of the Transportation Research Board, pp 63-77, Issue 2437, Washington DC, 2014.

8. Marzougui, D., C.D. Kan, and K.S. Opiela, *Vehicle Dynamics Investigations to Develop Guidelines for Crash Testing Cable Barriers on Sloped Surfaces*, Working Paper NCAC 2010-W-009, National Crash Analysis Center, George Washington University, Ashburn, Virginia, August 2010.
9. Karcher, J., *Vehicle Dynamics Modeling and Simulation for the Safety Evaluation, Selection, and Placement of Cable Barrier Systems*, Master's Thesis, The George Washington University, 2009.
10. Marzougui, D., C.D. Kan, and K.S. Opiela, *Evaluation of the Influences of Cable Barrier Design and Placement on Vehicle to Barrier Interface*, NCAC Document 2008-W-001, National Crash Analysis Center, George Washington University, Washington, D.C., 2008.
11. Marzougui, D., K.S. Opiela, C.C. Story, C.D. Kan, and E. Arispe, *Testing and Analysis of Sloped Terrain Effects on Vehicle Trajectories and Kinematics*, Internal Report, National Crash Analysis Center, George Mason University, Washington, D.C., 2014.
12. Bligh, R.P., and W.L. Menges, *MASH TL-3 Testing and Evaluation of the Midwest Cable Median Barrier*, Test Report No. 478730-1, Project No. 22-14(04), Texas A&M Transportation Institute, Texas A&M University, College Station, TX, December 2011.

Comparison of Human Occupant Kinematics in Laboratory Impact and Run-Off-Road Crash Configurations

RUDOLF REICHERT
CING-DAO (STEVE) KAN
DHAIFER MARZOUGUI
KENNETH OPIELA

George Mason University Center for Collision Safety and Analysis

An increasing number of passive safety requirements resulted in major improvements in vehicle safety. Advances in roadside hardware designs, road infrastructure, and crash avoidance systems have also improved road safety over the years. Despite these efforts, over 17,000 people are killed annually in roadway departure crashes in the United States [1]. The first step in the effort to reduce fatalities and serious injuries in run-off-road crashes is to evaluate occupant kinematics and occupant interactions. Current laboratory crash tests evaluate near-side occupants only. Current roadside hardware tests and simulations often do not include analysis of occupant kinematics despite the fact that well-validated dummy and human occupant models exist.

A mid-size sedan vehicle is equipped with human occupant models on the driver and passenger side and furnished with relevant restraint systems. Using this integrated occupant-vehicle model, occupant kinematics and interactions are first evaluated for laboratory side impact crash configurations. The same model is then exercised in a roadside hardware configuration, where the vehicle hits a New Jersey (NJ) barrier at a 25 degree angle.

This paper describes the methodologies used to conduct the integrated occupant-vehicle simulations. It provides insight into two areas that are not the main focus of today's vehicle and roadside hardware developments: [1] the evaluation of both near-side and far-side occupant, and [2] occupant kinematics and interactions during run-off-road accidents compared to laboratory impacts.

INTRODUCTION

An increasing number of passive safety regulations and consumer information requirements, such as Federal Motor Vehicle Safety Standard (FMVSS) requirements, New Car Assessment Program (NCAP) and Insurance Institute for Highway Safety (IIHS) ratings, resulted in major advances in vehicle structure integrity, safer interior vehicle designs, and advanced restraint systems. Advances in roadside hardware designs using the Manual for Assessing Safety Hardware (MASH) [2], road infrastructure, and crash avoidance systems have also improved road safety over the years. The fatality rate, which describes the number of fatalities per 100 million miles traveled, decreased from 5.39 in 1964 to 1.1 in 2013 [3]. Despite these efforts, over 17,000 people are killed annually in roadway departure crashes in the United States (U.S.), and many more in other countries [1]. The first step in the effort to reduce fatalities and serious injuries in run-off-road crashes is to evaluate occupant kinematics and occupant interactions. Current laboratory crash tests assess frontal and side impact configurations with near-side occupants only. Current roadside hardware tests and simulations often do not include analysis of occupant kinematics.

In addition to anthropomorphic test devices (ATD), which are a standard measuring device for assessing injury risk, well-validated human occupant models, such as Toyota's Total Human Model for Safety (THUMS) and the Global Human Body Model (GHBM), exist.

In this paper, a mid-size sedan vehicle is equipped with human occupant models on the driver and front passenger sides and furnished with relevant restraint systems. Near side occupant position refers to the seating position on the struck side and far side occupant refers to the seating position on the non-struck side of the vehicle. The structural vehicle model has been validated using full scale crash test results from various frontal, side, and roof crash configurations. Using this integrated occupant-vehicle model, occupant kinematics and interactions are first evaluated for two laboratory side impact crash configurations, where the vehicle hits a stationary rigid pole laterally at a 90 degree and 75 degree angle, respectively. The pole is aligned with the center of gravity of the near-side occupant. These configurations represent an accident where a vehicle strikes a tree, for example, in a run-off-road crash. In addition, the same integrated simulation model with human occupant models seated on the front driver and front passenger seats is used to evaluate a roadside hardware configuration where the vehicle travels at a speed of 100 km/h and hits a New Jersey barrier at an angle of 25 degrees. Occupant kinematics, interactions between near-side and far-side occupants, and occupant interactions with the vehicle are analyzed and compared for the selected impact configurations.

The conducted analysis explains the methodologies used to conduct the integrated occupant-vehicle crash analysis using human occupant models. It provides insight into two areas which are not in the main focus in today's vehicle and roadside hardware developments: [1] the evaluation of both near-side and far-side occupants and their potential interactions, and [2] insight into occupant kinematics and occupant-to-vehicle interactions in run-off-road and roadside hardware impact configurations.

RELATED WORK

Integrated occupant-vehicle simulation is a state-of-the-art technique in vehicle and restraint system development to evaluate injury risk and improve passive safety in laboratory crash test configurations using dummy models [4]. Furthermore, well-validated human occupant models have been shown to be capable of replicating and predicting injury risk in real world accident configurations [5].

The use of finite element simulation has become a valuable tool to evaluate roadside hardware devices under National Cooperative Highway Research Program (NCHRP) and MASH [6]. In the past, detailed occupant and restraints system models have generally not been included in such analysis.

Accident data analysis shows that about 34% of MAIS 3+ injuries in side crashes occur in far-side crashes, i.e. where occupants were seated on the non-struck side during an impact [7]. The Abbreviated Injury Scale (AIS) describes the severity of injuries ranging from minor (AIS 1), moderate (AIS 2), serious (AIS 3), severe (AIS 4), critical (AIS 5) to fatal (AIS 6) [8]. Furthermore, accurate prediction of occupant head kinematics is critical for better understanding of injury mechanisms in side impacts, especially for far-side occupants [9]. Many research studies evaluate injury risk of far-side occupants in absence of near-side occupants [10].

Despite the fact that all necessary tools and models exist, it can be concluded that more research needs to be conducted using detailed human occupant models on both near-side and

far-side seating positions in run-off-road configurations, in comparison with laboratory crash test load cases. The results presented in this paper combine traditional integrated occupant-vehicle simulation techniques with the use of validated human occupant models in run-off-road impact configurations to gain insight into potential injury risk in such impact events.

METHODS

The methodology used to conduct the research presented in this paper is outlined in this section. This includes the description of the integrated occupant-vehicle simulation technique using modular LS-DYNA input decks, the reverse engineering process for developing detailed vehicle models and relevant restraints, the validation methodology used, and a brief description of the THUMS human occupant model.

Integrated Occupant-Vehicle Simulation

The integrated occupant-vehicle simulation method used to conduct the research described in this paper is shown in Figure 1. The modular simulation model structure takes advantage of the available “*INCLUDE” option within LS-DYNA [11]. Vehicle model, driver and passenger occupant models, relevant restraint system models, the barrier model, and initial conditions for the respective crash configuration are defined in the main input deck. With this technique, the various components can be replaced or modified in an efficient manner without having to rebuild the entire integrated occupant-vehicle model. All simulations presented in this paper have been run with the nonlinear, explicit finite element code LS-DYNA with a minimum time-step of 0.7 microseconds using 16cpu on a high-performance computer system.

A so-called “seat squash” simulation is conducted to obtain a seat model that accounts for the deformation caused by the occupant. The deformed seat is integrated together with the occupant into the combined occupant-vehicle simulations.

“Belt fit” is used to place the seat belt around the occupants in the final seating positions. Driver and passenger seat belt models, including pre-tensioner and belt force limiter, run realistically through buckle and d-ring.

Appropriate contact definitions and friction parameters are used to ensure physically realistic interaction between components.

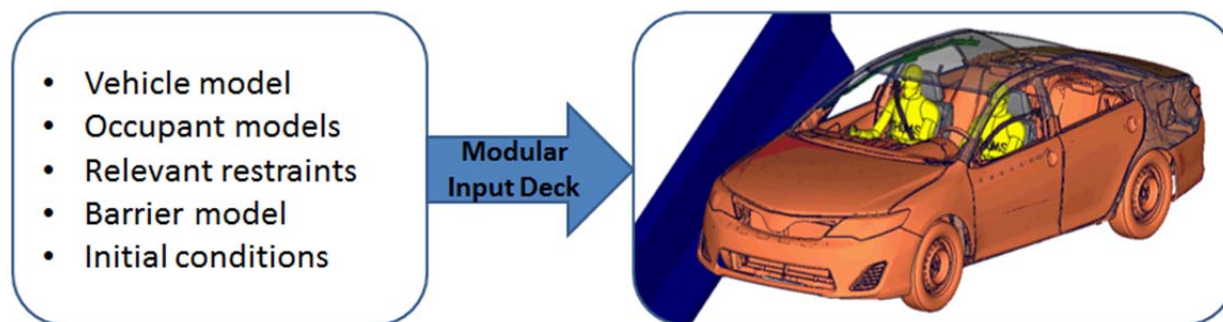


FIGURE 1 Integrated Occupant-Vehicle Model.

Model Development – Reverse Engineering Process

A reverse engineering process has been applied to develop the mid-size sedan vehicle model used in this research. A digitizing device has been used to scan all relevant components of the physical vehicle, including their internal structure. Accurate CAD surfaces and the respective finite element mesh of all components have been generated. Material thicknesses and mass distribution have been assigned to the individual parts and components, which are assembled using adequate connections according to the physical vehicle. Measured center of gravity (C.G.) location and inertial properties of the entire vehicle have been verified. Material property data for major structural parts was obtained by cutting specimens from the actual vehicle components and conducting material coupon tests. The model consists of 1086 parts and about 2.25 million nodes and elements. Additional details regarding the reverse engineering process, modeling approach, and validation process can be found in [12].

A similar reverse engineering methodology has been used to develop relevant airbag models. First, dimensions and folding patterns of the respective airbag are recorded. Second, the geometry of the unfolded airbag is digitized. Third, the flat airbag model is meshed, representing the so-called “reference geometry” in LS-DYNA. Fourth, the airbag is folded using OASYS Primer. The respective airbag model is implemented into the vehicle environment using additional pre-simulations. Fifth, the airbag deployment characteristics are evaluated with respect to numerical and physical validity. Finally, the airbag model is validated using available test data.

Validation Methodology

In order to validate the developed vehicle model, a variety of load cases, including frontal oblique impact configurations, side barrier, and side pole impacts have been configured and compared to respective full scale crash test results. First, a visual analysis of test pictures, test movies, and simulation animations was used to compare overall vehicle kinematics and crash characteristics. Time history data plots, in combination with test videos and simulation animations, were used to evaluate crash modes and structural energy absorption mechanisms.

The objective curve correlation software “CORA” (CORrelation and Analysis) was used to rate how well test and simulation results compare [13]. CORA was developed by the Partnership for Dummy technology and Biomechanics (PDB) and takes phase shift, size, and shape, as well as the comparison of values at each time increment, into account. Using these methods, an “objective rating” is given that indicates how well a curve (e.g., simulation) compares to a reference curve (e.g., test). Rating results range between 0 and 1, where 0 means no correlation and 1 means (close to) perfect correlation.

Human Occupant Model THUMS

The Total HUMAN Model for Safety (THUMS) [14] was used to conduct the integrated occupant-vehicle simulations presented in this paper. THUMS was developed by Toyota Motor Corporation and is distributed by Livermore Software Technology Corporation. It represents a 50th percentile adult male occupant with a height of 175 cm and a weight of 77 kg.

It enables simulation of human body kinematics and injury responses in vehicle crashes. The academic version 4.0, which contains all skeletal bones, structures, and internal organs,

consists of about 1.7 million elements and about 1,300 parts. The impact responses have been validated by Toyota for each body region using test data from the literature.

RESULTS

Correlation results between test and simulation for a 2012 Toyota Camry, which are the basis for the validity of the results presented in this paper, are exemplarily documented for oblique frontal impact configurations and for an oblique pole side impact load case in this section. The vehicle model conforms to MASH requirements for a “1500A” test vehicle. The validated vehicle model has been equipped with a THUMS 50th percentile human occupant model on the front driver and front passenger seats, both with relevant restraints. The resulting integrated occupant-vehicle model has been exercised in three different impact configurations.

First, results of a 90 degree pole side impact configuration, where the vehicle travels with a speed of 29 km/h laterally into a fixed rigid pole with a diameter of 254mm, are presented. According to the FMVSS testing protocol, the vehicle is oriented in such a way that the head C.G. of the near-side occupant is aligned with the center of the pole.

Second, results of a 75 degree oblique pole side impact configuration, where the vehicle travels with a speed of 32 km/h into a stationary rigid pole with a diameter of 254mm, are analyzed. The vehicle direction of travel is 75 degree lateral with respect to the vehicle longitudinal axis. According to the associated regulatory impact configuration, where the vehicle is positioned in the described manner on a so-called “flying floor”, vehicle and pole are positioned in such a way that the near-side occupant’s head C.G. aligns with the center of the pole.

Third, a New Jersey barrier frontal oblique impact configuration, which is generally used to assess roadside hardware according to MASH, is evaluated with the integrated occupant-vehicle model. The Toyota Camry travels with a speed of 100km/h in longitudinal vehicle direction and hits the New Jersey barrier at an angle of 25 degrees on the front right side of the vehicle in this load case.

Vehicle Model Validation

A detailed finite element model of a 2012 Toyota Camry was developed using the previously described reverse engineering process. The model consists of 2.25 million elements representing the geometry, thicknesses, material characteristics, and connections of all relevant structural, suspension, and interior components of the mid-size sedan. The model has gone through a thorough validation process using test results of 10 different frontal, side, and roof crush impact configurations (10).

As an example, validation results from the National Highway Traffic Safety Administration’s (NHTSA’s) left and right oblique frontal impact configuration are shown in Figure 2. A stationary Toyota Camry is impacted by a Research Moving Deformable Barrier (RMDB), which travels at a speed of 90 km/h into the front driver side and front passenger sides, respectively, in this test setup. The Toyota Camry was positioned with a 15 degree angle relative to the RMDB and impacted with a 35% overlap. Model year and engine type were the same in test and simulation. The vehicle weight of 1768 kg in the simulation compares well with 1758 kg in the

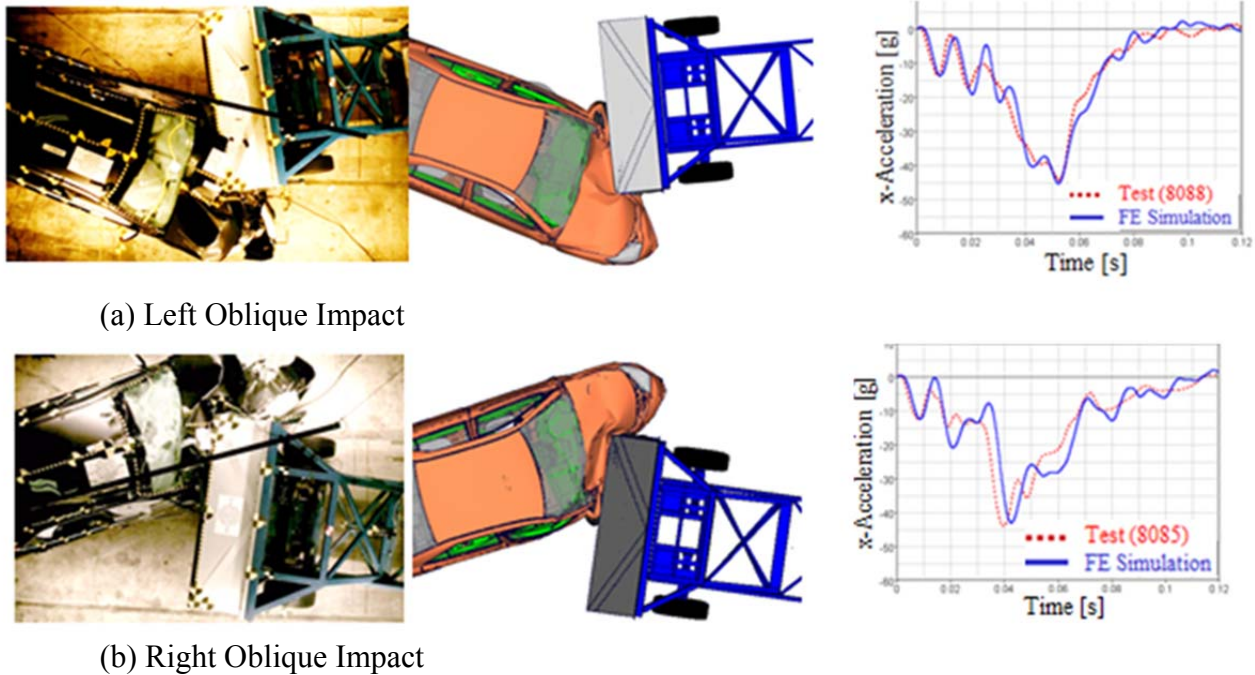


FIGURE 2 Test versus Simulation Results in (a) Left and (b) Right Oblique Impact

test. The C.G. location in the x direction, measured relative to the front axle, was 1252 mm in the test and 1247 mm in the simulation.

Figure 2a shows the top view comparison of vehicle and barrier deformation in test and simulation at about 100 milliseconds (ms) for the left side oblique impact. The barrier with a mass of 2500 kg shows little deformation, whereas the impacted front structure of the vehicle shows a similar deformation pattern in test and simulation. The vehicle pulse comparison on the right shows the time history acceleration data at the rear of the vehicle. Test and simulation show good correlation with a CORA rating of 0.93. Furthermore, similar vehicle kinematics with respect to yaw motion, i.e. rotation around the vehicle z-axis, could be observed.

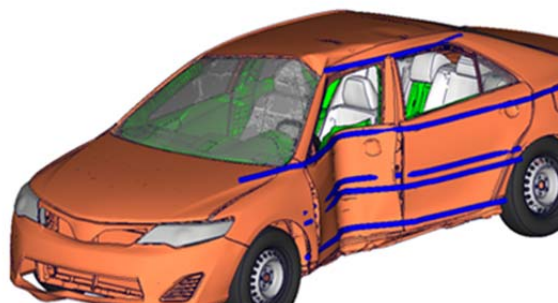
Similarly, Figure 2b shows the comparison of test and simulation in the right oblique frontal impact configuration. Again, good correlation of test and simulation results with respect to vehicle deformation, vehicle kinematics, and vehicle pulse time history data with a CORA rating of 0.90 can be observed.

Validation results for a 32 km/h, 75 degree oblique pole side impact configuration are described using available full scale test data. The weight of for the tested vehicle was exactly matched in the simulation. The C.G. location measured from the front axle was 1182 mm in the simulation compared to 1166 mm in the test. The location of the fixed rigid pole in the test was matched in the simulation. Post-crash deformation pattern of the tested vehicle and the vehicle deformation pattern at a time of 200 ms in the simulation are shown in Figures 3a and 3b.

Test vehicle exterior crush measurements have been taken after the crash at the height of the sill top, the occupant hip point, mid door, window sill, and window top. The different measurement heights are depicted with yellow markers on the tested vehicle in Figure 3a. The measured intrusion profiles from the test have been extracted and overlaid with the simulation in



(a) Test result



(b) Simulation results with overlaid test results

FIGURE 3 Test versus Simulation Results in 75 Degree Oblique Side Pole Impact

Figure 3b. The lines, shown in blue, represent intrusions measured in the full-scale crash test and correlate well with the intrusions seen in the simulation. Similar deformation pattern and intrusion depth in the roof, door, and sill areas could be observed in test and simulation.

Integrated Simulation for Pole Side Impact (90 Degree)

Figures 4a and 4b show the integrated occupant-vehicle model in the 90 degree pole side impact configuration at 0 ms and 180 ms, respectively. The vehicle, which travels with an initial speed of 29 km/h into the stationary rigid pole, experiences a change in velocity, i.e. the difference of initial velocity and rebound velocity, of $\Delta v_y = 36$ km/h in lateral vehicle direction and $\Delta v_x = 6$ km/h in longitudinal vehicle direction. The maximum local intrusion at the passenger door is about 250 mm.

Figures 4c-4f show a sequence of the occupant kinematics and interactions at selected times which represent characteristic occupant interactions. The near-side human occupant on the passenger seat is shown in yellow, the far-side human occupant on the driver seat is shown in turquois, the side airbags are shown in beige, and the pole is depicted in blue.

The near-side occupant impacts the struck door after 60 ms and the head is protected from hitting the pole by the deployed side curtain airbag. The far-side occupant has, to some extent, translated out of the center of the driver seat at this time, as shown in Figure 4c.

At 110 ms (Figure 4d), it can be observed that the near-side occupant has rebounded from the struck vehicle side and the far-side occupant has slid out of the seat belt and traveled towards the middle of the vehicle. Contact between the driver and passenger head and upper body occur at this time.

After 140ms (Figure 4e), the near-side occupant experiences a second impact against the intruding door, and a potential second impact of the head with the curtain airbag, door, or pole occurs at this time due to the previous interaction with the far-side occupant. The far-side occupant has moved further towards the struck side, leaning behind the upper body of the near-side occupant. Interaction with the middle interior console and the pelvis seat belt cause a significant amount of pitch motion of the far-side occupant.

The near-side occupant has rebounded from the struck side for the second time after 180 ms with head and upper body still leaning towards the intruding pole (Figure 4f). The far-side occupant is leaning in a similar manner with the head and upper body towards the struck vehicle

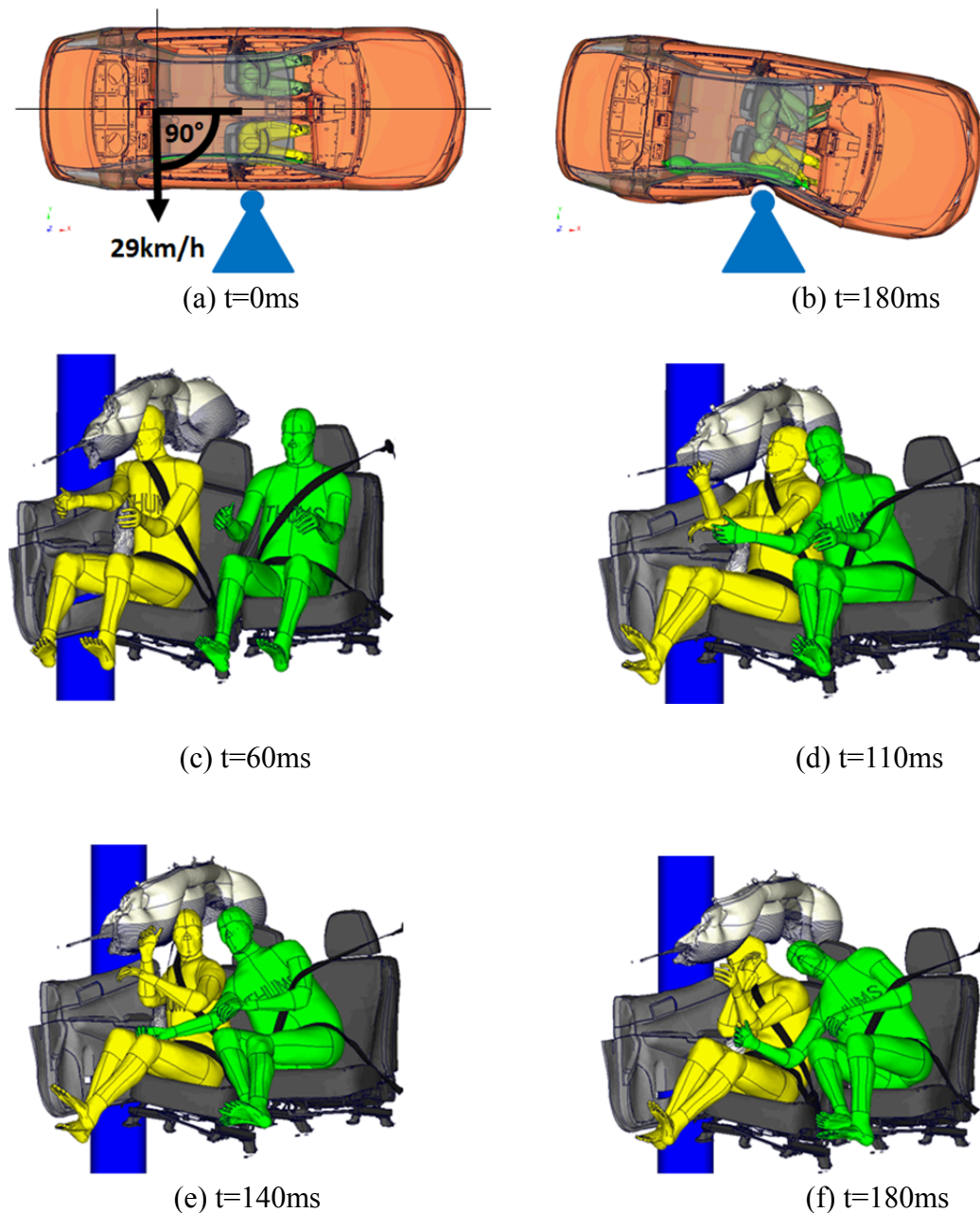


FIGURE 4 Pole Side Impact (90 degree)

side. The head is positioned between the back of the near-side occupant and the passenger seat backrest at this time.

Integrated Simulation for Oblique Pole Side Impact (75 Degree)

Figures 5a and 5b show the integrated occupant-vehicle model in the 75 degree pole side impact configuration at 0ms and 180ms, respectively. The vehicle, which travels with an initial speed of 32 km/h at a 75 degree angle relative to the vehicle longitudinal axis into the stationary pole,

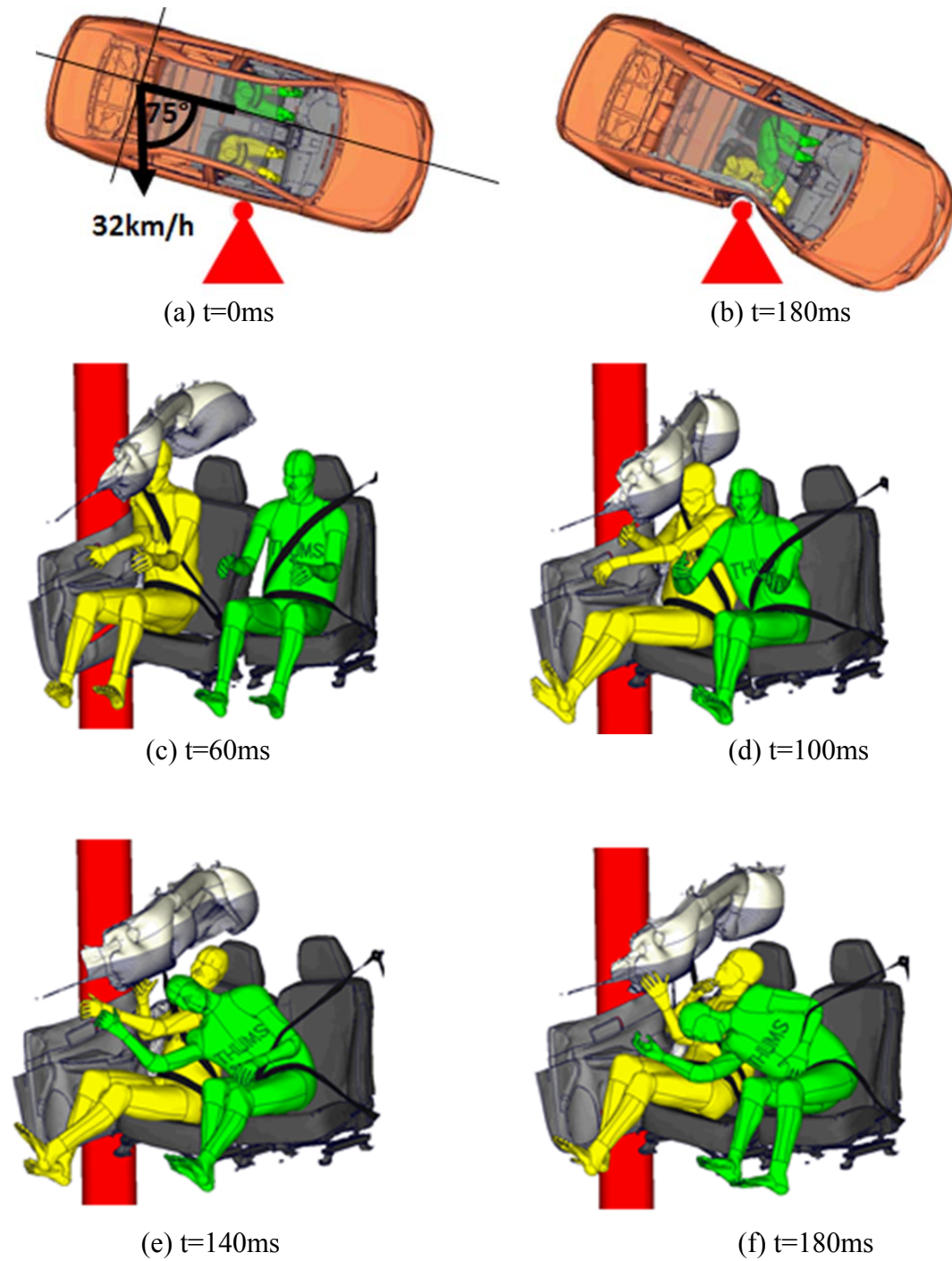


FIGURE 5 Oblique Pole Side Impact (75 degree)

experiences a change in velocity of $\Delta v_y = 38$ km/h in lateral vehicle direction and $\Delta v_x = 8$ km/h in longitudinal vehicle direction. The maximum local intrusion at the passenger door is about 300 mm.

Figures 5c-5f show a sequence of occupant kinematics and interactions. The near-side human occupant impacts the struck door after 60 ms with the head being protected from hitting the pole by the deployed side curtain airbag (Figure 5c). The far-side occupant has translated to some extent out of driver seat towards the struck side and the driver torso seat belt is positioned at the left shoulder.

After 100ms (Figure 5d), it can be noted that the near-side occupant has rebounded from the struck vehicle side and the far-side occupant has slid out of the torso seat belt and traveled towards the middle of the vehicle. The head of the far-side occupant hits the upper left arm of the near-side occupant and the abdomen strikes the middle interior console of the vehicle.

After 140 ms (Figure 5e), the near-side occupant has further rebounded away from the intruding vehicle structure and the far-side occupant has further slipped out of the torso seat belt, leaning towards the impacted side with the upper body positioned in front of the near-side occupant. No contact between the heads of driver and passenger has occurred.

After 180ms (Figure 5f), the near-side occupant is positioned in the middle of the passenger seat with the face and upper body facing towards the intruding pole. The far-side occupant is leaning with the head and upper body towards the struck vehicle side in front of the upper body of the near-side occupant. Interaction with the middle interior console and the pelvis seat belt cause a significant amount of pitch motion of the far-side occupant and the torso seat belt has slid further down towards the left lower arm.

Integrated Simulation for New Jersey Barrier Oblique Frontal Impact

Figures 6a and 6b show the integrated occupant-vehicle model in the New Jersey barrier frontal oblique impact configuration at 0 ms and 180 ms, respectively. The vehicle, which travels with an initial speed of 100 km/h at an angle of 25 degree into a fixed New Jersey barrier, experiences a change in velocity of $\Delta v_y = 25$ km/h in lateral vehicle direction and $\Delta v_x = 25$ km/h in longitudinal vehicle direction. Due to the redirection of the vehicle, a large amount of vehicle yaw motion, but no significant local intrusion at the struck side of the vehicle, was observed.

Figures 6c-6f show a sequence of occupant kinematics and interactions. The near-side human occupant impacts the struck vehicle side after 60 ms and the head makes contact with the deployed curtain airbag (Figure 6c). Both occupants have moved out of the center of their seat in both frontal and lateral vehicle direction at this time.

After 100ms (Figure 6d), the near-side occupant starts rebounding from the struck side and experienced more forward motion, with the neck bending forward and the head facing downward. The far-side occupant has slipped out of the torso seat belt, leaning with the head and neck towards the impacted side. No significant contact between occupants occurred.

At 140ms (Figure 6e), it can be observed that the near-side occupant has rebounded backwards in longitudinal vehicle direction with the head still facing downward. The head of the far-side occupant contacts the shoulder of the near-side occupant at this time.

After 180 ms (Figure 6f), the near-side occupant has further rebounded in lateral as well as in longitudinal vehicle direction.

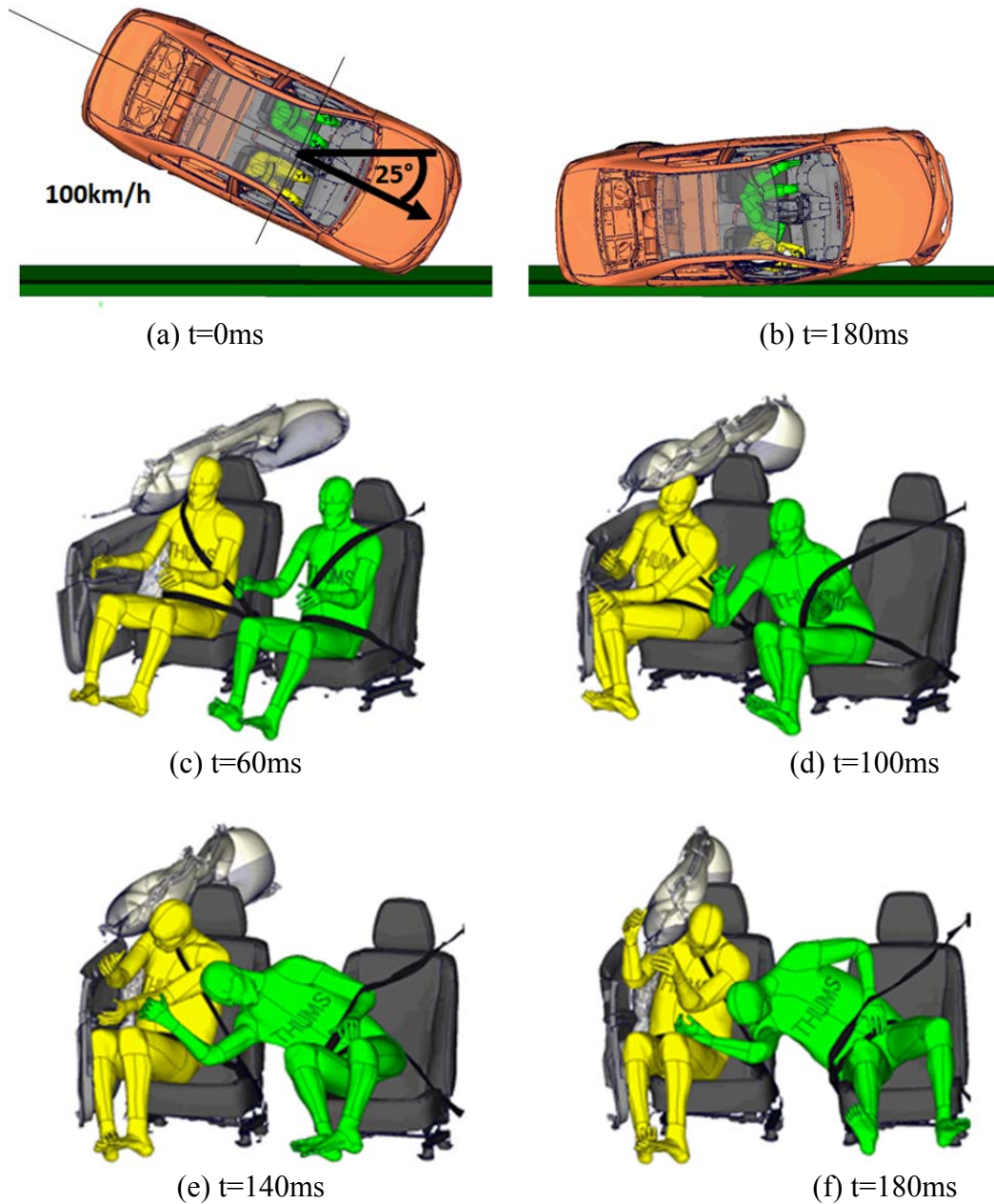


FIGURE 6 New Jersey Barrier Oblique Frontal Impact (25 degree)

DISCUSSION

All three evaluated run-off-road configurations show realistic near-side and far-side occupant kinematics and interactions. Driver and passenger experience a significant amount of lateral movement relative to the vehicle, which is the result of a large amount of change in velocity in vehicle y-direction, i.e. $\Delta v_y = 36$ km/h for the 90 degree pole side impact, 38 km/h for the 75 degree oblique pole side impact, and 25 km/h for the oblique frontal impact into a New Jersey barrier.

Similarities and differences of the evaluated configurations are discussed using occupant kinematics. As expected, the most severe occupant-to-occupant interaction could be observed for the 90 degree side pole configuration. Due to the same longitudinal seating position used for driver and passenger, severe head-to-head contact could be observed. In addition, occupant-to-occupant interaction caused the near-side occupant to rebound back to the struck vehicle side, which can lead to further injury risk due to interaction with the intruding door or outside vehicle objects.

The severity of occupant-to-occupant interaction and resulting injury risk is influenced by the initial seating position. For example, it can be expected that little or no head-to-head contact would occur in the same 90 degree side pole impact if a 5th percentile female near-side occupant, seated in full forward seating position, and a 95th percentile male far-side occupant, seated in full backward longitudinal seating position, were involved.

For the 75 degree oblique side pole configuration less severe occupant-to-occupant interaction has been observed. Driver and passenger heads do not come into contact due to the oblique character of the impact. Again, it can be expected that initial seating position influences the amount of interaction and related injury risk. Possible head-to-head contact can be expected for a near-side occupant seated full forward and a far-side occupant seated full backward, for example.

In the 100 km/h, 25 degree, oblique frontal configuration, the vehicle is redirected during the impact due to the small impact angle. Near-side and far-side occupants experience a larger amount of change in velocity in longitudinal vehicle direction, which causes more forward motion of the occupants, when compared to the side pole configurations. It can be expected that the influence of initial seating position in this load case is less significant than in the side pole configurations due to the limited amount of lateral vehicle intrusion.

While vehicle airbag sensors are usually configured to fire frontal airbags in full frontal and offset frontal impacts and side airbags in side impact configurations, airbag deployment depends on the algorithms used for a respective vehicle in frontal oblique impact configurations and in New Jersey barrier roadside hardware impacts. In order to be consistent, no frontal airbag deployment has been assumed for all three analyzed load cases in this study.

In addition to the analyses of occupant kinematics, selected injury criteria have been evaluated, as outlined in Figure 7. Maximum chest deflection, Brain Injury Criterion (BRIC), and Head Injury Criteria (HIC15) with associated probability of sustaining a AIS 3 or more severe head injury, have been assessed for the near and far-side occupants and compared for the three impact configurations. Injury Assessment Reference Values (IARV), which are considered to be used as an upper injury limit for a 50th percentile side impact dummy [15] are listed in the second column in Figure 7.

Chest deflection for the far-side occupants are small for all three impact configuration, since no contact with the intruding structure of the vehicle occurs. The 90 degree pole configuration shows the largest chest deflection for the near-side occupant due to the purely lateral nature of the impact. The New Jersey barrier configuration shows the lowest chest injury values, since no significant intrusion of the door can be observed.

BRIC is a new injury criteria based on the rotational velocity of the head [16]. As expected from the analysis of occupant kinematics, highest values occur in the 90 degree pole configuration for near and far-side occupants, caused by the head-to-head contact after 110 ms.

Similarly, the highest HIC15 values can be observed in the 90 degree pole impact. Consequently, a high risk of AIS 3+ head injuries exists. 75 degree pole and New Jersey barrier configurations show small risk of head injury, based on the HIC15 value, since no direct head-to-head contact occurs. The far-side occupant in the New Jersey barrier impact experiences

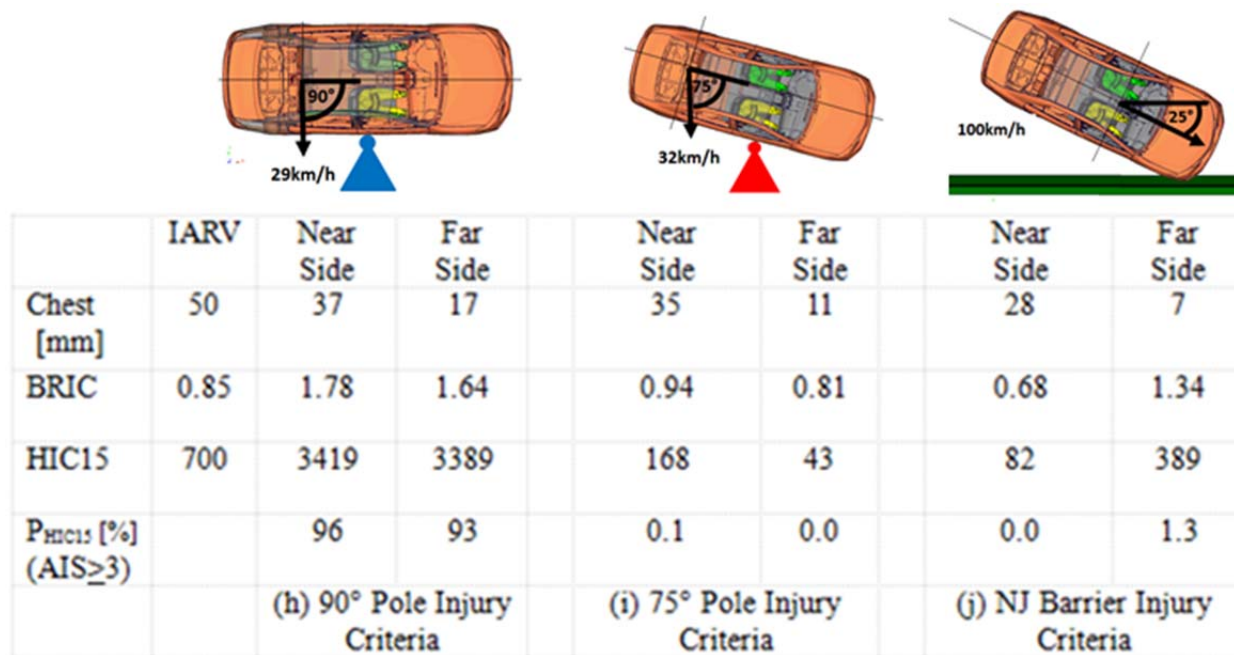


FIGURE 7 Near-Side and Far-Side Occupant Injury Criteria

contact with the shoulder of the near-side occupant after 140ms which is responsible for a moderately increased HIC15 value.

CONCLUSION

An integrated occupant-vehicle model, which consists of a validated 2012 Toyota Camry sedan, THUMS human occupants on the driver and front passenger seat, and relevant restraints (seatbelts, side and curtain airbag), has been used to evaluate occupant kinematics and interactions in three different run-off-road impact conditions. Potential injury risk due to occupant-to-occupant and occupant-to-vehicle interaction has been identified for two laboratory side pole impact load cases, representing the impact with a tree for example, and an oblique frontal New Jersey barrier load case.

The described integrated occupant-vehicle simulation method enables realistic simulation of run-off-road impacts and analysis of occupant kinematics, interactions, and potential injury mechanisms. The technique can be used to bridge the gap between real world accidents and laboratory crash testing to analyze occupant injury risk, vehicle performance, and effectiveness of roadside hardware devices.

The model can be used for further related research. For example, it can be setup without seatbelts and airbags to compare the results with the flail space model, which is widely used to assess injury risk in crash tests of roadside safety hardware.

The presented research gives insight into occupant kinematics and interactions for near-side and far-side occupants in three selected run-off-road crashes. It goes beyond laboratory impact tests, which generally are equipped with near-side occupants only. It also goes beyond

roadside hardware assessment according to MASH, which is generally not used for detailed occupant risk analysis. Additional research using a variety of different vehicle types, roadside hardware devices, impact angles, impact speeds, seating positions, restraint systems, and occupant types is necessary to better understand vehicle and occupant kinematics and related injury mechanisms. This will allow developing effective countermeasures that can further improve passive safety and contribute to reducing the number of people killed and injured in roadway departure crashes in the United States and around the world.

ACKNOWLEDGMENTS

The authors would like to thank the Federal Highway Administration (FHWA) and the National Highway Traffic Safety Administration (NHTSA) of the U.S. Department of Transportation (DoT) for supporting modeling and simulation efforts presented in this paper.

REFERENCES

1. Transportation Research Board (TRB), "Call for Abstracts," First International Roadside Safety Conference (IRSC), 2016
2. American Association of State Highway and Transportation Officials (AASHTO), "Manual for Assessing Safety Hardware," 1st ed., Washington, D.C., 2009
3. U.S. Department of Transportation, "Traffic Safety Facts", DOT HS 812 101, December 2014
4. Reichert, R., Kan, C.-D., Marzougui, D., et al, "Methodologies and Examples for Efficient Short and Long Duration Integrated Occupant-Vehicle Crash Simulation," 13th International LS-DYNA Users Conference, Detroit, 2014
5. Reichert, R., Morgan, R., Park, C.-K., Digges, K., and Kan, C.-D., "Thoracic and Abdominal Injuries to Drivers in Between-rail Frontal Crashes," IRCOBI Conference Sweden, 2013
6. Marzougui, D., Kan, C.-D., and Opiela, K., "Comparison of Crash Test and Simulation Results for Impact of Silverado Pickup into New Jersey Barrier Under Manual for Assessing Safety Hardware," Journal of the Transportation Research Board, No. 2309, Washington, D.C., 2012
7. Digges, K., and Gabler, H., "Opportunities for Reducing Casualties in Far-side Crashes," SAE Technical Paper 2006-01-0450, 2006, doi:10.4271/2006-01-0450
8. AAAM: The Abbreviated Injury Scale – 2005, Update 2008. Des Plaines, IL. 2008.
9. Iwamoto, M., and Nakahira, Y., 2015, "Development and Validation of the Total HUMAN Model for Safety (THUMS) Version 5 Containing Multiple 1D Muscles for Estimating Occupant Motions with Muscle Activation During Side Impacts," Toyota Central R&D Labs., Inc., Stapp Car Crash Journal, Vol. 59, 2015
10. Katagiri, M., Zhao, J., and Wiik, R., "Parametric Study for far side occupant protection using GHBM human body model," TK Holdings, Inc., 2016 Government Industry Meeting, Washington, DC, 2016
11. Hallquist, J., LS-DYNA Keyword User Manual, Livermore Software Technology Corporation, 2013
12. Reichert, R., Mohan, P., Marzougui, D., Kan, C.-D., et al, "Validation of a Toyota Camry Finite Element Model for Multiple Impact Configurations," SAE Technical Paper 2016-01-1534, 2016, doi:10.4271/2016-01-1534
13. Thunert, C., "CORA Release 3.6 User's Manual," Version 3.6, GNS mbH, Partnership for Dummy Technology and Biomechanics (PDB), 2012
14. Toyota Motor Corporation, "Total Human Model for Safety (THUMS)," AM50 Pedestrian/Occupant Model, Academic Version 4.0, 2011

15. Department Of Transportation, National Highway Traffic Safety Administration [Docket No. NHTSA-2015-0119] New Car Assessment Program, Request for Comments, January, 2017
16. Takhoumts, E.G., Hasija, V., Moorhouse, K., McFadden, J., Craig, M., “Development of Brain Injury Criteria (BrIC)”, Proceedings of the 57th Stapp Car Crash Conference, Orlando, FL, November 2013.

Investigation of Potential Mitigation of Driver Injury in Heavy Truck Frontal and Rollover Crashes

NATHAN SCHULZ

CHIARA SILVESTRI DOBROVOLNY

D. BLOWER

Texas A&M Transportation Institute

Advanced crash avoidance technologies (ACATs) for trucks have been developed in recent years and are beginning to be deployed. Prior to the development of standards for heavy truck crashworthiness and occupant protection, additional characterization of the crash-injury problem, current medium/heavy truck crashworthiness, and the potential benefits of crashworthy structures in heavy straight trucks and in truck cabs and trailers is needed. The goal of the project is to determine the nature of truck crashes that would remain after full deployment of ACATs, and to assess them in terms of truck driver injury and prevention. Then, using finite element analysis and computer simulation, exemplar tractor-semitrailer crashes were simulated to identify opportunities to improve occupant protection.

A full truck cabin model was developed and employed in our FE computer simulations to analyze occupant behavior and injury risk during frontal and rollover crashes. An integral part of this truck cabin model was the development of the occupant compartment components as no publicly available heavy truck models exist that contains interior components in the cabin. Additionally, researchers provided a methodology that can be employed and /or adapted to conduct future research within heavy truck occupant safety with use of computational analysis. Analysis of restraint systems during frontal and rollover crashes revealed unacceptable results according to current injury criteria standards and future work needs to be conducted to develop more effective restraint systems to increase occupant safety.

Experience with Inclusion of Instrumented Anthropomorphic Test Devices in Roadside Safety Barrier Testing with Heavy Trucks

CHIARA SILVESTRI DOBROVOLNY

NATHAN SCHULZ

ROGER P. BLIGH

D. LANCE BULLARD

Texas A&M Transportation Institute

According to the Census of Fatal Occupational Injuries for 2013 from the Bureau of Labor Statistics, truck driving accounts for the second most fatal occupational injuries annually. Truck driving has a fatality rate per worker over four times the national average, with a large majority of fatalities occurring in traffic crashes.

Through the years, there have been numerous safety technologies implemented to make driving safer among passenger vehicles (such as the inclusion of seatbelt and airbag systems). In addition to these technologies, various efforts were made to have passenger vehicles more crashworthy. National standards (FMVSS) and star-rating programs (NCAP) have been established to help with the objective to build safer vehicle and reduce the probability of serious injuries in traffic crashes. These improvements, however, are required only for passenger vehicles, and significant less development is supported to protect truck drivers in crashes. That is, there has been no development of crashworthiness features for trucks that is comparable to that for light vehicles. No NCAP testing has been developed or required for heavy trucks.

Within this research effort, an instrumented anthropomorphic test device (ATD) was placed in single unit trucks and heavy trucks employed in roadside safety barrier controlled testing. The objectives of this study were to better predict occupant injury in such impact events and to more realistically evaluate heavy truck occupant dynamics and possible interaction with roadside barriers. The researchers developed a methodology for positioning the instrumented ATD, as well as the seat and steering wheel, similar to the one currently mandate for NCAP testing of light vehicles. Positioning of the seat, steering wheel, and ATD were recorded through manual and computerized measurements, and was documented with photos, as required per NCAP testing of passenger cars.

Impacts of the heavy truck vehicles against roadside safety barriers were developed according to the testing requirements dictated by the AASHTO *Manual for Assessing Safety Hardware* (MASH) which specifies guidelines for crash tests and gives evaluation criteria for safety devices. The tests performed and reported in this study were conducted at 50 mph and 56 mph nominal impact speeds, and 15 degrees nominal orientation angles between the heavy trucks and the roadside barriers. In addition to the evaluation of occupant impact velocity and ridedown acceleration estimated through the concept of the flail space model adopted by MASH, occupant injury risk was also more realistically estimated through the instrumentations of the ATD, which have a humanlike response to impact and can be used to assess the potential for injury to different body regions.

Data, videos, evaluations from this research study can be employed to better understand heavy truck occupant dynamics, injury modes, and interaction with passive restraint systems as a result of oblique impacts with real-world deployed roadside safety barriers.

Evaluation of a 31-inch W-Beam Guardrail for Placement on a 3H:1V Sloped Terrain through FEA

CHIARA SILVESTRI DOBROVOLNY

NATHAN SCHULZ

D. ARRINGTON

Texas A&M Transportation Institute

The goal of this study was to develop a 31-inch W-beam guardrail system to be placed with a 3H:1V slope in front of the barrier. The structural capacity and the occupant risk factors of such a proposed guardrail system were evaluated with respect to the American Association of State Highway and Transportation Officials (AASHTO) Manual for Assessing Safety Hardware (MASH) TL-3 criteria. Finite element computer models of new guardrail designs for evaluation when placed on a 3H:1V sloped terrain configuration were developed and impact simulations were conducted to support their evaluation according to MASH standards evaluation criteria.

Three barrier designs for placement on a 3H:1V slope were suggested for evaluation through predictive computer simulations. All systems appear to be crashworthy and likely to pass safety evaluation criteria required for MASH. Depending on the desired system post distance location from the 3H:1V slope break, the researchers recommend evaluation of selected design through full-scale crash testing according to MASH TL-3 criteria. The information compiled from this research will provide the Federal Highway Administration (FHWA) and State Departments of Transportation with a W-beam guardrail design as a crashworthy system to be placed with a 3H:1V slope in front of a barrier.

Development of Crash Modification Functions for the Safety Performance of Treatments on Rural Two-Lane Roads

JIGUANG ZHAO
KIM KOLODY
CH2M HILL

HENRY BROWN
CARLOS SUN
University of Missouri

The treatment of shoulder rumble stripes, shoulder widening (from 0 to 2 feet) and pavement resurfacing (RSR) was deployed to more than 400 centerline miles of rural two-lane highways in Illinois. The safety performance of the RSR treatment was evaluated with the empirical Bayesian before and after study method based on the roadway characteristics and traffic and crash data collected. Crash modification factors (CMF) for 20 categories of crash severity and/or collision types were calculated. Generally, the RSR treatment effectively improves safety performance of rural two-lane roads, especially for fatal and injury crashes. Meanwhile, the RSR treatment is more effective for run-off road and head-on crashes than for total crashes.

A cumulative residual (CURE) analysis reveals that fixed-value CMFs for all annual average daily traffics (AADT) range are likely to conclude with biased estimation on the RSR's safety performance. The crash modification function (CMFunction) was introduced in this study, and a sample size of 16 was selected to develop the CMFunction based on the sensitivity analysis results. CMFunctions were developed for two collision types under different severity levels. The CURE plot indicates that CMFunctions produce unbiased crash frequency prediction results and, therefore, are more reliable than fixed-value CMFs.

Assessing Verification and Validation Comparisons of Crash Test and Simulation Results for Commonly Used, NCHRP 350-Approved Longitudinal Barriers under MASH Requirements

DHAIFER MARZOUGUI
George Mason University

CING-DAO (STEVE) KAN
George Mason University

KENNETH S. OPIELA
Transportation Consultant

In an effort to assess the efficacy of the crashworthiness requirements in the new Manual for Assessing of Safety Hardware (MASH) funding was provided for the testing of seven commonly-used longitudinal barriers in NCHRP Project 22-14(3). Each of these barriers had been previously approved under NCHRP Report 350 crashworthiness requirements. These crash tests were conducted using the Silverado pick-up truck as the 2270P test vehicle to exploit the unique opportunity to further validate the newly developed Chevrolet Silverado quad-cab pick-up truck finite element (FE) model. The Silverado conforms with all the generic specifications for a 2270P MASH test vehicle. In another effort, FHWA provided funding to simulate each of the seven crash tests to allow comparison of crash test and simulation results for validation purposes. These comparisons further confirmed that the 2270P vehicle model could be used to effectively replicate MASH Test 3-11 impacts for various types of longitudinal barriers. The comparisons of crash test data and simulation results also provided an opportunity to assess the new verification and validation (V&V) procedure for the individual cases. This paper provides a comparison of a set of V&V summaries in the interest of better understanding their relevance and implications of the findings and to support further implementation of the procedures.

The results for the seven barriers were compared using “traditional” methods, as well as the new verification and validation (V&V) procedures. The individual V&V comparisons suggest that the structured assessment across multiple factors reflected in the PIRT tables and statistical measures of test and simulation results provided a more robust validation. This analysis was motivated by a concern that there may not be a full appreciation of how the metrics were derived or the implications of variations in the results. Some variations across the tests were expected due to the differences in barrier design features, but since they all involved Test 3-11, the differences were assumed to be minor. Questions are raised in the comparison of specific results across tests that need to be answered for effective use of the V&V procedures and to establish a common understanding among roadside safety professionals about the implications of the V&V results.

INTRODUCTION

Background

Over the years, agencies have undertaken crash testing of roadside hardware to assess its safety effectiveness when impacted by an errant vehicle. Protocols and crashworthiness requirements evolved to address changing conditions, address a broad set of barriers, allow testing of new designs, and (to some extent) stretch the safety envelope. The most recent set of crashworthiness testing protocols and criteria are embodied in the Manual for Assessing Safety Hardware (MASH) which was adopted by AASHTO in October 2009 [1].

MASH provides an update of the procedures and criteria for assessing the safety performance of roadside hardware that were embodied in NCHRP Report 350 “Recommended Procedures for the Safety Performance Evaluation of Roadside Safety Appurtenances” [2]. The effort reported here was intended to see if consistent results using the V&V procedure developed under NCHRP Project 22-24 could be obtained [3]. The comparison of the results of seven similar crash tests and the corresponding simulations of the tests provided the basis. This was considered important for the effective implementation of the V&V procedures and applications of it, such as considering acceptance for improvements to previously tested hardware based upon simulations of the new versions of the hardware.

For more than 20 years, the FHWA has promoted the use of crash simulations based upon finite element models as a means to develop innovative designs and to evaluate their performance. To do so, requires finite element models of vehicles and the hardware. These models have been developed to describe the vehicle and test articles as a collection of elements that reflect the geometry of the items, the nature of connections between adjacent elements, the characteristics of the materials that make up the element, and properties associated with the relationships between elements (e.g., joints, fracture mechanics). Models have become more detailed through advances in the modeling techniques and simulations more accurate as a result of a steady evolution of software capabilities. Detailed models of the vehicle and barriers tested were available from previous analyses to support this effort.

Objectives

The primary objective of the effort reported here was to assess the efficacy of the V&V procedures across a set of comparisons of seven commonly used longitudinal barriers. In this effort, all crash test data originated from a single testing agency and all the crash simulations were undertaken by a single organization using the same computer and software platform. The intent of this effort was to assess the consistency and understanding of the results across a set of comparisons. While the features of the seven barriers differed to some extent, the MASH test requirements for each were the same. It was assumed that since not all the barriers “passed” the requirements it might be possible to better discern the efficacy of the V&V procedures. The outcomes of the assessment were hoped to promote efforts to enhance the procedures and support a rational implementation process. The resources available for this effort did not permit efforts to revise the procedures.

Approach

Research sponsored by the FHWA used the newly developed FE model of the 2007 Chevy Silverado pick-up truck in simulations of MASH test 3-11 with the seven, commonly-used, longitudinal barriers tested under the auspices of NCHRP Project 22-14(3). The requirements for MASH Test 3-11 for longitudinal barriers involved an impact angle of 25 degrees and a speed of 100 km/h (62 mph). Data and video from the crash tests were obtained for the comparisons. The simulations were set-up to replicate the crash test and to generate similar metrics. The comparisons followed traditional methods as well as those recommended by the new V&V procedure. The results for each step of the V&V procedure were tabulated to facilitate comparisons across the set of results. This allowed the consistency for the various aspects to be compared between individual cases as well as across cases. This effort focused on a cross sectional review of the individual results from the seven longitudinal barriers to assess the efficacy of factors, the consistency of results, and the potential implications of any inferences derived.

CRASH TEST DESCRIPTIONS

Full-scale crash tests of a 2007 Chevrolet Silverado quad-cab pick-up truck into seven commonly-used, NCHRP 350 approved barriers were conducted at the Texas A&M Transportation Institute under NCHRP Project 22-14(3) “Evaluation of Existing Roadside Hardware Using Updated Criteria” [4]. These tests involved the following longitudinal barriers based upon recommendations by TTI to the NCHRP project panel:

- New Jersey Shaped Concrete Barrier (Test 476460-1-4)
- G-9 Thrie Beam (Test 476460-1-8)
- G4(2W) (Test 476460-1-5)
- Penn DOT Transition (Test 476460-1-3)
- G4(1S) Median (Test 476460-1-9)
- G2 Weak Post (Test 476460-1-7)
- G3 Box Beam (Test 476460-1-6)

Table 1 provides a summary of the results from the seven tests. Column 2 indicates the specifics of the impact conditions from the test. Column 3 paraphrases the test reports relative to the outcomes of the test. For those tests that failed under the MASH criteria, notes or recommendations cited in the test reports relative to retrofit options are cited.

CRASH SIMULATIONS

Vehicle Model

In 2009, a detailed finite element (FE) model of a 2007 Chevy Silverado pick-up truck was developed. The model was developed jointly by FHWA and NHTSA to serve multiple purposes for studying and advancing vehicle and highway safety research. The model consists of over 300,000

TABLE 1 Summary of MASH Silverado Crash Tests and Outcomes

Barrier	Test Set-up	Outcome
New Jersey Shaped Concrete Barrier Test Number: TTI 476460-1-4 Test Date: 1/30/2009	A 2007 Chevrolet Silverado quad-cab pick-up truck traveling at a speed of 62.6 mph impacting a 32-inch concrete New Jersey shaped barrier at an impact angle of 25.2 degrees.	The 32-inch New Jersey shape barrier contained and redirected the 2270P vehicle. The vehicle did not penetrate, underride, override the installation. No measurable deflection of the barrier occurred. No detached elements, fragments, or other debris were present to penetrate or show potential for penetrating the occupant compartment, or to present a hazard to other in the area. Maximum occupant compartment deformation was 2.0 inches at the right kick panel. The 2270P vehicle remained upright during and after the collision event. Maximum roll and pitch angles were 29 and -16 degrees, respectively. Occupant risk factors were within the limits specified in MASH. The 2270P exited the barrier within the exit box. MASH Evaluation: PASS
G-9 Thrie Beam Test Number: TTI 476460-1-8 Test Date: 2/26/2009	A 2007 Chevrolet Silverado 4-door pickup truck traveling at a speed of 63.3 mph impacting a thrie-beam barrier at an impact angle of 26.4 degrees. The impact speed and angle were within the acceptable limits prescribed in <i>MASH</i> . However, the impact condition represented an impact severity 15.3 percent greater than the target <i>MASH</i> condition.	The G9 thrie beam guardrail did not perform acceptably when impacted by the 2270P vehicle. After being contained and redirected, the 2270P Silverado pickup rolled 360 degrees. Maximum dynamic deflection of the thrie-beam barrier during the test was 33.2 inches. Maximum occupant compartment deformation was 3.56 inches in the right rear passenger area. MASH Evaluation: FAIL Retrofit Note: If the speed and angle in the test were nearer to target impact conditions, the vehicle may not have rolled over.
G4(2W) Test Number: TTI 476460-1-5 Test Date: 3/04/2009	A 2007 Chevrolet Silverado 4-door pickup truck traveling at a speed of 64.4 mph impacting a G4(2w) barrier at an impact angle of 26.1 degrees. The impact speed and angle were within the acceptable limits prescribed in <i>MASH</i> . However, the impact condition represented an impact severity 16.4 percent greater than the target <i>MASH</i> condition.	The G4(2W) W-beam guardrail did not perform acceptably when impacted by the 2270P vehicle. The vehicle penetrated the guardrail after the W-beam rail element ruptured and then subsequently rolled 180 degrees. MASH Evaluation: FAIL Retrofit Note: Modifications that have demonstrated improved performance in crash tests include increasing the rail height to 31 inches, moving the rail splices to mid-span of the posts, and using 12 inch deep block-outs. It is believed any one or more of these changes will improve the performance of the G4(2W) W-beam guardrail. Additionally, it is known that W-beam guardrail has historically been performing at or very near 100 percent of structural design capacity. If the speed and angle in the test were nearer to target impact conditions, the rail may not have ruptured.

Continued on next page.

TABLE 1 (continued) Summary of MASH Silverado Crash Tests and Outcomes

Barrier	Test Set-up	Outcome
Penn DOT Transition Test Number: TTI 476460-1-3 Test Date: 3/31/2009	A 2007 Chevrolet Silverado 4-door pickup truck traveling at a speed of 62.8 mph impacting a G4(2w) barrier at an impact angle of 25.7 degrees. The impact speed and angle were within the acceptable limits prescribed in <i>MASH</i> .	The W-beam transition to concrete bridge parapet successfully contained and redirected the 2270P vehicle. The vehicle did not penetrate, override, or underide the installation. Maximum dynamic deflection was 3.8 inches. No detached elements, fragments, or other debris were present to penetrate or to show potential for penetrating the occupant compartment, or to present a hazard to others in the area. Maximum occupant compartment deformation was 0.6 inches in the left rear area at hip height. The 2270P vehicle remained upright during and after the collision event. Maximum roll angle was 54 degrees. Occupant risk factors were within the limits specified in <i>MASH</i> . The vehicle exited the W-beam transition within the exit box. MASH Evaluation: PASS
G4(1S) Median Test Number: TTI 476460-1-9 Test Date: 4/14/2009	A 2007 Chevrolet Silverado 4-door pickup truck traveling at a speed of 64.0 mph impacting a G4(1S) barrier at an impact angle of 25.1 degrees. The impact speed and angle were within the acceptable limits prescribed in <i>MASH</i> . However, the impact condition represented an impact severity 7.5 percent greater than the target <i>MASH</i> condition.	The G4(1S) W-beam median barrier did not perform acceptably when impacted by the 2270P vehicle. The 2270P Silverado pickup truck overrode the installation. In the test, a guardrail post was impacted by the left front tire and the vehicle climbed the post and w-beam rail element. However, in the G4(1S) W-beam median barrier, the addition of the rear W-beam rail element provides additional stiffness and constrains the lateral displacement of the posts. Because the rail cannot readily detach from the posts, the rail is pulled down by the posts and the effective rail height is reduced in the region of impact. MASH Evaluation: FAIL Retrofit Note: If the speed and angle in the test were nearer to target impact conditions, the vehicle may not have vaulted. A 30 inch tall version of the G4(1S) W-beam median barrier incorporating a rub-rail will prevent the wheel from contacting the face of the posts and thus help mitigate vehicle-post snagging and it will also increase the barrier stiffness, which should reduce post displacement and rail deflection. However, the rub-rail may still permit the pickup to climb the barrier.

Continued on next page.

TABLE 1 (continued) Summary of MASH Silverado Crash Tests and Outcomes

Barrier	Test Set-up	Outcome
G2 Weak Post Test Number: TTI 476460-1-7 Test Date: 5/01/2009	A 2007 Chevrolet Silverado 4-door pickup truck traveling at a speed of 62.4 mph impacting the Modified G2 Weak Post W-Beam guardrail at an impact angle of 24.6 degrees. The impact speed and angle were within the acceptable limits prescribed in <i>MASH</i> . The impact occurred 21 ft-4 inches upstream of the splice at the one-third point (31 inches upstream of post 12).	The Modified G2 Weak Post W-Beam guardrail performed acceptably by containing and redirecting the vehicle. The vehicle did not penetrate, underride or override the weak post W-beam guardrail. Maximum dynamic deflection of the rail during the test was 8.6 ft. There was no debris from the test installation that penetrated or show potential for penetrating the occupant compartment, or presented a hazard to others in the area. Maximum occupant compartment deformation was 0.25 inches in the lateral area across the cab at the driver's side hip area. The 2270P vehicle remained upright during and after the collision event. Maximum roll angle was -12 degrees. Occupant risk factors were within the limits specified in <i>MASH</i> . The 2270P vehicle remained within the exit box. MASH Evaluation: PASS
G3 Weak-Post Box Beam Test Number: TTI 476460-1-6 Test Date: 5/15/2009	A 2007 Chevrolet Silverado 4-door pickup truck traveling at a speed of 63.2 mph impacting a G3 box beam barrier at an impact angle of 25.4 degrees. The impact speed and angle were within the acceptable limits prescribed in <i>MASH</i> .	The G3 Weak Post Box-Beam guardrail performed acceptably by containing and redirecting the vehicle. The vehicle did not penetrate, underride or override the weak post guardrail. Maximum dynamic deflection of the rail during the test was 4.8 ft. Two rail brackets detached from their posts, but they did not penetrate or show potential for penetrating the occupant compartment, or present a hazard to others in the area. Maximum occupant compartment deformation was 0.75 inches in the lateral area across the cab at the driver's side kick panel. The vehicle remained upright during and after the collision event. Maximum roll angle was -14 degrees. Occupant risk factors were within the limits specified in <i>MASH</i> . The vehicle exited within the exit box. MASH Evaluation: PASS

elements representing the vehicle and its components, including the steering and suspension subsystems [5]. This model was initially validated following traditional protocols of comparison the full frontal impact with a vertical wall required under the NHTSA New Car Assessment Program (NCAP) and the simulated results. In addition, validation efforts included comparison of the inertial properties of the vehicle (before tear-down) and in its simulated form, component response tests for the front & rear suspension, and non-destructive bump & terrain tests. These validation tests indicated that the model was a solid representation of the real vehicle [6, 7, 8].

The opportunity arose to take the validation efforts one step further by collaboration with another project aimed at assessing the impact of the new crashworthiness criteria prescribed in the MASH. In this project, seven tests of safety hardware previously approved under criteria outlined in NCHRP Report 350 were to be tested under MASH using the larger pick-up truck (i.e., 2270 kg over 2000 kg). In these tests, a Chevrolet Silverado meeting the generic requirements for a 2270P vehicle under MASH was used. There had been no previous experience with crash testing using the Silverado. The simulation of these tests was intended to provide another round of validation for the Silverado FE model and thereby provide enhanced confidence in its capability to support the design and evaluation of roadside safety hardware to meet MASH requirements.

Barrier Hardware Models

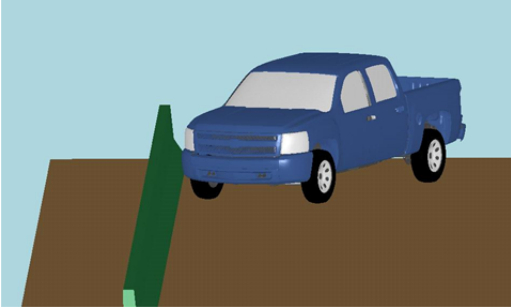
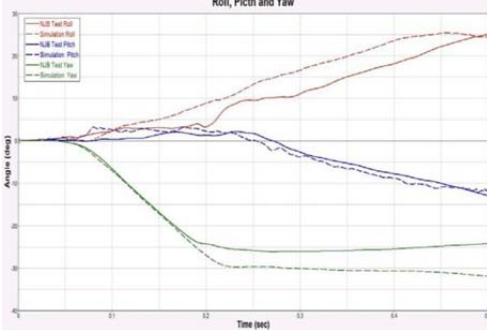
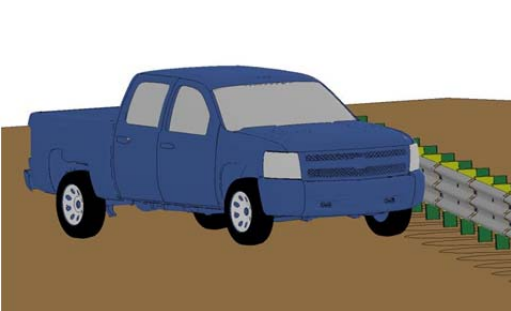
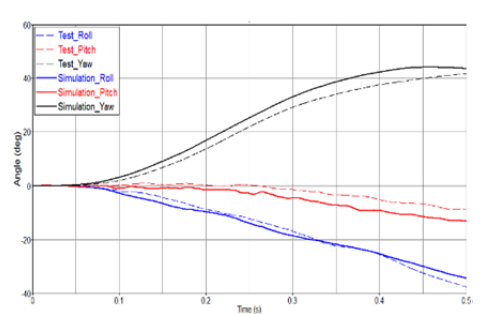
Crash simulations require models of both the vehicle and the barrier to be impacted. The National Crash Analysis Center (NCAC) developed finite element models for many roadside barriers over its twenty-year history. These models provided the basis for the creation of an FE model for each of the seven barriers analyzed in this effort. The models were updated to reflect the exact dimensions, materials, and connections as used in the barriers that were tested. Representations of these models can be seen in Table 2. In some cases, there had been extensive use of the barrier models in previous studies (e.g., concrete safety shapes, w-beam guardrails), so the efficacy of the models for roadside impacts had been solidly established. Details of these barrier models are documented elsewhere.

Simulation Results

The ultimate validation of an FE model for roadside hardware analysis purposes is the direct comparison to an actual crash test involving the same vehicle, barrier, and impact conditions. In this case, there were seven longitudinal barrier tests executed by the same agency over a short period of time and simulations for each also undertaken by a single agency all run on the same computer and software platform (thus, eliminating any variations in the results from the computational side). The comparison of the crash tests with the Silverado and the simulation of them are separately documented for each of the seven barriers [9 - 15].

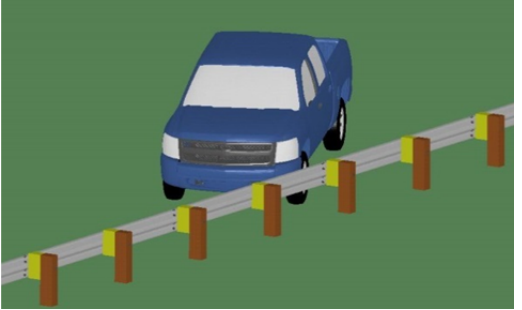
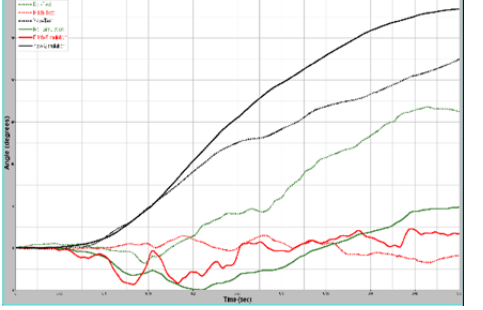
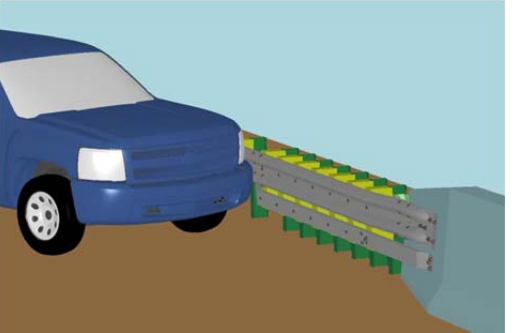
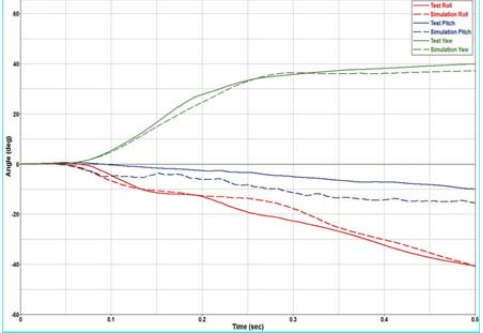
The results from these simulations for the seven barriers are summarized in Table 2. In this table, a representation of the simulation model is provided, along with the key “traditional” validation comparisons, namely visual and graphical comparisons. The visual comparisons involved typical side-by-side comparisons of the simulated versus actual test results in sequential views from varying perspectives. Where the sequential views showed similar behavior of the vehicle for each of the time step of the impact event, it was considered to be an indication of model validity. For example, when the nature of the interaction of the vehicle’s bumper with the

TABLE 2 Summary of Crash Simulation Results for the Seven Longitudinal Barriers

Test	Model Set-up	Roll, Pitch, & Yaw Comparisons	Outcome
NJ Concrete Barrier			<p>The simulation of a MASH 3-11 test into a New Jersey-shaped barrier demonstrated that the Silverado FE model was stable and displayed no unusual behavior. Visual comparison of the test and the simulation (best compared by viewing the video & animation) showed that there was very similar behavior at each time step in the crash event. Traditional comparison of graphs of roll, pitch, and yaw measures reflected good correlations between the crash test data and simulation results. The validation effort indicated that the simulations provide a good representation of the Test 3-11 impacts for the New Jersey barrier.</p>
G-9 Thrie Beam			<p>The simulation of a MASH 3-11 test into a G9 Thrie Beam barrier demonstrated that the Silverado FE model was stable and displayed no unusual behavior. Visual comparison of the test and the simulation (best compared by viewing the video and animation) showed that there was very similar behavior at all time steps in the crash event. The traditional comparison of graphs of roll, pitch, and yaw measures reflected good correlations between the crash test data and simulation results. The validation effort indicated that the simulations provide a good representation of the Test 3-11 impacts for the G9 Thrie Beam barrier. The simulation results indicated that the barrier would NOT pass on all evaluation measures for MASH Test 3-11, appropriately reflecting the test results. The additional simulation for nominal test parameters indicated that the outcome would be the same and that test parameters would be similar.</p>

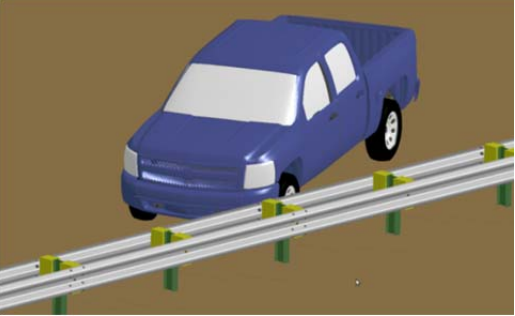
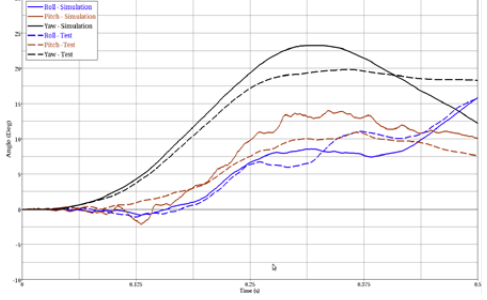
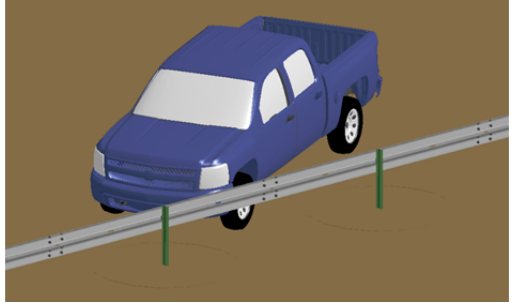
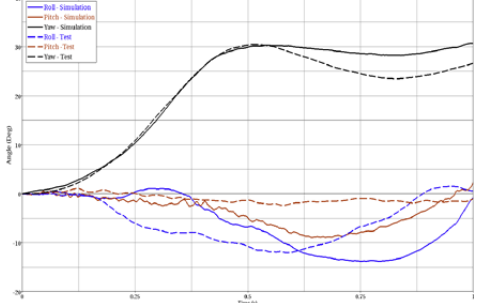
Continued on next page.

TABLE 2 (continued) Summary of Crash Simulation Results for the Seven Longitudinal Barriers

Test	Model Set-up	Roll, Pitch, & Yaw Comparisons	Outcome
G4(2W)			<p>The simulation of a MASH 3-11 test into a G4(2w) W-Beam barrier demonstrated that Silverado FE model was stable and displayed no unusual behavior. Visual comparison of the test and the simulation (best compared by viewing the video and animation) showed that there was very similar behavior at all time steps in the crash event. The traditional comparison of graphs of roll, pitch, and yaw measures reflected good correlations between the crash test data and simulation results. The validation effort indicated that the simulations provide a good representation of the Test 3-11 impacts for the G4(2w) W-Beam barrier. The simulation results indicated that the barrier would pass on all evaluation measures for MASH Test 3-11.</p>
Penn DOT Transition			<p>The simulation of a MASH 3-21 test into a W-Beam transition demonstrated that the Silverado FE model was stable and displayed no unusual behavior. Visual comparison of the test and the simulation (best compared by viewing the video and animation) showed that there was very similar behavior at all time steps in the crash event. The traditional comparison of graphs of roll, pitch, and yaw measures reflected good correlations between the crash test data and simulation results. The validation effort indicated that the simulations provide a good representation of the Test 3-12 impacts for the W-beam transition. The simulation results indicated that the barrier would pass on all evaluation measures for MASH Test 3-21 (which are identical to those Test 3-11).</p>


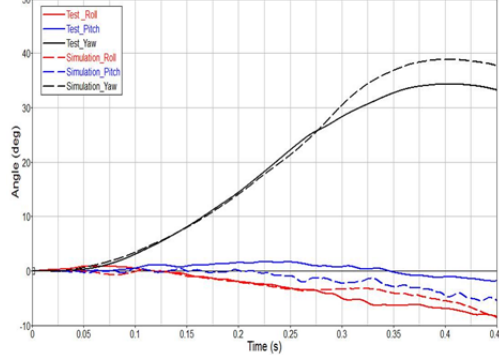
Continued on next page.

TABLE 2 (continued) Summary of Crash Simulation Results for the Seven Longitudinal Barriers

Test	Model Set-up	Roll, Pitch, & Yaw Comparisons	Outcome
G4(1S) Median			<p>The simulation of a MASH 3-11 test into a G4(1S) Median W-Beam barrier demonstrated that the Silverado FE model was stable and displayed no unusual behavior. Visual comparison of the test and the simulation (best compared by viewing the video and animation) showed that there was very similar behavior at all time steps in the crash event. The traditional comparison of graphs of roll, pitch, and yaw measures reflected good correlations between the crash test data and simulation results. The validation effort indicated that the simulations provide a good representation of the Test 3-11 impacts for the New Jersey barrier. The simulation results indicated that the barrier would pass on all evaluation measures for MASH Test 3-11.</p>
G2 Weak Post			<p>The simulation of a MASH 3-11 test into a G2 Weak Post W-Beam barrier demonstrated that the Silverado FE model was stable and displayed no unusual behavior. Visual comparison of the test and the simulation (best compared by viewing the video and animation) showed that there was very similar behavior at all time steps in the crash event. The traditional comparison of graphs of roll, pitch, and yaw measures reflected good correlations between the crash test data and simulation results. The validation effort indicated that the simulations provide a good representation of the Test 3-11 impacts for the G2 Weak Post W-Beam barrier. The simulation results indicated that the barrier would pass on all evaluation measures for MASH Test 3-11.</p>

Continued on next page.

TABLE 2 (continued) Summary of Crash Simulation Results for the Seven Longitudinal Barriers

Test	Model Set-up	Roll, Pitch, & Yaw Comparisons	Outcome
G3 Box Beam			<p>This simulation of a MASH 3-11 test into a G3 Weak Post Box Beam barrier demonstrated that the Silverado FE model was stable and displayed no unusual behavior. Visual comparison of the test and the simulation (best compared by viewing the video and animation) showed that there was very similar behavior at all time steps in the crash event. The traditional comparison of graphs of roll, pitch, and yaw measures reflected good correlations between the crash test data and simulation results. The validation effort indicated that the simulations provide a good representation of the Test 3-11 impacts for the G3 Weak Post Box Beam barrier. The simulation results indicated that the barrier would pass on all evaluation measures for MASH Test 3-11.</p>

barrier or the degree of roll are similar the model is providing a good representation of the real event. The text in the “Outcome” column summarize these observations for each simulation.

The second level involved comparisons of the yaw, pitch, and roll measures for the vehicle between the simulation and the full-scale test. These resultant graphs are shown in the third column with dashed lines used to represent the actual crash test data and solid lines for the simulated results. The red lines compare pitch angles over the duration of the crash event, similarly, the roll rates are compared by the blue lines, and the yaw rates indicated by the black lines. Across all the barriers, the pitch, roll, and yaw rates were similar and were judged to indicate that the models provided a good representation of the crash event.

COMPARISON OF RESULTS

The verification & validation (V&V) procedure recommended by NCHRP Project 22-24 “Guidelines for Verification and Validation of Crash Simulations Used in Roadside Safety Applications” [3] was used to compare the results of the crash against the computer simulation at a third level. While the longitudinal barriers tested were not identical, it was believed that they were similar enough to assess the consistency of V&V procedure results. This assessment was undertaken to determine if the procedure provided appropriate and unambiguous results to establish confidence in them or identify needs for modifications. Since such results will be used to make decisions about barrier crashworthiness, they need to be sound.

Model Verification & Validation Procedure and Results

The following sections provide a brief explanation of V&V procedure outputs along with a brief discussion of the meaning of the comparison, metrics, graphs, and tables. The validation efforts involve analytical comparisons of the simulation results and the crash test data as well as structured evaluations of the simulation process and assessment of MASH-based Phenomena Importance Ranking Tests (PIRTS) as described below.

Analytical Comparisons

The V&V procedures first involve analytic comparisons of the numerical, time-based data using the RSVVP software package to undertake various statistical comparisons of paired sets of time-based data. It undertakes the necessary data adjustments, and then applies a series of statistical tests to determine how well it compares. The software allows various types of single-channel data to be analyzed including the common crash test and simulation metrics that comprises:

- X-acceleration – change in acceleration in the forward direction of travel of the vehicle
- Y-acceleration – change in acceleration in the lateral direction of travel of the vehicle
- Z-acceleration – change in acceleration in the vertical direction of travel of the vehicle
- Yaw rate – change in angular rate about the vehicle vertical axis
- Roll rate – change in angular rate about the vehicle longitudinal axis
- Pitch rate – change in angular rate about the vehicle lateral axis

The typical outputs of the RSVVP software for single- and multi-channel data on accelerations and rates provide several summary graphs comparing the actual test and simulation data as well as measures of its variations including:

- Time history plot – provides comparison of the simulated results and test curves captured during the crash event. Each data point is a measure of the acceleration or angular rate recorded.
- Plot of integrated time histories – Integrating the change of acceleration data allows the changes in velocity to be plotted.
- MPC Metrics – The Geers approach is used to provide a statistical measure of “goodness of fit” between the two curves based on magnitude (M), phase (P), and comprehensive (C, combined magnitude and phase) parameters. A value of less than 40 for M, and P is considered passing the criteria. ANOVA Metrics – A second “goodness of fit” metric is assessed using Analysis of Variance considering the average and standard deviations of residuals between the curves. Values of less than 5% for the average residual and 35% for the standard deviation are considered passing the criteria.
- Residuals Plots – These plots show the time history (i.e., the residual versus time and in histogram format where the percentage of the residual is plotted against the percentage of its occurrence, and the cumulative of the residual (sum of all residuals up to that point in time) is plotted versus time.

Using research derived measures of “appropriate” correlation, these RSVVP results set the benchmark for determining the validity of modeled results on each of the common six test (single-channel) data items as well as a multi-channel comparison of combined effect. Since not all measurements have the same importance in the tests, (e.g. in some tests little roll, pitch, x-acceleration, etc. are observed), these low magnitude channels could fail the evaluation metrics even if the simulation is valid. To overcome this problem, a multi-channel comparison, where each channel is given a weighting factor based on magnitude, is incorporated in the validation process.

Structured Summaries

In addition to comparing the time history from the transducers mounted on the vehicle, the V & V procedure established a structured scheme for summarizing the results and comparing the individual verification and validation checks. These are in the form of tables which summarize the specifics of the data sets compared and define all the evaluations that have to be met before the model is considered valid. These include:

- Table A - Fundamental documentation of the test and simulation datasets being compared,
- Table B – Defines the factors that are important for to meet the selected crashworthiness criteria.
- Table C – Provides the solution verification in which the simulation results are checked to ensure that there are no discrepancies in simulations such as in the energies (kinetic, internal, hourglass, total, etc.) and mass of the components that would indicate computation error.

- Table D - Statistical measures for comparison of multi- or single-channel data, and
- Table E –“Phenomena Importance Ranking Table (PIRT).” In the PIRT evaluations in which different phenomena and measurements related to test performance criteria (MASH in this case) are compared between the simulation and the test.
- Table F - Composite score indicating the results of the process.

A full set of these tables and other results from the validations for the seven barriers are documented elsewhere [9-15].

Observations Summary

The results from the seven comparisons provide an opportunity to review the viability of the V&V procedures. The following observations or questions arise when looking at the seven sets of results that have been tabulated. The general objectives of the V&V procedures are important, but the question remains – have the testing and simulation processes evolved sufficiently to be compared stringently on a set of qualitative and quantitative factors. Some specific observations are highlighted below.

Input Summary (Tables A and B)

These tables are primarily summaries of test conditions. As such, there is not much to review, but questions that arise include:

- Is it necessary to better document the test instrumentation and filtering process (or at least cite the source)? These may be cited in test reports, but will they be conveniently available to the persons reviewing these results to help understand any unusual variations?
- There are readily available various versions of finite element models for vehicles and barriers. Is it necessary to more specifically cite FE model references? Is the current basis reference by release date sufficient? Did the model come from an accepted source?
- Was the model modified in any way? What level of detail was used? Given that the input files for the simulation model are extremely large, there is generally no easy way to identify all alterations in a model.
- Should there be levels of importance placed on the individual factors? Should the procedure be implemented in stages such that initially a subset of factors are the focus? Additional factors could be added over time. How should marginal results be noted?
- There is a need to assure that consistent answers are given for the qualitative factors. Some of the simulation questions might lead to ambiguous answers.

Simulation Metrics (Table C)

It is also possible to assess the validity of the model by analyzing the distribution of energy associated with the crash event. The laws of physics dictate that the total energy is balanced. Typically, an energy balance graph is generated to provide the energy summary. It indicates a relatively constant energy suggesting there are no usual characterizations in the structure of the model that would be an unrealistic sink (point of dissipation) of the energy. The kinetic energy associated with the motion of the vehicle typically drops off as the velocity is decreased

during the crash. Further, there is typically an increase in internal energy as components of the vehicle absorb energy through deformation. Sliding energy, which associated with friction contact forces between the vehicle and barrier, also typically increases during the simulations. The sum of internal and sliding energy increase, as it would be expected, is equal to the reduction in kinetic energy.

Table 3 summarizes the simulation results assessment for all seven barriers compared. For each barrier, the individual test and simulation results are included in the table. General questions that arise from the results in this table include:

- Are the appropriate units defined?
- The typical energy balance graph is not a reporting requirement. It seems that it should be.
- Is there a need for a more rigorous assessment of the time points in the crash event relative to the shape of the curves?

This section may be considered critical for ascertaining whether the simulators understand the tools and software. It is also critical that those interpreting the results recognize inconsistencies or the clues that may suggest a weak or inappropriate model.

RSVVP Statistical Analyses (Table D)

Table 4 summarizes the results of the RSVVP comparisons for all seven barriers compared. For each barrier, the individual test and simulation results are included in the table in adjacent columns. It can be noted that “Y” and “N” are included in pairs of related cells to indicate whether the results pass the criterion for being considered statistically similar. The following observations are noted:

- None of the barriers passed all the acceleration and rate metrics as indicated by none of the columns having all “Y’s.” Since not all the measured traces are critical for the barrier performance (i.e some of have small magnitudes), not meeting all criteria is not expected. This could be observed even when comparing traces from two tests with the same impact configuration (repeat tests).
- All of the barriers, passed on the multi-criteria evaluation as indicated by “Y’s” in all the cell pairs in the lower rows of the table. The weighting factors may be providing a useful analytic means to consider relative importance. Are these weighting factors well enough understood and adequate for the different barrier types and roadside devices? Have the effects of the various weighing methods on the outcomes been assessed?
- None of the z-acceleration metrics passed as indicated by the rows shaded all red. This could be attributed to the fact that the z- acceleration typically has smaller magnitude than the x and y accelerations. Could this be also associated with other factors such as a measurement problem or an insufficient understanding of effects of the vehicle as a sprung-mass?

More general questions related to the statistical analyses include:

- What is the sensitivity of the results relative to the pass/fail criteria?

TABLE 3 Simulation Energy Balance Summary Comparison for the Evaluation of the Seven Longitudinal Barriers

RSVVP Crashworthiness Evaluation Summary								
Test Conditions`	Test Reference:	TTI 476460-1-4	TTI 476460-1-8	TTI 476460-1-5	TTI 476460-1-3	TTI 476460-1-6	TTI 476460-1-9	TTI 476460-1-7
	Barrier:	New Jersey CMB	G9 Thrie Beam Guardrail	G4 (2W) Guardrail	Penn DOT Transition	G3 Weak post Box Beam	G4(1s) Median Guardrail	G2 Weak Post Guardrail
	Vehicle:	Silverado 2270	Silverado 2270	Silverado 2270	Silverado 2270	Silverado 2270	Silverado 2270	Silverado 2270
	Impact:	100kmh/25°	100kmh/25°	100kmh/25°	100kmh/25°	100kmh/25°	100kmh/25°	100kmh/25°
Evaluation Criteria								
Total energy of the analysis solution (i.e., kinetic, potential, contact, etc.) must not vary more than 10 percent from the beginning of the run to the end of the run	3.0	4.5	6.0	2.9	3.3	3.5	3.1	
	Yes	Yes	Yes	Yes	Yes	Yes	Yes	
Hourglass Energy of the analysis solution at the end of the run is less than 5 % of the total initial energy at the beginning of the run	1.0	12.0	6.0	6.2	8.1	5.7	6.1	
	Yes	No	Yes	No	No	No	No	
The part/material with the highest amount of hourglass energy at any time during the run is less than 5 % of the total initial energy at the beginning of the run.	NA	NA	NA	6.0	5.8	5.4	5.8	
	Yes	Yes	Yes	No	No	No	No	

Continued on next page.

TABLE 3 (continued) Simulation Energy Balance Summary Comparison for the Evaluation of the Seven Longitudinal Barriers

Evaluation Criteria							
Mass added to the total model is less than 5 % the total model mass at the start of the run.	0	0	0	0	0	0	0
	Yes	NA	NA	Yes	Yes	Yes	Yes
The part/material with the most mass added had less than 10 % of its initial mass added.	NA	NA	NA	NA	NA	NA	NA
	Yes	Yes	Yes	Yes	Yes	Yes	Yes
The moving parts/materials in the model have less than 5 % of mass added to the initial moving mass of the model.	NA	NA	NA	NA	NA	NA	NA
	Yes	Yes	Yes	Yes	Yes	Yes	Yes
There are no shooting nodes in the solution?	NA	NA	NA	NA	NA	NA	NA
	Yes	Yes	Yes	Yes	Yes	Yes	Yes
There are no solid elements with negative volumes?	NA	NA	NA	NA	NA	NA	NA
	Yes	Yes	Yes	Yes	Yes	Yes	Yes

TABLE 4 Analytical Evaluation Summary for the Seven Longitudinal Barriers

RSVVP Crashworthiness Evaluation Summary									
Test Conditions	Reference:	TTI 476460-1-4	TTI 476460-1-8	TTI 476460-1-5	TTI 476460-1-3	TTI 476460-1-6	TTI 476460-1-9	TTI 476460-1-7	
	Barrier:	New Jersey CMB	G9 Thrie Beam Guardrail	G4 (2W) Guardrail	Penn DOT Transition	G3 Weak post Box Beam	G4(1s) Median Guardrail	G2 Weak Post Guardrail	
	Vehicle:	Silverado 2270	Silverado 2270	Silverado 2270	Silverado 2270	Silverado 2270	Silverado 2270	Silverado 2270	
	Impact:	100kmh/25°	100kmh/25°	100kmh/25°	100kmh/25°	100kmh/25°	100kmh/25°	100kmh/25°	
Single Channel Sprauge-Geer Metrics (Magnitude & Phase Value <= 40.0)									
X-Acceleration	Magnitude	37.7	34.9	2.4	20.3	99.7	11.3	57.5	
	Phase	34.7 Y	31.1 Y	33.5 Y	23.1 Y	32.5 N	29.4 Y	41.3 N	
Y-Acceleration	Magnitude	3.4	45.2	22.8	66.8	3.4	13.5	27.4	
	Phase	35.0 Y	53.0 N	40.6 N?	43.9 N	35.0 Y	23.1 Y	30.9 Y	
Z-Acceleration	Magnitude	29.0	66.9	39.7	51.6	29.0	78.5	139.6	
	Phase	49.9 N	49.8 N	53.1 N	45.3 N	49.9 N	40.2 N	49.5 N	
Roll Rate	Magnitude	8.6	9.9	31.6	2.4	16.1	27.0	4.5	
	Phase	29.4 Y	14.3 Y	38.2 Y	22.1 Y	8.4 Y	11.1 Y	11.9 Y	
Pitch Rate	Magnitude	60.0	46.2	150.5	60.4	8.6	5.9	0.3	
	Phase	33.5 N	37.0 N	53.8 N	40.2 N	29.4 Y	26.2 Y	47.5 Y	
Yaw Rate	Magnitude	16.1	7.8	29.7	3.7	60.0	55.3	195.6	
	Phase	8.4 Y	3.8 Y	13.1 Y	8.2 Y	33.5 N	32.5 N	47.2 N	
Single Channel ANOVA Metrics (Mean & SD Residual Value <= 0.5 and SD Residual Value < 0.35)									
X-Acceleration	Mean Residual	0.0	0.01	0.01	0.01	0.03	0.01	0.02	
	SD Residual	0.25 Y	0.24 Y	0.26 Y	0.17 Y	0.38 Y	0.33 Y	0.26 Y	
Y-Acceleration	Mean Residual	0.12	0.4	-0.1	0.38	0.06	0.01	0.01	
	SD Residual	0.23 Y	0.58 N	0.22 Y	0.60 N	0.35 Y	0.34 Y	0.40 N	
Z-Acceleration	Mean Residual	0.09	0.02	0.02	0.08	0.01	0.02	0.04	
	SD Residual	0.42 N	0.29 Y	0.43 N	0.32 Y	0.69 N	0.52 N	0.88 N	

Continued on next page.

TABLE 4 (*continued*) **Analytical Evaluation Summary for the Seven Longitudinal Barriers**

Single Channel ANOVA Metrics (Mean & SD Residual Value <= 0.5 and SD Residual Value < 0.35)															
Roll Rate	Mean Residual	0.02		0.02		0.14		0.02		0.05		0.04		0.03	
	SD Residual	0.22	Y	0.2	Y	0.34	Y	0.34	Y	0.31	Y	0.24	Y	0.16	Y
Pitch Rate	Mean Residual	0.0		0.05		0.05		0.06		0.13		0.07		0.06	
	SD Residual	0.55	N	0.28	Y	0.97	N	0.32	Y	0.84	N	0.33	Y	0.54	N
Yaw Rate	Mean Residual	0.08		0.03		0.13		0.03		0.06		0.07		0.02	
	SD Residual	0.12	Y	0.07	Y	0.28		0.13	Y	0.17	Y	0.53	N	0.55	N
Multi-Channel Summary (Same Criterion as above)															
Sprauge-Geer Metrics	Magnitude	19		25.5		25.5		27.7		30.0		21.8		27.9	
	Phase	34.7	Y	22.7	Y	22.7	Y	24.3	Y	20.9	Y	24.1	Y	25.0	Y
ANOVA Metrics	Mean Residual	0.01		0.02		0.0		0.04		0.02		-1.4		0.01	
	SD Residual	0.24	Y	0.21	Y	0.21	Y	0.25	Y	0.34	Y	0.34	Y	0.27	Y

- Do the RSVVP metrics apply to all types of barriers? To date, most of V&V studies were focused on longitudinal barriers?
- Where there are variations, how can the source of the variation be determined? The crash test results are typically labeled “known” solution, but it is known that crash test can have problems with sensors and data capture instruments.
- Are there other metrics that should be considered?
- Do the patterns on pass and fail reveal anything about the efficacy of the factors selected?
- In testing, there is generally no instrumentation on the barrier. Does that suggest that effects might be missed? Might such metrics be critical to end treatments and crash cushions as they function by absorbing energy?
- Are the evaluation criteria equally appropriate for crash events of varying durations?

Table 5 uses color to depict the lack of consistency in the results. The green cells have passing levels on the various criterion. The red cells have failing measures. The yellow cells would be failing, but they might be considered on the margin. Altering the criterion slightly, would change the outcomes. Seven cases is too few to make such decisions, but it should be recognized that there is a need to track such results over a larger set of cases.

PIRTS Review (Table E)

Table 6 summarizes the results of the PIRT comparisons for all seven barriers compared. For each barrier, the individual test and simulation results are included in the table. These are based upon the MASH criteria, so there is a well-established basis for their inclusion. One might ask:

- Do the PIRTs address all the critical questions for comparing crash tests and simulations? Are too many/too few aspects being considered?
- Should a “marginal” pass be defined given the complexity of the process and the many factors that can influence the results?
- Should a sensitivity analysis be undertaken to ascertain that acceptance criteria are appropriate?

Overall Summaries (Table F)

Table 7 summarizes the results of the PIRT comparisons for all seven barriers compared. For each barrier, the individual test and simulation results are included in the table.

- It would seem that it would be appropriate to include notes to the summary to highlight any significant findings or issues.

General

Considering the overall application of these procedures, a number of concerns arise. These include:

TABLE 5 Sensitivity of Analytical Evaluation for the Seven Longitudinal Barriers

RSVVP Crashworthiness Evaluation Summary									
Test Conditions	Test Reference:	TTI 476460-1-4	TTI 476460-1-8	TTI 476460-1-5	TTI 476460-1-3	TTI 476460-1-6	TTI 476460-1-9	TTI 476460-1-7	
	Barrier:	New Jersey CMB	G9 Thrie Beam Guardrail	G4 (2W) Guardrail	Penn DOT Transition	G3 Weak post Box Beam	G4(1s) Median Guardrail	G2 Weak Post Guardrail	
	Vehicle:	Silverado 2270	Silverado 2270	Silverado 2270	Silverado 2270	Silverado 2270	Silverado 2270	Silverado 2270	
	Impact:	100kmh/25°	100kmh/25°	100kmh/25°	100kmh/25°	100kmh/25°	100kmh/25°	100kmh/25°	
Single Channel Sprauge-Geer Metrics (Magnitude & Phase Value <= 40.0)									
X-Acceleration	Magnitude	37.7	34.9	2.4	20.3	99.7	11.3	57.5	
	Phase	34.7 Y	31.1 Y	33.5 Y	23.1 Y	32.5 N	29.4 Y	41.3 N	
Y-Acceleration	Magnitude	3.4	45.2	22.8	66.8	3.4	13.5	27.4	
	Phase	35.0 Y	53.0 N	40.6 N?	43.9 N	35.0 Y	23.1 Y	30.9 Y	
Z-Acceleration	Magnitude	29.0	66.9	39.7	51.6	29.0	78.5	139.6	
	Phase	49.9 N	49.8 N	53.1 N	45.3 N	49.9 N	40.2 N	49.5 N	
Roll Rate	Magnitude	8.6	9.9	31.6	2.4	16.1	27.0	4.5	
	Phase	29.4 Y	14.3 Y	38.2 Y	22.1 Y	8.4 Y	11.1 Y	11.9 Y	
Pitch Rate	Magnitude	60.0	46.2	150.5	60.4	8.6	5.9	0.3	
	Phase	33.5 N	37.0 N	53.8 N	40.2 N	29.4 Y	26.2 Y	47.5 Y	
Yaw Rate	Magnitude	16.1	7.8	29.7	3.7	60.0	55.3	195.6	
	Phase	8.4 Y	3.8 Y	13.1 Y	8.2 Y	33.5 N	32.5 N	47.2 N	
Single Channel ANOVA Metrics (Mean & SD Residual Value <= 0.5 and SD Residual Value < 0.35)									
X-Acceleration	Mean Residual	0.0	0.01	0.01	0.01	0.03	0.01	0.02	
	SD Residual	0.25 Y	0.24 Y	0.26 Y	0.17 Y	0.38 Y	0.33 Y	0.26 Y	
Y-Acceleration	Mean Residual	0.12	0.4	-0.1	0.38	0.06	0.01	0.01	
	SD Residual	0.23 Y	0.58 N	0.22 Y	0.60 N	0.35 Y	0.34 Y	0.40 N	
Z-Acceleration	Mean Residual	0.09	0.02	0.02	0.08	0.01	0.02	0.04	
	SD Residual	0.42 N	0.29 Y	0.43 N	0.32 Y	0.69 N	0.52 N	0.88 N	
Roll Rate	Mean Residual	0.02	0.02	0.14	0.02	0.05	0.04	0.03	
	SD Residual	0.22 Y	0.2 Y	0.34 Y	0.34 Y	0.31 Y	0.24 Y	0.16 Y	

Continued on next page.

TABLE 5 (continued) Sensitivity of Analytical Evaluation for the Seven Longitudinal Barriers

Single Channel ANOVA Metrics (Mean & SD Residual Value <= 0.5 and SD Residual Value < 0.35)									
Pitch Rate	Mean Residual	0.0	0.05	0.05	0.06	0.13	0.07	0.06	
	SD Residual	0.55 N	0.28 Y	0.97 N	0.32 Y	0.84 N	0.33 Y	0.54 N	
Yaw Rate	Mean Residual	0.08	0.03	0.13	0.03	0.06	0.07	0.02	
	SD Residual	0.12 Y	0.07 Y	0.28 Y	0.13 Y	0.17 Y	0.53 N	0.55 N	
Multi-Channel Summary (Same Criterion as above)									
Sprauge-Geer Metrics	Magnitude	19	25.5	25.5	27.7	30.0	21.8	27.9	
	Phase	34.7 Y	22.7 Y	22.7 Y	24.3 Y	20.9 Y	24.1 Y	25.0 Y	
ANOVA Metrics	Mean Residual	0.01	0.02	0.0	0.04	0.02	-1.4	0.01	
	SD Residual	0.24 Y	0.21 Y	0.21 Y	0.25 Y	0.34 Y	0.34 Y	0.27 Y	

TABLE 6 MASH PIRTs Evaluation Summary for the Seven Longitudinal Barriers

Test Conditions	Reference:	TTI 476460-1-4		TTI 476460-1-8		TTI 476460-1-5		TTI 476460-1-3		TTI 476460-1-6		TTI 476460-1-9		TTI 476460-1-7	
	Barrier:	New Jersey CMB		G9 Thrie Beam Guardrail		G4 (2W) Guardrail		Penn DOT Transition		G3 Weak post Box Beam		G4(1s) Median Guardrail		G2 Weak Post Guardrail	
	Vehicle:	Silverado 2270		Silverado 2270		Silverado 2270		Silverado 2270		Silverado 2270		Silverado 2270		Silverado 2270	
	Impact:	100kmh/25°		100kmh/25°		100kmh/25°		100kmh/25°		100kmh/25°		100kmh/25°		100kmh/25°	
Structural Adequacy															
A1	Test article should contain & redirect the vehicle; the vehicle should not penetrate,	Yes	Yes	Yes	Yes	No	No	Yes	Yes	Yes	Yes	No	No	Yes	Yes
A2	The relative difference in the maximum dynamic deflection is less than 20 percent. (m)	0.0	0.0	0.84	0.74	0.84	0.75	0.14	0.17	1.45	1.32	0.59	0.53	2.62	2.27
A3	The relative difference in the length of vehicle-barrier contact is less than 20 percent. (m)	0.25	0.25	6.8	5.1	6.8	5.7	2.75	2.62	15.6	14.2	3.6	3.4	1.44	1.32
A4	The relative difference in the number of broken or significantly bent posts is less than 20 %.	NA	NA	3	3	3	3	0	0	11	11	3	3	12	10
A5	Barrier did not fail	Yes	Yes	Yes	Yes	Yes	Yes	Yes	Yes	Yes	Yes	Yes	Yes	Yes	Yes
A6	There were no failures of connector elements (Answer Yes or No).	NA	NA	No	No	No	No	Yes	Yes	NA	NA	No	No	No	No
A7	There was no significant snagging between the vehicle wheels and barrier elements	Yes	Yes	No	No	No	No	Yes	Yes	Yes	Yes	Yes	Yes	Yes	Yes
A8	There was no significant snagging between vehicle body components and barrier elements	Yes	Yes	Yes	Yes	Yes	Yes	Yes	Yes	Yes	Yes	Yes	Yes	Yes	Yes
Occupant Risk															
D	Detached elements, fragments or other debris from the test article should not penetrate or ...	Yes	Yes	Yes	Yes	Yes	Yes	Yes	Yes	Yes	Yes	Yes	Yes	Yes	Yes
F1	The vehicle should remain upright during and after the collision although moderate roll,	Yes	Yes	No	No	No	No	Yes	Yes	Yes	Yes	Yes	Yes	No	No
F2	The relative difference between the maximum roll of the vehicle is less than 20 percent.	25	26	38	38	38	34	41	41	25	289	15	15	12	11
F3	The relative difference between the maximum pitch of the vehicle is less than 20 percent.	13	12	9	13	9	13	10	15	13	12	10	14	2	3
F4	The relative difference between the maximum yaw of the vehicle is less than 20 percent.	26	32	42	45	42	45	40	41	26	32	20	23	30	30
H1	Longitudinal and lateral occupant impact velocities (OIV) should fall below the ...	Yes	Yes	Yes	Yes	Yes	Yes	Yes	Yes	Yes	Yes	Yes	Yes	Yes	Yes
H2	Longitudinal OIV (m/s) - Relative difference is less than 20 % absolute difference is less than 2 m/s	4.3	4.3	5.2	5.4	5.2	6.4	5.0	6.8	3.4	4.2	5.2	6.4	2.9	4.4
H3	Lateral OIV (m/s)- - Relative difference is less than 20 % or absolute difference is less than 2 m/s	9.2	2.8	5.3	5.8	5.3	5.8	8.7	3.8	4.6	3.9	5.2	5.0	3.2	3.1
I1	Longitudinal and lateral occupant ridedown accelerations (ORA) should fall below the ...	Yes	Yes	Yes	Yes	Yes	Yes	Yes	Yes	Yes	Yes	Yes	Yes	Yes	Yes
I2	Longitudinal ORA (g) - Relative difference is less than 20 % or absolute difference is ...	5.6	8.4	6.9	6.9	9.8	8.1	4.9	3.4	4.2	5.2	5.2	6.3	3.4	8.5
I3	Lateral ORA (g) - Relative difference is less than 20 % absolute difference is less than ...	9.6	11.5	7.7	6.7	7.7	6.7	16.4	8.9	7.2	7.1	5.3	5.8	4.5	6.6
Vehicle Trajectory															
L	The occupant impact velocity in the longitudinal direction should not exceed 40 ...'s.	Yes	Yes	Yes	Yes	Yes	Yes	Yes	Yes	Yes	No	No	Yes	Yes	Yes

TABLE 7 Overall V&V Comparison Summary

Crashworthiness Evaluation Summary								
Test Conditions	Reference:	TTI 476460-1-4	TTI 476460-1-8	TTI 476460-1-5	TTI 476460-1-3	TTI 476460-1-6	TTI 476460-1-9	TTI 476460-1-7
	Barrier:	New Jersey CMB	G9 Thrie Beam Guardrail	G4 (2W) Guardrail	Penn DOT Transition	G3 Weak post Box Beam	G4(1s) Median Guardrail	G2 Weak Post Guardrail
	Vehicle:	Silverado 2270	Silverado 2270	Silverado 2270	Silverado 2270	Silverado 2270	Silverado 2270	Silverado 2270
	Impact:	100kmh/25°	100kmh/25°	100kmh/25°	100kmh/25°	100kmh/25°	100kmh/25°	100kmh/25°
Structural Adequacy								
	Table C - Verification	Yes	Yes	Yes	Yes	Yes	Yes	Yes
	Table D – RSVVP	Yes	Yes	Yes	Yes	Yes	Yes	Yes
	Table E – PIRT	Yes	No	Yes	No	Yes	Yes	Yes
	Overall	Yes	No	No	Yes	Yes	Yes	No

- There appears that all available tables are setup for the application to comparison of longitudinal barriers. Other roadside hardware devices, such as end treatments, crash cushions, etc. have different evaluation criterion. Is there a need to develop PIRTs for these other devices? How will these be established?
- Are the statistical metrics and the selected acceptance criterion viable for comparing crash tests and simulations?
- Is there a need to undertake a sensitivity analysis across the various types of barriers to determine whether they are appropriate?
- The process does not assess the relative contributions of various components when evaluating a barrier system. Does that imply that the procedures may be of limited value in evaluating incremental improvements?

SUMMARY & CONCLUSIONS

The verification and validation procedures seem to meet a long standing need to provide a better way for the safety community to more specifically judge the validity of simulation results, but there are concerns that the procedure may not adequately address all types of barriers and test options. There appears to be a need for continued development and assessment of the procedure to reflect the overall understanding of the barrier design, testing, and crashworthiness evaluation processes.

There has been an interest in establishing a more rigorous process for determining the validity of simulation results for some time. The research under NCHRP Project 22-24 has clearly raised the bar and rationally assessed various statistical metrics and linked them to the evolved crashworthiness evaluation processes. This should not be construed to mean that the procedures are ready for implementation. Some concerns that arise include:

- There have been limited published verification and validation efforts. The Silverado simulations represent an opportunity to compare seven independent sets of results.
- One should note that the research and most of the applications of the procedure have been for longitudinal barriers. This includes all of the case cited in the research. The obvious question is then, do these same evaluation criteria apply to all barriers?
- Who should develop the PIRTs for the comparisons of end treatments, crash cushions, TMAs, breakaway devices, and other roadside hardware.
- Is the V&V procedure providing adequate and understandable information for those who will make judgments relative to new or improved roadside hardware?

The verification and validation procedures were also assessed by comparing a set of results for common longitudinal barriers for MASH Test 3-11. It was noted that:

- The RSVVP software is a useful tool for comparing sets of time-based data. It includes features that facilitate time adjustments of the data.
- The pass/fail thresholds seem appropriate but it will take a longer term logging of results over many tests to detect patterns that might suggest the current criteria are too loose or too stringent. Other pass/fail thresholds may be needed for other types of barriers.

- The software does not support “self-documentation” of the comparison results. The outputs may be improved by including additional information such as the title of the project, the name or initials of the analyst, the date of execution so that each output can be clearly associated with its project. Time and date stamps are critical to tracking revisions or reruns.

- It may be useful to consider the readability of the output pages relative to font sizes and axis markings.

- Automation of inputs and outputs to the software be very helpful to analysts and would save time and effort.

Further efforts might be considered useful to:

- Increased focus on the metrics compared. There may be metrics unique to a type of impact that should get more attention.

- There is a need to confirm that the pass/fail criteria are appropriately set. This may only be possible when many more comparisons have been completed.

- It may be appropriate to make provisions for explanations of any deviations from the “passing” criteria.

It would seem that further work is necessary for an effective implementation of the V&V procedure in a decision-making role. It is imperative that all simulation efforts be subjected to the comparisons prescribed in the procedure to develop further experience with the procedures and consensus on the meaning of the results.

Other questions will follow related to future roles for simulation in barrier design and analysis:

- Is there a role for simulation in enhancing the effectiveness of commonly-used barriers under changing vehicle fleet characteristics?

- How can simulation tools be used for retrofit analysis? Is it a sensitivity issue? Is there a basic scheme that could be applied? Who will undertake such evaluations?

- Should there be a periodic review of V&V accepted hardware? Based upon in-service results?

- Is there a need to maintain a DB of these results for tracking effectiveness changes over time?

- Is there a greater role for the use of simulations in future evaluations and acceptance?

- How best can the process be implemented and aggregate results compiled for further evaluation of the efficacy of the results?

While these procedures provide a far more robust means for comparing test and simulation results, there seems to be the need to monitor results from its application to further enhance the procedures to assure a high-level of confidence in the results.

ACKNOWLEDGMENTS

The authors wish to acknowledge the Federal Highway Administration (FHWA) and National Highway Traffic Safety Administration (NHTSA) of the U.S. Department of Transportation for supporting these modeling and simulation efforts.

REFERENCES

1. AASHTO, Manual for Assessing Safety Hardware (MASH), published by the American Associations of State Highway & Transportation Officials, Washington, DC, 2010.
2. Ross HEJ, Sicking DL, Zimmer RA, Michie JD; Recommended Procedures for the Safety Performance Evaluation of Highway Features,” National Cooperative Highway Research Program Report 350. Transportation Research Board, National Research Council, Washington, D.C., 1993.
3. Ray, M.L., et al; “Guidelines for Verification and Validation of Crash Simulations Used in Roadside Safety Applications,” Report from NCHRP Project 22-24, Transportation Research Board, Washington, DC, 2010
4. Bullard, D.L.; Bligh, R.P.; Menges, W.L.; & Huag, R.; Volume I: Evaluation of Existing Roadside Safety Hardware Using Updated Criteria – Technical Report, Texas Transportation Institute, TTI Project 476460-0001, College State, TX, March 2010.
5. Modeling, Testing, & Validation of the 2007 Chevy Silverado Finite Element Model, Working Paper NCAC 2009-W-005 prepared for FHWA, 2009.
6. Component & Full-Scale Tests of the 2007 Chevrolet Silverado Suspension System, Working Paper (NCAC 2009-R-004) prepared for FHWA, 2009.
7. Development & Validation of a Model of a 2007 Chevy Silverado Pick-up Truck Working Paper (NCAC 2009-R-002) prepared for FHWA, 2009. June 2011.
8. Extended Validation of the 2007 Silverado Finite Element Model Working Paper (NCAC 2012-W-003) prepared for FHWA, 2011, August 2011.
9. Marzougui, D.; Kan, C.D.; Opiela, K.S.; Simulation of MASH Test 3-11 of a Chevy Silverado into a New Jersey Shaped Concrete Barrier , Working Paper (NCAC 2010-W-001) prepared for the FHWA; December 2012.
10. Marzougui, D.; Kan, C.D.; Opiela, K.S.; Simulation of MASH Test 3-11 of a Chevy Silverado into a G9 Thrie Beam Guardrail, Working Paper (NCAC 2010-W-015) prepared for the FHWA; December 2012.
11. Marzougui, D.; Kan, C.D.; Opiela, K.S.; Simulation of MASH Test 3-11 of a Chevy Silverado into a G4(2W) W-Beam Guardrail, (NCAC 2010-W-002) prepared for the FHWA; December 2012.
12. Marzougui, D.; Kan, C.D.; Opiela, K.S.; Simulation of MASH Test 3-11 of a Chevy Silverado into a W-Beam Transition, (NCAC 2010-W-004) prepared for the FHWA; December 2012.
13. Marzougui, D.; Kan, C.D.; Opiela, K.S.; Simulation of MASH Test 3-11 of a Chevy Silverado into a G3 Weak Post Box Beam Guardrail, (NCAC 2010-W-014) prepared for the FHWA; December 2012.
14. Marzougui, D.; Kan, C.D.; Opiela, K.S.; Simulation of MASH Test 3-11 of a Chevy Silverado into a Modified G2 Weak Post W-Beam Guardrail, (NCAC 2010-W-013) prepared for the FHWA;
15. Marzougui, D.; Kan, C.D.; Opiela, K.S.; Simulation of MASH Test 3-11 of a Chevy Silverado into a G4(1S) W-Beam Median Barrier, (NCAC 2010-W-003) prepared for the FHWA;
16. AASHTO, Roadside Design Guide, published by the American Associations of State Highway & Transportation Officials, Washington, DC, 2006.

Applying Finite Element Analysis to Assess the Crash Performance of Modified R350 TL4 Bridge Rail Design in Accordance with the Federal-Aid Reimbursement Eligibility Process

CHUCK PLAXICO
Roadsafe LLC

This paper discusses design modifications made to the curb-mounted Oregon 3-tube bridge rail (BR208) to increase its strength capacity. Finite element analysis (FEA) was used to evaluate the crash performance of the modified design based on impact conditions and assessment procedures specified in NCHRP Report 350 (R350) for Test Level 4 (TL4). This assessment was carried out according to the Federal-Aid Reimbursement Eligibility Process recently instituted by the Federal Highway Administration (FHWA). The primary focus of this paper is on the application of these procedures to evaluate modifications to existing barrier hardware designs using FEA.

The proposed design options were adopted from another R350 TL4 design (i.e., New York Department of Transportation four-rail curbless bridge railing) and were here evaluated for the Oregon 3-tube bridge rail. The modifications included closer post spacing, stronger tube rails, and increased reinforcing for the curb/deck. Initial strength calculations for the modified design were carried out according to Appendix A13 of the AASHTO LRFD Bridge Design Specifications 2012 which indicated that the proposed design would be approximately 50 percent stronger than the baseline system. The crash analyses were carried out using the non-linear dynamic explicit FEA software LSDYNA.

A *baseline* finite element model of the BR208 bridge rail was developed and validated through comparison with results from full-scale crash tests using the procedures outlined in NCHRP Web-Document 179 to ensure that the model results were accurate, predictive and valid. The available full-scale test data for the validation task included Tests 404201-7 (Test 4-10), 404201-8 (Test 4-11) and 404201-9 (Test 4-12) which were performed under *Report 350* TL4 test conditions. Once the baseline model was validated, the model of the bridge rail was updated to reflect the proposed modifications. FEA was again used to evaluate the crash performance of the modified design regarding structural capacity, occupant risk measures and vehicle stability. The results of the analyses were also directly compared to those from full-scale crash tests on the original BR208 bridge rail design to determine if the design changes meet the FHWA criteria for “inconsequential or positive” change.

Based on the results of the analyses, the design modifications presented herein were determined to meet all structural capacity, occupant risk measures and vehicle stability criteria set forth in R350. The design modifications are further considered to be non-significant, regarding the changes to the original R350 TL4 design, since the effects of the changes were shown to be inconsequential to the performance of the system. These results are currently under review by the FHWA and their consultants and a determination of federal-aid eligibility will be forthcoming.

Roadside Safety Implications of Future Vehicle Designs

DHAIFER MARZOUGUI
CING-DAO (STEVE) KAN
FADI TAHAN
KENNETH OPIELA
George Mason University

Vehicle designs are consistently changing to address a variety of needs. These changes, however, can have implications on safety aspects. For example, there have been recent efforts to make vehicles lighter to meet new fuel economy requirements under government standards. While lighter vehicles will use less fuel (or energy), generally they are believed to offer less safety [albeit that weight itself may not be the controlling factor]. This effort was a spin-off of a previously undertaken efforts to assess safety impacts of proposed light-weighting measures for future vehicle designs. The efforts focused on occupant risk metrics associated with the New Car Assessment Program (NCAP). Since NCAP does not include an angular impact test reflective of most roadside crashes, it was considered important to assess the implications on safety for this type of impact. Vehicles with changes to reduce weight that were developed in the previous efforts were subjected to 25-degree impact angle at 50, 70, and 100 km/h speeds for three commonly-used types of longitudinal barriers (new Jersey-shaped concrete barrier, w-beam guardrail, and a w-beam transition). Changes in the roll, pitch, and yaw parameters were plotted and compared to understand the effects of light weighting on safety. Three vehicle types corresponding to barrier crashworthiness test vehicles were considered. Roll, pitch, and yaw measures of vehicle behavior derived from the simulations were the primary analysis metric. The results indicated the differences in roll, pitch, and yaw, but consistent trends were not apparent. A preliminary analysis of occupant risk effects was undertaken and minor effects were noted.

Comparing Objective and Subjective Roadway Data Collection Methods Using Cost–Benefit Analysis for the Proposed Safety Countermeasures

NILOO PARVIN

Iowa State University

The U.S. Roadway Assessment Program, have conducted numerous research efforts in the field of road safety to establish a methodology to determine built-in level of safety for the roads as well as tools to identify cost-effective safety improvements. Road infrastructure attributes that are known to have an impact on the likelihood and severity of crashes, can be modelled systematically. Level of safety of the road can be shown through RAP Start Rating method, giving one star to least and five star to safest roads.

The Second Strategic Highway Research Program Roadway Information Dataset (RID) includes a variety of safety-related roadway attributes collected by a mobile data collection vendor. RID covers about 12,500 centerline miles in the six Naturalistic Driving Study sites and met high accuracy requirements by implementing a quality assurance plan. Additionally, manual data coding using videologs/street view images is another common method of data collection. Although this method of data collection can be achieved with a low budget, the accuracy of data is in question due to subjectivity of the coder.

Using cost-benefit analysis, this study aims to compare the objective data collection approach of utilizing a mobile data collection vendor with high quality assurance processes versus the subjective approach of coding data manually. Star ratings are calculated for a sample of rural roads of North Carolina using RID and the manually coded dataset. The more accurate the input road inventory data is, the more proper safety countermeasure suggestion from the RAP tool will be expected. The cost-effectiveness of investing in high quality data will be determined with the comparison of the proposed countermeasures.

Performance Characteristics of Posts Embedded in Soil for Use in Computer Simulation

KARLA A. LECHTENBERG

JOHN D. REID

RONALD K. FALLER

*Midwest Roadside Safety Facility
University of Nebraska–Lincoln*

Computer simulation is utilized during the design phases of many projects. Researchers have relied primarily on strong-axis performance of posts embedded in soil to verify post-soil reactions during an impact. As computer simulation becomes more prominently used, there is a need to refine the performance of a post embedded in soil. The primary objective of this research study was to determine the post-soil impact reaction of W6x8.5 steel posts and 6-in. x 8-in. Southern Yellow Pine (SYP) posts, specifically along the weak axis, as well as the post-soil impact reaction of W6x8.5 posts in the strong axis.

Five bogie tests were conducted on W6x8.5 ASTM A992 steel posts with a length of 72 in. with embedment depths ranging between of 24 and 40 in. Four bogies tests were conducted on 6-in. x 8-in. SYP posts embedded at depths ranging between 30 and 40 in. The target impact conditions were an impact speed of 20 mph and an impact angle of 0 degrees creating weak-axis bending. The posts were impacted 24 $\frac{1}{8}$ in. above the groundline and perpendicular to the web of the post. For strong-axis evaluation, a total of eight dynamic component tests were performed - two tests with the 40-in. embedment depth and six with a 36-in. embedment depth. For two of the six 36-in. embedment tests, the load height was increased from 24 $\frac{1}{8}$ in. to 28 $\frac{1}{8}$ in.

A compacted, coarse crushed limestone material as recommended by the *Manual for Assessing Safety Hardware* (MASH) was utilized for all tests. For each test, acceleration data was used to determine force vs. displacement and energy vs. displacement and failure mechanisms of the post-soil system were noted. Post-soil interaction forces and energy dissipation characteristics of the posts were compared. Conclusions were made that pertain to the wood and steel posts impacted along the weak and strong axes in order to establish soil-post characteristics to be utilized during computer simulation modeling.

INTRODUCTION

Soil strength is known to be critical to the performance of soil-based systems. A soil strength requirement was introduced in the American Association of State Highway and Transportation Officials (AASHTO) *Manual for Assessing Safety Hardware* (MASH) [1], which is the current impact safety standards for evaluating highway safety features. However, this means that crash testing of a soil-based system is conducted under idealized conditions. This idealized crash testing may not encompass the real-world installation conditions for these soil-based systems.

In addition, computer simulation has been and is utilized during the design phases of many projects. Researchers have relied primarily on strong-axis performance of posts embedded in soil to verify post-soil reactions during an impact. As computer simulation becomes more prominently used, there is a need to refine the performance of a post embedded in soil. Thus, collecting data for the performance of a post impacted in the weak-axis is necessary.

Similarly, in order to optimize the post-soil interaction and maximize the lateral load supported by the post, it is often desirable for a steel post to rotate in the soil rather than bend and form a plastic hinge. Once the post bends under plastic deformation, the entire post is no longer rotating in the soil. Eventually, the post-soil resistance drops significantly as the steel post deforms due to lateral torsional buckling. An excessive post embedment would increase the soil resistance and reduce the capability of the entire post to rotate in the soil. On the contrary, a shallow post embedment would result in limited soil resistance during rotation and increase the propensity for the post to be removed from the ground. Therefore, it was desired to gain an understanding of the post-soil interaction characteristics associated with posts with reduced embedment depths.

RESEARCH OBJECTIVE

The primary objective of this research study was to determine the soil-post impact reaction of W6x8.5 (W150x12.6) steel posts and 6-in. x 8-in. (152-mm x 203-mm) Southern Yellow Pine (SYP) posts, specifically along the weak-axis, as well as the post-soil impact reaction of W6x8.5 posts in the strong axis with reduced embedment depths. Dynamic component testing was utilized to determine the post-soil behavior of steel and wood posts placed in compacted, soil material representative of that used for the AASHTO MASH full-scale testing [1]. This post testing program was used to investigate the dynamic response of the posts as well as to determine the point when a post will rotate through the soil instead of yielding or fracturing.

WEAK-AXIS DYNAMIC COMPONENT TESTING

Bogie tests were undertaken on W6x8.5 (W152x12.6) steel posts and 6-in. x 8-in. (152-mm x 203-mm) SYP posts impacted along the weak axis at varying embedment depths to determine their dynamic properties.

Five bogie tests were conducted on 72-in. (1,829-mm) long W6x8.5 (W152x12.6) ASTM A992 steel posts with embedment depths ranging from 24 to 40 in. (610 to 1,016 mm). Four bogie tests were then conducted on 72-in. (1,829-mm) long 6-in. x 8-in. (152mm x 203mm) SYP posts embedded at depths ranging from 30 to 40 in. (762 to 1,016 mm). A compacted, coarse crushed limestone material, as recommended by MASH, was utilized for all tests [1]. The target impact conditions were an impact speed of 20 mph (32.2 km/h) and an impact angle of 0 degrees, creating weak-axis bending. The posts were impacted 24 $\frac{7}{8}$ in. (632 mm) above the groundline and perpendicular to the web of the post. The dynamic component testing matrix is shown in Table 1.

Steel Post Weak-Axis Impact Results

Five bogie component tests were conducted on W6x8.5 (W152x12.6) steel posts with different embedment depths ranging between 24 and 40 in. (610 and 1,016 mm). All five posts were impacted perpendicular to the web of the post, creating weak-axis bending in order to determine the weak-axis characteristics of the steel post. All five posts rotated through the soil. However, the posts with embedment depths of 34 and 40 in. (864 and 1,016 mm) yielded significantly. The

TABLE 1 Test Matrix and Results

Test No.	Post Description	Impact Orientation	Embedment Depth in. (mm)	Peak Force kips (kN)	Average Force @ 15 in. kip (kN)	Total Energy kips-in. (kJ)	Maximum Deflection in. (mm)	Failure Type
WAP-1	W6x8.5 (W152x12.6)	Weak axis	40 (1016)	5.8 (25.8)	3.81 (16.9)	110.1 (12.4)	36.5 (927)	Post yielding - Flange tearing
WAP-2	W6x8.5 (W152x12.6)	Weak axis	34 (864)	9.7 (43.1)	3.74 (16.6)	113.1 (12.8)	41.5 (1054)	Post yielding - Flange tearing
WAP-3	W6x8.5 (W152x12.6)	Weak axis	28 (711)	12.2 (54.3)	3.74 (16.6)	103.1 (11.6)	41.5 (1054)	Rotation in Soil - Minor yielding
WAP-4	W6x8.5 (W152x12.6)	Weak axis	24 (610)	15.4 (68.5)	4.56 (20.3)	95.1 (10.7)	41.2 (1046)	Rotation in Soil - Minor yielding
WAP-5	W6x8.5 (W152x12.6)	Weak axis	24 (610)	15.4 (68.5)	4.19 (18.6)	87.7 (9.9)	41.0 (1041)	Rotation in Soil - Slight yielding
SYPW-1	6-in. x 8-in. (152 mm x 203 mm)	Weak axis	40 (1016)	14.3 (63.6)	NA	82.1 (9.3)	10.5 (267)	Post fracture near groundline
SYPW-4	6-in. x 8-in. (152 mm x 203 mm)	Weak axis	37 (940)	12.5 (55.6)	NA	45.4 (5.1)	6.9 (175)	Post fracture below groundline
SYPW-3	6-in. x 8-in. (152 mm x 203 mm)	Weak axis	34 (864)	15.9 (70.7)	7.15 (31.8)	162.5 (18.4)	40.3 (1024)	Post rotation through soil
SYPW-2	6-in. x 8-in. (152 mm x 203 mm)	Weak axis	30 (762)	15.7 (69.8)	6.33 (28.2)	121.1 (13.7)	36.6 (930)	Post rotation through soil
MH-1	W6x8.5 (W152x12.6)	Strong Axis	40 (1016)	14.0 (62.3)	9.5 (42.3)	230.6 (26.1)	36.3 (922)	Rotation in Soil - Yielding
MH-4	W6x8.5 (W152x12.6)	Strong Axis	40 (1016)	12.9 (57.4)	9.5 (42.3)	230.7 (26.1)	39.0 (991)	Rotation in Soil - Yielding
MH-2	W6x8.5 (W152x12.6)	Strong Axis	36 (914)	11.5 (51.2)	7.9 (35.1)	165.9 (18.7)	36.7 (932)	Post rotation through soil
MH-3	W6x8.5 (W152x12.6)	Strong Axis	36 (914)	11.6 (51.6)	8.6 (38.3)	214.3 (24.2)	39.5 (1,003)	Post rotation through soil
MH-5	W6x8.5 (W152x12.6)	Strong Axis	36 (914)	12.2 (54.3)	8.5 (37.8)	177.8 (20.1)	36.8 (935)	Post rotation through soil
MH-6	W6x8.5 (W152x12.6)	Strong Axis	36 (914)	13.8 (61.4)	8.8 (39.1)	176.6 (20.0)	31.0 (787)	Post rotation through soil
MH-7	W6x8.5 (W152x12.6)	Strong Axis	36 (914)	10.9 (48.5)	7.2 (32.0)	146.7 (16.6)	33.3 (846)	Post rotation through soil
MH-8	W6x8.5 (W152x12.6)	Strong Axis	36 (914)	12.2 (54.3)	8.3 (36.9)	178.0 (20.1)	33.8 (859)	Post rotation through soil

results are summarized in Table 1. Force vs. deflection and energy vs. deflection curves are shown in Figure 1 and Figure 2, respectively. Further testing analysis discussion can be found in the reference report [2].

It is important to understand the process and factors that reduce the bogie's kinetic energy. The energy in the system begins in the form of kinetic energy from the bogie moving in relation to the post system. When the bogie impacts the post, the bogie's kinetic energy is converted into other forms of energy. The two most prominent being the energy transferred from the bogie to the soil when the post rotates through the soil, and the energy absorbed through plastic deformation of the post. Other less prominent energies include friction between the bogie and the post and rolling friction. The system behavior resulted in varying amounts of energies absorbed by the system with total absorbed energies ranging between 87.7 and 113.1 kip-in. (9.8 and 12.8 kJ).

System behavior is determined by the post behavior, which is dependent on post embedment depth. When the embedment depth was 40 and 34 in. (1,016 and 864 mm), as used in test nos. WAP-1 and WAP-2, the posts had relatively low rotation in the soil and bent backward near the groundline. As a result of the similar behavior, the two systems absorbed approximately the same amount of total energy with values of 110.1 and 113.1 kip-in. (12.4 and 12.8 kJ), respectively. The majority of the energy was converted from kinetic energy into plastic energy from the post bending backward because the post had relatively very little rotation in the soil.

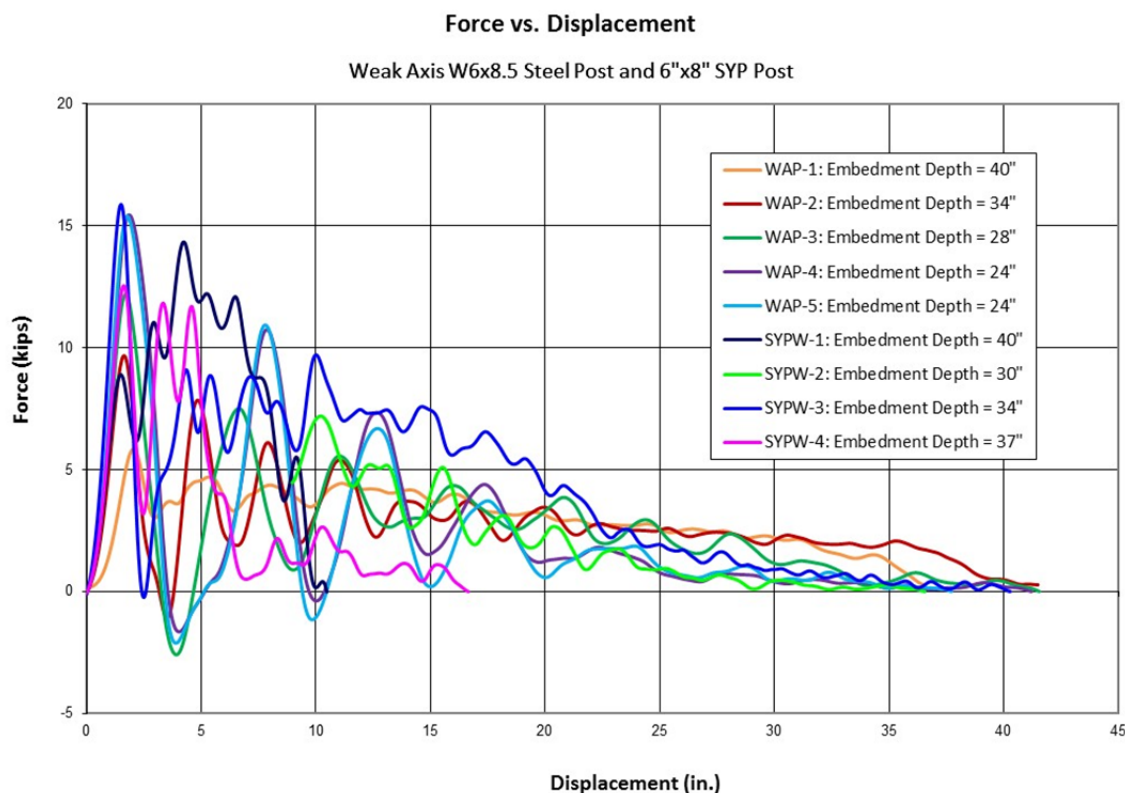


FIGURE 1 Force vs. Deflection Comparison, Weak Axis Impact.

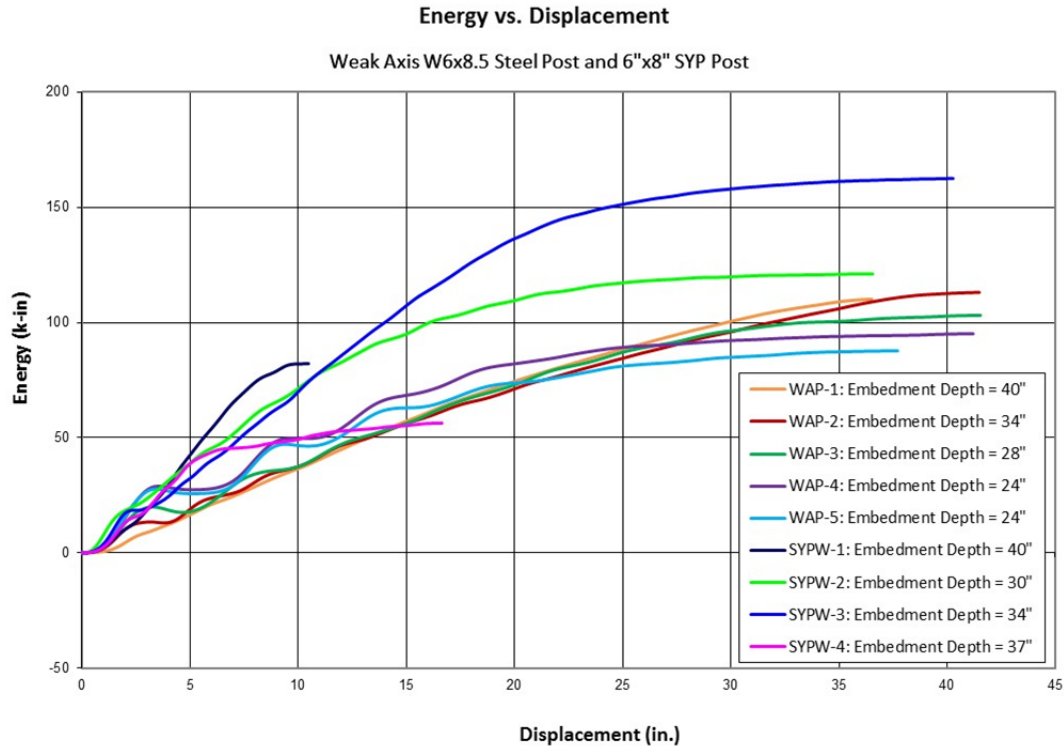


FIGURE 2 Energy vs. Deflection Comparison, Weak Axis Impact.

When embedment depths of 24 and 28 in. (610 and 711 mm) were used, as observed in test nos. WAP-3 through WAP-5, the posts rotated through the soil with minor post bending. The shallower embedded posts, which rotated through the soil, absorbed noticeably less energy than the posts that bent with plastic deformation, as reported in Table 1.

The resistive force reached its maximum amplitude between the first 1.7 and 2.0 in. (43 and 51 mm) of deflection, as shown in Figure 1. Generally, the amplitude of the initial peak is inversely proportional to the embedment depth. This could be attributed to the inertial effects of the bogie impacting the post. As the embedment depth decreases, additional mass is located above the bogie impact location. This additional mass above the impact point may increase the inertia required to initially displace the post, causing a higher initial resistive force. However, the deeper embedded posts provided greater resistive forces throughout the later stages of the impact event.

Wood Post Weak-Axis Impact Results

Four bogie component tests were conducted on 6-in. x 8-in. (152-mm x 203-mm) SYP post with different embedment depths ranging between 30 and 40 in. (762 and 1,016 mm). All four posts were impacted perpendicular to the weak axis of the post, creating weak-axis bending in order to determine the weak-axis characteristics of the wood post. All four posts rotated through the soil. However, the posts with embedment depths of 37 and 40 in. (940 and 1,016 mm) fractured completely. The results are summarized in Table 1. Force vs. deflection and energy vs. deflection

curves are shown in Figure 1 and Figure 2, respectively. Further testing analysis discussion can be found in the reference report [2].

Similar to the steel posts, it is important to understand the process and factors that reduce the bogie's kinetic energy. The energy in the system begins in the form of kinetic energy from the bogie moving in relation to the post system. When the bogie impacts the post, the bogie's kinetic energy is converted into other forms of energy. The two most prominent being the energy transferred from the bogie to the soil when the post rotates through the soil and the energy absorbed by the wood post during bending and fracturing. Other less prominent energies include friction between the bogie and the post and rolling friction. The system behavior resulted in varying amounts of energies absorbed by the system with total absorbed energies ranging between 45.4 and 162.5 kip-in. (5.1 and 18.4 kJ).

System behavior is determined by post behavior, which is dependent on post embedment depth. When the embedment depth was 30 and 34 in. (762 and 864 mm), as used in test nos. SYPW-2 and SYPW-3, the post experienced large rotations through the soil. The 34-in. (864-mm) embedded post allowed more energy absorption than the 30-in. (762-mm) embedded post because the deeper post displaced an additional 4 in. (102 mm) of soil compared to the shallower post during rotation. This additional soil provided greater resistive forces while the post rotated through the soil. The total energy absorbed by the 34-in. and 30-in. (864-mm and 762-mm) embedment systems were 162.0 kip-in and 121.1 kip-in (18.4 kJ and 13.7 kJ), respectively.

When deeper embedment depths of 37 and 40 in. (940 and 1016 mm) were used, such as in test nos. SYPW-1 and SYPW-4, the post fractured completely with little rotation through the soil. The values of the peak force were relatively similar regardless of post behavior, as reported in Table 1. However, the deeper embedded posts, which fractured, did not provide resistive forces for as long of a duration as the posts that rotated through the soil, as shown in Figure 4. As a result, the posts that fractured absorbed noticeably less energy than the posts that rotated through the soil.

STRONG-AXIS DYNAMIC COMPONENT TESTING

Bogie tests were undertaken on W6x8.5 (W152x12.6) steel posts impacted along the strong axis at varying embedment depths to determine their dynamic properties. Eight dynamic component tests were conducted on W6x8.5 (W152x12.6) ASTM A992 steel post at two different embedment depths. A compacted, coarse crushed limestone material, as recommended by MASH [1], was utilized for all tests. The target impact conditions were an impact speed of 20 mph (32.2 km/h) and an impact angle of 90 degrees, creating a classical "head-on" or full frontal impact and strong-axis bending. Six of the tests were impacted 24 $\frac{7}{8}$ in. (632 mm) above the groundline while the final two tests were impacted 28 $\frac{7}{8}$ in. (733 mm) above the groundline. All eight tests were impacted perpendicular to the flange of the post. The dynamic component testing matrix are shown in Table 1.

Steel Post Strong-Axis Impact Results

Eight bogie component tests were conducted on W6x8.5 (W152x12.6) steel posts at two different embedment depths and two different impact heights. All either posts were impacted perpendicular to the flange of the post, creating strong-axis bending in order to establish the

strong-axis characteristics of the steel post. All eight posts rotated through the soil. However, the posts with embedment depths of 40 in. (1,016 mm) yielded significantly. The results from the bogie testing matrix are summarized in Table 1. The force vs. deflection and energy vs. deflection comparison curves are shown in Figure 3 and Figure 4. Further testing analysis discussion can be found in the reference report [3].

Recall, system behavior is determined by the post behavior, which is dependent on post embedment depth. When the bogie impacts the post, the bogie's kinetic energy is converted into other forms of energy, specifically energy transferred from the bogie to the soil when the post rotates through the soil and the energy absorbed through plastic deformation of the post. Therefore, the system behavior resulted in varying amounts of energies absorbed by the system with average total absorbed energies ranging between 162.4 and 230.7 kip-in. (18.3 and 26.1 kJ).

The steel posts with a 40-in. (1,016-mm) embedment depth, as used in test nos. MH-1 and MH-4, had relatively low rotation in the soil and bent backward near the groundline. The two systems absorbed an average total energy of 230.65 kip-in. (26.1 kJ) through a maximum deflection of 37.7 in. (596 mm). The average post-soil resistance of these posts was 9.5 kips (42.3 kN) through 15 in. (381 mm) of deflection.

Test nos. MH-2, MH-3, MH-5, and MH-6 were conducted on posts with a reduced embedment depth of 36 in. (914 mm) while maintaining an impact height of 24 $\frac{7}{8}$ in. (733 mm). These posts rotated through the soil with minor post bending. As observed with the weak-axis impacts, the shallower embedded posts absorbed noticeably less energy than the posts that bent with plastic deformation.

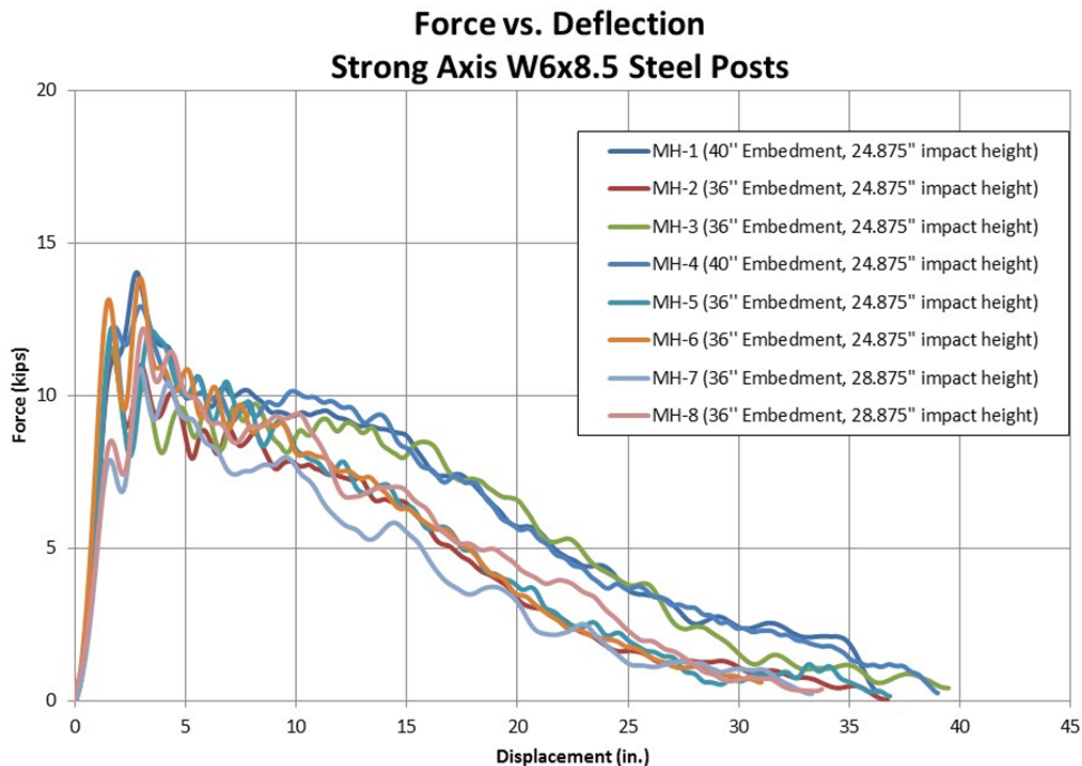


FIGURE 3 Force vs. Deflection Comparison, W6x8.5 Posts, Strong Axis Impact.

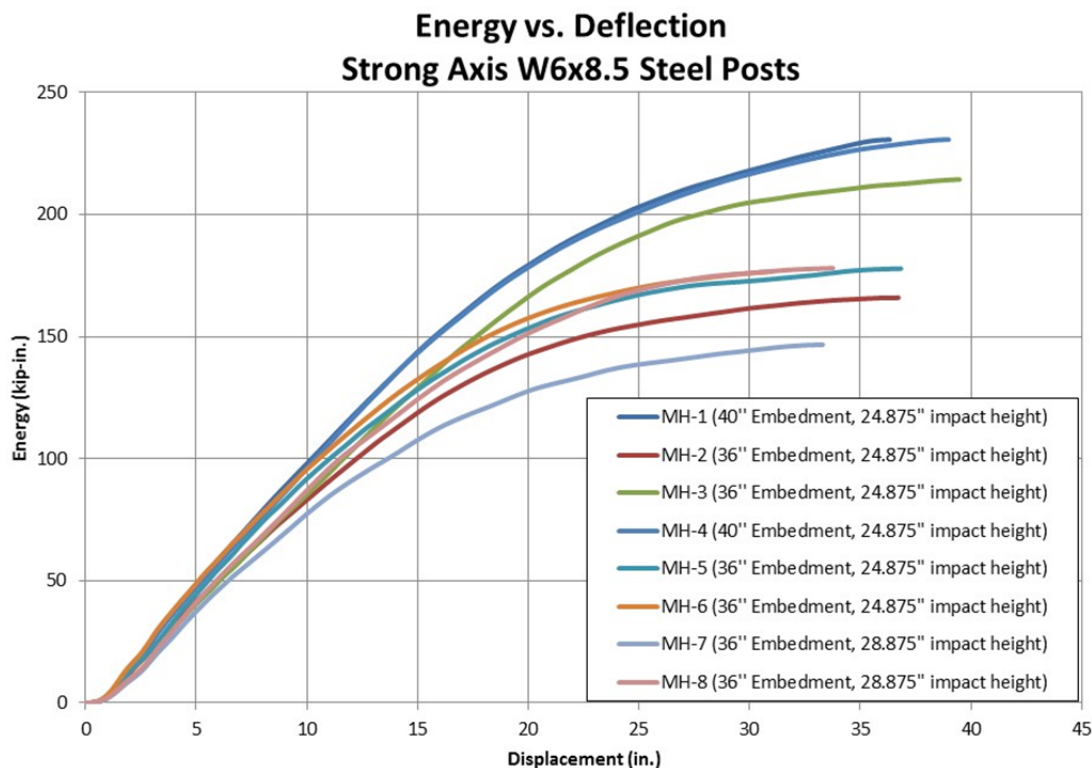


FIGURE 4 Energy vs. Deflection Comparison, W6x8.5 Posts, Strong Axis Impact.

When the reduced embedment depth of 36 in. (914 mm) was used in combination with an increased impact height of 28 $\frac{7}{8}$ in. (733 mm), as used in test nos. MH-7 and MH-8, the posts also rotated through the soil without bending. These posts observed a 17.9 percent reduction in force resistance when compared to the posts with a 40-in. (1,016-mm) embedment depth. The total energy absorbed by these posts was 162.4 kip-in. (18.3 kJ) through a maximum deflection of 33.6 in. (853 mm). These tests even had lower resistance and energy absorption than the posts with a reduced embedment depth of 36 in. (914 mm) and an impact height of 24 $\frac{7}{8}$ in. (733 mm).

SUMMARY OF DYNAMIC COMPONENT TESTING RESULTS

The objectives of this research study was to determine the soil-post impact reaction of W6x8.5 (W152x12.6) steel posts and 6-in. x 8-in. (152-mm x 203-mm) SYP posts along the weak axis and to determine the soil-post impact reaction characteristics for steel posts with reduced embedment depths and increased load heights along the strong axis. The first phase of the study contained of a total of five bogie tests on W6x8.5 (W152x12.6) steel posts embedded at depths ranging from 24 to 40 in. (610 to 1,016 mm), and four bogie tests conducted on 6-in. x 8-in. (152-mm x 203-mm) SYP posts embedded at depths ranging from 30 to 40 in. (762 to 1,016 mm). All posts of the first phase were impacted along the weak axis. The second phase of the study involved a total of eight dynamic component tests on 72-in. (1,829-mm) long W6x8.5 (W152x12.6) posts embedded at different depths and impacted at different heights. Two tests were conducted with an embedment depth of 40 in. (1,016 mm) with an impact height of 24 $\frac{7}{8}$ in.

(632 mm), four tests were conducted on posts with an embedment depth of 36 in. (914 mm) with an impact height of 24 $\frac{7}{8}$ in. (632 mm), and two tests were conducted on posts with an embedment depth of 36 in. (914 mm) with an impact height of 28 $\frac{7}{8}$ in. (733 mm). All posts of the second phase were impacted along the strong axis.

Phase 1 – Weak-Axis Soil-Post Impact Reaction Characteristics

During the weak-axis testing phase, the SYP post systems with embedment depths of 34 and 30 in. (864 and 762 mm), followed by the steel W6x8.5 (W152x12.6) post systems with embedment depths of 40 and 34 in. (1,016 and 864 mm), produced the greatest energy dissipations of 162.5, 121.1, 110.1 and 113.1 kip-in. (18.4, 13.7, 12.4 and 12.8 kJ), respectively. The post systems that absorbed the most energy among the nine tests were 6-in. x 8-in. (152-mm x 203-mm) SYP posts at 30 and 34 in. (762 and 864 mm) embedment depths. These posts rotated through the soil without fracturing. However, the W6x8.5 (W152x12.6) steel post systems with embedment depths of 40 and 34 in. (1016 and 864 mm) absorbed the most energy among the steel post systems. These embedment depths allowed the post to yield and provided more energy absorption than the steel post systems that rotated through the soil.

When impacted along the weak axis, the wood post systems absorbed more energy when rotation through the soil was witnessed compared to the wood post systems that fractured. However, the steel post system absorbed more energy when the post yielded compared to when the steel post rotated through the soil.

Phase 2 – Strong-Axis Soil-Post Impact Reaction Characteristics

During the strong-axis testing phase, the two W6x8.5 (W152x12.6) posts with a 40-in. (1,016-mm) embedment depth yielded. Both posts developed plastic hinges approximately 10 in. (254 mm) below groundline. None of the posts with the 36-in. (914-mm) embedment depths yielded. Even the posts with the increased load height remained undamaged.

As expected, the posts with a reduced embedment depth resulted in lower post-soil interaction forces when impacted along the strong axis. In fact, the average resistance force was decreased approximately 12 percent as compared to the average forces recorded during the 40-in. (1,016-mm) embedment depth tests. The resistance was further reduced during the tests when the load height was increased. The tests with the increased impact height of 28 $\frac{7}{8}$ in. (733 mm) showed average resistance forces approximately 20 percent lower than those with a 40-in. (1,016-mm) embedment depth and an impact height of 24 $\frac{7}{8}$ in. (632 mm).

STRONG AXIS VS. WEAK AXIS CHARACTERISTIC COMPARISON

Dynamic testing of 6-in. x 8-in. rectangular SYP posts impacted in the strong axis was undertaken in a previous study [4]. Therefore, these tests were not repeated. Test nos. GWB-14 and GWB-15 were performed with 6-in. x 8-in. (152-mm x 203-mm) wood posts. A summary of the bogie testing of the 6-in. x 8-in. rectangular SYP posts is shown in Table 2. The force vs. deflection and energy vs. deflection curves for strong-axis and weak-axis impacts of the W6x8.5 (W152x12.6) steel and 6-in. x 8-in. (152-mm x 203-mm) wood posts with embedment depths of 40 in. (1,016 mm) are shown in Figure 5 and Figure 6, respectively.

TABLE 2 Testing Results - 6-in. x 8-in. (152-mm x 203-mm) Wood Posts with 40-in. (1,016-mm) Embedment Depth [4]

Test No.	Post Description	Impact Orientation	Embedment Depth in. (mm)	Peak Force kips (kN)	Average Force @ 15 in. kip (kN)	Total Energy kips-in. (kJ)	Maximum Deflection in. (mm)	Failure Type
GWB-14	6-in. x 8-in. (152 mm x 203 mm)	Strong Axis	40 (1016)	14.6 (65.0)	11.6 (51.5)	232.0 (26.2)	31.7 (805)	Post rotation through soil
GWB-15	6-in. x 8-in. (152 mm x 203 mm)	Strong Axis	40 (1016)	13.5 (60.2)	11.3 (50.5)	225.6 (25.5)	30.0 (761)	Post rotation through soil

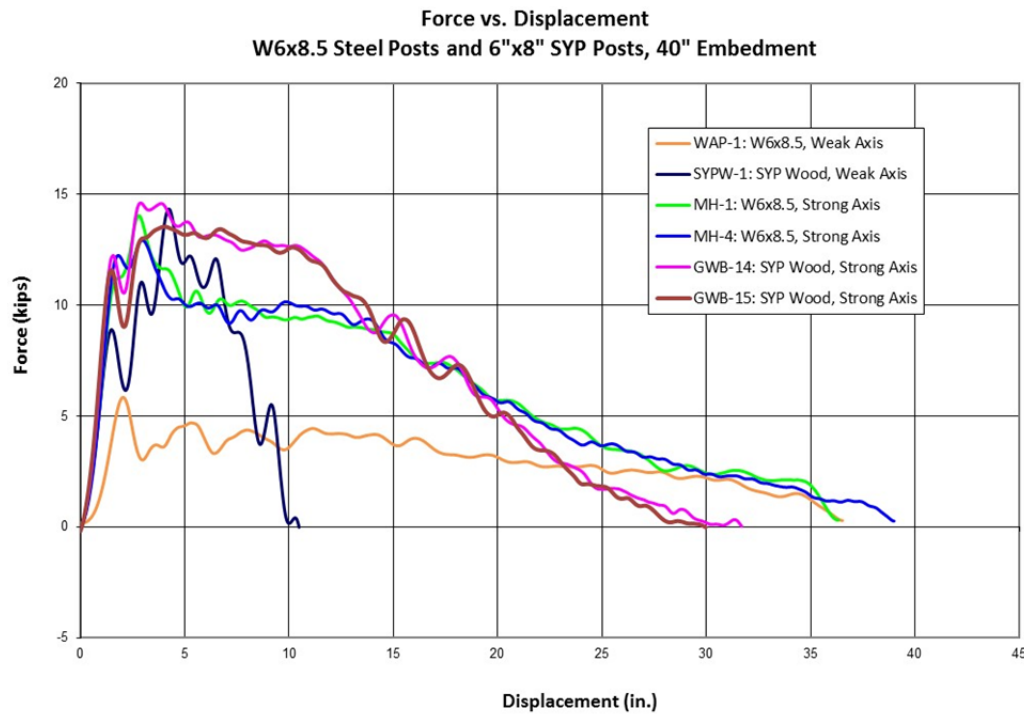


FIGURE 5 Force vs. Deflection Comparison, W6x8.5 and 6-in. x 8-in. SYP Posts, 40-in. Embedment.

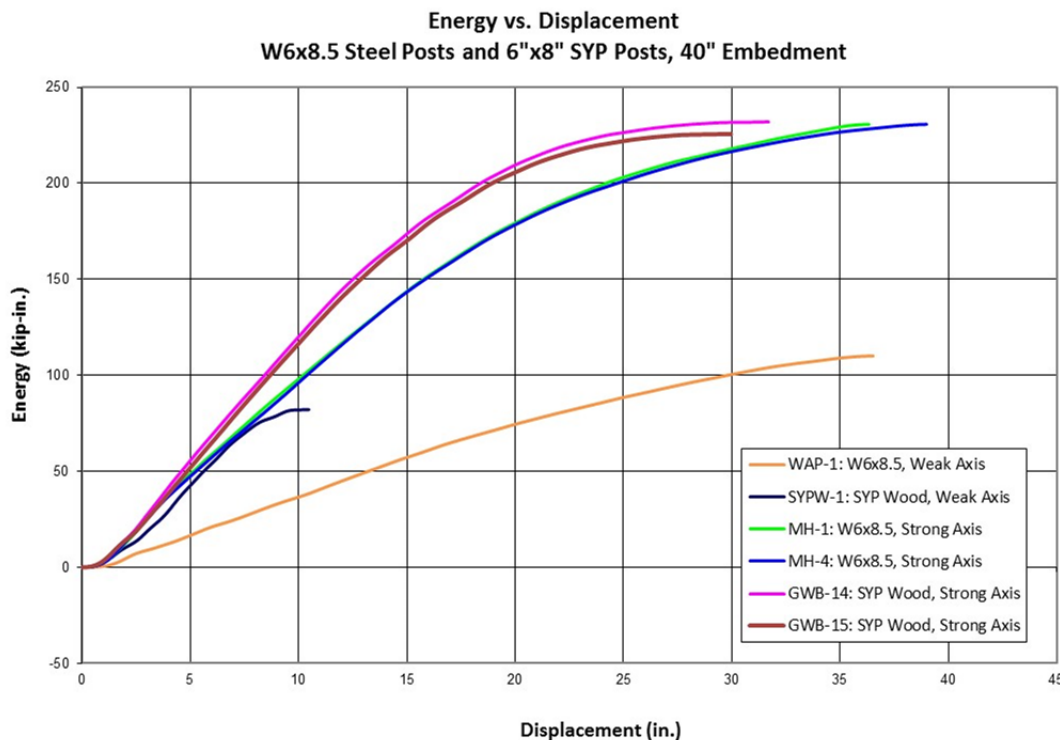


FIGURE 6 Energy vs. Deflection Comparison, W6x8.5 and 6-in. x 8-in. SYP Posts, 40-in. Embedment.

The force vs. deflection curves for all four strong-axis impact tests were similar in both shape and magnitude, but the forces in the wood posts were slightly higher between deflections of 3 and 13 in. (76 and 330 mm). The energy vs. deflection curves for both post types were similar in shape and magnitude, and almost overlapped for the first 5 in. (127 mm) of deflection. From 5 in. to 25 in. of deflection, the amount of energy absorbed by the steel post was slightly less than of the wood post. However, the total absorbed energies were also similar, ranging from 225.6 k-in. to 232.0 k-in. (25.5 kJ to 26.2 kJ). This slight difference in the soil resistance could be attributed to the fact that the wood post study was conducted a few years prior to the steel post strong-axis impact study.

The dynamic testing comparison indicated that the soil resistances for 6-in. x 8-in. (152-mm x 203-mm) wood posts and a W6x8.5 (W152x12.6) steel posts are similar when impacted in the strong axis. This supports the common assumption that 6-in. x 8-in. (152-mm x 203-mm) wood posts and W6x8.5 (W152x12.6) steel posts provide equivalent resistances for guardrail systems.

On the other hand, the force vs. deflection and energy vs. deflection curves for the two weak-axis impact test were quite different in both shape and magnitude, as shown in Figure 6. The forces in the weak-axis impacted wood post were very similar to those of a strong-axis impact of both the steel and wood posts. However, the wood post was only able to withstand soil resistance for approximately 10 in. (254 mm) of deflection as which point the post fractured. The total absorbed energy for the wood posts in a weak-axis impact was approximately 25 percent less than that of the steel post even though it fractured. It was shown that the soil resistance of the steel post in the weak-axis was approximately half of the resistance in the strong axis. This is

slightly greater than what one might expect when looking at only the material properties of a W6x8.5 (W152x12.6) steel posts.

CONCLUSIONS

Dynamic component testing was utilized to determine the post-soil behavior of steel and wood posts placed in compacted, soil material when impacted in both the strong-axis and weak-axis. Wood posts absorb more energy when rotation through the soil occurred when compared to wood posts that fractured. However, steel posts absorb more energy when the post yielded when compared to steel posts that rotate through the soil. The resistance of wood posts impacted in the weak axis is similar to that of wood and steel posts impacted in the strong axis until the point of wood post fracture. Further, the resistance of the steel post in the weak axis is approximately half of the resistance in the strong axis. Steel posts also absorb less energy when impacted at an increased impact height. Finally, the soil-post characteristics of both steel and wood posts in both the strong and weak axes for strong soil were established to be utilized during computer simulation modeling.

DISCLAIMER

The contents of this report reflect the views of the authors who are responsible for the facts and the accuracy of the data presented herein. The contents do not necessarily reflect the official views or policies of the Nebraska Department of Roads, the Mid-America Transportation Center (MATC), or the Federal Highway Administration (FHWA), U.S. Department of Transportation. This report does not constitute a standard, specification, regulation, product endorsement, or an endorsement of manufacturers.

ACKNOWLEDGMENTS

The authors wish to acknowledge several sources that made a contribution to this project: (1) the Nebraska Department of Roads, the Mid-America Transportation Center (MATC), and the Federal Highway Administration (FHWA), U.S. Department of Transportation for sponsoring this research project and (2) MwRSF personnel for installing the posts and conducting the component tests.

REFERENCES

1. *Manual for Assessing Safety Hardware (MASH)*, American Association of State Highway and Transportation Officials (AASHTO), Washington, D.C., 2009.
2. Humphrey, B.M., Lechtenberg, K.A., Reid, J.D., and Faller, R.K., *Performance Characteristics of Posts Embedded in Soil*, Final Report to Nebraska Department of Roads and Mid-America Transportation Center, Research Report No. TRP-03-301-15, Midwest Roadside Safety Facility, University of Nebraska-Lincoln, Lincoln, Nebraska, August 12, 2015.

3. Schmidt, T.L., Mongiardini, M., Bielenberg, R.W., Lechtenberg, K.A., Reid, J.D., and Faller, R.K., *Dynamic Testing of MGS W6x8.5 Posts at Decreased Embedment*, Final Report to Nebraska Department of Roads, Research Report No. TRP-03-271-12, Midwest Roadside Safety Facility, University of Nebraska-Lincoln, Lincoln, Nebraska, December 17, 2012.
4. Homan, D.M., Thiele, J.C., Faller, R.K., Rosenbaugh, S.K., Rohde, J.R., Arens, S.W., Lechtenberg, K.A., Sicking, D.L., and Reid, J.D. *Investigation and Dynamic Testing of Wood and Steel Posts for MGS on a Wire-Faced, MSE Wall*, Draft Final Report to Federal Highway Administration, Central Federal Lands Highway Division, Research Report No. TRP-03-231-11, Midwest Roadside Safety Facility, University of Nebraska-Lincoln, Lincoln, Nebraska, February 2012.

Impact Resistance of Guardrail Posts on Sloped Ground

CHUNG R. SONG

TEWODROS Y. YOSEF

University of Nebraska–Lincoln

RONALD K. FALLER

MOJDEH PAJOUH

KARLA A. LECHTENBERG

Midwest Roadside Safety Facility

University of Nebraska–Lincoln

The American Association of State Highway and Transportation Officials (AASHTO) *Manual for Assessing Safety Hardware* (MASH) recommend guardrail posts to be installed at least 2 ft. off from the slope break point. This width is difficult to achieve occasionally in terrains with sloping ground. As a result, guardrail design and installations in sloping ground may need to deviate from the desirable conditions, leading to, non-optimal guardrail installations in some cases. Thus, understanding the behavior of guardrail posts in sloping ground enables the determination of favorable guardrail design and installation. This research presents the result of non-linear finite element study on the impact behavior of guardrail posts in elasto-plastic soil medium.

The behavior of guardrail posts installed in sloping ground is complex due to the relative displacement of the post and the soil, the non-linear behavior of the soil, and the relative movement of the post and the soil at the interfaces. The problem gets further multifaceted in the presence of transient impact loads.

Three dimensional non-linear explicit finite element analyses were performed to investigate the impact behavior of guardrail posts in sloping ground under a transient lateral impact loading condition. The explicit non-linear finite element code, LS-DYNA was used for simulating the behavior. Standard steel guardrail posts of different lengths at different distances from the slope break point were considered for different undrained shear strength of the soil. The model used a piecewise linear plasticity material model for the steel guardrail post and extended Drucker-Prager model with the associated flow rule with dedicated interface elements.

From results of the nonlinear finite element analysis, an optimal guardrail post embedment length with respect to the ground slope angle was recommended. Finally, tentative design guidelines for embedment depth and mass inertia of the guardrail post were recommended.

Behavior and Performance of Wood and Composite Blockouts Raised on Posts during Component Pendulum Impact Testing

CHIARA SILVESTRI DOBROVOLNY

NATHAN SCHULZ

DUSTY ARRINGTON

ROGER P. BLIGH

Texas A&M Transportation Institute

With recent changes and clarifications about appropriate height for beam guardrail, there are more and more existing locations identified where rail height is below the recommended heights. Pavement overlays create additional locations where this occurs. Raising blockout on the post is a cost effective means to adjust the rail height, however there is not any known analysis of how this might affects rail performance.

The purpose of this research study was to analyze the behavior and performance of a post-blockout-rail system when the blockout is raised on the post as a mean for adjusting rail height. The researchers made use of the pendulum testing facility to test raised wood blockouts on wood and steel posts, as well as composite blockouts on steel posts. Tests were performed on 8-inch deep blockout raised on posts embedded in soil. Force-displacement data was recorded and evaluated to understand the strength of the raised blockout on the post system and its capability to transmit the impact forces into the soil. Recorded data from the pendulum testing was also used to help calibrate the FE models which were later employed to predict the behavior of raised wood blockouts on posts during full-scale impact events according to both NCHRP Report 350 and MASH testing standards. Given the proprietary characteristics, composite blockouts were not modeled for predictive FE computer simulations; however, engineering analysis was developed for recommendation of their use when raised on posts.

The information compiled from this research will enable the Departments of Transportation to determine whether raising blockouts on posts can be chosen as a low-cost safety means to adjust rail height when below recommended value, without compromising the rail system performance.

Evaluation of Soil Conditions and Post Embedment Depth on Guardrail Post Performance

ALI O. ATAHAN

Istanbul Technical University

MURAT ORNEK

Iskenderun Technical University

MURAT BUYUK

Sabanci University

ERCAN EPSILELI

Turkish DOT Kayseri Branch

Road Restraint Systems, RRS, are designed to provide the highest level of safety for traveling vehicles as well as vulnerable road users during a collision event. Steel guardrail systems are one of the most widely used road restraint systems in the world. The acceptability of these systems are evaluated through full-scale crash tests and during a crash event. Design parameters, such as post type, soil characteristics, guardrail properties, post-soil interaction and post embedment depth play an important role on the test outcome. Due to the differences in these parameters for a particular guardrail design crash test results vary significantly.

In this paper, effect of guardrail system parameters, such as post embedment depth, post type and soil characteristics on dynamic impact behavior of three different guardrail designs are evaluated. Field tests as well as finite element simulation results were used to compare impact performance of these designs. Three different post geometries, three different soil properties and seven different post embedment depths are assessed as test parameters. A 1000 kg pendulum device was used to apply the dynamic load on guardrail posts. Acceleration as well as post movement were recorded to make comparisons between designs.

Field and simulation test results showed that soil properties and post embedment depth have significant effect on guardrail post behavior during an impact test. Simulation results were found to be in a close agreement with the field test results. Optimum post embedment depth charts were constructed based on soil properties and post type. Full-scale crash testing is recommended to verify research findings.

Development of the Australian and New Zealand Standard for Safety Barriers and Associated Devices

ROD TROUTBECK

Troutbeck & Associates

JULIAN CHISNALL

New Zealand Transport Agency

The Australian and New Zealand Standard AS/NZS 3845 Part 1, published in 2015, addressed road safety barriers. Part 2 of the same standard is intended to be published in 2016 or 2017 and describes the acceptance process for truck mounted attenuators, truck rear under-run protection devices, permanent bollards, longitudinal channelizing devices, sign support structures and poles. Both parts of the standard are based on the MASH testing protocol but also provide for testing under other protocols. An important element of the standard is the additional issues that an assessor should consider when accepting the barrier system or device for use on Australian or New Zealand roads. This paper discusses the background to the standard with reasons why the committee (Standards Australia/Standards NZ joint committee CE-033) chose the approach taken.

WHY ASSESS SAFETY BARRIERS AND OTHER ROAD SAFETY DEVICES?

In the USA, run-off-road and cross centreline (head-on) crashes account for approximately 81 per cent of rural crashes (1). In New Zealand, run-off-road and cross centreline (head-on) crashes account for approximately 70% of all deaths and serious injuries on the New Zealand road network, with head-on crashes resulting in a greater number of fatalities per crash in comparison to run-off-road. The statistics are similar in Australia (2). Reducing this level of avoidable trauma is a key action for all road authorities in Australia and New Zealand.

The community at large has been demanding a higher level of road safety driven by the United Nations Decade of Action and encompassed in the National Road Safety Strategy (2) for Australia and the Safer Journeys Strategy (3) in New Zealand. The strong support for the Safe System approach to road safety that has been incorporated into these strategies looks to develop roads and roadsides such that they reflect the frailty of humans and that people make mistakes. An over riding principle is that nobody should be injured or seriously injured as a result of a road crash. The trend is to look towards barriers to provide the safer roadsides (4). The cost of providing sufficiently wide clear zones to ensure a low and acceptable risk to the community is becoming excessive. Additionally, the effectiveness of clear zone treatments has been challenged by Doecke and Woolley (5). Within this political and social environment, it is appropriate that the barriers and devices that we use on our roads are fit for purpose and have been assessed competently.

The Federal Highway Administration (FHWA) reviews crash testing undertaken on a road safety hardware system and issues a letter of eligibility for reimbursement of federal funds when used on federally funded projects (6) in the United States. The FHWA further indicates that the states should undertake their own assessment of road safety hardware to determine if they are

appropriate for their roads. Many states seem to simply rely on the FHWA eligibility letter as evidence of the system's acceptability.

The Europeans used the CE Mark to indicate that the road safety hardware has been tested to the CEN1317 requirements. This multipart standard does not assess durability of the product and this aspect is left to the purchaser to quantify. Unfortunately, within the European Union, it is sometimes difficult to exclude products because of their durability (7).

In Australia and New Zealand, the joint Standards Committee CE-033 considered there should be a thorough assessment of road safety hardware systems that covered a range of characteristics and uses. Part 1 of the Australian and New Zealand Standard AS/NZS 3845.1:2015 (8) provides guidance on this topic in relation to permanent and temporary road safety barrier systems including longitudinal road safety barriers, terminals, crash cushions, interfaces including transitions, and longitudinal barrier gate systems. Part 2 of the Standard (9) relates to permanent and temporary safety devices including bollards, longitudinal channelizing devices, truck or trailer mounted attenuators, truck rear under-run protection devices, sign support structures and poles.

FIRST EDITION OF THE STANDARD

The first edition of the joint Standard AS/NZS 3845:1999 (10) provided Australian and New Zealand Road Authorities with a common statement as to what constitutes an acceptable road safety barrier or crash attenuator. The principal method of assessment documented in AS/NZS 3845:1999 was through consideration of the results from full scale crash testing to the US NCHRP 350 protocol (11). The Standard listed the requirements for documentation to accompany a road safety barrier or crash attenuator. This list was useful to road authorities as the requirements assist installation design and maintenance procedures.

The Standard was produced at a time when most Australian and New Zealand road authorities were using standard public domain (non-proprietary) W-beam road safety barrier systems derived from US standard designs. In Australia, the most common semi-rigid barrier system comprised W-Beam guardrail mounted on steel block-outs and steel posts developed from the US standard design G4(1S), but using steel block-outs and posts with a different cross section. In New Zealand, the standard road safety barrier system comprised W-Beam guardrail mounted on timber posts and block-outs based on US standard design G4(2W).

At the time AS/NZS 3845:1999 was published, neither public domain design had been fully tested to the prevailing test protocol (NCHRP 350). As a consequence, the joint Standards Committee, CE-033, chose to make the W-beam systems "deemed to comply" at NCHRP 350 Test Level 3 without any full scale testing to establish their worth. In fact, later testing in the US (12) demonstrated that a barrier system similar to the Australian system failed to meet NCHRP 350 TL3 testing protocol with a 2000 kg vehicle. Later testing of a public domain steel barrier with plastic block-outs and mid-span splices has passed NCHRP 350 TL3 testing protocol. The New Zealand variant passed the NCHRP 350 TL3 testing protocol, but the test results (12) were "marginal" due to the instability of the impact test vehicle (2000kg pickup).

The First Edition of the standard contained a number of detailed drawings, which could have been used by a manufacturer to construct the W-beam and Thrie-beam public domain barriers, terminals based on the Modified Eccentric Loader Terminal (MELT) and transitions between W-beam systems and bridge parapets. Unfortunately, the detailed description of the components in these public domain systems caused some manufacturers to argue that using these

elements in another barrier system would make it compliant with the standard without further testing.

On the face of it, this may seem to be irresponsible, however, the experience with the systems was that the barrier was performing satisfactorily and there are advantages in having common components. It may be fairer to say that there was no adverse publicity and few if any reports of vehicles breaching the systems when it was considered that the barriers should have contained them. At the time of writing the first edition, the engineering profession and barrier suppliers generally accepted the “deemed to comply” status of these barriers, terminals and transitions.

Another issue in the development of the 1999 edition of the Standard was the use of Test Level 0. This was criticised internationally as being too weak to be a barrier and general international comment was that NCHRP 350 TL1 should be the minimum standard. However, the reason for introducing the TL0 level was because there were a number of plastic water filled barriers being sold or proposed to be sold in Australasia that did not meet TL1 and were unlikely to contain or redirect 1600 kg vehicles impacting the barrier at 50 km/h and 25° (the TL0 vehicle impact test parameters); that is 20 per cent less energy than NCHRP 350 TL1. It was thought that TL0 would eliminate the very poor water filled barriers and cause manufacturers and suppliers to strive for TL0 and then TL1 barriers. In hindsight, the introduction of the TL0 test level was not useful, and instead the Standard should have encouraged development to TL1 in the first instance.

DEVELOPMENT OF THE SECOND EDITION OF THE STANDARD

The impetus for the rewriting of the Australian and New Zealand Standard was that MASH (13) was being developed under the NCHRP 22-14 project. The Australian and New Zealand Standards committee CE-033 had knowledge of the changes through the paper published in Transportation Research Record (14, 15). The First Edition of the Australian and New Zealand Standard had used NCHRP 350 as the testing protocol and when the MASH was published, the AS/NZS 3845:1999 would be referencing a superceded document.

Part 1 of the new Standard (8) is based on the 1999 version. Much of the content is very similar to the earlier edition but based on more current thinking.

In the early meetings of the Committee CE-033 there was discussion as to whether the updated Australian and New Zealand Standard should adopt the US NCHRP 350 or the European CEN 1317 test protocol (MASH had not been published at that stage). The aspects of the CEN1317 that appealed were the heavy vehicle testing requirements and the fact that a 1500 kg vehicle was frequently used. It was felt that 1500 kg car was a common vehicle in Australia and New Zealand and therefore using this vehicle type would be more appropriate for Australian and New Zealand conditions. The final consensus was to adopt the MASH test protocol as NCHRP 350 had been referenced previously and that vehicles with a mass of MASH 2270P test vehicle were not uncommon. Additionally, the 1500kg vehicle was available as an optional test vehicle in MASH and covered in the test protocol requirements.

It was also felt that devices other than road safety barriers should be evaluated by this Standard and this would be better if the Standard was published in two parts. Part 1 (8) provided information on the acceptability of longitudinal permanent and temporary barriers (rigid, semi-rigid and flexible), terminals, crash cushions, interfaces between longitudinal barrier systems and barrier gates. Part 2 is used to evaluate permanent bollards, safety fences that separate

pedestrians and vehicles, longitudinal channelizing devices, truck and trailer mounted attenuators, truck rear under-run protection devices, sign support structures and poles.

CONTENT OF PART 1 OF THE SECOND EDITION

The major changes were the deletion of any reference to barriers being considered ‘deemed to comply’ to a particular test level, the removal of public domain barriers and components from the standard and an enlarged section on the assessment of the safety barriers.

Deemed to comply notation was removed because the committee considered that all road safety barrier systems should be evaluated against the same standard and test protocol. A system should not be accepted as performing to a particular level without full-scale testing. In service performance may demonstrate weaknesses in a barrier system but it does not predict a performance test level that can be used for comparison. So long as inferior products were included in the Standard, there was insufficient impetus for road authorities to either use better performing systems or for manufacturers to develop better systems (16). Since this aspect was removed from the standard, additional MASH TL3 steel post road safety barriers have been designed and tested promoting more competition in the market place and potentially lower prices for W-beam systems.

The Standard clearly states that: *“A successful full-scale testing program alone does not qualify a road safety system as suitable.”* The committee felt that while the testing is important, and without successful full scale testing a system could not be considered to be acceptable, there may be other aspects affecting the acceptability of performance. For instance, a road safety barrier alone without an acceptable terminal would not be an acceptable “system”.

In section 4.6, the standard states that the evaluation of a road safety barrier system should consider:

1. Documentation supplied in accordance with this Standard.
2. Any full-scale test results that are not in accordance with Clause 4.5 or verified using engineering calculations, computer simulation analysis, laboratory testing, bogie or pendulum tests or component structural tests in the case of modification in accordance with Clause 4.4.2.
3. Reasons to waive the required tests by this Standard.
4. The expected ability to withstand a second impact before being repaired.
5. Whether the road safety barrier system can reduce the severity of injuries to vulnerable road users.
6. The durability of components.
7. Workplace, health and safety requirements during installation and maintenance.
8. The ease with which maintenance can be undertaken including the requirement to use specialized tools and the expected time to replace damaged components after an impact.
9. Whether the road safety barrier system can be installed on a range of foundations or whether posts can be used in a range of foundation conditions.”

Some of these issues could cause the barrier system to be unacceptable. In particular, a barrier system that presents Workplace Health and Safety issues would be unacceptable. However, in most cases the consideration of these points informs users. A road authority might consider a barrier system for a particular site that has more durable components or that the barrier system is

more able to take a second impact. Test requirements for a second impact have not been specified and there is no requirement for a second impact test. On their own initiative, some manufacturers have undertaken a second reduced energy impact. Similarly, some manufacturers have provided details about durability. These are not pass/fail requirements but are informative.

This list is also a prompt to manufacturers when designing a barrier system or promoting the use of a system. Interestingly, some manufacturers have looked at a barrier's ability to redirect a second impact (albeit at a lower energy level than the first). The commentary to the Standard (section D4.6) lists second order issues that a road authority could consider. However, these are more for interest rather than for evaluation.

The current standard indicates that MASH is the "*basis of testing procedures for road safety barrier systems*". It is expected that the MASH protocol will be used. However, the Standard leaves the way open for the evaluation of barrier systems tested to EN1317. Test levels should be seen as a continuum of impact energy and performance. A barrier tested to EN1317 might give the assessor the view that the barrier system is performing better than a MASH TL3 but not as well as a TL4 system. It is noted that energy and vehicle differences need to be accounted for in quantifying the performance of the barrier to the Standard. To some engineers, this is a difficult concept, as they would prefer to not make this comparison. However, the CE-033 Committee did not want to preclude European products from entering the Australian and New Zealand market place, but felt that the barrier's performance needs to be described on a common basis with other accepted products. It may be that it is not necessary to provide a notional MASH performance level, but simply state the types of locations where installations would be acceptable. This position is also acceptable to the authors.

An important addition to the Standard is the recommended testing of motorcyclist protection devices. The standard utilises the CEN Technical Specification CEN/TS 1317-8 developed by the CEN Technical Committee CEN/TC 226 (17). However, the Australian and New Zealand standard also included measurements of thorax compression (18, 19) as the research found that approximately half the riders tended to be upright on the bike during impact and not sliding along the ground as in tests specified by the TS1317.8.

The standard also recommends that in-service performance evaluations are undertaken that conform to the processes in Chapter 7 of MASH (13) or Ray, Weir and Hopp (20).

CONTENT OF PART 2 OF THE SECOND EDITION

Part 2 of the standard covers method of testing and evaluation for other road safety devices not directly addressed by the previous standard. The CE-033 committee considered that a number of permanent and temporary road safety devices used on Australian and New Zealand roads should be assessed for their crashworthiness using accepted protocols and against a common set of evaluation criteria. Bollards, longitudinal channelizing devices, truck or trailer mounted attenuators, truck rear under-run protection devices, sign support structures and poles were selected for inclusion in the first edition of Part 2 of the new Standard.

Part 2 follows a similar format to Part 1 and while using MASH test procedures as the basis for assessment of these other devices, it also recognises the potential for products tested to EN 1317 or NCHRP 350 could be acceptable for use.

The evaluation of Longitudinal Channelizing Devices (LCDs) is in accordance with MASH using Tests 70, 71 and 72 for non-interconnected LCDs tested as "Work Zone Traffic

Control Devices” and Tests 90 and 91 for connected units. Similarly, the MASH evaluation process was used for truck and trailer mounted attenuators (Tests 50 through 54).

Bollards required careful consideration of their likely real-world use(s) and thus impact scenarios. The CE-033 committee concluded that the two most likely scenarios were:

1. bollards placed in a line essentially parallel to a traffic lane so that an errant vehicle would be expected to impact only one bollard; or
2. bollards used in a line or placed in a group, generally perpendicular to a traffic lane such that an errant vehicle may impact more than one bollard at the same time (bollard array).

When testing a single bollard, the test vehicle impacts head-on without an offset, i.e. the centreline of the MASH standard test vehicle is directed at the bollard. The MASH evaluation criteria used are B, C, D, F, H, and I (see Table 1). Importantly the same occupant protection criteria are used as would be used for crash cushions and longitudinal barriers. This allows Road Authorities to more clearly appreciate any differences in performance between device types and barriers.

In case (b) above, when two bollards can be impacted at approximately the same time, the test vehicle is required to impact the bollards spaced at half the test vehicle’s width with each bollard impacted at a quarter vehicle offset. With this bollard configuration, it would be essentially impossible to impact three bollards with the smaller MASH vehicle. The number of bollards impacted in real life installations would depend on the dimensions of the impacting vehicle. Consequently, in real life the impact conditions could vary significantly. It is therefore important to set a test condition that would provide at least some guidance. Road Authorities would need to consider the results of these tests carefully. Figure 1 below illustrates a common urban scenario where bollards have been installed to protect a kerbside dining area.

Again, test parameters were then developed based on the MASH protocol. However, only the MASH light car (1100C) was considered in the critical impact scenario for occupant protection criteria (H and I). It is likely that the test level for the one or two bollard tests would be different. In practical terms this would mean that a row of bollards parallel to the traffic lane, or standing alone could be acceptable for errant vehicle speeds that would differ from the appropriate vehicle speeds when bollards are perpendicular to the road and more than one bollard can be impacted.



FIGURE 1 Bollard array protecting a kerbside dining area.

TABLE 1 Synopsis of MASH Evaluation Criteria

Evaluation Factors	Evaluation Criteria *
Structural Adequacy	Test article should contain, redirect or arrest the vehicle in a controlled fashion without penetrating, under-riding or vaulting the test article
	The test article should readily activate in a predictable manner
	Test article performance may be by redirection, controlled penetration, or controlled stopping of the vehicle.
Occupant Risk	Detached elements or debris from the test article should not penetrate the occupant compartment, or present undue hazard to others.
	Detached elements or debris from the test article or vehicle should cause the driver to lose control.
	The vehicle should remain essentially upright throughout collision.
	It is not essential that the vehicle remain upright throughout collision.
	Occupant Impact Velocities (OIV) should satisfy the stated limits:
	The Occupant Ride Down Acceleration should satisfy the stated limits:
Vehicle trajectory	Vehicle trajectory behind the test article is acceptable.

* Consult MASH for complete description

The inclusion of truck rear under-run protection devices (or RUPDs) in the new Standard was a much debated issue, but ultimately the decision was made that to ensure satisfactory performance of such devices when specified, a full scale crash test protocol was required and at the time of writing, none existed to the committee's or the authors' knowledge. The derived test protocol was based on MASH using evaluation criteria C, D and F and where the impacting vehicle does not penetrate more than 500 mm underneath the rear of the truck.

The Standard recommends evaluating breakaway poles and sign supports using the MASH requirements for such devices, and energy absorbing poles using MASH crash cushion type requirements.

APPLICATION OF THE STANDARD

Using test results from a similar product

The best evaluation should consider all available information. This then leads to a question as to whether tests from other devices that act in a similar way should be used in the evaluation. It might be reasonably expected that they will operate similarly, but small differences in the hardware design can make a difference to the test outcome. It would seem to be wrong to fail or condition a product based on the testing of another product. Therefore, the results from another product should not be used to fail a system.

On the other hand, if one product shows a major concern, it would be appropriate to check if the concern is likely to arise with similar products. In our view, if the concern is serious then it would be worthwhile investigating the issue with the manufacturer and establishing if the concern is warranted. In any case it is not appropriate to share confidential information from one manufacturer to another, and this discussion needs to be done carefully and respectful of confidentiality.

At times there is a need to assess a family of products belonging to the same family. Crash cushions are a typical example. Often a manufacturer will propose a number of different configurations to cover a range of impact conditions and hazard widths. Not all configurations will be tested and the assessment will need to look at the justification for extending crash tests across the family of products. A well-documented case with energy and momentum calculations will assist in the assessment.

In recent times, some manufacturers have provided development testing to assist the evaluation. These tests may or may not have acceleration data, but will generally have good video footage. They do provide another view of the operation of the barrier system. It has been said that a manufacturer needs to have testing to establish compliance with a testing protocol as well as other testing which documents the performance of the system over a broader range of site and impact conditions (warranty testing). This latter testing gives the manufacture peace of mind and an ability to better describe unfavourable site conditions and what to do about it. Typically, this information is commercial in confidence, although some suppliers have been willing to share this information with others. In many respects this warranty testing is as important as compliance testing. The warranty testing could also be gained from an in-depth assessment of crashes into the barrier system. Either way it is important that manufacturers gather information about a broader range of impacts than just those in the compliance testing realm and use this information to inform designers and installers. These development tests should not be required to be reported. However, these tests may explain an issue for the assessors, although this should be used infrequently.

Installations on embankments and in weaker soils

When installing road safety barrier systems, it is often assumed that the soil conditions will match the AASHTO M147 standard soils (21) used in the testing. Essentially the crash test performance is only pertinent to installations with similar soil conditions to those used in the tests. It is generally accepted that the soil, foundation or footing characteristics can significantly affect the performance of a road safety barrier (or device). A test can be easily made to fail if the posts or fixings are not embedded in material that can resist the impact forces. When the material used in the foundations or footings differs from that used in the testing then information provided by the barrier system supplier or the road authority should specify the characteristics of the appropriate foundation material. The footings should be designed using this information.

Testing roadside safety hardware in strong soil conditions provides a baseline for comparison across tested systems. A stronger soil induces higher vehicle decelerations and occupant forces providing a "worst-practical" condition for most barrier types. MASH recommends that barrier systems adjacent to slopes are also tested in strong soil conditions with weaker soils able to be used when the typical system installation will only be in a weak soil condition.

This issue becomes particularly important for road safety barriers installed at the batter hinge point or on an embankment. Some barrier system suppliers have successfully tested their product in these site conditions. However, the expected performance of the barrier will be a function of the soil characteristics on the embankment, which is often not compacted to the same extent as the shoulder. Accordingly, there is a greater variation in the ability of the embankment to resist post loads and for the barrier system to operate in a predictable manner, and it is the right of a road authority to specify the conditions where barriers can be installed on embankments or not at all. Figure 2 from the NZ Transport Agency Technical Advice Note 16-01 (22) illustrates

examples. Conversely, it is appropriate for the barrier system manufacturers to develop systems that allow the barriers to be located further from the travelled lanes as this can reduce the cost of road construction or reduce the cost of road upgrades.

Care is required when installing barriers in weaker soils. Some systems are more tolerant when installed in softer soils depending on the post footings. There needs to be a greater effort to provide more information on this issue. Clause 2.5.4 of the Standard states:

(a) For systems that contain posts, the documentation shall include the load to which the post can be tested that ensures that it provides the necessary support to the system.

(b) For tests on wire rope barriers, the documentation shall include a test load to be exerted on the anchors to confirm their adequacy.”

The Standard continues in Clause 4.3.2 and requires Section 3.3.2 of MASH to apply with the additional requirement:

“For all road safety barrier systems that utilize posts, a load/deformation plot shall be provided based on the same soil conditions used for the crash testing. The post shall be loaded until it yields.”

Greater understanding of the post soil interaction will assist in providing more effective barrier system designs.

Road authorities commonly encounter installations where the ground conditions do not reasonably replicate the crash test soil conditions. Some have prepared additional design guidance to the sector on the appropriate techniques to apply to such situations, e.g. NZ Transport Agency Technical Advice Note 16-01 (22). Such guidance also provides clarity around roles and responsibilities within the design domain, something the new Standard has improved over its predecessor with clear definitions of the key roles within the road safety hardware sector.



FIGURE 2 Post failures (21).

CONCLUDING REMARKS

As our understanding of the interaction between errant vehicles and the road safety hardware systems and devices on our roads improves, there is a greater acceptance that design and testing standards must evolve, as is evidenced by the progression through NCHRP 230 (23), NCHRP 350 (8), EN 1317 (24) and now MASH (13), reflecting changes in our understanding and the vehicle fleet. There is increased pressure on many road authorities to raise speed limits and allow longer heavier trucks to improve network efficiency. We must also recognise industry's conflicting desires to minimise research and development investment and maintain profitability whilst still producing compliant products.

The introduction of Safe System philosophies has prompted research (5) demonstrating that roadside safety design based solely on clear zones is not as effective a solution as originally thought. Improvements in vehicle design and increased driver training standards have contributed to reductions in fatal and serious crashes, but run off road crashes still account for significant numbers of death and serious injuries on our road networks. Acknowledgement of this is driving increasing installation of road safety hardware to improve the safety performance of our roading networks.

The newer road safety barrier systems and devices are complex engineered systems, but nonetheless they are generally designed to pass the respective test protocols, not protect errant users from all situations. The test protocols and the standards that reflect them must be cognisant of these factors and balance commercial pressures against protection of the travelling public.

Continued evolution of testing protocols that better replicate real world fleets and crash scenarios is necessary to ensure improved safety performance across our networks. Equally, formal standards, such as AS/NZS3845, are needed to ensure those improved standards are able to be specified and met by all parties.

Personal view

The paper reflects the personal views of the authors and not necessarily that of their respective organisations/employers, Standards Australia, Standards New Zealand or any Australasian Road Authority.

REFERENCES

1. Liu, C., and R. Subramanian, Factors related to fatal single vehicle run-off the road crashes NHTSA Technical Report NVS-421 National Highway Traffic Safety Administration, Washington DC, 2009
2. Australian Transport Council. *National Road Safety Strategy 2011 – 2020*. Australian Transport Council, 2015
3. Ministry of Transport. *Safer Journeys – New Zealand's Road Safety Strategy 2010 – 2020*. New Zealand Government, Wellington, New Zealand, 2010
4. Jurewicz, C., L. Steinmetz, C. Phillips, P. Cairney, G. Veith, and J. McLean. Improving Roadside Safety: Summary Report. Austroads Research Report AP-R437-14. Austroads Sydney, Australia. 2014
5. Doecke, S., and J. Woolley J. Effective use of clear zones and barriers in a Safe System's context. *Proc Australasian Road Safety Research, Policing and Education Conference*, Canberra, Australia. 2010
6. Federal Highway Administration. *Open letter to all in the highway safety and roadside design community*. May 18 2015 www.safety.fhwa.dot.gov Accessed 16 August 2016

7. Everitt, T., 2013, Presentation made to TRB sub-committee AFB20(2) Roadside Safety Design – International Research
8. Standards Australia / Standards New Zealand. *Road Safety Barrier Systems and Devices; Part 1 Road safety barrier systems*. Joint Australian New Zealand Standard AS/NZS 3845, Part 1 2015
9. Standards Australia / Standards New Zealand. *Road Safety Barrier Systems and Devices; Part 2 Road safety devices*. Joint Australian / New Zealand Standard AS/NZS 3845 Part 2, in press.
10. Standards Australia / Standards New Zealand. *Road Safety Barrier Systems*. Joint Australian / New Zealand Standard AS/NZS 3845 1999
11. Ross, H. E. Jr, D.L. Sicking, R. A. Zimmer, and J. D. Michie. *Recommended Procedures for the Safety Performance Evaluation of Highway Features*, National Cooperative Highway Research Program Report 350 Transportation Research Board, Washington, D.C. 1993
12. Bullard, D.L., R. Bligh, W. Menges, and R. Haug. *Evaluation of Existing Roadside Safety Hardware Using Updated Criteria - Technical Report, Volume 1* (Web only document 157). National Cooperative Highway Research Program Project 22-14. Transportation Research Board of the National Academies, Washington, D.C. 2010
13. AASHTO. *Manual for Assessing Safety Hardware (MASH)*. Washington, D.C., U.S.A.: American Association of State Highway and Transportation Officials 2009
14. Mak, K., and R P Bligh. Assessment of NCHRP Report 350 test vehicles. In *Transportation Research Record: Journal of the Transportation Research Board*, No. 197 Transportation Research Board of the National Academies, Washington, D.C., 2002, pp. 33-37.
15. Mak, K., and R P Bligh. Assessment of NCHRP Report 350 test conditions. In *Transportation Research Record: Journal of the Transportation Research Board*, No. 197 Transportation Research Board of the National Academies, Washington, D.C., 2002, pp. 38-43.
16. Wallace, H. *The Public Benefit of Road Safety Barrier Innovation*. Paper presented at the International Workshop on Roadside Safety Design and Devices, 2015. Eds: Troutbeck and Burbridge. Transportation Research Board Circular, Transportation Research Board of the National Academies, Washington, D.C. (in press).
17. European Committee for Standardisation. *Road restraint systems - Part 8: Motorcycle road restraint systems which reduce the impact severity of motorcyclist collisions with safety barriers*. Technical specification CEN/TS 1317-8. 2011
18. Grzebieta R.H., M. Bambach, and A. McIntosh. Motorcycle Impacts into Roadside Barriers: Is The European Crash Test Standard Comprehensive Enough?, *Journal of the Transportation Research Board*, TRR 2013 pp 84–91 2013.
19. Bambach M., R. H. Grzebieta, and A. McIntosh. Injury typology of fatal motorcycle collisions with roadside barriers in Australia and New Zealand. *Accident Analysis & Prevention*, V.20, pp 253–260. 2012.
20. Ray M.H., J. Weir, and J.Hopp. *In service Performance of Traffic barriers*, NCHRP Report 490, Transportation Research Board of the National Academies, Washington, D.C. 2003.
21. American Association of State Highway and Transportation Officials (AASHTO), *Aggregate and soil-aggregate subbase, base, and surface courses: M147-70* Standard Specifications for Transportation Materials and Methods of Sampling and Testing, Washington, D. C., 1990.
22. NZ Transport Agency. *Notice to Industry: Wire Rope Safety Barrier Systems – post footing issues*. NZ Transport Agency Technical Advice Note #16-01, <http://www.nzta.govt.nz/resources/16-01-notice-to-industry-wire-rope-safety-barrier-systems-post-foo-ting-issues>, Accessed 21 October 2016
23. Michie, J.D., *Recommended Procedures for the Safety Performance Evaluation of Highway Appurtenances*, NCHRP Report 230, Transportation Research Board of the National Academies, Washington, D.C. (March 1981)
24. European Committee for Standardisation. *Road restraint systems - Part 1 : Terminology and general criteria for test methods Motorcycle road restraint systems which reduce the impact severity of motorcyclist collisions with safety barriers*. European Standard EN 1317-1. 2010.

Evaluation of a MASH Test Level 4 Sound Wall Barrier Using Simulation

NAUMAN M. SHEIKH

Texas A&M Transportation Institute

Sound walls are used to mitigate noise hazard for residential areas adjacent to major highways. A sound wall may be mounted on top of a crashworthy roadside barrier that has previously passed the pertinent crash testing criteria. However, with the addition of the sound wall structure, there may be additional safety concerns due to the interaction of an impacting vehicle with the barrier mounted sound wall structure. Such hazard should be evaluated through full-scale simulation, and if required, through full-scale crash testing. In this presentation, a design of a sound wall barrier system attached to an F-shape concrete barrier is presented. The safety performance of the sound wall system was evaluated through full-scale finite element simulation analyses for MASH test level 4 criteria. Details of the simulation model and results of the analyses performed are presented.

Evaluation of Head and Brain Injury Using Empirical and Analytical Predictors in Human Body Model

DAVIDE BENETTON

BENEDETTA AROSIO

MARCO ANGHILERI

*La.S.T., Transport Safety Laboratory, Department of Aerospace Science & Technology
Politecnico di Milano*

MARIO MONGIARDINI

GARRETT MATTOS

*Transport and Road Safety (TARS) Research Center
University of New South Wales*

The investigation of brain injuries has been approached through finite element (FE) model of human being. The Total Human Model for Safety (THUMS) is a highly accurate FE human model. Due to the high computational cost consumption of the whole body model and due to the focus on head and brain damage, the isolated FE head was used.

This study investigates the distribution of IntraCranial Pressure (ICP), Maximum Principal Strain (MPS), and Cumulative Strain Damage Measure (CSDM); those were used to compare the brain damage to the worldwide used head injury criteria: HIC and the linear acceleration signals. Acceleration components were measured through accelerometer elements embedded in the head CG of THUMS.

HIC is a fail/pass criterion of head injuries widely used in assessment of cadaver and dummy tests, since it is a good predictor of skull fracture. However, the risk of the occupant who sustained a brain injury without skull fracture might be greater than the ones who sustained a skull fracture without a brain injury. That means brain tissue damage needs more attention.

In order to evaluate the reliability level of the selected physical injury metrics, simulations of three-direction pendulum impact (frontal, lateral and upper impact), whose results were previously analysed with Hybrid III experimental and numerical simulations, were conducted using THUMS. The Abbreviated Injury Scale (AIS) has been considered for the correlation between HIC and the injury parameters (CSDM and ICP).

INTRODUCTION

Several mathematical models of the human body have been developed to produce biofidelic predictions of human behaviour in a crash and to improve the understanding of human impact responses and injury mechanisms. Human models are cost-effective alternatives to Post Mortem Human Subject (PMHS) and Anthropomorphic Test Devices (ATDs) tests, once they have been validated. Accurate human body models have the additional potential to predict physical variables related to injury and to evaluate dynamics (e.g., pressure, volume deformation, brain damage) that cannot be analysed with ATDs nor with volunteers.

One of the Finite Element (FE) human body models that has been developed is the Total Human Model for Safety (THUMS), produced by Toyota Central R&D. THUMS has been continuously improved since its initial development in 1997 and is one of the most detailed human body models commercially available. High-Resolution Computer Tomography (HRCT) scans were used to accurately represent the geometry of the human body and its internal organs. Starting with Version 4 it is possible to simulate not only bone fractures and internal organ injuries, but also head injuries. In this study, THUMS version 4.02 AM50 (Adult Male, 50th percentile), standing version was used, which is characterised by a finer mesh and an improved stability compared to previous versions [1]. A data set of a 39-year old male [1] was selected for the AM50 model. The male, 50th percentile version of THUMS has a height of 1.73 m, a weight of 77.3 kg and a Body Mass Index of 25.8 kg/m².

Usually, in crashworthiness analysis concerning human being, only the severity of the injury is notified, using the injury criteria. One of the main reasons for the diffuse adoption of injury criteria is the fact that they can be easily evaluated from the ATD's measurement recorders. Consequently, their evaluation using FE Hybrid III is quite straightforward as well. On the other hand, such parameters have some limits: they are referred to an injury that is localized in specific areas, such as the head CG, the upper neck or the lower neck, which is where the sensors are mounted on the ATD and they do not describe the real damage to which the subject of the accident undergoes. For example, the physical response of the neck to an impact, as the intra-cervical movement, is not considered. Another example is related to the worldwide used HIC, which describe head injuries related to skull fracture but other important internal brain damage, such as Diffuse Axonal Injury (DAI) have no influence on HIC value.

To overcome the limits of empirical injury metrics, analytical predictors can be considered. Analytical injury metrics compute the injury basing on simulated stress or strain in tissue structures. Those injury predictors can be computed only by human body simulations, since they represent kinematics of the human body in a realistic way.

The model considered in this study is THUMS. The version model available (v4.02) provides a means to calculate injury metrics analytically.

The objective of the present work is to investigate if THUMS can be considered as a reliable substitute of the Hybrid III ATD in crash analysis simulations, whether a valid and available correlation between the classical injury criteria and its responses in different scenarios exists. The analysis conducted in this study can be considered as the first step towards this direction. More investigations and comparisons are necessary as further step of the work.

METHODS

Brain Injuries

Several head impact scenarios on human cadaver heads have been carried out to measure accelerations of the head and the related HIC. Numerical methods, in particular FE simulations with ATD models, have proven to be not successful techniques for biomechanical analysis of the brain under various types of loading and they gave no remarkable insight into what happens to the brain and to the neck in impact situations. On the other hand, human body model has more biofidelic responses but usually have no possibility to evaluate empirical injury metrics. The evaluation of head and brain injuries related to measured values (such as HIC, acceleration based

criterion) depends on the presence of element that allow the kinematical evaluation of empirical predictors. Hence, in order to assess the accelerations and the forces in THUMS, one LS-DYNA element seatbelt accelerometer was introduced in the head CG (for accelerations evaluation) and two cross sections were placed in the upper and lower neck, at the correspondence of the upper and the lower intervertebral discs (due to forces measurement, as depicted in Figure 1). Since a sensitivity analysis related to those measurement elements and their position was performed and validated [2], no further investigation was conducted here.

Thanks to the element added in the model in the head CG, THUMS become able to predict HIC and not only the analytical predictions generated by FE human model, such as Cumulative Strain Damage Measure (CSDM) and IntraCranial Brain Pressure (ICP).

The brain part of THUMS, which include both the white and the grey matters, was used to attempt to reproduce brain injury outcomes by relating mechanical input and kinematic parameters to localized tissue deformation and damage.

The comparison between empirical injury metrics and analytical predictors have been made through the abbreviated injury scale (AIS); the AIS was introduced by the Association for the Advancement of Automotive Medicine (AAAM) as an anatomically-based coding system to classify and describe the severity of head and brain injuries. AIS codes range from 0, no injury, to 6, fatal injury. It is summarized in Table 1 [3].

Two analytical predictors were considered in this study: Cumulative Strain Damage Measure (CSDM) and InterCranial Brain Pressure (ICP). CSDM was proposed by Takhounts et al. [4] to establish a kinematically based injury metric to predict Diffuse Axonal Injuries (DAI). This criterion is a cumulative (non-decreasing) measure that is time dependant and quantifies the volume fraction of the brain that exceeds a given threshold; its computation requires the initial brain volume and the actual maximum first principal strain of the elements of the whole FE brain model. Those data are both available in THUMS simulation; in particular, the Kelvin-Maxwell linear viscoelastic material formulation selected by THUMS developers for its brain material, allows a direct computation of CSDM.

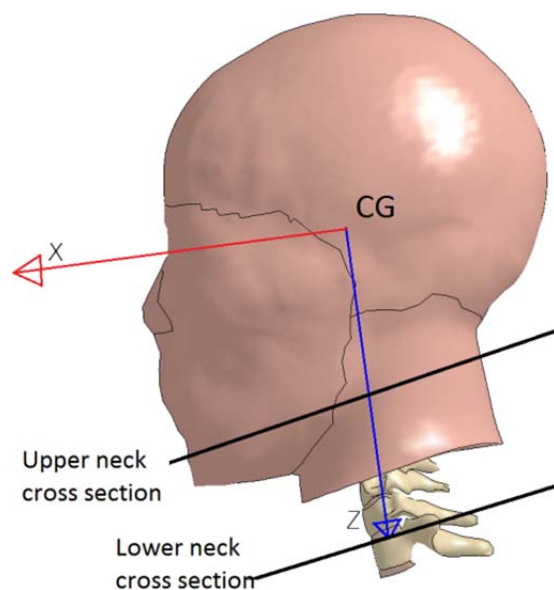


FIGURE 1 Measurement elements introduced in THUMS.

TABLE 1 Level of consciousness in relation with HIC

HIC	AIS	Level of Brain Concussion and Head Injury
135 - 519	1	Headache or dizziness; light brain injuries, light cervical injuries
520 - 899	2	Concussion with or without skull fracture; less than 15 minutes unconsciousness, corneal tiny cracks, detachment of retina, face or nose fracture without shifting – linear fracture-
900 – 1254	3	Concussion with or without skull fracture, more than 15 minutes unconsciousness, neurological damages, not severe, closed and shifted or impressed skull fracture or other injury indications in skull fracture, loss of vision shifted and/or open face bone fracture with antral or orbital implications, cervical fracture without damage of spinal cord
1,255 – 1574	4	Closed and shifted or impressed skull fracture with severe neurological injuries
1,575 – 1,859	5	Concussion with or without skull fracture with hemorrhage in skull and/or critical neurological indications; unconsciousness greater than 12 hours
> 1,860	6	Nonsurvivable

$$CSDM(\epsilon_0) = \frac{\sum_{k=1}^N V_k \varphi_k^\epsilon(t, \epsilon_0)}{\sum_{k=1}^N V_k} \leq 1$$

The CSDM can be computed as where

N: total number of elements in the part considered (in this case, in the brain)

V_k : volume of the k-th element

$$\varphi_k^\epsilon = \max H(|\epsilon_k(\tau) - \epsilon_0|)$$

φ_k^ϵ : function given by in which

$\tau \in [0, t]$ time instant

H: unit Heaviside step function

ϵ_0 : prescribed threshold level of strain ($\epsilon_0 = 0.1 - 0.25$)

Because of the cumulative character of the function, the CSDM always increases during an impact. It means that $0 \leq CSDM(t_1) \leq CSDM(t_2) \leq 1$, for every $t_1 < t_2$. A damaged volume –a volume is considered damaged once it passes the given threshold–, even if the strain in that element reduces at a later time, it is still considered to be damaged.

The brain parts considered in this study are the whole white and grey matters. In THUMS, brain material is modelled as viscoelastic. CSDM was used here for the entire brain but is theorised to be most associated with injury to the corpus callosum. Some suggested values for brain injury threshold are given from literature [3, 6] and reported in Table 2.

The determination of such tolerance levels cannot be calculated in-vivo, but must be estimated afterwards, sometimes with the assistance of numerical human model themselves.

TABLE 2 Threshold Values for Brain Injury Predictors

Criterion	Threshold Value	Predicted Injury
Intercranial pressure	> 235 kPa < 173 kPa	Severe or fatal injury minor injury
Strain	> 0.15 ÷ 0.25	Injury
Shear stress	11 to 16.6 kPa	Injury
CSDM	55% brain volume damaged	55% probability of concussion

Numerical Simulations

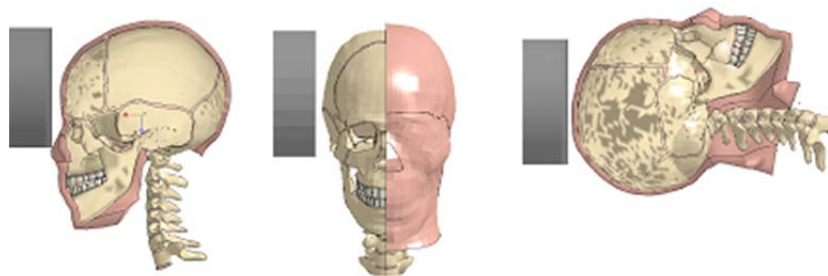
The brain injuries analysis has been conducted using a collection of measures from simulated head impact tests. THUMS head was assumed being impacted with a 23-kg aluminium impactor from three different directions (Figure 2). Further, three different impact velocities in each direction were investigated: 3 m/s, 3.5 m/s, 4 m/s.

Previously, impacts at 1.428 m/s have been analysed in order to have comparable data with available data of head impact tests conducted on Hybrid III anthropomorphic test device [2]; however, those were not considered for brain injury visualization, since the damage they caused were neither relevant nor diffuse.

The CSDM values were collected at the final instant of every simulation, since at that time the total number of element in the brain volume that are damaged is reached.

Figure 3 represents the CSDM visualization for frontal impact in the three velocities considered.

The numerical results from the simulations performed are reported in Table 3. Different values of ϵ_0 were used for the CSDM evaluation and compared. It can be highlighted that impact results are in accordance with the universally adopted HIC only for frontal impact. As described in Table 3, the obtained frontal impact results with $\epsilon_0 = 0.2$ (mean strain threshold between the suggested span) were coherent with the HIC values measured from the numerical accelerometer introduced in THUMS CG brain [2]. Frontal impact at impactor speed between 3.5 and 4 m/s shows HIC values related to AIS2, AIS3 in accordance with the CSDM (more than 55% brain volume damaged). The same relation was not experienced in lateral and upper impact. Hence, a detailed analysis of non-frontal impact is highly recommended to understand the lack of correlation. Considering the HIC threshold value (1000) the results obtained from THUMS are quite similar to the HIII for frontal impacts but the differences for the non-frontal impacts are

**FIGURE 2 Head impact scenarios analyzed.**

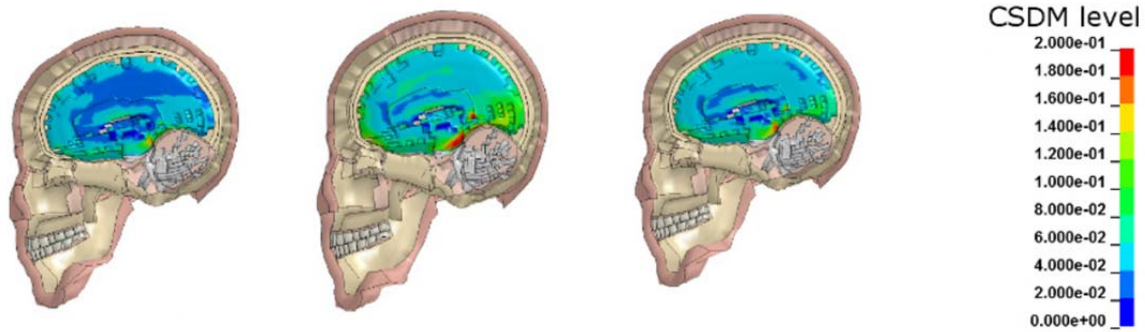


FIGURE 3 CSDM in frontal impact at 3 m/s (left), 3.5 m/s (center), 4 m/s (right).

TABLE 3 HIC / CSDM Comparison

Impact Direction	Impactor Speed [m/s]	HIC _{THUMS}	CSDM _{0.15}	CSDM _{0.20}	CSDM _{0.25}	HIC _{HIII}
Frontal	3	432	0.73	0.32	0.09	186
	3.5	712	0.78	0.48	0.16	823
	4	1069	0.84	0.62	0.24	1699
Lateral	3	737	0.15	0.02	0.00	823
	3.5	1084	0.29	0.06	0.01	583
	4	1547	0.45	0.16	0.03	835
Upper	3	650	0.01	0.00	0.00	4315
	3.5	1065	0.02	0.00	0.00	4742
	4	1599	0.20	0.04	0.00	1400

important. These differences could be related to the fact that HIC was originally defined for frontal impact scenarios.

Moreover, for all the impact analysed (frontal, lateral and upper impacts), the CSDM values increased with the augmentation of velocity.

In addition to CSDM, also ICP was considered as a brain injury criterion. The IntraCranial Pressure is the pressure inside the skull in general and in particular in the brain tissue. ICP can be considered related to CSDM since changes in ICP are attributed to volume changes in brain elements.

Due to the description reported in Table 2, also the ICP (Figure 4) has been classified as reliable since its visualization depicted brain damage coherent with the severity of the impact and the acceleration measured (Table 1 and Figure 4). While also a numerical value (percentage of volume that resulted damaged) was computed for CSDM injury predictor, for ICP this was not possible. However, the simulations visualisation of ICP allowed a qualitative description of the pressure trend in THUMS brain. The higher the velocity of impact, the higher the pressure in the brain reached during the impact time-history (Figure 4).

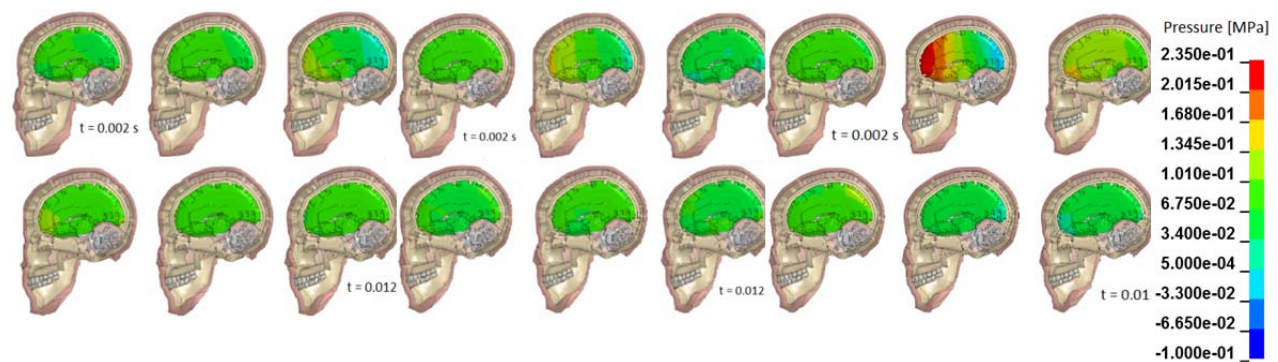


FIGURE 4 ICP in frontal impact at 3 m/s (left), 3.5 m/s (centre), 4 m/s (right).

CONCLUSIONS

Since THUMS provides for the evaluation of the internal organ damage, the qualitative visualization of damage could also support the development of protection systems nearby critical human body areas.

In addition, the analysis and definition of new and/or updated threshold values should be evaluated, since a lot of the present threshold scores are based on data recoded by Col. John Paul Stapp research, animal concussion tests, PMHS and low level exposed volunteers tests and dummy experimental tests, which cannot be considered totally reliable compared to real human body. The new and/or updated thresholds for brain injury should be based on the two additional injury metrics analysed in this study: CSDM and ICP, once the validation of those parameters have been done in low-level damage through comparison with human body data.

Hence, it is suggested that also analytical predictors (CSDM and ICP in particular) should be considered to complement the injury prediction based on the universally-adopted HIC criterion. The combination of multiple injury metrics is highly recommended. It is suggested to deeply analyse non-frontal impacts to understand the relation between empirical and analytical damage predictors.

ACKNOWLEDGMENT

This research, in particular THUMS simulations, includes computations using the Linux HPC cluster Katana from the Faculty of Science at the University of New South Wales.

REFERENCES

1. THUMS AM 50 Pedestrian/Occupant Model, Academic Version 4.02 20150527, May 2015, TOYOTA MOTOR CORPORATION, Toyota Central R&D Labs. Inc.
2. B. Arosio, 'Anthropomorphic Test Device and Total Human Model Head and Neck Injury Analysis Based on Experimental and Numerical Activities', Master Thesis, Politecnico di Milano, December 2015.

3. M. Lashkari, F. Frahmmand, and K. Kangarlou. "Finite element modeling of the human brain under impact conditions." IRJABS, International Research Journal of Applied and Basic Sciences, 6:875–881, 2013.
4. E. G. Takhounts, R. H. Eppinger, J. Q. Campbell, R. E. Tannous, E. D. Power, and L. S. Shook. On the development of the simon finite element head model. Stapp Car Crash Journal, 47:107–133, October 2003.
5. A. Rezaei, G. Karami, and M. Ziekewski, 'Examination of brain injury thresholds in terms of the severity of head motion and the brain stresses', *IBIA, International Brain Injury Association*, Fargo, ND, North Dakota State University, Mechanical Engineering Department.

Integrated Interior and Restraint Modeling for Occupant Risk Analysis

RUDOLF REICHERT

*Center for Collision Safety and Analysis
George Mason University*

An increasing number of passive safety regulation and consumer information requirements, such as Federal Motor Vehicle Safety Standard (FMVSS) regulations, New Car Assessment Program (NCAP) and Insurance Institute for Highway Safety (IIHS) ratings, resulted in major advances in vehicle structure integrity, safer interior vehicle design, and advanced restraint systems. Improvements in road side hardware designs, road infrastructure, and crash avoidance systems have also improved road safety over the years. Despite these efforts, over 17,000 people are killed in roadway departure crashes in the United States (U.S.). In order to further reduce fatalities and serious injuries in run off and other road crashes, it is necessary to use state of the art simulation models for vehicle structures, interiors, restraints, and occupants.

Using integrated occupant vehicle simulation models to analyze road departure crashes, such as configurations used to evaluate road side hardware according to the *Manual for Assessing Safety Hardware* (MASH), has the potential to further improve road safety. As a pre-requisite, detailed interior and restraint system simulation models that realistically represent the physical characteristics of hardware components, are needed. For example, airbag folding patterns, airbag deployment characteristics, material properties and connections need to be modeled genuinely.

In 2013, NHTSA released a report that detailed the development of an integrated occupant vehicle model for the analysis of safety in crashes (“Development of Integrated Vehicle-Occupant Model for Crashworthiness Safety Analysis”, Reichert, Park, and Morgan, DOT HS 812 087, December 2014). The resulting occupant-vehicle finite element model, with detailed interior and restraint component models, was used to conduct a range of sensitivity and occupant studies using a variety of dummy and human body finite element models. This effort has been the basis of several follow on studies to evaluate test procedures, performance metrics, and injury countermeasures.

In this presentation, modeling techniques for developing detailed interior and restraint models are outlined. For instance, techniques for seat modeling using mechanisms for positioning, airbag modeling using folding and vehicle integration techniques, and seat-belt modeling including belt fitting techniques, are provided. Examples, for using these models in integrated occupant vehicle simulations in various crash configurations in combination with different Anthropomorphic Test Devices (ATDs) and human body models are presented.

The state of the art techniques have been used to analyze kinematics and potential injury risk for near-side and far-side human occupants in run off road impact configurations including a 20 degree frontal oblique impact into a New Jersey Barrier according to MASH. Results of this study with the title “Comparison of Human Occupant Kinematics in Laboratory Impact and Run-Off-Road Crash Configurations” will also be presented and published at the First International Roadside Safety Conference (IRSC) 2017.

Comparison of Hybrid III and Human Body Model in Head Injury Encountered in Pendulum Impact and Inverted Drop Tests

BENEDETTA AROSIO

DAVIDE BENETTON

MARCO ANGHILERI

*La.S.T., Transport Safety Laboratory, Department of Aerospace Science & Technology
Politecnico di Milano*

MARIO MONGIARDINI

GARRETT MATTOS

RAPHAEL GZERBIETA

*Transport and Road Safety (TARS) Research Center
University of New South Wales*

The aim of this study is to investigate and compare head, neck and brain behavior in two different impact situations between Hybrid III and Total Human Model for Safety (THUMS). Two scenarios were considered: three-direction impact and three-height drop tests. The head responses were evaluated through the HIC and the linear acceleration signals; for THUMS brain damage was also analyzed.

Experimental tests were performed with a Hybrid III 50th percentile Anthropomorphic Test Device (ATD). The obtained results were used to compare the responses of the two Finite Element (FE) models under investigation. Simulations were performed using the non-linear explicit FE solver LS-DYNA.

To evaluate accelerations and forces in THUMS, it is necessary to model virtual sensors. A sensitivity analysis was carried out considering both the position at which the kinematic data were measured as well as different computational methods for collecting them. Due to the high sensitivity to the specific position where the neck loads are collected in THUMS, it is suggested that virtual sensors be embedded in THUMS at standard locations. The upper neck position results as the most appropriate for neck loads measurement. THUMS responses in the analyzed impact result more similar to human behavior whereas Hybrid III provided unreliable results, in particular in non-frontal impact.

INTRODUCTION

Traumatic Brain Injuries (TBI) and cervical spine and head injuries may lead to severe consequences. Since head and neck injuries can occur under various circumstances, they have been studied extensively. Before the introduction of Anthropomorphic Test Devices (ATDs), head and neck injuries have been studied using animals [1], Post-Mortem Human Subject (PMHS) [2] and live volunteers [1].

The introduction of ATDs increased the repeatability of the tests and started a new method to investigate crash simulations and fatalities. Even if ATDs are based on the human body, they are characterized by limited biofidelity, due to the necessity to implement a durable platform for repeatable testing. The durability and reliability requirements, which make an ATDs biofidelity such limited, are also reflected in the mathematical models of the ATDs, such as the

one exploited for this study, the Hybrid III. In addition, the computational models are useless unless it has been proven they can accurately replicate results of experimental testing. Due to that, this study investigates the differences in responses and injury criteria values between Hybrid III ATD head-form and its numerical counterpart (LSTC.H3 103008V1.0 Rigid FE 50th, downloadable from Livermore Software Technology Corporation (LSTC) website, and partially improved at Transport Safety Laboratory, La.S.T.) as a first step.

The second part of this study deals with the investigation of the differences in response, relative to the two specific impact scenarios analyzed, between a dummy FE model and a human body FE model, with particular focus on head responses.

Several mathematical models of the human body have been developed to produce biofidelic predictions of human behavior in a crash and to improve the understanding of human impact responses and injury mechanisms. Human models are cost-effective alternatives to PMHS tests, and avoid the ethical issues associated with the use of deceased human subjects. They provide an efficient method to perform many virtual tests without the challenges associated with physical experimentation. Accurate human body models have the additional potential to predict physical variables related to injury and to evaluate brain dynamics (e.g., pressure, volume deformation, brain damage) that cannot be analyzed with ATDs.

One of the FE human body models that has been developed is the Total HUMAN Model for Safety (THUMS), produced by Toyota Central R&D. THUMS has been continuously improved since its initial development in 1997 and is one of the most detailed human body models commercially available. High-Resolution Computer Tomography (HRCT) scans were used to accurately represent the geometry of the human body and its internal organs. A data set of a 39-year old male [3] was selected for the AM50 model.

Starting with Version 4 it is possible to simulate not only bone fractures and internal organ injuries, but also head/brain injuries. In this study, THUMS version 4.02 AM50 (Adult Male, 50th percentile) standing version was used, which is characterized by a finer mesh and an improved stability compared to previous versions [3]. The male, 50th percentile version of THUMS has a height of 1.73 m, a weight of 77.3 kg and a Body Mass Index of 25.8 kg/m².

It should be noted that usually in accident database only the severity of the injury is notified, using the injury criteria. One of the main reasons for the diffuse adoption of injury criteria is the fact that they can be easily evaluated from the measurement recorded from the Hybrid III ATD. Consequently, their evaluation using the corresponding FE model is quite straightforward as well. On the other hand, such parameters have some limits: they are referred to an injury that is localized in specific areas, such as the head CG, the upper neck or the lower neck, which is where the sensors are mounted on the ATD. For example, the physical response of the neck to an impact, as the intra-cervical movement, is not considered. This is not a limit for THUMS, since its behavior better resembles the human one. Thus, THUMS can be considered as a more reliable substitute of the Hybrid III in crash analysis simulations, whether a valid and available correlation between the classical injury criteria and its responses in different scenarios exists. The analysis conducted in this study can be considered as the first step towards this direction. More investigations and comparisons are necessary.

METHODS

The comparison between Hybrid III ATD, its numerical model and THUMS was carried out considering pendulum impact tests to the head and neck component at three different directions, and inverted drop tests of the whole body at three different drop heights.

All the experimental tests were conducted with a Hybrid III 50th percentile ATD, which is firmly established as a device for estimating the human response to both inertial and axial loadings [4]. The experimental tests conducted had the main purpose of creating a collection of data regarding the dummy responses in some simple impact configurations, in order to evaluate the level of reliability of the Hybrid III used in simulations.

For numerical head impacts, the head and neck component of FE Hybrid III and THUMS (v4.02, pedestrian model) were used. The whole body was used for drop tests.

The LS-DYNA non-linear explicit finite element solver version 971 R8.0 was used for all simulations.

Head accelerations and neck forces and moments were measured during both the experimental tests and the numerical simulations. They are required for the evaluation of injury criteria, which related the mechanical responses of crash test dummies in terms of risk to life or injury to a human being. Hence, calculating head accelerations and neck loadings is fundamental to understand and predict head and neck injuries as consequences of the crash event on a living human being.

THUMS simulations were preceded by a sensitivity analysis carried out considering both the position at which the accelerations and forces should be measured, as well as different computational methods for collecting them.

Experimental Tests

The experimental tests took place entirely at La.S.T., at Politecnico di Milano. In the experimental tests, the Hybrid III 50th percentile male was used. Currently, it is the most widely used and available human surrogate for dynamic tests.

The focus of this investigation was the response of the ATD head and neck components: the main head and neck injury criteria has been evaluated and compared with those calculated by means of numerical simulations.

The Hybrid III head (FIGURE 1) was instrumented according to the Code of Federal Regulations [5]:

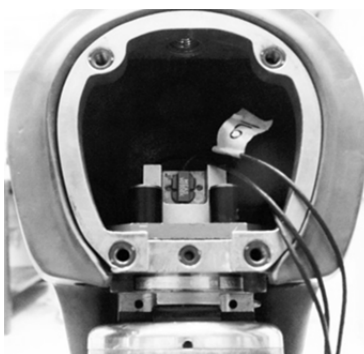


FIGURE 1 Hybrid III head instrumentation.

- three accelerometers in a triaxial array for the evaluation of x, y and z-axis accelerations [g];
- one six-axis upper neck load cell, model IF-205, for the evaluation of x, y and z-axis forces [N] and moments [Nm].

Data was recorded using a Data Acquisition System (DAS) and processed according to the SAE J211 standards [6].

The tests performed can be divided in two groups:

- pendulum impact tests on the head and neck component;
- inverted drop tests on the whole body.

Pendulum Impact Tests

The head and neck geometric characteristics are collected in Table 1. The head is composed by a single-piece anthropomorphic skull and a monolithic cap, both aluminum made, and covered by vinyl skin. The two parts are separated to allow easy access for instrumentation [7]. The Hybrid III neck is composed by rubber and aluminum discs which simulate the human vertebrae and which should have anthropomorphic response. Inside the neck, a steel cable runs through the central axis of the neck and it acts to limit the rotation at large angles [19].

The same procedure has been followed for all the tests: the impactor (Figure 3) was released at a defined height and impacted the target with a velocity dependent on its initial position. The pendulum velocity at impact was measured through high-speed videos at 400 fps.

To confirm the repeatability of the tests, the head was hit three times per position; frontal, lateral, and from overhead, as shown in Figure 2. As an example, three x-axis accelerations and forces measured in frontal impact and post-processed in Matlab® are shown in Figure 4 (reference system is depicted in Figure 3) [20].

All the signals have been filtered according to SAE J211 [6]:

- acceleration signals: CFC1000;
- force signals: CFC600.

Linear acceleration peaks and HIC₁₅ were calculated for each head impact and compared with the numerical simulations results.

Inverted drop test

The drop tests were conducted in three different configurations with respect to the drop height and two different configurations with respect to the angular inclination of the surface of impact. In addition, for tilted planes of impact, three different scenarios were evaluated with respect to

TABLE 1 Head and neck geometric characteristics

	Mass [kg]	Diameter [mm]	Width [mm]	Length [mm]
Head	4.54	190	155	203
Neck	1.54	82.3	-	123.8



FIGURE 2 Experimental configuration for pendulum impact tests.

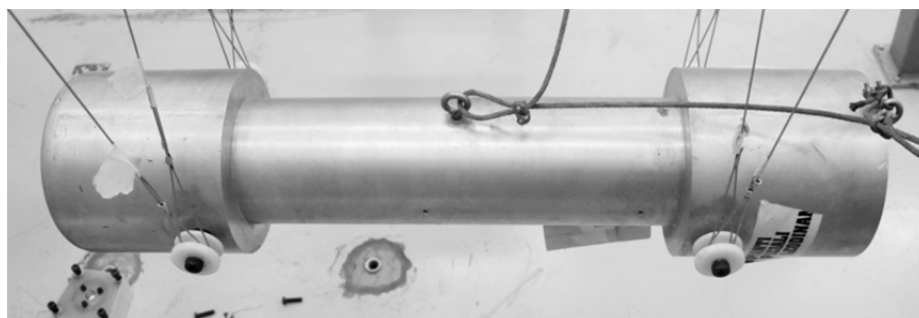


FIGURE 3 Impactor used in the pendulum impact tests.

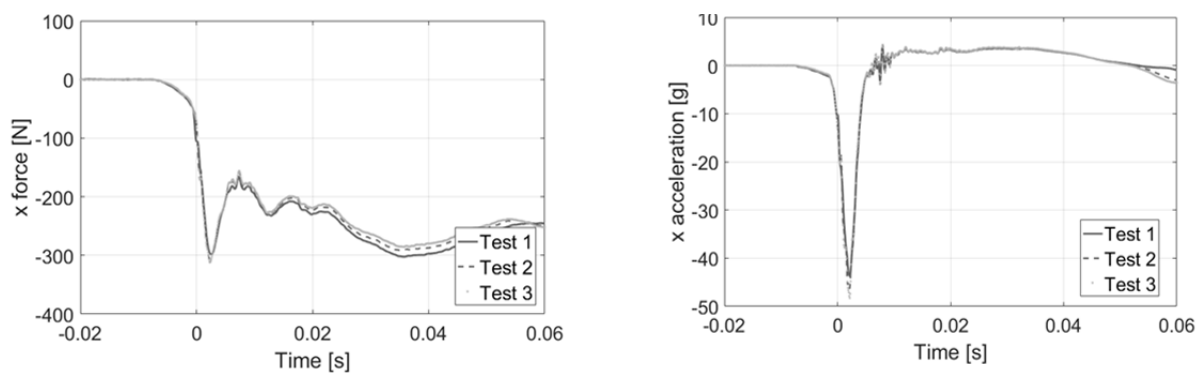


FIGURE 4 Frontal pendulum impact test:
x-axis forces (left) and x-axis accelerations (right)

TABLE 2 Impactor geometry characteristics

Mass [kg]	Diameter [mm]	Length [mm]	Height from ground [mm] ^a
23	150	700	737

a. Evaluated in the impactor equilibrium position

the orientation of the dummy about its z-axis (Figure 5). Also for the drop tests, each scenario was tested three times for repeatability purpose.

The dummy was hung by its feet at the desired drop height and a quick release mechanism started the free fall. This initial position let the dummy head to be the first to impact the ground.

The dummy arms and legs were tied with tape to the torso and to themselves, respectively.

Hence, potential asymmetry issues related to limbs movements far from the z-axis were avoided as much as possible. As expected, the head accelerations reduced with higher drop heights. In addition, the maximum acceleration peak was postponed in time at increased heights. A similar trend happened with the neck forces (Figure 6).

Numerical Reconstruction with Hybrid III and THUMS

By definition, Hybrid III and THUMS are two FE models of different structures. Similar to the actual ATD, the Hybrid III numerical model has many components devoted to measuring forces, moments and accelerations. On the other hand, since THUMS is a model of the actual human body rather than an ATD, it does not include any sort of instrumentation such as accelerometers or load cells.

In the Hybrid III model, acceleration signals were recorded through an accelerometer element located in the head CG, whereas the forces and moments that are measured by the upper neck load cell in the actual ATD were obtained through the reaction load of kinematical joints positioned at the occipital condyle. The comparison performed confirmed what has been described by Sances et al. [8] and Paver et al. [9], that the Hybrid III forces transmitted to the neck (both in the ATD and in the numerical model) are substantially higher than the failure forces measured in the PMHS by the following scale factors:

- extension: 3-5 times stiffer;
- flexion: 3-4 times stiffer;
- lateral bending: 5-6 times stiffer.

As such, a scale factor of 4.5 was deemed appropriate for comparing the Hybrid III and THUMS neck forces.

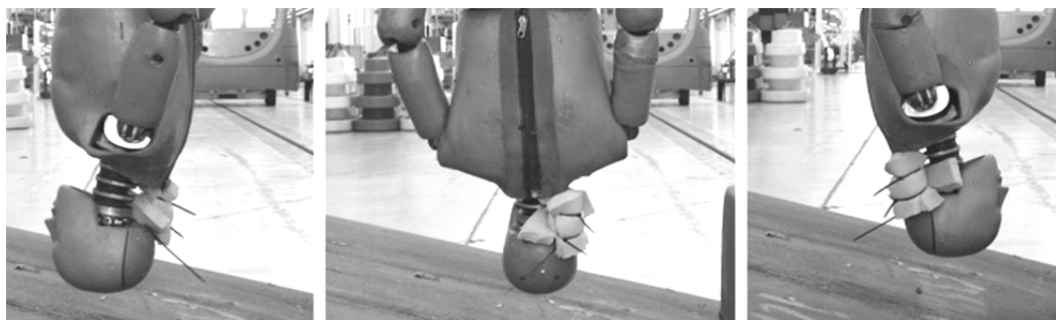


FIGURE 5 Experimental test configuration, drop tests.

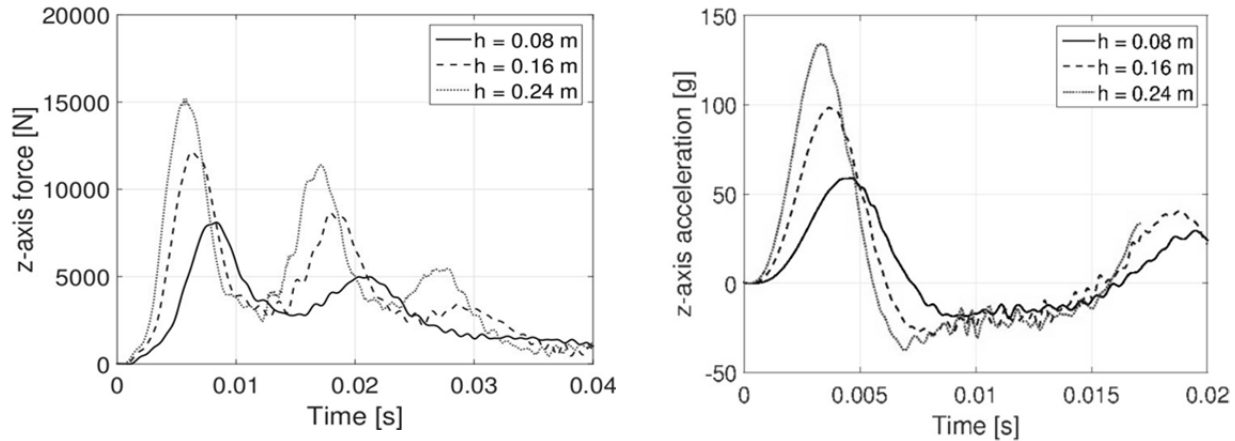


FIGURE 6 Drop test, horizontal plane: z-axis head forces (left) and accelerations (right) at the three different heights.

The stiffer behavior of the Hybrid III neck compared to THUMS is qualitatively shown in Figure 7.

To compensate for the absence of instrumentation in THUMS, a sensitivity analysis was conducted.

The sensitivity analysis was carried out considering both measured accelerations and forces and both the position at which those should be measured as well as different computational methods for collecting them.

For the accelerations signals, the values in the head CG was necessary. A coordinate system centered in the head CG was created and used as reference. Head accelerations were measured through a LS-DYNA element seatbelt accelerometer that was defined close to the location of the head CG. A sensitivity analysis related to the position of the accelerometer element and its associated rigid part was conducted. Once the head CG of THUMS was identified, a node in the CG coordinate positions was created. On the base of the definition of seatbelt accelerometer in LS-DYNA, three nodes were created in order to define the local coordinate system to which the accelerations will be referred and all of them were unified in one node-set and constrained to a unique rigid part: by definition, a seatbelt element accelerometer has to be fixed to a rigid part.

Since only one rigid part in THUMS was near the head CG in the sagittal plane of the head (symmetric with respect to the model sagittal axis, positioned at the base of the head), two different rigid parts were created to compare the results and to understand the relation between the accelerometer measurements and the position of the rigid part picked. In order to select the best rigid part for the seatbelt accelerometer definition, a sensitivity analysis was conducted, comparing the accelerations derived from the three different simulation configurations.

Finally, the approach followed was to refer the seatbelt accelerometer to the rigid part created in the neighborhood of the CG, as depicted in Figure 8. This part was specifically created by the union of two existing parts which were on the left and on the right side of the sagittal plane; the part was made rigid for the purpose.

To compensate for the absence of a load cell element, the forces at each cervical level of the neck were captured using two different techniques, both based on the definition of cross

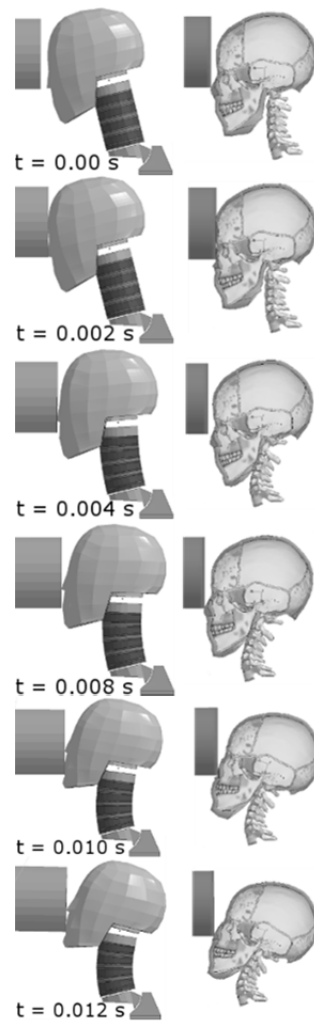


FIGURE 7 Simulated pendulum frontal impact: Hybrid III (left), THUMS (right).

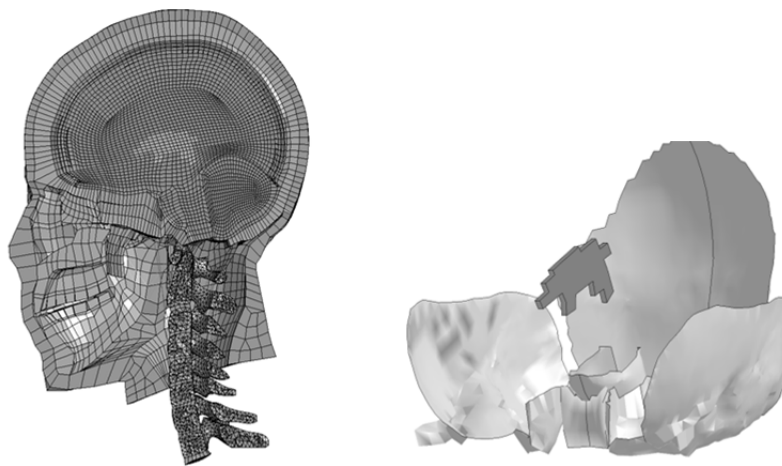


FIGURE 8 Part selected for the element seatbelt accelerometer.

section in LS-DYNA. These techniques were validated for the analysis of neck response of the Global Human Body Model Consortium (GHBMC) during a simulated rotary-wing aircraft impact [13].

Three different cross sections were created at each vertebral level of the cervical spine to evaluate force contributions from different anatomical components of the neck (Figure 9):

- vertebrae cross sections;
- Inter-Vertebral Disc (IVD) cross sections;
- planes cross sections.

Based on the analysis of the simulation results, the upper neck and the lower neck IVD cross sections were selected for the collection of neck forces and moments (Cart 1 and Cart 5 in Figure 9). Results showed that the measurements of forces and moments in THUMS vary significantly based on the locations where such numerical data are collected. On the other hand, due to the limited biofidelity of Hybrid III, neck measures seemed to be less sensitive to the specific measurement location [20].

Quantitative comparisons between THUMS and FE Hybrid III was conducted considering LS-DYNA output such as linear accelerations in the head, hence the HIC_{15} , and forces in the neck.

RESULTS

The results of this study indicate that Hybrid III FE model, with a few adaptations, can correctly represent the behavior of the correspondent actual ATD for frontal impacts, as indicated in the comparison of the HIC values (Table 3) and accelerations.

Unfortunately, a wider discrepancy between FE ATD and the actual ATD was obtained for non-frontal impact tests, as indicated in Table 3.

The performance of THUMS head and neck in the reconstructed experimental conditions, compared with the Hybrid III results, highlighted some important aspects:

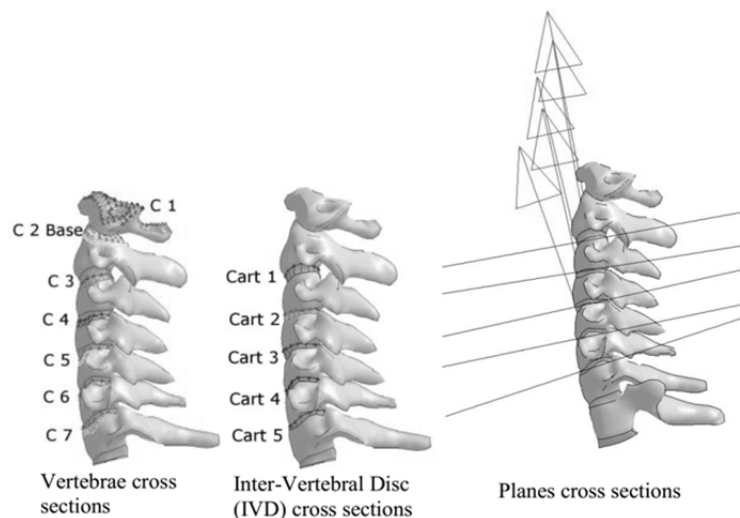


FIGURE 9 Cross sections at different neck components.

TABLE 3 HIC Hybrid III comparison between actual ATD and FE model, at $v = 1.428$ m/s.

Velocity [m/s]	Direction	Hybrid III	THUMS
1.248	Frontal	22.3	30.54
	Lateral	28.8	66.70
	Upper	76.8	66.8
3	Frontal	185.55	432.3
	Lateral	324.1	737.5
	Upper	4315.9	650
3.5	Frontal	823.5	712.9
	Lateral	583.7	1083.9
	Upper	4742.7	1065
4	Frontal	1699.9	1069.5
	Lateral	835.4	1547.2
	Upper	1400.8	1599

TABLE 4 HIC comparison between FE model of Hybrid III and THUMS

Direction	HIC experimental	HIC numerical
Frontal	21.3	22.3
Lateral	17.2	28.8
Upper	21.6	76.8

- the Hybrid III behavior, in particular the forces in the neck, is different from PMHS and THUMS and shows higher stiffness in every scenario analyzed;
- the Hybrid III responses (HIC) in frontal impacts are quite similar to THUMS (hence, to PMHS), but for the non-frontal impacts the differences are important;
- due to the previous result, HIC values in Hybrid III can be considered acceptable only for frontal impacts (Table 4).

The results of the study have been based on a single adult male occupant model only. Future work can include investigations of the pendulum impact tests and drop tests to other occupant sizes.

CONCLUSIONS

For the pendulum impact, a correlation was found between the ATD Hybrid III and its correspondent numerical model for only frontal impacts.

Although the analysis of human behavior is characterized by many random parameters, the development of a human FE model, such as THUMS, can be very useful for crashworthiness analysis and in the analysis of human body behavior in general. THUMS should help better understanding human injury mechanism during crashes through highly reliable reconstructions.

It is suggested to embed virtual sensors in THUMS, such as indicated in this work, to allow the evaluation of empirical injury criteria. Those virtual sensors should be used in

combination with analytical injury predictors, whose evaluation is possible in THUMS but not in ATD numerical models.

Injury evaluation and consequent injury prevention systems based only on HIC values, whose threshold values are based on Hybrid III results, could give misjudgment of the severity of the event or wrong estimation of the intensity of the trauma: the data on which they were evaluated are not completely reliable. This happens in particular in non-frontal impact scenarios.

It is suggested to compare the injury evaluation with more than one threshold and more than one analytical predictor.

ACKNOWLEDGMENTS

This research, in particular THUMS simulations, includes computations using the Linux HPC cluster Katana from the Faculty of Science at the University of New South Wales.

REFERENCES

1. A. Eichberger, M. Darok, E. P. Leinsinger and H. Steffan, 'Neck injury criterion validation using human subjects and dummies.', 2000, *Frontiers in Wiplash Trauma*, pp. 409-434.
2. A. M. Loyd, R. W. Nightingale, Y. Song, J. F. Luck, H. Cutcliffe, B. S. Myers and C. Bass, 'The response of the adult and ATD heads to impacts onto a rigid surface.', June 2014, *Accident Analysis and Prevention*.
3. THUMS AM 50 Pedestrian/Occupant Model, Academic Version 4.02 20150527, May 2015, TOYOTA MOTOR CORPORATION, Toyota Central R&D Labs. Inc..
4. P. J. Bishop, R. Wells, 'The Hybrid III Anthropometric Neck in the Evaluation of Head First Collisions', SAE Technical Paper, 860201, 1986.
5. National Highway Transport Safety Administration, 'Test condition and instrumentation', 49.B C.F.R. 572.11, 1977.
6. National Highway Transport Safety Administration, 'Head restraint', 49 C.F.R. 571.202a, 2009.
7. Humanetics® online documentation, <http://www.humaneticsatd.com/crash-test-dummies/frontalimpact/hybrid-iii-50th>.
8. J. A. Sances, F. Carlin, S. Kumaresan, 'Biomechanical Analysis of Head-Neck Force in Hybrid III Dummy During Inverted Vertical Drops.', 2001, *Biomechanical Science Instrumentation*, pp. 459-494.
9. J. G. Paver, D. Friedman, G. Mattos, J. Caplinger, 'The development of IARV's for the Hybrid III Neck Modified for Dynamic Rollover Crash Testing.', 2010, Icrash.
10. A. M. Loyd, W. Nightingale, Y. Song, J. F. Luck, H. Cutcliffe, B. S. Myers and C. Bass, 'The response of the adult and ATD heads to impacts onto a rigid surface.', June 2014, *Accident Analysis and Prevention*.
11. N. Yoganandan, Jr. A. Sances and F. Pintar, 'Biomechanical Evaluation of the Axial Compressive Responses of the Human Cadaveric and Manikin Necks.', August 1989, *Journal of biomechanical engineering*.
12. F. A. Pintar, A. Sances, N. Yoganandan, J. Reinartz, D. J. Maiman, J. K. Suh, G. Unger, J. F. Cusick, S. J. Larson, 'Biodynamics of the Total Human Cadaveric Cervical Spine.', 2010, SAE Technical Paper.
13. N. A. White, 'Simulated Automobile and Rotarywing Aircraft Impacts: Dynamic Neck Response After Surgical Treatment for Cervical Spondylosis.', 2013, *PhD Thesis*, Virginia Polytechnic Institute and State University, Blacksburg, VA.

14. E. G. Takhounts, M. J. Craig, K. Moorhouse, J. McFadden, V. Hasija, 'Development of Brain Injury Criteria (BrIC).', November 2013, *Stapp Car Crash Journal*, Vol. 57, pp 243-266.
15. F. A. Bandak, R. H. Eppinger, 'A Three Dimensional Finite Element Analysis of the Human Brain Under Combined Rotational and Translational Acceleration.', 1994, Warrendale, PA: Society of Automotive Engineers, SAE Technical Paper.
16. M. Lashkari, F. Frahmmand, K.Kangarlou, 'Finite Element Modelling of the Human Brain Under Impact Conditions.', 2013, *IRJABS, Internationale Research Journal of Applied and Basic Sciences*, pp 875-881.
17. A. Rezaei, G. Karami, and M. Ziekewski, 'Examination of brain injury thresholds in terms of the severity of head motion and the brain stresses', *IBIA, International Brain Injury Association*, Fargo, ND, North Dakota State University, Mechanical Engineering Department.
18. E. G. Takhounts, R. H. Eppinger, J. Q. Campbell, R. E. Tannous, E. D. Power, and L. S. Shook, 'On the development of the SIMon finite element head model.', October 2003, *Stapp Car Crash Journal*
19. E. K. Spittle, D. Jo Miller, B. W. Shipley, Jr. Ints Kaleps, 'Hybrid II and Hybrid III dummy neck properties for computer modelling', Vulnerability Assessment Branch, Biodynamics & Biocommunications Division, February 1992.
20. B. Arosio, 'Anthropomorphic Test Device and Total Human Model Head and Neck Injury Analysis based on Experimental and Numerical Activities', Master Thesis, Politecnico di Milano, December 2015.
21. L. Zhang, A. I. King, K. H. Yang. 'A proposed injury threshold for mild traumatic brain injury', in *Journal of Biomechanical Engineering*, pp 226–236, April 2004.

Vehicle Technologies and Safety Considerations

See Me Save Me
Improving the Safety of Cyclists

HARPREET SINGH DHUNNA
Avoid Accident

Cyclists are hard to be seen on the roads during night, rain, fog and hazy weather. Mostly these vehicles do not have any lights which could alert the other drivers to feel their presence on roads. They especially cyclist became almost invisible during the night when head lights from other side makes driver almost blind.

Description Most of the Indian population lives in rural areas and small cities. Walking and cycling remain the dominant modes of transport in small cities and rural areas.² The pedal bicyclist constitutes a significant share of total traffic on Indian roads accounting for 15-35% of total trips.³ The incidence of head injuries in cyclists ranges from 14- 36% of the total injuries. **Method** We have chosen one district to make the cyclists visible on the roads. The focus is on the labor class especially and the students riding it to schools We involved traffic police and media to make it success . We choose the spot where the labor and workers with cycles are stationed We fix high quality reflective on the cycles to make it visible on roads. And also we guide them about the driving precautions to be observed on roads riding at night and during fog.

Results: Aids to improve pedestrians and cyclist visibility have been used to avert potential collisions Visibility aids have the potential to increase visibility and enable drivers to detect pedestrians and cyclists earlier. “Fluorescent materials in yellow, red and orange colours improve detection and recognition in the daytime. Retroreflective materials enhance recognition.

Heavy Vehicle Encroachment Trajectories

MALCOLM H. RAY
CHRISTINE E. CARRIGAN
CHUCK A. PLAXICO
RoadSafe, LLC

The potential path a vehicle may take during a roadside encroachment could be influenced by the driver's response and alertness, the roadside terrain and material and the vehicle's handling characteristics. Using real-world trajectories incorporates all these factors into the trajectories. Currently, RSAPv3 uses 890 reconstructed trajectories of passenger vehicle encroachments from the FHWA rollover study, NCHRP Project 17-11 and NCHRP Project 17-22. There are no heavy vehicle trajectories in these data since the studies were limited to passenger vehicle encroachments.

Understanding a heavy vehicle trajectory during an encroachment is crucial to several aspects of roadside safety including selecting the appropriate test level for roadside hardware. Vehicles which travel a short distance or have a high departure speed will have more energy than vehicles that travel a longer distance or have a lower departure speed. Using passenger vehicle trajectories to represent heavy vehicle trajectories would include some trajectories that are unlikely for heavy vehicles. Passenger vehicles are smaller, have better braking and acceleration characteristics as well as different inertial properties so their encroachment and path characteristics are likely different than heavy vehicles.

This paper explores ways of estimating heavy vehicle trajectories in the absence of field-collected data. Field observations, of course, would be preferred but until such time as research is performed to collect such data, the approach described herein can be used to estimate the path of heavy vehicles in roadside and median encroachments.

INTRODUCTION

The vehicle's path during an encroachment is incorporated into the third version of the Roadside Safety Analysis Program's (RSAPv3) conditional probability model using field-measured vehicle trajectories. The potential path may be influenced by the driver's response and alertness, the roadside terrain and material and the vehicle's ability to respond. Using real-world trajectories incorporates all these factors into the trajectories and therefore makes the RSAPv3 procedure more realistic than simply plotting straight-line trajectories as was done in earlier versions of RSAP.

Each trajectory stored in the RSAPv3 database includes information such as the vehicle path, departure angle, departure speed, roadside terrain, and the posted speed limit of the road, among other on-road and off-road features. Knowledge of the path and vehicle departure speed allows RSAPv3 to compute the speed and position of the vehicle as it moves along the roadside and detect any intersections with hazards that might be located along the vehicle path. Vehicles which travel a short distance or have a high departure speed would have a higher energy when striking a roadside hazard than vehicles that travel a longer distance or have a lower departure speed. Knowledge of the vehicle path, departure speed, and angle are necessary to determine (1) the probability of a roadside hazard of being struck at difference offsets; (2) the range of energies

the hazard may be subjected to; and (3) the length of need of the barrier required to shield the hazard.

Currently, the RSAPv3 trajectory database is populated with the trajectories collected under NCHRP Project 17-22 which generated a run-off road (ROR) crash reconstruction database of 890 passenger vehicle cases. The data came from the FHWA rollover study, NCHRP Project 17-11 and new cases added under NCHRP Project 17-22. (1; 2) Both NCHRP 17-11 and 17-22 were limited to the study of passenger vehicles so, unfortunately, trajectory data is not available for heavy vehicles. Using passenger vehicle trajectories to represent heavy vehicle trajectories would include some trajectories that are unlikely for heavy vehicles. Passenger vehicles are smaller, have better braking and acceleration characteristics as well as different inertial properties so their encroachment and path characteristics are likely to be different than heavy vehicles. Understanding a heavy vehicle trajectory during an encroachment is crucial to several aspects of roadside safety including barrier test level section.

There are three methods of obtaining the necessary heavy vehicle trajectories for developing roadside guidance:

1. Collect new heavy vehicle trajectory data,
2. Find crash or encroachment databases that include heavy vehicle trajectories or
3. Assume heavy vehicles have similar trajectories to passenger vehicles if limited to reasonable speeds and angles.

While the first option is most likely to provide the highest quality data, it is exceedingly demanding of both time and funding for this unfunded effort. The third alternative is to selectively use passenger vehicle trajectories which meet certain criteria to represent vehicle trajectories. This paper explores the second and third options examining the available sources of heavy vehicle trajectories and presents a method for selecting representative trajectories. A database of presumptive truck trajectories that can be used in the development of future roadside safety guidance is developed. Comparisons are also made to a handful of real-world heavy vehicle encroachment trajectories.

AVAILABLE HEAVY VEHICLE TRAJECTORY SOURCES

Wright conducted a study of heavy vehicle crashes for the Georgia Department of Transportation in 1985. (3) One objective of the study was to “identify types of roadway and specific roadway and traffic characteristics most closely associated with large truck crashes.” While Wright did gather the roadway characteristics of these crashes, he did not gather the heavy vehicle paths. Wright’s study, therefore, does not include the information needed to create a database of heavy vehicle trajectories. The only database available with some of the required information for heavy vehicles is the Large Truck Crash Causation Study (LTCCS). (4) The LTCCS data includes scene diagrams which could be used to approximate a trajectory.

NCHRP 17-22 Data

The current passenger trajectory database is searched by RSAPv3 to identify trajectories which are appropriate for the situation based on similarity to the following segment characteristics (5):

- Roadside terrain,
- On-road horizontal curve radius,
- On-road vertical grade, and
- Posted speed limit.

Ray *et al.* found, through examination of the trajectory database, that passenger vehicles encroach onto the roadside at a wide range of speeds.(5) The average departure speed typically corresponds to approximately 90 percent of the posted speed when the speed limit was 50 mph or higher, and approximately 97 percent of the posted speed when the posted speed was 45 mph. (5) Figure 1 and Figure 2 provide the summary statistics for the departure speed and angle by

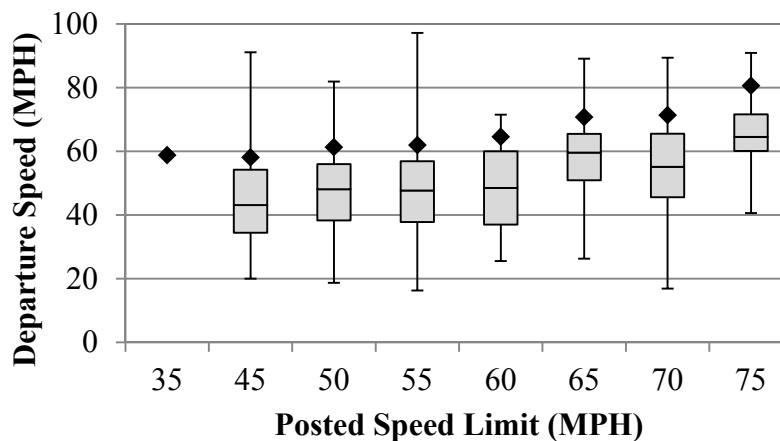


FIGURE 1 Passenger vehicle encroachment speed by posted speed limit.

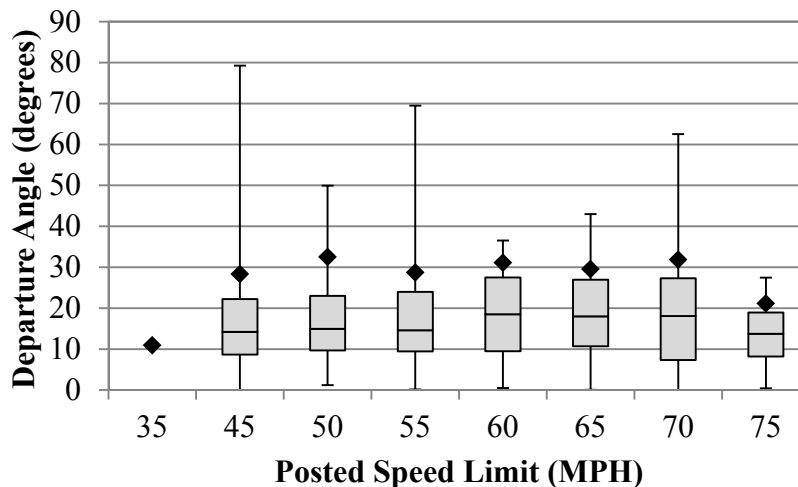


FIGURE 2 Passenger vehicle departure angle by posted speed limit.

the posted speed limit for passenger vehicle trajectories in the 17-22 database. Notice that the 35 mi/hr category has very little data, therefore, only a black diamond is shown.

Ray *et al.* in NCHRP 22-12(03), “Guidelines for Test Level 2 through 5 Bridge Railings” and Mak and Sicking when developing BCAP recognized that heavy vehicles cannot obtain the same departure speed and angle as passenger vehicles due to the many differences in handling, braking and power characteristics between passenger vehicles and heavy vehicles. They used the following simple point-mass procedure for limiting the possible encroachment angles based on the vehicle type, offset from the road, available friction and departure speed: (6; 7)

$$\theta_{max} = \cos^{-1}\left[1 - \frac{S_o f_{max} g}{V^2}\right]$$

where:

- Θ_{max} = The maximum likely encroachment angle in degrees,
- S_o = The vehicle offset from the edge of the travelled way in feet,
- f_{max} = The maximum available coefficient of friction,
- g = The gravity constant (i.e., 32.2 ft/s²) and
- V = The departure velocity in ft/s.

Based on 1989 AASHTO Guide Specification for Bridge Railing procedure, the maximum available side friction for SUTs was taken as 0.6 and the maximum available side friction for TTs was taken as 0.45. The vehicle offset, S_o , was taken to be half a typical 12-ft lane width which amounts to assuming that the heavy vehicles departed from the lane adjacent to the roadside or median. Θ_{max} was then calculated for each of the 890 passenger vehicle trajectories in the RSAPv3 trajectory database. If the actual departure angle was greater than Θ_{max} , the trajectory was eliminated as a possible representation of SUT or TT encroachments. The result was that 315 trajectories were deemed suitable for representing SUT trajectories (i.e., RSAPv3 trajectory grid 4) and are summarized in Figure 3 and Figure 4. The 890 original RSAPv3 trajectories were reduced to 253 which were deemed suitable for representing heavy vehicle trajectories (i.e., RSAPv3 trajectory grid 3) and are summarized in Figure 5 and Figure 6.

LTCCS Data

The Federal Motor Carrier Safety Administration (FMCSA) and the National Highway Traffic Safety Administration (NHTSA) compiled a nationally representative sample of large truck crashes in the Large Truck Crash Causation Study (LTCCS). (4) The data include scaled scene diagrams and a description of the circumstances. The NCHRP 17-54, “Consideration of Roadside Features in the Highway Safety Manual” research team studied the dataset as a potential source for heavy vehicle trajectories. (6) It was believed that the LTCCS scene diagrams could be used to provide road departure and trajectory data for heavy vehicles that could be incorporated into the RSAPv3 trajectory database.

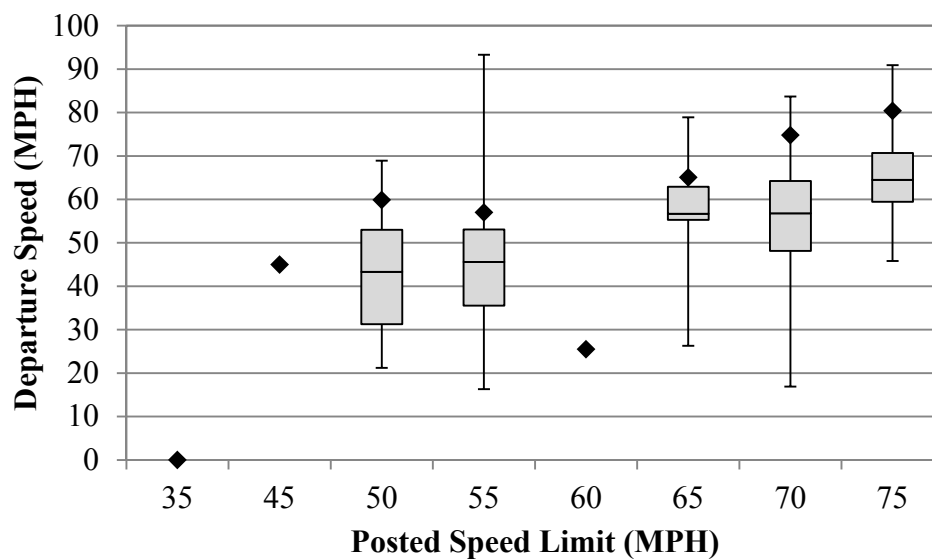


FIGURE 3 RSAPv3 SUT trajectory table departure speed by posted speed limit.

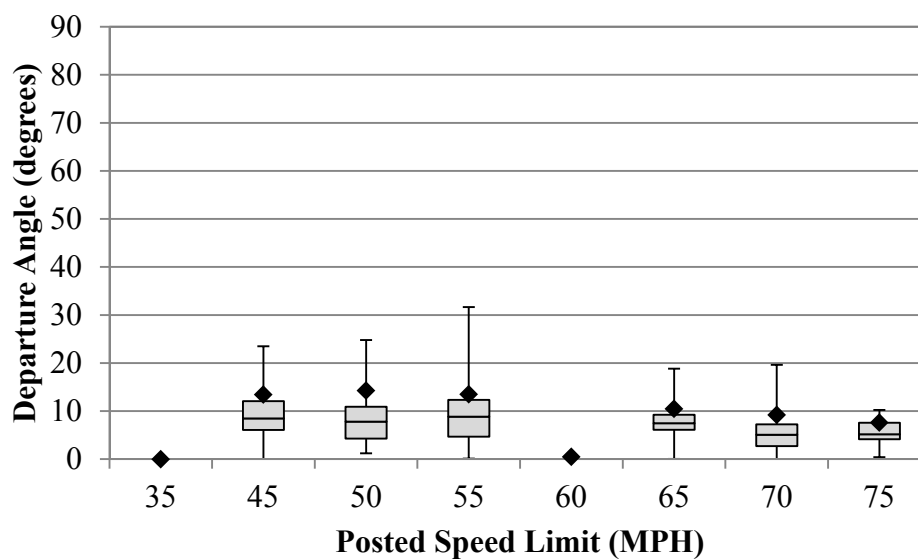


Figure 4. RSAPv3 SUT Trajectory Table Departure Angle by Posted Speed Limit.

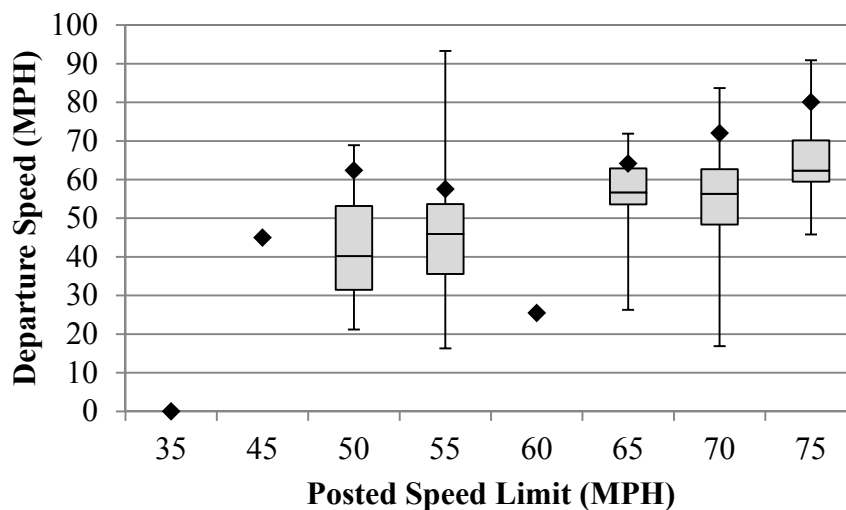


FIGURE 5 RSAPv3 TT trajectory table departure speed by posted speed limit.

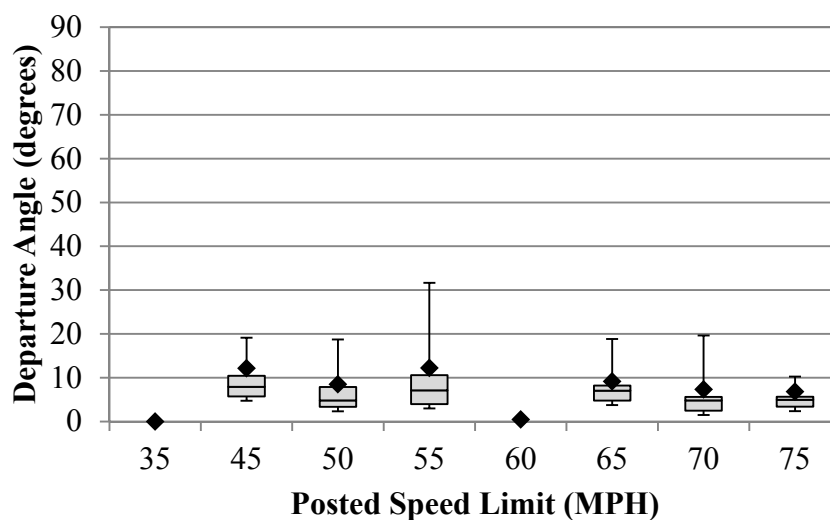


FIGURE 6 RSAPv3 TT trajectory table departure angle by posted speed limit.

Sixty eight single large truck left departure crashes were found in the data. Table 1 shows the body types for the 68 LTCCS cases that involved running off the left side of the roadway. Class 6 Single Unit Trucks (SUTs) comprised just over 16 percent of the cases and Classes 8-10 tractor-trailer trucks (TTs) comprised 72 percent of the cases so there is a 4.5 to one ratio of TT to SUTs which is consistent with the mix data found on highways within the United States (8)

The departure angle was estimated by drawing two tangents from the point of departure. One tangent was drawn with respect to the trajectory path and the other tangent was drawn with respect to the roadway edge of travel. The angle between these two tangent lanes represents the

TABLE 1 Distribution of LTCCS Body Types

Heavy Vehicle Type	Frequency	Percentage
Single unit truck ($4,500\text{kg} < \text{GVWR} \leq 8,850\text{kg}$)	4	5.88
Single unit truck ($8,850\text{kg} < \text{GVWR} \leq 12,000\text{kg}$)	2	2.94
Single unit truck ($\text{GVWR} > 12,000\text{kg}$)	11	16.18
Single unit truck (GVWR unknown)	1	1.47
Truck-tractor with no cargo trailer	1	1.47
Truck-tractor pulling one trailer	49	72.06
Total	68	100.00

departure angle. The roadside terrain and departure speed are not recorded in the LTCCS data although the posted speed limit is known for 66 of the 68 cases. While the NCHRP 17-54 research team concluded that further study of the dataset would not have satisfied the objectives of that project, but direct knowledge of heavy vehicle departure angles and heavy vehicles paths during encroachments are valuable clues into the behavior of heavy vehicles during an encroachment and this already collected data is considered in this study.

The departure angles for the 66 cases where posted speed limit is known are summarized in Figure 7. The gray vertical bars in these figures indicate the range of values which fall between the start of the second quartile and the end of the third quartile of the reported speed and angle for each posted speed limit. The black horizontal line at the middle of the gray vertical bars represents the median values for each posted speed limit. The black diamonds are located at the 85th percentile value and the thin black vertical lines represent the range in values (i.e., maximum and minimum) in the dataset. The mean encroachment angle for these 66 heavy vehicles was 12.6 degrees. A Posted Speed Limit (PSL) of 55 mi/hr experiences the widest departure angle range, with values observed between 5 and 40 degrees. Apart from one data point in the 55 mi/hr posted speed limit group and the entire 25 mi/hr speed limit group, all the encroachment angles were less than 33 degrees and the 85th percentile encroachment angles were less than 30 degrees.

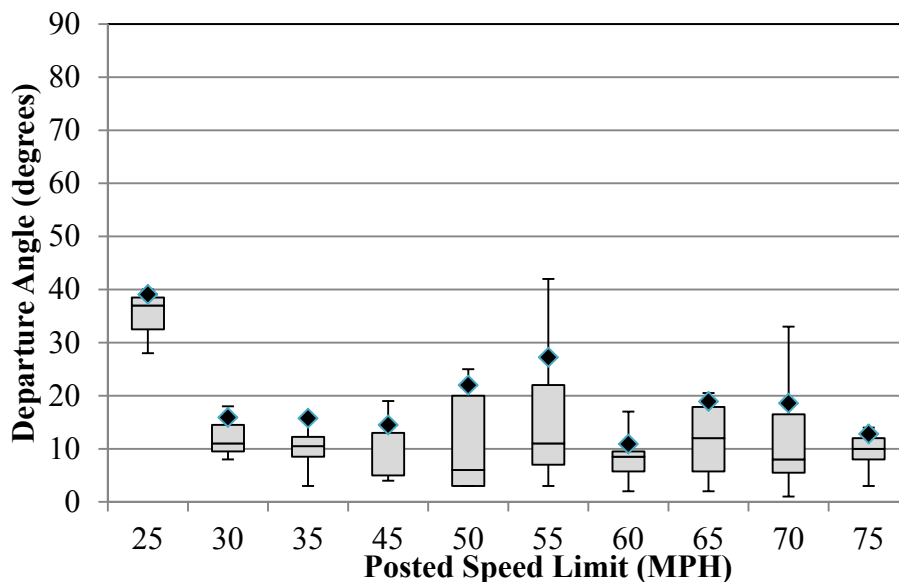
**FIGURE 7 LTCCS Heavy Vehicle Departure Angle by posted speed limit.**

Figure 8 shows a histogram of the passenger vehicle posted speed limits for the 68 left-side departure crashes in the LTCCS. Figure 8 shows the 25 and 30 mi/hr speed limit groups contain three cases each so the angle distribution for those speed limits in Figure 7 is drawn from a small sample. The speed limit group with the largest frequency are the 55 mi/hr roadways followed by the 35, 60, 45 and 70 mi/hr roadways respectively.

While the departure speed is not known from the LTCCS data, if one assumes that the encroachment speed is no greater than the travel speed, an encroachment speed can be assumed using the known posted speed limit for each of these collected heavy vehicle paths. It was found in NCHRP 12-90, Guidelines for Shielding Bridge Piers, that the measured mean travel speed of heavy vehicles is 0.96 times the posted speed limit for passenger vehicles with a standard deviation of $0.05 \cdot \text{PSL}$. (9) The speed distribution study from NCHRP 12-90 can be used to assign a reasonable distribution of heavy vehicle departure speeds to the 66 LTCCS cases based on the reported passenger vehicle posted speed.

The speed distribution was applied to the 66 LTCCS cases as follows. Each case in the LTCCS subset of 66 left-departure crashes with known speed limits was replicated in the RSAPv3 trajectory table three times. One group of cases was assigned an departure speed equal to the 15th percentile travel speed in that speed limit group, the next was assigned an departure speed equal to the 50th percentile travel speed in that speed limit group and the last was assigned an departure speed equal to the 85th percentile travel speed in that speed limit group. These three speeds result in approximately a normal distribution centered on the observed mean of $0.96 \cdot \text{PSL}$. Table 2 shows the recommended departure speed assignments for the LTCCS cases. The 66 LTCCS cases, therefore, have been transformed into 198 trajectories which have a normal speed distribution centered on $0.96 \cdot \text{PSL}$.

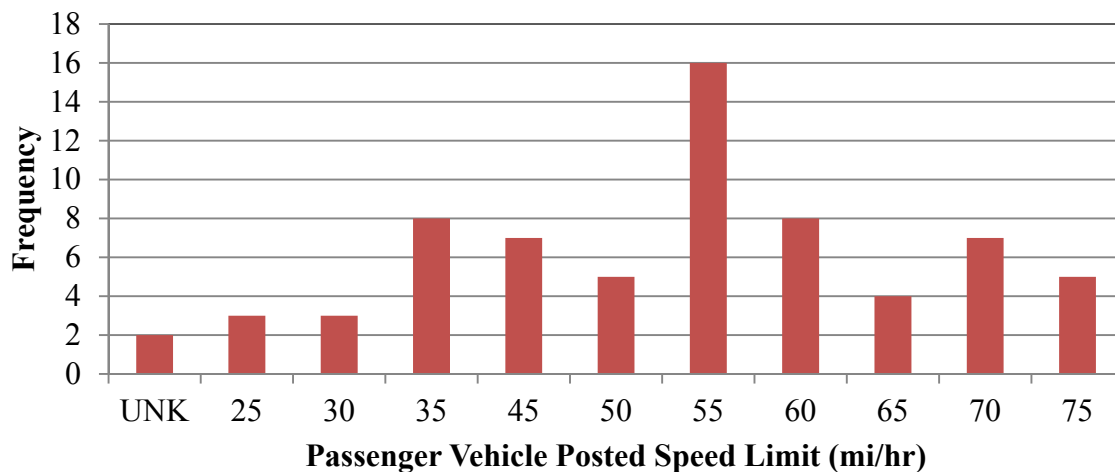


FIGURE 8 Histogram of passenger vehicle posted speed limits in the LTCCS.

TABLE 2 Recommended Departure Speeds for the LTCCS Cases

Posted Speed Limit (mi/hr)	LTCCS Case Freq.	Percentile		
		15 th	50 th	85 th
25	3	20.25	24	27.75
30	3	25.05	28.8	32.55
35	8	29.85	33.6	37.35
45	7	39.45	43.2	46.95
50	5	44.25	48	51.75
55	16	49.05	52.8	56.55
60	8	53.85	57.6	61.35
65	4	58.65	62.4	66.15
70	7	63.45	67.2	70.95
75	5	68.25	72	75.75
Total	66			

The LTCCS data also lacks roadside terrain information. The hard-copy case files for the 68 left-side departure cases were reviewed. The case files include photographs which, while not detailed enough to measure the slopes, are detailed enough to at least characterized the slopes as flat, relatively flat (i.e., less than 6:1) or greater than 6:1. Of the 68 cases, 40 (60 percent) were deemed to be flat, 28 percent appeared to be flatter than 6:1 and 12 (12 percent) appeared steeper than 6:1. The majority of the cases selected from the LTCCS data are, therefore, at least relatively flat and traversable (i.e., 88 percent). The use of these heavy vehicle trajectories derived from flat terrain allows the vehicle to interact with the roadside for a longer period without rolling over, therefore is a conservative assumption which is appropriate for developing roadside guidance. It is important to understand these assumptions should not be extended to the behavior of heavy vehicles on slopes.

Summary

The maximum encroachment angle used in NCHRP 22-12(03) for both single-unit trucks and truck-trailer trucks is 32 degrees. (6) The maximum encroachment angle used by Mak and Sicking in BCAP was 36 degrees.(7) Note that with the exception of the 25 mi/hr speed limit category in Figure 7 and a single maximum value in the 55 mi/hr speed limit category, all the other departure angles measured in the LTCCS database were less than 36 degrees so the LTCCS data appears to confirm the simple point-mass approach that Ray *et al.* and Sicking and Mak used in earlier studies. The maximum departure speed for the filtered database was 93 mi/hr and the mean was 47 mi/hr.

RESULTS

The approach taken in NCHRP 22-12(03) for converting passenger vehicle trajectories to heavy vehicle trajectories by limiting the speed and angle of the trajectories allowed for the inclusion of a large dataset collected under NCHRP 17-22. (10; 1; 2) The NCHRP 22-12(03) approach, however, did not include any vehicle paths from heavy vehicles. The LTCCS heavy vehicle paths, while lacking detailed data on the departure speeds, were used to supplement the covered heavy vehicle trajectories and are incorporated into trajectory grids 3 and 4 of RSAPv3 for use. These trajectory grids include heavy vehicle paths, departure angle and speed limitations discussed above. The heavy vehicle trajectories are summarized in Table 3.

CONCLUSIONS

The current RSAPv3 trajectory database includes 198 tractor trailer truck trajectories based on the vehicle paths in the LTCCS crash database combined with 253 passenger vehicle trajectories that were screened to represent reasonable tractor-trailer truck trajectories resulting in 451 available tractor trailer truck trajectories over a range of posted speed limits and encroachment angles (i.e., RSAPv3 trajectory grid 3). Similarly, the current RSAPv3 trajectory database includes 198 single-unit truck trajectories based on the vehicle paths in the LTCCS crash database combined with 315 passenger vehicle trajectories that were screened to represent reasonable single-unit truck trajectories resulting in 513 available single-unit truck trajectories over a range of posted speed limits and encroachment angles (i.e., RSAPv3 trajectory grid 4). While addition data collection to obtain more real-world heavy vehicle trajectories is highly desirable and recommended, the 964 heavy vehicle trajectories available in RSAPv3 represent the best available interim solution for modeling heavy vehicle trajectories.

TABLE 3 Number of Trajectories Used for Heavy Vehicles in RSAPv3

Posted Speed Limit (mi/hr)	SUT Trajectories		TT Trajectories	
	LTCCS	17-22	LTCCS	17-22
25	6	-	6	-
30	6	-	6	-
35	24	-	24	-
45	21	80	21	69
50	15	23	15	16
55	48	142	48	111
60	24	1	24	1
65	12	17	12	13
70	21	35	21	30
75	15	15	15	11
Total	198	315	198	253
	513		451	

REFERENCES

- 1 Roger Bligh and Shaw-Pin Miaou, "Determination of Safe/Cost Effective Roadside Slopes and Associated Clear Distances," NCHRP Project 17-11(2), National Cooperative Highway Research Program, Transportation Research Board, Washington, D.C., 2008.
- 2 Mak, K.K., Sicking, D.L., and B. A. Coon, "Identification of Vehicular Impact Conditions Associated with Serious Ran-off-Road Crashes," National Cooperative Highway Research Program Report 665, Transportation Research Board, Washington, D.C., 2010.
- 3 Wright, P., "Large Truck Safety and Roadway Elements," Project 8404, Georgia Department of Transportation, accessed online April 2014, https://smartech.gatech.edu/jspui/bitstream/1853/34604/1/e-20-656_297552.pdf, 1985.
- 4 National Highway Traffic Safety Administration, "Large Truck Crash Causation Survey Case Viewer." <http://www-nass.nhtsa.dot.gov/nass/ltrcs/SearchForm.aspx>. Accessed 12/28/2012.
- 5 Ray, M. H., Carrigan, C. E., Plaxico, C. A., Johnson, T. O., "Engineer's Manual: Roadside Safety Analysis Program (RSAP) Update," <http://rsap.roadsafellc.com/RSAPv3EngineersManual.pdf>, Roadsafellc LLC, Canton, ME, December 2012.
- 6 Ray, M.H., Carrigan, C.E., , "Consideration of Roadside Features in the Highway Safety Manual," NCHRP Project 17-54, National Cooperative Highway Research Program, Transportation Research Board, Washington, D.C., (in progress).
- 7 Mak, K. K. and Sicking, D. L., "Evaluation of Performance Level Selection Criteria for Bridge Railings," Draft Final Report (Unpublished), NCHRP Project 22-08, National Cooperative Highway Research Program, Washington, D.C., September 1993.
- 8 C.E. Carrigan and M.H. Ray, "Assessment of the MASH Heavy Vehicles for Field Relevancy," Transportation Research Board Annual Meeting Compendium of Papers, Transportation Research Board, Washington, D.C., (expected 2017).
- 9 Ray, M.H., Carrigan, C.E., Plaxico, C.A., "Guidelines for Shielding Bridge Piers," NCHRP Project 12-90, National Cooperative Highway Research Program, Transportation Research Board, Washington, D.C., (in progress).
- 10 Ray, M.H., Carrigan, C.E., Plaxico, C.A., "Recommended Guidelines for the Selection of Test Levels 2 through 5 Bridge Railings," NCHRP Project 22-12(03), National Cooperative Highway Research Program, Transportation Research Board, Washington, D.C., (in press).

Intelligent Transportation System Technology Application for Notification of Vehicles with Right-of-Way

CHIARA SILVESTRI DOBROVOLNY

RICHARD ZIMMER

HASSAN CHARARA

GARRETT ACKNER

Texas A&M Transportation Institute

Emergency vehicles (ambulances, firefighter's trucks, police cars, etc...) are faced with time restrictions and therefore run the risk of collision with other vehicles, especially on heavy traffic roads and intersections. Emergency vehicles must be granted the right of way when they are on an emergency call, but recognition of an upcoming emergency vehicle might not occur smoothly in certain situations. Emergency vehicles often overpass other vehicles and cross intersections despite facing a "red" light. Owing to limited visibility or distracted driving (cell phone usage or loud volume on stereo), the general traffic might not be in an ideal situation to clearly see and/or hear the approaching emergency vehicle. Such scenarios threaten the occurrence of a crash involving an emergency vehicle causing loss of valuable time and creating additional emergencies with occasionally considerable costs associated to lost of special equipment.

Crash data analysis was developed to determine the nature of some of those accidents involving emergency vehicle, to understand their general dynamics and determine which crash scenarios are mostly recurrent. Also, interviews were conducted to emergency personnel with the experience of conducting or riding on emergency vehicles to better understand ruling of emergency vehicles right-of-the-way, as well as their responsibility when on an emergency code on busy roads.

The researchers evaluated a practical application of V2V technology associated to notification of vehicles with right-of-way and conducted basic testing at the Texas A&M Transportation Institute's Riverside Proving Ground test bed to assess V2V technology in such instances.

Different driving scenarios were re-created with the involvement of existing commercial off-the-shelf technology to conveniently detect and alert other vehicles of an approaching emergency vehicle (or vehicle with right-of-way). The vehicles employed for this study were equipped with an On-Board-Unit (OBU). The OBU positioned in the emergency vehicle was designed to strategically send messages to other vehicles to alert them of the upcoming emergency vehicle. The OBU on the receiving vehicle was activated with audible alert notifying the driver of the oncoming emergency vehicle and its direction relatively to the receiving vehicle. Reception of the transmitted signal was limited to a certain distance radius so that only vehicles operating within this boundary would be alerted and affected. In all replicated scenarios, this intra-vehicle communication system promptly alerted drivers of the upcoming presence of an emergency vehicle, potentially avoiding and/or limiting potential crashes, thus contributing to the increase in roadside safety and traffic conditions.

The National Academies of
SCIENCES • ENGINEERING • MEDICINE

The **National Academy of Sciences** was established in 1863 by an Act of Congress, signed by President Lincoln, as a private, nongovernmental institution to advise the nation on issues related to science and technology. Members are elected by their peers for outstanding contributions to research. Dr. Marcia McNutt is president.

The **National Academy of Engineering** was established in 1964 under the charter of the National Academy of Sciences to bring the practices of engineering to advising the nation. Members are elected by their peers for extraordinary contributions to engineering. Dr. C. D. Mote, Jr., is president.

The **National Academy of Medicine** (formerly the Institute of Medicine) was established in 1970 under the charter of the National Academy of Sciences to advise the nation on medical and health issues. Members are elected by their peers for distinguished contributions to medicine and health. Dr. Victor J. Dzau is president.

The three Academies work together as the National Academies of Sciences, Engineering, and Medicine to provide independent, objective analysis and advice to the nation and conduct other activities to solve complex problems and inform public policy decisions. The Academies also encourage education and research, recognize outstanding contributions to knowledge, and increase public understanding in matters of science, engineering, and medicine.

Learn more about the National Academies of Sciences, Engineering, and Medicine at **www.national-academies.org**.

The **Transportation Research Board** is one of seven major programs of the National Academies of Sciences, Engineering, and Medicine. The mission of the Transportation Research Board is to increase the benefits that transportation contributes to society by providing leadership in transportation innovation and progress through research and information exchange, conducted within a setting that is objective, interdisciplinary, and multimodal. The Board's varied committees, task forces, and panels annually engage about 7,000 engineers, scientists, and other transportation researchers and practitioners from the public and private sectors and academia, all of whom contribute their expertise in the public interest. The program is supported by state transportation departments, federal agencies including the component administrations of the U.S. Department of Transportation, and other organizations and individuals interested in the development of transportation.

Learn more about the Transportation Research Board at **www.TRB.org**.



TRANSPORTATION RESEARCH BOARD
500 Fifth Street, NW
Washington, DC 20001

The National Academies of
SCIENCES • ENGINEERING • MEDICINE

The nation turns to the National Academies of Sciences, Engineering, and Medicine for independent, objective advice on issues that affect people's lives worldwide.

www.national-academies.org